

this document downloaded from

vulcanhammer.info

the website about
Vulcan Iron Works
Inc. and the pile
driving equipment it
manufactured

Visit our companion site
<http://www.vulcanhammer.org>

Terms and Conditions of Use:

All of the information, data and computer software ("information") presented on this web site is for general information only. While every effort will be made to insure its accuracy, this information should not be used or relied on for any specific application without independent, competent professional examination and verification of its accuracy, suitability and applicability by a licensed professional. Anyone making use of this information does so at his or her own risk and assumes any and all liability resulting from such use. The entire risk as to quality or usability of the information contained within is with the reader. In no event will this web page or webmaster be held liable, nor does this web page or its webmaster provide insurance against liability, for any damages including lost profits, lost savings or any other incidental or consequential damages arising from the use or inability to use the information contained within.

This site is not an official site of Prentice-Hall, Pile Buck, or Vulcan Foundation Equipment. All references to sources of software, equipment, parts, service or repairs do not constitute an endorsement.



U.S. Department of Transportation
Federal Highway Administration

Publication No. FHWA NHI-05-042
April 2006

NHI Courses No. 132021 and 132022 **Design and Construction of Driven Pile Foundations**

Reference Manual – Volume I



National Highway Institute

NOTICE

The contents of this report reflect the views of the authors, who are responsible for the facts and the accuracy of the data presented herein. The contents do not necessarily reflect policy of the Department of Transportation. This report does not constitute a standard, specification, or regulation. The United States Government does not endorse products or manufacturers. Trade or manufacturer's names appear herein only because they are considered essential to the objective of this document.

1. REPORT NO. FHWA-NHI-05-042	2. GOVERNMENT ACCESSION NO.	3. RECIPIENT'S CATALOG NO.	
4. TITLE AND SUBTITLE Design and Construction of Driven Pile Foundations – Volume I		5. REPORT DATE April 2006	
		6. PERFORMING ORGANIZATION CODE	
7. AUTHOR(S) P.J. Hannigan, G.G. Goble, G.E. Likins, and F. Rausche		8. PERFORMING ORGANIZATION REPORT NO.	
9. PERFORMING ORGANIZATION NAME AND ADDRESS Ryan R. Berg & Associates, Inc. 2190 Leyland Alcove Woodbury, MN 55125		10. WORK UNIT NO.	
		11. CONTRACT OR GRANT NO. DTFH61-02-T-63020	
12. SPONSORING AGENCY NAME AND ADDRESS National Highway Institute Federal Highway Administration U.S. Department of Transportation Washington, D.C.		13. TYPE OF REPORT & PERIOD COVERED Final Report	
		14. SPONSORING AGENCY CODE	
15. SUPPLEMENTARY NOTES FHWA Technical Consultants: J.A. DiMaggio, P.E. and C. Dumas, P.E. COTR - L. Jones <i>This manual is an update and revision of FHWA-HI-97-021 prepared by Goble Rausche Likins and Associates, Inc. Authors: P.J. Hannigan, G.G. Goble, G. Thendean, G.E. Likins and F. Rausche</i> FHWA Technical Consultant: J.A. DiMaggio			
16. ABSTRACT This manual is the reference text used for the FHWA NHI course Nos. 130221 Driven Pile Foundations – Design and Construction and 130222 Driven Pile Foundations – Construction Monitoring and reflects the current practice for pile foundations. The manual is also intended to serve as the FHWA's primary reference of recommended practice for driven pile foundations. The Design and Construction of Driven Pile Foundations manual is directed to geotechnical, structural, and construction engineers involved in the design and construction of pile supported structures. This manual is intended to serve as a practical reference of driven pile foundations. Volume I of the manual addresses design aspects including subsurface exploration, laboratory testing, static analyses, as well as specifications and foundation report preparation. Volume II covers construction aspects including dynamic formulas, wave equation analysis, dynamic pile testing, static load testing, Statnamic testing, Osterberg cell testing, as well as pile driving equipment, pile driving accessories, and pile installation inspection. Step by step procedures are included to facilitate use of most analysis procedures.			
17. KEY WORDS pile foundations, foundation deign, static analysis, foundation construction inspection		18. DISTRIBUTION STATEMENT No restrictions.	
19. SECURITY CLASSIF. Unclassified	20. SECURITY CLASSIF. Unclassified	21. NO. OF PAGES 968	22. PRICE

U.S. - SI Conversion Factors

From English	To SI	Multiply by	Quantity	From SI	To English	Multiply by
ft	m	0.3048	Length	m	ft	3.2808
inch	mm	25.40		mm	inch	0.039
ft ²	m ²	0.0929	Area	m ²	ft ²	10.764
inch ²	mm ²	645.2		mm ²	in ²	0.0015
ft ³	m ³	0.028	Volume	m ³	ft ³	35.714
inch ³	mm ³	16387		mm ³	inch ³	61x10 ⁻⁶
ft ⁴	m ⁴	0.0086	Second Moment of Area	m ⁴	ft ⁴	115.856
inch ⁴	mm ⁴	416231		mm ⁴	inch ⁴	2x10 ⁻⁶
lbm	kg	0.4536	Mass	kg	lbm	2.2046
lbm/ft ³	kg/m ³	16.02	Mass Density	kg/m ³	lbm/ft ³	0.062
lb	N	4.448	Force	N	lb	0.2248
kip	kN	4.448		kN	kip	0.2248
lbs/ft	N/m	14.59	Force/Unit- Length	N/m	lbs/ft	0.0685
kips/ft	kN/m	14.59		kN/m	kips/ft	0.0685
lbs/in ²	kPa	6.895	Force/Unit- Area; Stress; Pressure; Elastic Mod.	kPa	lbs/in ²	0.145
kips/in ²	MPa	6.895		MPa	kips/in ²	0.145
lbs/ft ²	Pa	47.88		Pa	lbs/ft ²	0.021
kips/ft ²	kPa	47.88		kPa	kips/ft ²	0.021

U.S. - SI Conversion Factors (continued)

From	To	Multiply by	Quantity	From	To	Multiply by
English	SI			SI	English	
lbs/ft ³	N/m ³	157.1	Force/Unit- Volume	N/m ³	lbs/ft ³	0.0064
kip/ft ³	kN/m ³	157.1		kN/m ³	kip/ft ³	0.0064
lb-inch	N-mm	112.98	Moment; or Energy	N-mm	lb-inch	0.0089
kip-inch	kN-mm	112.98		kN-mm	kip-inch	0.0089
lb-ft	N-m	1.356		N-m	lb-ft	0.7375
kip-ft	kN-m	1.356		kN-m	kip-ft	0.7375
ft-lb	Joule	1.356		Joule	ft-lb	0.7375
ft-kip	kJoule	1.356		kJoule	ft-kip	0.7375
s/ft	s/m	3.2808	Damping	s/m	s/ft	0.3048
blows/ft	blows/m	3.2808	Blow count	blows/m	blows/ft	0.3048

PREFACE

Engineers and contractors have been designing and installing pile foundations for many years. During the past three decades this industry has experienced several major improvements including newer and more accurate methods of predicting capacities, highly specialized and sophisticated equipment for pile driving, and improved methods of construction control.

In order to take advantage of these new developments, the FHWA developed a manual in connection with Demonstration Project No. 66, Design and Construction of Driven Pile Foundations. The primary purpose of the 1985 Manual was to support educational programs conducted by FHWA for transportation agencies. These programs consisted of (1) a workshop for geotechnical, structural, and construction engineers, and (2) field demonstrations of static and dynamic load testing equipment. Technical assistance on construction projects in areas covered by this Demonstration Project was provided to transportation agencies on request. A second purpose of equal importance was to serve as the FHWA's standard reference for highway projects involving driven pile foundations.

The original Manual was written by Suneel N. Vanikar with review and comment from Messrs. Ronald Chassie, Jerry DiMaggio, and Richard Cheney.

1996 Edition

After a decade of use, the Manual was updated in 1996. The manual was modified to include new developments that had taken place in the intervening years and to take advantage of the experience gained in using the Manual in the many workshops that were presented by Demonstration Project 66. The 1996 version of the Manual was prepared by Goble, Rausche, Likins, and Associates, Inc. under contract with the FHWA.

The authors' recognize the efforts of the project technical manager, Mr. Jerry DiMaggio, FHWA Principal Geotechnical Engineer, who provided invaluable guidance and input for the new manual. The authors' also acknowledge the additional contributions of the following technical review panel members of the 1996 manual listed in alphabetical order:

Mr. Chien-Tan Chang - FHWA
Mr. Tom Cleary - New Hampshire DOT
Mr. Chris Dumas - FHWA
Mr. Sam Holder - FHWA
Mr. Paul Passe - Florida DOT
Mr. Suneel Vanikar - FHWA

Mr. Richard Cheney - FHWA
Mr. Kerry Cook - FHWA
Mr. Carl Ealy - FHWA
Mr. Paul Macklin - Colorado DOT
Mr. Jan Six - Oregon DOT

The following individuals of the author's internal peer review team are also acknowledged for their technical advice and contributions in preparing the 1996 version of the manual.

Dr. Joseph Caliendo - Utah State University
Dr. D. Michael Holloway - InSituTech
Mr. Robert Lukas - Ground Engineering Consultants

Lastly, the authors' wish to thank the following Goble, Rausche, Likins, and Associates, Inc. employees for their vital contributions and significant effort in preparing the manual: Ms. Barbara Strader, Ms. Beth Richardson, Mr. Scott Webster, Mr. Neil Harnar, Mr. Jay Berger and Mr. Joe Beno.

2006 Edition

The 2006 version of the Manual is the third major version of the manual and was prepared by GRL Engineers, Inc. under contract with Ryan R Berg & Associates, Inc. The 2006 version of the Manual was once again updated to include new developments that had taken place since 1996 and to again serve a dual purpose. First, as a workshop participant's manual for the FHWA's National Highway Institute Courses on Driven Pile Foundations, and second to serve as FHWA's primary reference of recommended practice for driven pile foundations.

The authors' again recognize the efforts of the FHWA project technical manager Mr. Chris Dumas, and of Mr. Jerry DiMaggio, FHWA Principal Bridge Engineer - Geotechnical.

The manual is presented in two volumes. Volume I addresses design aspects and Volume II presents topics related to driven pile installation, monitoring, and inspection.

Design and Construction of Driven Pile Foundations - Volume I

Table of Contents	Page
1. NEED FOR A PILE MANUAL.....	1-1
1.1Scope of Manual	1-3
1.2Information Sources.....	1-4
 2. OVERVIEW OF PILE FOUNDATION AND DESIGN AND CONSTRUCTION	 2-1
2.1Design of Pile Foundations.....	2-1
2.2Construction of Pile Foundations.....	2-1
2.3Foundation Specialist Involvement in Pile Foundation Projects.....	2-2
2.4Driven Pile Design-Construction Process	2-2
2.5Communication...	2-14
References.....	2-16
 3. ECONOMICS OF FOUNDATIONS FOR HIGHWAY STRUCTURES	 3-1
3.1Foundation Alternatives	3-1
3.2Examples of Cost Savings by Utilizing Modern Design and Construction Control Practices.....	 3-2
3.3.1... Definition of Foundation Support Cost	3-3
3.3.2... Cost Optimization for One Pile Section.....	3-3
3.3.3... Cost Optimization for Multiple Pile Types and/or Pile Sections	3-13
3.4Use of Value Engineering Proposals	3-15
3.5Design – Build Contracts	3-17
References	3-18
 4. SUBSURFACE EXPLORATIONS.....	 4-1
4.1Subsurface Properties for Pile Design	4-1
4.2Subsurface Exploration Phases.....	4-3
4.2.1... Planning the Exploration Program (office work)	4-3
4.2.2... Field Reconnaissance Survey.....	4-3
4.2.3... Detailed Site Exploration.....	4-5
4.3Guidelines for Minimum Structure Exploration Programs	4-8
4.4Methods of Subsurface Exploration.....	4-10
4.5Soil and Rock Sampling.....	4-10
4.5.1... Disturbed Soil Samplers.....	4-12
4.5.2... Undisturbed Soil Samplers.....	4-20
4.5.3... Rock Core Samplers.....	4-24
4.6Ground Water Monitoring	4-24

Table of Contents		Page
4.7	Summarization and Interpretation of Subsurface Profile.....	4-25
4.8	Additional Subsurface Explorations	4-26
	References	4-28
5.	IN-SITU TESTING	5-1
5.1	Cone Penetration Test (CPT) and (CPTu).....	5-1
5.1.1...	Equipment Description and Operation	5-3
5.1.2...	Interpretation of CPT/CPTu Test Results.....	5-6
5.1.3...	Advantages and Disadvantages of CPT/CPTu Tests.....	5-6
5.2	Pressuremeter Test - (PMT)	5-9
5.3	Dilatometer Test - (DMT)	5-10
5.4	Vane Shear Test	5-11
5.5	Dynamic Cone Test	5-12
	References	5-13
6.	LABORATORY TESTING	6-1
6.1	Types of Tests	6-2
6.1.1...	Classification and Index Tests	6-2
6.1.2...	Shear Strength Tests	6-2
6.1.3...	Consolidation Tests.....	6-6
6.1.4...	Electro Chemical Classification Tests	6-6
6.2	Laboratory Testing for Pile Driveability Considerations	6-7
	References	6-9
7.	FOUNDATION DESIGN PROCEDURE	7-1
7.1	Foundation Design Approach	7-1
7.2	Consideration of Spread Footing Foundation	7-5
7.3	Establishment of a Need for a Deep Foundation	7-5
	References	7-9
8.	PILE TYPES FOR FURTHER EVALUATION.....	8-1
8.1	Overview of Typical Pile Types.....	8-1
8.2	Timber Piles.....	8-14
8.3	Steel H-Piles.....	8-16
8.4	Steel Pipe Piles.. ..	8-18
8.5	Precast Concrete Piles	8-21
8.5.1...	Prestressed Concrete Piles.....	8-22
8.5.2...	Reinforced Concrete Piles	8-25
8.5.3...	Spun-Cast Concrete Cylinder Piles.....	8-27

Table of Contents		Page
8.6	Cast-In-Place Concrete Piles.....	8-29
8.6.1...	Cased Driven Shell Concrete Piles	8-29
8.6.2...	Uncased Concrete Piles.....	8-33
8.7	Composite Piles.	8-35
8.7.1...	Precast Concrete - Steel Piles	8-35
8.7.2...	Wood Composite Piles.....	8-36
8.7.3...	Tapertube Pile	8-36
8.7.4...	Pipe – Corrugated Shell Piles	8-37
8.7.5 ..	Composite Tapered Precast Tip - (TPT).....	8-38
8.8	Design Considerations in Aggressive Subsurface Environments ...	8-38
8.8.1...	Corrosion of Steel Piles.....	8-39
8.8.2...	Sulfate and Chloride Attack on Concrete Piles	8-44
8.8.3...	Insects and Marine Borers Attack on Timber Piles	8-46
8.8.4...	Design Options for Piles Subject to Degradation or Abrasion	8-47
8.9	Selection of Pile Type and Size for Further Evaluation.....	8-48
References....	8-52
9.	STATIC ANALYSIS METHODS	9-1
9.1	Basics of Static Analysis	9-2
9.2	Events During and After Pile Driving.....	9-5
9.2.1...	Cohesionless Soils.....	9-5
9.2.2...	Cohesive Soils	9-6
9.3	Load Transfer	9-8
9.4	Effective Overburden Pressure.....	9-10
9.5	Considerations in Selection of Design Soil Strength Parameters	9-11
9.6	Factors of Safety	9-13
9.7	Design of Single Piles.....	9-17
9.7.1...	Ultimate Capacity of Single Piles	9-17
9.7.1.1	Bearing Capacity of Piles In Cohesionless Soils .	9-17
9.7.1.1a ..	Meyerhof Method Based on Standard Penetration Test (SPT) Data	9-18
9.7.1.1b ..	Brown Method	9-23
9.7.1.1c ..	Nordlund Method	9-25
9.7.1.2	Ultimate Capacity of Piles in Cohesive Soils	9-42
9.7.1.2a ..	Total Stress - α -Method	9-42
9.7.1.3	Effective Stress Method.....	9-51
9.7.1.4	Ultimate Capacity of Piles in Layered Soils	9-56

Table of Contents		Page
9.7.1.5The DRIVEN Computer Program	9-56
9.7.1.6Ultimate Capacity of Piles on Rock.....	9-58
9.7.1.7Methods Based on Cone Penetration Test (CPT) Data	9-65
9.7.1.7a	..Elsami and Fellenius Method.....	9-66
9.7.1.7b	..Nottingham and Schmertmann Method	9-68
9.7.1.7c	..Laboratoire des Ponts et Chaussees (LPC)	9-75
9.7.2	... Uplift Capacity of Single Piles	9-81
9.7.3	... Ultimate Lateral Capacity of Single Piles	9-82
9.7.3.1Lateral Capacity Design Methods.....	9-85
9.7.3.2Broms' Method.....	9-86
9.7.3.3Reese's LPILE Method	9-100
9.8Design of Pile Groups.....	9-116
9.8.1	... Axial Compression Capacity of Pile Groups.....	9-118
9.8.1.1Pile Group Capacity in Cohesionless Soils.....	9-118
9.8.1.2Pile Group Capacity in Cohesive Soils	9-120
9.8.1.3Block Failure of Pile Groups	9-122
9.8.2	... Settlement of Pile Groups	9-124
9.8.2.1Elastic Compression of Piles	9-124
9.8.2.2Settlements of Pile Groups in Cohesionless Soils	9-125
9.8.2.2a	..Method Based on SPT Test Data	9-125
9.8.2.2b	..Method Based on CPT Test Data	9-125
9.8.2.3Settlement of Pile Groups in Cohesive Soils.....	9-126
9.8.2.4Time Rate of Settlement in Cohesive Soils.....	9-132
9.8.2.5Settlement of Pile Groups in Layered Soils	9-133
9.8.2.6Settlement of Pile Groups Using the Janbu Tangent Modulus Approach.....	9-138
9.8.2.7Settlement of Pile Groups Using the Neutral Plane Method.....	9-144
9.8.3	... Uplift Capacity of Pile Groups	9-147
9.8.3.1Group Uplift Capacity by AASHTO Code.....	9-147
9.8.3.2Tomlinson Group Uplift Method	9-148
9.8.4	... Lateral Capacity of Pile Groups	9-150
9.9Special Design Considerations	9-156
9.9.1	... Negative Shaft Resistance or Downdrag	9-156
9.9.1.1Methods for Determining Negative Shaft Resistance.....	9-159

Table of Contents		Page
9.9.1.1a ..	Traditional Approach to Negative Shaft Resistance	9-159
9.9.1.1b ..	Alternative Approach to Negative Shaft Resistance.....	9-163
9.9.1.2	Methods for Reducing Negative Shaft Resistance Forces	9-166
9.9.2 ..	Vertical Ground Movements from Swelling Soils.....	9-169
9.9.3 ..	Lateral Squeeze of Foundation Soil.....	9-169
9.9.3.1	Solutions to Prevent Tilting.....	9-170
9.9.4 ..	Ultimate Capacity of Piles in Soils Subject to Scour.....	9-171
9.9.5 ..	Soil and Pile Heave	9-173
9.9.6 ..	Seismic Considerations	9-175
9.10	Additional Design and Construction Considerations	9-177
9.10.1.	Time Effects on Pile Capacity	9-177
9.10.1.1 ..	Soil Setup	9-177
9.10.1.2 ..	Relaxation	9-179
9.10.1.3 ..	Estimation of Pore Pressures During Driving	9-180
9.10.2.	Effects of Predrilling, Jetting and Vibratory Installation on Pile Capacity.....	9-182
9.10.3.	Effects of Site Dewatering on Pile Capacity and Adjacent Structures.....	9-183
9.10.4	Densification Effects on Pile Capacity and Installation Conditions	9-184
9.10.5	Plugging of Open Pile Sections.....	9-184
9.10.6	Design Considerations Due to Pile Driving Induced Vibrations	9-188
9.10.7	Design Considerations Due to Pile Driving Noise.....	9-191
9.10.8	Pile Driveability.....	9-192
9.10.8.1	Factors Affecting Driveability.....	9-193
9.10.8.2	Methods for Determining Pile Driveability.....	9-194
9.10.8.3	Driveability Versus Pile Type.....	9-195
References.....	9-196
10. ...	STRUCTURAL ASPECTS OF DRIVEN PILE FOUNDATIONS	10-1
10.1	Driving Stresses.	10-1
10.2	Factors Affecting Allowable Design Stresses	10-2
10.3	AASHTO Allowable Design and Driving Stresses.....	10-3
10.3.1.	Steel H-piles.....	10-3
10.3.2.	Steel Pipe Piles (unfilled).....	10-4

Table of Contents		Page
10.3.3. Steel Pipe Piles (top driven and concrete filled).....		10-5
10.3.4. Precast, Prestressed Concrete Piles.....		10-6
10.3.5. Conventionally Reinforced Concrete Piles		10-8
10.3.6. Timber Piles		10-9
10.4Geotechnical and Structural Loads.....		10-10
10.5Layout of Pile Groups		10-12
10.6Preliminary Design of Pile Caps		10-13
10.7Structural Properties of Piles		10-18
10.8Design of Piles for Combined Axial and Lateral Loads		10-19
10.8.1. Structural Design of Driven Piles for Axial Loads by ASD...		10-19
10.8.2. Structural Design of Driven Piles for Combined Axial and . Lateral Loads by ASD		10-21
. 10.8.2.1 ..Timber Piles.....		10-22
. 10.8.2.2 ..Steel Piles.....		10-23
. 10.8.2.3 ..Prestressed Concrete Piles		10-25
. 10.8.2.3.1..Concrete Pile Interaction Analysis		10-27
10.9Unsupported Length and Buckling.....		10-28
10.9.1. Timber Piles		10-29
10.9.2. Steel Piles		10-29
10.9.3. Prestressed Concrete Piles.....		10-29
References.....		10-30
11...CONTRACT DOCUMENTS		11-1
11.1Overview of Plan and Specification Requirements		11-1
11.2Background and Reasons For Specification Improvement.....		11-3
11.3Generic Driven Pile Specification.....		11-6
References.....		11-42
12...PILE FOUNDATION DESIGN SUMMARY		12-1
12.1Introduction.....		12-1
12.2Block 1 - Establish Global Project Performance		12-1
12.3Block 2 – Define Project Geotechnical Site Conditions.....		12-5
12.4Block 3 – Determine Preliminary Foundation Loads at . the Substructure Level		12-6
12.5Block 4 - Develop and Execute Subsurface Exploration Program for Feasible Foundation Systems.....		12-6
12.6Block 5 - Evaluate Information and Select Candidate Foundation Systems for Further Evaluation.....		12-8
12.7Block 6 - Deep Foundation Type		12-8

Table of ContentsPage

12.8Block 7 – Select Candidate Driven Pile Types and . Sections for Further Study	12-8
12.9Block 8 - Select Static Analysis Method and Calculate . Ultimate Capacity Versus Depth	12-9
12.10 ..Block 9 - Identify Most Economical Candidate Pile Types . and/or Sections	12-9
12.11 ..Block 10 – Calculate Driveability of Candidate Pile Types.....	12-9
12.12 ..Block 11 – Select 1 to 2 Final Candidate Pile Types for Trial . Group Sizing	12-10
12.13 ..Block 12 – Evaluate Capacity, Settlement, and Performance of . Trial Pile Groups	12-11
12.14 ..Block 13 – Size and Estimate Pile Cap Cost for Trial Pile Groups..	12-11
12.15 ..Block 14 – Summarize Total Cost of Final Candidate Piles.....	12-11
12.16 ..Block 15 – Select and Optimize Final Pile Type, Capacity . And Group Configuration	12-12
. 12.16.1 ...Single Pile Capacity.....	12-12
. 12.16.2 ...Pile Group Capacity.....	12-12
. 12.16.3 ...Group Settlement Calculations	12-17
. 12.16.4 ...Lateral Pile Capacity Analysis	12-18
. 12.16.5 ...Uplift Capacity Calculations	12-19
. 12.16.6 ...Negative Shaft Resistance	12-19
. 12.16.7 ...Lateral Squeeze Evaluation.....	12-21
. 12.16.8 ...Group Lateral Response Evaluation.....	12-21
12.17 ..Block 16 – Does Optimized Design Meet all Requirements?.....	12-21
12.18 ..Block 17 – Prepare Plans and Specifications, Set Field . Capacity Determination Procedure	12-22
12.19 ..Block 18 – Contractor Selection.....	12-22
12.20 ..Block 19 – Perform Wave Equation Analysis of Contractor’s . Equipment Submission	12-23
12.21 ..Block 20 – Set Preliminary Driving Criteria	12-23
12.22 ..Block 21 – Drive Test Pile and Evaluate Capacity	12-23
12.23 ..Block 22 – Adjust Driving Criteria or Design	12-23
12.24 ..Block 23 – Construction Control	12-23
12.25 ..Block 24 – Post Construction Evaluation and Review	12-24
 13... FOUNDATION DESIGN REPORT PREPARATION	 13-1
13.1Guidelines for Foundation Design Report Preparation	13-1
13.2Parts of a Foundation Design Report.....	13-2
13.3Geotechnical Report Reviews.....	13-8

Table of Contents	Page
13.4Information Made Available to Bidders	13-9
References.....	13-10

List of Appendices

APPENDIX A... List of FHWA Pile Foundation Design and Construction References	A-1
APPENDIX B... List of ASTM Pile Design and Testing Specifications.....	B-1
APPENDIX C-1 Information and Data on Various Pile Types, Metric Units.....	C1-1
APPENDIX C-2 Information and Data on Various Pile Types, U.S. Units.....	C2-1
APPENDIX D .. Pile Hammer Information	D-1
APPENDIX E... Subsurface Exploration Results for Peach Freeway Design Problem	E-1
APPENDIX F .. Peach Freeway Example Problem Calculations	F-1
APPENDIX G .. Driven Pile Foundation Design by LRFD	G-1

List of Tables Page

Table 3-1	Cost Saving Recommendations for Pile Foundations	3-4
Table 4-1	Summary of Field or Laboratory Tests for Pile Design Parameters	4-2
Table 4-2	Subsurface Exploration Phases	4-4
Table 4-3	Sources of Subsurface Information and Use	4-6
Table 4-4	Example Field Reconnaissance Report Form.....	4-7
Table 4-5	Methods of Subsurface Explorations	4-11
Table 4-6	Empirical Values for ϕ , D_r , and Unit Weight of Granular Soils Based on Corrected N' (after Bowles, 1977)	4-19
Table 4-7	Empirical Values For Unconfined Compressive Strength (q_u) and Consistency of Cohesive Soils Based on Uncorrected N (after Bowles, 1977).....	4-20
Table 4-8	Undisturbed Soil Samples.....	4-23
Table 5-1	Summary of In-Situ Test Methods	5-2
Table 5-2	Drill Rig with 45 kN (10 kip) Push Capacity.....	5-5
Table 5-3	Truck with 180 kN (40 kip) Push Capacity	5-5
Table 6-1	Laboratory Tests on Soils for Foundation Design	6-3
Table 6-2	Typical Values of Sensitivity from Sowers (1979)	6-8
Table 7-1	Foundation Types and Typical Uses.....	7-4
Table 8-1	Technical Summary of Piles	8-3
Table 8-2	Preservative Assay Retention Requirements (AWPI, 2002)	8-46
Table 8-3	Pile Type Selection Based on Subsurface and Hydraulic Conditions.....	8-50
Table 8-4	Pile Type Selection Pile Shape Effects	8-51
Table 9-1	Recommended Factor of Safety Based on Construction Control Method	9-14
Table 9-2	Methods of Static Analysis for Piles in Cohesionless Soils	9-19
Table 9-3	Input Factors for Brown's Method	9-24
Table 9-4a	Design Table for Evaluating K_s for Piles when $\omega = 0^\circ$ and $V = 0.0093$ to 0.0930 m^3/m (0.10 to 1.00 ft^3/ft).....	9-37
Table 9-4b	Design Table for Evaluating K_s for Piles when $\omega = 0^\circ$ and $V = 0.093$ to 0.0930 m^3/m (1.0 to 10.0 ft^3/ft)	9-38
Table 9-5	Methods of Static Analysis for Piles in Cohesive Soils.....	9-43
Table 9-6	Approximate Range of β and N_t Coefficients (Fellenius, 1991)	9-53
Table 9-7	Engineering Classification for In-Situ Rock Quality	9-64

List of Tables	Page
Table 9-8 C_{sc} Values for Elsami and Fellenius Method	9-67
Table 9-9 CPT C_f Values	9-69
Table 9-10 Driven Pile Type Categories for LPC Method	9-76
Table 9-11(a)... Curve Selection Based on Pile Type and Insertion Procedures for Clay and Silt	9-76
Table 9-11(b)... Curve Selection Based on Pile Type and Insertion Procedures for Sand and Gravel	9-77
Table 9-12 Cone Bearing Capacity Factors for LPC Method	9-77
Table 9-13 Values of Coefficients n_1 and n_2 for Cohesive Soils	9-87
Table 9-14 Values of K_h For Cohesionless Soils	9-87
Table 9-15 Representative Values of ϵ_{50} for Clays	9-112
Table 9-16 Representative p-y Modulus Values, k, for Clays and Sands ...	9-113
Table 9-17 Time Factor (T)	9-133
Table 9-18 Typical Modulus and Stress Exponent Values	9-141
Table 9-19 Laterally Loaded Pile Groups Studies	9-153
Table 9-20 Soil Setup Factors (after Rausche et al., 1996)	9-179
Table 10-1 Maximum Allowable Stresses For Steel H-Piles	10-4
Table 10-2 Maximum Allowable Stresses For Unfilled Steel Pipe Piles	10-5
Table 10-3 Maximum Allowable Stresses For Top Driven, Concrete Filled, Steel Pipe Piles	10-6
Table 10-4 Maximum Allowable Stresses For Precast, Prestressed, Concrete Piles	10-7
Table 10-5 Maximum Allowable Stresses For Conventionally Reinforced Concrete Piles	10-8
Table 10-6 Maximum Allowable Stresses For Timber Piles	10-9
Table 12-1(a)... North Abutment Pile Capacity Summary for 11.5 m Pile Embedment	12-13
Table 12-1(b)... North Abutment Pile Length Summary for a 1,780 kN Ultimate Pile Capacity	12-13
Table 12-2(a)... Pier 2 Pile Capacity Summary for 10.0 m Pile Embedment	12-14
Table 12-2(b)... Pier 2 Pile Length Summary for a 1,780 kN Ultimate Pile	12-14
Table 12-2(c)... Pier 2 Pile Capacity Summary Before and After Channel Degradation Scour Based on Nordlund Method	12-14
Table 12-3(a)... Pier 3 Pile Capacity Summary for 13.0 m Pile Embedment	12-15
Table 12-3(b)... Pier 3 Pile Length Summary for a 1,780 kN Ultimate Pile Capacity	12-15

List of Tables Page

Table 12-4(a)... South Abutment Pile Capacity Summary for a 17.5 m Pile Embedment.....	12-16
Table 12-4(b)... South Abutment Pile Length Summary for a 1,780 kN Ultimate Pile Capacity.....	12-16

List of Figures Page

Figure 2.1	Driven Pile Design and Construction Process.....	2-4
Figure 2.2	Design Stage Communication.....	2-14
Figure 2.3	Construction Stage Communication.....	2-15
Figure 3.1	Example Soil Profile.....	3-5
Figure 3.2a	Ultimate Capacity in kN Versus Pile Penetration Depth in Meters	3-6
Figure 3.2b	Ultimate Capacity in Tons Versus Pile Penetration Depth in Feet	3-6
Figure 3.3	Pile Cost Versus Pile Penetration Depth.....	3-7
Figure 3.4a	Ultimate Pile Capacity (kN) and Pile Support Cost – Ultimate Versus Depth (m).....	3-8
Figure 3.4b	Ultimate Pile Capacity (tons) and Pile Support Cost – Ultimate Versus Depth (ft).....	3-8
Figure 3.5a	Allowable Design Load in kN Versus Depth Based on Construction Control	3-9
Figure 3.5b	Allowable Design Load in Tons Versus Depth Based on Construction Control	3-9
Figure 3.6a	Pile Support Cost – Design Versus Allowable Design Load in kN	3-11
Figure 3.6b	Pile Support Cost – Design Versus Allowable Design Load in Tons	3-11
Figure 3.7	Pile Cap Cost as a Function of Column Load	3-12
Figure 3.8a	Pile Support Cost – Ultimate (\$/kN) vs Depth (m) for Two H-pile Sections.....	3-16
Figure 3.8b	Pile Support Cost – Ultimate (\$/ton) vs Depth (ft) for Two H-pile Sections.....	3-16
Figure 4.1	SPT Procedure from Mayne, <i>et al.</i> , (2002)	4-12
Figure 4.2	SPT Hammer Types	4-13
Figure 4.3	Split Barrel Sampler from Mayne, <i>et al.</i> , (2002)	4-13
Figure 4.4	Energy Measurements on Automatic SPT Hammer	4-15
Figure 4.5	SPT Test Results for Safety and Automatic Hammers (after Finno, 1989)	4-16
Figure 4.6	Chart for Correction of N-values in Sand for Influence of Effective Overburden Pressure (after Peck, <i>et al.</i> , 1974).....	4-18
Figure 4.7a	Thin Wall Open Tube (after FHWA, 1972).....	4-21
Figure 4.7b	Various Diameter Thin Wall Tubes from Mayne, <i>et al.</i> , (2002) .	4-21
Figure 4.8	Pitcher Sampler from Mayne, <i>et al.</i> , (2002)	4-22
Figure 4.9	Rigid and Swivel Type Double Tube Core Barrels (after FHWA, 1972).....	4-24
Figure 4.10	Example Subsurface Profile.....	4-27

List of Figures.....Page

Figure 5.1a	Terminology Regarding the Cone Penetrometer (from Robertson and Campanella, 1989)	5-4
Figure 5.1b	Cone Penetrometers (from Mayne, <i>et al.</i> , 2002).....	5-4
Figure 5.2	Simplified Soil Classification Chart for Standard Electronic Friction Cone (after Robertson <i>et al.</i> , 1986).....	5-7
Figure 5.3	Typical CPT Data Presentation.....	5-8
Figure 5.4	Pressuremeter Test Schematic.....	5-9
Figure 5.5	Dilatometer Test Equipment	5-10
Figure 5.6	Vane Shear Test Equipment and Procedure (after Mayne <i>et al.</i> , 2002).....	5-11
Figure 7.1	Situations in which Deep Foundations may be Needed (modified from Vesic, 1977)	7-7
Figure 8.1	Pile Classification System	8-2
Figure 8.2	Timber Piles	8-14
Figure 8.3	H-piles with Driving Shoes	8-16
Figure 8.4	Typical Closed-End Pipe Pile.....	8-19
Figure 8.5	Large Diameter Open End Pile Piles	8-19
Figure 8.6	760 mm (30 inch) Diameter Spin Fin Pile	8-21
Figure 8.7	Typical Prestressed Concrete Piles (after PCI, 1993).....	8-23
Figure 8.8	Square Precast, Prestressed Concrete Pile.....	8-24
Figure 8.9	Typical Conventionally Reinforced Concrete Piles (after PCA, 1951).....	8-26
Figure 8.10	Typical Spun-Cast Concrete Cylinder Pile Section	8-28
Figure 8.11	Concrete Cylinder Pile	8-28
Figure 8.12	Tapered Monotube Section with Add-on Sections	8-32
Figure 8.13	Square Concrete Pile with Embedded H-pile Section at Pile Toe.....	8-36
Figure 8.14	Tapered Tube Pile	8-37
Figure 8.15	Soil Sampling and Testing Protocol for Corrosion Assessment of Steel Piles in Non-Marine Applications.....	8-41
Figure 8.16	Procedure for Uniform or Macrocell Corrosion Assessment of Steel Piles in Non-Marine Applications	8-42
Figure 8.17	Procedure for Determination of Electrochemical Testing, Corrosion Monitoring and Corrosion Mitigation Techniques	8-43
Figure 8.18	Loss of Thickness by Corrosion for Steel Piles in Seawater (after Morley and Bruce, 1983)	8-45
Figure 9.1	Situation Where Two Static Analyses are Necessary - Due to Scour	9-4

List of Figures.....Page

Figure 9.2	Situation Where Two Static Analyses are Necessary - Due to Fill Materials	9-4
Figure 9.3	Compaction of Cohesionless Soils During Driving of Piles (Broms 1966)	9-7
Figure 9.4	Disturbance of Cohesive Soils During Driving of Piles (Broms 1966)	9-7
Figure 9.5	Typical Load Transfer Profiles	9-9
Figure 9.6	Effective Overburden Pressure Diagram - Water Table Below Ground Surface	9-12
Figure 9.7	Effective Overburden Pressure Diagram - Water Table Above Ground Surface	9-12
Figure 9.8	Soil Profile for Factor of Safety Discussion	9-15
Figure 9.9	Nordlund's General Equation for Ultimate Pile Capacity	9-27
Figure 9.10	Relation of δ/ϕ and Pile Displacement, V, for Various Types of Piles (after Nordlund, 1979)	9-32
Figure 9.11	Design Curve for Evaluating K_δ for Piles when $\phi = 25^\circ$ (after Nordlund, 1979)	9-33
Figure 9.12	Design Curve for Evaluating K_δ for Piles when $\phi = 30^\circ$ (after Nordlund, 1979)	9-34
Figure 9.13	Design Curve for Evaluating K_δ for Piles when $\phi = 35^\circ$ (after Nordlund, 1979)	9-35
Figure 9.14	Design Curve for Evaluating K_δ for Piles when $\phi = 40^\circ$ (after Nordlund, 1979)	9-36
Figure 9.15	Correction Factor for K_δ when $\delta \neq \phi$ (after Nordlund, 1979)	9-39
Figure 9.16	Chart For Estimating α_t Coefficient and Bearing Capacity Factor N'_q (Chart modified from Bowles, 1977)	9-40
Figure 9.17	Relationship Between Maximum Unit Pile Toe Resistance and Friction Angle for Cohesionless Soils (after Meyerhof, 1976)	9-41
Figure 9.18	Adhesion Values for Piles in Cohesive Soils (after Tomlinson, 1979)	9-46
Figure 9.19a	Adhesion Factors for Driven Piles in Clay – SI Units (after Tomlinson, 1980)	9-47
Figure 9.19b	Adhesion Factors for Driven Piles in Clay – US Units (after Tomlinson, 1980)	9-48
Figure 9.20	Chart for Estimating β Coefficient versus Soil Type ϕ' Angle (after Fellenius, 1991)	9-53
Figure 9.21	Chart for Estimating N_t Coefficient versus Soil Type ϕ' Angle (after Fellenius, 1991)	9-54

List of Figures.....Page	
Figure 9.22	DRIVEN Project Definition Screen 9-58
Figure 9.23	DRIVEN Soil Profile Screen – Cohesive Soil 9-58
Figure 9.24	DRIVEN Cohesive Soil Layer Properties Screen 9-59
Figure 9.25	DRIVEN Soil Profile Screen – Cohesionless Soil..... 9-59
Figure 9.26	DRIVEN Cohesionless Soil Layer Properties Screen 9-60
Figure 9.27	DRIVEN Pile Selection Drop Down Menu and Pile Detail Screen 9-60
Figure 9.28	DRIVEN Toolbar Output and Analysis Options 9-62
Figure 9.29	DRIVEN Tabular Output Screen 9-62
Figure 9.30	DRIVEN Graphical Output for End of Driving..... 9-63
Figure 9.31	DRIVEN Graphical Output for Restrike 9-63
Figure 9.32	Penetrometer Design Curves for Pile Side Friction in Sand (after FHWA Implementation Package, FHWA-TS-78-209)..... 9-70
Figure 9.33	Design Curve for Pile Side Friction in Clay (after Schmertmann, 1978) 9-71
Figure 9.34	Illustration of Nottingham and Schmertmann Procedure for Estimating Pile Toe Capacity (FHWA-TS-78-209) 9-72
Figure 9.35	Maximum Unit Shaft Resistance Curves for LPC Method..... 9-78
Figure 9.36	Soil Resistance to a Lateral Pile Load (adapted from Smith, 1989) 9-83
Figure 9.37	Ultimate Lateral Load Capacity of Short Piles in Cohesive Soils 9-91
Figure 9.38	Ultimate Lateral Load Capacity of Long Piles in Cohesive Soils 9-92
Figure 9.39	Ultimate Lateral Load Capacity of Short Piles in Cohesionless Soils..... 9-93
Figure 9.40	Ultimate Lateral Load Capacity of Long Piles in Cohesionless Soils..... 9-94
Figure 9.41	Load Deflection Relationship Used in Determination of Broms' Maximum Working Load 9-95
Figure 9.42	Lateral Deflection at Ground Surface of Piles in Cohesive Soils 9-97
Figure 9.43	Lateral Deflection at Ground Surface of Piles in Cohesionless Soils..... 9-98
Figure 9.44	LPILE Pile-Soil Model 9-101
Figure 9.45	Typical p-y Curves for Ductile and Brittle Soil (after Coduto 1994)..... 9-102
Figure 9.46	Graphical Presentation of LPILE Results (after Reese, et al. 2000) 9-104

List of Figures.....Page

Figure 9.47	Comparison of Measured and COM624P Predicted Load-Deflection Behavior versus Depth (after Kyfor <i>et al.</i> 1992)	9-105
Figure 9.48	LPILE Main Screen	9-106
Figure 9.49	LPILE Data Menu and Project Title Window	9-107
Figure 9.50	LPILE Data Menu and Pile Property and Pile Section Windows	9-107
Figure 9.51	LPILE Loading Type and Distributed Loads Input Screens.....	9-109
Figure 9.52	LPILE Pile Head Boundary Conditions and Loading Input Screen	9-109
Figure 9.53	LPILE Soil Layers and Individual Soil Property Input Screens..	9-111
Figure 9.54	LPILE Analysis Type Input Screen.....	9-114
Figure 9.55	LPILE Computation Menu Screen.....	9-115
Figure 9.56	Stress Zone from Single Pile and Pile Group (after Tomlinson, 1994)	9-117
Figure 9.57	Overlap of Stress Zones for Friction Pile Group (after Bowles, 1988)	9-119
Figure 9.58	Measured Dissipation of Excess Pore Water Pressure in Soil Surrounding Full Scale Pile Groups (after O'Neill, 1983) ...	9-121
Figure 9.59	Three Dimensional Pile Group Configuration (after Tomlinson, 1994)	9-123
Figure 9.60	Equivalent Footing Concept.....	9-127
Figure 9.61	Typical e-log p Curve from Laboratory Consolidation Test	9-128
Figure 9.62	Pressure Distribution Below Equivalent Footing for Pile Group (adapted from Cheney and Chassie, 1993)	9-130
Figure 9.63	Values of the Bearing Capacity Index, C', for Granular Soil (modified after Cheney and Chassie, 1993).....	9-135
Figure 9.64	The Non-Linear Relation Between Stress and Strain in Soil (after Fellenius, 1990)	9-138
Figure 9.65	Neutral Plane (after Goudrealt and Fellenius, 1994).....	9-145
Figure 9.66	Uplift of Pile Group in Cohesionless Soil (after Tomlinson, 1994)	9-149
Figure 9.67	Uplift of Pile Group in Cohesive Soils (after Tomlinson, 1994)	9-149
Figure 9.68	Illustration of p-multiplier Concept for Lateral Group Analysis	9-151
Figure 9.69	Typical Plots of Load versus Deflection and Bending Moment versus Deflection for Pile Group Analysis (adapted from Brown and Bollman, 1993)	9-155
Figure 9.70(a)..	Common Downdrag Situation Due to Fill Weight.....	9-158

List of Figures.....Page

Figure 9.70(b).. Common Downdrag Situation Due to Ground Water Lowering	9-158
Figure 9.71 Pressure Distribution Chart Beneath the End of a Fill (after Cheney and Chassie, 1993)	9-161
Figure 9.72 Geofoam Blocks for Embankment Construction	9-167
Figure 9.73 Over-sized Collar for Bitumen Coating Protection.....	9-168
Figure 9.74 Examples of Abutment Tilting Due to Lateral Squeeze.....	9-170
Figure 9.75 Local and Channel Degradation Scour	9-173
Figure 9.76 Balance of Forces on Pile Subject to Heave (after Haggerty and Peck, 1971)	9-175
Figure 9.77 Excess Pore Water Pressure due to Pile Driving (after Poulos and Davis, 1980)	9-181
Figure 9.78 Plugging of Open End Pipe Piles (after Paikowsky and Whitman, 1990)	9-187
Figure 9.79 Plugging of H-Piles (after Tomlinson, 1994)	9-187
Figure 9.80 Predicted Vibration Levels for Class II and Class III Soils (after Bay, 2003)	9-190
Figure 10.1 Pile Group with General Loads	10-11
Figure 10.2 Assumed Material Stress Strain Curves	10-27
Figure 10.3 Pile Interaction Diagram.....	10-28
Figure 11.1a Pile and Driving Equipment Data Form – SI Version	11-13
Figure 11.1b Pile and Driving Equipment Data Form – US Version.....	11-14
Figure 12.1 Driven Pile Design and Construction Process.....	12-2
Figure 12.2 Peach Freeway Subsurface Profile.....	12-7

LIST OF SYMBOLS

- A - Pile cross sectional area.
- A_b - Brown's regression analysis factor based on soil type.
- A_p - Pile cross section area at pile toe of an unplugged pile section.
- A_s - Pile shaft exterior surface area.
- A_{si} - Pile shaft interior surface area.
- A_t - Pile toe area.
- A_{tp} - Actual steel area at pile toe.
- B - Width of pile group.
- B_b - Brown's regression analysis factor based on soil type.
- B_d - Projected width of pile group at depth d.
- b - Pile diameter.
- b_f - Distance from midpoint of slope to centerline of embankment fill.
- b_o - Critical punching shear perimeter.
- C - Wave speed of pile material.
- C_f - Conversion factor for cone tip resistance to sleeve friction.
- C_c - Compression index.
- C_{cr} - Recompression index.
- C_d - Pile perimeter at depth d.

LIST OF SYMBOLS

- C_F - Correction factor for K_δ when $\delta \neq \phi$.
- C_N - Correction factor for SPT N value.
- C_s - Dimensionless shape factor.
- C_{sc} - Shaft correlation coefficient.
- C_{tc} - Toe correction coefficient.
- C_v - Coefficient of consolidation.
- c - Cohesion.
- c' - Effective cohesion.
- c_a - Adhesion or shear stress between the pile and soil at failure.
- c_u - Undrained shear strength or can be determined from $q_u/2$.
- c_{u1} - Average undrained shear strength around pile group.
- c_{u2} - Undrained shear strength below pile toe level.
- D - Pile embedded length.
- D_B - Pile embedded length into bearing stratum.
- D_r - Relative density.
- d - Depth.
- Δd - Length of pile segment.
- E - Modulus of elasticity of pile material.
- E_r - Manufacturers rated hammer energy.

LIST OF SYMBOLS

- E_s - Soil modulus.
- e - Void ratio.
- e_c - Eccentricity of applied load for free-headed pile.
- e_0 - Initial void ratio.
- F_{vs} - Reduction factor for vibratory installed piles.
- F_p - Plug mobilization factor.
- F_z - Largest factored axial load of the superstructure.
- f_s - Cone unit sleeve friction.
- \bar{f}_s - Average cone unit sleeve friction.
- f'_c - Ultimate compression strength for concrete.
- f_n - Negative unit shaft resistance over the shaft surface area.
- f_{pe} - Effective prestress after losses.
- f_s - Positive unit shaft resistance over the shaft surface area.
- f_{si} - Interior unit shaft resistance.
- f_{so} - Exterior unit shaft resistance.
- f_y - Yield stress of pile material for steel.
- H - Original thickness of stratum.
- H_v - Maximum vertical drainage path in cohesive layer.
- h - Ram stroke.

LIST OF SYMBOLS

- h_f - Height of embankment fill.
- I - Moment of inertia.
- I_f - Influence factor for group embedment.
- j - Stress exponent.
- K - Ratio of unit pile shaft resistance to cone unit sleeve friction for cohesionless soils.
- K_c - Cone bearing capacity factor.
- K_h - Coefficient of horizontal subgrade reaction.
- K_o - Coefficient of earth pressure at rest.
- K_p - Rankine passive pressure coefficient.
- K_δ - Coefficient of lateral earth pressure.
- k - Slope of soil modulus.
- L - Total pile length.
- ΔL - Length of pile between two measuring points under no load conditions.
- M_u - Bending moment.
- M_x - Factored moment about the x-axis acting on the pile cap.
- M_y - Factored moment about the y-axis acting on the pile cap.
- M_y - Broms resisting moment of the pile.
- m_n - Dimensionless modulus number.
- m_r - Dimensionless recompression modulus number.

LIST OF SYMBOLS

- N - Uncorrected field SPT resistance value.
- N_{60} - SPT resistance value corrected for 60% energy transfer.
- N' - Corrected SPT resistance value.
- \bar{N}' - Average corrected SPT resistance value.
- N_b - Number of hammer blows per 25 mm.
- N_c - Dimensionless bearing capacity factor.
- N'_q - Dimensionless bearing capacity factor.
- N_t - Toe bearing capacity coefficient.
- n - Number of piles in pile group.
- n_1 - Empirical coefficient for calculating the coefficient of subgrade reaction.
- n_2 - Empirical coefficient for calculating the coefficient of subgrade reaction.
- P_m - P-multiplier for p-y curve.
- p - Soil resistance per unit pile length.
- Δp - Change in pressure.
- p_c - Preconsolidation pressure.
- p_d - Effective overburden pressure at the center of depth increment d .
- p_f - Design foundation pressure.
- p_i - Pressure.
- p_o - Effective overburden pressure.

LIST OF SYMBOLS

- \bar{p}_o - Average effective overburden pressure.
- p_t - Total overburden pressure, also effective overburden pressure at the pile toe.
- Q - Load.
- ΔQ - Load increment.
- Q_a - Allowable design load of a pile.
- Q_d - Dead load on a pile.
- Q_l - Live load on a pile.
- Q_m - Maximum allowable lateral working load.
- Q_n - Drag load on a pile.
- Q_u - Ultimate pile capacity.
- Q_{ug} - Ultimate pile group capacity.
- q_c - Cone tip resistance.
- \bar{q}_c - Average cone tip resistance.
- q_E - cone tip resistance after correction for pore pressure and effective stress
- q_{Eg} - geometric average of the corrected cone tip resistance over the influence zone.
- q_L - Limiting unit toe resistance.
- q_t - Unit toe resistance over the pile toe area.
- q_u - Unconfined compressive strength.
- R_f - Friction ratio or f_s/q_c .

LIST OF SYMBOLS

- R_s - Ultimate pile shaft resistance.
- R_t - Ultimate pile toe resistance.
- R_u - Ultimate soil resistance.
- S - Section modulus about an axis perpendicular to the load plane.
- SRD - Soil resistance to driving.
- S_t - Sensitivity of a cohesive soil.
- s - Estimated total settlement.
- s_b - Set per blow.
- s_f - Settlement at failure.
- T - Theoretical time factor for percentage of primary consolidation.
- t - Time for settlement to occur.
- t_{cap} - Thickness of pile cap.
- U - Displacement.
- u - Pore water pressure (neutral pressure).
- V - Volume of soil displaced per unit length of pile.
- v - Design shear stress.
- v_c - Nominal shear strength of concrete.
- W_c - Estimated weight of pile cap.
- W_g - Effective weight of pile/soil block.

LIST OF SYMBOLS

- W_s - Estimated weight of soil above pile cap.
- w_p - Weight of soil plug.
- w - Width of pile cap.
- y - Lateral soil (or pile) deflection.
- Z - Length of pile group.
- Z_d - Projected length of pile group at depth d .
- z - Pile spacing.
- α - An empirical adhesion factor.
- α' - Ratio of pile unit shaft resistance to cone unit sleeve friction for cohesive soils.
- α_t - Dimensionless factor in Nordlund method (dependent on pile depth-width relationship).
- β - Beta shaft resistance coefficient.
- β_h - Dimensionless length factor for lateral load analysis.
- Δ - Elastic compression.
- Δu_m - Maximum excess pore pressure.
- δ - Friction angle between pile and soil.
- ϵ - Strain.
- ϵ_{50} - Strain at $1/2$ maximum principal stress.
- η - Dimensionless length factor for lateral load analysis.
- η_g - Pile group efficiency.

LIST OF SYMBOLS

- γ - Total unit weight of soil.
- γ' - Buoyant unit weight of soil.
- γ_D - Dry unit weight of soil.
- γ_f - Unit weight of embankment fill.
- γ_w - Unit weight of water.
- σ - Normal or total overburden stress (pressure).
- σ' - Effective stress or $(\sigma - u)$.
- σ_a - Maximum allowable stress in compression parallel to the wood grain.
- σ'_p - Preconsolidation pressure or stress.
- σ'_{vc} - Vertical consolidation stress.
- σ'_1 - Effective stress after stress increase.
- σ'_o - Effective stress prior to stress increase.
- σ'_r - Constant reference stress.
- τ - Shear strength of soil.
- ϕ - Angle of internal friction of soil.
- ϕ' - Effective angle of internal friction of soil.
- ψ - Ratio of undrained shear strength divided by effective overburden pressure, c_u/p_o' .
- ω - Angle of pile taper from vertical.

LIST OF SYMBOLS

Chapter 1 NEED FOR A PILE MANUAL

In 1985 the Federal Highway Administration published the first edition of this manual. Twenty years have elapsed since the original manual was developed and seven years since the last published update. Changes in pile design, construction, and performance requirements make it necessary to once again update the manual. Significant changes in practice addressed by this edition of the manual include:

routine use of higher strength pile materials and higher foundation loads, emphasis on a rational economic evaluation of the foundation design, updates in software programs for pile foundation analysis and design, use and quantification of soil set-up in foundation design and construction, improvements in pile installation equipment and equipment performance monitoring, increased use of instrumented static load test programs.

The goals of the original manual are unchanged. It is useful to repeat them here with modest updating.

1. There exists a vast quantity of information on the subject of pile foundations which presently is not compiled in a form which is useful to most practicing engineers. There are proven rational design procedures, information on construction materials, equipment and techniques, and useful case histories. Unfortunately, much of this information is fragmented and scattered. Standard textbooks and other publications on the subject tend to be theoretically oriented; practicing design and construction engineers often find them lacking in practical aspects.
2. Many of the methods currently in practice often lead to unnecessarily conservative designs because they are based solely on experience and tradition with little theoretical background. Newer and more rational design procedures and techniques can be applied to provide more economical pile systems which will safely support the applied structural loads without excessive safety factors.
3. During fiscal year 2000, FHWA and the State Transportation departments spent approximately 8.8 billion dollars for constructing, replacing, or rehabilitating bridges. Of that amount approximately 2.6 billion dollars were spent on bridge substructures and of that, at least 1.3 billion dollars were spent on foundations. In addition, city and county governments, whose practices closely follow the State practices, spend large

amounts on construction of bridges. There are opportunities for substantial savings in foundation construction costs, specifically in the area of pile foundations.

Cost savings can be achieved by the use of improved methods of design and construction technology. A minimum of fifteen percent of the substructure cost can be easily saved by utilizing such methods and, in most cases, the savings are more significant.

4. A comprehensive manual has been needed for some time to transfer available technology and to upgrade the level of expertise in pile foundations. This manual is intended to fulfill that need as well as to establish minimum design standards.
5. Design criteria for major and unusual bridge structures are becoming more complex and sophisticated. Extreme design events such as scour, debris loading, vessel impact, and seismic events require that foundation performance be evaluated under lateral and uplift loading, group behavior, and substructure - superstructure interaction. This new series of performance criteria frequently results in foundations which are more costly, more complex to design, and more difficult to construct.
6. The loading conditions noted above can have a substantial impact on the structural design of the piles. In the past, driven piles have usually been designed structurally for axial loads only using an allowable stress approach. The allowable stresses had been set primarily to assure pile drivability. Modern pile driving hammers may make it possible to exceed these traditional allowable stresses. However, the requirement that piles be analyzed for combined horizontal and axial loads requires a change in the evaluation procedure. The pile top is subjected to both horizontal and axial loads and in a pile group the pile resistance to lateral loads varies with each pile row. Of course this complicates the geotechnical analysis. It also complicates the structural analysis of the pile. A combined bending and axial load analysis of the structural behavior of the pile must be made. Particularly for concrete piles this analysis must be made based on an ultimate strength analysis and it is not always obvious which pile is the critical one. Excellent software is now available to perform the necessary analyses.
7. The final selection of a design should involve a cost evaluation. In the past, such evaluations have been implied but they were not a routine part of the design process. Methods have been developed to perform cost evaluations of pile foundations that include the effects of soil set-up. These concepts will be presented in this edition of the manual.

The original manual represented a major advance in that it included the most modern technology for pile design that was available. At the same time, the manual presented this technology so that it was usable to the practicing engineer. The work was very successful helping many transportation departments to modernize their design procedures.

1.1 SCOPE OF MANUAL

Since most piles used for highway structures are driven piles, and to keep this manual to a manageable size, this manual is limited to driven piles. The manual has been divided into two volumes. Volume I covers the design of pile foundations and Volume II covers installation, construction control, and inspection. However, sufficient information is provided in Volume I so that spread footings and drilled/bored piles, *e.g.*, drilled shafts, auger cast piles, *etc.*, can be considered in the foundation type selection process. This manual is intended to serve as a reference to all practical aspects of the design and construction of driven pile foundations.

All aspects of pile foundation design and construction, including subsurface exploration and laboratory testing, geotechnical and structural design analysis, foundation report preparation, and construction monitoring are covered in a systematic manner. Theoretical discussions have been included only where necessary. Specific recommendations are made wherever appropriate. Workshop exercises are included to provide hands-on knowledge to workshop participants and manual users.

It is important for design and construction engineers and pile construction inspectors to be familiar with pile driving equipment, accessories and inspection procedures. A separate section on this subject is included in this manual to fulfill this need.

During the period that the first edition of this manual was in use, several changes occurred in design requirements. For example, more stringent requirements for scour, vessel impact and seismic events have been implemented in design. The scour requirements make pile driveability analysis more critical. For vessel impact and seismic considerations, both pile uplift and lateral analyses are becoming more important. It has become much more common to consider the effects of soil strength changes with time in the design and construction process. In the past ten years, a better understanding of pile group behavior has been gained and this knowledge is now being put into practice. Finally, this edition of the manual is presented in both Systems International (SI) and customary U.S. English units.

As with the previous document, this edition is still the basis for a course on the design of driven pile foundations. This course will continue the original goal of modernizing transportation department practice in this area. Also, new engineers continue to join transportation department organizations and require updating of their knowledge in the practical aspects of pile design and installation.

The use of Load and Resistance Factor Design (LRFD) for highway bridges has been approved by the Subcommittee for Bridges and Structures of the American Association of State Highway and Transportation Officials (AASHTO). It has been mandated that all bridge design be based on this approach by October 2007. This design philosophy includes foundations and, of course, driven piles. This manual will continue to follow the working stress design philosophy. However, an overview of LRFD design of driven pile foundations is provided in Appendix G. NHI Course 130082A, LRFD for Highway Bridge Substructures and Earth Retaining Structures, has been developed on the use of LRFD in foundation design and is now available.

1.2 INFORMATION SOURCES

The information presented in this manual has been collected from several sources. The information has been condensed, modified and updated as needed. The sources include state-of-the-art technical publications, manufacturers' literature, existing Federal Highway Administration (FHWA), National Highway Institute (NHI) and Transportation Research Board (TRB) publications, standard textbooks, and information provided by State and Federal transportation engineers. Reference lists are provided at the end of each chapter. Many of the documents used in the development or updating of this manual, as well as useful industry links are available at www.fhwa.dot.gov/bridge/geo.htm.

Chapter 2

OVERVIEW OF PILE FOUNDATION DESIGN AND CONSTRUCTION

2.1 DESIGN OF PILE FOUNDATIONS

As stated by Professor R. B. Peck, “driving piles for a foundation is a crude and brutal process”. The interactions among the piles and the surrounding soil are complex. Insertion of piles generally alters the character of the soil and intense strains are set up locally near the piles. The non-homogeneity of soils, along with the effects of the pile group and pile shape, adds further difficulties to the understanding of soil-pile interaction.

Broad generalizations about pile behavior are unrealistic. An understanding of the significance of several factors involved is required to be successful in the design of pile foundations. Because of the inherent complexities of pile behavior, it is necessary to use practical semi-empirical methods of design, and to focus attention on significant factors rather than minor or peripheral details. The foundation engineer must have a thorough understanding of foundation loads, subsurface conditions including soil/rock properties and behavior, the significance of special design events, foundation performance criteria, and current practices in foundation design and construction in the area where the work is to be done to arrive at the optimum foundation solution.

2.2 CONSTRUCTION OF PILE FOUNDATIONS

Construction of a successful driven pile foundation that meets the design objectives depends on relating the requirements of the static analysis methods presented on the plans to the dynamic methods of field installation and construction control. The tools for obtaining such a foundation must be explicitly incorporated into the plans and specifications as well as included in the contract administration of the project.

A pile foundation must be installed to meet the design requirements for compressive, lateral and uplift capacity. This may dictate driving piles for a required ultimate capacity or to a predetermined length established by the designer. It is equally important to avoid pile damage or foundation cost overruns by excessive driving. These objectives can all be satisfactorily achieved by use of wave equation analysis, dynamic monitoring of pile driving, and static load testing. Commonly used dynamic formulas, such as Engineering News formula, have proven unreliable as pile capacities increased and more sophisticated pile installation equipment was routinely used by contractors.

Knowledgeable construction supervision and inspection are the keys to proper installation of piles. State-of-the-art designs and detailed plans and specifications must be coupled with good construction supervision to achieve desired results.

Post construction review of pile driving results versus predictions regarding pile driving resistances, pile length, field problems, and load test capacities is essential. These reviews add to the experience of all engineers involved on the project and will enhance their skills. In addition, the implementation of LRFD in pile foundation design with rationally determined resistance factors makes it possible to use data from the post construction review to improve the resistance factors. Particularly, if substantial amounts of dynamic testing is done for job quality control then that data can feed directly back into improved resistance factors.

2.3 FOUNDATION SPECIALIST INVOLVEMENT IN PILE FOUNDATION PROJECTS

The input of an experienced foundation specialist from the planning stage through project design and construction is essential to produce a successful driven pile foundation. A foundation specialist has both a structural and geotechnical background in design and construction. The foundation specialist is the most knowledgeable person for selecting the pile type, estimating pile length, and choosing the most appropriate method to determine ultimate pile capacity. Therefore, the foundation specialist should be involved throughout the design and construction process. In some project phases, *i.e.* preliminary explorations, preliminary design, and final design, the foundation specialist will have significant involvement. In other project phases, such as construction, and post construction review, the foundation specialist's involvement may be more of a technical services role. The foundation specialist's involvement provides the needed continuity of design personnel in dealing with design issues through the construction stage.

2.4 DRIVEN PILE DESIGN-CONSTRUCTION PROCESS

The driven pile design and construction process has aspects that are unique in all of structural design. Because the driving characteristics are related to pile capacity for most soils, they can be used to improve the accuracy of the pile capacity estimate. In general, the various methods of determining pile capacity from dynamic data such as driving resistance with wave equation analysis and dynamic measurements are considerably more accurate than the static analysis methods based on subsurface exploration information. It must be clearly understood that the static analysis based on the subsurface exploration

information usually has the function of providing an *estimate* of the pile length prior to going to the field. The final driving criterion is usually a blow count that is established after going to the field and the individual pile penetrations may vary depending on the soil variability. Furthermore, pile driveability is a very important aspect of the process and must be considered during the design phase. If the design is completed, a contractor is selected, and then the piles cannot be driven, large costs can be generated. It is absolutely necessary that the design and construction phases be linked in a way that does not exist elsewhere in construction.

The driven pile design-construction process is outlined in the flow chart of Figure 2.1. This flow chart will be discussed block by block using the numbers in the blocks as a reference and it will serve to guide the designer through all of the tasks that must be completed.

Block 1: Establish Global Project Performance Requirements

The first step in the entire process is to determine the general structure requirements.

1. Is the project a new bridge, a replacement bridge, a bridge renovation, a retaining wall, a noise wall, or sign or light standard?
2. Will the project be constructed in phases or all at one time?
3. What are the general structure layout and approach grades?
4. What are the surficial site characteristics?
5. Is the structure subjected to any special design events such as seismic, scour, downdrag, debris loading, vessel impact, *etc.*? If there are special design events, the design requirements should be reviewed at this stage so that these can be factored into the site investigation.
6. Are there possible modifications in the structure that may be desirable for the site under consideration?
7. What are the approximate foundation loads? What are the deformation or deflection requirements (total settlement, differential settlement, lateral deformations)?
8. Are there site environmental considerations that must be considered in the design (specific limitation on noise, vibrations, *etc.*)?

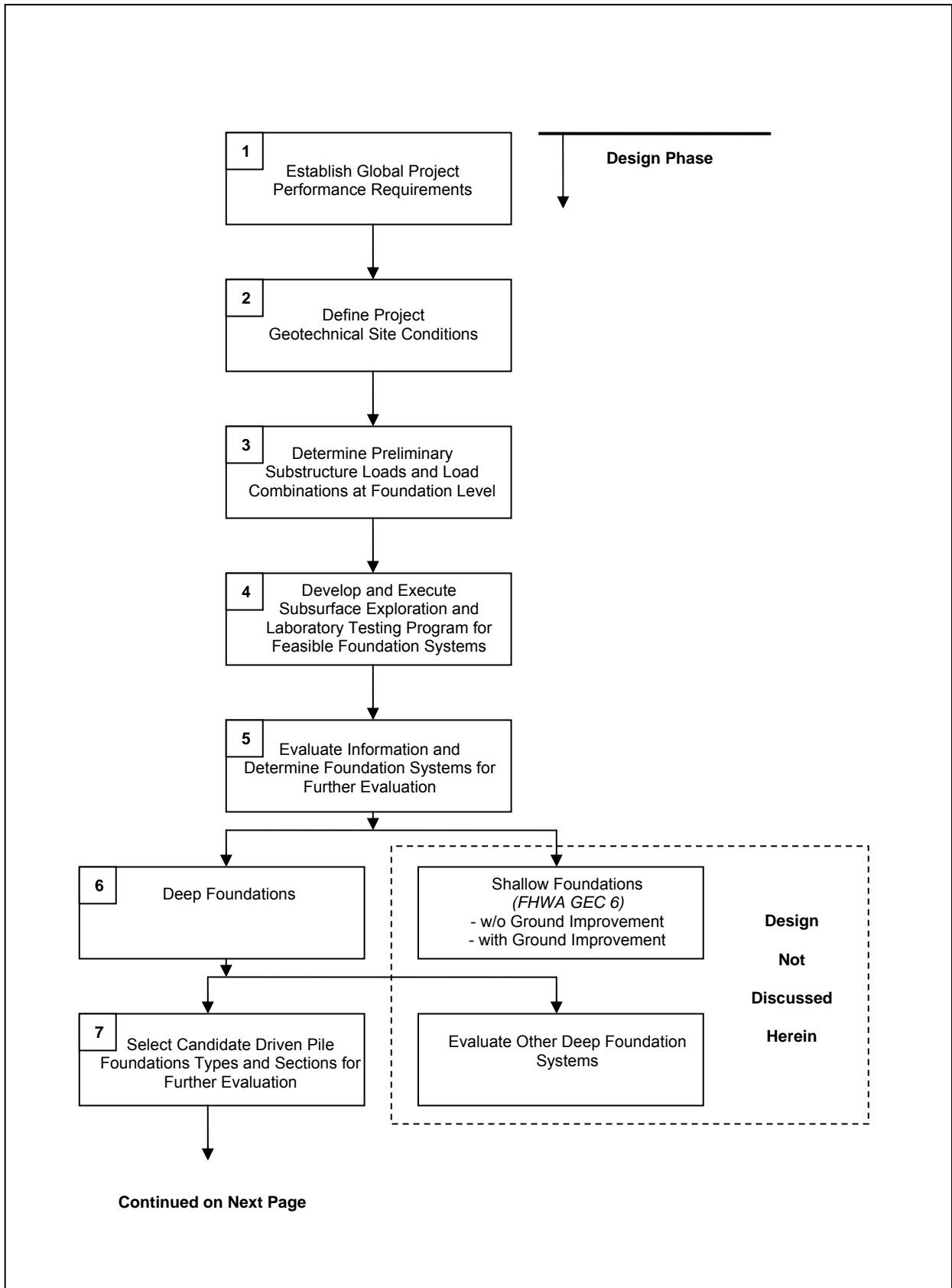


Figure 2.1 Driven Pile Design and Construction Process

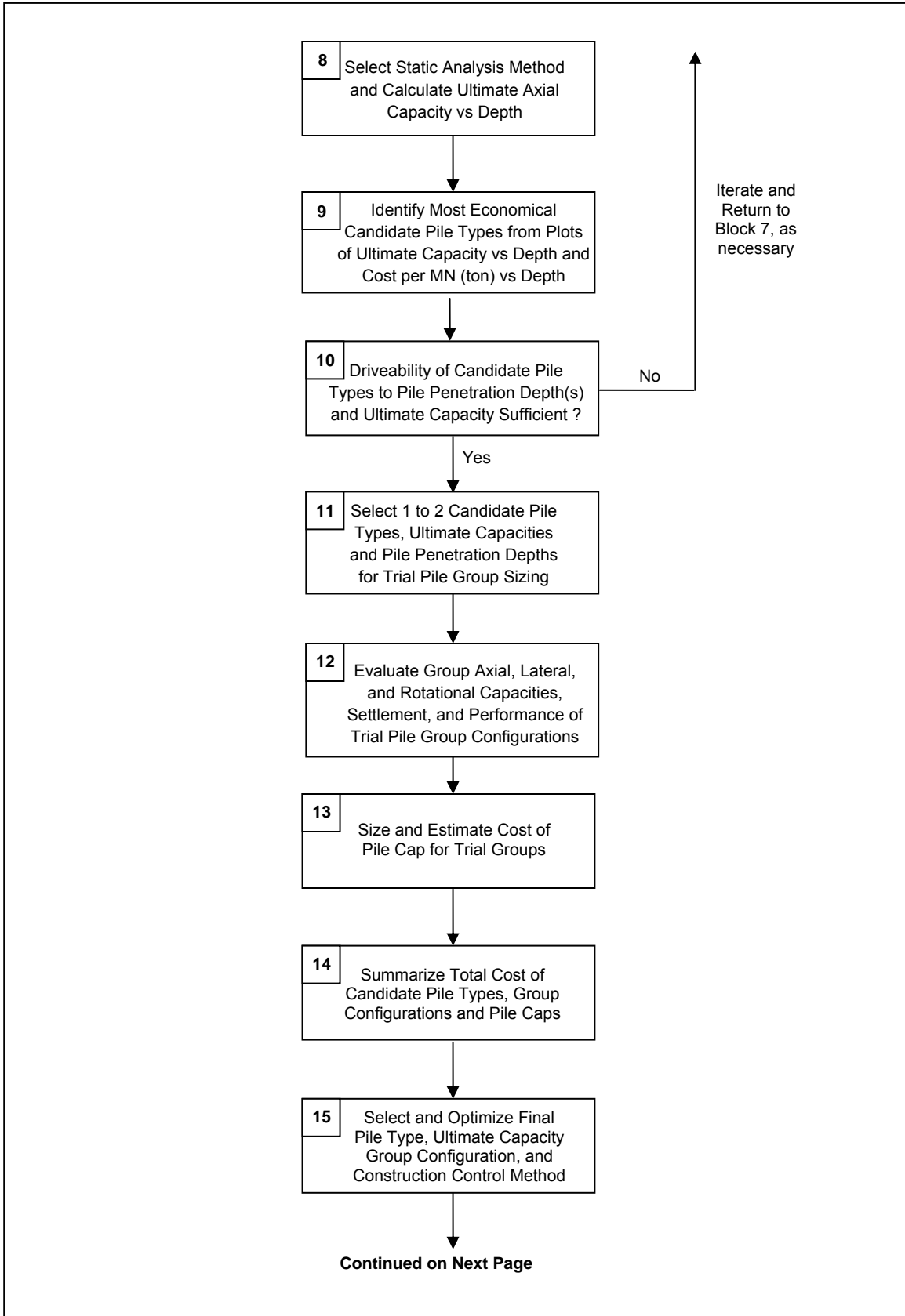


Figure 2.1 Driven Pile Design and Construction Process (continued)

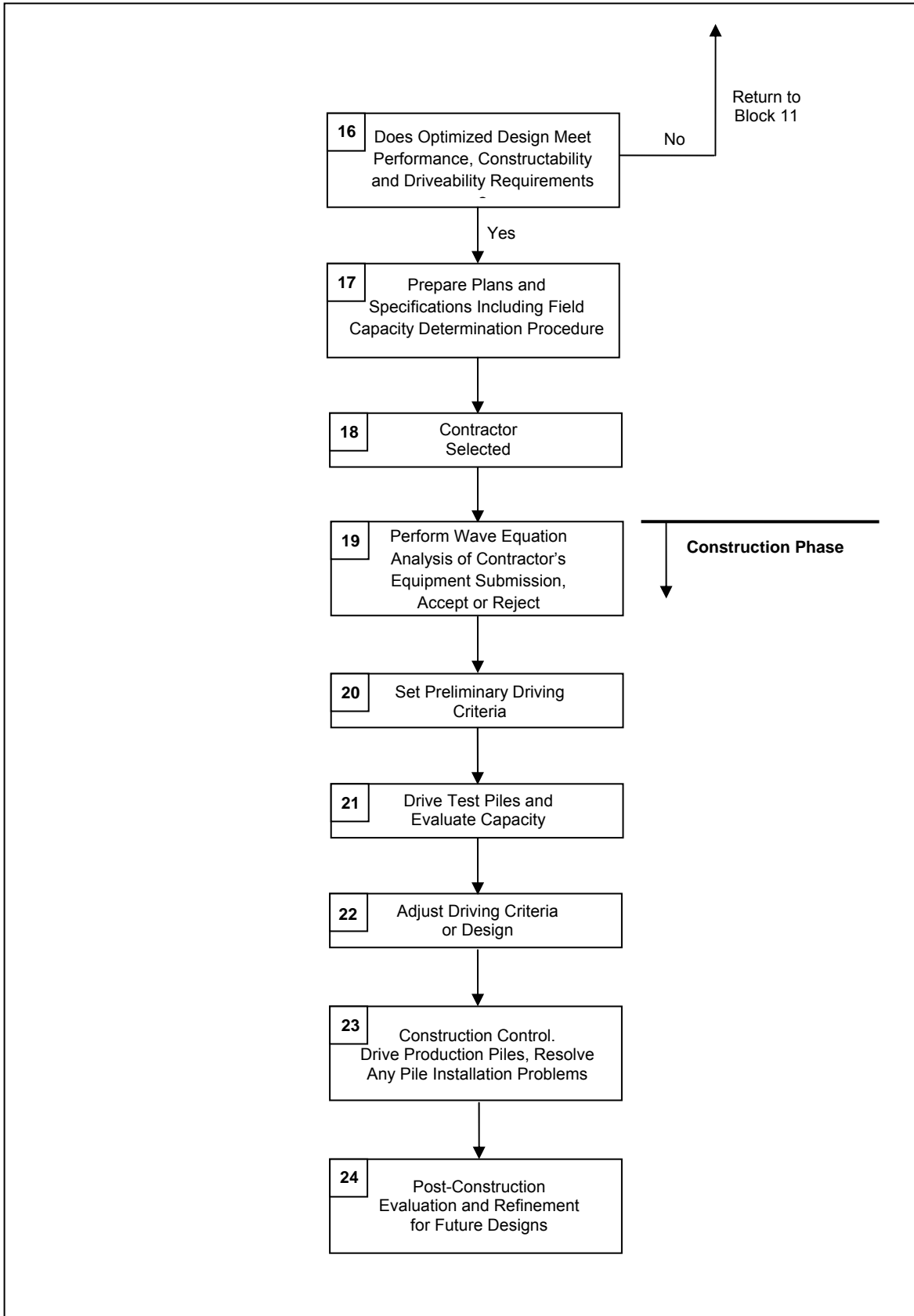


Figure 2.1 Driven Pile Design and Construction Process (continued)

Block 2: Define Project Geotechnical Site Conditions

A great deal can be learned about the foundation requirements with even a very general understanding of the site geology. For small structures, this may involve only a very superficial investigation such as a visit to the site. The foundation design for very large structures may require extensive geologic studies.

Frequently there is information available on foundations that have been constructed in the area. This information can be of assistance in avoiding problems. Both subsurface exploration information and foundation construction experience should be collected prior to beginning the foundation design. Unfortunately, this step is not often done in practice.

Block 3: Determine Preliminary Substructure Loads and Load Combinations

Substructure loads and reasonable vertical and lateral deformation requirements should be established at this time. This issue was considered in Block 1. The result of that effort has probably matured in the intervening time (which might be quite long for some projects) and is now better defined. It is imperative that the foundation specialist obtain a completely defined and unambiguous set of foundation loads and performance requirements in order to proceed through the foundation design process. Accurate load information and performance criteria are essential in the development and implementation of an adequate subsurface exploration program for the planned structure.

Block 4: Develop and Execute Subsurface Exploration Program for Feasible Foundation Systems

Based on the information obtained in Blocks 1-3, it is possible to make decisions regarding the necessary information that must be obtained for the feasible foundation systems at the site. The subsurface exploration program and the associated laboratory testing must meet the needs of the design problem that is to be solved at a cost consistent with the size of the structure. The results of the subsurface exploration program and the laboratory testing are used to prepare a subsurface profile and identify critical cross sections. These tasks are covered in greater detail in Chapters 4, 5, and 6.

Block 5: Evaluate Information and Select Candidate Foundation Systems

The information collected in Blocks 1-4 must be evaluated and candidate foundation systems selected. The first question to be decided is whether a shallow or a deep foundation is required. This question will be answered based primarily on the strength and compressibility of the site soils, the proposed loading conditions, the project performance criteria and the foundation cost. If settlement is not a problem for the structure, then a

shallow foundation will probably be the most economical solution. Ground improvement techniques in conjunction with shallow foundations should also be evaluated. Shallow and deep foundation interaction with approach embankments must also be considered. If the performance of a shallow foundation exceeds the structure performance criteria, a deep foundation must be used. The design of shallow foundations and ground improvement techniques are not covered in this manual. Information on design consideration for shallow foundations can be found in Kimmerling (2002), and in Munfakh *et al.*, (2001). Information on ground improvement techniques can be found in Elias *et al.*, (2004). The problem of selecting the proper foundation system is discussed in detail in Chapter 7.

Block 6: Deep Foundations

The decision among deep foundation types is now divided between driven piles and other deep foundation systems. These other deep foundation systems are primarily drilled shafts, but would also include micropiles, auger cast piles, and other drilled-in deep foundation systems. The questions that must be answered in deciding between driven piles and other deep foundation systems will center on the relative costs of available, possible systems. Foundation support cost can be conveniently calculated based on a cost per unit of load carried. In addition, constructability must be considered. This manual is concerned with driven piles so the other types of deep foundations will not be discussed here. Design guidance on drilled shafts can be found in O'Neil and Reese (1999). For micropile design guidance refer to Sabatini *et al.*, (2005), and for auger cast piles refer to in Brown and Dapp (2006). The need for and selection of a deep foundation system is discussed in Chapter 7.

Block 7: Select 2 to 5 Candidate Driven Pile Types for Further Evaluation

At this point on the flow chart, the primary concern is for the design of a driven pile foundation. The pile type must be selected consistent with the applied load per pile. Consider this problem. The general magnitude of the column or pier loads is known from the information obtained in Blocks 1 and 3. However, a large number of combinations of pile capacities and pile types can satisfy the design requirements. Should twenty, 1000 kN (225 kip) capacity piles be used to carry a 20,000 kN (4,500 kip) load, or would it be better to use ten, 2000 kN (450 kip) capacity piles? This decision should consider both the structural capacity of the pile and the realistic geotechnical capacities of the pile type for the soil conditions at the site, the cost of the available alternative piles, and the capability of available construction contractors to drive the selected pile. Of course, there are many geotechnical factors that must also be considered. At this point in the design process, 2 to 5 candidate pile types and/or sections that meet the general project requirements should be

selected for further evaluation. Pile type and selection considerations are covered in Chapter 8.

At this stage the loads must also be firmly established. In Block 1, approximate loads were determined which were refined in Block 3. At those stages of the design process the other aspects of the total structural design were probably not sufficiently advanced to establish the final design loads. By the time that Block 6 has been reached, the structural engineer should have finalized the various loads. One common inadequacy that is sometimes discovered when foundation problems arise is that the foundation loads were never really accurately defined at the final stage of the foundation design.

If there are special design events to be considered, they must be included in the determination of the loads. Vessel impact will be evaluated primarily by the structural engineer and the results of that analysis will give pile loads for that case. There may be stiffness considerations in dealing with vessel impact since the design requirement is basically a requirement that some vessel impact energy be absorbed.

Scour presents a different requirement. The loads due to the forces from the stream must be determined as specified in the AASHTO Standard Specification for Highway Bridges, Section 3.18 and this should be included in the structural engineer's load determination process. The depth of scour must also be determined as directed in AASHTO Specification, Section 4.3.5. In the design process, it must be assured that after scour the pile will still have adequate capacity.

In many locations in the country, seismic loads will be an important contributor to some of the critical pile load conditions. Since the 1971 San Fernando Earthquake, much more emphasis has been placed on seismic design considerations in the design of highway bridges. The AASHTO Standard Specifications for Highway Bridges has been substantially expanded to improve the determination of the seismic loads. Usually the structural engineer will determine the seismic requirements. Frequently the behavior of the selected pile design will affect the structural response and hence the pile design loads. In this case, there will be another loop in the design process that includes the structural engineer. The geotechnical engineer should review the seismic design requirements in Division I-A of the AASHTO Bridge Design Specification for a general understanding of the design approach.

Block 8: Select Static Analysis Method and Calculate Ultimate Capacity vs Depth

A static analysis method(s) applicable to the pile type(s) under consideration and the soil conditions at the site should now be selected. Static analysis methods are covered in detail

in Chapter 9. The ultimate axial capacity versus depth should then be calculated for all candidate pile types and sections.

Block 9: Identify Most Economical Candidate Pile Types and/or Sections

The next step is to develop and evaluate plots of the ultimate axial static capacity versus pile penetration depth and the pile support cost versus pile penetration depth for each candidate pile type and/or section. The support cost, which is the cost per kN (ton) supported, is the ultimate capacity at a given penetration depth divided by the pile cost to reach that penetration depth. The pile cost can be calculated from the unit cost per meter (ft) multiplied by the pile length to the penetration depth. These plots should be evaluated to identify possible pile termination depths to obtain the lowest pile support cost. This process is introduced in Chapter 3.

Block 10: Calculate Driveability of Candidate Pile Types

Candidate pile types should now be evaluated for driveability. Can the candidate pile type and/or section be driven to the required capacity and penetration depth at a reasonable pile penetration resistance (blow count) without exceeding allowable driving stresses for the pile material? This analysis is performed using the wave equation program. All of the necessary information is available except the hammer selection. Since the hammer to be used on the job will only be known after the contractor is selected, possible hammers must be tried to make sure that the pile is driveable to the capacity and depth required.

Pile driveability is introduced in Chapter 9 with additional details on the use of wave equation analysis to check pile driveability described in Chapter 16. Allowable pile driving stresses are presented in Chapter 10.

If candidate pile types or sections do not meet driveability requirements they are dropped from further evaluation or modified sections must be chosen and evaluated. For H-piles and pipe piles, it may be possible to increase the pile section without increasing the soil resistance to driving. For concrete piles, an increase in section usually means a larger pile size, and therefore, an increase in soil resistance must also be overcome. Hence, some section changes may cause the design process to revisit Block 8. If all candidate pile types fail to meet driveability requirements, the design process must return to Block 7 and new candidate pile types must be selected.

Block 11: Select 1 to 2 Final Candidate Pile Types for Trial Group Sizing

The most viable candidate pile types and/or sections from the cost and driveability evaluations in Blocks 9 and 10 should now be evaluated for trial group sizing using the final loads and performance requirements. Multiple pile penetration depths and the resulting ultimate capacity at those depths should be used to establish multiple trial pile group configurations for each candidate pile type. These trial configurations should then be carried forward to Block 13.

Block 12: Evaluate Capacity, Settlement, and Performance of Trial Groups

The trial group configurations should now be evaluated for axial group capacity, group uplift, group lateral load performance, and settlement. These computations and analysis procedures are described in Chapter 9.

Block 13: Size and Estimate Pile Cap Cost for Trial Groups

The size and thickness of the pile cap for each trial group should be evaluated, and the resulting pile cap cost estimated. It is not necessary to design the cap reinforcement at this time only to determine cap size. Pile cap cost is a key component in selecting the most cost effective pile type and should not be overlooked. A procedure for preliminary sizing of pile caps is provided in Chapter 10.

Block 14: Summarize Total Cost of Final Candidate Piles

The total cost of each candidate pile should now be determined. A given pile type may have several total cost options depending upon the pile penetration depths, ultimate capacities, group configurations, and pile cap sizes carried through the design process. The cost of any special construction considerations and environmental restrictions should also be included in the total cost for each candidate pile.

Block 15: Select and Optimize Final Pile Type, Capacity, and Group Configuration

Select the final pile foundation system including pile type, section, length, ultimate capacity and group configuration for final design. A complete evaluation of the group lateral and rotational resistance should be performed. The design should be optimized for final structure loads, performance requirements, and construction efficiency.

Block 16: Does Optimized Design Meet All Requirements?

The final pile type, section, capacity and group configuration optimized in Block 15 should be evaluated so that all performance requirements have been achieved. If the optimization process indicated that a reduced pile section could be used, the driveability of the optimized pile section must be checked by a wave equation driveability analysis. This analysis should also consider what influence the group configuration (pile spacing) and construction procedures (i.e., cofferdams, etc.) may have on pile installation conditions.

Block 17: Prepare Plans and Specifications, Set Field Capacity Determination Procedure

When the design has been finalized, plans and specifications can be prepared and the procedures that will be used to verify pile capacity can be defined. It is important that all of the quality control procedures are clearly defined for the bidders to avoid claims after construction is underway. In the former use of the dynamic formula, the pile load specified was a design or working load since a factor of safety was contained in the formula. Modern methods of pile capacity determination always use ultimate loads with a factor of safety (or in LRFD a resistance factor) selected and applied. This should also be made clear in the project specifications so that the contractor has no question regarding the driving requirements. Procedures should be in place that address commonly occurring pile installation issues such as obstructions and driveability. Construction specifications are discussed in Chapter 11 and the preparation of the foundation report is covered in Chapter 13.

Block 18: Contractor Selection

After the bidding process is complete, a successful contractor is selected.

Block 19: Perform Wave Equation Analysis of Contractor's Equipment Submission

At this point the engineering effort shifts to the field. The contractor will submit a description of the pile driving equipment that he intends to use on the project for the engineer's evaluation. Wave equation analysis is performed to determine the driving resistance that must be achieved in the field to meet the required capacity and pile penetration depth. Driving stresses are determined and evaluated. If all conditions are satisfactory, the equipment is approved for driving. Some design specifications make this information advisory to the contractor rather than mandatory. Chapters 10, 11, and 16 provide additional information in this area.

On smaller projects, a dynamic formula may be used to evaluate driveability and the modified Gates Formula should be used. If a dynamic formula is used, then driveability and hammer selection will be based on the driving resistance given by the formula only, since stresses are not determined. Dynamic formula usage is covered in Chapter 15.

Block 20: Set Preliminary Driving Criteria

Based on the results of the wave equation analysis of Block 19 (or on smaller projects the modified Gates Formula) and any other requirements in the design, the preliminary driving criteria can be set.

Block 21: Drive Test Pile and Evaluate Capacity

The test pile(s), if required, are driven to the preliminary criteria developed in Block 19. Driving requirements may be defined by penetration depth, driving resistance, dynamic monitoring results or a combination of these conditions. The capacity can be evaluated by driving resistance from wave equation analysis, the results of dynamic monitoring, static load test, the modified Gates Formula, or a combination of these. Dynamic monitoring is described in Chapter 17. Static load test procedures are discussed in greater detail in Chapter 18 and dynamic formulas are covered in Chapter 15.

Block 22: Adjust Driving Criteria or Design

At this stage the final conditions can be set or, if test results from Block 21 indicate the capacity is inadequate, the driving criteria may have to be changed. In a few cases, it may be necessary to make changes in the design as far back as Block 8.

In some cases, it is desirable to perform preliminary field testing before final design. When the job is very large and the soil conditions are difficult, it may be possible to achieve substantial cost savings by having results from a design stage test pile program, including actual driving records at the site, as part of the bid package.

Block 23: Construction Control

After the driving criterion is set, the production pile driving begins. Quality control and assurance procedures have been established and are applied. Construction inspection items are discussed in greater detail in Chapter 23. Problems may arise and must be handled as they occur in a timely fashion.

Block 24: Post-Construction Evaluation and Refinement of Design

After completion of the foundation construction, the design should be reviewed and evaluated for its effectiveness in satisfying the design requirements and also its cost effectiveness.

2.5 COMMUNICATION

Good communication between all parties involved in the design and construction of a pile foundation is essential to reach a successful completion of the project. In the design stage, communication and interaction is needed between the structural, geotechnical, geologic, hydraulic, and construction disciplines, as well as with consultants, drill crews and laboratory personnel. In the construction stage, structural, geotechnical and construction disciplines need to communicate for a timely resolution of construction issues as they arise. Figures 2.2 and 2.3 highlight some of the key issues to be communicated in the design and construction stages.

DESIGN STAGE COMMUNICATION						
Subject	Structural	Geotechnical	Hydraulic	Construction	Field Crews	Laboratory
Preliminary Structure Loads and Performance Criteria.	X	X	X			
Determination of Scour Potential.	X	X	X			
Determination of Special Design Event Requirements.	X	X	X			
Review of Past Construction Problems in Project Area.	X	X	X	X		
Implementation of Subsurface Exploration and Testing Programs.	X	X	X	X	X	X
Determination of Pile Type, Length and Capacity.	X	X				
Effect of Approach Fills on Design.	X	X				
Prepare Plans and Specifications.	X	X	X	X		

Figure 2.2 Design Stage Communication

CONSTRUCTION STAGE COMMUNICATION			
Subject	Structural	Geotechnical	Construction
Establish Appropriate Methods of Construction Control and Quality Assurance.	X	X	X
Perform Wave Equation Analysis of Contractors Driving System to Establish Driving Criteria.	X	X	X
Perform Static Load Test(s) and/or Dynamic Monitoring and Adjust Driving Criteria.	X	X	X
Resolve Pile Installation Problems / Construction Issues.	X	X	X

Figure 2.3 Construction Stage Communication

REFERENCES

- Brown D. and Dapp S. (2006). Geotechnical Engineering Circular No. 8, Continuous Flight Auger Piles, Federal Highway Administration, U.S. Department of Transportation, Office of Bridge Technology, Washington D.C. (publication pending)
- Elias, V., Welsh, J., Warren, J., Lukas, R., Collin, J.G., and Berg, R.R. (2004). Ground Improvement Methods, National Highway Institute, Federal Highway Administration, U.S. Department of Transportation, Washington, D.C., 1002.
- Kimmerling, R.E. (2002). Geotechnical Engineering Circular No. 6, Shallow Foundations, Federal Highway Administration, U.S. Department of Transportation, Office of Bridge Technology, Washington D.C., 310.
- Munfakh, G., Arman, A., Collin, J.G., Hung, J.C-J., and Brouillette, R.P. (2001). Shallow Foundations Reference Manual, National Highway Institute, Federal Highway Administration, U.S. Department of Transportation, Washington, D.C., 222.
- O'Neil, M.W. and Reese, L.C. (1999). Drilled Shafts: Construction Procedures and Design Methods, Report No. FHWA-IF-99-025, U.S. Department of Transportation, Federal Highway Administration, Office of Infrastructure / Office of Bridge Technology, Washington, D.C., 758
- Sabatini, P.J., Tanyu, B., Armour, T., Groneck, P., and Keeley, J. (2005). Micropile Design and Construction – Final Draft, National Highway Institute, Federal Highway Administration, Arlington, VA

Chapter 3

ECONOMICS OF FOUNDATIONS FOR HIGHWAY STRUCTURES

Foundation design and construction involve engineering, economic, and constructability considerations pertinent to the particular site in question. The engineering considerations are addressed by determining the foundation loads and performance requirements, development of the foundation design parameters, and design analysis. The design analysis coupled with past experience will provide several feasible foundation alternatives.

The next step involves an economic evaluation of potential foundations. Several foundation alternatives may be satisfactory for the subsurface conditions while also meeting superstructure requirements. However, of all the foundation alternatives, generally only one will have the least possible cost.

Last, the constructability of a potential foundation must be considered. A potential foundation solution may appear to be the most economical from purely a design perspective, but may not be most economical when limitations on construction activities are fully considered. Constructability issues such as impact on adjacent structures, equipment, access, methods, work hours, etc., must be considered in design.

3.1 FOUNDATION ALTERNATIVES

To determine the most feasible foundation alternatives, both shallow foundations and deep foundations should be considered. Deep foundation alternatives include driven piles, drilled shafts, micropiles, and auger cast piles. Proprietary deep foundations systems should not be excluded as they may be the most economical alternative in a given condition. This manual covers the design and construction of driven pile foundations. Therefore, design and construction procedures for shallow foundations, drilled shafts, micropiles and auger cast piles will not be covered herein. Additional details on spread footings for highway bridges may be found in FHWA/RD-86/185 Spread Footings for Highway Bridges by Gifford *et al.* (1987) and Geotechnical Engineering Circular No. 6, Shallow Foundations by Kimmerling (2002). The FHWA/ADSC publication FHWA-IF-99-025 by O'Neill and Reese (1999) summarizes design methods and construction procedures for drilled shafts. Details on micropiles can be found in FHWA-NHI-05-039 by Sabatini, *et al.*, (2005), and auger cast piles details are summarized in Brown and Dapp (2006).

A cost evaluation of all feasible foundation alternatives using the foundation support cost approach is essential in the selection of the optimum foundation system.

Cost analyses of all feasible alternatives may lead to the elimination of some foundations qualified under the engineering study. Other factors that must be considered in the final foundation selection are availability of materials and equipment, local contractor and construction force experience, as well as any environmental limitations/considerations on construction access or activities.

For major projects, if the estimated foundation support costs of alternatives during the design stage are within 15 percent of each other, then alternate foundation designs should be considered for inclusion in the contract documents. If an alternate design is included in the contract documents, both designs should be adequately detailed. For example, if two pile foundation alternatives are detailed, the bid quantity pile lengths should reflect the estimated pile lengths for each alternative. Otherwise, material costs and not the installed foundation cost will likely determine the low bid. Use of alternate foundation designs will generally provide the most cost effective foundation system.

Proprietary pile types should not be routinely excluded from consideration. In a given soil condition, a proprietary system may be the most economical foundation type. Therefore, a proprietary system should be considered as a viable foundation alternate when design analyses indicate the cost to be within 15% of a conventional design. A conventional design alternate should generally be included with a proprietary design alternate in the final project documents to stimulate competition.

3.2 EXAMPLES OF COST SAVINGS BY UTILIZING MODERN DESIGN AND CONSTRUCTION CONTROL PRACTICES

There are many factors which enter into the cost of a structure foundation. A failure to understand and consider any one of them will add to the total cost of the work. Use of overly conservative designs and inappropriate construction practices may result in significantly greater foundation costs. These practices are also often associated with increased risk of large change orders or claims.

Use of modern design and construction methods, techniques, and equipment provides an efficient foundation system without compromising safety or the service life of the structure. Modern methods allow significant cost savings through better quality control, optimization of pile type, and optimization of pile section. Outdated pile foundation practices usually lead

either to extremely conservative and inefficient piling systems or unsafe foundations. Opportunities for rational design, construction, and cost savings exist in several areas of pile foundations. These opportunities are summarized in Table 3-1.

Transportation agencies that are taking advantage of modern design and construction control methods have reduced foundation costs while obtaining greater confidence in the safety and the service life of their structures.

3.3 OPTIMIZATION OF FOUNDATION COST

3.3.1 Definition of Foundation Support Cost

A rational comparison of potential foundation systems can be made based on the foundation support cost of each candidate foundation type. The foundation support cost is defined as the total cost of the foundation divided by the load the foundation supports in MN (tons). The total foundation cost should include all costs associated with a given foundation system including the need for excavation or retention systems, pile caps and cap size, environmental restrictions on construction activities, etc. A detailed case history describing the foundation support cost concept can be found in Komurka (2004).

For driven pile foundation projects, the total foundation support cost can be separated into three major components; the pile support cost, the pile cap support cost, and the construction control method support cost.

3.3.2 Cost Optimization for One Pile Section

Figure 3.1 presents a layered soil profile that will be used to illustrate the cost optimization process. The first step in the cost optimization of a selected pile section is to perform a static analysis to determine the ultimate capacity versus the pile penetration depth. Static analysis methods are described in greater detail in Chapter 9. A static analysis was performed for the example soil profile presented in Figure 3.1 using the DRIVEN computer program. Figure 3.2 presents the results of this static analysis and consists of a plot of the calculated ultimate pile capacity versus pile penetration depth. The ultimate capacity versus depth results are for a HP 360 x 174 (HP 14x117) H-pile.

Several logical pile penetration termination depths and associated ultimate pile capacities are apparent in Figure 3.2a (SI units) or 3.2b (US units). Piles could be driven to the medium dense sand layer at a depth of 18 m (59 ft) for an ultimate pile capacity of 650 kN

TABLE 3-1 COST SAVING RECOMMENDATIONS FOR PILE FOUNDATIONS			
Factor	Inadequacy of Older Methods	Cost Saving Recommendations	Remarks
A. Design structural load capacity of piles.	1. Allowable pile material stresses may not address site specific considerations.	1. Use realistic allowable stresses for pile materials in conjunction with adequate construction control procedures, (i.e., load testing, dynamic pile monitoring and wave equation). 2. Determine potential pile types and carry candidate pile types forward in the design process. 3. Optimize pile size for loads.	1. Rational consideration of Factors A and B may decrease cost of a foundation by 25 percent or more. 2. Significant cost savings can be achieved by optimization of pile type and section for the structural loads with consideration of pile driveability requirements.
B. Design geotechnical capacity of soil and rock to carry load transferred by piles.	1. Inadequate subsurface explorations and laboratory testing. 2. Rules of thumb and prescription values used in lieu of static design may result in overly conservative designs. 3. High potential for change orders and claims.	1. Perform thorough subsurface exploration including in-situ and laboratory testing to determine design parameters. 2. Use rational and practical methods of design. 3. Perform wave equation driveability analysis. 4. Use design stage pile load testing on large pile driving projects to determine load capacities (load tests during design stage).	1. Reduction of safety factor can be justified because some of the uncertainties about load carrying capacities of piles are reduced. 2. Rational pile design will generally lead to shorter pile lengths and/or smaller number of piles.
C. Alternate foundation design.	1. Alternate foundation designs are rarely used even when possibilities of cost savings exist by allowing alternates in contract documents.	1. For major projects, consider inclusion of alternate foundation designs in the contract documents if estimated costs of feasible foundation alternatives are within 15 percent of each other.	1. Alternative designs often generate more competition which can lead to lower costs.
D. Plans and specifications.	1. Unrealistic specifications. 2. Uncertainties due to inadequate subsurface explorations force the contractors to inflate bid prices.	1. Prepare detailed contract documents based on thorough subsurface explorations, understanding of contractors' difficulties and knowledge of pile techniques and equipment. 2. Provide subsurface information to the contractor.	1. Lower bid prices will result if the contractor is provided with all the available subsurface information. 2. Potential for contract claims is reduced with realistic specifications.
E. Construction determination of pile load capacity during installation.	1. Often used dynamic formulas such as Engineering News are unreliable. Correlations between	1. Eliminate use of dynamic formulas for construction control as experience is gained with the wave equation analysis. 2. Use wave equation analysis coupled with dynamic monitoring for construction control and load capacity evaluation. 3. Use pile load tests on projects to substantiate capacity predictions by wave equation and dynamic monitoring.	1. Reduced factor of safety may allow shorter pile lengths and/or smaller number of piles. 2. Pile damage due to excessive driving can be eliminated by using dynamic monitoring equipment. 3. Increased confidence and lower risk results from improved construction control.

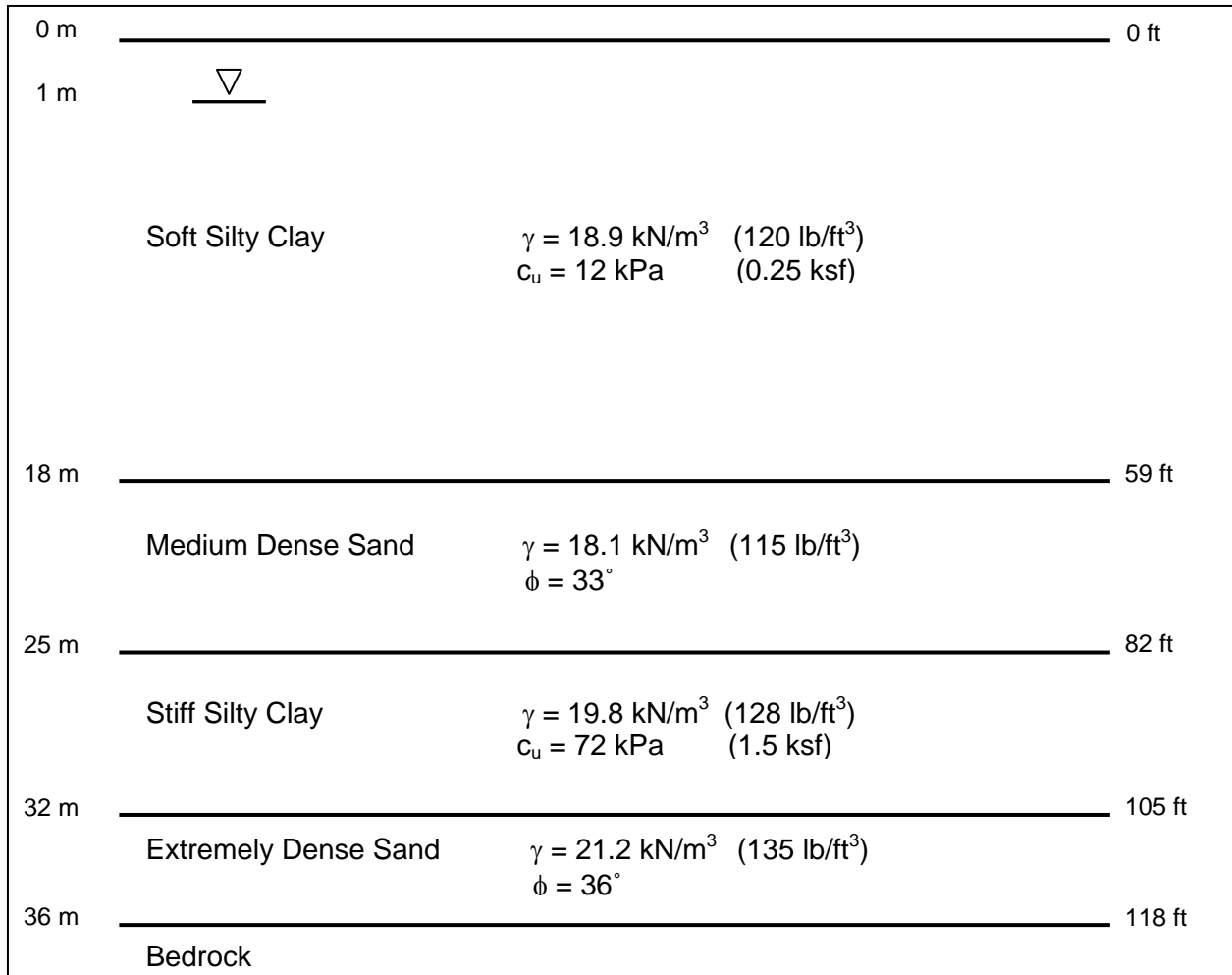


Figure 3.1 Example Soil Profile

(73 tons); seated into the medium dense sand layer near a depth of 21 m (69 ft) for 1100 kN (124 tons); driven through the medium dense sand layer and underlying stiff clay layer and into the extremely dense sand layer at 32 m (105 ft) for 3080 kN (346 tons); or driven to bedrock near 36 m (118 ft) for 5780 kN (650 tons). A rational economic assessment of these potential pile termination depths and ultimate pile capacities is needed for cost effective design. For most pile types, the pile cost can usually be assumed as linear with depth based on unit price as illustrated in Figure 3.3. However, this may not be true for very long concrete piles or long, large section steel piles. These exceptions may require the cost analysis to reflect special transportation, handling, or splicing costs for the concrete piles or extra splice time and cost for steel piles.

The pile cost at a given depth from Figure 3.3 can be divided by the ultimate capacity at that same depth from Figure 3.2a or 3.2b to obtain a plot of the pile support cost in dollars per ultimate kN supported or dollars per ultimate ton supported versus depth. Since pile

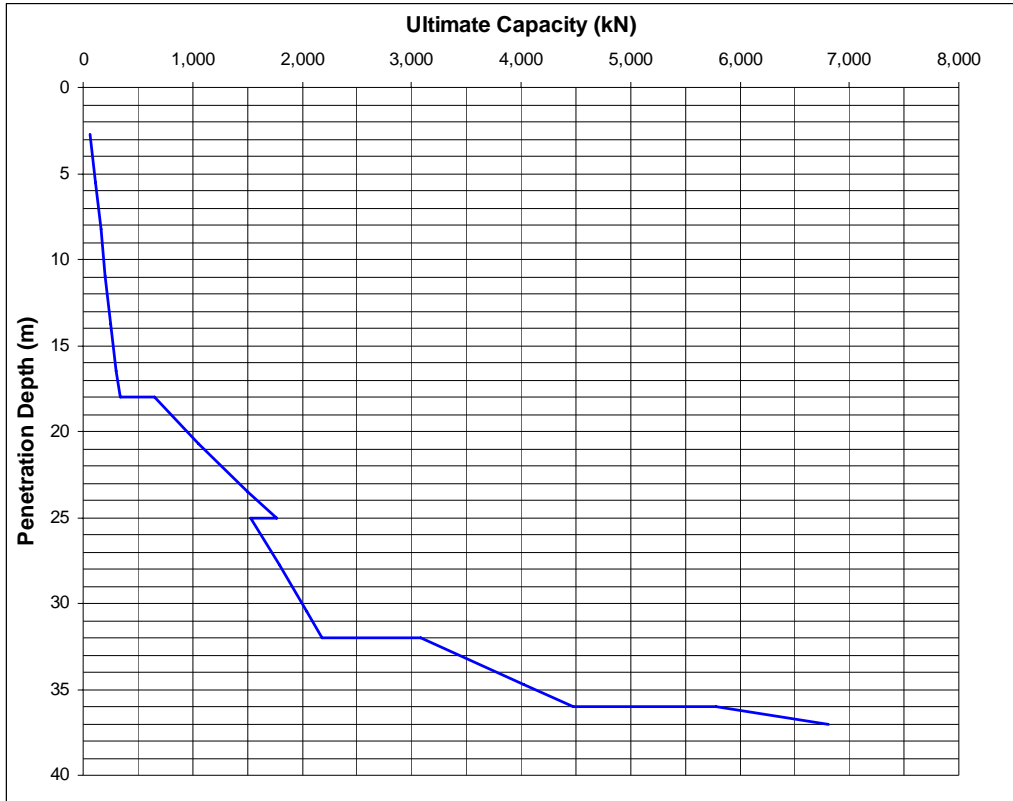


Figure 3.2a Ultimate Capacity in kN Versus Pile Penetration Depth in Meters.

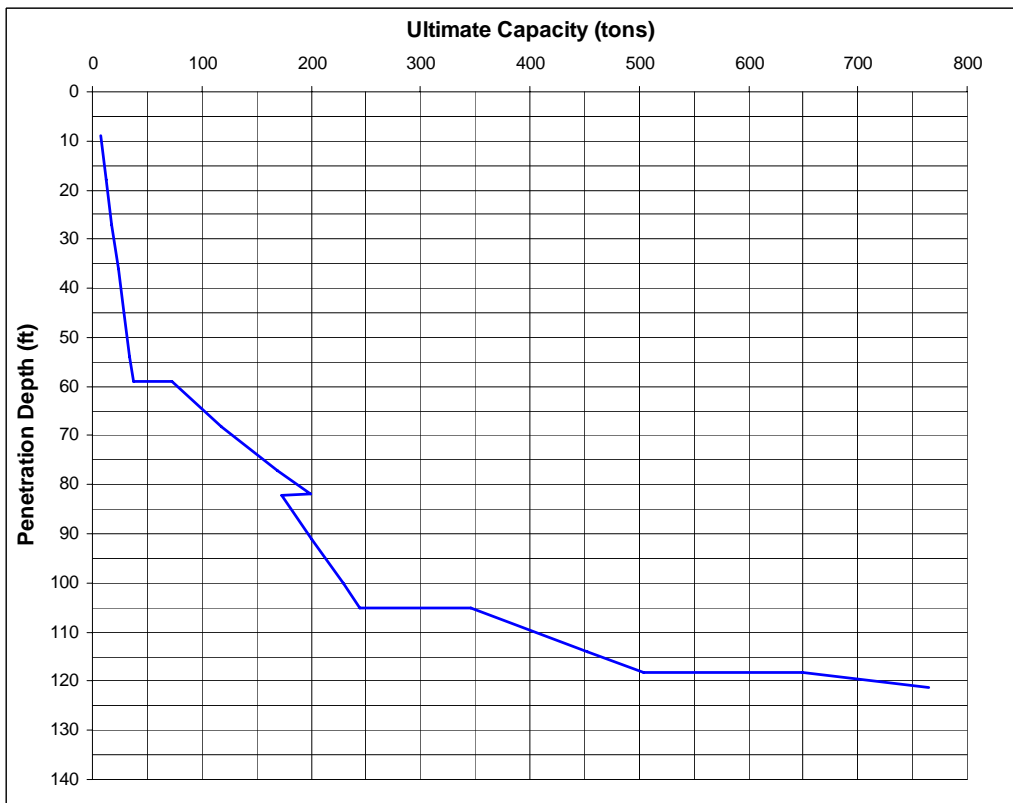


Figure 3.2b Ultimate Capacity in Tons Versus Pile Penetration Depth in Feet.



Figure 3.3 Pile Cost versus Pile Penetration Depth

capacities are ultimate capacities, this is the pile support cost – ultimate. Figure 3.4a (SI units) and 3.4b (US units) present plots of the pile support cost – ultimate versus depth and the ultimate pile capacity versus depth. For the pile section evaluated, a general conclusion can quickly be reached that longer, higher capacity piles appear more cost effective than shorter piles. At the 18 m depth and an ultimate pile capacity of 650 kN (73 tons), the pile section has a pile support cost – ultimate of \$4.28 per kN (\$38.05 per ton). At a depth of 21 m (69 ft) and an ultimate capacity of 1100 kN (124 tons), the pile section has a pile support cost – ultimate of \$3.03 per kN (\$26.99 per ton). The pile support cost – ultimate drops to \$1.59 per kN (\$14.19 per ton) at a depth of 32 m (105 ft) and an ultimate capacity of 3080 kN (346 tons). The pile support cost – ultimate continues to decrease to \$0.96 per kN (\$8.51 per ton) at a depth of 36 m (118 ft) and an ultimate pile capacity of 5780 kN (650 tons).

The next step in the optimization process is to plot the allowable design load versus pile penetration depth for different construction control methods as illustrated in Figures 3.5a and 3.5b for SI and US units. These figures also identify the maximum allowable AASHTO design loads based on the construction control method. Methods for determining the

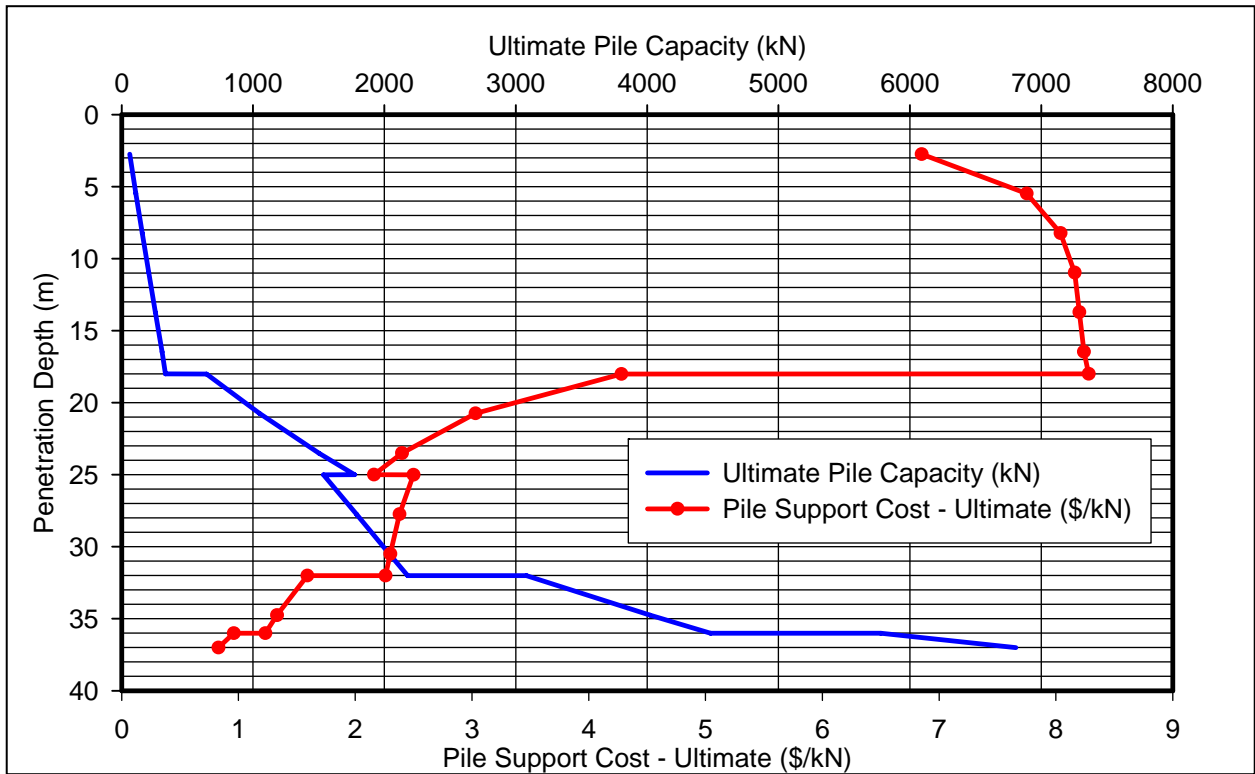


Figure 3.4a Ultimate Pile Capacity (kN) and Pile Support Cost - Ultimate Versus Depth (m)

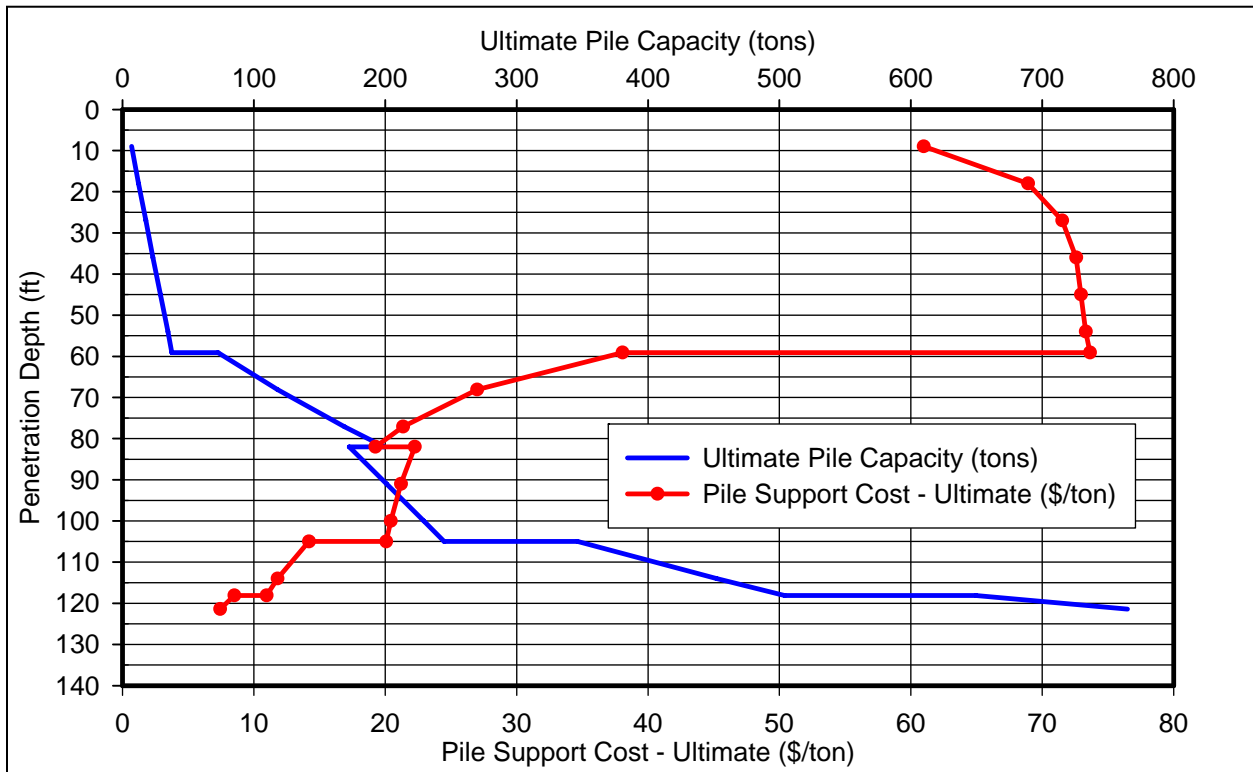


Figure 3.4b Ultimate Pile Capacity (tons) and Pile Capacity – Ultimate Versus Depth (ft)

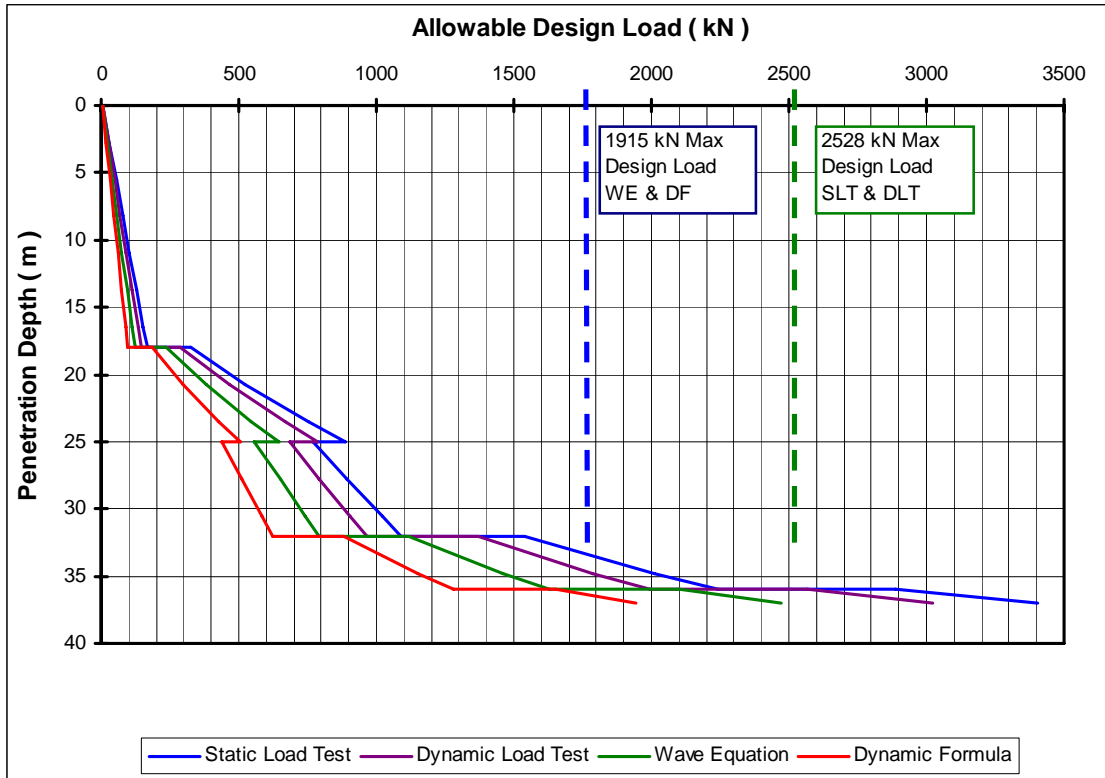


Figure 3.5a. Allowable Design Load in kN Versus Depth Based on Construction Control

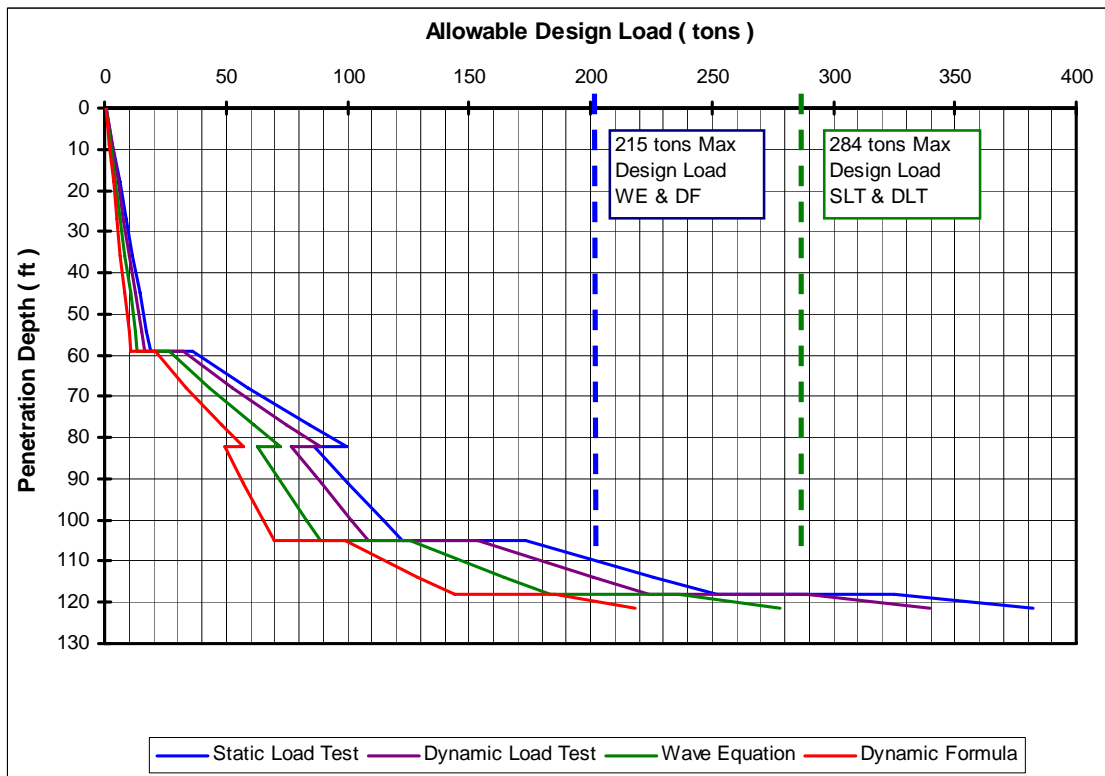


Figure 3.5b. Allowable Design Load in Tons Versus Depth Based on Construction Control

AASHTO maximum allowable design load on a given pile type are provided in Chapter 10. Design loads greater than the AASHTO limits should not be considered.

For the H-pile section used in the example, the maximum allowable design load varies from $0.25 F_y A_s$ for construction control with either wave equation (WE) or dynamic formula (DF) to $0.33 F_y A_s$ for construction control with either a dynamic load test (DLT) or static load test (SLT). These maximum allowable design loads are identified by the dashed vertical lines in Figures 3.5a and 3.5b. The allowable design load plots appear from right to left in order of the highest factor of safety to lowest factor of safety, i.e., dynamic formula (FS=3.5), wave equation (FS=2.75), dynamic load test (FS=2.25), and static load test (FS=2.0).

For the example give, the estimated pile penetration depth for the maximum design load allowed by each of the construction control methods are as follows:

Construction Control Method	Pile Depth	Maximum Design Load
Gates Dynamic Formula	36.9 m (121 ft)	1915 kN (215 tons)
Wave Equation	36 m (118 ft)	1915 kN (215 tons)
Dynamic Load Test	36 m (118 ft)	2528 kN (284 tons)
Static load Test	36 m (118 ft)	2528 kN (284 tons)

The pile support cost in dollars per allowable kN (ton) versus the allowable design load as a function of the construction control method should then be plotted as illustrated in Figures 3.6a (SI units) and 3.6b (US units). Since design loads are used, the pile support cost in these plots is the pile support cost – design. These plots allow a quick evaluation of the most cost effective construction control methods for a given design load. The dashed horizontal lines in these plots also indicate the maximum allowable design load that can be used on the pile section with a construction control method. Allowable design loads greater than the values indicated by the dashed line are not permissible for that construction control method but may be possible for a construction control method that uses a lower factor of safety. Figures 3.6a and 3.6b illustrate, the pile support cost at the maximum allowable design load for the pile section ranges from lowest to highest using dynamic formula, dynamic load test, wave equation analysis and then static load test as the method of construction control.

The next step in the optimization process is to determine the approximate pile cap size and cost for the required number of piles. Sections 10.5 and 10.6 of Chapter 10 discuss preliminary layout of pile groups and sizing of pile caps. The pile cap support cost can then be approximated using bid price information per cubic yard of reinforced concrete. The pile

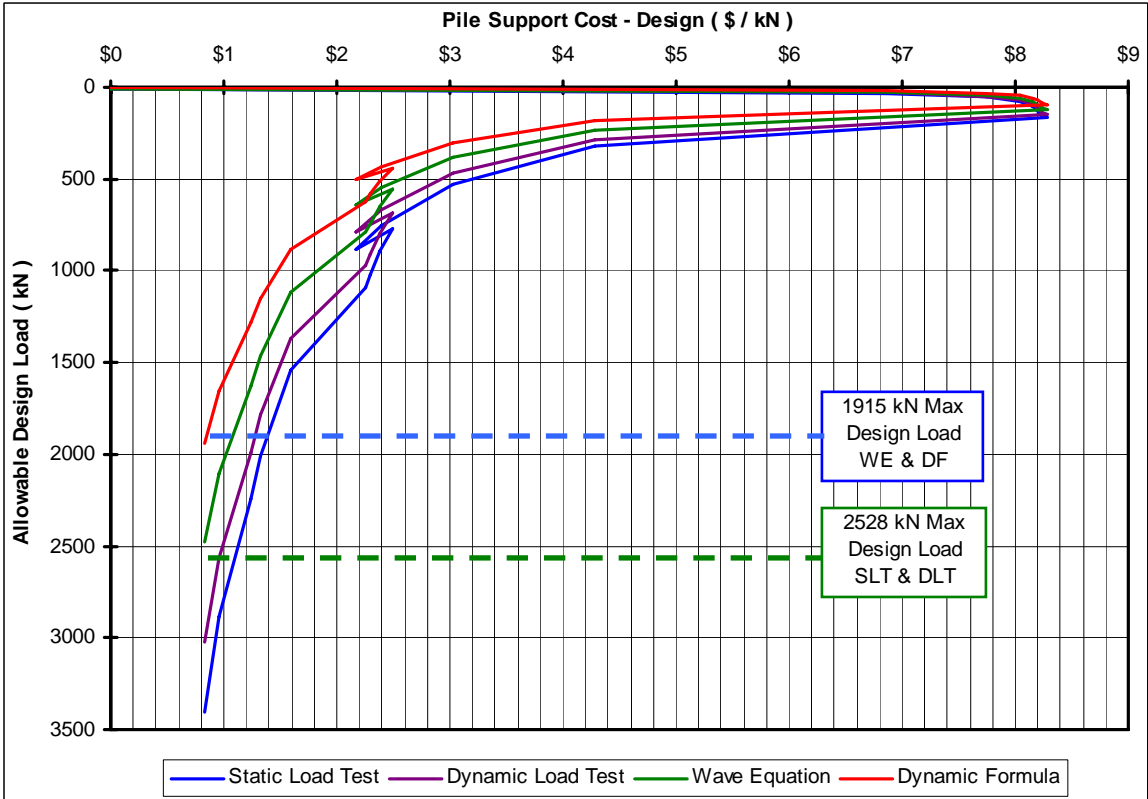


Figure 3.6a Pile Support Cost – Design Versus Allowable Design Load in kN

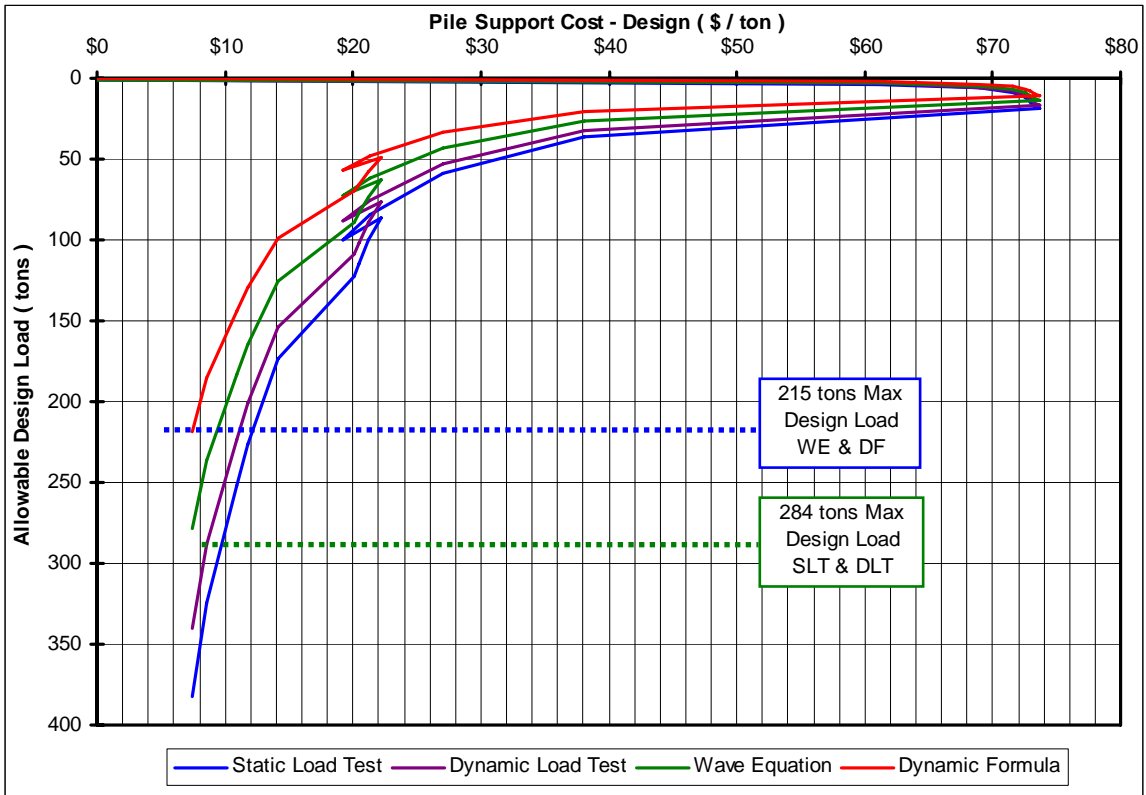


Figure 3.6b Pile Support Cost – Design Versus Allowable Design Load in Tons

cap support cost should also include construction considerations in addition to material costs. For example, the cost of excavations, cofferdams or retention systems, utility relocations, and removal and disposal of any contaminated soils should be included in the pile cap support where applicable.

For a common pile section and loads, a graph of approximate pile cap support cost as a function of column load could also be developed to allow for quicker cost estimates. An example plot of pile cap support cost versus column load for various pipe pile design loads is presented in Figure 3.7. This plot was specifically developed for 273 mm (10.75 inch), 324 mm (12.75 inch), 356 mm (14 inch), and 406 mm (16 inch) O.D., concrete filled pipe piles. The chart considers that 273 mm (10.75 inch) O.D. piles were used for design load up to an including 890 kN (100 tons), 324 mm (12.75 inch) O.D. piles were used for a design load of 1335 kN (150 tons), 356 mm (14 inch) O.D. pipe piles were used for a design load of 1780 kN (200 tons), and 406 mm (16 inch) O.D. pipe piles were used for a design load of 2224 kN (250 tons). Pile spacing was set at 3 times the pile diameter.

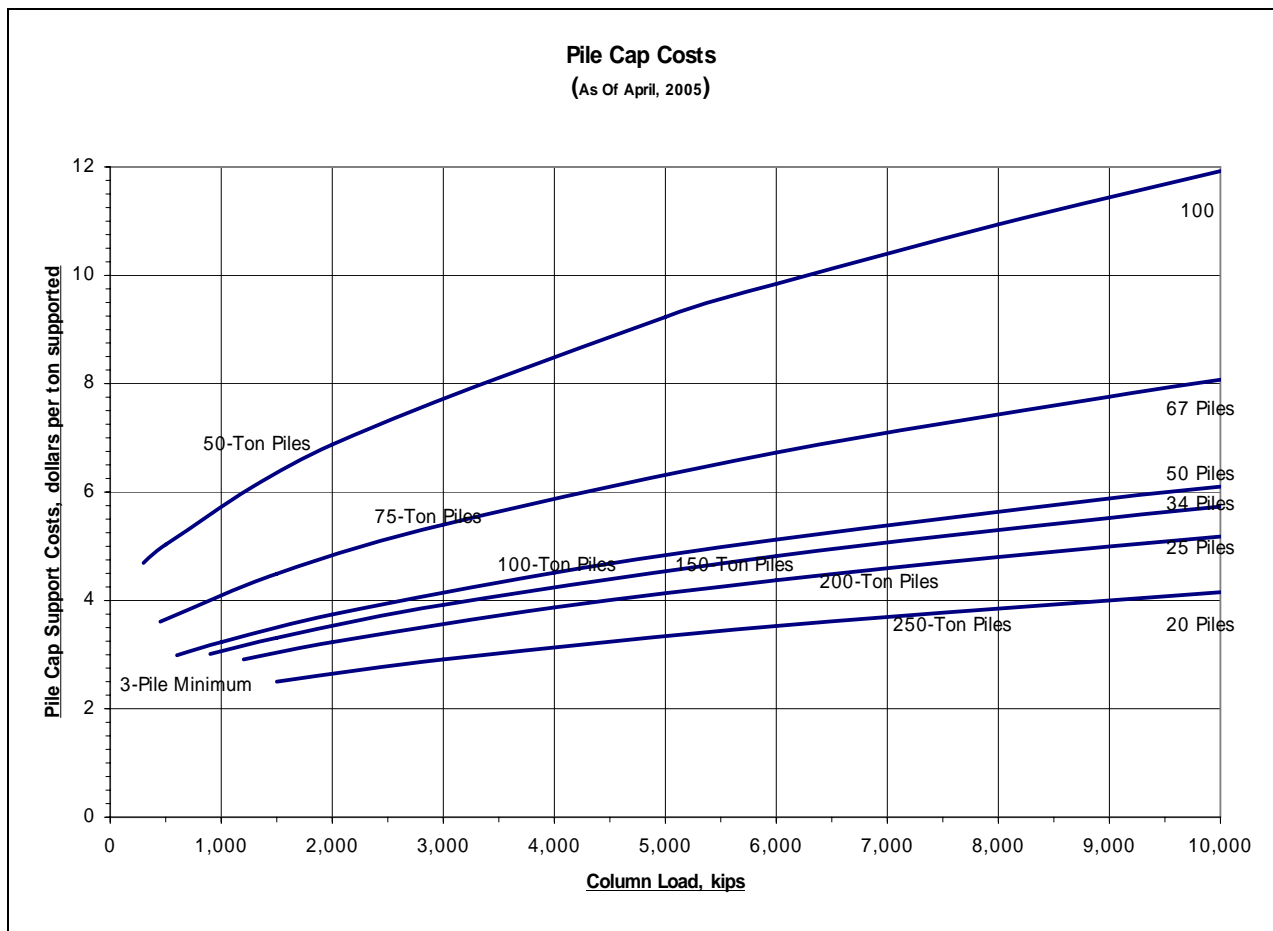


Figure 3.7 Pile Cap Cost as a Function of Column Load and Pile Design Load

The cost optimization process requires an evaluation of the total foundation support cost including the number of piles required, the pile cap size, cost of the construction control method, construction costs such as cofferdams, cost of any environmental restrictions, utility relocation costs, etc.

For example, consider a four span structure where preliminary estimates indicate maximum vertical column loads of 20,000 kN (2,250 tons). For the potential pile termination depths and ultimate capacities discussed in Figure 3.2a and 3.2b, determine the approximate number of piles, pile cost, cap cost, construction control method cost, and total cost. An example cost computation for this example is presented in Table 3-2.

The construction control methods being considered for the four span bridge include:

- a) one static load test (at up to 3 times design load) and wave equation analyses (SLT),
- b) dynamic testing of one test pile at each substructure location during initial driving and during restrike with signal matching and wave equation analyses (DLT),
- c) wave equation analyses for each substructure location (WE),
- d) the modified Gates dynamic formula (DF).

A review of Table 3-2 indicates high capacity piles driven to bedrock at 36 m (118 ft) for support of the maximum design load allowed on the section of 2528 kN (284 tons) with either dynamic load tests or a static load test for construction control will be the most cost effective. This cost evaluation example was based only on axial load considerations. In some cases, a minimum number of piles may be required to resist lateral load performance requirements. A wave equation analysis of pile driveability should also be performed to confirm that the pile can be driven to the required depth and capacity. Pile driveability is discussed later in Chapters 9 and 16.

Additional factors and their effect on the design economics that should be factored into the final section selection in the above example include construction limitations on time or space and any minimum penetration depth requirements for uplift loads (section driveability). Similar foundation support cost evaluations of other viable shallow and deep foundation systems should be performed for optimization of the final design.

3.3.3. Cost Optimization for Multiple Pile Types and/or Pile Sections

The steps described above for optimization of one pile section should be followed for economic evaluation and optimization of all candidate pile type and sections. Rational

Table 3-2 Example Cost Computation for Foundation Optimization

Pile Penetration Depth (m)	Ultimate Pile Capacity (kN)	Construction Control Method (C.C.M.)	Allowable Design Load (kN)	Approx. Number of Piles	Pile Support Cost at \$154/m	Approx. Pile Cap Support Cost	Cost of C.C.M. Tests	C.C.M. Support Cost Per Substructure Unit	Total Foundation Cost
18	650	SLT	325	62	\$ 171,864	\$ 23,062	\$ 25,000	\$ 6,250	\$ 201,176
		DLT	289	70	\$ 194,040	\$ 24,750	\$ 15,000	\$ 3,750	\$ 222,540
		WE	236	85	\$ 235,620	\$ 25,875	\$ 2,000	\$ 500	\$ 261,995
		DF	186	108	\$ 299,376	\$27,000	\$ 200	\$ 50	\$ 326,426
21	1100	SLT	550	37	\$ 119,658	\$ 18,000	\$ 30,000	\$ 7,500	\$ 145,158
		DLT	489	41	\$ 132,594	\$ 19,125	\$ 15,000	\$ 3,750	\$ 155,469
		WE	400	50	\$ 161,700	\$ 21,375	\$ 2,000	\$ 500	\$ 183,575
		DF	314	64	\$ 206,976	\$ 23,060	\$ 200	\$ 50	\$ 230,086
32	3080	SLT	1540	13	\$ 64,064	\$ 9,340	\$ 35,000	\$ 8,750	\$ 82,154
		DLT	1369	15	\$ 73,920	\$ 9,560	\$ 15,000	\$ 3,750	\$ 87,230
		WE	1120	18	\$ 88,704	\$ 9,900	\$ 2,000	\$ 500	\$ 99,104
		DF	880	23	\$ 113,344	\$ 10,460	\$ 200	\$ 50	\$ 123,854
36	5780	SLT	2890*	8	\$ 44,352	\$ 6,190	\$ 40,000	\$ 10,000	\$ 60,542
		DLT	2609*	8	\$ 44,352	\$ 6,190	\$ 15,000	\$ 3,750	\$ 54,292
		WE	2101**	11	\$ 60,984	\$ 8,440	\$ 2,000	\$ 500	\$ 69,924
		DF	1651	13	\$ 72,072	\$ 9,340	\$ 200	\$ 50	\$ 81,462

* - load limited to maximum allowable of 2528 kN

** - load limited to maximum allowable of 1915 kN

economic evaluation and optimized selection of the pile type and section can be made by following the single pile procedure provided above for each candidate pile type.

A real four span structure such as the one used in the single pile optimization example may have abutment loads that are about $\frac{1}{2}$ the pier loads. In this case, the minimum number of piles may govern the foundation design at the abutments. Figures 3.8a and 3.8b provide comparison plots of the pile support cost – ultimate versus depth for the HP 360 x 174 (HP 14x117) H-pile used in the single pile optimization example along with an HP 360 x 108 (HP 14x73) H-pile. The HP 360 x 108 section has a lower pile support cost – ultimate at the same depth compared to the HP 360 x 174 section. Hence, if the minimum number of piles governs the foundation design at the abutments, use of shorter, lower capacity, smaller section piles may be more cost effective.

Use of the foundation support cost concept allows sound economic and engineering decisions to be made in evaluating candidate pile types or sections, and in selecting the optimum structure foundation. The foundation support cost concept is a decision making process, not an estimating process. Therefore, the accuracy in the cost estimates is not as important as the relative difference between the cost estimates as long as consistent cost estimating methodology is maintained between all foundation alternatives.

3.4 USE OF VALUE ENGINEERING PROPOSALS

Value engineering is a cost saving technique that can be used either in the pre-bid or post bid stage of a contract. Value engineering consists of a five step logical thought process used to obtain the desired performance for the lowest cost achievable.

Value engineering can readily be applied to foundation engineering by allowing the use of value engineering change proposals in design or construction contracts. The obvious benefit of value engineering to the owner is a lower cost foundation. The consultant or contractor reward for an alternative foundation solution is typically a percentage of the cost savings realized by the owner.

For value engineering to be successful, the owner must be assured that the foundation performance criteria (total settlement, differential settlement, and lateral deformations) remain satisfied. This requires the owner to engage knowledgeable experts to review and comment on submittals as well as to be actively involved in resolution of technical details. In some cases, design verification testing or more sophisticated construction control may be required in order to confirm foundation performance criteria. Lastly, the review of submitted proposals must also be completed in a reasonable time period.

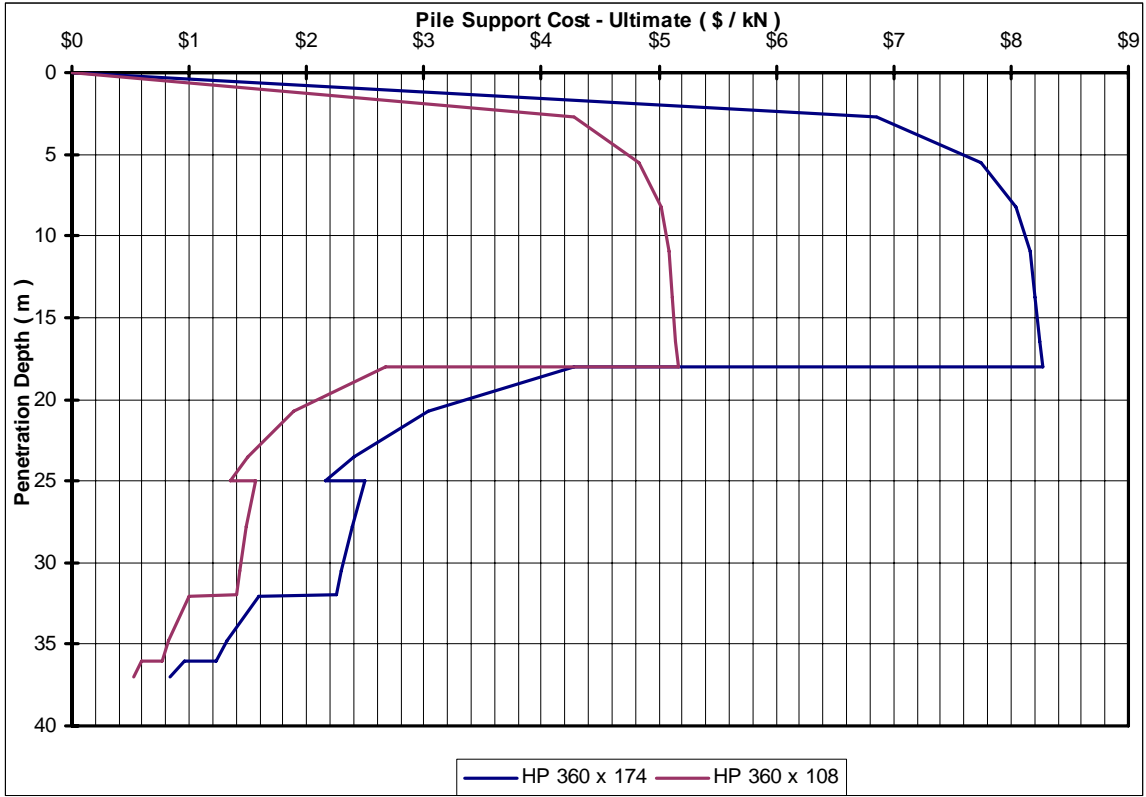


Figure 3.8a Pile Support Cost – Ultimate (\$/kN) vs Depth (m) for Two H-pile Sections

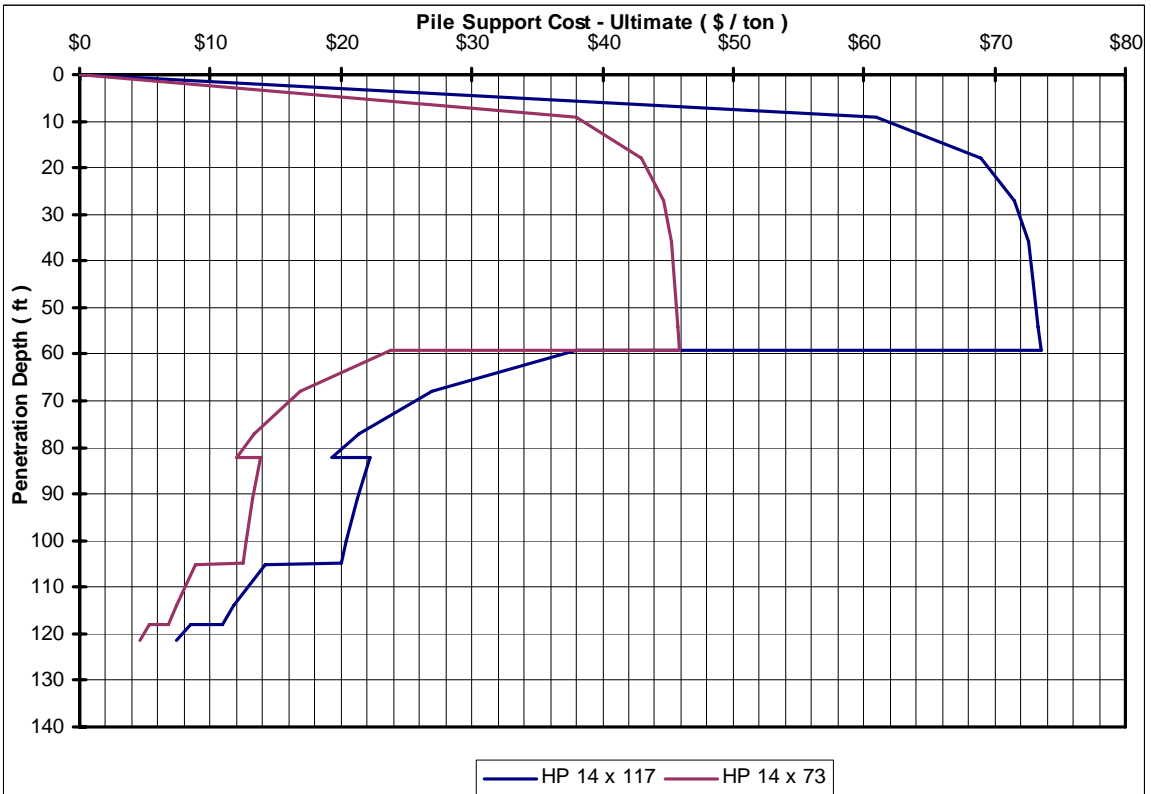


Figure 3.8b Pile Support Cost – Ultimate (\$/ton) vs Depth (ft) for Two H-pile Sections

Significant cost savings can result from value engineering. However, the cost savings should not be achieved by acceptance of unproven pile types, splices, *etc.* Proposed substitutions should be of equivalent quality and have a documented performance record in similar foundation installation conditions.

3.5 DESIGN - BUILD CONTRACTS

Another potential cost saving method is the use of design - build contracts. In this approach, the owner details the general project scope and performance requirements and solicits design - build proposals. Advantages associated with design – build contracts include quicker delivery of the project, use of new cost effective solutions to design and construction issues, and use of the contractor’s knowledge of special equipment or procedures.

Some of the greatest difficulties in design - build contracts surround the scope of the subsurface exploration program, adequate definition of the project performance requirements, and determining the minimum requirements of the quality control and assurance program. Therefore, it is important for the owner in design – build contracts to understand and clearly communicate the project scope, performance requirements, and desired end product as well as method of measurement for payment. Failure to do so may result in a constructed product not meeting the owner’s expectations or failing to meet the agreed-upon budget.

REFERENCES

- Brown D. and Dapp S. (2006). Geotechnical Engineering Circular No. 8, Continuous Flight Auger Piles, Federal Highway Administration, U.S. Department of Transportation, Office of Bridge Technology, Washington D.C. (publication pending)
- Gifford, D.G., Wheeler, J.R., Kraemer, S.R. and McKown, A.F. (1987). Spread Footings for Highway Bridges. FHWA Report No. FHWA/RD-86/185, U.S. Department of Transportation, Federal Highway Administration, Office of Engineering and Highway Operations Research and Development, McLean, 229.
- Kimmerling, R.E. (2002). Geotechnical Engineering Circular No. 6, Shallow Foundations, Federal Highway Administration., U.S. Department of Transportation, Office of Bridge Technology, Washington, D.C., 310.
- Komurka, V.E. (2004). Incorporating Set-up and Support Cost Distributions into Driven Pile Design. American Society of Civil Engineers, ASCE, Geotechnical Special Publication No. 125, Current Practices and Future Trends in Deep Foundations, 16-49.
- O'Neill, M.W. and Reese, L.C. (1999). Drilled Shafts: Construction Procedures and Design Methods. Publication No. FHWA-IF-99-023, U.S. Department of Transportation, Federal Highway Administration, Office of Infrastructure/Office of Bridge Technology, Washington, DC, 758.
- Sabatini, P.J., Tanyu, B., Armour, P., Groneck, P., and Keeley, J. (2005). Micropile Design and Construction – Final Draft, National Highway Institute, Federal Highway Administration, Arlington, VA (publication pending)
- Vanikar, S.N. and Wilson, L. (1986). State-of-the-Art Pile Load Test Program for the Third Lake Washington Bridge, Public Roads, Vol. 50, No. 1., 21-23.

Chapter 4

SUBSURFACE EXPLORATIONS

The design of a structure's foundation requires adequate knowledge of the subsurface conditions at the construction site. If the designer has the appropriate information, then an economical foundation system can be designed. The absence of a thorough foundation study or adequate geotechnical data often leads to (1) a foundation system with a large factor of safety which is generally a more expensive foundation and in some cases one that may be difficult to construct, or to (2) an unsafe foundation, or to (3) construction disputes and claims.

A thorough foundation study consists of a subsurface exploration program (which includes borings, sampling, groundwater measurements, and in-situ testing); laboratory testing; geotechnical analysis of all data; a determination of design properties; and design recommendations. This chapter covers the subsurface exploration portion of a foundation design study in a concise manner. A more detailed treatment of this chapter's subject matter may be found in the AASHTO Manual on Subsurface Investigations (1988) and in FHWA publication FHWA-NHI-01-031, Subsurface Investigations – Geotechnical Site Characterization (2002). Chapter 5 of this manual focuses on in-situ testing which is also considered part of a subsurface exploration, and Chapter 6 discusses laboratory testing. This chapter assumes that a decision with regard to the foundation type, *i.e.*, shallow or deep has not yet been made.

4.1 SUBSURFACE PROPERTIES FOR PILE DESIGN

Static analysis procedures described in Chapter 9 of this manual are used to estimate a pile foundations ability to support the applied compression, uplift, and lateral loads. Knowledge of the subsurface stratigraphy, soil classification and index properties, shear strength, compressibility, stress history, and the ground water table location is required for design. In addition, the pile selection process described in Chapter 8 will require knowledge of the aggressiveness of the subsurface environment on possible foundation types. The subsurface exploration program must be planned to delineate the subsurface stratigraphy and retrieve quality soil and rock samples so that the design soil profile and soil parameters can be subsequently developed.

Table 4-1 provides a summary of the design parameters needed for pile design as well as the sampling and/or test methods commonly used to obtain the design parameter. Subsurface stratigraphy and soil classification including gradation, Atterberg limits, and moisture content must be determined so that applicable pile design methods for capacity

and settlement computations are utilized for the subsurface conditions. Accurate determination of the effective friction angle or undrained shear strength of the soil strata is particularly important for piles designed to carry their loads through shaft resistance or for foundations subject to significant uplift loading. For pile foundations designed to transfer a majority of their load through end bearing on soil or rock, the soil strength parameters of the bearing layer or determination of the rock quality is important. Knowledge of the preconsolidation pressure of cohesive deposits is important in pile foundation designs that transfer load to or are supported above cohesive layers. Many of the design methods are effective stress based procedures that require information on soil unit weights and water table location. A pile foundation design will be more efficient when the subsurface parameters described in Table 4-1 are adequately and accurately defined.

TABLE 4-1 SUMMARY OF FIELD OR LABORATORY TESTS FOR PILE DESIGN PARAMETERS			
Design Parameter or Information Needed	Subsurface Material		
	Cohesionless	Cohesive	Rock
Subsurface stratigraphy	SPT, CPT _u , CPT, DMT	SPT, CPT _u , CPT, DMT	Rock Core
Classification	Lab	Lab	Lab
Gradation	Lab	Lab	
Atterberg Limits		Lab	
Moisture Content	Lab	Lab	
Unit Weight, γ	SPT, DMT	USS-Lab	USS-Lab
Sensitivity		VST, USS-Lab	
Effective friction angle, ϕ'	SPT, CPT _u , CPT, DMT	USS-Lab	USS-Lab
Undrained shear strength, c_u		Lab	
Preconsolidation pressure, p_c		USS-Lab, DMT, CPT _u , CPT	
Rock quality, RQD			Rock Core
Groundwater table elevation	Well / Piezometer	Well / Piezometer	Well / Piezometer

Table Key:

- SPT – Standard Penetration Test (Section 4.4.1)
- CPT_u – Cone Penetration Test with pore water pressure measurements (Section 5.1)
- CPT – Cone Penetration Test (Section 5.1)
- DMT – Dilatometer Test (Section 5.3)
- VST – Vane Shear Test (Section 5.4)
- Lab – Laboratory test on a disturbed or undisturbed soil sample (Chapter 6)
- USS-Lab – Laboratory test on undisturbed soil sample (Section 4.4.2 and Chapter 6)

4.2 SUBSURFACE EXPLORATION PHASES

There are three major phases in a subsurface exploration program. These phases are (1) planning the exploration program (office work), (2) completing a field reconnaissance survey, and (3) performing a detailed site exploration program (boring, sampling, and in-situ testing). Each phase should be planned so that a maximum amount of information can be obtained at a minimum cost. Each phase also adds to, or supplements, the information from the previous phase. Table 4-2 lists the purpose of each exploration phase.

4.2.1 Planning the Exploration Program (office work)

The purpose of this phase is to obtain information about the proposed structure and general information on the subsurface conditions. The structural information can be obtained from studying the preliminary structure plan prepared by the bridge design office and by meeting with the structural designer. Approach embankment preliminary design and performance requirements can be obtained from the roadway office. General information about the subsurface conditions can be obtained from a variety of sources listed in Table 4-3. **The planning phase prepares the engineer for the field reconnaissance survey, and identifies possible problems and areas to scrutinize.**

4.2.2 Field Reconnaissance Survey

The purpose of this phase is to substantiate the information gained from the office phase and to plan the detailed site exploration program. The field reconnaissance for a structure foundation exploration should include:

- a. Inspection of nearby structures to determine their performance with the particular foundation type used.
- b. Inspection of existing structure footings and stream banks for evidence of scour (for stream crossings) and movement. Large boulders in a stream are often an indication of obstructions which may be encountered in pile installations.
- c. Visual examination of terrain for evidence of landslides.
- d. Recording of the location, type and depth of existing structures which may be affected by the new structure construction.

TABLE 4-2 SUBSURFACE EXPLORATION PHASES

Phase	Activity	Purpose	Remarks
1.	Planning the exploration (Office Work).	<p>A. Obtain structure information. Determine:</p> <ol style="list-style-type: none"> 1. Type of structure. 2. Preliminary location of piers and abutments. 3. Loading and special design events. 4. Allowable differential settlement, lateral deformations, and other performance criteria. 5. Any special features and requirements. <p>B. Obtain drilling records for nearby structures and from local well drillers.</p> <p>C. Perform literature reviews including maintenance records, pile driving records, scour history, etc.</p> <p>Obtain overall picture of subsurface conditions in the area.</p>	See Table 4-2 for sources of information.
2.	Field Reconnaissance Survey	<p>Verify information gained from the office phase and plan the detailed subsurface exploration.</p> <p>A. Observe, verify and collect information regarding:</p> <ol style="list-style-type: none"> 1. Topographic and geologic features. 2. New and old construction in the area including utilities. Performance of existing structures. 3. Drilling equipment required, cost, and access for the equipment. <p>B. If appropriate, conduct geophysical testing to obtain preliminary subsurface information.</p>	Field reconnaissance is often conducted by a multi-disciplined team.
3.	Detailed Subsurface Exploration	<p>Develop a preliminary boring plan based on phases 1 and 2. Conduct a preliminary evaluation for viable foundation systems including ground improvement. Determine subsurface requirements for all of the viable foundation systems. The boring plan should be modified if needed as the borings are performed and detailed subsurface information is obtained.</p> <p>The subsurface exploration should provide the following:</p> <ol style="list-style-type: none"> 1. Depth and thickness of strata (subsurface profile). 2. In-situ field tests to determine soil design parameters. 3. Samples to determine soil and rock design parameters. 4. Groundwater levels including perched, regional, and any artesian conditions. 	For major structures, the pilot boring program is often supplemented with control and verification boring programs.

- e. Relating site conditions to proposed boring operations. This includes recording the locations of both overhead and below ground utilities, site access, private property restrictions, and other obstructions.
- f. Recording of any feature or constraint which may impact the constructability of potential foundation systems.

Table 4-4 contains an example of a field reconnaissance form modified from the AASHTO Foundation Investigation Manual (1978) for recording data pertinent to a site.

4.2.3 Detailed Site Exploration

The purpose of any boring program is not just to drill a hole, but to obtain representative information on the subsurface conditions, to recover disturbed and undisturbed soil samples, and to permit in-situ testing. This information provides factual basis upon which all subsequent steps in the pile design and construction process are based. It's quality and completeness are of paramount importance. Each step in the process directly or indirectly relies on this data.

The first step in this phase is to prepare a preliminary boring, sampling, and in-situ testing plan. For major structures, pilot borings are usually performed at a few select locations during the preliminary planning stage. These pilot borings establish a preliminary subsurface profile and thus identify key soil strata for testing and analysis in subsequent design stage borings. During the design stage of major structures, a two phase boring program is recommended. First, control borings are performed at key locations identified in the preliminary subsurface profile to determine what, if any, adjustments are appropriate in the design stage exploration program. Following analysis of the control boring data, verification borings are then performed to fill in the gaps in the design stage exploration program.

TABLE 4-3 SOURCES OF SUBSURFACE INFORMATION AND USE

Source No.	Source	Use
1.	Preliminary structure plans prepared by the bridge design office.	Determine: 1. Type of structure. 2. Preliminary locations of piers and abutments. 3. Footing loads and special design events. 4. Allowable differential settlement, lateral deformations, and performance criteria. 5. Any special features and requirements.
2.	Construction plans and records for nearby structures.	Foundation type, old boring data, construction information including construction problems.
3.	Topographic maps prepared by the United States Coast and Geodetic Survey (USC and GS), United States Geological Survey (USGS) and State Geology survey.	Existing physical features shown; find landform boundaries and determine access for exploration equipment. Maps from different dates can be used to determine topographic changes over time.
4.	County agricultural soil survey maps and reports prepared by the United States Department of Agriculture (USDA).	Boundaries of landforms shown; appraisal of general shallow subsurface conditions.
5.	Air photos prepared by the United States Geological Survey (USGS) or others.	Detailed physical relief shown; gives indication of major problems such as old landslide scars, fault scarps, buried meander channels, sinkholes, or scour; provides basis for field reconnaissance.
6.	Well drilling record or water supply bulletins from state geology or water resources department.	Old well records or borings with general soils data shown; estimate required depth of explorations and preliminary cost of foundations.
7.	Geologic maps and Geology bulletins.	Type, depth and orientation of rock formations.

TABLE 4-4 EXAMPLE FIELD RECONNAISSANCE REPORT FORM

Bridge Foundation Investigation
 Field Reconnaissance Report
 _____ Department of Transportation

Project No: _____ County _____ Sta. No. _____

Reported By: _____ Date _____

- | | |
|--|--|
| <p>1. Staking of Line
 Well Staked _____
 Poorly Staked (We can work) _____
 Request Division to Restake _____</p> <p>2. Bench Marks
 In Place: Yes _____ No _____
 Distance from bridge - m (ft) _____</p> <p>3. Property Owners
 Granted Permission: Yes _____ No _____
 Remarks on Back _____</p> <p>4. Utilities
 Will Drillers Encounter Underground or
 Overhead Utilities? Yes _____ No _____
 Maybe _____ At Which Holes? _____
 What Type? _____
 Who to See for Definite Location _____

 _____</p> <p>5. Geologic Formation</p> <p>6. Surface Soils
 Sand _____ Clay _____ Sandy Clay _____
 Muck _____ Silt _____ Other _____</p> <p>7. General Site Description
 Topography
 Level _____ Rolling _____ Hillside _____
 Valley _____ Swamp _____ Gullied _____
 Groundcover
 Cleared _____ Farmed _____ Buildings _____
 Heavy Woods _____ Light Woods _____
 Other _____
 Remarks on Back _____</p> <p>8. Bridge Site
 Replacing _____
 Widening _____
 Relocation _____
 Check Appropriate Equipment
 Truck Mounted Drill Rig _____
 Track Mounted Drill Rig _____
 Failing 1500 _____
 Truck Mounted Skid Rig _____
 Skid Rig _____
 Rock Coring Rig _____
 Wash Boring Equipment _____
 Water Wagon _____
 Pump _____
 Hose _____ m (ft)</p> | <p>8. Bridge Site - Continued
 Cut Section - m (ft) _____
 Fill Section - m (ft) _____
 If Stream Crossing:
 Will Pontoons Be Necessary? _____
 Can Pontoons Be Placed in Water Easily? _____

 Can Cable Be Stretched Across Stream?
 How Long? _____

 Is Outboard Motorboat Necessary? _____
 Current:
 Swift _____ Moderate _____ Slow _____
 Describe Streambanks scour.
 If Present Bridge Nearby:
 Type of Foundation _____
 Any Problems Evident in Old Bridge Including
 Scour _____
 (describe on back)
 Is Water Nearby for Wet Drilling - m (ft) _____
 Are Abandoned Foundations in Proposed
 Alignment? _____</p> <p>9. Ground Water Table
 Close to Surface - m (ft) _____
 nearby Wells - Depth - m (ft) _____
 Intermediate Depth - m (ft) _____
 Artesian head - m (ft) _____</p> <p>10. Rock
 Boulders Over Area? Yes _____ No _____
 Definite Outcrop? Yes _____ No _____
 (show sketch on back)
 What kind? _____</p> <p>11. Special Equipment Necessary</p> <p>12. Remarks on Access
 (Describe any Problems on Access)</p> <p>13. Debris and Sanitary Dumps
 Stations _____
 Remarks _____

 _____</p> <p>Reference: Modified from 1978 AASHTO Foundation
 Investigation Manual</p> |
|--|--|

4.3 GUIDELINES FOR MINIMUM STRUCTURE EXPLORATION PROGRAMS

The cost of a subsurface exploration program is comparatively small in relation to the foundation cost. For example, the cost of one 60 mm (2.4 inch) diameter boring is less than the cost of one 305 mm (12 inch) diameter pile. However, in the absence of adequate boring data, the design engineer must rely on extremely conservative designs with high safety factors. At the same time, the designer assumes enormous risk and uncertainty during the project's construction.

The number of borings required, their spacing, and sampling intervals depend on the uniformity of soil strata and loading conditions. Erratic subsurface conditions require closely spaced borings. Structures sensitive to settlements or subjected to heavy loads require detailed subsurface knowledge. In these cases borings should be closely spaced. Rigid rules for number, spacing, and depth of borings cannot be established. However, the following are general "guidelines" useful in preparing a boring plan.

1. A minimum of one boring with sampling should be performed at each pier or abutment. The boring pattern should be staggered at opposite ends of adjacent footings. Pier and abutment footings over 30 m (100 ft) in length require borings at the extremities of the substructure units.
2. Estimate required boring depths from data gathered in the planning and field reconnaissance phases. Confirmation of boring depth suitability for design purposes should be made by the geotechnical engineer as soon as possible after field crews initiate a boring program. Although less preferred, it may be possible for field crews to adjust boring depths using a resistance criteria such as: "Structure foundation borings shall be terminated when a minimum SPT resistance of 50 blows per 300 mm (1 ft) has been maintained for 7.5 m (25 ft). (This rule is intended for preliminary guidance to drillers. For heavy structures with high capacity piles, the borings must go deeper. A resistance criteria may also be inappropriate in some geologic conditions such as sites with boulder fields.)
3. All borings should extend through unsuitable strata, such as unconsolidated fill, peat, highly organic materials, soft fine grained soils and loose coarse-grained soils to reach hard or dense materials. Where stiff or dense soils are encountered at shallow depths, one or more borings should be extended through this material to a depth where the presence of underlying weaker strata cannot affect stability or settlement of the structure.

4. Standard Penetration Test (SPT) samples should be obtained at 1.5 m (5 ft) intervals or at changes in material with the test data recorded in accordance with AASHTO T206. For spread footing design or embankment evaluations, continuous sampling over the 6 m (20 ft) should be performed. Undisturbed tube samples should be obtained in accordance with AASHTO T207 at sites where cohesive soils are encountered. The location and frequency of undisturbed soil sampling should be based on project requirements.
5. When rock is encountered at shallow depths, additional borings or other investigation methods such as probes, test pits, or geophysical tests may be needed to define the rock profile. When feasible, borings should extend a minimum of 3 m (10 ft) into rock having an average core recovery of 50% or greater with an NX-core barrel providing a 54 mm (2-1/8 inch) diameter core.
6. Drill crews should maintain a field drilling log of boring operations. The field log should include a summary of drilling procedures including SPT hammer type, sample depth and recovery, strata changes, and visual classification of soil samples. The field log should also include pertinent driller's observations such as location of ground water table, boulders, loss of drilling fluids, artesian pressures, *etc.* Disturbed and undisturbed soil samples as well as rock cores should be properly labeled, placed in appropriate storage containers (undisturbed tube samples should be sealed in the field), and properly transported to the soils laboratory.
7. The water level reading in a bore hole should be made during drilling, at completion of the bore hole, and a minimum of 24 hours after completion of the bore hole. Long term readings may require installation of an observation well or piezometer in the bore hole. More than one week may be required to obtain representative water level readings in low permeability cohesive soils or in bore holes stabilized with some drilling muds.
8. All bore holes should be properly backfilled and sealed following completion of the subsurface exploration program, data collection, and analysis. Bore hole sealing is particularly important where groundwater migration may adversely affect the existing groundwater conditions (aquifer contamination) or planned construction (integrity of tremie seals in future cofferdams).

These guidelines should result in subsurface exploration data that clearly identify subsurface stratigraphy and any unusual conditions, allow laboratory assessments of soil strength and compressibility, and document the groundwater table conditions. This information permits a technical evaluation of foundation options and probable costs.

4.4 METHODS OF SUBSURFACE EXPLORATION

The most widely used method of subsurface exploration is drilling holes into the ground from which samples are collected for visual classification and laboratory testing. Table 4-5 summarizes the advantages and disadvantages of four commonly used soil boring methods, as well as rock coring, test pits and geophysical methods.

4.5 SOIL AND ROCK SAMPLING

One of the main purposes of a subsurface exploration program is to obtain **quality** soil and rock samples. Quality samples are important because soil identification and stratification, strength, and compressibility are all evaluated from samples recovered in the exploration program.

Soil samples are divided into two categories, disturbed and undisturbed. Disturbed samples are those which have experienced large structural disturbance during sampling operations and may be used for identification/classification tests. The primary disturbed sampling method is the split barrel sampler used in the Standard Penetration Test (SPT). The penetration resistance values obtained from the Standard Penetration Test are called N values. These N values provide an indication of soil density or consistency and shear strength. The recommended test procedures outlined in AASHTO T206 should be rigidly followed so that consistent, reliable SPT N values are obtained. SPT N values are commonly used for design of pile foundation design in granular soils. **SPT N values are NOT RECOMMENDED for pile design in cohesive soils.**

Undisturbed samples are those in which structural disturbance is kept to an absolute minimum. Undisturbed samples are used for consolidation tests and strength tests such as direct shear, triaxial shear and unconfined compression as well as for determining unit weight. Strength tests provide shear strength design parameters which are used in static analysis methods for pile foundation design. Consolidation tests provide parameters needed to estimate settlements of embankments, spread footings, or pile groups. Unit weight information is used in determining the effective overburden pressure.

Rock cores obtained from borings allow a qualitative evaluation of rock mass and distinguish between boulders and bedrock. Rock Quality Designation (RQD) values determined from cores indicate rock soundness and characteristics and may thereby be useful in estimating the compressive strength of the rock mass. Unconfined compression tests may also be performed on recovered, high quality core samples.

TABLE 4-5 METHODS OF SUBSURFACE EXPLORATIONS*

Method	Depth	Type of Samples Taken	Advantages	Disadvantages	Remarks
1. Seismic 2. Resistivity	Usually less than 30 m.(100 ft)	No samples are taken.	1. Less expensive than borings. 2. Complements borings. 3. Data obtained very quickly.	1. Indirect method of exploration, no samples are taken. 2. Interpretation of data is critical and requires substantial experience.	Main uses are described in AASHTO (1988). Additional limitations of seismic methods are: 1. Soil layers must increase in seismic velocities with depth. 2. The layer must be thick.
3. Wash Boring	Depends on the equipment.. Most equipment can drill to depths of 30 m (100 ft) or more.	Disturbed and undisturbed.	1. Borings of small and large diameter. 2. Equipment is relatively inexpensive. 3. Equipment is light. 4. Washwater provides an indication of change in materials. 5. Method does not interfere with permeability tests.	1. Slow rate of progress. 2. Not suitable for materials containing stones and boulders.	Hole advanced by a combination of the chopping action of a light bit and jetting action of the water coming through the bit.
4. Rotary Drilling	Depends on the equipment. Most equipment can drill to depths of 60 m (200 ft) or more.	Disturbed and undisturbed.	1. Suited for borings 100 to 150 mm (4 to 6 inches) in diameter. 2. Most rapid method in most soils and rock. 3. Relatively uniform hole with little disturbance to the soil below the bottom of hole. 4. Experienced driller can detect changes based on rate of progress.	1. Drilling mud if used does not provide an indication of material change as the washwater does. 2. Use of drilling mud hampers the performance of permeability tests.	Hole advanced by rapid rotation of drilling bit and removal of material by water or drilling mud. Rock coring is performed by rotary drilling.
5. Auger Borings	Depends on the equipment. Most equipment can drill to depths of 30 to 60 m (100 to 200 ft).	Disturbed and undisturbed.	1. Boring advanced without water or drilling mud. 2. Hollow stem auger acts as a casing.	1. Difficult to detect change in material. 2. Heavy equipment required. 3. Water level must be maintained in boring equal to or greater than existing water table to prevent sample disturbance.	Hole advanced by rotating and simultaneously pressing an auger into the ground either mechanically or hydraulically.
6. Continuous Sample Method of Advance	Depends on the equipment.	Disturbed and undisturbed.	Almost continuous record of the soil profile can be obtained.	Generally much slower in soils and more expensive than other methods.	Boring advanced by wash method, rotary drilling or auger method and continuous samples are taken.
7. Rock Coring	Rotary drilling equipment is used to drill to depths of 60 m (200 ft) or more.	Continuous rock cores.	Helps differentiate between boulders and bedrock.	Can be slow and fairly expensive.	Several types of core barrels are used including wire line core barrels for deep drilling.
8. Test Pits	Usually less than 6 m (20 ft) .	Disturbed samples and undisturbed block samples.	Least sample disturbance. Valuable in erratic soil deposits such as old fills, landfills, and residual soil deposits.	1. Limited depth. 2. Slower and expensive.	Power equipment used to excavate the pits. Test pits should be located so as not to disturb bearing stratum if footing foundations are feasible.

*Excluding in-situ tests.

4.5.1 Disturbed Soil Samplers

The split barrel sampler used in the Standard Penetration Test (SPT) is the primary disturbed soil sampler. The SPT test consists of driving a 51 mm (2 inch) O.D., 35 mm I.D., (1-3/8 inch) split-spoon sampler into the soil with a 64 kg (140 lb) mass dropped 760 mm (30 inches). The sampler is generally driven 450 mm (18 inches), and the blow count for each 150 mm (6 inch) increment is recorded. The number of blows required to advance the sampler from a penetration depth of 150 mm (6 inches) to a penetration depth of 450 mm (18 inches) is the SPT resistance value, N. A schematic of the Standard Penetration Test Procedure is provided in Figure 4.1, SPT hammer types are illustrated in Figure 4.2, and Figure 4.3 contains a picture of the split barrel sampler.

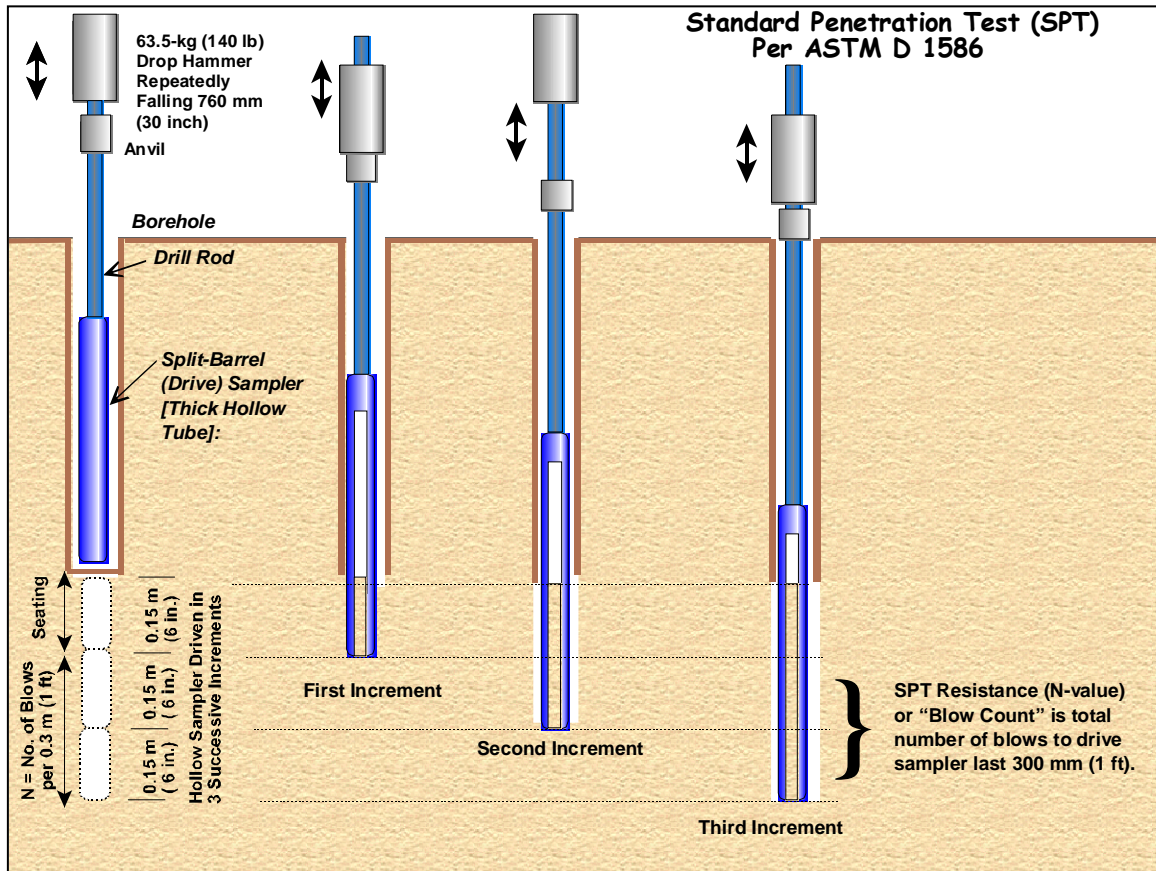


Figure 4.1 SPT Procedure from Mayne et. al., (2002)

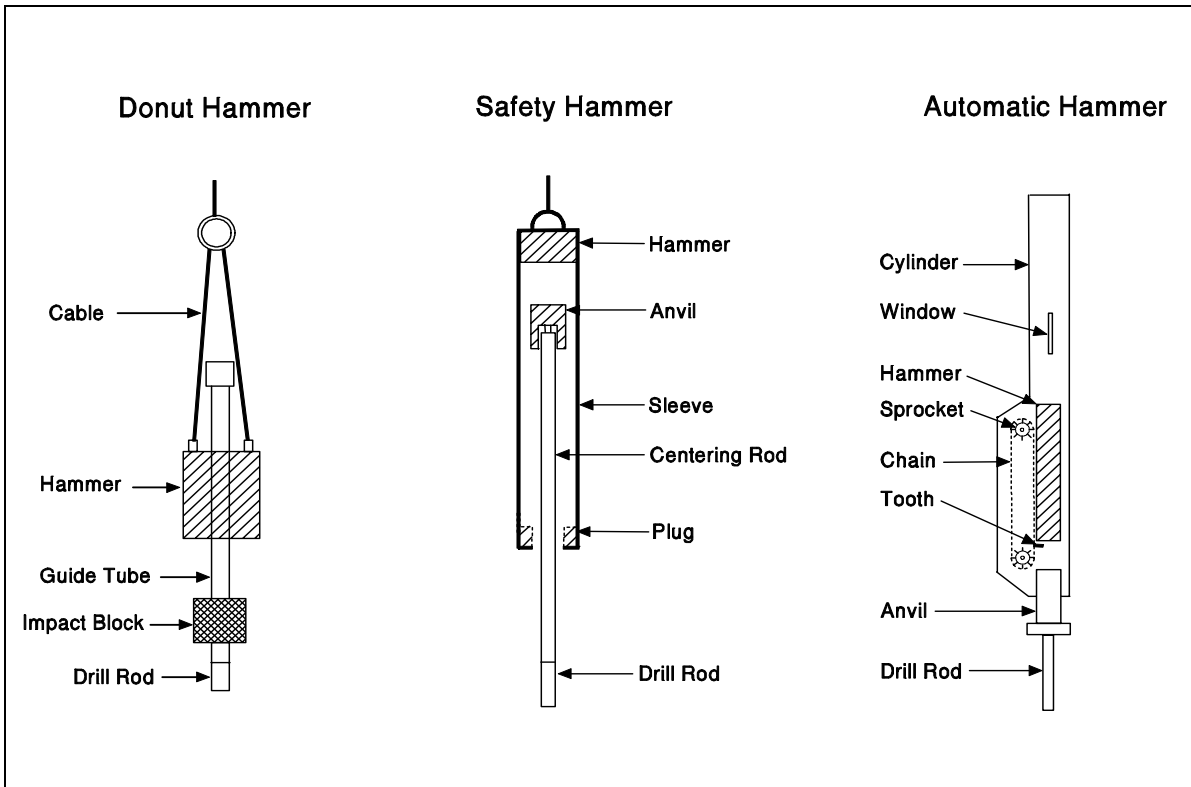


Figure 4.2 SPT Hammer Types



Figure 4.3 Split Barrel Sampler from Mayne et. al., (2002)

The SPT hammer type and operational characteristics have a significant influence on the resulting SPT N values. There are two main hammer types currently in use in the US, the safety hammer and the automatic hammer. A third hammer type, the donut hammer, was used almost exclusively prior to about 1970. However, it is seldom used now due to safety considerations. Figure 4.2 provides illustrations of these SPT hammer types. Numerous measurement studies on SPT energy transfer have been performed. In general, these studies have indicated that the typical energy transfer from donut, safety, and automatic hammers are on the order of 45%, 60%, and 80% of the SPT test potential energy, respectively. It should not be assumed that all SPT hammers of a given type will have the energy transfer values noted above. Energy transfer for a given hammer type can and does vary according to hammer maintenance, hammer manufacturer, driller, and operating procedures. Because of these variations, it is recommended that SPT hammers undergo a yearly calibration in accordance with ASTM D 4633-05 to document hammer performance. It may be particularly advantageous to conduct these calibrations prior to undertaking major projects. A photograph of energy transfer measurements being taken during a SPT sampling event is provide in Figure 4.4.

The pile design charts and methods provided in Chapter 9 that use SPT N values are based on safety hammer correlations, i.e., 60% energy transfer. SPT N values established on the basis on 60% energy transfer are referred to as N_{60} . SPT N values can be converted to N_{60} values based on energy transfer measurements as follows:

$$N_{60} = N (\text{ETR} / 60\%)$$

Where: N = field measured SPT N value
ETR = energy transfer ratio, i.e., transfer energy / potential energy (%)

The significance of the SPT hammer type and energy transfer on N values is apparent in a pile capacity prediction symposium reported by Finno (1989). For this event, two soil borings were drilled less than 10 m (33 ft) apart in a uniform sand soil profile. SPT N values were obtained using a safety hammer in one boring and an automatic hammer in the other boring.

Figure 4.5 presents a plot of the SPT N values versus depth from these two borings. The SPT N values from the safety hammer range from 1.9 to 2.7 times the comparable N value from the automatic hammer. **This significant variation in N values clearly indicates that the type of SPT hammer used should be recorded on all drilling logs.** It is recommended that N values be corrected and reported as N_{60} values whenever possible.



Figure 4.4 Energy Measurements on Automatic SPT Hammer

Cheney and Chassie (2000) list the following common errors that can influence SPT test results:

1. Effect of overburden pressure. Soils of the same density will give smaller SPT N values near the ground surface.
2. Variations in the 760 mm (30 inch) free fall of the drive weight, since this is often done by eye on older equipment using a rope wrapped around a power takeoff (cathead) from the drill motor. Newer automatic hammer equipment does this automatically.

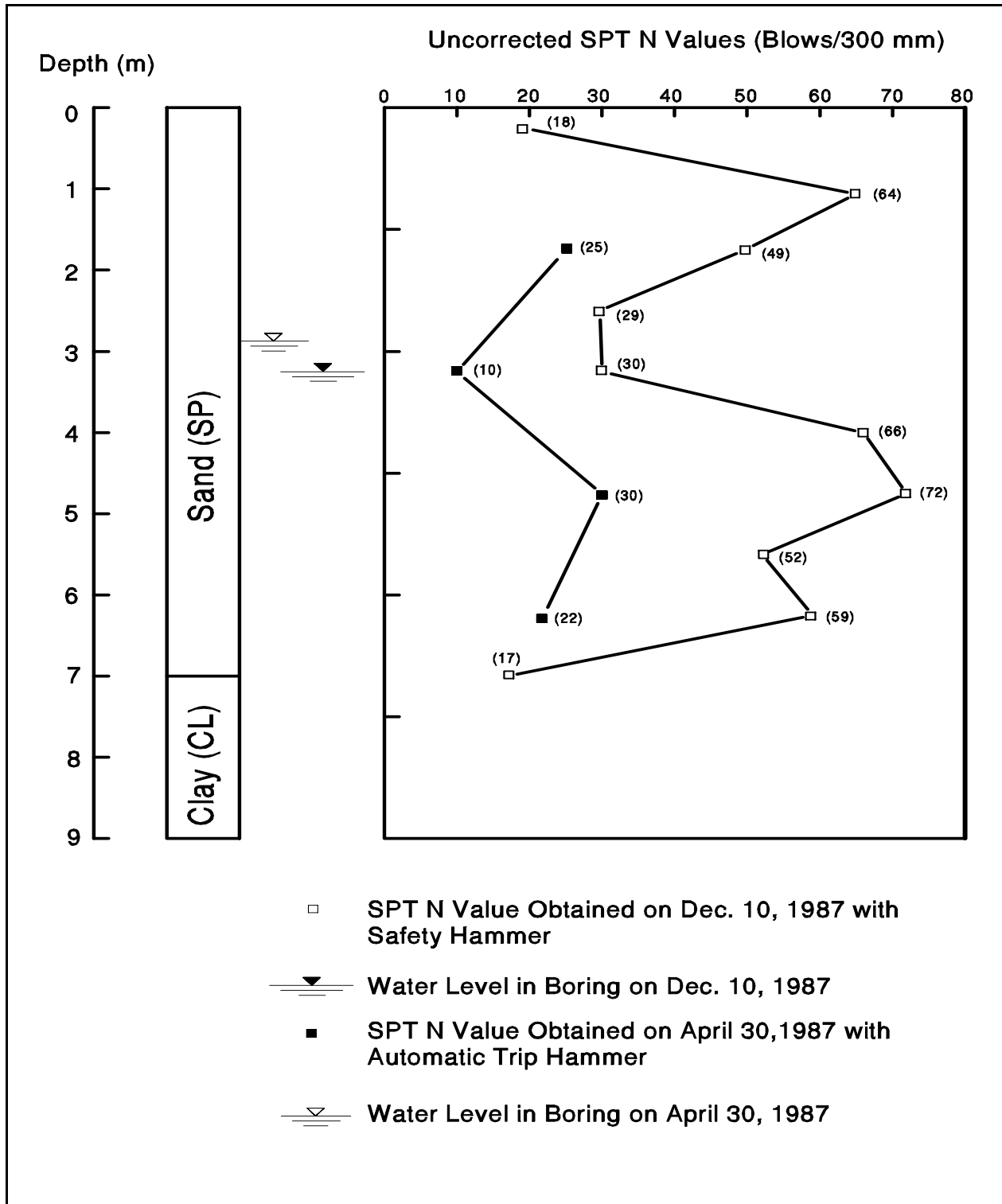
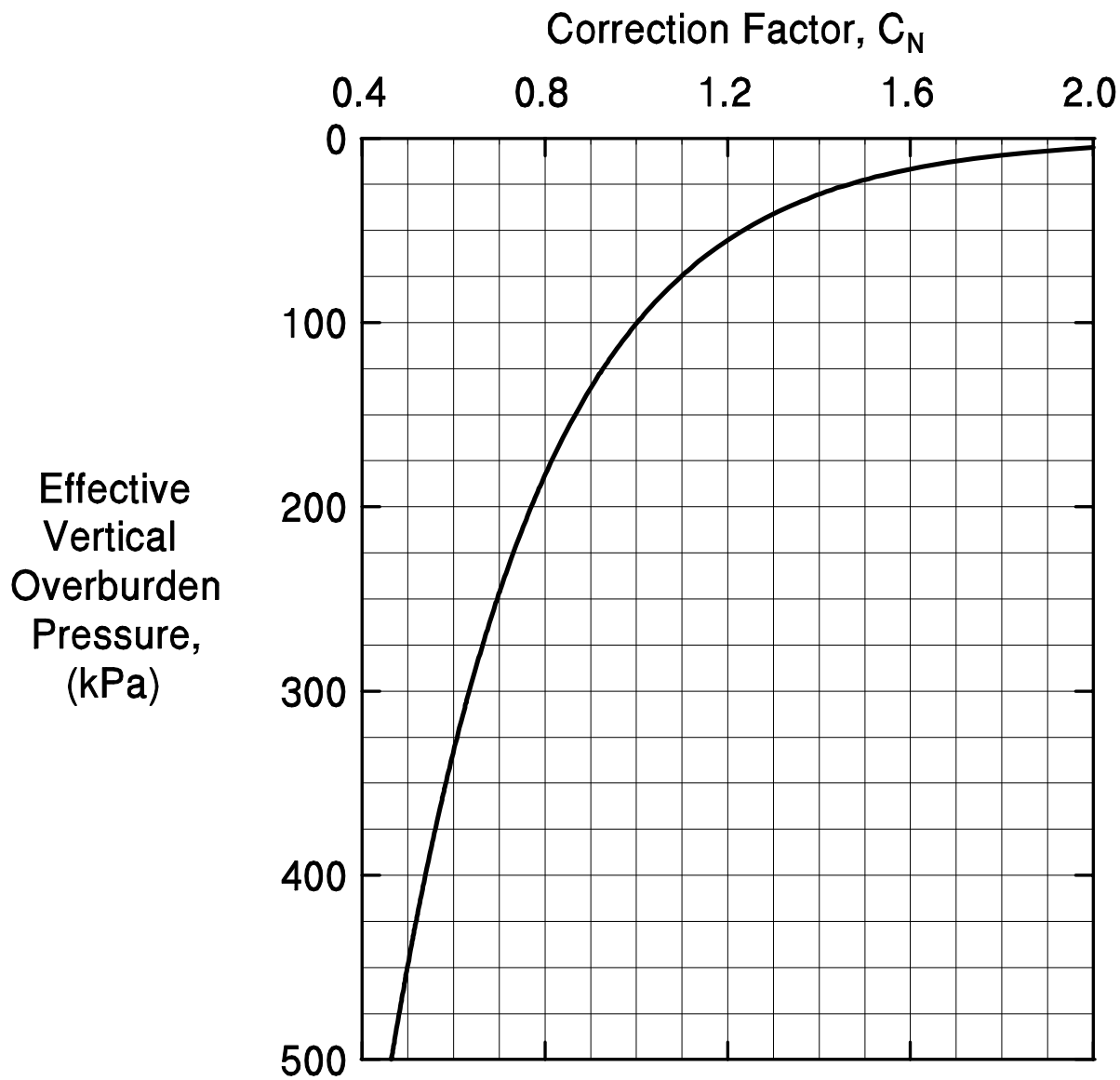


Figure 4.5 SPT Test Results for Safety and Automatic Hammers (after Finno, 1989)

3. Interference with the free fall of the drive weight by the guides or the hoist rope. New equipment eliminates rope interference.
4. Use of a drive shoe that is badly damaged or worn from too many drivings to "refusal" (SPT N values exceeding 100).
5. Failure to properly seat the sampler on undisturbed material at the bottom of the boring.
6. Inadequate cleaning of loosened material from the bottom of the boring.
7. Failure to maintain sufficient hydrostatic pressure in the borehole during drilling or during drill rod extraction. Unbalanced hydrostatic pressures between the borehole drill water and the ground water table can cause the test zone to become "quick". This can happen when using the continuous-flight auger with the end plugged and maintaining a water level in the hollow stem below that in the hole
8. SPT results may not be dependable in gravel. Since the split-spoon inside diameter is 35 mm (1-3/8 inch), gravel sizes larger than 35 mm (1-3/8 inch) will not enter the spoon. Therefore, soil descriptions may not reflect actual gravel content of the deposit. Also, gravel pieces may jam the end of the spoon which may get plugged and cause the SPT blow count to be erroneously high.
9. Samples retrieved from dilatant soils (fine sands, sandy silts) which exhibit unusually high blow count should be examined in the field to determine if the sampler drive shoe is plugged. Poor sample recovery is an indication of plugging.
10. Careless work on the part of the drill crew.

The use of reliable qualified drillers and adherence to recommended sampling practice cannot be overemphasized. State agencies which maintain their own drilling personnel and equipment achieve much more reliable, consistent results than those who routinely let boring contracts to the low bidder.

A correction of field N values is also necessary to account for the effects of overburden pressures when estimating physical properties in cohesionless soils. The corrected N' value is determined by multiplying the field N value by the correction factor obtained from Figure 4.6. All N' values referred to in this manual are the corrected for overburden pressure.



$N' = C_n(N)$

Where: N' = corrected SPT N value.
 C_n = correction factor for overburden pressure.
 N = uncorrected or field SPT value.

NOTE: Maximum correction factor is 2.0. 100 kPa = 1 TSF

Figure 4.6 Chart for Correction of N-values in Sand for Influence of Effective Overburden Pressure (after Peck *et al.*, 1974)

Correlations of cohesive soil physical properties with N values are crude and, therefore, correction of N values in cohesive soils is not necessary.

The corrected N' values and uncorrected N values (blows / 300 mm) (blows / ft) may be used to estimate the relative density of cohesionless soils and consistency of cohesive soils, respectively. Table 4-6 contains an empirical relationship between N' value, and the relative density, angle of internal friction and unit weight of granular soils. It is emphasized that for soils containing gravel sized particles, this table may yield unreliable results. In those cases, the correlations should be used for rough estimation purposes only. Static analysis procedures to calculate the ultimate capacity of pile foundations in cohesionless soils using SPT N' values are presented in Chapter 9.

Table 4-7 contains an empirical relationship between the uncorrected N value and the unconfined compressive strength and saturated unit weight of cohesive soils. The undrained shear strength is one half of the unconfined compressive strength. Correlation of N values to the undrained shear strength of clays is crude and unreliable for design. It should be used only for preliminary estimating purposes. Undisturbed cohesive samples should be obtained for laboratory determination of accurate shear strength and unit weight.

Description	Very Loose	Loose	Medium	Dense	Very Dense
Relative density D_r	0 - 0.15	0.15 - 0.35	0.35 - 0.65	0.65 - 0.85	0.85 - 1.00
Corrected Standard Penetration N' value	0 to 4	4 to 10	10 to 30	30 to 50	50+
Approximate angle of internal friction ϕ *	25 - 30°	27 - 32°	30 - 35°	35 - 40°	38 - 43°
Range of approximate moist unit weight γ kN/m ³ (lb/ft ³)	11.0 - 15.7 (70 - 100)	14.1 - 18.1 (90 - 115)	17.3 - 20.4 (110 - 130)	17.3 - 22.0 (110 - 140)	20.4 - 23.6 (130 - 150)

Correlations may be unreliable in soils containing gravel. See Section 9.5. of Chapter 9.

* Use larger values for granular material with 5% or less fine sand and silt.

TABLE 4-7 EMPIRICAL VALUES FOR UNCONFINED COMPRESSIVE STRENGTH (q_u) AND CONSISTENCY OF COHESIVE SOILS BASED ON UNCORRECTED N (after Bowles, 1977)						
Consistency	Very Soft	Soft	Medium	Stiff	Very Stiff	Hard
q_u , kPa (ksf)	0 – 24 (0 – 0.5)	24 – 48 (0.5 – 1.0)	48 – 96 (1.0 – 2.0)	96 – 192 (2.0 – 4.0)	192 – 384 (4.0 – 8.0)	384+ (8.0+)
Standard Penetration N value	0 - 2	2 - 4	4 – 8	8 - 16	16 - 32	32+
γ (saturated), kN/m ³ (lb/ft ³)	15.8 - 18.8 (100 – 120)	15.8 - 18.8 (100 – 120)	17.3 - 20.4 (110 – 130)	18.8 - 22.0 (120 – 140)	18.8 - 22.0 (120 – 140)	18.8 - 22.0 (120 – 140)
The undrained shear strength is 1/2 of the unconfined compressive strength.						

Correlations are unreliable. Use for preliminary estimates only.

4.5.2 Undisturbed Soil Samplers

Undisturbed samples of cohesive soils should be obtained for accurate shear strength, compressibility, and unit weight determinations. Several types of undisturbed soil samplers are used in conjunction with boring operations.

- a. Thin wall open tube (Figures 4.7a and 4.7b).
- b. Piston samplers.
- c. Pitcher sampler (Figure 4.9)

Thin wall open tube or Shelby tube samplers are the most common method for obtaining relatively undisturbed cohesive soil samples. These tubes have a beveled front cutting edge and are slowly pushed into the soil using a drill rig's hydraulic system. Thin wall open tube samplers are best suited for sampling medium soft to medium stiff cohesive soils. Sample recovery and/or sample disturbance may be unacceptable in very soft soils. Thin wall tube samples also often have difficulty sampling very hard or gravelly soils. Additional details on thin wall tube sampling are described in AASHTO T207 or ASTM D-1587.

Piston samplers were developed to prevent soil from entering the sampling tube before the sample depth and to reduce sample loss during tube extraction. They are basically a thin wall tube sampler with a piston, rod, and a modified sampler head. There are numerous types of piston samplers; free or semi-fixed piston samplers, fixed-piston samplers, and retractable piston samplers. In addition, piston samplers may be mechanically activated

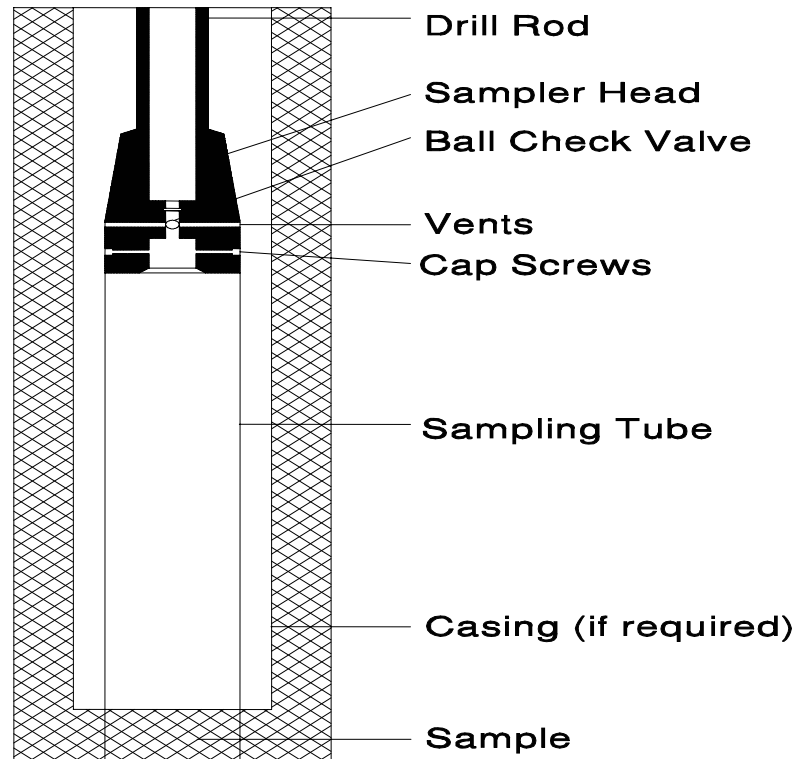


Figure 4.7a Thin Wall Shelby Tube Schematic (after FHWA, 1972)



Figure 4.7b Various Diameter Shelby Tubes from Mayne, et. al., (2002)

such as the Horslev fixed piston sampler, or hydraulically operated such as the Osterberg fixed piston sampler. Free piston samplers are most effective for sampling stiff clays or partially saturated silts and clays. Fixed piston samplers are particularly useful for sampling soft soils where sample recovery is often difficult, and can also be used in stiff clays and silts.

The Pitcher sampler is a core barrel sampler that may be used for sampling a broad range of materials including undisturbed samples of stiff to hard clays, soft rocks and cemented sands. This sampler consists of a rotating outer core barrel with an inner thin walled sampling tube. The sampling tube leads the core barrel when sampling soft soils and the core barrel leads the sampling tube when sampling hard materials. This makes the Pitcher sampler particularly attractive for sampling materials with alternating hard and soft layers. Table 4-8 provides a summary of various undisturbed soil samplers, and their advantages and disadvantages.

Great care is necessary in extraction, handling, and in transporting undisturbed samples to avoid disturbing the natural soil structure. Tubes should be pressed and not hammered. Proper storage and transport should be done with the tube upright and encased in an insulated box with cushioning material. Each tube should be physically separated from adjacent tubes.



Figure 4.8. Pitcher Sampler from Mayne, et. al., (2002)

TABLE 4-8 UNDISTURBED SOIL SAMPLES				
Sampler	Soil Types Suitable for Sampler	Advantages	Disadvantages	Remarks
Thin wall open tube sampler Figure 4.5.	Soils having some cohesion unless they are too hard or too gravelly for sampler penetration	<ol style="list-style-type: none"> 1. Small area ratio of tube permits obtaining sample with minimum disturbance. 2. Procedure is simple and requires very little time. 	<ol style="list-style-type: none"> 1. Excess or disturbed soil may enter the sampler and cause disturbance. Excess material prevents accurate measurement of recovery length. 2. When using in a bore hole filled with water or drilling fluid, an excess hydrostatic pressure will develop over the sample. 3. Check valve may clog, and may not reduce the hydrostatic pressures. 	Not suited for use in boulders, gravels and coarse soils.
Samplers with stationary pistons.	Soft soils	<ol style="list-style-type: none"> 1. Disturbed soil is prevented from entering the tube which decreases sample disturbance. 2. Atmospheric and hydrostatic pressures over sample area are reduced, which increases recovery ratio. 3. Any downward movement of the sample creates a partial vacuum over the sample and reduces the danger of losing the sample. 4. Much easier to determine recovery ratio since the length of rods can be easily measured. 	<ol style="list-style-type: none"> 1. The apparatus is complicated to use. 2. The insertion, clamping and withdrawal of the rods is time consuming. 	When a piston sampler is needed, the fixed piston sampler is preferable to other types of piston samplers to minimize sample disturbance.
Samplers with free pistons.	Stiff soils	<ol style="list-style-type: none"> 1. Entrance of disturbed and mixed soil is prevented when the sampler is lowered into position. 2. Recovery ratio is easily determined. 3. The piston is more effective than check valve in reducing pressure over the sample. 4. Easier to operate than the fixed piston. 	Additional weight is placed on the soil sample by the weight of the drill rods.	Similar to the fixed piston sampler with the exception that the piston is not fixed when the sample is taken; it is free to ride on top of the sample.
Samplers with retracted pistons.	Stiff soils	<ol style="list-style-type: none"> 1. The sampler is simpler in construction and operation than the stationary or free piston sampler as the piston head is held in place by a screw-type connection. 2. The piston prevents the entrance of disturbed soil into the tube when the tube is being placed into position for sampling. 	<ol style="list-style-type: none"> 1. The retraction of the piston may cause failure in soft soils as the soil may flow into the sampler. 2. The soil displaced during the positioning of the piston sampler may flow into the sampler when the piston is withdrawn. 3. If there is water leakage into the drill rod, excess hydrostatic pressure will develop over the sample. 	Piston is withdrawn just before the beginning of the actual sampling process.
Hydraulic piston sampler.	Soft soils	Eliminates need for center rod required to hold piston on a conventional piston-type sampler. This results in less time required to retrieve a sample.	<ol style="list-style-type: none"> 1. There are no means to determine the amount of penetration of the sampling tube into the soil stratum, since there are no visible signs of movement at the top of the hole. 2. Percent recovery is hard to establish, particularly for short pushes which do not fill the sampler. The weight of water in the drill steel causes the sampler to extend to its full length during retrieval from the hole. 	The sampling technique is the same as for the stationary piston sampler. The activation of the sampling tube is performed by water pressure applied to the sampler through its attached drill steel.
Pitcher.	Stiff to hard clays and soft rocks. Cemented sands.	<ol style="list-style-type: none"> 1. Inner thin wall sampling tube leads outer core barrel in softer soils. 2. Outer core barrel leads sampling tube in hard soils. 	<ol style="list-style-type: none"> 1. Sensitive soil samples may be damaged by vibrations of core barrel during sampling. 2. Water sensitive soils may be in continuous contact with drilling fluid. 	Well adapted to sampling alternating layers of hard and soft soils.

4.5.3 Rock Core Samplers

Rock Core Samplers (core barrels) are available in various diameters and length. The most widely used types are:

- a. Single tube.
- b. Double tube, rigid type (Figure 4.9).
- c. Double tube, swivel type (Figure 4.9).
- d. Wire line barrels.

Double tube or wire line core barrels which are capable of recovering rock cores of at least 54 mm in diameter should be used in subsurface exploration for structural projects.

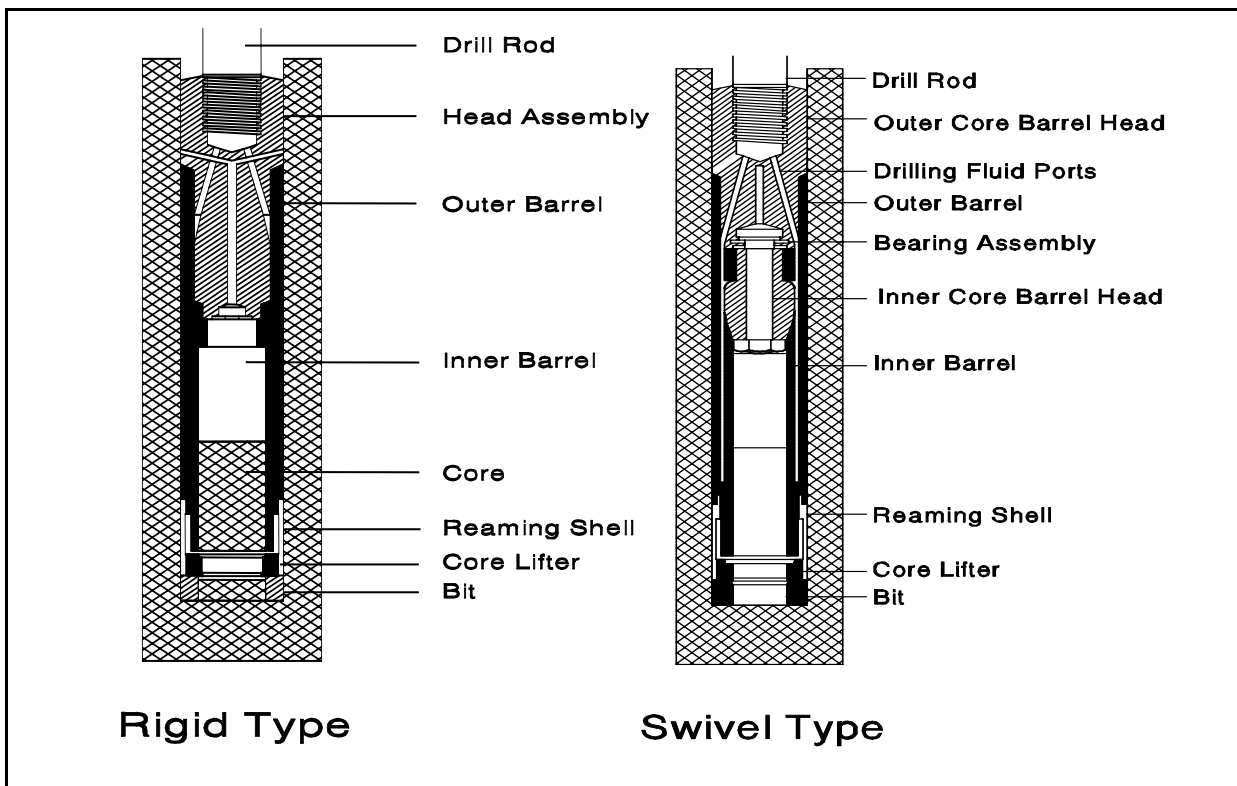


Figure 4.9 Rigid and Swivel Type Double Core Barrels (after FHWA, 1972)

4.6 GROUND WATER MONITORING

Accurate ground water level information is needed for the estimation of soil densities, determination of effective soil pressures and for the preparation of effective stress diagrams. This information is vital for performing foundation design. Water levels will also

indicate the construction difficulties which may be encountered in excavations and the dewatering effort required.

In most structure foundation explorations, water levels should be monitored during drilling of the boring, upon completion of the boring, and 24 hours after the completion of boring. More than one week may be required to obtain representative water level readings in low permeability cohesive soils or in bore holes stabilized with some drilling muds. In these cases, an observation well or piezometer should be installed in a boring to allow long term ground water monitoring. An observation well is typically used to monitor changes in the water level in a select aquifer whereas a piezometer is used to monitor changes in the hydrostatic pressure in a confined aquifer or specific stratum.

An observation well is usually a slotted section of small diameter PVC pipe installed in a bore hole. The bottom section of the slotted PVC pipe is capped and solid PVC sections are used to extend the observation well from the top of the slotted PVC section to a height above grade. The annulus between the slotted section and the sides of the bore hole is backfilled with sand. Once the sand is above the slotted PVC section, a bentonite seal is placed in the annulus sealing off the soil stratum in which the water table fluctuations will be monitored. The annulus above the bentonite seal is usually backfilled with grout or auger cuttings. The water level reading in the observation well will be the highest of the water table in any soil layer that the slotted section penetrates. The top section may be cast into a concrete surface seal that includes a locking removeable cover to prevent damage. The ground surface at the top of the pipe is usually sloped away from the pipe.

Piezometers are generally used to monitor hydrostatic pressure changes in a specific soil stratum. Piezometers may be either pneumatic or vibrating wire diaphragm devices. These piezometers may be installed in a sand pocket with a bentonite seal similar to an observation well. More recently, single and multiple piezometers are being installed in a single bore hole using a cement-bentonite grout. Additional information on piezometers is available in FHWA-NHI-01-031, Subsurface Investigations – Geotechnical Site Characterization by Mayne et.al (2002).

4.7 SUMMARIZATION AND INTERPRETATION OF SUBSURFACE PROFILE

A subsurface profile is a visual representation of subsurface conditions interpreted from subsurface explorations and laboratory testing. A complete subsurface profile should delineate the subsurface stratigraphy; the subsurface material classifications; the shear strength, compressibility, and stress history for each layer; and the ground water table location for foundation design.

A subsurface profile should be developed in stages. First, a rough profile is established from the drillers logs. This helps discover any obvious gaps while the drilling crew is at the site so that additional work can be performed immediately. When borings are completed and laboratory classification and moisture content data is received, the initial soil profile should be revised. Soil stratification and accurate soil descriptions are established at this stage. Overcomplication of a profile by noting minute variations between adjacent soil samples should be avoided. A vertical scale of 10 mm equal to 1 to 3 m (1 inch equals to 10 to 25 ft) a horizontal scale equal to the vertical scale are recommended.

After the soil layer boundaries and descriptions have been established, a determination of the extent and details of additional laboratory testing, such as consolidation and shear strength tests, is made. The final soil profile should include the average physical properties of the soil deposits including unit weight, shear strength, *etc.*, as well as a visual description of each deposit. The observed ground water level and the presence of items such as boulders, voids, and artesian pressures should also be noted. A well developed soil profile is necessary to design a cost-effective foundation. Uncertainties in the development of a subsurface profile usually indicate that additional explorations and/or laboratory testing are required. An example of a subsurface profile is presented in Figure 4.10.

The subsurface conditions presented in a subsurface profile are accurate only at the location of the borings. Interpretation between boring locations as shown in Figure 4.10 is often done for analysis purposes. However, where soil and/or rock profiles vary considerably between boring locations, this interpretation and presentation may be misleading. Interpreted soil profiles, when presented, should clearly note that the soil profile is only accurate at the boring locations, and that the interpreted profile between boring locations cannot be fully relied upon.

4.8 ADDITIONAL SUBSURFACE EXPLORATIONS

During the final design process, additional subsurface explorations may need to be performed to finalize the design soil profile and design soil parameters. Additional subsurface exploration and design soil profile development may be needed for the design of a foundation type not originally considered, due to a design change caused by environmental restrictions, or simply for a cost optimization of the foundation design.

The additional subsurface exploration program may consist of additional soil borings, and/or in-situ testing, and/or geophysical methods to supplement the original information. Additional laboratory tests may also be conducted to delineate soil properties of key strata.

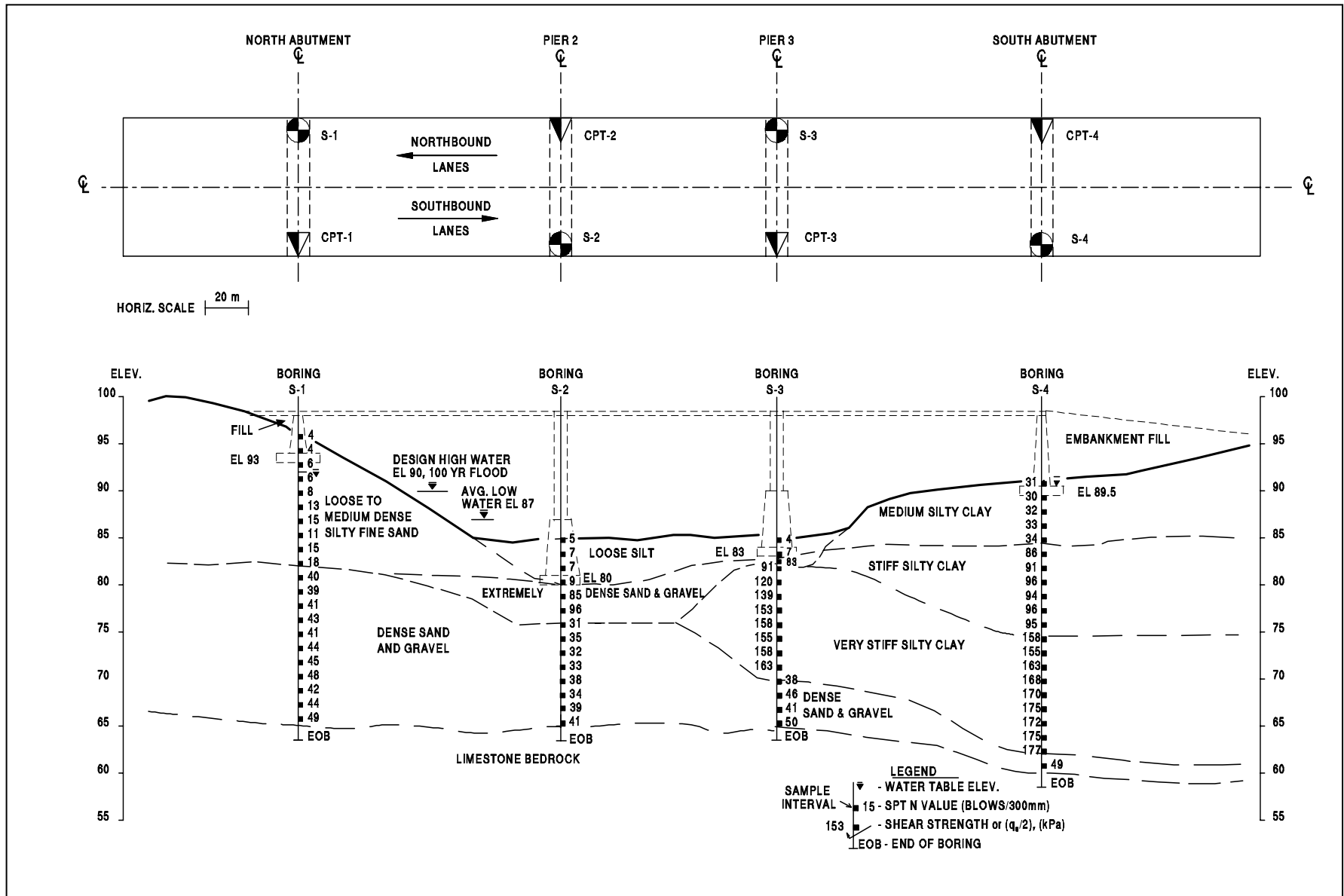


Figure 4.10. Example Subsurface Profile.

REFERENCES

- American Association of State Highway and Transportation Officials [AASHTO], (1988). Manual on Subsurface Investigations. AASHTO Highway Subcommittee on Bridges and Structures, Washington, D.C., 391.
- American Association of State Highway and Transportation Officials [AASHTO], (1978). Manual on Foundation Investigations. AASHTO Highway Subcommittee on Bridges and Structures, Washington, D.C.
- American Association of State Highway and Transportation Officials [AASHTO], (1995). Standard Methods of Test for Penetration Test and Split-Barrel Sampling of Soils, AASHTO T206.
- American Association of State Highway and Transportation Officials [AASHTO], (1995). Standard Method of Test for Thin-Walled Tube Sampling of Soils, AASHTO T207.
- American Society for Testing and Materials [ASTM], (2005). ASTM D-4633, Standard Test Method for Energy Measurement for Dynamic Penetrometers, Philadelphia, PA.
- Bowles, J.E. (1977). Foundation Analysis and Design. Second Edition, McGraw-Hill Book Company, New York, 85-86.
- Canadian Geotechnical Society (1985). Canadian Foundation Engineering Manual. Second Edition, BiTech Publishers, Ltd, Vancouver, 43-68.
- Cheney, R.S. and Chassie, R.G. (2000). Soils and Foundations Workshop Reference Manual. Publication No. FHWA HI-00-045, U.S. Department of Transportation, National Highway Institute, Federal Highway Administration, Washington, D.C., 358.
- Finno, R.J. (1989). Subsurface Conditions and Pile Installation Data, Predicted and Observed Axial Behavior of Piles. Results of a Pile Prediction Symposium, ASCE Geotechnical Special Publication No. 23, Richard J. Finno, Editor, 1-74.
- Fang, H.Y. (1991). Foundation Engineering Handbook. Second Edition, Van Nostrand Reinhold Company, New York.
- Federal Highway Administration (1972). Soils Exploration and Testing - Demonstration, Project No. 12.
- Mayne, P.W., Christopher, B.R., and DeJong, J. (2002). Subsurface Investigations – Geotechnical Site Characterization. Report No. FHWA-NHI-01-031, U.S. Department of Transportation, Federal Highway Administration, Washington, D.C., 300.

Peck, R.B., Hanson, W.E., and Thornburn, T.H. (1974). Foundation Engineering. Second Edition, John Wiley & Sons, Inc., New York.

Chapter 5

IN-SITU TESTING

In-situ testing provides soil parameters for the design of structure foundations especially in conditions where standard drilling and sampling methods cannot be used to obtain high quality undisturbed samples. Undisturbed samples from non-cohesive soils are difficult to obtain, trim, and test in the laboratory. Soft saturated clays, saturated sands and intermixed deposits of soil and gravel are also difficult to sample without disturbance. Therefore, representative strength test data is difficult to obtain on these soils in the laboratory. To overcome these difficulties, test methods have been developed to evaluate soil properties, especially strength and compressibility, in-situ.

In-situ testing methods can be particularly effective when used to supplement conventional exploration programs. The speed of in-situ testing in conjunction with no laboratory testing significantly reduces the subsurface exploration program time and cost. In addition, in-situ methods help identify key strata for further conventional sampling and laboratory tests.

Primary in-situ tests that provide data for foundation design are the cone penetration test (CPT), the cone penetration test with pore pressure measurements (CPTu), and the vane shear (VST). Other lesser used in-situ testing devices include the pressuremeter test (PMT), the dilatometer test (DMT), and the dynamic cone penetrometer test. Specific pile design procedures using CPT data are discussed in Chapter 9 of this manual.

The intent of this chapter is to provide a brief summary of in-situ test methods used for deep foundation design. For CPT/CPTu testing a brief summary of the equipment, operation, application, advantages and disadvantages is also provided. The applicability, advantages and disadvantages of all the in-situ testing methods are also briefly summarized in Table 5-1. For a detailed discussion of a particular in-situ testing method, the reader is referred to the publications listed at the end of this chapter. NHI course 132031, Subsurface Investigations – Geotechnical Site Characterization and the accompanying course manual by Mayne, et.al, (2002) provide a thorough coverage of in-situ testing methods.

5.1 CONE PENETRATION TEST (CPT) AND (CPTu)

The cone penetration test (CPT) was first introduced in the U.S. in 1965. By the mid 1970's, the electronic cone began to replace the mechanical cone. In the early 1980's, the

TABLE 5-1 SUMMARY OF IN-SITU TEST METHODS						
Type of Test	Best Suited for	Not Applicable for	Information that can be Obtained for Pile Foundation Design	Advantages	Disadvantages	Remarks
Cone Penetration Test (CPT)	Sand, silt, and clay	Gravel, very dense deposits, rubble fills, and rock.	Continuous evaluation of subsurface stratigraphy. Correlations for determination of in-situ density and friction angle of sands, undrained shear strength of clays, and liquefaction potential.	<ol style="list-style-type: none"> 1. Cone can be considered as a model pile. 2. Quick and simple test. 3. Can reduce number of borings. 4. Relatively operator independent. 	<ol style="list-style-type: none"> 1. Does not provide soil samples. 2. Should be used in conjunction with soil borings in an exploration program. 3. Local correlations can be important in data interpretation. 	Well suited to the design of axially loaded piles. ASTM D-3441 (mechanical cones) and ASTM D-5778 (electronic cones).
Cone Penetration Test with Pore Pressure Measurements (CPTu)	Sand, silt, and clay	Gravel, very dense deposits, and rubble fills.	Finer delineation of continuous subsurface stratigraphy compared to CPT. Correlations for determination of in-situ density and friction angle of sands, undrained shear strength of clays, and liquefaction susceptibility.	<ol style="list-style-type: none"> 1. Same advantages as CPT. 2. Pore pressure measurements can be used to assess soil setup effects. 3. Can help determine if penetration is drained or undrained. 	<ol style="list-style-type: none"> 1. Same disadvantages as CPT. 2. Location and saturation of porous filter can influence pore pressure measurements. 	Probably best in-situ test method for the design of axially loaded piles. ASTM D-5778.
Pressuremeter Test (PMT)	Sand, silt, clay and soft rock.	Organic soils and hard rock.	Bearing capacity from limit pressure and compressibility from pressure meter deformation modulus.	<ol style="list-style-type: none"> 1. Tests can be performed in and below hard strata that may stop other in-situ testing devices. 2. Tests can be made on non-homogenous soil deposits. 	<ol style="list-style-type: none"> 1. Bore hole preparation very important. 2. Limited number of tests per day. 3. Limited application for axially loaded pile design. 	Good application for laterally loaded pile design. ASTM D-4719.
Dilatometer Test (DMT)	Low to medium strength sand and clay	Dense deposits, gravels and rock.	Correlations for soil type, earth pressure at rest, over consolidation ratio, undrained shear strength, and dilatometer modulus.	<ol style="list-style-type: none"> 1. Quick, inexpensive test. 2. Relatively operator independent. 	<ol style="list-style-type: none"> 1. Less familiar test method. 2. Intended for soils with particle sizes smaller than fine gravel. 3. Limited application for axially loaded pile design. 	May be potentially useful for laterally loaded pile design. ASTM standard in progress.
Vane Shear Test	Soft clay	Silt, sand, and gravel	Undrained shear strength.	<ol style="list-style-type: none"> 1. Quick and economical. 2. Compares well with unconfined compression test results at shallow depths. 	<ol style="list-style-type: none"> 1. Can be used to depths of only 4 to 6 m (13 to 20 ft) without casing bore hole. 	Test should be used with caution in fissured, varved, and highly plastic clays. AASHTO T223.
Dynamic Cone Test	Sand and gravel	Clay	Qualitative evaluation of soil density. Qualitative comparison of stratigraphy.	<ol style="list-style-type: none"> 1. Can be useful in soil conditions where static cone (CPT) reaches refusal. 	<ol style="list-style-type: none"> 1. An unknown fraction of resistance is due to side friction. 2. Overall use is limited. 	Not recommended for final pile design. No AASHTO or ASTM standard.

piezo-cone or cone penetration test with pore pressure measurements (CPTu) became readily available. Since that time, the CPT/CPTu has developed into one of the most popular in-situ testing devices. Part of this popularity is due to the CPT's ability to provide large quantities of useful data quickly and at an economical cost. Depending upon equipment capability as well as soil conditions, 100 to 350 m (330 to 1150 ft) of penetration testing may be completed in one day

5.1.1 Equipment Description and Operation

Cone penetration testing can be separated into two main categories:

- a. Electronic cones.
- b. Mechanical cones.

Electronic cones are now the dominant cone type used in cone penetration testing. Hence, mechanical cones will not be discussed further in this chapter. Electronic cones may be further divided into two primary types, the standard friction cone (CPT), and the piezo-cone (PCPT or more commonly CPTu).

In the CPT test, a cone with a 1000 mm^2 (1.5 in^2) base and a 60° tip attached to a series of rods is continuously pushed into the ground. Typically, a hydraulic ram with 45 to 180 kN (10 to 40 kips) of thrust capability is used to continuously advance the cone into the ground at a rate of 20 mm (0.8 in/sec). A friction sleeve with a surface area of 15000 mm^2 (22.5 in^2) is located behind the conical tip. Built in load cells are used to continuously measure the cone tip resistance, q_c , and the sleeve friction resistance, f_s . The friction ratio, R_f , is the ratio of f_s/q_c and is commonly used in the interpretation of test results.

The piezo-cone (CPTu), is essentially the same as the standard electronic friction cone and continuously measures the cone tip resistance, q_c , and the sleeve friction resistance, f_s , during penetration. In addition to these values, the piezo-cone includes porous filter piezo-elements that may be located at the cone tip, on the cone face, behind the cone tip, or behind the friction sleeve. These porous filter elements are used to measure pore pressure, u , during penetration. Careful porous element and cavity saturation is essential to obtain reliable pore pressure measurements.

A general schematic and picture of a cone penetrometer is presented in Figures 5.1a and 5.1b. Typical penetration depths for a 45 kN (10 kip) and 180 kN (40 kip) thrust capability

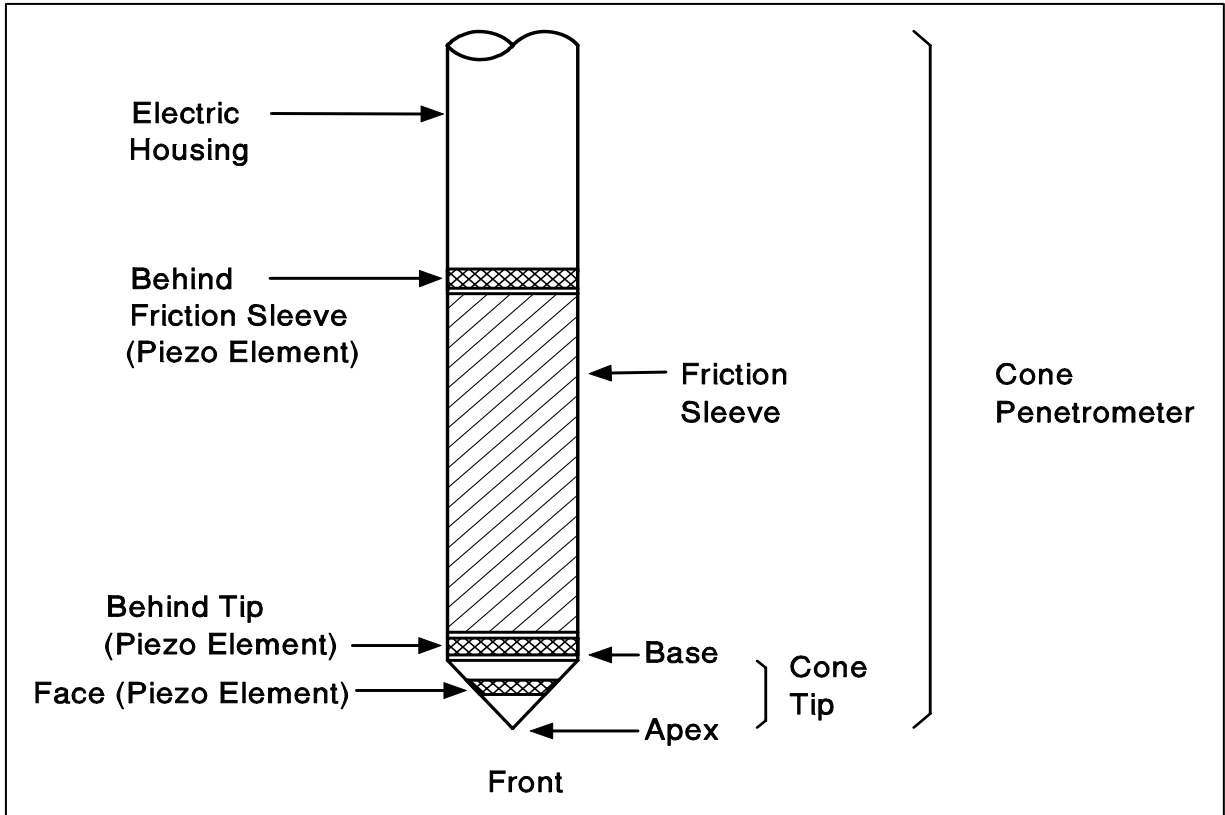


Figure 5.1a Terminology Regarding the Cone Penetrometer (from Robertson and Campanella, 1989)



Figure 5.1b Cone Penetrometers (from Mayne et. al., 2002)

are presented in Tables 5-2 and 5-3, respectively. Additional information on CPT/CPTu testing and analysis may be found in FHWA-SA-91-043, The Cone Penetrometer Test, by Briaud and Miran (1991). Test procedures may be found in ASTM D-3441 for mechanical cones and ASTM D-5778 for electronic cones.

TABLE 5-2 DRILL RIG WITH 45 kN (10 kip) PUSH CAPACITY						
	Soil					
	Clay			Sand		
Depth m (ft)	Soft	Stiff	Hard	Loose	Medium	Dense
1 (3.3)	*	*	*	*	*	
3 (9.8)	*	*		*	*	
4 (13.1)	*	*		*	*	
6 (19.7)	*			*	*	
9 (29.5)	*			*		
12 (39.4)	*			*		
15 (49.2)	*			*		
18 (59.0)	*					
21 (68.9)	*					
24 (78.7)						

TABLE 5-3 TRUCK WITH 180 kN (40 kip) PUSH CAPACITY						
	Soil					
	Clay			Sand		
Depth m (ft)	Soft	Stiff	Hard	Loose	Medium	Dense
4 (13.1)	*	*	*	*	*	*
9 (19.7)	*	*	*	*	*	*
18 (59.0)	*	*	*	*	*	*
27 (88.6)	*	*		*	*	
36 (118.1)	*			*		
46 (150.9)	*			*		
61 (200.1)	*					
76 (249.3)	*					
91 (298.4)						

Tables 5-2 and 5-3 (modified from Briaud and Miran, 1991)

5.1.2 Interpretation of CPT/CPTu Test Results

- a. CPT/CPTu data can provide a continuous profile of the subsurface stratigraphy. A simplified soil classification chart for a standard electronic friction cone is presented in Figure 5.2. Typical CPT test results are presented in Figure 5.3.
- b. From correlations with CPT/CPTu data, evaluations of in-situ relative density, D_r , and friction angle, ϕ , of cohesionless soils as well as the undrained shear strength, c_u , of cohesive soils can be made. Correlations for determination of other soil properties, liquefaction susceptibility, and estimates of SPT values may also be determined. The accuracy of these correlations may vary depending upon geologic conditions. Correlation confirmation with local conditions is therefore important.

5.1.3 Advantages and Disadvantages of CPT/CPTu Tests

The primary advantage of CPT/CPTu testing is the ability to rapidly develop a continuous profile of subsurface conditions more economically than any other subsurface exploration or in-situ testing tools. Determination of in-situ soil strength parameters from correlations with CPT/CPTu data is another advantage. The CPT/CPTu test can also reduce the number of conventional borings needed on a project, or focus attention on discrete zones for detailed soil sampling and testing. Lastly, CPT/CPTu results are relatively operator independent.

Limitations of CPT/CPTu testing include the inability to push the cone in dense or coarse soil deposits. To penetrate dense layers, cones are sometimes pushed in bore holes advanced through the dense strata. Another limitation is that soil samples are not recovered for confirmation of cone stratigraphy. For meaningful pore pressure measurements, careful preparation to ensure saturation of the porous elements and cone cavities is required. Local correlations are also important in data interpretation.

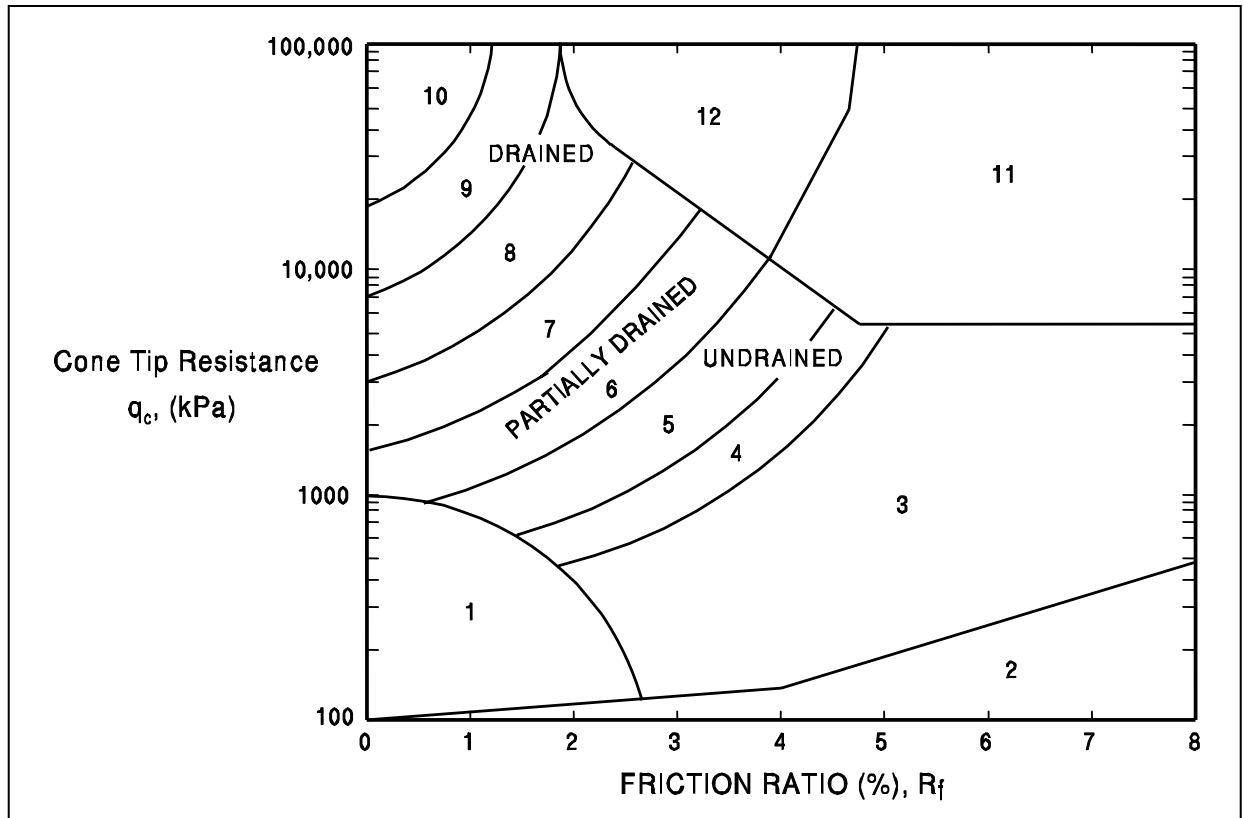


Figure 5.2 Simplified Soil Classification Chart for Standard Electronic Friction Cone (after Robertson et al., 1986)

Zone	q_c/N	Soil Behavior Type
1)	2	sensitive fine grained
2)	1	organic material
3)	1	clay
4)	1.5	silty clay to clay
5)	2	clayey silt to silty clay
6)	2.5	sandy silt to clayey silt
7)	3	silty sand to sandy silt
8)	4	sand to silty sand
9)	5	sand
10)	6	gravelly sand to sand
11)	1	very stiff fine grained
12)	2	sand to clayey sand

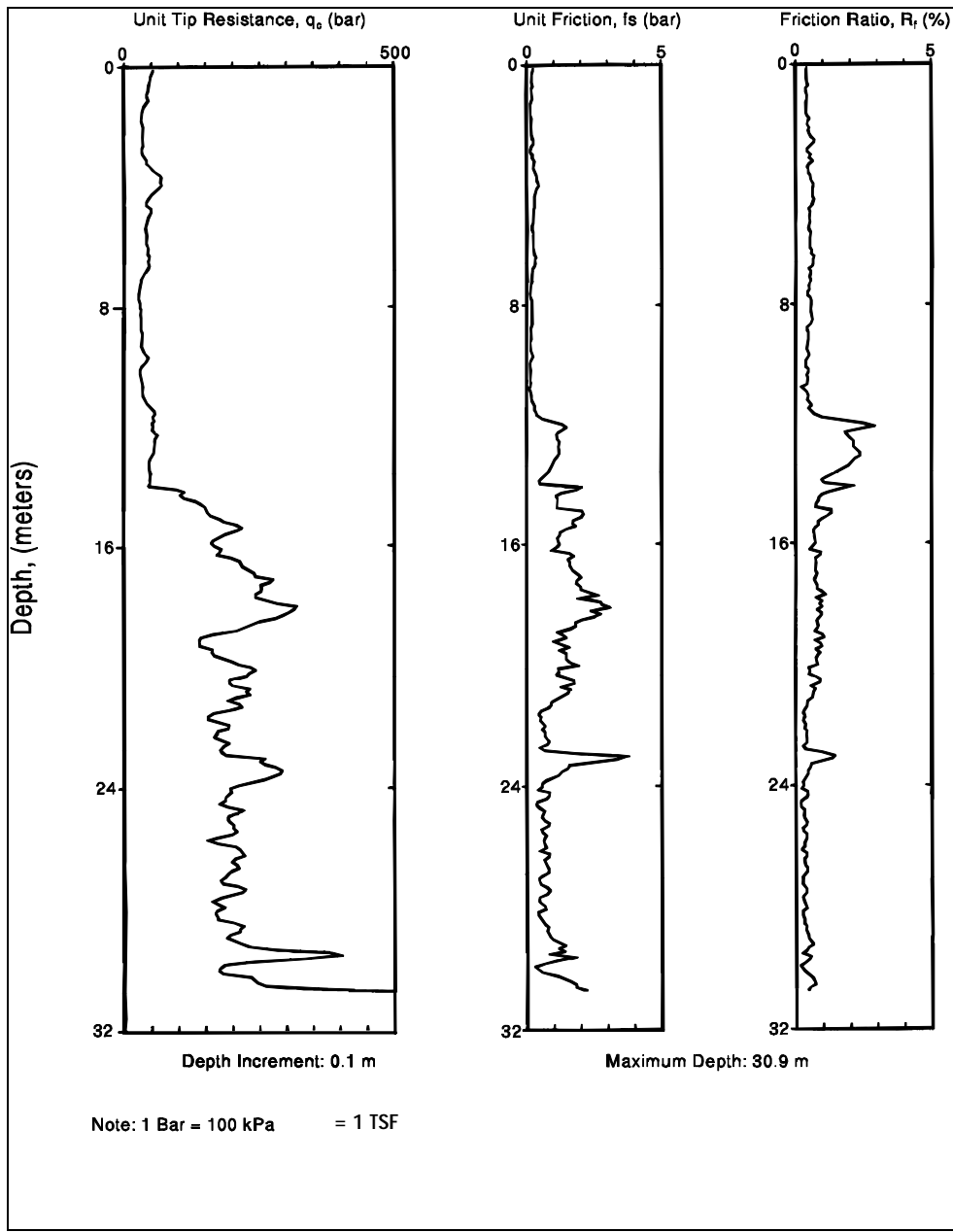


Figure 5.3 Typical CPT Data Presentation

5.2 PRESSUREMETER TEST - (PMT)

The pressuremeter test (PMT) is an in-situ device used to evaluate soil and rock properties. The pressuremeter has been used in Europe for many years and was introduced into the U.S. in the mid 1970's. The pressuremeter imparts lateral pressures to the soil, and the soil shear strength and compressibility are determined by interpretation of a pressure-volume relationship. The test allows a determination of the load-deformation characteristics of soil in axi-symmetric conditions. Deposits such as soft clays, fissured clays, sands, gravels and soft rock can be tested with pressuremeters. A pressuremeter test produces information on the elastic modulus of the soil as well as the at rest horizontal earth pressure, the creep pressure, and the soil limit pressure. A schematic of the pressuremeter test is presented in Figure 5.4.

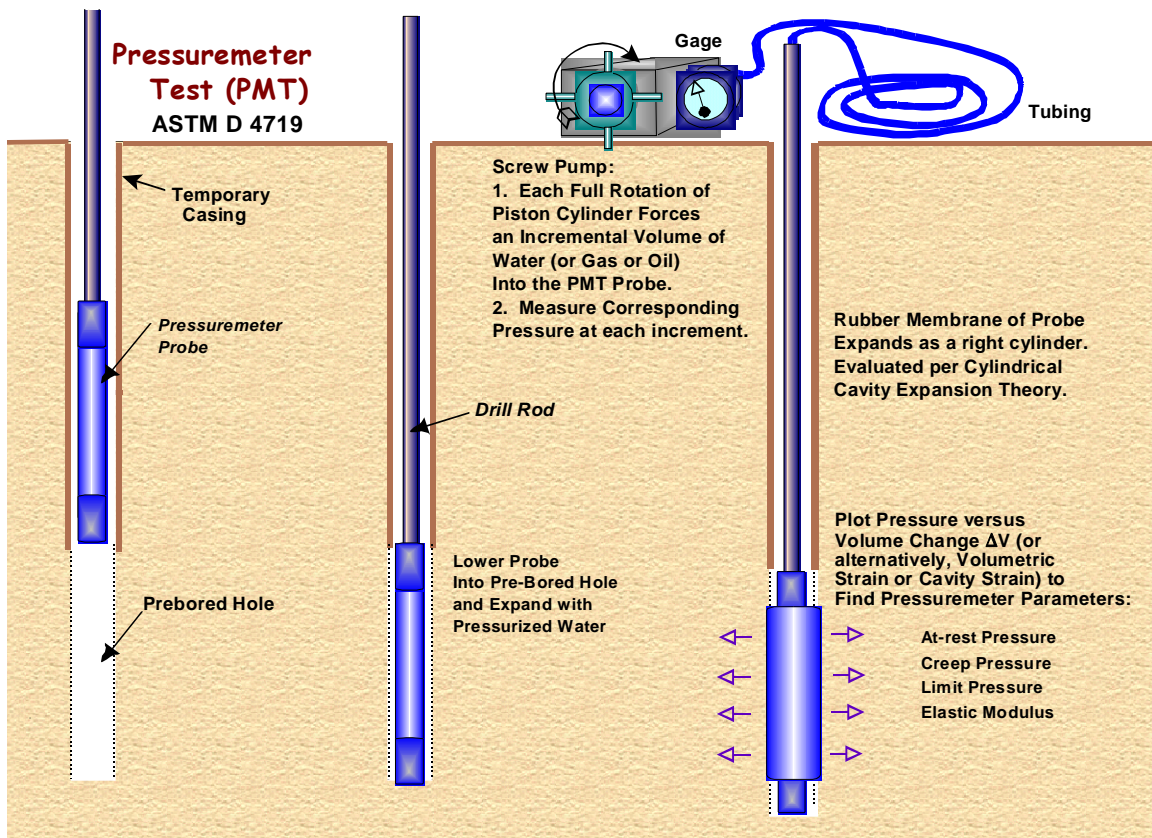


Figure 5.4 Pressuremeter Test Schematic

The utilization of test results is based upon semi-empirical correlations from a large number of tests and observations on actual structures. For piles subjected to lateral loads, the pressuremeter test is a useful design tool and can be used for determination of p-y curves. For design of vertically loaded piles, the pressuremeter test has limited value. Pile design

procedures using pressuremeter data have been developed and may be found in FHWA-IP-89-008, The Pressuremeter Test for Highway Applications, by Briaud (1989). Details on test procedures may be found in ASTM D-4719, Standard Test Method for Pressuremeter Testing in Soils.

5.3 DILATOMETER TEST - (DMT)

The dilatometer test is an in-situ testing device that was developed in Italy in the early 1970's and first introduced in the U.S. in 1979. Like the CPT, the DMT is generally hydraulically pushed into the ground although it may also be driven. When the DMT can be pushed into the ground with tests conducted at 200 mm (8 inch) increments, 30 to 40 m (100 to 130 ft) of DMT sounding may be completed in a day. The primary utilization of the DMT in pile foundation design is the delineation of subsurface stratigraphy and interpreted soil properties. However, it would appear that the CPT/CPTu is generally better suited to this task than the DMT. The DMT may be a potentially useful test for design of piles subjected to lateral loads. Design methods in this area show promise, but are still in the development stage. For design of axially loaded piles, the dilatometer test has limited direct value. A picture of dilatometer test equipment is presented in Figure 5.5.



Figure 5.5 Dilatometer Test Equipment

5.4 VANE SHEAR TEST

The vane shear test is an in-situ test for determining the undrained shear strength of soft to medium clays. Figure 5.6 is a schematic drawing of the essential components and test procedure. The test consists of forcing a four-bladed vane into undisturbed soil and rotating it until the soil shears. Two shear strengths are usually recorded, the peak shearing strength and the remolded shearing strength. These measurements are used to determine the sensitivity of clay. This allows analysis of the soil resistance to be overcome during pile driving in clays which is useful for pile driveability analyses. It is necessary to measure skin friction along the steel connector rods which must be subtracted to determine the actual shear strength. The vane shear test generally provides the most accurate undrained shear strength values for clays with undrained shear strengths less than 50 kPa (1 ksf). The test procedure has been standardized in AASHTO T223-74 and ASTM D-2573.

It should be noted that the sensitivity of a clay determined from a vane shear test provides insight into the set-up potential of the clay deposit. However, the sensitivity value is a qualitative and not a quantitative indicator of soil set-up.

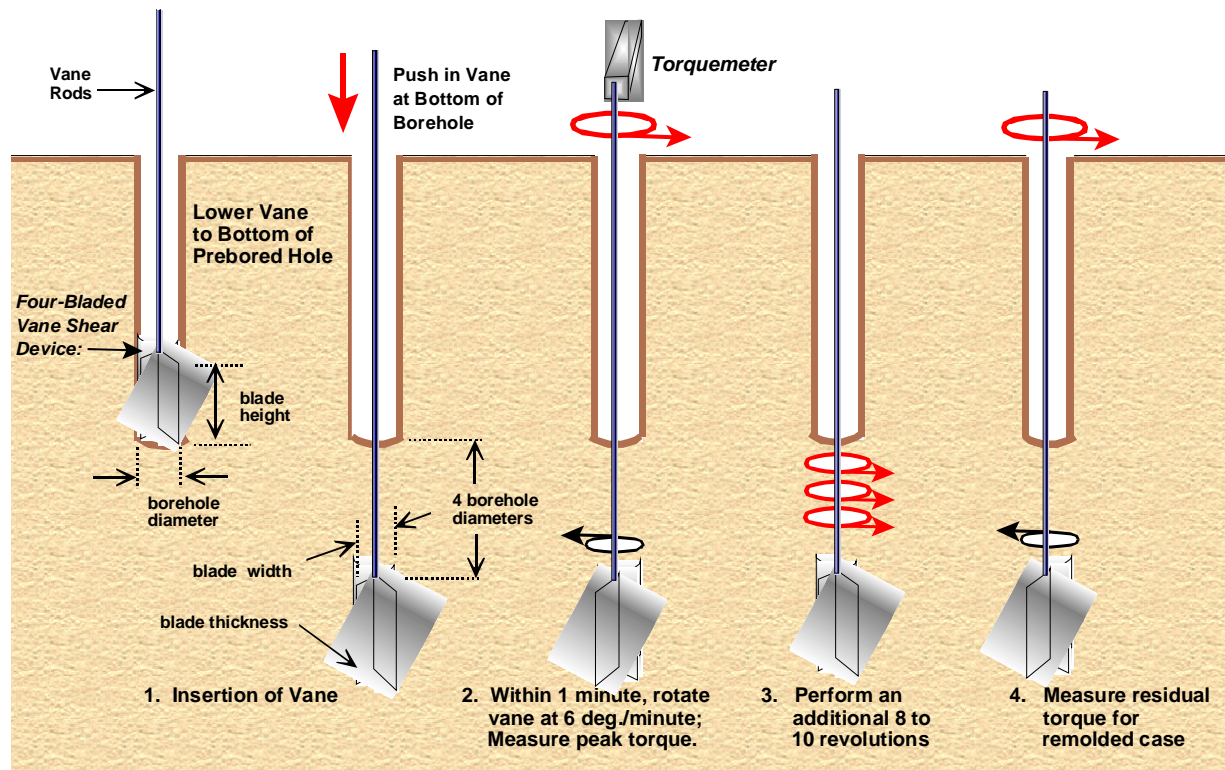


Figure 5.6 Vane Shear Test Equipment and Procedure (after Mayne et al., 2002)

5.5 DYNAMIC CONE TEST

There are two types of dynamic penetrometers with conical points. The dynamic cone type that is most often used has a shaft diameter that is smaller than the cone diameter. Theoretically, due to the cone being larger than the shaft, the penetrometer measures only point resistance. A lesser used cone type has a shaft and cone of the same diameter. This type of dynamic cone penetrometer records both skin friction and point resistance, but the two components cannot be analyzed independently. Equations have been developed for determining bearing capacity of pile foundations by using the dynamic cone test data, but are not used extensively. The dynamic cone penetrometer is not recommended for final foundation design unless specific local correlations with load tests to geotechnical failure have been taken.

REFERENCES

- American Association of State Highway and Transportation Officials [AASHTO], (1988). Manual on Subsurface Investigations. AASHTO Highway Subcommittee on Bridges and Structures, Washington, D.C., 391.
- Briaud, J-L. (1989). The Pressuremeter Test for Highway Applications. Report No. FHWA-IP-89-008, U.S. Department of Transportation, Federal Highway Administration, Office of Implementation, McLean, 156.
- Briaud, J-L. and Miran, J. (1991). The Cone Penetrometer Test. Report No. FHWA-SA-91-043, U.S. Department of Transportation, Federal Highway Administration, Office of Technology Applications, Washington, D.C., 161.
- Briaud, J-L. and Miran, J. (1992). The Flat Dilatometer Test. Report No. FHWA-SA-91-044, U.S. Department of Transportation, Federal Highway Administration, Office of Technology Applications, Washington, D.C., 102.
- Canadian Geotechnical Society (1985). Canadian Foundation Engineering Manual. Second Edition, BiTech Publishers Ltd., Vancouver, 45-62.
- Mayne, P.W., Christopher, B.R., and DeJong, J. (2002). Subsurface Investigations – Geotechnical Site Characterization. Report No. FHWA-NHI-01-031, U.S. Department of Transportation, Federal Highway Administration, Washington D.C., 300.
- Schmertman, J.H. (1988). Guidelines for Using the CPT, CPTU, and Marchetti DMT for Geotechnical Design. Report No. FHWA-PA-022+84-24, U.S. Department of Transportation, Federal Highway Administration, Volumes I-IV, Washington, D.C., 731.
- Robertson P.K., Campanella, R.G., Gillespie, D. and Grieg, J. (1986). Use of Piezometer Cone Data. Proceedings of In-Situ '86, ASCE Specialty Conference, Use of In-Situ Tests in Geotechnical Engineering, Special Publication No. 6, Blacksburg, 1263-1280.
- Robertson P.K. and Campanella, R.G. (1989). Guidelines for Geotechnical Design using the Cone Penetrometer Test and CPT with Pore Pressure Measurement. Fourth Edition, Hogentogler & Company, Inc., Columbia, 193.
- U.S. Department of Transportation (1972). Soil Exploration and Testing. Federal Highway Administration, Demonstration Project No. 12, Arlington.

Chapter 6 LABORATORY TESTING

The trend to higher capacity piles and greater pile penetration depths required for special design events reinforces the importance of accurately determining soil shear strength and consolidation properties. For cohesionless materials, the SPT and CPT will be the primary tools for strength and compressibility analysis. These tests should be complemented with appropriate laboratory index tests. For cohesive soils, the use of SPT resistance values for estimation and evaluation of soil shear strength and compressibility cannot be recommended as the basis for a final design. **In cohesive soils, traditional laboratory tests on undisturbed samples yield the best results for evaluation of strength and compressibility properties.**

In laboratory testing, the quality of test results is far more important than the quantity of test results. Inaccurate test results may lead to misjudgments in the design stage and/or problems in the construction stage. Owners and designers of structure foundations have a quality assurance responsibility over activities affecting the quality of laboratory test results. Quality control procedures for in-house or consultant laboratories should be in place for:

- Handling and storage of soil samples.
- Sample preparation for testing.
- Establishment of, and adherence to testing procedures.
- Documentation of equipment calibration and maintenance.
- Training and qualification of laboratory personnel.
- Laboratory test result review and checking.
- Reporting of laboratory test results.

The purpose of this chapter is to present a summary of laboratory tests performed to determine basic soil properties as well as soil shear strength and consolidation properties. For detailed information on laboratory testing, additional references are listed at the end of this chapter.

6.1 TYPES OF TESTS

Laboratory tests can be generally categorized as follows:

1. Soil classification and index tests.
2. Shear strength tests.
3. Consolidation tests.
4. Electro chemical classification tests.

The following subsections briefly describe each type of test. Table 6-1 summarizes the advantages, disadvantages and applications of soil classification, strength and compressibility tests.

6.1.1 Classification and Index Tests

For foundation design, soils are usually classified according to the Unified Soil Classification system. The classification of soil determines the type of material, its general characteristics, and whether any further testing for consolidation and strength properties are needed. The following tests are useful in classifying soils:

- a. Moisture content (AASHTO T265).
- b. Particle size analysis (mechanical and hydrometer analysis) AASHTO T88.
- c. Atterberg limits (liquid and plastic limits) AASHTO T89 and T90.
- d. Unit weight (AASHTO T38).

6.1.2 Shear Strength Tests

The shear strength of a soil is a measure of the soil's ability to resist sliding along internal surfaces within the mass.

TABLE 6-1 LABORATORY TESTS ON SOILS FOR FOUNDATION DESIGN

Test Category	Test	Classification or Design Parameters Provided by Test	Advantages	Disadvantages	Direct* Applications	Standard Test Procedure	Soil Types best suited for
Classification and Index Tests (both disturbed and undisturbed samples used unless noted)	Liquid limit	Liquid limit	Assists in correct soil classification.	----	Classification	AASHTO T89-68	Cohesive soils and silts
	Plastic limit	Plastic limit	Assists in correct soil classification.	----	Classification	AASHTO T90-70	Cohesive soils and silts
	Moisture content	Moisture content	Can assist in soil shear strength judgements and water table determination.	----	Classification	AASHTO T265-79	Cohesive soils and silts
	Particle size analysis (mechanical and hydrometer analysis)	Grain size curves	Assists in soil classification.	---	Classification	AASHTO T88-72	Cohesive and cohesionless soils
	Unit weight (Undisturbed samples only)	Dry density	Can assist in soil shear strength judgements.	----	Effective stress computations.	AASHTO T38	Cohesive soils
Shear strength (undisturbed samples used)	Triaxial compression test (UU, CU, or CD tests **)	Cohesion c or c' ; Angle of internal friction ϕ or ϕ' . (In terms of total or effective stresses).	<ol style="list-style-type: none"> 1. Models in-situ conditions better than other two tests. 2. Drainage control 3. Pore water pressure can be measured. 4. More accurate than other two methods. 	<ol style="list-style-type: none"> 1. Expensive. 2. Complicated test procedure. 3. Difficult to use for sands and silts. 	Static capacity calculations for deep foundations.	AASHTO T234-70	Cohesive soils
	Direct shear test	Cohesion, c' ; Angle of internal friction, ϕ' . (In terms of effective stresses).	Simple and quick test.	<ol style="list-style-type: none"> 1. Predetermined failure plane. 2. Poor drainage control. 	Static capacity calculations for deep foundations.	AASHTO T236-72	Cohesionless soils (sands and silts)
	Unconfined compression test	Unconfined compression strength and shear strength.	<ol style="list-style-type: none"> 1. Simple, quick, inexpensive test to measure strength of cohesive soils. 2. More uniform stresses and strains on sample than direct shear test. 3. Failure surface tends to develop at weakest portion of samples unlike the forced shear plane of direct shear test. 	<ol style="list-style-type: none"> 1. No lateral confining pressure during test. 2. Pore water pressures and saturation cannot be controlled. 3. Test results, especially with depth, are conservative and misleading due to release of confining stress when sample is removed from below ground and tested. 	Static capacity calculations for deep foundations.	AASHTO T208-70	Cohesive soils
Consolidation (undisturbed samples used)	Consolidation	Compression index. Recompression index. Coefficient of secondary compression. Coefficient of consolidation. Preconsolidation pressure. Swelling index.	----	----	Computation of foundation settlement and time rate of settlement.	AASHTO T216-74	Cohesive soils

* - All test results permit empirical and engineering judgement guidance with regard to pile installation and construction monitoring.

** - UU = Unconsolidated Undrained, CU = Consolidated Undrained, and CD= Consolidated Drained

For the design of foundations, a knowledge of the soil shear strength is essential. Shear tests on soil are performed to determine the cohesion, c , and the angle of internal friction, ϕ . Cohesion is the interparticle attraction effect and is independent of the normal stress, σ , but considerably dependent on water content and strain rate. The internal friction angle depends on the interlocking of soil grains and the resistance to sliding between the grains.

Internal friction depends on the roughness of grains and normal stress. The shear strength of a soil is defined as follows:

$$\tau = c + \sigma \tan \phi$$

For pile foundation design, the resistance along the pile shaft and at the pile toe are a function of τ , c and ϕ parameters.

Effective stress, σ' , is defined as the soil grain to soil grain pressure and is equal to the total overburden pressure, σ , minus the pore water pressure (neutral pressure), u . This may be expressed in equation form as:

$$\sigma' = \sigma - u$$

The pore water has no shear strength and is incompressible. Only the intergranular stress (effective stress) is effective in resisting shear or limiting compression of the soil. When pore water drains from soil during consolidation, the decrease in water pressure increases the level of effective stress. Effective stress is important in both laboratory testing and in design, since it correlates directly with soil behavior. An increase in effective stress causes densification and an increase in shear strength.

Three test methods are commonly used to measure shear strength in the laboratory. In order of increasing cost and test sophistication they are as follows:

- a. Unconfined compression test (AASHTO T208).
- b. Direct shear test (AASHTO T236).
- c. Triaxial compression test (AASHTO T234).

The unconfined compression test is the most widely used laboratory test to evaluate soil shear strength. In the unconfined compression test, an axial load is applied on a cylindrical soil sample while maintaining a zero lateral or confining pressure. The axial loading is

increased to failure and the shear strength is then considered to be one half the axial stress at failure. Unconfined compression tests are performed only on cohesive soil samples.

Unconfined compression tests on cohesive samples recovered from large depths or samples with a secondary structure, such as sand seams, fissures, or slickensides, can give misleadingly low shear strengths. This is due to the removal of the in-situ confining stress normally present. Triaxial compression tests provide better information on soil shear strength in these cases.

The direct shear test is performed by placing a sample of soil into a shear box which is split into two parts at mid-height. A normal load is then applied to the top of the sample and one half of the shear box is pulled or pushed horizontally past the other half. The shear stress is calculated from the horizontal force divided by the sample area and is plotted versus horizontal deformation. A plot of at least three normal stresses and their corresponding maximum shear stresses provides the shear strength parameters c and ϕ . Bowles (1977) notes that the ϕ values determined from plain strain direct shear tests are approximately 1.1 times the ϕ values determined from triaxial tests. Direct shear tests are primarily performed on recompacted granular soils. Direct shear tests are generally not recommended for cohesive soils due to limitations on drainage control during shear.

The most versatile shear strength test is the triaxial compression test. The triaxial test allows a soil sample to be subjected to three principal stresses under controlled conditions. A cylindrical test specimen is encased in a rubber membrane and is then subjected to a confining pressure. Drainage from the sample is controlled through its two ends. The shearing force is applied axially and increased to failure. A plot of normal stress versus shear stress is developed and parameters c and ϕ are determined. In triaxial tests where full drainage is allowed during shear, or in undrained tests with pore pressure measurements during shear, the effective stress parameters c' and ϕ' can be determined. In shear testing, the drainage, consolidation, and loading conditions are selected to simulate field conditions. Triaxial compression tests are classified according to the consolidation and drainage conditions allowed during testing. The three test types normally conducted are unconsolidated undrained (UU), consolidated undrained (CU) and consolidated drained (CD). The unconfined compression test may theoretically be considered a UU test performed with no confining pressure. Direct shear tests are usually consolidated under a normal stress then sheared either very slowly to model drained conditions, or rapidly to model undrained conditions.

Total stress and effective stress pile design methods are presented in Chapter 9. The total stress methods use undrained shear strengths. Effective stress design methods use drained shear strength data. Therefore, selection of the shear strength tests to be performed should consider the analysis method(s) that will be used.

6.1.3 Consolidation Tests

To estimate the amount and rate at which a cohesive soil deposit will consolidate under an applied load of a structure, a one dimensional consolidation test (AASHTO T216) is usually performed. In this test, a saturated soil sample is constrained laterally while being compressed vertically. The vertical compression is measured and related to the void ratio of the soil. Loading the sample results in an increased pore water pressure within the voids of the sample. Over a period of time, as the water is squeezed from the soil, this excess water pressure will dissipate resulting in the soil grains (or skeleton) supporting the load. The amount of water squeezed from the sample is a function of load magnitude and compressibility of soil skeleton. The rate of pressure dissipation is a function of the permeability of the soil.

The results from the test are used to plot void ratio, e , versus pressure, p , on a semi-log scale to determine the preconsolidation pressure, p_c , and compression index, C_c . An illustration of a typical e -log p curve is presented in Figure 9.61. A plot of log time versus sample compression is used to determine coefficient of consolidation. Consolidation test results can be used to estimate magnitude and settlement rate of pile foundations in cohesive soils. A settlement design example using consolidation test data is presented in Chapter 9.

6.1.4 Electro Chemical Classification Tests

The soil and groundwater can contain constituents detrimental to pile materials. Electro chemical classification tests can be used to determine the aggressiveness of the subsurface conditions and the potential for pile deterioration. These electro chemical tests include:

- a. pH (AASHTO T289).
- b. Resistivity (AASHTO T288).
- c. Sulfate ion content (AASHTO T290).

- d. Chloride ion content (AASHTO T291).

Additional discussion of the influence of environmental conditions on pile selection are presented in Section 8.8 of Chapter 8.

6.2 LABORATORY TESTING FOR PILE DRIVEABILITY CONSIDERATIONS

As noted earlier in this chapter, pile foundations are increasingly being driven to greater depths and greater capacities. Laboratory tests to determine the remolded shear strength of cohesive soils and the gradation and fine content of cohesionless soils are important in assessing the pile driveability and the potential soil setup effects (changes in pile capacity with time).

Remolded Shear Strength of Cohesive Soils

Cohesive soils may lose a significant portion of their shear strength when disturbed or remolded, as during the pile driving process. The ability to estimate the soil strength at the time of driving and the resulting strength gain with time or soil set-up is a key component of economical pile design in cohesive soils. Soil-set-up is discussed further in Section 9.10.1.1. **The sensitivity of a cohesive soil can provide a qualitative but not quantitative indication of potential soil set-up.** Sensitivity determined in-situ with a vane shear device as described in Section 5.4 of Chapter 5 provides the best assessment of cohesive soil sensitivity. However, the sensitivity of a cohesive soil can also be determined from laboratory tests on undisturbed and remolded samples.

The sensitivity of a cohesive soil, S_t , is defined as:

$$S_t = (q_u \text{ undisturbed}) / (q_u \text{ remolded})$$

Table 6-2 contains typical values of sensitivity as reported by Sowers (1979) which may be useful for preliminary estimates of remolded shear strength. Terzaghi and Peck, (1967) noted that clays with sensitivities less than 16 generally regain a portion to all of their original shear strength with elapsed time. Based upon typical sensitivity values reported by Terzaghi and Peck as well as by Sowers, the remolded shear strength of many cohesive soils during pile driving would be expected to range from about 1/3 to 1/2 the undisturbed shear strength.

TABLE 6-2 TYPICAL VALUES OF SENSITIVITY FROM SOWERS (1979)	
Clay of medium plasticity, normally consolidated	2-8
Highly flocculent, marine clays	10-80
Clays of low to medium plasticity, overconsolidated	1-4
Fissured clays, clays with sand seams	0.5-2

To determine site specific soil sensitivity from laboratory data, remolded soil specimens having the same moisture content as the undisturbed specimen should be tested in unconfined compression.

Gradation of Cohesionless Soils

The gradation and fine content of cohesionless soils provide useful information in assessing pile driveability. Soils with a high fine content generally have lower angles of internal friction than lower fine content soils of similar density. A high fine content can also affect soil drainage and pore pressures during shear, and thus, the effective stresses acting on a pile during driving. Depending upon soil density, cohesionless soils with high fine contents are also more likely to demonstrate soil set-up than cohesionless soils with little or no fines. The gradation and angularity of the soil grains also influences the angle of internal friction.

Routine laboratory grain size analyses (mechanical and hydrometer) can quantify gradation and fine content. With this information, better engineering assessments of pile driveability and soil setup potential in cohesionless soils can be made.

REFERENCES

- American Association of State Highway and Transportation Officials [AASHTO], (1988). Manual on Subsurface Investigations. AASHTO Highway Subcommittee on Bridges and Structures, Washington, D.C., 391.
- Bowles, J.E. (1977). Foundation Analysis and Design. Second Edition, McGraw-Hill Book Company.
- Cheney, R.S. and Chassie, R.G. (2000). Soils and Foundations Workshop Reference Manual. Publication No. FHWA HI-00-045, U.S. Department of Transportation, National Highway Institute, Federal Highway Administration, Washington, D.C., 358.
- Holtz, R.D. and Kovacs, W.D. (1981). An Introduction to Geotechnical Engineering. Prentice Hall, Inc., Englewood Cliffs, 283-665.
- Sowers, G.F. (1979). Introductory Soil Mechanics and Foundations. Geotechnical Engineering, Fourth Edition, MacMillan Publishing Co. Inc., New York, 217.
- Terzaghi, K. and Peck, R.B. (1967). Soil Mechanics in Engineering Practice. Second Edition, John Wiley & Sons Inc., New York, 51-52.

Chapter 7 FOUNDATION DESIGN PROCEDURE

A foundation is the interfacing element between the superstructure and the underlying soil or rock. The loads transmitted by the foundation to the underlying soil must not cause soil shear failure or damaging deformations of the superstructure. It is essential to systematically consider various foundation types and to select the optimum alternative based on the superstructure requirements, the subsurface conditions, and foundation cost.

Foundation types may include shallow foundations consisting of spread footing or mat foundations with or without ground improvement; or deep foundations consisting of driven piles, micropiles, or drilled shafts.

Subsequent chapters of this manual provide guidance on pile foundation design and construction. Guidance for other foundation solutions is contained in the following documents:

Spread Footings	FHWA-SA-02-054	Kimmerling (2002)
	FHWA-NHI-01-023	Munfakh et al. (2001)
	FHWA- RD-86-185	Gifford et al. (1987)
Ground Improvement	FHWA-NHI-04-001	Elias et. al (2004)
Micropiles	FHWA-NHI-05-039	Sabatini et al. (2005)
	FHWA-RD-96-016 to 019	Bruce and Juran (1997)
Drilled Shafts	FHWA-IF-99-025	O'Neil and Reese (1999)
Auger Cast Piles	GEC 8	Brown and Dapp (2006)

Complete references for the above design manuals are provided at the end of this chapter. Information on the availability of these documents is provided at www.fhwa.dot.gov/bridge/geopub.htm

7.1 FOUNDATION DESIGN APPROACH

The following design approach is recommended to determine the optimum foundation alternative.

1. Determine the foundation loads to be supported, structure layout, and special requirements such as limits on total and differential settlements, lateral deformations, lateral loads, scour, seismic performance, and time constraints on construction. **This step is often partially overlooked or vaguely addressed. A complete knowledge of these issues is of paramount importance.**
2. Evaluate the subsurface exploration and the laboratory testing data. Ideally, the subsurface exploration and laboratory testing programs were performed with knowledge of the loads to be transmitted to, and supported by the soil and/or rock materials.
3. Prepare a final soil profile and critical cross sections. Determine soil layers suitable or unsuitable for spread footings, pile foundations, or drilled shafts. Also consider if ground improvement techniques could modify unsuitable layers into suitable support layers.
4. Consider and prepare alternative designs.

Shallow Foundations: a. Spread footings.
 (without ground improvement) b. Mat foundations.

Shallow Foundations: a. Spread footings.
 (with ground improvement) b. Mat foundations.

Deep Foundations: a. Pile foundations.
 i. Candidate pile types
 ii. Viable pile sections
 b. Drilled shafts.
 c. Micropile.

Table 7-1 summarizes shallow and deep foundation types and uses, as well as applicable and non-applicable subsurface conditions.

5. Prepare cost estimates for feasible alternative foundation designs including all associated substructure costs. The cost estimates should be developed using the concept of foundation support cost that was introduced in Chapter 2. The foundation support cost should include all associated substructure costs required for foundation construction such as sheeting or cofferdam requirements, cap requirement and size, and the effect of environmental or construction limitations such as noise restrictions or abatement procedures, bubble nets, etc.

6. Select the optimum foundation alternative. Generally the most economical alternative (lowest foundation support cost) should be selected and recommended. However, the ability of the local construction force as well as the availability of materials and equipment should also be considered.

For major projects, if the estimated costs of feasible foundation alternatives (during the design stage) are within 15 percent of each other, then alternate foundation designs should be considered for inclusion in the contract documents. The most economical foundation design will then be determined by construction demand and material pricing rather than subtleties in the design estimate.

TABLE 7-1 FOUNDATION TYPES AND TYPICAL USES*

Foundation Type	Use	Applicable Soil Conditions	Non-suitable or Difficult Soil Conditions
Spread footing, wall footings.	Individual columns, walls, bridge piers.	Any conditions where bearing capacity is adequate for applied load. May use on single stratum; firm layer over soft layer, or weaker layer over firm layer. Check immediate, differential and consolidation settlements.	Any conditions where foundations are supported on soils subject to scour or liquefaction. Bearing layer located below ground water table.
Mat foundation.	Same as spread and wall footings. Very heavy column loads. Usually reduces differential settlements and total settlements.	Generally soil bearing value is less than for spread footings. Over one-half area of structure covered by individual footings. Check settlements.	Same as footings.
Pile foundations (shaft resistance, toe resistance or combination).	In groups to transfer heavy column and bridge loads to suitable soil layers. Also to resist uplift and/or lateral loads.	Poor surface and near surface soils. Soils suitable of load support 5 to 90 m (15 to 300 ft) below ground surface. Check settlement of pile groups.	Shallow depth to hard stratum. Sites where pile driving vibrations or heave may adversely impact adjacent facilities. Boulder fields.
Drilled shafts (shaft resistance, toe resistance or combination).	Larger column loads than for piles. Cap sometimes eliminated by using drilled shafts as column extension.	Poor surface and near surface soils. Soils and/or rock of suitable load support located 8 to 90 m (25 to 300 ft) below ground surface.	Deep deposits of soft clays and loose water bearing granular soils. Caving formations difficult to stabilize. Artesian conditions. Boulder fields.
Micropiles.	Often used for seismic retrofitting, underpinning, and in low head room situations.	Any soil, rock, or fill conditions including areas with rubble fill, boulders, and karstic conditions.	High slenderness ratio may present buckling problems from loss of lateral support in liquefaction susceptible soils.

* Modified from Bowles (1977).

7.2 CONSIDERATION OF SPREAD FOOTING FOUNDATION

The feasibility of using spread footings for foundation support should be considered in any foundation selection process. Spread footings are generally more economical than deep foundations (piles and drilled shafts); spread footings in conjunction with ground improvement techniques should also be considered. **Deep foundations should not be used indiscriminately for all subsurface conditions and for all structures.** There are subsurface conditions where pile foundations are very difficult and costly to install, and other conditions when they may not be necessary.

7.3 ESTABLISHMENT OF A NEED FOR A DEEP FOUNDATION

The first difficult problem facing the foundation designer is to establish whether or not the site conditions dictate that a deep foundation must be used. Vesic (1977) summarized typical situations in which piles may be needed. These typical situations as well as additional uses of deep foundations are shown in Figure 7.1.

Figure 7.1(a) shows the most common case in which the upper soil strata are too compressible or too weak to support heavy vertical loads. In this case, deep foundations transfer loads to a deeper dense stratum and act as toe bearing foundations. In the absence of a dense stratum within a reasonable depth, the loads must be gradually transferred, mainly through soil resistance along shaft, Figure 7.1(b). An important point to remember is that deep foundations transfer load through unsuitable layers to suitable layers. The foundation designer must define at what depth suitable soil layers begin in the soil profile.

Deep foundations are frequently needed because of the relative inability of shallow footings to resist inclined, lateral, or uplift loads and overturning moments. Deep foundations resist uplift loads by shaft resistance, Figure 7.1(c). Lateral loads are resisted either by vertical deep foundations in bending, Figure 7.1(d), or by groups of vertical and battered foundations, which combine the axial and lateral resistances of all deep foundations in the group, Figure 7.1(e). Lateral loads from overhead highway signs and noise walls may also be resisted by groups of deep foundations, Figure 7.1(f).

Deep foundations are often required when scour around footings could cause loss of bearing capacity at shallow depths, Figure 7.1(g). In this case the deep foundations must extend below the depth of scour and develop the full capacity in the support zone below the level of expected scour. FHWA scour guidelines by Richardson and Davis (2001) require the geotechnical analysis of bridge foundations to be performed on the basis that all stream bed materials in the scour prism have been removed and are not available for bearing or lateral support. Costly damage and the need for future underpinning can be avoided by properly designing for scour conditions.

Soils subject to liquefaction in a seismic event may also dictate that a deep foundation be used, Figure 7.1(h). Seismic events can induce significant lateral loads to deep foundations. During a seismic event, liquefaction susceptible soils offer less lateral resistance as well as reduced shaft resistance to a deep foundation. Liquefaction effects on deep foundation performance must be considered for deep foundations in seismic areas.

Deep foundations are often used as fender systems to protect bridge piers from vessel impact, Figure 7.1(i). Fender system sizes and group configurations vary depending upon the magnitude of vessel impact forces to be resisted. In some cases, vessel impact loads must be resisted by the bridge pier foundation elements. Single deep foundations may also be used to support navigation aids.

In urban areas, deep foundations may occasionally be needed to support structures adjacent to locations where future excavations are planned or could occur, Figure 7.1(j). Use of shallow foundations in these situations could require future underpinning in conjunction with adjacent construction.

Deep foundations are used in areas of expansive or collapsible soils to resist undesirable seasonal movements of the foundations. Deep foundations under such conditions are designed to transfer foundation loads, including uplift or down-drag, to a level unaffected by seasonal moisture movements, Figure 7.1(k).

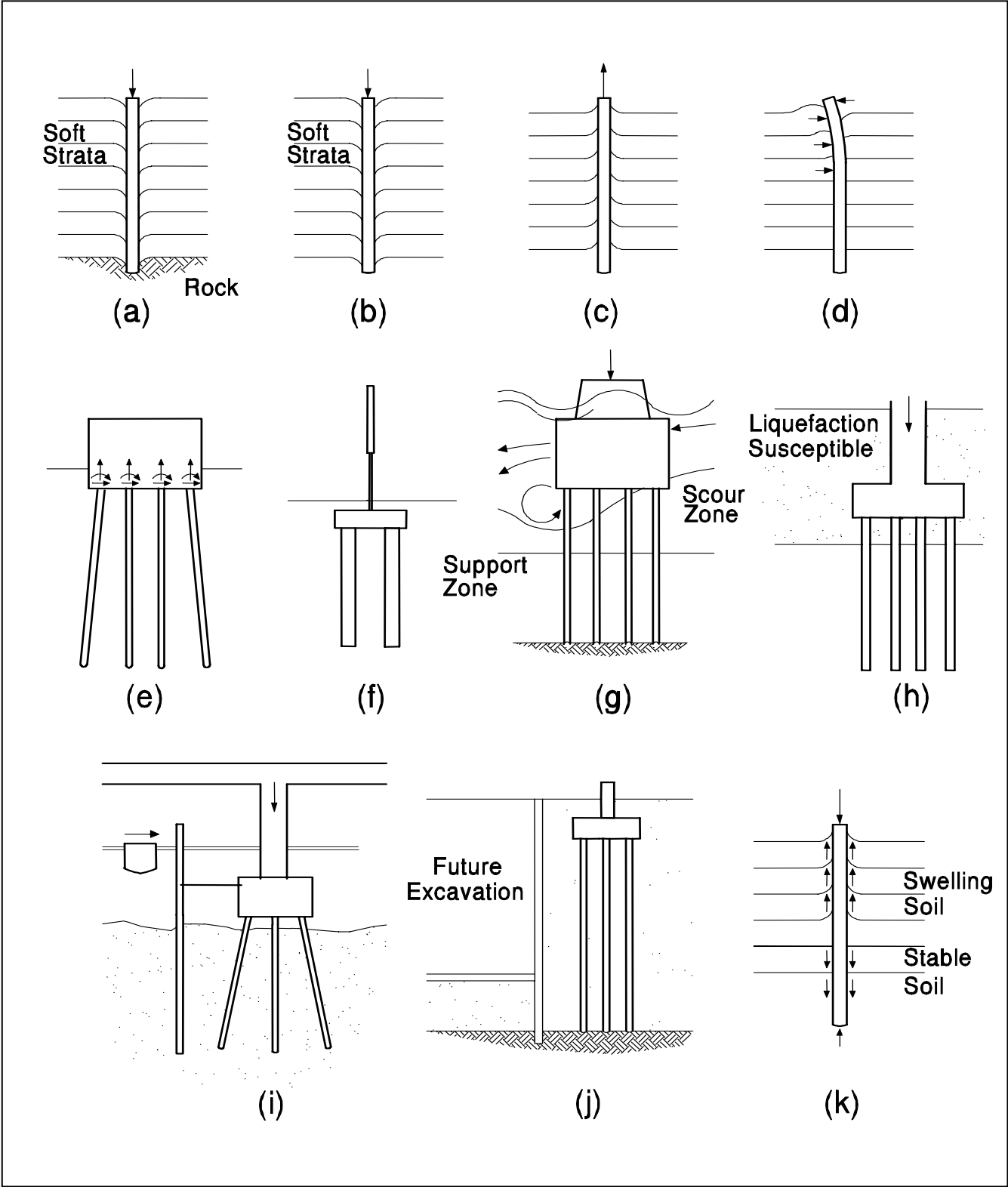


Figure 7.1 Situations in which Deep Foundations may be Needed (modified from Vesic, 1977)

In many instances either a shallow or deep foundation alternative is technically feasible. Under these circumstances, an evaluation of the shallow foundation should include; (1) the dimensions and depth of shallow footings based on allowable bearing capacity, (2) the magnitude and time-rate of settlement under anticipated loads, and (3) detailed cost analysis including such factors as need for cofferdams, overall substructure cost, dewatering and foundation seals, construction time, construction risk and claims potential. A comparative analysis of feasible deep foundation alternatives should also be made. The cost analyses of feasible alternatives should have a significant role in final selection of the foundation type.

Because this manual deals only with driven pile foundations, other types of foundations will not be discussed further.

REFERENCES

- Bowles, J.E. (1977). Foundation Analysis and Design. Third Edition, McGraw-Hill Book Company, New York, 4-5.
- Brown, D. and Dapp, S. (2006). Geotechnical Engineering Circular No. 8, Continuous Flight Auger Piles, Federal Highway Administration, U.S. Department of Transportation, Federal Highway Administration, Office of Bridge Technology, Washington D.C.
- Bruce D.A. and Juran, I. (1997). Drilled and Grouted Micropiles: State-of-Practice Review, Volumes I-IV. Report No. FHWA-RD-96-016 to 019, U.S. Department of Transportation, Federal Highway Administration, Office of Engineering R&D, McLean, VA
- Cheney, R.S. and Chassie, R.G. (2000). Soils and Foundations Workshop Reference Manual. Publication No. FHWA HI-00-045, U.S. Department of Transportation, National Highway Institute, Federal Highway Administration, Washington, D.C., 358.
- Elias, V., Welsh, J., Warren, J., Lukas, R., Collin, J.G., and Berg, R.R. (2004). Ground Improvement Methods, National Highway Institute, Federal Highway Administration, U.S. Department of Transportation, Washington, D.C., 1002.
- Gifford D.G., Wheeler, J.R., Kraemer, S.R. and McKown, A.F. (1987). Spread Footings for Highway Bridges. Report No. FHWA-RD-86-185, U.S. Department of Transportation, Federal Highway Administration, Office of Engineering and Highway Operations Research and Development, McLean, VA, 229.
- Kimmerling, R.E. (2002). Geotechnical Engineering Circular No. 6, Shallow Foundations, Federal Highway Administration, U.S. Department of Transportation, Federal Highway Administration, Office of Bridge Technology, Washington D.C., 310.
- Munfakh, G., Arman, A., Collin, J.G., Hung, J.C-J., and Brouillette, R.P. (2001). Shallow Foundations Reference Manual, National Highway Institute, Federal Highway Administration, U.S. Department of Transportation, Washington, D.C. 222.
- O'Neil, M.W. and Reese, L.C. (1999). Drilled Shafts: Construction Procedures and Design Methods, Report No. FHWA-IF-99-025, U.S. Department of Transportation, Federal Highway Administration, Office of Infrastructure/Office of Bridge Technology, Washington D.C., 758.

Richardson, E.V. and Davis, S.R. (2001). FHWA NHI-01-001, Evaluating Scour at Bridges, HEC-18. Office of Technology Applications, Federal Highway Administration, Washington, D.C.

Sabatini, P.J., Tanyu, B., Armour., P., Groneck, P., and Keeley, J., (2005). Micropile Design and Construction – Final Draft, National Highway Institute, Federal Highway Administration, Arlington, VA

Vesic, A.S. (1977). Design of Pile Foundations. National Cooperative Highway Research Program, Transportation Research Board, National Research Council, Washington, D.C., Synthesis of Highway Practice No. 42.

Chapter 8

PILE TYPES FOR FURTHER EVALUATION

The economic selection of a pile foundation type and section for a structure should be based on the specific soil conditions as well as the foundation loading requirements, final performance criteria, construction limitations and time, as well as the foundation support cost. This chapter focuses on the characteristics of driven pile foundation types typically used for highway structures. Design data useful in the selection and design of specific pile types is included in Appendices C-1 (SI units) and C-2 (US units). Additional details on pile splices and toe protection devices are presented in Chapter 22.

8.1 OVERVIEW OF TYPICAL PILE TYPES

Piles can be broadly categorized in two main types: foundation piles for support of structural loads and sheet piles for earth retention systems. Discussion of sheet piles is outside the scope of this manual.

There are numerous types of foundation piles. Figure 8.1 shows a pile classification system based on type of material, configuration, installation technique and equipment used for installation. Foundation piles can also be classified on the basis of their method of load transfer from the pile to the surrounding soil mass. Load transfer can be by shaft resistance, toe bearing resistance or a combination of both.

Table 8-1 modified from NAVFAC (1982) summarizes characteristics and uses of common pile types. The table is for preliminary guidance only, and should be confirmed by local practice. In addition, the design load should be determined by geotechnical engineering principles, limiting stresses in the pile material, and type and function of structure. Uncased cast-in-place concrete piles, although outside the scope of this driven pile manual, are included in this chapter because all feasible pile types should be considered in any selection process.

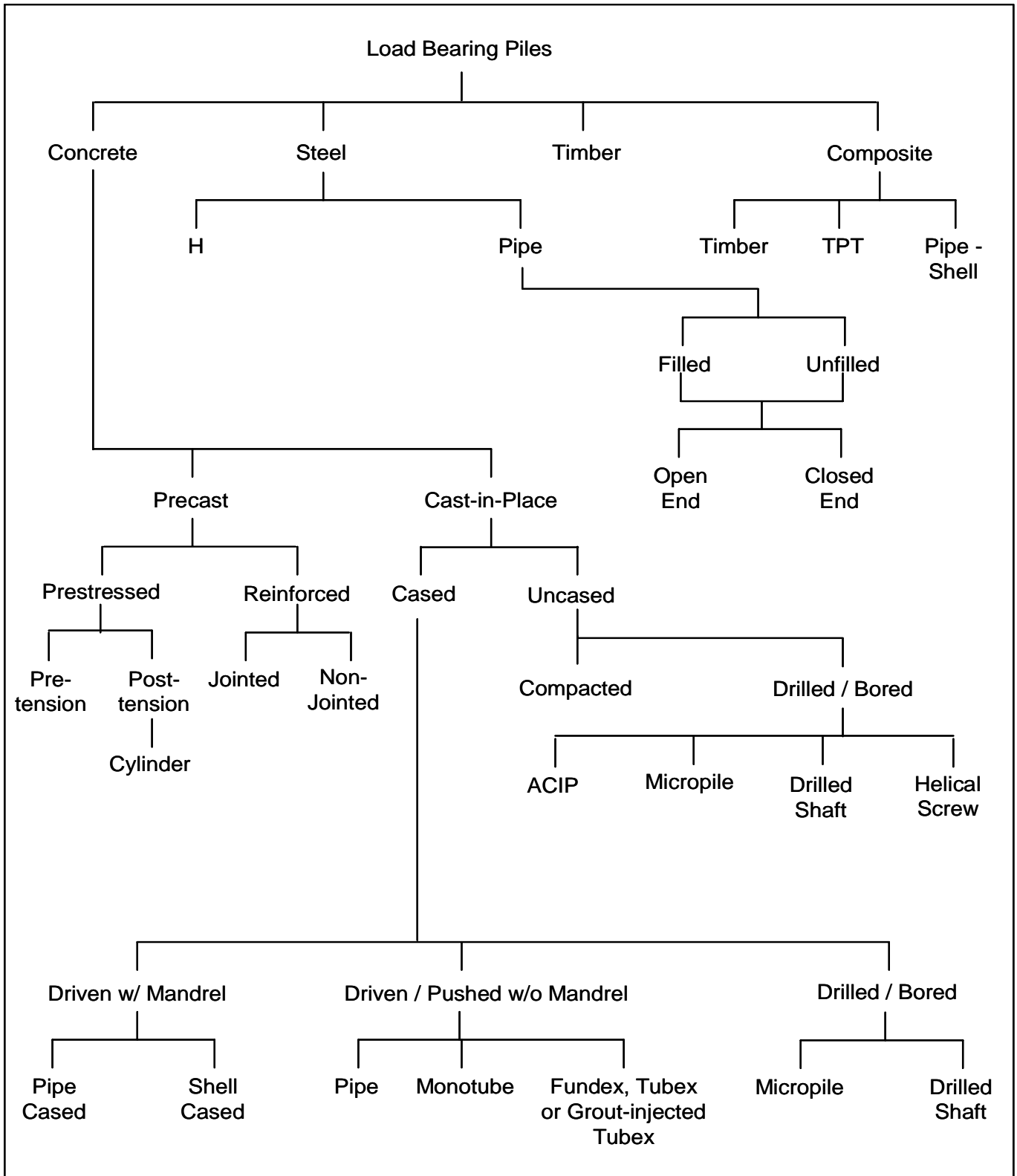
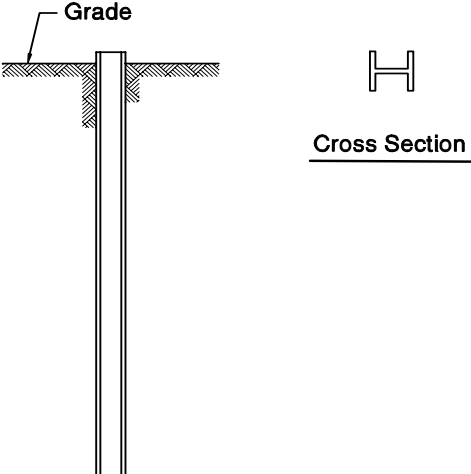


Figure 8.1 Pile Classification Chart

TABLE 8-1 TECHNICAL SUMMARY OF PILES*		
PILE TYPE	TIMBER	TYPICAL ILLUSTRATION
TYPICAL LENGTHS	5 m - 23 m (15 – 75 ft) Southern Pine 5 m - 37 m (15 – 120 ft) Douglas Fir	
MATERIAL SPECIFICATIONS	ASTM-D25 AWPA UC4A, UC4B UC4C, UC5A, UC5B and UC5C.	
MAXIMUM STRESSES	See Chapter 10.	
TYPICAL AXIAL DESIGN LOADS	100 kN - 500 kN (20 – 110 kips)	
DISADVANTAGES	<ul style="list-style-type: none"> • Difficult to splice. • Vulnerable to damage in hard driving; both pile head and toe may need protection. • Intermittently submerged piles are vulnerable to decay unless treated. 	
ADVANTAGES	<ul style="list-style-type: none"> • Comparatively low in initial cost. • Permanently submerged piles are resistant to decay. • Easy to handle. 	
REMARKS	<ul style="list-style-type: none"> • Best suited for friction piles in granular material. 	

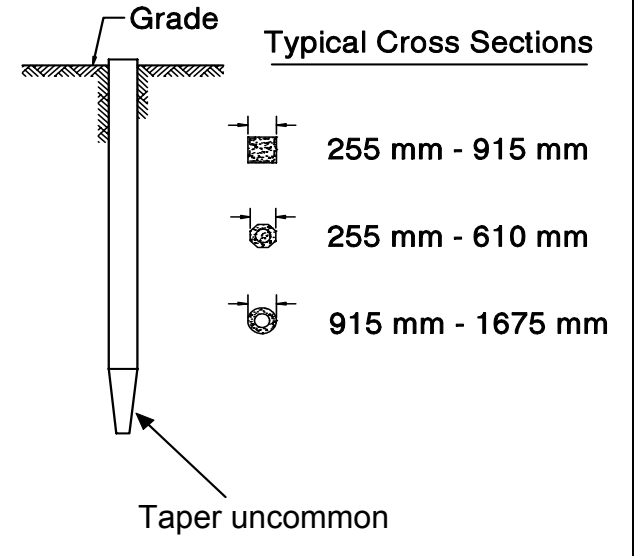
* Table modified and reproduced from NAVFAC DM 7.2 (1982)

TABLE 8-1 TECHNICAL SUMMARY OF PILES* (CONTINUED)		
PILE TYPE	STEEL - H SECTIONS	TYPICAL ILLUSTRATION
TYPICAL LENGTHS	5 m - 40 m (15 – 130 ft)	
MATERIAL SPECIFICATIONS	ASTM - A572, A588, or A690 Grade 50 (A36 steel is no longer produced)	
MAXIMUM STRESS	See Chapter 10.	
TYPICAL AXIAL DESIGN LOADS	600 kN - 2,500 kN (130 – 560 kips)	
DISADVANTAGES	<ul style="list-style-type: none"> • Vulnerable to corrosion where exposed HP section may be damaged or deflected by major obstructions. 	
ADVANTAGES	<ul style="list-style-type: none"> • Available in various lengths and sizes. • High capacity. • Small soil displacement. • Easy to splice. • Able to penetrate through light obstructions. • Pile toe protection will assist penetration through harder layers and some obstructions. 	
REMARKS	<ul style="list-style-type: none"> • Best suited for toe bearing on rock. • Allowable capacity should be reduced in corrosive environments. • Use as a friction pile in granular materials often results in cost overruns. 	

* Table modified and reproduced from NAVFAC DM 7.2 (198

TABLE 8-1 TECHNICAL SUMMARY OF PILES* (CONTINUED)		
PILE TYPE	STEEL PIPE PILES	TYPICAL ILLUSTRATION
TYPICAL LENGTHS	5 m - 40 m (15 - 130 ft)	<p>200 mm - 1220 mm</p> <p>Grade</p> <p>Cross Section of Plain Pipe Pile Shell Thickness 8 mm - 25 mm</p> <p>300 mm - 900 mm</p> <p>Cross Section of Pipe Pile with Core</p> <p>Socket Required for High Vertical Loads only.</p> <p>Rock</p> <p>End Closure may be Flat Plate, Conical Point, or Omitted</p>
MATERIAL SPECIFICATIONS	ASTM A252, Grade 2 or 3 - for pipe. ACI 318 - for concrete (if filled). ASTM A572 - for core (if used).	
MAXIMUM STRESSES	See Chapter 10.	
TYPICAL AXIAL DESIGN LOADS	800 kN - 2,500 kN (180 - 560 kips) with or without concrete fill and without cores. 2,500 kN - 15,000 kN (560 - 3400 kips) concrete filled with cores.	
DISADVANTAGES	<ul style="list-style-type: none"> • Soil displacement for closed end pipe. 	
ADVANTAGES	<ul style="list-style-type: none"> • Closed end pipe can be internally inspected after driving. • Low soil displacement for open end installation. • Open end pipe with cutting shoe can be used against obstructions. • Open end pipe can be cleaned out and driven further. • High load capacities. • Easy to splice. 	
REMARKS	<ul style="list-style-type: none"> • Provides high bending resistance where unsupported length is loaded laterally. • Open end not recommended as a friction pile in granular material. 	

* Table modified and reproduced from NAVFAC DM 7.2 (1982)

TABLE 8-1 TECHNICAL SUMMARY OF PILES* (CONTINUED)		
PILE TYPE	PRESTRESSED/PRECAST CONCRETE	TYPICAL ILLUSTRATION
TYPICAL LENGTHS	15 m - 40 m (50 – 130 ft) for prestressed. 10 m - 15 m (30 - 50 ft) for reinforced.	 <p>The diagram shows a vertical pile extending from the ground level (Grade) downwards. The pile has a slight taper at the bottom. To the right of the pile, three cross-sectional views are shown, labeled 'Typical Cross Sections'. The top cross-section is a square with dimensions 255 mm - 915 mm. The middle cross-section is a circle with dimensions 255 mm - 610 mm. The bottom cross-section is a larger circle with dimensions 915 mm - 1675 mm. An arrow points to the tapered bottom of the pile with the text 'Taper uncommon'. Below the diagram is the note: 'Note: Reinforcing may be Prestressed'.</p>
MATERIAL SPECIFICATIONS	ACI 318 - for concrete. ASTM - A82, A615, A722, and A884 - for reinforcing steel. ASTM - A416, A421, and A882 - for prestressing.	
MAXIMUM STRESSES	See Chapter 10.	
TYPICAL AXIAL DESIGN LOADS	400 kN - 4,500 kN (90 – 1000 kips) for prestressed. 400 kN - 1,000 kN (90 – 225 kips) for reinforced.	
DISADVANTAGES	<ul style="list-style-type: none"> • Unless prestressed, vulnerable to handling damage. • Relatively high breakage rate, especially when piles are to be spliced. • Considerable displacement. • Difficult to splice when insufficient length ordered. 	
ADVANTAGES	<ul style="list-style-type: none"> • High load capacities. • Corrosion resistance obtainable. • Hard driving possible. 	
REMARKS	<ul style="list-style-type: none"> • Cylinder piles are well suited for bending resistance. 	

* Table modified and reproduced from NAVFAC DM 7.2 (1982)

TABLE 8-1 TECHNICAL SUMMARY OF PILES* (CONTINUED)		
PILE TYPE	CAST-IN-PLACE CONCRETE (MANDREL DRIVEN SHELL)	TYPICAL ILLUSTRATION
TYPICAL LENGTHS	3 m - 40 m (10 - 130 ft), but typically in the 15 m - 25 m (50 - 80 ft) range.	
MATERIAL SPECIFICATIONS	ACI 318 - for concrete.	
MAXIMUM STRESSES	33% of 28-day strength of concrete, with increase to 40% of 28-day strength provided: <ul style="list-style-type: none"> • Casing is a minimum of 12 gage thickness. • Casing is seamless or with welded seams. • Ratio of steel yield strength to concrete is not less than 6. • Pile diameter not greater than 450 mm (18 in). 	
TYPICAL AXIAL DESIGN LOADS	Designed for a wide loading range but generally in the 400-1400 kN (90 - 315 kip) range.	
DISADVANTAGES	<ul style="list-style-type: none"> • Difficult to splice after concreting. • Redriving not recommended. • Thin shell vulnerable during driving to excessive earth pressure or impact. • Considerable displacement. 	
ADVANTAGES	<ul style="list-style-type: none"> • Initial economy. • Tapered sections provide higher resistance in granular soil than uniform piles. • Can be inspected after driving. • Relatively less waste of steel. • Can be designed as toe bearing or friction pile. 	
REMARKS	<ul style="list-style-type: none"> • Best suited as friction pile in granular materials. 	

* Table modified and reproduced from NAVFAC DM 7.2 (1982)

TABLE 8-1 TECHNICAL SUMMARY OF PILES* (CONTINUED)		
PILE TYPE	CAST-IN-PLACE CONCRETE (SHELLS DRIVEN WITHOUT A MANDREL)	TYPICAL ILLUSTRATION
TYPICAL LENGTHS	5 m - 25 m (15 - 80 ft)	
MATERIAL SPECIFICATIONS	ACI 318 - for concrete. ASTM A252 - for steel pipe.	
MAXIMUM STRESSES	See Chapter 10.	
TYPICAL AXIAL DESIGN LOADS	500 kN - 1350 kN (110 - 300 kips)	
DISADVANTAGES	<ul style="list-style-type: none"> • Difficult to splice after concreting. • Considerable displacement. 	
ADVANTAGES	<ul style="list-style-type: none"> • Can be redriven. • Shell not easily damaged if fluted. 	
REMARKS	<ul style="list-style-type: none"> • Best suited for friction piles of medium length. 	

* Table modified and reproduced from NAVFAC DM 7.2 (1982)

TABLE 8-1 TECHNICAL SUMMARY OF PILES* (CONTINUED)		
PILE TYPE	COMPOSITE PILES	TYPICAL ILLUSTRATION
TYPICAL LENGTHS	15 m - 65 m (50 - 210 ft)	<p style="text-align: center;">Typical Combinations</p> <p>The illustration shows four cross-sectional diagrams of composite piles. Each diagram has a horizontal line representing the ground level, labeled 'Grade'. 1. Top-left: A pile with a rectangular section above ground labeled 'Precast Concrete' and a narrow 'HP Section' below ground. 2. Top-right: A pile with a wider rectangular section above ground labeled 'Cased or Uncased Concrete' and a narrow 'Timber' section below ground. 3. Bottom-left: A pile with a wider rectangular section above ground labeled 'Concrete Filled Steel Shell' and a narrow 'HP Section' below ground. 4. Bottom-right: A pile with a wider rectangular section above ground labeled 'Steel Pipe Concrete Filled' and a narrow 'HP Section' below ground.</p>
MATERIAL SPECIFICATIONS	ASTM A572 - for HP section. ASTM A252 - for steel pipe. ASTM D25 - for timber. ACI 318 - for concrete.	
MAXIMUM STRESSES	33% of 28-day strength of concrete. 62 MPa (9 ksi) for structural and pipe sections if thickness is greater than 4 mm (0.16 inches).	
TYPICAL AXIAL DESIGN LOADS	300 kN - 1,800 kN (70 - 400 kips)	
DISADVANTAGES	<ul style="list-style-type: none"> • Difficult to attain good joints between two materials except for concrete H or pipe composite piles. 	
ADVANTAGES	<ul style="list-style-type: none"> • Considerable length can be provided at comparatively low cost for wood composite piles. • High capacity for some composite piles. • Internal inspection for pipe composite piles. 	
REMARKS	<ul style="list-style-type: none"> • The weakest of any material used shall govern allowable stresses and capacity. 	

* Table modified and reproduced from NAVFAC DM 7.2 (1982)

TABLE 8-1 TECHNICAL SUMMARY OF PILES* (CONTINUED)		
PILE TYPE	DRILLED SHAFTS	TYPICAL ILLUSTRATION
TYPICAL LENGTHS	5 m to 65 m or more (15 – 200 ft)	
MATERIAL SPECIFICATIONS	ACI 318 - for concrete. ASTM A82, A615, A722, and A884 for reinforcing steel.	
MAXIMUM STRESSES	33% of 28-day strength of concrete.	
TYPICAL AXIAL DESIGN LOADS	1,500 kN - 20,000 kN (330 – 4500 kips) or more.	
DISADVANTAGES	<ul style="list-style-type: none"> • Requires relatively more extensive inspection. • Construction procedures are critical to quality. • Boulders can be a serious problem, especially in small diameter shafts. • Mobilization of end bearing on a long shaft can require substantial displacement of shaft head. 	
ADVANTAGES	<ul style="list-style-type: none"> • Length variations easily accommodated. • High bearing capacity and bending resistance. • Availability of several construction methods. • Can be continued above ground as a column. 	
REMARKS	<ul style="list-style-type: none"> • No driving observations (blow count) available to aid in assessing capacity. • Not recommended in soft clays and loose sands. 	

* Table modified and reproduced from NAVFAC DM 7.2 (1982)

TABLE 8-1 TECHNICAL SUMMARY OF PILES* (CONTINUED)		
PILE TYPE	AUGER PLACED, PRESSURE INJECTED CONCRETE PILES (CFA PILES)	TYPICAL ILLUSTRATION
TYPICAL LENGTHS	5 m - 25 m (15 – 80 ft)	<p>The illustration shows a vertical pile with a wider base. A horizontal line at the top is labeled 'Grade'. A circular cross-section is shown to the right, labeled 'Typical Cross Section' with a diameter of '460 mm to 760 mm'. An arrow points to the base of the pile with the text 'Workmanship is critical to integrity'. Below the pile, text states 'CFA pile may be designed for load support through shaft resistance or a combination of shaft resistance and end bearing.'</p>
MATERIAL SPECIFICATIONS	ACI 318 - for concrete. ASTM A82, A615, A722, & A884 - for reinforcing steel.	
MAXIMUM STRESSES	33% of 28-day strength of concrete.	
TYPICAL AXIAL DESIGN LOADS	260 kN - 875 kN (60 – 200 kips)	
DISADVANTAGES	<ul style="list-style-type: none"> • Greater dependence on quality workmanship. • Not suitable through peat or similar highly compressible material. • Requires more extensive subsurface exploration. • No driving observation (blow count) to aid in assessing capacity. 	
ADVANTAGES	<ul style="list-style-type: none"> • Economy. • Zero displacement. • Minimal vibration to endanger adjacent structures. • High shaft resistance. • Good contact on rock for end bearing. • Visual inspection of augured material. 	
REMARKS	<ul style="list-style-type: none"> • Best suited as a friction pile in granular material. 	

* Table modified and reproduced from NAVFAC DM 7.2 (1982)

TABLE 8-1 TECHNICAL SUMMARY OF PILES (CONTINUED)		
PILE TYPE	MICROPILES	TYPICAL ILLUSTRATION
TYPICAL LENGTHS	12 m - 25 m (40 - 100 ft)	<p>The illustration shows a side view of three micropiles extending from a horizontal line labeled 'Grade'. Below this, a 'Cross Section' is detailed. It shows two circular cross-sections. The left one is labeled 'Steel Reinforcing Bar' with a diameter dimension of '130 - 230 mm'. The right one is labeled 'Steel Pipe (typically 100 - 180 mm)' with an outer diameter dimension of '150 - 230 mm'. Both are surrounded by a shaded area labeled 'Grout'.</p>
MATERIAL SPECIFICATIONS	ASTM C150 - for Portland cement. ASTM C595 - for blended hydraulic cement. ASTM A615 - for reinforcing steel.	
TYPICAL AXIAL DESIGN LOADS	300 kN - 1100 kN (70 - 250 kips)	
DISADVANTAGES	<ul style="list-style-type: none"> • Cost 	
ADVANTAGES	<ul style="list-style-type: none"> • Low noise and vibrations. • Small amount of spoil. • Excellent for sites with low headroom and restricted access. • Applicability to soil containing rubble and boulders, karstic areas. 	
REMARKS	<ul style="list-style-type: none"> • Can be used for any soil, rock or fill condition. 	

TABLE 8-1 TECHNICAL SUMMARY OF PILES* (CONTINUED)		
PILE TYPE	PRESSURE INJECTED FOOTINGS	TYPICAL ILLUSTRATION
TYPICAL LENGTHS	3 m - 15 m (10 – 50 ft)	<p>430 mm - 660 mm 300 mm - 500 mm</p> <p>Grade</p> <p>Concrete Compacted by Ramming Casing Corrugated Shell or Pipe</p> <p><u>Uncased Shaft</u> <u>Cased Shaft</u></p>
MATERIAL SPECIFICATIONS	ACI 318 - for concrete. ASTM A252 for steel pipe.	
MAXIMUM STRESSES	33% of 28-day strength of concrete. 62 MPa (9 ksi) for pipe shell if thickness is greater than 4 mm (0.16 inches).	
TYPICAL AXIAL DESIGN LOADS	600 kN - 1,200 kN (135 – 270 kips)	
DISADVANTAGES	<ul style="list-style-type: none"> • Base of footing cannot be made in clay or when hard spots (e.g., rock ledges) are present in soil. • When clay layers must be penetrated to reach suitable material, special precautions are required for shafts in groups. 	
ADVANTAGES	<ul style="list-style-type: none"> • Provides means for placing high capacity footings on bearing stratum without necessity for excavation or dewatering. • High blow energy available for overcoming obstructions. • Great uplift resistance if suitably reinforced. 	
REMARKS	<ul style="list-style-type: none"> • Best suited for granular soils where bearing is achieved through compaction around base. • Minimum spacing 1.5 m (5 ft) on center. 	

* Table modified and reproduced from NAVFAC DM 7.2 (1982)

8.2 TIMBER PILES

Timber piles are usually of round, tapered cross section made from tree trunks of Southern Pine or Douglas Fir driven with the small end down. Southern Pine timber piles can be found to lengths up to 23 meters (75 ft), and some west coast Douglas Fir may be up to 37 meters (120 ft) in length. Oak and other timber types have also been used for piles, but that is infrequent today. ASTM D25, Standard Specification for Round Timber Piles, presents guidelines on minimum timber pile dimensions, straightness, knot sizes, *etc.* AWPAC3, Piles, Preservative Treatment by Pressure Process, contains penetration and retention values for the various preservatives. Figure 8.2 presents a photograph of timber piles.



Figure 8.2 Timber Piles

Timber piles are best suited for modest loads when used as friction piles in sands, silts and clays. The taper of timber piles is effective in increasing the shaft resistance, particularly in loose sands. They are not recommended as piles to be driven through dense gravel, boulders, or till, or for toe bearing piles on rock since they are vulnerable to damage at the pile head and toe in hard driving. Overdriving of timber piles can result in the crushing of fibers or brooming at the pile head. This can be controlled by using a helmet with cushion material and/or metal strapping around the head of the pile. In hard driving situations, a metal shoe should be

attached to the pile toe. Timber piles are favored for the construction of bridge fender systems and small jetties due to the good energy absorption properties of wood.

Timber pile splices are difficult and generally undesirable. However, splice details are discussed in Chapter 22.

Durability is generally not a design consideration if a timber pile is below the permanent water table. However, when a timber pile is subjected to alternate wetting and drying cycles or located above the water table, damage and decay by insects may result. Such damage reduces the service life of timber piles significantly unless the pile is treated with a wood preservative. The most common treatments for timber piling are Creosote, Chromated Copper Arsenate (CCA) for Southern Pine, and Ammoniacal Copper Zinc Arsenate (ACZA) for Douglas Fir. Creosote cannot be used alone in southern waters because of attack by *limnoria tripundtata*, but should be used as part of a dual treatment with CCA or ACZA. If cracking of the pile shaft or head occurs and extends below the prescribed pile cut-off level, the initial preservative treatment will not be effective, and the trimmed end of the pile should be treated a second time.

According to Graham (1995), the durability of round timber piling is a function of site-specific conditions:

1. Foundation piles permanently submerged in ground water will typically last indefinitely.
2. Fully embedded, treated foundation piles partially above the ground water with a concrete cap will typically last on the order of 100 years or longer.
3. Treated trestle piles over land will generally last as long as utility poles in the area, *i.e.*, about 75 years in northern areas and about 40 years in southern areas of the United States.
4. Treated piles in fresh water will typically last about five to ten years less than land trestle piles in the same area.
5. For treated piles in brackish water, the longevity should be determined by the experience in the area.

6. Treated marine piles will typically last about 50 years in northern climates and 25 years in southern climates of the United States.

8.3 STEEL H-PILES

Steel H-piles consist of rolled wide flange sections that have flange widths approximately equal the section depth. In most H-pile sections, the flange and web thicknesses are the same. They are manufactured in standard sizes ranging from 200 to 360 mm (8 to 14 inches). In some cases, W-sections are also used for piles. Figure 8.3 contains a photograph of H-piles with driving shoes. A summary of standard H-pile sections including properties needed for design is provided in Appendix C.



Figure 8.3 H-piles with Driving Shoes

H-piles produced today typically meet the requirements of ASTM A572, Grade 50 steel. ASTM A36 steel H-piles are no longer readily available. Steel sections

meeting the requirements of ASTM A588 and ASTM A690 are also available. These steels are high strength, low alloy steels developed for improved corrosion resistance in atmospheric (ASTM A588) and marine (ASTM A690) environments. However, ASTM A588 and A690 steels are typically hard to obtain, and long lead times may be necessary if they are specified. ASTM A572, A588 and A690 steels are all Grade 50 steels. Therefore, it is possible to use the higher strength of the Grade 50 steel if the pile can be installed to sufficient capacity as limited by the soil. Steel H-Piles are very effective when driven into soft rock. They can be driven very hard with modern high impact velocity hammers with little likelihood of pile toe damage.

H-piles are suitable for use as toe bearing piles, and as combination shaft resistance and toe bearing piles. Since H-piles generally displace a minimum amount of soil, they can be driven more easily through dense granular layers and very stiff clays than displacement piles. In addition, the problems associated with soil heave during foundation installation are often reduced by using H-piles. However, sometimes H-piles will "plug". That is, the soil being penetrated will adhere to the web and the inside flange surfaces creating a closed-end, solid section. The pile will then drive as if it were a displacement pile below the depth of plug formation. Plugging can have a substantial effect on both the soil resistance during driving and the ultimate static pile capacity.

Experience indicates that corrosion is not a practical problem for steel piles driven in natural soil, due primarily to the absence of oxygen in the soil. However, in fill materials at or above the water table, moderate corrosion may occur and protection may be needed. As noted above, high strength, low alloy steels are available for improved corrosion resistance. Another common protection method requires the application of pile coatings before and after driving. Coal-tar epoxies, fusion bonded epoxies, metallized zinc, metallized aluminum and phenolic mastics are some of the pile coatings available. Encasement by cast-in-place concrete, precast concrete jackets, or cathodic protection can also provide protection for piles extending above the water table. Another design option for piles subject to corrosion is to select a heavier section than that required by the design loads, anticipating the loss of material caused by corrosion. Corrosion losses can be estimated using the information provided in Section 8.8.1.

One advantage of H-piles is the ease of extension or reduction in pile length. This makes them suitable for nonhomogeneous soils with layers of hard strata or natural

obstructions. Splices are commonly made by full penetration groove welds so that the splice is as strong as the pile in both compression and bending. The welding should always be done by properly qualified welders. Proprietary splices are also commonly used for splicing H-piles. Chapter 22 presents information on typical splices. A steel load transfer cap is not required by AASHTO if the pile head is embedded 305 mm (12 inches) into the concrete pile cap. Pile toe reinforcement using commercially manufactured cast pile shoes is recommended for H-piles driven through or into very dense soil or soil containing boulders or other obstructions. Pile shoes are also used for penetration into sloping rock surfaces. Chapter 22 provides details on available driving shoes.

The disadvantages of H-piles include a tendency to deviate when natural obstructions are encountered. Field capacity verification of H-piles used as friction piles in granular soils based on the penetration resistance (blow count) can also be problematic, and can result in significant length overruns. An H-pile in a granular profile will often not plug during the dynamic loading of pile installation but may plug under the slower static loading condition. Length for length, steel piles tend to be more expensive than concrete piles. On the other hand, steel's high design load for a given weight can reduce pile driving costs.

8.4 STEEL PIPE PILES

Pipe piles consist of seamless, welded or spiral welded steel pipes in diameters typically ranging from 200 to 1220 mm (8 to 48 inches). Still larger sizes are available, but they are not commonly used in land or nearshore applications. Typical wall thicknesses range from 4.5 to 25 mm (0.188 to 1 inch) with wall thicknesses of up to 64 mm (2.5 inches) possible. Open end pipe piles as large as 1830 to 3050 mm (72 to 120 inches) have been used on large projects with significant vessel impact and/or seismic design considerations. Pipe piles should be specified by grade with reference to ASTM A252. In some situations, a contractor may propose to supply used pipe not produced under ASTM standards. Pipe piles not meeting ASTM standards must be evaluated by an engineer for general condition, driveability, and weldability prior to approval. Figure 8.4 contains a picture of a typical smaller diameter closed-end pipe pile and Figure 8.5 presents a photograph of a large open end pipe pile. Appendix C includes a table of dimensions and design properties for pipe piles.



Figure 8.4 Typical Closed-End Pipe Pile



Figure 8.5 Large Diameter Open End Pipe Piles

Steel pipe piles can be used in friction, toe bearing, a combination of both, or as rock socketed piles. They are commonly used where variable pile lengths are required since splicing is relatively easy. Common offshore or nearshore applications of pipe piles include their use as bridge foundation piles, fender systems, and large diameter mooring dolphins. With the increased ductility requirements for earthquake resistant design, pipe piles are being used extensively in seismic areas.

Pipe piles may be driven either open or closed end. If the capacity from the full pile toe area is required, the pile toe should be closed with a flat plate or a conical tip. Pipe piles may be left open or filled with concrete, and they can also have a structural shape such as an H-section inserted into the concrete. Open end pipe piles can be socketed into bedrock (rock socketed piles). In driving through dense materials, open end piles may form a soil plug. The plug makes the pile act like a closed end pile and can significantly increase the pile toe resistance. Plugging is discussed in greater detail in Section 9.10.5. The plug should not be removed unless the pile is to be filled with concrete. Most often, pipe piles are driven from the pile head. However, closed end pipe piles can also be bottom driven using a mandrel.

A closed end pipe pile is generally formed by welding a 12 to 25 mm (0.5 to 1 inch) thick flat steel plate or a conical point to the pile toe. When pipe piles are driven to weathered rock or through boulders, a cruciform end plate or a conical point with rounded nose is often used to prevent distortion of the pile toe. Open ended piles can also be reinforced with steel cutting shoes to provide protection from damage.

Typically, pipe piles are spliced using full penetration groove welds. Proprietary splicing sleeves are available and should be used only if the splice can provide full strength in bending (unless the splice will be located at a distance below ground where bending moments are small). Typical pile splices are described in Chapter 22. The discussion presented under H-piles on corrosion is also applicable to steel pipe piles.

The spin fin pile, Figure 8.6, is a variation of a pipe pile recently introduced along the west coast. It is a pipe pile with an outside thread made of fins that gradually wind around the lower portion of the pile. During driving the pile rotates, but in response to uplift the pile is prevented from twisting. This results in a plugging effect that increases the pile's uplift capacity.



Figure 8.6 760 mm (30 inch) Diameter Spin Fin Pile

8.5 PRECAST CONCRETE PILES

This general classification covers both conventionally reinforced concrete and prestressed concrete piles. Both types can be manufactured by various methods and can be produced in a number of different cross sections. However, precast reinforced concrete piles are rarely used in the U.S. Concrete piles are sometimes cast with a hollow core. The hollow core may be used for a jet pipe (if continuous), for reducing section weight, for placing instrumentation during construction, or for determining pile damage. Precast concrete piles are usually of constant cross section but can also include a tapered section near the pile toe.

Precast concrete piles are suitable for use as friction piles when driven in sand, gravel, or clays. In boulder conditions, a short piece of structural H-section or

"stinger" may be cast into or attached to the pile toe for penetrating through the zone of cobbles and boulders. A rock shoe or "Oslo point" cast into the pile toe can assist seating of concrete piles into a rock surface. Precast concrete piles are capable of high capacities when used as toe bearing piles.

Concrete piles are considered resistant to corrosion but can be damaged by direct chemical attack (from organic soil, industrial wastes or organic fills), electrolytic action (chemical or stray direct currents), or oxidation. There have been cases where concrete piles exhibited serious corrosion problems in sea water. It is desirable in this case that the concrete be as dense as possible. Concrete can be protected from chemical attack by use of special cements and by special coatings as discussed in Section 8.8.

A necessary consideration when dealing with hollow core precast concrete piles driven in water includes the evaluation of internal pressures within the cylinder which can reach bursting pressures and cause vertical cracks during driving. Another concern for piles driven through water is water jet cracking. If a pile is under high tension stresses during driving, small cracks can open and close during each hammer blow. If the cracks are large enough, water can enter the cracks and subsequently be expelled at high velocities. Water jet pressures will often cause concrete deterioration near the cracks. This process can also be accelerated by the high impact compressive forces induced by driving. A high prestressing force in concrete piles can help reduce this danger by resisting tension stresses during driving and thereby reducing the risk of crack development.

8.5.1 Prestressed Concrete Piles

Prestressed concrete piles consist of a configuration similar to a conventional reinforced concrete pile except that the longitudinal reinforcing steel is replaced by the prestressing steel. The prestressing steel may be in the form of strands or wires which are enclosed in a conventional steel spiral and placed in tension. Prestressing steel must conform to ASTM A416, A421, and A882. Due to the effects of prestressing, these piles can usually be made lighter and longer than reinforced concrete piles of the same size.

In cases of extreme environmental conditions epoxy coating has been used on prestressing strand. If this coating is used it should be dusted with sand before the

epoxy sets. Then the strand will have sufficient bond strength to carry the prestress development bond stresses. If an epoxy coating has been used on the strand it should also be used on the tie or spiral reinforcement. However, epoxy coating should not be necessary for prestressed piles since the prestressing force will keep the concrete in compression making deterioration less likely.

Prestressed sections vary from the most common solid square section to a solid octagonal section. In addition, large sections are available but often these sections have internal circular voids.

Prestressed piles can either be pretensioned or post-tensioned. Pretensioned piles are usually cast to their full length in permanent casting beds. Post-tensioned piles are usually manufactured in sections, most commonly cylindrical, and assembled and prestressed to the required pile lengths at the manufacturing plant or on the job site. Figure 8.7 shows typical prestressed concrete pile sections and a square prestressed concrete pile is shown in Figure 8.8. Design data for typical prestressed concrete pile sections is presented in Appendix C

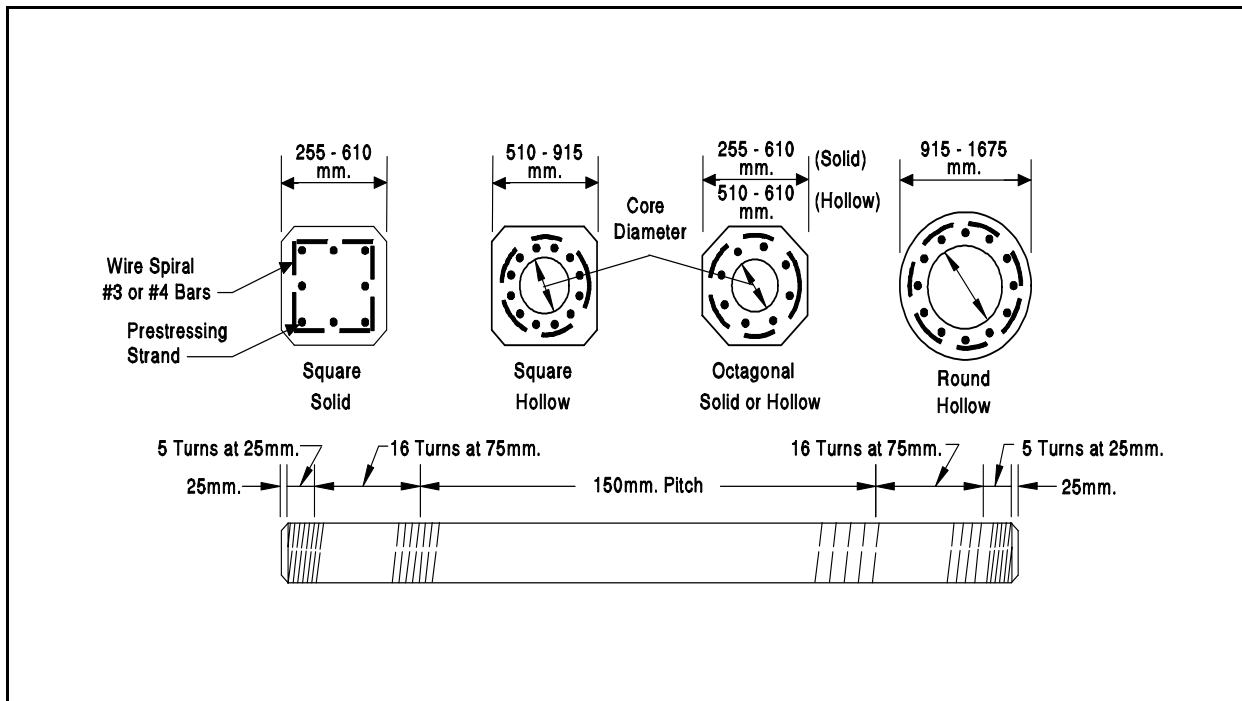


Figure 8.7 Typical Prestressed Concrete Piles (after PCI, 1993)



Figure 8.8 Square Prestressed Concrete Pile

The primary advantage of prestressed concrete piles compared to conventional reinforced concrete piles is durability. Since the concrete is under continuous compression, hairline cracks are kept tightly closed and thus prestressed piles are usually more resistant to weathering and corrosion than conventionally reinforced piles. This characteristic of prestressed concrete removes the need for special steel coatings since corrosion is not as serious a problem as for reinforced concrete. Another advantage of prestressing is that the tensile stresses which can develop in the concrete under certain driving and handling conditions are less critical.

Prestressed concrete piles are more vulnerable to damage from striking hard layers of soil or obstructions during driving than reinforced concrete piles. This is due to the decrease in axial compression capacity which results from the application of the prestressing force. When driven in soft soils, care must also be used since large tension stresses can be generated in easy driving.

Prestressed concrete piles cutoff and splicing problems are considered much more serious by contractors that drive them infrequently than by those that drive only this pile type. Special reinforcement required at the pile head in seismic areas can pose

problems if actual lengths vary significantly from the planned length. In these cases, a splice detail must be included so that the seismic reinforcement is extended into the pile cap.

8.5.2 Reinforced Concrete Piles

These piles are manufactured from concrete and have reinforcement consisting of a steel cage made up of several longitudinal bars and lateral or tie steel in the form of individual hoops or a spiral. Steel reinforcing for reinforced concrete piles is governed by ASTM A82, A615, and A884. High yield strength steel reinforcement must conform to ASTM A722 and may be used to resist uplift loads. Figure 8.9 shows a typical reinforced concrete pile.

Reinforced concrete piles as compared to prestressed piles are more susceptible to damage during handling and driving because of tensile stresses. Advantages of reinforced concrete piles include their lower net compressive stresses during driving and under service loads, and a reduced danger of pile head cracking. In addition, these piles are easier to splice than prestressed piles and thus may be used when variable pile lengths are needed. To avoid corrosion of the reinforced concrete joints, splices should be located below the ground surface, or if under water, the mudline. Segmental pile sections can be used to produce piles with varied lengths to accommodate variable soil conditions, and are easily transported to job sites.

The most common type of jointed pile is a square cross section made of high density concrete with each successive unit of shorter length. Typical pile cross sections range from 250 to 400 mm (10 to 16 inches), but sizes above and below this range are produced. Joints between these pile sections can be of the mechanical type, including bayonet fittings or wedges. The joints must be well aligned or energy will be lost during driving and bending stresses may be introduced due to an eccentric connection. These piles are best suited for friction piles in sand, gravel and clay.

Another jointed reinforced concrete pile type utilizes a hexagonal section. The advantages of this cross sectional shape are an improved stress distribution over the pile section and an improved resistance to torsional loading.

Special precautions should be taken when placing piles during cold weather. If piles are driven through ice and water before reaching soil, the air and concrete

may be at low temperatures relative to the soil and water. Such temperature gradients can cause concrete to crack due to non-uniform shrinkage and expansion. Although most reinforced concrete piles are jointed, there are occasions when non-jointed piles are more economical due to the cost of pile segments. Often for a very large job when thousands of piles will be used, piles can be economically cast on site. Most non-jointed piles have a square cross section and are difficult to change

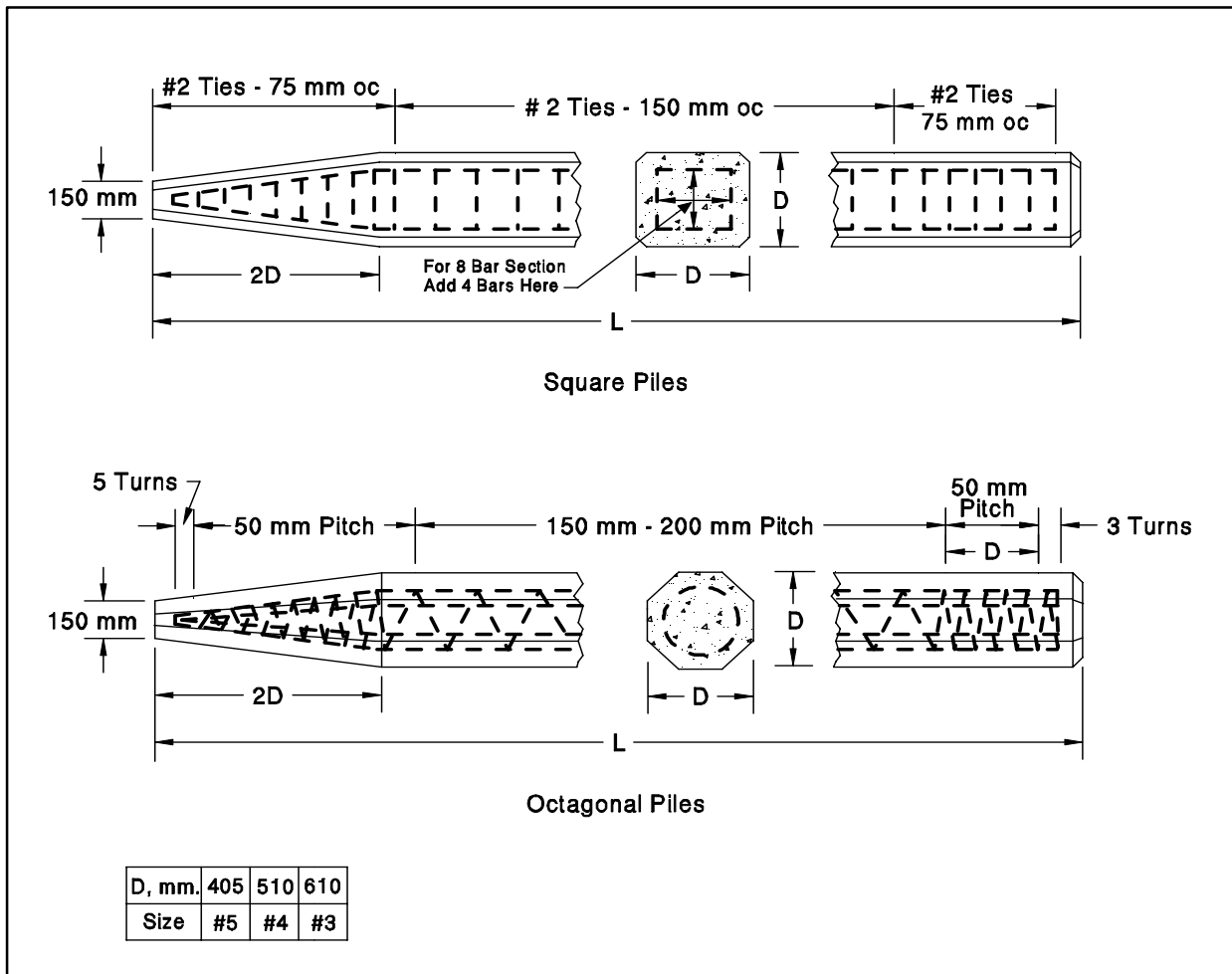


Figure 8.9 Typical Conventionally Reinforced Concrete Pile Details (after PCA, 1951)

in length. Only a few splicing procedures exist if a situation arises where a reinforced concrete pile must be lengthened. The first method of pile lengthening involves the breakdown of the projecting pile head to provide a suitable lap for reinforcing steel. Concrete is cast to form a joint. A second option is to butt the two piles together within a steel sleeve, and use an epoxy cement to join the two piles. The last lengthening method involves the use of dowel bars to be inserted into drilled holes with epoxy cement to form the joint. If piles are lengthened, the connecting pile sections must be carefully aligned, since excessive bending

stresses may result if any eccentricity exists. Splicing problems tend to become less severe or even non-existent when contractors develop experience and techniques. Special reinforcement required at the pile head in seismic areas can pose problems if actual lengths vary significantly from the planned length. In these cases, a splice detail must be included so that the seismic reinforcement is extended into the pile cap.

Reinforced concrete piles are used infrequently in the United States. However, in Europe, Australia, and many Asian countries reinforced concrete piles are used routinely based on economic considerations.

8.5.3 Spun-Cast Concrete Cylinder Piles

Concrete cylinder piles are post-tensioned, hollow concrete piles which are cast in sections, bonded with a plastic joint compound, and then post tensioned in lengths containing several segments. Special concrete is cast by a process unique to cylinder piles which achieves high density and low porosity. The pile is spun centrifugally in the casting process to obtain the high density. The pile is virtually impervious to moisture. Results of chloride ion penetration and permeability tests on prestressed cylinder piles indicate that the spun cylinder piles have excellent resistance to chloride intrusion. Figure 8.10 shows the typical configuration of a cylinder pile. A photograph of a concrete cylinder piles is presented in Figure 8.11. Appendix C provides appropriate engineering design data.

Not all cylinder piles are centrifugally cast. There is now a system where the pile is cast in a bed with forms. These piles are produced to the required length in a single piece and are pretensioned instead of being post tensioned like the spun-cast piles. These piles will not have the high density low porosity concrete that is characteristic of spun-cast cylinder piles and will therefore not have the same resistance to chloride intrusion.

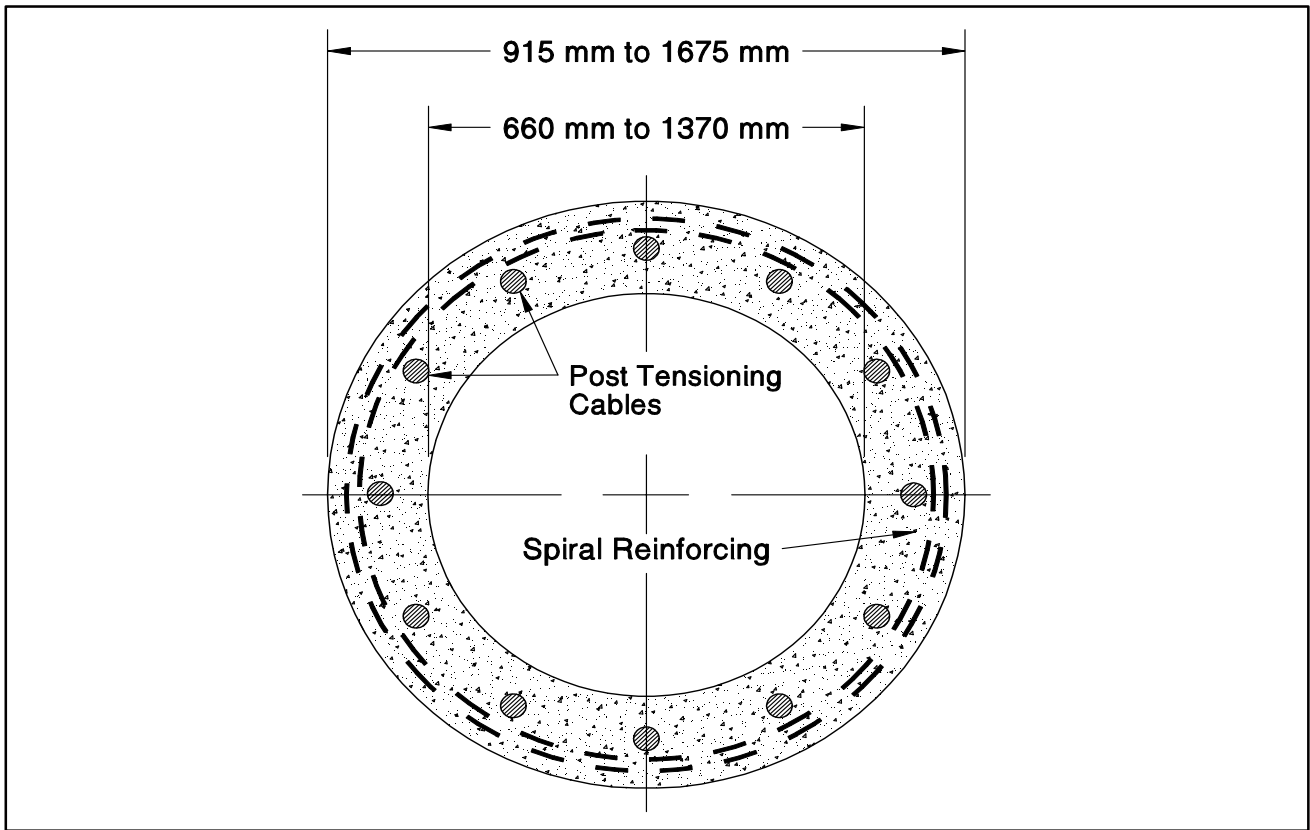


Figure 8.10 Typical Spun-Cast Concrete Cylinder Pile Section



Figure 8.11 Concrete Cylinder Pile

Generally spun-cast cylinder piles are used for marine structures or land trestles and have high resistance to corrosion. In freeze-thaw conditions however, the long term resistance of cylindrical piles is required. The piles typically extend above ground and are designed to resist a combination of axial loads and bending moments. They are available in diameters of 915 to 1675 mm (36 to 66 inches).

Cylinder piles are sometimes quite difficult to drive. However, they usually extend directly to the superstructure support level avoiding the need for a pile cap, which can result in substantial cost savings. Jetting is often used to install cylinder piles to the desired depth. When used, jetting must be controlled to minimize degradation of the lateral soil resistance.

8.6 CAST-IN-PLACE CONCRETE PILES

Cast-in-place concrete piles are installed by placing concrete in a steel shell that has been driven or inserted into a bored hole in the ground. The steel shell or casing may be left in place or withdrawn after the concrete is placed. Concrete is also placed in predrilled holes that are uncased. Predetermination of pile lengths is not as critical as for precast concrete piling.

8.6.1 Cased Driven Shell Concrete Piles

The cased driven shell concrete pile is the most widely used type of cast-in-place concrete pile. There are two principal types of cased piles. One type is driven without a mandrel and the other is driven with a mandrel. A mandrel is usually a heavy tubular steel section inserted into the pile that greatly improves the pile driveability. After driving, the mandrel is removed. Shells driven without mandrels have thicknesses in the range of 3 to 64 mm (0.12 to 2.5 inches). Shells driven with mandrels are much thinner, often 10 to 24 gage or 3.3 to 0.5 mm (0.13 to 0.02 inches) thick. The mandrel driven shells are usually corrugated circumferentially. This results in excellent frictional characteristics and increased collapse strength prior to concrete placement.

After driving, a shell pile is inspected internally along its full length before concrete is placed. Reinforcing steel is required only when the concrete in the pile may be under tension from such conditions as uplift, high lateral loads, or for unsupported

pile lengths. Reinforcing steel may also be used to provide additional axial load capacity.

a. Mandrel Driven Shell Concrete Piles

Mandrel driven shells can be used in most soil conditions except where obstacles such as cobbles and boulders are present that could damage the thin shells during driving. In addition, these thin shells are susceptible to collapse under hydrostatic pressure prior to concrete placement. They are best suited for friction piles in granular material.

The pile shells for mandrel driven piles are often produced from sections of corrugated steel and can be of constant diameter, steadily decreasing in diameter from the pile head to the pile toe, or diameter decreasing in discrete steps over the pile length. Typical tapers are on the order of 25 mm (1 inch) per 2.5 meter (8 ft) length. It is also possible to have different lengths for each section. Separate shell sections are usually screw-connected and waterproofed with an O-ring gasket. The Step Taper, Armco Hel-Cor, Republic Corwel and Guild pile are among the piles driven with mandrels.

The properties of the reusable mandrels dictate the driveability of these shell pile sections. This can result in a significant cost advantage for a mandrel driven shell pile since the mandrels result in improved pile driveability and load capacity at low material costs. Construction control of mandrel driven piles should include a wave equation analysis that accounts for the improved pile driveability from the mandrel. A dynamic formula should not be used for construction control of mandrel driven piles. Mandrel driven piles may be costly if it is necessary to drive piles to an unanticipated depth that exceeds the mandrel length available at the job site.

b. Monotube - Cased Concrete Piles

The Monotube pile, shown in Figure 8.12, is a proprietary pile driven without a mandrel. Monotubes are longitudinally fluted and are tapered over the lower pile length. These piles are available in 3 to 9 gage shell thicknesses or roughly 6 mm to 4 mm (0.23 to 0.15 inches). The fluted and tapered design of Monotube piles has several functional advantages. The flutes add

stiffness necessary for handling and driving lightweight piles. The flutes also increase the surface area while the tapered section improves the capacity per unit length in compression loading. The flutes are formed by cold working when the pile is manufactured. The cold working increases the yield point of the steel to more than 345 MPa (50 ksi), further improving the pile driveability. Monotube sections are spliced by a frictional connection and a fillet weld between a non-tapered extension and the lower pile section into which it is inserted. The manufacturer's recommended splicing detail should be followed. Additional design data for the Monotube pile is included in Appendix C.

c. Pipe - Cased Concrete Piles

Another variation of the cased, cast-in-place pile is the concrete filled pipe pile. These pipe piles can be driven either open or closed end. Closed end piles can be driven conventionally from the pile head, can be bottom driven with a mandrel, or by a mandrel engaged at both the pile head and toe. Open end piles are usually driven from the pile head. Piles that are driven open ended, may require internal clean out if the pile will be concrete filled to some distance below grade. Before concrete placement, steel reinforcement and uplift resisting dowels can be added, as necessary. Open end pipe piles are seldom cleaned out full length unless a rock socket is planned or short pile lengths are used.

d. Fundex Tubex or Grout-Injected Tubex Piles

The Fundex pile is a unique form of a pipe-cased, cast-in-place concrete pile. Instead of the pile being driven into the ground with a hammer, it is screwed into the ground with a special iron drill point which is welded to the end of the first section of pipe. A drill table then forces the pile into the ground utilizing a constant vertical load and torque. When the first pipe section reaches a depth providing sufficient headroom for the attachment of a second pipe section, the second section is welded to the first and drilling is resumed. Depending on the soil conditions, the pipe casing can be installed either grouted or non-grouted. Grouting can be used along the entire pile length or only in the bearing layer of the soil. The grout shell is created by pressure-injecting cement grout throughout the specified pile depth. Once the pile reaches its final design penetration, grouting is

stopped and steel reinforcement is placed. The drill point is left in place at the toe of the pile, providing a waterproof pile toe for concrete filling of the pipe casing.



Figure 8.12 Tapered Monotube Section With Add-on Sections

Some of the advantages of the Fundex Tubex piles include vibrationless and quiet installation, drilling equipment that can be used in confined spaces, and a removable mast that allows installation with only 6 meters (20 ft) of overhead clearance. In addition, the grout-injected Tubex pile can make use of a bentonite-water slurry to lessen frictional drag during installation when grout is not being injected into the soil surrounding the pile wall.

e. Driven and Drilled-In Caisson Piles

The Drilled-In Caisson is a special type of high capacity, cased, cast-in-place pile used for large engineering structures. The casing of this pile is usually a heavy-walled pipe fitted with a drive shoe which is driven to bedrock and sealed off within the rock. Once the casing reaches bedrock, it is cleaned out and a socket is drilled into the rock with rotary drilling

equipment. Next the rock socket is cleaned, and a steel H-shaped core or reinforcing cage is placed before filling the rock socket and cased pipe with concrete.

8.6.2 Uncased Concrete Piles

There are several types of cast-in-place piles that can be classified as uncased piles. Two principal types of uncased piles are bored piles and compacted concrete piles.

a. Bored Piles

Bored piles are installed by drilling or augering a hole in the ground and filling it with concrete. Bored pile installations should be performed carefully by an experienced contractor and with experienced inspection. Bored piles are susceptible to problems such as necking (smaller pile diameter at some locations along their length), grout contamination by soil, or bore hole collapse. Bored, uncased piles have a high degree of risk for structural integrity. There are several types of bored piles and they do not have the advantage of capacity determination from driving observations.

- (1) Auger Cast-in-Place (ACIP) piles are usually installed by turning a continuous-flight hollow-stem auger into the ground to the required depth. As the auger is withdrawn, grout or concrete is pumped under pressure through the hollow stem, filling the hole from the bottom up. Vertical reinforcing steel is pushed down into the grout or concrete shaft before it hardens. Uplift tension reinforcing can be installed by placing a single high strength steel bar through the hollow stem of the auger before grouting. After reinforcing steel is placed, the pile head is cleaned of any lumps of soil which may have fallen from the auger. Then the pile head is formed with a temporary steel sleeve to protect the fresh grout from contamination, or it is formed to the ground surface above the cutoff grade and later trimmed off to the cutoff elevation.
- (2) Drilled shafts are installed by mechanically drilling a hole to the required depth and filling the hole with concrete. Sometimes an

enlarged base is formed mechanically to increase the toe bearing area. Drilling slurry or a temporary liner can be used when the sides of the hole are unstable. Reinforcing steel is installed as a cage inserted prior to concrete placement. Drilled shafts are often used where large toe bearing capacities can be achieved, such as on rock or in glacial tills. They are also used where support is primarily developed through shaft resistance in granular and cohesive soils, and rock. Drilled shafts are sometimes designed with a permanent steel casing.

- (3) Drilled and grouted piles (micropiles) are installed by rotating a casing with a cutting edge into the soil or by percussion methods. Soil cuttings are removed with circulating drilling fluid. Reinforcing steel is then inserted and a sand-cement grout is pumped through a tremie. The bored hole is filled from the bottom up while the casing is withdrawn. These piles are principally used for underpinning work, seismic retrofitting and landslide stabilization. Several types of micropiles leave the casing in place for added bending resistance and axial capacity.
- (4) Helical Screw cast-in-place piles are formed using the Atlas Piling System. The helical piles are displacement piles formed using a single-start auger head with a short flight. The auger head is carried on a hollow stem which transmits a large torque and compressive force as it is screwed into the ground to the required depth. After reinforcement is placed, concrete is poured through the end of the hollow auger and the auger is slowly unscrewed and removed. This process leaves behind a screw-threaded cast-in-place pile with large threads which provide increased surface area for improved shaft resistance. In fact, for a given pile size and volume of concrete, pile capacities are greater than for traditionally constructed bored piles. The disadvantage of this pile type is that the restricted diameter of the reinforcement cage limits the bending capacity.

b. Compacted Concrete Pile

The compacted concrete pile is installed by bottom driving a temporary steel casing into the ground using a drop weight driving on a zero slump concrete plug at the bottom of the casing. When the required depth has been

reached, the steel casing is restrained from above and the concrete plug is driven out the bottom of the tube. An enlarged base is formed by adding and driving out small batches of zero slump concrete.

Steel reinforcing is then installed prior to adding more concrete to the shaft. It is suggested that widely spaced bars be used to allow the low workability mix to penetrate to the exterior of the piles. After the base is formed and reinforcement is placed, concrete continues to be added and the uncased shaft is formed by compacting the concrete with a drop weight in short lifts as the casing is being withdrawn. Alternatively, if a high workability mix is used to complete the pile, a vibrator can be clamped to the top of the tube and used to compact the concrete into place as the casing is withdrawn.

This type of driven, cast-in-place pile is often referred to as a Franki pile or pressure injected footing. The best site conditions for these piles are loose to medium dense granular soils.

8.7 COMPOSITE PILES

In general, a composite pile is made up of two or more sections of different materials or different pile types. Depending upon the soil conditions, various composite sections may be used. The upper pile section is often precast concrete, steel pipe, or corrugated shell. The lower pile section may consist of steel H, steel pipe, or timber pile. Composite piles have limited application and are generally used only under special conditions.

8.7.1 Precast Concrete - Steel Piles

One of the more commonly used composite piles consists of a lower section of steel H, or pipe pile embedded in an upper pile section of precast concrete. These composite sections are often used when uplift requirements dictate penetration depths that a displacement pile cannot achieve, or in waterfront construction where surficial soil layers have high corrosion potential. A photograph of a composite square concrete pile with H-pile stinger is presented in Figure 8.13.

8.7.2 Wood Composite Piles

Timber-steel or timber-concrete composite sections are sometimes used as foundation piles. It is common to have a timber section below the groundwater level with either a concrete or corrosion protected steel upper section. In the case of the composite timber-concrete pile, an untreated timber pile is first driven below the permanent ground water level, then a corrugated steel shell is connected to the pile head of the timber section with a wedge ring driven into the wood. After driving, the shell is filled with concrete to the cutoff elevation and the pile is complete.



Figure 8.13 Square Concrete Pile With Embedded H-pile Section at Pile Toe

8.7.3 Tapertube Pile

Another composite pile type is the Tapertube pile, Figure 8.14. This pile consists of a tapered, 12 sided polygon over the lower section with conventional steel pipe pile material as the upper add-on sections. The 4.6 to 9.1 m (15 to 30 ft) long tapered section steel is available with pile toe diameters ranging from 203 to 356 mm (8 to

14 in) and pile head diameters of 305 to 610 mm. The tapered tube section has a yield strength of 345 MPa (50 ksi), and the upper pipe sections conform to ASTM A252 Grade 3 steel. The tapered and pipe sections are connected using a full penetration weld.



Figure 8.14 Tapered Tube Pile

8.7.4 Pipe - Corrugated Shell Piles

This composite pile consists of a pipe pile for the lower section and a corrugated shell for the upper portion of the pile. A variety of pipe and shell diameters can be used to accommodate a range of loading conditions. The pipe-shell pile is mandrel driven. The mandrel provides a guide for alignment of the two pile sections provided it extends to the pipe pile head or partially into the pipe pile. Possible pile joints include; a sleeve joint, a welded joint, and a drive-sleeve joint. Once the pipe and shell are driven and connected, they are filled with concrete to cutoff grade and any excess shell is removed.

8.7.5 Composite Tapered Precast Tip - (TPT)

The most common form of this composite pile consists of a round, tapered, precast concrete tip, attached at the bottom of a pile shaft. The pile shaft may consist of pipe pile or thin corrugated shell. The precast tip is driven to its designed depth with a mandrel, then the pile shaft is socketed into the precast tip and filled with concrete. Enlarged tip piles can be particularly effective if downdrag forces are present. In addition to the reduced shaft resistance created by driving the enlarged tip, the shaft can be coated or wrapped with a material to further resist downdrag. The enlarged tip provides significant toe bearing capacity.

8.8 DESIGN CONSIDERATIONS IN AGGRESSIVE SUBSURFACE ENVIRONMENTS

In every design, consideration should be given to the possible deterioration of the pile over its design life due to the surrounding environment. This section will address design considerations in aggressive subsurface environments where corrosion, chemical attack, abrasion, and other factors can adversely affect pile durability after installation. An assessment of the in-situ soil conditions, fill materials, and groundwater properties is necessary to completely categorize an aggressive subsurface condition.

An aggressive environment can generally be identified by soil resistivity and pH tests. If either the pH or soil resistivity tests indicate the subsurface conditions are aggressive, then the pile selection and foundation design should be based on an aggressive subsurface environment. The design of pile foundations in an aggressive environment is a developing field. Therefore, a corrosion/degradation specialist should be retained for major projects with pile foundations in aggressive environments.

Whenever the pH value is 4.5 or less, the foundation design should be based on an aggressive subsurface environment. Alternatively, if the resistivity is less than 2000 ohms-cm the site should also be treated as aggressive. When the soil resistivity test results are between 2000 and 5000 ohms-cm then chloride ion content and sulfate ion content tests should be performed. If these test results indicate a chloride ion content greater than 100 parts per million (ppm) or a sulfate ion content greater than 200 ppm, then the foundation design should be based on an

aggressive subsurface environment. Resistivity values greater than 5000 ohms-cm are considered non-aggressive environments. Electro chemical classification tests for aggressive environments are described in Chapter 6.

Contaminated soil and groundwater can cause significant damage to foundation piles in direct contact with the aggressive chemicals. Acidic groundwater is common at sites with either organic soils or industrial contamination. The subsurface exploration program should indicate if the soil or groundwater is contaminated. If industrial contamination is found, the maximum likely concentrations should be determined as well as an estimate of the lateral and vertical extent of the contamination.

8.8.1 Corrosion of Steel Piles

Steel piles driven through contaminated soil and groundwater conditions may be subject to high corrosion rates and should be designed appropriately. Corrosion of steel or steel reinforced piles may also occur if piles are driven into disturbed ground or fill, if piles are located in a marine environment, or if piles are subject to alternate wetting and drying from tidal action. Corrosion rates are a function of the ambient temperature, pH, access to oxygen, and chemistry of the aqueous environment surrounding the steel member.

For steel piles buried in fill or disturbed natural soils, a conservative estimate of the corrosion rate is 0.08 mm per year (0.003 inches per year). Morley (1979) reported corrosion rates of 0.05 mm per year (0.002 inches per year) for steel piles immersed in fresh water, except at the waterline in canals where the rate was as high as 0.34 mm per year (0.013 inches per year). The high rate at the water line was attributed to debris abrasion and/or cell action between other parts of the structure.

AASHTO Standard R 27-01 (2004) provides a recommended assessment procedure for evaluating corrosion of steel piling in non-marine applications. This recommended procedure consists of a Phase I and Phase II assessment. In the Phase I assessment, information on the location of the pile cap relative to the groundwater table, the soil characteristics, and soil contaminants is obtained. This information is used to determine if a Phase II assessment is required.

If the pile cap is at or above the water table, a Phase II assessment is performed to evaluate the corrosivity of the site. The Phase II assessment consists of collecting continuous soil samples to a depth of 1 meter below the water table and conducting

laboratory tests on the recovered samples. The site sampling and testing protocol is outlined in Figure 8.15. After collecting the necessary information, the possibility of uniform or macrocell corrosion is evaluated using the flow chart presented in Figure 8.16. The final step in the evaluation process includes determining the necessity for electrochemical testing, corrosion monitoring, and mitigation techniques. A flow chart of this process is presented in Figure 8.17.

It should be noted that the flow charts do not cover all possibilities for corrosion of steel piling at a site. Factors not covered include chemical contamination, stray DC currents, and the presence of high concentrations of microbes. When these conditions are present on a project, a corrosion specialist should be consulted.

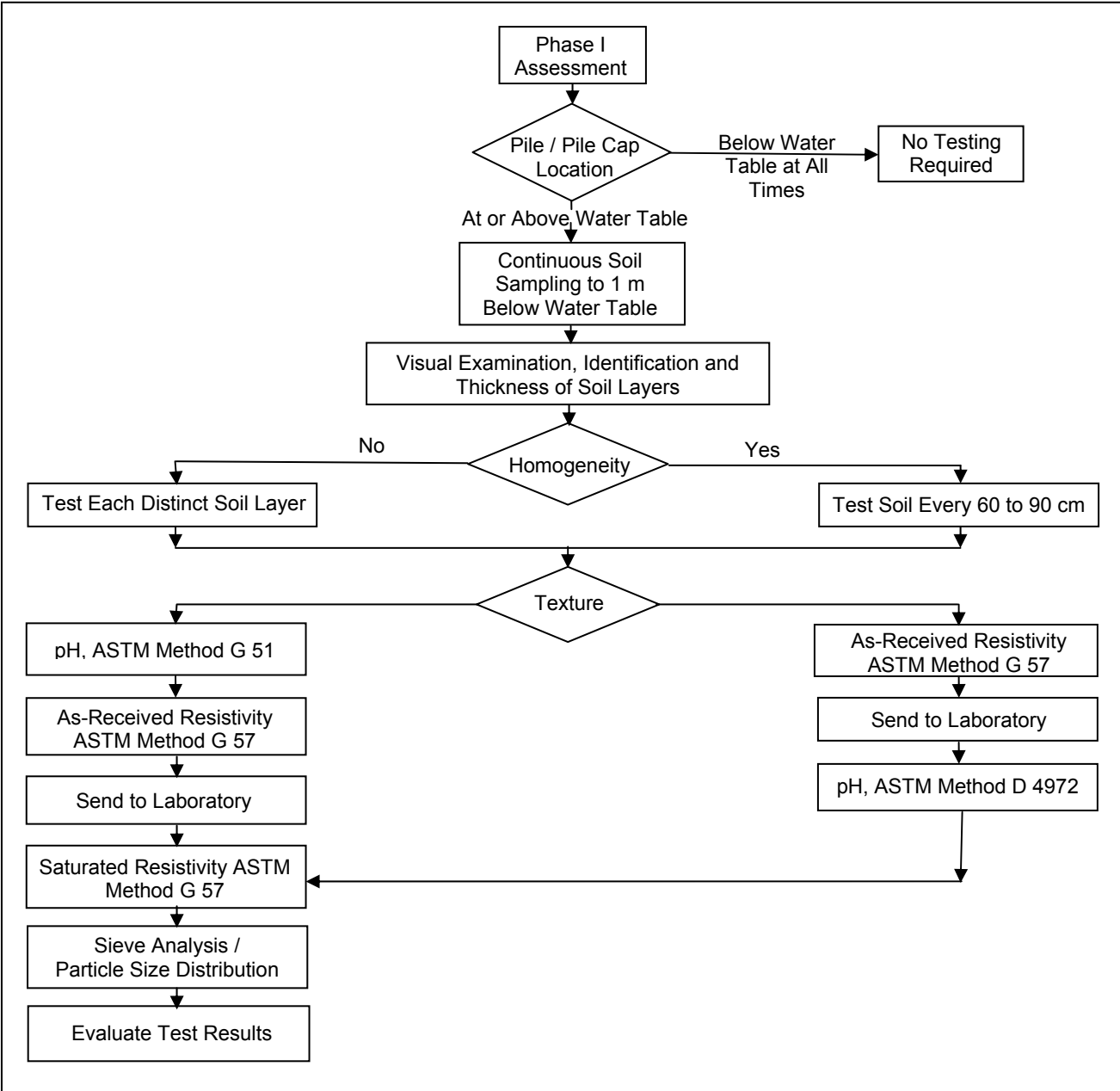


Figure 8.15 Soil Sampling and Testing Protocol for Corrosion Assessment of Steel Piles in Non-Marine Applications

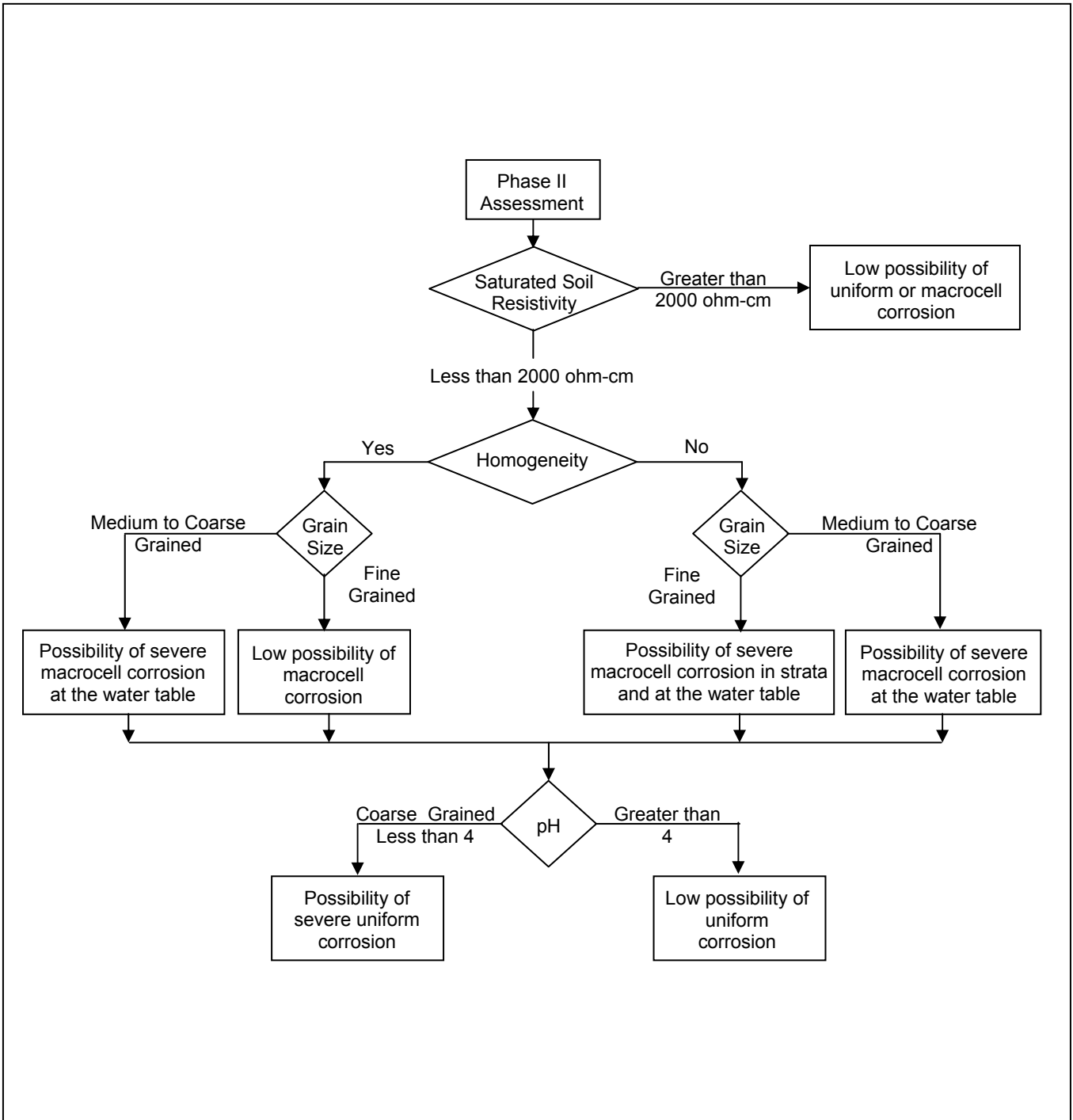


Figure 8.16 Procedure for Uniform or Macrocell Corrosion Assessment of Steel Piles in Non-Marine Applications

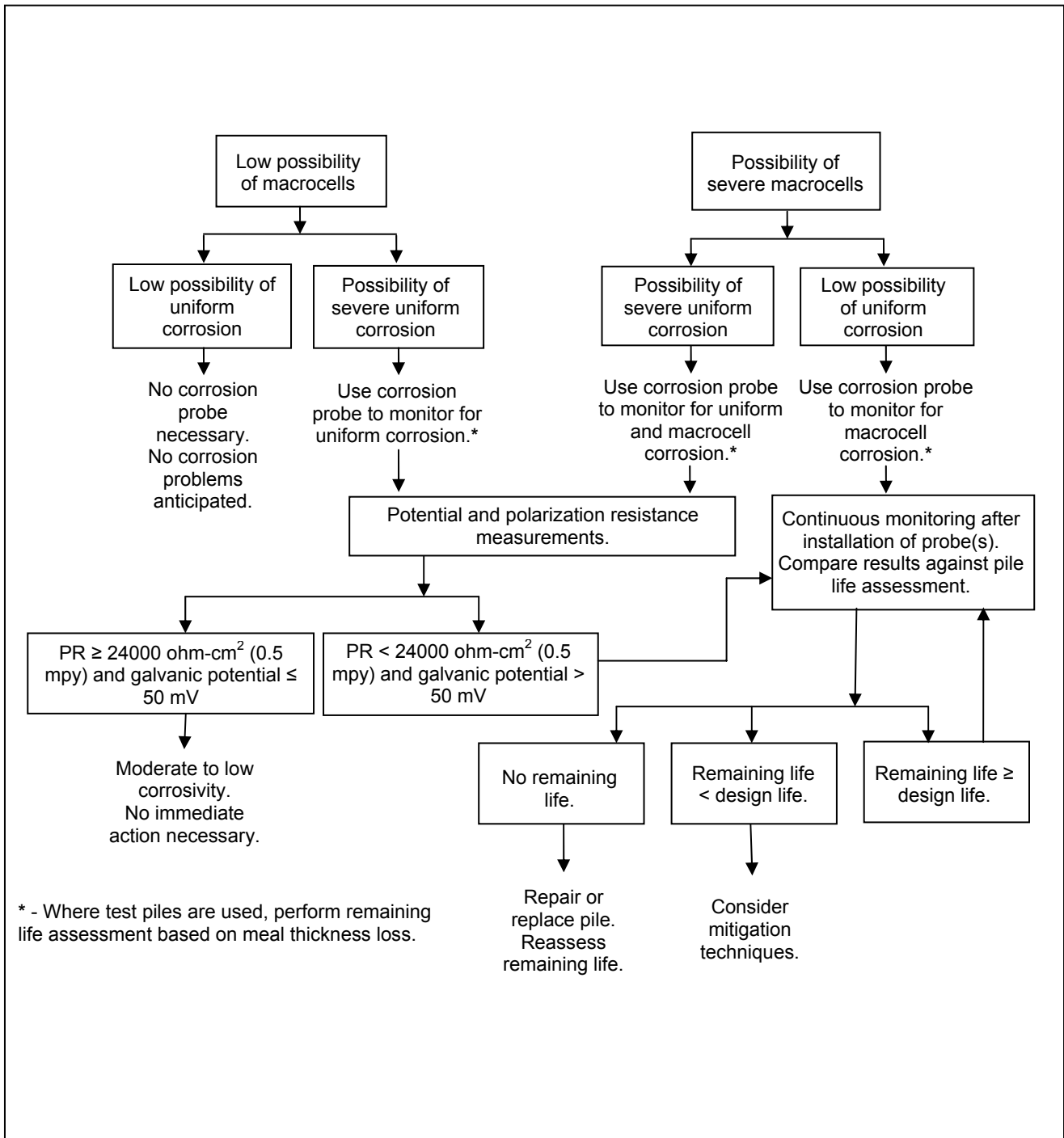


Figure 8.17 Procedure for Determination of Electrochemical Testing, Corrosion Monitoring and Corrosion Mitigation Techniques

ASHTO Standard R 27-01 (2004) should be consulted for a detailed step by step procedure of corrosion evaluation process and estimation of remaining service life. Additional insight into the corrosion of steel piles in non-marine environments is also presented in NCHRP Report 408 by Beavers and Dunn (1998).

For steel piles in marine environments (salt water), separate zones, each with a different corrosion rate, are present along the length of the pile. Tomlinson (1994) identifies these zones as follows:

1. Atmospheric zone: exposed to the damp atmospheric conditions above the highest water level but subject to airborne spray.
2. Splash zone: above the mean high tide, but exposed to waves, spray, and from passing ships.
3. Intertidal zone: between mean high and low tides.
4. Continuous immersion zone: below lowest low tide.
5. Underground zone: below the mudline.

Figure 8.18, after Morley and Bruce (1983), summarizes average and maximum probable marine corrosion rates in these zones as well as in the low water zone.

In corrosive environments, the designer should apply one of the design options for piles in corrosive environments discussed in Section 8.8.4.

8.8.2 Sulfate and Chloride Attack on Concrete Piles

Attack on precast and cast-in-place concrete occurs in soils with high sulfate or chloride concentrations. Factors influencing the rate of attack of sulfates or chlorides on concrete piles include the pH of the soil, the solubility of the sulfate or chloride, the movement of the groundwater relative to the piles, and the density of the pile concrete.

The reaction between concrete and sulfate begins with sulfate ions in solution. Once the sulfate ions in the groundwater come in contact with portland cement, an

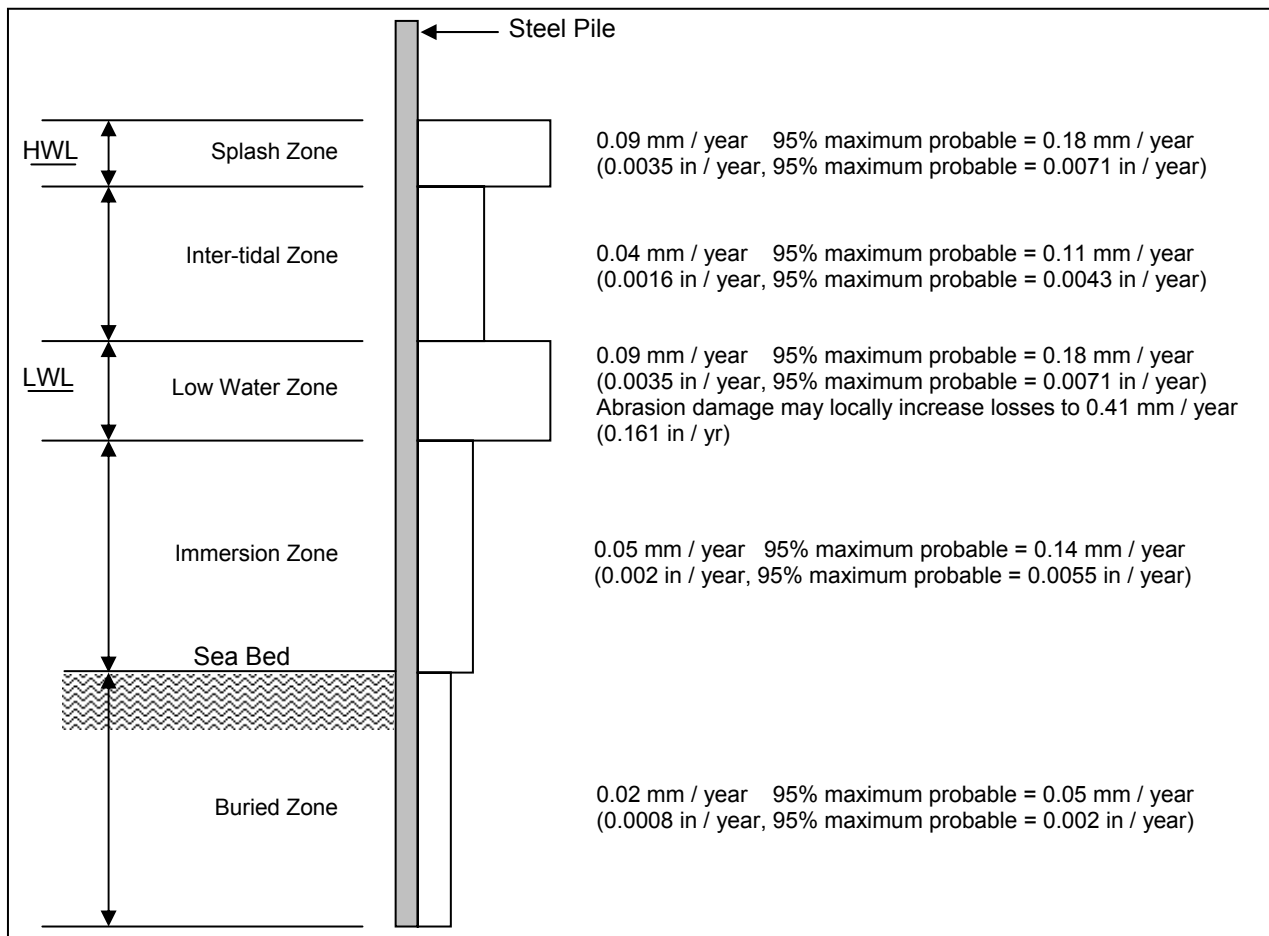


Figure 8.18 Loss of Thickness by Corrosion for Steel Piles in Seawater (after Morley and Bruce, 1983)

expansive chemical reaction takes place. Expansion of concrete often leads to cracking and spalling which can significantly reduce the available structural capacity of a pile foundation.

One method of reducing sulfate attack is to use a dense concrete which is less permeable to sulfate ions. Other possible deterrents include using sulfate-resisting cement, using cement with 25% pozzolanic material, or creating a physical barrier between the concrete and the groundwater with some sort of pile sleeve.

Chlorides are commonly found in soils, groundwater, or industrial wastes. Instead of attacking concrete, chlorides cause corrosion of reinforcement steel with consequential expansion and bursting of concrete as the products of steel corrosion are formed. Once corrosion begins, it continues at an accelerated rate. This can lead to a loss of bond between steel and concrete and extreme reduction of pile

capacity. Protective measures which can reduce corrosion include increased concrete cover around the reinforcing steel, and the use of galvanized, or epoxy coated reinforcement.

8.8.3 Insects and Marine Borers Attack on Timber Piles

Timber piles are subject to insect attack on land by termites and beetles, or in water by marine borers. Incidences of marine borer attack on timber piles have reemerged in some areas as previously polluted water has improved. As mentioned in Section 8.2, arsenate and creosote pressure treatments are the most effective means of protecting timber piles from premature deterioration. In southern waters, creosote must be combined with other preservative treatments because of attack by limnoria tripundata. Table 8-2 provides a summary of AWPI recommended preservative treatments depending upon foundation use, preservative, and wood

Use Category	Creosote (pcf)		Waterborne (CCA or ACZA) (pcf)	
	Southern Pine	Douglas Fir	Southern Pine CCA	Douglas Fir ACZA
Foundation	12	17	0.8	1.0
Land & Fresh Water	12	17	0.8	1.0
Marine (Saltwater) N. of Delaware ¹ or San Francisco ¹	16	16	1.5	1.5
S. of New Jersey ² or San Francisco ²	20	20	2.5	2.5
Dual Treatment ³	20	20	1.0	1.0
Comments: 1. Where Teredo is expected and Limnoria tripunctata is not expected, creosote or creosote solutions provide adequate protection. 2. Where Teredo and Limnoria tripunctata are expected and where pholad attack is not expected, either dual treatment, or high retentions of CCA for Southern Pine or ACZA for Douglas Fir provide maximum protection. 3. In those areas where Limnoria tripunctata and pholad attack is expected or known, dual treatment provides the maximum protection.				

species. Environmental damage from pressure treatments must be a consideration when selecting protection methods.

When designing with timber piles, the wood species is usually not specified unless a specific species of wood is more suitable for design loads and/or environmental conditions. Certain species are not suitable for preservative treatment, while others may provide increased durability. As expected, ASTM standards for timber piles vary with geologic region, as land and fresh water piles have less stringent preservative treatment requirements than piles used in marine environments.

If timber piles are installed in other aggressive environments such as environments containing chemical wastes, a timber pile specialist should be consulted in determining the appropriate preservative treatment.

8.8.4 Design Options for Piles Subject to Degradation or Abrasion

When a pile must be installed in an aggressive or abrasive environment, several design options can be considered. These design options include:

- a. A heavier steel section than required can be used to provide extra thickness (H and pipe sections). This method is not effective in running water with active bedload to scour the corroded surface.
- b. Cathodic protection of steel piles in soil below the water table or in marine environments. Note that this method of protection tends to be a costly solution and requires periodic anode replacement.
- c. Concrete encasement of steel piles above the mud line. This method may alter the impact absorbing properties of the pile.
- d. Use of copper-bearing steel is effective against atmospheric corrosion but cost is greater than conventional steel.
- e. Sleeving or encapsulating of reinforced, cast-in-place piles through use of metal casings or polymer or fiberglass jackets isolates contaminants from concrete.

- f. Use of a low water/cement ratio, resistant aggregate, and minimum air content consistent with the environment to improve abrasion resistance of precast concrete piles
- g. Use of a protective metallic or epoxy paint (isocyanate-cured) or fusion bonded epoxy coating on exposed sections of the pile. This method has the same limitations as (b) in running water.
- h. Use of coal-tar epoxies for corrosion protection in marine environments.

Protective coatings cannot be replaced after a pile is driven. Therefore, if a protective coating is used, the coating should be designed to be durable enough to remain undamaged during pile transportation, handling, and placement in the leads for driving as well as resistant to the abrasion resulting from pile driving. The designer should also note that the shaft resistance on a coated pile may be significantly different than on an uncoated pile, depending on the coating.

8.9 SELECTION OF PILE TYPE AND SIZE FOR FURTHER EVALUATION

The selection of appropriate pile types for any project involves the consideration of several design and installation factors including pile characteristics, subsurface conditions and performance criteria. This selection of elimination process should consider the factors listed in Tables 8-1, 8-3 and 8-4. Table 8-1 summarizes typical pile characteristics and uses. Table 8-3 provides pile type recommendations for various subsurface conditions. Table 8-4 presents the placement effects of pile shape characteristics.

In addition to the considerations provided in the tables, the problems posed by the specific project location and topography must be considered in any pile selection process. Following are some of the usually encountered problems:

1. Vibrations from driven pile installation may affect pile type selection, use of installation, and special techniques such as predrilling and/or vibration monitoring of adjacent structures.
2. Remote areas may restrict driving equipment size and, therefore, pile size.

3. Local availability of certain materials and capability of contractors may have decisive effects on pile selection.
4. Waterborne operations may dictate use of shorter pile sections due to pile handling limitations.
5. Steep terrain may make the use of certain pile equipment costly or impossible.

Often several different pile types meet all the requirements for a particular structure. In such cases, the final choice should be made on the basis of a cost analysis that assesses the over-all cost of the foundation alternatives. This requires that candidate pile types be carried forward in the design process for determination of the pile section requirements for design loads and constructability. The cost analysis should also include uncertainties in execution, time delays, cost of load testing programs, as well as the differences in the cost of pile caps and other elements of the structure that may differ among alternatives. For major projects, alternate foundation designs should be considered for inclusion in the contract documents if there is a potential for cost savings.

TABLE 8-3* PILE TYPE SELECTION BASED ON SUBSURFACE AND HYDRAULIC CONDITIONS	
TYPICAL PROBLEM	RECOMMENDATIONS
Boulders overlying bearing stratum	Use heavy nondisplacement pile with a point and include contingent predrilling item in contract.
Loose cohesionless soil	Use tapered pile to develop maximum skin friction.
Negative shaft resistance	Use smooth steel pile to minimize drag adhesion. Use bitumen coating or plastic wrap (if feasible) as pile-soil bond breaker or increase design stress. Avoid use of batter piles.
Deep soft clay	Use rough concrete piles to increase adhesion and rate of pore water dissipation.
Artesian pressure	Use solid prestressed concrete pile, tapered piles with sufficient collapse strength or thick wall closed end pipe with flush boot plate depending upon local practice. H-piles without driving shoes may also be viable selection. Do not use mandrel driven thin-wall shells, as generated hydrostatic pressure may cause shell collapse. Pile heave also common to closed-end pile.
Scour	Use uniform section pile with sufficient structural strength to act as a column through scour zone. Do not use tapered piles unless a large part of the taper extends well below scour depth; design permanent pile capacity to mobilize soil resistance below scour depth.
Coarse gravel deposits	Use prestressed concrete piles where hard driving is expected. In coarse soils use of H-piles and open end pipe piles often results in excessive pile lengths.

* Table modified and reproduced (Cheney and Chassie, 1993).

TABLE 8-4* PILE TYPE SELECTION PILE SHAPE EFFECTS		
SHAPE CHARACTERISTICS	PILE TYPE	PLACEMENT EFFECT
Displacement	Closed end steel pipe	Increase lateral ground stress.
	Precast concrete	Densifies cohesionless soils, remolds and weakens cohesive soils temporarily. Setup time for large pile groups in sensitive clays may be up to six months.
Nondisplacement	Steel H	Minimal disturbance to soil.
	Open end steel pipe	Not suited for friction piles in coarse granular soils. Piles often have low driving resistances in these deposits making field capacity verification difficult thereby often resulting in excessive pile lengths.
Tapered	Timber Monotube Tapertube Thin-wall shell	Increased densification of soil, high capacity for short length in granular soils.

* Table modified and reproduced (Cheney and Chassie, 1993).

REFERENCES

- American Concrete Institute (1974). Recommendations for Design, Manufacture and Installation of Concrete Piles. ACI-543.
- American Wood Preservers Institute [AWPI] (2002), Timber Pile Design and Construction Manual.
- AASHTO Standard R 27-01, Standard Recommended Practice for Assessment of Corrosion of Steel Piling for Non-Marine Applications (2004), AASHTO Standard Specifications for Transportation Materials and Methods of Sampling and Testing, Part 1B: Specifications, 24th Edition.
- Beavers, J.A. and Durr, C.L. (1998). Corrosion of Steel Piling in Non-Marine Applications. NCHRP Report 408, National Cooperative Highway Research Program, Transportation Research Board, Washington, D.C.
- Chellis, R.D. (1961). Pile Foundations. McGraw-Hill Book Company.
- Cheney, R.S. and Chassie, R.G. (2000). Soils and Foundations Workshop Reference Manual. Publication No. FHWA HI-00-045, U.S. Department of Transportation, National Highway Institute, Federal Highway Administration, Washington, D.C., 358.
- Department of the Navy, Naval Facilities Engineering Command, NAVFAC (1982). Foundations and Earth Structures, Design Manual DM 7.2.
- Fleming, W.G.K., Weltman, A.J., Randolph, M.F. Elson, W.K. (1992). Piling Engineering, John Wiley and Sons, Inc., New York.
- Fuller, F.M. (1983). Engineering of Pile Installations. McGraw-Hill, New York. 286.
- Graham, J. (1995). Personal Communication.
- Portland Cement Association [PCA], (1951). Concrete Piles: Design, Manufacture and Driving.

PCI (1993), Precast/Prestressed Concrete Institute Journal, Volume 38, No. 2, March-April, 1993.

Prakash, S. and Sharma, H. (1990). Pile Foundations in Engineering Practice. John Wiley and Sons, Inc., New York.

Morley, J., (1979). The Corrosion and Protection of Steel Piling, British Steel Corporation, Teesside Laboratories.

Morley, J. and Bruce, D.W., (1983). Survey of Steel Piling Performance in Marine Environments, Final Report, Commission of the European Communities, Document EUR 8492 EN.

Rausche, F. (1994). Design, Installation and Testing of Nearshore Piles. Proceedings of the 8th Annual Symposium on Deep Foundations, Vancouver.

Tomlinson, M.J., (1994). Pile Design and Construction Practice, Fourth Edition, E & FN Spon, London 357-372.

Transportation Research Board, (1977). Design of Pile Foundations NCHRP Synthesis of Highway Practice No. 42.

Chapter 9

STATIC ANALYSIS METHODS

Static analysis methods can be categorized as analytical methods that use soil strength and compressibility properties to determine pile capacity and performance. This chapter will focus on analysis methods for determining compression, uplift, and lateral load capacity of single piles and pile groups. Important considerations are as follows:

1. Static analysis methods are an integral part of the design process. Static analysis methods are necessary to determine the most cost effective pile type and to estimate the number of piles and the required pile lengths for the design of substructure elements. The foundation designer must have knowledge of the design loads and the structure performance criteria in order to perform the appropriate static analyses.
2. Many static analysis methods are available. The methods presented in this chapter are relatively simple methods that have proven to provide reasonable agreement with full scale field results. Other more sophisticated analysis methods may be used and in some cases may provide better results. Regardless of the method used, it is important to continually apply experience gained from past field performance of the analysis method.
3. Designers should fully understand the basis for, the limitations of, and the applicability of a chosen method. A selected method should also have a proven agreement with full scale field results.

Construction procedures can have a significant influence on the behavior of pile foundations. The analysis methods described in this chapter lead to successful designs of deep foundations only if adequate construction techniques are used. Construction inspection should be an integral part of the design and construction of any foundation. Static load tests, wave equation analysis or dynamic monitoring for construction control should, whenever possible, be used to confirm the results of a static design method. These items are discussed in greater detail in subsequent chapters.

The first few sections of this chapter will briefly cover background information. Static analysis procedures for piles subject to compression, uplift and lateral loads will be covered, as well as pile group settlement. The influence of special design events on static design will be discussed. Limited guidance on design in liquefaction susceptible soils will be provided. However, seismic design is a special design event beyond the scope of this

manual. Last, the chapter will address construction issues pertinent to static analysis methods and foundation design.

9.1 BASICS OF STATIC ANALYSIS

There are four general types of static analyses covered in this chapter. Static analyses are performed to determine:

1. Ultimate axial compression capacity of a pile or pile group. These calculations are performed to determine the long term capacity of a foundation as well as to determine the soil resistance provided from soil layers subject to scour, liquefaction, or that are otherwise unsuitable for long term support. Static analyses are used to establish minimum pile penetration requirements, pile lengths for bid quantities, as well as to estimate the ultimate soil resistance at the time of driving (SRD).
2. Ultimate uplift capacity of a pile or pile group. These calculations are performed to determine the soil resistance to uplift or tensile loading which, in some cases, may also determine the minimum pile penetration requirements.
3. Ultimate lateral resistance of a pile or pile group. These soil-structure interaction analysis methods consider the soil strength and deformation behavior as well as the pile structural properties and are used in pile section selection.
4. Settlement of a pile group. These calculations are performed to estimate the foundation deformation under load the structure loads.

The static capacity of a pile can be defined as the sum of soil/rock resistances along the pile shaft and at the pile toe available to support the imposed loads on the pile. As noted above, static analyses are performed to determine the ultimate capacity of an individual pile and of a pile group as well as the deformation response of a pile group to the applied loads.

The ultimate capacity of an individual pile and of a pile group is the smaller of: (1) the capacity of surrounding soil/rock medium to support the loads transferred from the pile(s) or, (2) the structural capacity of the pile(s). Soil-structure interaction analysis methods are used to determine the deformation response of piles and pile groups to lateral loads. The results from these analyses as well as the results of static analysis of pile group settlement are compared to the performance criteria established for the structure.

The static pile capacity from the sum of the soil/rock resistances along the pile shaft and at the pile toe can be estimated from geotechnical engineering analysis using

1. Laboratory determined shear strength parameters of the soil and rock surrounding the pile.
2. Standard Penetration Test data.
3. In-situ test data (*i.e.*, CPT/CPTU).

On many projects, multiple static analyses are required for a design. First, a static analysis is necessary to determine the number and length of piles necessary to support the structure loads. A second static analysis may also be required to determine the total soil resistance the pile will encounter during installation. This second analysis enables the design engineer to determine the necessary capability of the driving equipment. Figures 9.1 and 9.2 illustrate situations that require two static analyses.

Figure 9.1 shows a situation where piles are to be driven for a bridge pier. In this case, the first static analysis performed should neglect the soil resistance in the soil zone subject to scour, since this resistance may not be available for long term support. The number of piles and pile lengths determined from this analysis will then be representative of the long term conditions in the event of scour. At the time of pile driving however, the scour zone soil will provide resistance to pile penetration. Therefore, a second static analysis is required to estimate the total resistance encountered by the pile during driving to the embedment depth determined in the first analysis. The second static analysis includes the soil resistance in the materials above the scour depth as well as the underlying strata.

Figure 9.2 shows another frequently encountered situation in which piles are driven through loose uncompacted fill material into the natural ground. The loose fill material offers unreliable resistance and is usually neglected in determining the number of piles and the pile lengths required. A second static analysis is then performed to determine total resistance encountered by the pile during driving, which includes the resistance in the fill material. In both examples, the soil resistance to be overcome during driving will be substantially greater than the required ultimate pile capacity.

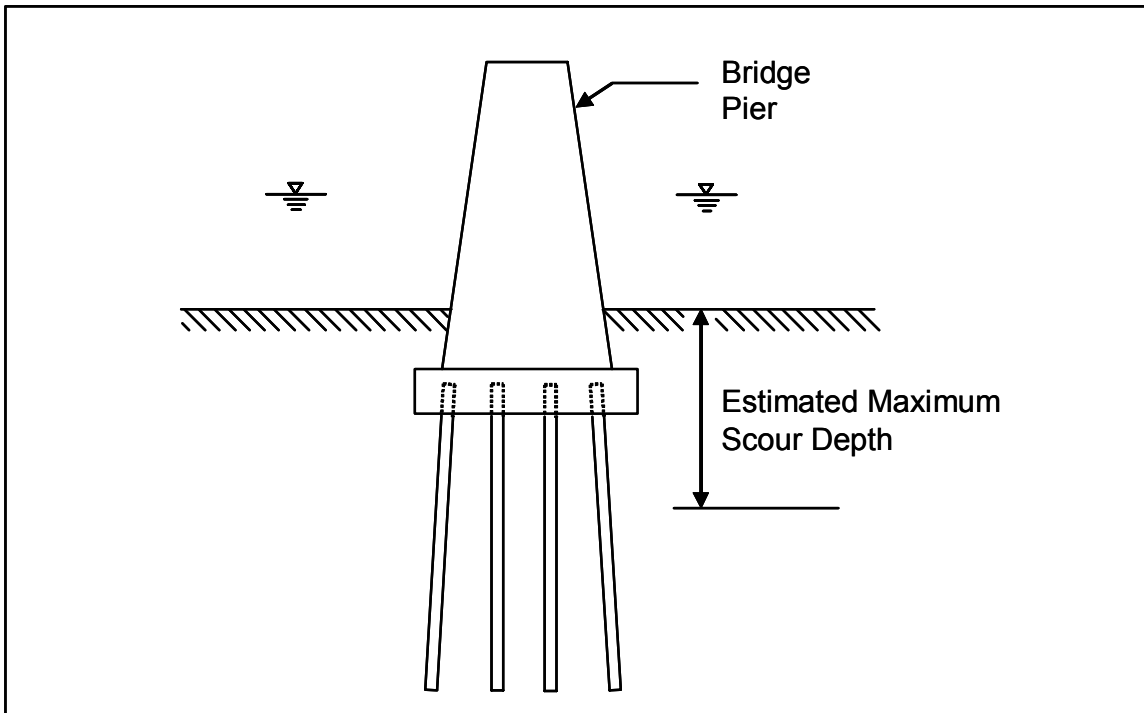


Figure 9.1 Situation Where Two Static Analyses are Necessary – Due to Scour

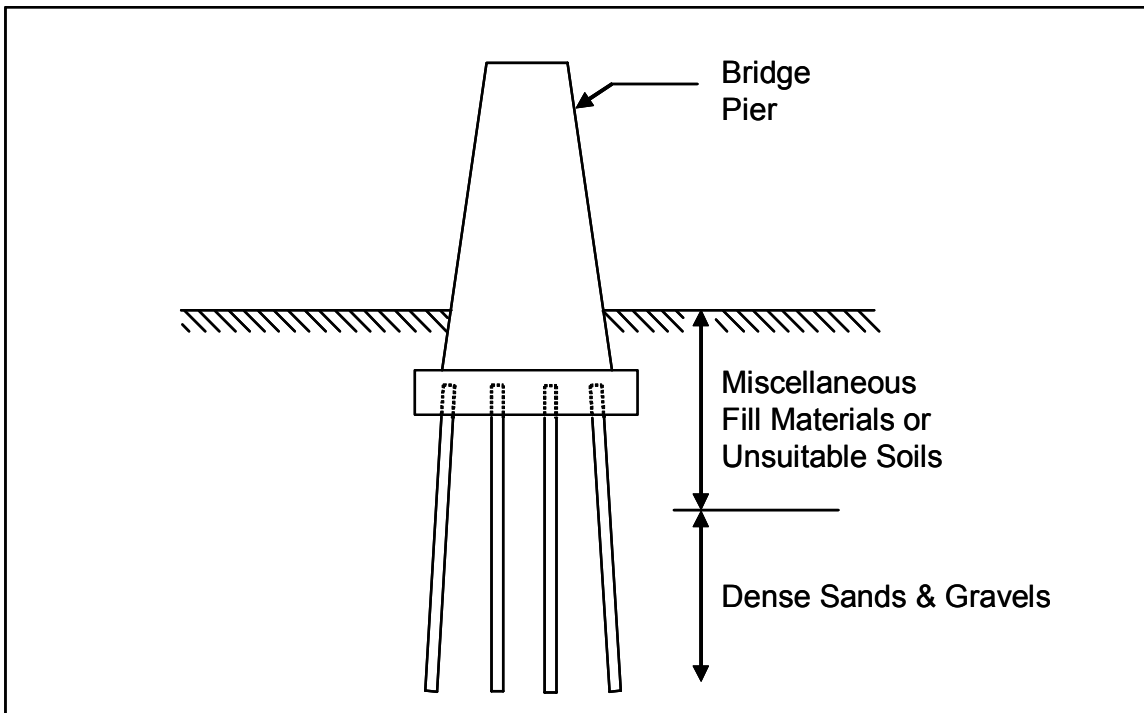


Figure 9.2 Situation Where Two Static Analyses are Necessary – Due to Fill Materials

The results of multiple static analyses should be considered in the development of project plans and specifications. For example, consider a case where scour, uplift loading, or some other special design event dictates that a greater pile penetration depth be achieved than that required for support of the axial compressive loads. The static analyses indicate that 2000 kN (450 kips) of soil resistance must be overcome to obtain the minimum penetration depth for a 1400 kN (315 kip) ultimate capacity pile. This information should be conveyed in the construction documents so that the driving equipment can be properly sized and so that the intent of the design is clearly and correctly interpreted by the contractor and construction personnel. Specifying only a 1400 kN (315 kip) ultimate capacity pile, without including a minimum penetration requirement and the soil resistance to be overcome, can lead to construction claims.

Prior to discussing static design methods for estimating pile capacity in detail, it is desirable to review events that occur in the pile-soil system during and after pile driving as well as basic load-transfer mechanisms.

9.2 EVENTS DURING AND AFTER PILE DRIVING

The soil in which a pile foundation is installed is almost always disturbed. Several factors influence the degree of disturbance. These include the soil type and density, the pile type (displacement, non-displacement), and the method of pile installation (driven, drilled, jetted). **For driven piles, substantial soil disturbance and remolding is unavoidable.**

9.2.1 Cohesionless Soils

The capacity of piles driven into cohesionless soil depends primarily on the relative density of the soil. During driving, the relative density of loose to medium dense cohesionless soil is increased close to the pile due to vibrations and lateral displacement of soil. This effect is most pronounced in the immediate vicinity of displacement piles. Broms (1966) and more recent studies found the zone of densification extends as far as 3 to 5.5 diameters away from the pile shaft and 3 to 5 diameters below the pile toe as depicted in Figure 9.3.

The increase in relative density increases the capacity of single piles and pile groups. The pile type selection also affects the amount of change in relative density. Piles with large displacement characteristics such as closed-end pipe and precast concrete increase the relative density of cohesionless material more than low displacement open-end pipe or steel H-piles.

The increase in horizontal ground stress, which occurs adjacent to the pile during the driving process, can be lost by relaxation in dense sand and gravels. The relaxation phenomenon occurs as the negative pore pressures generated during driving are dissipated. The negative pore pressures occur because of volume change and dilation of dense sand. The phenomena can be explained by considering the following effective stress shear strength equation.

$$\tau = c + (\sigma - u) \tan \phi$$

Where: τ = Shear strength of soil.
 c = Cohesion.
 σ = Vertical (normal) pressure.
 u = Pore water pressure.
 ϕ = Angle of internal friction.

Negative pore pressures temporarily increase the soil shear strength, and therefore pile capacity, by changing the $(\sigma - u) \tan \phi$ component of shear strength to $(\sigma + u) \tan \phi$. As negative pore pressures dissipate, the shear strength and pile capacity decrease.

The pile driving process can also generate high positive pore water pressures in saturated cohesionless silts and loose to medium dense fine sands. Positive pore pressures temporarily reduce the soil shear strength and the pile capacity. This phenomena is identical to the one described below for cohesive soils. The gain in capacity with time or soil set-up is generally quicker for sands and silts than for clays because the pore pressures dissipate more rapidly in cohesionless soils than in cohesive soils.

9.2.2 Cohesive Soils

When piles are driven into saturated cohesive materials, the soil near the piles is disturbed and radially compressed. For soft or normally consolidated clays, the zone of disturbance is generally within one pile diameter around the pile. For piles driven into saturated stiff clays, there are also significant changes in secondary soil structure (closing of fissures) with remolding and loss of previous stress history effects in the immediate vicinity of pile. Figure 9.4 illustrates the disturbance zone for piles driven in cohesive soils as observed by Broms (1966). This figure also notes the ground heave that can accompany driving displacement piles in cohesive soils.

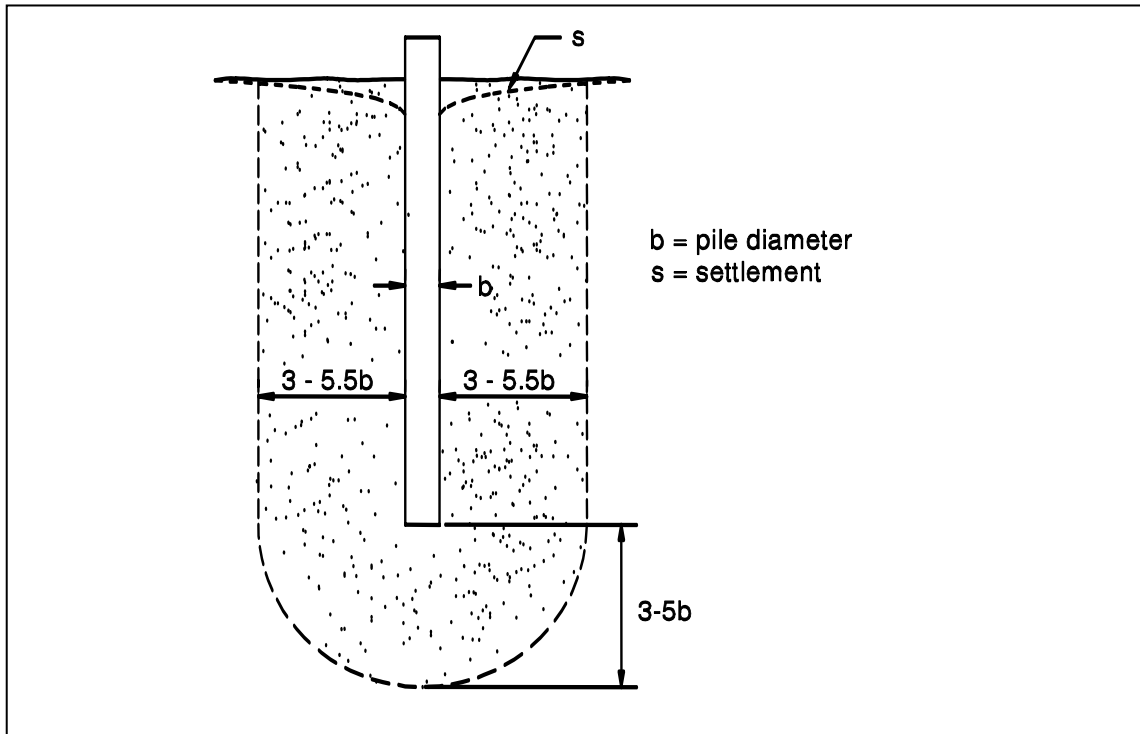


Figure 9.3 Compaction of Cohesionless Soils During Driving of Piles (Broms, 1966)

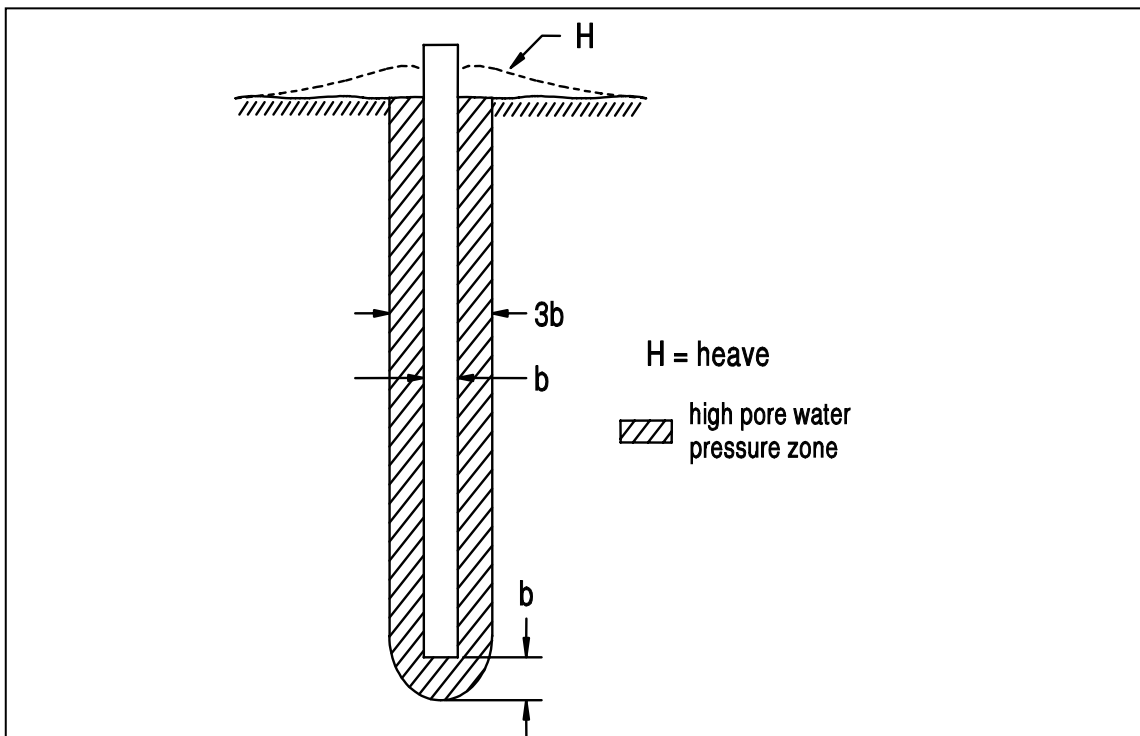


Figure 9.4 Disturbance of Cohesive Soils During Driving of Piles (Broms, 1966)

The disturbance and radial compression generate high pore pressures (positive pore pressures) which temporarily reduce soil shear strength, and therefore the load capacity of the pile. As reconsolidation of clay around the pile occurs, the high pore pressures are diminished, which leads to an increase in shear strength and pile capacity (setup). This phenomenon is opposite to "relaxation" described for cohesionless soils. The zone and magnitude of soil disturbance are dependent on the soil properties of soil sensitivity, driving method, and the pile foundation geometry. Limited data available for partially saturated cohesive soils indicates that pile driving does not generate high pore pressures and hence significant soil setup does not occur.

9.3 LOAD TRANSFER

The ultimate pile capacity, Q_u , of a pile in homogeneous soil may be expressed by the sum of the shaft resistance R_s and toe resistance R_t , or

$$Q_u = R_s + R_t$$

This may also be expressed in the form

$$Q_u = f_s A_s + q_t A_t$$

where f_s is the unit shaft resistance over the shaft surface area, A_s , and q_t is the unit toe resistance over the pile toe area, A_t . The above equations for pile bearing capacity assume that both the pile toe and the pile shaft have moved sufficiently with respect to the adjacent soil to simultaneously develop the ultimate shaft and toe resistances. Generally, the displacement needed to mobilize the shaft resistance is smaller than that required to mobilize the toe resistance. This simple rational approach has been commonly used for all piles except very large diameter piles.

Figure 9.5 illustrates typical load transfer profiles for a single pile. The load transfer distribution can be obtained from a static load test where strain gages or telltale rods are attached to a pile at different depths along the pile shaft. Figure 9.5 shows the measured axial load, Q_u , in the pile plotted against depth. The shaft resistance transferred to the soil is represented by R_s , and R_t represents the resistance at the pile toe. In Figure 9.5(a), the load transfer distribution for a pile with no shaft resistance is illustrated. In this case the full axial load at the pile head is transferred to the pile toe. In Figure 9.5(b), the axial load

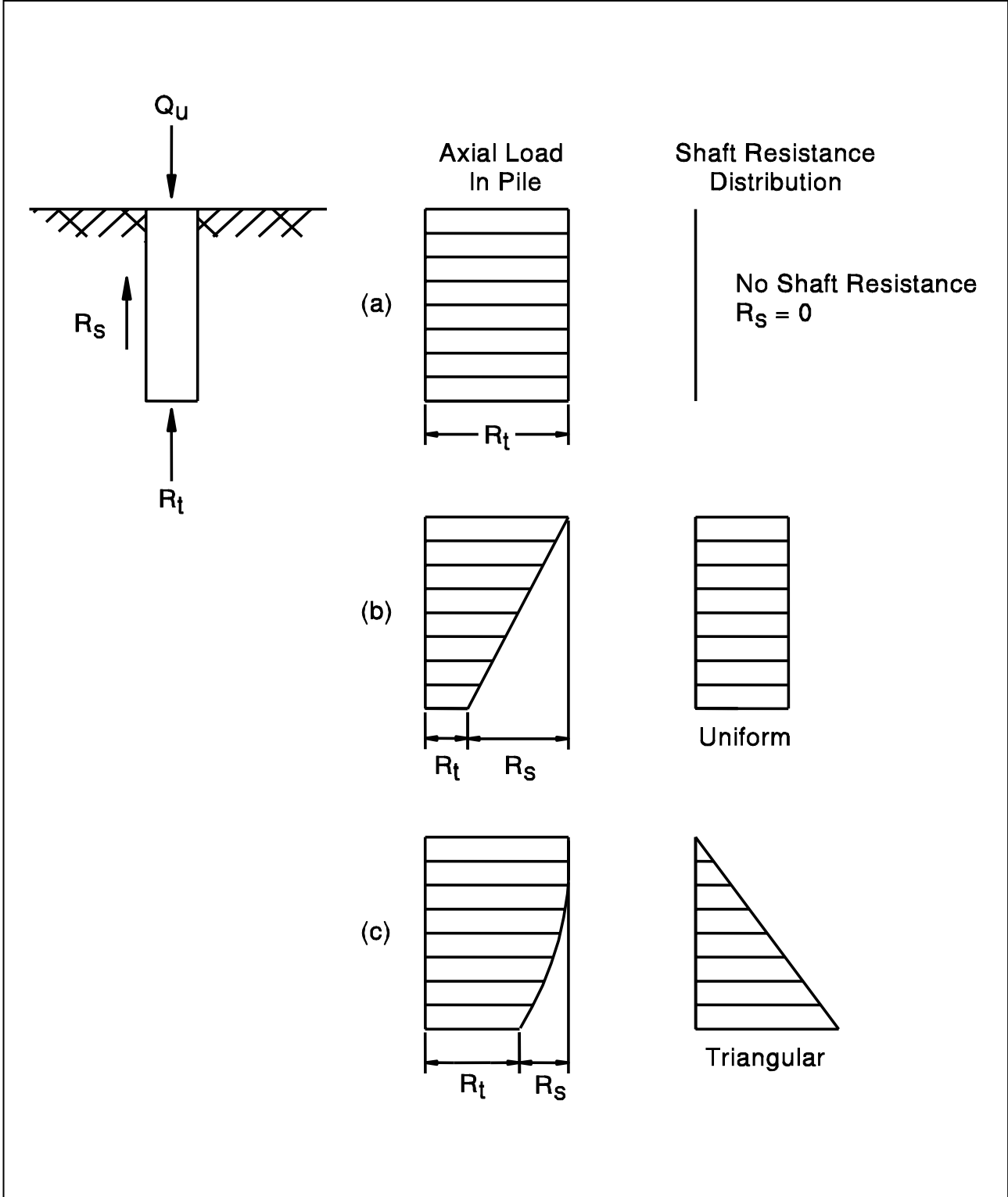


Figure 9.5 Typical Load Transfer Profiles

versus depth for a uniform shaft resistance distribution typical of a cohesive soil is illustrated. Figure 9.5(c) presents the axial load in the pile versus depth for a triangular shaft resistance distribution typical of cohesionless soils.

9.4 EFFECTIVE OVERBURDEN PRESSURE

The effective overburden pressure at a given depth below ground surface is the vertical stress at that depth due to the weight of the overlying soils. A plot of effective overburden pressure versus depth is called a " p_o Diagram" and is used in many static pile capacity and settlement calculations. Therefore, an understanding of how to construct and use a p_o Diagram is important.

Information needed to construct a p_o Diagram includes the total unit weight and thickness of each soil layer as well as the depth of the water table. The soil layer thickness and depth of the water table should be available from the project boring logs. The total unit weight of each soil layer may be obtained from density tests on undisturbed cohesive samples or estimated from Standard Penetration Test (SPT) N values in conjunction with the soil visual classification.

The first step in constructing a p_o Diagram is to calculate the total overburden pressure, p_t , versus depth. This is done by summing the product of the total unit weight times the layer thickness versus depth. Similarly, the pore water pressure, u , is summed versus depth by multiplying the unit weight of water, γ_w , of 9.8 kN/m^3 (62.4 lbs/ft^3), times the water height. The effective overburden pressure, p_o , at any depth is then the total overburden pressure minus the pore water pressure at that depth.

The effective overburden pressure at any depth is determined by summing the weights of all layers above that depth as follows:

1. For soil deposits above the static water table:

$$p_o = (\text{total soil unit weight, } \gamma)(\text{thickness of soil layer above the desired depth}).$$

2. For soil deposits below the static water table:

$$p_o = (\text{total soil unit weight, } \gamma)(\text{depth}) - (\text{unit weight of water, } \gamma_w)(\text{height of water}).$$

This may also be expressed as the buoyant or effective unit weight, γ' , ($\gamma' = \gamma - \gamma_w$):
 $p_o = (\text{buoyant unit weight, } \gamma') (\text{depth}).$

Figures 9.6 and 9.7 present examples of p_o diagrams for cases where the water table is above and below the ground surface level.

9.5 CONSIDERATIONS IN SELECTION OF DESIGN SOIL STRENGTH PARAMETERS

Most of the static analysis methods in cohesionless soils directly or indirectly utilize the soil friction angle, ϕ , in calculation of pile capacity. The soil friction angle may be determined from laboratory tests as described in Chapter 6, or may be estimated using corrected Standard Penetration Test (SPT) N values and the empirical values in Table 4-6. The designer should be aware of the many factors that can influence SPT N values discussed in Section 4.5.1 of Chapter 4 when selecting a design friction angle based on SPT values.

In coarse granular deposits, the selection of the design friction angle should be done conservatively. A comparison of ultimate pile capacities from static load test results with static analysis predictions indicates that static analyses often overpredict the shaft resistance in these deposits. This is particularly true for coarse granular deposits comprised of uniform sized or rounded particles. Cheney and Chassie (1993) recommend limiting the shearing resistance by neglecting particle interlock forces. For shaft resistance calculations in gravel deposits, this results in a maximum ϕ angle of 32° for gravels comprised of soft rounded particles, and in a maximum ϕ angle of 36° for hard angular gravel deposits. The ϕ angle used to calculate the toe resistance is determined using normal procedures.

Static analysis methods used for design of pile foundations in cohesive soils require accurate assessment of the soil shear strength and consolidation properties. This information should be obtained from laboratory tests on undisturbed samples as described in Chapter 6 and/or from in-situ testing as described in Chapter 5. Designs based solely on strength and compressibility information estimated from SPT N values from disturbed soil samples should be avoided.

Additional guidance on the selection of design soil strength parameters may be found in Geotechnical Engineering Circular 5 by Sabatini *et al.* (2002).

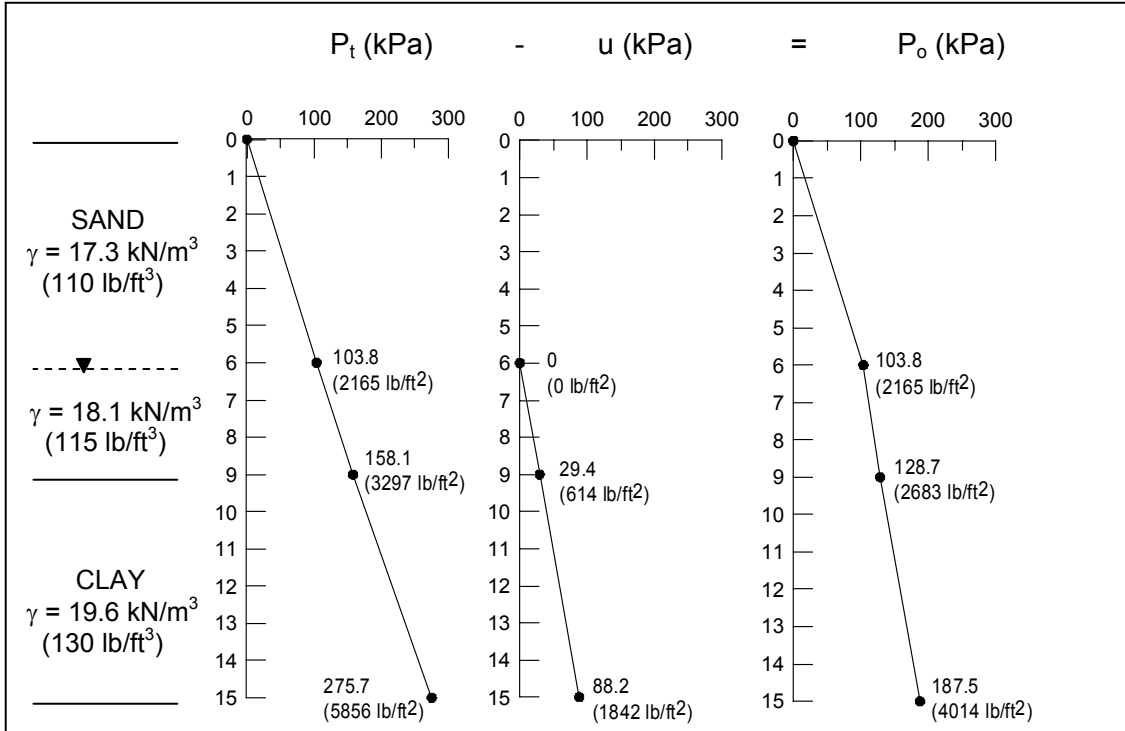


Figure 9.6 Effective Overburden Pressure Diagram – Water Table Below Ground Surface

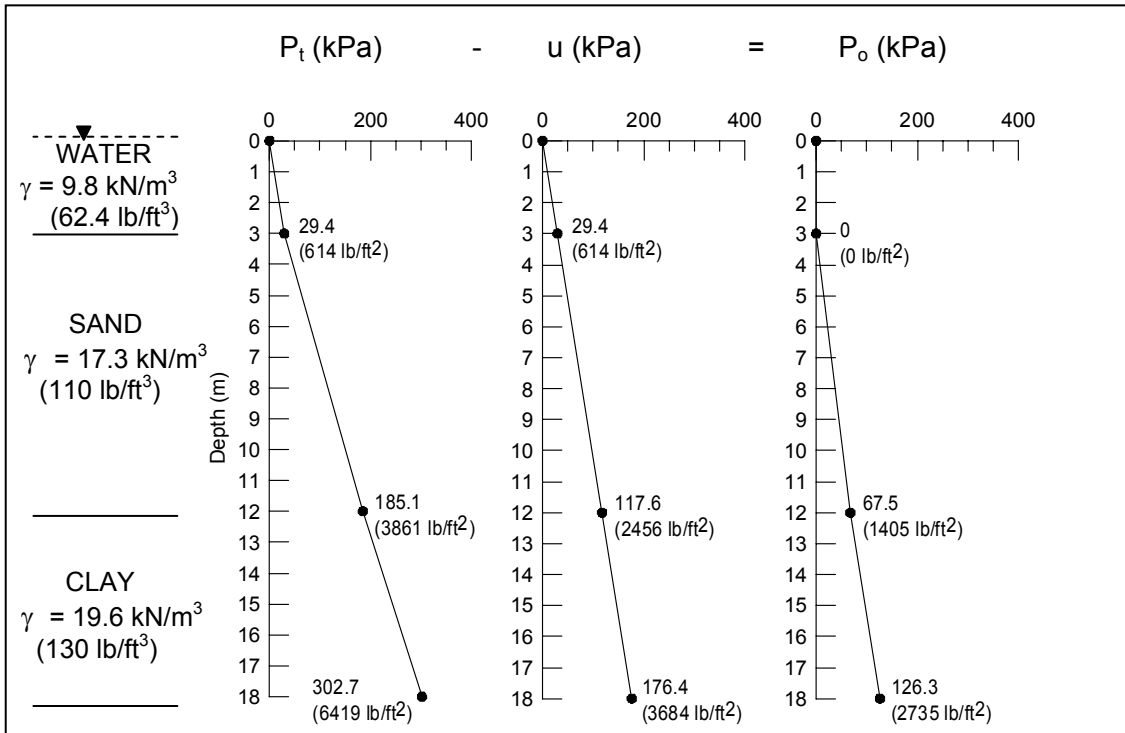


Figure 9.7 Effective Overburden Pressure Diagram – Water Table Above Ground Surface

The capacity of a pile when driven in many soil formations is not the same as the long term pile capacity. This is due to the soil disturbance created during installation as described in Section 9.2 of this chapter. For design in cohesive soils, the sensitivity of the cohesive soils should be determined as discussed in Section 6.2 of Chapter 6. Knowledge of the soil sensitivity allows a more accurate static analysis of the driving resistance in cohesive soils. Increases and decreases on pile capacity with time are known as soil setup and relaxation, respectively. These time effects are discussed in greater detail in Section 9.10.1. For a cost effective foundation design with any static analysis method, it is of paramount importance that the foundation designer logically select the soil strength parameters and include consideration of time dependent soil strength changes.

9.6 FACTORS OF SAFETY

Static analysis results yield an ultimate pile capacity or soil resistance. The allowable soil resistance (pile design load) is selected by dividing the ultimate pile capacity in suitable soil support layers by a factor of safety. The range in the factor of safety has primarily depended upon the reliability of the particular static analysis method with consideration of the following items.

1. The level of confidence in the input parameters. (This is a function of the type and extent of the subsurface exploration and laboratory testing of soil and rock materials.)
2. Variability of the soil and rock.
3. Method of static analysis.
4. Effects of and consistency of the proposed pile installation method.
5. Level of construction monitoring (static load test, dynamic analysis, wave equation analysis, Gates dynamic formula).

A large number of static analysis methods are documented in the literature with specific recommendations on the factor of safety to be used with each method. These recommended factors of safety have routinely disregarded the influence of the construction control method used to complement the static analysis computation. As part of the overall design process, it is important that the foundation designer qualitatively assess the validity of the chosen design analysis method and the reliability of the geotechnical design parameters.

While the range in static analysis factors of safety was from 2 to 4, most of the static analysis methods recommended a factor of safety of 3. As foundation design loads have increased over time, the use of high factors of safety has often resulted in pile installation problems. In addition, experience has shown that construction control methods have a significant influence on pile capacity. Therefore, the factor of safety used in a static analysis calculation should be based upon the construction control method specified. Provided that the procedures recommended in this manual are used for the subsurface exploration and analysis, the factors of safety in Table 9-1 are recommended, based on the specified construction control method. These factors of safety are discussed in greater detail in Chapter 14. The factor of safety for other test methods not included in Table 9-1 should be determined by the individual designer.

Table 9-1 Recommended Factor of Safety Based on Construction Control Method	
Construction Control Method	Factor of Safety
Static load test (ASTM D-1143) with wave equation analysis	2.00
Dynamic testing (ASTM D-4945) with wave equation analysis	2.25
Indicator piles with wave equation analysis	2.50
Wave equation analysis	2.75
Gates dynamic formula	3.50

The pile design load should be supported by soil resistance developed only in soil layers that contribute to long term load support. The soil resistance from soils subject to scour, or from soil layers above soft compressible soils should not be considered. The following example problem will be used to clarify the use of the factor of safety in static pile capacity calculations for determination of the pile design load as well as for determination of the soil resistance to pile driving.

Consider a pile to be driven through the soil profile described in Figure 9.8. The proposed pile type penetrates through a sand layer subject to scour in the 100 year flood overlying a very soft clay layer unsuitable for long term support and into competent support materials. Hence the soil resistances from the scour susceptible and soft clay layers do not contribute to long term load support and should not be included in the soil resistance for support of the design load. In this example, static load testing with wave equation analysis will be used for construction control. Therefore a factor of safety of 2.0 should be applied to the soil resistance calculated in suitable support layers in the static analysis. It should be noted

that this approach is for scour conditions under the 100 year or overtopping flood events and that a different approach would apply for the superflood or 500 year event. Additional discussion on scour considerations is provided in Section 9.9.4 of this chapter.

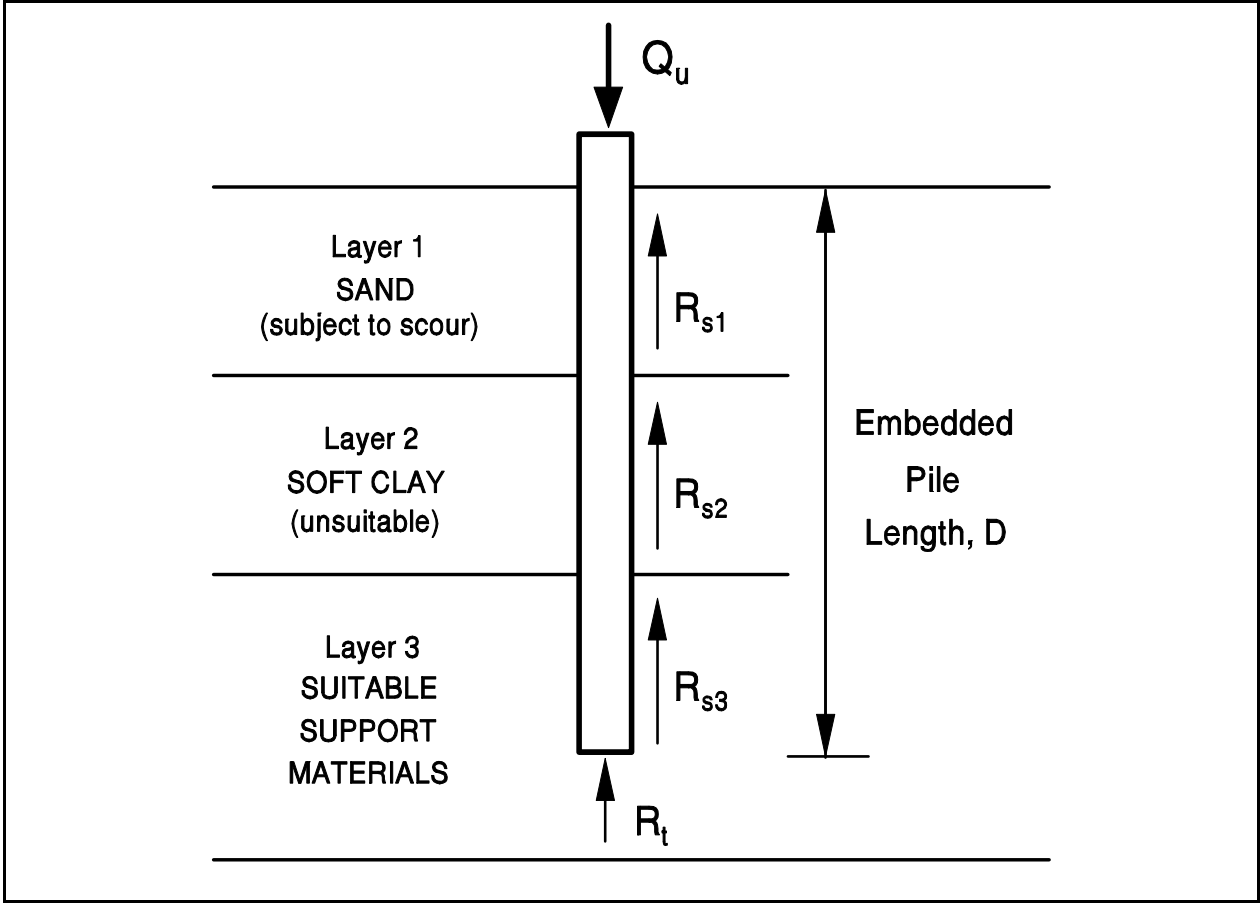


Figure 9.8 Soil Profile for Factor of Safety Discussion

In the static analysis, a trial pile penetration depth is chosen and an ultimate pile capacity, Q_u , is calculated. This ultimate capacity includes the soil resistance calculated from all soil layers including the shaft resistance in the scour susceptible layer, R_{s1} , the shaft resistance in the unsuitable soft clay layer, R_{s2} as well as the resistance in suitable support materials along the pile shaft, R_{s3} , and at the pile toe resistance, R_t .

$$Q_u = R_{s1} + R_{s2} + R_{s3} + R_t$$

The design load, Q_a , is the sum of the soil resistances from the suitable support materials divided by a factor of safety, FS. As noted earlier, a factor of safety of 2.0 is used in the equation below because of the planned construction control with static load testing.

$$Q_a = (R_{s3} + R_t) / (FS=2)$$

The design load may also be expressed as the sum of the ultimate capacity minus the calculated soil resistances from the scour susceptible and unsuitable layers divided by the factor of safety.

$$Q_a = (Q_u - R_{s1} - R_{s2}) / (FS=2)$$

The result of the static analysis is then the estimated pile penetration depth, D , the design load for that penetration depth, Q_a , and the calculated ultimate capacity, Q_u .

For preparation of construction plans and specifications, the calculated ultimate capacity, Q_u , is specified. Note that if the construction control method changes after the design stage, the required ultimate capacity and the required pile penetration depth for the ultimate capacity will also change. This is apparent when the previous equation for the design load is expressed in terms of the ultimate capacity as follows:

$$Q_u = R_{s1} + R_{s2} + (Q_a)(FS=2)$$

A static analysis should also be used to calculate the soil resistance to driving, SRD, that must be overcome to reach the estimated pile penetration depth necessary to develop the ultimate capacity. This information is necessary for the designer to select a pile section with the driveability to overcome the anticipated soil resistance and for the contractor to properly size equipment. Driveability aspects of design are discussed in Section 9.10.7.

In the soil resistance to driving calculation, a factor of safety is not used. The soil resistance to driving is the sum of the soil resistances from the scour susceptible and unsuitable layers plus the soil resistance in the suitable support materials to the estimated penetration depth.

$$SRD = R_{s1} + R_{s2} + R_{s3} + R_t$$

Soil resistances in this calculation should be the resistance at the time of driving. Hence time dependent changes in soil strengths due to soil setup or relaxation should be considered. For the example presented in Figure 9.8, the driving resistance from the unsuitable clay layer would be reduced by the sensitivity of the clay. Therefore, R_{s2} would

be $R_{s2} / 2$ for a clay with a sensitivity of 2. The soil resistance to driving to depth D would then be as follows

$$\text{SRD} = R_{s1} + R_{s2}/2 + R_{s3} + R_t$$

This example problem considers only the driving resistance at the final pile penetration depth. In cases where piles are driven through hard or dense layers above the estimated pile penetration depth, the soil resistance to penetrate these layers should also be calculated. Additional information on the calculation of time dependent soil strength changes is provided in Section 9.10.1 of this chapter.

9.7 DESIGN OF SINGLE PILES

9.7.1 Ultimate Capacity of Single Piles

Numerous static analysis methods are available for calculating the ultimate capacity of a single pile. The following sections of this chapter will detail analysis methods for piles in cohesionless, cohesive, and layered soil profiles using readily available SPT or laboratory test information. Additional methods based on cone penetration test results are also presented. As noted earlier, designers should fully understand the basis for, the limitations of, and the applicability of a chosen method. The selected method should also have a proven agreement with full scale field results in soil conditions similar to the project being designed, with the pile type being evaluated, and the pile installation conditions (impact driving, vibratory driving, etc.) to be used.

9.7.1.1 Bearing Capacity of Piles in Cohesionless Soils

The ultimate bearing capacity of a single pile in a cohesionless soil is the sum of shaft and toe resistances ($Q_u = R_s + R_t$). The calculation assumes that the shaft resistance and toe bearing resistance can be determined separately and that these two factors do not affect each other. Many analytical and empirical methods have been developed for estimating pile capacity in cohesionless materials. Table 9-2 describes some of the available methods. Each of the methods presented in Table 9-2 is also discussed in subsequent subsections.

9.7.1.1a Meyerhof Method Based on Standard Penetration Test (SPT) Data

Existing empirical correlations between Standard Penetration Test (SPT) results and static pile load tests can be used for preliminary estimates of static pile capacity for cohesionless soils. These correlations are based on the analyses of numerous pile load tests in a variety of cohesionless soil deposits. The Meyerhof (1976) method is quick and is easy to use. However, because the method is based on SPT test data which can be influenced by numerous factors, this method should only be used for preliminary estimates and not for final design.

Meyerhof (1976) reported that the average unit shaft resistance, f_s , of driven displacement piles, such as closed-end pipe piles and precast concrete piles, in kPa is:

$$f_s = 2\bar{N}' \leq 100 \text{ kPa}$$

The average unit shaft resistance of driven nondisplacement piles, such as H-piles, in kPa is:

$$f_s = \bar{N}' \leq 100 \text{ kPa}$$

where \bar{N}' is the average corrected SPT resistance value, in blows per 300 mm (1 ft), along the embedded length of pile. Typically, the soil profile is delineated into 3 to 6 m (10 to 20 ft) thick layers, and the average unit shaft resistance is calculated for each soil layer.

TABLE 9-2 METHODS OF STATIC ANALYSIS FOR PILES IN COHESIONLESS SOILS

Method	Approach	Method of Obtaining Design Parameters	Advantages	Disadvantages	Remarks
Meyerhof Method	Empirical	Results of SPT tests.	Widespread use of SPT test and input data availability. Simple method to use.	Non reproducibility of N values. Not as reliable as the other methods presented in this chapter.	Due to non reproducibility of N values and simplifying assumptions, use should be limited to preliminary estimating purposes.
Brown Method	Empirical	Results of SPT tests based of N_{60} values.	Widespread use of SPT test and input data availability. Simple method to use.	N_{60} values not always available.	Simple method based on correlations with 71 static load test results. Details provided in Section 9.7.1.1b.
Nordlund Method.	Semi-empirical	Charts provided by Nordlund. Estimate of soil friction angle is needed.	Allows for increased shaft resistance of tapered piles and includes effects of pile-soil friction coefficient for different pile materials.	No limiting value on unit shaft resistance is recommended by Nordlund. Soil friction angle often estimated from SPT data.	Good approach to design that is widely used. Method is based on field observations. Details provided in Section 9.7.1.1c.
Effective Stress Method.	Semi-empirical	Soil classification and estimated friction angle for β and N_t selection.	β value considers pile-soil friction coefficient for different pile materials. Soil resistance related to effective overburden pressure.	Results effected by range in β values and in particular by range in N_t chosen.	Good approach for design. Details provided in Section 9.7.1.3.
Methods based on Cone Penetration Test (CPT) data.	Empirical	Results of CPT tests.	Testing analogy between CPT and pile. Reliable correlations and reproducible test data.	Limitations on pushing cone into dense strata.	Good approach for design. Details provided in Section 9.7.1.7.

Meyerhof (1976) recommended that the unit toe resistance, q_t , in kPa for piles driven into sands and gravels may be approximated by:

$$q_t = 400\bar{N}'_o + \frac{(40\bar{N}'_B - 40\bar{N}'_o)D_B}{b} \leq 400\bar{N}'_B$$

Where: \bar{N}'_o = Average corrected SPT N' value for the stratum overlying the bearing stratum.

\bar{N}'_B = Average corrected SPT N' value of the bearing stratum.

D_B = Pile embedment depth into the bearing stratum in meters.

b = Pile diameter in meters.

The limiting value of $400\bar{N}'_B$ is reached when the embedment depth into the bearing stratum reaches 10 pile diameters. The above equation applies when the pile toe is located near the interface of two strata with a weaker stratum overlying the bearing stratum. For piles driven in a uniform cohesionless stratum, the unit toe resistance can be calculated as follows:

$$q_t = \frac{40\bar{N}'_B D_B}{b} \leq 400\bar{N}'_B$$

It is recommended that the average corrected SPT N' value, \bar{N}'_B , be calculated by averaging N' values within the zone extending 3 diameters below the pile toe. For piles driven into non-plastic silts, Meyerhof recommended the unit toe resistance, q_t , be limited to $300\bar{N}'_B$ instead of the $400\bar{N}'_B$ given in the above equation.

STEP BY STEP PROCEDURE FOR USING METHOD BASED ON SPT DATA

STEP 1 Correct SPT field N values for overburden pressure.

Use correction factors from Figure 4.6 to obtain corrected SPT N' values.

STEP 2 Compute the average corrected SPT N' value, \bar{N}' , for each soil layer. Along the embedded length of pile, delineate the soil profile into layers based on soil density indicated by N'. The individual soil layers should be selected between 3 and 6 m (10 to 20 ft) thick.

STEP 3 Compute unit shaft resistance, f_s (kPa) for driven, displacement piles from:

$$f_s = 2\bar{N}' \leq 100 \text{ kPa}$$

for driven, non-displacement piles such as H-piles, use:

$$f_s = \bar{N}' \leq 100 \text{ kPa}$$

STEP 4 Compute ultimate shaft resistance, R_s (kN).

$$R_s = f_s A_s$$

Where: A_s = Pile shaft surface area.
= (pile perimeter)(embedded length).

For H-piles in cohesionless soils, the "box" area should generally be used for shaft resistance calculations. Additional discussion on the behavior of open pile sections is presented in Section 9.10.5.

STEP 5 Compute average corrected SPT N' values, \bar{N}'_O and \bar{N}'_B , near pile toe.

In cases where the pile toe is situated near the interface of a weaker stratum overlying the bearing stratum, compute the average corrected SPT N' value for the stratum overlying the bearing stratum, \bar{N}'_O , and the average corrected SPT N' value for the bearing stratum, \bar{N}'_B .

In uniform cohesionless soils, compute the average corrected SPT N' value by averaging N' values within the zone extending 3 diameters below the pile toe.

STEP 6 Compute unit toe resistance, q_t (kPa).

For weaker stratum overlying the bearing stratum compute q_t from:

$$q_t = 400\bar{N}'_o + \frac{(40\bar{N}'_B - 40\bar{N}'_o)D_B}{b} \leq 400\bar{N}'_B$$

For piles in a uniform cohesionless deposit compute q_t from:

$$q_t = \frac{40\bar{N}'_B D_B}{b} \leq 400\bar{N}'_B$$

For piles driven into non-plastic silts, the unit toe resistance, q_t , should be limited to $300\bar{N}'_B$ instead of $400\bar{N}'_B$.

STEP 7 Compute ultimate toe resistance, R_t (kN).

$$R_t = q_t A_t$$

Where: A_t = Pile toe area.

For steel H and unfilled open end pipe piles, use only steel cross section area at pile toe unless there is reasonable assurance and previous experience that a soil plug will form at the pile toe. Additional discussion on plug formation in open pile sections is presented in Section 9.10.5. The assumption of a soil plug would allow the use of a box area at H pile toe and total pipe cross section area for open end pipe pile.

STEP 8 Compute ultimate pile capacity, Q_u (kN).

$$Q_u = R_s + R_t$$

STEP 9 Compute allowable design load, Q_a (kN).

$$Q_a = \frac{Q_u}{\text{Factor of Safety}}$$

Use Factor of Safety based on the construction control method as detailed in Section 9.6.

In using the Meyerhof method, it should be remembered that it is intended to be used only for preliminary capacity and length estimates. Limiting values often apply for the unit shaft and toe resistances and they should be used. It should also be remembered that the Standard Penetration Test is subject to many errors. Thus, judgment must be exercised when performing capacity calculations based on SPT results.

9.7.1.1b Brown Method

The Brown Method (2001) is a simple empirical method that uses Standard Penetration Test N_{60} values for calculating unit shaft resistance and unit end bearing values. The Brown Method was based on capacity correlations with 71 static load tests from Caltrans projects in a wide variety of soil types. The pile types included closed end pipe, open end pipe, H-piles, and precast concrete piles. The method considers compression and uplift loading as well as pile installation method (impact driving and partial vibratory installation).

Brown reported that the average unit shaft resistance, f_s , is:

$$f_s = F_{vs} (A_b + B_b N_{60})$$

N_{60} is the SPT N value corrected for 60% energy transfer and F_{vs} is a reduction factor for vibratory installed piles. A_b and B_b were determined from regression analyses on the data base and depend upon the soil type as noted in Table 9-3. Limits on the value of N_{60} were also recommended. If N_{60} is greater than 50, a value of 50 should be used and if N_{60} is less than 3, use 3. Brown recommended that the shaft resistance for H-piles be calculated using the “box” perimeter rather than the actual pile/soil contact area and for open end pipe piles Brown recommended using only the external surface area. The shaft resistance, R_s , is then:

$$R_s = f_s A_s$$

Where A_s is the pile shaft surface area (recommended pile perimeter noted above multiplied by length).

TABLE 9-3 INPUT FACTORS FOR BROWN'S METHOD							
Loading Condition	Installation Method	Soil Type	F _{vs}	A _b		B _b	
				kPa	(ksf)	kPa/bpf	(ksf/bpf)
Compression	Impact	Clay to Sand	1.0	26.6	0.555	1.92	0.040
"	"	Gravelly Sand to Boulders	1.0	42.6	0.888	42.6	0.888
"	"	Rock	1.0	138.0	2.89	138.0	2.89
Tension	Impact	Clay to Sand	1.0	25.0	0.522	1.8	0.0376
"	"	Gravelly Sand to Boulders	1.0	40.0	0.835	0.0	0.0
"	"	Rock	1.0	130	2.71	0.0	0.0
"	Vibratory	Clay to Sand	0.68	25.0	0.522	1.8	0.0376
"	"	Gravelly Sand to Boulders	0.68	40.0	0.835	0.0	0.0
"	"	Rock	0.68	130.0	2.71	0.0	0.0

Brown (2001) recommended that the unit toe resistance, q_t , for impact driven piles in MPa be calculated as:

$$q_t = 0.17 N_{60}$$

In US units, the unit toe resistance, q_t , in ksf is calculated:

$$q_t = 3.55 N_{60}$$

For vibratory installed piles this unit toe resistance should then be multiplied by 0.56. The pile toe resistance, R_t , is then calculated as follows:

$$R_t = q_t (A_t + A_{tp} F_p)$$

Brown recommended the actual steel area at the pile toe be used for A_t on H-piles and open end pipe piles. On these open end sections, the resistance on the soil plug is

calculated from the unit toe resistance multiplied by the soil plug area at the pile toe, A_{tp} , and a plug mobilization factor, F_p , of 0.42 for open end pipe piles or 0.67 for H-piles.

While the simplicity of Brown's method is attractive, it is recommended that the method be used only for preliminary length estimates until a greater experience base is obtained with the method results. Caltrans continues to study and expand on Brown's work as reported by Olson and Shantz (2004).

9.7.1.1c Nordlund Method

The Nordlund Method (1963) is based on field observations and considers the shape of pile taper and its soil displacement in calculating the shaft resistance. The method also accounts for the differences in soil-pile coefficient of friction for different pile materials. The method is based on the results of several load test programs in cohesionless soils. Several pile types were used in these test programs including timber, H, closed end pipe, Monotubes and Raymond step taper piles. These piles, which were used to develop the method's design curves, had pile widths generally in the range of 250 to 500 mm (10 to 20 inches). The Nordlund Method tends to overpredict pile capacity for piles with widths larger than 600 mm (24 inches).

According to the Nordlund Method, the ultimate capacity, Q_u , of a pile in cohesionless soil is the sum of the shaft resistance, R_s and the toe resistance, R_t . Nordlund suggests the shaft resistance is a function of the following variables:

1. The friction angle of the soil.
2. The friction angle on the sliding surface.
3. The taper of the pile.
4. The effective unit weight of the soil.
5. The pile length.
6. The minimum pile perimeter.
7. The volume of soil displaced.

These factors are considered in the Nordlund equation as illustrated in Figure 9.9.

The Nordlund Method equation for computing the ultimate capacity of a pile is as follows:

$$Q_u = \sum_{d=0}^{d=D} K_{\delta} C_F p_d \frac{\sin(\delta + \omega)}{\cos \omega} C_d \Delta d + \alpha_t N'_q A_t p_t$$

Where:

- d = Depth.
- D = Embedded pile length.
- K_{δ} = Coefficient of lateral earth pressure at depth d.
- C_F = Correction factor for K_{δ} when $\delta \neq \phi$.
- p_d = Effective overburden pressure at the center of depth increment d.
- δ = Friction angle between pile and soil.
- ω = Angle of pile taper from vertical.
- ϕ = Soil friction angle.
- C_d = Pile perimeter at depth d.
- Δd = Length of pile segment.
- α_t = Dimensionless factor (dependent on pile depth-width relationship).
- N'_q = Bearing capacity factor.
- A_t = Pile toe area.
- p_t = Effective overburden pressure at the pile toe.

For a pile of uniform cross section ($\omega=0$) and embedded length D, driven in soil layers of the same effective unit weight and friction angle, the Nordlund equation becomes:

$$Q_u = (K_{\delta} C_F p_d \sin \delta C_d D) + (\alpha_t N'_q A_t p_t)$$

The soil friction angle ϕ influences most of the calculations in the Nordlund method. In the absence of laboratory test data, ϕ can be estimated from corrected SPT N' values. Therefore, Figure 4.6 in Chapter 4 should be used for correcting field N values. The corrected SPT N' values may then be used in Table 4-6 of Chapter 4 to estimate the soil friction angle, ϕ .

Nordlund developed this method in 1963 and updated it in 1979 and has not placed a limiting value on the shaft resistance. However, Nordlund has recommended that the effective overburden pressure, p_t , used for computing the pile toe resistance be limited to 150 kPa (3 ksf).

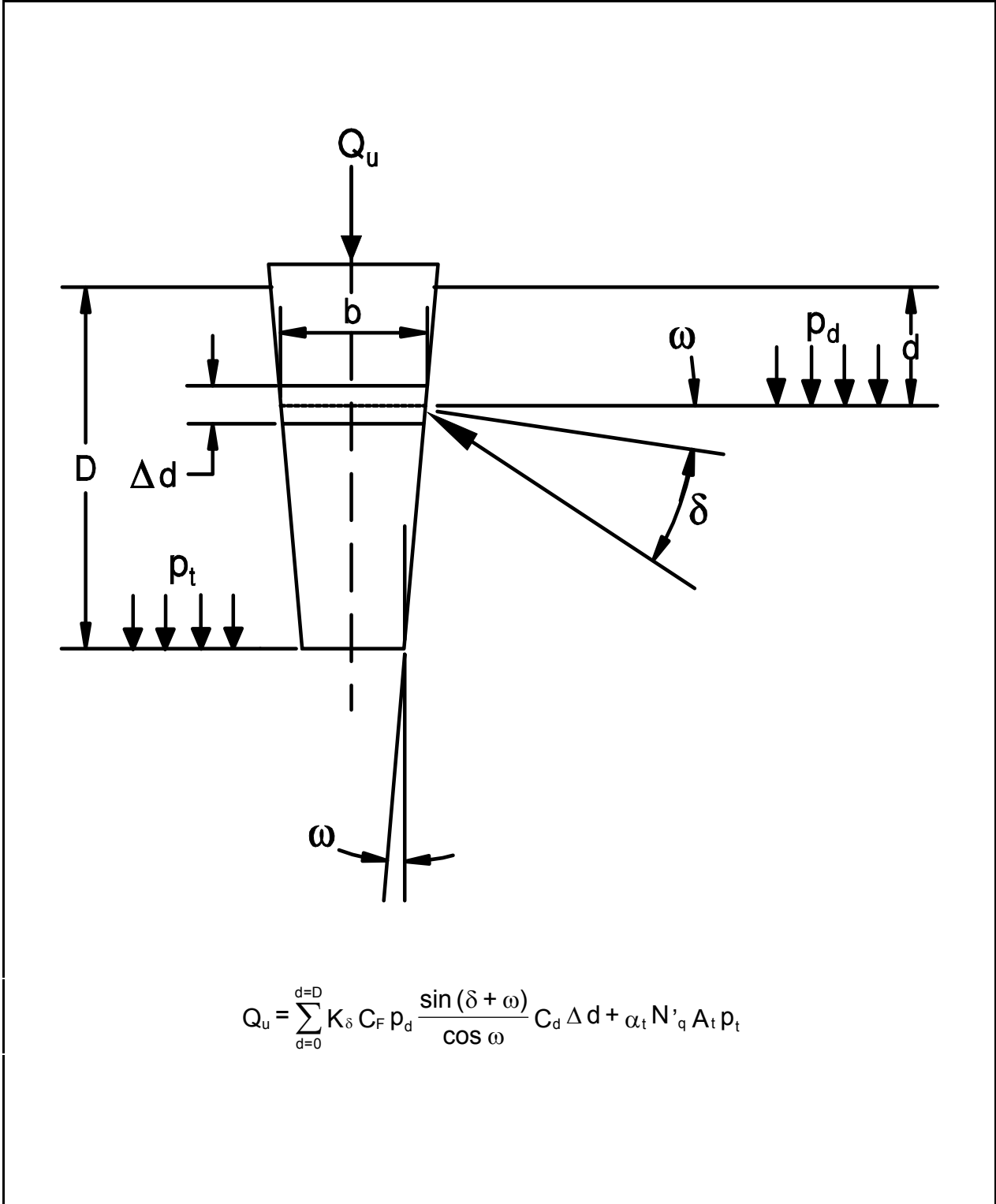


Figure 9.9 Nordlund's General Equation for Ultimate Pile Capacity

STEP BY STEP PROCEDURE FOR USING NORDLUND METHOD

Steps 1 through 6 are for computing the shaft resistance and steps 7 through 9 are for computing the pile toe resistance.

- STEP 1 Delineate the soil profile into layers and determine the ϕ angle for each layer.
- Construct p_o diagram using procedure described in Section 9.4.
 - Correct SPT field N values for overburden pressure using Figure 4.6 from Chapter 4 and obtain corrected SPT N' values. Delineate soil profile into layers based on corrected SPT N' values.
 - Determine ϕ angle for each layer from laboratory tests or in-situ data.
 - In the absence of laboratory or in-situ test data, determine the average corrected SPT N' value, \bar{N}' , for each soil layer and estimate ϕ angle from Table 4-6 in Chapter 4.
- STEP 2 Determine δ , the friction angle between pile and soil based on displaced soil volume, V , and the soil friction angle, ϕ .
- Compute volume of soil displaced per unit length of pile, V .
 - Enter Figure 9.10 with V and determine δ/ϕ ratio for pile type.
 - Calculate δ from δ/ϕ ratio.
- STEP 3 Determine the coefficient of lateral earth pressure, K_δ , for each ϕ angle.
- Determine K_δ for ϕ angle based on displaced volume, V , and pile taper angle, ω , using either Figure 9.11, 9.12, 9.13, or 9.14 and the appropriate procedure described in Step 3b, 3c, 3d, or 3e.
 - If the displaced volume is 0.0093, 0.093, or 0.930 m^3/m (0.1, 1.0 or 10.0 ft^3/ft) which correspond to one of the curves provided in Figures 9.11 through 9.14

and the ϕ angle is one of those provided, K_δ can be determined directly from the appropriate figure.

- c. If the displaced volume is 0.0093, 0.093, or 0.930 m³/m (0.1, 1.0 or 10.0 ft³/ft) which correspond to one of the curves provided in Figures 9.11 through 9.14 but the ϕ angle is different from those provided, use linear interpolation to determine K_δ for the required ϕ angle. Tables 9-4a and 9-4b also provide interpolated K_δ values at selected displaced volumes versus ϕ angle for uniform piles ($\omega = 0$).
- d. If the displaced volume is other than 0.0093, 0.093, or 0.930 m³/m (0.1, 1.0 or 10.0 ft³/ft) which correspond to one of the curves provided in Figures 9.11 through 9.14 but the ϕ angle corresponds to one of those provided, use log linear interpolation to determine K_δ for the required displaced volume. An example of this procedure may be found in Appendix F.2.1.2. Tables 9-4a and 9-4b also provide interpolated K_δ values at selected displaced volumes versus ϕ angle for uniform piles ($\omega = 0$).
- e. If the displaced volume is other than 0.0093, 0.093, or 0.930 m³/m (0.1, 1.0 or 10.0 ft³/ft) which correspond to one of the curves provided in Figures 9.11 through 9.14 and the ϕ angle does not correspond to one of those provided, first use linear interpolation to determine K_δ for the required ϕ angle at the displaced volume curves provided for 0.0093, 0.093, or 0.930 m³/m (0.1, 1.0 or 10.0 ft³/ft). Then use log linear interpolation to determine K_δ for the required displaced volume. An example of this procedure may be found in Appendix F.2.1.2. Tables 9-4a and 9-4b also provide interpolated K_δ values at selected displaced volumes versus ϕ angle for uniform piles ($\omega = 0$).

STEP 4 Determine the correction factor, C_F , to be applied to K_δ if $\delta \neq \phi$.

Use Figure 9.15 to determine the correction factor for each K_δ . Enter figure with ϕ angle and δ/ϕ value to determine C_F .

STEP 5 Compute the average effective overburden pressure at the midpoint of each soil layer, p_d (kPa).

Note: A limiting value is not applied to p_d .

STEP 6 Compute the shaft resistance in each soil layer. Sum the shaft resistance from each soil layer to obtain the ultimate shaft resistance, R_s (kN).

$$R_s = K_\delta C_F p_d \sin \delta C_d D$$

(for uniform pile cross section)

For H-piles in cohesionless soils, the "box" area should generally be used for shaft resistance calculations. Additional discussion on the behavior of open pile sections is presented in Section 9.10.5.

STEP 7 Determine the α_t coefficient and the bearing capacity factor, N'_q , from the ϕ angle near the pile toe.

- a. Enter Figure 9.16(a) with ϕ angle near pile toe to determine α_t coefficient based on pile length to diameter ratio.
- b. Enter Figure 9.16(b) with ϕ angle near pile toe to determine, N'_q .
- c. If ϕ angle is estimated from SPT data, compute the average corrected SPT N' value over the zone from the pile toe to 3 diameters below the pile toe. Use this average corrected SPT N' value to estimate ϕ angle near pile toe from Table 4-5.

STEP 8 Compute the effective overburden pressure at the pile toe, p_t (kPa).

Note: The limiting value of p_t is 150 kPa (3 ksf).

STEP 9 Compute the ultimate toe resistance, R_t (kN).

- a. $R_t = \alpha_t N'_q A_t p_t$
- b. limiting $R_t = q_L A_t$

q_L value is obtained from:

1. Entering Figure 9.17 with ϕ angle near pile toe determined from laboratory or in-situ test data.
 2. Entering Figure 9.17 with ϕ angle near the pile toe estimated from Table 4-6 and the average corrected SPT N' near toe as described in Step 7.
- c. Use lesser of the two R_t values obtained in steps a and b.

For steel H and unfilled open end pipe piles, use only steel cross section area at pile toe unless there is reasonable assurance and previous experience that a soil plug will form at the pile toe. Additional discussion on plug formation in open pile sections is presented in Section 9.10.5. The assumption of a soil plug would allow the use of a box area at H pile toe and total pipe cross section area for open end pipe pile.

STEP 10 Compute the ultimate pile capacity, Q_u (kN).

$$Q_u = R_s + R_t$$

STEP 11 Compute the allowable design load, Q_a (kN).

$$Q_a = \frac{Q_u}{\text{Factor of Safety}}$$

The factor of safety used in the calculation should be based upon the construction control method to be specified. Recommended factors of safety were described in Section 9.6.

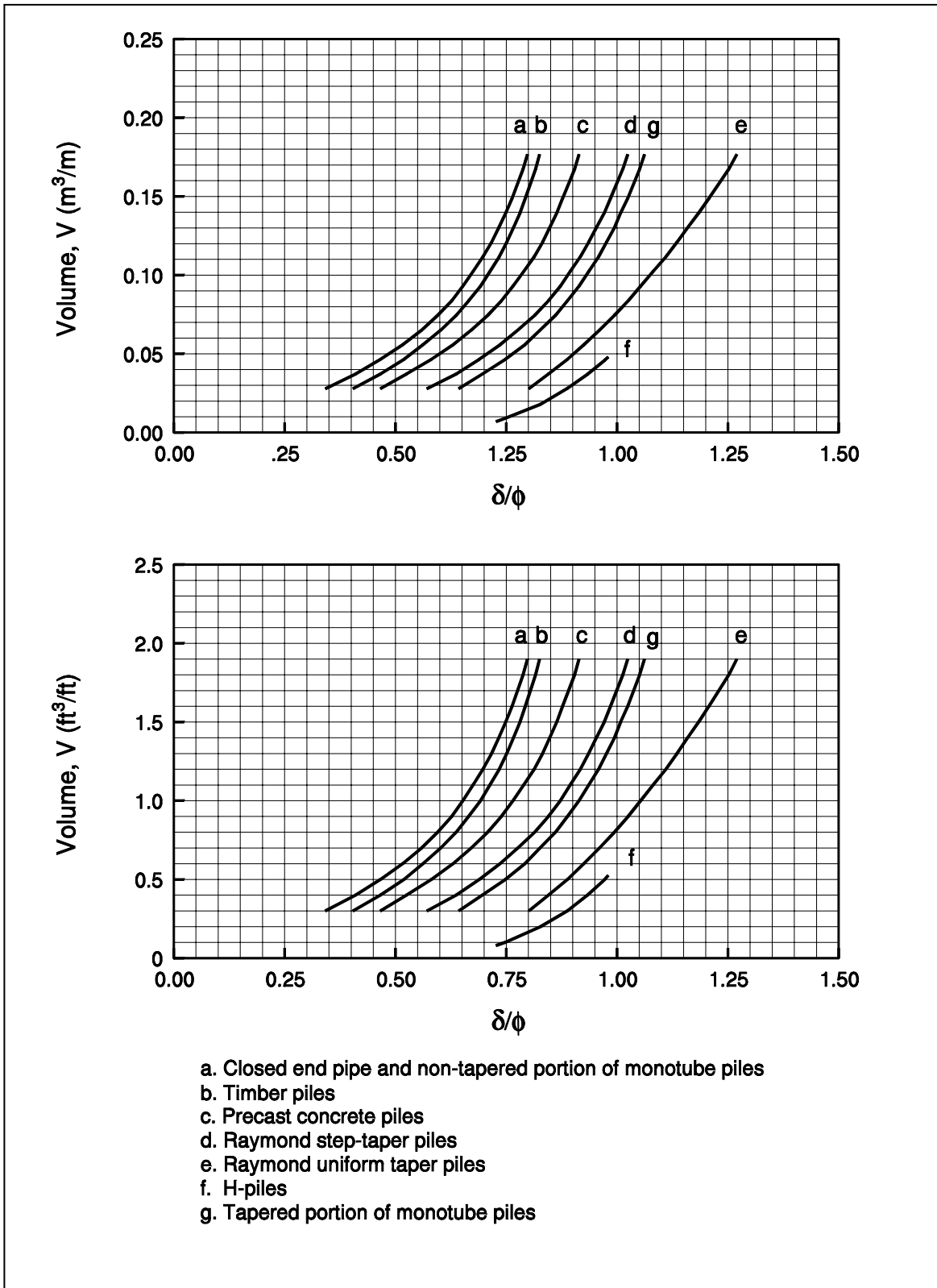


Figure 9.10 Relationship of δ/ϕ and Pile Soil Displacement, V , for Various Types of Piles (after Nordlund, 1979)

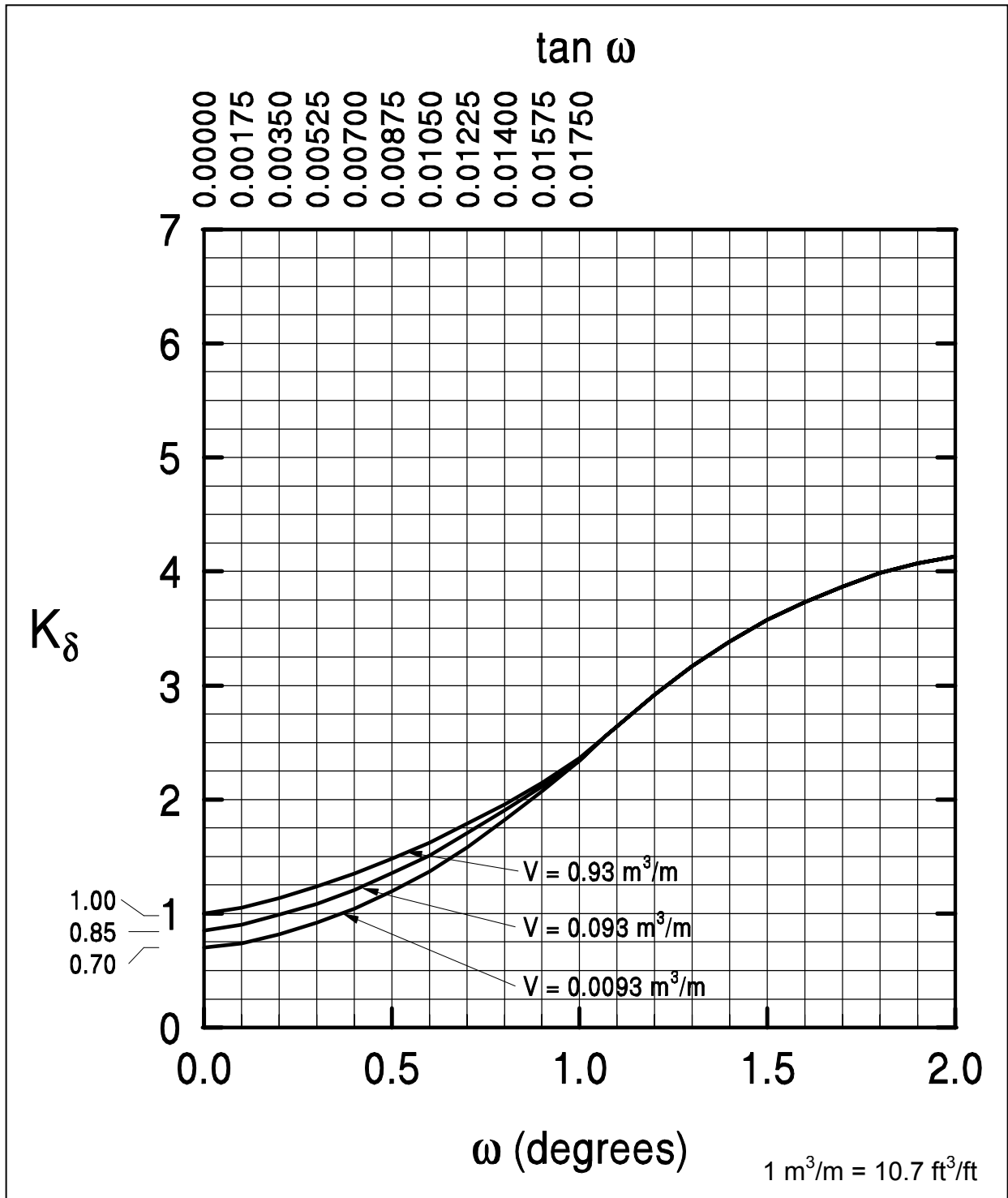


Figure 9.11 Design Curve for Evaluating K_δ for Piles when $\phi = 25^\circ$ (after Nordlund, 1979)

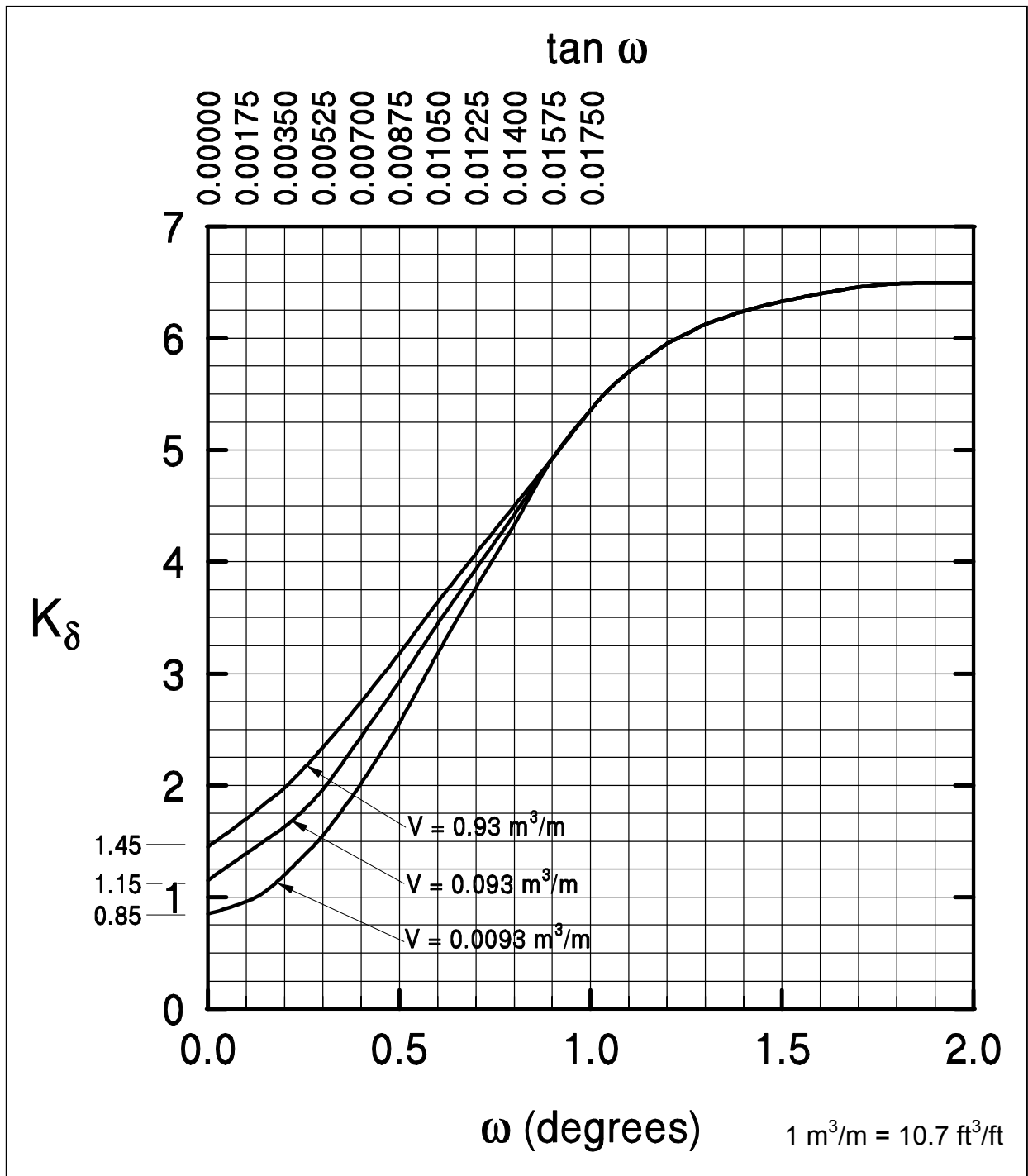


Figure 9.12 Design Curve for Evaluating K_δ for Piles when $\phi = 30^\circ$ (after Nordlund, 1979)

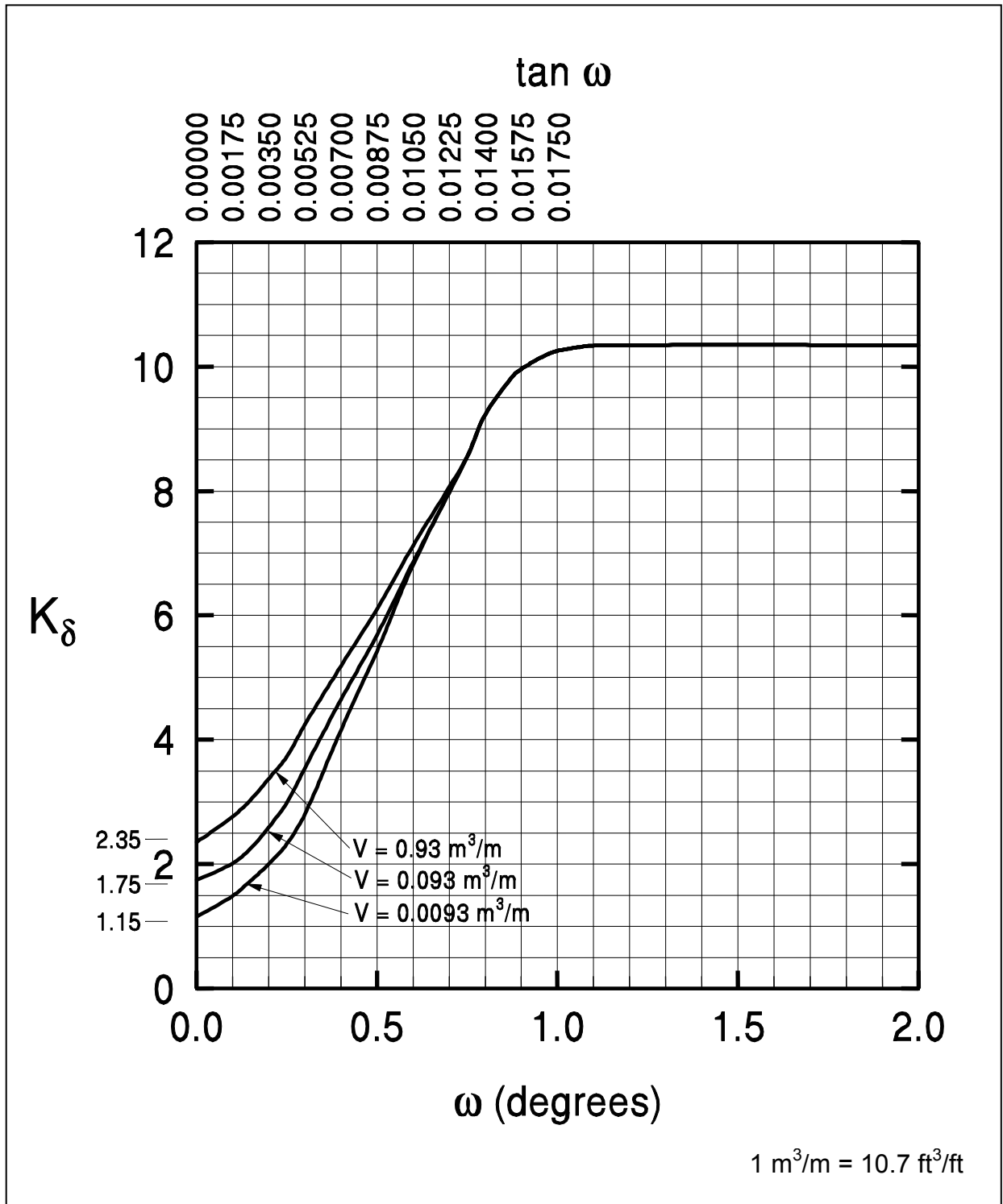


Figure 9.13 Design Curve for Evaluating K_δ for Piles when $\phi = 35^\circ$ (after Nordlund, 1979)

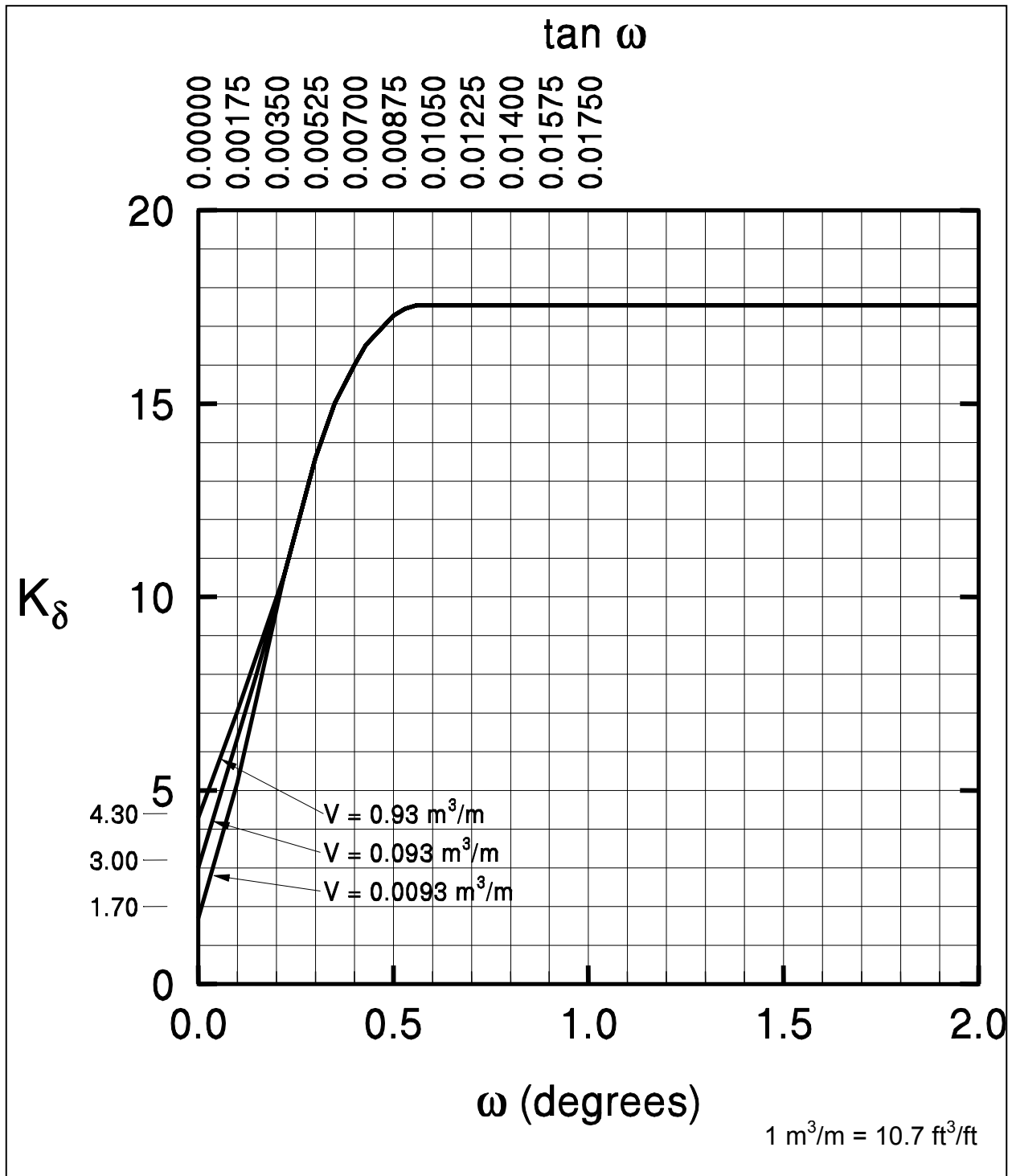


Figure 9.14 Design Curve for Evaluating K_δ for Piles when $\phi = 40^\circ$ (after Nordlund, 1979)

Table 9-4(a) Design Table for Evaluating K_{δ} for Piles when $\omega = 0^{\circ}$ and $V = 0.0093$ to $0.0930 \text{ m}^3/\text{m}$ (0.10 to $1.00 \text{ ft}^3/\text{ft}$)

ϕ	Displaced Volume -V, m^3/m , (ft^3/ft)									
	0.0093 (0.10)	0.0186 (0.20)	0.0279 (0.30)	0.0372 (0.40)	0.0465 (0.50)	0.0558 (0.60)	0.0651 (0.70)	0.0744 (0.80)	0.0837 (0.90)	0.0930 (1.00)
25	0.70	0.75	0.77	0.79	0.80	0.82	0.83	0.84	0.84	0.85
26	0.73	0.78	0.82	0.84	0.86	0.87	0.88	0.89	0.90	0.91
27	0.76	0.82	0.86	0.89	0.91	0.92	0.94	0.95	0.96	0.97
28	0.79	0.86	0.90	0.93	0.96	0.98	0.99	1.01	1.02	1.03
29	0.82	0.90	0.95	0.98	1.01	1.03	1.05	1.06	1.08	1.09
30	0.85	0.94	0.99	1.03	1.06	1.08	1.10	1.12	1.14	1.15
31	0.91	1.02	1.08	1.13	1.16	1.19	1.21	1.24	1.25	1.27
32	0.97	1.10	1.17	1.22	1.26	1.30	1.32	1.35	1.37	1.39
33	1.03	1.17	1.26	1.32	1.37	1.40	1.44	1.46	1.49	1.51
34	1.09	1.25	1.35	1.42	1.47	1.51	1.55	1.58	1.61	1.63
35	1.15	1.33	1.44	1.51	1.57	1.62	1.66	1.69	1.72	1.75
36	1.26	1.48	1.61	1.71	1.78	1.84	1.89	1.93	1.97	2.00
37	1.37	1.63	1.79	1.90	1.99	2.05	2.11	2.16	2.21	2.25
38	1.48	1.79	1.97	2.09	2.19	2.27	2.34	2.40	2.45	2.50
39	1.59	1.94	2.14	2.29	2.40	2.49	2.57	2.64	2.70	2.75
40	1.70	2.09	2.32	2.48	2.61	2.71	2.80	2.87	2.94	3.0

Table 9-4(b) Design Table for Evaluating K_{δ} for Piles when $\omega = 0^{\circ}$ and $V = 0.093$ to $0.930 \text{ m}^3/\text{m}$ (1.0 to $10.0 \text{ ft}^3/\text{ft}$)

ϕ	Displaced Volume $-V$, m^3/m (ft^3/ft)									
	0.093 (1.0)	0.186 (2.0)	0.279 (3.0)	0.372 (4.0)	0.465 (5.0)	0.558 (6.0)	0.651 (7.0)	0.744 (8.0)	0.837 (9.0)	0.930 (10.0)
25	0.85	0.90	0.92	0.94	0.95	0.97	0.98	0.99	0.99	1.00
26	0.91	0.96	1.00	1.02	1.04	1.05	1.06	1.07	1.08	1.09
27	0.97	1.03	1.07	1.10	1.12	1.13	1.15	1.16	1.17	1.18
28	1.03	1.10	1.14	1.17	1.20	1.22	1.23	1.25	1.26	1.27
29	1.09	1.17	1.22	1.25	1.28	1.30	1.32	1.33	1.35	1.36
30	1.15	1.24	1.29	1.33	1.36	1.38	1.40	1.42	1.44	1.45
31	1.27	1.38	1.44	1.49	1.52	1.55	1.57	1.60	1.61	1.63
32	1.39	1.52	1.59	1.64	1.68	1.72	1.74	1.77	1.79	1.81
33	1.51	1.65	1.74	1.80	1.85	1.88	1.92	1.94	1.97	1.99
34	1.63	1.79	1.89	1.96	2.01	2.05	2.09	2.12	2.15	2.17
35	1.75	1.93	2.04	2.11	2.17	2.22	2.26	2.29	2.32	2.35
36	2.00	2.22	2.35	2.45	2.52	2.58	2.63	2.67	2.71	2.74
37	2.25	2.51	2.67	2.78	2.87	2.93	2.99	3.04	3.09	3.13
38	2.50	2.81	2.99	3.11	3.21	3.29	3.36	3.42	3.47	3.52
39	2.75	3.10	3.30	3.45	3.56	3.65	3.73	3.80	3.86	3.91
40	3.00	3.39	3.62	3.78	3.91	4.01	4.10	4.17	4.24	4.30

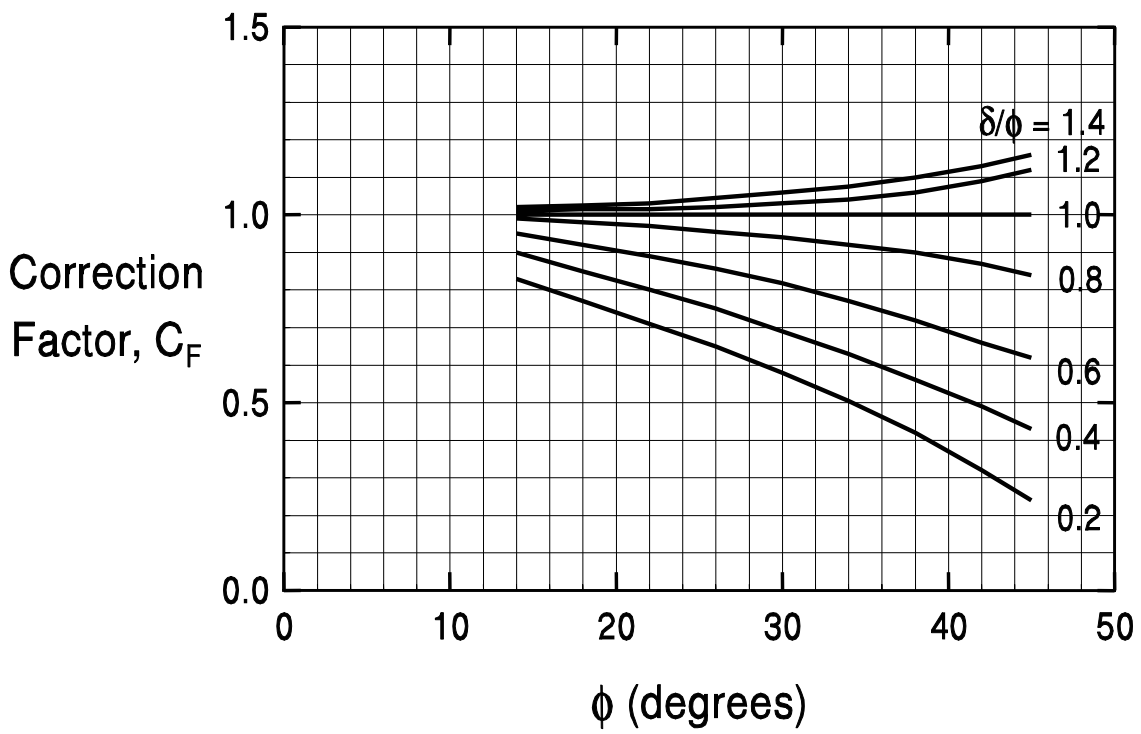


Figure 9.15 Correction Factor for K_δ when $\delta \neq \phi$ (after Nordlund, 1979)

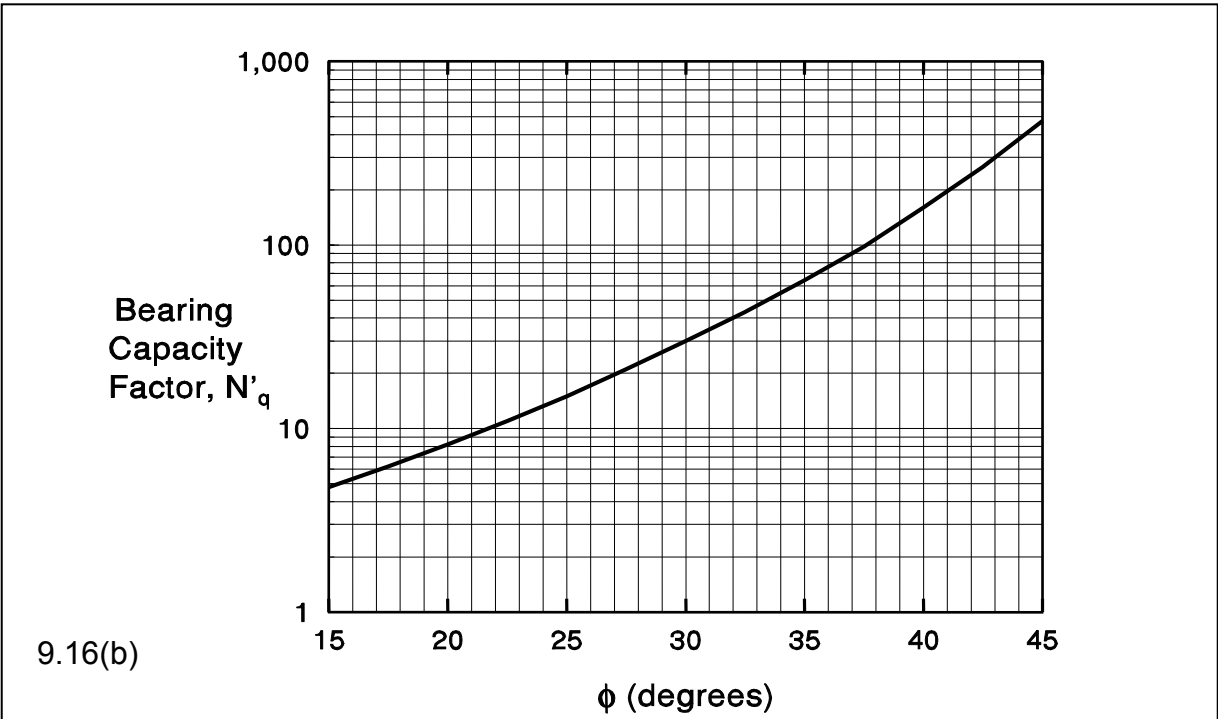
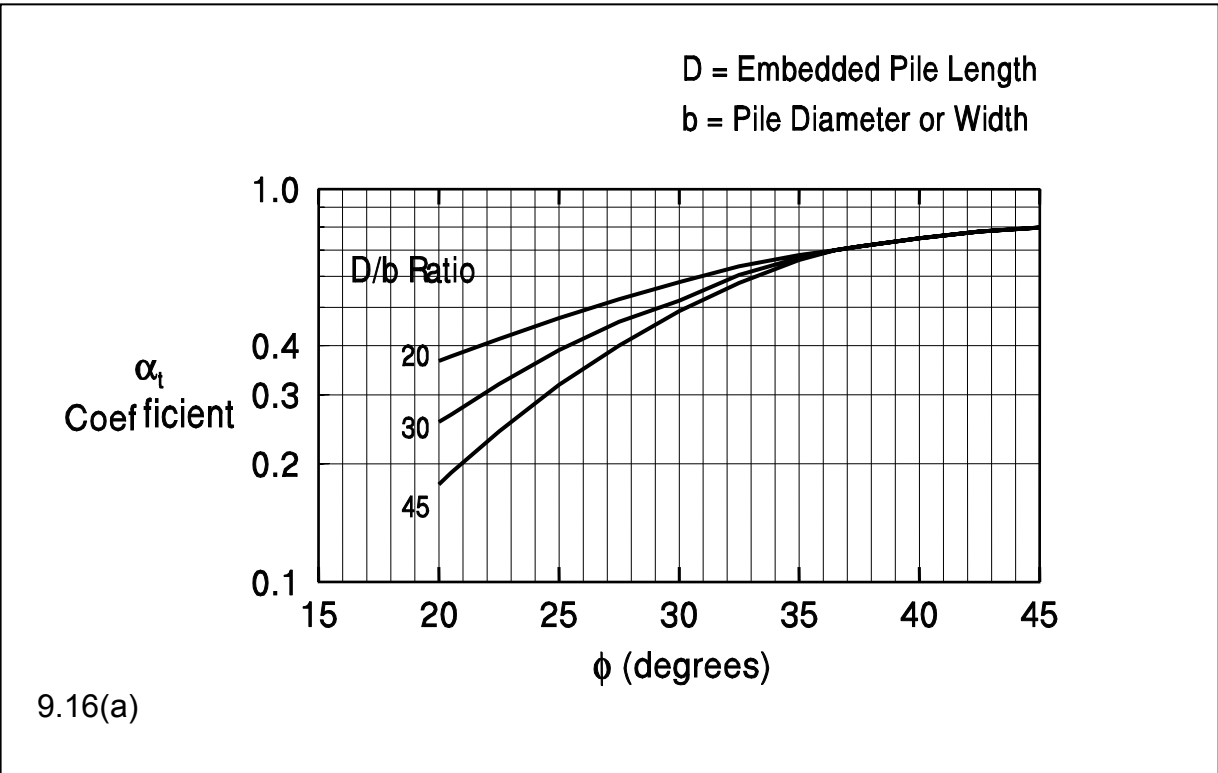


Figure 9.16 Chart for Estimating α_t Coefficient and Bearing Capacity Factor N'_q (Chart modified from Bowles, 1977)

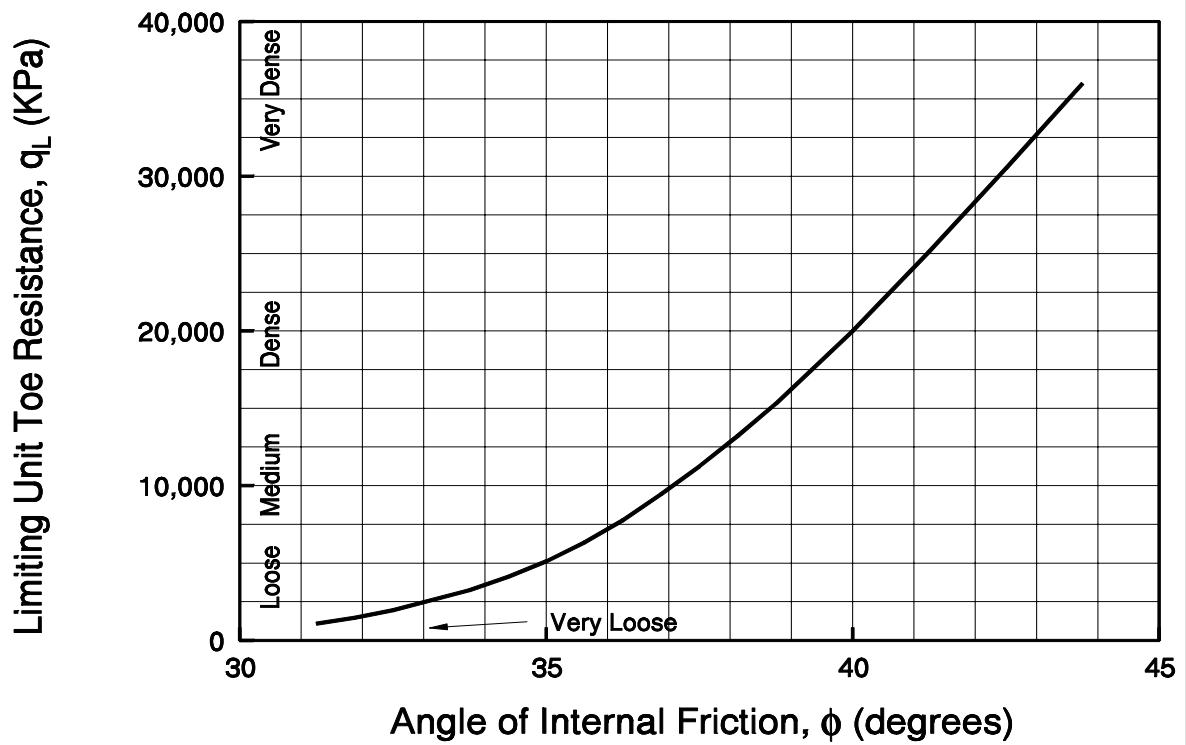
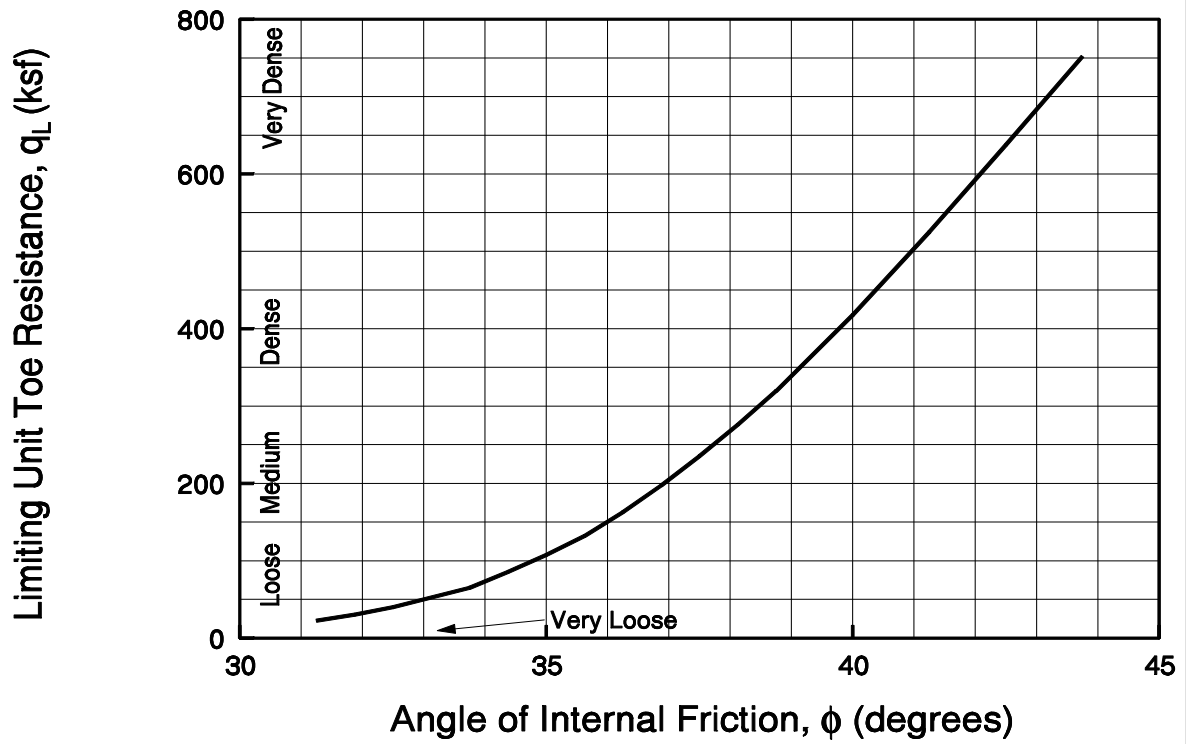


Figure 9.17 Relationship Between Maximum Unit Pile Toe Resistance and Friction Angle for Cohesionless soils (after Meyerhof, 1976)

9.7.1.2 Ultimate Capacity of Piles in Cohesive Soils

The ultimate capacity of a pile in cohesive soil may also be expressed as the sum of the shaft and toe resistances or $Q_u = R_s + R_t$. The shaft and toe resistances can be calculated from static analysis methods using soil boring and laboratory test data in either total stress or effective stress methods. The α -Method is a total stress method that uses undrained soil shear strength parameters for calculating static pile capacity in cohesive soil. The α -Method will be presented in Section 9.7.1.2a. The effective stress method uses drained soil strength parameters for capacity calculations. Since the effective stress method may be used for calculating static pile capacity in cohesive as well as cohesionless soils, this method will be presented in Section 9.7.1.3. Alternatively, in-situ CPT test results can also be used to calculate pile capacity in cohesive soils from cone sleeve friction and cone tip resistance values. CPT based methods are discussed in Section 9.7.1.7. An overview of design methods for cohesive soils is presented in Table 9-5.

The shaft resistance of piles driven into cohesive soils is frequently as much as 80 to 90% of the total capacity. Therefore, it is important that the shaft resistance of piles in cohesive soils be estimated as accurately as possible.

9.7.1.2a Total Stress - α -Method

For piles in clay, a total stress analysis is often used where ultimate capacity is calculated from the undrained shear strength of the soil. This approach assumes that the shaft resistance is independent of the effective overburden pressure and that the unit shaft resistance can be expressed in terms of an empirical adhesion factor times the undrained shear strength.

The unit shaft resistance, f_s , is equal to the adhesion, c_a , which is the shear stress between the pile and soil at failure. This may be expressed in equation form as:

$$f_s = c_a = \alpha c_u$$

in which α is an empirical adhesion factor for reduction of the average undrained shear strength, c_u , of undisturbed clay along the embedded length of the pile. The coefficient α depends on the nature and strength of the clay, pile dimension, method of pile installation, and time effects. The values of α vary within wide limits and decrease rapidly with increasing shear strength.

TABLE 9-5 METHODS OF STATIC ANALYSIS FOR PILES IN COHESIVE SOILS					
Method	Approach	Method of Obtaining Design Parameters	Advantages	Disadvantages	Remarks
α -Method (Tomlinson Method).	Empirical, total stress analysis.	Undrained shear strength estimate of soil is needed. Adhesion calculated from Figures 9.18 and 9.19.	Simple calculation from laboratory undrained shear strength values to adhesion.	Wide scatter in adhesion versus undrained shear strengths in literature.	Widely used method described in Section 9.7.1.2a.
Effective Stress Method.	Semi-Empirical, based on effective stress at failure.	β and N_t values are selected from Table 9-6 based on drained soil strength estimates.	Ranges in β and N_t values for most cohesive soils are relatively small.	Range in N_t values for hard cohesive soils such as glacial tills can be large.	Good design approach theoretically better than undrained analysis. Details in Section 9.7.1.3.
Methods based on Cone Penetration Test data.	Empirical.	Results of CPT tests.	Testing analogy between CPT and pile. Reproducible test data.	Cone can be difficult to advance in very hard cohesive soils such as glacial tills.	Good approach for design. Details in Section 9.7.1.7.

It is recommended that Figure 9.18 generally be used for adhesion calculations, unless one of the special soil stratigraphy cases identified in Figure 9.19 is present at a site. In cases where either Figures 9.18 or 9.19 could be used, the inexperienced user should select and use the smaller value obtained from either figure. All users should confirm the applicability of a selected design chart in a given soil condition with local correlations between static capacity calculations and static load tests results.

In Figure 9.18, the adhesion, c_a , is expressed as a function of the undrained shear strength, c_u , with consideration of both the pile type and the embedded pile length, D , to pile diameter, b , ratio. The embedded pile length used in Figure 9.18 should be the minimum value of the length from the ground surface to the bottom of the clay layer, or the length from the ground surface to the pile toe.

Figures 9.19a and 9.19b present the adhesion factor, α , versus the undrained shear strength of the soil in kPa and ksf, respectively, as a function of unique soil stratigraphy and pile embedment. The adhesion factor from these soil stratigraphy cases should be used only for determining the adhesion in a stiff clay layer in that specific condition. For a soil profile consisting of clay layers of significantly different consistencies such as soft clays over stiff clays, adhesion factors should be determined for each individual clay layer.

The top graph in Figures 9.19a and 9.19b may be used to select the adhesion factor when piles are driven through a sand or sandy gravel layer and into an underlying stiff clay stratum. This case results in the highest adhesion factors as granular material is dragged into the underlying clays. The greater the pile penetration into the clay stratum, the less influence the overlying granular stratum has on the adhesion factor. Therefore, for the same undrained shear strength, the adhesion factor decreases with increased pile penetration into the clay stratum.

The middle graph in Figures 9.19a and 9.19b should be used to select the adhesion factor when piles are driven through a soft clay layer overlying a stiff clay layer. In this case, the soft clay is dragged into the underlying stiff clay stratum thereby reducing the adhesion factor of the underlying stiff clay soils. The greater the pile penetration into the underlying stiff clay soils, the less the influence the overlying soft clays have on the stiff clay adhesion factor. Therefore, the stiff clay adhesion factor increases with increasing pile penetration into the stiff clay soils.

Last, the bottom graph in Figures 9.19a and 9.19b may be used to select the adhesion factor for piles driven in stiff clays without any different overlying strata. In stiff clays, a gap often forms between the pile and the soil along the upper portion of the pile shaft. In this case, the shallower the pile penetration into a stiff clay stratum the greater the effect the gap has on the shaft resistance that develops. Hence, the adhesion factor for a given shear strength is reduced at shallow pile penetration depths and increased at deeper pile penetration depths.

In highly overconsolidated clays, undrained shear strengths may exceed the upper limits of Figures 9.18 and 9.19. In these cases, it is recommended that adhesion factor, α , be calculated according to API Recommended Practice 2A (1993). API recommends the adhesion factor be computed using the following equations based on Ψ , the ratio of the undrained shear strength of the soil, c_u , divided by the effective overburden pressure, p_o' .

$$\alpha = 0.5 \Psi^{-0.5} \quad \text{for } \Psi \leq 1.0$$

$$\alpha = 0.5 \Psi^{-0.25} \quad \text{for } \Psi > 1.0$$

API stipulates that α be ≤ 1.0 . In addition, API recommends the above equations be applied with care in soils with high c_u / p_o' ratios as limited load test data is available for soils with c_u / p_o' ratios greater than 3.

In the case of H piles in cohesive soils, the shaft resistance should not be calculated from the surface area of the pile, but rather from the "box" area of the four sides. The shaft resistance for H-piles in cohesive soils consists of the sum of the adhesion, c_a , times the flange surface area along the exterior of the two flanges, plus the undrained shear strength of the soil, c_u , times the area of the two remaining sides of the "box", due to soil-to-soil shear along these faces. This computation can be approximated by determining the adhesion using the appropriate corrugated pile curve in Figure 9.18 and multiplying the adhesion by the H-pile "box" area. Additional information on the behavior of open pile sections is presented in Section 9.10.5.

In clays with large shrink-swell potential, static capacity calculations should ignore the shaft resistance from the adhesion in the shrink-swell zone. During dry times, shrinkage will create a gap between the clay and the pile in this zone and therefore the shaft resistance should not be relied upon for long term support.

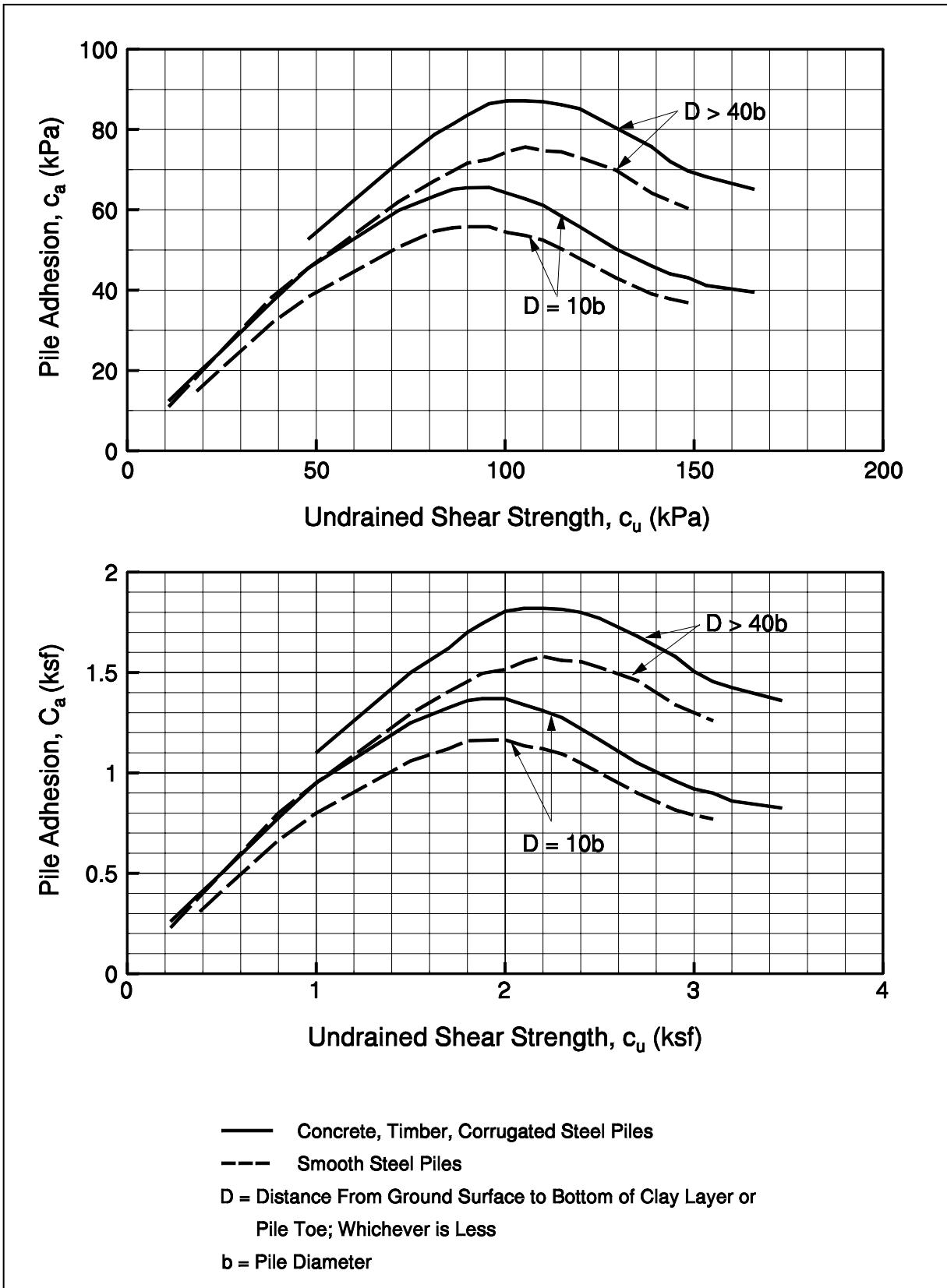


Figure 9.18 Adhesion Values for Piles in Cohesive Soils (after Tomlinson, 1979)

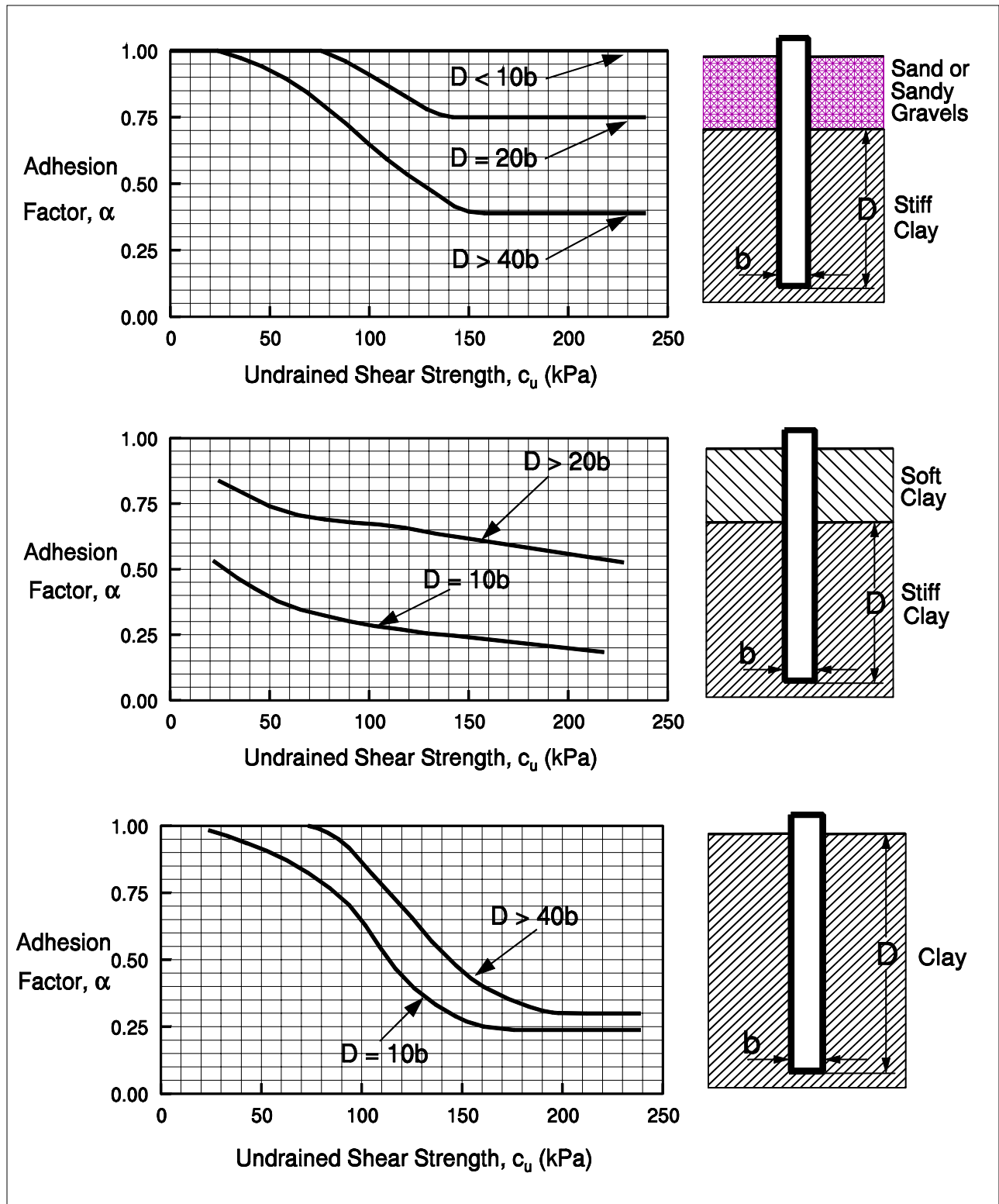


Figure 9.19(a) Adhesion Factors for Driven Piles in Clay –SI Units (Tomlinson, 1980)

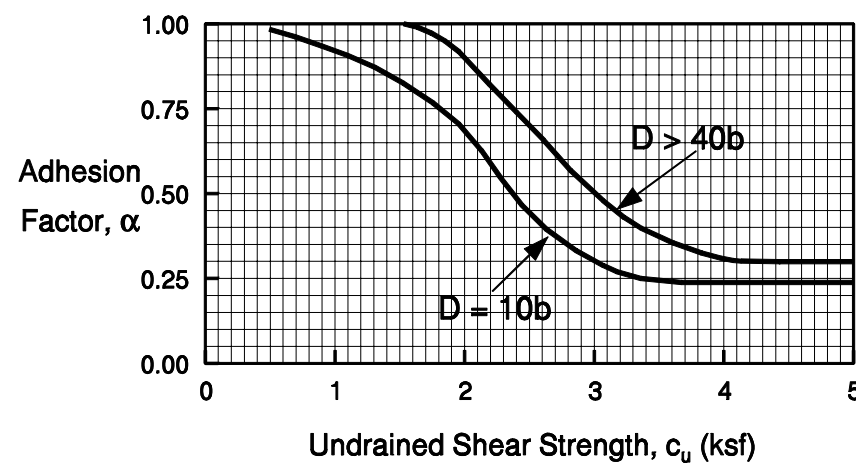
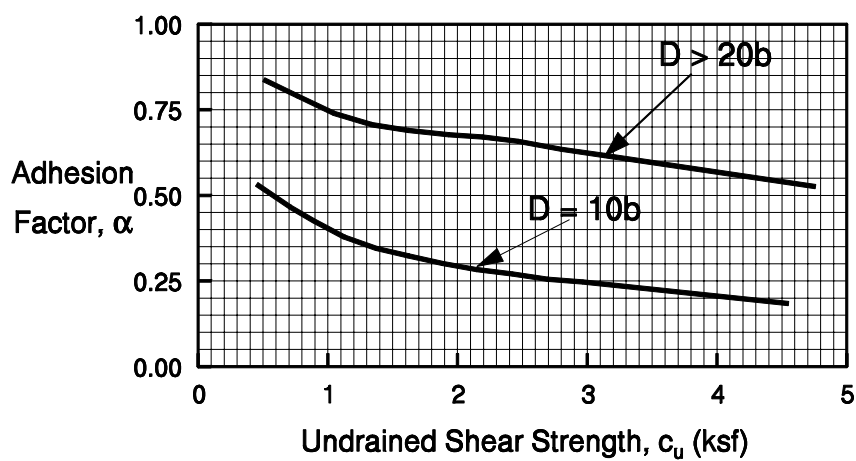
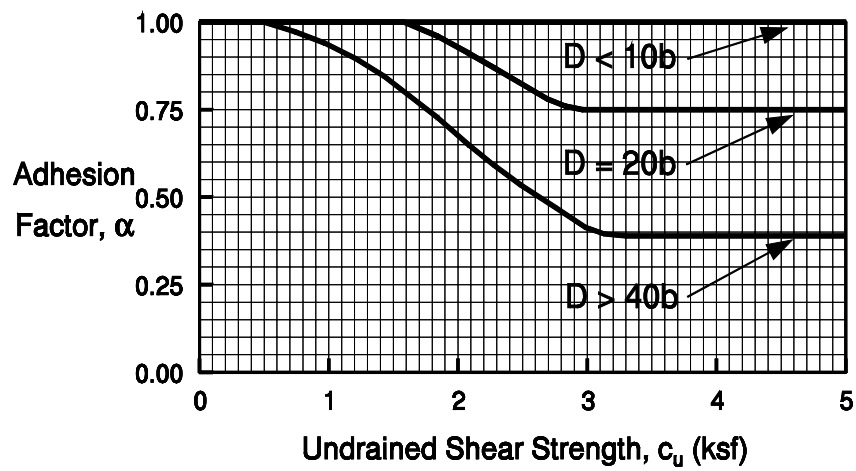


Figure 9.19(b) Adhesion Factors for Driven Piles in Clay - US Units (Tomlinson, 1980)

The unit toe resistance in a total stress analysis for homogeneous cohesive soil can be expressed as:

$$q_t = c_u N_c$$

The term N_c is a dimensionless bearing capacity factor which depends on the pile diameter and the depth of embedment. The bearing capacity factor, N_c , is usually taken as 9 for deep foundations.

It should be remembered that the movement required to mobilize the toe resistance is several times greater than that required to mobilize the shaft resistance. At the movement required to fully mobilize the toe resistance, the shaft resistance may have decreased to a residual value. Therefore, the toe resistance contribution to the ultimate pile capacity in cohesive soils is sometimes ignored except in hard cohesive deposits such as glacial tills.

STEP BY STEP PROCEDURE FOR - "α-METHOD"

STEP 1 Delineate the soil profile into layers and determine the adhesion, c_a , from Figure 9.18 or adhesion factor, α , from Figure 9.19a or 9.19b for each layer.

Enter appropriate figure with the undrained shear strength of the soil, c_u , and determine adhesion or adhesion factor based on the embedded pile length in clay, D , and pile diameter ratio, b . Use the curve for the appropriate soil and embedment condition.

STEP 2 For each soil layer, compute the unit shaft resistance, f_s in kPa (ksf).

$$f_s = c_a = \alpha c_u$$

Where: c_a = Adhesion.

STEP 3 Compute the shaft resistance in each soil layer and the ultimate shaft resistance, R_s , in kN (kips), from the sum of the shaft resistance from each layer.

$$R_s = f_s A_s$$

Where: A_s = Pile-soil surface area in m^2 (ft^2) from (pile perimeter) (length). A discussion on the behavior of open pile sections in cohesive soils is presented in Section 9.10.5.

STEP 4 Compute the unit toe resistance, q_t in kPa (ksf).

$$q_t = 9 c_u$$

Where: c_u = Undrained shear strength of soil at the pile toe.
in kPa (ksf)

STEP 5 Compute the ultimate toe resistance, R_t in kN (kips).

$$R_t = q_t A_t$$

Where: A_t = Area of pile toe in m^2 (ft^2).

For open pile sections, refer to the discussion of pile plugging presented in Section 9.10.5.

STEP 6 Compute the ultimate pile capacity, Q_u in kN (kips).

$$Q_u = R_s + R_t$$

STEP 7 Compute the allowable design load, Q_a in kN (kips).

$$Q_a = \frac{Q_u}{\text{Factor of Safety}}$$

The factor of safety in this static calculation should be based on the specified construction control method as described in Section 9.6 of this chapter.

9.7.1.3 Effective Stress Method

Static capacity calculations in cohesionless, cohesive, and layered soils can also be performed using an effective stress based method. Effective stress based methods were developed to model the long term drained shear strength conditions. Therefore, the effective soil friction angle, ϕ' , should be used in parameter selection.

In an effective stress analysis, the unit shaft resistance is calculated from the following expression:

$$f_s = \beta \bar{p}_o$$

Where: β = Bjerrum-Burland beta coefficient = $K_s \tan \delta$.
 \bar{p}_o = Average effective overburden pressure along the pile shaft, in kPa (ksf).
 K_s = Earth pressure coefficient.
 δ = Friction angle between pile and soil.

The unit toe resistance is calculated from:

$$q_t = N_t p_t$$

Where: N_t = Toe bearing capacity coefficient.
 p_t = Effective overburden pressure at the pile toe in kPa (ksf).

Recommended ranges of β and N_t coefficients as a function of soil type and ϕ' angle from Fellenius (1991) are presented in Table 9-6. Fellenius notes that factors affecting the β and N_t coefficients consist of the soil composition including the grain size distribution, angularity and mineralogical origin of the soil grains, the original soil density and density due to the pile installation technique, the soil strength, as well as other factors. Even so, β coefficients are generally within the ranges provided and seldom exceed 1.0.

For sedimentary cohesionless deposits, Fellenius states N_t ranges from about 30 to a high of 120. In very dense non-sedimentary deposits such as glacial tills, N_t can be much higher, but can also approach the lower bound value of 30. In clays, Fellenius notes that the toe resistance calculated using an N_t of 3 is similar to the toe resistance calculated from a traditional analysis using undrained shear strength. Therefore, the use of a relatively low N_t coefficient in clays is recommended unless local correlations suggest higher values are appropriate.

Graphs of the ranges in β and N_t coefficients versus the range in ϕ' angle as suggested by Fellenius are presented in Figure 9.20 and 9.21, respectively. These graphs may be helpful in selection of β or N_t . The inexperienced user should select conservative β and N_t coefficients. As with any design method, the user should also confirm the appropriateness of a selected β or N_t coefficient in a given soil condition with local correlations between static capacity calculations and static load tests results.

It should be noted that the effective stress method places no limiting values on either the shaft or toe resistance.

STEP BY STEP PROCEDURE FOR THE EFFECTIVE STRESS METHOD

STEP 1 Delineate the soil profile into layers and determine ϕ' angle for each layer.

- a. Construct p_o diagram using previously described procedure in Section 9.4.
- b. Divide soil profile throughout the pile penetration depth into layers and determine the effective overburden pressure, p_o , in kPa (ksf) at the midpoint of each layer.
- c. Determine the ϕ' angle for each soil layer from laboratory or in-situ test data.
- d. In the absence of laboratory or in-situ data for cohesionless layers, determine the average corrected SPT N' value for each layer and estimate ϕ' angle from Table 4-6 in Chapter 4.

STEP 2 Select the β coefficient for each soil layer.

- a. Use local experience to select β coefficient for each layer.
- b. In the absence of local experience, use Table 9-6 or Figure 9.20 to estimate β coefficient from ϕ' angle for each layer.

STEP 3 For each soil layer compute the unit shaft resistance, f_s in kPa (ksf).

$$f_s = \beta p_o$$

TABLE 9-6 APPROXIMATE RANGE OF β AND N_t COEFFICIENTS (Fellenius, 1991)			
Soil Type	ϕ'	B	N_t
Clay	25 - 30	0.23 - 0.40	3 - 30
Silt	28 - 34	0.27 - 0.50	20 - 40
Sand	32 - 40	0.30 - 0.60	30 - 150
Gravel	35 - 45	0.35 - 0.80	60 - 300

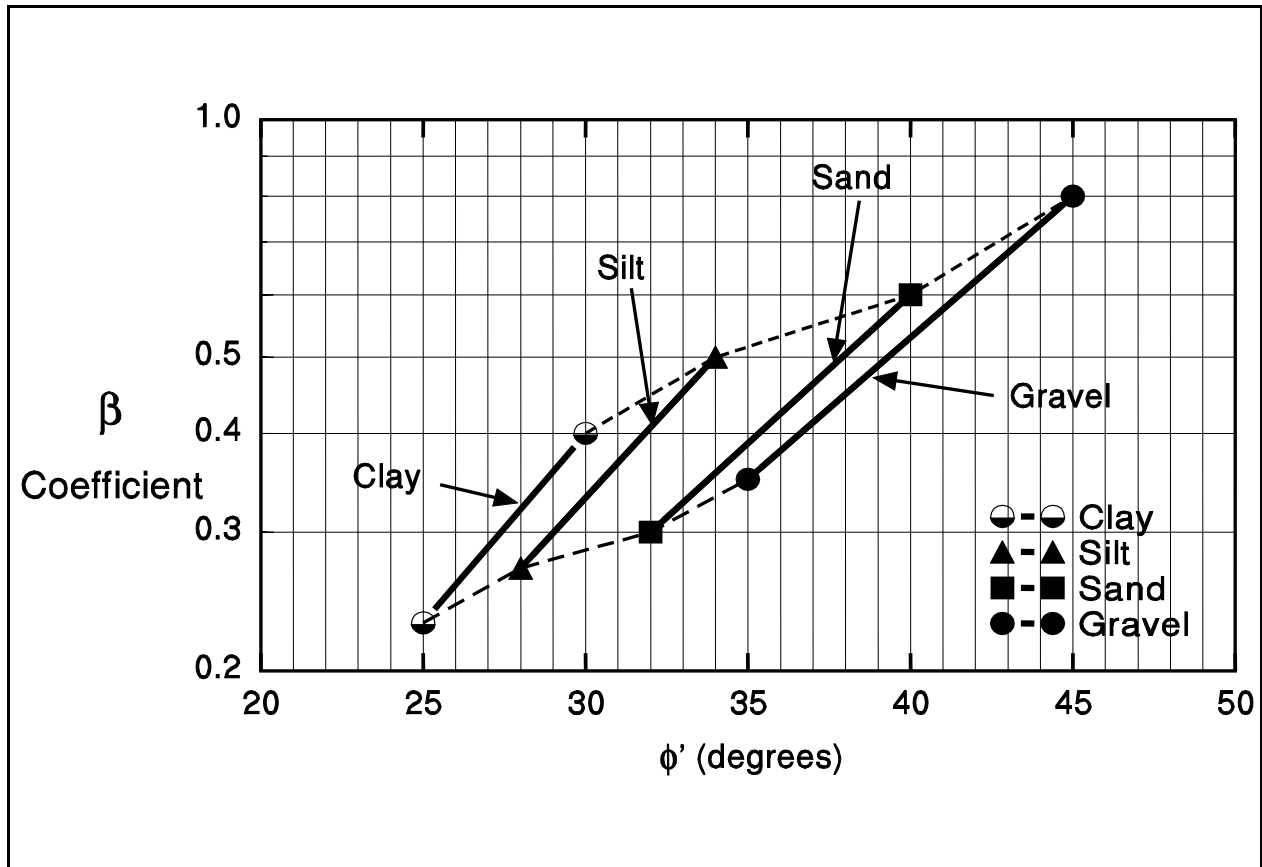


Figure 9.20 Chart for Estimating β Coefficient versus Soil Type ϕ' (after Fellenius, 1991)

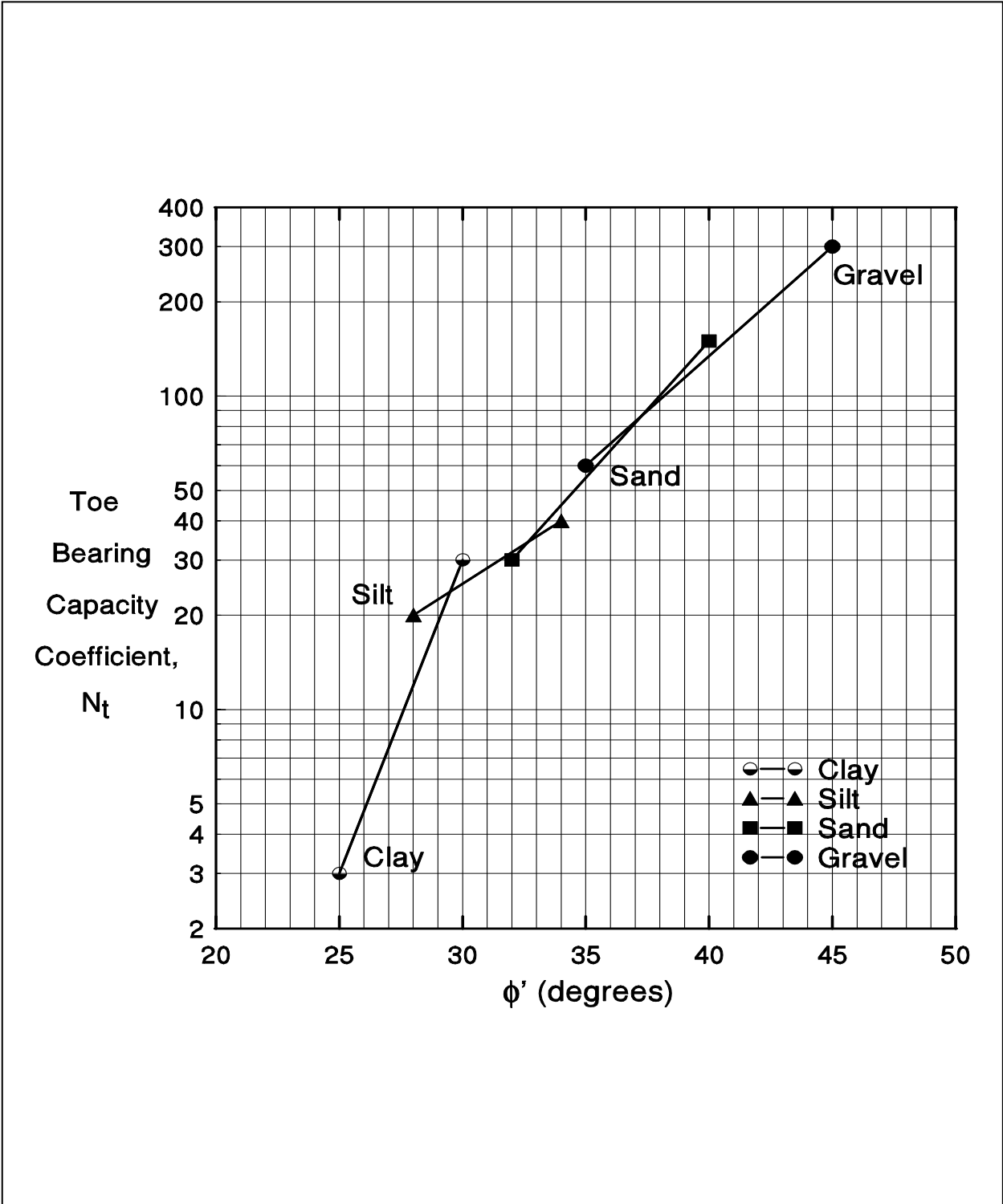


Figure 9.21 Chart for estimating N_t Coefficients versus Soil Type ϕ' Angle (after Fellenius, 1991)

STEP 4 Compute the shaft resistance in each soil layer and the ultimate shaft resistance, R_s in kN (kips) from the sum of the shaft resistance from each soil layer.

$$R_s = f_s A_s$$

Where: A_s = Pile-soil surface area in m^2 (ft^2) from (pile perimeter) (length).

Refer to Section 9.10.5 for additional information on the behavior of open pile sections.

STEP 5 Compute the unit toe resistance, q_t in kPa (ksf).

$$q_t = N_t p_t$$

- a. Use local experience to select N_t coefficient.
- b. In the absence of local experience, estimate N_t from Table 9-6 or Figure 9.21 based on ϕ' angle.
- c. Calculate the effective overburden pressure at the pile toe, p_t in kPa (ksf).

STEP 6 Compute the ultimate toe resistance, R_t in kN (kips).

$$R_t = q_t A_t$$

Where: A_t = Area of the pile toe in m^2 (ft^2).

For open pile sections, refer to the additional information on pile plugging presented in Section 9.10.5.

STEP 7 Compute the ultimate pile capacity, Q_u in kN (kips).

$$Q_u = R_s + R_t$$

STEP 8 Compute the allowable design load, Q_a in kN (kips).

$$Q_a = \frac{Q_u}{\text{Factor of Safety}}$$

The factor of safety in this static calculation should be based on the specified construction control method as described in Section 9.6 of this chapter.

9.7.1.4 Ultimate Capacity of Piles in Layered Soils

The ultimate capacity of piles in layered soils can be calculated by combining the methods previously described for cohesionless and cohesive soils. For example, a hand calculation combining the Nordlund method from Section 9.7.1.1b for cohesionless soil layers with the α -method from Section 9.7.1.2a for cohesive soil layers could be used. The effective stress method as described in Section 9.7.1.3 could also be used for layered soil profiles. Last, the CPT based methods presented in Section 9.7.1.7 could be used in a layered soil profile.

9.7.1.5 The DRIVEN Computer Program

The FHWA developed the computer program DRIVEN in 1998 for calculation of static pile capacity. The DRIVEN program can be used to calculate the capacity of open and closed end pipe piles, H-piles, circular or square solid concrete piles, timber piles, and Monotube piles. The program results can be displayed in both tabular and graphical form. Analyses may be performed in either SI or English units and can be switched between units during analyses. The DRIVEN Program User's Manual by Mathias and Cribbs (1998) is provided in FHWA-SA-98-074. The DRIVEN manual and software Version 1.2, released in March 2001, can be downloaded from: www.fhwa.dot.gov/bridge/geosoft.htm.

In the DRIVEN program, the user inputs the soil profile consisting of the soil unit weights and strength parameters including the percentage strength loss during driving. For the selected pile type, the program calculates the pile capacity versus depth for the entire soil profile using the Nordlund and α -methods in cohesionless and cohesive layers, respectively. Using the user input soil strength losses, the program calculates the ultimate pile capacity at the time of driving as well as during restrike.

The DRIVEN program includes several analysis options that facilitate pile design. These options include:

Soft compressible soils: The shaft resistance from unsuitable soil layers defined by the user is subtracted from the ultimate pile capacity calculation.

Scourable soils: Based on a user input depth, the calculated shaft resistance from scourable soils due to local scour is subtracted from the ultimate pile capacity calculation. In the case of channel degradation scour, the reduction in pile capacity from the loss of shaft resistance in the scour zone as well as the influence of the reduced effective overburden pressure from soil removal on the capacity calculated in the underlying layers is considered.

Pile Plugging: DRIVEN handles pile plugging based on the recommendations presented in Section 9.10.5 of this manual.

The initial DRIVEN program screen is the project description screen illustrated in Figure 9.22. In this screen the user inputs the project information as well as identifies the number of soil layers. Inputs for three water table elevations are provided. The water table at the time of drilling is used for correction of SPT N values for overburden pressure if that option is selected by the user. The water table at the time of restrike / driving affects the effective overburden pressure in the static capacity calculations at those times. The static calculation at the time of driving includes soil strength losses and the restrike static calculations would include the long term soil strength. The water table at the ultimate condition is used in the effective overburden pressure for the static capacity calculation under an extreme event.

The soil profile screen for a two layer soil profile is shown in Figure 9.23 for a cohesive soil. A mouse click on the select graph option will result in the cohesive soil layer properties screen shown in Figure 9.24 to appear. The user can then select how the adhesion is calculated. The general adhesion option uses the Tomlinson data presented in Figure 9.18. The three underlying options correspond to the Tomlinson data presented in Figures 9.19a, 9.19b, and 9.19c, respectively. The bottom option allows the user to enter an adhesion value of their choice.

The soil profile screen for a two layer profile with cohesionless soil properties is presented in Figure 9.25. The user can input the same or different soil friction angles to be used in the shaft resistance and end bearing calculations in the layer. The user can also user to input SPT N values and let the program compute the soil friction angle using a correlation developed by Peck, Hanson and Thornburn in 1974 as shown in Figure 9.26. However, it is recommended that the user manually select the soil friction angle rather than use this program option as factors influencing the N value - ϕ angle correlation such as SPT hammer type and sample recovery are not considered by the program.

Project Definiton

Client Information

Client: FHWA Pile Manual

Project Name: Student Exercise #4

Project Manager: CED

Date: 02/19/2005

Computed By: PJH

Soil Layers

Soil Layers: 2

Water Tables

Depth at top of boring: 0.0

Depth at Time of Drilling: 1.000 m

Depth for Restrike/Driving: 1.000 m

Depth for Ultimate: 1.000 m

Unit System

SI English

Optional Design Considerations

Soft Compressible Soils Overlying the Bearing Strata

Scourable Soil Overlying the Bearing Strata

Figure 9.22 DRIVEN Project Definition Screen

Soil Profile

Soil Layer Profile

Soil Layer #1

Layer General Data

Depth to bottom of layer: 14.000 m

Total unit weight of soil: 19.800 kN/m³

Driving strength loss: 43.000 %

Layer Soil Type

Cohesive Cohesionless

Undrained Shear Strength: 130.000 kPa

Pile Type: Pipe Pile - Closed End

Figure 9.23 DRIVEN Soil Profile Screen – Cohesive Soil

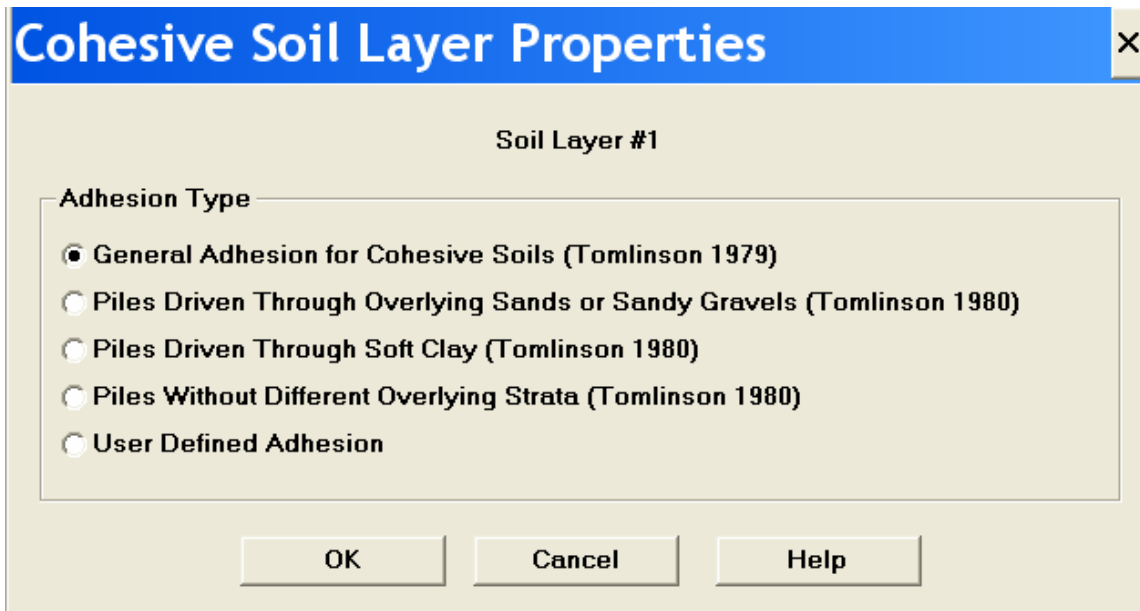


Figure 9.24 DRIVEN Cohesive Soil Layer Properties Screen

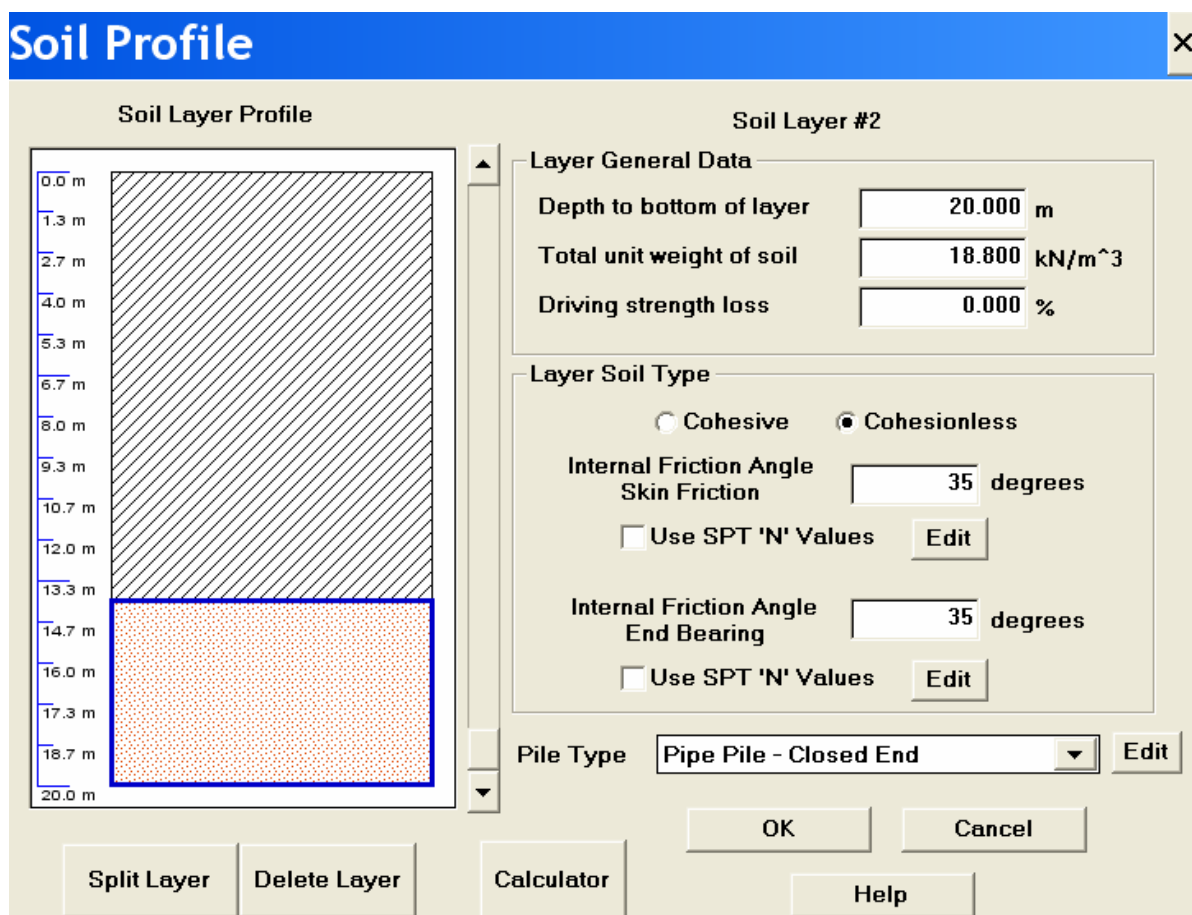


Figure 9.25 DRIVEN Soil Profile Screen – Cohesionless Soil

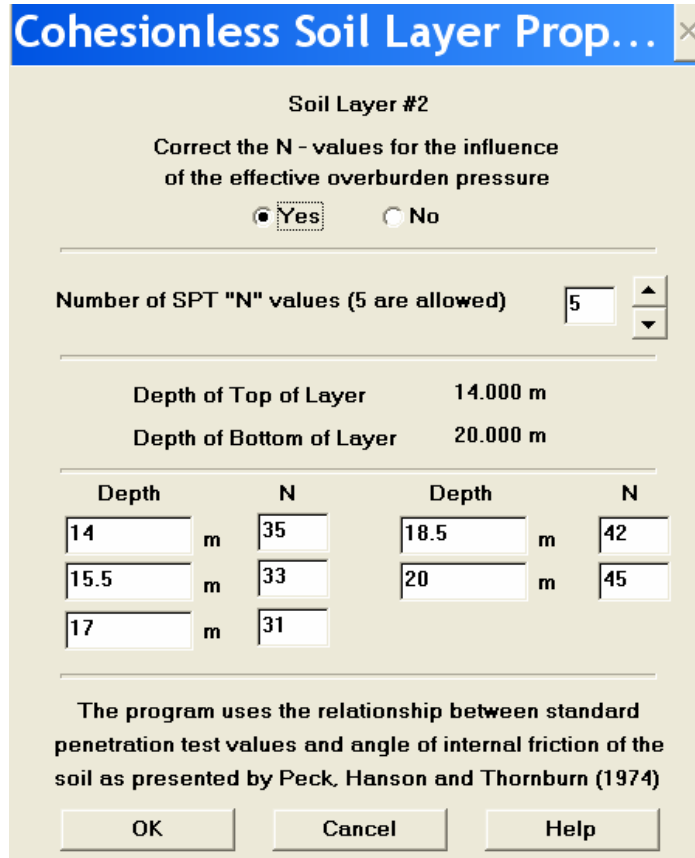


Figure 9.26 DRIVEN Cohesionless Soil Layer Properties Screen

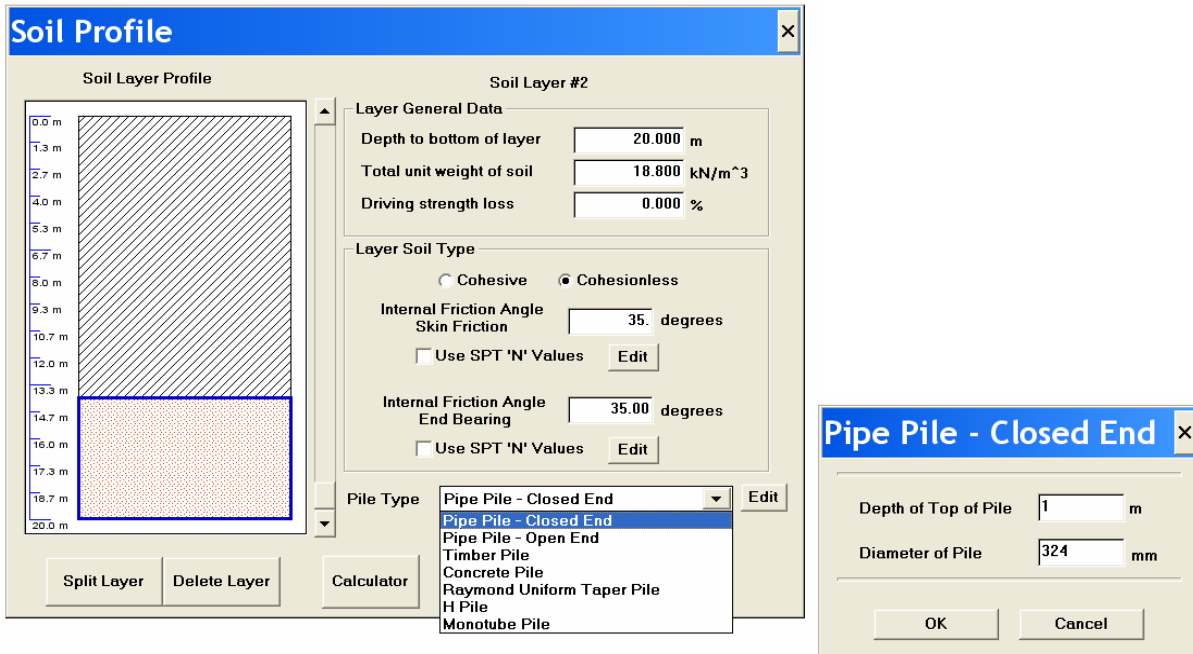


Figure 9.27 Driven Pile Selection Drop Down Menu and Pile Detail Screen

Both cohesive and cohesionless soil profile screens request the user to provide the percentage strength loss of the soil type during driving. This is sometimes difficult for the program user to quantify. Insight into appropriate driving strength loss values can be gathered from the soil setup factors presented in Table 9-19 of Section 9.10.1.1. The percent driving strength loss needed for input into DRIVEN can be then be calculated from:

$$\% \text{ Driving Strength Loss} = 1 - [1 / \text{setup factor}]$$

After the soil input has been entered, the user must select a pile type from a drop down menu. A pile detail screen will appear for the pile type selected requesting additional information on the depth to the top of the pile and the pile properties. These DRIVEN screens are presented in Figure 9.27.

Once all soil and pile information is entered, the user can review the static capacity calculations in tabular or graphical form by a mouse click on the appropriate icon in the program toolbar. The icons for tabular and graphical output are identified in Figure 9.28. The tabular output screen is shown in Figure 9.29. A summary of the analysis input and results will be printed if the user clicks on the report button. Analysis output can also be presented graphically as shown in Figures 9.30 and 9.31 for driving and restrike static analyses, respectively. The ultimate capacity versus depth from shaft resistance, toe resistance, and the combined shaft and toe resistance can be displayed by clicking on “skin friction”, “end bearing”, and “total capacity”. Capacity changes with time or from extreme events can be reviewed by clicking on “restrike”, “driving”, and “ultimate” in the plot set area.

The program also generates the soil input file required for a driveability study in the GRLWEAP wave equation program. The GRLWEAP file created by DRIVEN is compatible with the Windows versions of GRLWEAP. However, the DRIVEN file must be identified as a pre 2002 input file in the current version of GRLWEAP.

Additional DRIVEN program capabilities are described in the DRIVEN Program User’s Manual by Mathias and Cribbs (1998).

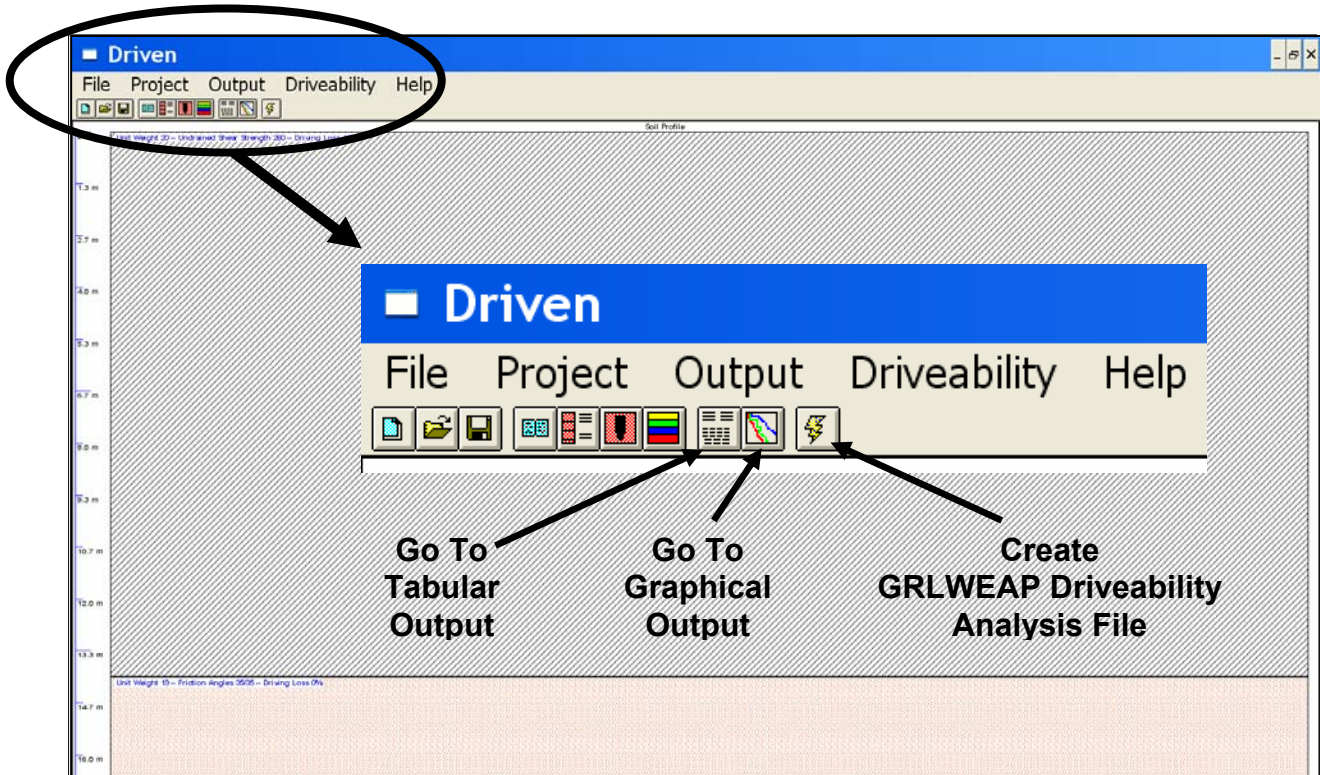


Figure 9.28 DRIVEN Toolbar Output and Analysis Options

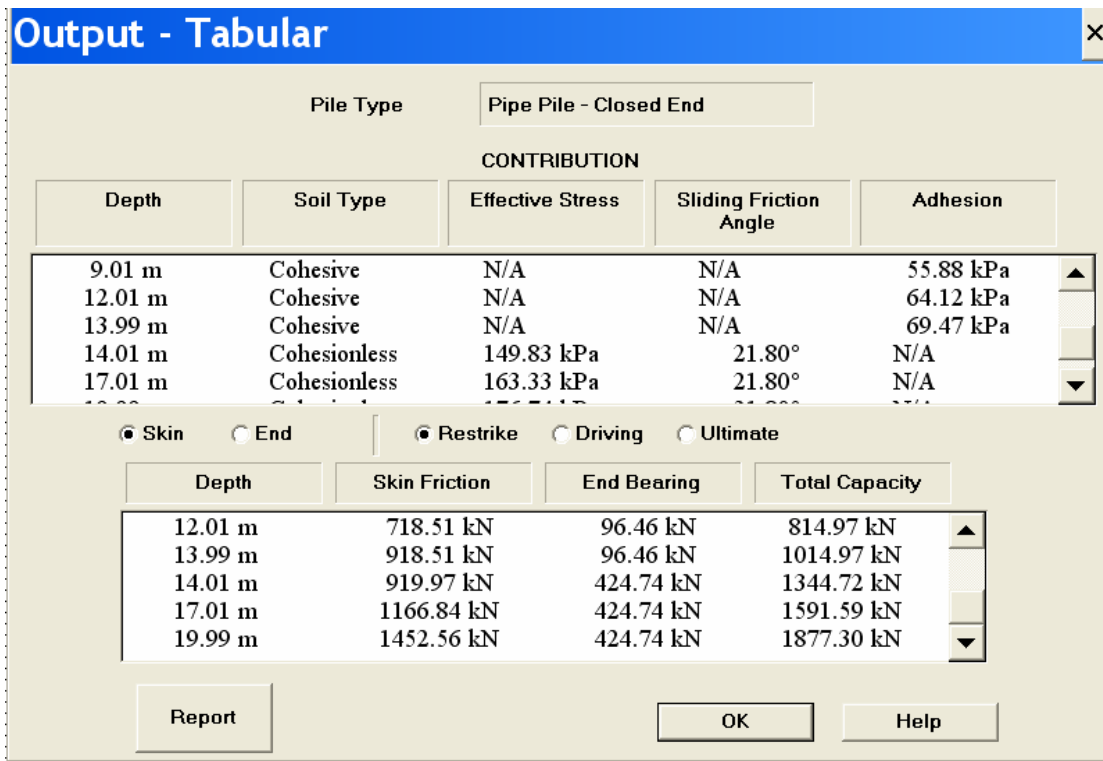


Figure 9.29 DRIVEN Tabular Output Screen

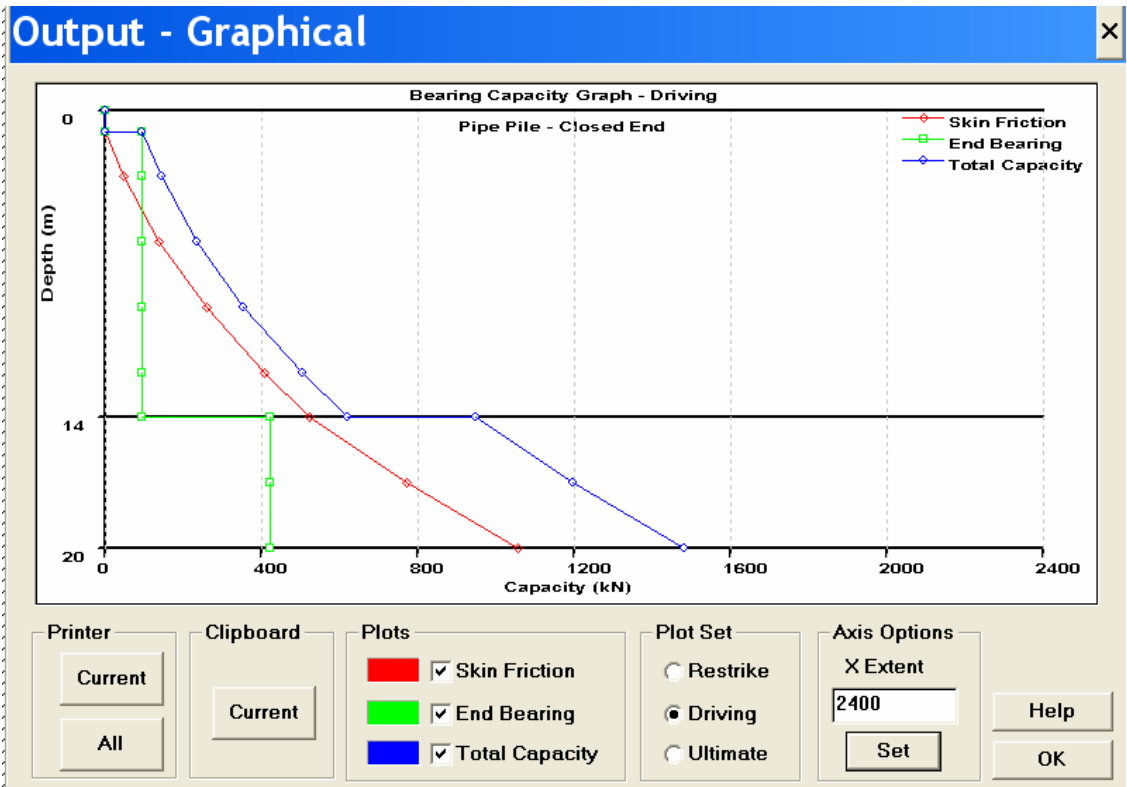


Figure 9.30 DRIVEN Graphical Output for End of Driving

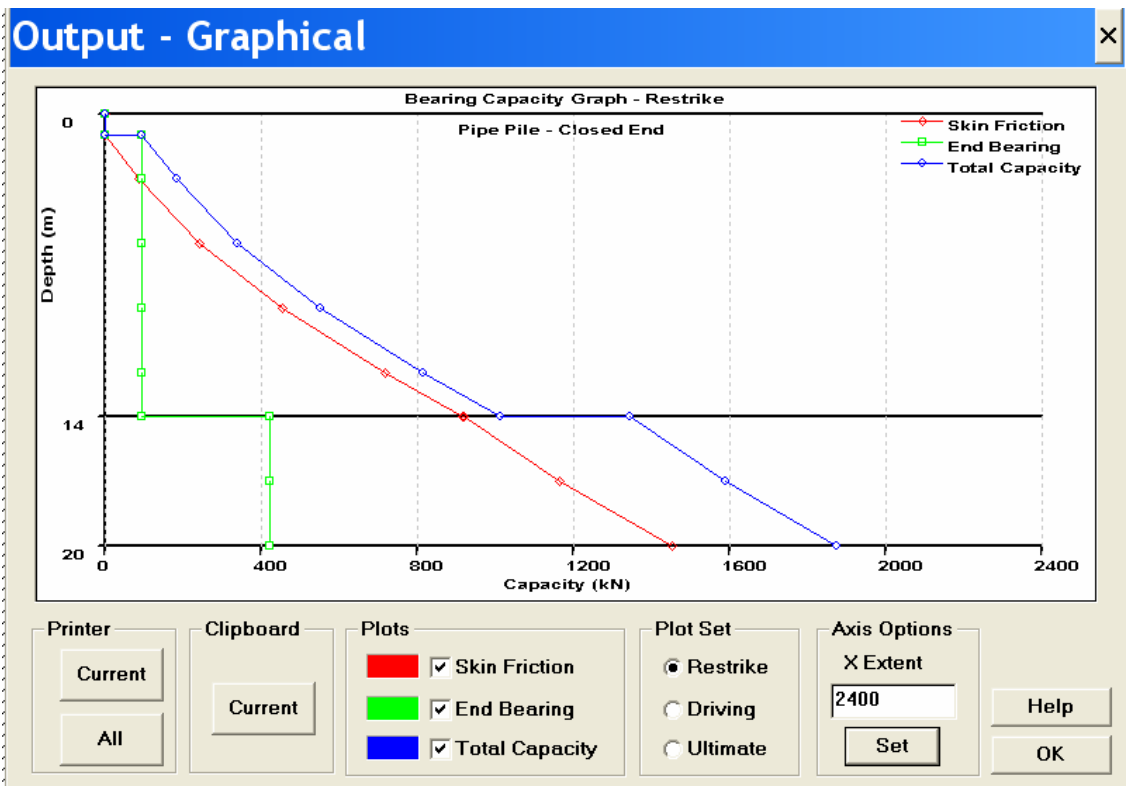


Figure 9.31 DRIVEN Graphical Output for Restrike.

9.7.1.6 Ultimate Capacity of Piles on Rock

Pile foundations on rock are normally designed to carry large loads. For pile foundations driven to rock, which include steel H-piles, pipe piles or precast concrete piles, the exact area in contact with the rock, the depth of penetration into rock, as well as the quality of rock are largely unknown. Therefore, the determination of load capacity of driven piles on rock should be made on the basis of driving observations, local experience and load tests.

Rock Quality Designation (RQD) Values can provide a qualitative assessment of rock mass as shown in Table 9-7. The RQD is only for NX size or larger core samples (double tube core barrel) and is computed by summing the length of all pieces of core equal to or longer than 102 mm (4 inches) and dividing by the total length of the coring run. The result is multiplied by 100 to get RQD in percent. Fresh, irregular breaks should be ignored and the pieces counted as intact lengths.

TABLE 9-7 ENGINEERING CLASSIFICATION FOR IN-SITU ROCK QUALITY	
RQD %	Rock Mass Quality
90-100	Excellent
75-90	Good
50-75	Fair
25-50	Poor
0-25	Very Poor

Except for soft weathered rock, the structural capacity of the pile will generally be lower than the capacity of rock to support loads for toe bearing piles on rock of fair to excellent quality as described in Table 9-7. The structural capacity, which is based on the allowable design stress for the pile material, will therefore govern the pile capacity in many cases.

Small diameter piles supported on fair to excellent quality rock may be loaded to their allowable structural capacity as described in Chapter 10. Piles supported on soft weathered rock, such as shale or other types of very poor or poor quality, should be designed based on the results of pile load tests.

9.7.1.7 Methods Based on Cone Penetration Test (CPT) Data

When subsurface exploration programs include in-situ testing with a static cone penetrometer test (CPT), the CPT data can be used to estimate static capacity of single piles under axial loading. The CPT provides especially useful data as a "model pile" pushed into the strata expected to contribute resistance for a driven pile. The cone penetration resistance often correlates well with that of a driven full-sized pile under static loading conditions.

At sites where the cone soundings satisfactorily penetrate to the depths contemplated for driven piles, the CPT results can provide valuable information for estimating static pile capacities. At locations where a shallow stratum causes "refusal" conditions for the CPT device, it is likely that pile driveability problems could develop in the same stratum.

There are two main approaches for using CPT data to pile design, indirect methods and direct methods. Indirect methods use CPT derived soil parameters such as soil friction angle and undrained shear strength along with bearing capacity and / or cavity expansion theories. Direct methods use cone resistance values to determine unit shaft and toe resistances. Eslami and Fellenius (1997) consider indirect methods less suitable for pile capacity evaluations than direct methods. They also note that there are five direct methods currently used for pile capacity evaluations in North America. These methods include the Nottingham and Schmertmann method, the Laboratoire des Ponts et Chaussées or LPC Method, the DeRuiter and Beringen method, the Meyerhof method, and the Tumay and Fakhroo method. However, all of these methods have limitations. Eslami and Fellenius (1997) identify the following difficulties associated with the current direct methods.

1. The five CPT methods are over a decade old and the method calibration was made with older cone than the modern cones now available.
2. The methods do not include a means of identify soil type from the CPT data.
3. All five methods specify extreme values be eliminated or filtered out potentially biasing the results.
4. The methods were developed prior to the piezocone and therefore neglect the pore pressure acting on the cone shoulder.
5. The CPT methods use total stress rather than effective stress values.

6. The methods were developed based on pile types and soil conditions in a local area and may therefore not perform as well outside of that locality.
7. All five methods require judgment in selecting the coefficient applied to the average cone resistance to determine unit toe resistance.

Elsami and Fellenius (1997) note several other specific limitations of particular methods. The methods presented in this the following sections of this manual include a new direct method based on CPTu measurements proposed Elsami and Fellenius, as well as the Nottingham and Schmertmann Method and the LPC Method. Additional information on the two older direct CPT methods may be found in FHWA publication FHWA-SA-91-043, "The Cone Penetrometer Test", by Briaud and Miran (1991). The UNICONE computer program performs ultimate pile capacity calculations for all five CPT and the one CPTu direct methods.

9.7.1.7a Elsami and Fellenius Method

In the Elsami and Fellenius method, the unit shaft resistance is correlated to the average effective cone tip resistance with a shaft correlation coefficient applied based on the soil profile. The unit shaft resistance is calculated from:

$$f_s = C_{sc} q_E$$

Where: C_{sc} = is the shaft correlation coefficient from Table 9-8.
 q_E = the cone tip resistance after correction for pore pressure on the cone shoulder and adjustment to effective stress.

The shaft resistance in a given soil layer is then:

$$R_s = f_s A_s$$

Where: A_s = Pile shaft surface area.
 = (pile perimeter)(embedded length).

The unit toe resistance is computed using a geometric averaging of the cone tip resistance over the influence zone at the pile toe after the cone tip resistances have been corrected

TABLE 9-8 C_{sc} VALUES FOR ELSAMI AND FELLENIUS METHOD	
Soil Type	C_{sc} (%)
Soft sensitive soil	8.0
Clay	5.0
Stiff clay and mixtures of clay and silt	2.5
Mixture of silt and sand	1.0
Sand	0.4

for pore pressure on the cone shoulder and effective stress. The zone of influence at the pile toe is based on the pile diameter, b , and ranges from $4b$ below the pile toe to $8b$ above the pile toe when the pile is installed through a weak zone overlying a dense zone. When a pile is driven through a dense soil into a weak soil, the zone of influence is from $4b$ below the pile toe to $2b$ above the pile toe. The unit toe resistance is calculated from:

$$q_t = C_{tc} q_{Eg}$$

Where: C_{tc} = toe correction coefficient equal to 1.0 in most cases.
 q_{Eg} = geometric average of the cone tip resistance over the influence zone after correction for pore pressure on the cone shoulder and adjustment to effective stress.

The toe correction coefficient is a function of the pile size since larger piles require greater movement to mobilize the pile toe resistance. For pile diameters, b , greater than 400 mm (16 inches), the toe correction coefficient should be calculated as follows:

SI units $C_{tc} = 1 / 3b$ (b in meters)

US Units $C_{tc} = 12 / b$ (b in inches)

The pile toe resistance is then computed from:

$$R_t = q_t A_t$$

Where: A_t = Pile toe area.

The ultimate pile capacity, Q_u , using the Elsami and Fellenius method is obtained by summing the shaft resistance from each soil layer plus the toe resistance or:

$$Q_u = R_s + R_t$$

9.7.1.7b Nottingham and Schmertmann Method

One empirical procedure used in U.S. practice was derived from work originally published by Nottingham and Schmertmann (1975), and summarized in publication FHWA-TS-78-209, "Guidelines for Cone Penetration Test, Performance and Design" by Schmertmann (1978). The ultimate shaft resistance, R_s , in cohesionless soils may be derived from unit sleeve friction of the CPT using the following expression:

$$R_s = K \left[\frac{1}{2} (\bar{f}_s A_s)_{0 \text{ to } 8b} + (\bar{f}_s A_s)_{8b \text{ to } D} \right]$$

Where: K = Ratio of unit pile shaft resistance to unit cone sleeve friction from Figure 9.32 as a function of the full penetration depth, D .

\bar{f}_s = Average unit sleeve friction over the depth interval indicated by subscript.

A_s = Pile-soil surface area over f_s depth interval.

b = Pile width or diameter.

D = Embedded pile length.

0 to $8b$ = Range of depths for segment from ground surface to a depth of $8b$.

$8b$ to D = Range of depths for segment from a depth equal to $8b$ to the pile toe.

The transfer function K , relating pile shaft resistance to CPT sleeve friction, varies as a function of total pile penetration (depth of embedment/pile diameter), pile material type, and type of cone penetrometer used. No limit was imposed on sleeve friction values in the procedure originally proposed by Nottingham and Schmertmann (1975).

If cone sleeve friction data is not available, R_s can be determined from the cone tip resistance as follows:

$$R_s = C_f \sum q_c A_s$$

Where: C_f is obtained from Table 9-9 and
 q_c = Average cone tip resistance along the pile length.
 A_s = Pile-soil surface area from (pile perimeter) (length).

TABLE 9-9 CPT C_f VALUES	
Type of Piles	C_f
Precast Concrete	0.012
Timber	0.018
Steel Displacement	0.012
Open End Steel Pipe	0.008

For shaft resistance in cohesive soils, the ultimate shaft resistance, R_s , is obtained from the sleeve friction values using the following expression:

$$R_s = \alpha' \bar{f}_s A_s$$

Where: α' = Ratio of pile shaft resistance to cone sleeve friction, patterned after Tomlinson's α -method.

The value of α' varies as a function of sleeve friction, f_s , value as shown in Figure 9.33. It is expected that this method of calculating pile shaft resistance is less appropriate in sensitive soils as the friction sleeve of the cone encounters severely disturbed soils behind the cone tip.

The estimation of pile toe ultimate capacity is described in Figure 9.34. In essence an elaborate averaging scheme is used to weight the cone tip resistance values, from 8 pile diameters above the pile toe, to as much as 3.75 pile diameters below the pile toe, favoring the lower cone tip resistance, q_c , values within the depth range. The authors make reference to a "limit" value of q_c between 5000 to 15000 kPa, that should be applied to the ultimate unit pile toe resistance, q_t , unless local experience warrants use of higher values. In the case of mechanical cone soundings in cohesive soils, the q_t value is reduced by 40 percent to account for end bearing effects on the base of the friction sleeve. As discussed in Section 9.10.5, careful consideration of soil plugging phenomena is needed in choosing the cross-sectional area over which q_t is applied for low displacement open ended pipe and H-piles.

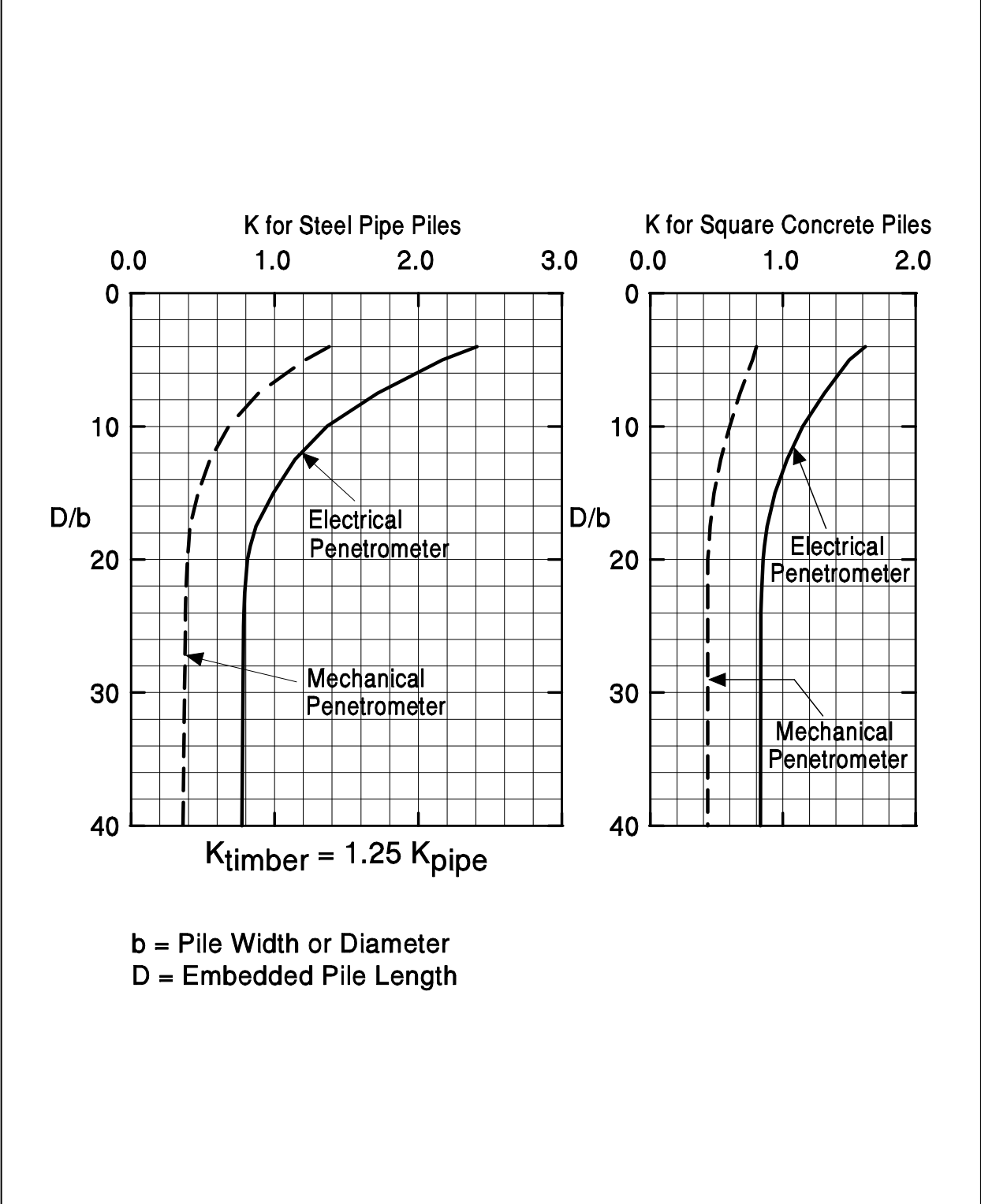


Figure 9.32 Penetrometer Design Curves for Pile Side Friction in Sand (after FHWA Implementation Package, FHWA-TS-78-209)

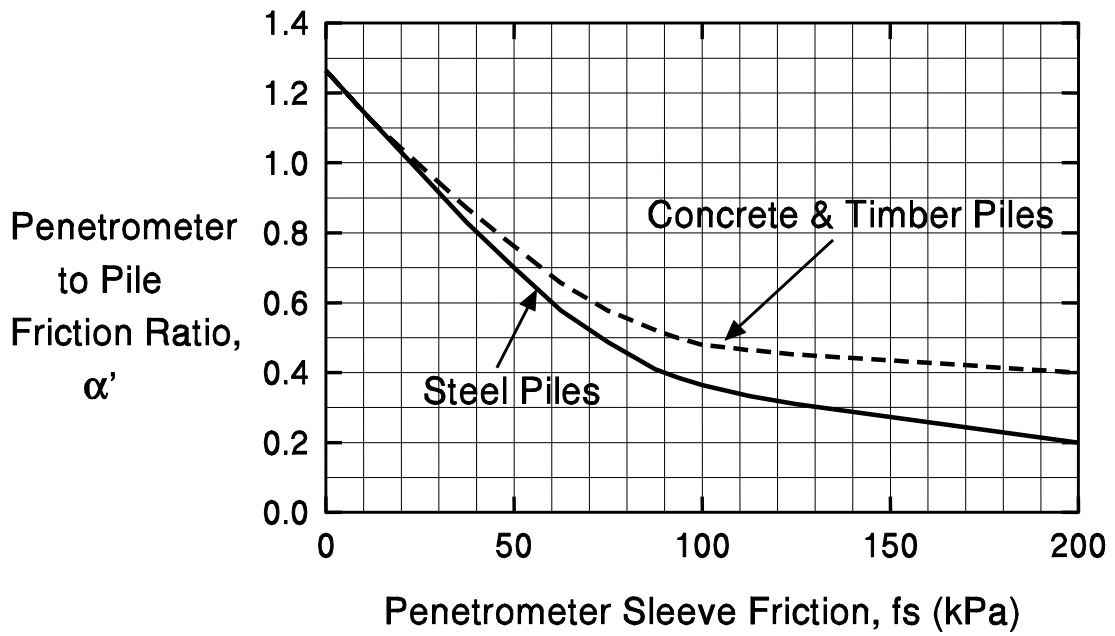


Figure 9.33 Design Curve for Pile Side Friction in Clay (after Schmertmann, 1978)

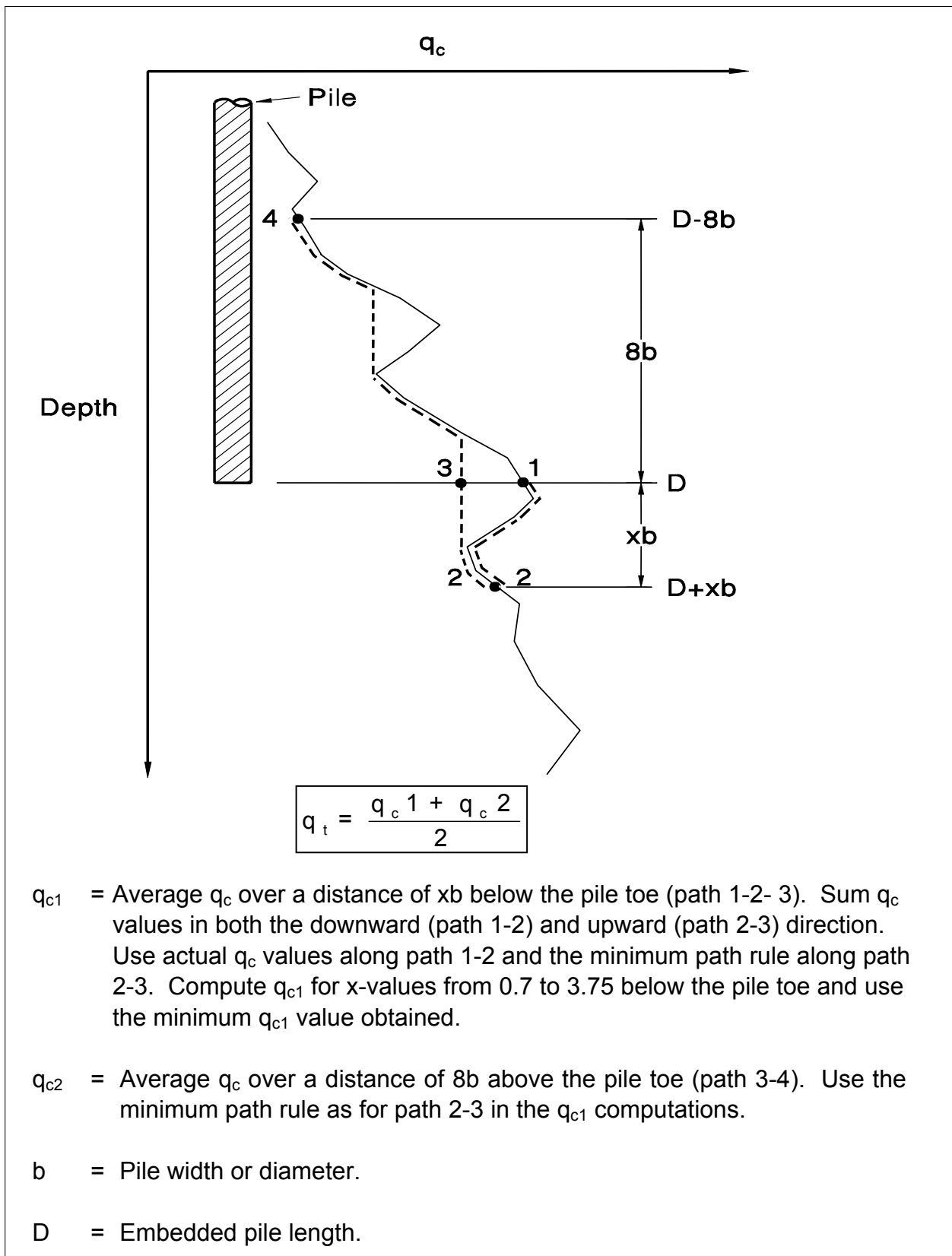


Figure 9.34 Illustration of Nottingham and Schmertmann Procedure for Estimating Pile Toe Capacity (FHWA-TS-78-209)

STEP BY STEP PROCEDURE FOR THE NOTTINGHAM AND SCHMERTMANN METHOD

STEP 1 Delineate the soil profile into layers using the cone tip resistance, q_t , and sleeve friction, f_s , values.

STEP 2 Compute the shaft resistance for each soil layer, R_s (kN).

- a. For piles in cohesionless soils, compute ultimate shaft resistance, R_s , using the average sleeve friction value for the layer, \bar{f}_s , and the K value. Note that K should be determined using the full pile penetration depth to diameter ratio from Figure 9.32, and not the penetration depth for the layer. Conversely, the depth d corresponds to the pile toe depth, or the depth to the bottom of the layer, whichever is less. For H-piles in cohesionless soils, the pile-soil surface area A_s , should be the "box" area.

$$R_s = K \left[\frac{1}{2} (\bar{f}_s A_s)_{0 \text{ to } 8b} + (\bar{f}_s A_s)_{8b \text{ to } d} \right]$$

For cohesionless layers below a depth of 8b, the above equation for shaft resistance in a layer reduces to:

$$R_s = K \bar{f}_s A_s$$

For piles in cohesionless soils without sleeve friction data, compute the ultimate shaft resistance from:

$$R_s = C_f \sum q_c A_s$$

Where: C_f is obtained from Table 9-9 and

q_c = Average cone tip resistance along the pile length.

- b. For piles in cohesive soils, compute the ultimate shaft resistance using the average sleeve friction value for the layer from:

$$R_s = \alpha' \bar{f}_s A_s$$

Where: α' determined from Figure 9.33.

STEP 3 Calculate the total pile shaft resistance from the sum of the shaft resistances from each soil layer.

STEP 4 Compute the unit pile toe resistance, q_t (kPa).

$$q_t = \frac{q_{c1} + q_{c2}}{2}$$

Where: q_{c1} and q_{c2} = Unit cone tip resistance.

Use procedure shown in Figure 9.24 to determine q_t .

STEP 5 Determine the ultimate toe resistance, R_t (kN).

$$R_t = q_t A_t$$

Where: A_t = Pile toe area.

For steel H and unfilled open ended pipe piles, use only the steel cross section area at the pile toe unless there is reasonable assurance and previous experience that a soil plug would form. For a plugged condition use the "box" area of the H pile and the full cross section area for pipe pile. Additional information on the plugging of open pile sections is presented in Section 9.10.5.

STEP 6 Determine ultimate pile capacity, Q_u (kN).

$$Q_u = R_s + R_t$$

STEP 7 Determine allowable design load, Q_a (kN).

$$Q_a = \frac{Q_u}{\text{Factor of Safety}}$$

The factor of safety in this static calculation should be based on the specified construction control method as described in Section 9.6 of this chapter.

9.7.1.7c Laboratoire des Ponts et Chaussees (LPC)

The LPC method was developed and presented by Bustamante and Gianeselli (1983), based on empirical criteria taking into consideration soil type, pile type, and level of cone tip resistance. The approach considers only cone tip resistance, q_c , and factors soil type, pile type, installation method, and q_c , into determination of ultimate shaft resistance along the pile, contributed layer-by-layer, based on a family of prescribed curves. The resistance at the pile toe is calculated as the product of q_c and a cone bearing factor, K_c , that varies by soil type and pile installation method.

In the LPC method, the pile is categorized based on pile type and installation procedure as indicated in Table 9-10. Next Tables 9-11(a) and 9-11(b) are used to determine the shaft resistance design curve in Figures 9.35(a) or 9.35(b) to be used for each soil layer, based on the soil type, pile category and cone tip resistance. In Table 9-11(a), the method provides no guidance on whether to use design curve 1 or 2 when q_c is between 700 and 1200 kPa (15 and 25 ksf). Therefore it is recommended to interpolate between curves 1 or 2 when q_c is between 700 and 1200 kPa (15 and 25 ksf) to determine the unit shaft resistance, f_s .

The unit toe resistance is calculated from the cone bearing capacity factor, K_c , obtained in Table 9-12, times the average cone resistance, q_c , within one pile diameter below the pile toe. This may be expressed in equation from as:

$$q_t = K_c q_c$$

In order to apply the CPT design procedures, it is necessary to characterize the subsurface materials as cohesive or cohesionless. The usual approach is to identify the "soil behavior" type as a function of cone tip resistance, q_c , and friction ratio, R_f . The friction ratio is the cone sleeve friction, f_s , divided by the cone tip resistance, or f_s/q_c . The soil classification chart presented in Figure 5.2 can then be used to characterize the soil as cohesive or cohesionless.

TABLE 9-10 DRIVEN PILE TYPE CATEGORIES FOR LPC METHOD		
Pile Type	Pile Description	Pile Installation Procedure
A	Driven prefabricated concrete piles.	Reinforced or prestressed concrete pile installed by driving or vibro-driving
B	Driven steel piles.	Pile made of steel only and driven in place: H pile, pipe pile or any shape obtained by welding sheet-pile sections.
C	Driven prestressed concrete tube piles.	Made of hollow cylinder elements of lightly reinforced concrete assembled together by prestressing before driving. Each element is generally 1.5 to 3 m (5 to 10 ft) long and 0.7 to 0.9 m (2.3 to 3 ft) in diameter; the thickness is approximately 0.15 m (0.5 ft). The piles are driven open-ended.

TABLE 9-11(a) CURVE SELECTION BASED ON PILE TYPE AND INSERTION PROCEDURES FOR CLAY AND SILT			
Curve No.	q_c in kPa (ksf)	Pile Type (see Table 9-9)	Comments on Insertion Procedure
1	<700 (<15 ksf)	A, B, C	
2	>1200 (>25 ksf)	A, B, C	For all steel piles, experience shows that, in plastic soils, f_s is often as low as curve 1. Therefore, use curve 1 in plastic soils when no previous load test data is available. For all driven concrete piles use curve 3 in low plasticity soils with sand or sand and gravel layers or containing boulders, and when $q_c > 2500$ kPa (52 ksf).
3	> 1200 (>25 ksf)	A	For all driven concrete piles in low plasticity soils with sand or sand and gravel layers or containing boulders, and when $q_c > 2500$ kPa (52 ksf).

TABLE 9-11(b) CURVE SELECTION BASED ON PILE TYPE AND INSERTION PROCEDURES FOR SAND AND GRAVEL			
Curve No.	q_c in kPa (ksf)	Pile Type (see Table 9-9)	Comments on Insertion Procedure
1	<3500 (<74 ksf)	A, B, C	
2	>3500 (>74 ksf)	A, B, C	For fine sands. Since steel piles can lead to very small values of f_s in such soils, use curve 1 unless higher values can be based on load test results. For concrete piles, use curve 2 for fine sands of $q_c > 7500$ kPa (157 ksf).
3	>7500 (>157 ksf)	A, B	For coarse gravelly sand or gravel only. For concrete piles, use curve 4 if it can be justified by a load test.
4	>7500 (>157 ksf)	A	Only for coarse gravelly sand and gravel and, if justified, by load test.

TABLE 9-12 CONE BEARING CAPACITY FACTORS FOR LPC METHOD	
Type of Soil	Cone Bearing Factor, K_c
Clay-silt	0.600
Sand-gravel	0.375

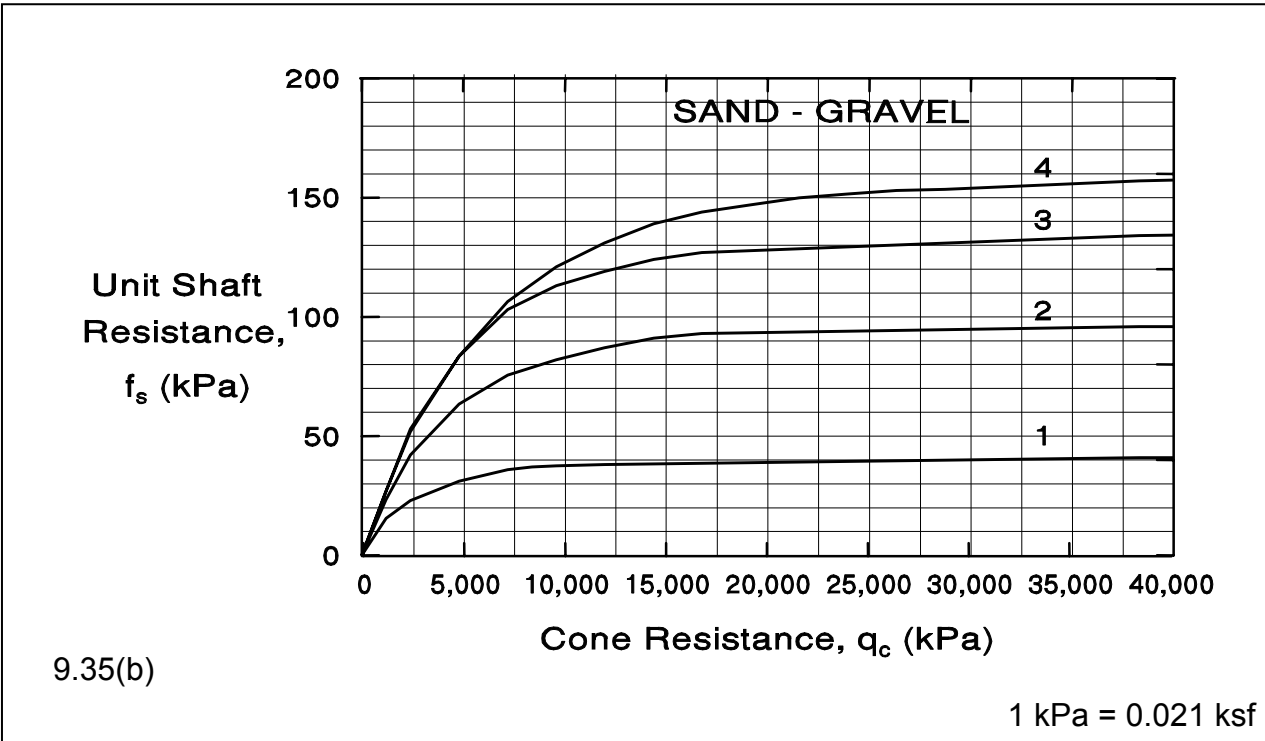
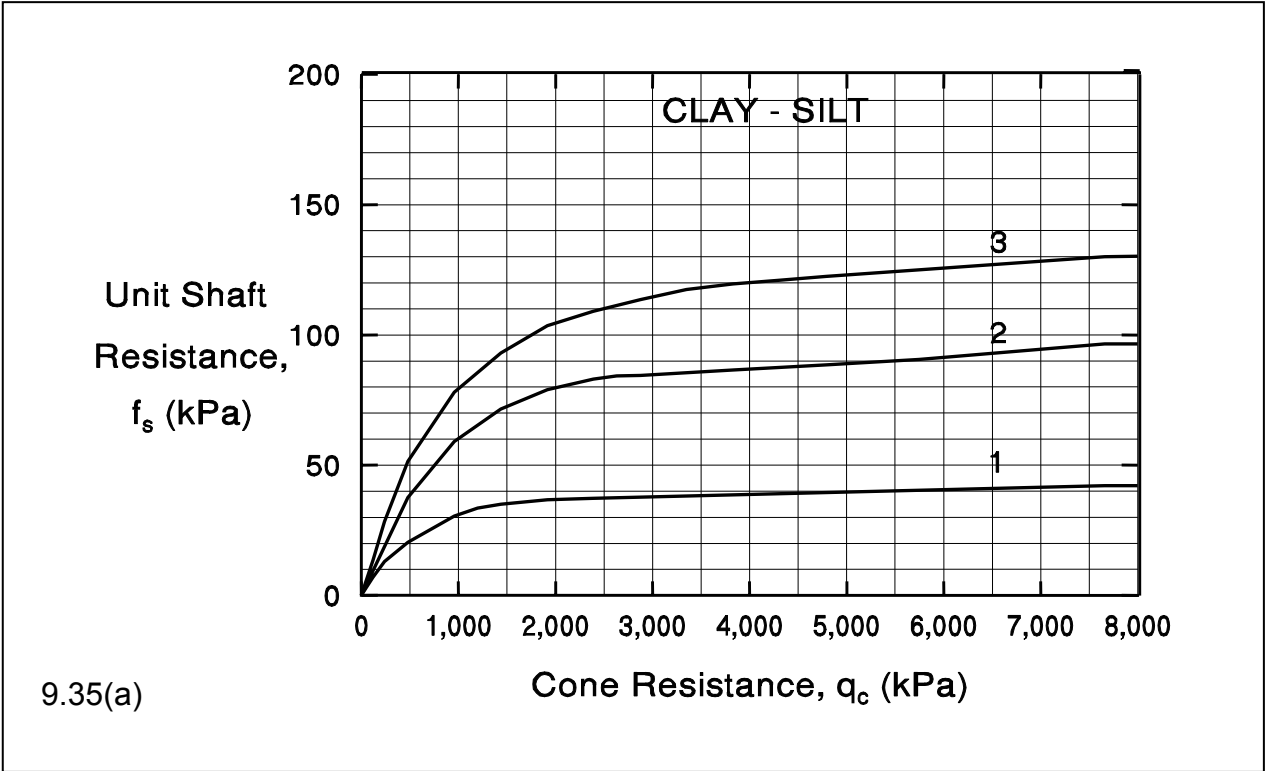


Figure 9.35 Maximum Unit Shaft Resistance Curves for LPC Method

STEP BY STEP PROCEDURE FOR THE LPC METHOD

STEP 1 Delineate the soil profile into layers using the cone tip resistance, q_c , and friction ratio, R_f , values.

Use Figure 5.2 to characterize each layer as cohesive or cohesionless.

STEP 2 Determine unit shaft resistance values for each soil layer, f_s (kPa).

a. Determine the average q_c value for each layer.

b. Use Table 9-11(a) or 9-11(b) to determine appropriate friction design curve in Figure 9.35(a), or Figure 9.35(b) based on pile type from Table 9-9 and soil characterization.

c. Enter Figures 9.35(a) or 9.35(b) with cone tip resistance, q_c , to determine layer unit shaft resistance, f_s (kPa).

STEP 3 Compute the shaft resistance in each soil layer and the ultimate shaft resistance, R_s (kN), from the sum of the shaft resistance from each soil layer.

$$R_s = f_s A_s$$

Where: A_s = Pile-soil surface area from pile perimeter and length.
For H-piles, the "box" area should be used.

STEP 4 Compute the unit pile toe resistance, q_t (kPa).

a. Average q_c value from pile toe to one diameter below pile toe.

b. Obtain cone bearing capacity factor, K_c , from Table 9-12.

c. Compute unit pile toe resistance from following equation.

$$q_t = K_c q_c$$

STEP 5 Compute the ultimate toe resistance, R_t in kN (kips).

$$R_t = q_t A_t$$

Where: A_t = Pile toe area in m^2 (ft^2).

Note: For steel H and unfilled open ended pipe piles, use only the steel cross section area at the pile toe unless there is reasonable assurance and previous experience that a soil plug would form. For a plugged condition use the "box" area of the H pile and the full cross section area for pipe pile. Additional discussion on plugging of open pile sections is presented in 9.10.5.

STEP 6 Compute the ultimate pile capacity, Q_u on kN (kips).

$$Q_u = R_s + R_t$$

STEP 7 Determine allowable design load, Q_a in kN (kips).

$$Q_a = \frac{Q_u}{\text{Factor of Safety}}$$

The factor of safety in this static calculation should be based on the specified construction control method as described in Section 9.6 of this chapter.

9.7.2 Uplift Capacity of Single Piles

The design of piles for uplift loading conditions has become increasingly important for structures subject to seismic loading. In some cases, the pile uplift capacity determines the minimum pile penetration requirements. Nicola and Randolph (1993) note that in fine grained cohesive soils, where loading is assumed to occur under undrained conditions, the shaft resistance is generally considered equal in compression and in uplift.

In noncohesive or free draining soils, the uplift capacity of a pile has been more controversial. Nicola and Randolph (1993) state that it has been customary to assume that the shaft resistance in uplift is approximately 70% of the shaft resistance in compression. Based upon a finite difference parametric study, they concluded that a reduction in shaft resistance for uplift in free draining soils should be used, and that piles have lower uplift capacity than their compression shaft resistance. Conversely, the American Petroleum Institute's (1993) recommended design practice considers the pile shaft resistance to be equal in uplift and compression loading. Likewise, Altaee, *et al.*, (1992) presented a case of an instrumented pile in sand where the shaft resistance was approximately equal in compression and uplift when residual stresses were considered.

Tomlinson (1994) notes that the shaft resistance under cyclic loading is influenced by the rate of application of load as well as the degree of degradation of soil particles at the soil-pile interface. Under cyclic or sustained uplift loading in clays, the uplift resistance can decrease from the peak value to a residual value. In sands, particle degradation or reorientation can also result in decrease in uplift capacity under cyclic or sustained uplift loading. Therefore, the designer should consider what effect, if any, sustained or cyclic uplift loading will have on soil strength degradation.

Based on the above issues, the design uplift capacity of a single pile should be taken as $\frac{1}{3}$ of the ultimate shaft resistance calculated from any of the static analysis methods presented in this chapter except for the Meyerhof (SPT) method which should not be used. If a tensile load test is done for design confirmation, the design uplift capacity may be increased to $\frac{1}{2}$ of the tensile load test failure load as defined in Chapter 18. Selection of the design uplift capacity should also consider the potential for soil strength degradation due to the duration or frequency of uplift loading, which may not influence the load test results.

The uplift capacity of pile groups is discussed in Section 9.8.3. Tensile load test procedures are described by Kyfor *et al.* (1992) in FHWA-SA-91-042 and in Chapter 18.

9.7.3 Ultimate Lateral Capacity of Single Piles

In addition to axial compression and uplift loads, piles are routinely subjected to lateral loads. Potential sources of lateral loads on bridge structures include vehicle acceleration and braking forces, wind loads, wave and current forces, debris loading, ice forces, vessel impact loads, construction procedures, thermal expansion and contraction, earth pressures on the backs of abutment walls, slope movements, and seismic events. These lateral loads can be of the same magnitude as axial compressive loads and therefore warrant careful consideration during design. The foundation deformation under lateral loading must also be within the established performance criterion for the structure.

Historically, designers often used prescription values for the lateral load capacity of vertical piles, or added batter piles to increase a pile group's lateral capacity when it was believed that vertical piles could not provide the needed lateral resistance. However, vertical piles can be designed to withstand significant lateral loads. Modern analysis methods should be employed in the selection of the pile type and pile section.

Coduto (1994) notes that a foundation system consisting of only vertical piles designed to resist both axial and lateral loads is more flexible, and thus more effective at resisting dynamic loads, as well as less expensive to build. Bollmann (1993) reported that the Florida Department of Transportation often uses only vertical piles to resist lateral loads, including ship impact loads because vertical piles are often less expensive than batter piles. In areas where seismic lateral shaking is a serious concern, batter piles can deliver excessively large horizontal forces to the structure during the earthquake event. This phenomenon was observed during the Loma Prieta earthquake of 1989 in California and discussed in greater detail by Hadjian *et al.* (1992). In earthquake areas, lateral loads should be resisted by ductile vertical piles, and batter piles should be avoided whenever possible.

Modern analysis methods are now readily available that allow the lateral load-deflection behavior of piles to be rationally evaluated. Lateral loads and moments on a vertical pile are resisted by the flexural stiffness of the pile and mobilization of resistance in the surrounding soil as the pile deflects. The flexural stiffness of a pile is defined by the pile's modulus of elasticity, E , and moment of inertia, I . The soil resistance to an applied lateral load is a combination of soil compression and shear resistance, as shown in Figure 9.36.

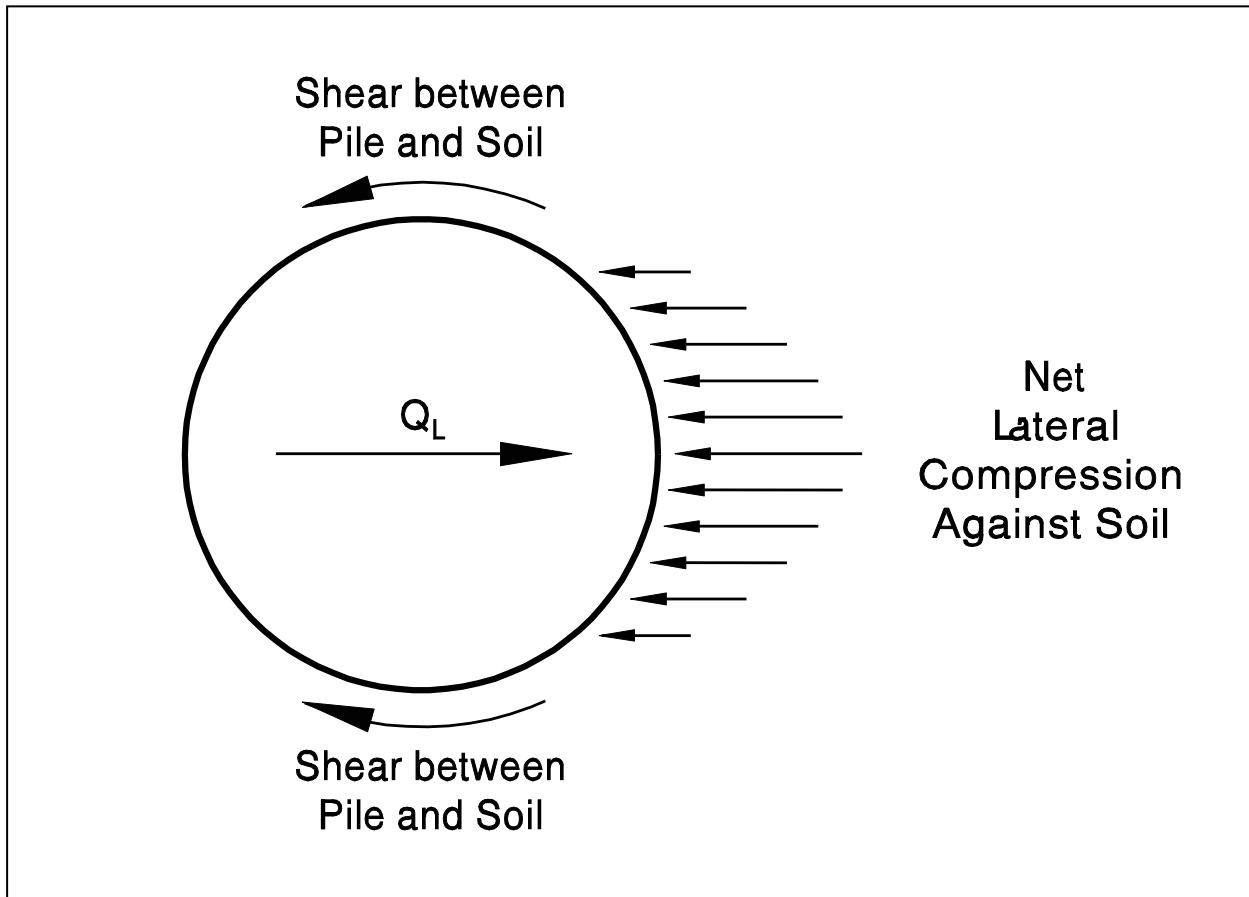


Figure 9.36 Soil Resistance to a Lateral Pile Load (adapted from Smith, 1989)

The design of laterally loaded piles must evaluate both the pile structural response and soil deformation to lateral loads. The factor of safety against both soil failure and pile structural failure must be determined. In addition, the pile deformation under the design loading conditions must be calculated and compared to foundation performance criteria.

The design of laterally loaded piles requires the combined skills of the geotechnical and structural engineer. It is inappropriate for the geotechnical engineer to analyze a laterally loaded pile without a full understanding of pile-structure interaction. Likewise it is inappropriate for the structural engineer to complete a laterally loaded pile design without a full understanding of how pile section or spacing changes may alter the soil response. Because of the interaction of pile structural and geotechnical considerations, the economical solution of lateral pile loading problems requires communication between the structural and geotechnical engineer.

Soil, pile, and load parameters have significant effects on the lateral load capacity of piles. The factors influencing these parameters are as follows:

1. Soil Parameters

- a. Soil type and physical properties such as shear strength, friction angle, density, groundwater level, and moisture content.
- b. Coefficient of horizontal subgrade reaction in kN/m^3 (lbs/in^3). This coefficient is defined as the ratio between a horizontal pressure per unit area of vertical surface in kN/m^2 (lbs/in^2) and the corresponding horizontal displacement in meters (inches). For a given deformation, the greater the coefficient, the greater the lateral load resistance.

2. Pile Parameters

- a. Physical properties such as shape, material, and dimensions.
- b. Pile head conditions (rotational constraint, if any).
- c. Method of pile placement such as driving, jetting, *etc.*
- d. Group action.

3. Lateral Load Parameters

- a. Static (monotonic or cyclic) or dynamic.
- b. Eccentricity (moment coupled with shear force).

9.7.3.1 Lateral Capacity Design Methods

The basic design approaches for lateral pile capacity analysis of vertical piles consist of lateral load tests or analytical methods. Both of these approaches are described in greater detail in the following sections.

1. Lateral Load Tests

Full scale lateral load tests can be conducted at a site during either the design or construction stage. The load-deformation data obtained is used to finalize or confirm the design for the particular site. Factors such as loading rate, cyclic (single or multi-directional) versus monotonic application of design forces, and magnitude of axial load should be considered in developing appropriate field testing procedures. These tests may be time-consuming, costly, and cannot be justified on all projects. Chapter 19 provides additional details on lateral load test procedures and interpretation.

2. Analytical Methods

The analytical methods are based on theory and empirical data and permit the rational consideration of various site parameters. Two common approaches are Broms' (1964a, 1964b) hand calculation method and Reese's (1984) computer solution. Both approaches consider the pile to be analogous to a beam on an elastic foundation. FHWA publication FHWA-IP-84-11 by Reese (1984) presents details of both methods.

Broms' method provides a relatively easy hand calculation procedure to determine lateral loads and pile deflections at the ground surface. Broms' method ignores the axial load on the pile. For small projects, Broms' method may be used. However, when there are definitive limits on the allowable pile movements, a more detailed load-deformation analysis may still be required.

Reese's method is a more rigorous computer analysis that now uses the LPILE computer program. Reese's method permits the inclusion of more complete modeling parameters of a specific problem. The program output provides distributions versus depth of moment, shear, soil and pile moduli, and soil resistance for the entire length of pile, including moments and shears in above ground sections.

For the design of all major pile foundation projects, Reese's more rigorous computer method should be used. The LPILE program is described in more detail in Section 9.7.3.3. Additional information on the LPILE program may be found in the program technical manual by Reese et al. (2000).

9.7.3.2 Broms' Method

The Broms' method is a straight forward hand calculation method for lateral load analysis of a single pile. The method calculates the ultimate soil resistance to lateral load as well as the maximum moment induced in the pile. Broms' method can be used to evaluate fixed or free head conditions in either purely cohesive or purely cohesionless soil profiles. The method is not conducive to lateral load analyses in mixed cohesive and cohesionless soil profiles. For long fixed head piles in sands, the method can also overpredict lateral load capacities (Long, 1996). Therefore, for mixed profiles and for long fixed head piles in sands, the LPILE program should be used. A step by step procedure developed by the New York State Department of Transportation (1977) on the application of Broms' method is provided below.

STEP BY STEP PROCEDURE FOR BROMS' METHOD

STEP 1 Determine the general soil type (*i.e.*, cohesive or cohesionless) within the critical depth below the ground surface (about 4 or 5 pile diameters).

STEP 2 Determine the coefficient of horizontal subgrade reaction, K_h , within the critical depth for cohesive or cohesionless soils.

a. Cohesive Soils:
$$K_h = \frac{n_1 n_2 80 q_u}{b}$$

Where: q_u = Unconfined compressive strength in kPa (lbs/ft²).

b = Width or diameter of pile in meters (ft).

n_1 and n_2 = Empirical coefficients taken from Table 9-13.

b. Cohesionless Soils:

Choose K_h from the Table 9-14. (The values of K_h given in Table 9-14 were determined by Terzaghi.)

TABLE 9-13 VALUES OF COEFFICIENTS n_1 AND n_2 FOR COHESIVE SOILS	
Unconfined Compressive Strength, q_u , in kPa (lbs/ft ²)	N_1
Less than 48 kPa (1000 lbs/ft ²)	0.32
48 to 191 kPa (1000 to 4000 lbs/ft ²)	0.36
More than 191 kPa (4000 lbs/ft ²)	0.40
Pile Material	N_2
Steel	1.00
Concrete	1.15
Wood	1.30

TABLE 9-14 VALUES OF K_h FOR COHESIONLESS SOILS		
Soil Density	K_h , in kN/m ³ (lbs/in ³)	
	Above Ground Water	Below Ground Water
Loose	1900 (7)	1086 (4)
Medium	8143 (30)	5429 (20)
Dense	17644 (65)	10857 (40)

STEP 3 Adjust K_h for loading and soil conditions.

a. Cyclic loading (for earthquake loading) in cohesionless soil:

1. $K_h = \frac{1}{2} K_h$ from Step 2 for medium to dense soil.

2. $K_h = \frac{1}{4} K_h$ from Step 2 for loose soil.

b. Static loads resulting in soil creep (cohesive soils):

1. Soft and very soft normally consolidated clays

$K_h = (\frac{1}{3} \text{ to } \frac{1}{6}) K_h$ from Step 2.

2. Stiff to very stiff clays

$K_h = (\frac{1}{4} \text{ to } \frac{1}{2}) K_h$ from Step 2.

STEP 4 Determine pile parameters.

- a. Modulus of elasticity, E , in MPa (lbs/in²).
- b. Moment of inertia, I , in meter⁴ (inches⁴).
- c. Section modulus, S , in meter³ (inches³) about an axis perpendicular to the load plane.
- d. Yield stress of pile material, f_y , in MPa (lb/in²) for steel or ultimate compression strength, f'_c , in MPa (lb/in²) for concrete.
- e. Embedded pile length, D , in meters (inches).
- f. Diameter or width, b , in meters (inches).
- g. Eccentricity of applied load e_c for free-headed piles - *i.e.*, vertical distance between ground surface and lateral load in meters (inches).
- h. Dimensionless shape factor C_s (for steel piles only):
 1. Use 1.3 for piles with circular cross section.
 2. Use 1.1 for H-section piles when the applied lateral load is in the direction of the pile's maximum resisting moment (normal to the pile flanges).
 3. Use 1.5 for H-section piles when the applied lateral load is in the direction of the pile's minimum resisting moment (parallel to the pile flanges).
- i. M_y , the resisting moment of the pile.
 1. $M_y = C_s f_y S$ in kN-m (in-lb) for steel piles.
 2. $M_y = f'_c S$ in kN-m (in-lb) for concrete piles.

STEP 5 Determine β_h for cohesive soils or η for cohesionless soils.

a. $\beta_h = \sqrt[4]{K_h b / 4EI}$ for cohesive soil, or

b. $\eta = \sqrt[5]{K_h / EI}$ for cohesionless soil.

STEP 6 Determine the dimensionless length factor.

a. $\beta_h D$ for cohesive soil, or

b. ηD for cohesionless soil.

STEP 7 Determine if the pile is long or short.

a. Cohesive soil:

1. $\beta_h D > 2.25$ (long pile).

2. $\beta_h D < 2.25$ (short pile).

Note: It is suggested that for $\beta_h D$ values between 2.0 and 2.5, both long and short pile criteria should be considered in Step 9, and then the smaller value should be used.

b. Cohesionless soil:

1. $\eta D > 4.0$ (long pile).

2. $\eta D < 2.0$ (short pile).

3. $2.0 < \eta D < 4.0$ (intermediate pile).

STEP 8 Determine other soil parameters over the embedded length of pile.

- a. The Rankine passive pressure coefficient for cohesionless soil, K_p .
 $K_p = \tan^2 (45 + \phi/2)$ where ϕ = angle of internal friction.
- b. The average effective unit weight of soil, γ' in kN/m^3 (lbs/in^3).
- c. The cohesion, c_u . in kPa (lbs/in^2).
 $c_u = 1/2$ the unconfined compressive strength, q_u .

STEP 9 Determine the ultimate lateral load for a single pile, Q_u .

- a. Short Free or Fixed-Headed Pile in Cohesive Soil.

Using D/b (and e_c/b for the free-headed case), enter Figure 9.37, select the corresponding value of $Q_u/c_u b^2$, and solve for Q_u in kN (lbs).

- b. Long Free or Fixed-Headed Pile in Cohesive Soil.

Using $M_y/c_u b^3$ (and e_c/b for the free headed case), enter Figure 9.38, select the corresponding value of $Q_u/c_u b^2$, and solve for Q_u in kN (lbs).

- c. Short Free or Fixed-Headed Pile in Cohesionless Soil.

Using D/b (and e_c/D for the free-headed case), enter Figure 9.39, select the corresponding value of $Q_u/K_p b^3 \gamma$ and solve for Q_u in kN (lbs).

- d. Long Free or Fixed-Headed Pile in Cohesionless Soil.

Using $M_y/b^4 \gamma K_p$, (and e_c/b for the free headed case), enter Figure 9.40, select the corresponding value of $Q_u/K_p b^3 \gamma$ and solve for Q_u in kN (lbs).

- e. Intermediate Free or Fixed-Headed Pile in Cohesionless Soil.

Calculate Q_u in kN (lbs) for both a short pile (Step 9c) and long pile (Step 9d) and use the smaller value.

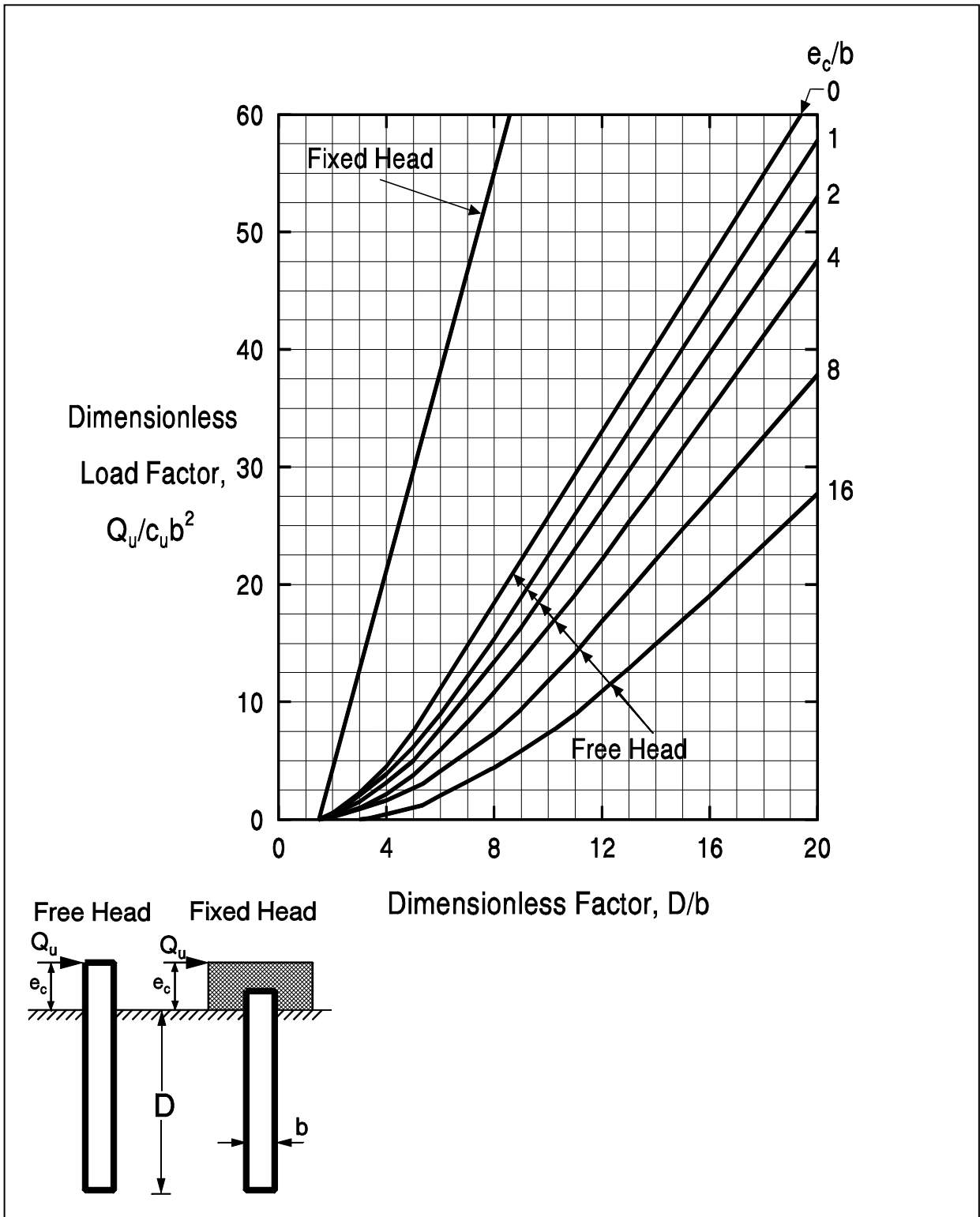


Figure 9.37 Ultimate Lateral Load Capacity of Short Piles in Cohesive Soils

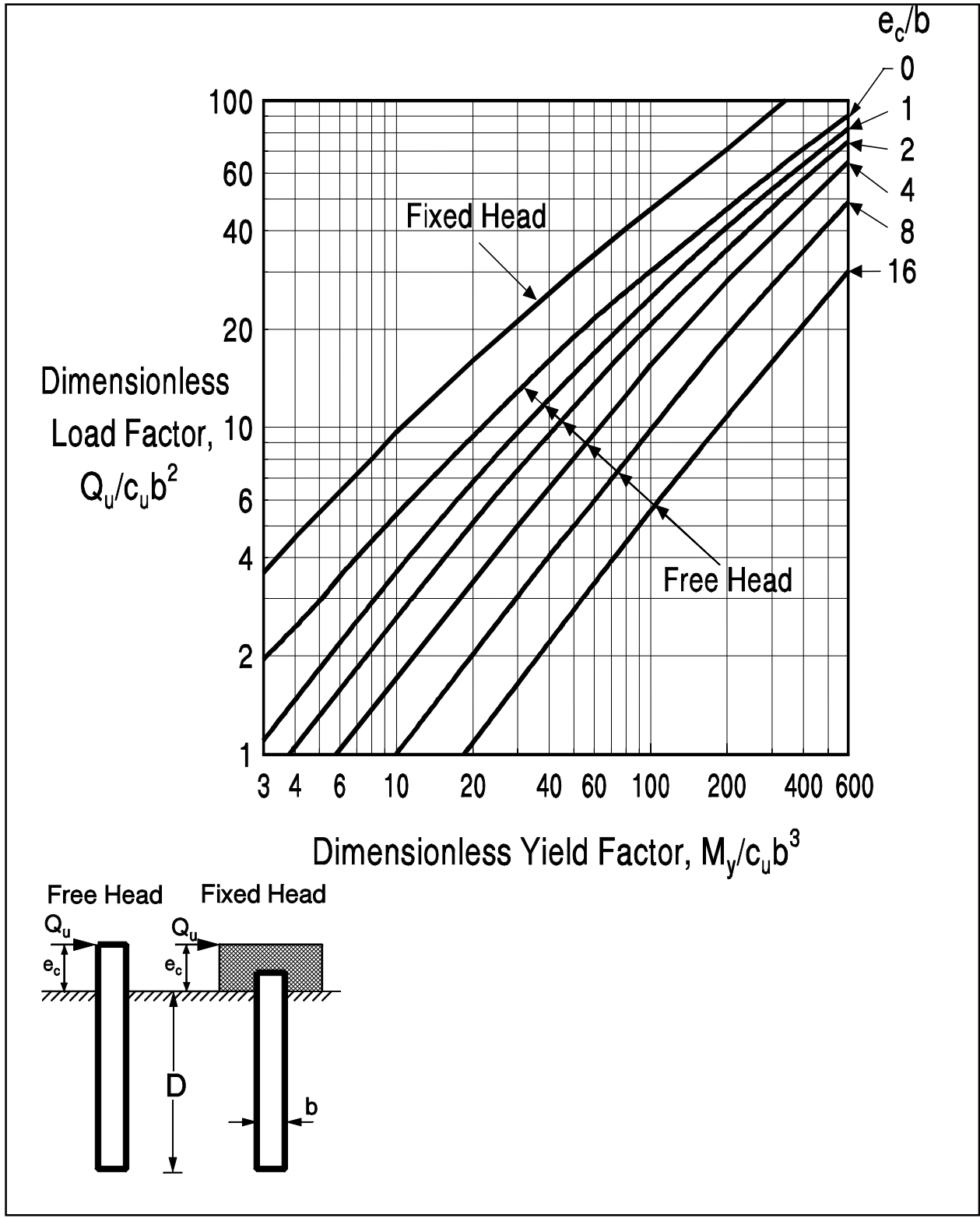


Figure 9.38 Ultimate Lateral Load Capacity of Long Piles in Cohesive Soils

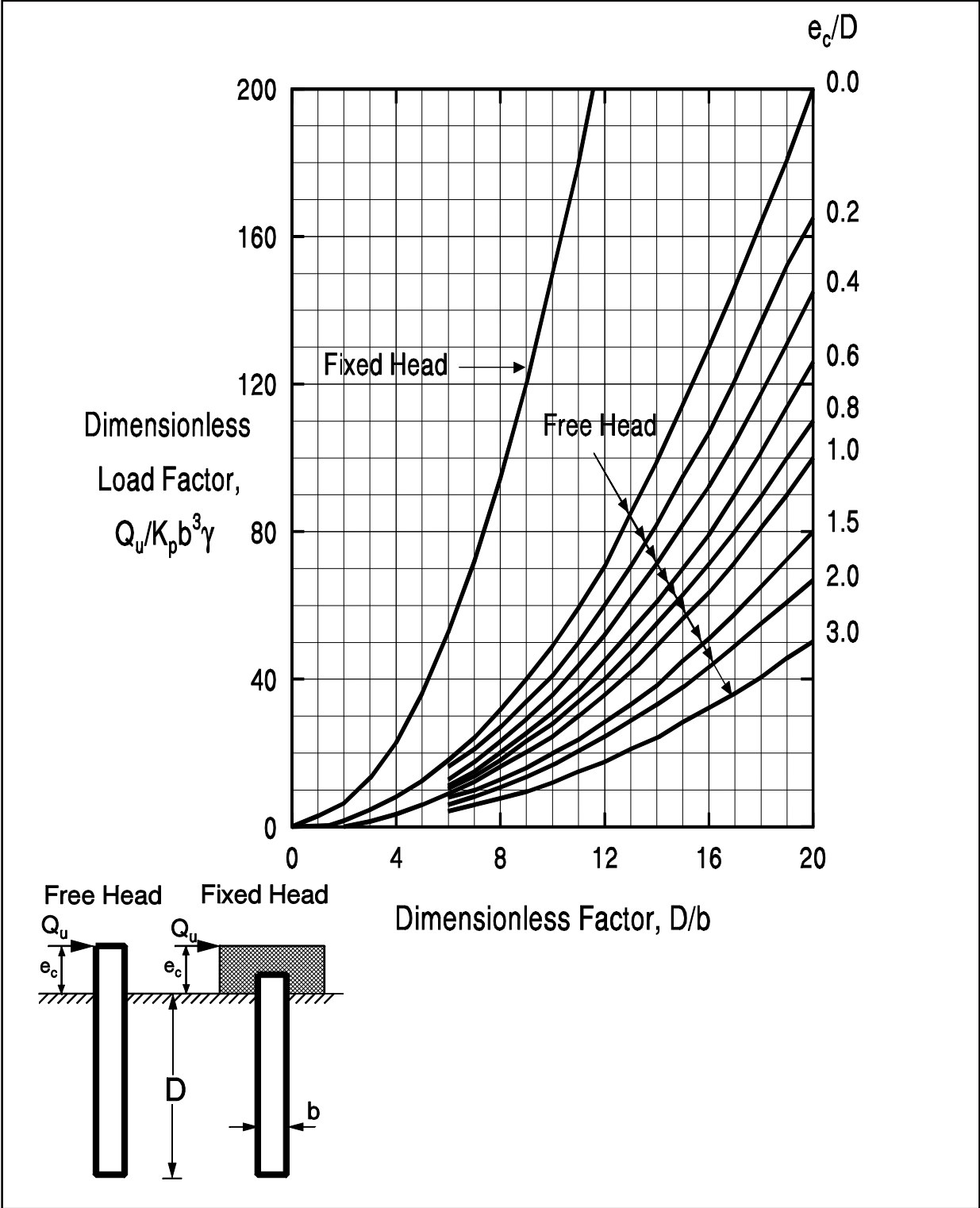


Figure 9.39 Ultimate Lateral Load Capacity of Short Piles in Cohesionless Soils

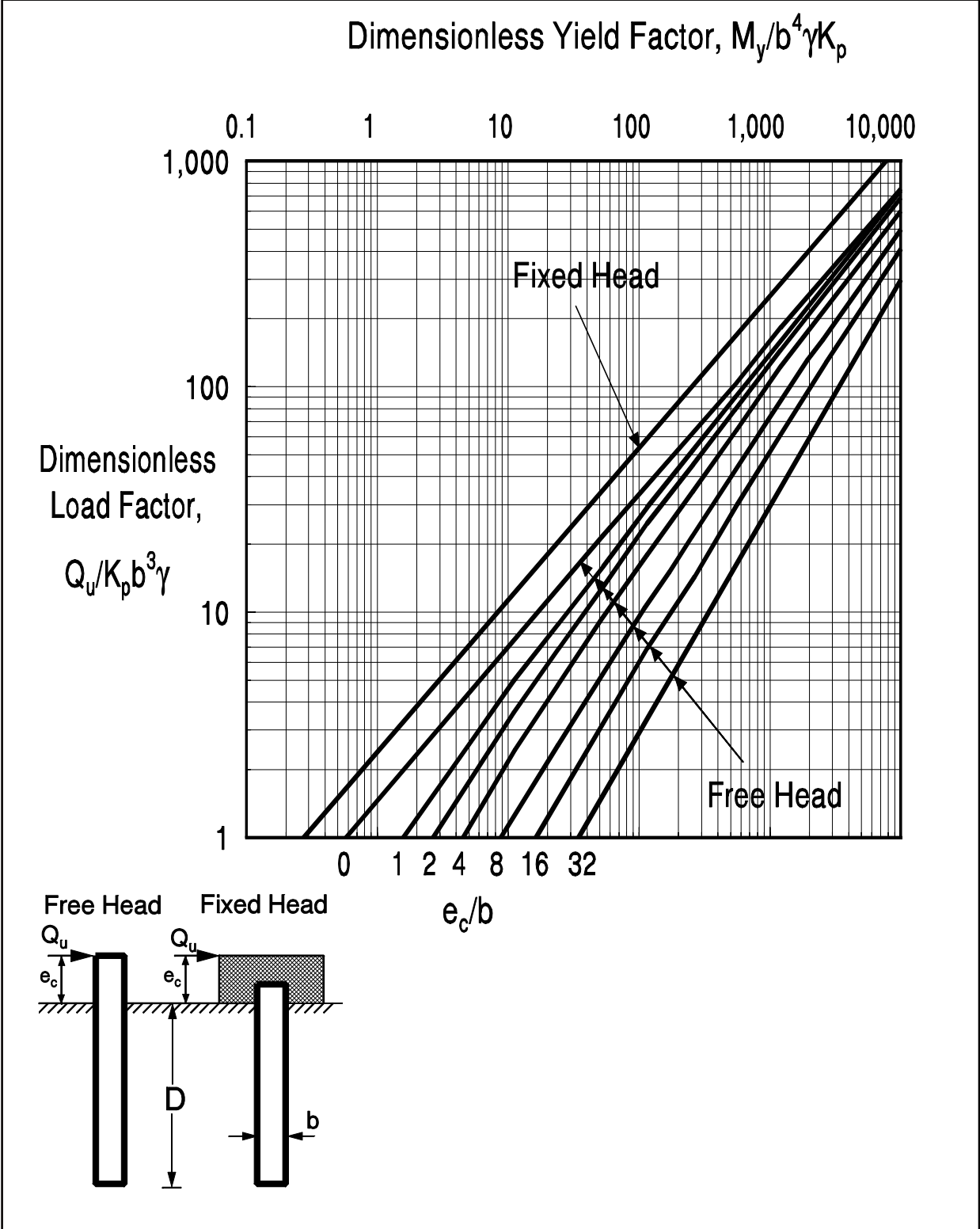


Figure 9.40 Ultimate Lateral Load Capacity of Long Piles in Cohesionless Soils

STEP 10 Calculate the maximum allowable working load for a single pile Q_m .

Calculate Q_m in kN (lbs) from the ultimate load Q_u in kN (lbs) determined in Step 9 as shown in Figure 9.41.

$$Q_m = \frac{Q_u}{2.5}$$

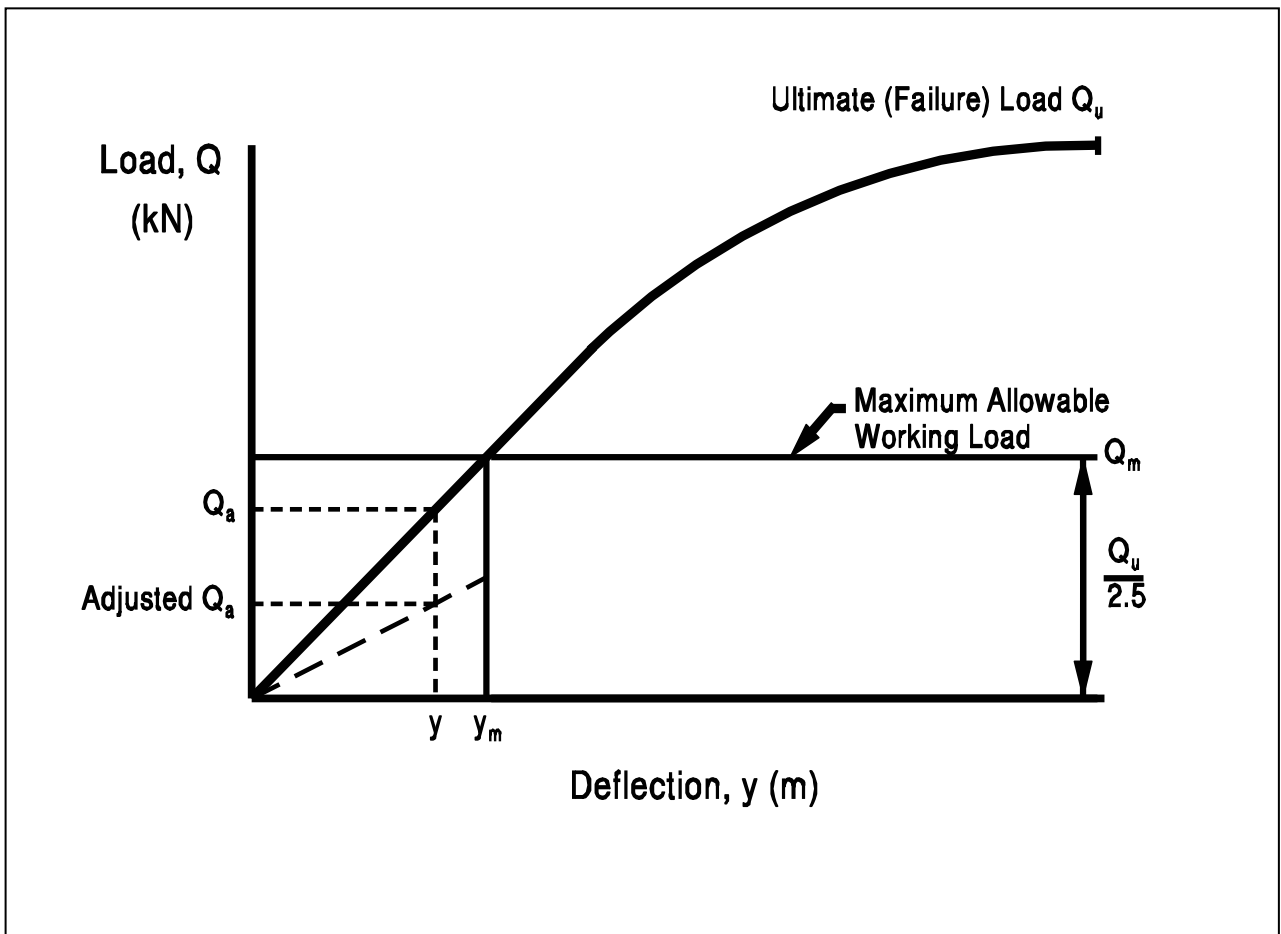


Figure 9.41 Load Deflection Relationship Used in Determination of Broms' Maximum Working Load

STEP 11 Calculate the working load for a single pile, Q_a in kN (lbs).

Calculate Q_a corresponding to a given design deflection at the ground surface, y , in meters (inches) or the deflection corresponding to a given design load. If Q_a and y are not given, substitute the value of Q_m in kN (lbs) from Step 10 for Q_a in the following cases and solve for y_m in meters (inches):

a. Free or Fixed-Headed Pile in Cohesive Soil.

Using $\beta_h D$ (and e_c/D for the free-headed case), enter Figure 9.42, select the corresponding value of $yK_h bD/Q_a$, and solve for Q_a in kN (lbs) or y in meters (inches).

b. Free or Fixed-Headed Pile in Cohesionless Soil.

Using ηD (and e_c/D for the free-headed case), enter Figure 9.43, select the corresponding value of $y(EI)^{3/5} K_h^{2/5}/Q_a D$, and solve for Q_a in kN (lbs) or y in meters (inches).

STEP 12 Compare Q_a to Q_m .

If $Q_a > Q_m$, use Q_m and calculate y_m (Step 11).

If $Q_a < Q_m$ use Q_a and y .

If Q_a and y are not given, use Q_m and y_m .

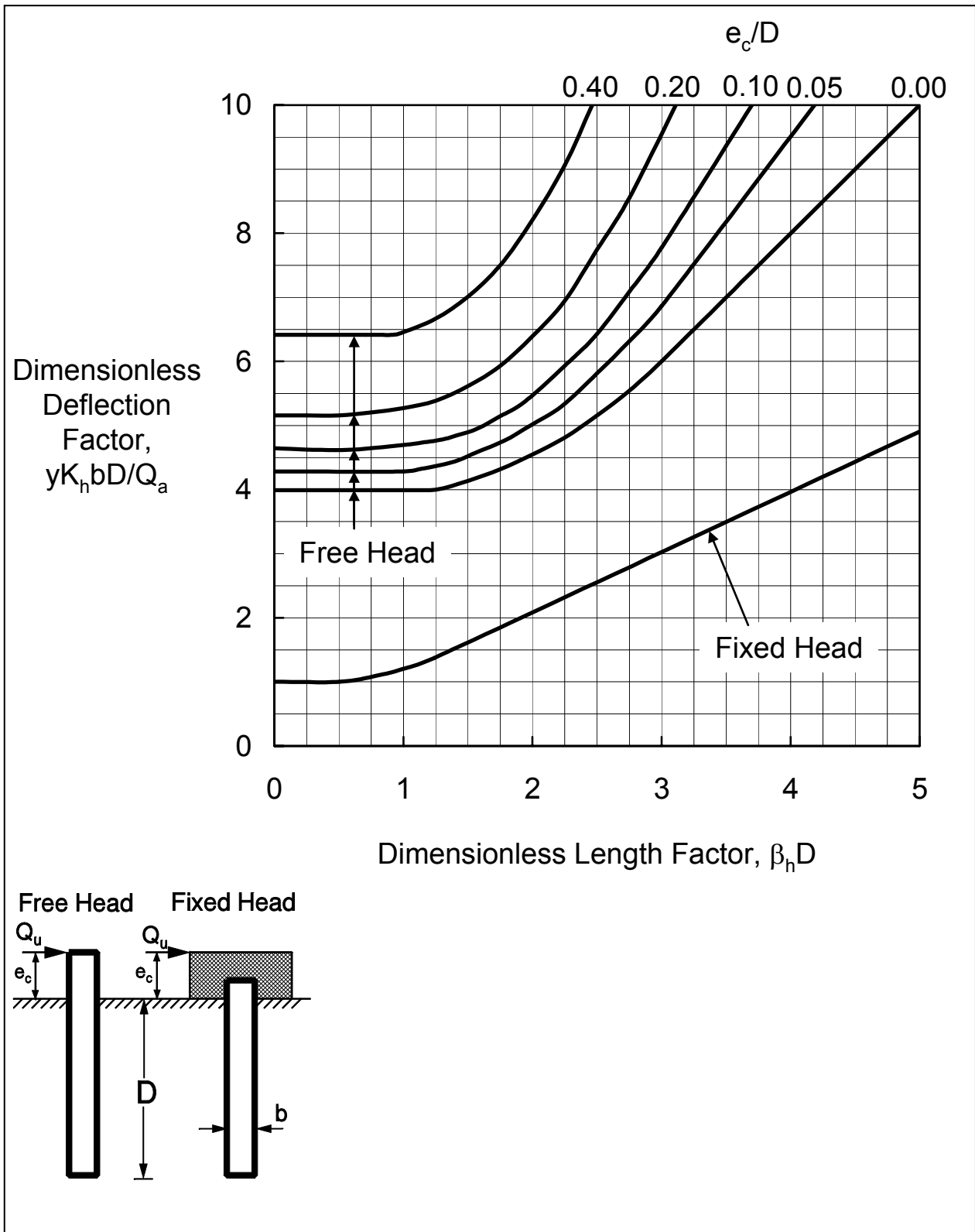


Figure 9.42 Lateral Deflection at Ground Surface of Piles in Cohesive Soils

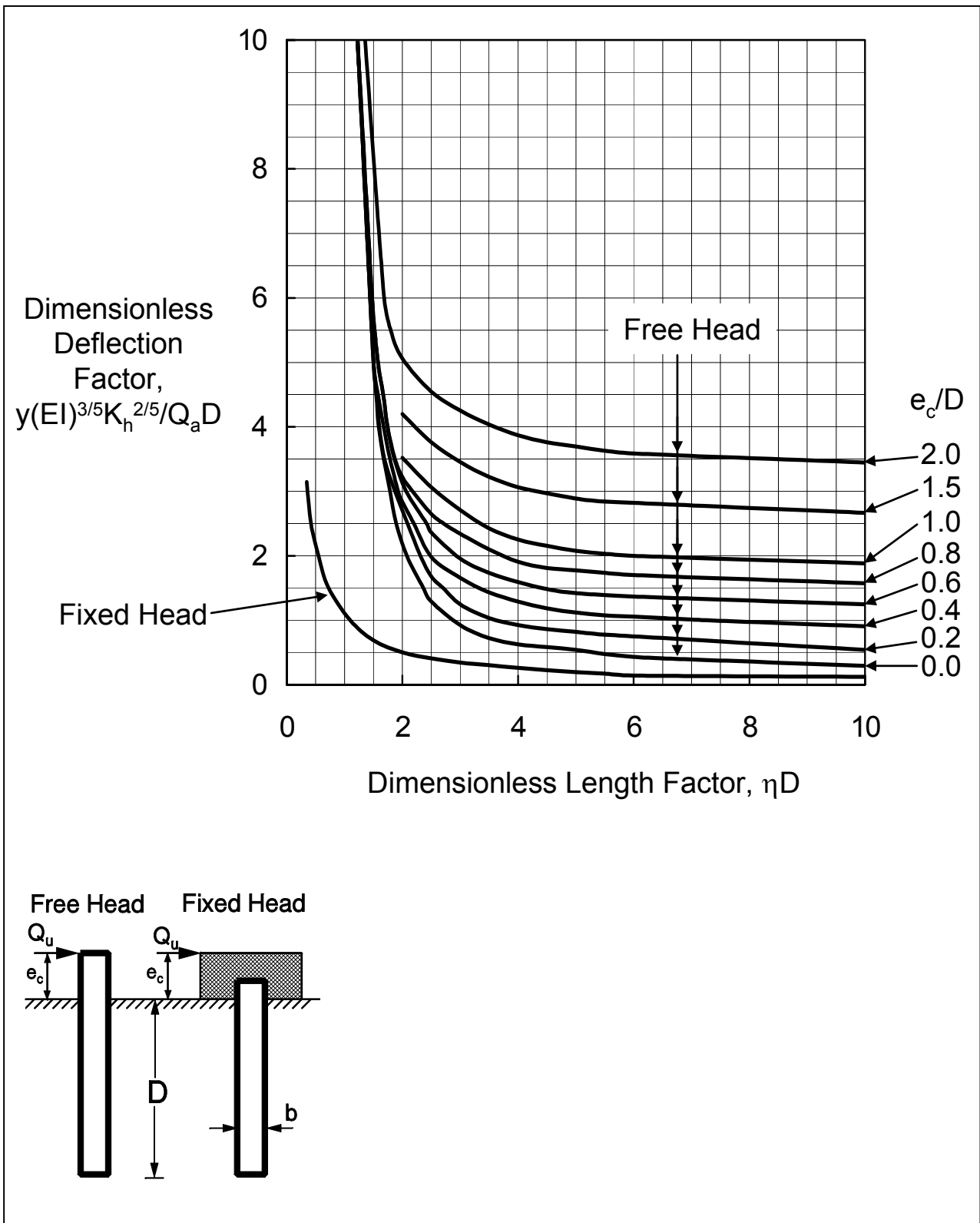
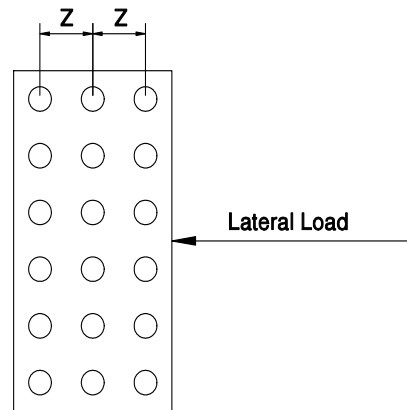


Figure 9.43 Lateral Deflection at Ground Surface of Piles in Cohesionless Soils

STEP 13 Reduce the allowable load from Step 12 for pile group effects and the method of pile installation.

- a. Group reduction factor determined by the center to center pile spacing, z , in the direction of load.

z	Reduction Factor
8b	1.0
6b	0.8
4b	0.5
3b	0.4



- b. Method of installation reduction factor.

1. For driven piles use no reduction.
2. For jetted piles use 0.75 of the value from Step 13a.

STEP 14 Determine pile group lateral capacity.

The total lateral load capacity of the pile group equals the adjusted allowable load per pile from Step 13b times the number of piles. The deflection of the pile group is the value selected in Step 12. It should be noted that no provision has been made to include the lateral resistance offered by the soil surrounding an embedded pile cap.

Special Note

Inspection of Figures 9.39 and 9.40 for cohesionless soils indicates that the ultimate load Q_u is directly proportional to the effective soil unit weight, γ . As a result, the ultimate load for short piles in submerged cohesionless soils will be about 50 percent of **the value** for the same soil in a dry state. For long **piles**, the reduction in Q_u is somewhat less than 50 percent due to the partially offsetting effect that the reduction in γ has on the dimensionless yield factor. In addition to these considerations, it should be noted that the coefficient of horizontal subgrade reaction K_h is less for the submerged case (Table 9-14) and thus the deflection will be greater than for the dry state.

9.7.3.3 Reese's LPILE Method

The interaction of a pile-soil system subjected to lateral load has long been recognized as a complex function of nonlinear response characteristics of both pile and soil. The most widely used nonlinear analysis method is the p-y method, where p is the soil resistance per unit pile length and y is the lateral soil or pile deflection. This method, illustrated in Figure 9.44, models the soil resistance to lateral load as a series of nonlinear springs.

Reese (1984, 1986) has presented procedures for describing the soil response surrounding a laterally loaded pile for various soil conditions by using a family of p-y curves. The procedures for constructing these curves are based on experiments using full-sized, instrumented piles and theories for the behavior of soil under stress.

The soil modulus E_s is defined as follows:

$$E_s = -\frac{p}{y}$$

The negative sign indicates that the soil resistance opposes pile deflection. The soil modulus, E_s , is the secant modulus of the p-y curve and is not constant except over a small range of deflections. Typical p-y curves are shown in Figure 9.45. Ductile p-y curves, such as curve A, are typical of the response of soft clays under static loading and sands. Brittle p-y curves, such as curve B, can be found in some stiff clays under dynamic loading conditions.

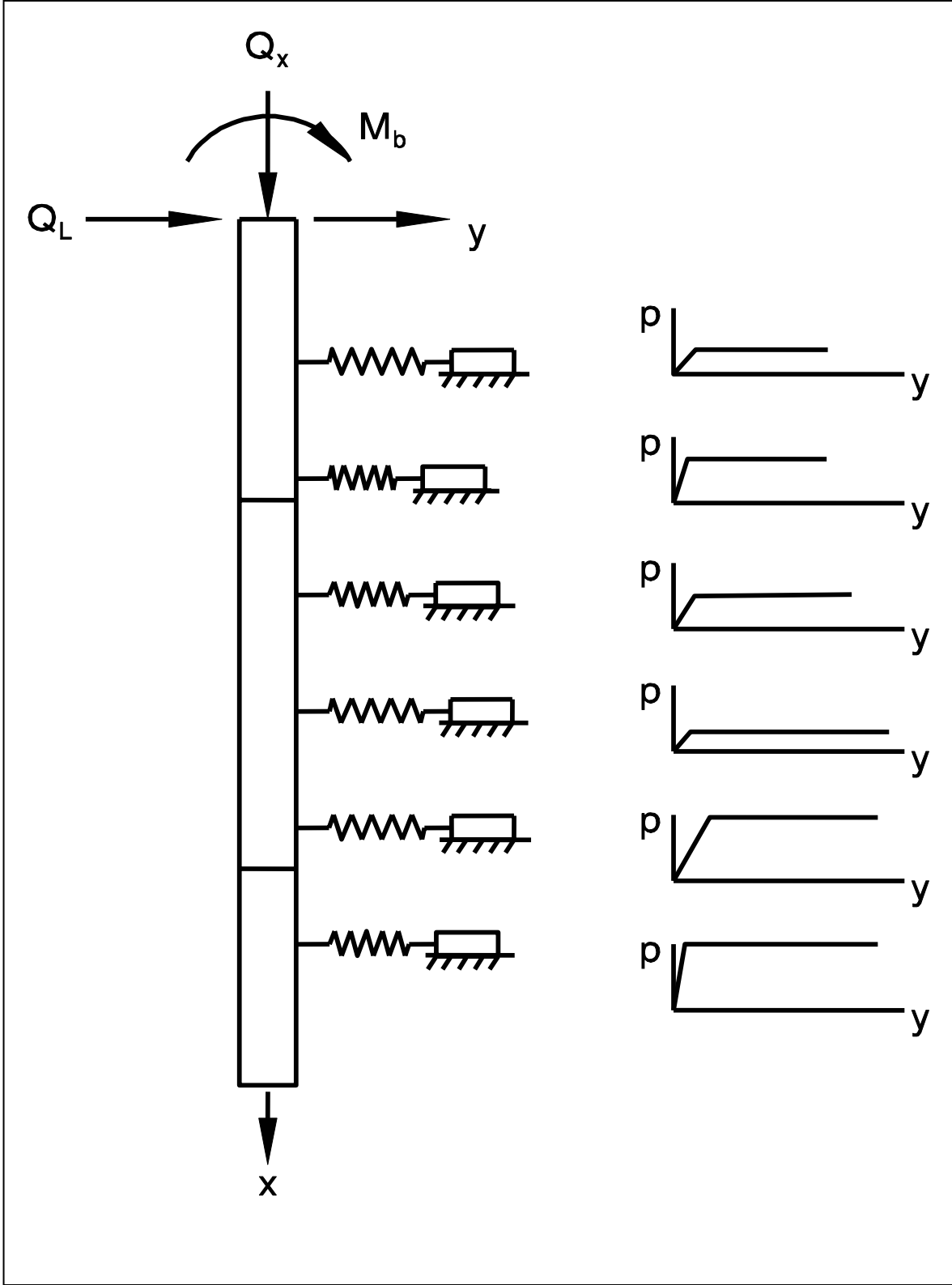


Figure 9.44 LPILE Pile-Soil Model

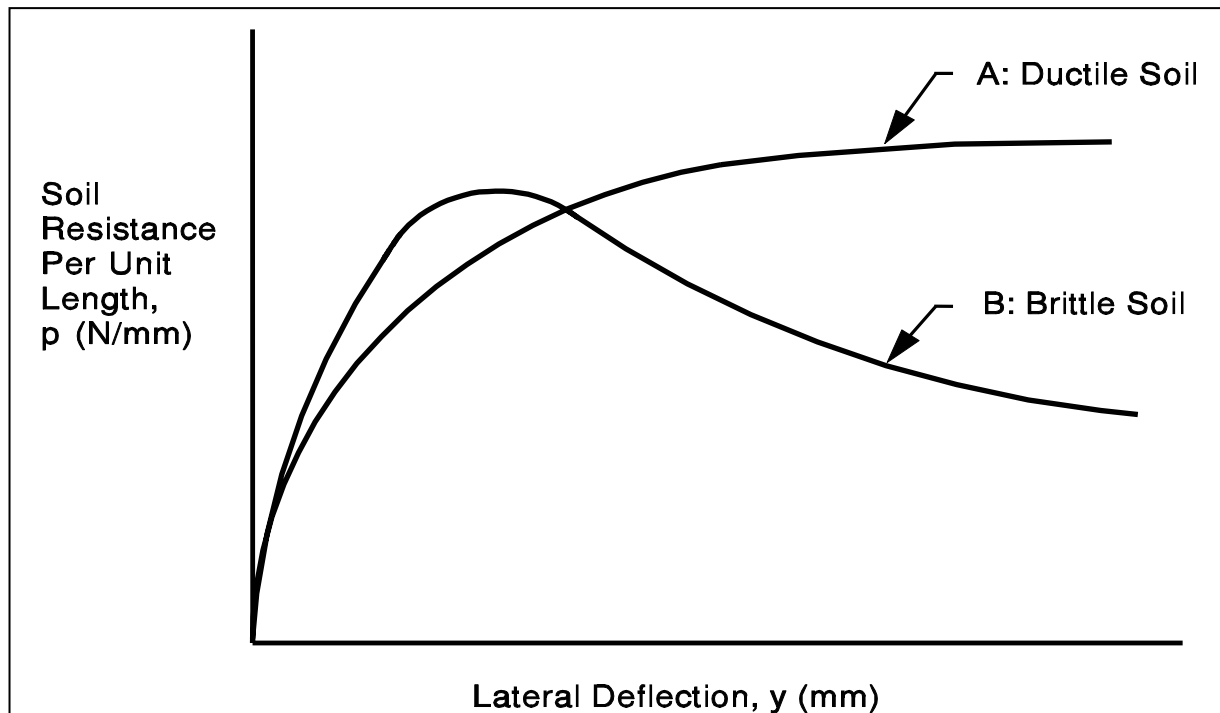


Figure 9.45 Typical p-y Curves for Ductile and Brittle Soil (after Coduto, 1994)

The factor most influencing the shape of the p-y curve is the soil properties. However, the p-y curves also depend upon depth, soil stress-strain relationships, pile width, water table location, and loading conditions (static or cyclic). Procedures for constructing p-y curves for various soil and water table conditions as well as static or cyclic loading conditions are provided in the LPILE program documentation by Reese et al., (2000).

Procedures for p-y curve development cover the following soil and water table conditions:

1. Soft clays below the water table.
2. Stiff clays below the water table.
3. Stiff clays above the water table.
4. Sands above or below the water table.

The LPILE program solves the nonlinear differential equations representing the behavior of the pile-soil system to lateral (shear and moment) loading conditions in a finite difference formulation using Reese's p-y method of analysis. The strongly nonlinear reaction of the surrounding soil to pile-soil deflection is represented by the p-y curve prescribed to act on each discrete element of the embedded pile. For each set of applied boundary (static)

loads the program performs an iterative solution which satisfies static equilibrium and achieves an acceptable compatibility between force and deflection (p and y) in every element.

The shape and discrete parameters defining each individual p - y curve may be input by the user or generated by the program. Layered soil systems are characterized by conventional geotechnical data including soil type, shear strength, density, depth, and stiffness parameters, and whether the loading conditions are monotonic or cyclic in nature.

In LPILE, the influence of applied loads (axial, lateral and moment) at each element can be modeled with flexural rigidity varying as a function of applied moment. In this manner, progressive flexural damage such as cracking in a reinforced concrete pile can be treated more rigorously. The LPILE program code includes a subroutine which calculates the value of flexural rigidity at each element under the boundary conditions and resultant pile-soil interaction conditions.

LPILE problem data is input through a series of menu-driven screens. Detailed information concerning the software can be found in the LPILE program user's manual by Reese et al. (2000). The user's manual includes useful guidelines for integrating LPILE analyses into the overall design process for laterally loaded deep foundations, and example problems.

The LPILE computer printout file summarizes the input information and the analysis results. The input data summarized includes the pile geometry and properties, and soil strength data. Output information includes the generated p - y curves at various depths below the pile head and the computed pile deflections, bending moments, stresses and soil moduli as functions of depth below the pile head. This information allows an analysis of the pile's structural capacity. Internally generated (or input) values of flexural rigidity for cracked or damaged pile sections are also output. Graphical presentations versus depth include the computed deflection, slope, moment, and shear in the pile, and soil reaction forces similar to those illustrated in Figure 9.46.

The LPILE analyses characterize the behavior of a single pile under lateral loading conditions. A detailed view is obtained of the load transfer and structural response mechanisms to design conditions. Considerable care is required in extrapolating the results to the behavior of pile groups (pile-soil-pile interaction, *etc.*), and accounting for the effects of different construction processes such as predrilling or jetting.

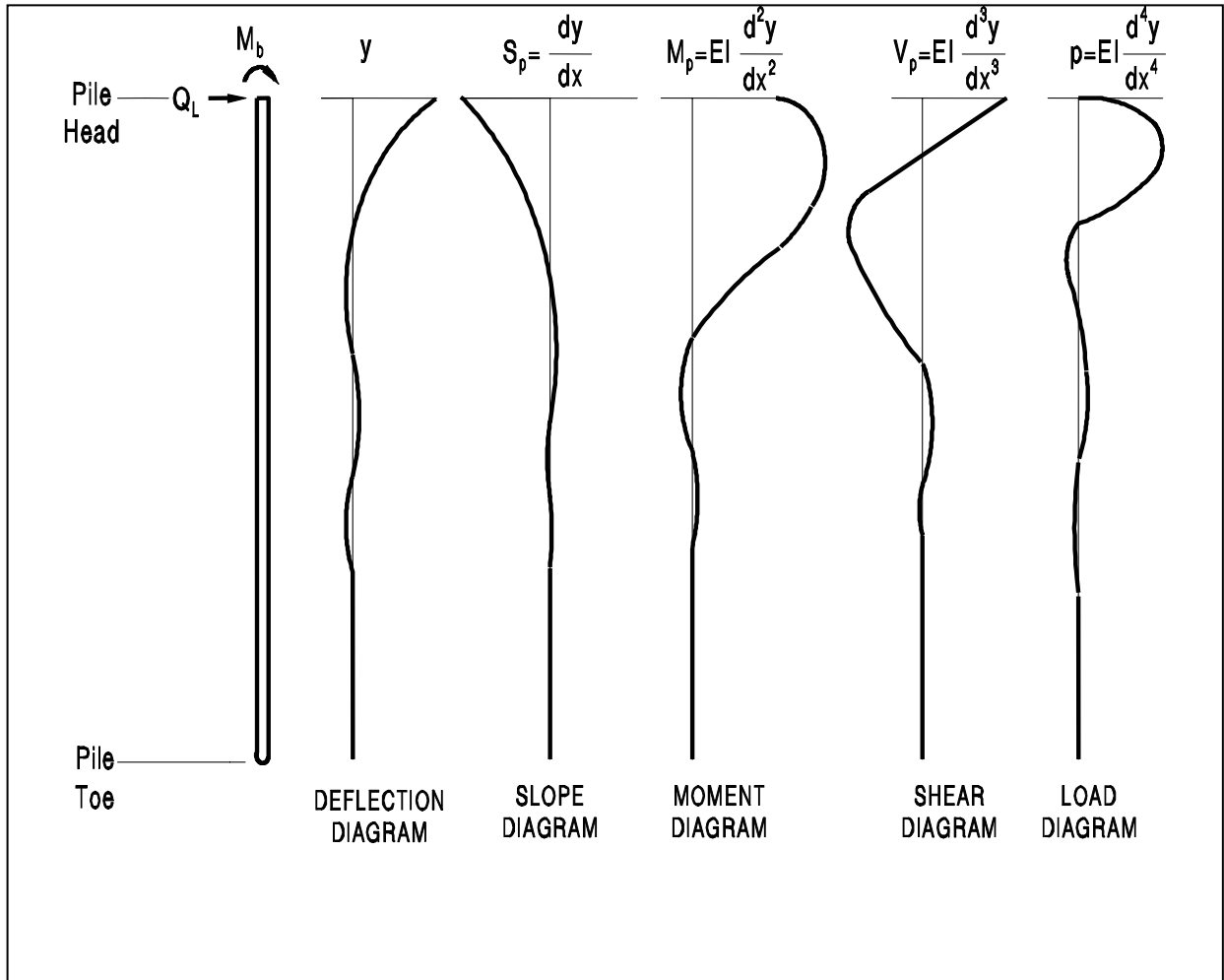


Figure 9.46 Graphical Presentation of LPILE Results (Reese, *et al.* 2000)

In any lateral analysis case, the analyst should verify that the intent of the modeling assumptions, all elastic behavior for example, is borne out in the analysis results. When a lateral load test is performed, the measured load-deflection results versus depth should be plotted and compared with the LPILE predicted behavior so that an evaluation of the validity of the p-y curves used for design can be made. Figure 9.47 illustrates a comparison between the measured load-deflection curve and one predicted by COM624P, the predecessor to the LPILE program

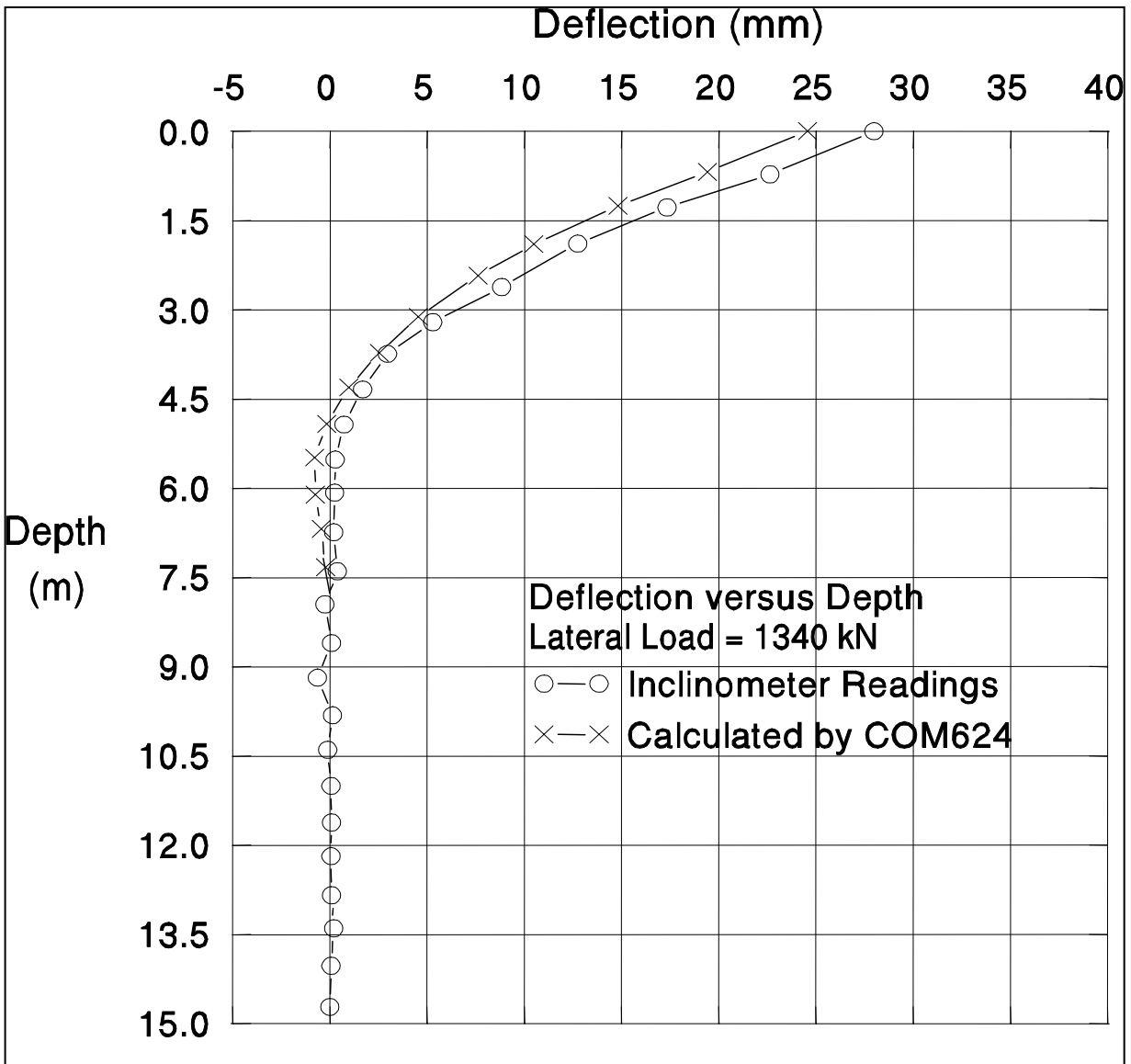


Figure 9.47 Comparison of Measured and COM624P Predicted Load-Deflection Behavior versus Depth (after Kyfor *et al.* 1992)

The opening LPILE program screen is presented in Figure 9.48. The main basic menu choices include; File, Data, Options, Computation, and Graphic. Clicking on the File menu allows the user to choice between a opening a new or existing file. File saving is also under the File menu options. A step by step procedure follows for performing a new LPILE analysis. The program user should also consult the LPILE technical and user's manuals by Reese *et al.* (2000).

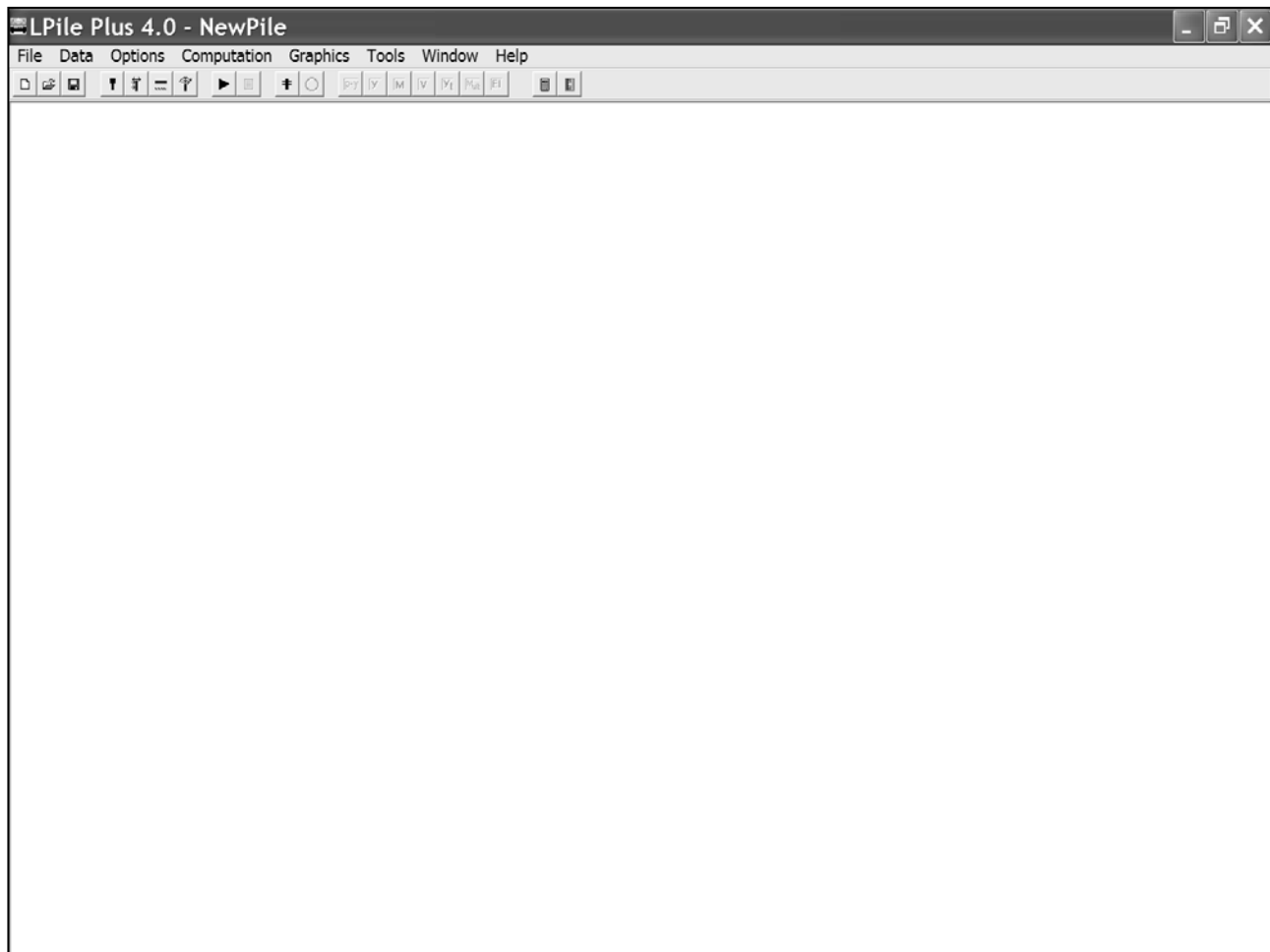


Figure 9.48 LPILE Main Screen

STEP BY STEP PROCEDURE FOR A BASIC LPILE ANALYSIS

- STEP 1 Click on the Options menu. A submenu will open to the right allowing the unit system for the analysis to be selected.
- STEP 2 Click on the Data menu to start data entry.
- STEP 3 Click on Title in the drop down window. The project title window will then appear as shown in Figure 9.49. A single line of text can then be entered to describe the project. After entering analysis description, click on the X to close the box.
- STEP 4 Next click on Pile Properties in the drop down window. The pile properties window will appear as shown in Figure 9.50.

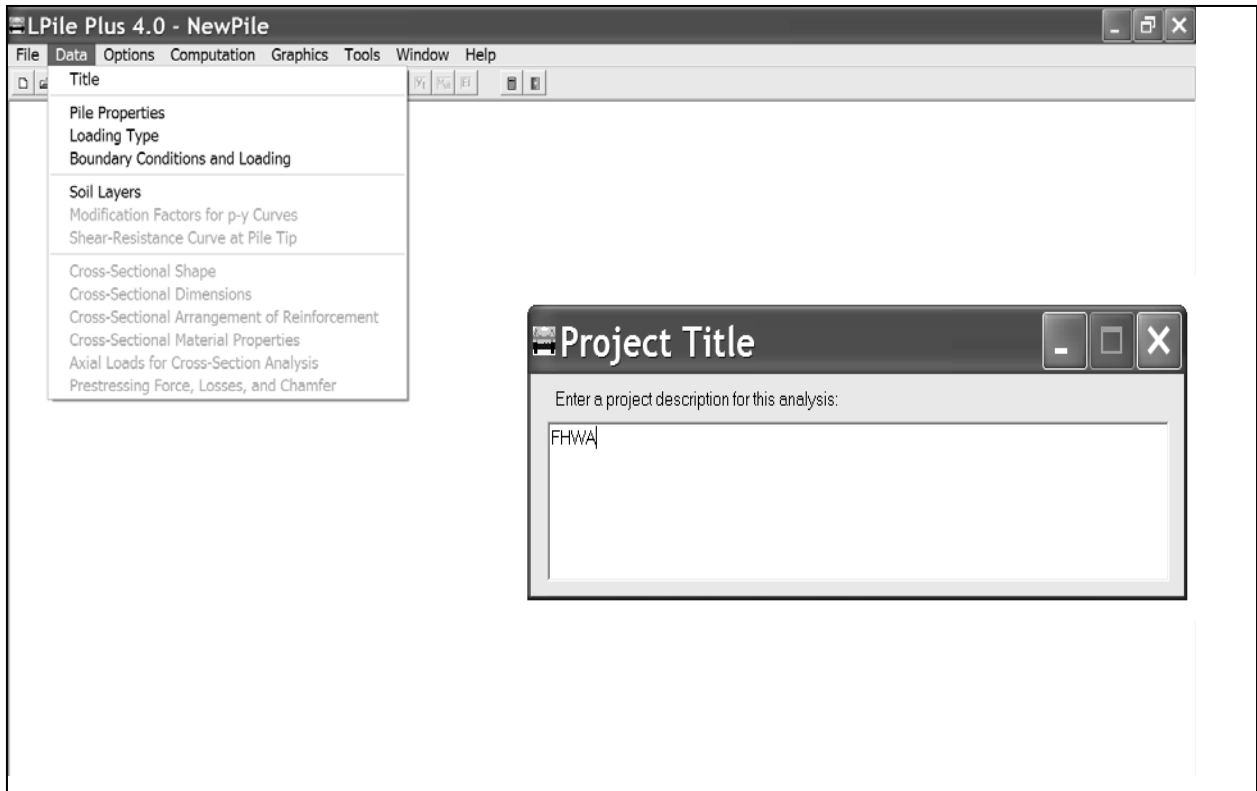


Figure 9.49 LPILE Data Menu and Project Title Window

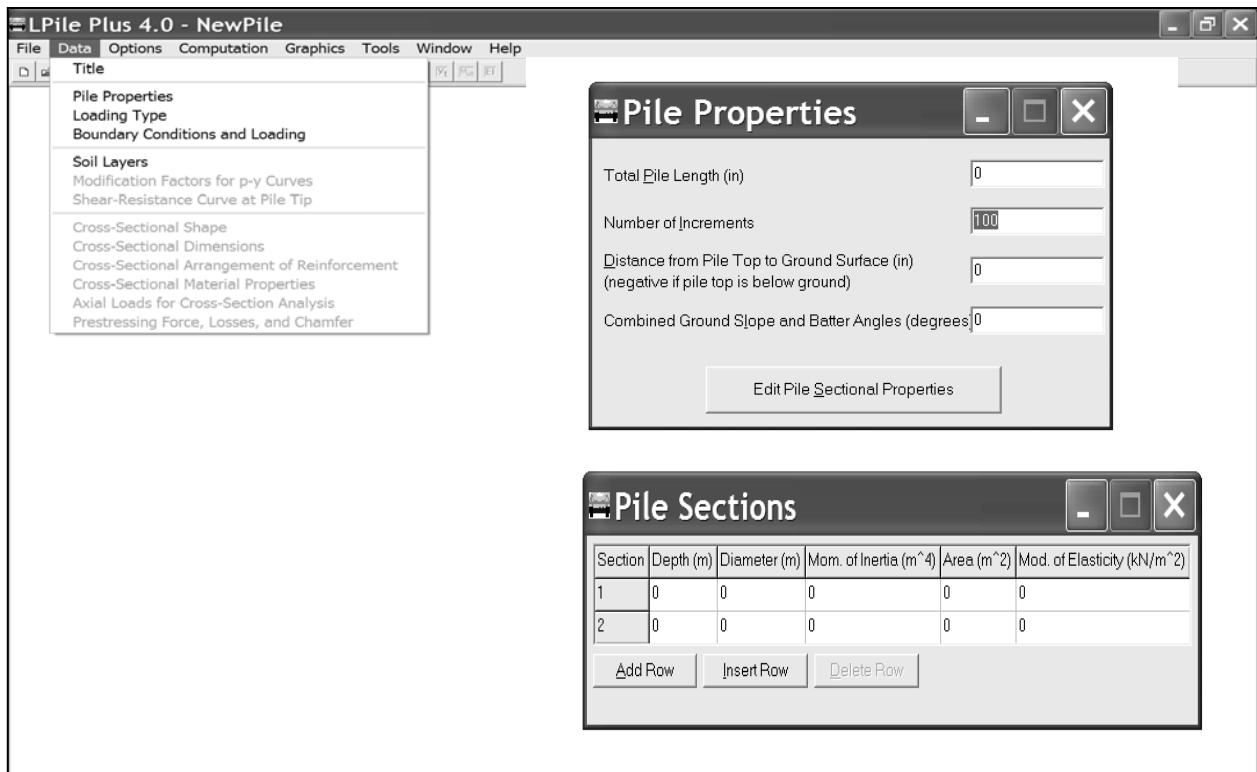


Figure 9.50 LPILE Data Menu and Pile Property and Pile Section Windows

- a. Enter the total pile length in meters (inches)
- b. Select the number of increments. The maximum number of increments a pile can be divided into is 300. Except for short piles, the number of increments is generally chosen between 80 and 200.
- c. Enter the distance from the pile head to the ground surface in meters (inches). Use a negative number if the pile head is below ground surface.
- d. If applicable, enter the combined ground slope and pile batter angle in degrees. The ground slope is defined as the angle between the sloping ground surface and a horizontal surface. The angle is positive if the pile moves downhill under the applied load and negative if the pile moves uphill. The pile batter angle from vertical is handled similarly. The batter angle is positive if the load is applied against the batter direction and negative if the load is applied with the batter direction.
- e. Click on the Edit Pile Sectional Properties box and the Pile Sections window will appear. Enter pile section information consisting of depth, diameter, moment of inertia, cross sectional area, and modulus of elasticity. For non-uniform piles, up to 10 rows of data can be entered by clicking on the Add Row box as necessary. Cross sectional area and moment of inertia data for most pile sections may be found in Appendix C.

STEP 5 Click on Loading Type in the Data menu. The Loading Type window will appear as shown in Figure 9.51.

- a. For each critical set of loading combinations, determine the axial loads, lateral loads, and bending moments to be analyzed. Load information should be supplied by the structural engineers.
- b. Select the type of loading, cyclic or static. If cyclic loading is selected, enter the number of cycles to be analyzed between 2 and 5000.
- c. If distributed lateral loads are to be analyzed, click on the “Include Distributed Lateral Loads” checkbox. This will activate a window that allows up to 10 combinations of depth and lateral load to be input. Depth entries must be in increasing order of depth.

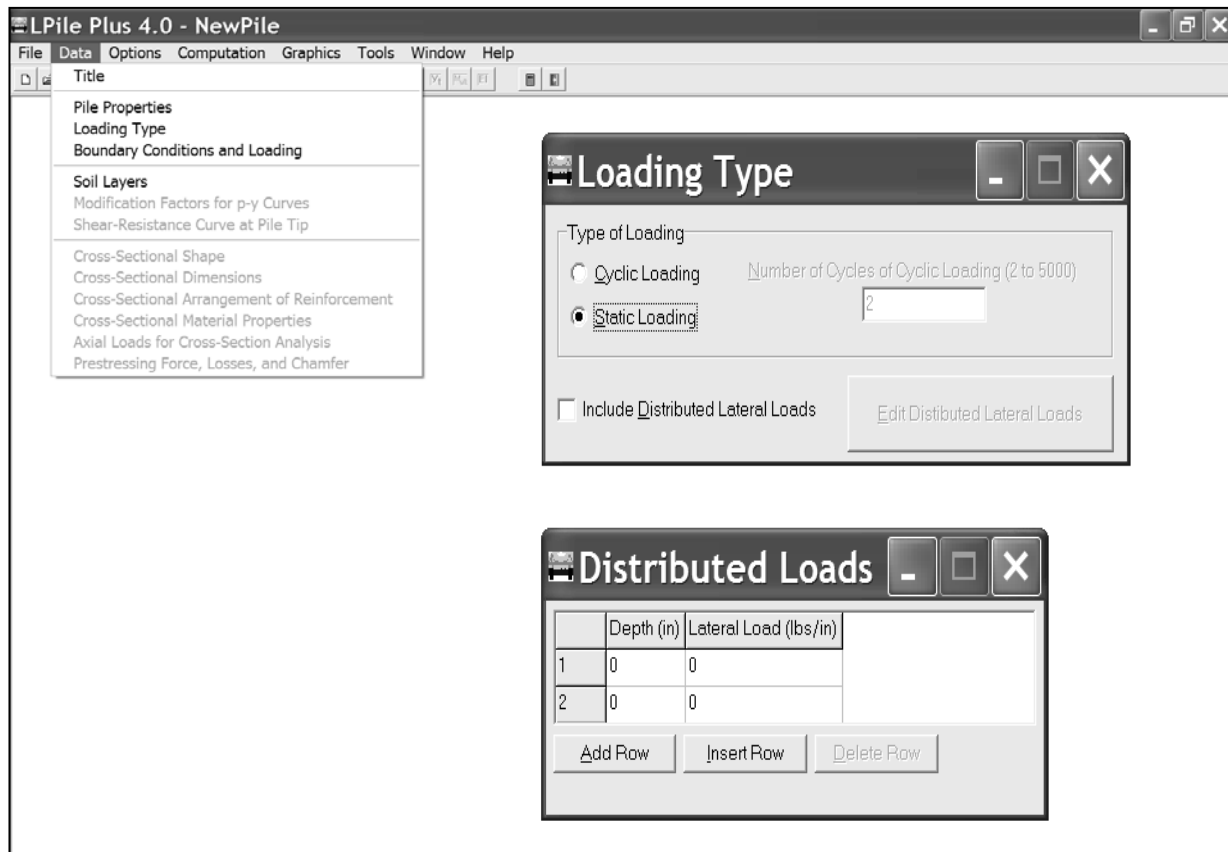


Figure 9.51 LPILE Loading Type and Distributed Loads Input Screens

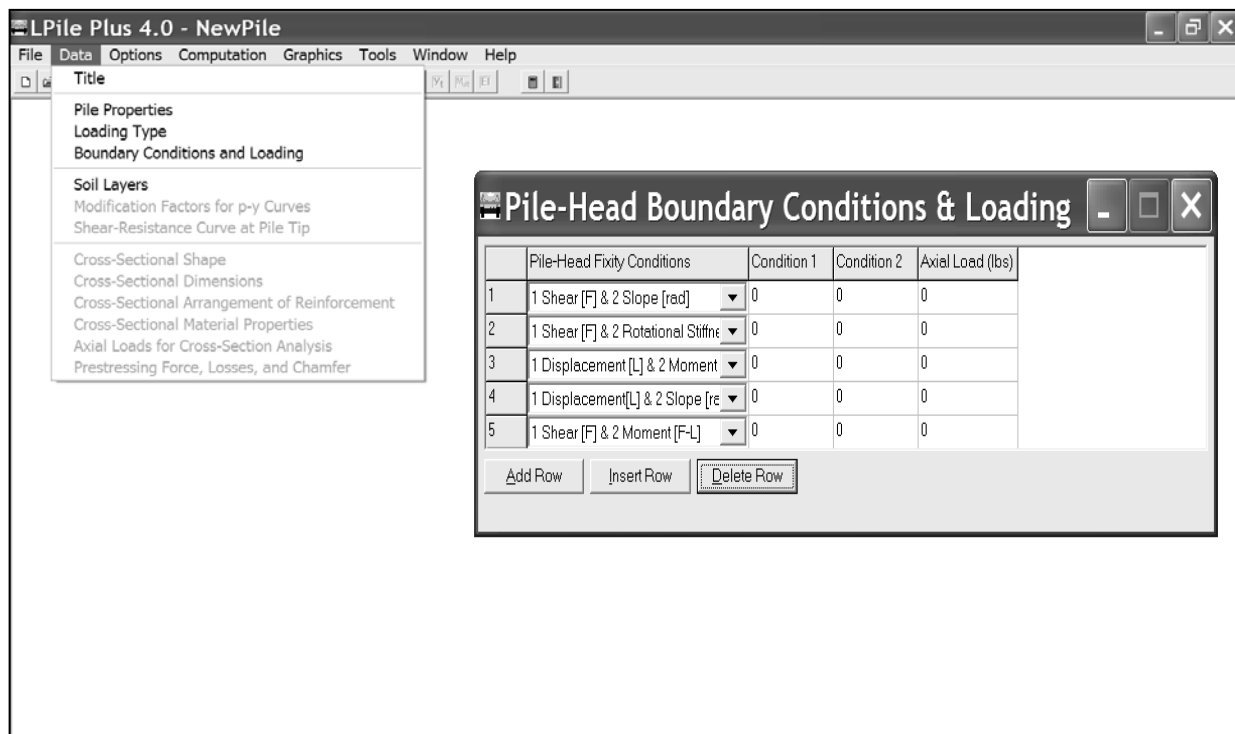


Figure 9.52 LPILE Pile Head Boundary Conditions and Loading Input Screen

STEP 6 Click on Boundary Conditions and Loading in the Data menu. The Pile Head Boundary Conditions window will appear as shown in Figure 9.52. The five available boundary condition options are depicted.

- a. Select the desired boundary condition from the dropdown list of choices. LPILE allows up to 10 rows of input boundary conditions to be analyzed. The boundary conditions are as follows:

The shear and moment case is selected to input values of applied load and applied moment at the pile head. This case is for a pile head that is free to rotate and move laterally.

The shear and slope case is selected to input values of applied lateral load and the slope of the applied load. A fixed head condition can be modeled by inputting a zero slope.

The shear and rotational stiffness case is selected to input the applied lateral load and the rotational stiffness at the pile head. A fixed head condition can be modeled by using a large rotational stiffness value. This boundary condition models an elastically restrained pile head.

The displacement and moment case is selected to input values of lateral displacement and moment at the pile head.

The displacement and slope case is selected to model lateral displacement and slope at the pile head.

- b. Enter the appropriate values for Condition 1 (first boundary condition, i.e. shear, displacement, etc.) and Condition 2 (second boundary condition, i.e. slope, rotational stiffness, etc.) along with the axial pile load. The axial pile load is used to evaluate secondary moments resulting from pile deflection.

STEP 7 Click on Soil Conditions in the Data menu. The soil layers window will then appear as shown in Figure 9.53. The nine available soil type selections are depicted and correspond to the p-y model that will be assigned to the layer.



Figure 9.53 LPILE Soil Layers and Individual Soil Property Input Screens

- For each soil layer, select the soil type and values for the top and bottom of each soil layer. Then click on data for soil properties line corresponding to the layer.
- For each soil type, a second soil property input window will appear. The user must input values for the effective unit weight and depending upon the soil type selected, values for the cohesive strength, the soil strain ϵ_{50} , the p-y modulus, the friction angle, the uniaxial compressive strength and Young's Modulus.

Values for ϵ_{50} , can be obtained from triaxial tests or an assumed value from Table 9-15 can be selected. Values for the p-y modulus, k, can be measured from laboratory or in-situ test data or assumed value from Table 9-16 can be chosen.

- c. After inputting the required soil information for the selected soil type, close the soil property box and return to the soil layer window. Add rows as appropriate for the soil model and repeat steps a and b for each layer

TABLE 9-15 REPRESENTATIVE VALUES OF ϵ_{50} FOR CLAYS		
Clay Consistency	Average Undrained Shear Strength, c_u in kPa (ksf)	ϵ_{50}
Soft Clay	12 – 24 (0.25 – 0.50)	0.02
Medium Clay	24 – 48 (0.50 - 1.0)	0.01
Stiff Clay	48 – 96 (1.0 – 2.0)	0.007
Very Stiff Clay	96 – 192 (2.0 – 4.0)	0.005
Hard Clay	192 – 383 (4.0 – 8.0)	0.004

STEP 8 Click on the Analysis Type in the Options menu. The Analysis Type window will then appear as shown in Figure 9.54. The four analysis type options available are as follows:

Type 1 – Computations of Pile Response with User Specified, Constant EI (Basic Modeling). This analysis uses the modulus of elasticity, E, and moment of inertia, I, that were input in the pile properties section.

Type 2 -- Computations of Ultimate Bending Moment of Cross Section (Section Design). Selection of this analysis method activates additional Data menu input screens (not described herein) on the pile cross sectional shape, the pile cross sectional dimensions, the rebar arrangement, the cross sectional material properties and the axial loads for the cross section analysis. This analysis option computes the ultimate bending moment and the nonlinear variation of flexural stiffness with applied moment.

TABLE 9-16 REPRESENTATIVE p-y MODULUS VALUES, k, FOR CLAYS AND SANDS				
Soil Type	Avg. Undrained Shear Strength, c_u in kPa (ksf)	Soil Condition Relative to Water Table	k - Static Loading in kN/m^3 (lb/in ³)	k - Cyclic Loading in kN/m^3 (lb/in ³)
Soft Clay	12 – 24 (0.25-0.50)	---	8,140 (30)	
Medium Clay	24 – 48 (0.50 -1.0)	---	27,150 (100)	
Stiff Clay	48 – 96 (1.0 – 2.0)	---	136,000 (500)	54,300 (200)
Very Stiff Clay	96 – 192 (2.0 – 4.0)	---	271,000 (1000)	108,500 (400)
Hard Clay	192 – 383 (4.0 – 8.0)	---	543,000 (2000)	217,000 (1000)
Loose Sand	---	Submerged	5,430 (20)	5,430 (20)
Loose Sand	---	Above	6,790 (25)	6,790 (25)
Medium Dense Sand	---	Submerged	16,300 (60)	16,300 (60)
Medium Dense Sand	---	Above	24,430 (90)	24,430 (90)
Dense Sand	---	Submerged	33,900 (125)	33,900 (125)
Dense Sand	---	Above	61,000 (225)	61,000 (225)

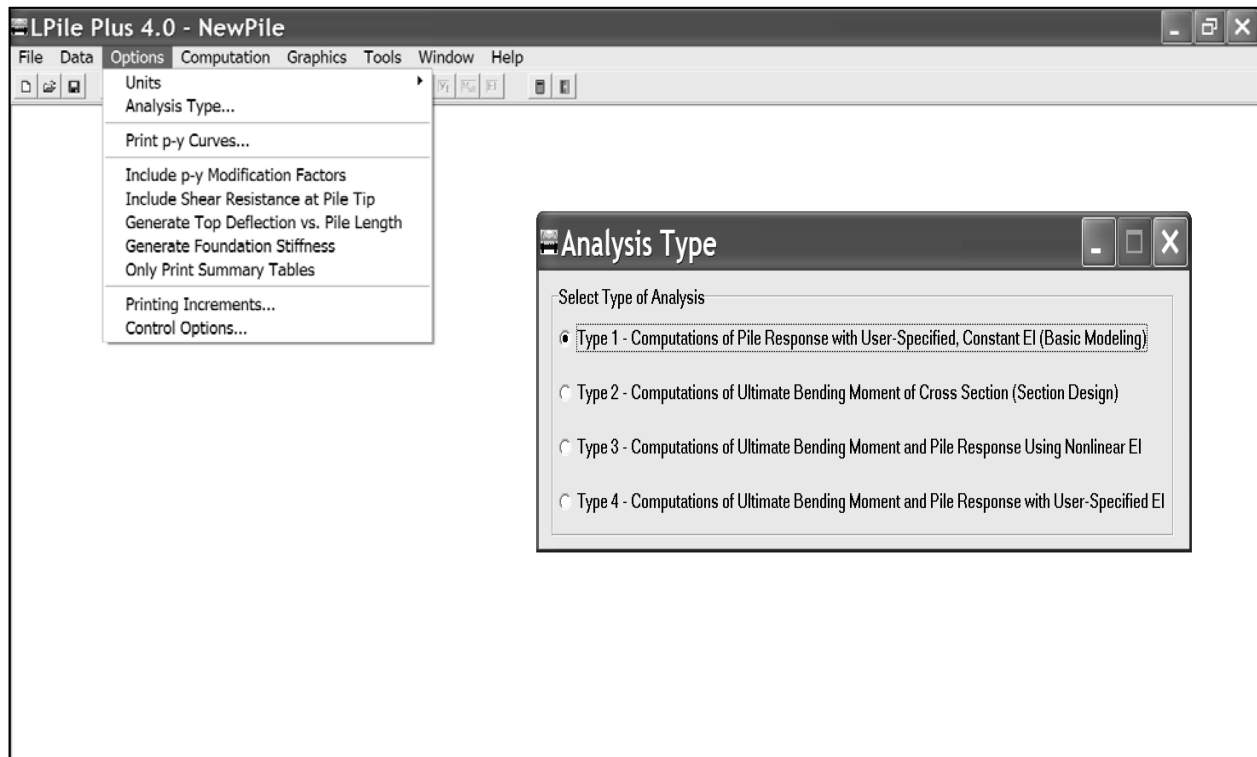


Figure 9.54 LPILE Analysis Type Input Screen

Type 3 – Computations of Ultimate Bending Moment and Pile Response Using Nonlinear EI. This analysis type, the pile cross section is analyzed to determine the ultimate bending moment and the variation of flexural stiffness with applied bending moment. LPILE then analyzes the laterally loaded pile using the nonlinear flexural stiffness values determined in the analysis of the cross section.

Type 4 – Computations of Ultimate Bending Moment and Pile Response with User-Specified EI. By selecting this analysis type, LPILE first analyses the pile cross section to determine the ultimate bending moment and the variation of flexural stiffness with applied bending moment. LPILE then analyzes the laterally loaded pile using the flexural stiffness computed by the user specified modulus of elasticity, E, and moment of inertia, I.

STEP 9 Click on Run Analysis in the Computations menu. After the analysis is completed, click on View Output Text File to review results. Results can also be printed after they are displayed on the screen. The LPILE Computation menu options are displayed in Figure 9.55.

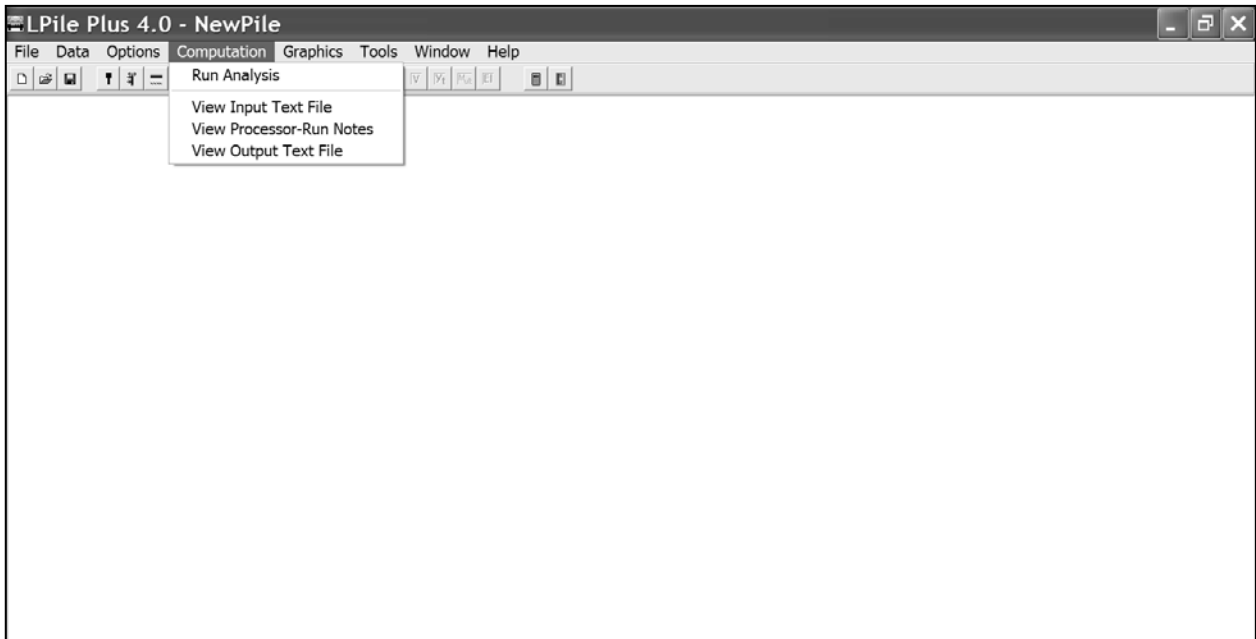


Figure 9.55 LPILE Computation Menu Screen

- STEP 10 Review output to determine the pile structural acceptability by finding the ultimate lateral load that produces a plastic hinge (ultimate bending moment).
- In this step the lateral, axial and bending moments used in the analysis should be ultimate values.
 - For concrete piles, the value of I for a cracked section can be determined directly by LPILE for each loading step. Alternatively, variations in E and I can be entered as a function of depth along the pile.
- STEP 11 Determine pile acceptability based on deflection under service loads.
- Use design loading conditions and not ultimate values for lateral and axial loads and bending moments.
 - Compare LPILE predicted movement with performance criteria.
- STEP 12 Optimize required pile section and pile penetration depth for lateral loading conditions to meet performance criteria as necessary.

After a basic LPILE analysis is performed, additional analyses can be used to refine the lateral pile design. Evaluation of pile group performance is discussed in Section 9.8.4.

9.8 DESIGN OF PILE GROUPS

The previous sections of this chapter dealt with design procedures for single piles. However piles for almost all highway structures are installed in groups, due to the heavy foundation loads. The next sections of this chapter will address the foundation design procedures for evaluating the axial compression capacity of pile groups as well as the settlement of pile groups under axial compression loads. The axial compression capacity and settlement of pile groups are interrelated and are therefore presented in sequence. Sections covering the design of pile groups for uplift and lateral load capacity will be presented following the axial compression capacity and settlement of pile group sections. At the present time, pile group design computations are primarily performed using computer programs designed for this purpose such as FB-Pier or Group 6.0 rather than the simple hand calculations presented in this manual.

The efficiency of a pile group in supporting the foundation load is defined as the ratio of the ultimate capacity of the group to the sum of the ultimate capacities of the individual piles comprising the group. This may be expressed in equation form as:

$$\eta_g = \frac{Q_{ug}}{nQ_u}$$

Where: η_g = Pile group efficiency.
 Q_{ug} = Ultimate capacity of the pile group.
 n = Number of piles in the pile group.
 Q_u = Ultimate capacity of each individual pile in the pile group.

If piles are driven into compressible cohesive soil or in dense cohesionless material underlain by compressible soil, then the ultimate axial compression capacity of a pile group may be less than that of the sum of the ultimate axial compression capacities of the individual piles. In this case, the pile group has a group efficiency of less than 1. In cohesionless soils, the ultimate axial compression capacity of a pile group is generally greater than the sum of the ultimate axial compression capacities of the individual piles comprising the group. In this case, the pile group has a group efficiency greater than 1.

The settlement of a pile group is likely to be many times greater than the settlement of an individual pile carrying the same load per pile as each pile in the pile group. Figure 9.56(a) illustrates that for a single pile, only a small zone of soil around and below the pile toe is subjected to vertical stress. Figure 9.56(b) illustrates that for a pile group, a considerable depth of soil around and below the pile group is stressed. The settlement of the pile group may be large, depending on the compressibility of the soils within the stressed zone.

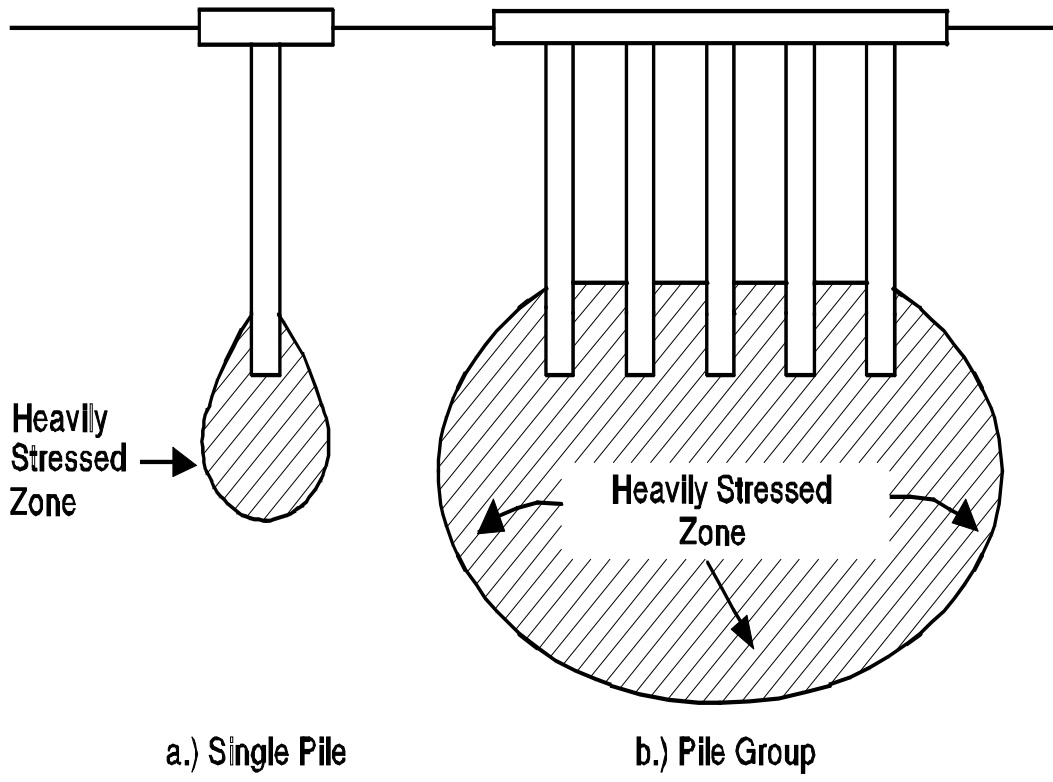


Figure 9.56 Stress Zone from Single Pile and Pile Group (after Tomlinson, 1994)

The soil medium supporting a pile group is also subject to overlapping stress zones from individual piles in the group. The overlapping effect of stress zones for a pile group supported by shaft resistance is illustrated in Figure 9.57.

9.8.1 Axial Compression Capacity of Pile Groups

9.8.1.1 Pile Group Capacity in Cohesionless Soils

In cohesionless soils, the ultimate group capacity of driven piles with a center to center spacing of less than 3 pile diameters is greater than the sum of the ultimate capacity of the individual piles. The greater group capacity is due to the overlap of individual soil compaction zones around each pile which increases the shaft resistance due to soil densification. Piles in groups at center to center spacings greater than three times the average pile diameter generally act as individual piles.

Design recommendations for estimating group capacity for driven piles in cohesionless soil are as follows:

1. The ultimate group capacity for driven piles in cohesionless soils not underlain by a weak deposit may be taken as the sum of the individual ultimate pile capacities, provided jetting or predrilling was not used in the pile installation process. Jetting or predrilling can result in group efficiencies less than 1. Therefore, jetting or predrilling should be avoided whenever possible and controlled by detailed specifications when necessary.
2. If a pile group founded in a firm bearing stratum of limited thickness is underlain by a weak deposit, then the ultimate group capacity is the smaller value of either the sum of the ultimate capacities of the individual piles, or the group capacity against block failure of an equivalent pier, consisting of the pile group and enclosed soil mass punching through the firm stratum into the underlying weak soil. From a practical standpoint, block failure in cohesionless soils can only occur when the center to center pile spacing is less than 2 pile diameters, which is less than the minimum center to center spacing of 2.5 diameters allowed by AASHTO code (2002). The method shown for cohesive soils in the Section 9.8.1.3 may be used to evaluate the possibility of a block failure.
3. Piles in groups should not be installed at center to center spacings less than 3 times the average pile diameter. A minimum center to center spacing of 3 diameters is recommended to optimize group capacity and minimize installation problems.

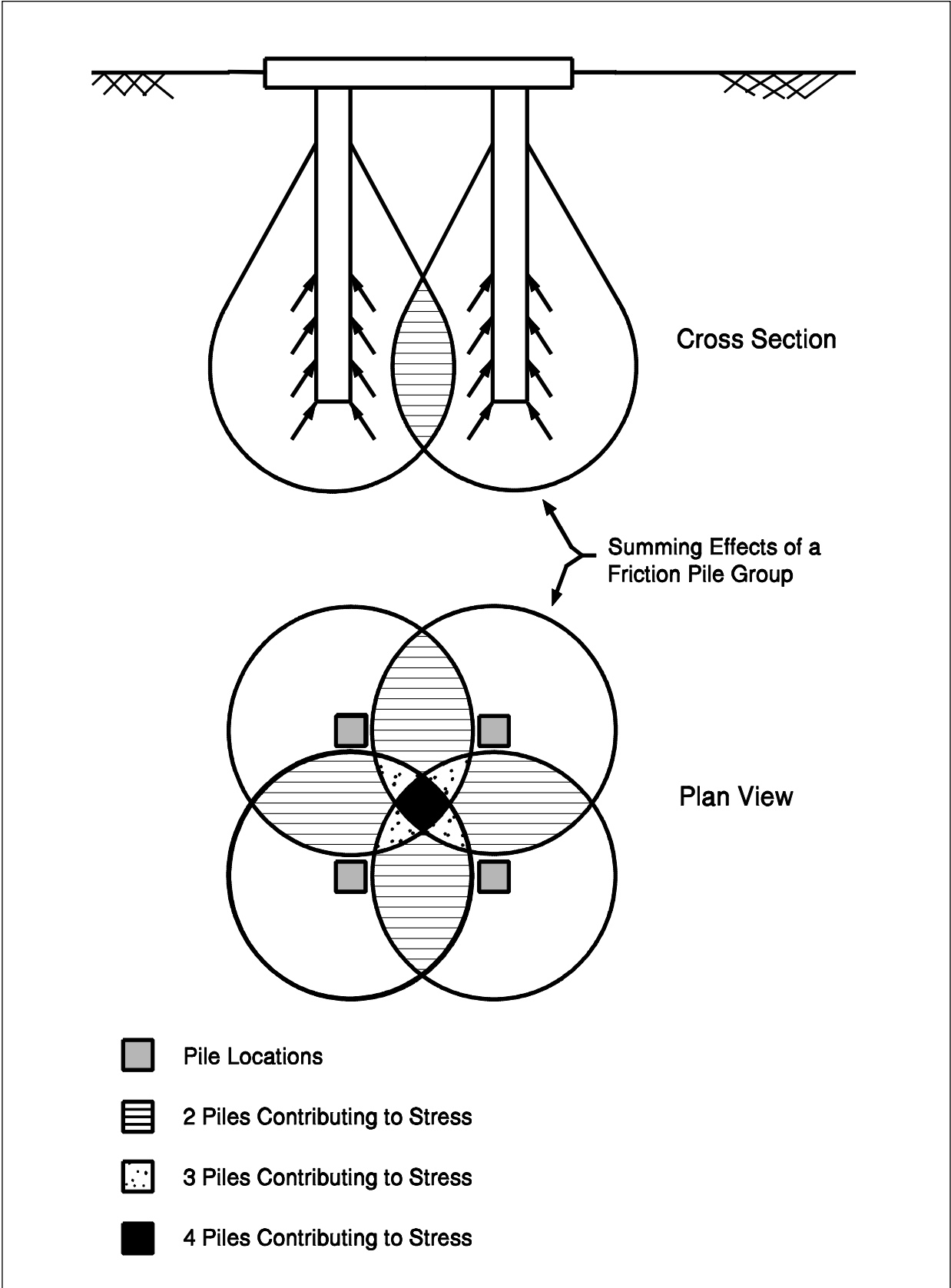


Figure 9.57 Overlap of Stress Zones for Friction Pile Group (after Bowles 1988)

9.8.1.2 Pile Group Capacity in Cohesive Soils

In the absence of negative shaft resistance, the group capacity in cohesive soil is usually governed by the sum of the ultimate capacities of the individual piles, with some reduction due to overlapping zones of shear deformation in the surrounding soil. Negative shaft resistance is described in section 9.9.1 and often occurs when soil settlement transfers load to the pile. AASHTO (2002) code states that the group capacity is influenced by whether the pile cap is in firm contact with the ground. If the pile cap is in firm contact with the ground, the soil between the piles and the pile group act as a unit.

The following design recommendations are for estimating ultimate pile group capacity in cohesive soils. The lesser of the ultimate pile group capacity, calculated from Steps 1 to 4, should be used.

1. For pile groups driven in clays with undrained shear strengths of less than 95 kPa (2 ksf) and the pile cap not in firm contact with the ground, a group efficiency of 0.7 should be used for center to center pile spacings of 3 times the average pile diameter. If the center to center pile spacing is greater than 6 times the average pile diameter, then a group efficiency of 1.0 may be used. Linear interpolation should be used for intermediate center to center pile spacings.
2. For piles in clays with undrained shear strengths less than 95 kPa (2 ksf), and the pile cap in firm contact with the ground, a group efficiency of 1.0 may be used.
3. For pile groups in clays with undrained shear strength in excess of 95 kPa (2 ksf), a group efficiency of 1.0 may be used regardless of the pile cap - ground contact.
4. Calculate the ultimate pile group capacity against block failure using the procedure described in Section 9.8.1.3.
5. Piles in cohesive soils should not be installed at center to center pile spacings less than 3.0 times the average pile diameter and not less than 1 meter (3.3 ft).

It is important to note that the driving of pile groups in cohesive soils can generate large excess pore water pressures. This can result in short term (1 to 2 months after installation) group efficiencies on the order of 0.4 to 0.8. As these excess pore pressures dissipate, the pile group efficiency will increase. Figure 9.58 presents observations on the dissipation of excess pore water pressure versus time for pile

groups driven in cohesive soils. Depending upon the group size, the excess pressures typically dissipate within 1 to 2 months after driving. However, in very large groups, full pore pressure dissipation may take up to a year.

If a pile group will experience the full group load shortly after construction, the foundation designer must evaluate the reduced group capacity that may be available for load support. In these cases, piezometers should be installed to monitor pore pressure dissipation with time. Effective stress capacity calculations can then be used to determine if the increase in pile group capacity versus time during construction meets the load support requirements.

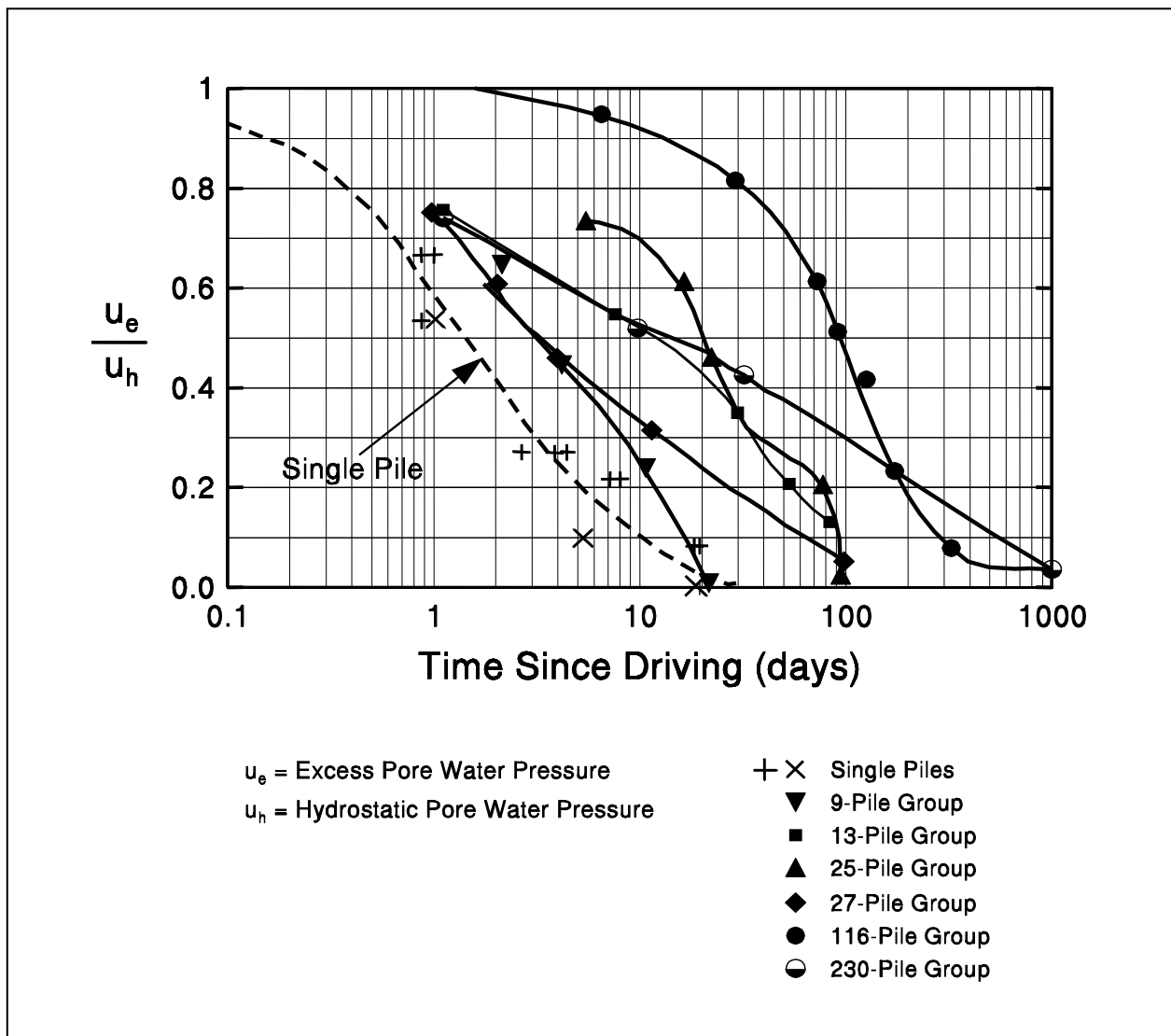


Figure 9.58 Measured Dissipation of Excess Pore Water Pressure in Soil Surrounding Full Scale Pile Groups (after O'Neill, 1983)

9.8.1.3 Block Failure of Pile Groups

Block failure of pile groups is generally only a design consideration for pile groups in soft cohesive soils or in cohesionless soils underlain by a weak cohesive layer. For a pile group in cohesive soil as shown in Figure 9.59, the ultimate capacity of the pile group against a block failure is provided by the following expression:

$$Q_{ug} = 2D (B + Z) c_{u1} + B Z c_{u2} N_c$$

Where:

- Q_{ug} = Ultimate group capacity against block failure.
- D = Embedded length of piles.
- B = Width of pile group.
- Z = Length of pile group.
- c_{u1} = Weighted average of the undrained shear strength over the depth of pile embedment for the cohesive soils along the pile group perimeter.
- c_{u2} = Average undrained shear strength of the cohesive soils at the base of the pile group to a depth of $2B$ below pile toe level.
- N_c = Bearing capacity factor.

If a pile group will experience the full group load shortly after construction, the ultimate group capacity against block failure should be calculated using the remolded or a reduced shear strength rather than the average undrained shear strength for c_{u1} .

The bearing capacity factor, N_c , for a rectangular pile group is generally 9. However, for pile groups with small pile embedment depths and/or large widths, N_c should be calculated from the following equation.

$$N_c = 5 \left[1 + \frac{D}{5B} \right] \left[1 + \frac{B}{5Z} \right] \leq 9$$

When evaluating possible block failure of pile groups in cohesionless soils underlain by a weak cohesive deposit, the weighted average unit shaft resistance for the cohesionless soils should be substituted for c_{u1} in calculating the ultimate group capacity. The pile group base strength determined from the second part of the ultimate group capacity equation should be calculated using the strength of the underlying weaker layer.

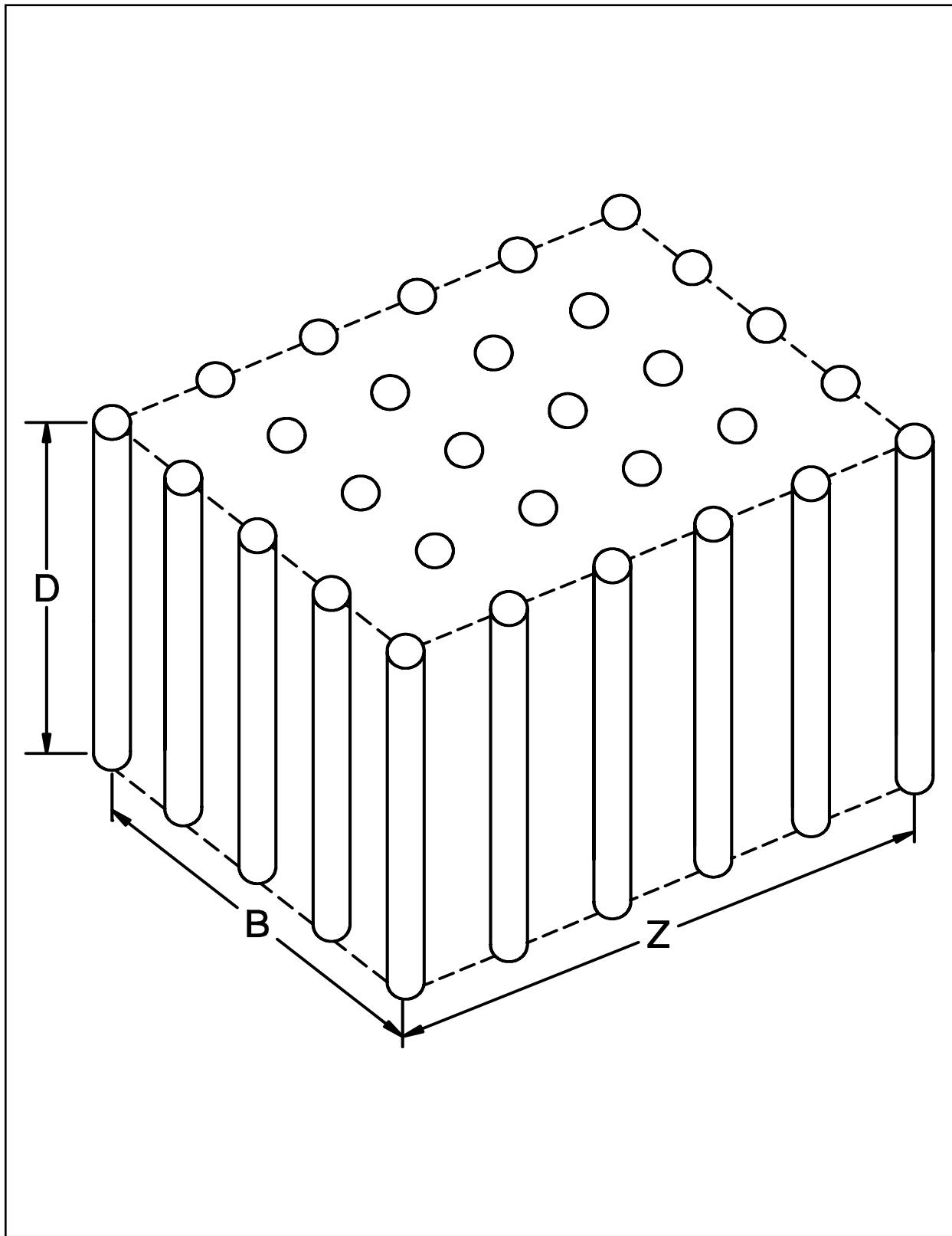


Figure 9.59 Three Dimensional Pile Group Configuration (after Tomlinson, 1994)

9.8.2 Settlement of Pile Groups

Pile groups supported in and underlain by cohesionless soils will produce only immediate settlements. This means the settlements will occur immediately as the pile group is loaded. Pile groups supported in and underlain by cohesive soils may produce both immediate settlements and consolidation settlements that occur over a period of time. In highly over-consolidated clays, the majority of the foundation settlement will occur immediately. Consolidation settlements will generally be the major source of foundation settlement in normally consolidated clays.

Methods for estimating settlement of pile groups are provided in the following sections. Methods for estimating single pile settlements are not provided because piles are usually installed in groups.

9.8.2.1 Elastic Compression of Piles

The pile group settlement methods discussed in the following sections only consider soil settlements and do not include the settlement caused by elastic compression of pile material due to the imposed axial load. Therefore, the elastic compression should also be computed and this settlement added to the group settlement estimates of soil settlement. The elastic compression can be computed by the following expression:

$$\Delta = \frac{Q_a L}{A E}$$

Where: Δ = Elastic compression of pile material in mm (in).
 Q_a = Design axial load in pile in kN (kips).
 L = Length of pile in mm (in).
 A = Pile cross sectional area in m^2 (in^2).
 E = Modulus of elasticity of pile material in kPa (ksi).

The modulus of elasticity for steel piles is 207,000 MPa (30,000 ksi). For concrete piles, the modulus of elasticity varies with concrete compressive strength and is generally on the order of 27800 MPa (4030 ksi). The elastic compression of short piles is usually quite small and can often be neglected in design.

9.8.2.2 Settlements of Pile Groups in Cohesionless Soils

9.8.2.2a Method Based on SPT Test Data

Meyerhof (1976) recommended that the settlement of a pile group in a homogeneous sand deposit not underlain by a more compressible soil at a greater depth may be conservatively estimated by the following expression:

$$s = \frac{0.96 p_f \sqrt{B} I_f}{\bar{N}'} \quad (\text{SI units}) \quad \text{or} \quad s = \frac{4 p_f \sqrt{B} I_f}{\bar{N}'} \quad (\text{US units})$$

For silty sand, use:
$$s = \frac{1.92 p_f \sqrt{B} I_f}{\bar{N}'} \quad (\text{SI units}) \quad \text{or} \quad s = \frac{8 p_f \sqrt{B} I_f}{\bar{N}'} \quad (\text{US units})$$

Where:

- s = Estimated total settlement in mm (in).
- p_f = Design foundation pressure in kPa (ksf). Group design load divided by group area.
- B = Width of pile group in m (ft).
- \bar{N}' = Average corrected SPT N' value within a depth B below pile toe.
- D = Pile embedment depth in m (ft).
- I_f = Influence factor for group embedment = $1 - [D / 8B] \geq 0.5$.

For piles in cohesionless soils underlain by cohesive deposits, the method presented in Sections 9.8.2.4 should be used.

9.8.2.2b Method Based on CPT Test Data

Meyerhof (1976) recommended the following relationship to estimate maximum settlements using cone penetration test results for saturated cohesionless soils.

$$(\text{SI units}) \quad s = \frac{42 p_f B I_f}{\bar{q}_c} \quad (\text{US units}) \quad s = \frac{p_f B I_f}{2 \bar{q}_c}$$

Where: s , p_f , B, and I_f are as defined in the previous method, and \bar{q}_c = Average static cone tip resistance in kPa (ksf) within a depth of B below the pile toe level.

9.8.2.3 Settlement of Pile Groups in Cohesive Soils

Terzaghi and Peck (1967) proposed that pile group settlements could be evaluated using an equivalent footing situated at a depth of $1/3 D$ above the pile toe. This concept is illustrated in Figure 9.60. For a pile group consisting of only vertical piles, the equivalent footing has a plan area $(B)(Z)$ that corresponds to the perimeter dimensions of the pile group as shown in Figure 9.59. The pile group load over this plan area is then the bearing pressure transferred to the soil through the equivalent footing. The load is assumed to spread within the frustum of a pyramid of side slopes at 30° and to cause uniform additional vertical pressure at lower levels. The pressure at any level is equal to the load carried by the group divided by the plan area of the base of the frustum at that level. Consolidation settlements are calculated based on the pressure increase in the underlying layers.

Consolidation settlements of cohesive soils are usually computed on the basis of laboratory tests. A typical plot of consolidation test results illustrating the relationships of the compression indices C_c and C_{cr} to void ratio, e , and pressure, p , are shown in Figure 9.61. For pressure increases less than the preconsolidation pressure, p_c , settlement is computed using a value of the compression index representing recompression, C_{cr} . For pressure increases greater than the preconsolidation pressure, settlement is computed using the compression index, C_c .

The following three equations are used to calculate settlements of cohesive soils depending upon the pressure increase and whether the soil is overconsolidated or normally consolidated. The terms used in these equations are as follows:

- s = Total settlement in mm (in).
- H = Original thickness of stratum in mm (in).
- C_{cr} = Recompression index.
- e_0 = Initial void ratio.
- p_o = Effective overburden pressure at midpoint of compressible stratum prior to pressure increase in kPa (ksf).
- p_c = Estimated preconsolidation pressure in kPa (ksf).
- C_c = Compression index.
- Δp = Average change in pressure in the compressible stratum in kPa (ksf).

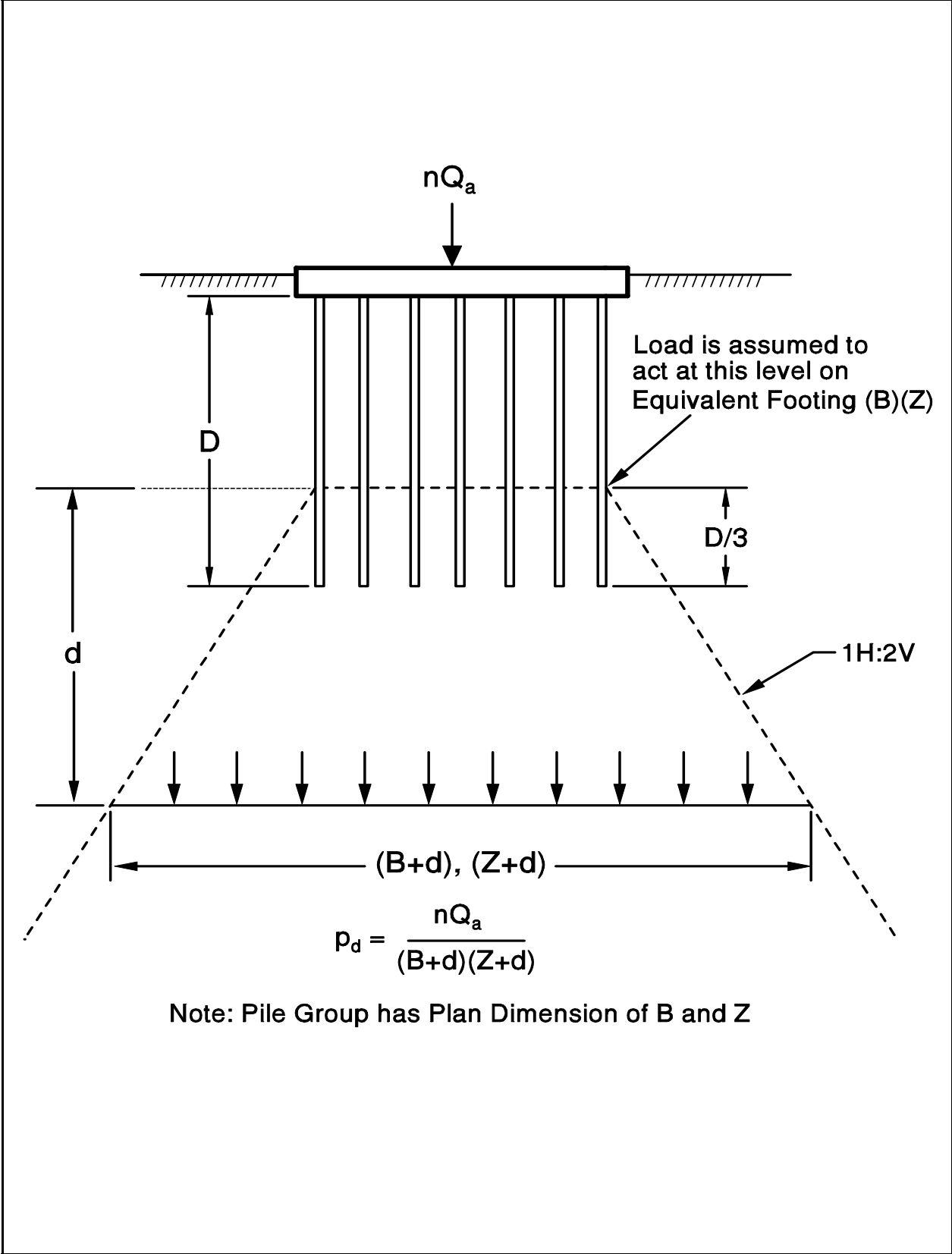


Figure 9.60 Equivalent Footing Concept

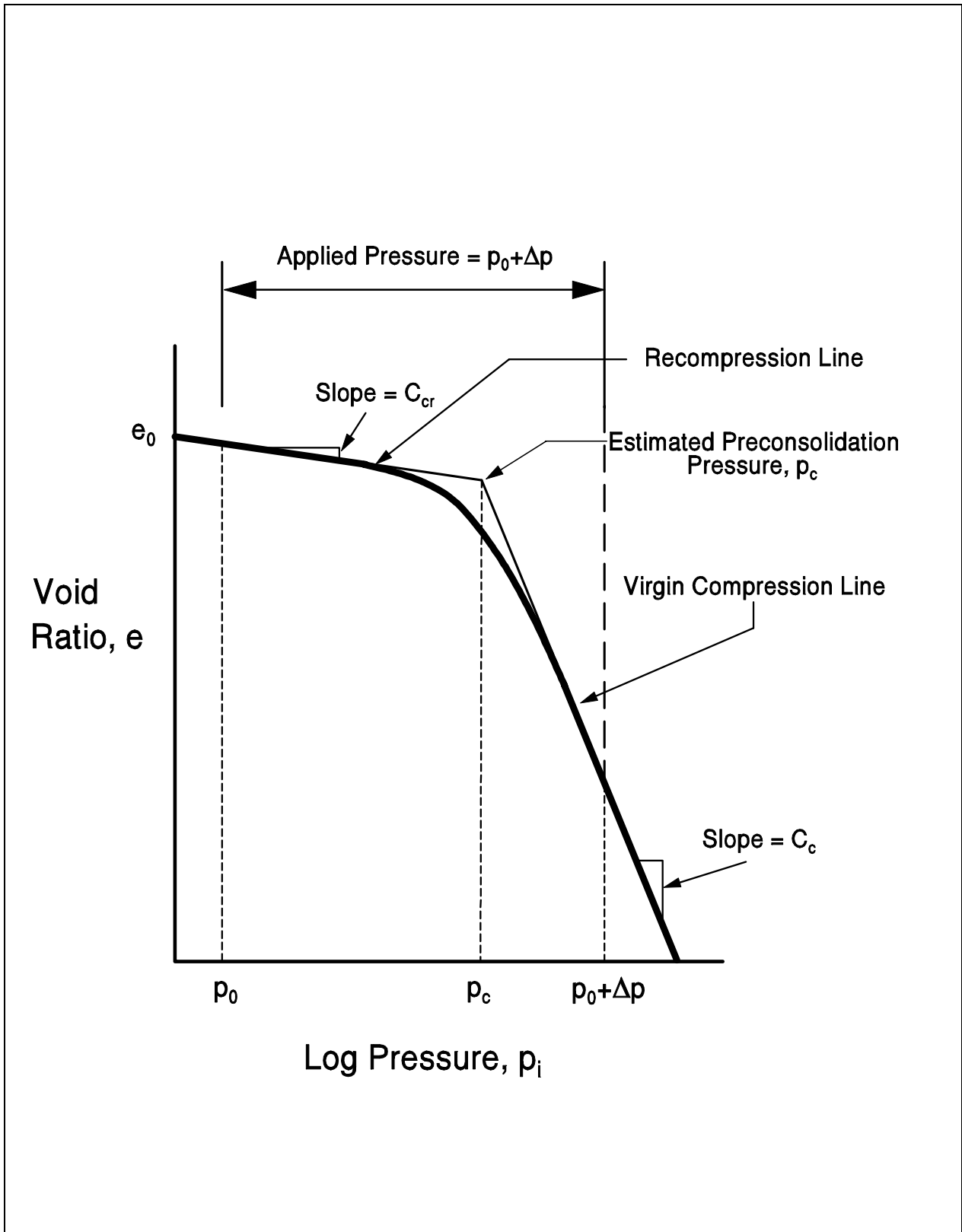


Figure 9.61 Typical e-log p Curve from Laboratory Consolidation Test

For overconsolidated cohesive soils where the pressure after the foundation pressure increase is greater than the soil preconsolidation pressure, settlements may be computed as follows:

$$s = H \left[\frac{C_{cr}}{1 + e_0} \log \frac{p_c}{p_o} \right] + H \left[\frac{C_c}{1 + e_0} \log \frac{p_o + \Delta p}{p_c} \right]$$

For overconsolidated cohesive soils where the pressure after the foundation pressure increase is less than the soil preconsolidation pressure, settlements should be computed using the following equation:

$$s = H \left[\frac{C_{cr}}{1 + e_0} \log \frac{p_o + \Delta p}{p_o} \right]$$

For normally consolidated cohesive soils, settlements should be computed from:

$$s = H \left[\frac{C_c}{1 + e_0} \log \frac{p_o + \Delta p}{p_o} \right]$$

Rather than fixing the equivalent footing at a depth of $\frac{1}{3} D$ above the pile toe for all soil conditions, the depth of the equivalent footing should be adjusted based upon soil stratigraphy and load transfer mechanism to the soil. Figure 9.62 presents the recommended location of the equivalent footing for the following load transfer and soil resistance conditions:

- a) toe bearing piles in hard clay or sand underlain by soft clay
- b) piles supported by shaft resistance in clay
- c) piles supported in shaft resistance in sand underlain by clay
- d) piles supported by shaft and toe resistance in layered soil profile

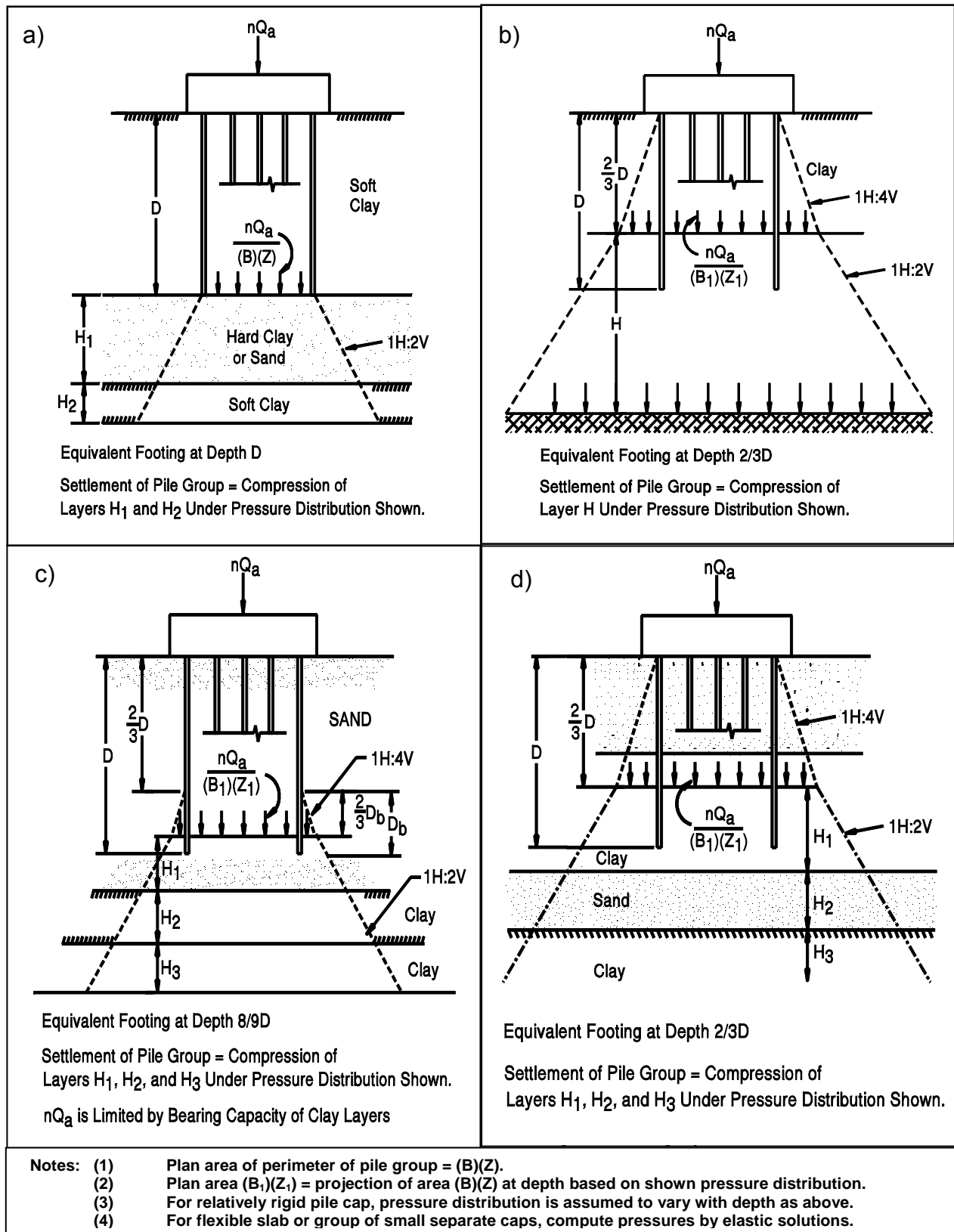


Figure 9.62 Pressure Distribution Below Equivalent Footing for a Pile Group (adapted from Cheney and Chassie, 1993)

STEP BY STEP PROCEDURE FOR PILE GROUP SETTLEMENT IN COHESIVE SOILS

STEP 1 Determine the new load imposed on soil by the pile group.

- a. Determine the location of the equivalent footing. For pile groups supported primarily by toe resistance, the equivalent footing is placed at the pile toe as illustrated in Figure 9.62(a). For pile groups supported primarily by shaft resistance, the equivalent footing is placed at a depth of $\frac{2}{3} D$ as shown in Figure 9.62(b).
- b. Determine the dimensions of the equivalent footing. For pile groups consisting only of vertical piles, the equivalent footing (unless modified for load transfer as in Figure 9.62(b)) has the same dimensions as the length and width of the pile group from Figure 9.59. For pile groups supported primarily by shaft resistance that include batter piles, the plan area of the footing should be calculated from the dimensions of the pile group at depth $\frac{2}{3} D$, including the plan area increase due to the pile batter. For toe bearing groups with batter piles, the equivalent footing area should be the dimensions of the pile group at depth D , including the area increase due to pile batter.
- c. Determine the pressure distribution to soil layers below the equivalent footing up to the depth at which the pressure increase from the equivalent footing is less than 10% of existing effective overburden pressure at that depth. Remember that the equivalent footing size may be increased and the footing pressure correspondingly reduced as a result of load transfer above the footing location or in groups with batter piles. The depth at which the pressure increase is less than 10% will provide the total thickness of cohesive soil layer or layers to be used in performing settlement computations. Note that the group design load should be used in determining the pressure distribution for settlement computations, and not the ultimate group load.

- d. Divide the cohesive soil layers in the affected pressure increase zone into several thinner layers of 1.5 to 3 meter (5 to 10 ft) thickness. The thickness of each layer is the thickness H for the settlement computation for that layer.
- e. Determine the existing effective overburden pressure, p_o , at midpoint of each layer.
- f. Determine the imposed pressure increase, Δp , at midpoint of each affected soil layer based on the appropriate pressure distribution.

STEP 2 Determine consolidation test parameters.

Plot results of consolidation test(s) as shown in Figure 9.61. Determine p_c , e_o , C_{cr} and C_c values from the consolidation test data.

STEP 3 Compute settlements.

Using the appropriate settlement equation, compute the settlement of each affected soil layer. Sum the settlements of all layers to obtain the total estimated soil settlement from the pile group. Add the elastic compression of the pile under the design load to obtain the total estimated pile group settlement.

9.8.2.4 Time Rate of Settlement in Cohesive Soils

Settlement analyses in cohesive soils should also evaluate the time required for the anticipated settlement to occur. In time rate computations, the time for 90% consolidation to occur is usually used to determine the total time required for primary settlement. The time rate of settlement of a cohesive soil deposit can be calculated from:

$$t = \frac{TH_v^2}{C_v}$$

Where: t = time for settlement to occur in days

T = theoretical time factor for percentage of primary consolidation to occur from Table 9-17

H_v = the maximum vertical drainage path in the cohesive layer in m (ft)
 C_v = the coefficient of consolidation in m^2/day (ft^2/day) from laboratory consolidation tests

The term H_v should not be confused with the term H used in the settlement equations for cohesive soils. H_v is the maximum distance water must travel from the compressible cohesive deposit to a more permeable layer. In the case of a cohesive layer overlain and underlain by a permeable granular layer, H_v would be $\frac{1}{2}$ the cohesive layer thickness. However if the cohesive layer were overlain by a permeable granular layer and underlain by a non-permeable rock layer, H_v would be the full thickness of the cohesive deposit. Additional discussion on time rate of consolidation can be found in the Soils and Foundation Workshop Manual, Report No. HI-88-009, Cheney and Chassie (2002).

TABLE 9-17 TIME FACTOR (T)	
Percent Primary Settlement	Time Factor (T)
10	0.008
20	0.031
30	0.071
40	0.126
50	0.197
60	0.287
70	0.403
80	0.567
90	0.848

9.8.2.5 Settlement of Pile Groups in Layered Soils

Piles are often installed in a layered soil profile consisting of cohesionless and cohesive soils or in soil profiles where an underlying soil stratum of different consistency is affected by the pile group loading. In these cases, group settlement will be influenced by the pressure increase in and compressibility of the affected layers. Figures 9.62(a), 9.62(c) and 9.62(d) may be used to determine the location of the equivalent footing and to evaluate the resulting pressure increase in a soil layer. The settlement of each layer

is then calculated using the appropriate settlement equation presented in Section 9.8.2.3 for cohesive layers and from the following equation for cohesionless layers.

$$s = H \left[\frac{1}{C'} \log \frac{p_o + \Delta p}{p_o} \right]$$

Where:

s	=	Total layer settlement in mm (in).
H	=	Original thickness of layer in mm (in).
C'	=	Dimensionless bearing capacity index from Figure 9.63, determined from average corrected SPT N' value N, for layer with consideration of SPT hammer type.
p _o	=	Effective overburden pressure at midpoint of layer prior to pressure increase in kPa (ksf).
Δp	=	Average change in pressure in the layer in kPa (ksf).

Cheney and Chassie (2002) report that FHWA experience with this method indicates the method is usually conservative and can overestimate settlements by a factor of 2. This conservatism is attributed to the use of the original bearing capacity index chart from Hough (1959) which was based upon SPT donut hammer data. Based upon average energy variations between SPT donut and safety hammers reported in technical literature, Figure 9.63 now includes a correlation between SPT N values from a safety hammer and bearing capacity index. The safety hammer values are considered N₆₀ values. This modification should improve the accuracy of settlement estimates with this method.

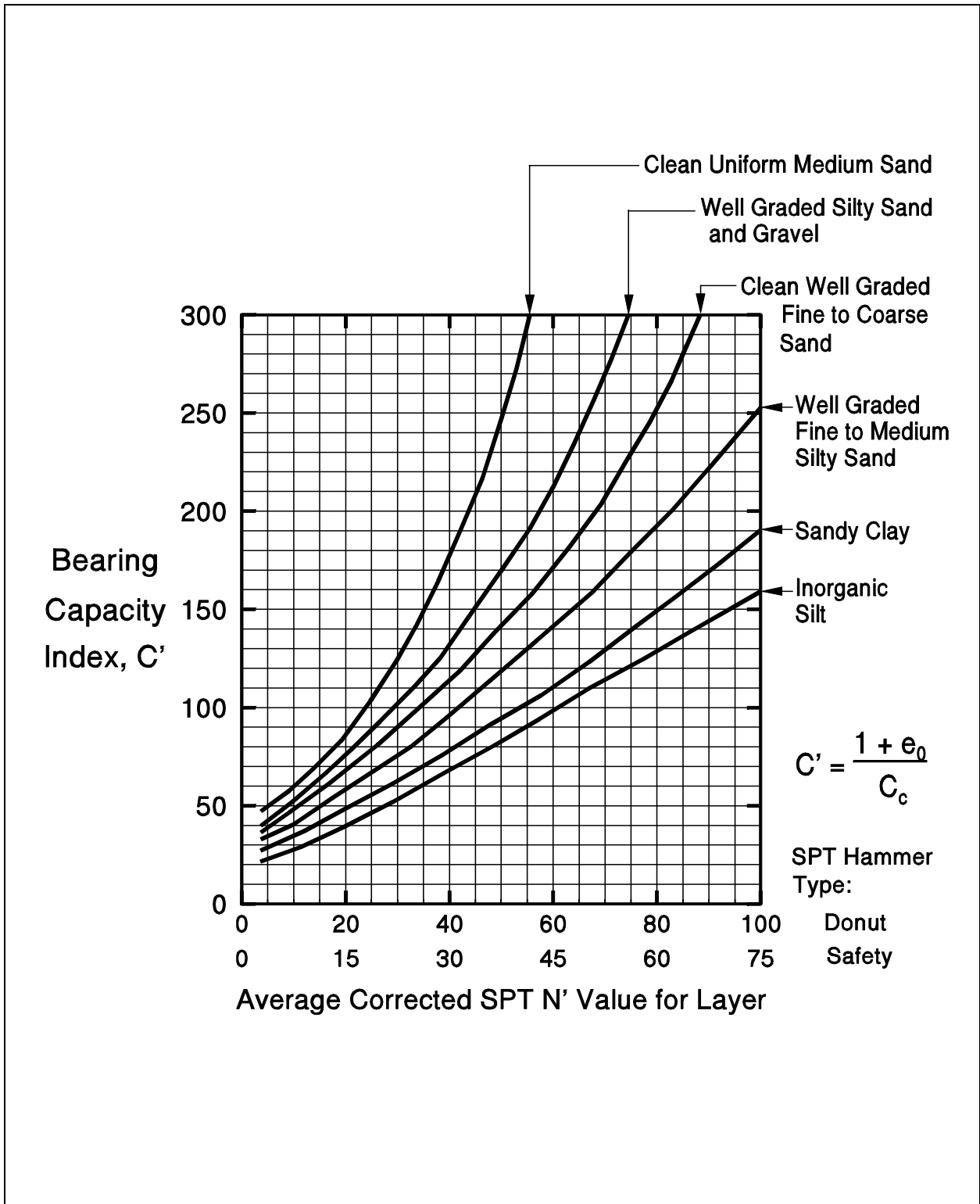


Figure 9.63 Values of the Bearing Capacity Index, C' , for Granular Soil (modified after Cheney and Chassie, 1993)

STEP BY STEP PROCEDURE FOR GROUP SETTLEMENT IN LAYERED SOIL PROFILES

STEP 1 Determine the new load imposed on soil by the pile group.

- a. Determine the location of the equivalent footing. For pile groups supported primarily by toe resistance, the equivalent footing is placed at the pile toe as illustrated in Figure 9.62(a). For pile groups supported primarily by shaft resistance in sands underlain by cohesive soils, the equivalent footing is placed at a depth of $8/9 D$ as shown in Figure 9.62(c). For pile groups in layered soils supported by a combination of shaft and toe resistance, the equivalent footing is placed at $2/3 D$ as shown in Figure 9.62(d).
- b. Determine the dimensions of the equivalent footing. For pile groups consisting only of vertical piles, the equivalent footing (unless modified for load transfer as in Figures 9.62(c) and 9.62(d)) has the same dimensions as the length and width of the pile group from Figure 9.59. For pile groups supported primarily by shaft resistance that include batter piles, the plan area of the footing should be calculated from the dimensions of the pile group at the equivalent footing depth that includes the plan area increase due to the pile batter. For toe bearing groups with batter piles, the equivalent footing area should be calculated from the dimensions of the pile group at depth D , including the plan area increase due to the pile batter.
- c. Determine the pressure distribution to soil layers below the equivalent footing up to the depth at which the pressure increase from the equivalent footing is less than 10% of existing effective overburden pressure at that depth. Remember that the equivalent footing size may be increased and the footing pressure correspondingly reduced as a result of load transfer above the footing location or in groups with batter piles. The depth at which the pressure increase is less than 10% will provide the total thickness of soil to be evaluated in the settlement computations. Note that the group design load should be used in determining the pressure distribution for settlement computations, and not the ultimate group capacity.

- d. Divide the soil layers in the affected pressure increase zone into several thinner layers of 1.5 to 3 meter (5 to 10 ft) thickness. The thickness of each layer is the thickness H for the settlement computation for that layer.
- e. Determine the existing effective overburden pressure, p_o , at midpoint of each soil layer.
- f. Determine the imposed pressure increase, Δp , at midpoint of each affected soil layer based on the appropriate pressure distribution.

STEP 2 Determine consolidation test parameters for each cohesive layer.

Plot results of consolidation test(s) as shown in Figure 9.61. Determine p_c , e_o , C_{cr} and C_c values from the consolidation test data.

STEP 3 Determine bearing capacity index for each cohesionless layer.

Determine the average corrected SPT N' value, \bar{N}' , for each cohesionless layer. Use N' or the appropriate SPT hammer type in Figure 9.63 to obtain the bearing capacity index for each layer. The safety hammer N values in Figure 9.63 are considered representative of N_{60} values.

STEP 4 Compute settlements.

Using the appropriate settlement equation, compute the settlement of each affected soil layer. Sum the settlements of all layers to obtain the total estimated soil settlement from the pile group. Add the elastic compression of the pile under the design load to obtain the total estimated pile group settlement.

9.8.2.6 Settlement of Pile Groups Using the Janbu Tangent Modulus Approach

The previous methods of group settlement analyses assume a linear relationship between induced stress and soil strain. However in most soils, a non-linear relationship exists between stress and strain. Figure 9.64 illustrates that a stress increase at a small original stress will result in a larger strain than the same stress increase applied at a greater original stress.

Janbu (1963, 1965) proposed a tangent modulus approach that is referenced in the Canadian Foundation Engineering Manual (1985). In this method, the stress strain relationship of soils is expressed in terms of a dimensionless modulus number, m , and a stress exponent, j . Values of the modulus number can be determined from conventional laboratory triaxial or oedometer tests. The stress exponent, j , can generally be taken as 0.5 for cohesionless soils and 0 for cohesive soils.

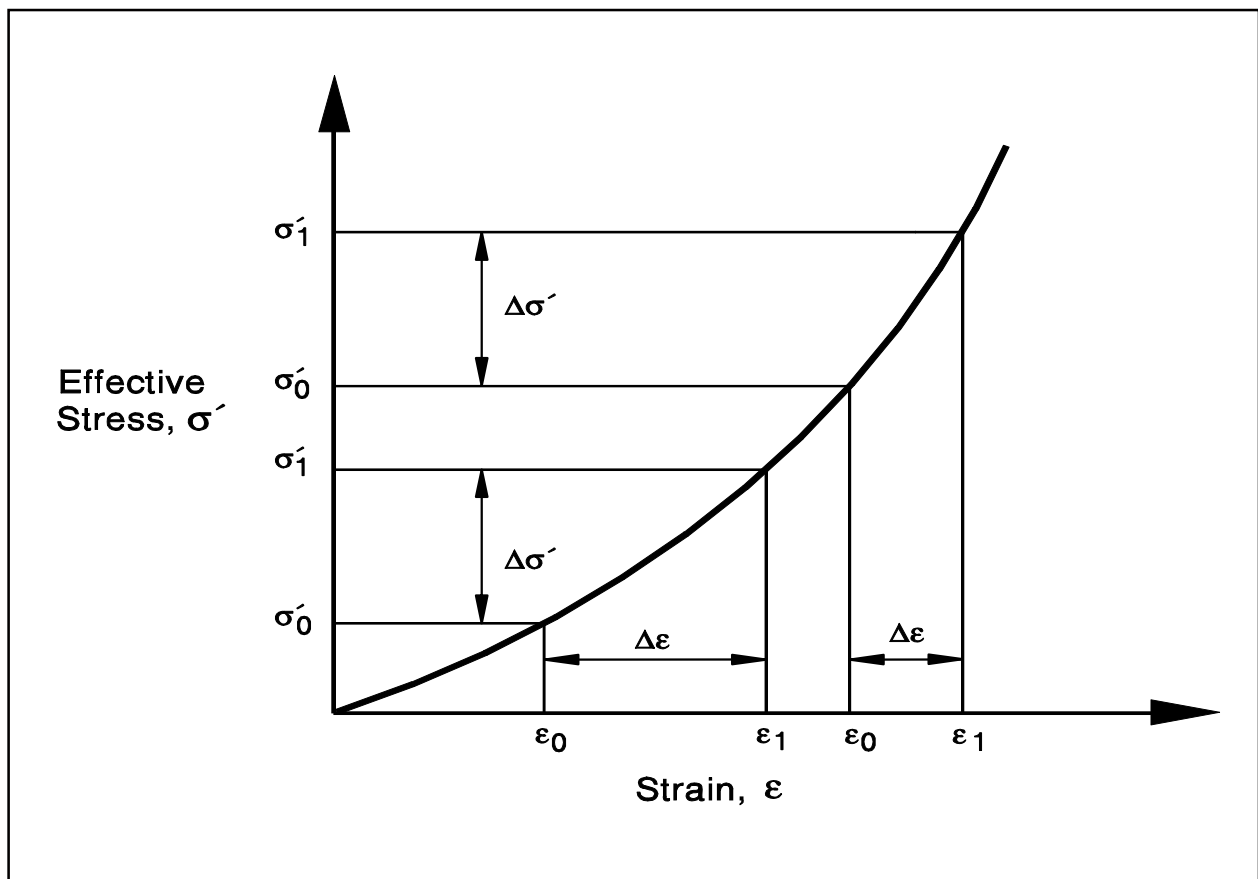


Figure 9.64 The Non-Linear Relation Between Stress and Strain in Soil (after Fellenius, 1990)

The following four equations are used to calculate the strain for normally and over consolidated, cohesionless and cohesive soils. The terms used in these four equations are as follows:

- ε = Strain from the increase in effective stress.
- m_n = Dimensionless modulus number.
- m_{nr} = Dimensionless recompression modulus number.
- j = Stress exponent.
- σ'_1 = New effective stress after stress increase, (kPa).
- σ'_0 = Original effective stress prior to stress increase, (kPa).
- σ'_p = Preconsolidation stress, (kPa).
- σ_r = Constant reference stress = 100 kPa.

For normally consolidated cohesionless soils, the strain induced by an increase in effective stress may be expressed as follows:

$$\varepsilon = \frac{1}{m_{nj}} \left[\left(\frac{\sigma'_1}{\sigma_r} \right)^j - \left(\frac{\sigma'_0}{\sigma_r} \right)^j \right]$$

For over consolidated cohesionless soils, the following equation should be used to calculate the strain induced by an increase in effective stress:

$$\varepsilon = \frac{1}{m_{nj}} \left[\left(\frac{\sigma'_1}{\sigma_r} \right)^j - \left(\frac{\sigma'_p}{\sigma_r} \right)^j \right] + \frac{1}{m_{nrj}} \left[\left(\frac{\sigma'_p}{\sigma_r} \right)^j - \left(\frac{\sigma'_0}{\sigma_r} \right)^j \right]$$

For cohesive soils, the stress exponent is zero, $j=0$. The strain induced by an increase in effective stress in a normally consolidated cohesive soil is then as follows:

$$\varepsilon = \frac{1}{m_n} \ln \left[\left(\frac{\sigma'_1}{\sigma'_0} \right) \right]$$

For over consolidated cohesive soils, the following equation should be used to calculate the strain induced by an increase in effective stress:

$$\varepsilon = \frac{1}{m_{nr}} \ln \left[\left(\frac{\sigma'_p}{\sigma'_0} \right) \right] + \frac{1}{m_n} \ln \left[\left(\frac{\sigma'_1}{\sigma_p} \right) \right]$$

In cohesionless soils, the modulus number can be calculated from the soil modulus of elasticity, E_s (kPa), and the previously described terms using the following equation:

$$m_n = \frac{E_s}{5[\sqrt{\sigma'_1} + \sqrt{\sigma'_0}]}$$

In cohesive soils, the modulus number, m_n , or recompression modulus number, m_{nr} , can be calculated from the initial void ratio, e_0 , and the compression index, C_c , or recompression index, C_{cr} . The modulus number is calculated from:

$$m_n = 2.30 \left[\frac{1 + e_0}{C_c} \right]$$

The recompression modulus number, m_{nr} , is calculated by substituting the recompression index, C_{cr} , for the compression index, C_c , in the above equation.

The Janbu tangent modulus approach is quite adaptable to calculating pile group settlements in any soil profile. For reference purposes, typical and normally conservative modulus number and stress exponent values from the Canadian Foundation Engineering Manual (1985) are presented in Table 9-18. These values may be useful for preliminary settlement estimates. A step by step procedure for this method follows.

TABLE 9-18 TYPICAL MODULUS AND STRESS EXPONENT VALUES			
Soil Type	Consistency	Range in Modulus Number, m_n	Stress Exponent, j
Glacial Till	Very Dense to Dense	1000 - 300	1.0
Gravel	---	400 - 40	0.5
Sand	Dense	400 - 250	0.5
Sand	Medium Dense	250 - 150	0.5
Sand	Loose	150 - 100	0.5
Silt	Dense	200 - 80	0.5
Silt	Medium Dense	80 - 60	0.5
Silt	Loose	60 - 40	0.5
Silty Clay & Clayey Silt	Hard - Stiff	60 - 20	0
Silty Clay & Clayey Silt	Stiff - Firm	20 - 10	0
Silty Clay & Clayey Silt	Soft	10 - 5	0
Marine Clay	Soft	20 - 5	0
Organic Clay	Soft	20 - 5	0
Peat	---	5 - 1	0

STEP BY STEP PROCEDURE FOR PILE GROUP SETTLEMENT BY JANBU METHOD

STEP 1 Determine the new load imposed on soil by the pile group.

- a. Determine the location of the equivalent footing. For pile groups supported primarily by toe resistance, the equivalent footing is placed at the pile toe as illustrated in Figure 9.62(a). For pile groups supported primarily by shaft resistance in sands underlain by cohesive soils, the equivalent footing is placed at a depth of $\frac{8}{9} D$ as shown in Figure 9.62(c). For pile groups in layered soils supported by a combination of shaft and toe resistance, the equivalent footing is placed at $\frac{2}{3} D$ as shown in Figure 9.62(d).
- b. Determine the dimensions of the equivalent footing. For pile groups consisting only of vertical piles, the equivalent footing (unless modified for load transfer as in Figures 9.62(c) and 9.62(d) has the same dimensions as the length and width of the pile group from Figure 9.59. For pile groups supported primarily by shaft resistance that include batter piles, the plan area of the footing should be calculated from the dimensions of the pile group at the equivalent footing depth that includes the plan area increase due to the pile batter. For toe bearing groups with batter piles, the equivalent footing area should be calculated from the dimensions of the pile group at depth D , including the plan area increase due to the pile batter.
- c. Determine the pressure distribution to soil layers below the equivalent footing up to the depth at which the pressure increase from the equivalent footing is less than 10% of existing effective overburden pressure at that depth. Remember that the equivalent footing size may be increased, and the footing pressure correspondingly reduced, as a result of load transfer above the footing location, or in groups with batter piles. The depth at which the pressure increase is less than 10% will provide the total thickness of the soil to be analyzed and the number of soil layers for settlement calculations. Note that the group design load should be used in determining the pressure distribution for settlement computations, and not the ultimate group capacity.

- d. Divide the soil layers in the affected pressure increase zone into several thinner layers of 1.5 to 3 (5 to 10 ft) meter thickness. The thickness of each layer is the thickness H for the settlement computation for that layer.
- e. Determine the existing effective stress, σ'_o , at midpoint of each soil layer.
- f. Determine the preconsolidation stress, σ'_p , at the midpoint of each soil layer and whether the soil layer is overconsolidated or normally consolidated.
- g. Determine the new effective stress, σ'_1 , at midpoint of each affected soil layer based on the equivalent footing pressure distribution.

STEP 2 Determine modulus number and stress exponent for each soil layer.

Use laboratory test data to compute modulus number for each layer. Preliminary settlement estimates can be made by using assumed modulus numbers based on soil type as indicated in Table 9-18.

STEP 3 Select the appropriate strain computation equation for each layer.

Select the strain equation applicable to each layer depending upon whether the soil layer is cohesive or cohesionless, and overconsolidated or normally consolidated.

STEP 4 Compute settlements.

Using the appropriate strain computation equation, compute the settlement, s , of each affected soil layer of thickness, H from: $s=(\varepsilon)(H)$. Sum the settlements of all layers to obtain the total estimated soil settlement from the pile group. Add the elastic compression of the pile under the design load to obtain the total estimated pile group settlement.

9.8.2.7 Settlement of Pile Groups Using the Neutral Plane Method

As the previous sections demonstrate, most of the group settlement methods select the depth of the equivalent footing based upon the assumed load transfer behavior. A preferred solution is to determine the depth of the neutral plane, and place the equivalent footing at or below the neutral plane location. The neutral plane occurs at the depth where the group dead load plus the load from negative shaft resistance is equal to the positive shaft resistance plus the toe resistance. The design should aim to locate the neutral plane in competent soils. When this is done, group settlements are usually well within acceptable limits.

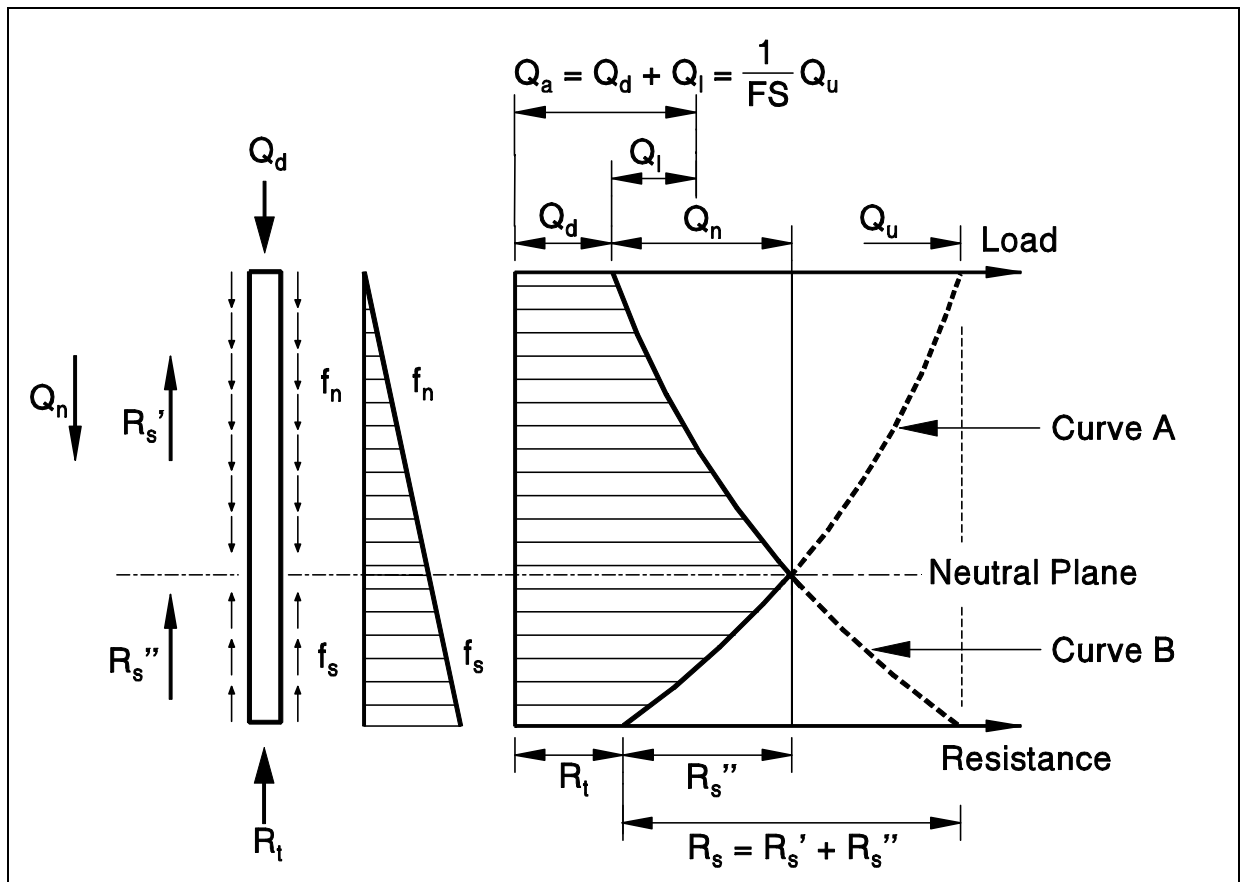
The position of the neutral plane and the resulting negative shaft resistance can be determined from a static calculation. As previously stated, the neutral plane is the depth at which the sum of dead load on the pile plus the negative shaft resistance is equal to the positive shaft plus the toe resistance. Above the neutral plane, the settlement of the soil is greater than the settlement of the pile. Any shaft resistance above the neutral plane is negative shaft resistance, since by definition the soil settlement is greater than the pile settlement. Therefore, the soil settlement transfers load to the pile. Below the neutral plane, the settlement of the soil is less than the settlement of the pile and load is transferred from the pile to the soil. Therefore, pile settlement is controlled by the soil compressibility below the neutral plane.

The following step by step procedure adapted from Goudreault and Fellenius (1994) is recommended for determination of the neutral plane.

STEP BY STEP PROCEDURE FOR DETERMINING THE NEUTRAL PLANE DEPTH

STEP 1 Perform a static capacity calculation.

- a. Determine the ultimate pile capacity, Q_u , from a static capacity calculation.
- b. Plot the load transfer versus depth by subtracting the shaft resistance at a given depth from the ultimate capacity. This computation is identified as Curve A in Figure 9.65.



Constructing the Neutral Plane

- | | |
|---------------------------|--|
| Q_a = Design Load | R_s = Shaft Resistance |
| Q_d = Dead Load | R_s' = Negative Shaft Resistance |
| Q_l = Live Load | R_s'' = Positive Shaft Resistance |
| Q_n = Drag Load | R_t = Toe Resistance |
| Q_u = Ultimate Capacity | f_n = Unit Negative Shaft Resistance |
| FS = Factor of Safety | f_s = Unit Shaft Resistance |

Figure 9.65 Neutral Plane (after Goudreault and Fellenius, 1994)

STEP 2 Determine the load transfer to the pile above the neutral plane.

- a. Determine the pile dead load, Q_d .
- b. Plot the load transfer to the pile versus depth by adding the shaft resistance at a given depth to the dead load. This computation is labeled as Curve B in Figure 9.65.

STEP 3 Determine the depth of the neutral plane.

- a. The depth where Curves A and B intersect is the depth of the neutral plane.
- b. The location of the neutral plane will move if the dead load is changed or the soil resistance versus depth is altered. Hence, design or construction decisions altering the dead load, or soil resistance versus depth, will require reevaluation of the neutral plane location under the changed conditions. Preaugering, jetting, use of bitumen coatings, *etc.* are but a few of the factors that can change the soil resistance versus depth and thus the neutral plane location.

Goudreault and Fellenius (1994) note that the magnitude of group settlement between the neutral plane and the pile toe level is generally small. This is because the piles below the neutral plane act as reinforcing elements and the compression of the pile-reinforced soil is small. Therefore, for most cases they recommend calculating the pile group settlements based on locating the neutral plane at the pile toe.

The group load is distributed below the neutral plane at a slope of 1H:2V. As in the previous methods, the soil materials below the equivalent footing at the neutral plane and the depth where the pressure increase is less than 10% should be evaluated for settlement. Group settlements are generally calculated based upon the pressure increase and the resulting strain as presented for the Janbu method in Section 9.8.2.6. However, the methods presented for layered soils in Section 9.8.2.5 could also be used.

9.8.3 Uplift Capacity of Pile Groups

The uplift capacity of a pile group is often a significant factor in determining the minimum pile penetration requirements and in some cases can control the foundation design. A few common conditions where group uplift capacity may significantly influence the foundation design include cofferdam seals that create large buoyancy forces, cantilever segmental bridge construction, and seismic, vessel impact, or debris loading. When piles with uplift loads are driven to a relatively shallow bearing stratum, uplift capacity may control the foundation design. Current AASHTO specifications (2002) for the determination of group uplift capacity are presented in Section 9.8.3.1. The AASHTO specifications for group uplift capacity are considered relatively conservative, particularly in cohesionless soils.

In cohesionless soils, Tomlinson's method presented in Section 9.8.3.2 will yield higher group uplift capacities than AASHTO specifications, and the Tomlinson method is recommended for design. Both AASHTO specifications and Tomlinson's method limit the group uplift capacity to the uplift capacity of an individual pile times the number of piles in the group. In the event this limit controls the group uplift capacity, an uplift load test may be cost effective and should be considered. With an uplift load test, a reduced safety factor is used to determine the uplift capacity. This should result in higher individual and group uplift capacities.

In cohesive soils, Tomlinson's method will yield similar results to AASHTO specifications. In the event the uplift capacity of an individual pile times the number of piles in the group limits the group uplift capacity, an uplift load test may again be cost effective and should be considered since an increase in the group uplift capacity would likely result.

9.8.3.1 Group Uplift Capacity by AASHTO Code

AASHTO specifications (2002) for service load design limit the uplift capacity of a pile group to the lesser value determined from any of the following:

1. The design uplift capacity of a single pile times the number of piles in a pile group. The design uplift capacity of a single pile is specified as $\frac{1}{3}$ the ultimate shaft resistance calculated in a static analysis method, or $\frac{1}{2}$ the failure load determined from an uplift load test.
2. $\frac{2}{3}$ the effective weight of the pile group and the soil contained within a block defined by the perimeter of the pile group and the embedded length of the piles.

3. $\frac{1}{2}$ the effective weight of the pile group and the soil contained within a block defined by the perimeter of the pile group and the embedded pile length plus $\frac{1}{2}$ the total soil shear resistance on the peripheral surface of the pile group.

9.8.3.2 Tomlinson Group Uplift Method

Tomlinson (1994) states that the ultimate uplift capacity of a pile group in cohesionless soils may be conservatively taken as the effective weight of the block of soil extending upward from the pile toe level at a slope of 1H:4V, as shown in Figure 9.66. For simplicity in performing the calculation, the weight of the piles within the soil block are considered equal to the weight of the soil. Tomlinson states that a factor of safety of 1 is acceptable in this calculation since the shear resistance around the perimeter of the group is ignored in the calculation. Tomlinson also recommended that the ultimate group uplift capacity determined from this calculation not exceed the sum of the ultimate uplift capacities of the individual piles comprising the pile group divided by an appropriate safety factor. It is recommended that a factor of safety of 2 be used if the ultimate uplift capacity of an individual pile is determined from an uplift load test and a factor of safety of 3 be used if based on the shaft resistance from a static calculation.

For pile groups in cohesive soils as shown in Figure 9.67, Tomlinson recommends the group uplift capacity be calculated based upon the undrained shear resistance of the block of soil enclosed by the group plus the effective weight of the pile cap and pile-soil block. This may be expressed in equation form as:

$$Q_{ug} = 2D (B + Z) C_{u1} + W_g$$

Where:

- Q_{ug} = Ultimate group capacity against block failure in uplift in kN (kips).
- D = Embedded length of piles in m (ft).
- B = Width of pile group in m (ft).
- Z = Length of pile group in m (ft).
- C_{u1} = Weighted average of the undrained shear strength over the depth of pile embedment along the pile group perimeter in kPa (ksf).
- W_g = Effective weight the pile/soil block including the pile cap weight in kN (kips).

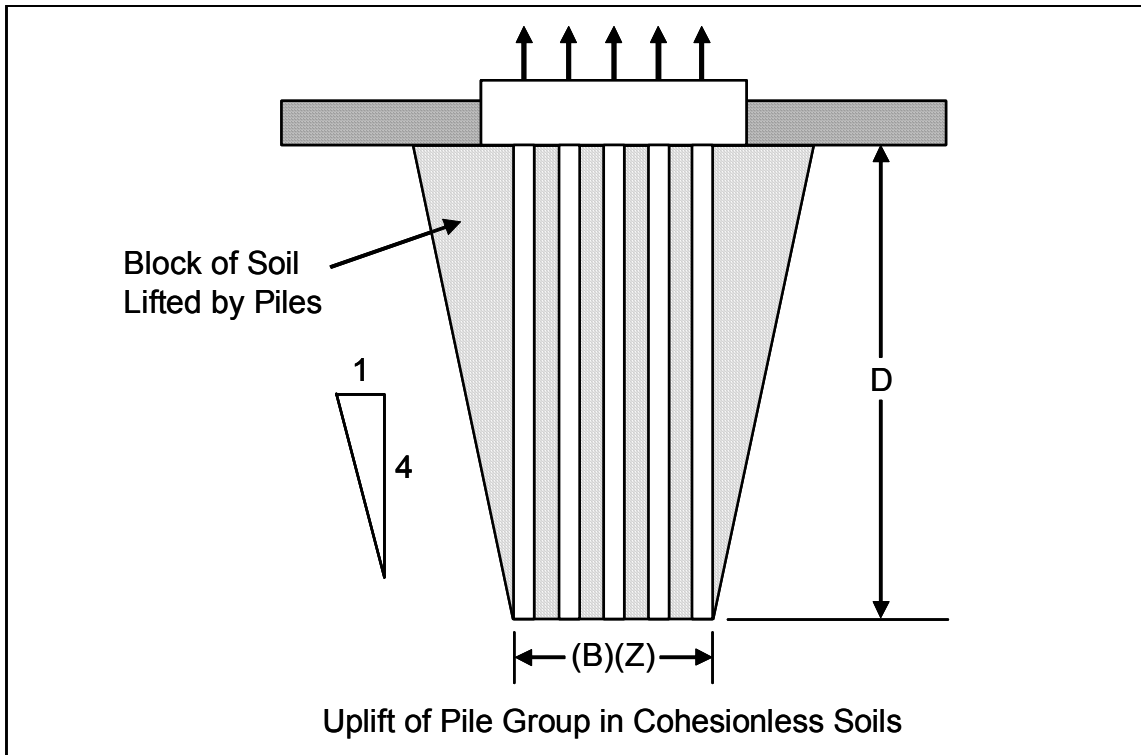


Figure 9.66 Uplift of Pile Group in Cohesionless Soil (after Tomlinson, 1994)

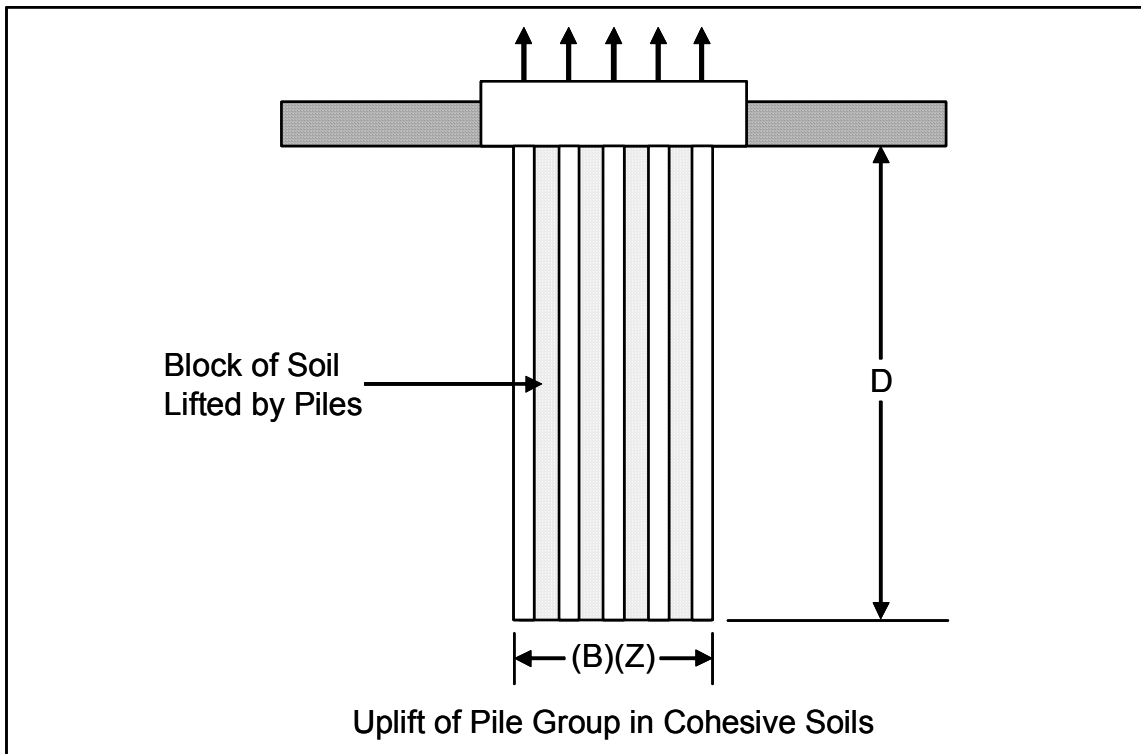


Figure 9.67 Uplift of Pile Group in Cohesive Soils (after Tomlinson, 1994)

Tomlinson states that a factor of safety of 2 should be used with this calculation to allow for possible weakening of the soil around the pile group as a result of the pile group installation. If long term sustained uplift loading is anticipated, a factor of safety of 2.5 to 3 is recommended. Tomlinson also recommends that the ultimate group uplift capacity determined from this calculation not exceed the sum of the ultimate uplift capacities of the individual piles comprising the pile group divided by an appropriate factor of safety. It is recommended that a factor of safety of 2 be used if the ultimate uplift capacity of an individual pile is determined from an uplift load test, and a factor of safety of 3 be used if based on the shaft resistance from a static calculation.

9.8.4 Lateral Capacity of Pile Groups

The ability of a pile group to resist lateral loads from vessel impact, debris, wind, or wave loading, seismic events, and other sources is a significant design issue. The deflection of a pile group under a lateral load is typically 2 to 3 times larger than the deflection of a single pile loaded to the same intensity. Holloway *et al.* (1981), and Brown *et al.* (1988) reported that piles in trailing rows of pile groups have significantly less resistance to a lateral load than piles in the lead row, and therefore exhibit greater deflections. This is due to the pile-soil-pile interaction that takes place in a pile group. The pile-soil-pile interaction results in the lateral capacity of a pile group being less than the sum of the lateral capacities of the individual piles comprising the group. Hence, laterally loaded pile groups have a group efficiency of less than 1.

The lateral capacity of an individual pile in a pile group is a function of its position in the group and the center to center pile spacing. Brown *et al.* (1988) proposed a p-multiplier, P_m , be used to modify the p-y curve of an individual pile based upon the piles row position. An illustration of the p-multiplier concept is presented in Figure 9.68. For piles in a given row, the same P_m value is applied to all p-y curves along the length of the pile. In a lateral load test of a 3 by 3 pile group in very dense sand with a center to center pile spacing of $3b$, Brown found the leading row of piles had a P_m of 0.8 times that of an individual pile. The P_m values for the middle and back row of the group were 0.4 and 0.3, respectively.

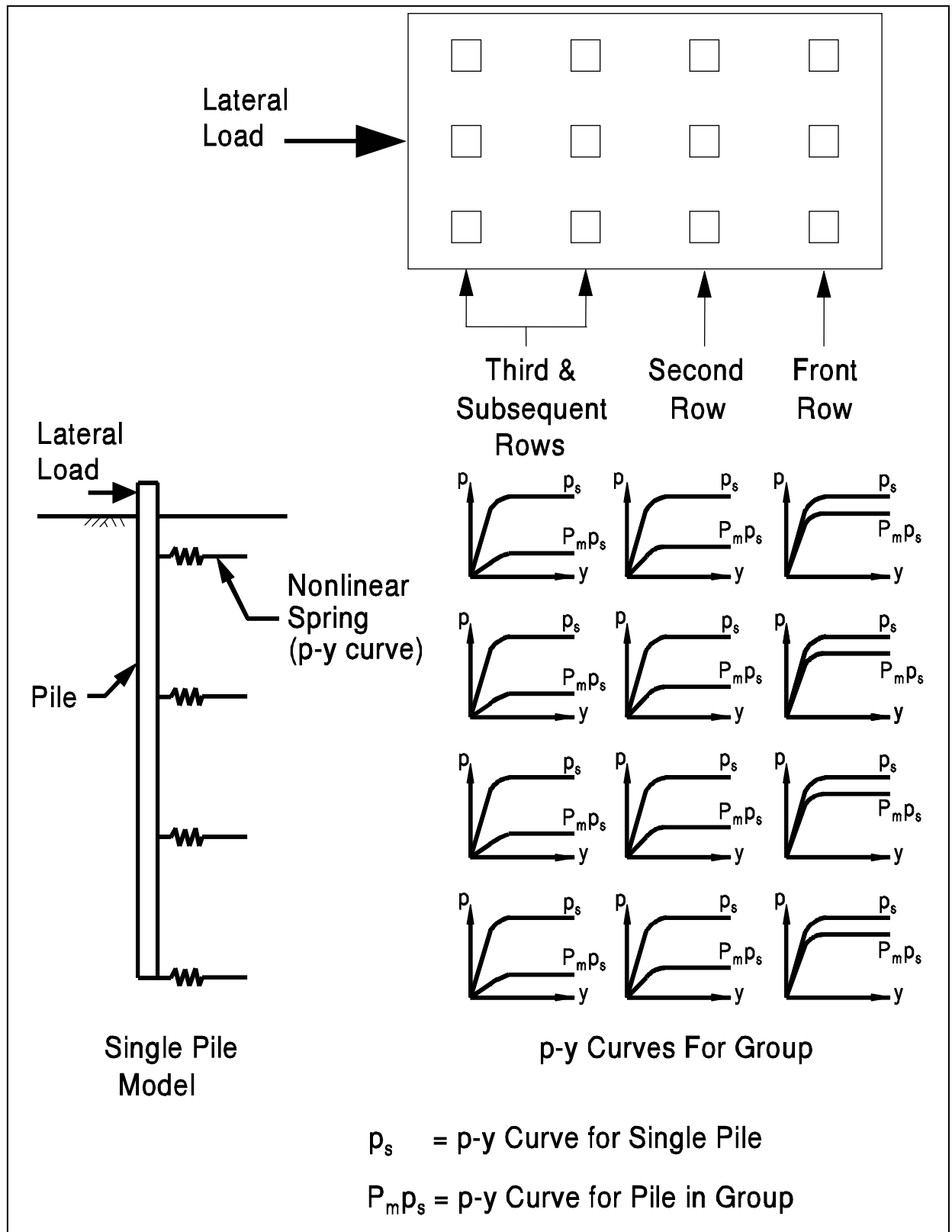


Figure 9.68 Illustration of p-multiplier Concept for Lateral Group Analysis

McVay, *et al.* (1995) performed centrifuge model tests on a 3 by 3 pile group having center to center pile spacings of 3b and 5b. A dense and loose sand condition were simulated in the centrifuge model tests. For the dense sand case at a center to center spacing of 3b, the centrifuge model test results were similar to Brown's field results. However, McVay also found that the P_m values were influenced by soil density and the center to center spacing. The P_m results from McVay's centrifuge tests as well as other recent results for vertical piles in 3 x 3 pile groups are summarized in Table 9-19. McVay's centrifuge tests indicated lateral load group efficiencies in sands on the order of 0.74 for a center to center pile of 3b and 0.93 for a center to center spacing of 5b. Field studies in cohesive soils have also shown that pile-soil-pile interaction occurs. Brown *et al.* (1987) reported P_m values of 0.7, 0.5, and 0.4 for the lead, second, and third row of a laterally loaded pile group in stiff clays.

The most recent work on this topic has included full scale lateral load testing of a 16 pile group in loose sand by Ruesta and Townsend (1997), and a 9 pile group in clayey silt by Rollins *et al.* (1998). A scaled model study of a cyclically laterally loaded pile group in medium clay has also been reported by Moss (1997). The center to center pile spacing, P_m results, and pile head deflections reported in these studies are included in Table 9-19. NCHRP Project 24-09 entitled "Static and Dynamic Lateral Loading of Pile Groups" was also recently completed Brown, *et al.* (2001). The objective of this study was to develop and validate an improved design method for pile groups subjected to static and dynamic lateral loads.

Brown and Bollman (1993) proposed a p-multiplier procedure for the design of laterally loaded pile groups. It is recommended that this approach, outlined in the step by step procedure that follows, be used for the design of laterally loaded pile groups. This procedure can be performed using multiple individual analyses with the LPILE program as illustrated in Appendix F.8. The analyses can also be performed with less effort using the FB-Pier or Group 6.0 computer programs.

The computer program FB-Pier was developed with FHWA support as the primary design tool for analysis of pile groups under axial and lateral loads. This program, which is a successor of the LPGSTAN program by Hoit and McVay (1994) is a non-linear, finite element analysis, soil structure interaction program. FB-Pier uses a p-multiplier approach in evaluation of laterally loaded pile groups under axial, lateral, and combined axial and lateral loads. The program is capable of analyzing driven pile and drilled shaft foundation supported sound walls, retaining walls, signs and high mast lighting. Additional information on FB-Pier program capabilities can be found at <http://bsi-web.ce.ufi.edu>.

TABLE 9-19 LATERALLY LOADED PILE GROUPS STUDIES					
Soil Type	Test Type	Center to Center Pile Spacing	Calculated p-Multipliers, P _m For Rows 1, 2, & 3+	Deflection in mm (in)	Reference
Stiff Clay	Field Study	3b	.70, .50, .40	51 (2)	Brown <i>et al</i> , (1987)
Stiff Clay	Field Study	3b	.70, .60, .50,	30 (1.2)	Brown <i>et al</i> , (1987)
Medium Clay	Scale Model-Cyclic Load	3b	.60, .45, .40	600 at 50 cycles (2.4)	Moss (1997)
Clayey Silt	Field Study	3b	.60, .40, .40	25-60 (1.0 - 2.4)	Rollins <i>et al</i> , (1998)
V. Dense Sand	Field Study	3b	.80, .40, .30	25 (1)	Brown <i>et al</i> , (1988)
M. Dense Sand	Centrifuge Model	3b	.80, .40, .30	76 (3)	McVay <i>et al</i> , (1995)
M. Dense Sand	Centrifuge Model	5b	1.0, .85, .70	76 (3)	McVay <i>et al</i> , (1995)
Loose M. Sand	Centrifuge Model	3b	.65, .45, .35	76 (3)	McVay <i>et al</i> , (1995)
Loose M. Sand	Centrifuge Model	5b	1.0, .85, .70	76 (3)	McVay <i>et al</i> , (1995)
Loose F. Sand	Field Study	3b	.80, .70, .30	25-75 (1-3)	Ruesta <i>et al</i> , (1997)

STEP BY STEP DESIGN PROCEDURE FOR LATERALLY LOADED PILE GROUPS USING LPILE

STEP 1: Obtain Lateral Loads.

STEP 2: Develop p-y curves for single pile.

- a. Obtain site specific single pile p-y curves from instrumented lateral pile load test at site.
- b. Use p-y curves based on published correlations with soil properties.
- c. Develop site specific p-y curves based on in-situ test data.

STEP 3: Perform LPILE analyses.

- a. Perform LPILE analyses using the P_m value for each row position to develop load-deflection and load-moment data.
- b. Based on current data, it is suggested that P_m values of 0.8 be used for the lead row, 0.4 for the second row, and 0.3 for the third and subsequent rows. These recommendations are considered reasonable for center to center pile spacing of $3b$ and pile deflections at the ground surface of .10 to .15 b . For larger center to center spacings or smaller deflections, these P_m values should be conservative.
- c. Determine shear load versus deflection behavior for piles in each row. Plot load versus pile head deflection results similar to as shown in Figure 9.69(a).

STEP 4: Estimate group deflection under lateral load.

- a. Average the load for a given deflection from all piles in the group (i.e., each of the four rows) to determine the average group response to a lateral load as shown in Figure 9.69(a).

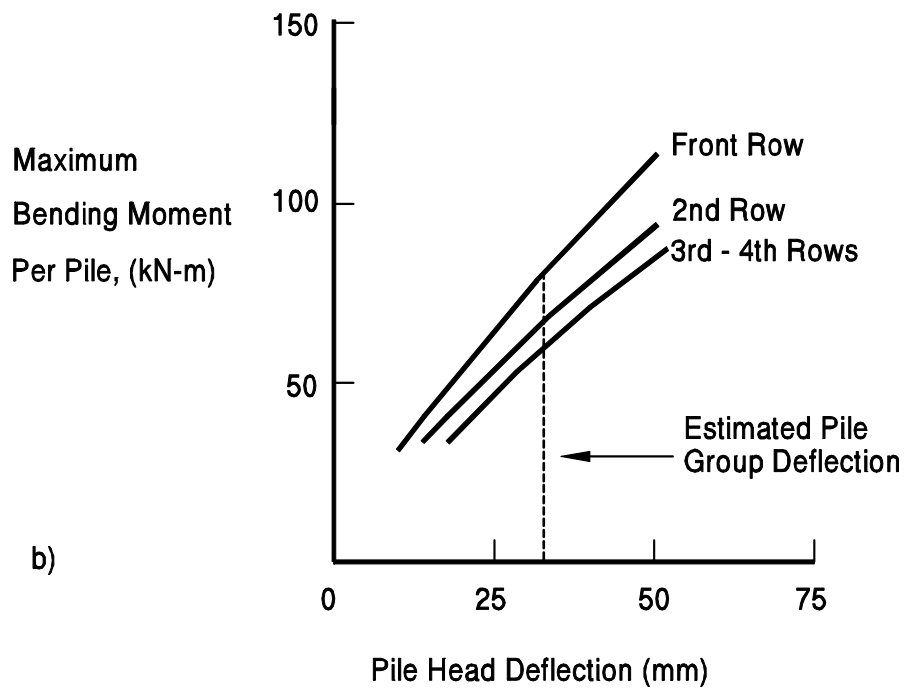
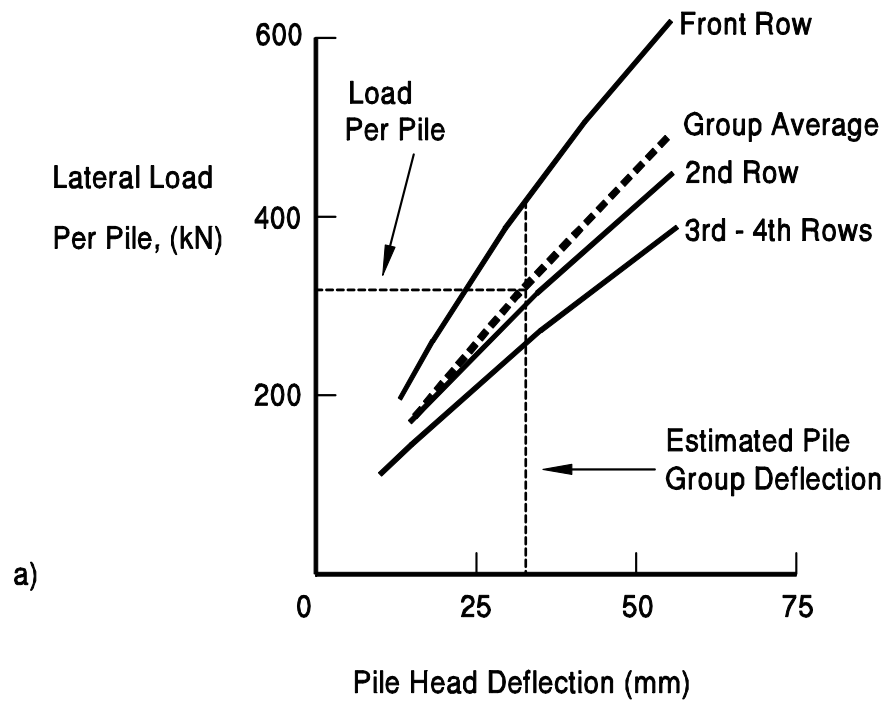


Figure 9.69 Typical Plots of Load versus Deflection and Bending Moment versus Deflection for Pile Group Analysis (adapted from Brown and Bollman, 1993)

Divide the lateral load to be resisted by the pile group by the number of piles in the group to determine the average lateral load resisted per pile.

Enter load-deflection graph similar to Figure 9.69(a) with the average load per pile to estimate group deflection using the group average load deflection curve.

STEP 5: Evaluate pile structural acceptability.

- a. Plot the maximum bending moment determined from LPILE analyses versus deflection for each row of piles as illustrated in Figure 9.69(b).
- b. Check the pile structural adequacy for each row of piles. Use the estimated group deflection under the lateral load per pile to determine the maximum bending moment for an individual pile in each row.
- c. Determine maximum pile stress from LPILE output associated with the maximum bending moment.
- d. Compare maximum pile stress with pile yield stress.

STEP 6: Perform refined pile group evaluation that considers superstructure substructure interaction.

9.9 SPECIAL DESIGN CONSIDERATIONS

In certain situations, additional design problems exist that must be analyzed. These special design considerations include negative shaft resistance, vertical ground movements from swelling soils, lateral squeeze of foundation soils, scour effects on pile capacity, pile heave, and seismic considerations.

9.9.1 Negative Shaft Resistance or Downdrag

When piles are installed through a soil deposit undergoing consolidation, the resulting relative downward movement of the soil around piles induces "downdrag" forces on the piles. These "downdrag" forces are also called negative shaft resistance. Negative

shaft resistance is the reverse of the usual positive shaft resistance developed along the pile surface. The downdrag force increases the axial load on the pile and can be especially significant on long piles driven through compressible soils. Therefore, the potential for negative shaft resistance must be considered in pile design. Batter piles should be avoided in soil conditions where large soil settlements are expected because of the additional bending forces imposed on the piles, which can result in pile deformation and damage.

Settlement computations should be performed to determine the amount of settlement the soil surrounding the piles is expected to undergo after the piles are installed. The amount of relative settlement between soil and pile that is necessary to mobilize negative shaft resistance is about 10 to 12 mm (0.4 to 0.5 in). At that movement, the maximum value of negative shaft resistance is equal to the soil-pile adhesion. The negative shaft resistance can not exceed this value because slip of the soil along the pile shaft occurs at this value. It is particularly important in the design of friction piles to determine the depth at which the pile will be unaffected by negative shaft resistance. Only below that depth can positive shaft resistance forces provide support to resist vertical loads.

The most common situation where large negative shaft resistance develops occurs when fill is placed over a compressible layer immediately prior to, or after piles are driven. This condition is shown in Figure 9.70(a). Negative shaft resistance can also develop whenever the effective overburden pressure is increased on a compressible layer through which a pile is driven; due to lowering of the ground water table as illustrated in Figure 9.70(b), for example.

Briaud and Tucker (1993) presented the following criteria for identifying when negative shaft resistance may occur. If any one of these criteria is met, negative shaft resistance should be considered in the design. The criteria are:

1. The total settlement of the ground surface will be larger than 100 mm (4 in).
2. The settlement of the ground surface after the piles are driven will be larger than 10 mm (0.4 in).
3. The height of the embankment to be placed on the ground surface exceeds 2 m (6.5 ft).
4. The thickness of the soft compressible layer is larger than 10 m (33 ft).

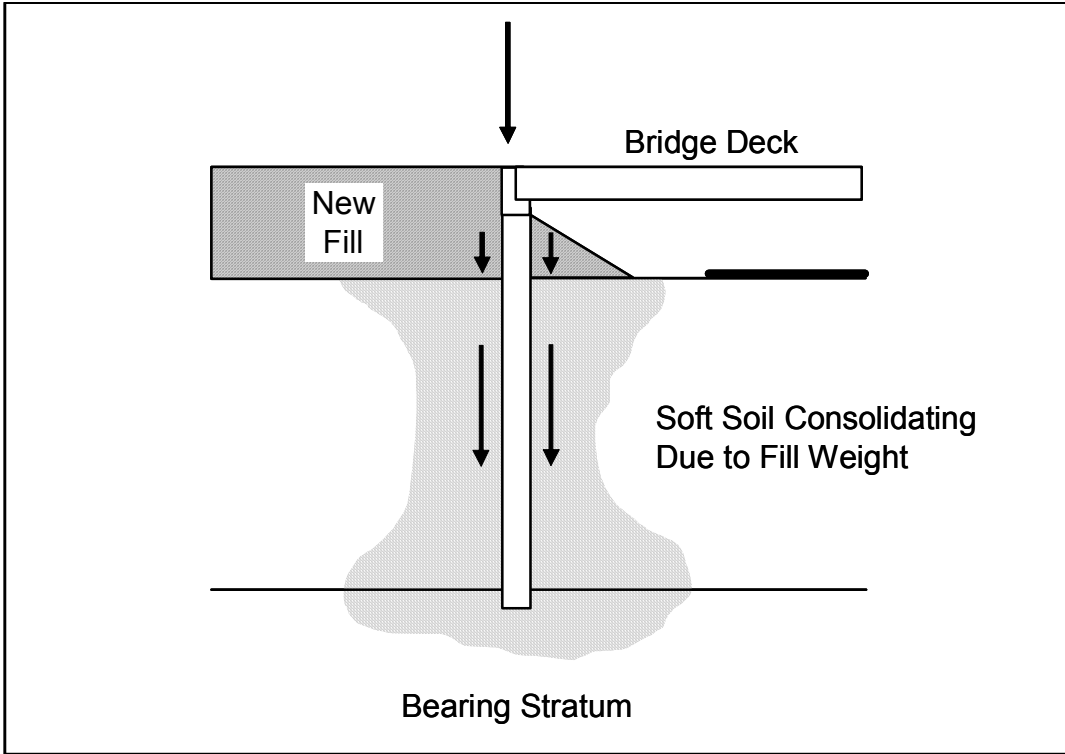


Figure 9.70(a) Common Downdrag Situation Due to Fill Weight

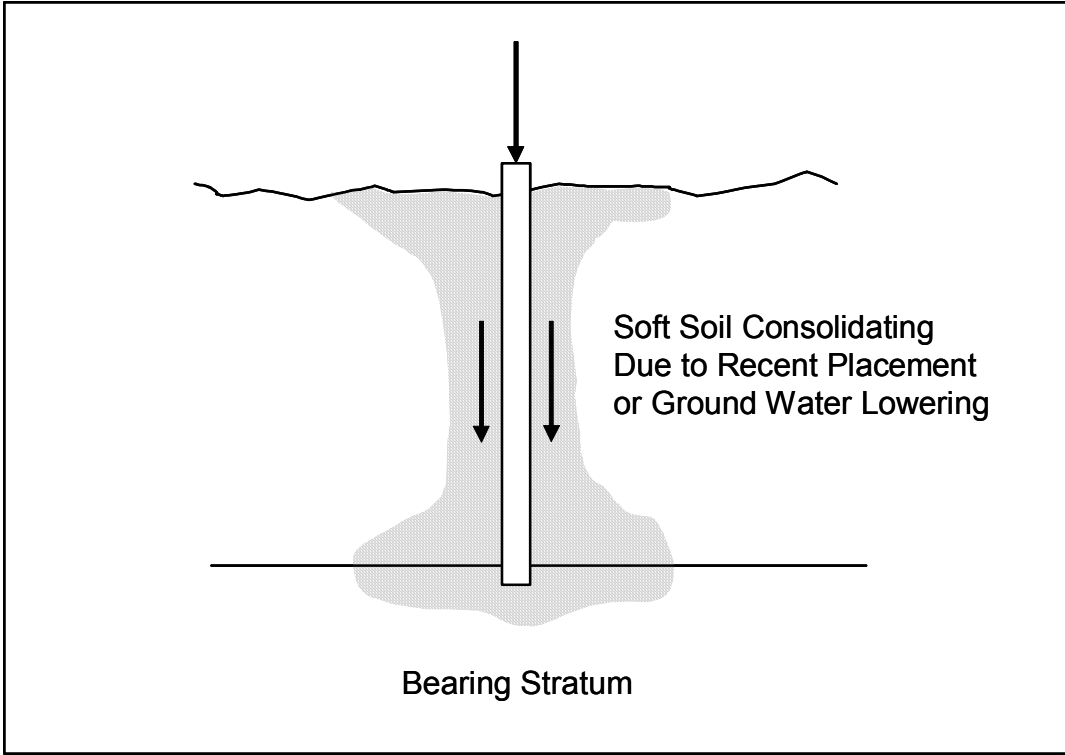


Figure 9.70(b) Common Downdrag Situation Due to Ground Water Lowering

5. The water table will be lowered by more than 4 m (13 ft).
6. The piles will be longer than 25 m (82 ft).

9.9.1.1 Methods for Determining Negative Shaft Resistance

Negative shaft resistance is similar to positive shaft resistance, except the direction of force is opposite. Two design approaches have been used for the design of pile foundations subject to negative shaft resistance. The traditional method has been to calculate the shaft resistance from the soil layers above the zone of consolidating soils, and add this resistance as a load the pile supports. In this approach, any of the previously discussed methods for computing positive pile shaft resistance in cohesive and cohesionless soils can be used. Newer methods of determining negative shaft resistance loads are based on the interrelationship between pile movement and the developed negative shaft resistance load, such as used in the NCHRP study entitled “Downdrag on Bitumen-Coated Piles” by Briaud and Tucker (1993).

9.9.1.1a Traditional Approach to Negative Shaft Resistance

The total stress α -method presented in Section 9.7.1.3 is often used for computing the negative shaft resistance or drag load in cohesive soils. In this approach, the adhesion calculated from the undrained shear strength of the soil times the pile perimeter is equated to the drag load from the consolidating soil layers. Similarly, the drag load from cohesionless layers above a consolidating soil layer is calculated from the shaft resistance in the cohesionless layers.

When selecting the undrained shear strength for calculation of the negative shaft resistance adhesion in the α -method, it is important to remember that the consolidating cohesive soil will have a higher undrained shear strength with time. The adhesion should be calculated using either the higher adhesion value, determined from the undrained shear strength at the time of the soil borings, or the estimated undrained shear strength of the soil after consolidation. Drag loads equal to 100% of the undrained shear strength of a soft clay, ie $\alpha = 1$, have been reported by Johansesen and Bjerrum (1965) for toe bearing piles driven to a relatively unyielding bearing layer. Engineering judgement should be exercised in determining drag loads so that the drag load is not grossly overestimated, resulting in an expensive foundation design, nor underestimated, resulting in a overloaded foundation.

STEP BY STEP DESIGN PROCEDURE FOR ANALYSIS OF DOWNDRAG LOADING

STEP 1 Establish the simplified soil profile and soil properties for computing settlement.

STEP 2 Determine the overburden pressure increase, Δp , versus depth due to the approach embankment fill.

The overburden pressure increase, Δp , is equal to the pressure coefficient, K_f , determined from the pressure distribution chart presented in Figure 9.71, multiplied by the height of fill, h_f , and the unit weight of fill, γ_f . The pressure distribution chart provides the pressure coefficient, K_f , at various depths below the bottom of the fill (xb_f), and also at various distances from the centerline of the fill. The depth below the bottom of the fill is given as a multiple of " b_f ", where b_f is the distance from the centerline of the fill to the midpoint of the fill side slope, as shown in Figure 9.71.

Alternatively, the FoSSA computer program (2005) could be used to determine the stress distribution and settlements from the embankment.

For downdrag loading settlement calculations, the overburden pressure increase, Δp , at various depths beneath the centerline of the fill needs to be calculated over the embedded pile length.

STEP 3 Perform settlement computations for the soil layers along the embedded pile length.

a. Determine consolidation test parameters for each soil layer from laboratory consolidation test results.

b. Compute settlement of each soil layer using the appropriate settlement equation provided in Section 9.8.2.3 for cohesive layers or Section 9.8.2.5 for cohesionless layers.

c. Compute the total settlement over the embedded pile length which is equal to the sum of the settlement from each soil layer. Do not include soil settlements below the pile toe level in this computation.

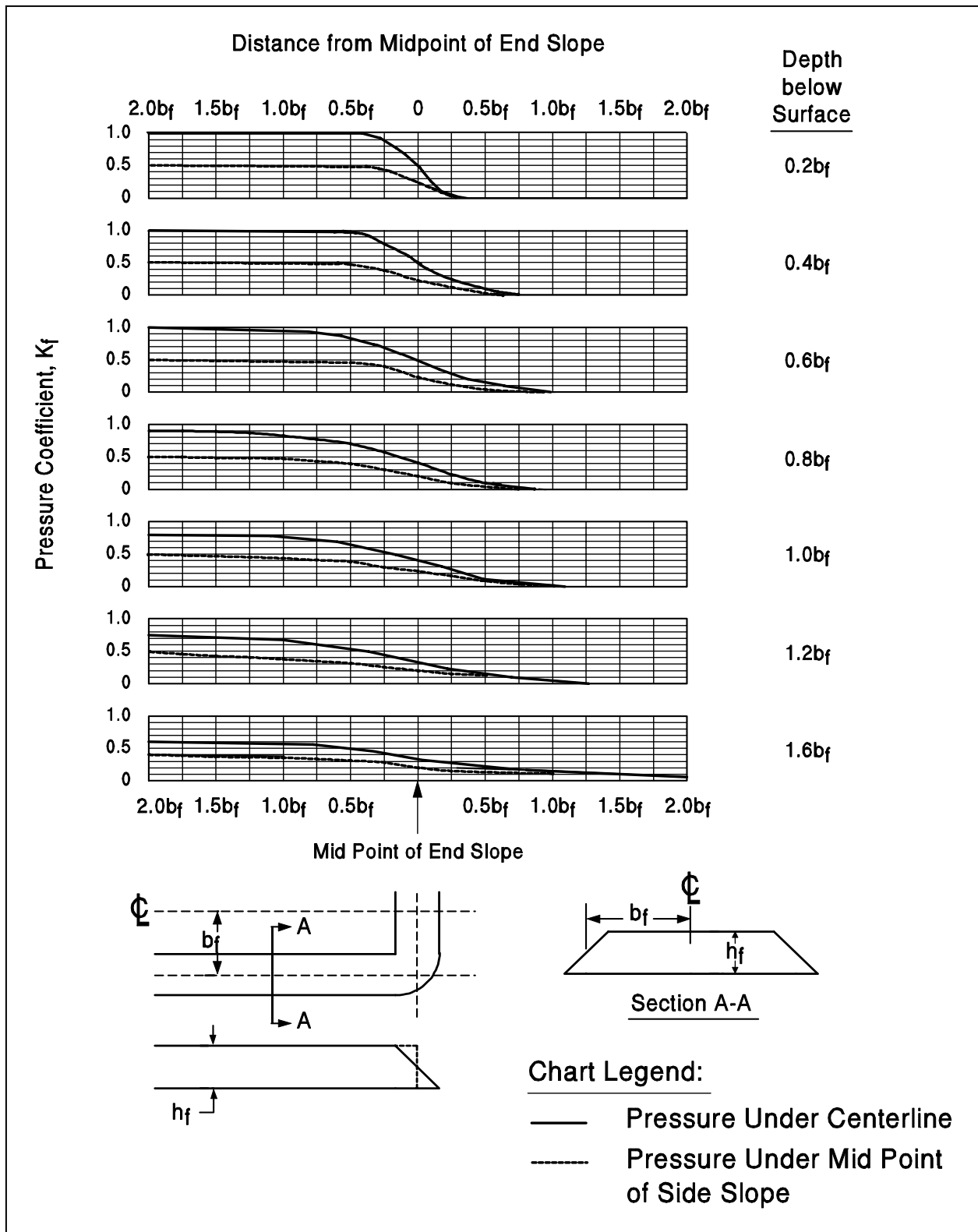


Figure 9.71 Pressure Distribution Chart Beneath the End of a Fill (after Cheney and Chassie, 1993)

STEP 4 Determine the pile length that will experience negative shaft resistance.

Negative shaft resistance occurs due to the settlement between soil and pile. The amount of settlement between soil and pile necessary to mobilize the negative shaft resistance is about 10 mm (0.4 in). Therefore, negative shaft resistance will occur on the pile shaft in each soil layer or portion of a soil layer with a settlement greater than 10 mm (0.4 in).

STEP 5 Determine magnitude of negative shaft resistance, Q_s^- .

The method used to calculate the ultimate negative shaft resistance over the pile length determined in Step 4 should be the same method used to calculate the ultimate positive shaft resistance, except that it will act in the opposite direction.

STEP 6 Calculate the ultimate pile capacity provided by the positive shaft resistance and the toe resistance, Q_u^+ .

Positive shaft and toe resistances will develop below the depth where the relative pile-soil movements are less than 10 mm (0.4 in). The positive soil resistances can be calculated on the pile length remaining below the negative shaft resistance depth from Step 4 using an appropriate static analysis method for the soil type as described in this chapter.

STEP 7 Calculate the net ultimate pile capacity, Q_u^{NET} , available to resist imposed loads.

$$Q_u^{NET} = Q_u^+ - Q_s^-$$

STEP 8 Consider alternatives to obtain higher net ultimate pile capacity.

Alternatives are described in Section 9.9.1.2 and include use of preloading or wick drains to reduce settlements prior to pile installation, use of lightweight fills to reduce settlements that cause downdrag loads, use of friction reducers to reduce downdrag loads, use of higher allowable material stress, and isolation of pile from consolidating soil.

An example calculation using this step by step procedure is included in Appendix F.6.

9.9.1.1b Alternative Approach to Negative Shaft Resistance

Dumas (2000) recommended an alternative approach for analysis and design of deep foundations subject to negative shaft resistance for highway structures. Dumas noted that design for negative shaft resistance can be a complex and time consuming process. In addition, the level of effort frequently employed in a detailed approach does not result in any appreciable economic advantage in foundation costs. Dumas recommended the design protocol presented below.

STEP 1 Determine ultimate deadload (DL_{Ult}) and live load (LL_{Ult}) per pile.

STEP 2 Determine the magnitude of negative shaft resistance, Q_s^- .

Assume an initial neutral plane (NP) at the soft to dense/stiff soil interface or at the top of the layer with approximately zero settlement.

STEP 3 Evaluate structural adequacy of pile.

The pile stress should not exceed the AASHTO recommended values (Chapter 10). It is important that this step be performed before soil resistance and pile toe estimations are performed. Extensive effort could be expended on these calculations, only to result in a structurally inadequate system.

$Q_{AllowStrc}$ = Maximum allowable ASD Stresses as per AASHTO.

$Q_{ReqAllowStrc}$ = maximum applied ASD stress demand on the pile. This will be the larger of two loading conditions:

LL +DL. Maximum stress will occur at the pile head.

DL + Q_{neg} . Maximum stress will occur at the NP.

If $Q_{AllowStrc} < Q_{ReqAllowStrc}$, then consider:

- Using higher strength materials. High performance concrete and high strength steel are commonly available.
- Using higher allowable stresses. For steel piles, AASHTO allows for considerable flexibility.
- Using a larger pile section without increasing the DL or LL, repeat Steps 2-3.

- d. Decreasing the DL and/or LL by adding more piles and repeat Steps 1-3. When evaluating this option, it is essential to consider the increased pile cap costs in the economic evaluation.
- e. Refining the location of the neutral plane. Refer to Steps R-1 to R-5. Repeat Steps 2-3.
- f. Specifying a construction sequence where primary consolidation settlement is completed prior to pile installation. For this approach to be effective, the iterative procedure for locating the neutral plane must be employed.
- g. Reducing the overall Q_s^- forces by using a bitumen coatings or other bond breaker.
- h. Reducing the overall settlement of the upper compressible soil (thereby decreasing Q_s^-) by a reducing the overburden load and/or by using light weight fill materials.

STEP 4 Determine the applied / required ultimate soil resistance (Q_{ReqUlt}).

The applied / required ultimate soil resistance (Q_{ReqUlt}):

If $(LL * FS_{AASHTO}) < (2 * Q_s^- * FS_{Neg})$, then

$$Q_{ReqUlt} = (DL * FS_{AASHTO}) + (Q_s^- * FS_{Neg})$$

otherwise

$$Q_{ReqUlt} = (DL + LL) * FS_{AASHTO}$$

STEP 5 Select an estimated minimum pile tip elevation for Q_{ReqUlt} calculated in Step 4.

STEP 6 Evaluate the adequacy of lateral resistance. It is recommended that LPILE p-y curve, or equivalent, be used.

STEP 7 Evaluate driveability and constructability. Determine if the pile can be driven without damage.

STEP 8 Calculate the cost associated with resisting the downdrag load (additional pile length, size, numbers, strength, lightweight fills, etc.) required to achieve acceptable soil or structural capacity. If costs are considered excessive, then consider items a through h of Step 3.

Iterative Procedure for Locating the Neutral Plane STEP R-1 to R-5

STEP R-1 Calculate and/or plot the soil settlement from the top of the bearing strata to the top of the pile.

STEP R-2 Calculate and/or plot pile settlements (W_n). Using the Q_{ReqUlt} from Step 4, and the estimated tip elevation from Step 5, calculate pile settlements (W_n). Remember, the initial neutral plane has been assumed to be located at the soft to dense/stiff soil interface--top of the layer with approximately zero settlement. W_n is the sum of pile toe movement and elastic shortening. If a linear curve is selected for load transfer in the base resistance and fully plastic curves are selected for load transfer in shaft resistance, a hand solution can be made without difficulty. More sophisticated t-z approaches incorporated in computer programs may be appropriate if the economic analysis in Step 8 warrants it.

STEP R-3 Determine the distance of the new neutral plane from the soft/dense soil interface (Z_n) graphically or by calculation. If the soft compressible layer is homogenous, the settlement can be considered linear (zero at the interface, and its maximum value at the pile top), and the following equation can be used.

$$Z_n = W_n / (\text{soil settlement at the pile top/depth of the soft layer})$$

STEP R-4 Using the new neutral plane, recalculate Q_s^- (Step 2), Q_{ReqUlt} (Step 4), the estimated pile toe elevation (Step 5), and Z_n (Steps R-2 & R-3).

STEP R-5. Repeat Step R-4 until reasonable convergence is achieved. Typically, 2 to 3 iterations.

9.9.1.2 Methods for Reducing Negative Shaft Resistance Forces

In situations where the negative shaft resistance on piles is large and a reduction in the pile design load is impractical, negative shaft resistance forces can be handled or reduced by using one or more of the following techniques:

a. Reduce soil settlement

Preconsolidation of compressible soils can be achieved by preloading and consolidating the soils **prior** to pile installation. This approach is often used for bridge foundations in fill sections. Wick drains are often used in conjunction with preloading in order to shorten the time required for consolidation. Additional information on wick drains is available in "Prefabricated Vertical Drains", FHWA RD 86/168 by Rixner *et al.* (1986) and in "Ground Improvement Methods" manual by Elias *et al.* (2004).

b. Use lightweight fill material

Construct structural fills using lightweight fill material to reduce the downdrag loads. Lightweight fill materials often used, depending upon regional availability, include geofoam, foamed concrete, wood chips, blast furnace slag, and expanded shales. Additional information on lightweight fills is available in Elias *et al.* (2004). Geofoam blocks being placed for embankment construction are shown in Figure 9.72.

c. Use a friction reducer

Bitumen coating and plastic wrap are two methods commonly used to reduce the friction at the pile-soil interface. Bitumen coatings should only be applied to the portion of the pile which will be embedded in the negative shaft resistance zone. Case histories on bitumen coatings have reported reductions in negative shaft resistance from as little as 47% to as much as 90%. Goudreault and Fellenius (1994) suggest that the reduction effect of bitumen may be analyzed by using an upper limit of 10 kPa (0.2 ksf) as the pile-soil shear resistance or adhesion in the bitumen coated zone.

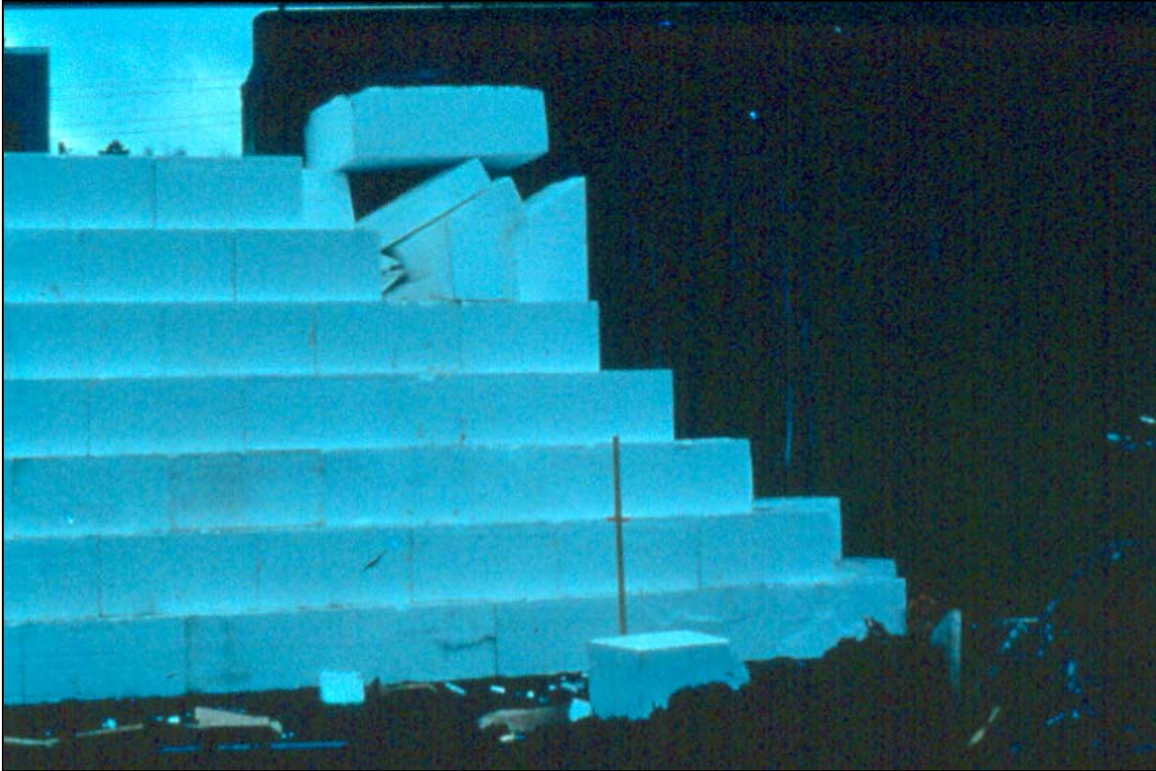


Figure 9.72 Geofabric Blocks for Embankment Construction

One of the major problems with bitumen coatings is protecting the coating during pile installation, especially when driving through coarse soils. An inexpensive solution to this problem is to weld an over-sized collar around the pile where the bitumen ends. The collar opens an adequate size hole to permit passage of the bitumen for moderate pile lengths in fine grained soils. Figure 9.73 presents a photograph on an over-sized collar between the uncoated lower pile section and white washed bitumen coating on the upper pile section.

Bitumen coatings can also present additional construction problems associated with field coating and handling. The bitumen coating used must have relatively low viscosity to permit slippage during soil consolidation, yet high enough viscosity and adherence to insure the coating will stick to the pile surface during storage and driving. The bitumen must also have sufficient ductility to prevent cracking and spalling of the bitumen during handling and driving. Therefore, the climate at the time of pile installation should be considered in selection of the proper bitumen coating. The use of bitumen coatings can be quite successful provided proper construction control methods are followed. However, Bitumen coatings should not be casually specified as the solution to downdrag loading.

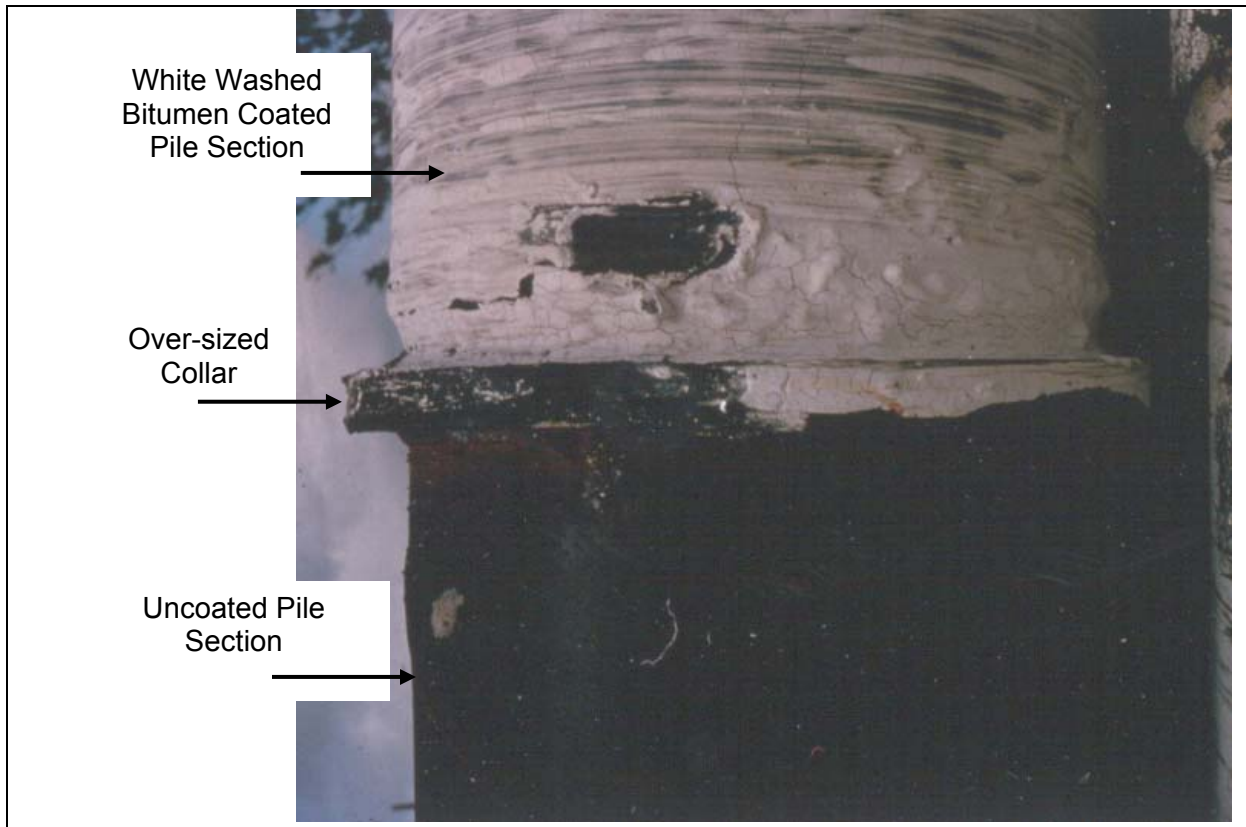


Figure 9.73 Over-sized Collar for Bitumen Coating Protection

Plastic wrap has proven to be an economically attractive friction reducer, particularly for abutment piles driven behind and before construction of MSE walls. Tawfig (1994) performed laboratory tests on 0.15 mm (0.006 in) thick polyethylene sheets used as a friction reducer. The laboratory test results indicated plastic wraps reduced the pile-soil shear resistance from between 78% for a one wrap layer to 98% for a two layer wrap with mineral oil lubricant of the pile-soil shear resistance. The laboratory test data indicated the pile-soil shear resistance of a one wrap layer was about 10 kPa (0.2 ksf) and only 1 kPa (0.02 ksf) for the lubricated two wrap system.

d. Increase allowable-pile stress

In piles where the allowable pile material strength has not been fully utilized, the pile design stress can be increased to offset the negative shaft resistance load. Increased structural capacity can also be obtained by using higher strength pile materials, or in the case of pipe piles, by using an increased wall thickness. Foundation settlement at the increased loading should be computed and checked against the foundation performance criteria.

- e. Prevent direct contact between soil and pile

Pile sleeves are sometimes used to eliminate direct contact between pile and soil. Bentonite slurry has been used in the past to achieve the same purpose. These methods are generally more expensive.

9.9.2 Vertical Ground Movements from Swelling Soils

Detrimental vertical ground movements can also occur in swelling soils subject to seasonal moisture changes, such as expansive clays. In this case, the swell pressures can induce uplift forces on the pile. For piles driven in swelling soils, bitumen coatings on the pile shaft through the swelling soil zone is effective in reducing the uplift forces.

9.9.3 Lateral Squeeze of Foundation Soil

Bridge abutments supported on piles driven through soft compressible cohesive soils may tilt forward or backward depending on the geometry of the backfill and the abutment. This problem is illustrated in Figure 9.74. Large horizontal movements may cause damage to the structure. The unbalanced fill loads shown in Figure 9.74 displace the soil laterally. This lateral displacement may bend the piles, causing the abutment to tilt toward or away from the fill.

The following rules of thumb are recommended for determining whether tilting will occur, as well as estimating the magnitude of horizontal movement.

1. Lateral squeeze and abutment tilting can occur if:

(SI Units)

$$[\gamma \text{ fill in kN/m}^3] [\text{fill height in m}] > 3 [\text{undrained shear strength of soft soil in kPa}]$$

(US Units)

$$[\gamma \text{ fill in lb/ft}^3] [\text{fill height in ft}] > 3 [\text{undrained shear strength of soft soil in psf}]$$

2. If abutment tilting can occur, the magnitude of the horizontal movement can be estimated by the following formula:

Horizontal Abutment Movement in mm (in) = 0.25 Vertical Fill Settlement in mm (in)

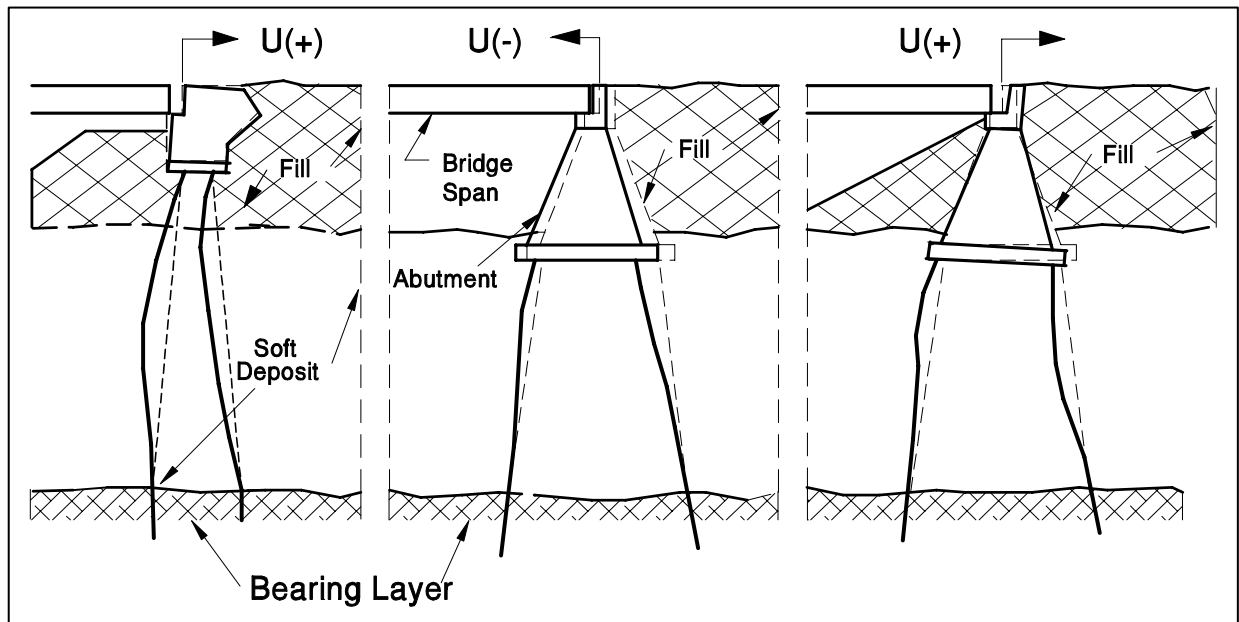


Figure 9.74 Examples of Abutment Tilting Due to Lateral Squeeze

9.9.3.1 Solutions to Prevent Tilting

- Delay installation of abutment piling until after fill settlement has stabilized (best solution).
- Provide expansion shoes large enough to accommodate the movement.
- Use steel H-piles to provide high tensile strength in flexure.
- Use lightweight fill to reduce driving forces.

9.9.4 Ultimate Capacity of Piles in Soils Subject to Scour

Scour is defined as the erosion of soil materials from the streambed and/or stream banks due to flowing water. Though often considered as being localized, scour may consist of multiple components including long term aggradation and degradation, local scour, contraction scour, and general scour. Aggradation and degradation involve the long term streambed elevation changes due to an abundance or deficit, respectively, in upstream sediment supply. Local scour involves the removal of material from the immediate vicinity of a substructure unit and can be either clear-water, free of disturbed upstream sediment, or live-bed scour, complicated by the transport of upstream sediment into the scour hole. In contrast, contraction scour and general scour involve erosion across all or most of the channel width and relate directly with the stream stratigraphy at the scour location. Contraction scour results from a contraction of flow, while general scour encompasses other short-term, non-localized lowering of the streambed.

Different materials, subject to any of the abovementioned types of scour, erode at different rates. In a flood event, loose granular soils can be eroded away in a few hours. Cohesive or cemented soils typically erode more gradually and over several cycles of flooding but can experience the same ultimate scour depths as those of cohesionless deposits. As noted earlier in this chapter, the ultimate capacity of a driven pile is due to soil resistance along the pile shaft and at the pile toe. Therefore, the erosion of the soil materials providing pile support can have significant detrimental effects on pile capacity and must clearly be evaluated during the design stage.

Depending on the type of scour and the scour susceptibility of the streambed soils, multiple static capacity calculations may be required to evaluate the ultimate capacity of a pile and toe establish pile penetration requirements. In the case of local scour, the soil in the scour zone provides resistance at the time of driving that cannot be counted on for long term support. Hence, shaft resistance in the scour zone, although included for driveability considerations, is ignored for design purposes. However, because the erosion is localized, pile capacity calculations should assume that the effective overburden pressure is unchanged. The effects of non-localized scour on long term pile capacity are more severe. In all of degradation, contraction scour, and general scour, a reduction in both the scour zone soil resistance and the effective overburden is applied to long term capacity calculations, due to the widespread removal of the streambed materials. This added reduction in effective stresses can have a significant effect on the calculated shaft and toe resistances. Figure 9.75 provides an illustration of localized and non-localized scour.

The FHWA publication FHWA NHI-01-001, "Evaluating Scour at Bridges" by Richardson and Davis (2001), more commonly known as HEC-18, recommends that the following pile design issues also be considered at bridge sites subject to scour.

1. For pile supported substructures subjected to scour, a reevaluation of the foundation design may require a change in the pile length, number, cross-sectional dimension and type based on the loading and performance requirements and site-specific conditions.
2. Piling should be designed for additional lateral restraint and column action because of the increase in unsupported pile length after scour. The unsupported pile length is discussed in Chapter 10.
3. Local scour holes at piers and abutments may overlap one another in some instances. If local scour holes do overlap, the scour is indeterminate and may be deeper. The topwidth of a local scour hole on each side of the pier ranges from 1.0 to 2.8 times the depth of local scour. A topwidth value of 2.0 times the depth of local scour on each side of a pier is suggested for practical applications.
4. Perform the bridge foundation analysis on the basis that all streambed material in the scour prism above the total scour line has been removed and is not available for pile capacity or lateral support. In areas where the local scour is confined to the proximity of the footing, the lateral ground stresses on the pile length which remains embedded may not be significantly reduced from the pre-local scour conditions.
5. Placing the top of the footing or pile cap below the streambed a depth equal to the estimated long term degradation and contraction scour depth will minimize obstruction to flood flows and resulting local scour. Even lower footing elevations may be desirable for pile supported footings when the piles could be damaged by erosion and corrosion from exposure to river or tidal currents. However, in deep water situations, it may be more cost effective to situate the pile cap above the mudline and design the foundation accordingly.
6. Stub abutments positioned in the embankment should be founded on piling driven below the elevation of the thalweg including long term degradation and contraction scour in the bridge waterway to assure structural integrity in the event the thalweg shifts and the bed material around the piling scours to the thalweg elevation.

The design event dictates the recommended design procedure for scour. For scour depths associated with earlier the 100-year flood event or the overtopping flood, the procedure illustrated in Section 9.6 should be followed where the factor of safety is linked to the construction control. For the superflood, or 500-year event, HEC-18 specifies a minimum factor of safety of 1.0. This minimum factor of safety is determined by dividing the maximum pile load by the sum of the shaft and toe resistances available below the scour depth. The shaft and toe resistances should be determined from an appropriate static analysis calculation as detailed earlier in this chapter.

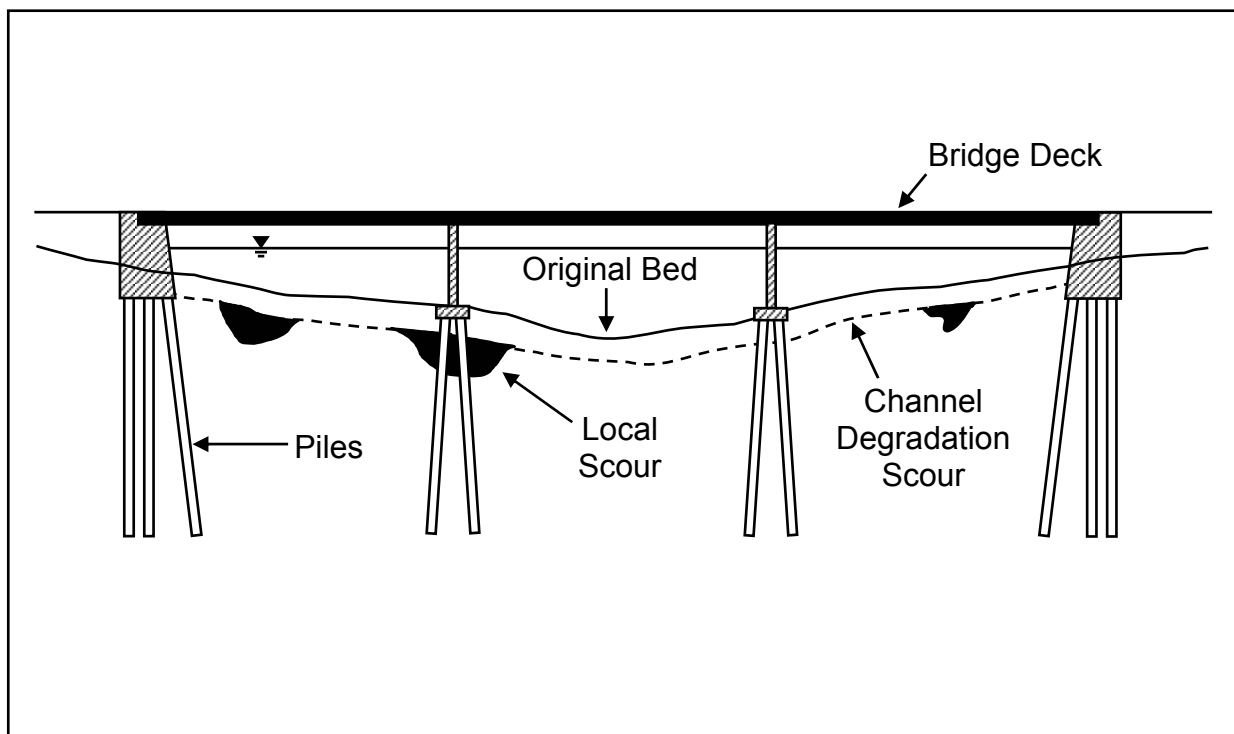


Figure 9.75 Local and Channel Degradation Scour

9.9.5 Soil and Pile Heave

As noted by Hagerty and Peck (1971), whenever piles are driven, soil is displaced. This can result in both upward movement (pile heave) and lateral movements of previously driven piles. These soil movements can be detrimental to the capacity of previously driven piles as well as to adjacent facilities. Obviously, the greater the volume of soil displaced by pile driving, the greater the potential for undesirable movements of previously driven piles, or damage to adjacent structures. Heave of toe bearing piles is particularly troublesome since the pile may be lifted from the bearing stratum, thereby greatly reducing the pile capacity and increasing the foundation settlement when

loaded. Haggerty and Peck noted that saturated, insensitive clays behave incompressibly during pile driving and have the greatest heave potential.

When piles are to be installed in cohesive soils, it is recommended that the potential magnitude of vertical and lateral soil movements be considered in the design stage. If calculations indicate that movements may be significant, use of an alternate low displacement pile, or specifying a modified installation procedure (such as predrilling to reduce the volume of displaced soil) should be evaluated. A step by step procedure adapted from Haggerty and Peck for estimating soil and pile heave in a saturated insensitive clay follows. The procedure assumes a regular pile driving sequence and a level foundation surface. The paper by Haggerty and Peck should be consulted for modifications to the recommended procedure for conditions other than those stated.

STEP BY STEP PROCEDURE FOR ESTIMATING SOIL AND PILE HEAVE

STEP 1 Calculate the estimated soil heave at the ground surface.

- a. Divide the volume of inserted piles by the volume of soil enclosed by the pile foundation to obtain the volumetric displacement ratio.
- b. Estimate the normalized soil heave (soil heave / pile length) from $\frac{1}{2}$ the volumetric displacement ratio calculated in Step 1a.
- c. Calculate the soil heave at the ground surface by multiplying the normalized soil heave in Step 1b by the average length of piles.

STEP 2 Determine the depth of no pile-soil movement.

- a. Figure 9.76 illustrates that a depth, d , exists where the potential upward pushing and downward resisting forces on the pile shaft are equal.
- b. Calculate the pile-soil adhesion along the entire pile shaft using the α -method described in Section 9.7.1.2a.
- c. Through multiple iterations determine the depth, d , where the adhesion from the upward pushing force equals the adhesion from the downward resisting force. Remember only shaft resistance is considered in calculating the downward resisting force.

STEP 3 Calculate the estimated pile heave.

- a. Calculate the percentage of pile length subject to heave from $(D-d) / D$ where D is the embedded pile length, and d is the equilibrium depth from Step 2c.
- b. Calculate the estimated pile heave by multiplying the estimated soil heave from Step 1c by the percentage of pile length subject to heave from Step 3a.

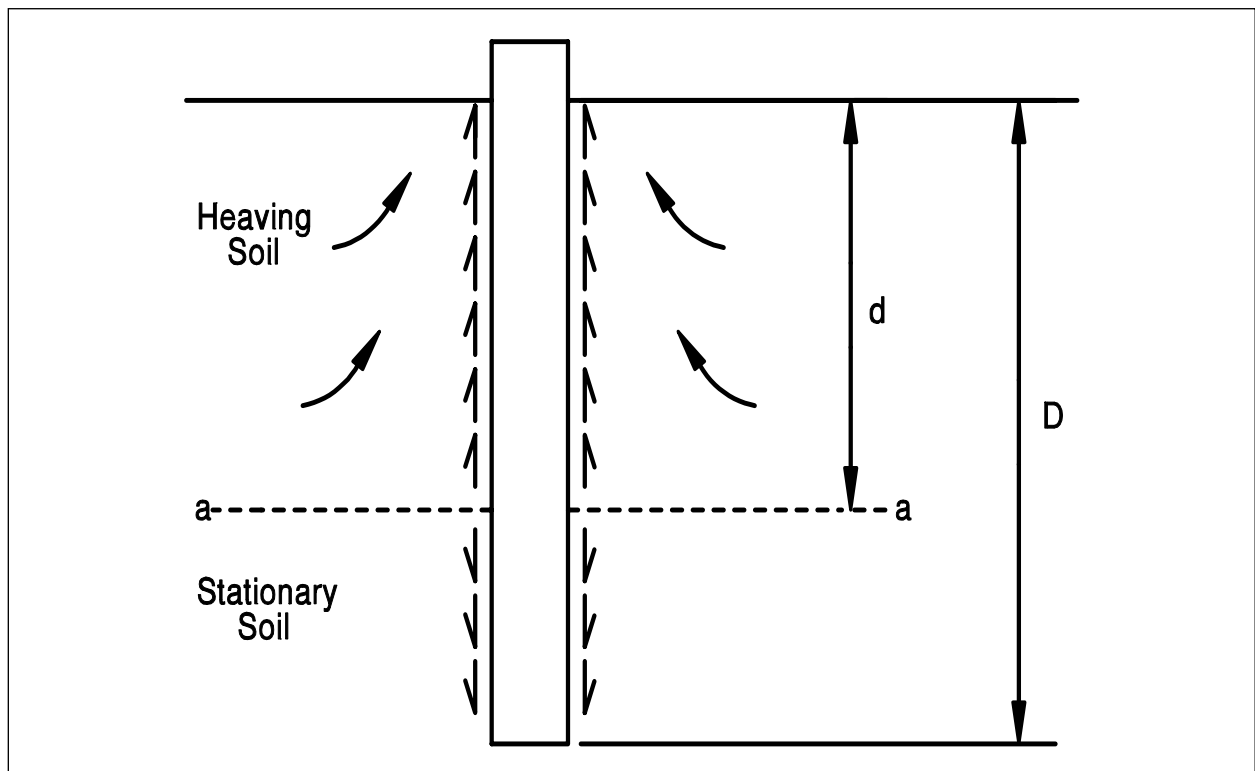


Figure 9.76 Balance of Forces on Pile Subject to Heave (after Haggerty and Peck, 1971)

9.9.6 Seismic Considerations

The design issues associated with pile foundation design for seismic events are significant and are beyond the scope of this manual. Other publications such as FHWA RD-86/102, Seismic Design of Highway Bridge Foundations by Lam and Martin (1986), and Division 1A - Seismic Design of AASHTO Standard Specification (1992) should be consulted for design guidance in seismically active areas. Geotechnical Engineering Circular No. 3 by Kavazanjian, *et al.*, (1997) provides additional guidance on geotechnical earthquake engineering. Pile foundation design issues in seismic events include liquefaction effects on pile capacity, ground movements, seismic induced foundation loads, and seismic

induced drag loads. This manual will therefore only briefly address the identification of liquefiable soils and the consequences of liquefaction on pile foundation design.

Soil types most susceptible to liquefaction can be described as saturated, very loose to medium dense, fine to medium grained sands and non-plastic silts. However, liquefaction has also occurred in saturated, very loose to medium dense gravels and certain clayey soils.

In seismically active areas where peak earthquake acceleration will be greater than 0.1g, the soil susceptibility to liquefaction should be evaluated. A commonly used procedure for identification of liquefaction susceptible soils was proposed by Seed *et al.* (1983). This liquefaction evaluation approach is detailed in the Commentary for Section 6, Division 1A of the AASHTO Standard Specifications (2002) as well as Lam and Martin (1986). If the soils are found to liquefy during the design event, the pile foundation must be designed to accommodate the loss of frictional resistance, seismic induced loads, as well as the anticipated vertical and horizontal displacements. Alternatively, the liquefaction potential may be mitigated through ground improvement techniques.

Pile foundations in liquefiable soils must penetrate through the zone of liquefaction and develop adequate capacity in the underlying soils. Evaluation of compression and uplift capacities during the seismic event can be made by assigning residual strength properties to the liquefiable layers. Residual strengths of sands and silty sands can be approximated from SPT resistance values using a correlation proposed by Seed (1987) and updated by Seed and Harder (1990).

Following a seismic event that induces soil liquefaction, the liquefied layer will consolidate. The soil resistance in and above the liquified layer will then become additional drag load that the pile must support. The pile foundation must be structurally capable of supporting this drag load and the foundation settlement resulting from the drag load must be within the structure's performance criteria.

Liquefaction induced lateral spread can impose significant bending moments in piles driven through liquefiable soils. Therefore, piles in liquefiable soils should be flexible and ductile in order to accommodate lateral loads. The maximum bending moment of piles in liquefiable soils is often evaluated in a LPILE analysis by assigning Reese's soft clay p-y curve with low residual shear strengths and high ϵ_{50} values to the liquefiable layer.

9.10 ADDITIONAL DESIGN AND CONSTRUCTION CONSIDERATIONS

The previous sections of this chapter addressed routine and special event static analysis procedures for pile foundation design. However, the designer should be aware of additional design and construction considerations that can influence the reliability of static analysis procedures in estimating pile capacity. These issues include the influence of time, predrilling or jetting, construction dewatering, soil densification, and the plugging of open pile sections on pile capacity. Pile driving induced vibrations can also influence the final design and static calculation results if potential vibration levels dictate changes in pile type or installation procedures. The closing section of this chapter focuses on pile driveability. Evaluation of pile driveability is a fitting final topic of this design chapter since all the previously described analyses are meaningless if the pile cannot be driven to the required depth and capacity without damage.

9.10.1 Time Effects on Pile Capacity

As noted in Section 9.2, the soil is greatly disturbed when a pile is driven into the soil. As the soil surrounding the pile recovers from the installation disturbance, a time dependent change in pile capacity often occurs. Frequently piles driven in saturated clays, and loose to medium dense silts or fine sands gain capacity after driving has been completed. This phenomenon is called soil setup. Occasionally piles driven into dense saturated fine sands, dense silts, or weak laminated rocks such as shale, will exhibit a decrease in capacity after the driving has been completed. This phenomenon is called relaxation. Case history discussions on soil setup and relaxation may be found in Fellenius *et al.* (1989), and Thompson and Thompson (1985), respectively.

9.10.1.1 Soil Setup

When saturated cohesive soils are compressed and disturbed due to pile driving, large excess pore pressures develop. These excess pore pressures are generated partly from the shearing and remolding of the soil and partly from radial compression as the pile displaces the soil. The excess pore pressures cause a reduction in the effective stresses acting on the pile, and thus a reduction in the soil shear strength. This results in a reduced pile capacity during, and for a period of time after, driving.

After driving, the excess pore pressures will dissipate primarily through radial flow of the pore water away from the pile. With the dissipation of pore pressures, the soil reconsolidates and increases in shear strength. This increase in soil shear strength results in an increase in the static pile capacity and is called soil setup. A similar decrease in

resistance to pile penetration with subsequent soil setup may occur in loose to medium dense, saturated, fine grained sands or silts. The magnitude of the gain in capacity depends on soil characteristics, pile material and pile dimensions.

Because the pile capacity may increase after the end of driving, pile capacity assessments should be made from static load testing or retapping performed **after** equilibrium conditions in the soil have been re-established. The time for the return of equilibrium conditions is highly variable and depends on soil type and degree of soil disturbance. Piezometers installed within three diameters of the pile can be used to monitor pore pressure dissipation with time. Effective stress static pile capacity calculation methods can be used to evaluate the increase in capacity with time once pore pressures are quantified.

Static load testing or restrike testing of piles in fine grained soils should not be conducted until after pore pressures dissipate and return to equilibrium. In the absence of site specific pore pressure data from piezometers, it is suggested that static load testing or retapping of piles in clays and other predominantly fine grained soils be delayed for at least two weeks after driving and preferably for a longer period. In sandy silts and fine sands, pore pressures generally dissipate more rapidly. In these more granular deposits, five days to a week is often a sufficient time delay.

Rausche, *et al.* (1996) calculated general soil setup factors based on the predominant soil type along the pile shaft. The soil setup factor was defined as the static load test failure load divided by the end-of-drive wave equation capacity. These results are presented in Table 9-20. The data base for this study was comprised of 99 test piles from 46 sites. The number of sites and the percentage of the data base in a given soil condition is included in the table. While these soil set-up factors may be useful for preliminary estimates, soil setup is better estimated based on site specific data gathered from pile retapping, dynamic measurements, static load testing, and local experience.

Komurka *et al.*, (2003) summarized the current practice in estimating and measuring soil setup in a report to the Wisconsin Highway Research Program. This report summarizes the mechanisms associated with soil setup development and reviews several empirical relationships for estimating set-up.

TABLE 9-20 SOIL SETUP FACTORS (after Rausche <i>et al.</i> , 1996)			
Predominant Soil Type Along Pile Shaft	Range in Soil Set-up Factor	Recommended Soil Set-up Factors*	Number of Sites and (Percentage of Data Base)
Clay	1.2 - 5.5	2.0	7 (15%)
Silt - Clay	1.0 - 2.0	1.0	10 (22%)
Silt	1.5 - 5.0	1.5	2 (4%)
Sand - Clay	1.0 - 6.0	1.5	13 (28%)
Sand - Silt	1.2 - 2.0	1.2	8 (18%)
Fine Sand	1.2 - 2.0	1.2	2 (4%)
Sand	0.8 - 2.0	1.0	3 (7%)
Sand - Gravel	1.2 - 2.0	1.0	1 (2%)

* Confirmation with Local Experience Recommended

9.10.1.2 Relaxation

The ultimate capacity of driven piles can also decrease with time following driving. This is known as relaxation and it has been observed in dense, saturated, fine grained soils such as non-cohesive silts and fine sands, as well as in some shales. In these cases, the driving process is believed to cause the dense soil near the pile toe to dilate (tendency for volume increase), thereby generating negative pore pressures (suction). The negative pore pressures temporarily increase the effective stresses acting on the pile, resulting in a temporarily higher soil strength and driving resistance. When these pore pressures dissipate, the effective stresses acting on the pile decrease, as does the pile capacity. Relaxation in weak laminated rocks has been attributed to a release of locked in horizontal stresses, Thompson and Thompson (1985).

Because the pile capacity may decrease (relaxation) after the end of driving, pile capacity assessments from static load testing or retapping should be made after equilibrium conditions in the soil have been re-established. In the absence of site specific pore pressure data from piezometers, it is suggested that static load testing or retapping of piles in dense silts and fine sands be delayed for five days to a week after driving, or longer if possible. In relaxation prone shales, it is suggested that static load testing or restrike testing be delayed a minimum of two weeks after driving.

Published cases of the relaxation magnitude of various soil types are quite limited. However, data from Thompson and Thompson (1985) as well as Hussein *et al.* (1993) suggest relaxation factors for piles founded in some shales can range from 0.5 to 0.9. The relaxation factor is defined as the static load test failure load divided by the pile capacity at the end of initial driving. Relaxation factors of 0.5 and 0.8 have also been observed in two cases where piles were founded in dense sands and extremely dense silts, respectively. The importance of evaluating time dependent decreases in pile capacity for piles founded in these materials cannot be over emphasized.

9.10.1.3 Estimation of Pore Pressures During Driving

According to Lo and Stermac (1965), the maximum pore pressure induced from pile driving may be estimated from the following equation.

$$\Delta u_m = \left[(1 - K_0) + \left(\frac{\Delta u}{p} \right)_m \right] p_i$$

Where: Δu_m = Maximum excess pore pressure in kPa (ksf).
 K_0 = Coefficient of earth pressure at-rest.
 $(\Delta u/p)_m$ = Maximum value of the pore pressure ratio, $\Delta u/p$, measured in a CU triaxial test with pore pressure measurements.
 p_i = Initial effective overburden pressure prior to pile driving in kPa (ksf).

Ismael and Klym (1979) presented a case history where the above procedure was used. They reported good agreement between measured excess pore pressures with estimates from the Lo and Stermac procedure.

Poulos and Davis (1980) summarized measurements of excess pore pressures due to pile driving from several case histories. In this compilation, the reported excess pore pressure measurements divided by the effective overburden pressure were plotted versus the radial

distance from the pile surface divided by the pile radius. These results are presented in Figure 9.77 and indicate that the excess pore pressure at the pile-soil interface can approach 1.4 to 1.9 times the effective overburden pressure, depending upon the clay sensitivity.

The foundation designer should evaluate the potential change in pile capacity with time. Once pore pressures are measured or estimated, effective stress static pile capacity calculation methods can be used to quantify the probable change in pile capacity with time.

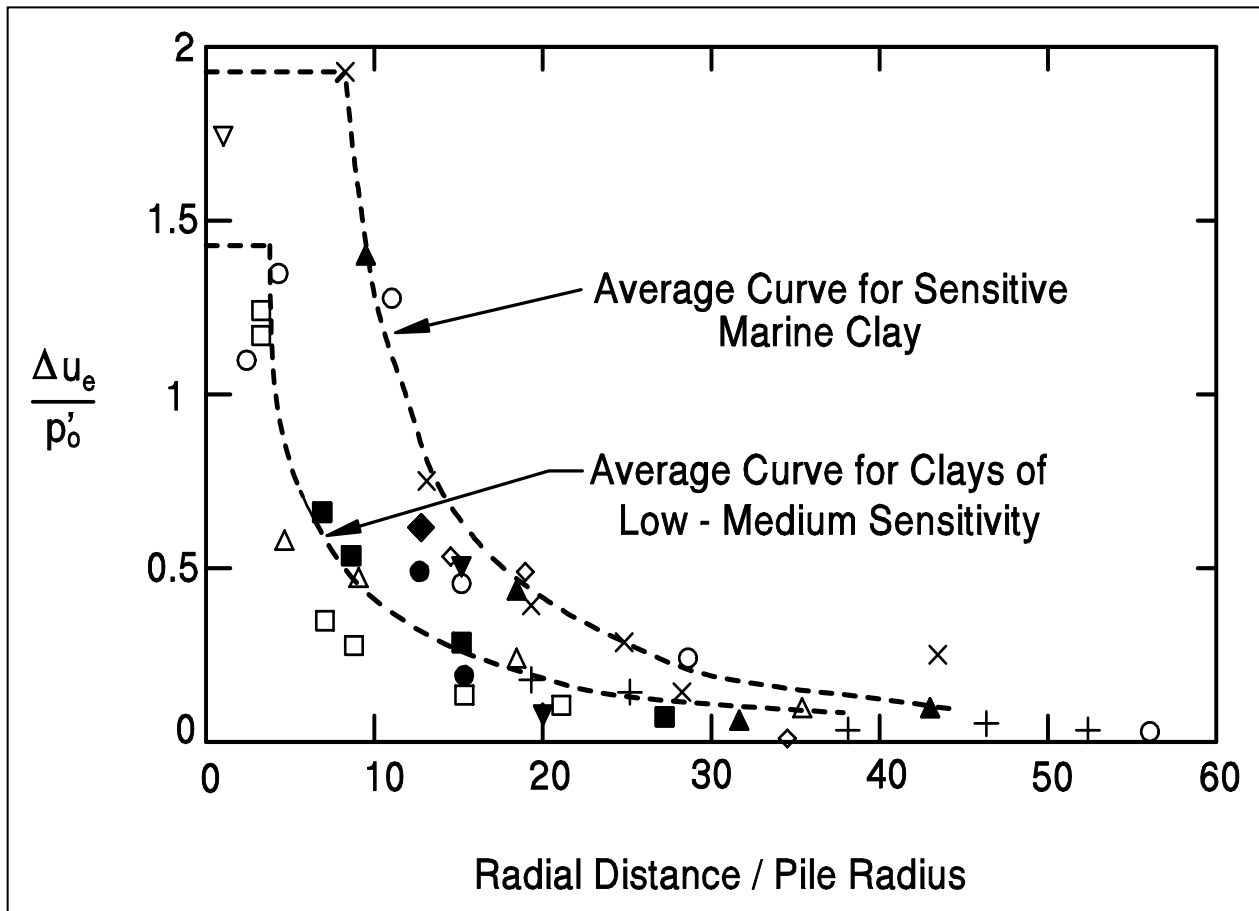


Figure 9.77 Excess Pore Water Pressure due to Pile Driving (after Poulos and Davis, 1980)

9.10.2 Effects of Predrilling, Jetting and Vibratory Installation on Pile Capacity

Piles are sometimes predrilled or jetted to a prescribed depth in order to attain the pile penetration depths required, as well as to reduce other foundation installation concerns, such as ground vibrations. Jetting is usually performed in cohesionless soils that can be freely eroded by water jets. Jetting, which can be very effective in sands, is usually ineffective in cohesive soils. For clays, and other drillable materials, such as thin layers of rock, predrilling the pile locations is more effective. The predrilled hole can be slightly smaller, equal to, or slightly larger than the pile diameter.

The use of predrilling or jetting will result in greater soil disturbance than considered in standard static pile capacity calculations. Therefore, when predrilling or jetting is contemplated, the effect of either of these construction procedures on calculated compression, uplift, and lateral pile capacity should be considered. Poulos and Davis (1980) report that the ultimate shaft resistance should be reduced by 50% of the originally calculated capacity in the jetted zone if the pile is jetted and then driven to the final penetration. McClelland *et al.* (1969) reported that a decrease in shaft resistance over a predrilled depth can range from 50 to 85% of that calculated without predrilling, depending upon the size of the predrilled hole. Hence, the probable reduction in compression, uplift, and lateral capacity from jetting or predrilling should be evaluated whenever predrilling or jetting is being considered.

Agencies are often requested to allow pile installation with a vibratory pile hammer instead of an impact hammer. Mosher (1987) summarized the results from five sites where piles were installed by both impact and vibratory hammers. This study concluded that for a significant majority of the cases, piles installed in sand with a vibratory hammer had a lower ultimate capacity than impact driven piles at the same site. Mosher also concluded that time dependent soil strength changes occurred equally for both installation methods. Hence, the capacity of the vibratory installed piles did not increase to the capacity of the impact driven piles with time. However, it was also observed that impact driving a vibratory installed pile would increase the capacity of the vibratory installed pile to that of an impact driven pile.

O'Neill and Vipulanandan (1989) performed a laboratory evaluation of piles installed with vibratory hammers. This laboratory study found impact driven piles had a 25% greater unit shaft resistance and a 15 to 20% higher unit toe resistance than vibratory installed piles in medium dense to dense, uniform, fine sand. However, in very dense, uniform, fine sand, the impact driven pile had a 20 to 30% lower unit shaft resistance and approximately a 30% lower unit toe resistance than the vibratory installed pile.

These two studies indicate use of vibratory pile installation rather than impact driving will affect the ultimate pile capacity that can be achieved at a given pile penetration depth. Therefore, communication between design and construction personnel should occur, and the influence of vibratory pile installation be evaluated when it is proposed. Impact driving a specific final depth of vibratory installed piles may provide a foundation that meets the engineer's performance requirements at reduced installation cost.

9.10.3 Effects of Site Dewatering on Pile Capacity and Adjacent Structures

When a site is dewatered during construction, a temporary increase in effective stresses will occur. This causes a corresponding temporary increase in soil shear strength that will result in piles driven in a dewatered site to develop a greater capacity at a shallower pile penetration depth as compared to the non-dewatered condition. The soil resistance to be overcome to reach a specified penetration depth will also be greater than in the non-dewatered condition. If not considered in the design stage, the selected pile type may not be driveable to the required penetration depth in the dewatered construction condition. When dewatering is terminated, the effective stresses acting on the pile will decrease as the water table rises. This will result in a decrease in the soil shear strength and a decrease in long term pile capacity. Hence piles driven to the ultimate capacity in the dewatered condition would have less than the required ultimate capacity once dewatering was terminated.

For projects where significant dewatering is required, the effects of the dewatering on pile capacity and pile driveability should be evaluated. In these cases, multiple static analyses should be performed to determine the pile capacity and driveability requirements under the short term dewatered condition, as well as the long term pile capacity after dewatering has been terminated.

Dewatering can also have negative impacts on nearby structures supported on deep and shallow foundations. The increase in effective stress can cause or increase negative shaft resistance loads on deep foundations or cause consolidation settlements that affect the performance of deep and shallow foundations systems. The potential dewatering effects on adjacent structures should be evaluated during the design phase.

9.10.4 Densification Effects on Pile Capacity and Installation Conditions

As illustrated in Figure 9.3, driving a pile in cohesionless soil influences the surrounding soils to a distance of about 3 to 5 pile diameters away from the pile. The soil displacement and vibrations resulting from driving pile groups in cohesionless soils can further densify cohesionless materials. The use of displacement piles also intensifies group densification effects in cohesionless soils.

Densification can result in the pile capacity as well as the resistance to pile penetration being significantly higher than that calculated for a single pile in the static capacity calculations. The added confinement provided by cofferdams or the sequence of pile installation can further aggravate a group densification problem. Piles should be installed from the center of the group outward in order to reduce group densification effects due to installation sequence. Densification can cause significant construction problems if scour, seismic, or other considerations require pile penetration depths that cannot be achieved.

Potential densification effects should be considered in the design stage. Studies by Meyerhof (1959) and Kishida (1967) indicate that an increase in the soil friction angle of up to 4 degrees would not be uncommon for piles in loose to medium dense sands. It is expected that the increase in soil friction angle would be less for dense sands or cohesionless soils with a significant fine content. Densification affects the soil resistance to be overcome during driving and should be evaluated through static analyses performed using higher soil strength parameters than used for design. Results from these static analyses may indicate that a low displacement pile should be used, the pile spacing should be increased, or that a pile installation aid should be specified in order to obtain the required pile penetration depth.

9.10.5 Plugging of Open Pile Sections

Open pile sections include open end pipe piles and H-piles. The use of open pile sections has increased, particularly where special design events dictate large pile penetration depths. When open pile sections are driven, they may behave as low displacement piles and "cookie cut" through the soil, or act as displacement piles if a soil plug forms near the pile toe. It is generally desired that open sections remain unplugged during driving and plugged under static loading conditions.

Stevens (1988) reported that plugging of pipe piles in clays does not occur during driving if pile accelerations (along the plug zone) are greater than 22g's. Holloway and Beddard (1995) reported that hammer blow size (impact force and energy) influenced the dynamic response of the soil plug. With a large hammer blow, the plug "slipped" under the dynamic event whereas under a lesser hammer blow the pile encountered toe resistance typically of a plugged condition. From a design perspective, these cases indicate that pile penetration of open sections can be facilitated if the pile section is designed to accommodate a large pile hammer. Wave equation analyses can provide calculated accelerations at selected pile segments.

Static pile capacity calculations must determine whether an open pipe section will exhibit plugged or unplugged behavior. Studies by O'Neill and Raines (1991), Raines *et al.* (1992), as well as Paikowsky and Whitman (1990) suggest that plugging of open pipe piles in medium dense to dense sands generally begins at a pile penetration to pile diameter ratio of 20, but can be as high as 35. For pipe piles in soft to stiff clays, Paikowsky and Whitman (1990) reported plugging occurs at penetration-to-pile diameter ratios of 10 to 20.

The above studies suggest that plugging in any soil material is probable under static loading conditions once the penetration to pile diameter ratio exceeds 20 in dense sands and clays, or 20 to 30 in medium sands. An illustration of the difference in the soil resistance mechanism that develops on a pipe pile with an open and plugged toe condition is presented in Figure 9.78. Paikowsky and Whitman (1990) recommend that the static capacity of an open end pipe pile be calculated from the lesser of the following equations:

Plugged Condition:
$$Q_u = f_{so} A_s + q_t A_t$$

Unplugged Condition:
$$Q_u = f_{so} A_s + f_{si} A_{si} + q_t A_p - w_p$$

- Where:
- Q_u = Ultimate pile capacity in kN (kips).
 - f_{so} = Exterior unit shaft resistance in kPa (ksf).
 - A_s = Pile exterior surface area in m^2 (ft^2).
 - f_{si} = Interior unit shaft resistance in kPa (ksf).
 - A_{si} = Pile interior surface area in m^2 (ft^2).
 - q_t = Unit toe resistance in kPa (ksf).
 - A_t = Toe area of a plugged pile in m^2 (ft^2).
 - A_p = Pile cross sectional area of an unplugged pile in m^2 (ft^2).
 - w_p = Weight of the plug kN (kips).

The soil stresses and displacements induced by driving an open pile section and a displacement pile section are not the same. Hence, a lower unit toe resistance, q_t , should be used for calculating the toe capacity of open end pipe piles compared to a typical closed end condition. The value of the interior unit shaft resistance in an open end pipe pile is typically on the order of 1/3 to 1/2 the exterior unit shaft resistance, and is influenced by soil type, pile diameter, and pile shoe configuration. These factors will also influence the length of soil plug that may develop.

For open end pipe piles in cohesionless soils, Tomlinson (1994) recommends that the static pile capacity be calculated using a limiting value of 5000 kPa (105 ksf) for the unit toe resistance, regardless of the pile size or soil density. Tomlinson states that higher unit toe resistances do not develop, because yielding of the soil plug rather than bearing capacity failure of the soil below the plug governs the capacity.

For open end pipe piles driven in stiff clays, Tomlinson (1994) recommends that the static pile capacity be calculated as follows when field measurements confirm a plug is formed and carried down with the pile:

$$Q_u = 0.8 c_a A_s + 4.5 c_u A_t$$

Where: Q_u = Ultimate pile capacity in kN (kips).
 c_a = Pile adhesion from Figure 9.18 in kPa (ksf).
 A_s = Pile-soil surface area in m^2 (ft^2).
 c_u = Average undrained shear strength at the pile toe in kPa (ksf).
 A_t = Toe area of a plugged pile in m^2 (ft^2).

Static pile capacity calculations for open end pipe piles in cohesionless soils should be performed using the Paikowsky and Whitman equations. Toe resistance should be calculated using the Tomlinson limiting unit toe resistance of 5000 kPa (105 ksf), once Meyerhof's limiting unit toe resistance, determined from Figure 9.17, exceeds 5000 kPa (105 ksf). For open end pipe piles in predominantly cohesive soils, the Tomlinson equation should be used.

The plugging phenomenon in H-piles can be equally difficult to analyze. However, the distance between flanges of an H-pile is smaller than the inside diameter of most open end pipe piles. Therefore, it can usually be assumed that an H-pile will be plugged under static

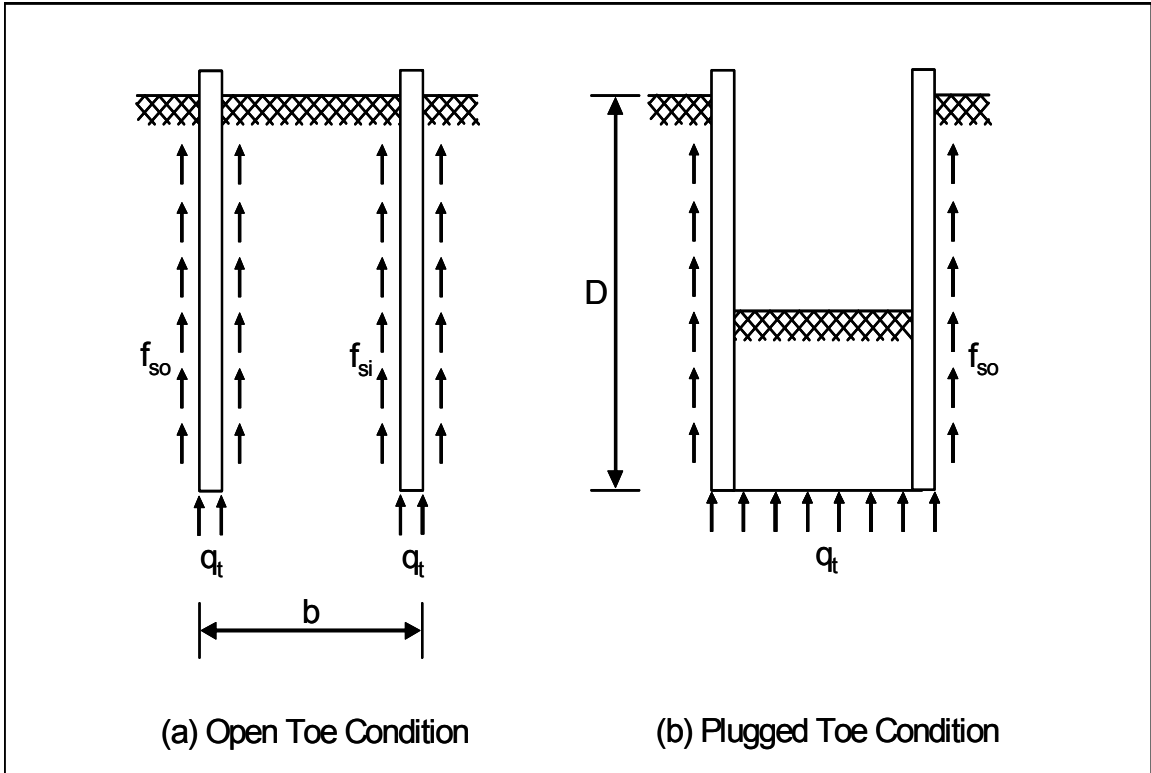


Figure 9.78 Plugging of Open End Pipe Piles (after Paikowsky and Whitman, 1990)

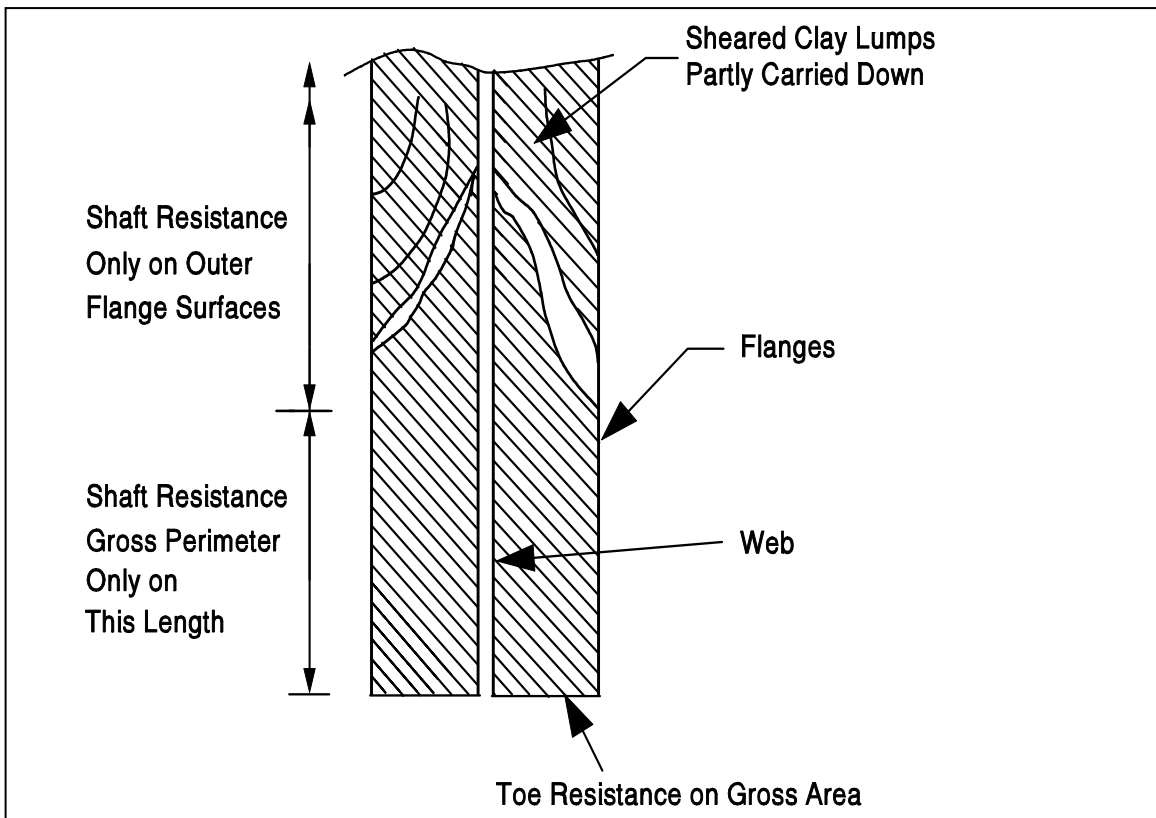


Figure 9.79 Plugging of H-Piles (after Tomlinson, 1994)

loading conditions and the “box” area of the pile toe can be used for static calculation of the toe capacity in cohesionless and cohesive soils. The toe capacity for H-piles driven to rock is usually governed by the pile structural strength, calculated based on the steel cross sectional area, and should not include the area of a soil plug, if any.

For H-piles in cohesionless soils, arching between the flanges can usually be assumed, and the "box" perimeter can be used for shaft resistance calculations. In most cohesive soils, the shaft resistance is calculated from the sum of the adhesion, c_a , along the exterior of the two flanges plus the undrained shear strength of the soil, c_u , times the surface area of the two remaining sides of the "box" due to soil-to-soil shear along these two faces. Figure 9.79 illustrates that calculation of H-piles in stiff clays can still be problematic. Sheared clay lumps can develop above the plug zone, in which case the shaft resistance may only develop along the exterior surfaces of the flanges in the sheared lump zone.

The above discussions highlight the point that a higher degree of uncertainty often exists for static pile capacity calculations of open pile sections than for displacement piles. Soil plug formation and plug response is often different under static and dynamic loading. This can complicate pile capacity evaluations of open pile sections with all dynamic methods (wave equation, dynamic testing, and dynamic formulas). Therefore, for large diameter open end pipe piles, greater than 450 mm (18 in), or for H-piles designed due carry their load primarily in shaft resistance, a static load test is recommended for capacity verification.

9.10.6 Design Considerations Due to Pile Driving Induced Vibrations

Since piles are driven by impact or vibratory hammers, ground vibrations of some magnitude are almost always induced into the surrounding soils during pile installation. Damage to nearby structures can result from two mechanisms:

- 1) Vibrations induced soil densification and settlement,
- 2) The effects of vibrations on the structure itself.

The ground vibration level where vibration induced soil densification and settlement or structural damage from direct vibrations occur depends upon the vibration magnitude and frequency as well as the type and condition of the existing structure or facility. The vibrations created by pile driving depend on the soil type, pile type and section, pile hammer, pile installation techniques, pile penetration resistance, the pile toe penetration depth, and the distance from the pile. Therefore, the distance from a pile driving operation

where these variables combine to potentially cause structure damage varies. For pile driving projects having structures or facilities within a potential damage zone, careful evaluation of the pile driving procedures and/or monitoring of ground vibrations during pile installations should be performed by personnel with vibration monitoring and mitigation experience.

Lacy and Gould (1985) found that vibration induced soil densification settlements and resulting structural damage can occur at peak particle velocities much less than 50 mm per second (2 inches per second) and that soil gradation is an important factor in this phenomenon. They reported that significant vibration induced settlements occurred at some sites with peak particle velocities measured on the ground surface as low as 2.5 to 5.1 mm per second (0.1 to 0.2 inches per second). Sands particularly susceptible to vibration induced densification were late Pleistocene deposits with uniformity coefficients of up to 4 or 5 and relative densities of up to 50 or 55%.

Wiss (1981) reported "safe" levels of ground vibration for structures have typically been recommended between 12 and 100 mm per second (0.5 and 4 inches per second). In many codes, such as NFPA 495 (2006), the maximum allowable particle velocity to prevent the onset or propagation of hairline cracks in plaster or drywall is a function of the vibration frequency. For example, a particle velocity of 25 mm per second (1 inch per second) at 30 Hz would be below NFPA 495 code limits but would be above code limits if the vibration frequency were 10 Hz.

Bay (2003) summarized relationships between peak particle velocity and the distance from the pile as a function of rated hammer energy. These results were plotted against typical damage thresholds for various types of structures. Charts for Class II and Class III soils were provided and are reproduced in Figures 9.80 top and bottom, respectively. Class II soils were defined as competent soils with Standard Penetration test N values of 5 to 15 blows per 0.3 m (ft). Class III soils are hard soils with SPT N values of 15 to 50 blows per 0.3 m (ft). Bay noted that stiff soil crusts near the ground surface can significantly increase the vibration levels from those noted in the charts. Bay noted other factors that can influence the vibration levels include nearby deep excavations, rock outcrops, and shallow bedrock. Soil-structure interaction should also be considered in assessing vibration levels and damage potential. Therefore, while informative, these charts should not be used to eliminate vibration monitoring.

If the potential for damaging ground vibrations is high, pile installation techniques should be specified to reduce vibration levels. Specifications could require predrilling or jetting as well

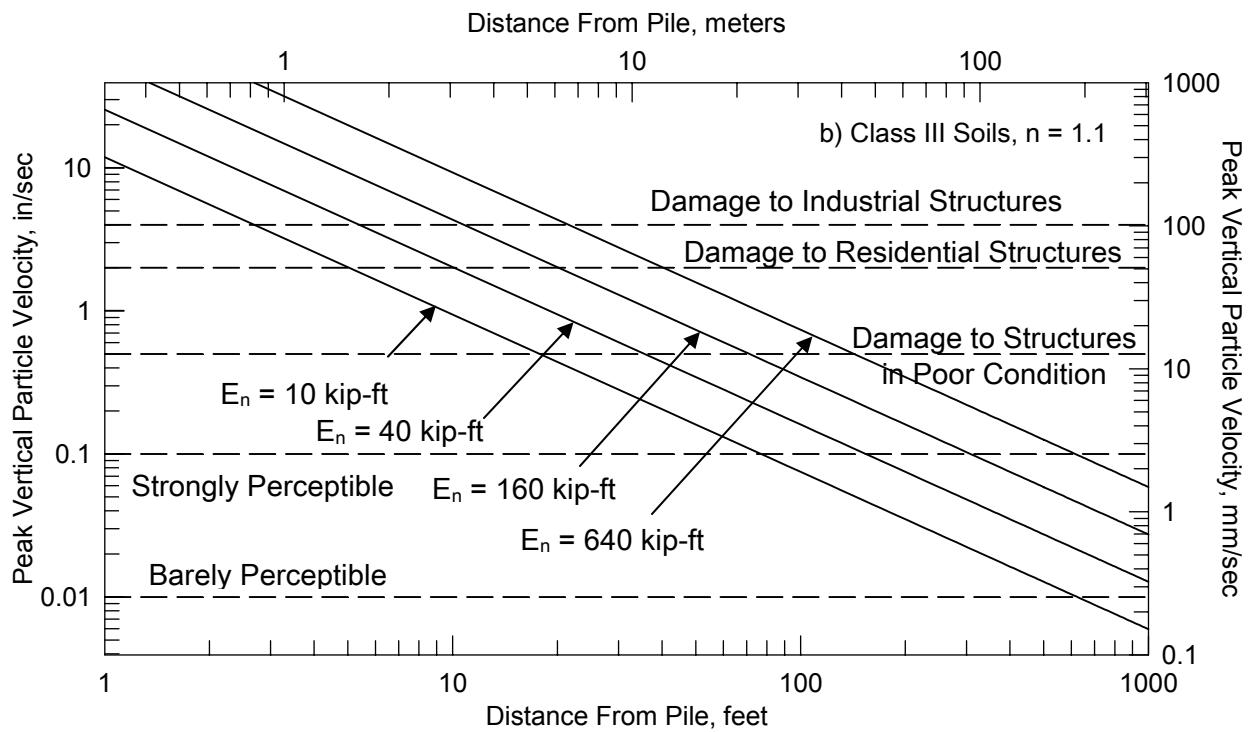
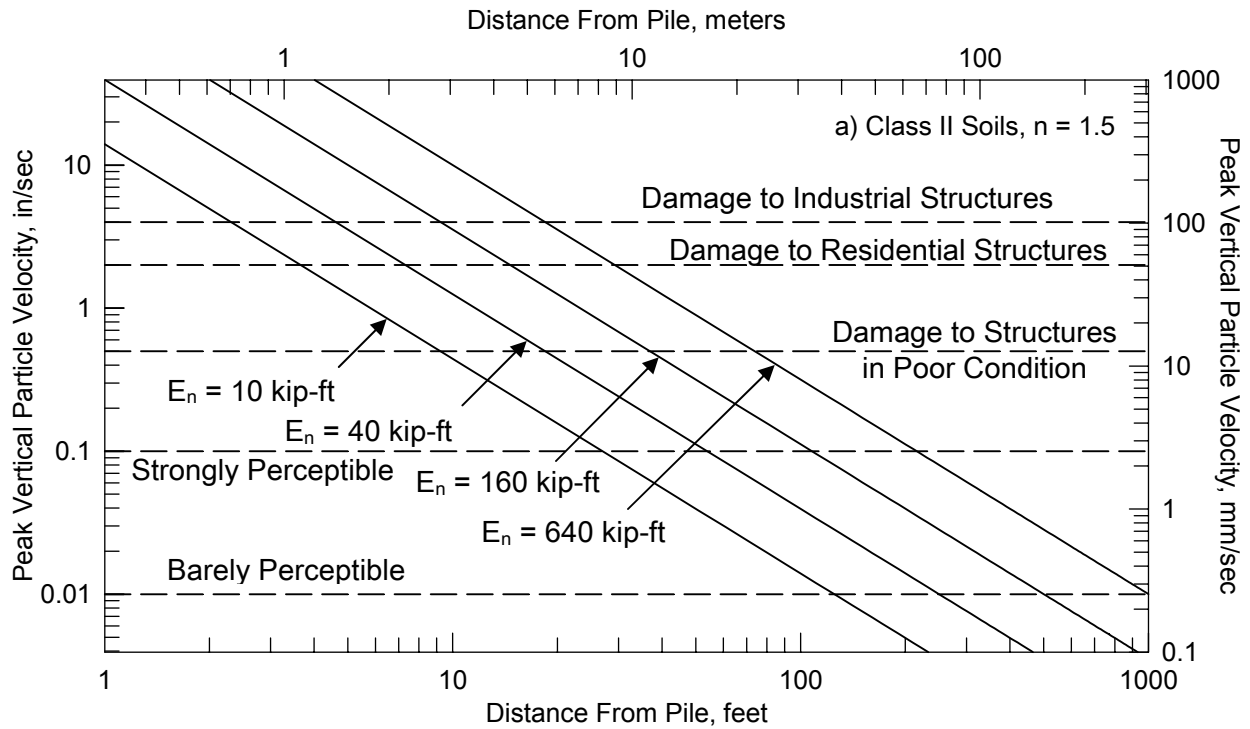


Figure 9.80 Predicted Vibration Levels for Class II and Class III Soils (after Bay, 2003)

as use of a different pile type or use of a specific type of pile hammer. Since predrilling and jetting influence compression, uplift, and lateral pile capacities, a determination of probable vibration levels and remediation measures should be evaluated in the design stage. A case history illustrating how a change in pile installation procedures reduced vibration induced soil densification and off-site settlement damage was reported by Lukas and Gill (1990).

NCHRP Project 20-5, *Dynamic Effects of Pile Installations on Adjacent Structures*, by Woods (1997), provides a synthesis of pile driving induced vibrations and typical mitigation practices. This synthesis noted that vibration problem management is the key to minimizing vibration damage, delays and claims. Two important elements in vibration management are a vibration specification with limits on the maximum peak particle velocity and a predriving survey of surrounding structures. An example vibration specification that details the requirements of a preconstruction survey as well as particle velocity controls is included in the NCHRP synthesis. The predriving survey needs to document conditions within the potential effected area. Woods reported that vibration damage a distance greater than on pile length away from driving is relatively uncommon but settlement damage in loose clean sands can occur up to 400 meters (1300 ft) away. Woods also concluded that piles with low impedances, EA/C , tend to transmit the hammer energy to the soils along the pile shaft and thus increase ground vibrations, whereas piles with higher impedances tend to more effectively transmit the hammer energy to the pile toe resulting in lower ground vibration levels. Hence, selection of a stiffer pile section at sites where vibrations are a concern may reduce vibration problems.

The Pile Driving Contractors Association (2006) is currently compiling a national pile driving noise and vibration database. The goal of this database is to allow contractors and designers to make reasonable assessments of the potential vibration effects from driven pile installations.

9.10.7 Design Considerations Due to Pile Driving Noise

Driven piles are installed by impact hammers. Noise levels associated with typical impact pile driving activities depend upon the hammer and pile type used. Noise from impact pile driving operations typically ranges from around 80 to 135 dBa. If local ordinances dictate allowable noise levels at or below this level, some driving equipment may not meet these requirements. Manufacturers of a few diesel and hydraulic hammers can provide optional noise suppression devices that may reduce the pile driving generated noise by about 10

dBa. Independently manufactured devices are also available. Additional information on noise suppression equipment is presented in Chapter 22.

In noise sensitive areas, the foundation designer should review any noise ordinances to determine if pile driving noise suppression devices would be necessary and if so, the impact this may have on the contractor's equipment selection and productivity. If limits on work hours, pile equipment type, or noise suppression equipment are required, costs associated with these limitations should be considered in the foundation selection process.

9.10.8 Pile Driveability

Greater pile penetration depths are increasingly being required to satisfy performance criteria in special design events such as scour, vessel impact, ice and debris loading, and seismic events. Therefore, the ability of a pile to be driven to the required penetration depth has become increasingly more important and must be evaluated in the design stage. Pile driveability refers to the ability of a pile to be driven to a desired penetration depth and/or capacity. All of the previously described static analysis methods are meaningless if the pile cannot be driven to the required design depth and ultimate capacity without sustaining damage. The limit of pile driveability is the maximum soil resistance a pile can be driven against without sustaining damage or a refusal driving resistance with a properly sized driving system.

Primary factors controlling the ultimate geotechnical capacity of a pile are the pile type and length, the soil conditions, and the method of installation. Since the pile type, length and method of installation can be specified, it is often erroneously assumed that the pile can be installed as designed to the estimated penetration depth. However, the pile must have sufficient driveability to overcome the soil resistance encountered during driving to reach the estimated or specified pile penetration depth. If a pile section does not have a driveability limit in excess of the soil resistance to be overcome during driving, it will not be driveable to the desired pile penetration depth. The failure to adequately evaluate pile driveability is one of the most common deficiencies in driven pile design practice.

In evaluating the driveability of a pile, the soil disturbance during installation and the time dependent soil strength changes should be considered. Both soil setup and relaxation have been described earlier in this chapter. For economical pile design, the foundation designer must match the soil resistance to be overcome at the time of driving with the pile impedance, the pile material strength, and the pile driving equipment.

9.10.8.1 Factors Affecting Driveability

A pile must satisfy two aspects of driveability. First, the pile must have sufficient stiffness to transmit driving forces large enough to overcome soil resistance. Second, the pile must have sufficient structural strength to withstand the driving forces without damage.

The primary controlling factor on pile driveability is the pile impedance, EA/C . Once the pile material is selected, and thus the pile modulus of elasticity, E , and the pile wave speed, C , only increasing the pile cross sectional area, A , will improve the pile driveability. For steel H-piles, the designer can improve pile driveability by increasing the H-pile section without increasing the H-pile size. The driveability of steel pipe piles can be improved by increasing the pipe wall thickness. For open ended pipe piles, an inside-fitting cutting shoe can improve driveability by delaying the formation of a soil plug and thereby reducing the soil resistance to be overcome. Most concrete piles are solid cross sections. Therefore, increasing the pile area to improve driveability is usually accompanied by an increase in the soil resistance to driving.

A lesser factor influencing pile driveability is the pile material strength. The influence of pile material strength on driveability is limited, since strength does not alter the pile impedance. However, a pile with a higher pile material strength can tolerate higher driving stresses that may allow a larger pile hammer to be used. This may allow a slightly higher capacity to be obtained before refusal driving conditions or pile damage occur.

Other factors that may affect pile driveability include the driving system characteristics such as ram weight, stroke, and speed, as well as the actual system performance in the field. The dynamic soil response can also affect pile driveability. Soils may have higher damping characteristics or elasticity than assumed, both of which can reduce pile driveability. Dynamic soil response is discussed in greater detail in Chapters 16 and 17.

Even if the pile structural capacity and geotechnical capacity both indicate a high pile capacity could be used, a high pile capacity may still not be obtainable because driving stresses may exceed allowable driving stress limits. A pile cannot be driven to an ultimate static capacity that is as high as the structural capacity of the pile because of the additional dynamic resistance or damping forces generated during pile driving. The allowable static design stresses in pile materials by various codes generally represent the static stress levels (pile capacity) which can be consistently developed with normal pile driving equipment and methods. Maximum allowable design and driving stresses are presented in Chapter 10.

9.10.8.2 Methods for Determining Pile Driveability

There are three available methods for predicting and/or checking pile driveability. As design tools, all of the methods have advantages and disadvantages and are therefore presented in order of increasing cost and reliability.

1. Wave Equation Analysis

This method, Goble and Rausche (1986), accounts for pile impedance and predicts driving stresses as well as the relationship of pile driving resistance versus ultimate pile capacity. Wave equation analyses performed in the design stage require assumptions on the hammer type and performance level, the drive system components, as well as the soil response during driving. These shortcomings are reflected in variations between predicted and actual field behavior. Even with these shortcomings, the wave equation is a powerful design tool that can and should be used to check driveability in the design stage, to design an appropriate pile section, or to specify driving equipment characteristics. Additional information on the wave equation, including its use as a construction control tool, is presented in Chapter 16.

2. Dynamic Testing and Analysis

Dynamic measurements can be made during pile installation to calculate driving stresses and to estimate static pile capacity at the time of driving. Time dependent changes in pile capacity can be evaluated if measurements are made during restrike tests. Additional signal matching analysis can also provide soil parameters for refined wave equation analysis. A shortcoming of this method as a design tool is that it must be performed during pile driving. Therefore, in order to use dynamic testing information to confirm driveability or to refine a design, a test program is required during the design stage. Additional details on dynamic testing and analysis, including its use as a construction control tool, is presented in Chapter 17.

3. Static Load Tests

Static load tests, Kyfor *et al.* (1992), are useful for checking driveability and confirming pile capacity prior to production pile driving. Test piles are normally driven to estimated lengths and load tested. The confirmation of pile driveability through static load testing is the most accurate method of confirming driveability and pile capacity since a pile is actually driven and load tested. However, this advantage also illustrates one of its shortcomings as a design tool, in that a test program is required during the design stage.

Other shortcomings associated with static load tests for determining driveability include:

- a. cost and time delay that limit their suitability to certain projects.
- b. assessment of driving stresses and extent of pile damage, if any, sustained by the pile is not provided by the test.
- c. can be misleading on projects where soil conditions are highly variable.

Additional details on static load testing, including its use as a construction control tool, is presented in Chapter 18. The Osterberg cell and the Statnamic test can also be used to evaluate pile capacity. These methods are discussed in Chapters 19 and 20, respectively.

As design and construction control tools, methods 1 and 2 offer additional information and complement static load tests. Used properly, methods 1 and 2 can yield significant savings in material costs or reduction of construction delays. These methods can be used to reduce the number of static load tests and also allow evaluation of increases in the maximum allowable design stresses. A determination of the increase (soil setup) or decrease (relaxation) in pile capacity with time can also be made if piles are retapped after initial driving.

9.10.8.3 Driveability Versus Pile Type

Driveability should be checked during the design stage of all driven piles. It is particularly important for closed end steel pipe piles where the impedance of the steel casing may limit pile driveability. Although the designer may attempt to specify a thin-wall pipe in order to save material cost, a thin wall pile may lack the driveability to develop the required ultimate capacity or to achieve the necessary pile penetration depth. Wave equation analyses should be performed in the design stage to select the pile section and wall thickness.

Steel H-piles and open pipe piles, prestressed concrete piles, and timber piles are also subject to driveability limitations. This is particularly true as allowable design stresses increase and as special design events require increased pile penetration depths. The driveability of long prestressed concrete piles can be limited by the pile's tensile strength.

REFERENCES

- Altaee, A., Evgin, E. and Fellenius, B.H. (1992). Axial Load Transfer for Piles in Sand, I: Tests on an Instrumented Precast Pile. *Canadian Geotechnical Journal*, Vol. 29, No. 1, 11-20.
- American Association of State Highway and Transportation Officials [AASHTO], (2002). *Standard Specifications for Highway Bridges. Division 1 and 2*, Washington, D.C.
- Bay, J.A. (2003). A Summary of the Research on Pile Driving Vibrations. *Proceedings of the Pile Driving Contractor's Association 7th Annual Winter Roundtable*, Atlanta, 13 pp.
- Bollman, H.T. (1993). Notes on Designing Deep Foundations for Lateral Loads. *Proceedings of Design of Highway Bridges for Extreme Events*, Crystal City, Virginia, 175-199.
- Bowles, J.E. (1977). *Foundation Analysis and Design. Second Edition*, McGraw-Hill Book Company.
- Bowles, J.E. (1988). *Foundation Analysis and Design. Fourth Edition*, McGraw-Hill Book Company, 1004.
- Briaud J-L. and Miran, J. (1992). The Cone Penetration Test. Report No. FHWA-SA-91-043, U.S. Department of Transportation, Federal Highway Administration, Office of Technology Applications, Washington, D.C., 161.
- Briaud, J-L. and Tucker, L.M. (1993). Downdrag on Bitumen-Coated Piles. Preliminary Draft Final Report, National Cooperative Highway Research Program NCHRP 24-5, Washington, D.C., 245.
- Briaud, J-L. and Tucker, L.M. (1986). *User's Manual for PILECPT*. Civil Engineering Department, Texas A&M University.
- Broms, B.B. (1964a). Lateral Resistance of Piles in Cohesive Soils. *American Society of Civil Engineers, Journal for Soil Mechanics and Foundation Engineering*, Vol. 90, SM2, 27-63.

- Broms, B.B. (1964b). Lateral Resistance of Piles in Cohesionless Soils. American Society of Civil Engineers, Journal for Soil Mechanics and Foundation Engineering, Vol. 90, SM3, 123-156.
- Broms, B.B. (1966). Methods of Calculating the Ultimate Bearing Capacity of Piles - A Summary. Sols-Sols No. 18-19, 21-32.
- Brown, D.A., O'Neill, M.W., Hoit, M., McVay, M., El Naggar, M.H., and Chakraborty, S. (2001). Static and Dynamic Lateral Loading of Pile Groups, NCHRP Report 461, Transportation Research Board – National Research Council, Washington, DC, 60.
- Brown, D.A., Reese, L.C. and O'Neill, M.W. (1987). Cyclic Lateral Loading of a Large-Scale Pile Group in Sand. American Society of Civil Engineers, Journal of Geotechnical Engineering, Vol. 113, No. 11, 1326-1343.
- Brown, D.A., Morrison, C. and Reese, L.C. (1988). Lateral Load Behavior of Pile Group in Sand. American Society of Civil Engineers, Journal of Geotechnical Engineering, Vol. 114, No. 11, 1261-1276.
- Brown, D.A. and Bollman, H.T. (1993). Pile-Supported Bridge Foundations Designed for Impact Loading. Appended Document to the Proceedings of Design of Highway Bridges for Extreme Events, Crystal City, Virginia, 265-281.
- Bustamante, M. and Gianselli, L. (1982). Pile Bearing Capacity Prediction by Means of Static Penetrometer CPT. Proceedings of the Second European Symposium on Penetration Testing, Amsterdam, 493-500.
- Canadian Foundation Engineering Manual (1985). Second Edition, Canadian Geotechnical Society, Technical Committee on Foundations, 456.
- Cheney, R.S. and Chassie, R.G. (2002). Soils and Foundation Workshop Manual. Second Edition, Report No. HI-88-009, U.S. Department of Transportation, Federal Highway Administration, Office of Engineering, Washington, D.C., 395.
- Coduto, D.P. (1994). Foundation Design: Principles and Practice. Prentice-Hall, Inc., Englewood Cliffs, 796.
- Dumas, C. (2000), Soil Downdrag on Deep Foundations, An Overview Perspective. Proceedings of the 18th ASCE / PennDOT Geotechnical Seminar, Hershey, PA, 19.

Elias, V., Welsh, J.P., Warren, J., Lukas, R.G., Collin J.G., and Berg, R.R. (2004). Ground Improvement Methods. National Highway Institute, Federal Highway Administration, U.S. Department of Transportation, Washington D.C., 102

FoSSA (2.0), (2005) ADAMA Engineering, Inc., Newark, DE

Fellenius, B.H., Riker, R.E., O'Brien, A.J. and Tracy, G.R. (1989). Dynamic and Static Testing in a Soil Exhibiting Set-up. American Society of Civil Engineers, Journal of Geotechnical Engineering, Vol. 115, No. 7, 984-1001.

Fellenius, B.H. (1991). Chapter 13 - Pile Foundations, Foundation Engineering Handbook. Second Edition. H.S. Fang, Editor, Van Nostrand Reinhold Publisher, New York, 511-536.

Goble, G.G. and Rausche, F. (1986). Wave Equation Analysis of Pile Driving - WEAP86 Program. U.S. Department of Transportation, Federal Highway Administration, Implementation Division, McLean, Volumes I-IV.

Gouderault, P. and Fellenius, B.H. (1990). UNIPILE Program for Unified Analysis of Piles and Pile Groups Considering Capacity, Negative Skin Friction, and Settlement, Users Manual. Bengt Fellenius Consultants, Inc., Ottawa.

Gouderault, P. and Fellenius, B.H. (1994). UNIPILE Program Background and Manual. Unisoft, Ltd., Ottawa.

Hadjian, A.H., Fallgren, R.B. and Tufenkjian, M.R. (1992). Dynamic Soil-Pile-Structure Interaction, The State-of-Practice. Geotechnical Special Publication No. 34, Piles Under Dynamic Loads, S. Prakash Editor, American Society of Civil Engineers, ASCE, 1-26.

Hagerty, D.J. and Peck, R.B. (1971). Heave and Lateral Movements Due to Pile Driving. American Society of Civil Engineers, ASCE, Journal of the Soil Mechanics and Foundations Division, SM11, November, 1513-1531.

Hoit, M.I. and McVay, M. (1994). LPGSTAN User's Manual. University of Florida, Gainesville.

Holloway, D.M. and Beddard, D.L. (1995). Dynamic Testing Results Indicator Pile Test Program - I-880. Proceedings of the 20th Annual Members Conference of the Deep Foundations Institute.

- Holloway, D.M., Moriwaki, Y., Stevens, J.B. and Perez, J-Y (1981). Response of a Pile Group to Combined Axial and Lateral Loading. Proceedings of the 10th International Conference on Soil Mechanics and Foundation Engineering, Boulimia Publishers, Stockholm, Vol. 2, 731-734.
- Hough, B.K. (1959). Compressibility as the Basis for Soil Bearing Value. American Society of Civil Engineers, Journal for Soil Mechanics and Foundation Engineering, Vol. 85, SM4, 11-39.
- Hussein, M.H., Likins, G.E. and Hannigan, P.J. (1993). Pile Evaluation by Dynamic Testing During Restrike. Eleventh Southeast Asian Geotechnical Conference, Singapore.
- Ismael, N.F. and Klym, T.W. (1979). Pore-Water Pressures Induced by Pile Driving. American Society of Civil Engineers, Journal of Geotechnical Engineering, Vol. 105, GT11, 1349-1354.
- Kavazanjian Jr., E., Matasovic, N., Hadj-Hamou, T., and Sabatini, P.J. (1997). Geotechnical Engineering Circular No. 3, Design Guidance: Geotechnical Earthquake Engineering for Highways, Volume I – Design Principals U.S. Department of Transportation, Office of Bridge Technology, Federal Highway Administration, Washington, D.C.
- Kishida, H. (1967). Ultimate Bearing Capacity of Piles Driven in Loose Sands, Soils and Foundations. Japanese Society of Soil Mechanics and Foundation Engineering, Vol. 7, No. 3, 20-29.
- Komurka, V.E., Wagner, A.B., and Edil, T.B. (2003). Estimating Soil/Pile Set-up, Final Report, Wisconsin Highway Research Program, 42.
- Kyfor, Z.G., Schnore, A.R., Carlo, T.A. and Bailey, P.F. (1992). Static Testing of Deep Foundations. Report No. FHWA-SA-91-042, U.S. Department of Transportation, Federal Highway Administration, Office of Technology Applications, Washington, D.C., 174.
- Lacy H.S. and Gould, J.P. (1985). Settlement from Pile Driving in Sands, Vibration Problems in Geotechnical Engineering. American Society of Civil Engineers, ASCE Special Technical Publication, New York, 152-173.

- Lam, I.P. and Martin, G.R. (1986). Seismic Design of Highway Bridge Foundations. Volume II - Design Procedures and Guidelines, Report No. FHWA/RD-86/102, U.S. Department of Transportation, Federal Highway Administration, Office of Engineering and Highway Operations, McLean, 181.
- Lo, K.Y. and Stermac, A.G. (1965). Induced Pore Pressures During Pile Driving Operations. Proceedings of the 6th International Conference on Soil Mechanics and Foundation Engineering, Vol. 2, Montreal, 285-289.
- Long, J.H. (1996). Personal Communication.
- Lukas, R.G. and Gill, S.A. (1992). Ground Movement from Piling Vibrations. Piling-European Practice and Worldwide Trends, The Institute of Civil Engineers, Thomas Telford House, London, 163-169.
- Mathias, D. and Cribbs, M. (1998). DRIVEN 1.0: A Microsoft Windows™ Based Program for Determining Ultimate Vertical Static Pile Capacity. Report No. FHWA-SA-98-074, U.S. Department of Transportation, Federal Highway Administration, Office of Technology Applications, Washington D.C. 112.
- McClelland, B., Focht, J.A. and Emrich, W.J. (1969). Problems in Design and Installation of Offshore Piles. American Society of Civil Engineers, ASCE, Journal of the Soil Mechanics and Foundations Division, SM6, 1491-1514.
- McVay, M., Casper, R. and Shang, T-I. (1995). Lateral Response of Three-Row Groups in Loose to Dense Sands at 3D and 5D Pile Spacing. American Society of Civil Engineers, Journal of Geotechnical Engineering, Vol. 121, No. 5, 436-441.
- Meyerhof, G.G. (1959). Compaction of Sands and Bearing Capacity of Piles. American Society of Civil Engineers, ASCE, Journal of the Soil Mechanics and Foundations Division, Vol. 85, SM6, December, 1-29.
- Meyerhof, G.G. (1976). Bearing Capacity and Settlement of Pile Foundations. American Society of Civil Engineers, ASCE, Journal of the Geotechnical Engineering Division, 195-228.
- Mosher, R.L. (1987). Comparison of Axial Capacity of Vibratory Driven Piles to Impact Driven Piles. USAEWES Technical Report ITL-877, 36.

- Moss, R.E.S. (1997). Cyclic Lateral Loading of Model Pile Groups in Clay Soil, Phase 2B. Master Thesis Research, Utah State University.
- New York State Department of Transportation, Engineering Research and Development Bureau (1977). Lateral Load Capacity of Vertical Pile Groups. Report NYSDOT-ERD-77-RR47.
- NFPA 495 (2006). Explosive Materials Code, Chapter 10, Ground Vibration, Airblast, and Flyrock, Quincy, 37-38
- Nordlund, R.L. (1963). Bearing Capacity of Piles in Cohesionless Soils. American Society of Civil Engineers, ASCE, Journal of the Soil Mechanics and Foundations Division, SM3, 1-35.
- Nordlund, R.L. (1979). Point Bearing and Shaft Friction of Piles in Sand. Missouri-Rolla 5th Annual Short Course on the Fundamentals of Deep Foundation Design.
- Nottingham, L.C. (1975). Use of Quasi-Static Friction Cone Penetrometer to Predict Load Capacity of Displacement Piles. Ph.D. dissertation to the Department of Civil Engineering, University of Florida, 552.
- Olson, R.E., and Shantz T.J., (2004). Axial Load Capacity of Piles in California in Cohesionless Soils, Geotechnical Special Publication No. 125, Current Practices and Future Trends in Deep Foundations, J.A. DiMaggio and M.H.Hussein Editors, American Society of Civil Engineers, ASCE, Reston, VA, 1-25.
- O'Neill, M.W. (1983). Group Action in Offshore Piles. Proceedings of the Conference on Geotechnical Practice in Offshore Engineering, S.G. Wright Editor, American Society of Civil Engineers, ASCE, New York, 25-64.
- O'Neill, M.W. and Vupulanandan, C. (1989). Laboratory Evaluation of Piles Installed with Vibratory Drivers. NCHRP Report 316, National Cooperative Highway Research Program, Transportation Research Board, Washington, D.C.
- O'Neill, M.W. and Raines, R.D. (1991). Load Transfer for Pipe Piles in Highly Pressured Dense Sand. American Society of Civil Engineers, Journal of Geotechnical Engineering, Vol. 117, No. 8, 1208-1226.

- Paikowsky, S.G. and Whitman, R.V. (1990). The effects of Plugging on Pile Performance and Design. Canadian Geotechnical Journal, Vol. 27, No. 4, 429-440.
- Peck, R.B., Hanson, W.E. and Thornburn, T. (1974). Foundation Engineering. Second Edition, John Wiley & Sons, New York, 215.
- Pile Driving Contractors Association [PDCA], (2006). National Pile Driving Noise and Vibration Database, www.piledrivers.org
- Poulos, H.G. and Davis, E.H. (1980). Pile Foundation Analysis and Design. John Wiley and Sons, New York, 18-51.
- Raines, R.D., Ugaz, O.G. and O'Neill, M.W. (1992). Driving Characteristics of Open-Toe Piles in Dense Sand. American Society of Civil Engineers, Journal of Geotechnical Engineering, Vol. 118, No. 1, 72-88.
- Rausche, F., Thendean, G., Abou-matar, H., Likins, G. and Goble, G. (1996). Determination of Pile Driveability and Capacity from Penetration Tests. FHWA Contract No. DTFH61-91-C-00047, Final Report, U.S. Department of Transportation, Federal Highway Administration.
- Reese, L.C. (1984). Handbook on Design of Piles and Drilled Shafts Under Lateral Load. Report No. FHWA-IP-84-11, U.S. Department of Transportation, Federal Highway Administration, Office of Implementation, Washington, D.C., 386.
- Reese, L.C. (1986). Behavior of Piles and Pile Groups Under Lateral Load. Report No. FHWA/RD-85/106, U.S. Department of Transportation, Federal Highway Administration, Office of Engineering and Highway Operations Research and Development, Washington, D.C., 311.
- Reese, L.C., Wang, S.T., Isenhower, W.M., Arrellage, J.A., (2000). Computer Program LPILE Plus Version 4.0 Technical Manual, Ensoft, Inc., Austin, Tx.
- Reese, L.C., Wang, S.T., Isenhower, W.M., Arrellage, J.A., (2000). Computer Program LPILE Plus Version 4.0 User's Guide, Ensoft, Inc., Austin, Tx.
- Richardson, E.V. and Davis, S.R. (2001). FHWA NHI-01-001, Evaluating Scour at Bridges, HEC-18. Office of Technology Applications, Federal Highway Administration, Washington, D.C.

- Rixner, J.J., Kraemer, S.R. and Smith, A.D. (1986). Prefabricated Vertical Drains Volume I, Engineering Guidelines. Report No. FHWA/RD-86/168, U.S. Department of Transportation, Federal Highway Administration, Office of Engineering and Highway Operations Research and Development, McLean, 117.
- Rollins, K.M., Peterson, K.T., and Weaver, T.J. (1989). Lateral Load Behavior of Full-Scale Pile Group in Clay. American Society of Civil Engineers, Journal of Geotechnical and Geoenvironmental Engineering, Vol. 124, No. 6, 468-478.
- Ruesta, P.F. and Townsend, F.C. (1997). Evaluation of Laterally Loaded Pile Group at Roosevelt Bridge. American Society of Civil Engineers, Journal of Geotechnical and Geoenvironmental Engineering, Vol. 123, No. 12, 1153-1161.
- Sabatini, P.J., Bachus, R.C., Mayne, P.W., Schweider, J.A., and Zettler, T.E. (2002). Geotechnical Engineering Circular No. 5, Evaluation of Soil and Rock Properties. U.S. Department of Transportation, Office of Bridge Technology, Federal Highway Administration, Washington, DC, 385.
- Schmertman, J.H. (1978). Guidelines For Cone Penetration Test, Performance, and Design. Report No. FHWA-TS-78-209, U.S. Department of Transportation, Federal Highway Administration, Washington, D.C., 145.
- Seed, H.B., Idriss, I.M. and Arango, I. (1983). Evaluation of Liquefaction Potential Using Field Performance Data. American Society of Civil Engineers, Journal of Geotechnical Engineering, Vol. 109, No. 3, 458-482.
- Seed, H.B. (1987). Design Problems in Soil Liquefaction. American Society of Civil Engineers, Journal of Geotechnical Engineering, Vol. 113, No. 8, 827-845.
- Seed, R.B. and Harder, L.F., Jr. (1990). SPT-Based Analysis of Cyclic Pore Pressure Generation and Undrained Residual Strength. Proceedings, H.B. Bolton Seed Memorial Symposium, J.M. Duncan Editor, BiTech Publishers, Vol. 2, 351-376.
- Smith, T.D. (1989). Fact or Friction: A Review of Soil Response to a Laterally Moving Pile. Foundation Engineering: Current Principles and Practices, F.H. Kulhawy Editor, American Society of Civil Engineers, ASCE, New York, Vol. 1, 588-598.

- Stevens, R.F. (1988). The Effect of a Soil Plug on Pile Driveability in Clay. Proceedings of the Third International Conference on the Application of Stress Wave Theory to Piles, B.H. Fellenius, Editor, BiTech Publishers, Vancouver, 861-868.
- Tawfig, K.S. (1994). Polyethylene Coating for Downdrag Mitigation on Abutment Piles. Proceedings of the International Conference on Design and Construction of Deep Foundations, Vol. 2, 685-698.
- Terzaghi, K. and Peck, R.B. (1967). Soil Mechanics in Engineering Practice. John Wiley and Sons, New York.
- Tomlinson, M.J. (1980). Foundation Design and Construction. Fourth Edition, Pitman Advanced Publishing Program.
- Tomlinson, M.J. (1994). Pile Design and Construction Practice. Fourth Edition, E & FN Spon, London, 411.
- Thompson, C.D. and Thompson, D.E. (1985). Real and Apparent Relaxation of Driven Piles. American Society of Civil Engineers, Journal of Geotechnical Engineering, Vol. 111, No. 2, 225-237.
- Thurman, A.G. (1964). Discussion of Bearing Capacity of Piles in Cohesionless Soils. American Society of Civil Engineers, ASCE, Journal of the Soil Mechanics and Foundations Division, SM1, 127-129.
- Urzua, A. (1992). SPILE A Microcomputer Program for Determining Ultimate Vertical Static Pile Capacity. Users Manual, Report No. FHWA-SA-92-044, U.S. Department of Transportation, Federal Highway Administration, Office of Engineering and Office of Technology Applications, Washington, D.C., 58.
- Woods, R.D. (1997). Dynamic Effects of Pile Installations on Adjacent Structures. NCHRP Synthesis 253, National Cooperative Highway Research Program, Transportation Research Board, Washington, D.C.
- Wiss, J.F. (1981). Construction Vibrations: State-of-the-Art. American Society of Civil Engineers, ASCE, Journal of the Geotechnical Engineering Division, February, 167-181.

Chapter 10

STRUCTURAL ASPECTS OF DRIVEN PILE FOUNDATIONS

The structural design of driven piles as a specific topic has not been emphasized extensively in the past. But, during last decade the structural design of piles has become more critical because lateral loads have been considered more carefully. An increased emphasis has been placed on the analysis of the effects of vessel impact, scour, and earthquake events in bridge design making the pile structural analysis more critical. Sometimes, these events will control the foundation design and the structural failure modes can govern the design. In such cases, the foundation design cannot be finalized by geotechnical considerations only so the foundation specialist needs an understanding of the structural aspects of driven pile design where substantial lateral loads are present.

This chapter deals with the static and dynamic structural pile capacity in terms of allowable stresses for pile materials. A driven pile has to remain within structural limits (stress and buckling) under static loading conditions during its service life as well as under dynamic, driving induced loads. Therefore, the material stress limits are placed on:

1. The maximum allowable driving stresses.
2. The maximum allowable design stress during the service life.

Driving stress limits, group layout, cap preliminary design, in-service stress limits, and buckling of piles are addressed in this chapter.

10.1 DRIVING STRESSES

In almost all cases, the highest stress levels occur in a pile during driving. High driving stresses are necessary to cause pile penetration. The pile must be stressed to overcome the ultimate soil resistance, plus any dynamic resistance forces, in order to be driven to support the pile design load. The high strain rate and temporary nature of the loading during pile driving allow a substantially higher driving stress limitation than for the static design case. Wave equation analyses can be used for predicting driving stresses prior to installation. During installation, dynamic testing can be used to monitor driving stresses.

10.2 FACTORS AFFECTING ALLOWABLE DESIGN STRESSES

Traditionally, the allowable design stress was determined by dividing the ultimate stress of the pile material by a factor of safety. The factor of safety was based on experience and included consideration of load and structural resistance variations. The allowable design stresses in this chapter are in conformance with AASHTO (2002) Standard Specification.

Allowable design stresses for piles, given in Article 4.5.7.3 of the AASHTO Standard Specification, are a function of the following variables:

1. Average section strength from an acceptance test such as:
 - a. f_y (yield strength) for steel piles.
 - b. f_c (unit ultimate strength from 28-day cylinder test for concrete).
 - c. Wood crushing strengths.
2. Reduction for defects such as knots in timber.
3. Reduction for section treatment such as preservation treatment of wood.
4. ϕ - factor which allows for variations in materials, construction dimensions, and calculation approximations. These items are partially under the engineer's control.
5. Factor of safety to account for the possibility that design service loads may be exceeded.
 - a. Among other causes, increase in load may occur due to overloads permitted on a bridge, pile mislocation, differential settlement and unaccounted negative shaft resistance or downdrag load.
 - b. Decrease in resistance offered by the pile may occur due to variability in pile material properties, corrosion, heave, or undetected driving induced damage.

10.3 AASTHO ALLOWABLE DESIGN AND DRIVING STRESSES

The limitations on maximum allowable static design stresses for driven piles in various codes generally represent the static capacity which can be consistently developed with traditional driving equipment and methods.

The pile material ultimate strength must be greater than the ultimate pile-soil resistance. In order that this is achieved, a factor of safety is applied to the material strength to obtain an allowable stress. The recommended AASHTO limits for maximum pile design stresses will generally keep the driving stresses within recommended limits. Allowable design stresses are covered in Article 4.5.7.3 of the AASHTO Standard Specification for Highway Bridges (2002) and driving stresses limits are presented in AASHTO Article 4.5.11.

10.3.1 Steel H-piles

a. Design Stresses

Table 10-1 contains the AASHTO recommended design and driving stresses for axially loaded steel H-piles in terms of the steel yield stress, f_y . AASHTO limits the maximum allowable design stress to $0.25 f_y$. In conditions where pile damage is unlikely, AASHTO allows the design stress to be increased to a maximum of $0.33 f_y$ provided static and/or dynamic load tests confirming satisfactory results are performed. As noted in Chapter 8, new H-piles now meet the requirements of ASTM A-572 steel with a yield strength of 345 MPa (50 ksi), and are no longer produced in A-36 steel. Design stresses of 86 to 114 MPa (12.5 to 16.5 ksi) are possible on these higher strength steel H-piles at 0.25 and $0.33 f_y$. For older A-36 steel with a yield stress of 248 MPa (36 ksi), a design stress of 0.25 to $0.33 f_y$ correspond to a design stress of 62 to 82 MPa (9.0 to 11.9 ksi).

b. Driving Stresses

AASHTO limits the maximum compression and tension driving stresses to $0.9 f_y$. For A-572 steel, this results in a maximum driving stress of 310 MPa (45 ksi) and, for older A-36 steel, this results in a maximum driving stress of 223 MPa (32.4 ksi).

TABLE 10-1 MAXIMUM ALLOWABLE STRESSES FOR STEEL H-PILES	
AASHTO (2002) Standard Specification Articles 4.5.7.3 and 4.5.11	
Design Stresses	$0.25 f_y$ $0.33 f_y$ If damage is unlikely, and confirming static and/or dynamic load tests are performed and evaluated by engineer.
Driving Stresses	$0.9 f_y$ 223 MPa (32.4 ksi) for ASTM A-36 ($f_y = 248$ MPa; 36 ksi) 310 MPa (45.0 ksi) for ASTM A-572 or A-690, ($f_y = 345$ MPa; 50 ksi)

10.3.2 Steel Pipe Piles (unfilled)

a. Design Stresses

Table 10-2 summarizes the AASHTO recommended design and driving stresses for axially loaded unfilled steel pipe piles in terms of the steel yield stress, f_y . The maximum AASHTO allowable design stress is limited to $0.25 f_y$. For ASTM A-252, Grade 2 steel with a yield stress of 241 MPa (35 ksi), this results in a maximum design stress of 60 MPa (8.75 ksi) and for Grade 3 steel with a yield stress of 310 MPa (45 ksi) this results in a design stress of 78 MPa (11.25 ksi). AASHTO allows the design stress to be increased to a maximum of $0.33 f_y$ in conditions where pile damage is unlikely. However, static and/or dynamic load tests confirming satisfactory results should be performed for design at this stress level. For ASTM A-252, Grade 2 steel, a design stress of $0.33 f_y$ corresponds to a design stress of 79 MPa (11.55 ksi) and for Grade 3 steel this corresponds to a design stress of 102 MPa (14.85 ksi).

b. Driving Stresses

AASHTO specifications limit the maximum allowable driving stresses to $0.9 f_y$. For A-252 Grade 2 steel, this results in a maximum driving stress of 217 MPa (31.5 ksi), and for Grade 3 steel, this corresponds to a maximum allowable driving stress of 279 MPa (40.5 ksi) .

TABLE 10-2 MAXIMUM ALLOWABLE STRESSES FOR UNFILLED STEEL PIPE PILES	
AASHTO (2002) Standard Specification Articles 4.5.7.3 and 4.5.11	
Design Stresses	$0.25 f_y$ $0.33 f_y$ If damage is unlikely, and confirming static and/or dynamic load tests are performed and evaluated by engineer.
Driving Stresses	$0.9 f_y$ 186 MPa (27.0 ksi) for ASTM A-252, Grade 1 ($f_y = 207$ MPa; 30 ksi) 217 MPa (31.5 ksi) for ASTM A-252, Grade 2 ($f_y = 241$ MPa; 35 ksi) 279 MPa (40.5 ksi) for ASTM A-252, Grade 3 ($f_y = 310$ MPa; 45 ksi)

10.3.3 Steel Pipe Piles (top driven and concrete filled)

a. Design Stresses

Table 10-3 summarizes AASHTO (2002) recommended design and driving stresses for axially loaded, top driven and concrete filled pipe piles in terms of the steel yield strength, f_y , and the concrete compressive strength, f'_c . These requirements are also applicable to Monotube piles. AASHTO limits the maximum allowable design stress to the sum of $0.25 f_y$ on the steel cross sectional area plus $0.40 f'_c$ on the concrete cross sectional area.

b. Driving Stresses

Concrete filled pipe piles are generally unfilled when driven. Hence, the AASHTO recommended driving stress for unfilled steel pipe piles apply.

TABLE 10-3 MAXIMUM ALLOWABLE STRESSES FOR TOP DRIVEN, CONCRETE FILLED, STEEL PIPE PILES	
	AASHTO (2002) Standard Specification Articles 4.5.7.3 and 4.5.11
Design Stresses	0.25 f_y (on steel area) <i>plus</i> 0.40 f'_c (on concrete area)
Driving Stresses	0.9 f_y 186 MPa (27.0 ksi) for ASTM A-252, Grade 1 ($f_y = 207$ MPa; 30 ksi) 217 MPa (31.5 ksi) for ASTM A-252, Grade 2 ($f_y = 241$ MPa; 35 ksi) 279 MPa (40.5 ksi) for ASTM A-252, Grade 3 ($f_y = 310$ MPa; 45 ksi)

10.3.4 Precast, Prestressed Concrete Piles

a. Design Stresses

Table 10-4 summarizes the AASHTO recommended design and driving stresses for axially loaded prestressed concrete piles in terms of the concrete compression strength, f'_c , and the effective prestress after losses, f_{pe} . Prestressed concrete piles fully embedded in soils providing lateral support are limited to a maximum design stress of $0.33 f'_c - 0.27 f_{pe}$ on the gross cross sectional area of the concrete. The concrete must have a minimum 28 day compression strength of 34.5 MPa (5.0 ksi)

b. Driving Stresses

AASHTO specifications limit the maximum allowable compression driving stress to 0.85 times the concrete compressive strength, f'_c , minus the effective prestress after losses, f_{pe} . In normal environments, tension driving stresses are limited to 0.25 times the square root of the concrete compressive strength plus the effective prestress after losses in SI units or 3 times the square root of the concrete compressive strength plus the effective prestress after losses in US units. In severe corrosive environments, maximum allowable tension stresses

10.3.5 Conventionally Reinforced Concrete Piles

a. Design Stresses

Table 10-5 summarizes the AASHTO recommended design and driving stresses for axially loaded reinforced concrete piles in terms of the concrete compression strength, f'_c , and the yield strength of the reinforcing steel, f_y . The recommended maximum allowable design stress is limited to $0.33 f'_c$ on the gross cross sectional area of the concrete. The concrete must have a minimum 28 day compression strength of 34.5 MPa (5.0 ksi).

b. Driving Stresses

AASHTO specifications limit the maximum allowable compression driving stress to $0.85 f'_c$ and the maximum tension driving stress to $0.70 f_y$.

Control of driving stresses is particularly important when driving reinforced concrete piles at high driving stress levels while penetrating through dense soil layers into underlying weaker soils. When the pile breaks through the dense layer with the hammer operating at a large stroke, the reduced pile toe resistance can cause a large tension stress to be reflected up the pile.

TABLE 10-5 MAXIMUM ALLOWABLE STRESSES FOR CONVENTIONALLY REINFORCED CONCRETE PILES	
	AASHTO (2002) Standard Specification Articles 4.5.7.3 and 4.5.11
Design Stresses	$0.33 f'_c$ (on gross concrete area) f'_c minimum of 34.5 MPa (5.0 ksi)
Driving Stresses	Compression Limit $< 0.85 f'_c$ Tension Limit $< 0.70 f_y$ (of steel reinforcement)

10.3.6 Timber Piles

a. Design Stresses

Table 10-6 summarizes AASHTO recommended design and driving stresses for axially loaded timber piles in terms of the maximum allowable design stress in compression parallel to the grain, σ_a . This value varies depending upon the timber species, and for the common species listed in the table below ranges from about 5.5 MPa to 8.3 MPa (0.8 to 1.2 ksi) The resulting maximum design load is based upon the allowable design stress times the pile toe area.

The engineer can specify species of timber piles but can seldom specify subspecies which have a wide range of strengths. There is a large natural variability of clear wood strength and natural growth imperfections which can also significantly affect wood strength. Therefore, while a high design stress may be allowed, engineering judgment must also be used, taking into account the above factors as well as the installation conditions.

b. Driving Stresses

AASHTO specifications limit maximum allowable compression and tension driving stresses to 3 times the allowable design stress from Table 10-6.

TABLE 10-6 MAXIMUM ALLOWABLE STRESSES FOR TIMBER PILES	
AASHTO (2002) Standard Specification Articles 4.5.7.3 and 4.5.11	
Design Stresses	5.5 to 8.3 MPa (0.8 to 1.2 ksi) (for pile toe area depending upon species) Southern Pine $\sigma_a = 8.3$ MPa (1.2 ksi) Douglas Fir $\sigma_a = 8.3$ MPa (1.2 ksi) Red Oak $\sigma_a = 7.6$ MPa (1.1 ksi) Eastern Hemlock $\sigma_a = 5.5$ MPa (0.8 ksi)
Driving Stresses	Compression Limit $< 3 \sigma_a$ Tension Limit $< 3 \sigma_a$ σ_a - AASHTO allowable working stress

10.4 GEOTECHNICAL AND STRUCTURAL LOADS

The problem of the design of a pile group subjected to a general set of loads is illustrated in Figure 10.1. The requirements that must be satisfied are:

1. The axial geotechnical capacity of the piles must be satisfactory in both compression and tension. Since moments are applied to the pile cap the individual pile loads will vary across the group. Bear in mind that a large number of load combinations can be present.
2. The lateral displacement of the pile group under service loads must not be excessive.
3. The structural strength of the piles under the effect of combined axial and lateral loads must be satisfactory. Since there are several load combinations it will usually not be obvious which pile in the group is critical in the structural case.

The first and second requirements will be satisfied in the geotechnical design process. However, it should be noted that several trial designs may be necessary to achieve a satisfactory and efficient design. In general, it can be seen from Figure 10.1 that it may be necessary to modify both pile capacity and pile spacing to obtain the best design. The larger the moments on the pile group the more complex the design process becomes. If the pile row spacing is larger the lateral load carried by the second and other rows is increased (see Table 9-19). On the other hand the pile cap cost will increase.

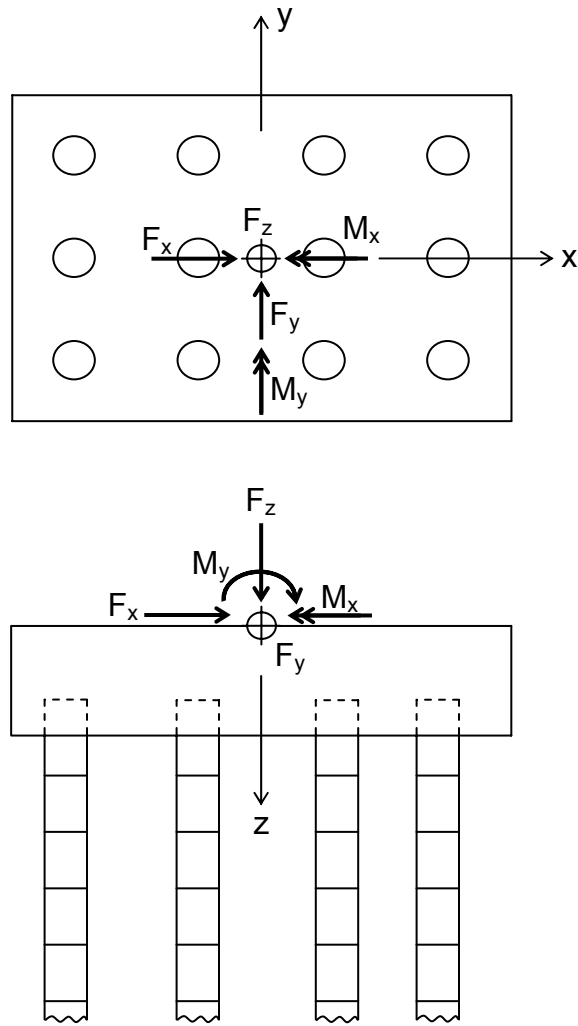


Figure 10.1. Pile Group with General Loads

10.5 LAYOUT OF PILE GROUPS

A group of piles is typically required to support large structural loads. An initial group layout must be determined to perform in-service stress checks. The possible loads are illustrated in Figure 10.1. The various load combinations, as given in Article 3.22 of the 2002 AASHTO Standard Specification, should be investigated to determine the pile stress conditions.

An initial, or trial, group layout may be computed dividing the factored axial load acting on the pile cap/group by the allowable capacity of a single pile, and then rounding the number up (say, by 15% or more, depending upon magnitude of the moments and lateral loads) to a constructible pile layout. Therefore, the number of piles is estimated as:

$$\frac{F_z}{Q_A} \cong \text{Number of piles (round-up)} \Rightarrow n$$

where:

F_z	=	largest factored, axial load of the superstructure
Q_A	=	allowable (geotechnical) axial load on a single pile
n	=	number of piles in group

Develop a trial configuration for the group of piles with this rounded-up number with a minimum center-to-center pile spacing of 0.75 m (2.5 ft) or 2.5 pile diameters, whichever is greater per AASHTO Article 4.5.15. Example pile group layouts can be found in CRSI Design Handbook (2002) and other sources.

This trial configuration should then be checked for single pile axial capacity adequacy under the combined superstructure axial loads and moments. The various factored load combinations, and not just the combination with the largest axial load, should be checked to determine the critical loading case. The maximum single pile axial load, q_s , may be computed as:

$$q_s = \frac{F_z + W_c + W_s}{n} \pm \frac{M_x y}{\sum y^2} \pm \frac{M_y x}{\sum x^2}$$

where:

F_z	=	factored, axial load of the superstructure acting upon the pile cap
W_c	=	estimated weight of pile cap

W_s	=	estimated weight of soil above pile cap, if applicable
n	=	number of piles in the group
M_x	=	factored, moment about the x axis acting on the pile cap
M_y	=	factored, moment about the y axis acting on the pile cap
x	=	distance along x-axis from the center of the column to each pile center
y	=	distance along y-axis from the center of the column to each pile center

Add one, or more, piles to the group or increase the pile spacing if $q_s > Q_A$ and recompute the maximum single pile axial load (q_s). If the moments in one direction are substantially larger than the other it may be desirable to make the cap unsymmetric.

10.6 PRELIMINARY DESIGN OF PILE CAPS

The purpose of this section is to provide guidelines to develop a preliminary size of a pile cap for the purposes of cost estimating. Information for complete, comprehensive structural design is beyond the scope of this manual, and not presented here.

The design and size of the pile cap is dependent on the pile group layout, pile loads, and superstructure loads. Thus, an iterative design is required to optimize overall economics. The horizontal dimensions of the pile cap for the trial pile group configuration may be estimated by using the minimum center-to-center pile spacing and, per AASTHO Article 4.5.15, a minimum edge of cap to pile distance of 230 mm (9 inches). Maximum width and/or length of pile cap may be dictated by project constraints.

The thickness of the pile cap is a sum of the pile embedment into the cap, clear space between the cap reinforcing steel and the top of (embedded) piles, and thickness required for structural support. Per AASTHO Article 4.5.15.1.2, the piles shall project not less than 300 mm (12 inches) into the cap after damaged pile material has been removed, though in special cases it may be reduced to 150 mm (6 inches). The reinforced concrete must be designed with consideration of flexure and shear, for the factored loads. Potential shear failures include punching about a single pile, punching about a pair of piles, punching of the (superstructure) column, and across the widths of the cap.

An initial, trial total (including pile embedment and 75 mm (3 inches) clear space between top of piles and reinforcing steel) thickness of the pile cap may be estimated from experience, agency guidelines or standards, or with the following equation.

$$t_{\text{cap}} \text{ (mm)} \approx \frac{Q_A \text{ (kN)}}{2} + 750$$

$$t_{\text{cap}} \text{ (inches)} \approx \frac{Q_A \text{ (tons)}}{6} + 30$$

This initial, trial thickness should be refined by examining punching shear, beam shear, and bending in the reinforced concrete pile cap. Equations for these preliminary calculation steps are shown below.

1. Determine dimensions for computations

a. Select a trial total thickness of cap, D.

b. Determine effective depth to concrete reinforcement, d.

$$d = D - \text{pile embedment} - \text{clear space} - \text{distance to center of steel}$$

i. assume pile embedment distance into cap = 300 mm (12 inches).
The pile embedment is suggested to be 12 inches. However, it can be as little as 150 mm (6 inches)

ii. assume clear space between top of pile and concrete reinforcement = 75 mm (3 inches)

iii. assume distance up to center of steel reinforcement = $1\frac{1}{2}$ x bar diameter

c. Determine critical punching shear perimeter, b_o , around the column. The shear force applied the shear perimeter is the load acting outside that perimeter.

i. For square columns

$$b_o = 4(c + d)$$

ii. For rectangular columns

$$b_o = 2(c_1 + c_2 + 2d)$$

iii. For circular column

$$b_o = (c_o + d)$$

with c = column side for square columns

c_1 = small column side for rectangular columns

c_2 = large column side for rectangular columns

c_o = column diameter

2. Check punching shear at $d/2$ from column

a. $v \leq v_c$ per AASHTO Article 8.15.5.6

b. compute total applied design shear stress at critical section, v

$$v = \frac{n_o Q_A}{b_o d}$$

c. nominal shear strength of concrete, per AASHTO Article 8.15.5.6.3

$$v_c = [0.8 + 2/\beta_c] \sqrt{f'_c} \leq 1.8 \sqrt{f'_c}$$

where: β_c = the ratio of the long side to the short side of the loaded area.

v = design shear stress

v_c = nominal shear strength of concrete

n_o = number of piles whose center lie outside of b_o

3. Check beam shear, per AASHTO Article 8.15.5.6.1

a. Determine beam shear distance from center of the column to the critical section, per AASHTO Article 4.4.11.3.2

$$\text{Beam Shear } D = \frac{c}{2} + \frac{d}{2}$$

for circular columns, use an equivalent area square section and c

b. For each direction of pile cap, check number of piles that lie outside of the critical section. Where the critical section passes through the pile cross

section, the applied load is proportioned based on the amount of pile section within the critical section as per AASHTO Article 4.4.11.3.2.

c. $v \leq v_c$ per AASHTO Article 8.15.5.6

d. Shear load and stress

$$V = n_c \times Q_A$$

$$v = \frac{n_c Q_A}{w d}$$

e. nominal shear strength of concrete subject to shear and bending, per AASHTO Article 8.15.5.2.1

$$v_c = 0.95 \sqrt{f'_c}$$

where:

- V = design shear load
- v = design shear stress
- v_c = nominal shear strength of concrete
- n_c = no. of piles whose center lie outside critical shear line plus the percentage of load from the piles that intersect the critical shear plane.
- w = width of pile cap (in applicable direction)

4. Check bending

a. Compute bending moment, for each direction of pile cap, from piles to edge of column.

$$M_u = \sum Q_A \text{ arm}$$

The term arm refers to the distance from the edge of the column to each pile.

The moment capacity of a reinforced concrete beam is determined based on the assumption of a rectangular distribution of the compression stress in the concrete at failure. The design must fail by yield in the tension steel to assure

ductility. The area of steel required per AASHTO Article 8.16.3.2 can be computed with the following equations:

$$M_u = \phi M_n = \phi \left[A_s f_y \left(d - \frac{a}{2} \right) \right]$$

where a is the depth of the rectangular compression stress block

$$a = \frac{A_s f_y}{0.85 f_c' b}$$

The equation for moment strength, M_n , can be solved for the area of steel, A_s . However, $a/2$ is small compared with d so an approximate value can be assumed for $a/2$, A_s can be calculated and the steel area adjusted to arrive at a satisfactory A_s . If $d - a/2$ is assumed to be $0.9d$, A_s will be quite close and it will be satisfactory for preliminary design. If an improved A_s is desired it can be obtained made by determining an improved a with a knowledge of the preliminary A_s and with the new a the next cycle of A_s can be determined and it will probably be final.

A_s/bd is called the reinforcement ratio, ρ . The case where failure occurs in the steel at the same time as in the concrete is called balanced design and the associated reinforcement ratio is ρ_b . Failure in the concrete is assumed to take place at 0.003 strain. The reinforcement ratio must be less than $0.75\rho_b$ to assure that the bending failure takes place by yielding in the steel. ρ_b can be determined from

$$\rho_b = [0.85\beta_1 f_c'] / f_y [87,000 / (87,000 + f_y)]$$

where β_1 is 0.85 for concrete strengths up to and including 4,000 psi. For concrete strengths above 4,000 psi it shall be reduced at a rate of 0.05 for each 1,000 psi but not less than 0.65. Values for ρ_b are available in concrete design textbooks or design manuals.

Per AASHTO Article 8.17.1.2, the minimum reinforcement should be at least one-third greater than that required by analysis to waive requirements of 8.17.2.1. Therefore, increase minimum area of steel to:

$$A_s = \frac{4}{3} (A_{s\text{-initial}})$$

The final, structural design of pile caps is beyond the scope of this manual. See AASHTO (2002), ACI (1997), etc. for guidance on detailed structural design.

10.7 STRUCTURAL PROPERTIES OF PILES

The largest stresses in piles occur at the greatest distance from the neutral axis. This is at the outer edge(s) of a single pile and at the outer edge of the outermost piles of a group. Under combined axial and bending loading, the pile area (A), the stiffness or moment of inertia (I), and distance from neutral axis to the edge of the section (c) must be defined to check maximum stress.

The moment of inertia for various shapes may be computed with the following equations.

for solid, circular sections:

$$I = \frac{\pi (\text{O.D.})^4}{64}$$

for (circular) pipe sections:

$$I = \frac{\pi [(\text{O.D.})^4 - (\text{I.D.})^4]}{64}$$

where : O.D. = outside diameter
 I.D. = inside diameter

for solid, square sections:

$$I = \frac{d^4}{3}$$

where : d = width/height of square

It is also convenient to compute the elastic section modulus (S) for the structural analysis. S is simply the moment of inertia divided by the distance to the outermost element, so

$$S = \frac{I}{c}$$

where : c = distance from centroid to outer edge

The structural properties of common pile sections are presented in Appendix C.

10.8 DESIGN OF PILES FOR COMBINED AXIAL AND LATERAL LOADS

10.8.1 Structural Design of Driven Piles for Axial Loads by ASD

Consider first the traditional limits that have been used historically for allowable stress design of piles. Code limitations were placed on the allowable axial pile stress under design load. Little if any emphasis was placed on geotechnical limitations and the allowable axial pile stress was based on an extended experience with the axial driving stresses. These limits were selected primarily to assure that the pile could be driven to a required capacity without damage. The resulting allowable stresses were misunderstood to be limits on the stresses that could be safely applied to the pile material from a structural point of view. This is not true. For example, the allowable stress that was commonly permitted on steel piles was $0.25 f_y$ but it is obvious that much higher design stresses could be applied to the steel before structural failure occurred. A commonly used allowable stress for laterally supported compression member is $0.6 f_y$. Even when a driveability analysis by wave equation was required these allowable stresses continued to be specified.

The actual explanation for the use of this allowable stress comes from the practice several decades ago of the use of 248 MPa (36 ksi) yield point steel with the traditional air hammer and a pile driving formula such as Engineering News. With the typical stroke of three feet for these hammers and an efficiency of about 65 percent, the effective, transmitted impact velocity will be about 3.0 to 3.7 meters/second (10 to 12 feet/second). This impact velocity will deliver a peak impact stress to the pile top of about 124 to 138 MPa (18 to 20 ksi). If a factor of safety of about 2.0 is assumed this produces a design stress of about 62 MPa (9 ksi) or $0.25 f_y$ for A36 steel with its 248 MPa (36 ksi) yield point. If a larger capacity is desired a higher impact stress is required and the common air hammers of forty years ago could not be depended on to achieve

that. This rather crude description will not cover all cases of pile driving but it, rather generally, defines how the limitation came about and these limitations were arrived at by experience not a rational analysis. With an allowable stress of this magnitude driving to a blow count defined by a dynamic formula with an air hammer, pile damage did not usually occur.

Today, many modern diesel or hydraulic hammers will deliver much higher impact velocities. But, some of the old traditional approaches are still with us. The AASHTO Standard Specification (2002) contains an allowable design stress of $0.25 f_y$ (Article 4.5.7.3). However, it also allows design stresses up to $0.33 f_y$ “in conditions where pile damage is unlikely.” With the advent of 345 MPa (50 ksi) steel, an allowable stress of about 83 MPa (12 ksi) becomes possible and $0.33 f_y$ gives a much larger allowable of 110 MPa (16 ksi). With a factor of safety of 2.0 the associated ultimate stress is 220 MPa (32 ksi). To achieve this ultimate stress a driving stress near the limiting value that can be achieved by a high impact velocity hammer will be required.

The allowable axial compression stresses for all pile types are given in Article 4.5.7.3 of the AASHTO Standard Specification. The allowable load on concrete filled steel pipe piles is $0.25 f_y A_s + 0.40 f_c A_c$. Prestressed concrete piles have an allowable load of $0.33 f_c A_c - 0.27 f_{pe} A_{ps}$. Allowable stresses for timber piles are given in Table 4.5.7.3A. And of course, the allowable steel stresses are limited to $0.25 f_y$ and $0.33 f_y$ as discussed above. This specification also specifies factors of safety on the geotechnical axial strength in Table 4.5.6.2A.

In addition to the allowable pile material stresses, the AASHTO Standard Specification states in Article 4.5.9 that the Engineer “should” evaluate “constructability” of a pile foundation using a wave equation analysis. Allowable maximum driving stresses are given in Article 4.5.11. It may be concluded that the limiting material design stresses are redundant except for the case where the geotechnical capacity is established by the use of a driving formula.

The Allowable Stress Design loads and load combinations to be used in design are specified in the first part of Table 3.22.1A. A total of 11 different load combinations are given and all of them must be satisfied. The details and definitions of the loads and their application are discussed in Section 3 of the AASHTO Standard Specification.

Consider a very brief summary of the structural design process for axial loads only that is implied by the AASHTO Standard Specification, Allowable Stress Design provisions.

1. A pile type and design load is selected for a pile.
2. The method of capacity determination is selected and, with that, the factor of safety is determined from the AASHTO Standard Specification, Table 4.5.6.2A.
3. The allowable stress for the pile material is obtained from the AASHTO Specification Article 4.5.7.3 and the pile cross section is selected to carry the required design load.
4. The pile length required to carry the ultimate axial load determined with the factor of safety applied to the specified design loads is determined from geotechnical considerations.
5. Driveability is then evaluated by wave equation analysis. It is possible that the limiting driving stresses can not be satisfied and a larger pile section or a smaller design load may have to be selected but this is unlikely. Thus, it can be seen that there is redundancy in specifying allowable pile stresses and also driveability limits. But, the driveability limits must be included.

10.8.2 Structural Design of Driven Piles for Combined Axial and Lateral Loads by ASD

In Article 4.5.6.5 of the AASHTO Standard Specification a lateral load analysis is specified to determine the horizontal displacement. Reference is made to an analysis to evaluate structural strength and deflection with a reference to the work of Reese (1984). References are also made to the approximate methods of Broms (1964) and Singh et al (1971). However, the statement is made that the strength analysis based on Broms or Singh is only appropriate in a preliminary analysis.

Over the past two decades it has become common to perform a structural analysis for lateral loads and extensive software has been developed to perform the analysis as referenced in Chapter 9 of this manual. Section 9.7.3.3 of Chapter 9 discusses the LPILE computer program for the analysis of single piles. The geotechnical design of pile groups is discussed in detail in Section 9.8 of Chapter 9. When designing pile groups for both axial and lateral loads the designer should be aware of the FB-Pier program developed at the University of Florida for the Florida DOT. This program can perform a general analysis of pile foundations and can include pile cap, pier and superstructure. A single pile analysis can be used and the pile group analyses can be

assembled from the single pile analysis. The lateral soil resistance will be affected by the shading from multiple rows of piles as discussed in Section 9.8.4 of Chapter 9.

The behavior of a single pile under the action of a lateral load is illustrated in Figure 9.44. The geotechnical engineer must represent the lateral soil resistance response using the soil model shown. Both the nonlinear soil response of the individual springs and the distribution of the resistance along the pile length must be defined. An additional consideration that must be established is the fixity condition at the pile head. In many cases of single piles the pile head may be free to rotate. However, if the pile head is embedded in a pile cap it is likely that the pile head will be fixed. The assumed pile head condition can radically affect the maximum moment in the pile. If the pile head is assumed fixed the maximum moment will be at the pile head while if the pile head is pinned the maximum moment will be at some point along the pile below the pile head. The pinned condition will produce a much smaller maximum moment in the pile than does the fixed head condition.

An approach to the structural design of pile groups subjected to a general set of loads will be discussed. As noted above, the AASHTO Standard Specification, Section 4, Foundations makes only a very general reference to this problem. Current practice will be covered using the requirements from the AASHTO Standard Specification Sections on the particular structural material. The limitations given in AASHTO Sections 8, 9, 10 and 13 provide guidance that can be used to govern driven pile structural design

The central problem becomes the analysis of an individual pile in the group for the combined bending and axial loads applied to that particular pile in the group.

10.8.2.1 Timber Piles

Consider first the analysis of a timber pile group. The structural design of timber piles is not covered specifically in the AASHTO Standard Specification. The stress in the pile can be calculated from the expression:

$$f_c = \frac{P}{A} \pm \frac{M_y}{S} \pm \frac{M_x}{S} \quad \text{Equation 10-1}$$

where P is the applied axial load on the pile, A is the pile cross sectional area, M_x and M_y are the moments about the x and y axes of the pile, respectively, and S is the section modulus of the pile cross section. The values for P are found by the analysis of

the pile group response to the vertical and moment loads on the pile cap shown in Figure 1. The values of M_x and M_y are determined by the lateral pile analysis discussed in Section 9.7.3 of Chapter 9 of this manual. Since the cross section is assumed circular the section modulus is independent of the reference axes. The allowable stress for timber is given in Article 13.7.3.2 of the AASHTO Standard Specification and is specified to be:

$$F'_c = F_c C_D C_P \quad \text{Equation 10-2}$$

where F_c is the allowable compression stress given in Table 13.5.2A for the wet service condition, C_D is the load duration factor given in Table 13.5.5A and C_P is the column stability factor given in Article 13.7.3.3.

10.8.2.2 Steel Piles

The structural design of steel piles is not discussed specifically in the AASHTO Standard Specification. The cross section design of compression members is discussed in AASHTO Article 10.35.2. (There are a number of limitations on plate thicknesses that must be satisfied.) Steel piles are designed for capacity to satisfy the requirements of AASHTO Article 10.36, Combined Stresses. These limitations are based on an allowable steel stress including the effect of combined bending and axial loads. The conditions that must be dealt with are as described for timber piles including the problem of dealing with a number of load combinations for a typical pile group shown in Figure 10.1. The three conditions presented above for timber piles in Equation 10-1 must also be satisfied for steel piles that are fully embedded in the ground.

For pipe piles:

$$f_c = \frac{P}{A} \pm \frac{M_y}{S} \pm \frac{M_x}{S} \quad \text{Equation 10-1}$$

For H-Piles:

$$f_c = \frac{P}{A} \pm \frac{M_y}{S_y} \pm \frac{M_x}{S_x} \quad \text{Equation 10-1a}$$

The determination of the structural capacity of a partially unsupported steel pile as specified in AASHTO Article 10.36 will be summarized here. Two interaction requirements must be satisfied as follows

$$\frac{f_a}{F_a} + \frac{C_{mx} f_{bx}}{\left(1 - \frac{f_a}{F'_e}\right) F_{bx}} + \frac{C_{my} f_{by}}{\left(1 - \frac{f_a}{F'_e}\right) F_{by}} \leq 1.0 \quad \text{Equation 10-3}$$

and

$$\frac{f_a}{0.472F_y} + \frac{f_{bx}}{F_{bx}} + \frac{f_{by}}{F_{by}} \leq 1.0 \text{ (at points of support)} \quad \text{Equation 10-4}$$

where

$$F'_e = \frac{\pi^2 E}{F.S. (K_b L_b / r_b)^2} \quad \text{Equation 10-5}$$

- f_a = computed axial stress;
- f_{bx} or f_{by} = computed compressive bending stress about the x axis and y axis, respectively;
- F_a = axial stress that would be permitted if axial force alone existed, regardless of the plane of bending;
- F_{bx}, F_{by} = compressive bending stress that would be permitted if bending moment alone existed about the x axis and the y axis, respectively, as evaluated according to AASHTO Table 10.32.1A
- F'_e = Euler buckling stress divided by a factor of safety;
- E = modulus of elasticity of steel;
- K_b = effective length factor in the plane of bending from AASHTO Appendix C;
- L_b = actual unbraced length in the plane of bending; The unbraced length must include the effect of the lateral soil resistance for the embedded length of the pile.
- r_b = Radius of gyration in the plane of bending;
- C_{mx}, C_{my} = coefficient about the x axis and y axis, respectively, whose value is taken from AASHTO Table 10.36A;
- $F.S.$ = Factor of safety = 2.12.

In most cases of driven pile design, the pile will be fully embedded so Equation 10-1 will govern.

The above limitations are familiar to the structural designer from their use in steel column design. The allowable stresses are given in Table 10.32.1A of the AASHTO Standard Specification (2002).

10.8.2.3 Prestressed Concrete Piles

The structural design of prestressed concrete piles is not discussed in the AASHTO Standard Specification. AASHTO contains two major Sections dealing with concrete structures – Sections 8 and 9. AASHTO Section 9 deals specifically with the design of prestressed concrete structures. However, it makes no mention of the design of either piles or prestressed concrete compression members, probably because prestressed concrete columns are not commonly used in bridge structures or any other structure for that matter. AASHTO Section 8 is titled Reinforced Concrete. It also does not deal specifically with piles but it does have a clear treatment of reinforced concrete compression members. The methods specified will be reviewed.

Allowable Stress Design is called Service Load Design in the AASHTO Standard Specification and it is covered in AASHTO Article 8.15. AASHTO Article 8.15.4, Compression Members, states, “The combined flexural and axial load capacity of compression members shall be taken as 35 percent of that computed in accordance the provisions of Article 8.16.4.” All of reinforced concrete performance is now analyzed on a strength basis so calculated stresses are not determined. To use the calculated strengths in the ASD format they are reduced to 35 percent of the ultimate values and compared with the working loads determined by ASD. Other provisions are also contained in this Article. The fundamental problem is that an elastic analysis of concrete compression members produces very poor results due to the substantial time dependent deformations that occur in concrete members loaded in compression. If the loads introduce both axial and bending forces the problems are particularly difficult.

In order to apply AASHTO Article 8.16.4 to prestressed concrete piles subjected to combined bending and axial loads some suggestions are offered. The design axial strength at zero eccentricity specified in AASHTO Equation (8-31) could be replaced by

$$P_0 = 0.85 f_c (A_g - A^*_s) - A^*_s f_{se} \quad \text{Equation 10-6}$$

where f'_c is the concrete cylinder strength, A_g is the area of the gross concrete section, A^*_s is the area of the prestressing steel and f_{se} is the effective prestress. In this strength estimate, the effective prestress force is subtracted from the axial compression strength of the concrete. In the extreme compression load case, the effective prestress would have been reduced by the compression deformations but probably there would still be prestress force active at the concrete compression failure. Therefore, this strength estimate should be conservative since the full effective prestress is subtracted from the capacity. The design axial strength at balanced conditions, P_b , given in AASHTO Equation (8-32) can be replaced by

$$P_b = 0.85 f'_c b a_b - A^*_{st} f_{se} \quad \text{Equation 10-7}$$

where b is the pile width, a_b is the distance from the extreme compression fiber to the bottom of the compression block and A^*_{st} is that portion of the prestressing steel that will act in tension in the balanced failure condition. The value of a_b can be estimated from

$$a_b = \frac{87,000}{(87,000 + f_{se})} \quad \text{Equation 10-8}$$

This estimate of a_b has been generated by Goble (2005). It should provide a conservative value of a_b . The expression for balanced moment can be estimated from

$$M_b = 0.85 f'_c b a_b (d - d'' - a_b/2) + A^*_{st} f_{se} d'' \quad \text{Equation 10-9}$$

where d is the distance from the extreme compression fiber to the tension prestressing steel, d'' is the distance from the tension prestressing steel to the centroid of the gross section and A^*_{st} is the area of the prestressing steel that acts in tension to resist the balanced moment.

With the above quantities determined the combined bending and axial capacity can be determined from the interaction expressions given in AASHTO Article 8.16.4.3. When the three values described above have been calculated it is a reasonably simple task to determine the allowable capacity. However, the analysis of a large pile group with a number of load combinations would be a time consuming task. Alternatively, the use of computer software such as FB Pier can give a much more reliable answer with considerably less effort.

10.8.2.3.1 Concrete Pile Interaction Analysis

In the general case, a pile cap will be loaded at its center with a vertical load, two orthogonal lateral loads and two orthogonal bending moments as shown in Figure 10.1. Actually, the loads may be applied at the column top but they can be transferred to the pile cap or the total structure can be analyzed. Horizontal soil resistance forces will be mobilized on the piles and may also act on the faces of the pile cap. Figure 10.1 illustrates this condition for a 12 pile group.

A numerical analysis can be performed by discretizing the piles into elements of finite length as shown in Figure 10.1. Soil resistance forces are prescribed along the pile lengths in the form of a response resistance-displacement relationship. The analysis process applies the forces to the pile cap incrementally and the displacements and member forces are determined in the analysis. Since the soil response will be nonlinear the loads must be applied incrementally until the maximum load is reached or failure occurs.

The analysis of the prestressed concrete section response to a combination of an axial load and two orthogonal moments is complex. A successful and practical approach to the analysis of the pile cross section is offered by the FB-Pier Program. The concrete and the prestressing steel stress strain relationships are assumed. An example is illustrated in Figure 10.2. For concrete, the FB-Pier program assumes a maximum concrete strength of $0.85f_c$ to include loading time effects on the concrete strength and all points on the stress strain curve are reduced to 85 percent of the short time values.

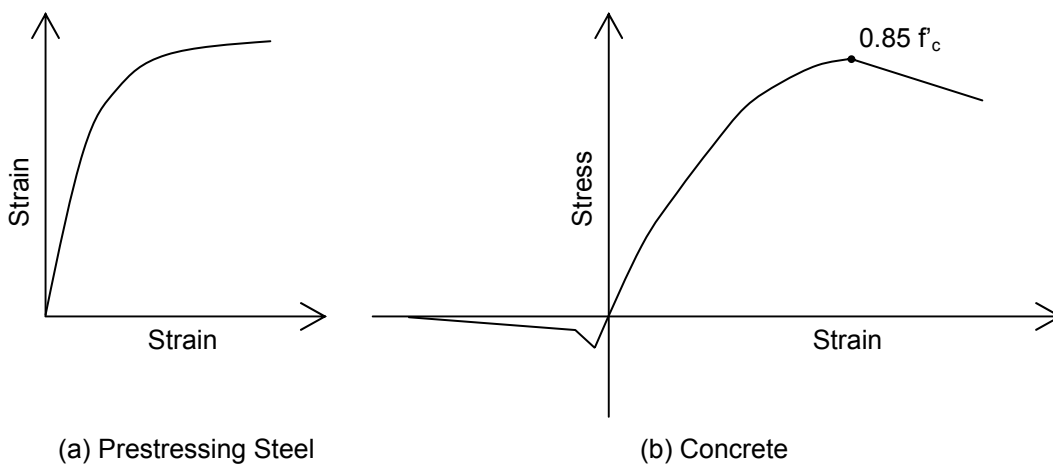


Figure 10.2 Assumed Material Stress Strain Curves

Bi-axial interaction diagrams are determined for each of an increasing set of axial loads up to the maximum axial strength condition. An illustration of one of these interaction diagrams for a particular axial load is shown in Figure 10.3. These diagrams are determined for the entire range of axial loads up to the axial failure case. With increasing axial load the maximum moment strength becomes smaller. A three dimensional interaction diagram can then be constructed with the axial load on the vertical axis and a particular interaction diagram at each level of axial load. Imagine a stack of these interaction diagrams. Thus, a three dimensional failure surface is defined. The equation of the failure surface can be generated by fitting a surface through the interaction diagrams at each level.

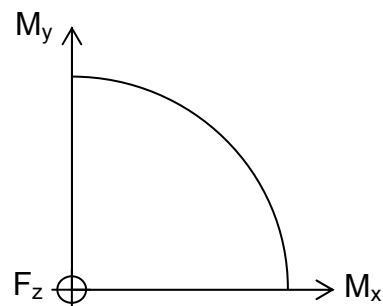


Figure 10.3 Pile Interaction Diagram

When the necessary failure surfaces are available the analysis at a particular load level can be checked by examining whether the vector of the forces on the section (axial, M_x and M_y) falls within or outside the failure envelope. The deformations associated with the three applied forces make it possible to determine the displacements associated with the various load levels. This elegant and powerful analysis algorithm produces excellent results. Well-designed graphics make it possible for the foundation specialist to easily evaluate the results.

The analysis has been discussed for prestressed concrete piles and they are probably the most challenging to deal with. FB-Pier can also analyze steel piles and concrete filled pipes using the same concepts described above.

10.9 UNSUPPORTED LENGTH AND BUCKLING

A pile or a pile group may have a portion of its length that is laterally unsupported. Examples of this are piles in water, piles after scour has occurred, and piles in very weak soil not capable of providing adequate lateral support to prevent buckling.

Potential buckling of the unsupported length of the pile, i.e., column length, must be checked. In these cases, the maximum supportable pile load may be controlled by buckling, and not by unit stress. The unbraced length must include the effect of the lateral soil resistance for the embedded length of the pile. A procedure for determining the effective length was proposed by Davisson and Robinson (1965).

Per Article 4.5.7.2 of AASHTO, the structural design provisions for compression members of AASHTO Sections 8, 9, 10, and 13 apply, except: timber piles shall be designed in accordance with Article 13.5 using the allowable unit stresses given in Article 13.2 and Table 4.5.7.3.A.

10.9.1 Timber Piles

For timber piles with unsupported length, the maximum allowable compression stress should be reduced by the column stability factor, C_P , of Equation 10-2. The formula for calculating the column stability factor is provided in AASHTO code Article 13.7.3.3.5.

10.9.2 Steel Piles

The maximum unsupported length for steel piles should be determined by satisfying the requirements of Equation 10-5, the Euler buckling stress formula.

10.9.3 Prestressed Concrete Piles

For prestressed concrete pile, it is recommended that maximum design stress computed from Table 10-4 be limited to L/r values of 60 where L is the unsupported length and r is the radius of gyration. For piles fully fixed at both ends, L may be taken as 0.5 times the length between the assumed points of fixity. For piles fully fixed at one end and hinged at the other, it is recommended that L be taken as 0.7 times the length between the hinge and assumed point of fixity.

REFERENCES

- ACI (1997), SP-17 Design Handbook: Beams, One-Way Slabs, Brackets, Footings, Pile Caps, Columns, Two-Way Slabs, and Seismic Design in Accordance with the Strength Design Method of 318-95; American Concrete Institute, Farmington Hills, MI, 482 p.
- American Association of State Highway and Transportation Officials [AASHTO], (2002). Standard Specifications for Highway Bridges, Seventeenth Edition, Washington D.C.
- Broms, B.B. (1964a). Lateral Resistance of Piles in Cohesive Soils. American Society of Civil Engineers, Journal for Soil Mechanics and Foundation Engineering, Vol. 90, SM2, 27-63.
- Broms, B.B. (1964b). Lateral Resistance of Piles in Cohesionless Soils. American Society of Civil Engineers, Journal for Soil Mechanics and Foundation Engineering, Vol. 90, SM3, 123-156.
- CRSI (2002), CRSI Design Handbook, Concrete Reinforcing Steel Institute, Schaumburg, IL.
- Davisson, M.T. and K.E. Robinson. (1965). "Bending and Buckling of Partially Embedded Piles." in Proceedings Sixth International Conference on Soil Mechanics and Foundation Engineering, University of Toronto Press. Montreal, pp 243-246.
- Goble, G.G. (2005). Personal communication.
- Reese, L.C. (1984). Handbook on Design of Piles and Drilled Shafts Under Lateral Load. Report No. FHWA-IP-84-11, U.S. Department of Transportation, Federal Highway Administration, Office of Implementation, Washington, D.C., 386.

Chapter 11 CONTRACT DOCUMENTS

11.1 OVERVIEW OF PLAN AND SPECIFICATION REQUIREMENTS

Pile foundations generally cannot be inspected after installation. Therefore, construction specifications and control are of prime importance for a successful pile foundation. Preparation of the contract plan details and construction specifications related to piling issues are the responsibility of the foundation designer in cooperation with materials and construction personnel. Project plans should include:

- Location of piles.
- Designation to identify piles.
- Pile cut off elevation.
- Estimated pile toe elevation.
- Minimum pile toe elevation.
- Required pile batter and direction.
- Orientation of H-piles.
- Ultimate pile capacity.
- Location of soil borings.
- Results of subsurface exploration.

It is the designer's responsibility to confirm that plans and specifications have been prepared using compatible language. This is particularly true in defining the required pile capacity, which is an important component of any driven pile specification. Problems can arise when modern dynamic methods, which use ultimate pile capacity, are mixed with specifications written for a dynamic formula that uses allowable pile capacity. For example, plans stating "piles shall be driven to a safe bearing of 1000 kN (225 kips)" may have been suitably worded when construction control was performed with the Engineering News formula, which uses the allowable design load. However, this type of wording with modern dynamic methods creates confusion and could result in piles being driven to only the design load, or to a claim for overdriving. Construction plans should therefore indicate the ultimate pile capacity. This ultimate capacity should include an appropriate factor of safety on the design load as well as the resistances from any unsuitable support layers.

This chapter includes a generic pile specification that was developed with input from State and Federal bridge and geotechnical engineers. The generic specification, originally released in 1985 as FHWA Geotechnical Guideline 13, has been slightly modified and updated as necessary. AASHTO (2002) contains similar specifications without commentary.

The intent of the attached generic specification is to provide designers and highway agencies with a comprehensive driven pile specification. Commentary sections are included where appropriate to explain the reasons behind development of particular sections of the specification and the relationship of the specification requirements to necessary pile design or construction activities. Note that only driven piles are covered by the specification. Other deep foundation types such as drilled shafts require completely different construction controls and should not be included in a driven pile specification.

A good driven pile specification should include the following basic components:

1. Pile Material Details
 - Material type and section.
 - Material grade and strength.
 - Splice details.
 - Toe protection requirement.
 - Coating details.
 - Transportation and handling.

2. Driving System Requirements
 - Hammer.
 - Hammer and pile cushions.
 - Helmet and inserts.
 - Pile leads.

3. Installation Issues
 - Driving sequence.
 - Pile location tolerances.
 - Pile alignment tolerances.
 - Pile cutoff.
 - Use of followers.
 - Use of jetting.
 - Use of spudding.
 - Predrilling.
 - Pile heave.

- Pile cap connection.
 - Pile rejection criteria
4. Capacity Verification
- Static load testing.
 - Dynamic testing.
 - Wave equation analysis.
 - Dynamic formulas.
5. Basis of Payment
- Method of measurement.
 - Payment items.

11.2 BACKGROUND AND REASONS FOR SPECIFICATION IMPROVEMENT

Older pile specifications placed the major responsibilities for pile capacity determination on the field staff. Little analysis was done in the design stage to provide accurate estimates of the required pile length to safely support the design load. Nor did many design analyses account for the actual soil resistance which had to be overcome to drive the pile to the estimated length, or the stresses generated in the pile during driving. Older specifications frequently placed the responsibility for determining what pile length to order on the contractor. Delays for reordering additional lengths or splices to reach final penetration requirements were considered incidental to the price bid for the item. This resulted in higher bid prices due to the unknown risks associated with the pile item.

Procedures, equipment, and analysis methods now exist to permit the designer to accurately establish pile section and length for any driving condition. Basic foundation design procedures are routinely followed by nearly all public agencies. Much of this design information is neither reflected in the pile specification of the agency nor utilized by the agencies construction staff. Many agencies perform detailed static analyses to determine pile length, but control the pile length actually installed in the field with the unreliable Engineering News formula. Changes are required in pile specifications to permit the cost effective use of modern construction control methods. The five areas of major change are briefly explained below as well as in commentary sections of the attached driven pile specification.

1. **Ordered Length Replaces Estimated Length:** Public highway agencies should assume responsibility for determining and placing in the contract documents the pile

length necessary to safely support the design load. Costs associated with overruns or underruns due to inaccurate length determination should not be borne by the contractor. The attached specification is based on the highway agency performing an adequate subsurface exploration and design analyses to rationally establish pile lengths during the design phase.

2. **Ultimate Pile Capacity Replaces Design Load:** Installation of piling to a predetermined length involves overcoming the design soil resistance, multiplied by the safety factor in suitable pile supporting layers, plus the resistance in any overlying layers unsuitable for long term support. The use of procedures involving design load, such as the Engineering News formula, should be replaced with ultimate load based methods. The ultimate pile load should be based on both the actual resistance to be overcome to reach the required penetration depth and the confidence in the method of construction control to be used. The attached specification is written in terms of ultimate load.
3. **Increased Emphasis on Approval of Driving Equipment:** The use of properly sized pile driving equipment will practically insure a successful installation of properly designed piles. Conversely, improperly sized pile driving equipment insures a pile project fraught with problems, regardless of how well the pile design was done. Too small a pile hammer results in extremely difficult, time consuming driving. Too large a pile hammer increases the risk of pile damage. The attached specification places great emphasis on a formal approval procedure for the hammer and driving system. This approval procedure is the most significant change to current specifications.
4. **Pile Capacity Control by Modern Methods Instead of Dynamic Formulas:** Good piling practice dictates use of the wave equation and dynamic pile testing to replace the use of dynamic formulas to monitor pile driving on all projects. Continued use of the Engineering News formula can only result in unreliable, costly pile foundations.

Highway agencies need to utilize modern methods in both design and construction control of pile foundations. The wave equation uses ultimate soil resistances, basic soil properties, and calculated pile lengths in conjunction with driving equipment characteristics to determine the necessary pile penetration resistance for the ultimate capacity, as well as the maximum pile stresses during driving. Dynamic pile testing provides a quick, reliable field test supplement and/or alternate to static load testing, as well as a supplement to wave equation analysis. Both methods are detailed in the attached specification, with commentary containing recommended safety factors applied to the pile design load based on the method of construction control selected.

5. **Separation of Payment into Fixed and Variable Cost Items Instead of Lump Sum**

Costs: Fair compensation for work performed in pile driving can only be accomplished by recognizing and providing bid items for contract costs which are fixed and contract costs which are variable. The currently popular payment methods used by highway agencies involve lumping fixed and variable costs into a single item. Such lump sum items, with variable contingencies, are recognized as high risk items by contractors who, to avoid a monetary loss, increase the price bid to cover the risk. The attached specification contains a list of bid items which separate the major fixed and variable costs to permit contractors to develop a low risk bid.

11.3 GENERIC DRIVEN PILE SPECIFICATION

<u>SECTION</u>	<u>CONTENTS</u>	<u>PAGE</u>
Section XXX.01	DESCRIPTION	11-7
	A. Pile Installation Plan	11-7
Section XXX.02	MATERIALS	11-9
Section XXX.03	EQUIPMENT FOR DRIVING PILES	11-9
	A. Pile Hammers	11-9
	B. Approval of Pile Driving Equipment	11-11
	1. Alternate Approval Method	11-17
	C. Drive System Components and Accessories	11-19
	1. Hammer Cushion	11-19
	2. Helmet	11-19
	3. Pile Cushion	11-20
	4. Leads	11-21
	5. Followers	11-21
	6. Jets	11-22
	7. Preboring	11-22
Section XXX.04	CONSTRUCTION METHODS	11-23
	A. Driven Pile Capacity	11-23
	1. Wave Equation	11-23
	2. Dynamic Formula	11-23
	B. Compression Load Tests	11-26
	1. Static Load Tests	11-26
	2. Dynamic Load Tests	11-28
	3. General	11-32
	C. Test Piles (Indicator Piles)	11-32
	D. Ultimate Pile Capacity	11-33
	E. Preparation and Driving	11-34
	1. General	11-34
	2. Preboring	11-34
	3. Location and Alignment Tolerance	11-35
	4. Heaved Piles	11-35
	5. Obstructions	11-36
	6. Installation Sequence	11-36
	7. Practical and Absolute Refusal	11-36
	F. Unsatisfactory Piles	11-36
	G. Splices	11-37
	H. Pile Shoes	11-38
	I. Cutoff Lengths	11-38
Section XXX.05	METHOD OF MEASUREMENT	11-38
	A. Timber, Steel, and Precast Concrete Piles	11-38
	1. Piles Furnished	11-38
	2. Piles Driven	11-39
	B. Cast in Place Pipe or Shell Concrete Piles	11-39
	C. Pile Shoes	11-39
	D. Load Tests	11-39
	E. Splices	11-40
	F. Furnishing Equipment for Driving Piles	11-40
Section XXX.06	BASIS OF PAYMENT	11-40

SECTION XXX.01 DESCRIPTION

This item shall consist of furnishing and driving foundation piles of the type and dimensions designated, including cutting off or building up foundation piles when required. Piling shall conform to and be installed in accordance with these specifications, and at the location, and to the elevation, penetration and/or capacity shown on the plans, or as directed by the Engineer.

The Contractor shall furnish the piles in accordance with an itemized order list which will be furnished by the Engineer, showing the number and length of all piles. When test piles are required, the pile lengths shown on the plans are for estimating purposes only and the actual lengths to be furnished for production piles will be determined by the Engineer after the test piles have been driven. The lengths given in the order list will be based on the lengths which are assumed after cutoff to remain in the completed structure. The Contractor shall, without added compensation, increase the lengths to provide for fresh heading and for such additional length as may be necessary to suit the Contractor's method of operation.

Commentary: *The objective of this specification is to provide criteria by which the Owner can assure that designated piles are properly installed and the Contractor can expect equitable compensation for work performed. The Owner's responsibility is to estimate the pile lengths required to safely support the design load. Pile lengths should be estimated based on subsurface explorations, testing and analysis which are completed during the design phase. Pile contractors who enter contractual agreements to install piles for an owner should not be held accountable or indirectly penalized for inaccuracies in estimated lengths. The Contractor's responsibility is to provide and install designated piles, undamaged, to the lengths specified by the Owner. This work is usually accomplished within an established framework of restrictions necessary to insure a "good" pile foundation. The price bid for this item of work will reflect the Contractor's estimate of both actual cost to perform the work and perceived risk.*

A. Pile Installation Plan

A Pile Driving Installation Plan shall be prepared by the Contractor and submitted to the Engineer no later than 30 days before driving the first pile. The Pile Driving Installation

Plan shall include the following:

1. List and size of proposed equipment including cranes, barges, driving equipment, jetting equipment, compressors, and predrilling equipment. Include manufacturer's data sheets on hammers.
2. Methods to determine hammer energy in the field for determination of pile capacity. Include in the submittal necessary charts and recent calibrations for any pressure measuring equipment.
3. Detailed drawings of any proposed followers.
4. Detailed drawings of any templates.
5. Details of proposed load test equipment and procedures, including recent calibrations of jacks and required load cells.
6. Sequence of driving of piles for each different configuration of pile layout.
7. Proposed schedule for test pile program and production pile driving.
8. Details of proposed features and procedures for protection of existing structures.
9. Required shop drawings for piles, cofferdams, etc.
10. Methods and equipment proposed to prevent displacement of piles during placement and compaction of fill within 4.5 m (15 ft) of the piles.
11. Methods to prevent deflection of battered piles due to their own weight and to maintain their as-driven position until casting of the pile cap is complete.
12. Proposed pile splice locations and details of any proprietary splices anticipated to be used.

SECTION XXX.02 MATERIALS

Materials shall meet the requirements in the following Subsections of Section XXX - Materials:

- Portland Cement Concrete
- Reinforcing Steel
- Structural Steel
- Castings for Pile Shoes
- Steel Shells for Cast in Place Piles
- Timber Piles
- Paint / Coatings
- Timber Preservative and Treatment

Commentary: *The appropriate sections of each agency's standard specifications should be included under the XXX.02 Materials Section. A generic materials section cannot be provided herein, considering the vast combinations of materials used in piling operations and the varying control methods used by individual highway departments. The above list contains the common material components. Additions or deletions may be required to this list based on the content of individual agency standard specifications and the pile type specified.*

SECTION XXX.03. EQUIPMENT FOR DRIVING PILES

A. Pile Hammers. Piles may be driven with air, steam, diesel, or hydraulic hammers. Gravity hammers, if specifically permitted in the contract, shall only be used to drive timber piles. When gravity hammers are permitted, the ram shall weigh between 900 and 1600 kg (2 and 3.5 kips) and the height of drop shall not exceed 4 m (13 ft). In no case shall the weight of gravity hammers be less than the combined weight of helmet and pile. All gravity hammers shall be equipped with hammer guides to insure concentric impact on the helmet.

Air/steam hammers shall be operated and maintained within the manufacturer's specified ranges. The plant and equipment furnished for air/steam hammers shall have sufficient capacity to maintain at the hammer, under working conditions, the volume and pressure specified by the manufacturer. The plant and equipment shall

be equipped with accurate pressure gauges which are easily accessible to the Engineer. The weight of the striking parts of air and steam hammers shall not be less than one third the weight of helmet and pile being driven, and in no case shall the striking parts weigh less than 1250 kg (2.75 kips).

Open end (single acting) diesel hammers shall be equipped with a device such as rings on the ram to permit the Engineer to visually determine hammer stroke at all times during pile driving operations. Also, the Contractor shall provide the Engineer a chart from the hammer manufacturer equating stroke and blows per minute for the open-end diesel hammer to be used. For open end diesel hammers, the contractor shall provide and maintain in working order for the Engineer's use, an approved device to automatically determine and display ram stroke.

Closed end (double acting) diesel hammers shall be equipped with a bounce chamber pressure gauge, in good working order, mounted near ground level so as to be easily read by the Engineer. Also, the Contractor shall provide the Engineer a chart, calibrated to actual hammer performance within 90 days of use, equating bounce chamber pressure to either equivalent energy or stroke for the closed-end diesel hammer to be used.

Hydraulic hammers shall have a power plant with sufficient capacity to maintain at the hammer, under working conditions, the volume and pressure specified by the manufacturer. The power plant and equipment shall be equipped with accurate pressure gauges which are easily accessible to the Engineer.

Commentary: *Pile inspectors frequently do not possess adequate knowledge or technical information concerning even the most basic details of the Contractor's hammer. Chapters 21 and 23 provide information on driving equipment and inspection. Highway agencies should also provide pile inspectors with basic manuals such as FHWA/RD-86/160 "The Performance of Pile Driving Systems: "Inspections Manual" or "Inspectors Manual for Pile Foundations" and "A Pile Inspectors Guide to Hammers, Second Edition" available from the Deep Foundation Institute, 120 Charlotte Place, Englewood Cliffs, NJ 07632.*

On large projects or on projects using high capacity piles, specifications should consider requiring kinetic energy readout devices for hammers as described in Section 21.16 of Chapter 21. Several manufacturers can

equip their hammers with these devices when requested. Any existing hammer can also be retrofitted with a kinetic energy readout device. These devices allow improved quality control and can detect changes in hammer performance over time that may necessitate adjustment to the pile installation criterion.

Non-impact hammers, such as vibratory hammers, or driving aids such as jets, followers and prebored holes shall not be used unless either specifically permitted in writing by the Engineer or stated in the contract documents. When permitted, such equipment shall be used for installing production piles only after the pile toe elevation for the ultimate pile capacity is established by load testing and/or test piles driven with an impact hammer. The Contractor shall perform, at his cost, such load tests and/or extra work required to drive test piles as determined by the Engineer as a condition of approval of the non-impact hammers or driving aids. Installation of production piles with vibratory hammers shall be controlled according to power consumption, rate of penetration, specified toe elevation, or other means acceptable to the Engineer which assure the ultimate pile capacity equals or exceeds the ultimate capacity of the test pile. In addition, one of every ten piles driven with a vibratory hammer shall be restruck with an impact hammer of suitable energy to verify the ultimate pile capacity as in XXX.04(D).

Commentary: *At present no formula exists to reliably predict the capacity of piles driven with vibratory hammers. Until reliable procedures are developed for vibratory installation, special precautions must be taken to insure foundation piles installed with vibratory hammers have both adequate capacity and structural integrity. On critical projects, highway agencies should consider the use of dynamic testing during restrrike to substantiate pile capacity and integrity.*

- B. Approval of Pile Driving Equipment. All pile driving equipment furnished by the Contractor shall be subject to the approval of the Engineer. It is the intent of this specification that all pile driving equipment be sized such that the project piles can be driven with reasonable effort to the ordered lengths without damage. Approval of pile driving equipment by the Engineer will be based on wave equation analysis and/or other judgments. In no case shall the driving equipment be transported to the project site until approval of the Engineer is received in writing. Prerequisite to such approval, the Contractor shall submit to the Engineer the necessary pile driving

equipment information at least 30 days prior to driving piles. The form which the Contractor shall complete with the above information is shown in Figure 11.1a (SI unit version) and Figure 11.1b (US unit version). If a follower is to be used, detailed drawings of the follower shall be included as part of this submittal.

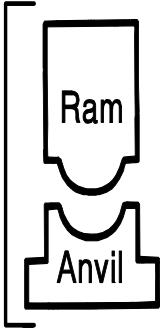
Commentary: *Use of wave equation analysis for approval of driving equipment can substantially reduce pile driving costs and pile driving claims by checking that the equipment mobilized to the job can drive the pile to the required penetration depth without damage. Public agencies should encourage Contractors to use wave equation analysis to select the optimum hammer for each project. In cases where disputes arise over rejection of pile driving equipment, the Engineer should request the Contractor to submit proof of the adequacy of the pile driving equipment. Such proof should consist of, but not be limited to, a wave equation analysis of the proposed driving equipment performed by a registered professional engineer. All costs of such submissions, if required, shall be the responsibility of the Contractor.*

The pile and driving equipment data form should be submitted for approval even if wave equation analysis will not be used for hammer approval. The approved form should be used by the pile inspector to check the proposed hammer and drive system components are as furnished and are maintained during the driving operation. Few agencies currently supply the pile inspector with any such information on which rational inspection can be based.

Contract No.: _____ Structure Name and/or No.: _____
 Project: _____ Pile Driving Contractor or Subcontractor: _____
 County: _____

(Piles driven by)

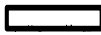
Hammer Components



Hammer

Manufacturer: _____ Model No.: _____
 Hammer Type: _____ Serial No.: _____
 Manufacturers Maximum Rated Energy: _____ (Joules)
 Stroke at Maximum Rated Energy: _____ (meters)
 Range in Operating Energy: _____ to _____ (Joules)
 Range in Operating Stroke: _____ to _____ (meters)
 Ram Weight: _____ (kg)
 Modifications: _____

Striker Plate



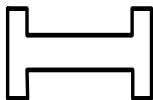
Weight: _____ (N) Diameter: _____ (mm)
 Thickness: _____ (mm)

Hammer Cushion



Material #1 _____ Material #2 _____
 (for Composite Cushion)
 Name: _____ Name: _____
 Area: _____ (cm²) Area: _____ (cm²)
 Thickness/Plate: _____ (mm) Thickness/Plate: _____ (mm)
 No. of Plates: _____ No. of Plates: _____
 Total Thickness of Hammer Cushion: _____

Helmet (Drive Head)



Weight: _____ including inserts (kN)

Pile Cushion



Material: _____
 Area: _____ (cm²) Thickness/Sheet: _____ (mm)
 No. of Sheets: _____
 Total Thickness of Pile Cushion: _____ (mm)

Pile



Pile Type: _____
 Wall Thickness: _____ (mm) Taper: _____
 Cross Sectional Area: _____ (cm²) Weight/Meter: _____

Ordered Length: _____ (m)
 Design Load: _____ (kN)
 Ultimate Pile Capacity: _____ (kN)

Description of Splice: _____

 Driving Shoe/Closure Plate Description: _____

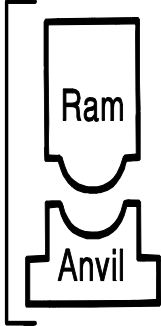
Submitted By: _____ Date: _____
 Telephone No.: _____ Fax No.: _____

Figure 11.1a Pile and Driving Equipment Data Form – SI Version

Contract No.: _____ Structure Name and/or No.: _____
 Project: _____ Pile Driving Contractor or Subcontractor: _____
 County: _____

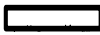
(Piles driven by)

Hammer Components



Hammer

Manufacturer: _____ Model No.: _____
 Hammer Type: _____ Serial No.: _____
 Manufacturers Maximum Rated Energy: _____ (ft-lbs)
 Stroke at Maximum Rated Energy: _____ (ft)
 Range in Operating Energy: _____ to _____ (ft-lbs)
 Range in Operating Stroke: _____ to _____ (ft)
 Ram Weight: _____ (kips)
 Modifications: _____



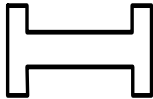
Striker Plate

Weight: _____ (kips) Diameter: _____ (in)
 Thickness: _____ (in)



Hammer Cushion

Material #1 _____ Material #2 _____
 (for Composite Cushion)
 Name: _____ Name: _____
 Area: _____ (in²) Area: _____ (in²)
 Thickness/Plate: _____ (in) Thickness/Plate: _____ (in)
 No. of Plates: _____ No. of Plates: _____
 Total Thickness of Hammer Cushion: _____



Helmet (Drive Head)

Weight: _____ including inserts (kips)



Pile Cushion

Material: _____
 Area: _____ (in²) Thickness/Sheet: _____ (in)
 No. of Sheets: _____
 Total Thickness of Pile Cushion: _____ (in)



Pile

Pile Type: _____
 Wall Thickness: _____ (in) Taper: _____
 Cross Sectional Area: _____ (in²) Weight/Ft: _____
 Ordered Length: _____ (ft)
 Design Load: _____ (kips)
 Ultimate Pile Capacity: _____ (kips)

Description of Splice: _____

 Driving Shoe/Closure Plate Description: _____

Submitted By: _____ Date: _____
 Telephone No.: _____ Fax No.: _____

Figure 11.1b Pile and Driving Equipment Data Form – US Version

The criteria, which the Engineer will use to evaluate the driving equipment from the wave equation results, consists of both the required number of hammer blows per 0.25 meter of penetration as well as the pile stresses at the required ultimate pile capacity. The required number of hammer blows indicated by the wave equation at the ultimate pile capacity shall be between 25 and 98 blows per 0.25 meter (30 and 120 blows per foot) for the driving equipment to be acceptable.

In addition, for the driving equipment to be acceptable the pile stresses which are indicated by the wave equation to be generated by the driving equipment shall not exceed allowable values. For steel piles, maximum compressive driving stresses shall not exceed 90% of the minimum yield strength of the pile material. For prestressed concrete piles in normal environments, tensile stresses shall not exceed 0.25 multiplied by the square root of the concrete compressive strength, f'_c plus the effective prestress value, f_{pe} , *i.e.* $(0.25 \sqrt{f'_c} + f_{pe})$. Both f'_c and f_{pe} in this equation must be in MPa. (In US units, tensile stresses shall not exceed 3 multiplied by the square root of the concrete compressive strength, f'_c plus the effective prestress value, f_{pe} , with both f'_c and f_{pe} in psi.) For prestressed concrete piles in severe corrosive environments, tensile stresses shall not exceed f_{pe} . Compressive stresses for prestressed concrete piles shall not exceed 85% of the compressive strength minus the effective prestress value, *i.e.* $(0.85 f'_c - f_{pe})$. For timber piles, the compressive driving stress shall not exceed three times the allowable static design strength listed on the plans. These criteria will be used in evaluating wave equation results to determine acceptability of the Contractor's proposed driving system.

The Contractor will be notified of the acceptance or rejection of the driving system within 14 calendar days of the Engineer's receipt of the Pile and Driving Equipment Data Form. If the wave equation analyses show that either pile damage or inability to drive the pile with a reasonable driving resistance to the desired ultimate capacity will result from the Contractor's proposed equipment or methods, the Contractor shall modify or replace the proposed methods or equipment at his expense until subsequent wave equation analyses indicate the piles can be reasonably driven to the desired ultimate capacity, without damage. The Engineer will notify the Contractor of the acceptance or rejection of the revised driving system within 7 calendar days of receipt of a revised Pile and Driving Equipment Data Form.

During pile driving operations, the Contractor shall use the approved system. No variations in the driving system will be permitted without the Engineer's written approval. Any change in the driving system will only be considered after the Contractor has submitted the necessary information for a revised wave equation analysis. The Contractor will be notified of the acceptance or rejection of the driving system changes within 7 calendar days of the Engineer's receipt of the requested change. The time required for submission, review, and approval of a revised driving system shall not constitute the basis for a contract time extension to the Contractor.

Commentary: *The ultimate pile capacity during driving is the soil resistance which must be overcome (including resistance from unsuitable layers and scour zone soils) to reach the pile penetration depth where the design load can be obtained with an acceptable safety factor. The safety factor selected will depend on design factors, such as quantity of subsurface information and geotechnical analysis, as well as construction factors such as the use of load tests, wave equation or dynamic formula to determine pile capacity. When proper foundation exploration procedures and static analyses such as those described in this manual are employed, the following safety factors on design load may be used, based on the pile construction control procedures specified:*

<u>Construction Control Method</u>	<u>Factor of Safety</u>
<i>Static load test (ASTM D-1143) with wave equation analysis</i>	2.00
<i>Dynamic testing (ASTM D-4945) with signal matching and wave equation analysis</i>	2.25
<i>Indicator piles with wave equation analysis</i>	2.50
<i>Wave equation analysis</i>	2.75
<i>Modified Gates dynamic formula</i>	3.50

The factor of safety for other test methods should be determined by the individual designer.

The ultimate pile capacity during driving is affected by:

- 1. The resistance in unsuitable soil layers overlying suitable support layers,*

2. *Temporary loss or increase in soil strength due to driving operations.*
3. *Pile installation methods which alter the in place soil resistance such as jetting, preboring, etc.*

The designer must estimate the ultimate pile capacity to be encountered during driving if pile driving resistance is to be used to determine pile capacity. Only on the most routine pile projects will the ultimate pile capacity be equal to the pile design load multiplied by the design safety factor. More typically, piles are used to penetrate upper soil layers which are unsuitable for load support due to either poor soil characteristics, or future loss of load support by scour or erosion. In such cases the resistance in unsuitable layers is not considered in determining the pile penetration necessary to support the design load at the appropriate safety factor. However, the estimated ultimate pile capacity to be encountered during driving must include the resistance to be encountered in penetrating those unsuitable layers, in addition to the design load multiplied by the safety factor. This ultimate pile capacity must be shown on the contract documents to permit the Contractor to properly size the driving equipment and the Engineer to judge the acceptability of the Contractor's driving equipment. Optimum pile installation generally occurs when the ultimate pile capacity is obtained with a driving effort below the point of maximum curvature (usually 60-100 blows per 0.25 meter or 75-120 blows per foot) of the wave equation bearing graph. Larger driving resistances result in negligible pile penetration per blow and generally inefficient driving conditions. Excessive driving resistances can also result in damage to the pile or the driving system.

1. **Alternate Approval Method:** An alternate method of driving equipment approval will be used when either the contract documents contain a provision that wave equation analysis will not be used for approval of driving equipment. The alternate approval method requires that the energy of the driving equipment submitted for approval on the Pile and Driving Equipment Data form, be rated by the manufacturer at or above the appropriate minimum energy level in Table 11-1 corresponding to the ultimate pile capacity shown on the plans.

TABLE 11-1 ALTERNATE APPROVAL METHOD Minimum Pile Hammer Requirements	
Ultimate Pile Capacity (kN)	Minimum Manufacturers Rated Hammer Energy (Joules)*
800 and under (180 kips)	-----
800 to 1350 (180 to 300 kips)	-----
1351 to 1850 (300 to 420 kips)	-----
1851 to 2400 (420 to 540 kips)	-----
2401 to 2650 (540 to 600 kips)	-----
2650 and over (600 kips)	-----

* Previously published tables which include specific values were based on assumptions which might not be appropriate for local conditions and were subject to misinterpretation.

Commentary: *A table of the minimum rated hammer energy vs. ultimate pile capacity should be developed using wave equation analyses of commonly available driving systems for the pile types, pile lengths, and pile loads routinely used by the specific agency. These analyses should model the typical soil and pile installation conditions. The wave equation results should be evaluated for driving stress levels and driving resistances to determine which hammer energies are too large (driving stress problems or driving resistances at ultimate capacity less than 25 blows per 0.25 meter (30 blows/ft.)) and which energies are too small (driving resistances at ultimate capacity greater than 98 blows per 0.25 meter (120 blows /ft.)).*

Once the specific table of energy values has been developed, it should only be considered for routine projects in uniform soil conditions or when the agency is in the process of phasing the wave equation analysis into standard use. Projects involving long piles or large ultimate pile capacities relative to the design load (such as scour piles or piles to be driven through embankments) should use job specific wave equation analysis to establish minimum driving equipment requirements. Piles to rock should also be evaluated by wave equation analysis to reduce the risk of pile damage from too large a hammer.

During pile driving operations, the Contractor shall use the approved system. If the Engineer determines the Contractor's hammer is unable to transfer sufficient energy to the pile, the hammer shall be removed from service until repaired to the satisfaction of the Engineer. No variations in the driving system will be permitted without the Engineer's written approval. Any changes in the driving system will be considered only after the Contractor has submitted a new Pile and Driving Equipment Data form. The Contractor will be notified of the acceptance or rejection of the proposed change in driving equipment within 7 calendar days of the Engineer's receipt of the form.

C. Drive System Components and Accessories

1. **Hammer Cushion:** Impact pile driving equipment designed to be used with a hammer cushion shall be equipped with a suitable thickness of hammer cushion material to prevent damage to the hammer or pile and to insure uniform driving behavior. Hammer cushions shall be made of durable manufactured materials, provided in accordance with the hammer manufacturer's guidelines. Wood, wire rope, and asbestos hammer cushions are specifically disallowed and shall not be used. A striker plate as recommended by the hammer manufacturer shall be placed on the hammer cushion to insure uniform compression of the cushion material. The hammer cushion shall be removed from the helmet and inspected in the presence of the Engineer when beginning pile driving at each structure or after each 100 hours of pile driving, whichever is less. Any reduction of hammer cushion thickness exceeding 25% of the original thickness shall be replaced by the Contractor before driving is permitted to continue.

Commentary: *For hammers requiring cushion material, mandatory use of a durable hammer cushion material which will retain uniform properties during driving is necessary to accurately relate driving resistance to pile capacity. Non-durable materials which deteriorate during driving cause erratic estimates of pile capacity and, if allowed to dissolve, result in damage to the pile or driving system.*

2. **Helmet:** Piles driven with impact hammers require an adequate helmet or drive head to distribute the hammer blow to the pile head. The helmet shall be axially aligned with the hammer and the pile. The helmet shall be guided by the leads and not be free-swinging. The helmet shall fit around the pile head in such a manner as to prevent transfer of torsional forces during driving, while maintaining

proper alignment of hammer and pile. An insert may be used with a helmet to adapt the helmet to different types or sizes of piles.

For steel and timber piling, the pile heads shall be cut squarely and a helmet, as recommended by the hammer manufacturer, shall be provided to hold the axis of the pile in line with the axis of the hammer.

For precast concrete and prestressed concrete piles, the pile head shall be plane and perpendicular to the longitudinal axis of the pile to prevent eccentric impacts from the helmet.

For special types of piles, appropriate helmets, mandrels or other devices shall be provided in accordance with the manufacturer's recommendations so that the piles may be driven without damage.

- 3. Pile Cushion:** The heads of concrete piles shall each be protected by a pile cushion having the same cross sectional area as the pile top. Pile cushions shall be made of plywood, hardwood, or composite plywood and hardwood materials. The minimum pile cushion thickness placed on the pile head prior to driving shall not be less than 100 mm (4 inches).

A new pile cushion shall be provided for each pile. In addition the pile cushion shall be replaced if, during the driving of any pile, the cushion is compressed more than one-half the original thickness or it begins to burn. Pile cushions shall be protected from the weather, and kept dry prior to use. Pile cushion shall not be soaked in any liquid unless approved by the Engineer. The use of manufactured pile cushion materials in lieu of a wood pile cushion shall be evaluated on a case by case basis.

A used pile cushion in good condition shall be used for restrrike tests. The used cushion shall be the same pile cushion from the end of initial driving unless that cushion condition has deteriorated. If the original cushion has deteriorated, a used cushion of similar thickness as the end of drive pile cushion shall be used.

Commentary: *A pile cushion is only needed for the protection of concrete piles. If the wave equation analysis of the Contractor's hammer indicates tension stresses exceed specification limits, the pile cushion may need to be substantially thicker than 100 mm (4 inches). Pile cushion thicknesses up*

to 460 mm (18 inches) have been used to mitigate tension stresses. Compressive stresses at the pile head can be controlled with a relatively thin pile cushion. However, wood pile cushions may become overly compressed and hard after about 1000 hammer blows. The physical characteristics of manufactured pile cushion materials should be determined by standard test procedures such as the Deep Foundations Institute standard "Testing of Pile Driving Cushion Material".

4. **Leads:** Piles shall be supported in line and position with leads while being driven. Pile driver leads shall be constructed in a manner that affords freedom of movement of the hammer while maintaining alignment of the hammer and the pile to insure concentric impact for each blow. Leads may be either fixed or swinging type. Swinging leads, when used, shall be fitted with a pile gate at the bottom of the leads and, in the case of batter piles, a horizontal brace may be required between the crane and the leads. The pile section being driven shall not extend above the leads. The leads shall be adequately embedded in the ground or the pile constrained in a structural frame such as a template to maintain alignment. The leads shall be of sufficient length to make the use of a follower unnecessary, and shall be so designed as to permit proper alignment of batter piles.
5. **Followers:** Followers shall only be used when approved in writing by the Engineer, or when specifically stated in the contract documents. In cases where a follower is permitted, the first pile in each bent and every tenth pile driven thereafter shall be driven full length without a follower, to determine that adequate pile penetration is being attained to develop the ultimate pile capacity.

The follower and pile shall be held and maintained in equal and proper alignment during driving. The follower shall be of such material and dimensions to permit the piles to be driven to the penetration depth determined necessary from the driving of the full length piles. When driving concrete piles, the cross sectional area of the steel follower shall be at least 20% of the cross sectional area of the concrete pile. When driving steel piles, the cross sectional area of the steel follower shall be greater than or equal to the cross section area of the steel pile. The lower end of the follower shall be equipped with a helmet or follower-pile connection suitable for the pile type being driven.

The final position and alignment of the first two piles installed with followers in each substructure unit shall be verified to be in accordance with the location tolerances in Section XXX.04(E) before additional piles are installed.

Commentary: *The use of a follower often causes substantial and erratic reductions in the hammer energy transmitted to the pile due to the follower flexibility, poor connection to the pile head, frequent misalignment, etc. Reliable correlations of driving resistance with ultimate pile capacity are very difficult when followers are used. Severe problems with pile alignment and location frequently occur when driving batter piles with a follower in a cofferdam unless a multi-tier template is used.*

6. **Jets:** Jetting shall only be permitted if approved in writing by the Engineer or when specifically stated in the contract documents. When jetting is not required in the contract documents, but approved after the Contractor's request, the Contractor shall determine the number of jets and the volume and pressure of water at the jet nozzles necessary to freely erode the material adjacent to the pile without affecting the lateral stability of the final in place pile. The Contractor shall be responsible for all damage to the site caused by unapproved or improper jetting operations. When jetting is specifically required in the contract documents, the jetting plant shall have sufficient capacity to deliver at all times a pressure equivalent to at least 700 kPa (100 psi) at two 19 mm (0.75 inch) jet nozzles. In either case, unless otherwise indicated by the Engineer, jet pipes shall be removed when the pile toe is a minimum of 1.5 m (5 ft) above prescribed toe elevation and the pile shall be driven to the required ultimate pile capacity with an impact hammer. Also, the Contractor shall control, treat if necessary, and dispose of all jet water in a manner satisfactory to the Engineer.

When jetting is used, the Contractor shall submit details of the proposed jetting and pile driving plan. Where practical, all piles in a pile group shall be jetted to the required penetration depth before beginning pile driving. When large pile groups or pile spacing and batter make this impractical, restrike tests on a select number of previously driven piles shall be performed to check pile capacity after jetting operations are completed.

7. **Preboring:** When stated in the contract documents, the Contractor shall prebore holes at pile locations to the depths shown on the plans. Prebored holes shall be of a size smaller than the diameter or diagonal of the pile cross section that is

sufficient to allow penetration of the pile to the specified depth. If subsurface obstructions, such as boulders or rock layers, are encountered, the hole diameter may be increased to the least dimension which is adequate for pile installation. Any void space remaining around the pile after completion of driving shall be filled with sand or other approved material. The use of spuds, a short strong driven member which is removed to make a hole for inserting a pile, shall not be permitted in lieu of preboring.

SECTION XXX.04 CONSTRUCTION METHODS

A. Driven Pile Capacity

1. **Wave Equation:** The ultimate pile capacity shall be determined by the Engineer, based on a wave equation analysis. Piles shall be driven with the approved driving equipment to the ordered length or other lengths necessary to obtain the required ultimate pile capacity. Jetting or other methods to facilitate pile penetration shall not be used unless specifically permitted either in the contract documents or approved by the Engineer after a revised driving resistance is established from the wave equation analysis. Adequate pile penetration shall be considered to be obtained when the specified wave equation resistance criteria is achieved within 1.5 m (5 ft) of the pile toe elevation, based on ordered length. Piles not achieving the specified resistance within these limits shall be driven to penetrations established by the Engineer.
2. **Dynamic Formula:** The ultimate pile capacity will only be determined by dynamic formula if either the contract documents contain a provision that dynamic formula shall be used or the Engineer approves dynamic formula use. In such cases, piles shall be driven to a penetration depth necessary to obtain the ultimate pile capacity according to the following formula:

Modified Gates Formula In SI Units

$$R_u = [6.7\sqrt{E_r} \log(10N_b)] - 445$$

Where: R_u = the ultimate pile capacity (kN).
 E_r = the manufacturer's rated hammer energy (Joules) at the **field**

observed ram stroke.

$\log(10N_b)$ = logarithm to the base 10 of the quantity 10 multiplied by N_b , the number of hammer blows per 25 mm at final penetration.

The number of hammer blows per 0.25 meter of pile penetration required to obtain the ultimate pile capacity shall be calculated as follows:

$$N_{qm} = 10 (10^x)$$

Where: $x = [(R_u + 445) / (6.7\sqrt{E_r})] - 1$

Modified Gates Formula In US Units

$$R_u = [1.75\sqrt{E_r} \log(10 N_b)] - 100$$

Where: R_u = the ultimate pile capacity (kips).

E_r = the manufacturer's rated hammer energy (ft-lbs) at the **field observed ram stroke**.

$\log(10N_b)$ = logarithm to the base 10 of the quantity 10 multiplied by N_b , the number of hammer blows per 1 inch at final penetration

The number of hammer blows per foot of pile penetration required to obtain the ultimate pile capacity shall be calculated as follows:

$$N_{ft} = 12 (10^x)$$

Where: $x = [(R_u + 100) / 1.75\sqrt{E} \log] - 1$

Commentary: *Driven pile capacity should be monitored in terms of ultimate pile capacity; not design load. The driving resistance at any penetration depth reflects the total capacity mobilized by the pile. This total capacity may include capacity mobilized temporarily in soil deposits unsuited for bearing, as well as suitable bearing layers. Therefore, the driving resistance should be*

established for the ultimate pile capacity that must be overcome in order to reach anticipated pile penetration depth. These ultimate capacities are determined by static analysis procedures. In the case of piles to be driven to a specified minimum pile toe elevation, the ultimate pile capacity must be computed by static analysis to include the capacity of all soil layers penetrated by the pile above the minimum pile toe elevation as well as the end bearing resistance at that depth. Also, the ultimate pile capacity is directly related to the maximum pile driving stress during installation. This stress is more critical than the stress caused after installation by the design load.

Good piling practices dictate use of the wave equation in place of dynamic formulas to monitor driven pile capacity for all projects. The driving resistance and maximum pile stresses should be determined for the ultimate pile capacity. Use of the wave equation will permit the use of lower safety factors on the design load and the minimum permissible pile section to resist the driving force. This will result in significant cost reductions due to savings in pile lengths and use of smaller pile sections. FHWA recommends that all agencies phase in wave equation analysis with an ultimate goal of eliminating use of dynamic formulas on all pile projects. Wave equation analysis is discussed in greater detail in Chapter 16 of this manual.

The Engineering News formula is recognized to be the least accurate and least consistent of all dynamic formula, yet the vast majority of all States continue to use this formula. The Washington State DOT study WA-RD-163.1 "Comparison of Methods for Estimating Pile Capacity" (1988) found that the Hiley, Gates, Janbu, and Pacific Coast Uniform Building code formulas all provide relatively more dependable results than the Engineering News formula. The dynamic formula contained in this specification is the modified Gates formula and it already includes the 80% efficiency factor on the rated energy, E , recommended by Gates.

The Gates formula was also studied by Olson and Flaate (1967) and found to be the most consistent of the dynamic formulas studied. However, all dynamic formulas are not suited for soft cohesive soils. Engineers planning to use dynamic formula should carefully read these

references to comprehend the limitations involved with their use. A design safety factor of 3.5 is recommended when using the modified Gates formula to determine the safe design load, i.e., if a design load of 1000 kN (225 kips) is required in the bearing layer, then an ultimate pile capacity of 3500 kN (788 kips) should be used in the modified Gates formula to determine the necessary driving resistance. The formula was selected for its relative accuracy, consistency and simplicity of use. However, the top priority for highway agencies should be to change from dynamic formulas to wave equation analysis.

B. Compression Load Tests*

** **Commentary:** Compression tests with the Osterberg Cell (Chapter 19) and Statnamic (Chapter 20) are not covered by this generic specification. The individual design should prepare the project specification for either of these test methods.*

1. **Static Load Tests:** Compression load tests shall be performed by procedures set forth in ASTM D-1143 using the quick load test method, except that the test shall be taken to plunging failure or the capacity of the loading system. Testing equipment and measuring systems shall conform to ASTM D-1143, except that the loading system shall be capable of applying 150% of the ultimate pile capacity or 9000 kN (2000 kips), whichever is less, and that a load cell and spherical bearing plate shall be used.

The Contractor shall submit to the Engineer for approval detailed plans prepared by a licensed professional engineer of the proposed loading apparatus. The submittal shall include calibrations for the hydraulic jack, load cell, and pressure gage conducted within 30 days of the load test. If requested by the Engineer, the jack, load cell, and pressure gage shall be recalibrated after the load test

The loading apparatus shall be constructed to allow the various increments of the load to be placed gradually, without causing vibration to the test pile. When the approved method requires the use of tension (reaction) piles, the tension piles, when feasible, shall be of the same type and diameter as the production piles, and shall be driven in the location of permanent piles. Timber or tapered piles installed in permanent locations shall not be used as tension piles.

While performing the load test, the contractor shall provide safety equipment and

employ adequate safety procedures. Adequate support for the load test plates, jack, and ancillary devices shall be provided to prevent them from falling in the event of a release of load due to hydraulic failure, test pile failure, or other cause.

The design load shall be defined as 50% of the failure load. The failure load for the pile shall be defined as follows: for piles 610 mm (24 inches) or less in diameter or width, the failure load of a pile tested under axial compressive load is that load which produces a settlement at failure of the pile head equal to:

$$\text{In SI units} \quad s_f = \Delta + (4.0 + 0.008b)$$

$$\text{In US Units} \quad s_f = \Delta + (0.15 + 0.008b)$$

Where: s_f = Settlement at failure in mm (inches).

b = Pile diameter or width in mm (inches).

Δ = Elastic deformation of total pile length in mm (inches).

For piles greater than 610 mm (24 inches) in diameter or width, the failure load can be defined as a pile head settlement equal to:

$$s_f = \Delta + (b / 30)$$

The top elevation of the test pile shall be determined immediately after driving and again just before load testing to check for heave. Any pile which heaves more than 6 mm (0.25 inches) shall be redriven or jacked to the original elevation prior to testing. Unless otherwise specified in the contract, a minimum 3-day waiting period shall be observed between the driving of any anchor piles or the load test pile and the commencement of the load test.

Commentary: *The pile capacity may increase (soil setup) or decrease (relaxation) after the end of driving. Therefore, it is essential that static load testing be performed **after** equilibrium conditions in the soil have re-established. Static load tests performed before equilibrium conditions have re-established will underestimate the long term pile capacity in soil setup*

conditions and overestimate the long term capacity in relaxation cases. For piles in clays, specifications should require at least 2 weeks or longer to elapse between driving and load testing. In sandy silts and sands, 5 days to a week is usually sufficient. Load testing of piles driven into shales should also be delayed for at least 2 weeks after driving. Additional discussion on time dependent changes in pile capacity may be found in Section 9.10.1.

Each static load test pile should be determining the load transferred to the pile toe. Instrumentation commonly consists of strain gages and/or telltale rods mounted at varying depths from the pile toe. Also, a load cell and spherical bearing plate should be mounted between the load frame and the pile head to verify the readings from the hydraulic jack pressure gauge. Due to jack ram friction, loads indicated by a jack pressure gauge are commonly 10% to 20% higher than the actual load imposed on the pile. Last, after completion of a load test on a non production pile, the static test pile should be pulled and checked for damage. The examination of the extracted pile will determine driving damage and its effect on capacity.

When static load tests are used to control production pile driving, the time required to analyze the load test results and establish driving criteria should be specified so that the delay time to the contractor is clearly identified. Static load testing is discussed in greater detail in Chapter 18 of this manual. A more detailed specification for static load testing may be found in FHWA-SA-91-042, Static Testing of Deep Foundations.

- 2. Dynamic Load Tests:** Dynamic measurements following procedures set forth in ASTM D-4945 will be taken by the Engineer during the driving of piles designated as dynamic load test piles.

Commentary: *When static load tests are specified, dynamic load tests are recommended to be performed on at least half the reaction piles prior to driving the static load test pile. The dynamic test results are used both to verify that the desired ultimate pile capacity can be attained at the proposed estimated static load test pile penetration depth and to fine tune the dynamic test equipment for site soil conditions. Dynamic monitoring of the load test pile during both initial driving and during restriking after completion of the static load test are also recommended. This allows correlation of static test*

results with dynamic test results. Signal matching techniques using the dynamic test data can further quantify dynamic soil parameters such as soil quake and damping for the site. When dynamic tests are specified on production piles, the first pile driven in each substructure foundation is recommended to be tested. Where uniform soil conditions exist across a site, the number of dynamic tests may be reduced based on recommendations from the geotechnical engineer.

*This section of the specifications applies to the Contractor's activities as they relate to the dynamic testing of piles. **If the dynamic tests are to be performed by an independent firm retained by the Contractor and not transportation department personnel, an additional specification section detailing the dynamic test analysis and reporting requirements must be added. In addition, testing personnel should have attained an appropriate level of expertise on the Foundation QA Examination for providers of dynamic testing services.** Dynamic tests and the Foundation QA Examination are discussed in greater detail in Chapter 17 of this manual.*

Prior to placement in the leads, the Contractor shall make each designated concrete and/or timber pile available for taking of wave speed measurements and for predrilling the required instrument attachment holes. Predriving wave speed measurements will not be required for steel piles. When wave speed measurements are made, the piling shall be in a horizontal position and not in contact with other piling. The Engineer will furnish the equipment, materials, and labor necessary for drilling holes in the piles for mounting the instruments. The instruments will be attached near the head of the pile with bolts placed in masonry anchors for the concrete piles, or through drilled holes on the steel piles, or with wood screws for timber piles.

The Contractor shall provide the Engineer reasonable means of access to the pile for attaching instruments after the pile is placed in the leads. A platform with minimum size of 1.2 x 1.2 m (4 x 4 ft) designed to be raised to the top of the pile while the pile is located in the leads shall be provided by the Contractor. Alternatively, Contractor's personnel following the Engineer's instructions can attach the instruments to the pile after it is placed in the leads. It is estimated that approximately 1 hour per pile will be needed for instrument attachment and removal.

The Contractor shall furnish electric power for the dynamic test equipment. The power supply at the outlet shall be 10 amp, 115 volt, 55-60 cycle, A.C. only. Field generators used as the power source shall be equipped with functioning meters for monitoring voltage and frequency levels.

The Contractor shall furnish a shelter to protect the dynamic test equipment from the elements. The shelter shall have a minimum floor size of 2.5 x 2.5 m (8 x 8 ft) and minimum roof height of 2 m (6.5 ft). The inside temperature of the shelter shall be maintained above 45 degrees. The shelter shall be located within 15 m (50 ft) of the test location.

With the dynamic testing equipment attached, the Contractor shall drive the pile to the design penetration depth or to a depth determined by the Engineer. The Engineer will use the ultimate pile capacity estimates at the time of driving and/or restriking from dynamic test methods to determine the required pile penetration depth for the ultimate pile capacity. The stresses in the piles will be monitored during driving with the dynamic test equipment to ensure that the values determined do not exceed the values in Section XXX.03(B). If necessary, the Contractor shall reduce the driving energy transmitted to the pile by using additional cushions or reducing the energy output of the hammer in order to maintain stresses below the values in Section XXX.03(B). If non-axial driving is indicated by dynamic test equipment measurements, the Contractor shall immediately realign the driving system.

The Contractor shall wait up to 24 hours (or a longer duration specified in the contract documents) and restrike the dynamic load test pile with the dynamic testing instruments attached. It is estimated that the Engineer will require approximately 30 minutes to reattach the instruments. A cold hammer shall not be used for the restrike. The hammer shall be warmed up before restrike begins by applying at least 20 blows to another pile or to timber mats placed on the ground. The maximum amount of penetration required during restrike shall be 150 mm (6 inches), or the maximum total number of hammer blows required will be 50, whichever occurs first. After restriking, the Engineer will either provide the cutoff elevation or specify additional pile penetration and testing.

Commentary: *For purposes of measurement and payment one dynamic test includes all data collected on one pile during both the initial pile driving and a restrike done up to 24 hours after the initial driving. Additional long term restrikes*

should be paid for as separate tests unless the restrrike schedule is specifically stated in the dynamic test specification.

The restrrike time and frequency should be clearly stated in the specifications and should be based on the time dependent strength change characteristics of the soil. The following restrrike durations are often used:

<u>Soil Type</u>	<u>Time Delay Until Restrike</u>
<i>Cleans Sands</i>	<i>1 Day</i>
<i>Silty Sands</i>	<i>2 Days</i>
<i>Sandy Silts</i>	<i>3-5 Days</i>
<i>Silty Clays</i>	<i>7-14 Days*</i>
<i>Shales</i>	<i>10-14 Days*</i>

** - Longer times sometimes required.*

The restrrike time interval is particularly important when dynamic testing is used for construction control. Specifying too short of a restrrike time for friction piles in fine grained deposits may result in pile length overruns. However, it is sometimes difficult for long term restrikes to be accommodated in the construction schedule. In these cases, multiple restrikes are sometimes specified on selected piles with shorter term restrikes at other locations.

The time necessary to analyze the dynamic test results and provide driving criteria to the contractor once restrikes are completed should also be stated in the specifications. This is important when the testing is done by agency personnel or their consultants as well as when the testing firm is retained by the contractor. In cases where the testing is retained by the contractor, the time required for the agency to review the test results and provide driving criteria should be specified relative to the agency's receiving the test results.

3. **General:** On completion of the load testing, any test or anchor piling not a part of the finished structure shall be removed or cut off at least 300 mm (1 ft) below either the bottom of footing or the finished ground elevation, if not located within the footing area.
- C. Test Piles (Indicator Piles). Test piles shall be driven when shown on the plans at the locations and to the penetration depths specified by the Engineer. All test piles shall be driven with impact hammers unless specifically stated otherwise in the plans. In general, the specified length of test piles will be greater than the estimated length of production piles in order to provide for variation in soil conditions. The driving equipment used for driving test piles shall be identical to that which the Contractor proposes to use on the production piling. Approval of driving equipment shall conform with the requirements of these Specifications. The Contractor shall excavate the ground at each test pile to the elevation of the bottom of the footing before the pile is driven.

Test piles shall be driven to a driving resistance established by the Engineer at the estimated pile toe elevation. Test piles which do not attain the driving resistance specified above at a depth of 0.25 meter (1 ft) above the estimated pile toe elevation shown on the plans shall be allowed to "set up" for 12 to 24 hours, or as directed by the Engineer, before being re-driven. A cold hammer shall not be used for re-drive. The hammer shall be warmed up before driving begins by applying at least 20 blows to another pile. If the specified driving resistance is not attained on re-driving, the Engineer may direct the Contractor to drive a portion or all of the remaining test pile length and repeat the "set up" re-drive procedure. Test piles driven to plan grade and not having the driving resistance required, shall be spliced and driven until the required capacity is obtained.

A record of driving of the test pile will be prepared by the Engineer, including the number of hammer blows per 0.25 meter (1 ft) for the entire driven length, the as-driven length of the test pile, cutoff elevation, penetration in ground, and any other pertinent information. The Contractor shall provide the information listed in Figure 11.1 of Section XXX.03(B) to the Engineer for inclusion in the record. If a re-drive is necessary, the Engineer will record the number of hammer blows per 25 mm (1 inch) of pile movement for the first 0.25 meter (1 ft) of re-drive. The Contractor shall not order piling to be used in the permanent structure until test pile data has been reviewed and pile order lengths are authorized by the Engineer. The Engineer will provide the pile order list within 7 calendar days after completion of all test pile driving specified in the contract documents.

Commentary: *Test piles are recommended on projects where: 1) large quantities or long length of friction piling are estimated, even if load tests are to be used at adjacent footings; 2) large ultimate soil resistance is expected in relation to the design load and, 3) where concrete piles are used.*

- D. Ultimate Pile Capacity. Piles shall be driven by the Contractor to the penetration depth shown on the plans or to a greater depth if necessary to obtain the ultimate pile capacity. The ultimate pile capacity shall be determined by the Engineer based on one of the methods listed in Section XXX.04(A).

Jetting or other methods shall not be used to facilitate pile penetration unless specifically permitted in the contract plans or in writing by the Engineer. The ultimate pile capacity of jetted piles shall be based on driving resistances recorded during impact driving after the jet pipes have been removed. Jetted piles not attaining the ultimate pile capacity at the ordered length shall be spliced, as required, at the Contractor's cost, and driven with an impact hammer until the ultimate pile capacity is achieved, as indicated by the appropriate criteria in Section XXX.04(A).

The ultimate pile capacity of piles driven with followers shall only be considered acceptable when the follower driven piles attain the same pile toe elevation as the full length piles driven without followers, installed per Section XXX.03(C), which attained the required ultimate pile capacity.

The ultimate pile capacity of piles driven with vibratory hammers shall be based on the driving resistance recorded during impact driving after the vibratory equipment has been removed from the first pile in each group of 10 piles. Vibrated piles not attaining the ultimate pile capacity at the ordered length shall be spliced, as required, at the Contractor's cost, and driven with an impact hammer until the ultimate pile capacity is achieved, as indicated by the appropriate criteria in Section XXX.04(A). When the ultimate pile capacity is attained, the remaining 9 piles shall be installed to similar depths with similar vibratory hammer power consumption and rate of penetration as the first pile.

E. Preparation and Driving

1. **General:** The heads of all piles shall be plane and perpendicular to the longitudinal axis of the pile before the helmet is attached. The heads of all concrete piles shall be protected with a pile cushion as described in Section XXX.03(C).

During pile driving, the pile cushion shall be changed as described in Section XXX.03(C) before excessive compression or damage takes place. Approval of a pile hammer relative to driving stress damage shall not relieve the Contractor of responsibility for piles damaged because of misalignment of the leads, failure of cushion materials, failure of splices, malfunctioning of the pile hammer, or other improper construction methods. Piles damaged for such reasons shall be rejected and replaced at the Contractor's expense when the Engineer determines that the damage impairs the strength of the pile.

2. **Preboring:** Augering, wet-rotary drilling, or other methods of preboring shall be used only when approved by the Engineer or in the same manner as used for any indicator piles or load test piles. When permitted, such procedures shall be carried out in a manner which will not impair the capacity of the piles already in place or the safety of existing adjacent structures.

Except for end bearing piles, preboring shall be stopped at least 1.5 m (5 ft) above the pile toe elevation, determined from the ordered length and the pile shall be driven with an impact hammer to a driving resistance specified by the Engineer. Where piles are to be end-bearing on rock or hardpan, preboring may be carried to the surface of the rock or hardpan, and the piles shall be restruck with an impact hammer to insure proper seating.

If the Engineer determines that preboring has disturbed the capacities of previously installed piles, those piles that have been disturbed shall be restored to conditions meeting the requirements of this specification by re-driving or by other methods acceptable to the Engineer. Redriving or other remedial measures shall be instituted after the preboring operations in the area have been completed. The Contractor shall be responsible for the costs of any necessary remedial measures, unless the preboring method was specifically included in the contract documents and properly executed by the Contractor.

3. **Location and Alignment Tolerance:** The pile head at cutoff elevation shall be within 50 mm (2 inches) of plan locations for bent caps supported by piles, and shall be within 150 mm (6 inches) of plan locations for all piles capped below final grade. The as-driven centroid of load of any pile group at cutoff elevation shall be within 5% of the plan location of the designed centroid of load. No pile shall be nearer than 100 mm (4 inches) from any edge of the cap. Any increase in size of cap to meet this edge distance requirement shall be at the Contractor's expense.

Piles shall be installed so that the axial alignment of the top 3 m (10 ft) of the pile is within 2% of the specified alignment. For piles that cannot be inspected internally after installation, an alignment check shall be made before installing the last 1.5 m (5 ft) of pile, or after installation is completed provided the exposed portion of the pile is not less than 1.5 m (5 ft) in length. The Engineer may require that driving be stopped in order to check the pile alignment. Pulling laterally on piles to correct misalignment, or splicing a properly aligned section on a misaligned section shall not be permitted.

If the location and/or alignment tolerances specified in the preceding paragraphs are exceeded, the extent of overloading shall be evaluated by the Engineer. If in the judgment of the Engineer, corrective measures are necessary, suitable measures shall be designed and constructed by the Contractor. The Contractor shall bear all costs, including delays, associated with the corrective action.

Commentary: *Conditions exist, such as soft overburden soils directly overlying a sloping bedrock, where final pile location and/or alignment may be beyond the contractor's control. These cases should be identified during the design stage with specifications tailored to meet the site and project requirements.*

4. **Heaved Piles:** Level readings to measure pile heave after driving shall be made by the Engineer at the start of pile driving operations and shall continue until the Engineer determines that such checking is no longer required. Level readings shall be taken immediately after the pile has been driven and again after piles within a radius of 5 m (16 ft) have been driven. If pile heave is observed, accurate level readings referenced to a fixed datum shall be taken by the Engineer on all piles immediately after installation and periodically thereafter as adjacent piles are driven to determine the pile heave range. All piles that have been heaved more than 6 mm (0.25 in) shall be redriven to the required resistance or penetration.

Concrete shall not be placed in pile casings until pile driving has progressed beyond a radius of 5 m (16 ft) from the pile to be concreted. If pile heave is detected for pipe or shell piles which have been filled with concrete, the piles shall be redriven to original position after the concrete has obtained sufficient strength and a proper hammer-pile cushion system, satisfactory to the Engineer, is used. All work performed in conjunction with redriving piles due to pile heave shall be paid for by the Department provided the initial driving was done in accordance with the specified installation sequence.

5. **Obstructions:** If piles encounter unforeseeable, isolated obstructions, the Department shall pay for the cost of obstruction removal and for all remedial design or construction measures caused by the obstruction.
6. **Installation Sequence:** The order of placing individual piles in pile groups shall be either starting from the center of the group and proceeding outwards in both directions or starting at the outside row and proceeding progressively across the group.
7. **Practical and Absolute Refusal:** Practical refusal is defined as 20 blows per 25 mm of penetration (20 blows per inch) with the hammer operated at its maximum fuel or energy setting, or at a reduced fuel or energy setting recommended by the Engineer based on pile installation stress control. In no case should driving continue for more than 75 mm (3 inches) at practical refusal driving conditions.

Absolute refusal is defined as a penetration resistance 50% greater than that of practical refusal, i.e. 30 blows per 25 mm (30 blows per inch). Driving should be terminated immediately once absolute refusal driving conditions are encountered.

- F. Unsatisfactory Piles. The method used in driving piles shall not subject the piles to excessive or undue abuse producing crushing and spalling of concrete, injurious splitting, splintering, and brooming of the wood, or deformation of the steel. Misaligned piles shall not be forced into proper position. Any pile damaged during driving by reason of internal defects, or by improper driving, or driven out of its proper location, or driven below the designated cutoff elevation, shall be corrected by the Contractor, without added compensation, by a method approved by the Engineer.

Commentary: *The following procedures may be used to correct unsatisfactory pile conditions:*

- 1. The pile may be withdrawn and replaced by a new and, when necessary, longer pile. In removing piles, jets may be used in conjunction with jacks or other devices for pulling in an effort to remove the whole pile.*
- 2. A second pile may be driven adjacent to the defective pile.*
- 3. The pile may be spliced or built up as otherwise provided herein, or a sufficient portion of the footing extended to properly embed the pile.*
- 4. All piles pushed up by the driving of adjacent piles, or by any other cause, shall be redriven.*

Piles which have been bent during installation shall be considered unsatisfactory unless the ultimate capacity is proven by load tests performed at the Contractor's expense. If such tests indicate inadequate capacity, corrective measures as determined by the Engineer shall be taken, such as use of bent piles at reduced capacity, installation of additional piles, strengthening of bent piles, or replacement of bent piles.

A concrete pile will be considered defective if a visible crack, or cracks, appears around the entire periphery of the pile, or if any defect is observed which, as determined by the Engineer, affects the strength or life of the pile.

G. Splices. Full length piles shall always be used where practical. In no case shall timber piles be spliced. Where splices are unavoidable for steel or concrete piles, their number, locations and details shall be subject to approval of the Engineer. Splices in steel piles and steel pile casings shall be welded in conformance with Section XXX. Splices for cast in place piles shall be watertight. Splices for concrete piles shall be made by the cement dowel method as detailed on the plans unless the Engineer approves alternate splices. Mechanical splices for concrete or steel piles may be approved by the Engineer if the splice can transfer the full pile strength in compression, tension and bending. Shop drawings of any proposed mechanical splice shall be submitted to the Engineer for approval.

H. Pile Shoes. Pile shoes of the type and dimensions specified shall be provided and installed when shown on the contract plans. Shoes for timber piles shall be metal and shall be fastened securely to the pile. Timber pile toes shall be carefully shaped to secure an even uniform bearing on the pile shoe. Steel pile shoes shall be fabricated from cast steel conforming to ASTM A 27.

Commentary: *H-pile shoes composed of steel plates welded to the flanges and webs are not recommended because this reinforcement provides neither protection nor increased strength at the critical area of the flange to web connection. Only prefabricated pile shoes made of ASTM A 27 cast steel have been proven reliable. The designer should select and detail on the plans the proper pile shoe to suit the application. Additional information on pile shoes is presented in Chapter 22 of this manual.*

I. Cutoff Lengths. The pile head of all permanent piles and pile casings shall be cutoff at the elevation shown on the plans or as ordered by the Engineer. All cutoff lengths shall become the property of the Contractor, and shall be removed by the Contractor from the site of the work.

Commentary: *Additional structural details for timber, steel, concrete and cast in place piles should be included by each agency in this driven pile specification, either directly or by reference to appropriate sections of the individual agency's standard specification. Typical items include: timber pile butt treatment and preservative treatment; precast concrete pile reinforcement, forming, casting, curing, and handling; steel pile field painting; cast in place pile details for shell, interior reinforcement and concrete.*

SECTION XXX.05. METHOD OF MEASUREMENT

A. Timber, Steel, and Precast Concrete Piles

1. **Piles Furnished:** The unit of measurement for payment for furnishing timber, steel, and precast concrete piles shall be the linear meter. The quantity to be paid for will be the sum of the lengths in meters of the piles, of the types and lengths ordered in writing by the Engineer, furnished in compliance with the material requirements of these specifications, stockpiled in good condition at the site of the work by the Contractor, and accepted by the Engineer. No allowance will be made

for that length of piles, including test piles, furnished by the Contractor to replace piles which were previously accepted by the Engineer, but are subsequently damaged prior to completion of the contract.

When extensions of piles are necessary, the extension length ordered in writing by the Engineer will be included in the linear meters of piling furnished.

2. Piles Driven: The units of measurement for driving timber, steel, and precast concrete piles shall be per linear meter (linear ft) of piling in place measured below the cutoff elevation. The measured length will be rounded to the nearest meter. Preboring, jetting or other methods used for facilitating pile driving procedures will not be measured and payment shall be considered included in the unit price bid for the Piles Driven pay item.

B. Cast in Place Pipe or Shell Concrete Piles. The quantity of cast in place pipe or shell concrete piles to be paid for will be the actual number of linear meters (linear ft) of steel pipe or shell piles driven, cast, and left in place in the completed and accepted work. Measurements will be made from the toe of the steel pipe or shell pile to the bottom of the cap or bottom of the footing, as the case may be.

No separate measurement will be made for reinforcing steel, excavation, drilling, cleaning of drilled holes, drilling fluids, sealing materials, concrete, casing, and or any other items required to complete the work. Preboring, jetting or other methods used for facilitating pile driving procedures will not be measured and payment shall be considered included in the unit price bid for the driven and cast in place pay item.

C. Pile Shoes. The number of pile shoes measured for payment shall be those shoes actually installed on piles and accepted for payment by the Engineer.

D. Load Tests. The quantity of load tests to be paid for will be the number of load tests completed and accepted, except that load tests made at the option of the Contractor will not be included in the quantity measured for payment.

Reaction and test piling which are not a part of the permanent structure will be included in the unit price bid for each load test. Reaction and test piling, which are a part of the permanent structure, will be paid for under the appropriate pay item.

E. Splices. The number of splices measured for payment shall be only those splices actually made as required to drive the piles in excess of the ordered length furnished by the Engineer.

F. Furnishing Equipment for Driving Piles. Payment will be made at the lump sum price bid for this item as follows: Seventy-five percent (75%) of the amount bid will be paid when the equipment for driving piles is furnished and driving of satisfactory piles has commenced. The remaining 25% will be paid when the work of driving piles is completed. The lump sum price bid shall include the cost of furnishing all labor, materials and equipment necessary for transporting, erecting, maintaining, replacing any ordered equipment, dismantling and removing of the entire pile driving equipment. The cost of all labor, including the manipulation of the pile driving equipment and materials in connection with driving piles, shall be included in the unit price bid per linear meter for the piles to be driven. The furnishing of equipment for driving sheet piling is not included in this work. Payment for furnishing and using a follower, augers or jetting will be considered as included in the unit price bid for piles.

SECTION XXX.06 BASIS OF PAYMENT

The accepted quantities, determined as provided above, will be paid for at the contract price per unit of measurement, respectively, for each of the particular pay items listed below that is shown in the bid schedule, which prices and payment will be full compensation for the work prescribed in this section. Payment will be made under:

Pay Item	Pay Unit
XXX(1) ____ piles, furnished	Linear meter (linear foot)
XXX(2) ____ piles, driven	Linear meter (linear foot)
XXX(3) ____ piles, driven & cast in place	Linear meter (linear foot)
XXX(4) ____ test piles, furnished	Linear meter (linear foot)
XXX(5) ____ test piles, driven	Linear meter (linear foot)
XXX(6) ____ test piles, driven & cast in place	Linear meter (linear foot)
XXX(7) Pile load test (static)	Each
XXX(8) Pile load test (rapid)	Each
XXX(9) Pile load test (dynamic)	Each
XXX(10) Splices	Each

XXX(11)	Pile Shoes	Each
XXX(12)	Furnishing Equipment for Pile Driving	Each

Commentary: *The above pile payment items have been chosen to separate the major fixed costs from the variable costs. Many highway agencies oversimplify pile payment by including all costs associated with the driving operation in the price per meter of pile installed. Contractors bidding such "simple" items need to break down the total cost of the mobilization, splices, shoes, etc., to a price per linear meter (linear ft) based on the total estimated quantity. If that quantity underruns, the contractor does not recover the full cost of mobilization, splices, shoes, etc. If that quantity overruns, the highway agency pays an unfair price for the overrun quantity. The use of separate items for operations of major fixed cost such as mobilization can substantially mitigate the inequitable impact of length variations. Similarly, the ordered pile length is the highway agency's responsibility. Separate payment for furnishing piles and driving piles compensates the contractor for actual materials used and installation costs, even when overruns or underruns occur.*

REFERENCES

- American Association of State Highway and Transportation Officials [AASHTO], (2002). Standard Specifications for Highway Bridges, 17th Edition, Division 2, AASHTO Highway Subcommittee on Bridges and Structures, Washington, D.C.
- American Society for Testing and Materials [ASTM], (1987). Standard Test Method for Piles Under Static Axial Compressive Load, ASTM D-1143.
- The Deep Foundations Institute, Equipment Applications Committee (1995). A Pile Inspector's Guide to Hammers, Second Edition.
- Fragasny, R.J., Higgins, J.D. and Argo, D.E. (1988). Comparison of Methods for Estimating Pile Capacity. Report No. WA-RD 163.1, Washington State Department of Transportation, Olympia, 62.
- Geotechnical Guideline 13 (1985). Geotechnical Engineering Notebook, U.S. Department of Transportation. Federal Highway Administration, Washington, D.C., 37.
- Kylor, Z.G., Schnore, A.R., Carlo, T.A. and Baily, P.F. (1992). Static Testing of Deep Foundations. Report No. FHWA-SA-91-042, U.S. Department of Transportation, Federal Highway Administration, Office of Technology Applications, Washington, D.C., 174.
- Olson, R.E. and Flaate, K.S. (1967). Pile Driving Formula for Friction Piles in Sands. American Society of Civil Engineers, Journal for Soil Mechanics and Foundation Engineering, Vol. 93, SM6, 279-296.
- Rausche, F., Likins, G.E., Goble, G.G. and Hussein, M. (1986). The Performance of Pile Driving Systems. Inspection Manual, Report No. FHWA/RD-86/160, U.S. Department of Transportation, Federal Highway Administration, Office of Research and Development, Washington, D.C., 92.

Chapter 12

PILE FOUNDATION DESIGN SUMMARY

12.1 INTRODUCTION

In this chapter, the total design process will be reviewed. However, this time the design process will be illustrated through a proposed bridge construction project. A condensed version of the Foundation Design Process flow chart presented in Figure 2.1 is repeated for convenience here as Figure 12.1. The proposed project is a bridge that will carry the imaginary Peach Freeway over Dismal Creek. This is a new freeway that is to be built in a city in the southeastern part of the United States. The alignment of the roadway has been defined and the foundation design now comes into consideration. The design process will be followed using Figure 12.1.

12.2 BLOCK 1 - ESTABLISH GLOBAL PROJECT PERFORMANCE

The general structure requirements will now be reviewed following the list from Chapter 2, Section 2.4.

1. The project is a new bridge.
2. The structure will be constructed at one time by a single contract.
3. The structure layout has not been finalized at the time that the foundation engineer first becomes involved. The alignment is quite well defined but the grades have not been established.
4. The foundation engineer has briefly visited the proposed site. Dismal Creek is a flat, shallow stream that, at low water, is more than 30 meters (98 ft) wide in the vicinity of the proposed bridge. At the north end of the structure there is a bank about eight meters high while on the south end the bank slopes up quite slowly. The new bridge will probably be about 80-100 meters (262-328 ft) long with an approach embankment required for the south approach. Bridge piers will probably be located in Dismal Creek.

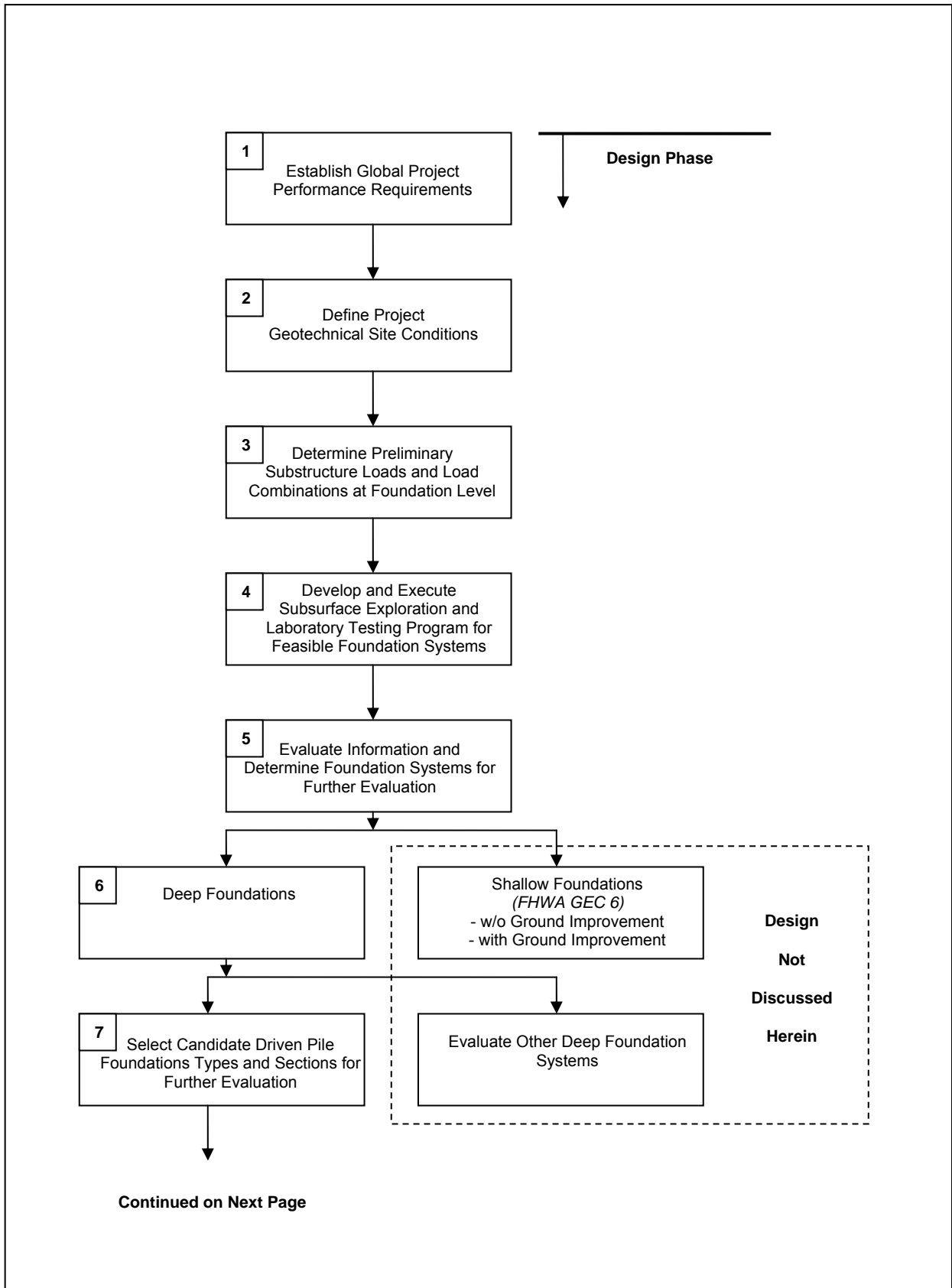


Figure 12.1 Driven Pile Design and Construction Process

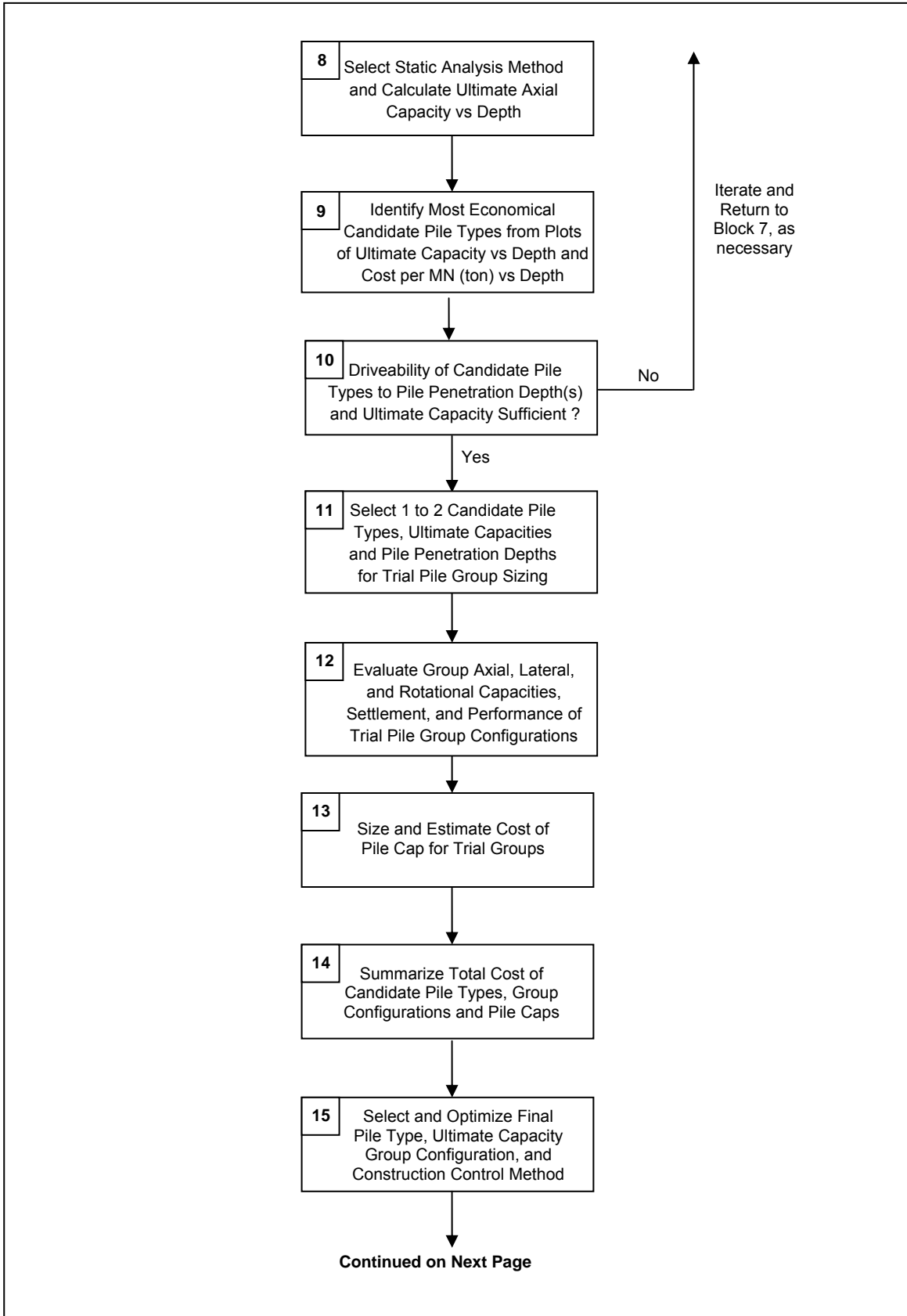


Figure 12.1 Driven Pile Design and Construction Process (continued)

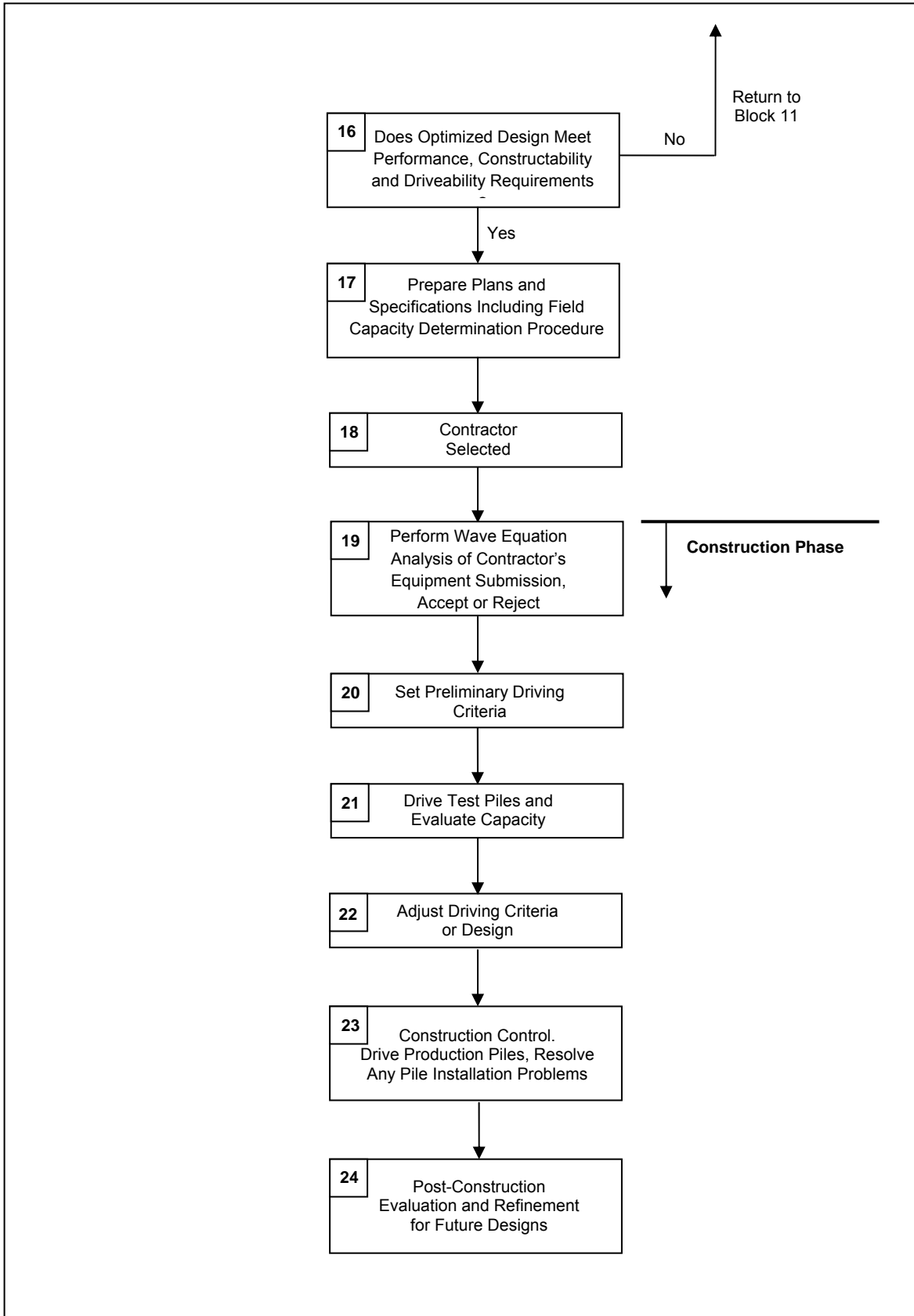


Figure 12.1 Driven Pile Design and Construction Process (continued)

5. Seismic and vessel impact loads are not a design consideration. However, scour and debris loading must be considered for the bridge piers.
6. As yet the structure is not sufficiently defined to consider modifications in the structure due to site considerations.
7. Foundation loads cannot be estimated very accurately at this time. A meeting with the bridge engineer indicates that, based on his experience, compression loads on the order of 10,000 to 15,000 kN (2248 to 3372 kips) per substructure location are likely. Typical deflection and deformation requirements are anticipated.
8. There are no special environmental conditions that must be considered in the design.

12.3 BLOCK 2 – DEFINE PROJECT GEOTECHNICAL SITE CONDITIONS

Published data from the sources listed in Table 4-2 has been reviewed in the office planning stage. Geologists have also been contacted to provide information regarding the site geology. At first glance, an extensive subsurface exploration would probably not be required for this modest sized structure. However, a field reconnaissance survey of the area has been made by the foundation engineer and the project bridge engineer. Field observations of the eroded stream banks indicated that the surficial soils on the north side of Dismal Creek consist of silty sands while silty clays were noted in the south stream bank. The granular upland soils on the north approach and the cohesive lowland soils on the south approach further suggest that the subsurface conditions may be quite complex. Therefore, it would be desirable that fairly extensive subsurface exploration be made. The foundation engineer expected the site to be underlain by limestone bedrock at a depth of 30 to 50 meters (98 to 164 ft), based on previous experience.

Agency files have been reviewed to determine if there are any existing soil borings in the area of the proposed bridge site. However, no previous subsurface information has been located. There are also no existing bridges in the vicinity of the planned structure to provide details on subsurface conditions or previous construction information and/or problems.

12.4 BLOCK 3 – DETERMINE PRELIMINARY FOUNDATION LOADS AT THE SUBSTRUCTURE LEVEL

Preliminary substructure loads and reasonable vertical and lateral deformation requirements are now available. Accurate load information and performance criteria are essential to the development and implementation of an adequate subsurface exploration program for the structure. The total axial compression loads have been established at 12,600 kN (2,830 kips) per substructure location. Other load conditions that include several combinations of axial and transverse loads result in axial compression, uplift, lateral, and moment loads at each substructure unit. These load combinations are too extensive to be repeated here. However, the lateral loads will range from 600 kN (135 kips) at the interior piers to 900 kN (202 kips) at the abutments. Maximum uplift loads on a pile group will be less than 1800 kN (405 kips).

The foundation performance requirements have also been established. Maximum pile group settlements less than 25 mm (1 inch) are required under the compression loads with maximum differential settlements between substructure units of 15 mm (0.60 inch). Maximum horizontal deflections of up to 10 mm (0.40 inch) are permissible under lateral loading.

12.5 BLOCK 4 - DEVELOP AND EXECUTE SUBSURFACE EXPLORATION PROGRAM FOR FEASIBLE FOUNDATION SYSTEMS

Based on the information generated in Blocks 1 to 3, a subsurface exploration program was planned. The foundation engineer requested that the bridge engineer provide additional information on the planned structural configuration. Since some time had elapsed since the initial discussions regarding the proposed structural configuration, it was possible to better define the structure geometry. The proposed bridge will be supported at two abutments and two interior piers. Due to the possibly complex subsurface conditions, both a soil boring and an in-situ cone penetration test will be performed at each substructure location.

The subsurface program was performed and results of the exploration are included in Appendix E. This data was evaluated and a subsurface profile was prepared and is given in Figure 12.2.

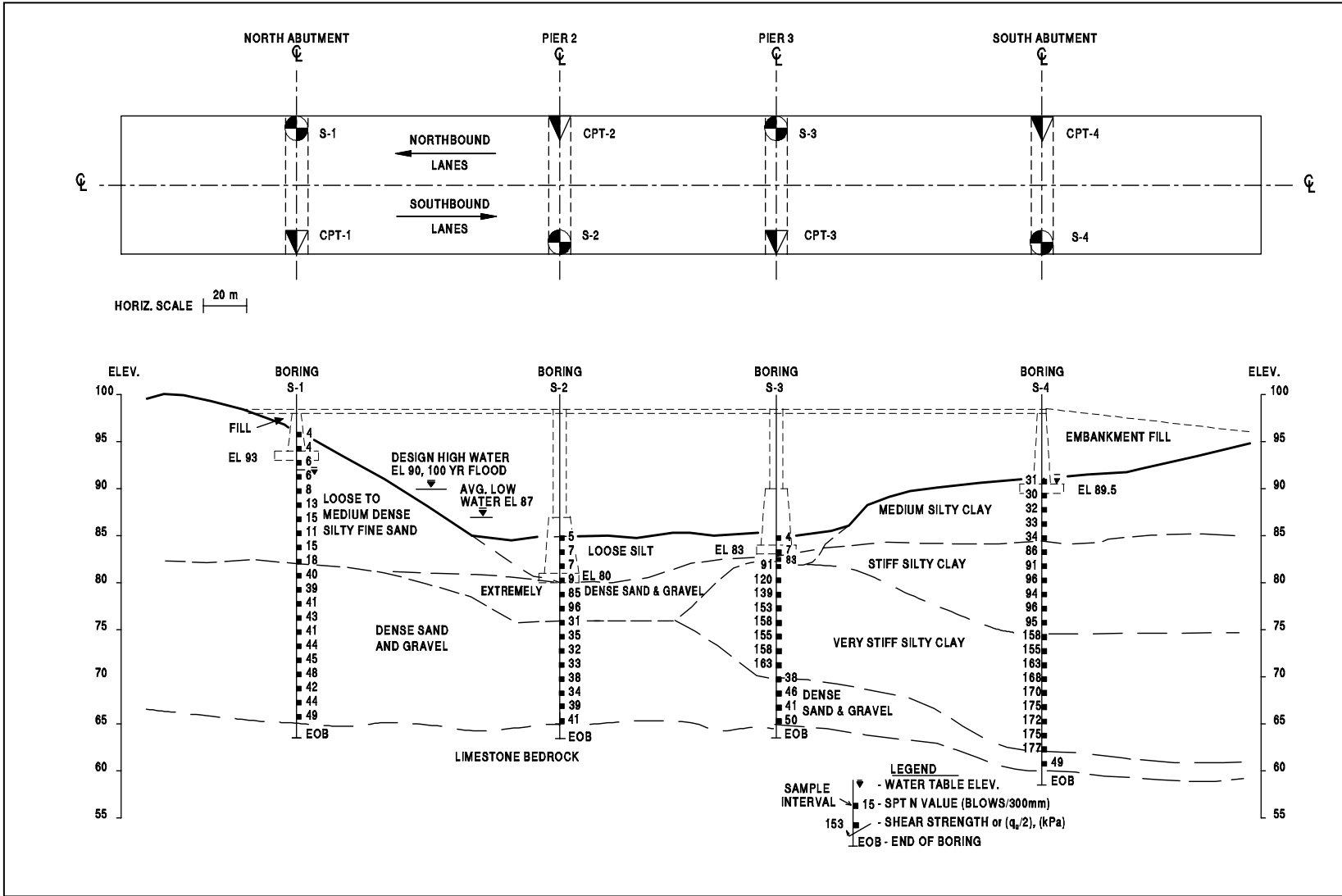


Figure 12.2 Peach Freeway Subsurface Profile.

12.6 BLOCK 5 - EVALUATE INFORMATION AND SELECT CANDIDATE FOUNDATION SYSTEMS FOR FURTHER EVALUATION

A decision must now be made regarding candidate foundation systems that will be evaluated. First, the foundation engineer met again with the bridge engineer to verify the final design loads and foundation locations. It was determined that the foundations will be located as anticipated at the last meeting. The Peach Freeway Bridge over Dismal Creek will be a three span structure supported at North and South Abutments and interior piers, Pier 2 and Pier 3. At the proposed bridge location, the only extreme event that must be considered is scour. The bridge is not in a region where seismic loads will influence the design and vessel impact is not a design consideration. Lateral loads will be induced by stream debris.

A hydraulics division study indicates that a shallow foundation should not be used under the two piers due to scour. In addition, settlement of a shallow foundation at Pier 3 is expected to be excessive. Therefore, the use of a shallow foundation was ruled out and a deep foundation will be required.

12.7 BLOCK 6 - DEEP FOUNDATION TYPE

A decision must now be made between the use of driven piles, drilled shafts, micropiles, or auger cast piles. Both driven piles and drilled shafts are commonly used in the region. A cost evaluation indicates that a driven pile option will be the most economical deep foundation type because of the complex subsurface conditions. Therefore, a driven pile foundation system is selected.

12.8 BLOCK 7 - SELECT CANDIDATE DRIVEN PILE TYPES AND SECTIONS FOR FURTHER STUDY

Five candidate pile types suitable for the subsurface conditions and loads are now chosen for further evaluation. The candidate pile types selected are 356 mm (14 inch) and 457 mm (18 inch) precast, prestressed concrete piles, 406 mm (16 inch) and 457 mm (18 inch) O.D. closed-end steel pipe piles, and a HP 360 x 152 (HP 14x102) H-pile.

12.9 BLOCK 8 - SELECT STATIC ANALYSIS METHOD AND CALCULATE ULTIMATE CAPACITY VERSUS DEPTH

Static pile capacity calculations have been performed for each candidate pile section to determine the ultimate capacity versus pile penetration depth at each substructure unit (*i.e.*, North Abutment, Pier 2, Pier 3, and South Abutment). The static analyses were performed using applicable static analysis methods for the candidate pile types and the subsurface conditions at each substructure location. Static analysis procedures are presented in Chapter 9.

12.10 BLOCK 9 – IDENTIFY MOST ECONOMICAL CANDIDATE PILE TYPES AND/OR SECTIONS

Pile support cost versus depth plots are now developed for each candidate pile type. The pile support cost in dollars per kN (ton) supported versus pile penetration depth plots are obtained by dividing the ultimate pile capacity at a given depth by the pile cost to reach that depth. Details of this process are presented in Chapter 3. Based on the pile support cost evaluations, 356 mm (14 inch) concrete piles appear the most cost effective pile type and section.

12.11 BLOCK 10 - CALCULATE DRIVEABILITY OF CANDIDATE PILE TYPES

The driveability of each candidate pile type, section(s) and lengths for the required ultimate pile capacity must now be evaluated using a wave equation program analysis. The soil resistance versus depth has been calculated for each substructure location using the DRIVEN program and then input into a wave equation program. Details on the DRIVEN program are given in Chapter 9 and the wave equation is presented in Chapter 16 of Volume II.

At this stage, driveability analysis results indicate that the proposed 356 mm (14 inch) concrete piles would work well at the abutments. Sample input and output screens for the North and South Abutments are shown in Appendices F.9.1 and F.9.4. Wave equation driveability studies in the North Abutment show penetration resistance with an assumed air hammer reach 111 blows per 0.25 m at the final penetration of 14.5 m below the surface.

Compression stresses reach 13.7 MPa and tension stresses reach 3 MPa. These stresses and the predicted penetration resistance are with FHWA recommended limits.

At the South Abutment, the predicted penetration resistance is predicted to reach 23 blows per 0.25 m at the end of driving if the hammer is run at full stroke. This value is lower than the FHWA required 25 blows per 0.25 m. If the hammer is equipped with and operated at a short stroke setting, the pile penetration resistance will be higher and acceptable. Stresses in compression and tension when driving at full stroke reach 13.4 and 5.7 MPa, both within recommended limits.

At the interior piers, however, the driveability of the concrete displacement piles through the extremely dense sand and gravel layer may be quite difficult. The driveability results at Pier 2 are presented and discussed in greater detail in Section 16.5.5. More complete input and output results of the driveability studies of Pier 2 and Pier 3 are included in Appendices F.9.2 and F.9.3, respectively. These results indicate concrete displacement piles would like encounter refusal driving conditions when penetrating the extremely dense sand and gravel layer. The driveability of the candidate pipe pile sections is worse since these piles have similar soil resistances to overcome but have a reduced pile impedance compared to the 356mm (14 inch) concrete pile. Therefore, the low displacement H-pile, may be necessary at the interior piers to meet pile penetration requirements dictated by scour. The HP 360 x 152 (14 x 102) H-pile section has a predicted penetration resistance of 31 blows/0.25 m at end of drive in Pier 2 and 21 blows/0.25 m in Pier 3. If the air hammer is equipped with and operated at a short stroke setting, the FHWA minimum pile penetration resistance requirements will be met in Pier 3. Compressive stresses in Piers 2 and 3 will reach 149 and 163 MPa, respectively.

Based on the driveability analysis results and earlier cost evaluations, both pipe pile sections and the 457 mm (18 inch) precast, prestressed concrete pile have been dropped from further evaluation.

12.12 BLOCK 11 – SELECT 1 TO 2 FINAL CANDIDATE PILE TYPES FOR TRIAL GROUP SIZING

The most viable candidate pile types and/or sections from the cost and driveability evaluations in Blocks 9 and 10 are now evaluated for trial group sizing using the final loads and performance requirements. The remaining candidate pile types are the 356 mm (14

inch) precast, prestressed concrete pile and the HP 360 x 152 (HP 14x102) H-pile. Multiple pile penetration depths and the resulting ultimate capacity at those depths are used to establish multiple trial pile group configurations for each the two remaining candidate pile types. Trial pile group sizing and configurations are discussed in Chapter 10. The trial group configurations are carried forward to Block 13.

12.13 BLOCK 12 - EVALUATE CAPACITY, SETTLEMENT, AND PERFORMANCE OF TRIAL PILE GROUPS

Trial group configurations for the two remaining candidate pile type are now evaluated for axial group capacity, group uplift, group lateral load performance, and settlement. These computations and analysis procedures are described in Chapter 9. Block 15 discusses these computations for the final pile type.

12.14 BLOCK 13 - SIZE AND ESTIMATE PILE CAP COST FOR TRIAL PILE GROUPS

The size and thickness of the pile cap for each trial group is now evaluated and the cost of the resulting pile cap is estimated. It is not necessary to design the cap reinforcement at this time only to determine cap size. Pile cap cost is a key component in selecting the most cost effective pile type and must not be overlooked. A procedure for preliminary sizing of pile caps is provided in Chapter 10.

12.15 BLOCK 14 - SUMMARIZE TOTAL COST OF FINAL CANDIDATE PILES

The total cost of the two remaining candidate pile types should now be determined. A given pile type may have several total cost options depending upon the pile penetration depths, ultimate capacities, group configurations, and pile cap sizes carried through the design process. The cost of any special construction considerations and environmental restrictions should also be included in the total cost for each final candidate pile type. An example of the cost optimization process for a single pile section is presented in Chapter 3. Based on the cost optimization process, the 356 mm (14 inch) precast, prestressed concrete piles are selected for final design.

12.16 BLOCK 15 – SELECT AND OPTIMIZE FINAL PILE TYPE, CAPACITY AND GROUP CONFIGURATION

Based on all of the available information, it is now time to select the final pile type as well as optimize the number of piles and pile group configuration. The selected pile type and section is the 356 mm (14 inch) precast, prestressed, concrete pile. The optimized pile group design consists of 24 piles arranged in three rows of eight piles each at each substructure location. The maximum compressive design load is 890 kN, the design uplift load is 100 kN, and the maximum lateral load is 40 kN per pile. A complete evaluation of the group lateral and rotational resistance should also be performed at this time. This final design should be optimized for final structure loads, performance requirements, and construction efficiency.

12.16.1 Single Pile Capacity

Construction control procedures have been selected that will make a factor of safety of 2.0 appropriate. Therefore, an ultimate axial capacity of 1780 kN (400 kips) is required. At Piers 2 and 3, the effect of scour on the static axial capacity should also be calculated. Static capacity calculation details are given in Appendix F (including the scour calculation at Pier 2) and summaries of the calculations are provided in Tables 12-1 to 12-4.

The capacity calculation summaries indicate different static analysis methods will yield different results. Therefore, designers should use a method they fully understand, including the method limitations. Based upon the analyses performed, pile penetration lengths of 11.5 m (38 ft) are selected for the North Abutment, 14 m (46 ft) for Pier 2 (after scour), 13 m (43 ft) for Pier 3 (total stress α -method so scour effect limited) and 21 m (69 ft) for the South Abutment (17.5 m (58 ft) if drag load not considered).

12.16.2 Pile Group Capacity

The North Abutment piles will be driven into a dense cohesionless soil at center to center pile spacings greater than 4 diameters. Therefore, the ultimate pile group capacity for the North Abutment may be taken as the sum of the ultimate capacities of the individual piles in the group as discussed in Section 9.8.1.1. Similarly, the Pier 2 piles will be driven into a dense cohesionless soil at center to center pile spacings greater than 4 diameters. Therefore, the ultimate pile group capacity at Pier 2 may also be taken as the sum of the ultimate capacities of the individual piles in the group.

At Pier 3, the piles will be driven through cohesive soils and into a dense cohesionless layer at center to center pile spacings of 4 diameters. Since the piles will be founded in a dense cohesionless layer, the pile group capacity should be equal to the sum of the ultimate capacities of the individual piles in the group. However, the possibility of block failure should be checked in accordance with the procedures detailed in Section 9.8.1.3 particularly if the dense layer is underlain by a weaker deposit.

TABLE 12-1(a) NORTH ABUTMENT PILE CAPACITY SUMMARY FOR 11.5 m PILE EMBEDMENT			
Method Used for Estimation of Pile Capacity	Calculated Pile Shaft Resistance (kN)	Calculated Pile Toe Resistance (kN)	Calculated Ultimate Pile Capacity (kN)
Meyerhof Method - SPT Data	418	854	1,272
Nordlund Method - SPT Data	898	940	1,838
Effective Stress Method - SPT Data	537	1,294	1,831
Driven Program – SPT Data	920	920	1,840
LPC CPT Program - CPT Data	780	511	1,291
Schmertmann Method - CPT Data	604	1,111	1,715

1 kip = 4.448 kN

TABLE 12-1(b) NORTH ABUTMENT PILE LENGTH SUMMARY FOR A 1,780 kN ULTIMATE PILE CAPACITY	
Method Used for Estimation of Pile Capacity	Calculated Pile Length for the 1,780 kN Ultimate Pile Capacity
Meyerhof Method - SPT Data	13.0 meters for 1,840 kN
Nordlund Method - SPT Data	11.5 meters for 1,838 kN
Effective Stress Method	11.5 meters for 1,831 kN
Driven Program - SPT Data	11.5 meters for 2,145 kN
LPC CPT Program - CPT Data	13.5 meters for 1,815 kN
Schmertmann Method - CPT Data	11.7 meters for 1,939 kN

1 ft = 0.305 m, 1 kip = 4.448 kN

TABLE 12-2(a) PIER 2 PILE CAPACITY SUMMARY FOR 10.0 m PILE EMBEDMENT

Method Used for Estimation of Pile Capacity	Calculated Pile Shaft Resistance (kN)	Calculated Pile Toe Resistance (kN)	Calculated Ultimate Pile Capacity (kN)
Meyerhof Method - SPT Data	1,134	1,676	2,810
Nordlund Method - SPT Data	984	854	1,838
Effective Stress Method	451	1,155	1,606
Driven Program - SPT Data	994	878	1,873

1 kip = 4.448 kN

TABLE 12-2(b) PIER 2 PILE LENGTH SUMMARY FOR A 1,780 kN ULTIMATE PILE

Method Used for Estimation of Pile Capacity	Calculated Pile Length for the 1,780 kN Ultimate Pile Capacity
Meyerhof Method - SPT Data	1.0 meters for 2,136 kN
Nordlund Method - SPT Data	10.0 meters for 1,838 kN
Effective Stress Method	12.5 meters for 1,847 kN
Driven Program - SPT Data	10.0 meters for 1,873 kN

1 ft = 0.305 m, 1 kip = 4.448 kN

TABLE 12-2(c) PIER 2 PILE CAPACITY SUMMARY BEFORE AND AFTER CHANNEL DEGRADATION SCOUR BASED ON NORDLUND METHOD

Pile Embedment	Ultimate Pile Capacity	
	Before Scour	After Scour
10 meters	1,838 kN	1,347 kN
14 meters	2,331 kN	1,887 kN

1 ft = 0.305 m, 1 kip = 4.448 kN

TABLE 12-3(a) PIER 3 PILE CAPACITY SUMMARY FOR 13.0 m PILE EMBEDMENT

Method Used for Estimation of Pile Capacity	Calculated Pile Shaft Resistance (kN)	Calculated Pile Toe Resistance (kN)	Calculated Ultimate Pile Capacity (kN)
Nordlund and α Method - SPT Data	1,171	635	1,806
Effective Stress Method	525	1,059	1,584
Driven Program - SPT Data	1,345	920	2,265
LPC CPT Program - CPT Data	1,189	841	2,030
Schmertmann Method - CPT Data	1,727	1,231	2,958

1 ft = 0.305 m, 1 kip = 4.448 kN

TABLE 12-3(b) PIER 3 PILE LENGTH SUMMARY FOR A 1,780 kN ULTIMATE PILE CAPACITY

Method Used for Estimation of Pile Capacity	Calculated Pile Length for the 1,780 kN Ultimate Pile Capacity
Nordlund and α Method - SPT Data	13.0 meters for 1,806 kN
Effective Stress Method	14.0 meters for 1,980 kN
Driven Program - SPT Data	13.0 meters for 2,265 kN
LPC CPT Program - CPT Data	12.5 meters for 1,826 kN
Schmertmann Method - CPT Data	10.2 meters for 1,808 kN

1 ft = 0.305 m, 1 kip = 4.448 kN

Note: Strata transitions from very stiff clay to dense sand and gravel at an embedded pile length of 13 m (43 ft).

TABLE 12-4(a) SOUTH ABUTMENT PILE CAPACITY SUMMARY FOR 17.5 m PILE EMBEDMENT			
Method Used for Estimation of Pile Capacity	Calculated Pile Shaft Resistance (kN)	Calculated Pile Toe Resistance (kN)	Calculated Ultimate Pile Capacity (kN)
α Method	1,648	182	1,830
Effective Stress Method	898	715	1,613
Driven Program	1,644	190	1,834
LPC CPT Program - CPT Data	1,361	328	1,689
Schmertmann Method - CPT Data	1,717	353	2,070

1 kip = 4.448 kN

TABLE 12-4(b) SOUTH ABUTMENT PILE LENGTH SUMMARY FOR A 1,780 kN ULTIMATE PILE CAPACITY	
Method Used for Estimation of Pile Capacity	Calculated Pile Length for the 1,780 kN Ultimate Pile Capacity
α Method	17.5 meters for 1,830 kN
Effective Stress Method	18.7 meters for 1,800 kN
Driven Program	17.5 meters for 1,834 kN
LPC CPT Program - CPT Data	19.5 meters for 1,807 kN
Schmertmann Method - CPT Data	15.2 meters for 1,828 kN

1 ft = 0.305 m, 1 kip = 4.448 kN

Note: These analyses do not consider the influence of downdrag loads on pile capacity which is discussed in Section 12.16.6.

At the South Abutment, the ultimate pile group capacity against block failure has been calculated and compared with the ultimate pile group capacity from the sum of the ultimate capacities of the individual piles times the group efficiency. Based on the design recommendations outlined in Section 9.8.1.2, a group efficiency of 1.0 was used. This calculation, included in Section F.2.4.1 of Appendix F, indicates that ultimate capacity

against block failure is greater than the ultimate capacity of the group. Therefore, block failure is not a design issue.

At all four substructure locations, the group capacity meets the design requirements.

12.16.3 Group Settlement Calculations

The optimized foundation layout resulted in a pile group having 3 rows of piles with 8 piles in each row. The piles are arranged at 1.5 m (5 ft) center to center spacing with a total pile group area of 3.36 m by 10.86 m (11.0 x 35.6 ft). Piles in a group are combined with a pile cap having a dimension of 4.5 m by 12 m (14.8 x 39.4 ft). The maximum pile group settlement should be less than 25 mm (1 inch) under the compression loads with maximum differential settlements of 15 mm (0.6 inch) between substructure units.

At the North Abutment, group settlement has been calculated using the Meyerhof Method detailed in Section 9.8.2.2. Results of this calculation are given in Appendix F.3.1 and indicate that the total pile group settlement is 12.2 mm (0.48 inch) due to soil compression and elastic pile compression. This is less than the maximum allowable settlement of 25 mm (1 inch).

At Pier 2, group settlement has also been calculated using the Meyerhof Method detailed in Section 9.8.2.2. Results of this calculation are given in Appendix F.3.2 and indicate that the total pile group settlement is 13.2 mm (0.52 inch) due to soil compression and elastic pile compression. This is less than the maximum allowable of 25 mm (1 inch).

At Pier 3, group settlement has been calculated using the equivalent footing method for layered soils described in Section 9.8.2.4 and the Meyerhof Method detailed in Section 9.8.2.2. Results of these calculations are given in Appendix F.3.3. The calculated settlement using the equivalent footing method is 16.1 mm (0.63 inch) including soil settlement and elastic pile compression. Most of this calculated settlement (12 mm or 0.47 inch) is in the clay layer. Since the piles are supported in an underlying dense sand and gravel layer where settlements are calculated to be 3.0 mm (0.12 inch), it is unlikely that the calculated settlement in the clay layer could develop due to the lack of strain compatibility between layers. The Meyerhof Method calculation indicates a group settlement of 9.0 mm (0.35 inch) including soil settlement and pile compression. In this soil profile, the Meyerhof Method calculation is considered a better indicator of probable foundation performance under load. Therefore the calculated settlement at Pier 3 of 9.0 mm (0.35 inch) is less than the maximum allowable of 25 mm (1 inch).

At the South Abutment, group settlement has been calculated using the equivalent footing method described in Section 9.8.2.3. Results of this calculation are provided in Appendix F.3.4 and indicate that the group settlement at the South Abutment is 28 mm (1.10 inch) including soil and pile compression. This is larger than the maximum allowable pile group settlement of 25 mm (1 inch). The group settlement will even be larger after the placement of the approach embankment fill materials behind the abutment wall. The settlement from embankment construction alone is calculated to be 500 mm (19.7 inches). Therefore, preloading of the South Abutment should be performed prior to pile installation.

With preloading of the South Abutment, group settlements could be kept within the foundation performance criteria. Differential settlements between substructure units have been calculated to be within the 15 mm (0.60 inch) criterion for differential settlement provided preloading at the South Abutment is performed.

12.16.4 Lateral Pile Capacity Analysis

The bridge division has determined that the group lateral loads range from 600 kN (135 kips) at the interior pile groups to 900 kN (202 kips) at the abutment pile groups. The maximum lateral load per pile is limited to 40 kN (9 kips). A horizontal deflection of up to 10 mm (0.40 inch) is permissible under lateral loading.

A simple Broms' Method lateral pile capacity analysis has been performed for the North Abutment piles. This calculation, included in Appendix F.4.1, indicates that the maximum lateral load per pile is 25 kN (6 kips) in order to meet the 10 mm (0.40 inch) deflection requirement. This lateral load is less than desired. Therefore, the group capacity of 600 kN (135 kips) based on 24 piles at 25 kN/pile (6 kips) is less than the 900 kN (202 kips) required, and more piles would be needed.

A more rigorous LPILE analysis was also performed to evaluate the lateral load capacity of the 356 mm (14 inch) square prestressed concrete piles at the North Abutment. This analysis is included in Appendix F.4.2 and indicates that the pile deflection under the 40 kN (9 kips) design load will be 3.2 mm (0.12 inch). The corresponding maximum moment and shear stress are -54.2 kN-m (40 kip-ft) and 14,500 kN/m² (304 kips/ft²). The deflection, moment and shear stress under the design load are acceptable. Hence, the LPILE analysis indicates a 40 kN (9 kips) design lateral load could be used whereas the Broms' Method indicated only a 25 kN (6 kips) design load.

An LPILE analysis was also performed to evaluate the lateral load capacity of the 356 mm (14 inch) square prestressed concrete pile at the South Abutment. This analysis is included in Appendix F.4.5 and indicates that the pile deflection under the 40 kN (9 kips) design load will be 1.9 mm (0.07 inch). The corresponding maximum moment and shear stress are - 44.4 kN-m (32.7 kip-ft) and 13,100 kN/m² (275.1 kips/ft²). The deflection, moment and shear stress under the design load are acceptable.

Additional LPILE analyses should be performed to evaluate the 356 mm (14 inch) concrete piles in Piers 2 and 3. These analyses are not included here.

12.16.5 Uplift Capacity Calculations

The maximum uplift load on a pile group is estimated to be 1,800 kN (405 kips) with a maximum uplift load per pile of 100 kN (23 kips). A calculation of the uplift capacity of the North Abutment pile group has been performed following AASHTO Code (2002) for service load design as outlined in Section 9.8.3.1. Following this procedure, the uplift capacity of the North Abutment pile group is 2,475 kN (556 kips), which is greater than the maximum uplift load of 1,800 kN (405 kips). Uplift calculation results are included in Appendix F.5.1.

A calculation of the uplift capacity of the Pier 2 pile group has also been performed in Appendix F.5.2. Following this procedure, the uplift capacity of the Pier 2 pile group is 2,616 kN (588 kips), which is greater than the maximum uplift load of 1,800 kN (405 kips).

At Pier 3, an uplift capacity calculation in accordance with AASHTO code yielded an uplift capacity of 3,354 kN (754 kips), which is greater than the maximum uplift load of 1,800 kN (405 kips). Uplift calculation results for Pier 3 are included in Appendix F.5.3.

A calculation of the uplift capacity of the South Abutment pile group has also been performed. The uplift capacity of the South Abutment pile group is 4,275 kN (961 kips), which is greater than the maximum uplift load of 1,800 kN (405 kips). Uplift calculation results for the South Abutment are included in Appendix F.5.4.

12.16.6 Negative Shaft Resistance

Piles at the South Abutment will be subjected to negative shaft resistance or downdrag loading due to soil settlement following the placement of 10 m (33 ft) of approach embankment material behind the abutment after pile installation. This settlement needs to

be estimated prior to determining the location of the negative and positive shaft resistances along the pile. The α -method is now used to estimate both the positive and negative shaft resistance components. The step by step procedure for the calculation of downdrag loading is presented in Section 9.9.1.1a.

Following this procedure, a drag load of 259 kN (58 kips) has been calculated. The net ultimate pile capacity for a 17.5 m (58 ft) embedded length available to resist imposed loads is then only 1,312 kN (295 kips) which is smaller than the required ultimate pile capacity. Therefore, alternatives such as preloading to reduce settlement and thereby the drag load, use of bitumen coatings to reduce pile-soil adhesion and thereby the drag load, or use of longer length piles to carry the drag load should be evaluated.

Calculations indicate use of bitumen coating to a depth of 5.5 m (18 ft) would reduce the negative shaft resistance to 78 kN (18 kips). However, the net ultimate pile capacity available to resist imposed loads on a 17.5 m (58 ft) embedded length pile is still only 1,493 kN (336 kips) which is less than the required ultimate pile capacity of 1780 kN (400 kips).

Calculations indicate the use of a 21 m (69 ft) long pile with a bitumen coating to a depth of 5.5 m (18 ft) would increase the ultimate pile capacity to 1,908 kN (429 kips). With these 21 m (69 ft) long piles, the net ultimate pile capacity available to resist imposed loads is 1,830 kN (411 kips). Hence, this alternate provides the required ultimate capacity. However, cost analyses of preloading, bitumen coatings, and longer piles in conjunction with meeting performance criteria requirements should be performed before making the final selection. The negative shaft resistance calculations are given in Appendix F.6.1.

A stub abutment instead of a full height abutment may also be a solution at the South Abutment. The stub abutment could be supported on a spread footing with specified embankment material and density control in the foundation area. A stub abutment with pile foundation is another alternative available for consideration.

This design problem illustrates the difficulties encountered in designing pile foundations in clay where substantial settlements occur and large drag loads are encountered by piles.

12.16.7 Lateral Squeeze Evaluation

The South Abutment should be evaluated for the potential for lateral squeeze following the guidelines presented in Section 9.9.3 of Chapter 9. Following these procedures, calculations presented in Appendix F.7.1 indicate that abutment tilting can occur. If piles are placed before any soil compression occurs, calculations indicate horizontal movement of 124 mm (4.9 inches), which is not tolerable. If piles are driven after 90% of vertical settlement has occurred, calculations indicate horizontal movements of 12.4 mm (0.49 inches). This is greater than the performance criteria but could be tolerated if provisions were made in the bridge shoe and expansion joint design.

12.16.8 Group Lateral Response Evaluation

The pile group response should be evaluated at all substructure units using the p-multiplier approach described in Section 9.8.4 or using software routines such as GROUP or FBPIER.

A series of LPILE analyses was performed to check the group deflection, moments and stresses imposed on the 356 mm (14 inch) square concrete piles in each row in the North Abutment. The lateral load on the group was assumed to act along the three pile axis and perpendicular to the eight pile axis. At the maximum lateral load on a single pile of 40 kN (9 kips), the calculations from Appendix F.8.1 show an estimated group deflection of 5.4 mm (0.21 inches), which corresponds to total stresses of 19,000; 16,000 and 14,500 kPa (2.75, 2.32, and 2.10 ksi) in the Front Row, Second Row and Third Row, respectively.

The deflection and total stresses are acceptable, but an analysis of the interaction between the substructure and superstructure should be performed. Analyses of lateral loading parallel to the eight pile axis, on the Piers and on the South Abutment should also be performed, but are not included here.

12.17 BLOCK 16 – DOES OPTIMIZED DESIGN MEET ALL REQUIREMENTS?

The selected pile lengths have now been checked for compression, lateral, and uplift loading as well as settlements. With preloading at the South Abutment group capacities and settlements are satisfactory. At this point the design has been found acceptable from a geotechnical perspective to meet the performance requirements. Pile lengths, loads and pile group configurations have been optimized.

A final pile driveability review of the design indicates the 356 mm (14 inch) concrete piles may be too difficult to install to the required penetration depths at the interior piers. Therefore, the interior pier foundations are re-designed and optimized using the second most cost effective option, the HP 360 x 152 (HP 14x102) H-piles. LPILE analyses for the H-piles at Piers 2 and 3 are performed and are presented in Appendix F.4.3. and F.4.4, respectively. To satisfy capacity requirements in the event of scour, the H-piles would need to be driven to within 1.5 meters of bedrock. Driveability results for the H-pile solution at Pier 2, are presented in Section 16.5.5 and Appendix F.9.2.3. These results indicate H-piles could be driven to bedrock. Therefore, the final design of the interior pier foundations was optimized using fewer higher capacity piles. This optimized H-pile design at the interior piers was found to meet all the design requirements including driveability. Therefore, all of the design requirements are now satisfied and the design is finalized.

12.18 BLOCK 17 - PREPARE PLANS AND SPECIFICATIONS, SET FIELD CAPACITY DETERMINATION PROCEDURE

The foundation design report should now be prepared. This report should summarize the results of the subsurface exploration program, laboratory test data, static analyses, a specific design and construction recommendations. The report should also highlight any special notes which should be incorporated into the plans or specifications which are also prepared at this time. For example, the preloading requirement at the South Abutment to reduce foundation settlements and drag loads should be clearly stated in the project plans and specifications.

Because of the variability of the subsurface site conditions, the foundation report recommended construction control using a static load test. Wave equation analysis is also required for driving system approval. In addition, dynamic testing has been specified during initial driving and restriking of two test piles per each substructure location. These test piles are to be driven in advance of production pile driving. The required ultimate pile capacity, driving stress limits, and testing methods are then incorporated into the plans and specifications.

12.19 BLOCK 18 - CONTRACTOR SELECTION

At this time the bidding process is completed, a successful contractor is selected.

12.20 BLOCK 19 - PERFORM WAVE EQUATION ANALYSIS OF CONTRACTOR'S EQUIPMENT SUBMISSION

The engineering effort now shifts to the field. The contractor has submitted the Pile Driving and Equipment Data form shown in Figure 11.1 for the engineer's evaluation of the proposed driving system. The design stage driveability studies were saved and can now be reanalyzed using the proposed driving system as part of the hammer approval process. Additional wave equation analyses are now performed to determine the driving resistance that must be achieved in the field to meet the required capacity and pile penetration depth. Driving stresses are also determined and checked against specification requirements. All conditions are satisfactory, and the equipment is approved for pile driving.

12.21 BLOCK 20 - SET PRELIMINARY DRIVING CRITERIA

Based on the results of the wave equation analysis of Block 19 along with minimum pile penetration requirements for scour, the preliminary driving criteria is set.

12.22 BLOCK 21 - DRIVE TEST PILE AND EVALUATE CAPACITY

Test piles are now driven using the preliminary driving criteria at each substructure location. Dynamic testing is performed on the test piles during initial driving and during restrike. The ultimate pile capacity is confirmed at each substructure unit by the dynamic test results and the correlating static load test.

12.23 BLOCK 22 - ADJUST DRIVING CRITERIA OR DESIGN

At this stage the final conditions can be set. If test results from Block 21 had indicated the capacity was inadequate, the driving criteria may have to be changed. In a few cases, it may be necessary to make changes in the design as far back as Block 7. If major changes are required, it will be necessary to repeat Blocks 19, 20, and 21.

12.24 BLOCK 23 - CONSTRUCTION CONTROL

After the driving criteria is set, the production pile driving proceeds following established quality control procedures.

12.25 BLOCK 24 – POST CONSTRUCTION EVALUATION AND REVIEW

After completion of the foundation construction, the design is reviewed and evaluated for its ability to satisfy the design requirements and its cost effectiveness.

Chapter 13

FOUNDATION DESIGN REPORT PREPARATION

A foundation design report should be prepared to present the results of the subsurface explorations, laboratory test data, analysis, and specific design and construction recommendations for the foundation system of a structure. The foundation report is referred to frequently during the design and construction period as well as in resolving post construction issues such as claims. It is therefore important that the foundation report be clear, concise and accurate. The foundation report is a very important document and should be prepared and reviewed accordingly.

As described in Chapter 12, the foundation design evolves as information is gathered and analyzed. Preliminary design recommendations based on, and/or transmitted with initial subsurface data does not constitute a foundation design report. A foundation design report should be developed with the full knowledge of loads, special design events, performance criteria and any site restrictions. Only with this full knowledge can a foundation design report be prepared with appropriate content and quality. The parts of a foundation design report are described in greater detail in Section 13.2.

The foundation report should be widely distributed to design, construction and maintenance engineers involved in the project. The foundation report should also furnish information regarding anticipated construction problems and solutions. This will provide a basis for the contractor's cost estimates.

The foundation design report should be completed and available to the designer prior to final design. The foundation drawings, special provisions, and foundation design report should all be cross-checked for compliance upon completion of final design documents. Conflicts between any of these documents greatly increases the potential for construction problems.

13.1 GUIDELINES FOR FOUNDATION DESIGN REPORT PREPARATION

1. The geotechnical engineer responsible for the report preparation should have a broad enough background in geotechnical and highway engineering to have knowledge of the foundation requirements and limitations for various types of structures. This includes knowledge in specifications, construction procedures, construction methods, quality control and assurance, and structural components.

2. The geotechnical engineer must have a clear and complete understanding of the compression, uplift and lateral load demands, performance criteria regarding deformations and constraints or restrictions.
3. The report should contain an interpretation and analysis of subsurface and site data. This includes a description of analysis and results in a summarized form.
4. The report should contain specific engineering recommendations for design.
5. Recommendations should be brief, concise, and definitive.
6. Reasons for recommendations and their supporting data should always be included.
7. Extraneous data of little use to the designer or Project Engineer should be omitted.
8. Discussion of soil materials and subsurface conditions which may be encountered during construction should be included.
9. Possible design and/or construction problems should be anticipated and recommendations for their solution should be included in the report.
10. The report should highlight any special notes which need to be placed on the plans or in the specifications.

13.2 PARTS OF A FOUNDATION DESIGN REPORT

A standard format provides uniformity of report writing as well as a checklist, so that major foundation design and construction considerations are not overlooked. The Soil and Foundations Workshop Manual FHWA HI-00-045 by Cheney and Chassie (2000) contains a foundation report outline that has been modified to include information from the AASHTO manual on Subsurface Investigations (1988). This modified outline is presented below and is recommended as a report preparation guide.

I. Table of Contents

II. Introduction

1. Summary of proposed construction, including foundation loading conditions (vertical and horizontal, static and dynamic, various combinations).

2. Summary of special design events: scour, seismic, vessel impact.
3. Foundation performance criteria (total and differential settlements, lateral deformation, vibration limits).

III. Scope of Explorations

1. Field explorations (summary of dates and methods, appended results).
2. Laboratory Testing (summary of types of tests, appended results).

IV. Interpretation of Subsurface Conditions

1. Description of formations.
2. Soil types.
3. Dip and strike of rock.
 - a. Regional.
 - b. Local.
4. Water table data.
 - a. Perched.
 - b. Regional.
 - c. Artesian.

V. Design Soil Parameters

1. Narrative to describe procedure for evaluating all factual data to establish design values.
 - a. Shear strength.
 - b. Compressibility.

VI. Design Analysis

1. Description of design procedures.
2. Summary of results.

3. Explanation of interpretation.

VII. Geotechnical Conclusions and Recommendations

1. Approach embankment considerations (primarily for fills over soft, weak subsoils).

a. Stability.

1. Excavation and replacement of unsuitable materials.
2. Counter berm.
3. Stage construction, time delay.
4. Other treatment methods: change alignment, lower grade, lightweight fill, *etc.*
5. Estimated factors of safety with and without treatment: estimated costs for treatment alternates, recommended treatment.

b. Settlement of subsoils.

1. Estimated settlement amount.
2. Estimated settlement time.
3. Surcharge height.
4. Special foundation treatment: vertical drains, soil densification, soil removal and replacement, *etc.*
5. Waiting periods.
6. Downdrag loads on deep foundations.
7. Lateral squeeze of soft subsoils.

c. Construction considerations.

1. Select fill material: gradation and compaction requirements.
2. Construction monitoring (instrumentation).

d. Special notes.

2. Spread footing support.

a. Elevation of bottom of footing: based on frost depth, scour depth, or depth to competent bearing material.

b. Allowable bearing pressure: based on settlement or bearing capacity, considering soil or rock type, adjacent foundations, water table, *etc.*

- c. Footing size used in computations.
- d. Estimated settlement of soil supported footings.
- e. Resistance to sliding of soil supported footings.
- f. Excavation, structural fill, and dewatering requirements.
- g. Special notes.

3. Pile foundation support.

- a. Method of pile support: shaft resistance, toe resistance, or both. Delineation of unsuitable support layers due to compressibility, scour, or liquefaction.
- b. Suitable pile types: reasons for choice and/or exclusion of types and optimization of the recommended section.
- c. Pile toe elevations.
 - 1. Estimated toe elevation, (average estimated values from static analyses with probable variation potential).
 - 2. Specified toe elevation, (toe elevation required due to underlying soft layers, negative shaft resistance, scour, lateral or uplift loads, piles uneconomically long, *etc.*).
- d. Estimated pile lengths.
- e. Allowable pile design loads for compression, uplift, and lateral loading.
- f. Estimated pile group settlement; very important for pile groups in cohesive soils and large groups in a cohesionless soil deposit underlain by compressible soils.
- g. Test piles to establish order lengths; specify test locations for maximum utility.
- h. Static pile load tests; specify test locations for maximum utility.
 - 1. Axial compression.

2. Axial tension.

3. Lateral.

- i. O-cell or Statnamic load tests; specify test locations.
- j. Dynamic pile load tests; specify test locations and retap frequency.
- k. Driving criteria; specify use of wave equation analysis or dynamic formula.
- l. Estimated soil resistance to overcome in order to reach estimated pile length.
- m. Preboring, pile toe reinforcement, or other requirements to reach pile penetration requirements or handle potential obstructions.
- n. Pile driving requirements: hammer size, tolerances, *etc.*
- o. Cofferdams and seals; seal design should consider potential conflicts between batter piles driven at alignment tolerance limits and depth of sheeting. Group densification inside sheeting for displacement piles in sands, or heave for displacement piles in clays should be considered.
- p. Corrosion effects or chemical attack; particular concern in marine environments, old dumps, areas with soil or groundwater contaminants.
- q. Effects of pile driving on adjacent construction; settlements from vibrations and development of excess pore water pressures in soil.
- r. Special notes.

4. Drilled shaft support.

- a. Method of drilled shaft support: shaft resistance, toe resistance, or both. Delineation of unsuitable support layers.
- b. Shaft diameter and configuration: straight shafts, belled, rock sockets.
- c. Anticipated support elevation and resulting shaft length.
- d. Specified or likely construction method: dry, casing, slurry.

- e. Allowable shaft load for compression, uplift, and lateral loading with consideration of construction method.
 - f. Estimated settlement.
 - g. Load tests; specify test locations for maximum utility.
 - 1. Axial compression (specify static, O-cell, Statnamic, or dynamic)
 - 2. Axial tension.
 - 3. Lateral.
 - h. Integrity tests; specify type, frequency, and access tube material and placement, (if required).
 - 1. Low strain pulse echo tests.
 - 2. Cross hole - sonic logging.
 - 3. Down hole - parallel seismic.
 - 4. High strain dynamic tests.
 - i. Anticipated construction difficulties due to boulders, obstructions, groundwater, artesian conditions, unstable ground, *etc.*
 - j. Special notes.
5. Special design considerations.
- a. Seismic design; design earthquake ground acceleration, liquefaction potential (loose saturated sands and silts).
 - b. Lateral earth pressures against retaining walls and high bridge abutments.

VIII. Construction Considerations

- 1. Water table: fluctuations, control in excavation, pumping, tremie seals, *etc.*
- 2. Excavations: safe slopes for open excavations, need for sheeting shoring, *etc.*
- 3. Adjacent structures: protection against damage from excavation, pile driving vibrations, drilled shaft ground loss, drainage, *etc.*
- 4. Special notes.

VIV. Appendix: Graphic Presentations

1. Map showing project location.
2. Detailed plan of the site showing proposed structure(s) borehole locations and existing structures.
3. Laboratory test data.
4. Finished boring logs and interpreted soil profile.

X. Report Distribution

Copies of the completed Foundation Report should be transmitted to:

1. Bridge design section.
2. Roadway design section.
3. Construction section.
4. Project engineer.
5. Residency or maintenance group.
6. Others, as required by agency policy.

13.3 GEOTECHNICAL REPORT REVIEWS

The FHWA developed a checklist to aid highway engineers in the review of geotechnical reports, plans, and special provisions. This document, FHWA ED-88-053 was originally produced in 1988 and revised in 2003. A copy of the document can be downloaded from: www.fhwa.dot.gov/bridge/checklist.htm

The review checklist and guidelines were developed to assist highway engineers in:

- Review of geotechnical reports and plan, specification, and estimate (PS&E) packages;

- Recognize potential cost saving opportunities;
- Identify potential claim problems and deficiencies in the geotechnical report, analysis, or design;
- Recognize when a geotechnical specialist should be consulted for additional technical guidance.

13.4 INFORMATION MADE AVAILABLE TO BIDDERS

The information developed during the foundation design is of value to contractors bidding on the project. Disagreement exists among owners, engineers and lawyers as to what information should be made available to the bidders. It is generally in the interest of the highway agency to release all pertinent information prior to the bid.

The finished boring logs and/or generalized soil profile should be included in the contract plans. Other subsurface information, such as soil and rock samples, results of field and laboratory testing and the foundation design report, should be made available for inspection by bidders.

Disclaimers should be used very carefully. "General" disclaimer clauses should be avoided. "Specific" disclaimer clauses are given more weight by the courts in settling contract disputes. A good example of a "specific" disclaimer is provided in the paragraph below. Refer to Cheney and Chassie (2000) for additional information.

"The observed water levels and/or conditions indicated on the subsurface profiles are as recorded at the time of exploration. These water levels and/or conditions may vary considerably, with time, according to the prevailing climate, rainfall or other factors and are otherwise dependent on the duration of and methods used in the explorations program."

REFERENCES

- American Association of State Highway and Transportation Officials [AASHTO], (1988). Manual on Subsurface Investigations. AASHTO Highway Subcommittee on Bridges and Structures, Washington, D.C., 391.
- Cheney, R.S. and Chassie, R.G. (2000). Soils and Foundations Workshop Reference Manual. Publication No. FHWA HI-00-045, U.S. Department of Transportation, National Highway Institute, Federal Highway Administration, Washington, D.C., 358.

APPENDIX A

List of FHWA Pile Foundation Design and Construction References

- Briaud, J-L. (1989). The Pressuremeter Test for Highway Applications. Report No. FHWA IP-89-008, U.S. Department of Transportation, Federal Highway Administration, Office of Implementation, McLean, 156.
- Briaud, J-L. and Miran, J. (1991). The Cone Penetrometer Test. Report No. FHWA-SA-91-043, U.S. Department of Transportation, Federal Highway Administration, Office of Technology Applications, Washington, D.C., 161.
- Briaud, J-L. and Miran, J. (1992). The Flat Dilatometer Test. Report No. FHWA-SA-91-44, U.S. Department of Transportation, Federal Highway Administration, Office of Technology Applications, Washington, D.C., 102.
- Briaud, J-L., Tucker, L., Lytton, R.L. and Coyle, H.M. (1985). Behavior of Piles and Pile Groups in Cohesionless Soils. Report No. FHWA/RD-83/038, U.S. Department of Transportation, Federal Highway Administration, Office of Research - Materials Division, Washington, D.C., 233.
- Cheney, R.S. and Chassie, R.G. (2000). Soils and Foundations Workshop Reference Manual. Publication No. FHWA HI-00-045, U.S. Department of Transportation, National Highway Institute, Federal Highway Administration, Office of Engineering, Washington, D.C., 358.
- Goble, G.G., and Rausche, F. (1986). Wave Equation Analysis of Pile Driving - WEAP86 Program. U.S. Department of Transportation, Federal Highway Administration, Implementation Division, McLean, Volumes I-IV.
- Kyfor, Z.G., Schnore, A.S., Carlo, T.A. and Bailey, P.F. (1992). Static Testing of Deep Foundations. Report No. FHWA-SA-91-042, U.S. Department of Transportation, Federal Highway Administration, Office of Technology Applications, Washington, D.C., 174.

- Lam, I.P. and Martin, G.R. (1986). Seismic Design of Highway Bridge Foundations. Volume II - Design Procedures and Guidelines, Report No. FHWA/RD-86/102, U.S. Department of Transportation, Federal Highway Administration, Office of Engineering and Highway Operations, McLean, 181.
- Mathias, D. and Cribbs, M. (1998). DRIVEN 1.0: A Microsoft Windows™ Based Program for Determining Ultimate Vertical Static Pile Capacity. Report No. FHWA-SA-98-074, U.S. Department of Transportation, Federal Highway Administration, Office of Technology Applications, Washington D.C. 112.
- Osterberg, J.O. (1995). The Osterberg Cell for Load Testing Drilled Shafts and Driven Piles. Report No. FHWA-SA-94-035, U.S. Department of Transportation, Federal Highway Administration, Office of Technology Applications, Washington, D.C., 92.
- Rausche, F., Likins, G.E., Goble, G.G. and Miner, R. (1985). The Performance of Pile Driving Systems. Main Report, U.S. Department of Transportation, Federal Highway Administration, Office of Research and Development, Washington, D.C., Volumes I-IV.
- Reese, L.C. (1984). Handbook on Design of Piles and Drilled Shafts Under Lateral Load. Report No. FHWA-IP-84 11, U.S. Department of Transportation, Federal Highway Administration, Office of Implementation, McLean, 386.
- Wang, S-T, and Reese, L.C. (1993). COM624P - Laterally Loaded Pile Analysis Program for the Microcomputer, Version 2.0. Report No. FHWA-SA-91-048, U.S. Department of Transportation, Federal Highway Administration, Office of Technology Applications, Washington, D.C., 504.

APPENDIX B

List of ASTM Pile Design and Testing Specifications

DESIGN

Standard Specification for Welded and Seamless Steel Pipe Piles.
ASTM Designation: A 252

Standard Specification for Round Timber Piles.
ASTM Designation: D 25

Standard Method for Establishing Design Stresses for Round Timber Piles.
ASTM Designation: D 2899

Standard Methods for Establishing Clear Wood Strength Values.
ASTM Designation: D 2555

TESTING

Standard Method for Testing Piles under Axial Compressive Load.
ASTM Designation: D 1143

Standard Method for Testing Individual Piles under Static Axial Tensile Load.
ASTM Designation: D 3689

Standard Method for Testing Piles under Lateral Load.
ASTM Designation: D 3966

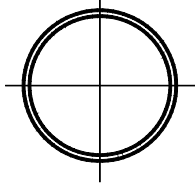
Standard Test Method for High Strain Dynamic Testing of Piles.
ASTM Designation: D 4945

Standard Test Method for Low Strain Dynamic Testing of Piles.
ASTM Designation: D 5882

APPENDIX C-1

Information and Data on Various Pile Types, Metric Units

	Page
Dimensions and Properties of Pipe Piles	C1-3
Data for Steel Monotube Piles.....	C1-17
Typical Prestressed Concrete Pile Sections.....	C1-18
Dimensions and Properties of H-Piles.....	C1-21



PIPE PILES

Approximate Pile Dimensions and Design Properties

Designation and Outside Diameter	Wall Thickness	Area A	Weight per Meter	Section Properties			Area of Exterior Surface	Inside Cross Sectional Area	Inside Volume	External Collapse Index
				I	S	r				
mm	mm	mm ²	N	mm ⁴ x 10 ⁶	mm ³ x 10 ³	mm	m ² /m	mm ²	m ³ /m	*
PP203	3.58	2,245	173	11.197	110.12	70.61	0.64	30,193	0.0301	266
	4.17	2,607	200	12.903	127.00	70.36	0.64	29,806	0.0298	422
	4.37	2,729	210	13.486	132.74	70.36	0.64	29,677	0.0296	487
	4.55	2,839	218	13.985	137.82	70.36	0.64	29,613	0.0296	548
	4.78	2,974	229	14.651	144.21	70.10	0.64	29,484	0.0293	621
	5.56	3,452	266	16.857	165.51	69.85	0.64	28,968	0.0291	874
PP219	2.77	1,884	145	10.989	100.45	76.45	0.69	35,806	0.0359	97
	3.18	2,155	166	12.570	114.55	76.45	0.69	35,548	0.0356	147
	3.58	2,426	187	14.069	128.47	76.20	0.69	35,290	0.0354	212
	3.96	2,678	206	15.484	141.42	75.95	0.69	35,032	0.0351	288
	4.17	2,813	216	16.233	148.30	75.95	0.69	34,903	0.0349	335
	4.37	2,949	227	16.982	155.02	75.95	0.69	34,774	0.0349	388
	4.55	3,065	236	17.648	160.92	75.95	0.69	34,645	0.0346	438
	4.78	3,213	247	18.481	168.79	75.69	0.69	34,452	0.0344	508
	5.16	3,465	266	19.813	180.26	75.69	0.69	34,258	0.0341	623
	5.56	3,729	287	21.269	195.01	75.44	0.69	33,935	0.0339	744
	6.35	4,245	326	24.017	219.59	75.18	0.69	33,419	0.0334	979
	7.04	4,684	360	26.389	240.89	74.93	0.69	33,032	0.0331	1,180
	7.92	5,258	404	29.344	267.11	74.68	0.69	32,452	0.0324	1,500
	8.18	5,420	417	30.177	275.30	74.68	0.69	32,258	0.0324	1,600
	8.74	5,775	444	31.967	291.69	74.42	0.69	31,935	0.0319	1,820
	9.53	6,271	482	34.506	314.63	74.17	0.69	31,419	0.0314	2,120
10.31	6,775	520	36.920	337.57	73.91	0.69	30,903	0.0309	2,420	
11.13	7,291	559	39.417	358.88	73.66	0.69	30,452	0.0304	2,740	
12.70	8,259	633	44.121	401.48	73.15	0.69	29,484	0.0293	3,340	
PP254	2.77	2,187	168	17.232	135.68	88.90	0.80	48,516	0.0484	62
	3.05	2,400	185	18.939	148.96	88.65	0.80	48,258	0.0482	83
	3.40	2,678	206	21.020	165.51	88.65	0.80	48,000	0.0479	116

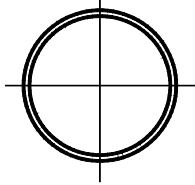
Pile design data converted to SI units from US units published in 1985 version of this manual.

Note: Designer must confirm section properties and local availability of selected pile section.

Material Specifications - ASTM A252

Example of suggested method of designation: PP219 x 2.77

* The External Collapse Index is a non-dimensional function of the diameter to wall thickness ratio and is for general guidance only. The higher the number, the greater is the resistance to collapse.



PIPE PILES

Approximate Pile Dimensions and Design Properties

Designation and Outside Diameter	Wall Thickness	Area A	Weight per Meter	Section Properties			Area of Exterior Surface	Inside Cross Sectional Area	Inside Volume	External Collapse Index
				I	S	r				
mm	mm	mm ²	N	mm ⁴ x 10 ⁶	mm ³ x 10 ³	mm	m ² /m	mm ²	m ³ /m	*
	3.58	2,820	217	22.102	173.70	88.65	0.80	47,871	0.0479	135
	3.81	2,994	230	23.434	185.17	88.39	0.80	47,677	0.0477	163
	4.17	3,271	251	25.515	201.56	88.39	0.80	47,419	0.0474	214
	4.37	3,426	263	26.680	209.75	88.39	0.80	47,226	0.0472	247
	4.55	3,562	274	27.721	217.95	88.14	0.80	47,097	0.0472	279
	4.78	3,742	287	29.053	229.42	88.14	0.80	46,903	0.0469	324
	5.16	4,033	310	31.217	245.81	87.88	0.80	46,645	0.0467	409
	5.56	4,342	334	33.507	263.83	87.88	0.80	46,322	0.0464	515
	5.84	4,555	350	35.088	276.94	87.88	0.80	46,129	0.0462	588
	6.35	4,942	380	37.919	298.24	87.63	0.80	45,742	0.0457	719
PP273	2.77	2,349	181	21.478	157.32	95.50	0.86	56,193	0.0562	50
	3.05	2,587	199	23.559	172.06	95.50	0.86	56,000	0.0559	67
	3.18	2,690	207	24.516	180.26	95.50	0.86	55,871	0.0559	76
	3.40	2,884	222	26.223	191.73	95.25	0.86	55,677	0.0557	93
	3.58	3,032	233	27.513	201.56	95.25	0.86	55,548	0.0554	109
	3.81	3,226	248	29.219	214.67	95.25	0.86	55,355	0.0554	131
	3.96	3,349	258	30.343	222.86	95.25	0.86	55,226	0.0552	148
	4.17	3,516	271	31.800	232.70	95.00	0.86	55,032	0.0549	172
	4.37	3,691	284	33.299	244.17	95.00	0.86	54,839	0.0549	199
	4.55	3,832	295	34.589	254.00	95.00	0.86	54,710	0.0547	224
	4.78	4,026	310	36.212	265.47	94.74	0.86	54,516	0.0544	260
	5.16	4,342	334	38.959	285.13	94.74	0.86	54,193	0.0542	328
	5.56	4,679	359	41.623	306.44	94.49	0.86	53,871	0.0539	414
	5.84	4,904	377	43.704	321.19	94.49	0.86	53,677	0.0537	480
	6.35	5,323	409	47.450	347.41	94.23	0.86	53,226	0.0532	605
	7.09	5,923	455	52.445	383.46	93.98	0.86	52,645	0.0527	781
	7.80	6,517	500	57.024	419.51	93.73	0.86	52,064	0.0522	951
	8.74	7,226	558	63.267	465.39	93.47	0.86	51,290	0.0514	1,180

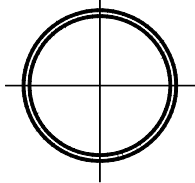
Pile design data converted to SI units from US units published in 1985 version of this manual.

Note: Designer must confirm section properties and local availability of selected pile section.

Material Specifications - ASTM A252

Example of suggested method of designation: PP219 x 2.77

* The External Collapse Index is a non-dimensional function of the diameter to wall thickness ratio and is for general guidance only. The higher the number, the greater is the resistance to collapse.



PIPE PILES

Approximate Pile Dimensions and Design Properties

Designation and Outside Diameter	Wall Thickness	Area A	Weight per Meter	Section Properties			Area of Exterior Surface	Inside Cross Sectional Area	Inside Volume	External Collapse Index
				I	S	r				
mm	mm	mm ²	N	mm ⁴ x 10 ⁶	mm ³ x 10 ³	mm	m ² /m	mm ²	m ³ /m	*
	9.27	7,678	591	67.013	489.97	93.22	0.86	50,903	0.0509	1,320
	11.13	9,162	704	78.668	576.82	92.71	0.86	49,419	0.0494	1,890
	12.70	10,389	799	88.241	645.65	92.20	0.86	48,193	0.0482	2,380
PP305	3.40	3,226	248	36.587	240.89	106.68	0.96	69,677	0.0697	67
	3.58	3,387	261	38.460	252.36	106.43	0.96	69,677	0.0695	78
	3.81	3,600	277	40.791	267.11	106.43	0.96	69,677	0.0695	94
	4.17	3,936	303	44.537	291.69	106.43	0.96	69,032	0.0690	123
	4.37	4,123	317	46.618	304.80	106.17	0.96	69,032	0.0687	142
	4.55	4,291	330	48.283	317.91	106.17	0.96	68,387	0.0687	161
	4.78	4,503	346	50.780	332.66	106.17	0.96	68,387	0.0685	186
	5.16	4,852	373	54.526	357.24	105.92	0.96	68,387	0.0682	235
	5.56	5,233	402	58.689	383.46	105.92	0.96	67,742	0.0677	296
	5.84	5,484	422	61.186	403.12	105.66	0.96	67,742	0.0675	344
	6.35	5,955	458	66.181	435.90	105.66	0.96	67,097	0.0670	443
	7.14	6,646	513	74.089	485.06	105.16	0.96	66,451	0.0662	616
7.92	7,420	568	81.581	534.22	104.90	0.96	65,806	0.0655	784	
PP324	2.77	2,794	215	36.004	222.86	113.54	1.02	79,355	0.0795	30
	3.18	3,200	246	41.124	254.00	113.28	1.02	79,355	0.0793	45
	3.40	3,426	264	44.121	272.03	113.28	1.02	78,710	0.0790	56
	3.58	3,607	277	46.202	285.13	113.28	1.02	78,710	0.0788	65
	3.81	3,832	295	49.115	303.16	113.29	1.02	78,710	0.0785	78
	3.96	3,981	306	50.780	314.63	113.03	1.02	78,710	0.0785	88
	4.17	4,181	322	53.278	329.38	113.03	1.02	78,064	0.0783	103
	4.37	4,387	337	55.775	345.77	113.03	1.02	78,064	0.0780	118
	4.55	4,562	351	58.272	358.88	113.03	1.02	78,064	0.0778	134
	4.78	4,787	368	60.770	376.90	112.78	1.02	77,419	0.0775	155
	5.16	5,162	397	65.765	404.76	112.78	1.02	77,419	0.0773	196
5.56	5,562	428	70.343	435.90	112.52	1.02	76,774	0.0768	246	

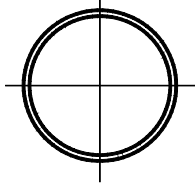
Pile design data converted to SI units from US units published in 1985 version of this manual.

Note: Designer must confirm section properties and local availability of selected pile section.

Material Specifications - ASTM A252

Example of suggested method of designation: PP219 x 2.77

* The External Collapse Index is a non-dimensional function of the diameter to wall thickness ratio and is for general guidance only. The higher the number, the greater is the resistance to collapse.



PIPE PILES

Approximate Pile Dimensions and Design Properties

Designation and Outside Diameter	Wall Thickness	Area A	Weight per Meter	Section Properties			Area of Exterior Surface	Inside Cross Sectional Area	Inside Volume	External Collapse Index
				I	S	r				
mm	mm	mm ²	N	mm ⁴ x 10 ⁶	mm ³ x 10 ³	mm	m ² /m	mm ²	m ³ /m	*
	5.84	5,839	449	73.673	455.56	112.52	1.02	76,774	0.0765	286
	6.35	6,336	487	79.916	493.25	112.27	1.02	76,129	0.0760	368
	7.14	7,097	546	89.074	550.61	112.01	1.02	75,484	0.0753	526
	7.92	7,871	605	98.231	606.32	111.76	1.02	74,193	0.0745	684
	8.38	8,323	639	103.225	639.10	111.51	1.02	74,193	0.0740	776
	8.74	8,646	665	107.388	663.68	111.51	1.02	73,548	0.0737	848
	9.53	9,420	723	116.129	717.75	111.25	1.02	72,903	0.0730	1,010
	10.31	10,131	781	124.869	771.83	111.00	1.02	72,258	0.0722	1,170
	11.13	10,905	840	133.610	825.91	110.74	1.02	71,613	0.0715	1,350
	12.70	12,389	955	150.676	929.15	109.98	1.02	69,677	0.0700	1,760
PP356	3.40	3,768	290	58.272	327.74	124.47	1.12	95,484	0.0956	42
	3.58	3,962	305	61.186	345.77	124.47	1.12	95,484	0.0953	49
	3.81	4,213	324	65.348	367.07	124.46	1.12	94,839	0.0951	59
	3.96	4,374	337	67.846	380.18	124.21	1.12	94,839	0.0948	66
	4.17	4,600	354	71.176	399.84	124.21	1.12	94,839	0.0948	77
	4.37	4,820	371	74.505	417.87	124.21	1.12	94,193	0.0946	89
	4.55	5,013	386	77.419	434.26	124.21	1.12	94,193	0.0943	101
	4.78	5,265	405	81.165	455.56	123.95	1.12	94,193	0.0941	117
	5.16	5,678	436	86.992	489.97	123.95	1.12	93,548	0.0936	147
	5.33	5,871	451	89.906	506.36	123.95	1.12	93,548	0.0936	163
	5.56	6,116	470	93.652	527.66	123.70	1.12	92,903	0.0933	815
	5.84	6,420	494	98.231	552.24	123.70	1.12	92,903	0.0928	215
	6.35	6,968	536	106.139	598.13	123.44	1.12	92,258	0.0923	277
	7.14	7,807	601	118.626	666.95	123.19	1.12	91,613	0.0916	395
	7.92	8,646	666	130.697	735.78	122.94	1.12	90,968	0.0906	542
	8.74	9,549	732	143.184	806.24	122.68	1.12	89,677	0.0898	691
	9.53	10,389	796	155.254	873.43	122.43	1.12	89,032	0.0890	835
	11.13	12,065	926	178.563	1,006.17	121.92	1.12	87,097	0.0873	1,130

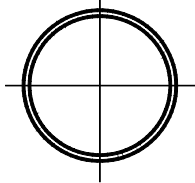
Pile design data converted to SI units from US units published in 1985 version of this manual.

Note: Designer must confirm section properties and local availability of selected pile section.

Material Specifications - ASTM A252

Example of suggested method of designation: PP219 x 2.77

* The External Collapse Index is a non-dimensional function of the diameter to wall thickness ratio and is for general guidance only. The higher the number, the greater is the resistance to collapse.



PIPE PILES

Approximate Pile Dimensions and Design Properties

Designation and Outside Diameter	Wall Thickness	Area A	Weight per Meter	Section Properties			Area of Exterior Surface	Inside Cross Sectional Area	Inside Volume	External Collapse Index
				I	S	r				
mm	mm	mm ²	N	mm ⁴ x 10 ⁶	mm ³ x 10 ³	mm	m ² /m	mm ²	m ³ /m	*
	11.91	12,839	989	190.218	1,070.08	121.67	1.12	86,451	0.0865	1,280
	12.70	13,678	1,052	201.456	1,132.35	121.41	1.12	85,806	0.0855	1,460
PP406	3.40	4,310	331	87.409	430.98	142.49	1.28	125,161	1.2542	28
	3.58	4,529	348	91.987	452.28	142.49	1.28	125,161	0.1252	33
	3.81	4,820	371	97.814	480.14	142.24	1.28	125,161	0.1249	39
	3.96	5,007	385	101.560	499.81	142.24	1.28	124,516	0.1247	44
	4.17	5,265	405	106.555	524.39	142.24	1.28	124,516	0.1244	52
	4.37	5,516	424	111.550	548.97	142.24	1.28	124,516	0.1242	60
	4.55	5,742	441	115.712	570.27	141.99	1.28	123,871	0.1239	67
	4.78	6,026	463	121.540	598.13	141.99	1.28	123,871	0.1237	78
	5.16	6,517	500	130.697	644.01	141.99	1.28	123,226	0.1232	98
	5.56	7,033	539	140.686	693.17	141.73	1.28	122,580	0.1227	124
	5.84	7,355	565	147.346	725.95	141.73	1.28	122,580	0.1224	144
	6.35	8,000	614	159.833	786.58	141.48	1.28	121,935	0.1217	185
	7.14	8,968	688	178.563	878.35	141.22	1.28	120,645	0.1207	264
	7.92	9,936	763	196.877	970.11	140.97	1.28	120,000	0.1199	362
	8.74	10,905	839	216.024	1,061.88	140.72	1.28	118,709	0.1189	487
	9.53	11,873	913	233.922	1,152.01	140.46	1.28	118,064	0.1179	617
	11.13	13,807	1,062	270.134	1,328.99	139.70	1.28	116,129	0.1159	874
11.91	14,775	1,135	287.616	1,414.20	139.45	1.28	114,838	0.1149	1,000	
12.70	15,679	1,208	304.681	1,499.42	139.19	1.28	114,193	0.1141	1,130	
PP457	3.58	5,104	392	131.113	573.55	160.27	1.44	159,355	0.1590	23
	4.37	6,213	478	159.417	696.45	160.02	1.44	158,064	0.1580	42
	4.78	6,775	522	173.569	760.36	160.02	1.44	157,419	0.1573	55
	5.16	7,291	563	186.888	817.71	159.77	1.44	156,774	0.1568	69
	5.56	7,871	607	201.456	879.99	159.77	1.44	156,129	0.1563	87
	5.84	8,259	637	211.029	922.59	159.51	1.44	156,129	0.1558	101
	6.35	8,968	692	228.511	999.61	159.51	1.44	155,484	0.1553	129

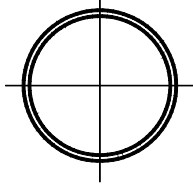
Pile design data converted to SI units from US units published in 1985 version of this manual.

Note: Designer must confirm section properties and local availability of selected pile section.

Material Specifications - ASTM A252

Example of suggested method of designation: PP219 x 2.77

* The External Collapse Index is a non-dimensional function of the diameter to wall thickness ratio and is for general guidance only. The higher the number, the greater is the resistance to collapse.



PIPE PILES

Approximate Pile Dimensions and Design Properties

Designation and Outside Diameter	Wall Thickness	Area A	Weight per Meter	Section Properties			Area of Exterior Surface	Inside Cross Sectional Area	Inside Volume	External Collapse Index
				I	S	r				
mm	mm	mm ²	N	mm ⁴ x 10 ⁶	mm ³ x 10 ³	mm	m ² /m	mm ²	m ³ /m	*
	7.14	10,065	776	255.566	1,117.60	159.26	1.44	154,193	0.1540	184
	7.92	11,163	860	282.205	1,235.58	158.75	1.44	152,903	0.1530	253
	8.74	12,323	947	309.676	1,353.57	158.50	1.44	151,613	0.1518	341
	9.53	13,420	1,030	335.899	1,468.28	158.24	1.44	150,967	0.1508	443
	10.31	14,452	1,113	361.705	1,581.35	157.99	1.44	149,677	0.1498	559
	11.13	15,615	1,199	387.928	1,704.25	157.73	1.44	148,387	0.1485	675
	11.91	16,646	1,281	413.318	1,802.58	157.48	1.44	147,742	0.1475	788
	12.70	17,743	1,364	437.043	1,917.29	157.23	1.44	146,451	0.1465	900
PP508	3.58	5,678	436	180.644	711.20	178.31	1.60	196,774	0.1969	17
	4.37	6,904	531	219.354	863.60	178.05	1.60	195,483	0.1957	30
	4.78	7,549	581	238.917	940.62	177.80	1.60	194,838	0.1952	40
	5.16	8,130	626	257.647	1,014.36	177.80	1.60	194,838	0.1947	50
	5.56	8,775	675	277.210	1,091.38	177.55	1.60	194,193	0.1939	63
	6.35	10,002	769	314.671	1,238.86	177.29	1.60	192,903	0.1926	94
	7.14	11,226	864	352.132	1,386.35	177.04	1.60	191,613	0.1914	134
	7.92	12,452	957	389.176	1,532.19	176.78	1.60	190,322	0.1901	184
	8.74	13,678	1,054	428.718	1,687.87	176.53	1.60	189,032	0.1889	247
	9.53	14,904	1,147	462.017	1,818.96	176.28	1.60	187,742	0.1879	321
	10.31	16,130	1,240	499.478	1,966.45	176.02	1.60	186,451	0.1866	409
	11.13	17,357	1,335	536.939	2,113.93	175.77	1.60	185,161	0.1854	515
	11.91	18,583	1,428	570.237	2,245.03	175.51	1.60	183,871	0.1841	618
12.70	19,743	1,520	607.698	2,392.51	175.26	1.60	183,225	0.1829	719	
PP559	4.37	7,613	585	292.611	1,047.13	196.09	1.76	237,419	0.2375	23
	4.78	8,323	639	318.833	1,142.18	195.83	1.76	236,774	0.2370	30
	5.56	9,678	743	370.030	1,324.07	195.58	1.76	235,483	0.2355	47
	6.35	11,034	847	420.394	1,504.33	195.33	1.76	234,193	0.2343	70
	7.14	12,389	951	470.342	1,687.87	195.07	1.76	232,903	0.2328	100
	7.92	13,744	1,055	520.289	1,868.13	194.82	1.76	231,612	0.2315	138

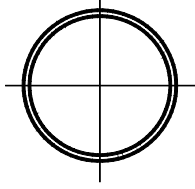
Pile design data converted to SI units from US units published in 1985 version of this manual.

Note: Designer must confirm section properties and local availability of selected pile section.

Material Specifications - ASTM A252

Example of suggested method of designation: PP219 x 2.77

* The External Collapse Index is a non-dimensional function of the diameter to wall thickness ratio and is for general guidance only. The higher the number, the greater is the resistance to collapse.



PIPE PILES

Approximate Pile Dimensions and Design Properties

Designation and Outside Diameter	Wall Thickness	Area A	Weight per Meter	Section Properties			Area of Exterior Surface	Inside Cross Sectional Area	Inside Volume	External Collapse Index
				I	S	r				
mm	mm	mm ²	N	mm ⁴ x 10 ⁶	mm ³ x 10 ³	mm	m ² /m	mm ²	m ³ /m	*
	8.74	15,099	1,161	570.237	2,048.38	194.56	1.76	230,322	0.2303	185
	9.53	16,454	1,264	620.185	2,212.25	194.31	1.76	229,032	0.2288	241
	10.31	17,743	1,366	670.133	2,392.51	194.06	1.76	227,741	0.2275	306
	11.13	19,162	1,472	715.918	2,572.77	193.55	1.76	225,806	0.2260	386
	11.91	20,454	1,574	765.866	2,736.64	193.29	1.76	224,516	0.2248	475
	12.70	21,809	1,675	811.651	2,900.51	193.04	1.76	223,225	0.2235	571
PP610	4.37	8,323	639	380.436	1,248.69	213.87	1.91	283,870	0.2834	18
	4.78	9,097	698	414.983	1,361.77	213.87	1.91	282,580	0.2834	23
	5.56	10,582	812	482.828	1,579.71	213.61	1.91	281,290	0.2809	36
	6.35	12,065	925	549.425	1,802.58	213.36	1.91	279,999	0.2809	54
	7.14	13,486	1,039	611.860	2,015.61	213.11	1.91	278,064	0.2784	77
	7.92	14,970	1,152	678.457	2,228.64	212.85	1.91	276,774	0.2759	106
	8.74	16,517	1,268	745.054	2,441.67	212.34	1.91	275,483	0.2759	142
	9.53	17,937	1,381	807.489	2,654.70	212.09	1.91	274,193	0.2734	185
	10.31	19,421	1,493	869.924	2,867.74	211.84	1.91	272,258	0.2734	235
	11.13	20,904	1,608	936.521	3,080.77	211.58	1.91	270,967	0.2709	296
	11.91	22,388	1,720	998.955	3,277.41	211.33	1.91	269,677	0.2684	364
	12.70	23,809	1,831	1,061.390	3,474.06	211.07	1.91	267,741	0.2684	443
PP660	6.35	13,033	1,003	699.269	2,113.93	231.14	2.08	329,677	0.3286	43
	7.14	14,646	1,126	782.515	2,359.74	230.89	2.08	327,741	0.3286	61
	7.92	16,259	1,249	865.761	2,621.93	230.63	2.08	326,451	0.3261	83
	8.74	17,872	1,376	949.008	2,884.12	230.38	2.08	324,515	0.3236	112
	9.53	19,485	1,498	1,032.254	3,129.93	230.12	2.08	323,225	0.3236	145
	10.31	21,034	1,620	1,111.338	3,375.74	229.87	2.08	321,290	0.3211	184
	11.13	22,711	1,745	1,194.584	3,621.54	229.62	2.08	319,999	0.3211	232
	11.91	24,260	1,866	1,277.830	3,867.35	229.36	2.08	318,064	0.3186	286
	12.70	25,873	1,987	1,356.914	4,113.15	229.11	2.08	316,774	0.3161	347
	14.27	28,969	2,228	1,510.920	4,588.38	228.60	2.08	313,548	0.3135	495

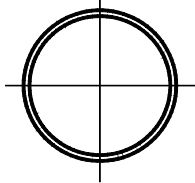
Pile design data converted to SI units from US units published in 1985 version of this manual.

Note: Designer must confirm section properties and local availability of selected pile section.

Material Specifications - ASTM A252

Example of suggested method of designation: PP219 x 2.77

* The External Collapse Index is a non-dimensional function of the diameter to wall thickness ratio and is for general guidance only. The higher the number, the greater is the resistance to collapse.



PIPE PILES

Approximate Pile Dimensions and Design Properties

Designation and Outside Diameter	Wall Thickness	Area A	Weight per Meter	Section Properties			Area of Exterior Surface	Inside Cross Sectional Area	Inside Volume	External Collapse Index
				I	S	r				
mm	mm	mm ²	N	mm ⁴ x 10 ⁶	mm ³ x 10 ³	mm	m ² /m	mm ²	m ³ /m	*
PP711	15.88	32,132	2,472	1,669.088	5,063.60	227.84	2.08	310,322	0.3110	656
	17.48	35,292	2,714	1,823.094	5,522.44	227.33	2.08	307,096	0.3060	814
	19.05	38,389	2,951	1,977.099	5,981.28	226.82	2.08	303,870	0.3035	970
	6.35	14,065	1,081	874.086	2,458.06	249.17	2.23	383,225	0.3838	34
	7.14	15,807	1,214	978.144	2,753.03	248.92	2.23	381,290	0.3813	48
	7.92	17,486	1,346	1,082.202	3,047.99	248.67	2.23	379,999	0.3788	66
	8.74	19,291	1,483	1,190.422	3,342.96	248.41	2.23	378,064	0.3788	89
	9.53	20,969	1,615	1,294.480	3,637.93	248.16	2.23	376,128	0.3763	116
	10.31	22,711	1,746	1,394.375	3,916.51	247.90	2.23	374,838	0.3737	147
	11.13	24,453	1,881	1,498.433	4,211.48	247.65	2.23	372,902	0.3737	185
	11.91	26,195	2,012	1,598.329	4,506.44	247.40	2.23	370,967	0.3712	228
	12.70	27,874	2,143	1,698.224	4,785.02	246.89	2.23	369,677	0.3687	277
	14.27	31,229	2,403	1,898.015	5,342.18	246.38	2.23	365,806	0.3587	395
	15.88	34,713	2,667	2,097.806	5,899.34	245.87	2.23	362,580	0.3612	544
	17.48	38,068	2,929	2,293.435	6,440.12	245.36	2.23	359,354	0.3587	691
	19.05	41,423	3,185	2,480.739	6,980.89	244.86	2.23	356,128	0.3562	835
	PP762	6.35	15,099	1,159	1,078.039	2,818.58	266.70	2.39	440,644	0.4415
7.14		16,904	1,302	1,207.071	3,162.70	266.70	2.39	439,354	0.4390	39
7.92		18,775	1,444	1,336.103	3,506.83	266.70	2.39	437,418	0.4365	54
8.74		20,646	1,590	1,465.135	3,850.96	266.70	2.39	435,483	0.4365	72
9.53		22,517	1,731	1,594.166	4,178.70	266.70	2.39	433,548	0.4340	94
10.31		24,324	1,873	1,719.036	4,522.83	266.70	2.39	431,612	0.4314	120
11.13		26,261	2,018	1,848.068	4,850.57	266.70	2.39	429,677	0.4289	150
11.91		28,066	2,159	1,972.937	5,178.31	264.16	2.39	427,741	0.4289	185
12.70		29,874	2,299	2,097.806	5,506.05	264.16	2.39	426,451	0.4264	225
14.27		33,550	2,578	2,343.383	6,145.15	264.16	2.39	422,580	0.4214	321
15.88		37,228	2,861	2,588.959	6,800.63	264.16	2.39	418,709	0.4189	443
17.48	40,907	3,143	2,834.536	7,439.73	264.16	2.39	415,483	0.4164	584	

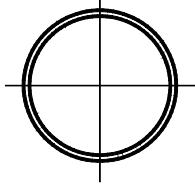
Pile design data converted to SI units from US units published in 1985 version of this manual.

Note: Designer must confirm section properties and local availability of selected pile section.

Material Specifications - ASTM A252

Example of suggested method of designation: PP219 x 2.77

* The External Collapse Index is a non-dimensional function of the diameter to wall thickness ratio and is for general guidance only. The higher the number, the greater is the resistance to collapse.



PIPE PILES

Approximate Pile Dimensions and Design Properties

Designation and Outside Diameter	Wall Thickness	Area A	Weight per Meter	Section Properties			Area of Exterior Surface	Inside Cross Sectional Area	Inside Volume	External Collapse Index
				I	S	r				
mm	mm	mm ²	N	mm ⁴ x 10 ⁶	mm ³ x 10 ³	mm	m ² /m	mm ²	m ³ /m	*
PP813	19.05	44,454	3,419	3,071.788	8,062.44	261.62	2.39	411,612	0.4114	719
	6.35	16,065	1,237	1,306.967	3,211.86	284.48	2.55	502,580	0.5017	23
	7.14	18,067	1,389	1,465.135	3,605.15	284.488	2.55	500,644	0.5017	32
	7.92	20,067	1,541	1,623.303	3,998.44	284.48	2.55	498,709	0.4992	44
	8.74	22,067	1,697	1,785.633	4,391.73	284.48	2.55	496,773	0.4967	60
	9.53	24,067	1,848	1,939.638	4,768.64	284.48	2.55	494,838	0.4942	77
	10.31	26,002	1,999	2,093.644	5,145.54	284.48	2.55	492,902	0.4916	98
	11.13	28,003	2,155	2,251.812	5,538.83	284.48	2.55	490,967	0.4916	124
	11.91	30,003	2,305	2,401.655	5,915.73	281.94	2.55	489,031	0.4891	152
	12.70	31,937	2,455	2,555.661	6,292.63	281.94	2.55	487,096	0.4866	185
	14.27	35,810	2,754	2,855.348	7,030.05	281.94	2.55	483,225	0.4841	264
	15.88	39,744	3,056	3,155.034	7,767.47	281.94	2.55	479,354	0.4791	364
	17.48	43,680	3,358	3,454.721	8,504.89	281.94	2.55	475,483	0.4741	487
19.05	47,488	3,653	3,741.921	9,209.53	281.94	2.55	471,612	0.4716	617	
PP864	6.35	17,099	1,315	1,569.192	3,637.93	302.26	2.71	568,386	0.5694	19
	7.14	19,228	1,477	1,760.659	4,080.38	302.26	2.71	566,450	0.5669	27
	7.92	21,293	1,638	1,947.963	4,522.83	302.26	2.71	564,515	0.5644	37
	8.74	23,485	1,804	2,143.592	4,965.28	302.26	2.71	562,580	0.5619	50
	9.53	25,551	1,965	2,330.896	5,391.34	302.26	2.71	559,999	0.5594	64
	10.31	27,615	2,126	2,518.200	5,833.79	302.26	2.71	558,063	0.5569	82
	11.13	29,808	2,291	2,705.504	6,276.25	302.26	2.71	556,128	0.5569	103
	11.91	31,873	2,451	2,888.646	6,702.31	302.26	2.71	554,192	0.5544	127
	12.70	33,938	2,611	3,071.788	7,111.99	299.72	2.71	551,612	0.5518	154
	14.27	38,068	2,929	3,433.909	7,964.11	299.72	2.71	547,741	0.5468	219
	15.88	42,262	3,251	3,800.193	8,799.85	299.72	2.71	543,225	0.5443	303
	17.48	46,454	3,572	4,158.152	9,635.59	299.72	2.71	539,354	0.5393	405
	19.05	50,519	3,887	4,495.299	10,438.56	299.72	2.71	535,483	0.5343	527
22.23	58,779	4,517	5,202.893	12,044.49	297.18	2.71	527,096	0.5268	767	

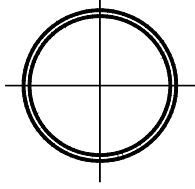
Pile design data converted to SI units from US units published in 1985 version of this manual.

Note: Designer must confirm section properties and local availability of selected pile section.

Material Specifications - ASTM A252

Example of suggested method of designation: PP219 x 2.77

* The External Collapse Index is a non-dimensional function of the diameter to wall thickness ratio and is for general guidance only. The higher the number, the greater is the resistance to collapse.



PIPE PILES

Approximate Pile Dimensions and Design Properties

Designation and Outside Diameter	Wall Thickness	Area A	Weight per Meter	Section Properties			Area of Exterior Surface	Inside Cross Sectional Area	Inside Volume	External Collapse Index
				I	S	r				
mm	mm	mm ²	N	mm ⁴ x 10 ⁶	mm ³ x 10 ³	mm	m ² /m	mm ²	m ³ /m	*
PP914	25.40	67,102	5,143	5,868.863	13,617.65	297.18	2.71	518,709	0.5192	1,010
	6.35	18,130	1,393	1,868.879	4,080.38	320.04	2.87	638,708	0.6396	16
	7.14	20,325	1,564	2,093.644	4,571.99	320.04	2.87	636,128	0.6371	23
	7.92	22,582	1,735	2,318.409	5,063.60	320.04	2.87	634,192	0.6346	31
	8.74	24,840	1,912	2,547.336	5,571.60	320.04	2.87	631,612	0.6321	42
	9.53	27,098	2,082	2,772.101	6,063.21	320.04	2.87	629,676	0.6296	54
	10.31	29,292	2,252	2,992.704	6,538.44	320.04	2.87	627,096	0.6271	69
	11.13	31,550	2,428	3,221.631	7,046.44	320.04	2.87	625,160	0.6246	87
	11.91	33,808	2,597	3,438.072	7,521.66	320.04	2.87	623,225	0.6221	107
	12.70	36,002	2,766	3,658.674	7,996.89	320.04	2.87	620,644	0.6221	129
	14.27	40,390	3,104	4,087.393	8,947.34	317.50	2.87	616,128	0.6171	184
	15.88	44,841	3,446	4,536.923	9,897.79	317.50	2.87	611,612	0.6120	254
	17.48	49,230	3,786	4,953.154	10,831.85	317.50	2.87	607,741	0.6070	341
	19.05	53,616	4,120	5,369.385	11,749.52	317.50	2.87	603,225	0.6020	443
	22.23	62,326	4,790	6,201.848	13,568.49	314.96	2.87	594,192	0.5945	674
	25.40	70,972	5,455	7,034.311	15,338.29	314.96	2.87	585,805	0.5870	900
31.75	87,747	6,770	8,574.367	18,845.12	312.42	2.87	568,386	0.5694	1,380	
PP965	6.35	19,099	1,471	2,197.702	4,555.60	337.82	3.03	709,676	0.7124	14
	7.14	21,485	1,652	2,464.090	5,112.76	337.82	3.03	709,676	0.7099	19
	7.92	23,809	1,833	2,730.478	5,653.54	337.82	3.03	709,676	0.7074	26
	8.74	26,261	2,019	3,001.029	6,227.08	337.82	3.03	703,224	0.7049	35
	9.53	28,582	2,199	3,263.254	6,767.86	337.82	3.03	703,224	0.7023	46
	10.31	30,971	2,379	3,525.480	7,308.63	337.82	3.03	703,224	0.6998	59
	11.13	33,358	2,564	3,796.031	7,865.79	337.82	3.03	696,773	0.6973	74
	11.91	35,680	2,743	4,054.094	8,406.56	337.82	3.03	696,773	0.6973	90
	12.70	38,002	2,922	4,328.807	8,930.95	337.82	3.03	696,773	0.6923	110
	14.27	42,649	3,279	4,828.285	9,996.11	335.28	3.03	690,321	0.6898	156
15.88	47,359	3,641	5,327.762	11,061.27	335.28	3.03	683,870	0.6848	216	

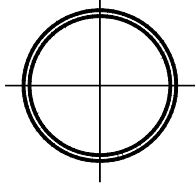
Pile design data converted to SI units from US units published in 1985 version of this manual.

Note: Designer must confirm section properties and local availability of selected pile section.

Material Specifications - ASTM A252

Example of suggested method of designation: PP219 x 2.77

* The External Collapse Index is a non-dimensional function of the diameter to wall thickness ratio and is for general guidance only. The higher the number, the greater is the resistance to collapse.



PIPE PILES

Approximate Pile Dimensions and Design Properties

Designation and Outside Diameter	Wall Thickness	Area A	Weight per Meter	Section Properties			Area of Exterior Surface	Inside Cross Sectional Area	Inside Volume	External Collapse Index
				I	S	r				
mm	mm	mm ²	N	mm ⁴ x 10 ⁶	mm ³ x 10 ³	mm	m ² /m	mm ²	m ³ /m	*
	17.48	52,003	4,001	5,827.240	12,110.04	335.28	3.03	677,418	0.6798	289
	19.05	56,649	4,354	6,326.718	13,142.43	335.28	3.03	677,418	0.6748	376
	22.23	65,810	5,063	7,325.673	15,174.42	332.74	3.03	664,515	0.6647	590
	25.40	74,843	5,767	8,283.005	17,206.42	332.74	3.03	658,063	0.6572	805
	31.75	92,909	7,160	10,156.047	20,975.44	330.20	3.03	638,708	0.6396	1,230
	38.10	110,974	8,533	11,945.842	24,744.47	327.66	3.03	620,644	0.6221	1,780
PP1016	7.92	25,098	1,930	3,188.333	6,276.25	355.60	3.20	787,095	0.7851	23
	8.74	27,679	2,126	3,508.831	6,898.95	355.60	3.20	780,644	0.7826	30
	9.53	30,131	2,316	3,812.680	7,505.28	355.60	3.20	780,644	0.7801	39
	10.31	32,583	2,505	4,120.691	8,111.60	355.60	3.20	780,644	0.7776	50
	11.13	35,099	2,701	4,453.676	8,734.31	355.60	3.20	774,192	0.7751	63
	11.91	37,551	2,890	4,745.038	9,324.24	355.60	3.20	774,192	0.7726	77
	12.70	40,002	3,078	5,036.400	9,914.17	355.60	3.20	767,740	0.7701	94
	14.27	44,906	3,454	5,619.124	11,094.04	353.06	3.20	767,740	0.7651	134
	15.88	49,874	3,836	6,243.471	12,273.91	353.06	3.20	761,289	0.7600	185
	17.48	54,842	4,215	6,826.195	13,453.78	353.06	3.20	754,837	0.7550	247
	19.05	59,681	4,588	7,408.919	14,600.87	353.06	3.20	748,386	0.7500	321
	22.23	69,682	5,336	8,574.367	16,878.68	350.52	3.20	741,934	0.7425	514
	25.40	79,360	6,078	9,698.192	19,172.86	350.52	3.20	729,031	0.7324	719
	31.75	98,070	7,549	11,904.219	23,433.50	347.98	3.20	709,676	0.7124	1,130
38.10	116,781	9,001	14,026.999	27,530.27	345.44	3.20	696,773	0.6923	1,620	
44.45	135,492	10,433	16,024.910	31,627.03	342.90	3.20	677,418	0.6748	2,140	
PP1067	7.92	26,389	2,027	3,696.135	6,931.73	373.38	3.35	864,514	0.8679	20
	8.74	29,034	2,233	4,066.581	7,619.98	373.38	3.35	864,514	0.8654	26
	9.53	31,615	2,433	4,412.053	8,291.85	373.38	3.35	864,514	0.8629	34
	10.31	34,260	2,632	4,786.661	8,947.34	373.38	3.35	864,514	0.8604	43
	11.13	36,905	2,837	5,161.270	9,635.59	373.38	3.35	858,063	0.8579	54
	11.91	39,486	3,036	5,494.255	10,291.08	373.38	3.35	851,611	0.8554	67

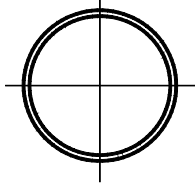
Pile design data converted to SI units from US units published in 1985 version of this manual.

Note: Designer must confirm section properties and local availability of selected pile section.

Material Specifications - ASTM A252

Example of suggested method of designation: PP219 x 2.77

* The External Collapse Index is a non-dimensional function of the diameter to wall thickness ratio and is for general guidance only. The higher the number, the greater is the resistance to collapse.



PIPE PILES

Approximate Pile Dimensions and Design Properties

Designation and Outside Diameter	Wall Thickness	Area A	Weight per Meter	Section Properties			Area of Exterior Surface	Inside Cross Sectional Area	Inside Volume	External Collapse Index
				I	S	r				
mm	mm	mm ²	N	mm ⁴ x 10 ⁶	mm ³ x 10 ³	mm	m ² /m	mm ²	m ³ /m	*
	12.70	42,067	3,234	5,827.240	10,946.56	373.38	3.35	851,611	0.8528	81
	14.27	47,229	3,630	6,534.833	12,257.52	373.38	3.35	845,160	0.8478	116
	15.88	52,390	4,030	7,242.427	13,568.49	370.84	3.35	838,708	0.8403	159
	17.48	57,616	4,430	7,950.020	14,863.07	370.84	3.35	838,708	0.8353	213
	19.05	62,713	4,822	8,615.991	16,141.26	370.84	3.35	832,256	0.8303	277
	22.23	72,908	5,608	9,947.931	18,681.25	368.30	3.35	819,353	0.8202	443
	25.40	83,231	6,390	11,279.872	21,139.31	368.30	3.35	812,902	0.8102	641
	31.75	103,232	7,939	13,818.883	25,891.56	365.76	3.35	793,547	0.7901	1,030
	38.10	123,233	9,468	16,316.272	30,643.81	363.22	3.35	767,740	0.7701	1,460
	44.45	142,589	10,978	18,688.791	35,068.32	360.68	3.35	748,386	0.7500	1,970
	50.80	161,945	12,468	20,978.064	39,328.95	360.68	3.35	729,031	0.7324	2,470
PP1118	8.74	30,453	2,341	4,661.792	8,373.79	391.16	3.51	948,385	0.9507	23
	9.53	33,163	2,550	5,078.023	9,111.21	391.16	3.51	948,385	0.9482	30
	10.31	35,873	2,759	5,494.255	9,832.24	391.16	3.51	941,934	0.9457	38
	11.13	38,647	2,974	5,910.486	10,586.04	391.16	3.51	941,934	0.9432	47
	11.91	41,357	3,182	6,326.718	11,323.46	391.16	3.51	941,934	0.9406	58
	12.70	44,067	3,390	6,742.949	12,044.49	391.16	3.51	935,482	0.9381	70
	15.88	54,971	4,225	8,324.629	14,928.62	388.62	3.51	929,030	0.9256	138
	19.05	65,810	5,056	9,906.308	17,698.03	388.62	3.51	916,127	0.9156	241
	22.23	76,779	5,881	11,487.987	20,483.83	388.62	3.51	903,224	0.9055	384
	25.40	87,102	6,702	12,986.420	23,269.63	386.08	3.51	896,772	0.8930	571
	31.75	108,394	8,328	15,983.287	28,513.49	383.54	3.51	870,966	0.8729	941
PP1219	38.10	129,040	9,936	18,855.284	33,757.35	381.00	3.51	851,611	0.8528	1,300
	44.45	149,686	11,524	21,602.411	38,673.47	381.00	3.51	832,256	0.8303	1,810
	50.80	170,333	13,092	24,266.292	43,425.72	378.46	3.51	812,902	0.8102	2,290
	57.15	190,334	14,641	26,846.927	48,014.10	375.92	3.51	793,547	0.7901	2,770
	8.74	33,228	2,555	6,076.979	9,979.72	426.72	3.84	1,135,482	1.1338	18
	9.53	36,196	2,784	6,618.080	10,864.62	426.72	3.84	1,129,030	1.1313	23

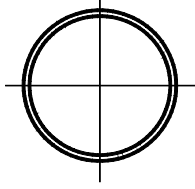
Pile design data converted to SI units from US units published in 1985 version of this manual.

Note: Designer must confirm section properties and local availability of selected pile section.

Material Specifications - ASTM A252

Example of suggested method of designation: PP219 x 2.77

* The External Collapse Index is a non-dimensional function of the diameter to wall thickness ratio and is for general guidance only. The higher the number, the greater is the resistance to collapse.



PIPE PILES

Approximate Pile Dimensions and Design Properties

Designation and Outside Diameter	Wall Thickness	Area A	Weight per Meter	Section Properties			Area of Exterior Surface	Inside Cross Sectional Area	Inside Volume	External Collapse Index
				I	S	r				
mm	mm	mm ²	N	mm ⁴ x 10 ⁶	mm ³ x 10 ³	mm	m ² /m	mm ²	m ³ /m	*
	10.31	39,164	3,012	7,159.181	11,733.14	426.72	3.84	1,129,030	1.1288	29
	11.13	42,196	3,247	7,700.281	12,634.43	426.72	3.84	1,122,578	1.1263	36
	11.91	45,164	3,474	8,241.382	13,502.94	426.72	3.84	1,122,578	1.1212	45
	12.70	48,132	3,702	8,740.860	14,371.46	426.72	3.84	1,116,127	1.1187	54
	15.88	60,004	4,615	10,863.640	17,861.90	426.72	3.84	1,109,675	1.1087	106
	19.05	71,617	5,523	12,944.797	21,139.31	424.18	3.84	1,096,772	1.0962	185
	22.23	83,876	6,427	14,984.331	24,580.60	424.18	3.84	1,083,869	1.0836	295
	25.40	95,490	7,325	16,982.242	27,858.01	421.64	3.84	1,070,966	1.0711	443
	31.75	118,717	9,108	20,894.818	34,248.96	419.10	3.84	1,051,611	1.0485	787
	38.10	141,299	10,871	24,682.524	40,476.05	416.56	3.84	1,025,804	1.0259	1,130
	44.45	163,881	12,614	28,345.360	46,539.26	416.56	3.84	1,006,450	1.0034	1,530
	50.80	186,463	14,339	31,883.327	52,274.73	414.02	3.84	980,643	0.9808	1,970
	57.15	208,400	16,043	35,296.425	57,846.34	411.48	3.84	961,288	0.9582	2,410
	63.50	230,336	17,729	38,626.276	63,254.07	408.94	3.84	935,482	0.9381	2,850

Pile design data converted to SI units from US units published in 1985 version of this manual.

Note: Designer must confirm section properties and local availability of selected pile section.

Material Specifications - ASTM A252

Example of suggested method of designation: PP219 x 2.77

* The External Collapse Index is a non-dimensional function of the diameter to wall thickness ratio and is for general guidance only. The higher the number, the greater is the resistance to collapse.

MONOTUBE PILES

Standard Monotube Weights and Volumes

TYPE	SIZE POINT DIAMETER x BUTT DIAMETER x LENGTH	Weight (N) per m				EST. CONC. VOL. m ³
		9 GA.	7 GA.	5 GA.	3 GA.	
F Taper 3.6 mm per Meter	216 mm x 305 mm x 7.62 m	248	292	350	409	0.329
	203 mm x 305 mm x 9.14 m	233	292	336	394	0.420
	216 mm x 356 mm x 12.19 m	277	321	379	452	0.726
	203 mm x 406 mm x 18.29 m	292	350	409	482	1.284
	203 mm x 457 mm x 22.86 m	-	379	452	511	1.979
J Taper 6.4 mm per Meter	203 mm x 305 mm x 5.18 m	248	292	336	394	0.244
	203 mm x 356 mm x 7.62 m	263	321	379	438	0.443
	203 mm x 406 mm x 10.06 m	292	350	409	467	0.726
	203 mm x 457 mm x 12.19 m	-	379	438	511	1.047
Y Taper 10.2 mm per Meter	203 mm x 305 mm x 3.05 m	248	292	350	409	0.138
	203 mm x 356 mm x 4.57 m	277	321	379	438	0.260
	203 mm x 406 mm x 6.10 m	292	350	409	482	0.428
	203 mm x 457 mm x 7.62 m	-	379	452	511	0.657

Extensions (Overall Length 0.305 m Greater than indicated)

TYPE	DIAMETER + LENGTH	9 GA.	7 GA.	5 GA.	3 GA.	m ³ /m
N 12	305 mm x 305 mm x 6.10 / 12.19 m	292	350	409	482	0.065
N 14	356 mm x 356 mm x 6.10 m / 12.19 m	350	423	496	598	0.088
N 16	406 mm x 406 mm x 6.10 m / 12.19 m	409	482	569	671	0.113
N 18	457 mm x 457 mm x 6.10 m / 12.19 m	-	555	642	759	0.145



Note: Designer must confirm section properties of selected pile section.

Pile design data converted to SI units from US units published in Monotube Pile Corporation Catalog 592.

MONOTUBE PILES

Physical Properties

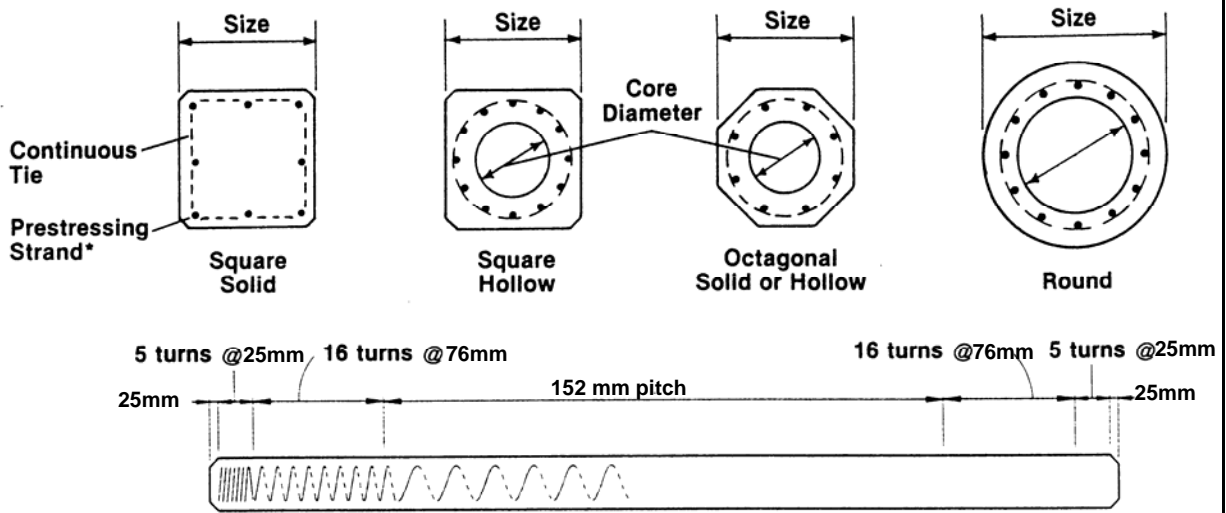
STEEL THICKNESS	POINTS		BUTTS OF PILE SECTIONS							
	203 mm	216 mm	305 mm				356 mm			
	A mm ²	A mm ²	A mm ²	I mm ⁴ x 10 ⁶	S mm ³ x 10 ³	r mm	A mm ²	I mm ⁴ x 10 ⁶	S mm ³ x 10 ³	r mm
9 GAUGE 3.797 mm	2,342	2,535	3,748	42.456	267.109	106	4,355	66.181	360.515	123
7 GAUGE 4.554 mm	2,839	3,077	4,497	50.780	319.548	106	5,252	80.749	437.535	124
5 GAUGE 5.314 mm	3,348	3,619	5,277	60.354	376.902	107	6,129	94.485	507.999	124
3 GAUGE 6.073 mm	3,787	4,245	5,781	61.602	396.567	103	6,839	99.479	550.605	121
CONCRETE AREA mm ²	27,290	30,518	65,161				87,742			

STEEL THICKNESS	POINTS		BUTTS OF PILE SECTIONS							
	203 mm	216 mm	406 mm				457 mm			
	A mm ²	A mm ²	A mm ²	I mm ⁴ x 10 ⁶	S mm ³ x 10 ³	r mm	A mm ²	I mm ⁴ x 10 ⁶	S mm ³ x 10 ³	r mm
9 GAUGE 3.797 mm	2,342	2,535	4,929	96.566	463.754	140	-	-	-	-
7 GAUGE 4.554 mm	2,839	3,077	5,923	115.712	555.521	140	6,710	168.157	712.837	158
5 GAUGE 5.314 mm	3,348	3,619	6,968	136.940	555.521	140	7,871	198.959	839.018	159
3 GAUGE 6.073 mm	3,787	4,245	7,742	144.849	706.282	137	8,774	209.781	907.843	155
CONCRETE AREA mm ²	27,290	30,518	113,548				144,516			

Note: Designer must confirm section properties of selected pile section.

Pile design data converted to SI units from US units published in Monotube Pile Corporation Catalog 592.

PRECAST/PRESTRESSED CONCRETE PILES



* Strand pattern may be circular or square.

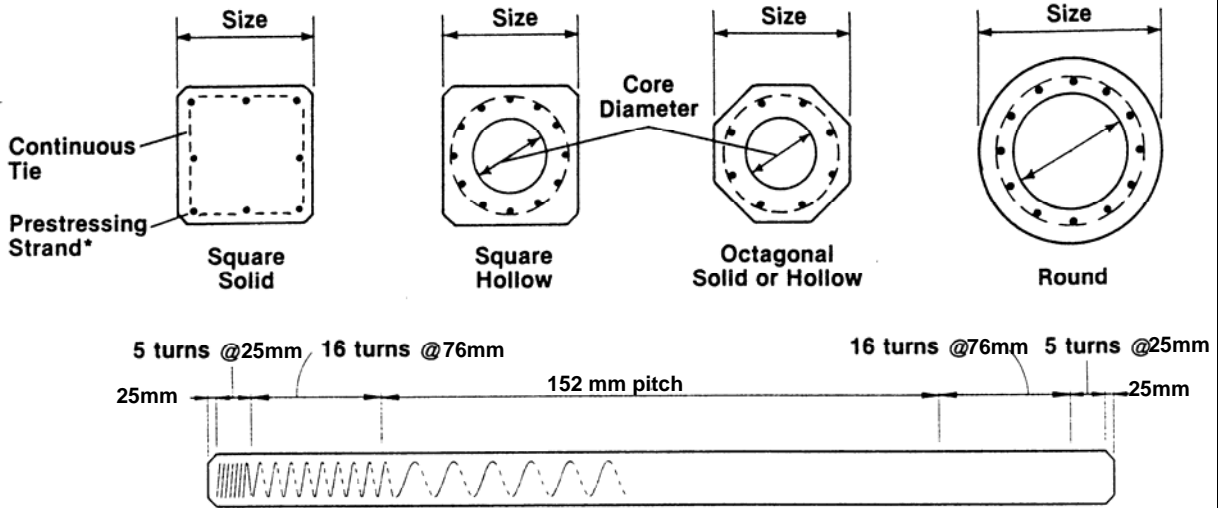
Typical Elevation

Size mm	Core Diameter mm	Section Properties					
		Area mm ²	Weight N/m	Moment of Inertia mm ⁴ x 10 ⁶	Section Modulus mm ³ x 10 ³	Radius of Gyration mm	Perimeter m
Square Piles							
254	Solid	64,516	1,518	346.721	2,736.640	73.4	1.015
305	Solid	92,903	2,189	719.248	4,719.474	87.9	1.219
356	Solid	126,451	2,977	1,332.357	7,488.888	102.6	1.423
406	Solid	165,161	3,896	2,273.040	11,192.365	117.3	1.625
457	Solid	209,032	4,932	3,641.193	15,928.226	132.1	1.829
508	Solid	258,064	6,085	5,549.614	21,843.956	146.6	2.033
508	279 mm	196,774	4,641	5,250.759	20,680.475	163.3	2.033
610	Solid	371,612	8,756	11,507.966	37,755.795	176.0	2.438
610	305 mm	298,709	7,034	11,084.243	36,362.895	192.5	2.438
610	356 mm	272,258	6,406	10,722.954	35,183.026	198.4	2.438
610	381 mm	257,419	6,056	10,473.631	34,363.673	201.7	2.438
762	457 mm	416,773	9,807	25,950.781	68,121.025	249.4	3.048
914	457 mm	672,257	15,834	56,114.240	122,739.109	289.1	3.658

Note: Designer must confirm section properties for a selected pile. Form dimensions may vary with producers, with corresponding variations in section properties.

Data converted to SI units from US unit properties in PCI (1993), Precast/Prestressed Concrete Institute Journal, Volume 38, No. 2, March-April, 1993.

PRECAST/PRESTRESSED CONCRETE PILES



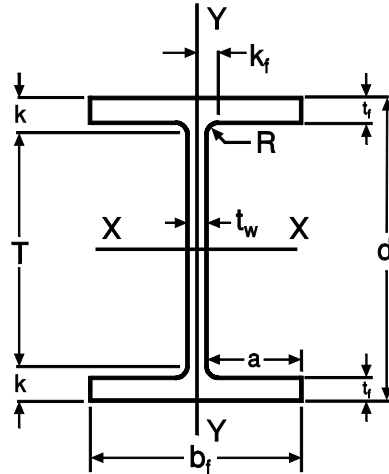
* Strand pattern may be circular or square.

		Section Properties					
Size mm	Core Diameter mm	Area mm ²	Weight N/m	Moment of Inertia mm ⁴ x 10 ⁶	Section Modulus mm ³ x 10 ³	Radius of Gyration mm	Perimeter m
Octagonal Piles							
254	Solid	53,548	1,240	231.008	1,818.964	65.8	0.841
305	Solid	76,774	1,824	472.006	3,097.155	78.5	1.009
356	Solid	104,516	2,466	876.167	4,932.506	91.4	1.180
406	Solid	136,774	3,210	1,495.103	7,357.792	104.6	1.347
457	Solid	172,903	4,086	2,374.600	10,471.334	117.1	1.515
508	Solid	213,548	5,035	3,650.350	14,371.455	130.8	1.682
508	279 mm	152,258	3,575	3,350.663	13,191.587	148.3	1.682
559	Solid	258,709	6,129	5,343.163	19,123.704	143.8	1.853
559	330 mm	172,903	4,086	4,761.688	17,042.547	165.9	1.853
610	Solid	307,741	7,224	7,567.087	24,826.402	156.7	2.021
610	381 mm	193,548	4,597	6,533.168	21,434.280	183.6	2.021
Round Piles							
914	660 mm	314,193	7,399	24,976.799	54,634.471	281.9	2.874
1,067	813 mm	374,838	8,829	42,153.005	79,034.810	335.3	3.353
1,219	965 mm	435,483	10,259	65,856.969	108,023.526	388.9	3.831
1,372	1118 mm	496,773	11,704	97,137.176	141,633.394	442.2	4.310
1,676	1372 mm	729,676	17,191	213,954.191	255,261.296	541.5	5.267

Note: Designer must confirm section properties for a selected pile. Form dimensions may vary with producers, with corresponding variations in section properties.

Data converted to SI units from US unit properties in PCI (1993), Precast/Prestressed Concrete Institute Journal, Volume 38, No. 2, March-April, 1993.

H-PILES



C1-20

Section Designation	Area A	Depth d	Web Thickness t_w	Flange		Distance				Fillet Radius R	Elastic Properties					
				Width b_f	Thickness t_f	T	k	k_f	a		X-X			Y-Y		
											I	S	r	I	S	r
mm x kg/m	mm ²	mm	mm	mm	mm	mm	mm	mm	mm	mm	mm ⁴ x 10 ⁶	mm ³ x 10 ³	mm	mm ⁴ x 10 ⁶	mm ³ x 10 ³	mm
HP360 x 174	22,200	361	20.4	378	20	277	42	30.2	179	20	511	2,830	152	183	968	91
HP360 x 152	19,400	356	17.9	376	18	277	40	29.0	179	20	442	2,480	151	158	840	90
HP360 x 132	16,900	351	15.6	373	16	277	37	27.8	179	20	378	2,150	150	135	724	89
HP360 x 108	13,800	346	12.8	370	13	277	34	26.4	179	20	306	1,770	148	108	584	88
HP310 x 125	15,800	312	17.4	312	17	244	34	23.7	147	15	270	1,730	131	88	565	75
HP310 x 110	14,000	308	15.4	310	15	244	32	22.7	147	15	236	1,530	130	77	497	74
HP310 x 93	11,800	303	13.1	308	13	244	30	21.6	148	15	196	1,290	129	64	414	74
HP310 x 79	9,970	299	11.0	306	11	244	28	20.5	148	15	162	1,080	127	53	343	73
HP250 x 85	10,800	254	14.4	260	14	196	29	20.2	123	13	123	969	107	42	325	63
HP250 x 62	7,980	246	10.5	256	11	96	25	18.3	123	13	88	711	105	30	234	61
HP200 x 53	6,810	204	11.3	207	11	158	23	15.7	98	10	50	487	86	17	161	50

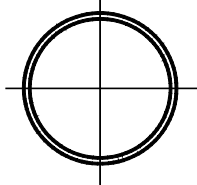
Note: Designer must confirm section properties for a selected pile.

Data obtained from FHWA Geotechnical Metrication Guidelines (1995) FHWA-SA-95-035.

APPENDIX C-2

Information and Data on Various Pile Types, US Units

	Page
Dimensions and Properties of Pipe Piles	C2-3
Data for Steel Monotube Piles.....	C2-17
Typical Prestressed Concrete Pile Sections.....	C2-19
Dimensions and Properties of H-Piles.....	C2-21



PIPE PILES

Approximate Pile Dimensions and Design Properties

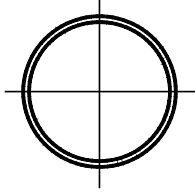
Designation and Outside Diameter	Wall Thickness	Area A	Weight per Foot	Section Properties			Area of Exterior Surface	Inside Cross Sectional Area	Inside Volume	External Collapse Index
				I	S	r				
in	in	in ²	lb	in ⁴	in ³	in	ft ² /ft	in ²	ft ³ /ft	*
PP8	0.141	3.48	11.83	26.9	6.72	2.78	2.09	46.8	0.0120	266
	0.164	4.04	13.72	31.0	7.75	2.77	2.09	46.2	0.0119	422
	0.172	4.23	14.38	32.4	8.10	2.77	2.09	46.0	0.0118	487
	0.179	4.40	14.95	33.6	8.41	2.77	2.09	45.9	0.0118	548
	0.188	4.61	15.69	35.2	8.80	2.76	2.09	45.7	0.0117	621
	0.219	5.35	18.20	40.5	10.1	2.75	2.09	44.9	0.0116	874
PP8-5/8	0.109	2.92	9.91	26.4	6.13	3.01	2.26	55.5	0.0143	97
	0.125	3.34	11.35	30.2	6.99	3.01	2.26	55.1	0.0142	147
	0.141	3.76	12.78	33.8	7.84	3.00	2.26	54.7	0.0141	212
	0.156	4.15	14.11	37.2	8.63	2.99	2.26	54.3	0.0140	288
	0.164	4.36	14.82	39.0	9.05	2.99	2.26	54.1	0.0139	335
	0.172	4.57	15.53	40.8	9.46	2.99	2.26	53.9	0.0139	388
	0.179	4.75	16.15	42.4	9.82	2.99	2.26	53.7	0.0138	438
	0.188	4.98	16.94	44.4	10.3	2.98	2.26	53.4	0.0137	508
	0.203	5.37	18.26	47.6	11.0	2.98	2.26	53.1	0.0136	623
	0.219	5.78	19.66	51.1	11.9	2.97	2.26	52.6	0.0135	744
	0.250	6.58	22.36	57.7	13.4	2.96	2.26	51.8	0.0133	979
	0.277	7.26	24.70	63.4	14.7	2.95	2.26	51.2	0.0132	1180
	0.312	8.15	27.70	70.5	16.3	2.94	2.26	50.3	0.0129	1500
	0.322	8.40	28.55	72.5	16.8	2.94	2.26	50.0	0.0129	1600
	0.344	8.95	30.42	76.8	17.8	2.93	2.26	49.5	0.0127	1820
	0.375	9.72	33.04	82.9	19.2	2.92	2.26	48.7	0.0125	2120
0.406	10.50	35.64	88.7	20.6	2.91	2.26	47.9	0.0123	2420	
0.438	11.3	38.30	94.7	21.9	2.90	2.26	47.2	0.0121	2740	
0.500	12.8	43.39	106.0	24.5	2.88	2.26	45.7	0.0117	3340	

Note: Designer must confirm section properties and local availability of selected pile section.

Material Specifications - ASTM A252

Example of suggested method of designation: PP8 x 0.141

* The External Collapse Index is a non-dimensional function of the diameter to wall thickness ratio and is for general guidance only. The higher the number, the greater is the resistance to collapse.



PIPE PILES

Approximate Pile Dimensions and Design Properties

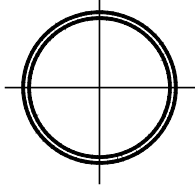
Designation and Outside Diameter	Wall Thickness	Area A	Weight per Foot	Section Properties			Area of Exterior Surface	Inside Cross Sectional Area	Inside Volume	External Collapse Index
				I	S	r				
in	in	in ²	lb	in ⁴	in ³	in	ft ² /ft	in ²	ft ³ /ft	*
PP10	0.109	3.39	11.51	41.4	8.28	3.50	2.62	75.2	0.0193	62
	0.120	3.72	12.66	45.5	9.09	3.49	2.62	74.8	0.0192	83
	0.134	4.15	14.12	50.5	10.10	3.49	2.62	74.4	0.0191	116
	0.141	4.37	14.85	53.1	10.60	3.49	2.62	74.2	0.0191	135
	0.150	4.64	15.78	56.3	11.30	3.48	2.62	73.9	0.0190	163
	0.164	5.07	17.23	61.3	12.30	3.48	2.62	73.5	0.0189	214
	0.172	5.31	18.05	64.1	12.80	3.48	2.62	73.2	0.0188	247
	0.179	5.52	18.78	66.6	13.30	3.47	2.62	73.0	0.0188	279
	0.188	5.80	19.70	69.8	14.00	3.47	2.62	72.7	0.0187	324
	0.203	6.25	21.24	75.0	15.00	3.46	2.62	72.3	0.0186	409
	0.219	6.73	22.88	80.5	16.10	3.46	2.62	71.8	0.0185	515
	0.230	7.06	24.00	84.3	16.90	3.46	2.62	71.5	0.0184	588
	0.250	7.66	26.03	91.1	18.20	3.45	2.62	70.9	0.0182	719
PP10-3/4	0.109	3.64	12.39	51.6	9.60	3.76	2.81	87.1	0.0224	50
	0.120	4.01	13.62	56.6	10.50	3.76	2.81	86.8	0.0223	67
	0.125	4.17	14.18	58.9	11.00	3.76	2.81	86.6	0.0223	76
	0.134	4.47	15.19	63.0	11.70	3.75	2.81	86.3	0.0222	93
	0.141	4.70	15.98	66.1	12.30	3.75	2.81	86.1	0.0221	109
	0.150	5.00	16.98	70.2	13.10	3.75	2.81	85.8	0.0221	131
	0.156	5.19	17.65	72.9	13.60	3.75	2.81	85.6	0.0220	148
	0.164	5.45	18.54	76.4	14.20	3.74	2.81	85.3	0.0219	172
	0.172	5.72	19.43	80.0	14.90	3.74	2.81	85.0	0.0219	199
	0.179	5.94	20.21	83.1	15.50	3.74	2.81	84.8	0.0218	224
	0.188	6.24	21.21	87.0	16.20	3.73	2.81	84.5	0.0217	260
	0.203	6.73	22.87	93.6	17.40	3.73	2.81	84.0	0.0216	328

Note: Designer must confirm section properties and local availability of selected pile section.

Material Specifications - ASTM A252

Example of suggested method of designation: PP8 x 0.141

* The External Collapse Index is a non-dimensional function of the diameter to wall thickness ratio and is for general guidance only. The higher the number, the greater is the resistance to collapse.



PIPE PILES

Approximate Pile Dimensions and Design Properties

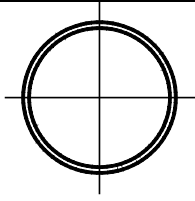
Designation and Outside Diameter	Wall Thickness	Area A	Weight per Foot	Section Properties			Area of Exterior Surface	Inside Cross Sectional Area	Inside Volume	External Collapse Index
				I	S	r				
In	in	in ²	lb	in ⁴	in ³	in	ft ² /ft	in ²	ft ³ /ft	*
PP10-3/4 (cont'd)	0.219	7.25	24.63	100.0	18.7	3.72	2.81	83.5	0.0215	414
	0.230	7.60	25.84	105.0	19.6	3.72	2.81	83.2	0.0214	480
	0.250	8.25	28.04	114.0	21.2	3.71	2.81	82.5	0.0212	605
	0.279	9.18	31.20	126.0	23.4	3.70	2.81	81.6	0.0210	781
	0.307	10.10	34.24	137.0	25.6	3.69	2.81	80.7	0.0208	951
	0.344	11.20	38.23	152.0	28.4	3.68	2.81	79.5	0.0205	1180
	0.365	11.90	40.48	161.0	29.9	3.67	2.81	78.9	0.0230	1320
	0.438	14.20	48.24	189.0	35.2	3.65	2.81	76.6	0.0197	1890
	0.500	16.10	54.74	212.0	39.4	3.63	2.81	74.7	0.0192	2380
PP12	0.134	5.00	16.98	87.9	14.7	4.20	3.14	108.0	0.0278	67
	0.141	5.25	17.86	92.4	15.4	4.19	3.14	108.0	0.0277	78
	0.150	5.58	18.98	98.0	16.3	4.19	3.14	108.0	0.0277	94
	0.164	6.10	20.73	107.0	17.8	4.19	3.14	107.0	0.0275	123
	0.172	6.39	21.73	112.0	18.6	4.18	3.14	107.0	0.0274	142
	0.179	6.65	22.60	116.0	19.4	4.18	3.14	106.0	0.0274	161
	0.188	6.98	23.72	122.0	20.3	4.18	3.14	106.0	0.0273	186
	0.203	7.52	25.58	131.0	21.8	4.17	3.14	106.0	0.0272	235
	0.219	8.11	27.55	141.0	23.4	4.17	3.14	105.0	0.0270	296
	0.230	8.50	28.91	147.0	24.6	4.16	3.14	105.0	0.0269	344
	0.250	9.23	31.37	159.0	26.6	4.16	3.14	104.0	0.0267	443
	0.281	10.30	35.17	178.0	29.6	4.14	3.14	103.0	0.0264	616
	0.312	11.50	38.95	196.0	32.6	4.13	3.14	102.0	0.0261	784
PP12-3/4	0.109	4.33	14.72	86.5	13.6	4.47	3.34	123.0	0.0317	30
	0.125	4.96	16.85	98.8	15.5	4.46	3.34	123.0	0.0316	45
	0.134	5.31	18.06	106.0	16.6	4.46	3.34	122.0	0.0315	56
	0.141	5.59	18.99	111.0	17.4	4.46	3.34	122.0	0.0314	65

Note: Designer must confirm section properties and local availability of selected pile section.

Material Specifications - ASTM A252

Example of suggested method of designation: PP8 x 0.141

* The External Collapse Index is a non-dimensional function of the diameter to wall thickness ratio and is for general guidance only. The higher the number, the greater is the resistance to collapse.



PIPE PILES

Approximate Pile Dimensions and Design Properties

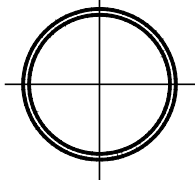
Designation and Outside Diameter	Wall Thickness	Area A	Weight per Foot	Section Properties			Area of Exterior Surface	Inside Cross Sectional Area	Inside Volume	External Collapse Index
				I	S	r				
in	in	in ²	lb	in ⁴	in ³	in	ft ² /ft	in ²	ft ³ /ft	*
PP12-3/4 (cont'd)	0.150	5.94	20.19	118	18.5	4.46	3.34	122	0.0313	78
	0.156	6.17	20.98	122	19.2	4.45	3.34	122	0.0313	88
	0.164	6.48	22.04	128	20.1	4.45	3.34	121	0.0312	103
	0.172	0.68	23.11	134	21.1	4.45	3.34	121	0.0311	118
	0.179	7.07	24.03	140	21.9	4.45	3.34	121	0.0310	134
	0.188	7.42	25.22	146	23.0	4.44	3.34	120	0.0309	155
	0.203	8.00	27.20	158	24.7	4.44	3.34	120	0.0308	196
	0.219	8.62	29.31	169	26.6	4.43	3.34	119	0.0306	246
	0.230	9.05	30.75	177	27.8	4.43	3.34	119	0.0305	286
	0.250	9.82	33.38	192	30.1	4.42	3.34	118	0.0303	368
	0.281	11.00	37.42	214	33.6	4.41	3.34	117	0.0300	526
	0.312	12.20	41.45	236	37.0	4.40	3.34	115	0.0297	684
	0.330	12.90	43.77	248	39.0	4.39	3.34	115	0.0295	776
	0.344	13.40	45.58	258	40.5	4.39	3.34	114	0.0294	848
	0.375	14.60	49.56	279	43.8	4.38	3.34	113	0.0291	1010
	0.406	15.70	53.52	300	47.1	4.37	3.34	112	0.0288	1170
	0.438	16.90	57.59	321	50.4	4.36	3.34	111	0.0285	1350
	0.500	19.20	65.42	362	56.7	4.33	3.34	108	0.0279	1760
PP14	0.134	5.84	19.84	140	20.0	4.90	3.67	148	0.0381	42
	0.141	6.14	20.87	147	21.1	4.90	3.67	148	0.0380	49
	0.150	6.53	22.19	157	22.4	4.90	3.67	147	0.0379	59
	0.156	6.78	23.07	163	23.2	4.89	3.67	147	0.0378	66
	0.164	7.13	24.23	171	24.4	4.89	3.67	147	0.0378	77
	0.172	7.47	25.40	179	25.5	4.89	3.67	146	0.0377	89
	0.179	7.77	26.42	186	26.5	4.89	3.67	146	0.0376	101
	0.188	8.16	27.73	195	27.8	4.88	3.67	146	0.0375	117
	0.203	8.80	29.91	209	29.9	4.88	3.67	145	0.0373	147
	0.210	9.10	30.93	216	30.9	4.88	3.67	145	0.0373	163

Note: Designer must confirm section properties and local availability of selected pile section.

Material Specifications - ASTM A252

Example of suggested method of designation: PP8 x 0.141

* The External Collapse Index is a non-dimensional function of the diameter to wall thickness ratio and is for general guidance only. The higher the number, the greater is the resistance to collapse.



PIPE PILES

Approximate Pile Dimensions and Design Properties

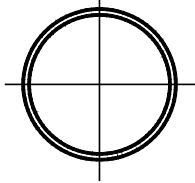
Designation and Outside Diameter	Wall Thickness	Area A	Weight per Foot	Section Properties			Area of Exterior Surface	Inside Cross Sectional Area	Inside Volume	External Collapse Index
				I	S	r				
in	in	in ²	lb	in ⁴	in ³	in	ft ² /ft	in ²	ft ³ /ft	*
PP14 (cont'd)	0.219	9.48	32.23	225	32.2	4.87	3.67	144	0.0372	815
	0.230	9.95	33.82	236	33.7	4.87	3.67	144	0.0370	215
	0.250	10.80	36.71	255	36.5	4.86	3.67	143	0.0368	277
	0.281	12.10	41.17	285	40.7	4.85	3.67	142	0.0365	395
	0.312	13.40	45.61	314	44.9	4.84	3.67	141	0.0361	542
	0.344	14.80	50.17	344	49.2	4.83	3.67	139	0.0358	691
	0.375	16.10	54.57	373	53.3	4.82	3.67	138	0.0355	835
	0.438	18.70	63.44	429	61.4	4.80	3.67	135	0.0348	1130
	0.469	19.90	67.78	457	65.3	4.79	3.67	134	0.0345	1280
	0.500	21.20	72.09	484	69.1	4.78	3.67	133	0.0341	1460
PP16	0.134	6.68	22.71	210	26.3	5.61	4.19	194	0.5000	28
	0.141	7.02	23.88	221	27.6	5.61	4.19	194	0.0499	33
	0.150	7.47	25.39	235	29.3	5.60	4.19	194	0.0498	39
	0.156	7.76	26.40	244	30.5	5.60	4.19	193	0.0497	44
	0.164	8.16	27.74	256	32.0	5.60	4.19	193	0.0496	52
	0.172	8.55	29.08	268	33.5	5.60	4.19	193	0.0495	60
	0.179	8.90	30.25	278	34.8	5.59	4.19	192	0.0494	67
	0.188	9.34	31.75	292	36.5	5.59	4.19	192	0.0493	78
	0.203	10.10	34.25	314	39.3	5.59	4.19	191	0.0491	98
	0.219	10.90	36.91	338	42.3	5.58	4.19	190	0.0489	124
	0.230	11.40	38.74	354	44.3	5.58	4.19	190	0.0488	144
	0.250	12.40	42.05	384	48.0	5.57	4.19	189	0.0485	185
	0.281	13.90	47.17	429	53.6	5.56	4.19	187	0.0481	264
	0.312	15.40	52.27	473	59.2	5.55	4.19	186	0.0478	362
	0.344	16.90	57.52	519	64.8	5.54	4.19	184	0.0474	487
	0.375	18.40	62.58	562	70.3	5.53	4.19	183	0.0470	617
	0.438	21.40	72.80	649	81.1	5.50	4.19	180	0.0462	874
	0.469	22.90	77.79	691	86.3	5.49	4.19	178	0.0458	1000
0.500	24.30	82.77	732	91.5	5.48	4.19	177	0.0455	1130	

Note: Designer must confirm section properties and local availability of selected pile section.

Material Specifications - ASTM A252

Example of suggested method of designation: PP8 x 0.141

* The External Collapse Index is a non-dimensional function of the diameter to wall thickness ratio and is for general guidance only. The higher the number, the greater is the resistance to collapse.



PIPE PILES

Approximate Pile Dimensions and Design Properties

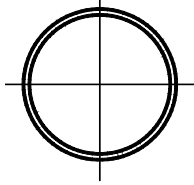
Designation and Outside Diameter	Wall Thickness	Area A	Weight per Foot	Section Properties			Area of Exterior Surface	Inside Cross Sectional Area	Inside Volume	External Collapse Index
				I	S	r				
in	in	in ²	lb	in ⁴	in ³	in	ft ² /ft	in ²	ft ³ /ft	*
PP18	0.141	7.91	26.89	315	35.0	6.31	4.71	247	0.0634	23
	0.172	9.63	32.75	383	42.5	6.30	4.71	245	0.0630	42
	0.188	10.50	35.76	417	46.4	6.30	4.71	244	0.0627	55
	0.203	11.30	38.58	449	49.9	6.29	4.71	243	0.0625	69
	0.219	12.20	41.59	484	53.7	6.29	4.71	242	0.0623	87
	0.230	12.80	43.65	507	56.3	6.28	4.71	242	0.0621	101
	0.250	13.90	47.39	549	61.0	6.28	4.71	241	0.0619	129
	0.281	15.60	53.18	614	68.2	6.27	4.71	239	0.0614	184
	0.312	17.30	58.94	678	75.4	6.25	4.71	237	0.0610	253
	0.344	19.10	64.87	744	82.6	6.24	4.71	235	0.0605	341
	0.375	20.80	70.59	807	89.6	6.23	4.71	234	0.0601	443
	0.406	22.40	76.29	869	96.5	6.22	4.71	232	0.0597	559
	0.438	24.20	82.15	932	104.0	6.21	4.71	230	0.0592	675
	0.469	25.80	87.81	993	110.0	6.20	4.71	229	0.0588	788
	0.500	27.50	93.45	1050	117.0	6.19	4.71	227	0.0584	900
PP20	0.141	8.80	29.91	434	43.4	7.02	5.24	305	0.0785	17
	0.172	10.70	36.42	527	52.7	7.01	5.24	303	0.0780	30
	0.188	11.70	39.78	574	57.4	7.00	5.24	302	0.0778	40
	0.203	12.60	42.92	619	61.9	7.00	5.24	302	0.0776	50
	0.219	13.60	46.27	666	66.6	6.99	5.24	301	0.0773	63
	0.250	15.50	52.73	756	75.6	6.98	5.24	299	0.0768	94
	0.281	17.40	59.18	846	84.6	6.97	5.24	297	0.0763	134
	0.312	19.30	65.60	935	93.5	6.96	5.24	295	0.0758	184
	0.344	21.20	72.21	1030	103.0	6.95	5.24	293	0.0753	247

Note: Designer must confirm section properties and local availability of selected pile section.

Material Specifications - ASTM A252

Example of suggested method of designation: PP8 x 0.141

* The External Collapse Index is a non-dimensional function of the diameter to wall thickness ratio and is for general guidance only. The higher the number, the greater is the resistance to collapse.



PIPE PILES

Approximate Pile Dimensions and Design Properties

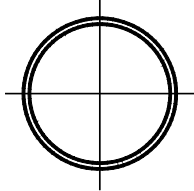
Designation and Outside Diameter	Wall Thickness	Area A	Weight per Foot	Section Properties			Area of Exterior Surface	Inside Cross Sectional Area	Inside Volume	External Collapse Index
				I	S	r				
in	in	in ²	lb	in ⁴	in ³	in	ft ² /ft	in ²	ft ³ /ft	*
PP20 (cont'd)	0.375	23.10	78.60	1110	111.0	6.94	5.24	291	0.0749	321
	0.406	25.00	84.96	1200	120.0	6.93	5.24	289	0.0744	409
	0.438	26.90	91.51	1290	129.0	6.92	5.24	287	0.0739	515
	0.469	28.80	97.83	1370	137.0	6.91	5.24	285	0.0734	618
	0.500	30.60	104.13	1460	146.0	6.90	5.24	284	0.0729	719
PP22	0.172	11.80	40.10	703	63.9	7.72	5.76	368	0.0947	23
	0.188	12.90	43.80	766	69.7	7.71	5.76	367	0.0945	30
	0.219	15.00	50.94	889	80.8	7.70	5.76	365	0.0939	47
	0.250	17.10	58.07	1010	91.8	7.69	5.76	363	0.0934	70
	0.281	19.20	65.18	1130	103.0	7.68	5.76	361	0.0928	100
	0.312	21.30	72.27	1250	114.0	7.67	5.76	359	0.0923	138
	0.344	23.40	79.56	1370	125.0	7.66	5.76	357	0.0918	185
	0.375	25.50	86.61	1490	135.0	7.65	5.76	355	0.0912	241
	0.406	27.50	93.63	1610	146.0	7.64	5.76	353	0.0907	306
	0.438	29.70	100.86	1720	157.0	7.62	5.76	350	0.0901	386
	0.469	31.70	107.85	1840	167.0	7.61	5.76	348	0.0896	475
PP24	0.500	33.80	114.81	1950	177.0	7.60	5.76	346	0.0891	571
	0.172	12.90	43.77	914	76.2	8.42	6.28	440	0.1130	18
	0.188	14.10	47.81	997	83.1	8.42	6.28	438	0.1130	23
	0.219	16.40	55.62	1160	96.4	8.41	6.28	436	0.1120	36
	0.250	18.70	63.41	1320	110.0	8.40	6.28	434	0.1120	54
	0.281	20.90	71.18	1470	123.0	8.39	6.28	431	0.1110	77
	0.312	23.20	78.93	1630	136.0	8.38	6.28	429	0.1100	106
	0.344	25.60	86.91	1790	149.0	8.36	6.28	427	0.1100	142
0.375	27.80	94.62	1940	162.0	8.35	6.28	425	0.1090	185	

Note: Designer must confirm section properties and local availability of selected pile section.

Material Specifications - ASTM A252

Example of suggested method of designation: PP8 x 0.141

* The External Collapse Index is a non-dimensional function of the diameter to wall thickness ratio and is for general guidance only. The higher the number, the greater is the resistance to collapse.



PIPE PILES

Approximate Pile Dimensions and Design Properties

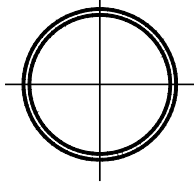
Designation and Outside Diameter	Wall Thickness	Area A	Weight per Foot	Section Properties			Area of Exterior Surface	Inside Cross Sectional Area	Inside Volume	External Collapse Index
				I	S	r				
In	in	in ²	lb	in ⁴	in ³	in	ft ² /ft	in ²	ft ³ /ft	*
PP24 (cont'd)	0.406	30.10	102.31	2090	175	8.34	6.28	422	0.109	235
	0.438	32.40	110.22	2250	188	8.33	6.28	420	0.108	296
	0.469	34.70	117.86	2400	200	8.32	6.28	418	0.107	364
	0.500	36.90	125.49	2550	212	8.31	6.28	415	0.107	443
PP26	0.250	20.20	68.75	1680	129	9.10	6.81	511	0.131	43
	0.281	22.70	77.18	1880	144	9.09	6.81	508	0.131	61
	0.312	25.20	85.60	2080	160	9.08	6.81	506	0.130	83
	0.344	27.70	94.26	2280	176	9.07	6.81	503	0.129	112
	0.375	30.20	102.63	2480	191	9.06	6.81	501	0.129	145
	0.406	32.60	110.98	2670	206	9.05	6.81	498	0.128	184
	0.438	35.20	119.57	2870	221	9.04	6.81	496	0.128	232
	0.469	37.60	127.88	3070	236	9.03	6.81	493	0.127	286
	0.500	40.10	136.17	3260	251	9.02	6.81	491	0.126	347
	0.562	44.90	152.68	3630	280	9.00	6.81	486	0.125	495
	0.625	49.80	169.38	4010	309	8.97	6.81	481	0.124	656
	0.688	54.70	185.99	4380	337	8.95	6.81	476	0.122	814
PP28	0.750	59.50	202.25	4750	365	8.93	6.81	471	0.121	970
	0.250	21.80	74.09	2100	150	9.81	7.33	594	0.153	34
	0.281	24.50	83.19	2350	168	9.80	7.33	591	0.152	48
	0.312	27.10	92.26	2600	186	9.79	7.33	589	0.151	66
	0.344	29.90	101.61	2860	204	9.78	7.33	586	0.151	89
	0.375	32.50	110.64	3110	222	9.77	7.33	583	0.150	116
	0.406	35.20	119.65	3350	239	9.76	7.33	581	0.149	147
	0.438	37.90	128.93	3600	257	9.75	7.33	578	0.149	185
0.469	40.60	137.90	3840	275	9.74	7.33	575	0.148	228	

Note: Designer must confirm section properties and local availability of selected pile section.

Material Specifications - ASTM A252

Example of suggested method of designation: PP8 x 0.141

* The External Collapse Index is a non-dimensional function of the diameter to wall thickness ratio and is for general guidance only. The higher the number, the greater is the resistance to collapse.



PIPE PILES

Approximate Pile Dimensions and Design Properties

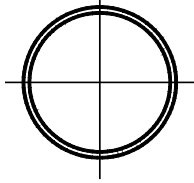
Designation and Outside Diameter	Wall Thickness	Area A	Weight per Meter	Section Properties			Area of Exterior Surface	Inside Cross Sectional Area	Inside Volume	External Collapse Index
				I	S	r				
In	in	in ²	lb	in ⁴	in ³	in	ft ² /ft	in ²	ft ³ /ft	*
PP28 (cont'd)	0.500	43.20	146.85	4080	292	9.72	7.33	573	0.147	277
	0.562	48.40	164.69	4560	326	9.70	7.33	567	0.143	395
	0.625	53.80	182.73	5040	360	9.68	7.33	562	0.144	544
	0.688	59.00	200.68	5510	393	9.66	7.33	557	0.143	691
	0.750	64.20	218.27	5960	426	9.64	7.33	552	0.142	835
PP30	0.250	23.40	79.43	2590	172	10.50	7.85	683	0.176	28
	0.281	26.20	89.19	2900	193	10.50	7.85	681	0.175	39
	0.312	29.10	98.93	3210	214	10.50	7.85	678	0.174	54
	0.344	32.00	108.95	3520	235	10.50	7.85	675	0.174	72
	0.375	34.90	118.65	3830	255	10.50	7.85	672	0.173	94
	0.406	37.70	128.32	4130	276	10.50	7.85	669	0.172	120
	0.438	40.70	138.29	4440	296	10.50	7.85	666	0.171	150
	0.469	43.50	147.92	4740	316	10.40	7.85	663	0.171	185
	0.500	46.30	157.53	5040	336	10.40	7.85	661	0.170	225
	0.562	52.00	176.69	5630	375	10.40	7.85	655	0.168	321
	0.625	57.70	196.08	6220	415	10.40	7.85	649	0.167	443
	0.688	63.40	215.38	6810	454	10.40	7.85	644	0.166	584
	0.750	68.90	234.29	7380	492	10.30	7.85	638	0.164	719
PP32	0.250	24.90	84.77	3140	196	11.20	8.38	779	0.200	23
	0.281	28.00	95.19	3520	220	11.20	8.38	776	0.200	32
	0.312	31.10	105.59	3900	244	11.20	8.38	773	0.199	44
	0.344	34.20	116.30	4290	268	11.20	8.38	770	0.198	60
	0.375	37.30	126.66	4660	291	11.20	8.38	767	0.197	77
	0.406	40.30	136.99	5030	314	11.20	8.38	764	0.196	98
	0.438	43.40	147.64	5410	338	11.20	8.38	761	0.196	124
	0.469	46.50	157.94	5770	361	11.10	8.38	758	0.195	152

Note: Designer must confirm section properties and local availability of selected pile section.

Material Specifications - ASTM A252

Example of suggested method of designation: PP8 x 0.141

* The External Collapse Index is a non-dimensional function of the diameter to wall thickness ratio and is for general guidance only. The higher the number, the greater is the resistance to collapse.



PIPE PILES

Approximate Pile Dimensions and Design Properties

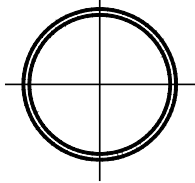
Designation and Outside Diameter	Wall Thickness	Area A	Weight per Foot	Section Properties			Area of Exterior Surface	Inside Cross Sectional Area	Inside Volume	External Collapse Index
				I	S	r				
in	in	in ²	lb	in ⁴	in ³	in	ft ² /ft	in ²	ft ³ /ft	*
PP32 (cont'd)	0.500	49.50	168.21	6140	384	11.10	8.38	755	0.194	185
	0.562	55.50	188.70	6860	429	11.10	8.38	749	0.193	264
	0.625	61.60	209.43	7580	474	11.10	8.38	743	0.191	364
	0.688	67.70	230.08	8300	519	11.10	8.38	737	0.189	487
	0.750	73.60	250.31	8990	562	11.10	8.38	731	0.188	617
PP34	0.250	26.50	90.11	3770	222	11.90	8.90	881	0.227	19
	0.281	29.80	101.19	4230	249	11.90	8.90	878	0.226	27
	0.312	33.00	112.25	4680	276	11.90	8.90	875	0.225	37
	0.344	36.40	123.65	5150	303	11.90	8.90	872	0.224	50
	0.375	39.60	134.67	5600	329	11.90	8.90	868	0.223	64
	0.406	42.80	145.67	6050	356	11.90	8.90	865	0.222	82
	0.438	46.20	157.00	6500	383	11.90	8.90	862	0.222	103
	0.469	49.40	167.95	6940	409	11.90	8.90	859	0.221	127
	0.500	52.60	178.89	7380	434	11.80	8.90	855	0.220	154
	0.562	59.00	200.70	8250	486	11.80	8.90	849	0.218	219
	0.625	65.50	222.78	9130	537	11.80	8.90	842	0.217	303
	0.688	72.00	244.77	9990	588	11.80	8.90	836	0.215	405
	0.750	78.30	266.33	10800	637	11.80	8.90	830	0.213	527
	0.875	91.10	309.55	12500	735	11.70	8.90	817	0.210	767
1.000	104.00	352.44	14100	831	11.70	8.90	804	0.207	1010	
PP36	0.250	28.10	95.45	4490	249	12.60	9.42	990	0.255	16
	0.281	31.50	107.20	5030	279	12.60	9.42	986	0.254	23
	0.312	35.00	118.92	5570	309	12.60	9.42	983	0.253	31
	0.344	38.50	131.00	6120	340	12.60	9.42	979	0.252	42

Note: Designer must confirm section properties and local availability of selected pile section.

Material Specifications - ASTM A252

Example of suggested method of designation: PP8 x 0.141

* The External Collapse Index is a non-dimensional function of the diameter to wall thickness ratio and is for general guidance only. The higher the number, the greater is the resistance to collapse.



PIPE PILES

Approximate Pile Dimensions and Design Properties

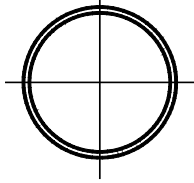
Designation and Outside Diameter	Wall Thickness	Area A	Weight per Foot	Section Properties			Area of Exterior Surface	Inside Cross Sectional Area	Inside Volume	External Collapse Index
				I	S	r				
in	in	in ²	lb	in ⁴	in ³	in	ft ² /ft	in ²	ft ³ /ft	*
PP36 (cont'd)	0.375	42.00	142.68	6660	370	12.60	9.42	976	0.2510	54
	0.406	45.40	154.34	7190	399	12.60	9.42	972	0.2500	69
	0.438	48.90	166.35	7740	430	12.60	9.42	969	0.2490	87
	0.469	52.40	177.97	8260	459	12.60	9.42	966	0.2480	107
	0.500	55.80	189.57	8790	488	12.60	9.42	962	0.2480	129
	0.562	62.60	212.70	9820	546	12.50	9.42	955	0.2460	184
	0.625	69.50	236.13	10900	604	12.50	9.42	948	0.2440	254
	0.688	76.30	259.47	11900	661	12.50	9.42	942	0.2420	341
	0.750	83.10	282.35	12900	717	12.50	9.42	935	0.2400	443
	0.875	96.60	328.24	14900	828	12.40	9.42	921	0.2370	674
	1.000	110.00	373.80	16900	936	12.40	9.42	908	0.2340	900
PP38	0.250	29.60	100.79	5280	278	13.30	9.95	1100	0.2840	14
	0.281	33.30	113.20	5920	312	13.30	9.95	1100	0.2830	19
	0.312	36.90	125.58	6560	345	13.30	9.95	1100	0.2820	26
	0.344	40.70	138.35	7210	380	13.30	9.95	1090	0.2810	35
	0.375	44.30	150.69	7840	413	13.30	9.95	1090	0.2800	46
	0.406	48.00	163.01	8470	446	13.30	9.95	1090	0.2790	59
	0.438	51.70	175.71	9120	480	13.30	9.95	1080	0.2780	74
	0.469	55.30	187.99	9740	513	13.30	9.95	1080	0.2780	90
	0.500	58.90	200.25	10400	545	13.30	9.95	1080	0.2760	110
	0.562	66.10	224.71	11600	610	13.20	9.95	1070	0.2750	156
	0.625	73.40	249.48	12800	675	13.20	9.95	1060	0.2730	216
	0.688	80.60	274.16	14000	739	13.20	9.95	1050	0.2710	289

Note: Designer must confirm section properties and local availability of selected pile section.

Material Specifications - ASTM A252

Example of suggested method of designation: PP8 x 0.141

* The External Collapse Index is a non-dimensional function of the diameter to wall thickness ratio and is for general guidance only. The higher the number, the greater is the resistance to collapse.



PIPE PILES

Approximate Pile Dimensions and Design Properties

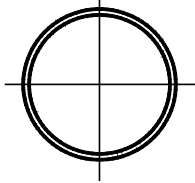
Designation and Outside Diameter	Wall Thickness	Area A	Weight per Foot	Section Properties			Area of Exterior Surface	Inside Cross Sectional Area	Inside Volume	External Collapse Index
				I	S	r				
in	in	in ²	lb	in ⁴	in ³	in	Ft ² /ft	in ²	ft ³ /ft	*
PP38 (cont'd)	0.750	87.8	298.37	15200	802	13.20	9.95	1050	0.269	376
	0.875	102.0	346.93	17600	926	13.10	9.95	1030	0.265	590
	1.000	116.0	395.16	19900	1050	13.10	9.95	1020	0.262	805
	1.250	144.0	490.61	24400	1280	13.00	9.95	990	0.255	1230
	1.500	172.0	584.73	28700	1510	12.90	9.95	962	0.248	1780
PP40	0.312	38.9	132.25	7660	383	14.00	10.50	1220	0.313	23
	0.344	42.9	145.69	8430	421	14.00	10.50	1210	0.312	30
	0.375	46.7	158.70	9160	458	14.00	10.50	1210	0.311	39
	0.406	50.5	171.68	9900	495	14.00	10.50	1210	0.310	50
	0.438	54.4	185.06	10700	533	14.00	10.50	1200	0.309	63
	0.469	58.2	198.01	11400	569	14.00	10.50	1200	0.308	77
	0.500	62.0	210.93	12100	605	14.00	10.50	1190	0.307	94
	0.562	69.6	236.71	13500	677	13.90	10.50	1190	0.305	134
	0.625	77.3	262.83	15000	749	13.90	10.50	1180	0.303	185
	0.688	85.0	288.86	16400	821	13.90	10.50	1170	0.301	247
	0.750	92.5	314.39	17800	891	13.90	10.50	1160	0.299	321
	0.875	108.0	365.62	20600	1030	13.80	10.50	1150	0.296	514
	1.000	123.0	416.52	23300	1170	13.80	10.50	1130	0.292	719
	1.250	152.0	517.31	28600	1430	13.70	10.50	1100	0.284	1130
1.500	181.0	616.77	33700	1680	13.60	10.50	1080	0.276	1620	
1.750	210.0	714.89	38500	1930	13.50	10.50	1050	0.269	2140	
PP42	0.312	40.9	138.91	8880	423	14.70	11.00	1340	0.346	20
	0.344	45.0	153.04	9770	465	14.70	11.00	1340	0.345	26
	0.375	49.0	166.71	10600	506	14.70	11.00	1340	0.344	34
	0.406	53.1	180.35	11500	546	14.70	11.00	1340	0.343	43

Note: Designer must confirm section properties and local availability of selected pile section.

Material Specifications - ASTM A252

Example of suggested method of designation: PP8 x 0.141

* The External Collapse Index is a non-dimensional function of the diameter to wall thickness ratio and is for general guidance only. The higher the number, the greater is the resistance to collapse.



PIPE PILES

Approximate Pile Dimensions and Design Properties

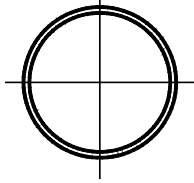
Designation and Outside Diameter	Wall Thickness	Area A	Weight per Foot	Section Properties			Area of Exterior Surface	Inside Cross Sectional Area	Inside Volume	External Collapse Index
				I	S	r				
in	in	in ²	lb	in ⁴	in ³	in	Ft ² /ft	in ²	ft ³ /ft	*
PP42 (cont'd)	0.438	57.2	194.42	12400	588	14.70	11.00	1330	0.342	54
	0.469	61.2	208.03	13200	628	14.70	11.00	1320	0.341	67
	0.500	65.2	221.61	14000	668	14.70	11.00	1320	0.340	81
	0.562	73.2	248.72	15700	748	14.70	11.00	1310	0.338	116
	0.625	81.2	276.18	17400	828	14.60	11.00	1300	0.335	159
	0.688	89.3	303.55	19100	907	14.60	11.00	1300	0.333	213
	0.750	97.2	330.41	20700	985	14.60	11.00	1290	0.331	277
	0.875	113.0	384.31	23900	1140	14.50	11.00	1270	0.327	443
	1.000	129.0	437.88	27100	1290	14.50	11.00	1260	0.323	641
	1.250	160.0	544.01	33200	1580	14.40	11.00	1230	0.315	1030
	1.500	191.0	648.81	39200	1870	14.30	11.00	1190	0.307	1460
PP44	1.750	221.0	752.27	44900	2140	14.20	11.00	1160	0.299	1970
	2.000	251.0	854.40	50400	2400	14.20	11.00	1130	0.292	2470
	0.344	47.2	160.39	11200	511	15.40	11.50	1470	0.379	23
	0.375	51.4	174.72	12200	556	15.40	11.50	1470	0.378	30
	0.406	55.6	189.03	13200	600	15.40	11.50	1460	0.377	38
	0.438	59.9	203.78	14200	646	15.40	11.50	1460	0.376	47
	0.469	64.1	218.04	15200	691	15.40	11.50	1460	0.375	58
	0.500	68.3	232.29	16200	735	15.40	11.50	1450	0.374	70
	0.625	85.2	289.53	20000	911	15.30	11.50	1440	0.369	138
	0.750	102.0	346.43	23800	1080	15.30	11.50	1420	0.365	241
0.875	119.0	403.00	27600	1250	15.30	11.50	1400	0.361	384	
1.000	135.0	459.24	31200	1420	15.20	11.50	1390	0.356	571	

Note: Designer must confirm section properties and local availability of selected pile section.

Material Specifications - ASTM A252

Example of suggested method of designation: PP8 x 0.141

* The External Collapse Index is a non-dimensional function of the diameter to wall thickness ratio and is for general guidance only. The higher the number, the greater is the resistance to collapse.



PIPE PILES

Approximate Pile Dimensions and Design Properties

Designation and Outside Diameter	Wall Thickness	Area A	Weight per Foot	Section Properties			Area of Exterior Surface	Inside Cross Sectional Area	Inside Volume	External Collapse Index
				I	S	r				
in	in	in ²	lb	in ⁴	in ³	in	Ft ² /ft	in ²	ft ³ /ft	*
PP44 (cont'd)	1.250	168.0	570.71	38400	1740	15.10	11.50	1350	0.348	941
	1.500	200.0	680.85	45300	2060	15.00	11.50	1320	0.340	1300
	1.750	232.0	789.65	51900	2360	15.00	11.50	1290	0.331	1810
	2.000	264.0	897.12	58300	2650	14.90	11.50	1260	0.323	2290
	2.250	295.0	1003.25	64500	2930	14.80	11.50	1230	0.315	2770
PP48	0.344	51.5	175.08	14600	609	16.80	12.60	1760	0.452	18
	0.375	56.1	190.74	15900	663	16.80	12.60	1750	0.451	23
	0.406	60.7	206.37	17200	716	16.80	12.60	1750	0.450	29
	0.438	65.4	222.49	18500	771	16.80	12.60	1740	0.449	36
	0.469	70.0	238.08	19800	824	16.80	12.60	1740	0.447	45
	0.500	74.6	253.65	21000	877	16.80	12.60	1730	0.446	54
	0.625	93.0	316.23	26100	1090	16.80	12.60	1720	0.442	106
	0.750	111.0	378.47	31100	1290	16.70	12.60	1700	0.437	185
	0.875	130.0	440.38	36000	1500	16.70	12.60	1680	0.432	295
	1.000	148.0	501.96	40800	1700	16.60	12.60	1660	0.427	443
	1.250	184.0	624.11	50200	2090	16.50	12.60	1630	0.418	787
	1.500	219.0	744.93	59300	2470	16.40	12.60	1590	0.409	1130
	1.750	254.0	864.41	68100	2840	16.40	12.60	1560	0.400	1530
	2.000	289.0	982.56	76600	3190	16.30	12.60	1520	0.391	1970
	2.250	323.0	1099.37	84800	3530	16.20	12.60	1490	0.382	2410
2.500	357.0	1214.85	92800	3860	16.10	12.60	1450	0.374	2850	

Note: Designer must confirm section properties and local availability of selected pile section.

Material Specifications - ASTM A252

Example of suggested method of designation: PP8 x 0.141

* The External Collapse Index is a non-dimensional function of the diameter to wall thickness ratio and is for general guidance only. The higher the number, the greater is the resistance to collapse.

Monotube Piles

Standard Monotube Weights and Volumes

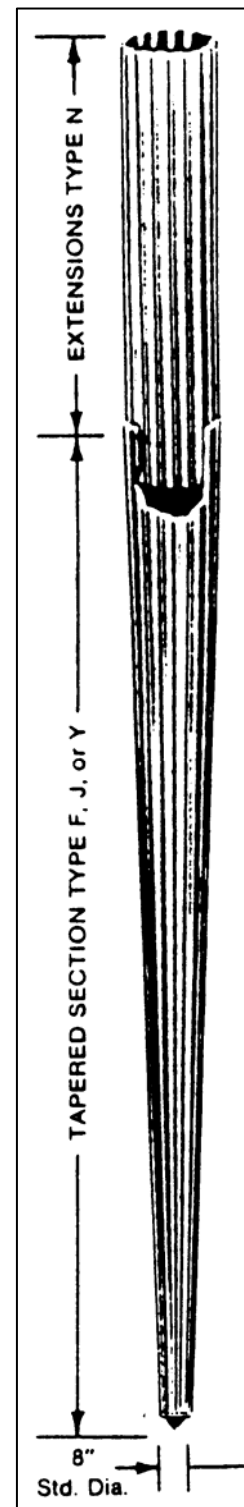
TYPE	SIZE POINT DIAMETER x BUTT DIAMETER x LENGTH	Weight (N) per m				EST. CONC. VOL. yd ³
		9 GA.	7 GA.	5 GA.	3 GA.	
F Taper 0.14 inch per foot	8½" x 12" x 25'	17	20	24	28	0.43
	8" x 12" x 30'	16	20	23	27	0.55
	8½" x 14" x 40'	19	22	26	31	0.95
	8" x 16" x 60'	20	24	28	33	1.68
	8" x 18" x 75'	--	26	31	35	2.59
J Taper 0.25 inch per foot	8" x 12" x 17'	17	20	23	27	0.32
	8" x 14" x 25'	18	22	26	30	0.58
	8" x 16" x 33'	20	24	28	32	0.95
	8" x 18" x 40'	--	26	30	35	1.37
Y Taper 0.40 inch per foot	8" x 12" x 10'	17	20	24	28	0.18
	8" x 14" x 15'	19	22	26	30	0.34
	8" x 16" x 20'	20	24	28	33	0.56
	8" x 18" x 25'	--	26	31	35	0.86

Extensions (Overall Length 1 Foot than indicated)

TYPE	DIAMETER + LENGTH	9 GA.	7 GA.	5 GA.	3 GA.	yd ³ /ft
N 12	12" x 12" x 20' / 40'	20	24	28	33	0.026
N 14	14" x 14" x 20' / 40'	24	29	34	41	0.035
N 16	16" x 16" x 20' / 40'	28	33	39	46	0.045
N 18	18" x 18" x 20' / 40'	--	38	44	52	0.058

Note: Designer must confirm section properties of selected pile section.

Pile design data converted to SI units from US units published in Monotube Pile Corporation Catalog 592.



MONOTUBE PILES

Physical Properties

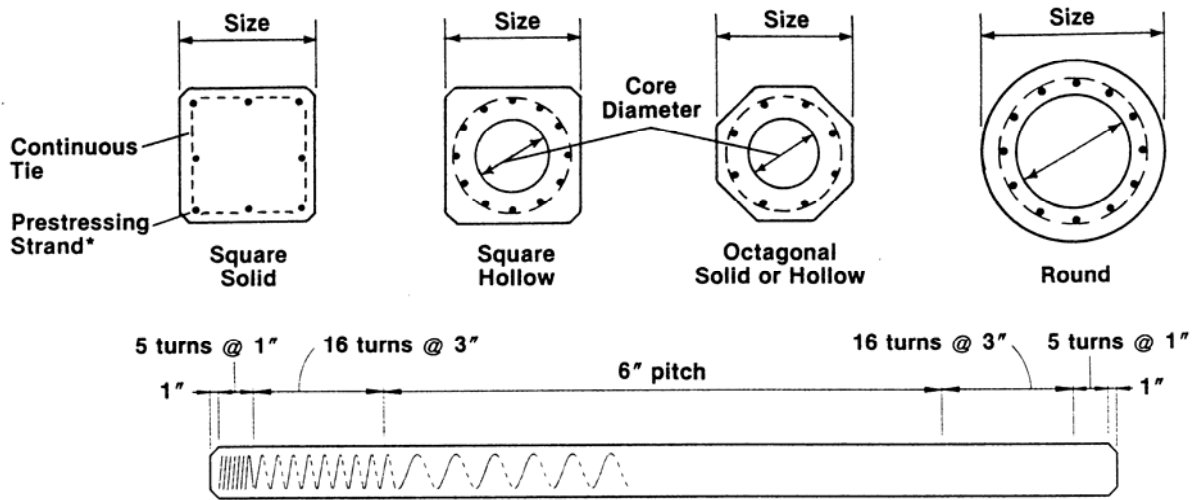
STEEL THICKNESS	POINTS		BUTTS OF PILE SECTIONS							
	8 in	8 ½ in	12 in				14 in			
	A in ²	A in ²	A in ²	I in ⁴	S in ³	r in	A in ²	I in ⁴	S in ³	r in
9 GAUGE (0.1495")	3.63	3.93	5.81	102	16.3	4.18	6.75	159	22.0	4.86
7 GAUGE (0.1793")	4.40	4.77	6.97	122	19.5	4.18	8.14	194	26.7	4.89
5 GAUGE (0.2391")	5.19	5.61	8.18	145	23.0	4.21	9.50	227	31.0	4.88
3 GAUGE (0.2391")	5.87	6.58	8.96	148	24.2	4.07	10.60	239	33.6	4.77
CONCRETE AREA in ²	42.3	47.3	101				136			

STEEL THICKNESS	POINTS		BUTTS OF PILE SECTIONS							
	8 in	8 ½ in	16 in				18 in			
	A in ²	A in ²	A in ²	I in ⁴	S in ³	r in	A in ²	I in ⁴	S in ³	r in
9 GAUGE (0.1495")	3.63	3.93	7.64	232	28.3	5.50	--	--	--	--
7 GAUGE (0.1793")	4.40	4.77	9.18	278	33.9	5.51	10.4	404	43.5	6.23
5 GAUGE (0.2391")	5.19	5.61	10.8	329	33.9	5.53	12.2	478	51.2	6.26
3 GAUGE (0.2391")	5.87	6.58	12.0	348	43.1	5.40	13.6	504	55.4	6.10
CONCRETE AREA in ²	42.3	47.3	176				224			

Note: Designer must confirm section properties of selected pile section.

Pile design data converted to SI units from US units published in Monotube Pile Corporation Catalog 592.

PRECAST/PRESTRESSED CONCRETE PILES



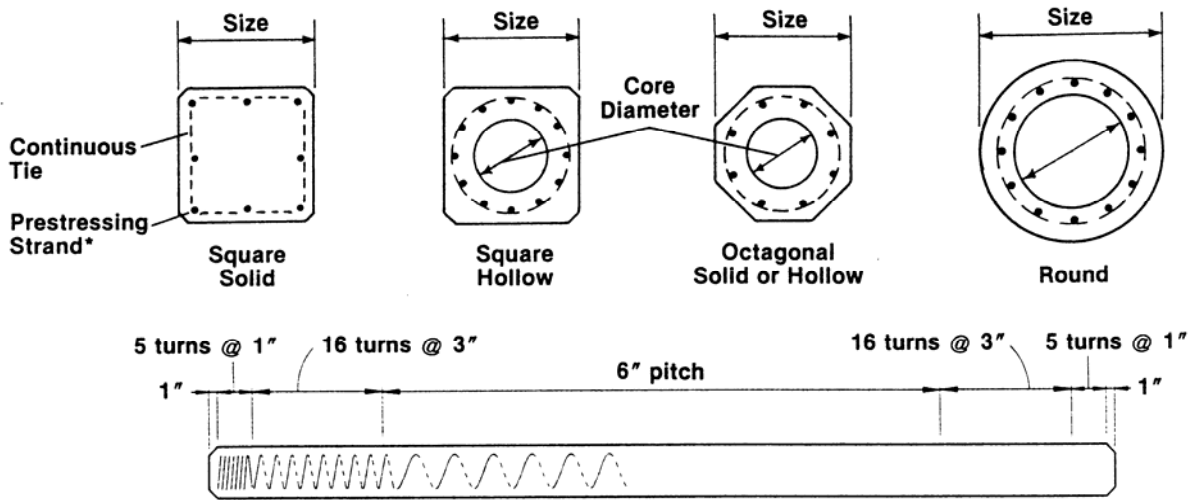
* Strand pattern may be circular or square.

Size in	Core Diameter in	Section Properties					
		Area in ²	Weight lb/ft	Moment of Inertia in ⁴	Section Modulus in ³	Radius of Gyration in	Perimeter ft
Square Piles							
10	Solid	100	104	833	167	2.89	3.33
12	Solid	144	150	1,728	288	3.46	4.00
14	Solid	196	204	3,201	457	4.04	4.67
16	Solid	256	267	5,461	683	4.62	5.33
18	Solid	324	338	8,748	972	5.20	6.00
20	Solid	400	417	13,333	1,333	5.77	6.67
20	11	305	318	12,615	1,262	6.43	6.67
24	Solid	576	600	27,648	2,304	6.93	8.00
24	12	463	482	26,630	2,219	7.58	8.00
24	14	422	439	25,762	2,147	7.81	8.00
24	16	399	415	25,163	2,097	7.94	8.00
30	18	646	672	62,347	4,157	9.82	10.00
36	18	1,042	1085	134,815	7,490	11.38	12.00

Note: Designer must confirm section properties for a selected pile. Form dimensions may vary with producers, with corresponding variations in section properties.

PCI (1993), Precast/Prestressed Concrete Institute Journal, Volume 38, No. 2, March-April, 1993.

PRECAST/PRESTRESSED CONCRETE PILES



* Strand pattern may be circular or square.

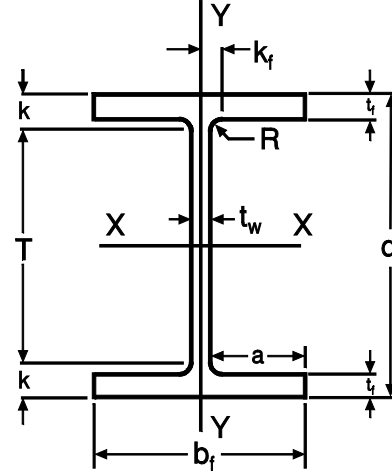
Typical Elevation

Size in	Section Properties						
	Core Diameter in	Area in ²	Weight lb/ft	Moment of Inertia in ⁴	Section Modulus in ³	Radius of Gyration in	Perimeter ft
Octagonal Piles							
10	Solid	83	85	555	111	2.59	2.76
12	Solid	119	125	1,134	189	3.09	3.31
14	Solid	162	169	2,105	301	3.60	3.87
16	Solid	212	220	3,592	449	4.12	4.42
18	Solid	268	280	5,705	639	4.61	4.97
20	Solid	331	345	8,770	877	5.15	5.52
20	11	236	245	8,050	805	5.84	5.52
22	Solid	401	420	12,837	1167	5.66	6.08
22	13	268	280	11,440	1040	6.53	6.08
24	Solid	477	495	18,180	1515	6.17	6.63
24	15	300	315	15,696	1308	7.23	6.63
Round Piles							
36	26	487	507	60,007	3,334	11.10	9.43
42	32	581	605	101,273	4,823	13.20	11.00
48	38	675	703	158,222	6,592	15.31	12.57
54	44	770	802	233,373	8,643	17.41	14.14
66	54	1,131	1,178	514,027	15,577	21.32	17.28

Note: Designer must confirm section properties for a selected pile. Form dimensions may vary with producers, with corresponding variations in section properties.

PCI (1993), Precast/Prestressed Concrete Institute Journal, Volume 38, No. 2, March-April, 1993.

H-PILES



C2-20

Section Designation	Area A	Depth d	Web Thickness t_w	Flange		Distance				Fillet Radius R	Elastic Properties					
				Width b_f	Thickness t_f	T	k	k_f	a		X-X			Y-Y		
											I	S	r	I	S	r
in x lb/ft	in ²	in	in	in	in	in	in	in	in	in	in ⁴	in ³	in	in ⁴	in ³	in
HP14 x 117	34.4	14.21	0.805	14.885	0.805	10.91	1.65	1.19	7.05	0.79	1220	172	5.96	443	59.5	3.59
HP14 x 102	30.0	14.01	0.705	14.785	0.705	10.91	1.57	1.14	7.05	0.79	1050	150	5.92	380	51.4	3.56
HP14 x 89	26.1	13.83	0.615	14.695	0.615	10.91	1.46	1.09	7.05	0.79	904	131	5.88	326	44.3	3.53
HP14 x 73	21.4	13.61	0.505	14.585	0.505	10.91	1.34	1.04	7.05	0.79	729	107	5.84	261	35.8	3.49
HP12 x 84	24.6	12.28	0.685	12.295	0.685	9.61	1.34	0.93	5.79	0.59	650	106	5.14	213	34.6	2.94
HP12 x 73	21.8	12.13	0.605	12.215	0.610	9.61	1.26	0.89	5.79	0.59	569	93	5.11	186	30.4	2.92
HP12 x 63	18.4	11.94	0.515	12.125	0.515	9.61	1.18	0.85	5.83	0.59	472	79	5.06	153	25.3	2.88
HP12 x 53	15.5	11.78	0.435	12.045	0.435	9.61	1.10	0.81	5.83	0.59	393	66	5.03	127	21.1	2.86
HP10 x 57	16.8	9.99	0.565	10.225	0.565	7.72	1.14	0.80	4.84	0.51	294	59	4.18	101	19.7	2.45
HP10 x 42	12.4	9.70	0.415	10.075	0.420	3.78	0.98	0.72	4.84	0.51	210	43	4.13	72	14.2	2.41
HP8 x 36	10.6	8.02	0.445	8.155	0.445	6.22	0.91	0.62	3.86	0.39	119	30	3.36	41	9.88	1.95

Note: Designer must confirm section properties for a selected pile.

AISC (1989), Manual of Steel Construction, Allowable Stress Design. Ninth Edition, American Institute of Steel Construction, Inc. 1989.

APPENDIX D

Pile Hammer Information

Table D-1 DIESEL HAMMER LISTING (sorted by Rated Energy)	D-3
Table D-2 EXTERNAL COMBUSTION HAMMER LISTING (sorted by Rated Energy)	D-11
Table D-3 VIBRATORY HAMMER LISTING (sorted by Power)	D-25
Table D-4 COMPLETE HAMMER LISTING (sorted by GRLWEAP ID Numbers)	D-29

Note: GRLWEAP hammer ID numbers correspond to those contained in Version 2003-1 of the GRLWEAP program.

TABLE D-1: DIESEL HAMMER LISTING (sorted by Rated Energy)									
Hammer Description				SI Units			US Units		
GRLWEAP ID	Hammer Manufacturer	Hammer Name	Hammer Type	Rated Energy kJ	Ram Weight kN	Eq. Rated Stroke m	Rated Energy ft-kips	Ram Weight kips	Eq. Rated Stroke ft
81	LINKBELT	LB 180	CED	10.98	7.70	1.43	8.10	1.73	4.68
120	ICE	180	CED	11.03	7.70	1.43	8.13	1.73	4.70
146	MKT	DE 10	OED	11.93	4.90	3.35	8.80	1.10	11.00
1	DELMAG	D 5	OED	14.24	4.90	2.93	10.51	1.10	9.62
36	DELMAG	D 6-32	OED	18.31	5.87	3.12	13.50	1.32	10.23
82	LINKBELT	LB 312	CED	20.36	17.18	1.19	15.02	3.86	3.89
147	MKT	DE 20	OED	21.70	8.90	2.74	16.00	2.00	9.00
402	BERMINGH	B200	OED	24.41	8.90	2.74	18.00	2.00	9.00
578	APE	D 8-32	OED	24.41	7.83	3.12	18.00	1.76	10.25
83	LINKBELT	LB 440	CED	24.68	17.80	1.39	18.20	4.00	4.55
122	ICE	440	CED	25.17	17.80	1.41	18.56	4.00	4.64
142	MKT 20	DE333020	OED	27.12	8.90	3.51	20.00	2.00	11.50
2	DELMAG	D 8-22	OED	27.25	7.83	3.67	20.10	1.76	12.05
151	MKT	DA 35B	CED	28.48	12.46	2.29	21.00	2.80	7.50
167	MKT	DA 35C	CED	28.48	12.46	2.29	21.00	2.80	7.50
422	BERMINGH	B2005	OED	28.48	8.90	3.20	21.00	2.00	10.50
148	MKT	DE 30	OED	30.37	12.46	3.05	22.40	2.80	10.00
50	FEC	FEC 1200	OED	30.50	12.24	2.49	22.50	2.75	8.18
127	ICE	30-S	OED	30.51	13.35	2.34	22.50	3.00	7.67
3	DELMAG	D 12	OED	30.65	12.24	3.29	22.61	2.75	10.80
401	BERMINGH	B23	CED	31.17	12.46	2.50	22.99	2.80	8.21
414	BERMINGH	B23 5	CED	31.17	12.46	2.50	22.99	2.80	8.21
121	ICE	422	CED	31.35	17.80	1.76	23.12	4.00	5.78

TABLE D-1: DIESEL HAMMER LISTING (sorted by Rated Energy)									
Hammer Description				SI Units			US Units		
GRLWEAP ID	Hammer Manufacturer	Hammer Name	Hammer Type	Rated Energy kJ	Ram Weight kN	Eq. Rated Stroke m	Rated Energy ft-kips	Ram Weight kips	Eq. Rated Stroke ft
149	MKT	DA35B SA	OED	32.27	12.46	3.96	23.80	2.80	13.00
150	MKT	DE 30B	OED	32.27	12.46	3.05	23.80	2.80	10.00
61	MITSUBIS	M 14	OED	34.23	13.22	2.59	25.25	2.97	8.50
350	HERA	1250	OED	34.37	12.50	2.75	25.35	2.81	9.02
101	KOBE	K 13	OED	34.48	12.77	2.70	25.43	2.87	8.86
139	ICE	32-S	OED	35.27	13.35	3.25	26.01	3.00	10.67
415	BERMINGH	B250 5	OED	35.60	11.13	3.20	26.25	2.50	10.50
84	LINKBELT	LB 520	CED	35.68	22.56	1.58	26.31	5.07	5.19
4	DELMAG	D 15	OED	36.74	14.69	3.29	27.09	3.30	10.80
51	FEC	FEC 1500	OED	36.74	14.69	2.50	27.09	3.30	8.21
143	MKT 30	DE333020	OED	37.97	12.46	3.51	28.00	2.80	11.50
62	MITSUBIS	MH 15	OED	38.15	14.73	2.59	28.14	3.31	8.50
403	BERMINGH	B225	OED	39.66	13.35	2.97	29.25	3.00	9.75
360	ICE	I-12	OED	40.95	12.55	3.51	30.20	2.82	11.50
123	ICE	520	CED	41.18	22.56	1.83	30.37	5.07	5.99
351	HERA	1500	OED	41.22	15.00	2.75	30.40	3.37	9.02
152	MKT	DA 45	CED	41.66	17.80	2.34	30.72	4.00	7.68
37	DELMAG	D 12-32	OED	42.48	12.55	3.60	31.33	2.82	11.81
153	MKT	DE 40	OED	43.39	17.80	3.05	32.00	4.00	10.00
144	MKT 33	DE333020	OED	44.75	14.69	3.51	33.00	3.30	11.50
38	DELMAG	D 12-42	OED	45.16	12.55	3.60	33.30	2.82	11.81
39	DELMAG	D 14-42	OED	46.84	13.75	3.60	34.55	3.09	11.81
154	MKT	DE 42/35	OED	47.46	15.58	4.11	35.00	3.50	13.50

TABLE D-1: DIESEL HAMMER LISTING (sorted by Rated Energy)									
Hammer Description				SI Units			US Units		
GRLWEAP ID	Hammer Manufacturer	Hammer Name	Hammer Type	Rated Energy kJ	Ram Weight kN	Eq. Rated Stroke m	Rated Energy ft-kips	Ram Weight kips	Eq. Rated Stroke ft
423	BERMINGH	B2505	OED	48.00	13.35	3.60	35.40	3.00	11.80
161	MKT	DA 55B	CED	51.80	22.25	2.33	38.20	5.00	7.64
168	MKT	DA 55C	CED	51.80	22.25	2.33	38.20	5.00	7.64
579	APE	D 16-32	OED	53.37	15.71	3.43	39.36	3.53	11.25
128	ICE	40-S	OED	54.24	17.80	3.10	40.00	4.00	10.17
145	MKT 40	DE333020	OED	54.24	17.80	3.51	40.00	4.00	11.50
160	MKT	DA55B SA	OED	54.24	22.25	3.66	40.00	5.00	12.00
5	DELMAG	D 16-32	OED	54.51	15.66	3.58	40.20	3.52	11.76
404	BERMINGH	B300	OED	54.66	16.69	3.28	40.31	3.75	10.75
410	BERMINGH	B300 M	OED	54.66	16.69	3.28	40.31	3.75	10.75
6	DELMAG	D 22	OED	55.06	21.85	2.90	40.61	4.91	9.50
124	ICE	640	CED	55.08	26.70	2.06	40.62	6.00	6.77
155	MKT	DE 42/35	OED	56.95	18.69	4.11	42.00	4.20	13.50
129	ICE	42-S	OED	56.96	18.20	3.18	42.00	4.09	10.42
40	DELMAG	D 19-32	OED	57.55	17.80	3.58	42.44	4.00	11.76
159	MKT	DE 50B	OED	57.63	22.25	3.35	42.50	5.00	11.00
571	APE	D 19-32	OED	58.07	18.65	3.12	42.82	4.19	10.25
580	APE	D 19-42	OED	58.07	18.65	3.23	42.82	4.19	10.60
63	MITSUBIS	M 23	OED	58.32	22.52	2.59	43.01	5.06	8.50
361	ICE	I-19	OED	58.56	17.84	3.75	43.19	4.01	12.30
412	BERMINGH	B400 4.8	OED	58.58	21.36	2.74	43.20	4.80	9.00
35	DELMAG	D 19-52	OED	58.63	17.80	3.61	43.24	4.00	11.86
41	DELMAG	D 19-42	OED	58.63	17.80	3.61	43.24	4.00	11.86

TABLE D-1: DIESEL HAMMER LISTING (sorted by Rated Energy)									
Hammer Description				SI Units			US Units		
GRLWEAP ID	Hammer Manufacturer	Hammer Name	Hammer Type	Rated Energy kJ	Ram Weight kN	Eq. Rated Stroke m	Rated Energy ft-kips	Ram Weight kips	Eq. Rated Stroke ft
349	HERA	1900	OED	60.23	18.65	3.23	44.41	4.19	10.60
413	BERMINGH	B400 5.0	OED	61.02	22.25	2.74	45.00	5.00	9.00
103	KOBE	K22-Est	OED	61.49	21.58	2.85	45.35	4.85	9.35
64	MITSUBIS	MH 25	OED	63.51	24.52	2.59	46.84	5.51	8.50
416	BERMINGH	B350 5	OED	64.00	17.80	3.60	47.20	4.00	11.80
7	DELMAG	D 22-02	OED	65.77	21.58	4.10	48.50	4.85	13.44
8	DELMAG	D 22-13	OED	65.77	21.58	4.10	48.50	4.85	13.44
52	FEC	FEC 2500	OED	67.79	24.48	2.77	50.00	5.50	9.09
157	MKT	DE 50C	OED	67.80	22.25	3.96	50.00	5.00	13.00
163	MKT 50	DE70/50B	OED	67.80	22.25	3.66	50.00	5.00	12.00
352	HERA	2500	OED	68.74	25.01	2.75	50.69	5.62	9.02
9	DELMAG	D 22-23	OED	69.45	21.58	4.10	51.22	4.85	13.44
104	KOBE	K 25	OED	69.86	24.52	2.85	51.52	5.51	9.35
85	LINKBELT	LB 660	CED	70.01	33.69	2.08	51.63	7.57	6.82
125	ICE	660	CED	70.01	33.69	2.08	51.63	7.57	6.82
405	BERMINGH	B400	OED	72.89	22.25	3.28	53.75	5.00	10.75
411	BERMINGH	B400 M	OED	72.89	22.25	3.28	53.75	5.00	10.75
46	DELMAG	D 21-42	OED	75.59	20.60	4.27	55.75	4.63	14.00
53	FEC	FEC 2800	OED	75.93	27.41	2.77	55.99	6.16	9.09
353	HERA	2800	OED	76.93	27.99	2.75	56.74	6.29	9.02
581	APE	D 25-32	OED	78.45	24.52	3.20	57.86	5.51	10.50
417	BERMINGH	B400 5	OED	80.00	22.25	3.60	59.00	5.00	11.80
162	MKT	DE 70B	OED	80.68	31.15	3.66	59.50	7.00	12.00

TABLE D-1: DIESEL HAMMER LISTING (sorted by Rated Energy)									
Hammer Description				SI Units			US Units		
GRLWEAP ID	Hammer Manufacturer	Hammer Name	Hammer Type	Rated Energy kJ	Ram Weight kN	Eq. Rated Stroke m	Rated Energy ft-kips	Ram Weight kips	Eq. Rated Stroke ft
11	DELMAG	D 30	OED	80.99	29.37	2.90	59.73	6.60	9.50
130	ICE	60-S	OED	81.35	31.15	3.18	59.99	7.00	10.42
65	MITSUBIS	M 33	OED	83.68	32.31	2.59	61.71	7.26	8.50
54	FEC	FEC 3000	OED	85.47	29.37	2.91	63.03	6.60	9.55
66	MITSUBIS	MH 35	OED	88.98	34.35	2.59	65.62	7.72	8.50
12	DELMAG	D 30-02	OED	89.76	29.37	4.10	66.20	6.60	13.44
13	DELMAG	D 30-13	OED	89.76	29.37	4.10	66.20	6.60	13.44
10	DELMAG	D 25-32	OED	89.96	24.52	4.19	66.34	5.51	13.76
131	ICE	70-S	OED	94.92	31.15	3.10	70.00	7.00	10.17
158	MKT	DE 70C	OED	94.92	31.15	3.96	70.00	7.00	13.00
164	MKT 70	DE70/50B	OED	94.92	31.15	3.66	70.00	7.00	12.00
572	APE	D 30-32	OED	95.01	29.41	3.23	70.07	6.61	10.60
354	HERA	3500	OED	96.26	35.02	2.75	70.99	7.87	9.02
107	KOBE	K 35	OED	97.88	34.35	2.85	72.18	7.72	9.35
126	ICE	1070	CED	98.45	44.50	2.21	72.60	10.00	7.26
55	FEC	FEC 3400	OED	98.99	33.29	2.97	73.00	7.48	9.76
14	DELMAG	D 30-23	OED	100.06	29.37	4.10	73.79	6.60	13.44
362	ICE	I-30	OED	102.27	29.41	3.84	75.42	6.61	12.60
15	DELMAG	D 30-32	OED	102.29	29.37	4.18	75.44	6.60	13.73
418	BERMINGH	B450 5	OED	105.61	29.37	3.60	77.88	6.60	11.80
132	ICE	80-S	OED	108.48	35.60	3.79	80.00	8.00	12.42
67	MITSUBIS	M 43	OED	109.04	42.10	2.59	80.41	9.46	8.50
16	DELMAG	D 36	OED	113.66	35.29	3.22	83.82	7.93	10.57

TABLE D-1: DIESEL HAMMER LISTING (sorted by Rated Energy)									
Hammer Description				SI Units			US Units		
GRLWEAP ID	Hammer Manufacturer	Hammer Name	Hammer Type	Rated Energy kJ	Ram Weight kN	Eq. Rated Stroke m	Rated Energy ft-kips	Ram Weight kips	Eq. Rated Stroke ft
17	DELMAG	D 36-02	OED	113.66	35.29	3.96	83.82	7.93	12.98
18	DELMAG	D 36-13	OED	113.66	35.29	6.09	83.82	7.93	19.98
573	APE	D 36-32	OED	113.98	35.29	3.23	84.06	7.93	10.60
68	MITSUBIS	MH 45	OED	115.84	44.72	2.59	85.43	10.05	8.50
421	BERMINGH	B550 C	OED	119.33	48.95	2.44	88.00	11.00	8.00
19	DELMAG	D 36-23	OED	120.00	35.29	3.96	88.50	7.93	12.98
133	ICE	90-S	OED	122.04	40.05	3.10	90.00	9.00	10.17
21	DELMAG	D 44	OED	122.25	42.28	2.90	90.16	9.50	9.52
20	DELMAG	D 36-32	OED	122.80	35.29	4.01	90.56	7.93	13.14
363	ICE	I-36	OED	122.96	35.33	3.69	90.67	7.94	12.10
419	BERMINGH	B500 5	OED	124.81	34.71	3.60	92.04	7.80	11.80
110	KOBE	K 45	OED	125.77	44.14	2.85	92.75	9.92	9.35
24	DELMAG	D 46-13	OED	130.90	45.12	3.94	96.53	10.14	12.94
134	ICE	100-S	OED	135.60	44.50	3.66	100.00	10.00	12.00
136	ICE	200-S	OED	135.60	89.00	1.83	100.00	20.00	6.00
355	HERA	5000	OED	137.48	50.02	2.75	101.38	11.24	9.02
420	BERMINGH	B550 5	OED	144.01	40.05	3.60	106.20	9.00	11.80
22	DELMAG	D 46	OED	145.20	45.12	3.22	107.08	10.14	10.57
23	DELMAG	D 46-02	OED	145.20	45.12	3.94	107.08	10.14	12.94
25	DELMAG	D 46-23	OED	145.20	45.12	3.94	107.08	10.14	12.94
574	APE	D 46-32	OED	145.75	45.12	3.23	107.48	10.14	10.60
364	ICE	I-46	OED	146.17	45.17	3.69	107.79	10.15	12.12
165	MKT 110	DE110150	OED	149.16	48.95	4.11	110.00	11.00	13.50

TABLE D-1: DIESEL HAMMER LISTING (sorted by Rated Energy)									
Hammer Description				SI Units			US Units		
GRLWEAP ID	Hammer Manufacturer	Hammer Name	Hammer Type	Rated Energy kJ	Ram Weight kN	Eq. Rated Stroke m	Rated Energy ft-kips	Ram Weight kips	Eq. Rated Stroke ft
356	HERA	5700	OED	156.68	57.00	2.75	115.55	12.81	9.02
135	ICE	120-S	OED	162.72	53.40	3.79	120.00	12.00	12.42
26	DELMAG	D 46-32	OED	165.69	45.12	3.99	122.19	10.14	13.10
27	DELMAG	D 55	OED	169.51	52.78	3.40	125.00	11.86	11.15
357	HERA	6200	OED	170.38	61.99	2.75	125.65	13.93	9.02
112	KOBE	KB 60	OED	176.53	58.87	3.00	130.18	13.23	9.84
140	ICE	120S-15	OED	179.60	66.75	3.73	132.45	15.00	12.25
70	MITSUBIS	MH 72B	OED	183.26	70.76	2.59	135.15	15.90	8.50
71	MITSUBIS	MH 80B	OED	202.86	78.32	2.59	149.60	17.60	8.50
166	MKT 150	DE110150	OED	203.40	66.75	4.11	150.00	15.00	13.50
358	HERA	7500	OED	206.09	74.98	2.75	151.99	16.85	9.02
28	DELMAG	D 62-02	OED	206.72	60.79	3.87	152.45	13.66	12.71
29	DELMAG	D 62-12	OED	206.72	60.79	3.87	152.45	13.66	12.71
575	APE	D 62-22	OED	218.94	60.79	3.60	161.46	13.66	11.82
30	DELMAG	D 62-22	OED	223.20	60.79	4.04	164.60	13.66	13.26
365	ICE	I-62	OED	223.71	64.97	4.34	164.98	14.60	14.25
137	ICE	205-S	OED	230.52	89.00	3.20	170.00	20.00	10.50
113	KOBE	KB 80	OED	235.37	78.50	3.00	173.58	17.64	9.84
359	HERA	8800	OED	241.93	88.02	2.75	178.42	19.78	9.02
31	DELMAG	D 80-12	OED	252.55	78.41	3.92	186.24	17.62	12.87
576	APE	D 80-23	OED	267.12	78.41	3.41	196.99	17.62	11.18
366	ICE	I-80	OED	288.01	78.77	4.11	212.40	17.70	13.50
32	DELMAG	D 80-23	OED	288.15	78.41	3.98	212.50	17.62	13.05

TABLE D-1: DIESEL HAMMER LISTING
(sorted by Rated Energy)

Hammer Description				SI Units			US Units		
GRLWEAP ID	Hammer Manufacturer	Hammer Name	Hammer Type	Rated Energy kJ	Ram Weight kN	Eq. Rated Stroke m	Rated Energy ft-kips	Ram Weight kips	Eq. Rated Stroke ft
577	APE	D 100-13	OED	333.98	98.03	3.41	246.30	22.03	11.18
33	DELMAG	D100-13	OED	360.32	98.21	4.11	265.72	22.07	13.50
43	DELMAG	D120-42	OED	409.23	117.70	3.60	301.79	26.45	11.81
582	APE	D 125-32	OED	416.69	122.64	3.40	307.29	27.56	11.15
45	DELMAG	D125-42	OED	425.29	122.64	4.15	313.63	27.56	13.60
44	DELMAG	D150-42	OED	511.66	147.16	3.60	377.33	33.07	11.81
42	DELMAG	D200-42	OED	667.21	196.20	5.13	492.04	44.09	16.83

TABLE D-2: EXTERNAL COMBUSTION HAMMER LISTING (sorted by Rated Energy)									
Hammer Description				SI Units			US Units		
GRLWEAP ID	Hammer Manufacturer	Hammer Name	Hammer Type	Rated Energy kJ	Ram Weight kN	Eq. Rated Stroke m	Rated Energy ft-kips	Ram Weight kips	Eq. Rated Stroke ft
301	MKT	No. 5	ECH	1.36	0.89	1.52	1.00	0.20	5.00
302	MKT	No. 6	ECH	3.39	1.78	1.91	2.50	0.40	6.25
303	MKT	No. 7	ECH	5.63	3.56	1.58	4.15	0.80	5.19
205	VULCAN	VUL 02	ECH	9.84	13.35	0.74	7.26	3.00	2.42
220	VULCAN	VUL 30C	ECH	9.84	13.35	0.74	7.26	3.00	2.42
521	DAWSON	HPH1200	ECH	11.82	10.24	1.16	8.72	2.30	3.79
304	MKT	9B3	ECH	11.87	7.12	1.67	8.75	1.60	5.47
305	MKT	10B3	ECH	17.78	13.35	1.33	13.11	3.00	4.37
522	DAWSON	HPH1800	ECH	18.62	14.69	1.27	13.73	3.30	4.16
567	HMC	19D	ECH	18.98	15.58	1.22	14.00	3.50	4.00
306	MKT	C5-Air	ECH	19.26	22.25	0.87	14.20	5.00	2.84
171	CONMACO	C 50	ECH	20.34	22.25	0.91	15.00	5.00	3.00
204	VULCAN	VUL 01	ECH	20.34	22.25	0.91	15.00	5.00	3.00
251	RAYMOND	R 1	ECH	20.34	22.25	0.91	15.00	5.00	3.00
221	VULCAN	VUL 50C	ECH	20.48	22.25	0.92	15.10	5.00	3.02
307	MKT	C5-Steam	ECH	21.97	22.25	0.99	16.20	5.00	3.24
380	BSP	HH 1.5	ECH	22.02	14.69	1.50	16.24	3.30	4.92
308	MKT	S-5	ECH	22.04	22.25	0.99	16.25	5.00	3.25
514	UDDCOMB	H2H	ECH	22.49	19.58	1.15	16.59	4.40	3.77
523	DAWSON	HPH2400	ECH	23.47	18.65	1.26	17.30	4.19	4.13
541	BANUT	3 Tonnes	ECH	23.48	29.41	0.80	17.32	6.61	2.62
309	MKT	11B3	ECH	25.97	22.25	1.17	19.15	5.00	3.83

TABLE D-2: EXTERNAL COMBUSTION HAMMER LISTING (sorted by Rated Energy)									
Hammer Description				SI Units			US Units		
GRLWEAP ID	Hammer Manufacturer	Hammer Name	Hammer Type	Rated Energy kJ	Ram Weight kN	Eq. Rated Stroke m	Rated Energy ft-kips	Ram Weight kips	Eq. Rated Stroke ft
222	VULCAN	VUL 65C	ECH	26.00	28.93	0.90	19.18	6.50	2.95
172	CONMACO	C 65	ECH	26.44	28.93	0.91	19.50	6.50	3.00
206	VULCAN	VUL 06	ECH	26.44	28.93	0.91	19.50	6.50	3.00
252	RAYMOND	R 1S	ECH	26.44	28.93	0.91	19.50	6.50	3.00
253	RAYMOND	R 65C	ECH	26.44	28.93	0.91	19.50	6.50	3.00
254	RAYMOND	R 65CH	ECH	26.44	28.93	0.91	19.50	6.50	3.00
223	VULCAN	VUL 65CA	ECH	26.53	28.93	0.92	19.57	6.50	3.01
550	ICE	70	ECH	28.48	31.15	0.91	21.00	7.00	3.00
561	HMC	28B	ECH	28.48	31.15	0.91	21.00	7.00	3.00
311	MKT	C826 Air	ECH	28.75	35.60	0.81	21.20	8.00	2.65
335	IHC	SC-30	ECH	29.57	16.73	1.77	21.81	3.76	5.80
542	BANUT	4 Tonnes	ECH	31.33	39.25	0.80	23.11	8.82	2.62
255	RAYMOND	R 0	ECH	33.05	33.38	0.99	24.38	7.50	3.25
310	MKT	C826 Stm	ECH	33.09	35.60	0.93	24.40	8.00	3.05
224	VULCAN	VUL 80C	ECH	33.19	35.60	0.93	24.48	8.00	3.06
256	RAYMOND	R 80C	ECH	33.19	35.60	0.93	24.48	8.00	3.06
257	RAYMOND	R 80CH	ECH	33.19	35.60	0.93	24.48	8.00	3.06
449	MENCK	MHF3-3	ECH	33.55	31.37	1.07	24.75	7.05	3.51
515	UDDCOMB	H3H	ECH	33.74	29.37	1.15	24.88	6.60	3.77
173	CONMACO	C 550	ECH	33.90	22.25	1.52	25.00	5.00	5.00
192	CONMACO	C 50E5	ECH	33.90	22.25	1.52	25.00	5.00	5.00
235	VULCAN	VUL 505	ECH	33.90	22.25	1.52	25.00	5.00	5.00
320	IHC	S-35	ECH	34.61	29.50	1.17	25.53	6.63	3.85

TABLE D-2: EXTERNAL COMBUSTION HAMMER LISTING (sorted by Rated Energy)									
Hammer Description				SI Units			US Units		
GRLWEAP ID	Hammer Manufacturer	Hammer Name	Hammer Type	Rated Energy kJ	Ram Weight kN	Eq. Rated Stroke m	Rated Energy ft-kips	Ram Weight kips	Eq. Rated Stroke ft
225	VULCAN	VUL 85C	ECH	35.24	37.91	0.93	25.99	8.52	3.05
175	CONMACO	C 80	ECH	35.26	35.60	0.99	26.00	8.00	3.25
207	VULCAN	VUL 08	ECH	35.26	35.60	0.99	26.00	8.00	3.25
312	MKT	S-8	ECH	35.26	35.60	0.99	26.00	8.00	3.25
591	APE	5.4mT	ECH	35.31	53.40	0.66	26.04	12.00	2.17
381	BSP	HH 3	ECH	35.31	29.41	1.20	26.04	6.61	3.94
530	Bruce	SGH-0312	ECH	35.31	29.41	1.20	26.04	6.61	3.94
535	BANUT	3000	ECH	35.31	29.41	1.20	26.04	6.61	3.94
481	JUNTTAN	HHK 3	ECH	36.00	29.46	1.22	26.55	6.62	4.01
560	HMC	28A	ECH	37.97	31.15	1.22	28.00	7.00	4.00
568	HMC	38D	ECH	37.97	31.15	1.22	28.00	7.00	4.00
543	BANUT	5 Tonnes	ECH	39.15	49.04	0.80	28.87	11.02	2.62
336	IHC	SC-40	ECH	40.50	24.52	1.65	29.86	5.51	5.42
551	ICE	75	ECH	40.68	33.38	1.22	30.00	7.50	4.00
313	MKT	MS-350	ECH	41.77	34.35	1.22	30.80	7.72	3.99
450	MENCK	MHF3-4	ECH	41.98	39.25	1.07	30.96	8.82	3.51
174	CONMACO	C 565	ECH	44.07	28.93	1.52	32.50	6.50	5.00
176	CONMACO	C 100	ECH	44.07	44.50	0.99	32.50	10.00	3.25
193	CONMACO	C 65E5	ECH	44.07	28.93	1.52	32.50	6.50	5.00
208	VULCAN	VUL 010	ECH	44.07	44.50	0.99	32.50	10.00	3.25
236	VULCAN	VUL 506	ECH	44.07	28.93	1.52	32.50	6.50	5.00
258	RAYMOND	R 2/0	ECH	44.07	44.50	0.99	32.50	10.00	3.25
314	MKT	S 10	ECH	44.07	44.50	0.99	32.50	10.00	3.25

TABLE D-2: EXTERNAL COMBUSTION HAMMER LISTING (sorted by Rated Energy)									
Hammer Description				SI Units			US Units		
GRLWEAP ID	Hammer Manufacturer	Hammer Name	Hammer Type	Rated Energy kJ	Ram Weight kN	Eq. Rated Stroke m	Rated Energy ft-kips	Ram Weight kips	Eq. Rated Stroke ft
506	HPSI	650	ECH	44.07	28.93	1.52	32.50	6.50	5.00
372	FAIRCHLD	F-32	ECH	44.14	48.28	0.91	32.55	10.85	3.00
226	VULCAN	VUL 100C	ECH	44.61	44.50	1.00	32.90	10.00	3.29
516	UDDCOMB	H4H	ECH	44.99	39.16	1.15	33.18	8.80	3.77
544	BANUT	6 Tonnes	ECH	47.00	58.87	0.80	34.66	13.23	2.62
536	BANUT	4000	ECH	47.12	39.25	1.20	34.75	8.82	3.94
482	JUNTTAN	HHK 4	ECH	47.96	39.25	1.22	35.37	8.82	4.01
227	VULCAN	VUL 140C	ECH	48.79	62.30	0.78	35.98	14.00	2.57
337	IHC	SC-50	ECH	49.92	32.44	1.54	36.81	7.29	5.05
177	CONMACO	C 115	ECH	50.68	51.18	0.99	37.38	11.50	3.25
315	MKT	S 14	ECH	50.88	62.30	0.82	37.52	14.00	2.68
552	ICE	110-SH	ECH	51.15	51.18	1.00	37.72	11.50	3.28
553	ICE	115-SH	ECH	51.46	51.18	1.01	37.95	11.50	3.30
441	MENCK	MHF5-5	ECH	52.45	49.04	1.07	38.68	11.02	3.51
451	MENCK	MHF3-5	ECH	52.45	49.04	1.07	38.68	11.02	3.51
209	VULCAN	VUL 012	ECH	52.88	53.40	0.99	39.00	12.00	3.25
178	CONMACO	C 80E5	ECH	54.24	35.60	1.52	40.00	8.00	5.00
237	VULCAN	VUL 508	ECH	54.24	35.60	1.52	40.00	8.00	5.00
545	BANUT	7 Tonnes	ECH	54.82	68.66	0.80	40.43	15.43	2.62
259	RAYMOND	R 3/0	ECH	55.09	55.63	0.99	40.63	12.50	3.25
517	UDDCOMB	H5H	ECH	56.23	48.95	1.15	41.47	11.00	3.77
182	CONMACO	C 140	ECH	56.95	62.30	0.91	42.00	14.00	3.00
210	VULCAN	VUL 014	ECH	56.95	62.30	0.91	42.00	14.00	3.00

TABLE D-2: EXTERNAL COMBUSTION HAMMER LISTING (sorted by Rated Energy)									
Hammer Description				SI Units			US Units		
GRLWEAP ID	Hammer Manufacturer	Hammer Name	Hammer Type	Rated Energy kJ	Ram Weight kN	Eq. Rated Stroke m	Rated Energy ft-kips	Ram Weight kips	Eq. Rated Stroke ft
382	BSP	HH 5	ECH	58.88	49.04	1.20	43.42	11.02	3.94
531	Bruce	SGH-0512	ECH	58.88	49.04	1.20	43.42	11.02	3.94
537	BANUT	5000	ECH	58.88	49.04	1.20	43.42	11.02	3.94
801	DKH	PH-5	ECH	58.88	49.04	1.20	43.42	11.02	3.94
316	MKT	MS 500	ECH	59.66	48.95	1.22	44.00	11.00	4.00
501	HPSI	110	ECH	59.66	48.95	1.22	44.00	11.00	4.00
489	JUNTTAN	HHK 5A	ECH	59.77	49.04	1.22	44.08	11.02	4.00
483	JUNTTAN	HHK 5	ECH	59.98	49.08	1.22	44.23	11.03	4.01
338	IHC	SC-60	ECH	60.96	59.19	1.03	44.95	13.30	3.38
371	FAIRCHLD	F-45	ECH	61.02	66.75	0.91	45.00	15.00	3.00
282	MENCK	MRBS 500	ECH	61.12	49.04	1.25	45.07	11.02	4.09
554	ICE	115	ECH	62.38	51.18	1.22	46.00	11.50	4.00
562	HMC	62	ECH	62.38	51.18	1.22	46.00	11.50	4.00
442	MENCK	MHF5-6	ECH	62.97	58.87	1.07	46.44	13.23	3.51
452	MENCK	MHF3-6	ECH	62.97	58.87	1.07	46.44	13.23	3.51
524	DAWSON	HPH6500	ECH	63.66	45.61	1.40	46.95	10.25	4.58
183	CONMACO	C 160	ECH	66.11	72.31	0.91	48.75	16.25	3.00
211	VULCAN	VUL 016	ECH	66.11	72.31	0.91	48.75	16.25	3.00
260	RAYMOND	R 150C	ECH	66.11	66.75	0.99	48.75	15.00	3.25
261	RAYMOND	R 4/0	ECH	66.11	66.75	0.99	48.75	15.00	3.25
271	MENCK	MH 68	ECH	66.68	34.35	1.94	49.18	7.72	6.37
518	UDDCOMB	H6H	ECH	67.48	58.74	1.15	49.76	13.20	3.77
179	CONMACO	C 100E5	ECH	67.80	44.50	1.52	50.00	10.00	5.00

TABLE D-2: EXTERNAL COMBUSTION HAMMER LISTING (sorted by Rated Energy)									
Hammer Description				SI Units			US Units		
GRLWEAP ID	Hammer Manufacturer	Hammer Name	Hammer Type	Rated Energy kJ	Ram Weight kN	Eq. Rated Stroke m	Rated Energy ft-kips	Ram Weight kips	Eq. Rated Stroke ft
238	VULCAN	VUL 510	ECH	67.80	44.50	1.52	50.00	10.00	5.00
507	HPSI	1000	ECH	67.80	44.50	1.52	50.00	10.00	5.00
228	VULCAN	VUL 200C	ECH	68.07	89.00	0.77	50.20	20.00	2.51
321	IHC	S-70	ECH	69.49	34.40	2.02	51.25	7.73	6.63
592	APE	7.2mT	ECH	69.64	72.09	0.97	51.35	16.20	3.17
191	CONMACO	C 160 **	ECH	70.21	76.81	0.91	51.78	17.26	3.00
538	BANUT	6000	ECH	70.68	58.87	1.20	52.13	13.23	3.94
484	JUNTTAN	HHK 6	ECH	71.94	58.87	1.22	53.05	13.23	4.01
443	MENCK	MHF5-7	ECH	73.44	68.66	1.07	54.16	15.43	3.51
453	MENCK	MHF3-7	ECH	73.44	68.66	1.07	54.16	15.43	3.51
339	IHC	SC-75	ECH	74.30	54.07	1.37	54.80	12.15	4.51
262	RAYMOND	R 5/0	ECH	77.12	77.88	0.99	56.88	17.50	3.25
180	CONMACO	C 115E5	ECH	77.97	51.18	1.52	57.50	11.50	5.00
184	CONMACO	C 200	ECH	81.36	89.00	0.91	60.00	20.00	3.00
212	VULCAN	VUL 020	ECH	81.36	89.00	0.91	60.00	20.00	3.00
231	VULCAN	VUL 320	ECH	81.36	89.00	0.91	60.00	20.00	3.00
239	VULCAN	VUL 512	ECH	81.36	53.40	1.52	60.00	12.00	5.00
317	MKT	S 20	ECH	81.36	89.00	0.91	60.00	20.00	3.00
502	HPSI	150	ECH	81.36	66.75	1.22	60.00	15.00	4.00
383	BSP	HH 7	ECH	82.44	68.66	1.20	60.79	15.43	3.94
532	Bruce	SGH-0712	ECH	82.44	68.66	1.20	60.79	15.43	3.94
802	DKH	PH-7	ECH	82.44	68.66	1.20	60.79	15.43	3.94
803	DKH	PH-7S	ECH	82.44	68.66	1.20	60.79	15.43	3.94

TABLE D-2: EXTERNAL COMBUSTION HAMMER LISTING (sorted by Rated Energy)									
Hammer Description				SI Units			US Units		
GRLWEAP ID	Hammer Manufacturer	Hammer Name	Hammer Type	Rated Energy kJ	Ram Weight kN	Eq. Rated Stroke m	Rated Energy ft-kips	Ram Weight kips	Eq. Rated Stroke ft
503	HPSI	154	ECH	83.53	68.53	1.22	61.60	15.40	4.00
490	JUNTTAN	HHK 7A	ECH	83.69	68.66	1.22	61.72	15.43	4.00
485	JUNTTAN	HHK 7	ECH	83.96	68.71	1.22	61.91	15.44	4.01
444	MENCK	MHF5-8	ECH	83.96	78.50	1.07	61.92	17.64	3.51
181	CONMACO	C 125E5	ECH	84.75	55.63	1.52	62.50	12.50	5.00
555	ICE	160-SH	ECH	86.78	71.20	1.22	64.00	16.00	4.00
556	ICE	160	ECH	86.78	71.20	1.22	64.00	16.00	4.00
563	HMC	86	ECH	86.78	71.20	1.22	64.00	16.00	4.00
322	IHC	S-90	ECH	89.36	44.23	2.02	65.90	9.94	6.63
283	MENCK	MRBS 750	ECH	91.90	73.56	1.25	67.77	16.53	4.10
272	MENCK	MH 96	ECH	94.14	49.04	1.92	69.43	11.02	6.30
384	BSP	HH 8	ECH	94.24	78.50	1.20	69.50	17.64	3.94
539	BANUT	8000	ECH	94.24	78.50	1.20	69.50	17.64	3.94
445	MENCK	MHF5-9	ECH	94.43	88.29	1.07	69.64	19.84	3.51
263	RAYMOND	R 30X	ECH	101.70	133.50	0.76	75.00	30.00	2.50
446	MENCK	MHF5-10	ECH	104.90	98.08	1.07	77.36	22.04	3.51
385	BSP	HH 9	ECH	106.00	88.29	1.20	78.17	19.84	3.94
491	JUNTTAN	HHK 9A	ECH	107.61	88.29	1.22	79.36	19.84	4.00
504	HPSI	200	ECH	108.48	89.00	1.22	80.00	20.00	4.00
512	HPSI	2000	ECH	108.48	89.00	1.22	80.00	20.00	4.00
595	APE	10-60	ECH	108.48	89.00	1.22	80.00	20.00	4.00
264	RAYMOND	R 8/0	ECH	110.18	111.25	0.99	81.25	25.00	3.25
340	IHC	SC-110	ECH	111.04	77.70	1.43	81.89	17.46	4.69

TABLE D-2: EXTERNAL COMBUSTION HAMMER LISTING (sorted by Rated Energy)									
Hammer Description				SI Units			US Units		
GRLWEAP ID	Hammer Manufacturer	Hammer Name	Hammer Type	Rated Energy kJ	Ram Weight kN	Eq. Rated Stroke m	Rated Energy ft-kips	Ram Weight kips	Eq. Rated Stroke ft
519	UDDCOMB	H8H	ECH	111.45	78.32	1.42	82.19	17.60	4.67
508	HPSI	1605	ECH	112.55	73.87	1.52	83.00	16.60	5.00
447	MENCK	MHF5-11	ECH	115.42	107.91	1.07	85.12	24.25	3.51
804	DKH	PH-10	ECH	117.75	98.08	1.20	86.84	22.04	3.94
520	UDDCOMB	H10H	ECH	117.81	98.12	1.20	86.88	22.05	3.94
533	Bruce	SGH-1012	ECH	117.81	98.12	1.20	86.88	22.05	3.94
540	BANUT	10000	ECH	117.81	98.12	1.20	86.88	22.05	3.94
557	ICE	220	ECH	119.33	97.90	1.22	88.00	22.00	4.00
564	HMC	119	ECH	119.33	97.90	1.22	88.00	22.00	4.00
486	JUNTTAN	HHK 10	ECH	119.90	98.12	1.22	88.42	22.05	4.01
323	IHC	S-120	ECH	121.19	59.99	2.02	89.37	13.48	6.63
185	CONMACO	C 300	ECH	122.04	133.50	0.91	90.00	30.00	3.00
213	VULCAN	VUL 030	ECH	122.04	133.50	0.91	90.00	30.00	3.00
232	VULCAN	VUL 330	ECH	122.04	133.50	0.91	90.00	30.00	3.00
505	HPSI	225	ECH	122.04	100.13	1.22	90.00	22.50	4.00
448	MENCK	MHF5-12	ECH	125.89	117.70	1.07	92.84	26.45	3.51
285	MENCK	MRBS 850	ECH	126.49	84.37	1.50	93.28	18.96	4.92
509	HPSI	2005	ECH	128.96	84.64	1.52	95.10	19.02	5.00
386	BSP	HH11-1.2	ECH	129.56	107.91	1.20	95.55	24.25	3.94
186	CONMACO	C 5200	ECH	135.60	89.00	1.52	100.00	20.00	5.00
194	CONMACO	C 200E5	ECH	135.60	89.00	1.52	100.00	20.00	5.00
240	VULCAN	VUL 520	ECH	135.60	89.00	1.52	100.00	20.00	5.00
265	RAYMOND	R 40X	ECH	135.60	178.00	0.76	100.00	40.00	2.50

TABLE D-2: EXTERNAL COMBUSTION HAMMER LISTING (sorted by Rated Energy)									
Hammer Description				SI Units			US Units		
GRLWEAP ID	Hammer Manufacturer	Hammer Name	Hammer Type	Rated Energy kJ	Ram Weight kN	Eq. Rated Stroke m	Rated Energy ft-kips	Ram Weight kips	Eq. Rated Stroke ft
492	JUNTTAN	HHK 12A	ECH	141.31	117.70	1.20	104.21	26.45	3.94
273	MENCK	MH 145	ECH	142.11	73.56	1.93	104.80	16.53	6.34
487	JUNTTAN	HHK 12	ECH	143.88	117.75	1.22	106.10	26.46	4.01
341	IHC	SC-150	ECH	148.28	108.14	1.37	109.35	24.30	4.50
558	ICE	275	ECH	149.16	122.38	1.22	110.00	27.50	4.00
565	HMC	149	ECH	149.16	122.38	1.22	110.00	27.50	4.00
324	IHC	S-150	ECH	149.24	73.87	2.02	110.06	16.60	6.63
805	DKH	PH-13	ECH	153.12	127.54	1.20	112.92	28.66	3.94
229	VULCAN	VUL 400C	ECH	154.04	178.00	0.87	113.60	40.00	2.84
393	BSP	HH11-1.5	ECH	161.78	107.91	1.50	119.31	24.25	4.92
214	VULCAN	VUL 040	ECH	162.72	178.00	0.91	120.00	40.00	3.00
233	VULCAN	VUL 340	ECH	162.72	178.00	0.91	120.00	40.00	3.00
387	BSP	HH14-1.2	ECH	164.87	137.33	1.20	121.59	30.86	3.94
493	JUNTTAN	HHK 14A	ECH	164.87	137.33	1.20	121.59	30.86	3.94
286	MENCK	MRBS1100	ECH	167.37	107.91	1.55	123.43	24.25	5.09
488	JUNTTAN	HHK 14	ECH	167.86	137.37	1.22	123.79	30.87	4.01
454	MENCK	MHF10-15	ECH	169.01	147.12	1.15	124.64	33.06	3.77
287	MENCK	MRBS1502	ECH	183.86	147.16	1.25	135.59	33.07	4.10
566	HMC	187	ECH	187.13	153.53	1.22	138.00	34.50	4.00
388	BSP	HH16-1.2	ECH	188.43	156.95	1.20	138.96	35.27	3.94
494	JUNTTAN	HHK 16A	ECH	188.43	156.95	1.20	138.96	35.27	3.94
274	MENCK	MH 195	ECH	191.36	98.12	1.95	141.12	22.05	6.40
325	IHC	S-200	ECH	197.49	97.90	2.02	145.64	22.00	6.62

TABLE D-2: EXTERNAL COMBUSTION HAMMER LISTING (sorted by Rated Energy)									
Hammer Description				SI Units			US Units		
GRLWEAP ID	Hammer Manufacturer	Hammer Name	Hammer Type	Rated Energy kJ	Ram Weight kN	Eq. Rated Stroke m	Rated Energy ft-kips	Ram Weight kips	Eq. Rated Stroke ft
461	MENCK	MHUT 200	ECH	199.85	117.75	1.70	147.38	26.46	5.57
187	CONMACO	C 5300	ECH	203.40	133.50	1.52	150.00	30.00	5.00
195	CONMACO	C 300E5	ECH	203.40	133.50	1.52	150.00	30.00	5.00
241	VULCAN	VUL 530	ECH	203.40	133.50	1.52	150.00	30.00	5.00
266	RAYMOND	R 60X	ECH	203.40	267.00	0.76	150.00	60.00	2.50
394	BSP	HH14-1.5	ECH	205.88	137.33	1.50	151.83	30.86	4.92
342	IHC	SC-200	ECH	206.80	134.39	1.54	152.51	30.20	5.05
510	HPSI	3005	ECH	209.23	137.33	1.52	154.30	30.86	5.00
495	JUNTTAN	HHK 18A	ECH	212.00	176.58	1.20	156.34	39.68	3.94
275	MENCK	MHU 220	ECH	215.70	111.83	1.93	159.07	25.13	6.33
455	MENCK	MHF10-20	ECH	225.29	196.11	1.15	166.14	44.07	3.77
395	BSP	HH16-1.5	ECH	235.30	156.95	1.50	173.53	35.27	4.92
389	BSP	HH 20	ECH	235.56	196.20	1.20	173.71	44.09	3.94
390	BSP	HH 20S	ECH	235.56	196.20	1.20	173.71	44.09	3.94
511	HPSI	3505	ECH	239.06	156.91	1.52	176.30	35.26	5.00
230	VULCAN	VUL 600C	ECH	243.27	267.00	0.91	179.40	60.00	2.99
215	VULCAN	VUL 060	ECH	244.08	267.00	0.91	180.00	60.00	3.00
234	VULCAN	VUL 360	ECH	244.08	267.00	0.91	180.00	60.00	3.00
288	MENCK	MRBS1800	ECH	257.39	171.68	1.50	189.81	38.58	4.92
242	VULCAN	VUL 540	ECH	271.20	182.01	1.49	200.00	40.90	4.89
326	IHC	S-280	ECH	278.40	133.77	2.08	205.31	30.06	6.83
806	DKH	PH-20	ECH	294.15	196.20	1.50	216.92	44.09	4.92
188	CONMACO	C 5450	ECH	305.10	200.25	1.52	225.00	45.00	5.00

TABLE D-2: EXTERNAL COMBUSTION HAMMER LISTING (sorted by Rated Energy)									
Hammer Description				SI Units			US Units		
GRLWEAP ID	Hammer Manufacturer	Hammer Name	Hammer Type	Rated Energy kJ	Ram Weight kN	Eq. Rated Stroke m	Rated Energy ft-kips	Ram Weight kips	Eq. Rated Stroke ft
290	MENCK	MRBS2502	ECH	306.39	245.24	1.25	225.95	55.11	4.10
291	MENCK	MRBS2504	ECH	306.39	245.24	1.25	225.95	55.11	4.10
391	BSP	HA 30	ECH	353.31	294.28	1.20	260.55	66.13	3.94
289	MENCK	MRBS2500	ECH	355.43	284.49	1.25	262.11	63.93	4.10
276	MENCK	MHU 400	ECH	392.64	225.66	1.74	289.55	50.71	5.71
327	IHC	S-400	ECH	396.77	196.69	2.02	292.60	44.20	6.62
462	MENCK	MHUT 400	ECH	400.18	234.52	1.71	295.12	52.70	5.60
243	VULCAN	VUL 560	ECH	406.80	278.13	1.46	300.00	62.50	4.80
245	VULCAN	VUL 3100	ECH	406.80	445.00	0.91	300.00	100.00	3.00
292	MENCK	MRBS3000	ECH	441.19	294.28	1.50	325.36	66.13	4.92
807	DKH	PH-30	ECH	441.19	294.28	1.50	325.36	66.13	4.92
392	BSP	HA 40	ECH	471.11	392.40	1.20	347.43	88.18	3.94
189	CONMACO	C 5700	ECH	474.60	311.50	1.52	350.00	70.00	5.00
328	IHC	S-500	ECH	496.41	246.09	2.02	366.09	55.30	6.62
596	APE	HI 400U	ECH	542.40	356.00	1.52	400.00	80.00	5.00
463	MENCK	MHUT 500	ECH	550.59	294.28	1.87	406.04	66.13	6.14
277	MENCK	MHU 600	ECH	588.01	343.36	1.71	433.64	77.16	5.62
808	DKH	PH-40	ECH	588.29	392.40	1.50	433.85	88.18	4.92
329	IHC	S-600	ECH	601.44	298.15	2.02	443.54	67.00	6.62
294	MENCK	MRBS4600	ECH	676.56	451.27	1.50	498.94	101.41	4.92
246	VULCAN	VUL 5100	ECH	678.00	445.00	1.52	500.00	100.00	5.00
190	CONMACO	C 6850	ECH	691.56	378.25	1.83	510.00	85.00	6.00
293	MENCK	MRBS3900	ECH	696.09	386.53	1.80	513.34	86.86	5.91

TABLE D-2: EXTERNAL COMBUSTION HAMMER LISTING (sorted by Rated Energy)									
Hammer Description				SI Units			US Units		
GRLWEAP ID	Hammer Manufacturer	Hammer Name	Hammer Type	Rated Energy kJ	Ram Weight kN	Eq. Rated Stroke m	Rated Energy ft-kips	Ram Weight kips	Eq. Rated Stroke ft
464	MENCK	MHUT700U	ECH	699.88	413.09	1.69	516.13	92.83	5.56
295	MENCK	MRBS5000	ECH	735.40	490.52	1.50	542.33	110.23	4.92
468	MENCK	MHU 800S	ECH	799.02	441.44	1.81	589.25	99.20	5.94
465	MENCK	MHUT700A	ECH	839.60	413.09	2.03	619.18	92.83	6.67
297	MENCK	MRBS7000	ECH	856.18	685.30	1.25	631.40	154.00	4.10
330	IHC	S-900	ECH	892.73	442.55	2.02	658.36	99.45	6.62
466	MENCK	MHUT1000	ECH	999.25	588.74	1.70	736.91	132.30	5.57
278	MENCK	MHU 1000	ECH	1000.32	565.02	1.77	737.70	126.97	5.81
247	VULCAN	VUL 5150	ECH	1017.00	667.50	1.52	750.00	150.00	5.00
296	MENCK	MRBS6000	ECH	1029.52	588.60	1.75	759.23	132.27	5.74
298	MENCK	MRBS8000	ECH	1176.66	784.85	1.50	867.74	176.37	4.92
469	MENCK	MHU 1200	ECH	1202.34	657.62	1.83	886.68	147.78	6.00
331	IHC	S-1200	ECH	1208.27	598.97	2.02	891.05	134.60	6.62
299	MENCK	MRBS8800	ECH	1294.34	863.34	1.50	954.53	194.01	4.92
332	IHC	S-1800	ECH	1586.93	738.70	2.15	1170.30	166.00	7.05
279	MENCK	MHU 1700	ECH	1666.35	922.17	1.81	1228.87	207.23	5.93
280	MENCK	MHU 2100	ECH	2098.53	1138.31	1.84	1547.59	255.80	6.05
467	MENCK	MHU2100S	ECH	2100.02	1010.51	2.08	1548.69	227.08	6.82
300	MENCK	MBS12500	ECH	2144.96	1226.33	1.75	1581.83	275.58	5.74
333	IHC	S-2300	ECH	2280.09	1130.30	2.02	1681.48	254.00	6.62
248	VULCAN	VUL 6300	ECH	2440.80	1335.00	1.83	1800.00	300.00	6.00
281	MENCK	MHU 3000	ECH	2944.75	1618.73	1.82	2171.65	363.76	5.97

TABLE D-3: VIBRATORY HAMMER LISTING (sorted by Power)									
Hammer Description				SI Units			US Units		
GRLWEAP ID	Hammer Manufacturer	Hammer Name	Hammer Type	Power kW	Ram Weight kN	Frequency Hz	Power kW	Ram Weight kips	Frequency Hz
770	APE	3	VIB	10.58	0.00	38.30	10.58	0.00	38.30
771	APE	6	VIB	10.58	0.04	38.30	10.58	0.01	38.30
700	ICE	23-28	VIB	21.00	0.45	26.70	21.00	0.10	26.70
720	HMC	3+28	VIB	21.00	0.49	26.80	21.00	0.11	26.80
750	MKT	V-2B	VIB	52.00	0.67	30.00	52.00	0.15	30.00
721	HMC	3+75	VIB	56.00	0.49	36.10	56.00	0.11	36.10
772	APE	15	VIB	59.67	0.49	30.00	59.67	0.11	30.00
773	APE	20	VIB	59.67	0.67	38.30	59.67	0.15	38.30
774	APE	20E	VIB	59.67	0.67	38.30	59.67	0.15	38.30
701	ICE	216	VIB	130.00	2.05	26.70	130.00	0.46	26.70
702	ICE	216E	VIB	130.00	2.05	26.70	130.00	0.46	26.70
751	MKT	V-5C	VIB	138.00	1.91	28.33	138.00	0.43	28.33
722	HMC	13+200	VIB	149.00	1.56	26.70	149.00	0.35	26.70
723	HMC	13S+200	VIB	149.00	1.56	26.70	149.00	0.35	26.70
703	ICE	11-23	VIB	164.00	2.05	31.70	164.00	0.46	31.70
724	HMC	13H+200	VIB	164.00	1.56	29.80	164.00	0.35	29.80
725	HMC	25+220	VIB	164.00	2.71	20.90	164.00	0.61	20.90
775	APE	50	VIB	194.00	1.02	30.00	194.00	0.23	30.00
776	APE	50E	VIB	194.00	1.02	30.00	194.00	0.23	30.00

TABLE D-3: VIBRATORY HAMMER LISTING (sorted by Power)									
Hammer Description				SI Units			US Units		
GRLWEAP ID	Hammer Manufacturer	Hammer Name	Hammer Type	Power kW	Ram Weight kN	Frequency Hz	Power kW	Ram Weight kips	Frequency Hz
777	APE	100	VIB	194.00	1.42	30.00	194.00	0.32	30.00
778	APE	100E	VIB	194.00	0.62	30.00	194.00	0.14	30.00
704	ICE	223	VIB	242.00	2.05	38.30	242.00	0.46	38.30
705	ICE	416L	VIB	242.00	4.09	26.70	242.00	0.92	26.70
708	ICE	44-30	VIB	242.00	5.79	20.00	242.00	1.30	20.00
726	HMC	26+335	VIB	242.00	3.16	25.60	242.00	0.71	25.60
727	HMC	26S+335	VIB	242.00	3.16	25.60	242.00	0.71	25.60
728	HMC	51+335	VIB	242.00	5.38	19.50	242.00	1.21	19.50
752	MKT	V-20B	VIB	242.00	35.60	28.33	242.00	8.00	28.33
779	APE	100HF	VIB	260.00	0.62	43.00	260.00	0.14	43.00
780	APE	150	VIB	260.00	0.62	30.00	260.00	0.14	30.00
781	APE	150T	VIB	260.00	0.76	30.00	260.00	0.17	30.00
706	ICE	812	VIB	375.00	8.10	26.70	375.00	1.82	26.70
707	ICE	815	VIB	375.00	8.19	26.70	375.00	1.84	26.70
709	ICE	44-50	VIB	377.00	5.79	26.70	377.00	1.30	26.70
729	HMC	51+535	VIB	377.00	5.38	26.40	377.00	1.21	26.40
730	HMC	51S+535	VIB	377.00	5.38	26.40	377.00	1.21	26.40
753	MKT	V-30	VIB	448.00	6.54	28.33	448.00	1.47	28.33
782	APE	150HF	VIB	466.00	1.42	43.00	466.00	0.32	43.00
783	APE	200	VIB	466.00	1.29	30.00	466.00	0.29	30.00

TABLE D-3: VIBRATORY HAMMER LISTING (sorted by Power)									
Hammer Description				SI Units			US Units		
GRLWEAP ID	Hammer Manufacturer	Hammer Name	Hammer Type	Power kW	Ram Weight kN	Frequency Hz	Power kW	Ram Weight kips	Frequency Hz
784	APE	200T	VIB	466.00	1.51	30.83	466.00	0.34	30.83
714	ICE	1412C	VIB	470.00	8.99	23.00	470.00	2.02	23.00
710	ICE	44-65	VIB	485.00	5.79	27.50	485.00	1.30	27.50
711	ICE	66-65	VIB	485.00	8.68	21.70	485.00	1.95	21.70
731	HMC	51+740	VIB	485.00	5.38	27.50	485.00	1.21	27.50
732	HMC	76+740	VIB	485.00	8.10	21.70	485.00	1.82	21.70
754	MKT	V-35	VIB	485.00	7.12	28.33	485.00	1.60	28.33
712	ICE	66-80	VIB	597.00	8.68	26.70	597.00	1.95	26.70
713	ICE	1412B	VIB	597.00	9.08	21.00	597.00	2.04	21.00
733	HMC	76+800	VIB	597.00	8.10	26.10	597.00	1.82	26.10
734	HMC	115+800	VIB	597.00	6.01	20.40	597.00	1.35	20.40
785	APE	200T HF	VIB	738.00	1.51	43.00	738.00	0.34	43.00
786	APE	300	VIB	738.00	1.51	25.00	738.00	0.34	25.00
787	APE	400B	VIB	738.00	3.47	23.33	738.00	0.78	23.33
788	APE	600	VIB	800.00	4.67	23.30	800.00	1.05	23.30
810	MGF	RBH 2400	VIB	975.00	23.99	23.50	975.00	5.39	23.50
735	HMC	230+1600	VIB	1193.00	11.97	20.40	1193.00	2.69	20.40
755	MKT	V-140	VIB	1341.00	20.78	23.33	1341.00	4.67	23.33
789	APE	Tan 400	VIB	1476.00	6.10	23.33	1476.00	1.37	23.33
790	APE	Tan 600	VIB	1800.00	9.39	23.30	1800.00	2.11	23.30

TABLE D-4: COMPLETE HAMMER LISTING (sorted by GRLWEAP ID Numbers)									
Hammer Description				SI Units			US Units		
GRLWEAP ID	Hammer Manufacturer	Hammer Name	Hammer Type	Rated Energy kJ	Ram Weight kN	Eq. Rated Stroke m	Rated Energy ft-kips	Ram Weight kips	Eq. Rated Stroke ft
1	DELMAG	D 5	OED	14.24	4.90	2.93	10.51	1.10	9.62
2	DELMAG	D 8-22	OED	27.25	7.83	3.67	20.10	1.76	12.05
3	DELMAG	D 12	OED	30.65	12.24	3.29	22.61	2.75	10.80
4	DELMAG	D 15	OED	36.74	14.69	3.29	27.09	3.30	10.80
5	DELMAG	D 16-32	OED	54.51	15.66	3.58	40.20	3.52	11.76
6	DELMAG	D 22	OED	55.06	21.85	2.90	40.61	4.91	9.50
7	DELMAG	D 22-02	OED	65.77	21.58	4.10	48.50	4.85	13.44
8	DELMAG	D 22-13	OED	65.77	21.58	4.10	48.50	4.85	13.44
9	DELMAG	D 22-23	OED	69.45	21.58	4.10	51.22	4.85	13.44
10	DELMAG	D 25-32	OED	89.96	24.52	4.19	66.34	5.51	13.76
11	DELMAG	D 30	OED	80.99	29.37	2.90	59.73	6.60	9.50
12	DELMAG	D 30-02	OED	89.76	29.37	4.10	66.20	6.60	13.44
13	DELMAG	D 30-13	OED	89.76	29.37	4.10	66.20	6.60	13.44
14	DELMAG	D 30-23	OED	100.06	29.37	4.10	73.79	6.60	13.44
15	DELMAG	D 30-32	OED	102.29	29.37	4.18	75.44	6.60	13.73
16	DELMAG	D 36	OED	113.66	35.29	3.22	83.82	7.93	10.57
17	DELMAG	D 36-02	OED	113.66	35.29	3.96	83.82	7.93	12.98
18	DELMAG	D 36-13	OED	113.66	35.29	6.09	83.82	7.93	19.98
19	DELMAG	D 36-23	OED	120.00	35.29	3.96	88.50	7.93	12.98

TABLE D-4: COMPLETE HAMMER LISTING (sorted by GRLWEAP ID Numbers)									
Hammer Description				SI Units			US Units		
GRLWEAP ID	Hammer Manufacturer	Hammer Name	Hammer Type	Rated Energy kJ	Ram Weight kN	Eq. Rated Stroke m	Rated Energy ft-kips	Ram Weight kips	Eq. Rated Stroke ft
20	DELMAG	D 36-32	OED	122.80	35.29	4.01	90.56	7.93	13.14
21	DELMAG	D 44	OED	122.25	42.28	2.90	90.16	9.50	9.52
22	DELMAG	D 46	OED	145.20	45.12	3.22	107.08	10.14	10.57
23	DELMAG	D 46-02	OED	145.20	45.12	3.94	107.08	10.14	12.94
24	DELMAG	D 46-13	OED	130.90	45.12	3.94	96.53	10.14	12.94
25	DELMAG	D 46-23	OED	145.20	45.12	3.94	107.08	10.14	12.94
26	DELMAG	D 46-32	OED	165.69	45.12	3.99	122.19	10.14	13.10
27	DELMAG	D 55	OED	169.51	52.78	3.40	125.00	11.86	11.15
28	DELMAG	D 62-02	OED	206.72	60.79	3.87	152.45	13.66	12.71
29	DELMAG	D 62-12	OED	206.72	60.79	3.87	152.45	13.66	12.71
30	DELMAG	D 62-22	OED	223.20	60.79	4.04	164.60	13.66	13.26
31	DELMAG	D 80-12	OED	252.55	78.41	3.92	186.24	17.62	12.87
32	DELMAG	D 80-23	OED	288.15	78.41	3.98	212.50	17.62	13.05
33	DELMAG	D100-13	OED	360.32	98.21	4.11	265.72	22.07	13.50
35	DELMAG	D 19-52	OED	58.63	17.80	3.61	43.24	4.00	11.86
36	DELMAG	D 6-32	OED	18.31	5.87	3.12	13.50	1.32	10.23
37	DELMAG	D 12-32	OED	42.48	12.55	3.60	31.33	2.82	11.81
38	DELMAG	D 12-42	OED	45.16	12.55	3.60	33.30	2.82	11.81
39	DELMAG	D 14-42	OED	46.84	13.75	3.60	34.55	3.09	11.81
40	DELMAG	D 19-32	OED	57.55	17.80	3.58	42.44	4.00	11.76
41	DELMAG	D 19-42	OED	58.63	17.80	3.61	43.24	4.00	11.86

TABLE D-4: COMPLETE HAMMER LISTING (sorted by GRLWEAP ID Numbers)									
Hammer Description				SI Units			US Units		
GRLWEAP ID	Hammer Manufacturer	Hammer Name	Hammer Type	Rated Energy kJ	Ram Weight kN	Eq. Rated Stroke m	Rated Energy ft-kips	Ram Weight kips	Eq. Rated Stroke ft
42	DELMAG	D200-42	OED	667.21	196.20	5.13	492.04	44.09	16.83
43	DELMAG	D120-42	OED	409.23	117.70	3.60	301.79	26.45	11.81
44	DELMAG	D150-42	OED	511.66	147.16	3.60	377.33	33.07	11.81
45	DELMAG	D125-42	OED	425.29	122.64	4.15	313.63	27.56	13.60
46	DELMAG	D 21-42	OED	75.59	20.60	4.27	55.75	4.63	14.00
50	FEC	FEC 1200	OED	30.50	12.24	2.49	22.50	2.75	8.18
51	FEC	FEC 1500	OED	36.74	14.69	2.50	27.09	3.30	8.21
52	FEC	FEC 2500	OED	67.79	24.48	2.77	50.00	5.50	9.09
53	FEC	FEC 2800	OED	75.93	27.41	2.77	55.99	6.16	9.09
54	FEC	FEC 3000	OED	85.47	29.37	2.91	63.03	6.60	9.55
55	FEC	FEC 3400	OED	98.99	33.29	2.97	73.00	7.48	9.76
61	MITSUBIS	M 14	OED	34.23	13.22	2.59	25.25	2.97	8.50
62	MITSUBIS	MH 15	OED	38.15	14.73	2.59	28.14	3.31	8.50
63	MITSUBIS	M 23	OED	58.32	22.52	2.59	43.01	5.06	8.50
64	MITSUBIS	MH 25	OED	63.51	24.52	2.59	46.84	5.51	8.50
65	MITSUBIS	M 33	OED	83.68	32.31	2.59	61.71	7.26	8.50
66	MITSUBIS	MH 35	OED	88.98	34.35	2.59	65.62	7.72	8.50
67	MITSUBIS	M 43	OED	109.04	42.10	2.59	80.41	9.46	8.50
68	MITSUBIS	MH 45	OED	115.84	44.72	2.59	85.43	10.05	8.50
70	MITSUBIS	MH 72B	OED	183.26	70.76	2.59	135.15	15.90	8.50
71	MITSUBIS	MH 80B	OED	202.86	78.32	2.59	149.60	17.60	8.50

TABLE D-4: COMPLETE HAMMER LISTING (sorted by GRLWEAP ID Numbers)									
Hammer Description				SI Units			US Units		
GRLWEAP ID	Hammer Manufacturer	Hammer Name	Hammer Type	Rated Energy kJ	Ram Weight kN	Eq. Rated Stroke m	Rated Energy ft-kips	Ram Weight kips	Eq. Rated Stroke ft
81	LINKBELT	LB 180	CED	10.98	7.70	1.43	8.10	1.73	4.68
82	LINKBELT	LB 312	CED	20.36	17.18	1.19	15.02	3.86	3.89
83	LINKBELT	LB 440	CED	24.68	17.80	1.39	18.20	4.00	4.55
84	LINKBELT	LB 520	CED	35.68	22.56	1.58	26.31	5.07	5.19
85	LINKBELT	LB 660	CED	70.01	33.69	2.08	51.63	7.57	6.82
101	KOBE	K 13	OED	34.48	12.77	2.70	25.43	2.87	8.86
103	KOBE	K22-Est	OED	61.49	21.58	2.85	45.35	4.85	9.35
104	KOBE	K 25	OED	69.86	24.52	2.85	51.52	5.51	9.35
107	KOBE	K 35	OED	97.88	34.35	2.85	72.18	7.72	9.35
110	KOBE	K 45	OED	125.77	44.14	2.85	92.75	9.92	9.35
112	KOBE	KB 60	OED	176.53	58.87	3.00	130.18	13.23	9.84
113	KOBE	KB 80	OED	235.37	78.50	3.00	173.58	17.64	9.84
120	ICE	180	CED	11.03	7.70	1.43	8.13	1.73	4.70
121	ICE	422	CED	31.35	17.80	1.76	23.12	4.00	5.78
122	ICE	440	CED	25.17	17.80	1.41	18.56	4.00	4.64
123	ICE	520	CED	41.18	22.56	1.83	30.37	5.07	5.99
124	ICE	640	CED	55.08	26.70	2.06	40.62	6.00	6.77
125	ICE	660	CED	70.01	33.69	2.08	51.63	7.57	6.82
126	ICE	1070	CED	98.45	44.50	2.21	72.60	10.00	7.26
127	ICE	30-S	OED	30.51	13.35	2.34	22.50	3.00	7.67
128	ICE	40-S	OED	54.24	17.80	3.10	40.00	4.00	10.17

TABLE D-4: COMPLETE HAMMER LISTING (sorted by GRLWEAP ID Numbers)									
Hammer Description				SI Units			US Units		
GRLWEAP ID	Hammer Manufacturer	Hammer Name	Hammer Type	Rated Energy kJ	Ram Weight kN	Eq. Rated Stroke m	Rated Energy ft-kips	Ram Weight kips	Eq. Rated Stroke ft
129	ICE	42-S	OED	56.96	18.20	3.18	42.00	4.09	10.42
130	ICE	60-S	OED	81.35	31.15	3.18	59.99	7.00	10.42
131	ICE	70-S	OED	94.92	31.15	3.10	70.00	7.00	10.17
132	ICE	80-S	OED	108.48	35.60	3.79	80.00	8.00	12.42
133	ICE	90-S	OED	122.04	40.05	3.10	90.00	9.00	10.17
134	ICE	100-S	OED	135.60	44.50	3.66	100.00	10.00	12.00
135	ICE	120-S	OED	162.72	53.40	3.79	120.00	12.00	12.42
136	ICE	200-S	OED	135.60	89.00	1.83	100.00	20.00	6.00
137	ICE	205-S	OED	230.52	89.00	3.20	170.00	20.00	10.50
139	ICE	32-S	OED	35.27	13.35	3.25	26.01	3.00	10.67
140	ICE	120S-15	OED	179.60	66.75	3.73	132.45	15.00	12.25
142	MKT 20	DE333020	OED	27.12	8.90	3.51	20.00	2.00	11.50
143	MKT 30	DE333020	OED	37.97	12.46	3.51	28.00	2.80	11.50
144	MKT 33	DE333020	OED	44.75	14.69	3.51	33.00	3.30	11.50
145	MKT 40	DE333020	OED	54.24	17.80	3.51	40.00	4.00	11.50
146	MKT	DE 10	OED	11.93	4.90	3.35	8.80	1.10	11.00
147	MKT	DE 20	OED	21.70	8.90	2.74	16.00	2.00	9.00
148	MKT	DE 30	OED	30.37	12.46	3.05	22.40	2.80	10.00
149	MKT	DA35B SA	OED	32.27	12.46	3.96	23.80	2.80	13.00
150	MKT	DE 30B	OED	32.27	12.46	3.05	23.80	2.80	10.00
151	MKT	DA 35B	CED	28.48	12.46	2.29	21.00	2.80	7.50

TABLE D-4: COMPLETE HAMMER LISTING (sorted by GRLWEAP ID Numbers)									
Hammer Description				SI Units			US Units		
GRLWEAP ID	Hammer Manufacturer	Hammer Name	Hammer Type	Rated Energy kJ	Ram Weight kN	Eq. Rated Stroke m	Rated Energy ft-kips	Ram Weight kips	Eq. Rated Stroke ft
152	MKT	DA 45	CED	41.66	17.80	2.34	30.72	4.00	7.68
153	MKT	DE 40	OED	43.39	17.80	3.05	32.00	4.00	10.00
154	MKT	DE 42/35	OED	47.46	15.58	4.11	35.00	3.50	13.50
155	MKT	DE 42/35	OED	56.95	18.69	4.11	42.00	4.20	13.50
157	MKT	DE 50C	OED	67.80	22.25	3.96	50.00	5.00	13.00
158	MKT	DE 70C	OED	94.92	31.15	3.96	70.00	7.00	13.00
159	MKT	DE 50B	OED	57.63	22.25	3.35	42.50	5.00	11.00
160	MKT	DA55B SA	OED	54.24	22.25	3.66	40.00	5.00	12.00
161	MKT	DA 55B	CED	51.80	22.25	2.33	38.20	5.00	7.64
162	MKT	DE 70B	OED	80.68	31.15	3.66	59.50	7.00	12.00
163	MKT 50	DE70/50B	OED	67.80	22.25	3.66	50.00	5.00	12.00
164	MKT 70	DE70/50B	OED	94.92	31.15	3.66	70.00	7.00	12.00
165	MKT 110	DE110150	OED	149.16	48.95	4.11	110.00	11.00	13.50
166	MKT 150	DE110150	OED	203.40	66.75	4.11	150.00	15.00	13.50
167	MKT	DA 35C	CED	28.48	12.46	2.29	21.00	2.80	7.50
168	MKT	DA 55C	CED	51.80	22.25	2.33	38.20	5.00	7.64
171	CONMACO	C 50	ECH	20.34	22.25	0.91	15.00	5.00	3.00
172	CONMACO	C 65	ECH	26.44	28.93	0.91	19.50	6.50	3.00
173	CONMACO	C 550	ECH	33.90	22.25	1.52	25.00	5.00	5.00
174	CONMACO	C 565	ECH	44.07	28.93	1.52	32.50	6.50	5.00
175	CONMACO	C 80	ECH	35.26	35.60	0.99	26.00	8.00	3.25

TABLE D-4: COMPLETE HAMMER LISTING (sorted by GRLWEAP ID Numbers)									
Hammer Description				SI Units			US Units		
GRLWEAP ID	Hammer Manufacturer	Hammer Name	Hammer Type	Rated Energy kJ	Ram Weight kN	Eq. Rated Stroke m	Rated Energy ft-kips	Ram Weight kips	Eq. Rated Stroke ft
176	CONMACO	C 100	ECH	44.07	44.50	0.99	32.50	10.00	3.25
177	CONMACO	C 115	ECH	50.68	51.18	0.99	37.38	11.50	3.25
178	CONMACO	C 80E5	ECH	54.24	35.60	1.52	40.00	8.00	5.00
179	CONMACO	C 100E5	ECH	67.80	44.50	1.52	50.00	10.00	5.00
180	CONMACO	C 115E5	ECH	77.97	51.18	1.52	57.50	11.50	5.00
181	CONMACO	C 125E5	ECH	84.75	55.63	1.52	62.50	12.50	5.00
182	CONMACO	C 140	ECH	56.95	62.30	0.91	42.00	14.00	3.00
183	CONMACO	C 160	ECH	66.11	72.31	0.91	48.75	16.25	3.00
184	CONMACO	C 200	ECH	81.36	89.00	0.91	60.00	20.00	3.00
185	CONMACO	C 300	ECH	122.04	133.50	0.91	90.00	30.00	3.00
186	CONMACO	C 5200	ECH	135.60	89.00	1.52	100.00	20.00	5.00
187	CONMACO	C 5300	ECH	203.40	133.50	1.52	150.00	30.00	5.00
188	CONMACO	C 5450	ECH	305.10	200.25	1.52	225.00	45.00	5.00
189	CONMACO	C 5700	ECH	474.60	311.50	1.52	350.00	70.00	5.00
190	CONMACO	C 6850	ECH	691.56	378.25	1.83	510.00	85.00	6.00
191	CONMACO	C 160 **	ECH	70.21	76.81	0.91	51.78	17.26	3.00
192	CONMACO	C 50E5	ECH	33.90	22.25	1.52	25.00	5.00	5.00
193	CONMACO	C 65E5	ECH	44.07	28.93	1.52	32.50	6.50	5.00
194	CONMACO	C 200E5	ECH	135.60	89.00	1.52	100.00	20.00	5.00
195	CONMACO	C 300E5	ECH	203.40	133.50	1.52	150.00	30.00	5.00
204	VULCAN	VUL 01	ECH	20.34	22.25	0.91	15.00	5.00	3.00

TABLE D-4: COMPLETE HAMMER LISTING (sorted by GRLWEAP ID Numbers)									
Hammer Description				SI Units			US Units		
GRLWEAP ID	Hammer Manufacturer	Hammer Name	Hammer Type	Rated Energy kJ	Ram Weight kN	Eq. Rated Stroke m	Rated Energy ft-kips	Ram Weight kips	Eq. Rated Stroke ft
205	VULCAN	VUL 02	ECH	9.84	13.35	0.74	7.26	3.00	2.42
206	VULCAN	VUL 06	ECH	26.44	28.93	0.91	19.50	6.50	3.00
207	VULCAN	VUL 08	ECH	35.26	35.60	0.99	26.00	8.00	3.25
208	VULCAN	VUL 010	ECH	44.07	44.50	0.99	32.50	10.00	3.25
209	VULCAN	VUL 012	ECH	52.88	53.40	0.99	39.00	12.00	3.25
210	VULCAN	VUL 014	ECH	56.95	62.30	0.91	42.00	14.00	3.00
211	VULCAN	VUL 016	ECH	66.11	72.31	0.91	48.75	16.25	3.00
212	VULCAN	VUL 020	ECH	81.36	89.00	0.91	60.00	20.00	3.00
213	VULCAN	VUL 030	ECH	122.04	133.50	0.91	90.00	30.00	3.00
214	VULCAN	VUL 040	ECH	162.72	178.00	0.91	120.00	40.00	3.00
215	VULCAN	VUL 060	ECH	244.08	267.00	0.91	180.00	60.00	3.00
220	VULCAN	VUL 30C	ECH	9.84	13.35	0.74	7.26	3.00	2.42
221	VULCAN	VUL 50C	ECH	20.48	22.25	0.92	15.10	5.00	3.02
222	VULCAN	VUL 65C	ECH	26.00	28.93	0.90	19.18	6.50	2.95
223	VULCAN	VUL 65CA	ECH	26.53	28.93	0.92	19.57	6.50	3.01
224	VULCAN	VUL 80C	ECH	33.19	35.60	0.93	24.48	8.00	3.06
225	VULCAN	VUL 85C	ECH	35.24	37.91	0.93	25.99	8.52	3.05
226	VULCAN	VUL 100C	ECH	44.61	44.50	1.00	32.90	10.00	3.29
227	VULCAN	VUL 140C	ECH	48.79	62.30	0.78	35.98	14.00	2.57
228	VULCAN	VUL 200C	ECH	68.07	89.00	0.77	50.20	20.00	2.51
229	VULCAN	VUL 400C	ECH	154.04	178.00	0.87	113.60	40.00	2.84

TABLE D-4: COMPLETE HAMMER LISTING (sorted by GRLWEAP ID Numbers)									
Hammer Description				SI Units			US Units		
GRLWEAP ID	Hammer Manufacturer	Hammer Name	Hammer Type	Rated Energy kJ	Ram Weight kN	Eq. Rated Stroke m	Rated Energy ft-kips	Ram Weight kips	Eq. Rated Stroke ft
230	VULCAN	VUL 600C	ECH	243.27	267.00	0.91	179.40	60.00	2.99
231	VULCAN	VUL 320	ECH	81.36	89.00	0.91	60.00	20.00	3.00
232	VULCAN	VUL 330	ECH	122.04	133.50	0.91	90.00	30.00	3.00
233	VULCAN	VUL 340	ECH	162.72	178.00	0.91	120.00	40.00	3.00
234	VULCAN	VUL 360	ECH	244.08	267.00	0.91	180.00	60.00	3.00
235	VULCAN	VUL 505	ECH	33.90	22.25	1.52	25.00	5.00	5.00
236	VULCAN	VUL 506	ECH	44.07	28.93	1.52	32.50	6.50	5.00
237	VULCAN	VUL 508	ECH	54.24	35.60	1.52	40.00	8.00	5.00
238	VULCAN	VUL 510	ECH	67.80	44.50	1.52	50.00	10.00	5.00
239	VULCAN	VUL 512	ECH	81.36	53.40	1.52	60.00	12.00	5.00
240	VULCAN	VUL 520	ECH	135.60	89.00	1.52	100.00	20.00	5.00
241	VULCAN	VUL 530	ECH	203.40	133.50	1.52	150.00	30.00	5.00
242	VULCAN	VUL 540	ECH	271.20	182.01	1.49	200.00	40.90	4.89
243	VULCAN	VUL 560	ECH	406.80	278.13	1.46	300.00	62.50	4.80
245	VULCAN	VUL 3100	ECH	406.80	445.00	0.91	300.00	100.00	3.00
246	VULCAN	VUL 5100	ECH	678.00	445.00	1.52	500.00	100.00	5.00
247	VULCAN	VUL 5150	ECH	1017.00	667.50	1.52	750.00	150.00	5.00
248	VULCAN	VUL 6300	ECH	2440.80	1335.00	1.83	1800.00	300.00	6.00
251	RAYMOND	R 1	ECH	20.34	22.25	0.91	15.00	5.00	3.00
252	RAYMOND	R 1S	ECH	26.44	28.93	0.91	19.50	6.50	3.00
253	RAYMOND	R 65C	ECH	26.44	28.93	0.91	19.50	6.50	3.00

TABLE D-4: COMPLETE HAMMER LISTING (sorted by GRLWEAP ID Numbers)									
Hammer Description				SI Units			US Units		
GRLWEAP ID	Hammer Manufacturer	Hammer Name	Hammer Type	Rated Energy kJ	Ram Weight kN	Eq. Rated Stroke m	Rated Energy ft-kips	Ram Weight kips	Eq. Rated Stroke ft
254	RAYMOND	R 65CH	ECH	26.44	28.93	0.91	19.50	6.50	3.00
255	RAYMOND	R 0	ECH	33.05	33.38	0.99	24.38	7.50	3.25
256	RAYMOND	R 80C	ECH	33.19	35.60	0.93	24.48	8.00	3.06
257	RAYMOND	R 80CH	ECH	33.19	35.60	0.93	24.48	8.00	3.06
258	RAYMOND	R 2/0	ECH	44.07	44.50	0.99	32.50	10.00	3.25
259	RAYMOND	R 3/0	ECH	55.09	55.63	0.99	40.63	12.50	3.25
260	RAYMOND	R 150C	ECH	66.11	66.75	0.99	48.75	15.00	3.25
261	RAYMOND	R 4/0	ECH	66.11	66.75	0.99	48.75	15.00	3.25
262	RAYMOND	R 5/0	ECH	77.12	77.88	0.99	56.88	17.50	3.25
263	RAYMOND	R 30X	ECH	101.70	133.50	0.76	75.00	30.00	2.50
264	RAYMOND	R 8/0	ECH	110.18	111.25	0.99	81.25	25.00	3.25
265	RAYMOND	R 40X	ECH	135.60	178.00	0.76	100.00	40.00	2.50
266	RAYMOND	R 60X	ECH	203.40	267.00	0.76	150.00	60.00	2.50
271	MENCK	MH 68	ECH	66.68	34.35	1.94	49.18	7.72	6.37
272	MENCK	MH 96	ECH	94.14	49.04	1.92	69.43	11.02	6.30
273	MENCK	MH 145	ECH	142.11	73.56	1.93	104.80	16.53	6.34
274	MENCK	MH 195	ECH	191.36	98.12	1.95	141.12	22.05	6.40
275	MENCK	MHU 220	ECH	215.70	111.83	1.93	159.07	25.13	6.33
276	MENCK	MHU 400	ECH	392.64	225.66	1.74	289.55	50.71	5.71
277	MENCK	MHU 600	ECH	588.01	343.36	1.71	433.64	77.16	5.62
278	MENCK	MHU 1000	ECH	1000.32	565.02	1.77	737.70	126.97	5.81

TABLE D-4: COMPLETE HAMMER LISTING (sorted by GRLWEAP ID Numbers)									
Hammer Description				SI Units			US Units		
GRLWEAP ID	Hammer Manufacturer	Hammer Name	Hammer Type	Rated Energy kJ	Ram Weight kN	Eq. Rated Stroke m	Rated Energy ft-kips	Ram Weight kips	Eq. Rated Stroke ft
279	MENCK	MHU 1700	ECH	1666.35	922.17	1.81	1228.87	207.23	5.93
280	MENCK	MHU 2100	ECH	2098.53	1138.31	1.84	1547.59	255.80	6.05
281	MENCK	MHU 3000	ECH	2944.75	1618.73	1.82	2171.65	363.76	5.97
282	MENCK	MRBS 500	ECH	61.12	49.04	1.25	45.07	11.02	4.09
283	MENCK	MRBS 750	ECH	91.90	73.56	1.25	67.77	16.53	4.10
285	MENCK	MRBS 850	ECH	126.49	84.37	1.50	93.28	18.96	4.92
286	MENCK	MRBS1100	ECH	167.37	107.91	1.55	123.43	24.25	5.09
287	MENCK	MRBS1502	ECH	183.86	147.16	1.25	135.59	33.07	4.10
288	MENCK	MRBS1800	ECH	257.39	171.68	1.50	189.81	38.58	4.92
289	MENCK	MRBS2500	ECH	355.43	284.49	1.25	262.11	63.93	4.10
290	MENCK	MRBS2502	ECH	306.39	245.24	1.25	225.95	55.11	4.10
291	MENCK	MRBS2504	ECH	306.39	245.24	1.25	225.95	55.11	4.10
292	MENCK	MRBS3000	ECH	441.19	294.28	1.50	325.36	66.13	4.92
293	MENCK	MRBS3900	ECH	696.09	386.53	1.80	513.34	86.86	5.91
294	MENCK	MRBS4600	ECH	676.56	451.27	1.50	498.94	101.41	4.92
295	MENCK	MRBS5000	ECH	735.40	490.52	1.50	542.33	110.23	4.92
296	MENCK	MRBS6000	ECH	1029.52	588.60	1.75	759.23	132.27	5.74
297	MENCK	MRBS7000	ECH	856.18	685.30	1.25	631.40	154.00	4.10
298	MENCK	MRBS8000	ECH	1176.66	784.85	1.50	867.74	176.37	4.92
299	MENCK	MRBS8800	ECH	1294.34	863.34	1.50	954.53	194.01	4.92
300	MENCK	MBS12500	ECH	2144.96	1226.33	1.75	1581.83	275.58	5.74

TABLE D-4: COMPLETE HAMMER LISTING (sorted by GRLWEAP ID Numbers)									
Hammer Description				SI Units			US Units		
GRLWEAP ID	Hammer Manufacturer	Hammer Name	Hammer Type	Rated Energy kJ	Ram Weight kN	Eq. Rated Stroke m	Rated Energy ft-kips	Ram Weight kips	Eq. Rated Stroke ft
301	MKT	No. 5	ECH	1.36	0.89	1.52	1.00	0.20	5.00
302	MKT	No. 6	ECH	3.39	1.78	1.91	2.50	0.40	6.25
303	MKT	No. 7	ECH	5.63	3.56	1.58	4.15	0.80	5.19
304	MKT	9B3	ECH	11.87	7.12	1.67	8.75	1.60	5.47
305	MKT	10B3	ECH	17.78	13.35	1.33	13.11	3.00	4.37
306	MKT	C5-Air	ECH	19.26	22.25	0.87	14.20	5.00	2.84
307	MKT	C5-Steam	ECH	21.97	22.25	0.99	16.20	5.00	3.24
308	MKT	S-5	ECH	22.04	22.25	0.99	16.25	5.00	3.25
309	MKT	11B3	ECH	25.97	22.25	1.17	19.15	5.00	3.83
310	MKT	C826 Stm	ECH	33.09	35.60	0.93	24.40	8.00	3.05
311	MKT	C826 Air	ECH	28.75	35.60	0.81	21.20	8.00	2.65
312	MKT	S-8	ECH	35.26	35.60	0.99	26.00	8.00	3.25
313	MKT	MS-350	ECH	41.77	34.35	1.22	30.80	7.72	3.99
314	MKT	S 10	ECH	44.07	44.50	0.99	32.50	10.00	3.25
315	MKT	S 14	ECH	50.88	62.30	0.82	37.52	14.00	2.68
316	MKT	MS 500	ECH	59.66	48.95	1.22	44.00	11.00	4.00
317	MKT	S 20	ECH	81.36	89.00	0.91	60.00	20.00	3.00
320	IHC	S-35	ECH	34.61	29.50	1.17	25.53	6.63	3.85
321	IHC	S-70	ECH	69.49	34.40	2.02	51.25	7.73	6.63
322	IHC	S-90	ECH	89.36	44.23	2.02	65.90	9.94	6.63
323	IHC	S-120	ECH	121.19	59.99	2.02	89.37	13.48	6.63

TABLE D-4: COMPLETE HAMMER LISTING (sorted by GRLWEAP ID Numbers)									
Hammer Description				SI Units			US Units		
GRLWEAP ID	Hammer Manufacturer	Hammer Name	Hammer Type	Rated Energy kJ	Ram Weight kN	Eq. Rated Stroke m	Rated Energy ft-kips	Ram Weight kips	Eq. Rated Stroke ft
324	IHC	S-150	ECH	149.24	73.87	2.02	110.06	16.60	6.63
325	IHC	S-200	ECH	197.49	97.90	2.02	145.64	22.00	6.62
326	IHC	S-280	ECH	278.40	133.77	2.08	205.31	30.06	6.83
327	IHC	S-400	ECH	396.77	196.69	2.02	292.60	44.20	6.62
328	IHC	S-500	ECH	496.41	246.09	2.02	366.09	55.30	6.62
329	IHC	S-600	ECH	601.44	298.15	2.02	443.54	67.00	6.62
330	IHC	S-900	ECH	892.73	442.55	2.02	658.36	99.45	6.62
331	IHC	S-1200	ECH	1208.27	598.97	2.02	891.05	134.60	6.62
332	IHC	S-1800	ECH	1586.93	738.70	2.15	1170.30	166.00	7.05
333	IHC	S-2300	ECH	2280.09	1130.30	2.02	1681.48	254.00	6.62
335	IHC	SC-30	ECH	29.57	16.73	1.77	21.81	3.76	5.80
336	IHC	SC-40	ECH	40.50	24.52	1.65	29.86	5.51	5.42
337	IHC	SC-50	ECH	49.92	32.44	1.54	36.81	7.29	5.05
338	IHC	SC-60	ECH	60.96	59.19	1.03	44.95	13.30	3.38
339	IHC	SC-75	ECH	74.30	54.07	1.37	54.80	12.15	4.51
340	IHC	SC-110	ECH	111.04	77.70	1.43	81.89	17.46	4.69
341	IHC	SC-150	ECH	148.28	108.14	1.37	109.35	24.30	4.50
342	IHC	SC-200	ECH	206.80	134.39	1.54	152.51	30.20	5.05
349	HERA	1900	OED	60.23	18.65	3.23	44.41	4.19	10.60
350	HERA	1250	OED	34.37	12.50	2.75	25.35	2.81	9.02
351	HERA	1500	OED	41.22	15.00	2.75	30.40	3.37	9.02

TABLE D-4: COMPLETE HAMMER LISTING (sorted by GRLWEAP ID Numbers)									
Hammer Description				SI Units			US Units		
GRLWEAP ID	Hammer Manufacturer	Hammer Name	Hammer Type	Rated Energy kJ	Ram Weight kN	Eq. Rated Stroke m	Rated Energy ft-kips	Ram Weight kips	Eq. Rated Stroke ft
352	HERA	2500	OED	68.74	25.01	2.75	50.69	5.62	9.02
353	HERA	2800	OED	76.93	27.99	2.75	56.74	6.29	9.02
354	HERA	3500	OED	96.26	35.02	2.75	70.99	7.87	9.02
355	HERA	5000	OED	137.48	50.02	2.75	101.38	11.24	9.02
356	HERA	5700	OED	156.68	57.00	2.75	115.55	12.81	9.02
357	HERA	6200	OED	170.38	61.99	2.75	125.65	13.93	9.02
358	HERA	7500	OED	206.09	74.98	2.75	151.99	16.85	9.02
359	HERA	8800	OED	241.93	88.02	2.75	178.42	19.78	9.02
360	ICE	I-12	OED	40.95	12.55	3.51	30.20	2.82	11.50
361	ICE	I-19	OED	58.56	17.84	3.75	43.19	4.01	12.30
362	ICE	I-30	OED	102.27	29.41	3.84	75.42	6.61	12.60
363	ICE	I-36	OED	122.96	35.33	3.69	90.67	7.94	12.10
364	ICE	I-46	OED	146.17	45.17	3.69	107.79	10.15	12.12
365	ICE	I-62	OED	223.71	64.97	4.34	164.98	14.60	14.25
366	ICE	I-80	OED	288.01	78.77	4.11	212.40	17.70	13.50
371	FAIRCHLD	F-45	ECH	61.02	66.75	0.91	45.00	15.00	3.00
372	FAIRCHLD	F-32	ECH	44.14	48.28	0.91	32.55	10.85	3.00
380	BSP	HH 1.5	ECH	22.02	14.69	1.50	16.24	3.30	4.92
381	BSP	HH 3	ECH	35.31	29.41	1.20	26.04	6.61	3.94
382	BSP	HH 5	ECH	58.88	49.04	1.20	43.42	11.02	3.94
383	BSP	HH 7	ECH	82.44	68.66	1.20	60.79	15.43	3.94

TABLE D-4: COMPLETE HAMMER LISTING (sorted by GRLWEAP ID Numbers)									
Hammer Description				SI Units			US Units		
GRLWEAP ID	Hammer Manufacturer	Hammer Name	Hammer Type	Rated Energy kJ	Ram Weight kN	Eq. Rated Stroke m	Rated Energy ft-kips	Ram Weight kips	Eq. Rated Stroke ft
384	BSP	HH 8	ECH	94.24	78.50	1.20	69.50	17.64	3.94
385	BSP	HH 9	ECH	106.00	88.29	1.20	78.17	19.84	3.94
386	BSP	HH11-1.2	ECH	129.56	107.91	1.20	95.55	24.25	3.94
387	BSP	HH14-1.2	ECH	164.87	137.33	1.20	121.59	30.86	3.94
388	BSP	HH16-1.2	ECH	188.43	156.95	1.20	138.96	35.27	3.94
389	BSP	HH 20	ECH	235.56	196.20	1.20	173.71	44.09	3.94
390	BSP	HH 20S	ECH	235.56	196.20	1.20	173.71	44.09	3.94
391	BSP	HA 30	ECH	353.31	294.28	1.20	260.55	66.13	3.94
392	BSP	HA 40	ECH	471.11	392.40	1.20	347.43	88.18	3.94
393	BSP	HH11-1.5	ECH	161.78	107.91	1.50	119.31	24.25	4.92
394	BSP	HH14-1.5	ECH	205.88	137.33	1.50	151.83	30.86	4.92
395	BSP	HH16-1.5	ECH	235.30	156.95	1.50	173.53	35.27	4.92
401	BERMINGH	B23	CED	31.17	12.46	2.50	22.99	2.80	8.21
402	BERMINGH	B200	OED	24.41	8.90	2.74	18.00	2.00	9.00
403	BERMINGH	B225	OED	39.66	13.35	2.97	29.25	3.00	9.75
404	BERMINGH	B300	OED	54.66	16.69	3.28	40.31	3.75	10.75
405	BERMINGH	B400	OED	72.89	22.25	3.28	53.75	5.00	10.75
410	BERMINGH	B300 M	OED	54.66	16.69	3.28	40.31	3.75	10.75
411	BERMINGH	B400 M	OED	72.89	22.25	3.28	53.75	5.00	10.75
412	BERMINGH	B400 4.8	OED	58.58	21.36	2.74	43.20	4.80	9.00
413	BERMINGH	B400 5.0	OED	61.02	22.25	2.74	45.00	5.00	9.00

TABLE D-4: COMPLETE HAMMER LISTING (sorted by GRLWEAP ID Numbers)									
Hammer Description				SI Units			US Units		
GRLWEAP ID	Hammer Manufacturer	Hammer Name	Hammer Type	Rated Energy kJ	Ram Weight kN	Eq. Rated Stroke m	Rated Energy ft-kips	Ram Weight kips	Eq. Rated Stroke ft
414	BERMINGH	B23 5	CED	31.17	12.46	2.50	22.99	2.80	8.21
415	BERMINGH	B250 5	OED	35.60	11.13	3.20	26.25	2.50	10.50
416	BERMINGH	B350 5	OED	64.00	17.80	3.60	47.20	4.00	11.80
417	BERMINGH	B400 5	OED	80.00	22.25	3.60	59.00	5.00	11.80
418	BERMINGH	B450 5	OED	105.61	29.37	3.60	77.88	6.60	11.80
419	BERMINGH	B500 5	OED	124.81	34.71	3.60	92.04	7.80	11.80
420	BERMINGH	B550 5	OED	144.01	40.05	3.60	106.20	9.00	11.80
421	BERMINGH	B550 C	OED	119.33	48.95	2.44	88.00	11.00	8.00
422	BERMINGH	B2005	OED	28.48	8.90	3.20	21.00	2.00	10.50
423	BERMINGH	B2505	OED	48.00	13.35	3.60	35.40	3.00	11.80
441	MENCK	MHF5-5	ECH	52.45	49.04	1.07	38.68	11.02	3.51
442	MENCK	MHF5-6	ECH	62.97	58.87	1.07	46.44	13.23	3.51
443	MENCK	MHF5-7	ECH	73.44	68.66	1.07	54.16	15.43	3.51
444	MENCK	MHF5-8	ECH	83.96	78.50	1.07	61.92	17.64	3.51
445	MENCK	MHF5-9	ECH	94.43	88.29	1.07	69.64	19.84	3.51
446	MENCK	MHF5-10	ECH	104.90	98.08	1.07	77.36	22.04	3.51
447	MENCK	MHF5-11	ECH	115.42	107.91	1.07	85.12	24.25	3.51
448	MENCK	MHF5-12	ECH	125.89	117.70	1.07	92.84	26.45	3.51
449	MENCK	MHF3-3	ECH	33.55	31.37	1.07	24.75	7.05	3.51
450	MENCK	MHF3-4	ECH	41.98	39.25	1.07	30.96	8.82	3.51
451	MENCK	MHF3-5	ECH	52.45	49.04	1.07	38.68	11.02	3.51

TABLE D-4: COMPLETE HAMMER LISTING (sorted by GRLWEAP ID Numbers)									
Hammer Description				SI Units			US Units		
GRLWEAP ID	Hammer Manufacturer	Hammer Name	Hammer Type	Rated Energy kJ	Ram Weight kN	Eq. Rated Stroke m	Rated Energy ft-kips	Ram Weight kips	Eq. Rated Stroke ft
452	MENCK	MHF3-6	ECH	62.97	58.87	1.07	46.44	13.23	3.51
453	MENCK	MHF3-7	ECH	73.44	68.66	1.07	54.16	15.43	3.51
454	MENCK	MHF10-15	ECH	169.01	147.12	1.15	124.64	33.06	3.77
455	MENCK	MHF10-20	ECH	225.29	196.11	1.15	166.14	44.07	3.77
461	MENCK	MHUT 200	ECH	199.85	117.75	1.70	147.38	26.46	5.57
462	MENCK	MHUT 400	ECH	400.18	234.52	1.71	295.12	52.70	5.60
463	MENCK	MHUT 500	ECH	550.59	294.28	1.87	406.04	66.13	6.14
464	MENCK	MHUT700U	ECH	699.88	413.09	1.69	516.13	92.83	5.56
465	MENCK	MHUT700A	ECH	839.60	413.09	2.03	619.18	92.83	6.67
466	MENCK	MHUT1000	ECH	999.25	588.74	1.70	736.91	132.30	5.57
467	MENCK	MHU2100S	ECH	2100.02	1010.51	2.08	1548.69	227.08	6.82
468	MENCK	MHU 800S	ECH	799.02	441.44	1.81	589.25	99.20	5.94
469	MENCK	MHU 1200	ECH	1202.34	657.62	1.83	886.68	147.78	6.00
481	JUNTTAN	HHK 3	ECH	36.00	29.46	1.22	26.55	6.62	4.01
482	JUNTTAN	HHK 4	ECH	47.96	39.25	1.22	35.37	8.82	4.01
483	JUNTTAN	HHK 5	ECH	59.98	49.08	1.22	44.23	11.03	4.01
484	JUNTTAN	HHK 6	ECH	71.94	58.87	1.22	53.05	13.23	4.01
485	JUNTTAN	HHK 7	ECH	83.96	68.71	1.22	61.91	15.44	4.01
486	JUNTTAN	HHK 10	ECH	119.90	98.12	1.22	88.42	22.05	4.01
487	JUNTTAN	HHK 12	ECH	143.88	117.75	1.22	106.10	26.46	4.01
488	JUNTTAN	HHK 14	ECH	167.86	137.37	1.22	123.79	30.87	4.01

TABLE D-4: COMPLETE HAMMER LISTING (sorted by GRLWEAP ID Numbers)									
Hammer Description				SI Units			US Units		
GRLWEAP ID	Hammer Manufacturer	Hammer Name	Hammer Type	Rated Energy kJ	Ram Weight kN	Eq. Rated Stroke m	Rated Energy ft-kips	Ram Weight kips	Eq. Rated Stroke ft
489	JUNTTAN	HHK 5A	ECH	59.77	49.04	1.22	44.08	11.02	4.00
490	JUNTTAN	HHK 7A	ECH	83.69	68.66	1.22	61.72	15.43	4.00
491	JUNTTAN	HHK 9A	ECH	107.61	88.29	1.22	79.36	19.84	4.00
492	JUNTTAN	HHK 12A	ECH	141.31	117.70	1.20	104.21	26.45	3.94
493	JUNTTAN	HHK 14A	ECH	164.87	137.33	1.20	121.59	30.86	3.94
494	JUNTTAN	HHK 16A	ECH	188.43	156.95	1.20	138.96	35.27	3.94
495	JUNTTAN	HHK 18A	ECH	212.00	176.58	1.20	156.34	39.68	3.94
501	HPSI	110	ECH	59.66	48.95	1.22	44.00	11.00	4.00
502	HPSI	150	ECH	81.36	66.75	1.22	60.00	15.00	4.00
503	HPSI	154	ECH	83.53	68.53	1.22	61.60	15.40	4.00
504	HPSI	200	ECH	108.48	89.00	1.22	80.00	20.00	4.00
505	HPSI	225	ECH	122.04	100.13	1.22	90.00	22.50	4.00
506	HPSI	650	ECH	44.07	28.93	1.52	32.50	6.50	5.00
507	HPSI	1000	ECH	67.80	44.50	1.52	50.00	10.00	5.00
508	HPSI	1605	ECH	112.55	73.87	1.52	83.00	16.60	5.00
509	HPSI	2005	ECH	128.96	84.64	1.52	95.10	19.02	5.00
510	HPSI	3005	ECH	209.23	137.33	1.52	154.30	30.86	5.00
511	HPSI	3505	ECH	239.06	156.91	1.52	176.30	35.26	5.00
512	HPSI	2000	ECH	108.48	89.00	1.22	80.00	20.00	4.00
514	UDDCOMB	H2H	ECH	22.49	19.58	1.15	16.59	4.40	3.77
515	UDDCOMB	H3H	ECH	33.74	29.37	1.15	24.88	6.60	3.77

TABLE D-4: COMPLETE HAMMER LISTING (sorted by GRLWEAP ID Numbers)									
Hammer Description				SI Units			US Units		
GRLWEAP ID	Hammer Manufacturer	Hammer Name	Hammer Type	Rated Energy kJ	Ram Weight kN	Eq. Rated Stroke m	Rated Energy ft-kips	Ram Weight kips	Eq. Rated Stroke ft
516	UDDCOMB	H4H	ECH	44.99	39.16	1.15	33.18	8.80	3.77
517	UDDCOMB	H5H	ECH	56.23	48.95	1.15	41.47	11.00	3.77
518	UDDCOMB	H6H	ECH	67.48	58.74	1.15	49.76	13.20	3.77
519	UDDCOMB	H8H	ECH	111.45	78.32	1.42	82.19	17.60	4.67
520	UDDCOMB	H10H	ECH	117.81	98.12	1.20	86.88	22.05	3.94
521	DAWSON	HPH1200	ECH	11.82	10.24	1.16	8.72	2.30	3.79
522	DAWSON	HPH1800	ECH	18.62	14.69	1.27	13.73	3.30	4.16
523	DAWSON	HPH2400	ECH	23.47	18.65	1.26	17.30	4.19	4.13
524	DAWSON	HPH6500	ECH	63.66	45.61	1.40	46.95	10.25	4.58
530	Bruce	SGH-0312	ECH	35.31	29.41	1.20	26.04	6.61	3.94
531	Bruce	SGH-0512	ECH	58.88	49.04	1.20	43.42	11.02	3.94
532	Bruce	SGH-0712	ECH	82.44	68.66	1.20	60.79	15.43	3.94
533	Bruce	SGH-1012	ECH	117.81	98.12	1.20	86.88	22.05	3.94
535	BANUT	3000	ECH	35.31	29.41	1.20	26.04	6.61	3.94
536	BANUT	4000	ECH	47.12	39.25	1.20	34.75	8.82	3.94
537	BANUT	5000	ECH	58.88	49.04	1.20	43.42	11.02	3.94
538	BANUT	6000	ECH	70.68	58.87	1.20	52.13	13.23	3.94
539	BANUT	8000	ECH	94.24	78.50	1.20	69.50	17.64	3.94
540	BANUT	10000	ECH	117.81	98.12	1.20	86.88	22.05	3.94
541	BANUT	3 Tonnes	ECH	23.48	29.41	0.80	17.32	6.61	2.62
542	BANUT	4 Tonnes	ECH	31.33	39.25	0.80	23.11	8.82	2.62

TABLE D-4: COMPLETE HAMMER LISTING (sorted by GRLWEAP ID Numbers)									
Hammer Description				SI Units			US Units		
GRLWEAP ID	Hammer Manufacturer	Hammer Name	Hammer Type	Rated Energy kJ	Ram Weight kN	Eq. Rated Stroke m	Rated Energy ft-kips	Ram Weight kips	Eq. Rated Stroke ft
543	BANUT	5 Tonnes	ECH	39.15	49.04	0.80	28.87	11.02	2.62
544	BANUT	6 Tonnes	ECH	47.00	58.87	0.80	34.66	13.23	2.62
545	BANUT	7 Tonnes	ECH	54.82	68.66	0.80	40.43	15.43	2.62
550	ICE	70	ECH	28.48	31.15	0.91	21.00	7.00	3.00
551	ICE	75	ECH	40.68	33.38	1.22	30.00	7.50	4.00
552	ICE	110-SH	ECH	51.15	51.18	1.00	37.72	11.50	3.28
553	ICE	115-SH	ECH	51.46	51.18	1.01	37.95	11.50	3.30
554	ICE	115	ECH	62.38	51.18	1.22	46.00	11.50	4.00
555	ICE	160-SH	ECH	86.78	71.20	1.22	64.00	16.00	4.00
556	ICE	160	ECH	86.78	71.20	1.22	64.00	16.00	4.00
557	ICE	220	ECH	119.33	97.90	1.22	88.00	22.00	4.00
558	ICE	275	ECH	149.16	122.38	1.22	110.00	27.50	4.00
560	HMC	28A	ECH	37.97	31.15	1.22	28.00	7.00	4.00
561	HMC	28B	ECH	28.48	31.15	0.91	21.00	7.00	3.00
562	HMC	62	ECH	62.38	51.18	1.22	46.00	11.50	4.00
563	HMC	86	ECH	86.78	71.20	1.22	64.00	16.00	4.00
564	HMC	119	ECH	119.33	97.90	1.22	88.00	22.00	4.00
565	HMC	149	ECH	149.16	122.38	1.22	110.00	27.50	4.00
566	HMC	187	ECH	187.13	153.53	1.22	138.00	34.50	4.00
567	HMC	19D	ECH	18.98	15.58	1.22	14.00	3.50	4.00
568	HMC	38D	ECH	37.97	31.15	1.22	28.00	7.00	4.00

TABLE D-4: COMPLETE HAMMER LISTING (sorted by GRLWEAP ID Numbers)									
Hammer Description				SI Units			US Units		
GRLWEAP ID	Hammer Manufacturer	Hammer Name	Hammer Type	Rated Energy kJ	Ram Weight kN	Eq. Rated Stroke m	Rated Energy ft-kips	Ram Weight kips	Eq. Rated Stroke ft
571	APE	D 19-32	OED	58.07	18.65	3.12	42.82	4.19	10.25
572	APE	D 30-32	OED	95.01	29.41	3.23	70.07	6.61	10.60
573	APE	D 36-32	OED	113.98	35.29	3.23	84.06	7.93	10.60
574	APE	D 46-32	OED	145.75	45.12	3.23	107.48	10.14	10.60
575	APE	D 62-22	OED	218.94	60.79	3.60	161.46	13.66	11.82
576	APE	D 80-23	OED	267.12	78.41	3.41	196.99	17.62	11.18
577	APE	D 100-13	OED	333.98	98.03	3.41	246.30	22.03	11.18
578	APE	D 8-32	OED	24.41	7.83	3.12	18.00	1.76	10.25
579	APE	D 16-32	OED	53.37	15.71	3.43	39.36	3.53	11.25
580	APE	D 19-42	OED	58.07	18.65	3.23	42.82	4.19	10.60
581	APE	D 25-32	OED	78.45	24.52	3.20	57.86	5.51	10.50
582	APE	D 125-32	OED	416.69	122.64	3.40	307.29	27.56	11.15
591	APE	5.4mT	ECH	35.31	53.40	0.66	26.04	12.00	2.17
592	APE	7.2mT	ECH	69.64	72.09	0.97	51.35	16.20	3.17
595	APE	10-60	ECH	108.48	89.00	1.22	80.00	20.00	4.00
596	APE	HI 400U	ECH	542.40	356.00	1.52	400.00	80.00	5.00
700	ICE	23-28	VIB	21.00	0.45	8.14	21.00	0.10	26.70
701	ICE	216	VIB	130.00	2.05	8.14	130.00	0.46	26.70
702	ICE	216E	VIB	130.00	2.05	8.14	130.00	0.46	26.70
703	ICE	11-23	VIB	164.00	2.05	9.66	164.00	0.46	31.70
704	ICE	223	VIB	242.00	2.05	11.67	242.00	0.46	38.30

TABLE D-4: COMPLETE HAMMER LISTING (sorted by GRLWEAP ID Numbers)									
Hammer Description				SI Units			US Units		
GRLWEAP ID	Hammer Manufacturer	Hammer Name	Hammer Type	Rated Energy kJ	Ram Weight kN	Eq. Rated Stroke m	Rated Energy ft-kips	Ram Weight kips	Eq. Rated Stroke ft
705	ICE	416L	VIB	242.00	4.09	8.14	242.00	0.92	26.70
706	ICE	812	VIB	375.00	8.10	8.14	375.00	1.82	26.70
707	ICE	815	VIB	375.00	8.19	8.14	375.00	1.84	26.70
708	ICE	44-30	VIB	242.00	5.79	6.10	242.00	1.30	20.00
709	ICE	44-50	VIB	377.00	5.79	8.14	377.00	1.30	26.70
710	ICE	44-65	VIB	485.00	5.79	8.38	485.00	1.30	27.50
711	ICE	66-65	VIB	485.00	8.68	6.61	485.00	1.95	21.70
712	ICE	66-80	VIB	597.00	8.68	8.14	597.00	1.95	26.70
713	ICE	1412B	VIB	597.00	9.08	6.40	597.00	2.04	21.00
714	ICE	1412C	VIB	470.00	8.99	7.01	470.00	2.02	23.00
720	HMC	3+28	VIB	21.00	0.49	8.17	21.00	0.11	26.80
721	HMC	3+75	VIB	56.00	0.49	11.00	56.00	0.11	36.10
722	HMC	13+200	VIB	149.00	1.56	8.14	149.00	0.35	26.70
723	HMC	13S+200	VIB	149.00	1.56	8.14	149.00	0.35	26.70
724	HMC	13H+200	VIB	164.00	1.56	9.08	164.00	0.35	29.80
725	HMC	25+220	VIB	164.00	2.71	6.37	164.00	0.61	20.90
726	HMC	26+335	VIB	242.00	3.16	7.80	242.00	0.71	25.60
727	HMC	26S+335	VIB	242.00	3.16	7.80	242.00	0.71	25.60
728	HMC	51+335	VIB	242.00	5.38	5.94	242.00	1.21	19.50
729	HMC	51+535	VIB	377.00	5.38	8.05	377.00	1.21	26.40
730	HMC	51S+535	VIB	377.00	5.38	8.05	377.00	1.21	26.40

TABLE D-4: COMPLETE HAMMER LISTING (sorted by GRLWEAP ID Numbers)									
Hammer Description				SI Units			US Units		
GRLWEAP ID	Hammer Manufacturer	Hammer Name	Hammer Type	Rated Energy kJ	Ram Weight kN	Eq. Rated Stroke m	Rated Energy ft-kips	Ram Weight kips	Eq. Rated Stroke ft
731	HMC	51+740	VIB	485.00	5.38	8.38	485.00	1.21	27.50
732	HMC	76+740	VIB	485.00	8.10	6.61	485.00	1.82	21.70
733	HMC	76+800	VIB	597.00	8.10	7.96	597.00	1.82	26.10
734	HMC	115+800	VIB	597.00	6.01	6.22	597.00	1.35	20.40
735	HMC	230+1600	VIB	0.00	11.97	6.22	0.00	2.69	20.40
750	MKT	V-2B	VIB	52.00	0.67	9.14	52.00	0.15	30.00
751	MKT	V-5C	VIB	138.00	1.91	8.63	138.00	0.43	28.33
752	MKT	V-20B	VIB	242.00	35.60	8.63	242.00	8.00	28.33
753	MKT	V-30	VIB	448.00	6.54	8.63	448.00	1.47	28.33
754	MKT	V-35	VIB	485.00	7.12	8.63	485.00	1.60	28.33
755	MKT	V-140	VIB	0.00	20.78	7.11	0.00	4.67	23.33
770	APE	3	VIB	10.58	0.00	11.67	10.58	0.00	38.30
771	APE	6	VIB	10.58	0.04	11.67	10.58	0.01	38.30
772	APE	15	VIB	59.67	0.49	9.14	59.67	0.11	30.00
773	APE	20	VIB	59.67	0.67	11.67	59.67	0.15	38.30
774	APE	20E	VIB	59.67	0.67	11.67	59.67	0.15	38.30
775	APE	50	VIB	194.00	1.02	9.14	194.00	0.23	30.00
776	APE	50E	VIB	194.00	1.02	9.14	194.00	0.23	30.00
777	APE	100	VIB	194.00	1.42	9.14	194.00	0.32	30.00
778	APE	100E	VIB	194.00	0.62	9.14	194.00	0.14	30.00
779	APE	100HF	VIB	260.00	0.62	13.11	260.00	0.14	43.00

TABLE D-4: COMPLETE HAMMER LISTING (sorted by GRLWEAP ID Numbers)									
Hammer Description				SI Units			US Units		
GRLWEAP ID	Hammer Manufacturer	Hammer Name	Hammer Type	Rated Energy kJ	Ram Weight kN	Eq. Rated Stroke m	Rated Energy ft-kips	Ram Weight kips	Eq. Rated Stroke ft
780	APE	150	VIB	260.00	0.62	9.14	260.00	0.14	30.00
781	APE	150T	VIB	260.00	0.76	9.14	260.00	0.17	30.00
782	APE	150HF	VIB	466.00	1.42	13.11	466.00	0.32	43.00
783	APE	200	VIB	466.00	1.29	9.14	466.00	0.29	30.00
784	APE	200T	VIB	466.00	1.51	9.40	466.00	0.34	30.83
785	APE	200T HF	VIB	738.00	1.51	13.11	738.00	0.34	43.00
786	APE	300	VIB	738.00	1.51	7.62	738.00	0.34	25.00
787	APE	400B	VIB	738.00	3.47	7.11	738.00	0.78	23.33
788	APE	600	VIB	800.00	4.67	7.10	800.00	1.05	23.30
789	APE	Tan 400	VIB	1476.00	6.10	7.11	1476.00	1.37	23.33
790	APE	Tan 600	VIB	1800.00	9.39	7.10	1800.00	2.11	23.30
801	DKH	PH-5	ECH	58.88	49.04	1.20	43.42	11.02	3.94
802	DKH	PH-7	ECH	82.44	68.66	1.20	60.79	15.43	3.94
803	DKH	PH-7S	ECH	82.44	68.66	1.20	60.79	15.43	3.94
804	DKH	PH-10	ECH	117.75	98.08	1.20	86.84	22.04	3.94
805	DKH	PH-13	ECH	153.12	127.54	1.20	112.92	28.66	3.94
806	DKH	PH-20	ECH	294.15	196.20	1.50	216.92	44.09	4.92
807	DKH	PH-30	ECH	441.19	294.28	1.50	325.36	66.13	4.92
808	DKH	PH-40	ECH	588.29	392.40	1.50	433.85	88.18	4.92
810	MGF	RBH 2400	VIB	975.00	23.99	7.16	975.00	5.39	23.50

APPENDIX E

Subsurface Exploration Results for Peach Freeway Design Problem

	Page
SOIL BORING LOGS	E-3
CONE PENETRATION TEST RESULTS	E-11

SUBSURFACE EXPLORATION LOG				BORING NO.	S - 1	SHEET NO.	1	OF 2
Region	6	Hammer Fall-Casing	--	Line	Baseline	Station	1223 + 88	
County	James	Hammer Fall-Sampler	--	Offset	20 m Rt	Surface Elev.	96.0 m	
Project	Peach Freeway	Wt. of Hammer-Casing	--	Water Tbl. Elev.	92.0 m	Date	10-3-1995	
Structure	Dismal River	Wt. of Hammer-Sampler	64 kg	SPT Hammer Type	Safety Hammer	Time	5:00 p.m.	
Date Start	10-1-1995	Core Barrel Type	Double Tube	Drill Rig Type	Rotary	Depth	4.0 m	
Date Finish	10-2-1995							
Backfill/Sealed	10-3-1995							

NO.	BLOWS ON SAMPLER PER 150 mm				N	DEPTH (m) (ft)	SOIL DESCRIPTION AND REMARKS	q _u (kPa) (tsf)	γ _D (kN/m ³) (pcf)	w _c (%)
	0-150	150-300	300-450	450						
SS-1	1	1	3	4	0	LOOSE TO MEDIUM DENSE, SILTY FINE SAND				
					1					
SS-2	1	2	2	4	2					
					3					
SS-3	2	2	4	6	4					
					5					
SS-4	2	3	3	6	6					
					7					
SS-5	2	3	5	8	8					
					9					
SS-6	3	6	7	13	10					
					11					
SS-7	4	7	8	15	12					
					13					
SS-8	3	5	6	11	14					
					15					
SS-9	6	7	8	15	16					
					17					
SS-10	7	9	9	18	18					
					19					
SS-11	10	19	21	40	20					
SS-12	15	19	20	39						
SS-13	15	20	21	41						
SS-14	16	21	22	43						

SUBSURFACE EXPLORATION LOG				BORING NO. <u>S - 1</u>		SHEET NO. <u>2</u> OF <u>2</u>				
Region <u>6</u>	Hammer Fall-Casing <u>--</u>		Line <u>Baseline</u>		Station <u>1223 + 88</u>					
County <u>James</u>	Hammer Fall-Sampler <u>--</u>		Offset <u>20 m Rt</u>		Surface Elev. <u>96.0 m</u>					
Project <u>Peach Freeway</u>	Wt. of Hammer-Casing <u>--</u>		Surface Elev. <u>96.0 m</u>		Water Tbl. Elev. <u>92.0 m</u>					
Structure <u>Dismal River</u>	Wt. of Hammer-Sampler <u>64 kg</u>		Date <u>10-3-1995</u>		Time <u>5:00 p.m.</u>					
Date Start <u>10-1-1995</u>	SPT Hammer Type <u>Safety Hammer</u>		Date <u>10-3-1995</u>		Time <u>5:00 p.m.</u>					
Date Finish <u>10-3-1995</u>	Core Barrel Type <u>Double Tube</u>		Date <u>10-3-1995</u>		Time <u>5:00 p.m.</u>					
Backfill/Sealed <u>10-3-1995</u>	Drill Rig Type <u>Rotary</u>		Date <u>10-3-1995</u>		Time <u>5:00 p.m.</u>					
		Depth <u>4.0 m</u>								
NO.	BLOWS ON SAMPLER PER 150 mm				DEPTH (m) (ft)	SOIL DESCRIPTION AND REMARKS	Q _u (kPa) (tsf)	γ _D (kN/m ³) (pcf)	W _c (%)	
	0	150	300	450						N
					20	DENSE SAND AND GRAVEL				
SS-15	15	19	22	41	21					
					22					
SS-16	17	21	23	44	23					
					24					
SS-17	18	20	25	45	25					
					26					
SS-18	19	23	25	48	27					
					28					
SS-19	15	21	21	42	29					
					30					
SS-20	17	21	23	44	31					
					32					
SS-21	20	23	26	49	33					
					34					
RUN 1					35		LIMESTONE BEDROCK			
					36		RUN 1 31.0-32.5m REC=83% RQD=81%			
					37		END OF BORING @32.5m			
					38		NOTES:			
					39		SPT N VALUES FROM SAFETY HAMMER.			
					40					

SUBSURFACE EXPLORATION LOG				BORING NO.	S - 2	SHEET NO.	1	OF 2
Region	6	Hammer Fall-Casing	--	Line	Baseline	Station	1225 + 13	
County	James	Hammer Fall-Sampler	--	Offset	20 m Lt	Surface Elev.	85.0 m	
Project	Peach Freeway	Wt. of Hammer-Casing	--	Water Tbl. Elev.	87.0 m	Date	10-3-1995	
Structure	Dismal River	Wt. of Hammer-Sampler	64 kg	Date	10-3-1995	Time	5:00 p.m.	
Date Start	10-3-1995	SPT Hammer Type	Safety Hammer	Depth	Surface			
Date Finish	10-3-1995	Core Barrel Type	Double Tube					
Backfill/Sealed	10-3-1995	Drill Rig Type	Rotary					

NO.	BLOWS ON SAMPLER PER 150 mm				N	DEPTH (m) (ft)	SOIL DESCRIPTION AND REMARKS	Q _u (kPa) (tsf)	γ _D (kN/m ³) (pcf)	W _c (%)
	0-150	150-300	300-450	450-600						
SS-1	2	2	3	5	0	0	LOOSE SILT			
					1					
SS-2	2	3	4	7	2	5				
					3					
SS-3	3	3	4	7	3	10				
					4					
SS-4	3	4	5	9	5	15				
					6					
SS-5	25	39	46	85	6	20		EXTREMELY DENSE SAND AND GRAVEL		
					7					
SS-6	33	41	55	96	8	25				
					9					
SS-7	12	13	18	31	9	30				
					10					
SS-8	15	16	19	35	11	35				
					12					
SS-9	11	16	16	32	12	40				
					13					
SS-10	12	15	18	33	14	45				
					15					
SS-11	15	17	21	38	15	50				
					16					
SS-12	13	16	18	34	17	55				
					18					
SS-13	17	19	20	39	18	60				
					19					
SS-14	16	19	22	41	20	65				

SUBSURFACE EXPLORATION LOG				BORING NO. <u>S - 2</u>		SHEET NO. <u>2</u> OF <u>2</u>			
Region	<u>6</u>	Hammer Fall-Casing	<u>--</u>	Line	<u>Baseline</u>				
County	<u>James</u>	Hammer Fall-Sampler	<u>--</u>	Station	<u>1225 + 13</u>				
Project	<u>Peach Freeway</u>	Wt. of Hammer-Casing	<u>--</u>	Offset	<u>20 m Lt</u>				
Structure	<u>Dismal River</u>	Wt. of Hammer-Sampler	<u>64 kg</u>	Surface Elev.	<u>85.0 m</u>				
Date Start	<u>10-3-1995</u>	SPT Hammer Type	<u>Safety Hammer</u>	Water Tbl. Elev.	<u>87.0 m</u>				
Date Finish	<u>10-3-1995</u>	Core Barrel Type	<u>Double Tube</u>	Date	<u>10-3-1995</u>				
Backfill/Sealed	<u>10-3-1995</u>	Drill Rig Type	<u>Rotary</u>	Time	<u>5:00 p.m.</u>				
				Depth	<u>Surface</u>				
NO.	BLOWS ON SAMPLER PER 150 mm				DEPTH (m) (ft)	SOIL DESCRIPTION AND REMARKS	q _u kPa (tsf)	γ _D kN/m ³ (pcf)	w _c %
	0	150	300	450					
					20	65			
RUN					21				
1					22	70			
RUN					23	75			
2					24	80			
					25	85			
					26	90			
					27	95			
					28	100			
					29	105			
					30	110			
					31	115			
					32	120			
					33	125			
					34				
					35				
					36				
					37				
					38				
					39				
					40				

LIMESTONE BEDROCK
 RUN 1 20.5-22.0m REC.=98%, RQD=67%
 RUN 2 22.0-23.5m REC.=100%, RQD=85%

END OF BORING @20.0m
 NOTES:
 SPT N VALUES FROM SAFETY HAMMER.

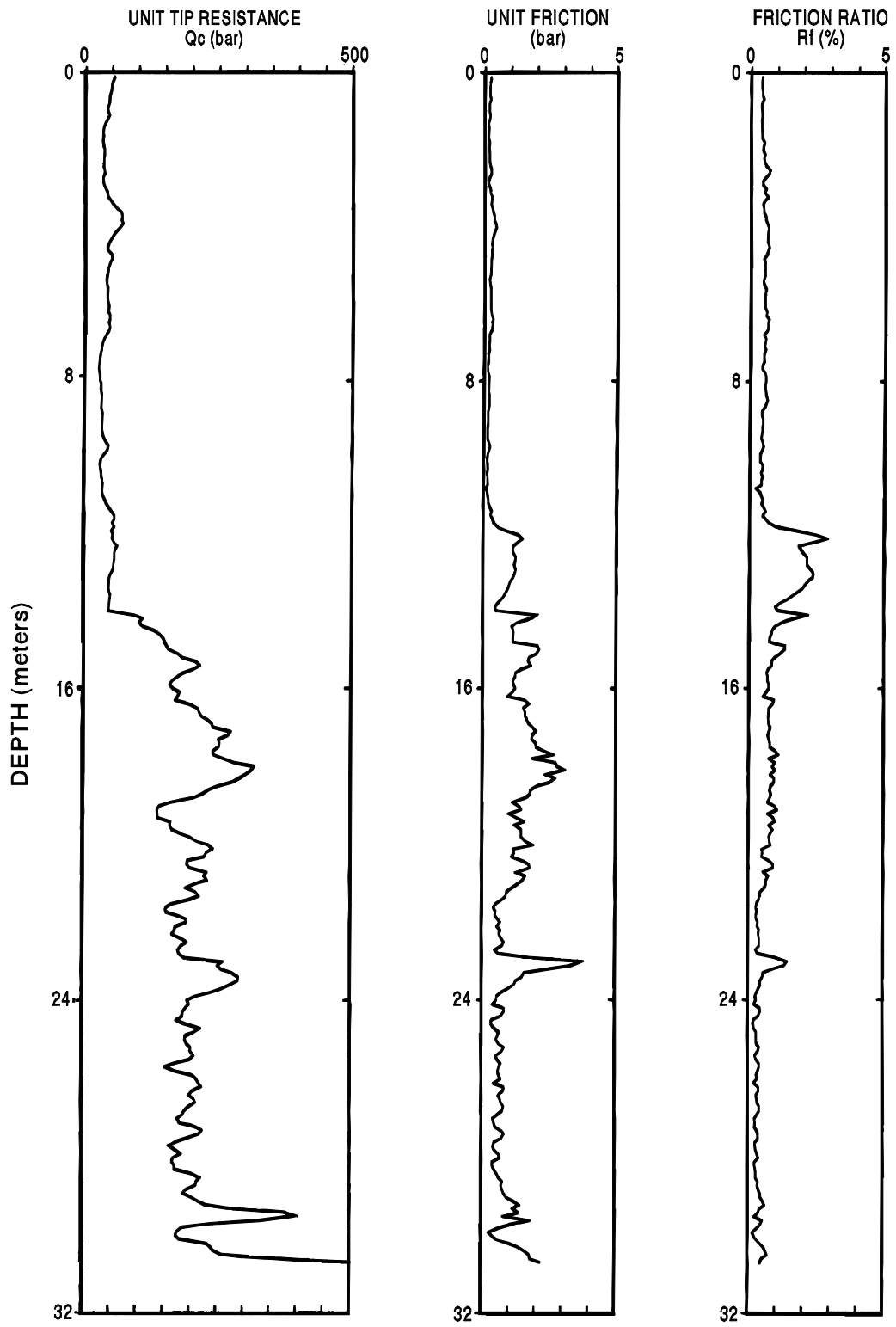
SUBSURFACE EXPLORATION LOG				BORING NO. <u>S - 3</u>		SHEET NO. <u>1</u> OF <u>2</u>	
Region <u>6</u>	Hammer Fall-Casing <u>--</u>		Line <u>Baseline</u>				
County <u>James</u>	Hammer Fall-Sampler <u>--</u>		Station <u>1226 + 13</u>				
Project <u>Peach Freeway</u>	Wt. of Hammer-Casing <u>--</u>		Offset <u>20 m Rt</u>				
Structure <u>Dismal River</u>	Wt. of Hammer-Sampler <u>64 kg</u>		Surface Elev. <u>85.0 m</u>				
Date Start <u>10-4-1995</u>	SPT Hammer Type <u>Safety Hammer</u>		Water Tbl. Elev. <u>87.0 m</u>				
Date Finish <u>10-4-1995</u>	Core Barrel Type <u>Double Tube</u>		Date <u>10-4-1995</u>				
Backfill/Sealed <u>10-4-1995</u>	Drill Rig Type <u>Rotary</u>		Time <u>5:00 p.m.</u>				
			Depth <u>Surface</u>				

NO.	BLOWS ON SAMPLER PER 150 mm				DEPTH (m) (ft)	SOIL DESCRIPTION AND REMARKS	Q _u (kPa) (tsf)	γ _D (kN/m ³) (pcf)	W _c (%)
	0-150	150-300	300-450	N					
SS-1	1	2	2	4	0 - 0				
					1 - 5	LOOSE SILT			
SS-2	2	3	4	7	2 - 5				
SS-3	38	41	42	83	3 - 10	EXTREMELY DENSE SAND AND GRAVEL			
UD-1					4 - 15	STIFF TO VERY STIFF SILTY CLAY	182 (1.90)	14.6 (93)	33
UD-2					5 - 15		240 (2.51)	15.1 (96)	31
UD-3					6 - 20		278 (2.90)	15.7 (100)	27
UD-4					8 - 25		307 (3.21)	16.2 (103)	24
UD-5					9 - 30		316 (3.30)	16.7 (106)	22
UD-6					11 - 35		311 (3.25)	16.3 (104)	23
UD-7					12 - 40		316 (3.30)	16.7 (106)	22
UD-8					14 - 45		326 (3.40)	17.0 (108)	21
SS-4	18	19	19	38	15 - 50	DENSE SAND AND GRAVEL			
					16 - 55				
SS-5	21	22	24	46	17 - 55				
SS-6	19	19	22	41	18 - 60				
					19 - 65				
SS-7	21	24	26	50	20 - 65				

SUBSURFACE EXPLORATION LOG		BORING NO. <u>S - 3</u>		SHEET NO. <u>2</u> OF <u>2</u>			
Region <u>6</u>	Hammer Fall-Casing <u>--</u>	Line <u>Baseline</u>					
County <u>James</u>	Hammer Fall-Sampler <u>--</u>	Station <u>1226 + 13</u>					
Project <u>Peach Freeway</u>	Wt. of Hammer-Casing <u>--</u>	Offset <u>20 m Rt</u>					
Structure <u>Dismal River</u>	Wt. of Hammer-Sampler <u>64 kg</u>	Surface Elev. <u>85.0 m</u>					
Date Start <u>10-4-1995</u>	SPT Hammer Type <u>Safety Hammer</u>	Water Tbl. Elev. <u>87.0 m</u>					
Date Finish <u>10-4-1995</u>	Core Barrel Type <u>Double Tube</u>	Date <u>10-4-1995</u>					
Backfill/Sealed <u>10-4-1995</u>	Drill Rig Type <u>Rotary</u>	Time <u>5:00 p.m.</u>					
		Depth <u>Surface</u>					
NO.	BLOWS ON SAMPLER PER 150 mm	DEPTH		SOIL DESCRIPTION AND REMARKS	Q _u kPa (tsf)	γ _D kN/m ³ (pcf)	W _c %
		(m)	(ft)				
	0 150 300 450 N	20	65				
RUN 1		21		LIMESTONE BEDROCK			
		22	70	RUN 1 20-21.5m REC.=90%, RQD=79%			
		23	75	END OF BORING @21.5m			
		24		NOTES:			
		25	80	SPT N VALUES FROM SAFETY HAMMER.			
		26	85				
		27					
		28	90				
		29	95				
		30					
		31	100				
		32	105				
		33					
		34	110				
		35	115				
		36					
		37	120				
		38	125				
		39					
		40	130				

SUBSURFACE EXPLORATION LOG				BORING NO. <u>S - 4</u>		SHEET NO. <u>1</u> OF <u>2</u>			
Region <u>6</u>		Hammer Fall-Casing <u>--</u>		Line <u>Baseline</u>					
County <u>James</u>		Hammer Fall-Sampler <u>--</u>		Station <u>1227 + 38</u>					
Project <u>Peach Freeway</u>		Wt. of Hammer-Casing <u>--</u>		Offset <u>20 m Lt</u>					
Structure <u>Dismal River</u>		Wt. of Hammer-Sampler <u>64 kg</u>		Surface Elev. <u>91.0 m</u>					
Date Start <u>10-5-1995</u>		SPT Hammer Type <u>Safety Hammer</u>		Water Tbl. Elev. <u>90.5 m</u>					
Date Finish <u>10-5-1995</u>		Core Barrel Type <u>Double Tube</u>		Date <u>10-6-1995</u>					
Backfill/Sealed <u>10-5-1995</u>		Drill Rig Type <u>Rotary</u>		Time <u>5:00 p.m.</u>					
				Depth <u>0.5 m</u>					
NO.	BLOWS ON SAMPLER PER 150 mm				DEPTH (m) (ft)	SOIL DESCRIPTION AND REMARKS	Q _u kPa (tsf)	γ _D kN/m ³ (pcf)	W _c %
	0	150	300	450					
UD-1					0	0	62	13.9	35
					1	5	(0.65)	(89)	
UD-2					2	5	60	13.6	38
					3	10	(0.63)	(87)	
UD-3					4	10	65	14.1	34
					5	15	(0.68)	(90)	
UD-4					6	20	67	14.4	32
					7	20	(0.70)	(92)	
UD-5					8	25	69	14.6	31
					9	25	(0.72)	(93)	
UD-6					10	30	172	14.9	30
					11	30	(1.79)	(95)	
UD-7					12	35	182	15.7	27
					13	35	(1.89)	(100)	
UD-8					14	40	192	16.3	24
					15	40	(2.00)	(104)	
UD-9					16	45	188	16.0	26
					17	45	(1.96)	(102)	
UD-10					18	50	192	16.3	24
					19	50	(2.00)	(104)	
UD-11					20	55	190	16.2	25
					21	55	(1.98)	(103)	
UD-12					22	60	316	16.7	22
					23	60	(3.30)	(106)	
UD-13					24	65	310	16.5	23
					25	65	(3.24)	(105)	
UD-14					26	65	326	17.0	21
					27	65	(3.40)	(108)	

SUBSURFACE EXPLORATION LOG				BORING NO. S - 4		SHEET NO. 2 OF 2				
Region 6		Hammer Fall-Casing --		Line Baseline						
County James		Hammer Fall-Sampler --		Station 1227 + 38						
Project Peach Freeway		Wt. of Hammer-Casing --		Offset 20 m Lt						
Structure Dismal River		Wt. of Hammer-Sampler 64 kg		Surface Elev. 91.0 m						
Date Start 10-5-1995		SPT Hammer Type Safety Hammer		Water Tbl. Elev. 90.5						
Date Finish 10-5-1995		Core Barrel Type Double Tube		Date 10-6-1995						
Backfill/Sealed 10-6-1995		Drill Rig Type Rotary		Time 5:00 p.m.						
				Depth 0.5 m						
NO.	BLOWS ON SAMPLER PER 150 mm				DEPTH		SOIL DESCRIPTION AND REMARKS	q _u kPa (tsf)	γ _D kN/m ³ (pcf)	W _c %
	0	150	300	N	(m)	(ft)				
	0	150	300		20	65				
UD-15					21	70	STIFF TO VERY STIFF SILTY CLAY	335 (3.50)	16.8 (107)	21
UD-16					22	75		340 (3.55)	17.0 (108)	20
UD-17					23	80		350 (3.65)	17.1 (109)	19
UD-18					24	85		345 (3.60)	17.0 (108)	20
UD-19					25	90		350 (3.65)	17.2 (110)	19
UD-20					26	95		354 (3.70)	17.3 (110)	18
SS-1	20	22	27	49	27	100	DENSE SAND AND GRAVEL			
RUN 1					28	105	LIMESTONE BEDROCK RUN 1 31-32.5m REC.=93%, RQD=88%			
					29	110	END OF BORING @32.5m			
					30	115	NOTES: SPT N VALUES FROM SAFETY HAMMER.			
					31	120				
					32	125				
					33	130				



Depth Increment: .1 m

Max Depth: 30.9 m

Licensed to: InSituTech Ltd.
Address: 5 del Valle
City: Orinda, CA 94563, U.S.A.

Interpreter Name: Mike Holloway

File Number: 202	Date: 8/21/89
Operator: DM HOLLOWAY	On Site Location: Peach Freeway CPT-1
Cone Type: 186	Comment: 93/2/1001

SUMMARY SHEET

'a' for calculating Q_t :	0.800
Value for Water Table (in m):	4.000
Valid Zone Classification based on:	R_f
Missing unit weight to start depth:	15.720
Method for calculating s_u :	N_k
Value of the constant N_k :	15.000
Define Zone 6 for Sand Parameters?	Yes
Sand Compressibility for calc D_r :	All sands

Soil Behavior Type Zone Numbers for R_f Zone and B_q Zone Classification

Zone #1 = Sensitive fine grained	Zone #7 = Sand with some silt
Zone #2 = Organic material	Zone #8 = Fine sand
Zone #3 = Clay	Zone #9 = Sand
Zone #4 = Silty clay	Zone #10 = Gravelly sand
Zone #5 = Clayey silt	Zone #11 = Very stiff fine grained *
Zone #6 = Silty sand	Zone #12 = Sand to clayey sand *

* Overconsolidated and/or cemented

NOTE: For 8011 classification, R_f values $>$ are assumed to be 8.

NOTE: Since U_2 (pore pressure) has not been defined, Q_t cannot be calculated, therefore, the value of Q_t has been made equal to q_c .

NOTE: ---- means out of range.

PEACH FREEWAY CPT-1											
Depth (meter)	q _c Average (bars)	f _s Average (bars)	R _f (%)	OS Average (bars)	EOS Average (bars)	R _f Zone (zone #)	SPT N (blow/.3 m)	SPT N1 (blow/.3 m)	Dr (%)	s _u (bars)	s _u /EOS (ratio)
0.25	49.900	0.195	0.391	0.054	0.054	8	12	18	89	----	----
0.50	46.867	0.190	0.405	0.103	0.103	8	12	18	78	----	----
0.75	43.900	0.180	0.410	0.152	0.152	8	11	17	71	----	----
1.00	42.633	0.167	0.391	0.201	0.201	8	11	17	66	----	----
1.25	38.650	0.150	0.388	0.251	0.251	8	10	15	60	----	----
1.50	33.600	0.130	0.387	0.299	0.299	7	11	17	54	----	----
1.75	32.450	0.145	0.447	0.346	0.346	7	11	17	51	----	----
2.00	34.700	0.157	0.451	0.393	0.393	7	12	18	51	----	----
2.25	34.250	0.165	0.482	0.440	0.440	7	11	17	49	----	----
2.50	34.400	0.220	0.640	0.487	0.487	7	11	17	47	----	----
2.75	32.150	0.150	0.467	0.534	0.534	7	11	17	44	----	----
3.00	36.633	0.180	0.491	0.582	0.582	7	12	18	47	----	----
3.25	44.200	0.245	0.554	0.630	0.630	8	11	15	51	----	----
3.50	58.667	0.267	0.455	0.679	0.679	8	15	20	58	----	----
3.75	67.250	0.360	0.535	0.728	0.728	8	17	21	61	----	----
4.00	63.733	0.393	0.617	0.777	0.777	8	16	19	58	----	----
4.25	49.750	0.305	0.613	0.826	0.802	8	12	14	51	----	----
4.50	41.733	0.263	0.631	0.874	0.825	7	14	16	45	----	----
4.75	48.500	0.250	0.515	0.922	0.849	8	12	13	49	----	----
5.00	43.733	0.223	0.511	0.972	0.874	8	11	12	46	----	----
5.25	40.200	0.200	0.498	1.020	0.897	7	13	14	43	----	----
5.50	39.667	0.193	0.487	1.067	0.920	7	13	13	42	----	----
5.75	41.350	0.215	0.520	1.115	0.943	8	10	10	43	----	----
6.00	42.400	0.217	0.511	1.164	0.968	8	11	11	43	----	----
6.25	43.950	0.250	0.569	1.213	0.993	8	11	11	44	----	----
6.50	44.600	0.283	0.635	1.261	1.016	7	15	14	44	----	----
6.75	41.550	0.225	0.542	1.309	1.039	7	14	13	42	----	----
7.00	32.767	0.170	0.519	1.356	1.061	7	11	10	35	----	----
7.25	29.100	0.150	0.515	1.403	1.084	7	10	9	31	----	----
7.50	26.567	0.123	0.464	1.450	1.107	7	9	8	28	----	----
7.75	26.350	0.125	0.474	1.497	1.129	7	9	8	28	----	----
8.00	28.900	0.160	0.554	1.544	1.152	7	10	9	30	----	----
8.25	29.950	0.160	0.551	1.591	1.175	7	10	9	31	----	----
8.50	31.033	0.183	0.591	1.639	1.197	7	10	8	31	----	----
8.75	31.400	0.145	0.462	1.686	1.220	7	10	8	31	----	----

PEACH FREEWAY cpt-1											
Depth (meter)	q _c Average (bars)	f _s Average (bars)	R _f (%)	OS Average (bars)	EOS Average (bars)	R _f Zone (zone #)	SPT N (blow/.3 m)	SPT N1 (blow/.3 m)	Dr (%)	s _u (bars)	s _u /EOS (ratio)
9.00	32.833	0.147	0.447	1.733	1.242	7	11	9	33	----	----
9.25	32.100	0.140	0.436	1.780	1.265	7	11	9	32	----	----
9.50	36.133	0.150	0.415	1.827	1.288	7	12	10	35	----	----
9.75	42.700	0.195	0.457	1.875	1.311	8	11	9	39	----	----
10.00	32.867	0.123	0.375	1.923	1.335	7	11	9	32	----	----
10.25	29.150	0.130	0.446	1.971	1.358	7	10	8	28	----	----
10.50	31.500	0.133	0.423	2.018	1.380	7	11	8	30	----	----
10.75	33.350	0.105	0.315	2.065	1.403	7	11	8	31	----	----
11.00	35.100	0.143	0.408	2.112	1.425	7	12	9	32	----	----
11.25	42.650	0.195	0.457	2.160	1.449	8	11	8	38	----	----
11.50	54.300	0.290	0.534	2.209	1.474	8	14	10	44	----	----
11.75	53.500	0.445	0.832	2.258	1.498	8	13	9	44	----	----
12.00	51.333	1.207	2.351	2.308	1.523	6	21	15	42	----	----
12.25	58.350	1.215	2.082	2.356	1.546	7	19	13	46	----	----
12.50	56.700	1.140	2.011	2.403	1.569	7	19	13	45	----	----
12.75	55.000	1.165	2.118	2.451	1.593	6	22	15	44	----	----
13.00	50.200	1.163	2.317	2.500	1.617	6	20	13	41	----	----
13.25	46.500	0.990	2.129	2.549	1.642	6	19	13	38	----	----
13.50	47.267	0.843	1.784	2.597	1.665	7	16	10	39	----	----
13.75	47.300	0.590	1.247	2.645	1.688	7	16	10	39	----	----
14.00	62.467	0.973	1.558	2.692	1.711	7	21	13	46	----	----
14.25	106.350	1.525	1.434	2.740	1.734	8	27	17	61	----	----
14.50	127.733	1.110	0.869	2.789	1.759	9	26	16	66	----	----
14.75	149.800	1.110	0.741	2.838	1.784	9	30	19	71	----	----
15.00	162.900	2.047	1.256	2.887	1.808	8	41	25	73	----	----
15.25	196.200	1.715	0.874	2.936	1.833	9	39	24	78	----	----
15.50	203.300	1.477	0.726	2.985	1.857	9	41	25	79	----	----
15.75	170.900	1.155	0.676	3.035	1.882	9	34	20	74	----	----
16.00	168.633	1.153	0.684	3.084	1.907	9	34	20	73	----	----
16.25	173.950	1.240	0.713	3.133	1.931	9	35	20	74	----	----
16.50	208.867	1.610	0.771	3.182	1.956	9	42	24	79	----	----
16.75	224.800	1.605	0.714	3.231	1.980	9	45	26	81	----	----
17.00	252.367	1.877	0.744	3.280	2.005	9	50	28	84	----	----
17.25	260.650	1.840	0.706	3.329	2.030	9	52	29	85	----	----
17.50	249.233	2.083	0.836	3.378	2.054	9	50	28	83	----	----

PEACH FREEWAY CPT-1											
Depth (meter)	q _c Average (bars)	f _s Average (bars)	R _f (%)	OS Average (bars)	EOS Average (bars)	R _f Zone (zone #)	SPT N (blow/.3 m)	SPT N1 (blow/.3 m)	Dr (%)	s _u (bars)	s _u /EOS (ratio)
17.75	252.400	2.275	0.901	3.428	2.079	9	50	28	84	----	----
18.00	305.000	2.860	0.938	3.477	2.103	9	61	33	89	----	----
18.25	297.400	2.555	0.859	3.526	2.128	9	59	32	88	----	----
18.50	254.833	2.123	0.833	3.575	2.153	9	51	27	83	----	----
18.75	214.850	1.705	0.794	3.624	2.177	9	43	23	78	----	----
19.00	148.067	1.310	0.885	3.673	2.202	9	30	16	67	----	----
19.25	139.100	1.125	0.809	3.722	2.226	9	28	15	66	----	----
19.50	162.450	1.390	0.856	3.771	2.251	9	32	17	70	----	----
19.75	173.100	1.450	0.838	3.821	2.276	9	35	18	71	----	----
20.00	214.933	1.657	0.771	3.870	2.300	9	43	22	78	----	----
20.25	236.350	1.165	0.493	3.919	2.325	9	47	24	80	----	----
20.50	204.867	1.427	0.696	3.968	2.349	9	41	21	76	----	----
20.75	214.700	1.515	0.706	4.017	2.374	9	43	22	77	----	----
21.00	221.533	1.477	0.667	4.066	2.399	9	44	22	78	----	----
21.25	201.300	1.015	0.504	4.115	2.423	9	40	20	75	----	----
21.50	192.700	0.710	0.368	4.164	2.448	9	39	20	74	----	----
21.75	154.550	0.465	0.301	4.214	2.472	9	31	16	67	----	----
22.00	186.733	0.577	0.309	4.263	2.497	9	37	19	72	----	----
22.25	172.050	0.615	0.357	4.312	2.522	9	34	17	70	----	----
22.50	180.900	0.713	0.394	4.361	2.546	9	36	18	71	----	----
22.75	180.450	0.615	0.341	4.410	2.571	9	36	18	71	----	----
23.00	209.567	2.040	0.973	4.459	2.595	9	42	21	75	----	----
23.25	255.250	2.870	1.124	4.508	2.620	9	51	26	81	----	----
23.50	286.267	1.450	0.507	4.558	2.646	10	48	24	84	----	----
23.75	267.100	1.085	0.406	4.610	2.672	10	45	23	82	----	----
24.00	213.833	0.607	0.284	4.661	2.699	10	36	18	75	----	----
24.25	195.400	0.615	0.315	4.711	2.724	9	39	20	72	----	----
24.50	183.033	0.630	0.344	4.760	2.749	9	37	19	70	----	----
24.75	205.600	0.395	0.192	4.810	2.774	10	34	17	74	----	----
25.00	197.667	0.590	0.298	4.860	2.800	9	40	20	72	----	----
25.25	198.400	0.730	0.368	4.909	2.825	9	40	20	72	----	----
25.50	203.167	0.617	0.304	4.958	2.849	9	41	21	73	----	----
25.75	164.050	0.675	0.411	5.008	2.874	9	33	17	67	----	----
26.00	197.300	0.653	0.331	5.057	2.898	9	39	20	72	----	----
26.25	219.850	0.645	0.293	5.107	2.924	10	37	19	75	----	----

PEACH FREEWAY CPT-1											
Depth (meter)	q _c Average (bars)	f _s Average (bars)	R _f (%)	OS Average (bars)	EOS Average (bars)	R _f Zone (zone #)	SPT N (blow/.3 m)	SPT N1 (blow/.3 m)	Dr (%)	s _u (bars)	s _u /EOS (ratio)
26.50	204.100	0.700	0.343	5.157	2.950	9	41	21	72	----	----
26.75	205.200	0.770	0.375	5.206	2.974	9	41	21	73	----	----
27.00	185.200	0.600	0.324	5.255	2.999	9	37	19	69	----	----
27.25	196.050	0.480	0.245	5.304	3.023	9	39	20	71	----	----
27.50	211.900	0.753	0.356	5.353	3.048	9	42	21	73	----	----
27.75	167.800	0.440	0.262	5.402	3.073	9	34	17	66	----	----
28.00	175.400	0.593	0.338	5.452	3.097	9	35	18	67	----	----
28.25	169.000	0.400	0.237	5.501	3.122	9	34	17	66	----	----
28.50	198.167	0.560	0.283	5.550	3.146	9	40	20	71	----	----
28.75	213.100	0.755	0.354	5.599	3.171	9	43	22	73	----	----
29.00	194.933	0.837	0.429	5.648	3.196	9	39	20	70	----	----
29.25	222.300	1.285	0.578	5.697	3.220	9	44	22	74	----	----
29.50	351.033	1.137	0.324	5.747	3.246	10	59	30	87	----	----
29.75	282.400	1.410	0.499	5.798	3.272	10	47	24	80	----	----
30.00	179.367	0.430	0.240	5.849	3.298	9	36	18	67	----	----
30.25	207.250	0.805	0.388	5.898	3.323	9	41	21	71	----	----
30.50	248.033	1.580	0.637	5.947	3.347	9	50	25	76	----	----
30.75	425.400	2.005	0.471	5.997	3.373	10	71	36	92	----	----

InSituTech

Engineer: DM HOLLOWAY

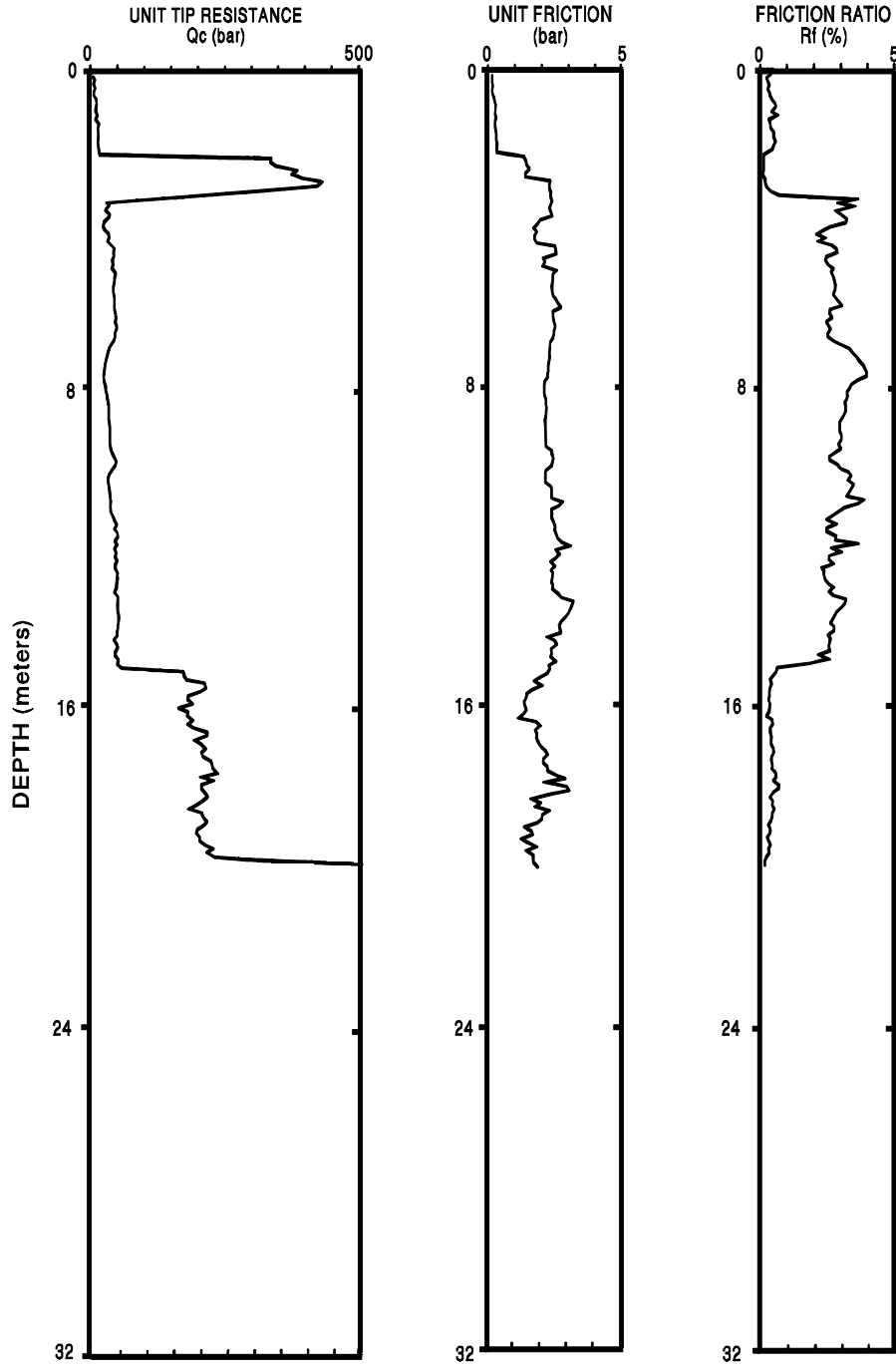
CPT Date: 8/22/89

Page No.: 1 / 1

Location: PEACH FREEWAY, CPT3

Cone Used: 186

Job No.: 93/2/1001



Depth Increment: .1 m

Max Depth: 19.9 m

Licensed to: InSituTech Ltd.
Address: 5 del Valle
City: Orinda, CA 94563, U.S.A.

Interpreter Name: Mike Holloway

File Number: 203 Date: 8/22/89
Operator: DM HOLLOWAY On Site Location: Peach Freeway CPT-3
Cone Type: 186 Comment: 93/2/1001

SUMMARY SHEET

'a' for calculating Q_t : 0.800
Value for Water Table (in m): 0.000
Valid Zone Classification based on: R_f
Missing unit weight to start depth: 15.720
Method for calculating s_u : Nk
Value of the constant Nk: 15.000
Define Zone 6 for Sand Parameters? Yes
Sand Compressibility for calc D_r : All sands

Soil Behavior Type Zone Numbers for R_f Zone and B_q Zone Classification

Zone #1	= Sensitive fine grained	Zone #7	= Sand with some silt
Zone #2	= Organic material	Zone #8	= Fine sand
Zone #3	= Clay	Zone #9	= Sand
Zone #4	= Silty clay	Zone #10	= Gravelly sand
Zone #5	= Clayey silt	Zone #11	= Very stiff fine grained *
Zone #6	= Silty sand	Zone #12	= Sand to clayey sand *

* Overconsolidated and/or cemented

NOTE: For 8011 classification, R_f values > are assumed to be 8.

NOTE: Since U_2 (pore pressure) has not been defined, Q_t cannot be calculated, therefore, the value of Q_t has been made equal to Q_c .

NOTE: ---- means out of range.

PEACH FREEWAY CPT-3											
Depth (meter)	q _c Average (bars)	f _s Average (bars)	R _f (%)	OS Average (bars)	EOS Average (bars)	R _f Zone (zone #)	SPT N (blow/.3 m)	SPT N1 (blow/.3 m)	D _r (%)	s _u (bars)	s _u /EOS (ratio)
0.25	12.400	0.110	0.887	0.051	0.027	6	5	8	60	----	----
0.50	11.867	0.117	0.983	0.098	0.049	6	5	8	50	----	----
0.75	13.900	0.155	1.115	0.145	0.072	6	6	9	49	----	----
1.00	12.633	0.157	1.240	0.193	0.094	6	5	8	42	----	----
1.25	13.650	0.150	1.099	0.240	0.117	6	5	8	41	----	----
1.50	13.600	0.137	1.005	0.287	0.140	6	5	8	39	----	----
1.75	12.450	0.145	1.165	0.334	0.162	6	5	8	34	----	----
2.00	121.367	0.490	0.404	0.382	0.186	9	24	36	97	----	----
2.25	339.750	1.265	0.372	0.432	0.211	10	57	86	125	----	----
2.50	384.400	1.287	0.335	0.483	0.238	10	64	96	127	----	----
2.75	427.650	2.150	0.503	0.534	0.265	10	71	107	128	----	----
3.00	236.633	2.180	0.921	0.585	0.290	9	47	71	110	----	----
3.25	34.200	2.245	6.564	0.634	0.315	3	34	51	----	2.238	7.108
3.50	35.333	2.267	6.415	0.683	0.339	3	35	53	----	2.311	6.805
3.75	27.250	1.810	6.642	0.732	0.364	3	27	41	----	1.768	4.856
4.00	33.733	1.660	4.921	0.781	0.389	3	34	51	----	2.198	5.653
4.25	34.750	1.655	4.763	0.830	0.413	4	23	35	----	2.262	5.472
4.50	41.733	2.363	5.663	0.879	0.438	3	42	63	----	2.725	6.221
4.75	38.500	1.900	4.935	0.928	0.462	3	39	59	----	2.506	5.416
5.00	40.400	2.133	5.281	0.978	0.487	3	40	60	----	2.629	5.396
5.25	40.200	2.200	5.473	1.027	0.512	3	40	60	----	2.613	5.104
5.50	39.667	2.193	5.529	1.076	0.536	3	40	60	----	2.573	4.798
5.75	41.350	2.365	5.719	1.125	0.561	3	41	62	----	2.682	4.782
6.00	42.400	2.317	5.464	1.174	0.585	3	42	61	----	2.748	4.695
6.25	43.950	2.250	5.119	1.223	0.610	3	44	62	----	2.848	4.669
6.50	44.600	2.283	5.120	1.272	0.635	3	45	62	----	2.889	4.551
6.75	41.550	2.225	5.355	1.321	0.659	3	42	56	----	2.682	4.068
7.00	32.767	2.170	6.623	1.371	0.684	3	33	43	----	2.093	3.061
7.25	29.100	2.150	7.388	1.420	0.708	3	29	37	----	1.845	2.605
7.50	26.567	2.123	7.992	1.469	0.733	3	27	33	----	1.673	2.283

PEACH FREEWAY CPT-3											
Depth (meter)	q _c Average (bars)	f _s Average (bars)	R _f (%)	OS Average (bars)	EOS Average (bars)	R _f Zone (zone #)	SPT N (blow/.3 m)	SPT N1 (blow/.3 m)	Dr (%)	s _u (bars)	s _u /EOS (ratio)
7.75	26.350	2.055	7.799	1.518	0.758	3	26	31	----	1.655	2.185
8.00	28.900	1.960	6.782	1.567	0.782	3	29	34	----	1.822	2.329
8.25	29.950	1.965	6.561	1.616	0.807	3	30	34	----	1.889	2.341
8.50	31.033	1.983	6.391	1.665	0.831	3	31	35	----	1.958	2.355
8.75	31.400	1.945	6.194	1.714	0.856	3	31	34	----	1.979	2.312
9.00	32.833	1.947	5.929	1.764	0.881	3	33	35	----	2.071	2.352
9.25	32.100	1.940	6.044	1.813	0.905	3	32	33	----	2.019	2.231
9.50	36.133	2.083	5.766	1.862	0.930	3	36	37	----	2.285	2.457
9.75	42.700	2.195	5.141	1.911	0.954	3	43	43	----	2.719	2.849
10.00	32.867	1.990	6.055	1.960	0.979	3	33	32	----	2.060	2.105
10.25	29.150	1.930	6.621	2.009	1.004	3	29	28	----	1.809	1.803
10.50	31.500	2.133	6.772	2.058	1.028	3	32	30	----	1.963	1.909
10.75	33.350	2.355	7.061	2.107	1.053	3	33	31	----	2.083	1.978
11.00	35.100	2.243	6.391	2.157	1.077	3	35	32	----	2.196	2.038
11.25	42.650	2.195	5.147	2.206	1.102	3	43	39	----	2.696	2.447
11.50	44.300	2.290	5.169	2.255	1.127	3	44	39	----	2.803	2.488
11.75	43.500	2.445	5.621	2.304	1.151	3	44	38	----	2.746	2.386
12.00	41.333	2.540	6.145	2.353	1.176	3	41	35	----	2.599	2.210
12.25	43.350	2.215	5.110	2.402	1.200	3	43	36	----	2.730	2.274
12.50	45.033	2.207	4.900	2.451	1.225	4	30	25	----	2.839	2.317
12.75	45.000	2.165	4.811	2.500	1.250	4	30	24	----	2.833	2.267
13.00	43.533	2.263	5.199	2.550	1.274	3	44	35	----	2.732	2.144
13.25	46.500	2.740	5.892	2.599	1.299	3	47	37	----	2.927	2.253
13.50	47.267	2.843	6.016	2.648	1.323	3	47	37	----	2.975	2.248
13.75	47.300	2.590	5.476	2.697	1.348	3	47	36	----	2.974	2.206
14.00	45.800	2.473	5.400	2.746	1.373	3	46	35	----	2.870	2.091
14.25	41.350	2.125	5.139	2.795	1.397	3	41	31	----	2.570	1.840
14.50	43.067	2.210	5.132	2.844	1.422	3	43	32	----	2.681	1.886
14.75	46.800	2.210	4.722	2.893	1.446	4	31	23	----	2.927	2.024
15.00	130.900	2.047	1.564	2.943	1.471	8	33	24	70	----	----
15.25	191.200	1.615	0.845	2.992	1.496	9	38	27	80	----	----

PEACH FREEWAY CPT-3											
Depth (meter)	q _c Average (bars)	f _s Average (bars)	R _f (%)	OS Average (bars)	EOS Average (bars)	R _f Zone (zone #)	SPT N (blow/.3 m)	SPT N1 (blow/.3 m)	Dr (%)	s _u (bars)	s _u /EOS (ratio)
15.50	195.967	1.477	0.754	3.041	1.520	9	39	27	81	----	----
15.75	180.900	1.155	0.638	3.090	1.545	9	36	25	78	----	----
16.00	170.967	1.153	0.675	3.139	1.569	9	34	23	76	----	----
16.25	181.450	1.240	0.683	3.188	1.594	9	36	24	78	----	----
16.50	203.867	1.610	0.790	3.237	1.619	9	41	27	81	----	----
16.75	194.800	1.605	0.824	3.286	1.643	9	39	26	80	----	----
17.00	205.700	1.877	0.912	3.336	1.668	9	41	27	81	----	----
17.25	220.650	1.840	0.834	3.385	1.692	9	44	28	83	----	----
17.50	219.233	2.083	0.950	3.434	1.717	9	44	28	82	----	----
17.75	212.400	2.275	1.071	3.483	1.742	9	42	27	81	----	----
18.00	208.333	2.527	1.213	3.532	1.766	9	42	26	80	----	----
18.25	197.400	1.555	0.788	3.581	1.791	9	39	24	79	----	----
18.50	194.833	1.790	0.919	3.630	1.815	9	39	24	78	----	----
18.75	209.850	1.705	0.812	3.679	1.840	9	42	25	80	----	----
19.00	194.733	1.310	0.673	3.729	1.865	9	39	23	78	----	----
19.25	204.100	1.125	0.551	3.778	1.889	9	41	24	79	----	----
19.50	217.450	1.390	0.639	3.827	1.914	9	43	25	81	----	----
19.75	273.100	1.450	0.531	3.877	1.939	10	46	27	87	----	----
20.00	505.050	1.545	0.306	3.928	1.966	10	84	48	----	----	----

InSituTech

Engineer: DM HOLLOWAY

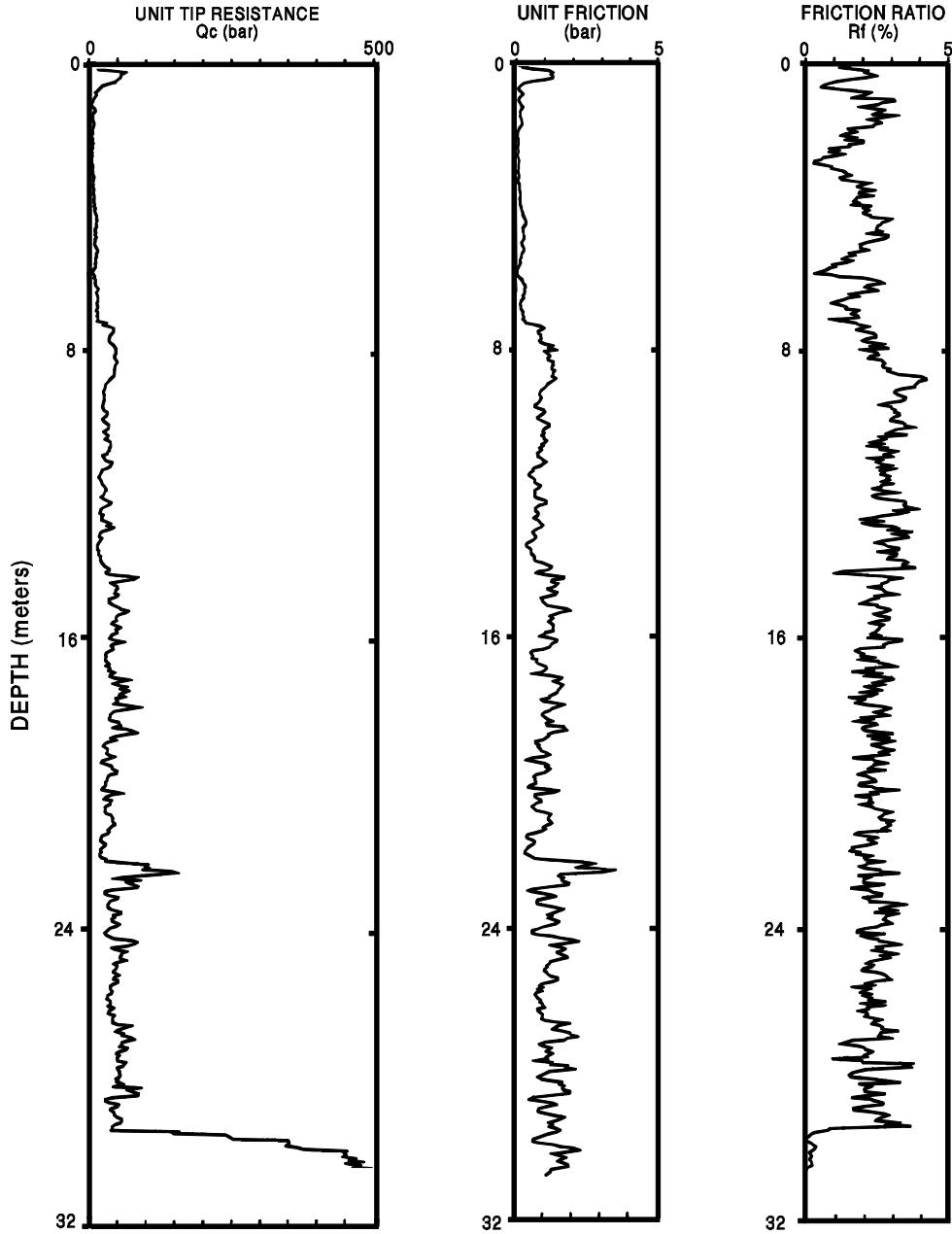
CPT Date: 8/19/89

Page No.: 1 / 1

Location: PEACH FREEWAY, CPT4

Cone Used: 186

Job No.: 93/2/1001



Depth Increment: .05 m

Max Depth: 30.7 m

Licensed to: InSituTech Ltd.
Address: 5 del Valle
City: Orinda, CA 94563, U.S.A.

Interpreter Name: Mike Holloway

File Number: 8 0 Date: 8/19/89
Operator: DM HOLLOWAY On Site Location: Peach Freeway CPT-4
Cone Type: 186 Comment: 93/2/1001

SUMMARY SHEET

'a' for calculating Q_t : 0.800
Value for Water Table (in m): 1.000
Valid Zone Classification based on: R_f
Missing unit weight to start depth: 15.720
Method for calculating s_u : Nk
Value of the constant Nk: 15.000
Define Zone 6 for Sand Parameters? Yes
Sand Compressibility for calc D_r : All sands

Soil Behavior Type Zone Numbers for R_f Zone and B_q Zone Classification

Zone #1 = Sensitive fine grained	Zone #7 = Sand with some silt
Zone #2 = Organic material	Zone #8 = Fine sand
Zone #3 = Clay	Zone #9 = Sand
Zone #4 = Silty clay	Zone #10 = Gravelly sand
Zone #5 = Clayey silt	Zone #11 = Very stiff fine grained *
Zone #6 = Silty sand	Zone #12 = Sand to clayey sand *

* Overconsolidated and/or cemented

NOTE: For soil classification, R_f values > 8 are assumed to be 8.

NOTE: Since U_2 (pore pressure) has not been defined, Q_t cannot be calculated, therefore, the value of Q_t has been made equal to Q_c .

NOTE: ---- means out of range.

PEACH FREEWAY CPT-4											
Depth (Meter)	q _c Average (bars)	f _s Average (bars)	R _f (%)	OS Average (bars)	EOS Average (bars)	R _f Zone (zone #)	SPT N (blow/.3 m)	SPT N1 (blow/.3 m)	D _r (%)	s _u (bars)	s _u /EOS (ratio)
0.25	56.040	2.612	4.661	0.054	0.054	4	37	56	----	3.732	69.071
0.50	29.040	0.964	3.320	0.103	0.103	5	15	23	----	1.929	18.700
0.75	12.560	0.417	3.320	0.151	0.151	4	8	12	----	0.827	5.468
1.00	6.480	0.345	5.327	0.198	0.198	3	6	9	----	0.419	2.110
1.25	8.820	0.463	5.252	0.246	0.221	3	9	14	----	0.572	2.586
1.50	8.240	0.457	5.544	0.293	0.244	3	8	12	----	0.530	1.174
1.75	6.900	0.325	4.713	0.340	0.266	3	7	11	----	0.437	1.642
2.00	5.960	0.208	3.487	0.387	0.289	3	6	9	----	0.372	1.286
2.25	5.160	0.189	3.663	0.434	0.312	3	5	8	----	0.315	1.011
2.50	4.520	0.110	2.442	0.481	0.334	3	5	8	----	0.269	0.806
2.75	5.560	0.085	1.536	0.527	0.355	1	3	5	----	0.336	0.946
3.00	6.720	0.208	3.098	0.572	0.376	3	7	11	----	0.410	1.091
3.25	6.780	0.258	3.808	0.619	0.398	3	7	11	----	0.411	1.032
3.50	7.680	0.336	4.370	0.666	0.421	3	8	12	----	0.468	1.111
3.75	7.900	0.329	4.162	0.713	0.443	3	8	12	----	0.479	1.080
4.00	10.220	0.459	4.495	0.761	0.467	3	10	15	----	0.631	1.350
4.25	12.000	0.648	5.397	0.810	0.492	3	12	18	----	0.746	1.517
4.50	10.800	0.599	5.544	0.860	0.516	3	11	17	----	0.663	1.284
4.75	10.040	0.577	5.745	0.909	0.541	3	10	15	----	0.609	1.126
5.00	11.100	0.495	4.456	0.958	0.565	3	11	17	----	0.676	1.196
5.25	10.840	0.421	3.880	1.007	0.590	3	11	16	----	0.656	1.111
5.50	9.040	0.268	2.962	1.055	0.614	4	6	8	----	0.532	0.867
5.75	6.360	0.108	1.701	1.102	0.636	4	4	5	----	0.351	0.551
6.00	9.740	0.469	4.811	1.149	0.659	3	10	13	----	0.573	0.869
6.25	13.120	0.637	4.852	1.198	0.683	3	13	17	----	0.795	1.165
6.50	13.420	0.448	3.337	1.246	0.706	4	9	11	----	0.812	1.149
6.75	13.160	0.411	3.125	1.293	0.729	4	9	11	----	0.791	1.086
7.00	16.120	0.537	3.330	1.340	0.751	4	11	13	----	0.985	1.311
7.25	35.860	1.482	4.133	1.388	0.775	4	24	28	----	2.298	2.965
7.50	34.820	1.692	4.859	1.437	0.800	3	35	40	----	2.226	2.783

PEACH FREEWAY CPT-4											
Depth (meter)	q _c Average (bars)	f _s Average (bars)	R _f (%)	OS Average (bars)	EOS Average (bars)	R _f Zone (zone #)	SPT N (blow/.3 m)	SPT N1 (blow/.3 m)	Dr (%)	s _u (bars)	s _u /EOS (ratio)
7.75	41.900	2.076	4.955	1.486	0.824	3	42	47	----	2.694	3.269
8.00	44.460	2.370	5.331	1.535	0.849	3	44	48	----	2.862	3.371
8.25	45.780	2.494	5.448	1.585	0.873	3	46	49	----	2.946	3.373
8.50	42.960	2.622	6.103	1.634	0.898	3	43	45	----	2.755	3.068
8.75	31.400	2.582	8.223	----	----	----	----	----	----	----	----
9.00	25.280	1.944	7.690	1.683	0.898	3	25	26	----	1.573	1.752
9.25	24.700	1.738	7.036	1.732	0.923	3	25	26	----	1.531	1.660
9.50	24.920	1.578	6.332	1.781	0.947	3	25	25	----	1.543	1.628
9.75	25.980	1.758	6.767	1.830	0.972	3	26	26	----	1.610	1.657
10.00	31.420	2.184	6.951	1.879	0.996	3	31	30	----	1.969	1.976
10.25	28.120	1.938	6.892	1.928	0.021	3	28	27	----	1.746	1.710
10.50	35.760	2.010	5.621	1.978	0.046	3	36	34	----	2.252	2.154
10.75	28.640	1.676	5.852	2.027	0.070	3	29	27	----	1.774	1.658
11.00	33.540	1.884	5.617	2.076	0.095	3	34	31	----	2.098	1.916
11.25	22.160	1.320	5.957	2.125	0.119	3	22	20	----	1.336	1.193
11.50	19.440	1.182	6.080	2.174	0.144	3	19	17	----	1.151	1.006
11.75	27.160	1.564	5.758	2.223	0.169	3	27	23	----	1.662	1.423
12.00	27.240	1.530	5.617	2.272	0.193	3	27	23	----	1.665	1.395
12.25	25.480	1.788	7.017	2.321	0.218	3	25	21	----	1.544	1.268
12.50	21.400	1.464	6.841	2.371	0.242	3	21	17	----	1.269	1.021
12.75	34.800	1.734	4.983	2.420	0.267	3	35	28	----	2.159	1.704
13.00	19.540	1.338	6.847	2.469	0.292	3	20	16	----	1.138	0.881
13.25	16.000	1.062	6.638	2.518	0.316	3	16	13	----	0.899	0.683
13.50	16.300	1.030	6.319	2.567	1.341	3	16	12	----	0.916	0.683
13.75	21.620	1.442	6.670	2.616	1.365	3	22	17	----	1.267	0.928
14.00	31.480	2.244	7.128	2.665	1.390	3	31	23	----	1.921	1.382
14.25	61.400	2.602	4.238	2.714	1.415	5	31	23	----	3.912	2.766
14.50	45.740	2.640	5.772	2.764	1.439	3	46	34	----	2.865	1.991
14.75	41.460	2.466	5.948	2.813	1.464	3	41	30	----	2.576	1.760
15.00	45.200	2.240	4.956	2.862	1.488	4	30	21	----	2.823	1.896
15.25	54.840	3.188	5.813	2.911	1.513	3	55	39	----	3.462	2.288

PEACH FREEWAY CPT-4											
Depth (meter)	q _c Average (bars)	f _s Average (bars)	R _f (%)	OS Average (bars)	EOS Average (bars)	R _f Zone (zone #)	SPT N (blow/.3 m)	SPT N1 (blow/.3 m)	Dr (%)	s _u (bars)	s _u /EOS (ratio)
15.50	44.960	2.530	5.627	2.960	1.538	3	45	31	----	2.800	1.821
15.75	43.120	2.408	5.584	3.009	1.562	3	43	30	----	2.674	1.712
16.00	42.380	2.494	5.885	3.058	1.587	3	42	28	----	2.621	1.652
16.25	33.980	1.820	5.356	3.107	1.611	3	34	23	----	2.058	1.277
16.50	29.100	1.292	4.440	3.157	1.636	4	19	13	----	1.730	1.057
16.75	34.500	1.968	5.704	3.206	1.661	3	35	23	----	2.086	1.256
17.00	45.820	2.352	5.133	3.255	1.685	3	46	30	----	2.838	1.684
17.25	55.860	3.070	5.496	3.304	1.710	3	56	36	----	3.504	2.049
17.50	53.160	2.690	5.060	3.353	1.734	4	35	22	----	3.320	1.914
17.75	62.300	2.602	4.177	3.402	1.759	5	31	19	----	3.927	2.232
18.00	37.040	2.150	5.805	3.451	1.784	3	37	23	----	2.239	1.255
18.25	46.560	2.264	4.863	3.500	1.808	4	31	19	----	2.871	1.588
18.50	64.020	3.082	4.814	3.550	1.833	4	43	26	----	4.031	2.199
18.75	32.000	1.844	5.763	3.599	1.857	3	32	19	----	1.893	1.019
19.00	30.440	1.768	5.808	3.648	1.882	3	30	18	----	1.786	0.949
19.25	28.940	1.534	5.301	3.697	1.907	3	29	17	----	1.683	0.883
19.50	42.220	2.222	5.263	3.746	1.931	3	42	24	----	2.565	1.328
19.75	30.340	1.482	4.885	3.795	1.956	3	30	17	----	1.770	0.905
20.00	27.260	1.326	4.864	3.844	1.980	3	27	15	----	1.561	0.788
20.25	36.500	1.944	5.326	3.893	2.005	3	37	21	----	2.174	1.084
20.50	30.500	1.482	4.859	3.943	2.030	3	31	17	----	1.770	0.872
20.75	33.600	1.936	5.762	3.992	2.054	3	34	19	----	1.974	0.961
21.00	39.780	2.348	5.902	4.041	2.079	3	40	22	----	2.383	1.146
21.25	27.360	1.592	5.819	4.090	2.103	3	27	15	----	1.551	0.738
21.50	22.380	1.064	4.754	4.139	2.128	3	22	12	----	1.216	0.571
21.75	18.540	0.782	4.218	4.188	2.153	3	19	10	----	0.957	0.444
22.00	46.920	2.124	4.527	4.237	2.177	4	31	16	----	2.846	1.307
22.25	116.780	5.476	4.689	4.288	2.204	11	117	62	----	----	----
22.50	71.180	3.778	5.308	4.341	2.232	11	71	37	----	----	----
22.75	61.100	2.856	4.674	4.393	2.259	4	41	21	----	3.780	1.674
23.00	38.180	1.962	5.139	4.442	2.284	3	38	19	----	2.249	0.985

PEACH FREEWAY CPT-4											
Depth (meter)	q _c Average (bars)	f _s Average (bars)	R _f (%)	OS Average (bars)	EOS Average (bars)	R _f Zone (zone #)	SPT N (blow/.3 m)	SPT N1 (blow/.3 m)	Dr (%)	s _u (bars)	s _u /EOS (ratio)
23.25	33.420	1.898	5.679	4.491	2.308	3	33	17	----	1.929	0.836
23.50	46.080	2.788	6.050	4.540	2.333	3	46	23	----	2.769	1.187
23.75	43.620	2.644	6.061	4.589	2.357	3	44	22	----	2.602	1.104
24.00	46.060	1.416	4.711	4.638	2.382	3	30	15	----	1.695	0.712
24.25	68.280	3.522	5.158	4.689	2.408	11	68	34	----	----	----
24.50	51.380	3.012	5.862	4.740	2.435	3	51	26	----	3.109	1.277
24.75	51.620	3.144	6.091	4.790	2.460	3	52	26	----	3.122	1.269
25.00	39.188	1.978	5.046	4.839	2.484	3	39	20	----	2.290	0.922
25.25	36.660	1.674	4.566	4.888	2.509	4	24	12	----	2.118	0.844
25.50	51.300	2.602	5.072	4.937	2.533	4	34	17	----	3.091	1.220
25.75	54.840	3.222	5.875	4.986	2.558	3	55	28	----	3.324	1.299
26.00	60.740	2.974	4.896	5.035	2.583	4	40	20	----	3.714	1.438
26.25	54.660	2.224	4.069	5.084	2.607	5	27	14	----	3.305	1.268
26.50	52.220	2.088	3.998	5.133	2.632	5	26	13	----	3.139	1.193
26.75	50.380	3.148	6.249	5.183	2.656	3	50	25	----	3.013	1.134
27.00	48.320	1.854	3.837	5.232	2.681	5	24	12	----	2.873	1.071
27.25	----	----	----	----	----	----	----	----	----	----	----
27.50	61.950	3.197	5.161	5.283	2.683	11	62	31	----	----	----
27.75	61.100	2.856	4.674	5.334	2.710	4	41	21	----	3.718	1.372
28.00	0.180	1.962	5.139	5.383	2.734	3	38	19	----	2.186	0.800
28.25	38.420	1.898	4.582	5.432	2.759	4	28	14	----	2.399	0.870
28.50	41.080	2.788	5.799	5.481	2.783	3	48	24	----	2.840	1.020
28.75	121.620	2.644	2.174	5.529	2.807	7	41	21	58	----	----
29.00	306.060	1.416	0.463	5.578	2.832	10	51	26	85	----	----
29.25	394.280	3.522	0.893	5.629	2.857	9	79	40	92	----	----
29.50	457.380	3.012	0.659	5.679	2.883	10	76	38	96	----	----
29.75	495.620	3.144	0.634	5.730	2.909	10	83	42	98	----	----
30.00	699.567	2.203	0.315	5.781	2.936	10	117	59	----	----	----

APPENDIX F

Peach Freeway Example Problem Calculations

	Page
F.1 INTRODUCTION	F-3
F.2 STATIC AXIAL PILE CAPACITY CALCULATIONS.....	F-7
F.2.1 North Abutment - Soil Boring S-1 (Cohesionless Soil).....	F-8
F.2.1.1 Meyerhof SPT Method	F-8
F.2.1.2 Nordlund Method	F-14
F.2.1.3 Effective Stress Method	F-26
F.2.1.4 Driven Computer Program	F-31
F.2.1.5 LPC CPT Method - Computer Program	F-37
F.2.1.6 Schmertmann Method	F-39
F.2.1.7 Summary of North Abutment Capacity Calculation Results	F-40
F.2.2 Pier 2 - Soil Boring S-2 (Cohesionless Soil).....	F-41
F.2.2.1 Meyerhof SPT Method (before scour).....	F-41
F.2.2.2 Nordlund Method (before scour at 10 m)	F-47
F.2.2.3 Nordlund Method (after scour at 10 m)	F-53
F.2.2.4 Nordlund Method (before scour at 14 m)	F-61
F.2.2.5 Nordlund Method (after scour at 14 m)	F-67
F.2.2.6 Effective Stress Method (before scour).....	F-73
F.2.2.7 Driven Computer Program (before scour).....	F-78
F.2.2.8 Summary of Pier 2 Capacity Calculation Results.....	F-82
F.2.3 Pier 3 - Soil Boring S-3 (Cohesive and Cohesionless Soil).....	F-84
F.2.3.1 Nordlund and α -Methods	F-84
F.2.3.2 Effective Stress Method	F-94
F.2.3.3 Driven Computer Program	F-99
F.2.3.4 LPC CPT Method - Computer Program	F-103
F.2.3.5 Schmertmann Method	F-105
F.2.3.6 Summary of Pier 3 Capacity Calculation Results.....	F-106

F.2.4	South Abutment - Soil Boring S-4 (Cohesive Soil).....	F-108
F.2.4.1	α -Method	F-108
F.2.4.2	Effective Stress Method	F-115
F.2.4.3	Driven Computer Program	F-120
F.2.4.3	LPC CPT Method - Computer Program	F-126
F.2.4.4	Schmertmann Method	F-128
F.2.4.5	Summary of South Abutment Capacity Calculation Results	F-130
F.3	GROUP SETTLEMENT CALCULATIONS.....	F-131
F.3.1	North Abutment - Meyerhof Method based on SPT Test Data.....	F-131
F.3.2	Pier 2 - Meyerhof Method based on SPT Test Data	F-136
F.3.3	Pier 3 - Equivalent Footing Method for Layered Soils	F-139
F.3.4	South Abutment - Equivalent Footing Method	F-151
F.4	LATERAL PILE CAPACITY ANALYSIS.....	F-161
F.4.1	Broms' Method - North Abutment.....	F-161
F.4.2	LPILE - North Abutment.....	F-168
F.4.3	LPILE - Pier 2 H-pile, X-X Axis and Y-Y Axis	F-179
F.4.4	LPILE - Pier 3 H-pile, X-X Axis and Y-Y Axis	F-195
F.4.5	LPILE - South Abutment	F-212
F.5	UPLIFT LOAD CALCULATIONS	F-223
F.5.1	North Abutment - AASHTO Code (1994).....	F-223
F.5.2	Pier 2 - AASHTO Code (1994).....	F-227
F.5.3	Pier 3 - AASHTO Code (1994).....	F-231
F.5.4	South Abutment - AASHTO Code (1994)	F-235
F.6	NEGATIVE SHAFT RESISTANCE CALCULATIONS	F-239
F.6.1	South Abutment - α -Method.....	F-239
F.7	LATERAL SQUEEZE CALCULATIONS.....	F-252
F.7.1	South Abutment - Investigation of Lateral Squeeze.....	F-252
F.8	LATERALLY LOADED PILE GROUP CALCULATION	
F.8.1	Laterally Loaded Pile Group, North Abutment Example Calculation ..	F-254
F.9	PRECONSTRUCTION DRIVEABILITY ANALYSES WITH GRLWEAP	F-287
F.9.1	North Abutment Preconstruction Driveability	F-287

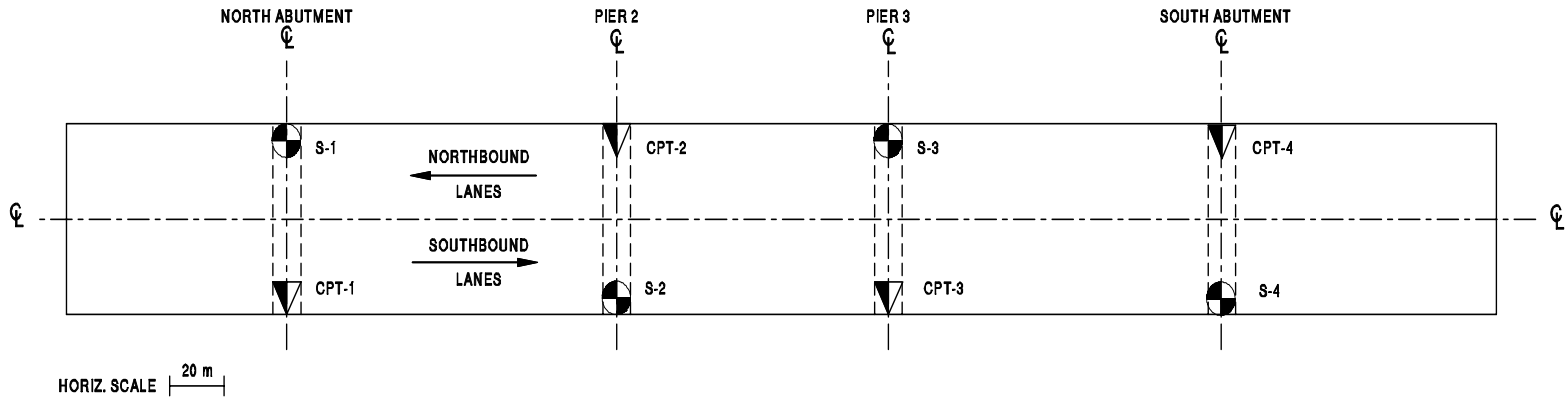
F.1 INTRODUCTION

The various design methods presented in Chapter 9 of the manual will be illustrated by applying these methods to foundation design problems for the Peach Freeway Bridge over Dismal Creek. In many real design problems, additional analyses beyond those presented in these example problems would be used to complete the actual foundation design. For example, group lateral load capacity evaluations are not completed at each substructure location in these example problems.

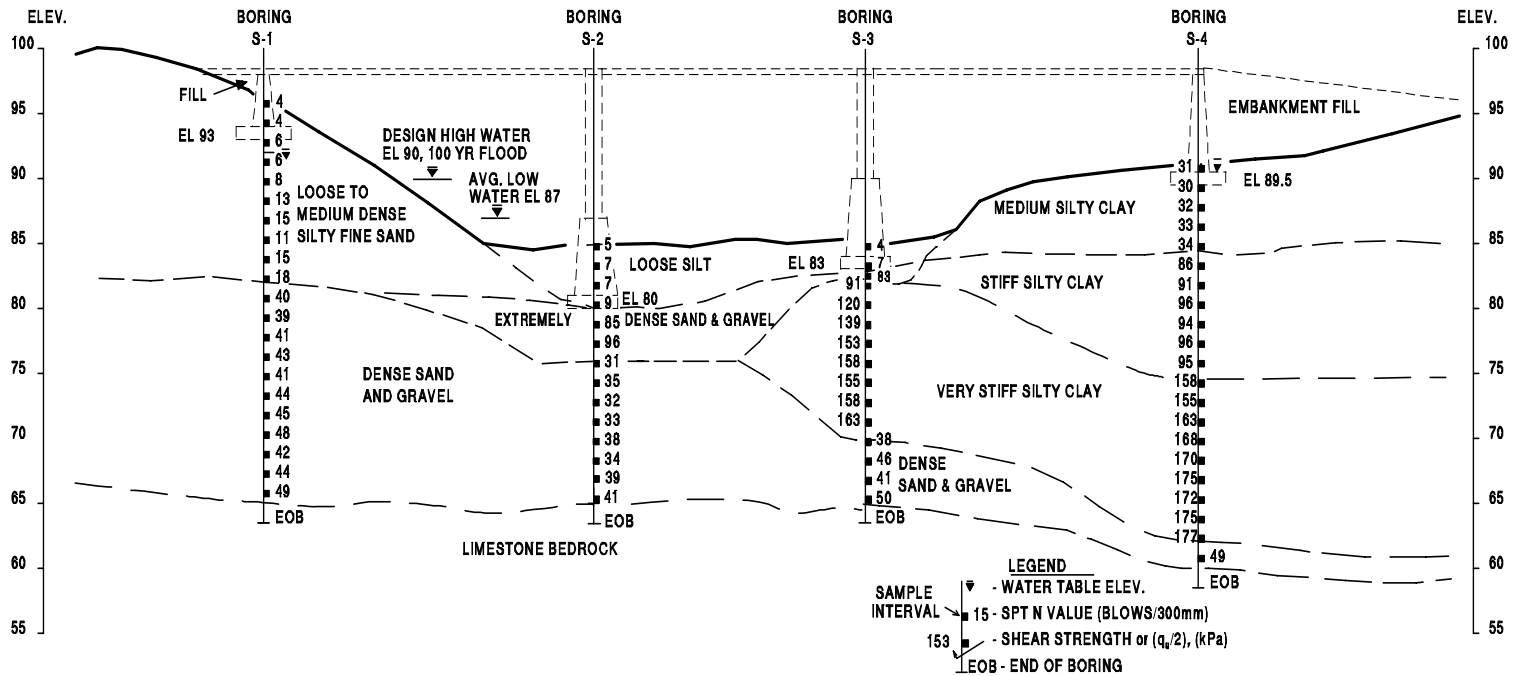
The Peach Freeway Bridge over Dismal Creek will be a three span structure supported at North and South Abutments and interior piers, Pier 2 and Pier 3. One soil boring and one cone penetration test were performed for each substructure location. The subsurface exploration results were included in Appendix E of this manual. The cone penetration test at Pier 2, CPT-2, encountered shallow refusal and therefore, a log of CPT-2 is not included in Appendix E. The subsurface profile developed from the subsurface exploration and laboratory testing program results is presented in Figure F.1.

The "bridge division" has estimated that the maximum compression loads per substructure unit will be 12,600 kN. Each substructure location will be supported on a pile group having three rows of eight piles per row. For abutment pile groups, fewer piles are often required in the middle and rear rows as compared to the front row. The maximum design compression load on any pile will be 890 kN. Lateral loads will range from 600 kN at the interior piers to 900 kN at the abutments with a maximum lateral load per pile of 40 kN. The maximum uplift load on a pile group will be 1,800 kN with a maximum uplift load per pile of 100 kN. Maximum pile group settlements less than 25 mm are required under the compression loads and horizontal deflections of up to 10 mm are permissible under lateral loading. The pile location plan for each substructure location is presented in Figure F.2.

Initial design estimates and local availability of materials indicate square, precast, prestressed concrete piles will probably be the most cost effective foundation type. This pile type should work well at the abutments because they will develop significant load support through both shaft and toe resistance. However, at the interior piers, the driveability of these displacement piles through the extremely dense sand and gravel layer will need to be carefully evaluated. A low displacement pile may be necessary at the interior piers to meet pile penetration requirements.



F-4



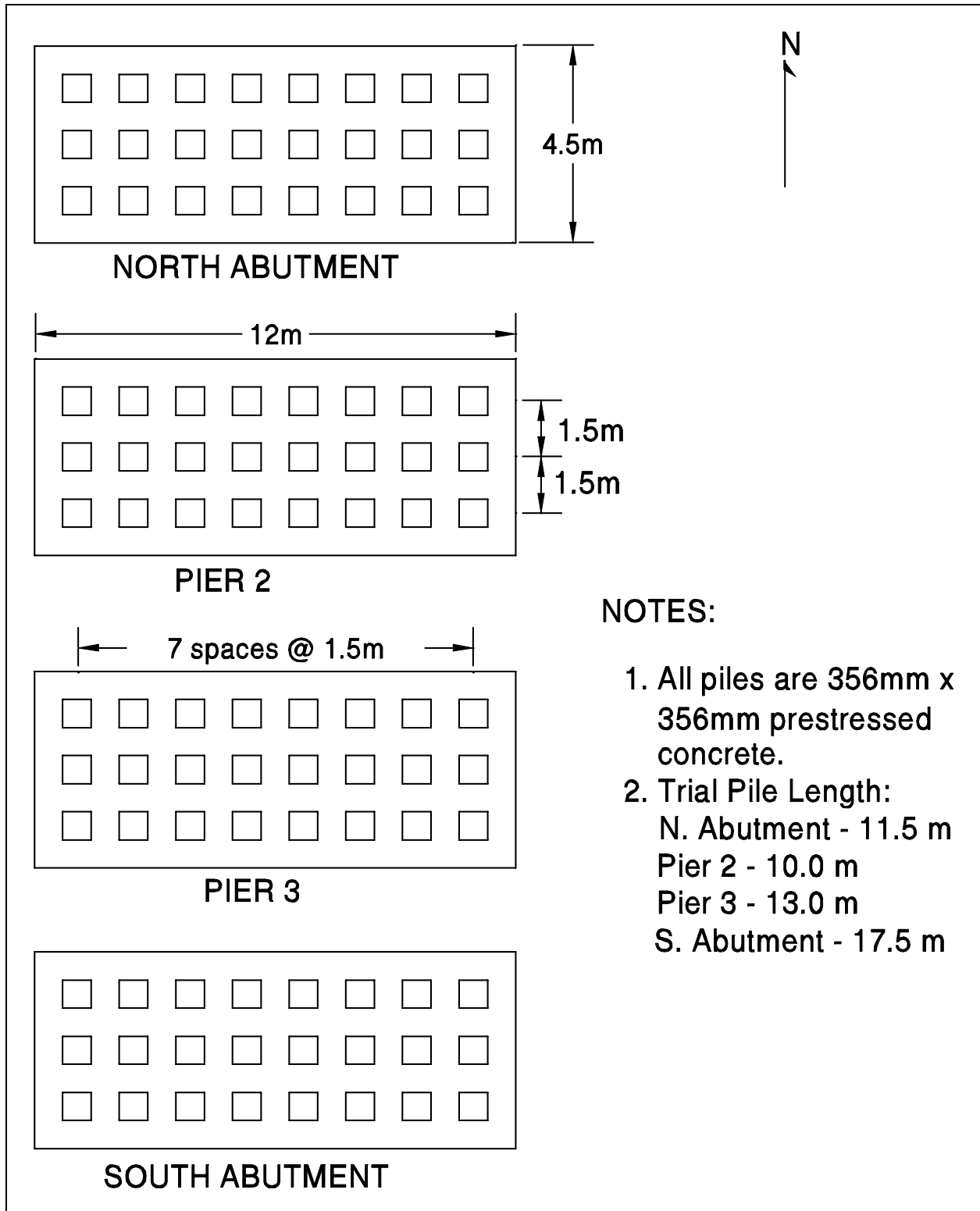


Figure F.2 Pile Foundation Plan

Section F.2 of this Appendix presents static capacity calculations using the applicable methods at each substructure location. Pile group settlement computations for each substructure location are provided in Section F.3. Section F.4 presents lateral pile capacity analyses performed for the North Abutment using both the Brom's Method and the LPILE program. Lateral capacity analysis for Pier 2, Pier 3 and the South Abutment using the LPILE program are also presented. Group uplift computation at each substructure location following AASHTO code are presented in Section F.5. Last, special design considerations of negative shaft resistance and lateral squeeze are presented for the South Abutment in Sections F.6 and F.7, respectively.

F.2 STATIC AXIAL PILE CAPACITY CALCULATIONS

The design load per pile group will be 12,600 kN. The bridge office has determined that the maximum axial design load to be imposed on a single pile will be 890 kN. (At the abutments, the design load on piles in the front row will be 890 kN, whereas the middle and rear rows of piles will have smaller design loads). Construction control will be based on static load test results and a factor of safety of 2.0 will be used on the design load. Therefore, static capacity calculations will be used to evaluate the required pile lengths for a 1780 kN ultimate pile capacity at each substructure location.

Several static axial capacity calculations and computer solutions will be used to determine the required pile length at each substructure unit (*i.e.*, North Abutment, Pier 2, Pier 3, and South Abutment). At Pier 2 location, the effect of scour on the static axial capacity will also be calculated. At all substructure location, pile group capacity will be evaluated. At the South Abutment location, the ultimate pile group capacity against block failure will be calculated and compared with the ultimate pile group capacity from the sum of the ultimate capacities of the individual piles.

The static capacity calculations for each substructure location are presented in the following sections.

F.2.1 North Abutment - Soil Boring S-1 (Cohesionless Soil)

F.2.1.1 Static Axial Pile Capacity Calculations by Meyerhof SPT Method

For the soil profile interpreted from Soil Boring S-1 shown in Figure F.3, perform a Meyerhof method pile capacity calculation for an embedded length of 11.5 meters. The pile top is 3 meters below the existing ground surface. The step-by-step method outlined in Section 9.7.1.1a should be followed.

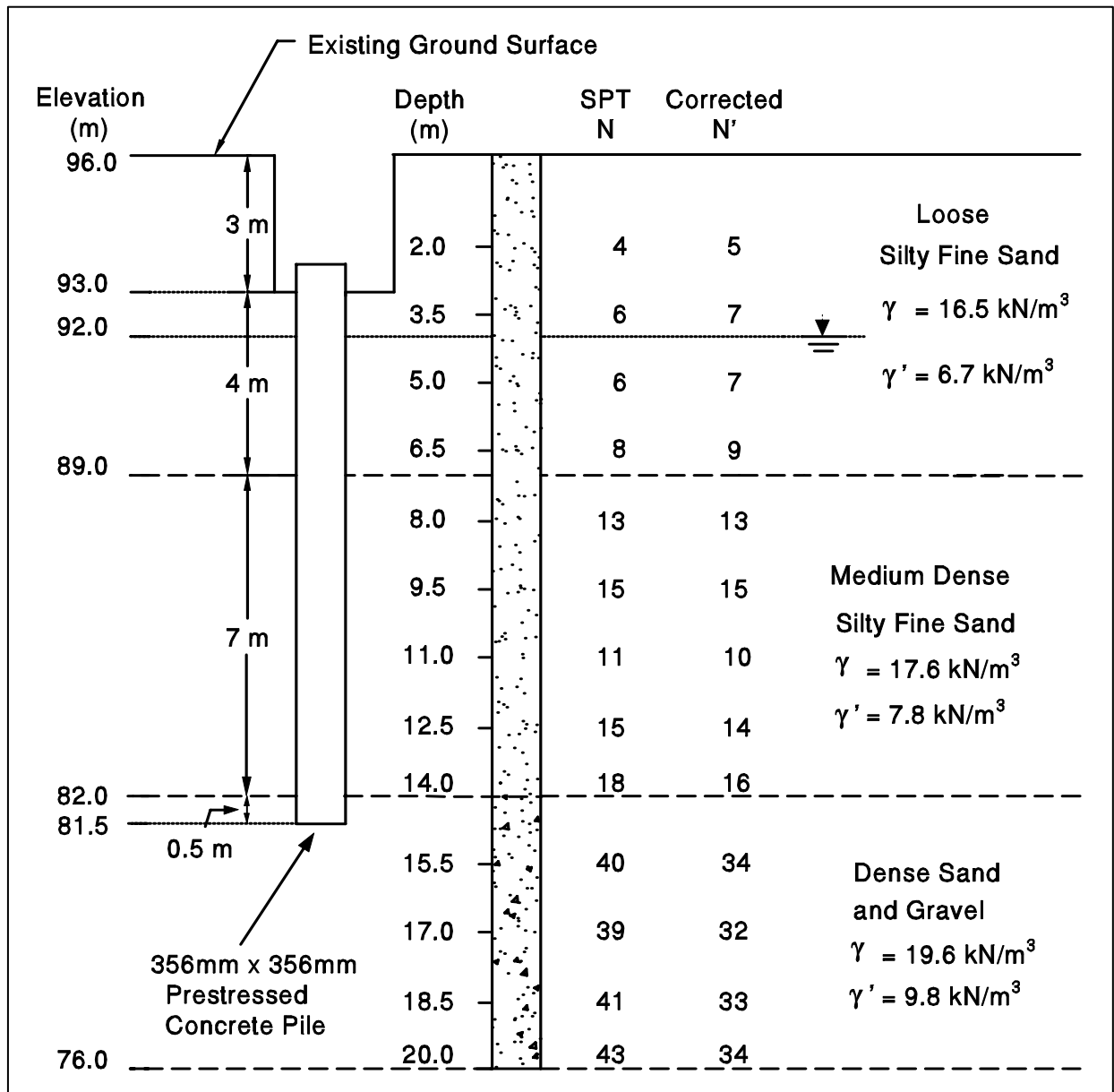


Figure F.3 Interpreted Soil Profile from Soil Boring S-1 at the North Abutment

STEP 1 Correct SPT field N values for overburden pressure.

Effective overburden pressures, p_o , are needed to correct SPT field N values. The method for calculating the effective overburden pressure is explained in Section 9.4. First, the soil profile should be delineated into layers based on soil type and density indicated by the corrected SPT N' value. However, since the corrected SPT N' value has yet to be calculated, the SPT field N' value should be used to estimate soil unit weights. Re-adjust the soil unit weight (if necessary) after the corrected SPT N' value has been obtained. The empirical correlation between soil unit weight and corrected SPT N' value is presented in Table 4-6. The effective overburden pressure diagram is presented below in Figure F.4.

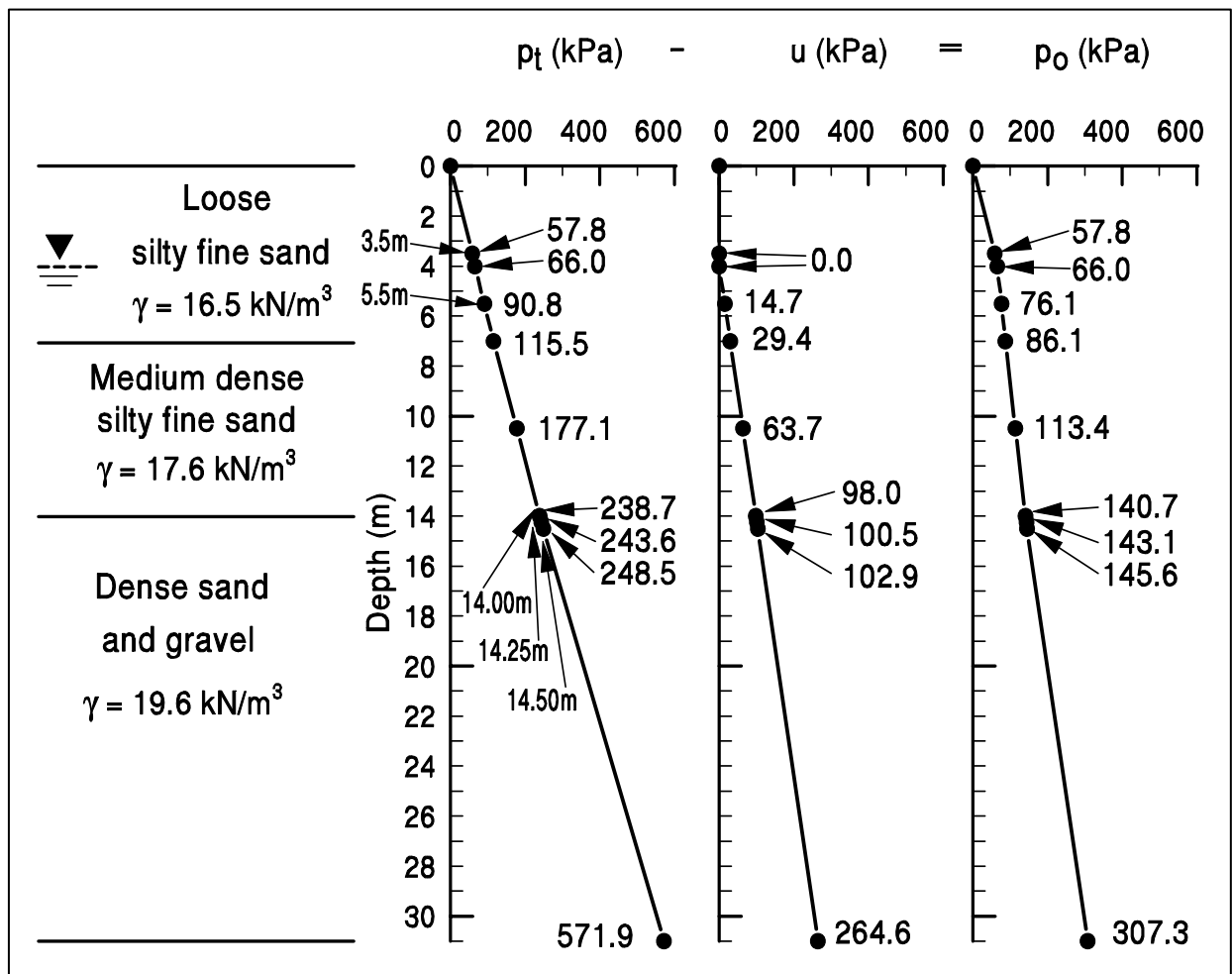


Figure F.4 Effective Overburden Pressure Diagram – North Abutment

STEP 1 (continued)

Use correction factors from Figure 4.6 (Chapter 4) to obtain corrected SPT N' values.

Depth (m)	p_o (kPa)	Field SPT N value	Correction Factor	Corrected SPT N' (Field SPT N x Correction Factor)
0.8	13.2	4	1.65	7
2.0	33.0	4	1.35	5
3.5	57.8	6	1.17	7
5.0	72.7	6	1.12	7
6.5	82.8	8	1.08	9
8.0	93.9	13	1.02	13
9.5	105.6	15	0.98	15
11.0	117.3	11	0.95	10
12.5	129.0	15	0.91	14
14.0	140.7	18	0.87	16
15.5	155.4	40	0.85	34
17.0	170.1	39	0.82	32
18.5	184.8	41	0.80	33
20.0	199.5	43	0.78	34
21.5	214.2	41	0.74	30
23.0	228.9	44	0.72	32
24.5	243.6	45	0.70	32
26.0	258.3	48	0.68	33
27.5	273.0	42	0.67	28
29.0	287.7	44	0.64	28
30.5	302.4	49	0.63	31

STEP 2 Compute the average corrected SPT N' value, \bar{N}' , for each soil layer.

Along the pile embedded length, the soil profile is delineated into three layers. Layer 1 is loose silty fine sand that is 4 meters thick, layer 2 is medium dense silty fine sand that is 7 meters thick, and layer 3 is dense sand and gravel that is 0.5 meter thick.

$$\bar{N}'_1 = \frac{7 + 7 + 9}{3} = 8$$

(Layer 1 - depth 3 to 7 m;
Loose silty fine sand)

$$\bar{N}'_2 = \frac{13 + 15 + 10 + 14 + 16}{5} = 14$$

(Layer 2 - depth 7 to 14 m;
Medium dense silty fine sand)

$$\bar{N}'_3 = 34$$

(Layer 3 - depth 14 to 14.5 m;
Dense sand and gravel)

STEP 3 Compute the unit shaft resistance, f_s (kPa), for each layer using the equation for driven displacement piles:

$$f_s = 2\bar{N}' \leq 100 \text{ kPa}$$

$$\text{Layer 1: } f_{s-1} = 2 (8) = 16 \text{ kPa}$$

$$\text{Layer 2: } f_{s-2} = 2 (14) = 28 \text{ kPa}$$

$$\text{Layer 3: } f_{s-3} = 2 (34) = 68 \text{ kPa}$$

STEP 4 Compute the ultimate shaft resistance, R_s (kN).

$$R_s = f_s A_s$$

$$\text{Layer 1: } R_{s1} = 16 \text{ kPa } (4)(0.356 \text{ m})(4 \text{ m}) = 91 \text{ kN}$$

$$\text{Layer 2: } R_{s2} = 28 \text{ kPa } (4)(0.356 \text{ m})(7 \text{ m}) = 279 \text{ kN}$$

$$\text{Layer 3: } R_{s3} = 68 \text{ kPa } (4)(0.356 \text{ m})(0.5 \text{ m}) = 48 \text{ kN}$$

$$\begin{aligned} \text{Total: } R_s &= R_{s1} + R_{s2} + R_{s3} = 91 \text{ kN} + 279 \text{ kN} + 48 \text{ kN} \\ &= 418 \text{ kN} \end{aligned}$$

STEP 5 Compute the average corrected SPT N' values, \bar{N}'_O and \bar{N}'_B , near pile toe.

The soil near the pile toe is a dense sand and gravel. Since the pile toe is situated near the interface of a weaker stratum overlying the bearing stratum, the average corrected SPT N' value for both the bearing stratum, \bar{N}'_B , and the overlying stratum, \bar{N}'_O , need to be calculated.

Average corrected SPT N' value for the overlying stratum:

$$\bar{N}'_O = \frac{13 + 15 + 10 + 14 + 16}{5} = 14$$

Average corrected SPT N' value for the bearing stratum:

$$\bar{N}'_B = 34$$

STEP 6 Compute the unit toe resistance, q_t (kPa).

Since a weaker stratum overlies the bearing stratum:

$$q_t = 400 \bar{N}'_O + \frac{(40 \bar{N}'_B - 40 \bar{N}'_O) D_B}{b} \leq 400 \bar{N}'_B$$

STEP 6 (continued)

$$= 400(14) + \frac{\{40(34) - 40(14)\}(0.5)}{0.356} \leq 400(34)$$

$$= 6,724 \leq 13,600 \rightarrow \text{so } q_t = 6,724 \text{ kPa}$$

STEP 7 Compute the ultimate toe resistance, R_t (kN).

$$\begin{aligned} R_t &= q_t A_t = 6,724 \text{ kPa} (0.356 \text{ m})(0.356 \text{ m}) \\ &= 854 \text{ kN} \end{aligned}$$

STEP 8 Compute the ultimate pile capacity, Q_u (kN).

$$\begin{aligned} Q_u &= R_s + R_t \\ &= 418 \text{ kN} + 854 \text{ kN} \\ &= 1,272 \text{ kN} \end{aligned}$$

Note: The ultimate capacity according to the Meyerhof method is less than the required 1780 kN ultimate capacity. The Meyerhof method would require a pile penetration depth of 13 meters for a 1,780 kN capacity.

STEP 9 Compute allowable design load, Q_a (kN).

$$Q_a = \frac{Q_u}{\text{Factor of Safety}} = \frac{1,272 \text{ kN}}{\text{Factor of Safety}}$$

Note: Factor of Safety should be selected based on the construction control method to be specified. Recommended factors of safety are described in Section 9.6.

F.2.1.2 Static Axial Pile Capacity Calculations by Nordlund Method

For the soil profile interpreted from Soil Boring S-1 as shown in Figure F.3. Perform a Nordlund method pile capacity calculation for an embedded length of 11.5 meters. Use the step-by-step method outlined in Section 9.7.1.1c.

STEP 1 Delineate the soil profile into layers and determine the ϕ angle for each layer.

- a. Construct p_o diagram using procedure described in Section 9.4. This is completed in Figure F.4.
- b. Correct SPT field N values for overburden pressure using Figure 4.6 from Chapter 4 and obtain corrected SPT N' values. For Soil Boring S-1, this has been done in the previous example (see Section F.2.1.1, Step 1).
- c. Determine the ϕ angle for each layer from laboratory tests or in-situ data.

Since the ϕ angle is not provided by either laboratory or in-situ data, it should be determined using the average corrected SPT N' value, \bar{N}' , as calculated below.

- d. In the absence of laboratory or in-situ test data, determine the average corrected SPT N' value, \bar{N}' , for each soil layer and estimate ϕ angle from Table 4-6 in Chapter 4.

As the example in Section F.2.1.1, the soil profile along the pile embedded length is delineated into three layers of 4.0, 7.0, and 0.5 meters thick. The average corrected SPT N' value for each soil layer is as follow.

Layer 1:	$\bar{N}'_1 = 8$	(Layer 1 - depth 3 to 7 m; Loose silty fine sand)
Layer 2:	$\bar{N}'_2 = 14$	(Layer 2 - depth 7 to 14 m; Medium dense silty fine sand)
Layer 3:	$\bar{N}'_3 = 34$	(Layer 3 - depth 14 to 14.5 m; Dense sand and gravel)

STEP 1 (continued)

Use the average corrected SPT N' value for each soil layer to estimate ϕ angle from Table 4-6 in Chapter 4.

$$\text{Layer 1: } \phi_1 = 29^\circ \quad \text{for } \bar{N}_1' = 8$$

$$\text{Layer 2: } \phi_2 = 31^\circ \quad \text{for } \bar{N}_2' = 14$$

$$\text{Layer 3: } \phi_3 = 36^\circ \quad \text{for } \bar{N}_3' = 34$$

STEP 2 Determine δ , the friction angle between pile and soil based on displaced soil volume, V , and the soil friction angle, ϕ .

- a. Compute the volume of soil displaced per unit length of pile, V .
Since this is a uniform cross section ($\omega = 0^\circ$) pile,

$$V = (0.356 \text{ m}) (0.356 \text{ m}) (1.0 \text{ m/m}) = 0.127 \text{ m}^3/\text{m}$$

For a non-uniform pile cross section ($\omega \neq 0^\circ$), the pile should be divided into sections and the volume for each section should be calculated.

- b. Enter Figure 9.10 with V and determine δ/ϕ ratio for pile type.

For a precast, prestressed concrete pile with $V = 0.127 \text{ m}^3/\text{m}$,

$$\delta/\phi = 0.84$$

- c. Calculate δ from δ/ϕ ratio.

$$\text{Layer 1: } \delta_1 = 0.84 (29^\circ) = 24.4^\circ$$

$$\text{Layer 2: } \delta_2 = 0.84 (31^\circ) = 26.0^\circ$$

$$\text{Layer 3: } \delta_3 = 0.84 (36^\circ) = 30.2^\circ$$

STEP 3 Determine the coefficient of lateral earth pressure, K_δ , for each ϕ angle.

- a. Determine K_δ for ϕ angle based on displaced volume, V , and pile taper angle, ω , using either Figure 9.11, 9.12, 9.13, or 9.14 and the appropriate procedure described in Step 3b, 3c, 3d, or 3e.

The pile taper angle, ω , = 0° .

For Layer 1:

$\phi_1 = 29^\circ$ and $V = 0.127 \text{ m}^3/\text{m}$, therefore use Step 3e.

First, use linear interpolation to determine K_δ for the required ϕ angle of 29° at the given displaced volume curves of 0.093 and $0.93 \text{ m}^3/\text{m}$.

For $V = 0.093 \text{ m}^3/\text{m}$:

$\phi = 25^\circ$ $K_\delta = 0.85$ (from Figure 9.11)

$\phi = 29^\circ$ $K_\delta =$ (using linear interpolation)

$\phi = 30^\circ$ $K_\delta = 1.15$ (from Figure 9.12)

Using linear interpolation to determine K_δ for $\phi = 29^\circ$:

$$K_\delta = 0.85 + \frac{(29 - 25)}{(30 - 25)}(1.15 - 0.85)$$
$$= 1.09$$

For $V = 0.93 \text{ m}^3/\text{m}$:

$\phi = 25^\circ$ $K_\delta = 1.00$ (from Figure 9.11)

$\phi = 29^\circ$ $K_\delta =$ (using linear interpolation)

$\phi = 30^\circ$ $K_\delta = 1.45$ (from Figure 9.12)

STEP 3 (continued)

Using linear interpolation to determine K_{δ} for $\phi = 29^{\circ}$:

$$\begin{aligned}K_{\delta} &= 1.0 + \frac{(29 - 25)}{(30 - 25)} (1.45 - 1.0) \\ &= 1.36\end{aligned}$$

Then use log linear interpolation to determine K_{δ} for $\phi = 29^{\circ}$ and $V = 0.127 \text{ m}^3/\text{m}$.

$$V = 0.093 \text{ m}^3/\text{m} \quad K_{\delta} = 1.09$$

$$V = 0.127 \text{ m}^3/\text{m} \quad K_{\delta} = \quad (\text{using log linear interpolation})$$

$$V = 0.93 \text{ m}^3/\text{m} \quad K_{\delta} = 1.36$$

Log linear interpolation for $V = 0.127 \text{ m}^3/\text{m}$:

$$\begin{aligned}K_{\delta 1} &= 1.09 + \frac{\log(0.127) - \log(0.093)}{\log(0.93) - \log(0.093)} (1.36 - 1.09) \\ &= 1.13\end{aligned}$$

Table 9-4b can be used to check the above calculations. From Table 9-4b, for $\phi = 29^{\circ}$:

$$V = 0.093 \text{ m}^3/\text{m} \quad K_{\delta} = 1.09 \text{ (from Table 9-4b)}$$

$$V = 0.127 \text{ m}^3/\text{m} \quad K_{\delta} = 1.13 \text{ (from log linear interpolation)}$$

$$V = 0.186 \text{ m}^3/\text{m} \quad K_{\delta} = 1.17 \text{ (from Table 9-4b)}$$

STEP 3 (continued)

For Layer 2:

$\phi_2 = 31^\circ$ and $V = 0.127 \text{ m}^3/\text{m}$, therefore use Step 3e.

First, use linear interpolation to determine K_δ for the required ϕ angle of 31° at the given displaced volume curves of 0.093 and $0.93 \text{ m}^3/\text{m}$.

For $V = 0.093 \text{ m}^3/\text{m}$:

$\phi = 30^\circ$ $K_\delta = 1.15$ (from Figure 9.12)

$\phi = 31^\circ$ $K_\delta =$ (using linear interpolation)

$\phi = 35^\circ$ $K_\delta = 1.75$ (from Figure 9.13)

Using linear interpolation to determine K_δ for $\phi = 31^\circ$:

$$\begin{aligned} K_\delta &= 1.15 + \frac{(31-30)}{(35-30)} (1.75 - 1.15) \\ &= 1.27 \end{aligned}$$

For $V = 0.93 \text{ m}^3/\text{m}$:

$\phi = 30^\circ$ $K_\delta = 1.45$ (from Figure 9.12)

$\phi = 31^\circ$ $K_\delta =$ (using linear interpolation)

$\phi = 35^\circ$ $K_\delta = 2.35$ (from Figure 9.13)

Using linear interpolation to determine K_δ for $\phi = 31^\circ$:

$$K_\delta = 1.45 + \frac{(31-30)}{(35-30)} (2.35 - 1.45) = 1.63$$

STEP 3 (continued)

Then use log linear interpolation to determine K_{δ} for $\phi = 31^{\circ}$ and $V = 0.127 \text{ m}^3/\text{m}$.

$$V = 0.093 \text{ m}^3/\text{m} \quad K_{\delta} = 1.27$$

$$V = 0.127 \text{ m}^3/\text{m} \quad K_{\delta} = \quad (\text{using log linear interpolation})$$

$$V = 0.93 \text{ m}^3/\text{m} \quad K_{\delta} = 1.63$$

Log linear interpolation for $V = 0.127 \text{ m}^3/\text{m}$:

$$\begin{aligned} K_{\delta 2} &= 1.27 + \frac{\log(0.127) - \log(0.093)}{\log(0.93) - \log(0.093)} (1.63 - 1.27) \\ &= 1.32 \end{aligned}$$

Table 9-4b can be used to check the above calculations. From Table 9-4b, for $\phi = 31^{\circ}$:

$$V = 0.093 \text{ m}^3/\text{m} \quad K_{\delta} = 1.27 \text{ (from Table 9-4b)}$$

$$V = 0.127 \text{ m}^3/\text{m} \quad K_{\delta} = 1.32 \text{ (from log linear interpolation)}$$

$$V = 0.186 \text{ m}^3/\text{m} \quad K_{\delta} = 1.38 \text{ (from Table 9-4b)}$$

STEP 3 (continued)

For Layer 3:

$\phi_3 = 36^\circ$ and $V = 0.127 \text{ m}^3/\text{m}$, therefore use Step 3e.

First, use linear interpolation to determine K_δ for the required ϕ angle of 36° at the given displaced volume curves of 0.093 and $0.93 \text{ m}^3/\text{m}$.

For $V = 0.093 \text{ m}^3/\text{m}$:

$$\phi = 35^\circ \quad K_\delta = 1.75 \quad (\text{from Figure 9.13})$$

$$\phi = 36^\circ \quad K_\delta = \quad (\text{using linear interpolation})$$

$$\phi = 40^\circ \quad K_\delta = 3.00 \quad (\text{from Figure 9.14})$$

Using linear interpolation to determine K_δ for $\phi = 36^\circ$:

$$\begin{aligned} K_\delta &= 1.75 + \frac{(36 - 35)}{(40 - 35)} (3.00 - 1.75) \\ &= 2.00 \end{aligned}$$

For $V = 0.93 \text{ m}^3/\text{m}$:

$$\phi = 35^\circ \quad K_\delta = 2.35 \quad (\text{from Figure 9.13})$$

$$\phi = 36^\circ \quad K_\delta = \quad (\text{using linear interpolation})$$

$$\phi = 40^\circ \quad K_\delta = 4.30 \quad (\text{from Figure 9.14})$$

Using linear interpolation to determine K_δ for $\phi = 36^\circ$:

$$K_\delta = 2.35 + \frac{(36 - 35)}{(40 - 35)} (4.30 - 2.35) = 2.74$$

STEP 3 (continued)

Then use log linear interpolation to determine K_δ for $\phi = 36^\circ$ and $V = 0.127 \text{ m}^3/\text{m}$.

$$V = 0.093 \text{ m}^3/\text{m} \quad K_\delta = 2.00$$

$$V = 0.127 \text{ m}^3/\text{m} \quad K_\delta = \quad \text{(using log linear interpolation)}$$

$$V = 0.93 \text{ m}^3/\text{m} \quad K_\delta = 2.74$$

Log linear interpolation for $V = 0.127 \text{ m}^3/\text{m}$:

$$\begin{aligned} K_{\delta 3} &= 2.00 + \frac{\log(0.127) - \log(0.093)}{\log(0.93) - \log(0.093)} (2.74 - 2.00) \\ &= 2.10 \end{aligned}$$

Table 9-4b can be used to check the above calculations. From Table 9-4b, for $\phi = 36^\circ$:

$$V = 0.093 \text{ m}^3/\text{m} \quad K_\delta = 2.00 \text{ (from Table 9-4b)}$$

$$V = 0.127 \text{ m}^3/\text{m} \quad K_\delta = 2.10 \text{ (from log linear interpolation)}$$

$$V = 0.186 \text{ m}^3/\text{m} \quad K_\delta = 2.22 \text{ (from Table 9-4b)}$$

STEP 4 Determine the correction factor, C_F , to be applied to K_δ if $\delta \neq \phi$.

Use Figure 9.15 to determine the correction factor for each K_δ . Enter figure with ϕ angle and $\delta/\phi=0.84$ to determine C_F .

Layer 1: For $\phi_1 = 29^\circ \rightarrow C_{F1} = 0.96$

Layer 2: For $\phi_2 = 31^\circ \rightarrow C_{F2} = 0.94$

Layer 3: For $\phi_3 = 36^\circ \rightarrow C_{F3} = 0.93$

STEP 5 Compute the average effective overburden pressure at the midpoint of each soil layer, p_d (kPa). (Note: a limiting value is not applied to p_d).

The effective overburden pressure at the midpoint of each soil layer is equal to the average effective overburden pressure of that layer. The effective overburden pressure versus depth for the North Abutment has been computed and tabulated in the previous example (see Section F.2.1.1, Step 1). The effective overburden pressure diagram for the North Abutment is presented in Figure F.4. Since the effective overburden pressure is non linear in layer 1, this layer should be split at the water table location into layer 1a and layer 1b. The effective overburden pressure is then calculated at the midpoint of each of these layers.

Layer 1a: $p_{d1a} = 57.8 \text{ kPa}$ (midpoint of layer 1a - at depth of 3.5 m)

Layer 1b: $p_{d1b} = 76.1 \text{ kPa}$ (midpoint of layer 1b - at depth of 5.5 m)

Layer 2: $p_{d2} = 113.4 \text{ kPa}$ (midpoint of layer 2 - at depth of 10.5 m)

Layer 3: $p_{d3} = 143.1 \text{ kPa}$ (midpoint of layer 3 - at depth of 14.25 m)

STEP 6 Compute the shaft resistance in each soil layer. Sum the shaft resistance from each soil layer to obtain the ultimate shaft resistance, R_s (kN).

$$R_s = K_\delta C_F p_d \sin \delta C_d D \quad (\text{for uniform pile cross section})$$

$$\text{where: } C_d = (4)(0.356 \text{ m}) = 1.424 \text{ m}$$

$$\begin{aligned} \text{Layer 1a: } R_{s1a} &= 1.13 (0.96) (57.8 \text{ kPa}) (\sin 24.4^\circ) (1.424 \text{ m}) (1 \text{ m}) \\ &= 37 \text{ kN} \end{aligned}$$

$$\begin{aligned} \text{Layer 1b: } R_{s1b} &= 1.13 (0.96) (76.1 \text{ kPa}) (\sin 24.4^\circ) (1.424 \text{ m}) (3 \text{ m}) \\ &= 146 \text{ kN} \end{aligned}$$

$$\begin{aligned} \text{Layer 2: } R_{s2} &= 1.32 (0.94) (113.4 \text{ kPa}) (\sin 26.0^\circ) (1.424 \text{ m}) (7 \text{ m}) \\ &= 615 \text{ kN} \end{aligned}$$

$$\begin{aligned} \text{Layer 3: } R_{s3} &= 2.10 (0.93) (143.2 \text{ kPa}) (\sin 30.2^\circ) (1.424 \text{ m}) (0.5 \text{ m}) \\ &= 100 \text{ kN} \end{aligned}$$

$$\begin{aligned} \text{Total: } R_s &= R_{s1a} + R_{s1b} + R_{s2} + R_{s3} \\ &= 37 \text{ kN} + 146 \text{ kN} + 615 \text{ kN} + 100 \text{ kN} \\ &= 898 \text{ kN} \end{aligned}$$

STEP 7 Determine the α_t coefficient and the bearing capacity factor, N'_q , from the ϕ angle near the pile toe.

Since the ϕ angle is not provided by either laboratory tests or in-situ data, the ϕ angle can be estimated from Table 4-6 using the average corrected SPT N' value over the zone from the pile toe to 3 diameter below the pile toe (1.065 meters). The soil near the pile toe is a dense sand and gravel.

$$\bar{N}'_{\text{toe}} = 34 \quad \rightarrow \quad \phi_{\text{toe}} = 36^\circ$$

a. Enter Figure 9.16(a) with ϕ angle near pile toe to determine α_t coefficient based on pile length to diameter ratio.

$$(D/b) = (11.5 \text{ m}) / (0.356 \text{ m}) = 32.3$$

$$\text{For } \phi_{\text{toe}} = 36^\circ \text{ and } (D/b) = 32.3 \quad \rightarrow \quad \alpha_t = 0.68$$

b. Enter Figure 9.16(b) with ϕ angle near pile toe to determine N'_q .

$$\text{For } \phi_{\text{toe}} = 36^\circ \quad \rightarrow \quad N'_q = 75$$

STEP 8 Compute the effective overburden pressure at the pile toe, p_t (kPa).

The effective overburden pressure at the pile toe should be limited to a maximum of 150 kPa.

The effective overburden pressure at the pile toe, p_t , has been computed in the previous example (Section F.2.1.1, Step 1):

$$p_t = 145.6 \text{ kPa} < 150 \text{ kPa} \quad \rightarrow \quad \text{OK}$$

STEP 9 Compute the ultimate toe resistance, R_t (kN).

$$\begin{aligned} \text{a. } R_t &= \alpha_t N'_q A_t p_t \\ &= 0.68 (75) (0.356 \text{ m})(0.356 \text{ m}) (145.6 \text{ kPa}) \\ &= 943 \text{ kN} \end{aligned}$$

$$\text{b. limiting } R_t = q_L A_t$$

Using the estimated $\phi=36^\circ$ and Figure 9.17, the limiting unit toe resistance is:

$$q_L = 7,400 \text{ kPa}$$

Therefore,

$$R_t = 7,400 \text{ kPa} (0.356 \text{ m})(0.356 \text{ m}) = 940 \text{ kN}$$

c. Use lesser of the two R_t values obtained in steps a and b which is:

$$R_t = 940 \text{ kN}$$

STEP 10 Compute the ultimate pile capacity, Q_u (kN).

$$\begin{aligned} Q_u &= R_s + R_t \\ &= 898 \text{ kN} + 940 \text{ kN} = 1,838 \text{ kN} \end{aligned}$$

STEP 11 Compute the allowable design load, Q_a (kN).

$$Q_a = \frac{Q_u}{\text{Factor of Safety}} = \frac{1,838 \text{ kN}}{\text{Factor of Safety}}$$

Note: Factor of Safety should be selected based on the construction control method to be specified. Recommended factors of safety are described in Section 9.6.

F.2.1.3 Static Axial Pile Capacity Calculations by Effective Stress Method

For the soil profile interpreted from Soil Boring S-1 as shown in Figure F.3. Perform an Effective Stress method pile capacity calculation for an embedded length of 11.5 meters. Use the step-by-step method outlined in Section 9.7.1.3.

STEP 1 Delineate the soil profile into layers and determine ϕ' angle for each layer.

- a. Use the procedure described in Section 9.4 to construct a p_o diagram.

For Soil Boring S-1, the p_o diagram has been constructed in Section F.2.1.1 - Step 1 and also presented in Figure F.4.

- b. Divide the soil profile throughout the pile penetration depth into layers and determine the effective overburden pressure, p_o , at the midpoint of each layer.

As the example in Section F.2.1.1, the soil profile along the pile embedded length is delineated into three layers of 4.0, 7.0, and 0.5 meter thick. Since the effective overburden pressure is non linear in layer 1, this layer should be split at the water table location into layer 1a and 1b. The average effective overburden pressure of each layer is equal to the effective overburden pressure at the midpoint of that layer, as follows.

Layer 1a: $p_{o1a} = 57.8 \text{ kPa}$ (midpoint of layer 1a - at depth of 3.5 m)

Layer 1b: $p_{o1b} = 76.1 \text{ kPa}$ (midpoint of layer 1b - at depth of 5.5 m)

Layer 2: $p_{o2} = 113.4 \text{ kPa}$ (midpoint of layer 2 - at depth of 10.5 m)

Layer 3: $p_{o3} = 143.1 \text{ kPa}$ (midpoint of layer 3 - at depth of 14.25 m)

- c. Determine the ϕ' angle for each soil layer from laboratory or in-situ test data.

Since the ϕ' angle is not provided by either laboratory or in-situ test data, the average corrected SPT N' value will be used to estimate the ϕ' angle.

STEP 1 (continued)

- d. In the absence of laboratory or in-situ test data for cohesionless soil layers, determine the average corrected SPT N' value for each soil layer and estimate the ϕ' angle from Table 4-6 in Chapter 4.

As in the previous example (Section F.2.1.1), the average corrected SPT N' value and the soil type for each soil layer is as follows.

Layer 1:	$\bar{N}_1' = 8$	(Layer 1 - depth 3 to 7 m; Loose silty fine sand)
Layer 2:	$\bar{N}_2' = 14$	(Layer 2 - depth 7 to 14 m; Medium dense silty fine sand)
Layer 3:	$\bar{N}_3' = 34$	(Layer 3 - depth 14 to 14.5 m; Dense sand and gravel)

Use the average corrected SPT N' value for each soil layer to estimate ϕ' angle from Table 4-6 in Chapter 4.

Layer 1:	$\phi_1' = 29^\circ$	for $\bar{N}_1' = 8$
Layer 2:	$\phi_2' = 31^\circ$	for $\bar{N}_2' = 14$
Layer 3:	$\phi_3' = 36^\circ$	for $\bar{N}_3' = 34$

STEP 2 Select the β coefficient for each soil layer.

- a. Use local experience to select β coefficient for each layer.

Assume no local experience.

STEP 2 (continued)

- b. In the absence of local experience, use Table 9-6 or Figure 9.20 to estimate β coefficient from ϕ' angle for each layer.

Use the soil type, the estimated ϕ' angle, and Table 9-6 or Figure 9.20 to estimate the β coefficient for each layer.

Layer 1: $\beta_1 = 0.30$ (For loose silty fine sand with $\phi_1' = 29^\circ$)

Layer 2: $\beta_2 = 0.33$ (For medium dense silty fine sand with $\phi_2' = 31^\circ$)

Layer 3: $\beta_3 = 0.40$ (For dense sand and gravel with $\phi_3' = 36^\circ$)

STEP 3 For each soil layer compute the unit shaft resistance, f_s (kPa).

$$f_s = \beta p_o$$

Layer 1a: $f_{s1a} = 0.30 (57.8 \text{ kPa}) = 17.34 \text{ kPa}$

Layer 1b: $f_{s1b} = 0.30 (76.1 \text{ kPa}) = 22.83 \text{ kPa}$

Layer 2: $f_{s2} = 0.33 (113.4 \text{ kPa}) = 37.42 \text{ kPa}$

Layer 3: $f_{s3} = 0.40 (143.1 \text{ kPa}) = 57.24 \text{ kPa}$

STEP 4 Compute the shaft resistance in each soil layer and the ultimate shaft resistance, R_s (kN), from the sum of the shaft resistance from each soil layer.

$$R_s = f_s A_s$$

where A_s = Pile-soil surface area from pile perimeter and length

Layer 1a: $R_{s1a} = 17.34 (4) (0.356 \text{ m}) (1 \text{ m}) = 25 \text{ kN}$

Layer 1b: $R_{s1b} = 22.83 (4) (0.356 \text{ m}) (3 \text{ m}) = 98 \text{ kN}$

STEP 4 (continued)

$$\text{Layer 2: } R_{s2} = 37.42 (4) (0.356 \text{ m}) (7 \text{ m}) = 373 \text{ kN}$$

$$\text{Layer 3: } R_{s3} = 57.24 (4) (0.356 \text{ m}) (0.5 \text{ m}) = 41 \text{ kN}$$

$$\begin{aligned} \text{Total: } R_s &= R_{s1a} + R_{s1b} + R_{s2} + R_{s3} \\ &= 25 \text{ kN} + 98 \text{ kN} + 373 \text{ kN} + 41 \text{ kN} \\ &= 537 \text{ kN} \end{aligned}$$

STEP 5 Compute the unit toe resistance, q_t (kPa).

$$q_t = N_t p_t$$

- a. Use local experience to select N_t coefficient.

Assume no local experience.

- b. In the absence of local experience, estimate N_t coefficient from Table 9-6 or Figure 9.21 based on ϕ' angle.

Table 9-6 or Figure 9.21 are a function of soil type and the ϕ' angle. The soil type for each layer can be obtained from the soil boring. The ϕ' angle for each layer can be obtained from laboratory tests or in-situ data. In the absence of either laboratory or in-situ test data, the ϕ' angle should be estimated from Table 4-6 in Chapter 4 using the average corrected SPT N' value, \bar{N}' , over the zone from the pile toe to 3 diameter below the pile toe (1.065 meters). The soil near the pile toe is a dense sand and gravel.

$$\bar{N}'_{\text{toe}} = 34 \quad \rightarrow \quad \phi'_{\text{toe}} = 36^\circ$$

Use the soil type, the estimated ϕ' angle, and Table 9-6 or Figure 9.21 to estimate the N_t coefficient.

$$N_t = 70 \quad (\text{For dense sand and gravel with } \phi'_{\text{toe}} = 36^\circ)$$

- c. Calculate the effective overburden pressure at the pile toe, p_t .

The effective overburden pressure at the pile toe, p_t , has been computed in the previous example (Section F.2.1.1, Step 1):

$$p_t = 145.6 \text{ kPa}$$

The unit toe resistance, q_t is:

$$\begin{aligned} q_t &= N_t p_t \\ &= 70 (145.6 \text{ kPa}) = 10,192 \text{ kPa} \end{aligned}$$

- STEP 6 Compute the ultimate toe resistance, R_t (kN).

$$\begin{aligned} R_t &= q_t A_t \\ &= 10,192 (0.356 \text{ m}) (0.356 \text{ m}) \\ &= 1,294 \text{ kN} \end{aligned}$$

- STEP 7 Compute the ultimate pile capacity, Q_u (kN).

$$\begin{aligned} Q_u &= R_s + R_t \\ &= 537 \text{ kN} + 1,294 \text{ kN} \\ &= 1,831 \text{ kN} \end{aligned}$$

- STEP 8 Compute the allowable design load, Q_a (kN).

$$Q_a = \frac{Q_u}{\text{Factor of Safety}} = \frac{1,831 \text{ kN}}{\text{Factor of Safety}}$$

Note: Factor of Safety should be selected based on the construction control method to be specified. Recommended factors of safety are described in Section 9.6.

F.2.1.4 Static Axial Pile Capacity Calculations by Driven Computer Program

Note: In the following tables, the depth corresponding to the pile tip is 14.5 m. The “driving strength loss (%)” factor used in Driven for Boring S-2 was selected based on Table 9-20. Because these soils are cohesionless sands and gravels, the soil set-up factor selected was 1.0. For this problem, the driving strength loss is therefore 0%. In the Driven results, the “Ultimate,” “Restrike” and “Driving” tables are the same because no strength was lost during driving to be regained when the restrike is performed and no effective stress losses due to scour are present.

DRIVEN 1.2 **GENERAL PROJECT INFORMATION**

Filename: C:\DRIVEN\S1.DVN
Project Name: Boring S-1 Project Date: 09/11/2003
Project Client: FHWA Manual
Computed By: BRR
Project Manager:

PILE INFORMATION

Pile Type: Concrete Pile
Top of Pile: 2.50 m
Length of Square Side: 356.00 mm

ULTIMATE CONSIDERATIONS

Water Table Depth At Time Of: - Drilling: 4.00 m
 - Driving/Restrike 4.00 m
 - Ultimate: 4.00 m
Ultimate Considerations: - Local Scour: 0.00 m
 - Long Term Scour: 0.00 m
 - Soft Soil: 0.00 m

ULTIMATE PROFILE

Layer	Type	Thickness	Driving Loss	Unit Weight	Strength	Ultimate Curve
1	Cohesionless	7.00 m	0.00%	16.50 kN/m ³	29.0/29.0	Nordlund
2	Cohesionless	7.00 m	0.00%	17.60 kN/m ³	31.0/31.0	Nordlund
3	Cohesionless	0.50 m	0.00%	19.60 kN/m ³	36.0/36.0	Nordlund
4	Cohesionless	5.50 m	0.00%	19.60 kN/m ³	36.0/36.0	Nordlund

RESTRIKE - SKIN FRICTION

Depth	Soil Type	Effective Stress At Midpoint	Sliding Friction Angle	Adhesion	Skin Friction
0.01 m	Cohesionless	0.00 kPa	0.00	N/A	0.00 kN
2.49 m	Cohesionless	0.00 kPa	0.00	N/A	0.00 kN
2.50 m	Cohesionless	41.25 kPa	24.43	N/A	0.00 kN
3.01 m	Cohesionless	45.46 kPa	24.43	N/A	14.68 kN
3.99 m	Cohesionless	53.54 kPa	24.43	N/A	50.52 kN
4.01 m	Cohesionless	66.04 kPa	24.43	N/A	51.35 kN
6.99 m	Cohesionless	76.02 kPa	24.43	N/A	194.85 kN
7.01 m	Cohesionless	86.14 kPa	26.11	N/A	196.07 kN
10.01 m	Cohesionless	97.84 kPa	26.11	N/A	426.25 kN
13.01 m	Cohesionless	109.53 kPa	26.11	N/A	711.46 kN
13.99 m	Cohesionless	113.35 kPa	26.11	N/A	816.55 kN
14.01 m	Cohesionless	140.74 kPa	30.32	N/A	819.63 kN
14.49 m	Cohesionless	143.09 kPa	30.32	N/A	915.98 kN
14.51 m	Cohesionless	145.64 kPa	30.32	N/A	920.06 kN
17.51 m	Cohesionless	160.33 kPa	30.32	N/A	1594.81 kN
19.99 m	Cohesionless	172.48 kPa	30.32	N/A	2245.97 kN

RESTRIKE - END BEARING

Depth	Soil Type	Effective Stress At Tip	Bearing Cap. Factor	Limiting End Bearing	End Bearing
0.01 m	Cohesionless	0.00 kPa	26.40	80.82 kN	0.00 kN
2.49 m	Cohesionless	0.00 kPa	26.40	80.82 kN	0.00 kN
2.50 m	Cohesionless	41.25 kPa	26.40	80.82 kN	77.01 kN
3.01 m	Cohesionless	49.67 kPa	26.40	80.82 kN	80.82 kN
3.99 m	Cohesionless	65.84 kPa	26.40	80.82 kN	80.82 kN
4.01 m	Cohesionless	66.07 kPa	26.40	80.82 kN	80.82 kN
6.99 m	Cohesionless	86.03 kPa	26.40	80.82 kN	80.82 kN
7.01 m	Cohesionless	86.18 kPa	35.20	125.39 kN	125.39 kN
10.01 m	Cohesionless	109.57 kPa	35.20	125.39 kN	125.39 kN
13.01 m	Cohesionless	132.97 kPa	35.20	125.39 kN	125.39 kN
13.99 m	Cohesionless	140.61 kPa	35.20	125.39 kN	125.39 kN
14.01 m	Cohesionless	140.79 kPa	77.60	919.89 kN	919.89 kN
14.49 m	Cohesionless	145.49 kPa	77.60	919.89 kN	919.89 kN
14.51 m	Cohesionless	145.69 kPa	77.60	919.89 kN	919.89 kN
17.51 m	Cohesionless	175.08 kPa	77.60	919.89 kN	919.89 kN
19.99 m	Cohesionless	199.38 kPa	77.60	919.89 kN	919.89 kN

RESTRIKE - SUMMARY OF CAPACITIES

Depth	Skin Friction	End Bearing	Total Capacity
0.01 m	0.00 kN	0.00 kN	0.00 kN
2.49 m	0.00 kN	0.00 kN	0.00 kN
2.50 m	0.00 kN	77.01 kN	77.01 kN
3.01 m	14.68 kN	80.82 kN	95.50 kN
3.99 m	50.52 kN	80.82 kN	131.34 kN
4.01 m	51.35 kN	80.82 kN	132.18 kN
6.99 m	194.85 kN	80.82 kN	275.67 kN
7.01 m	196.07 kN	125.39 kN	321.45 kN
10.01 m	426.25 kN	125.39 kN	551.64 kN
13.01 m	711.46 kN	125.39 kN	836.84 kN
13.99 m	816.55 kN	125.39 kN	941.94 kN
14.01 m	819.63 kN	919.89 kN	1739.51 kN
14.49 m	915.98 kN	919.89 kN	1835.86 kN
14.51 m	920.06 kN	919.89 kN	1839.95 kN
17.51 m	1594.81 kN	919.89 kN	2514.69 kN
19.99 m	2245.97 kN	919.89 kN	3165.86 kN

DRIVING - SKIN FRICTION

Depth	Soil Type	Effective Stress At Midpoint	Sliding Friction Angle	Adhesion	Skin Friction
0.01 m	Cohesionless	0.00 kPa	0.00	N/A	0.00 kN
2.49 m	Cohesionless	0.00 kPa	0.00	N/A	0.00 kN
2.50 m	Cohesionless	41.25 kPa	24.43	N/A	0.00 kN
3.01 m	Cohesionless	45.46 kPa	24.43	N/A	14.68 kN
3.99 m	Cohesionless	53.54 kPa	24.43	N/A	50.52 kN
4.01 m	Cohesionless	66.04 kPa	24.43	N/A	51.35 kN
6.99 m	Cohesionless	76.02 kPa	24.43	N/A	194.85 kN
7.01 m	Cohesionless	86.14 kPa	26.11	N/A	196.07 kN
10.01 m	Cohesionless	97.84 kPa	26.11	N/A	426.25 kN
13.01 m	Cohesionless	109.53 kPa	26.11	N/A	711.46 kN
13.99 m	Cohesionless	113.35 kPa	26.11	N/A	816.55 kN
14.01 m	Cohesionless	140.74 kPa	30.32	N/A	819.63 kN
14.49 m	Cohesionless	143.09 kPa	30.32	N/A	915.98 kN
14.51 m	Cohesionless	145.64 kPa	30.32	N/A	920.06 kN
17.51 m	Cohesionless	160.33 kPa	30.32	N/A	1594.81 kN
19.99 m	Cohesionless	172.48 kPa	30.32	N/A	2245.97 kN

DRIVING - END BEARING

Depth	Soil Type	Effective Stress At Tip Factor	Bearing Cap.	Limiting End Bearing	End Bearing
0.01 m	Cohesionless	0.00 kPa	26.40	80.82 kN	0.00 kN
2.49 m	Cohesionless	0.00 kPa	26.40	80.82 kN	0.00 kN
2.50 m	Cohesionless	41.25 kPa	26.40	80.82 kN	77.01 kN
3.01 m	Cohesionless	49.67 kPa	26.40	80.82 kN	80.82 kN
3.99 m	Cohesionless	65.84 kPa	26.40	80.82 kN	80.82 kN
4.01 m	Cohesionless	66.07 kPa	26.40	80.82 kN	80.82 kN
6.99 m	Cohesionless	86.03 kPa	26.40	80.82 kN	80.82 kN
7.01 m	Cohesionless	86.18 kPa	35.20	125.39 kN	125.39 kN
10.01 m	Cohesionless	109.57 kPa	35.20	125.39 kN	125.39 kN
13.01 m	Cohesionless	132.97 kPa	35.20	125.39 kN	125.39 kN
13.99 m	Cohesionless	140.61 kPa	35.20	125.39 kN	125.39 kN
14.01 m	Cohesionless	140.79 kPa	77.60	919.89 kN	919.89 kN
14.49 m	Cohesionless	145.49 kPa	77.60	919.89 kN	919.89 kN
14.51 m	Cohesionless	145.69 kPa	77.60	919.89 kN	919.89 kN
17.51 m	Cohesionless	175.08 kPa	77.60	919.89 kN	919.89 kN
19.99 m	Cohesionless	199.38 kPa	77.60	919.89 kN	919.89 kN

DRIVING - SUMMARY OF CAPACITIES

Depth	Skin Friction	End Bearing	Total Capacity
0.01 m	0.00 kN	0.00 kN	0.00 kN
2.49 m	0.00 kN	0.00 kN	0.00 kN
2.50 m	0.00 kN	77.01 kN	77.01 kN
3.01 m	14.68 kN	80.82 kN	95.50 kN
3.99 m	50.52 kN	80.82 kN	131.34 kN
4.01 m	51.35 kN	80.82 kN	132.18 kN
6.99 m	194.85 kN	80.82 kN	275.67 kN
7.01 m	196.07 kN	125.39 kN	321.45 kN
10.01 m	426.25 kN	125.39 kN	551.64 kN
13.01 m	711.46 kN	125.39 kN	836.84 kN
13.99 m	816.55 kN	125.39 kN	941.94 kN
14.01 m	819.63 kN	919.89 kN	1739.51 kN
14.49 m	915.98 kN	919.89 kN	1835.86 kN
14.51 m	920.06 kN	919.89 kN	1839.95 kN
17.51 m	1594.81 kN	919.89 kN	2514.69 kN
19.99 m	2245.97 kN	919.89 kN	3165.86 kN

ULTIMATE - SKIN FRICTION

Depth	Soil Type	Effective Stress At Midpoint	Sliding Friction Angle	Adhesion	Skin Friction
0.01 m	Cohesionless	0.00 kPa	0.00	N/A	0.00 kN
2.49 m	Cohesionless	0.00 kPa	0.00	N/A	0.00 kN
2.50 m	Cohesionless	41.25 kPa	24.43	N/A	0.00 kN
3.01 m	Cohesionless	45.46 kPa	24.43	N/A	14.68 kN
3.99 m	Cohesionless	53.54 kPa	24.43	N/A	50.52 kN
4.01 m	Cohesionless	66.04 kPa	24.43	N/A	51.35 kN
6.99 m	Cohesionless	76.02 kPa	24.43	N/A	194.85 kN
7.01 m	Cohesionless	86.14 kPa	26.11	N/A	196.07 kN
10.01 m	Cohesionless	97.84 kPa	26.11	N/A	426.25 kN
13.01 m	Cohesionless	109.53 kPa	26.11	N/A	711.46 kN
13.99 m	Cohesionless	113.35 kPa	26.11	N/A	816.55 kN
14.01 m	Cohesionless	140.74 kPa	30.32	N/A	819.63 kN
14.49 m	Cohesionless	143.09 kPa	30.32	N/A	915.98 kN
14.51 m	Cohesionless	145.64 kPa	30.32	N/A	920.06 kN
17.51 m	Cohesionless	160.33 kPa	30.32	N/A	1594.81 kN
19.99 m	Cohesionless	172.48 kPa	30.32	N/A	2245.97 kN

ULTIMATE - END BEARING

Depth	Soil Type	Effective Stress At Tip	Bearing Cap. Factor	Limiting End Bearing	End Bearing
0.01 m	Cohesionless	0.00 kPa	26.40	80.82 kN	0.00 kN
2.49 m	Cohesionless	0.00 kPa	26.40	80.82 kN	0.00 kN
2.50 m	Cohesionless	41.25 kPa	26.40	80.82 kN	77.01 kN
3.01 m	Cohesionless	49.67 kPa	26.40	80.82 kN	80.82 kN
3.99 m	Cohesionless	65.84 kPa	26.40	80.82 kN	80.82 kN
4.01 m	Cohesionless	66.07 kPa	26.40	80.82 kN	80.82 kN
6.99 m	Cohesionless	86.03 kPa	26.40	80.82 kN	80.82 kN
7.01 m	Cohesionless	86.18 kPa	35.20	125.39 kN	125.39 kN
10.01 m	Cohesionless	109.57 kPa	35.20	125.39 kN	125.39 kN
13.01 m	Cohesionless	132.97 kPa	35.20	125.39 kN	125.39 kN
13.99 m	Cohesionless	140.61 kPa	35.20	125.39 kN	125.39 kN
14.01 m	Cohesionless	140.79 kPa	77.60	919.89 kN	919.89 kN
14.49 m	Cohesionless	145.49 kPa	77.60	919.89 kN	919.89 kN
14.51 m	Cohesionless	145.69 kPa	77.60	919.89 kN	919.89 kN
17.51 m	Cohesionless	175.08 kPa	77.60	919.89 kN	919.89 kN
19.99 m	Cohesionless	199.38 kPa	77.60	919.89 kN	919.89 kN

ULTIMATE - SUMMARY OF CAPACITIES

Depth	Skin Friction	End Bearing	Total Capacity
0.01 m	0.00 kN	0.00 kN	0.00 kN
2.49 m	0.00 kN	0.00 kN	0.00 kN
2.50 m	0.00 kN	77.01 kN	77.01 kN
3.01 m	14.68 kN	80.82 kN	95.50 kN
3.99 m	50.52 kN	80.82 kN	131.34 kN
4.01 m	51.35 kN	80.82 kN	132.18 kN
6.99 m	194.85 kN	80.82 kN	275.67 kN
7.01 m	196.07 kN	125.39 kN	321.45 kN
10.01 m	426.25 kN	125.39 kN	551.64 kN
13.01 m	711.46 kN	125.39 kN	836.84 kN
13.99 m	816.55 kN	125.39 kN	941.94 kN
14.01 m	819.63 kN	919.89 kN	1739.51 kN
14.49 m	915.98 kN	919.89 kN	1835.86 kN
14.51 m	920.06 kN	919.89 kN	1839.95 kN
17.51 m	1594.81 kN	919.89 kN	2514.69 kN
19.99 m	2245.97 kN	919.89 kN	3165.86 kN

F.2.1.5 Static Axial Pile Capacity Calculations by LPC CPT Method - Computer Program

L.P.C. CPT Method

Page 1/2

Peach Freeway CPT-1 at North Abutment -- 356 mm-square PCPS

Concrete Pile

Installation Method: 9 - Driven Prefabricated Piles (Concrete)

Depth to Water Table: 4.0 meter

Pile No.	Toe Area (m ²)	Perimeter (m)
1	0.127	1.424

Depth to Bottom of Layer (m)	Soil Type
14.021	5
30.785	7

Depth (m)	Cone Tip Resistance (kPa)
.0	3,926.20
5.0	3,926.20
10.0	3,399.48
11.5	3,591.00
13.0	5,171.04
14.0	5,075.28
15.0	13,071.24
16.0	15,369.48
17.0	20,588.40
18.0	23,078.16
20.0	19,199.88
23.0	17,188.92
24.0	24,466.68
27.0	18,050.80

Peach Freeway CPT-1 at North Abutment -- 356 mm-square PCPS

Concrete Pile

Depth (m)	Unit Friction (kPa)	Toe Bearing (kPa)	Shaft Resistance (kN)	Toe Resistance (kN)	Ultimate Capacity (kN)
0.00	60.66	2,355.70	0.0	298.0	298.0
5.00	36.96	1,474.70	347.4	186.4	533.8
10.00	17.05	1,292.76	539.5	163.7	703.2
11.50	35.96	1,484.28	596.0	187.7	783.7
13.00	40.75	2,312.60	678.3	292.2	970.6
14.00	40.46	3,413.84	735.7	431.5	1,167.2
15.00	62.72	4,677.88	824.7	591.1	1,415.8
16.00	63.58	6,171.73	914.5	780.6	1,695.1
17.00	65.60	7,340.00	1,006.1	928.3	1,934.4
18.00	66.55	7,986.38	1,099.1	1,010.1	2,109.2
20.00	65.07	7,445.34	1,287.7	941.6	2,229.3
23.00	64.30	7,411.82	1,563.5	936.7	2,500.2
24.00	67.08	8,158.75	1,657.3	1,031.5	2,688.8
27.00	64.64	6,846.84	1,938.0	866.0	2,804.0

Note: Depth is referenced from the original ground surface.

F.2.1.6 Static Axial Pile Capacity Calculations by Schmertmann Method

Location: Peach Freeway CPT-1 at North Abutment.

Depth (m)	fs (avg) (bars)	Unit Friction (bars)	Increment Friction (kN)	Shaft Resist. (kN)	qc (avg) (bars)	qc1 (min) (bars)	qc2 (bars)	Toe Resistance (kN)	Ultimate Capacity (kN)
12.00	1.21	1.03	35.86	286	51.33				
12.25	1.22	1.03	36.00	322	58.35				
12.50	1.14	0.97	33.78	356	56.70				
12.75	1.17	0.99	34.52	390	55.00				
13.00	1.16	0.99	34.46	425	50.20	47.37	23.63	430	855
13.25	0.99	0.84	29.34	454	46.50				
13.50	0.84	0.72	24.98	479	47.27				
13.75	0.59	0.50	17.48	497	47.30				
14.00	0.97	0.83	28.83	526	62.47				
14.25	1.53	1.30	45.19	571	106.35				
14.50	1.11	0.94	32.89	604	127.73				
14.75	1.11	0.94	32.89	637	149.80				
15.00	2.05	1.74	60.66	697	162.90	173.94	68.33	1,467	2,164
15.25	1.72	1.46	50.82	748	196.20				
15.50	1.48	1.26	43.77	792	203.30				
15.75	1.16	0.98	34.23	826	170.90	169.20	98.38	1,620	2,446
16.00	1.15	0.98	34.17	860	168.63				
16.25	1.24	1.05	36.75	897	173.95				
16.50	1.61	1.37	47.71	945	208.87	216.83	129.36	2,096	3,041
16.75	1.61	1.36	47.56	992	224.80				
17.00	1.88	1.60	55.62	1,048	252.37				
17.25	1.84	1.56	54.53	1,102	260.65	252.40	173.18	2,577	3,679
17.50	2.08	1.77	61.73	1,164	249.23				
17.75	2.28	1.93	67.42	1,231	252.40				
18.00	2.86	2.43	84.75	1,316	305.00				
18.25	2.56	2.17	75.71	1,392	297.40				
18.50	2.12	1.80	62.91	1,455	254.83				
18.75	1.71	1.45	50.52	1,505	214.85				
19.00	1.31	1.11	38.82	1,544	148.70				

Note: Depth is referenced from the original ground surface.

F.2.1.7 Summary of North Abutment Capacity Calculation Results

Summary of Pile Capacity Estimates with an Embedded Pile Length of 11.5 meters

Method Used for Estimation of Pile Capacity	Calculated Pile Shaft Resistance (kN)	Calculated Pile Toe Resistance (kN)	Calculated Ultimate Pile Capacity (kN)
Meyerhof Method - SPT Data	418	854	1,272
Nordlund Method - SPT Data	898	940	1,838
Effective Stress Method - SPT Data	537	1,294	1,831
Driven Program - SPT Data	920	920	1,840
LPC CPT Program - CPT Data	780	511	1,291
Schmertmann Method - CPT Data	604	1,111	1,715

Summary of Pile Length Estimates for the 1,780 kN Ultimate Pile Capacity

Method Used for Estimation of Pile Capacity	Calculated Pile Length for the 1,780 kN Ultimate Pile Capacity
Meyerhof Method - SPT Data	13.0 meters for 1,840 kN
Nordlund Method - SPT Data	11.5 meters for 1,838 kN
Effective Stress Method	14.5 meters for 1,840 kN
Driven Program - SPT Data	11.5 meters for 1,840 kN
LPC CPT Program - CPT Data	13.5 meters for 1,815 kN
Schmertmann Method - CPT Data	11.7 meters for 1,939 kN

The ultimate pile group capacity at the North Abutment may be taken as the sum of the ultimate capacities of the individual piles in the group as discussed by the design recommendation for estimating group capacity in cohesionless soil presented in Section 9.8.1.1.

F.2.2 Pier 2 - Soil Boring S-2 (Cohesionless Soil)

F.2.2.1 Static Axial Pile Capacity Calculations by Meyerhof SPT Method (before scour)

For the soil profile interpreted from Soil Boring S-2 as shown in Figure F.5. Perform a Meyerhof method pile capacity calculation for an embedded length of 10 meters. Assume that scour has not occurred. Use the step-by-step method outlined in Section 9.7.1.1a.

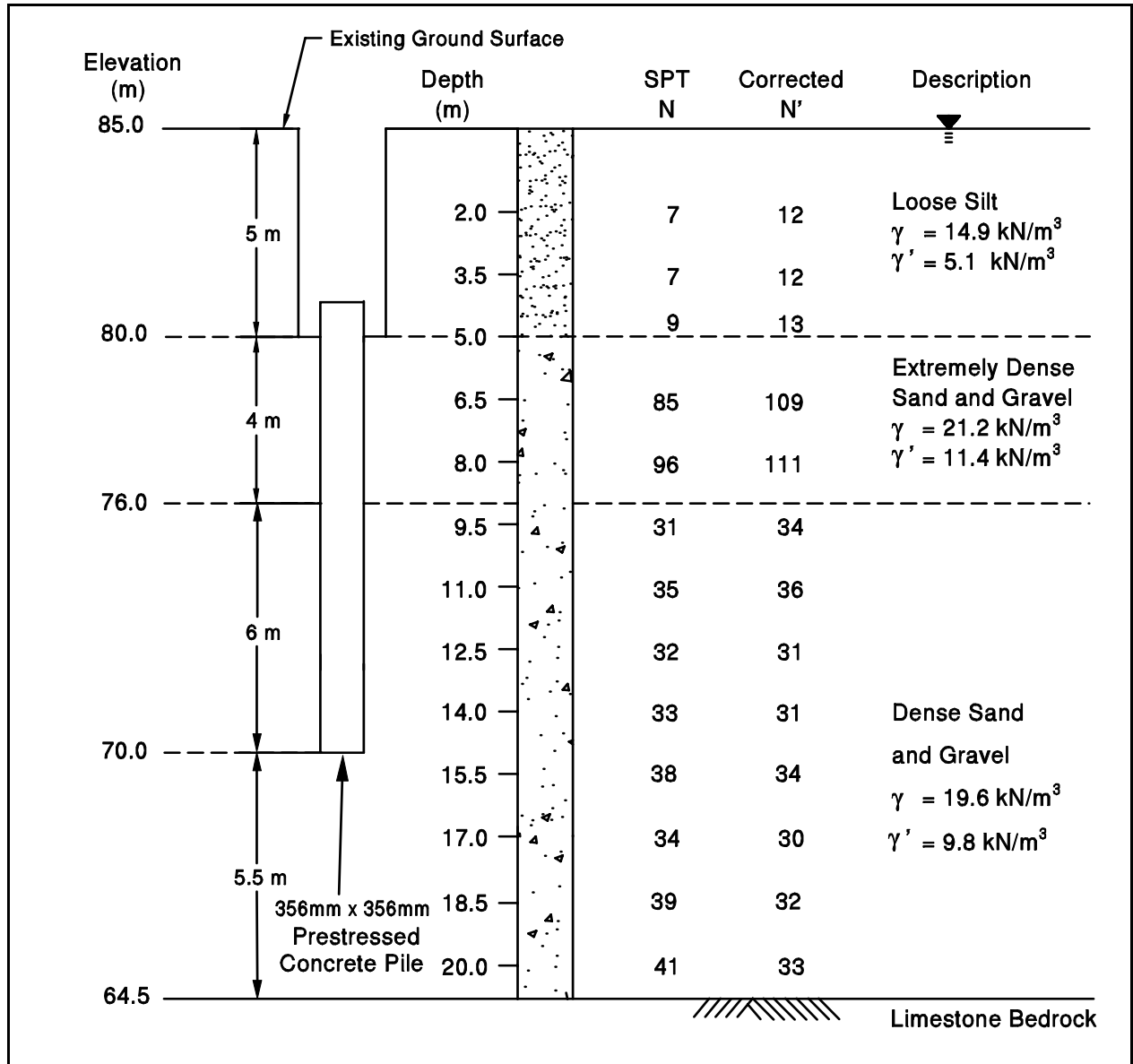


Figure F.5 Interpreted Soil Profile from Soil Boring S-2 at Pier 2

STEP 1 Correct SPT field N values for overburden pressure.

Effective overburden pressures, p_o , are needed to correct SPT field N values. The method for calculating the effective overburden pressure is explained in Section 9.4 and an example was presented earlier in Section F.2.1.1. The effective overburden pressure diagram and the soil layers are presented in Figure F.6 below.

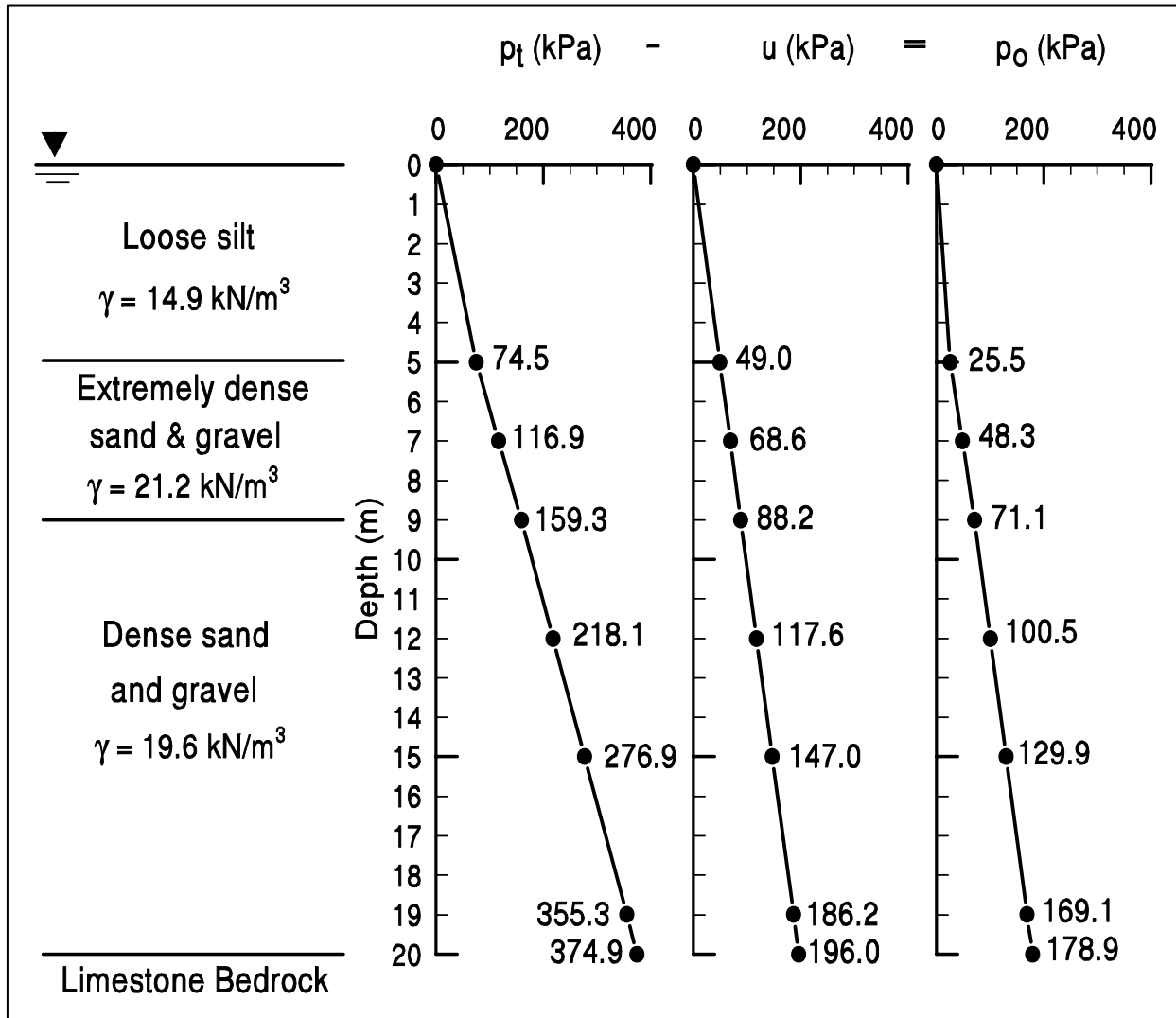


Figure F.6 Effective Overburden Pressure Diagram – Pier 2

STEP 1 (continued)

Use correction factors from Figure 4.6 (Chapter 4) to obtain corrected SPT N' values.

Depth (m)	p_o (kPa)	Field SPT N value	Correction Factor	Corrected SPT N' (Field SPT N x Correction Factor)
2.0	10.2	7	1.75	12
3.5	17.9	7	1.65	12
5.0	25.5	9	1.43	13
6.5	42.6	85	1.28	109
8.0	59.7	96	1.16	111
9.5	76.0	31	1.09	34
11.0	90.7	35	1.04	36
12.5	105.4	32	0.98	31
14.0	120.1	33	0.95	31
15.5	134.8	38	0.90	34
17.0	149.5	34	0.87	30
18.5	164.2	39	0.83	32
20.0	178.9	41	0.81	33

STEP 2 Compute the average corrected SPT N' value, \bar{N}' , for each soil layer.

Along the pile embedded length, the soil profile is delineated into two layers. Layer 1 is extremely dense sand and gravel that is 4 meters thick, and layer 2 is dense sand and gravel that is 6 meters thick.

$$\bar{N}'_1 = \frac{109 + 111}{2} = 110 \quad \begin{array}{l} \text{(Layer 1 - depth 5 to 9 m;} \\ \text{Extremely dense sand and gravel)} \end{array}$$

$$\bar{N}'_2 = \frac{34 + 36 + 31 + 31}{4} = 33 \quad \begin{array}{l} \text{(Layer 2 - depth 9 to 15 m;} \\ \text{Dense sand and gravel)} \end{array}$$

STEP 3 Compute unit shaft resistance, f_s (kPa), using the equation for driven displacement piles:

$$f_s = 2\bar{N}' \leq 100 \text{ kPa}$$

$$\text{Layer 1: } f_{s1} = 2 (110) = 220 \text{ kPa, so use } f_{s1} = 100 \text{ kPa}$$

$$\text{Layer 2: } f_{s2} = 2 (33) = 66 \text{ kPa}$$

STEP 4 Compute ultimate shaft resistance, R_s (kN).

$$R_s = f_s A_s$$

$$\text{Layer 1: } R_{s1} = 100 \text{ kPa } (4) (0.356 \text{ m }) (4 \text{ m }) = 570 \text{ kN}$$

$$\text{Layer 2: } R_{s2} = 66 \text{ kPa } (4) (0.356 \text{ m }) (6 \text{ m }) = 564 \text{ kN}$$

$$\begin{aligned} \text{Total: } R_s &= R_{s1} + R_{s2} = 570 \text{ kN} + 564 \text{ kN} \\ &= 1,134 \text{ kN} \end{aligned}$$

STEP 5 Compute average corrected SPT N' value, \bar{N}'_O and \bar{N}'_B near pile toe.

When the pile is embedded to more than 10 pile diameters into the bearing stratum, the effect of overlying stratum becomes irrelevant. The unit toe resistance is governed by the limiting unit toe resistance of the bearing stratum that is $400\bar{N}'_B$.

The average corrected SPT N' value for the bearing stratum should be calculated from the average N' value within the zone extending 3 pile diameters below the pile toe or in this case 1.065 meter. The average corrected SPT N' value for the bearing stratum which consists of dense sand and gravel is:

$$\bar{N}'_B = \frac{34 + 36 + 31 + 31 + 34}{5} = 33$$

STEP 6 Compute unit toe resistance, q_t (kPa).

$$q_t = \frac{40\bar{N}'_B D_B}{b} \leq 400\bar{N}'_B$$
$$= \frac{40\bar{N}'_B (6 \text{ m})}{0.356 \text{ m}} = 674\bar{N}'_B, \text{ so use } q_t = 400\bar{N}'_B$$

$$q_t = 400 (33) = 13,200 \text{ kPa}$$

STEP 7 Compute ultimate toe resistance, R_t (kN).

$$R_t = q_t A_t = 13,200 \text{ kPa} (0.356 \text{ m})(0.356 \text{ m})$$
$$= 1,676 \text{ kN}$$

STEP 8 Compute ultimate pile capacity, Q_u (kN).

$$\begin{aligned} Q_u &= R_s + R_t \\ &= 1,134 \text{ kN} + 1,676 \text{ kN} \\ &= 2,810 \text{ kN} \end{aligned}$$

STEP 9 Compute allowable design load, Q_a (kN).

$$Q_a = \frac{Q_u}{\text{Factor of Safety}} = \frac{2,810 \text{ kN}}{\text{Factor of Safety}}$$

Note: Factor of Safety should be selected based on the construction control method to be specified. Recommended factors of safety are described in Section 9.6.

F.2.2.2 Static Axial Pile Capacity Calculations by Nordlund Method (before scour at 10 m)

For the soil profile interpreted from Soil Boring S-2 as shown in Figure F.5. Perform a Nordlund method pile capacity calculation for an embedded length of 10 meters. Assume that scour has not occurred. Use the step-by-step method outlined in Section 9.7.1.1b.

STEP 1 Delineate the soil profile into layers and determine the ϕ angle for each layer.

- a. Construct p_o diagram using the procedure described in Section 9.4. This is completed in Figure F.6.
- b. Correct SPT field N values for overburden pressure using Figure 4.6 from Chapter 4 and obtain corrected SPT N' values. For Soil Boring S-2, this has been done in the previous example (see Section F.2.2.1, Step 1).
- c. Determine ϕ angle for each layer from laboratory tests or in-situ data.

Since the ϕ angle is not provided by either laboratory or in-situ data, it should be determined using the average corrected SPT N' value, \bar{N}' , as calculated below.

- d. In the absence of laboratory or in-situ test data, determine the average corrected SPT N' value, \bar{N}' , for each soil layer and estimate ϕ angle from Table 4-6 in Chapter 4.

As the example in Section F.2.2.1, the soil profile along the pile embedded length is delineated into two layers of 4, and 6 meters thick. The average corrected SPT N' value for each soil layer is as follows:

Layer 1: $\bar{N}'_1 = 110$ (Layer 1 - depth 5 to 9 m;
Extremely dense sand and gravel)

Layer 2: $\bar{N}'_2 = 33$ (Layer 2 - depth 9 to 15 m;
Dense sand and gravel)

Use the average corrected SPT N' value for each soil layer to estimate ϕ angle from Table 4-6 in Chapter 4.

STEP 1 (continued)

Based on Table 4-6, the ϕ angle is indicated to be as high as 43° when N' is greater than 50. However, as discussed in Section 9.5, in soil layers with greater than 50% gravel the ϕ angle for shaft resistance calculations should be limited to:

36° for hard angular gravel, and
32° for soft rounded gravel.

A limiting friction angle should be used for layer 1.

Layer 1: $\phi_1 = 36^\circ$ limiting friction angle for hard angular gravel

For layer 2, the friction angle is computed from Table 4-6:

Layer 2: $\phi_2 = 35^\circ$ for $\bar{N}_2' = 33$

STEP 2 Determine δ , the friction angle between pile and soil based on displaced soil volume, V , and the soil friction angle, ϕ .

- a. Compute volume of soil displaced per unit length of pile, V .
Since this is a uniform cross section ($\omega = 0^\circ$) pile,

$$V = (0.356 \text{ m})(0.356 \text{ m})(1.0 \text{ m/m}) = 0.127 \text{ m}^3/\text{m}$$

For a non-uniform pile cross section ($\omega \neq 0^\circ$), the pile should be divided into sections and the volume for each section should be calculated.

- b. Enter Figure 9.10 with V and determine δ/ϕ ratio for pile type.

For a precast, prestressed concrete pile with $V = 0.127 \text{ m}^3/\text{m}$

$$\delta/\phi = 0.84$$

STEP 2 (continued)

c. Calculate δ from δ/ϕ ratio.

$$\text{Layer 1: } \delta_1 = 0.84 (36^\circ) = 30.2^\circ$$

$$\text{Layer 2: } \delta_2 = 0.84 (35^\circ) = 29.4^\circ$$

STEP 3 Determine the coefficient of lateral earth pressure, K_δ , for each ϕ angle.

a. Determine K_δ for ϕ angle based on displaced volume, V , and pile taper angle, ω , using either Figure 9.11, 9.12, 9.13, or 9.14 and the appropriate procedure described in Step 3b, 3c, 3d, or 3e.

The pile taper angle, ω , = 0° .

For Layer 1:

$$\phi_1 = 36^\circ \quad \text{and} \quad V = 0.127 \text{ m}^3/\text{m}, \text{ therefore use Step 3e.}$$

A step by step procedure for determining K_δ using the linear interpolation and the log linear interpolation is presented in Section F.2.1.2 - Step 3.

$$\text{For } \phi_1 = 36^\circ, \omega = 0^\circ, \text{ and } V = 0.127 \text{ m}^3/\text{m}:$$

$$K_{\delta 1} = 2.10$$

For Layer 2:

$$\phi_2 = 35^\circ \quad \text{and} \quad V = 0.127 \text{ m}^3/\text{m}, \text{ therefore use Step 3d.}$$

A step by step procedure for determining K_δ using the log linear interpolation is presented in Section F.2.1.2 - Step 3.

$$\text{For } \phi_2 = 35^\circ, \omega = 0^\circ, \text{ and } V = 0.127 \text{ m}^3/\text{m}:$$

$$K_{\delta 2} = 1.83$$

STEP 4 Determine the correction factor, C_F , to be applied to K_δ if $\delta \neq \phi$.

Use Figure 9.15 to determine the correction factor for each K_δ . Enter figure with ϕ angle and $\delta/\phi=0.84$ to determine C_F .

Layer 1: For $\phi_1 = 36^\circ \rightarrow C_{F1} = 0.92$

Layer 2: For $\phi_2 = 35^\circ \rightarrow C_{F2} = 0.93$

STEP 5 Compute the average effective overburden pressure at the midpoint of each soil layer, p_d (kPa). (Note: a limiting value is not applied to p_d).

The effective overburden pressure at the midpoint of each soil layer is equal to the average effective overburden pressure of that layer. The effective overburden pressure versus depth for Pier 2 has been computed and tabulated in the previous example (see Section F.2.2.1 - Step 1). The effective overburden pressure diagram for Pier 2 is presented in Figure F.6.

Layer 1: $p_{d1} = 48.3$ kPa (midpoint of layer 1 - at depth of 7.0 m)

Layer 2: $p_{d2} = 100.5$ kPa (midpoint of layer 2 - at depth of 12.0 m)

STEP 6 Compute the shaft resistance in each soil layer. Sum the shaft resistance from each soil layer to obtain the ultimate shaft resistance, R_s (kN).

$$R_s = K_\delta C_F p_d \sin \delta C_d D \quad (\text{for uniform pile cross section})$$

$$\text{where : } C_d = (4) (0.356 \text{ m}) = 1.424 \text{ m}$$

$$\begin{aligned} \text{Layer 1: } R_{s1} &= 2.10 (0.92) (48.3 \text{ kPa}) (\sin 30.2^\circ) (1.424 \text{ m}) (4 \text{ m}) \\ &= 267 \text{ kN} \end{aligned}$$

$$\begin{aligned} \text{Layer 2: } R_{s2} &= 1.83 (0.93) (100.5 \text{ kPa}) (\sin 29.4^\circ) (1.424 \text{ m}) (6 \text{ m}) \\ &= 717 \text{ kN} \end{aligned}$$

STEP 6 (continued)

$$\begin{aligned}\text{Total: } R_s &= R_{s1} + R_{s2} \\ &= 267 \text{ kN} + 717 \text{ kN} = 984 \text{ kN}\end{aligned}$$

STEP 7 Determine the α_t coefficient and the bearing capacity factor, N'_q , from the ϕ angle near the pile toe.

Since the ϕ angle is not provided by either laboratory tests or in-situ data, the ϕ angle can be estimated from Table 4-6 using the average corrected SPT N' value over the zone from the pile toe to 3 diameter below the pile toe (1.065 meters). The soil near the pile toe is a dense sand and gravel.

$$\bar{N}'_{\text{toe}} = 34 \rightarrow \phi_{\text{toe}} = 36^\circ$$

- a. Enter Figure 9.16(a) with ϕ angle near pile toe to determine α_t coefficient based on pile length to diameter ratio.

$$(D/b) = (10.0 \text{ m}) / (0.356 \text{ m}) = 28.1$$

$$\text{For } \phi_{\text{toe}} = 36^\circ \text{ and } (D/b) = 28.1 \rightarrow \alpha_t = 0.69$$

- b. Enter Figure 9.16(b) with ϕ angle near pile toe to determine N'_q .

$$\text{For } \phi_{\text{toe}} = 36^\circ \rightarrow N'_q = 75$$

STEP 8 Compute the effective overburden pressure at the pile toe, p_t (kPa).

The effective overburden pressure at the pile toe should be limited to a maximum of 150 kPa.

The effective overburden pressure at the pile toe, p_t , has been computed in the previous example (Section F.2.2.1, Step 1):

$$p_t = 129.9 \text{ kPa} < 150 \text{ kPa} \rightarrow \text{OK}$$

STEP 9 Compute ultimate toe resistance, R_t (kN).

$$\begin{aligned} \text{a. } R_t &= \alpha_t N'_q A_t p_t \\ &= 0.69 (75) (0.356 \text{ m }) (0.356 \text{ m }) (129.9 \text{ kPa }) \\ &= 854 \text{ kN} \end{aligned}$$

$$\text{b. limiting } R_t = q_L A_t$$

Using the estimated $\phi=36^\circ$ and Figure 9.17, the limiting unit toe resistance is:

$$q_L = 7,400 \text{ kPa}$$

Therefore,

$$R_t = 7,400 \text{ kPa } (0.356 \text{ m }) (0.356 \text{ m }) = 940 \text{ kN}$$

c. Use lesser of the two R_t values obtained in steps a and b which is:

$$R_t = 854 \text{ kN}$$

STEP 10 Compute the ultimate pile capacity, Q_u (kN).

$$\begin{aligned} Q_u &= R_s + R_t \\ &= 984 \text{ kN} + 854 \text{ kN} = 1,838 \text{ kN} \end{aligned}$$

STEP 11 Compute the allowable design load, Q_a (kN).

$$Q_a = \frac{Q_u}{\text{Factor of Safety}} = \frac{1,838 \text{ kN}}{\text{Factor of Safety}}$$

Note: Factor of Safety should be selected based on the construction control method to be specified. Recommended factors of safety are described in Section 9.6.

F.2.2.3 Static Axial Pile Capacity Calculations by Nordlund Method (after scour at 10 m)

For the soil profile interpreted from Soil Boring S-2 after scour as shown in Figure F.7. Perform a Nordlund method pile capacity calculation for an embedded length of 10 meters. Assume that channel degradation scour has removed the 5 meter thick loose silt layer. Use the step-by-step method outlined in Section 9.7.1.1b.

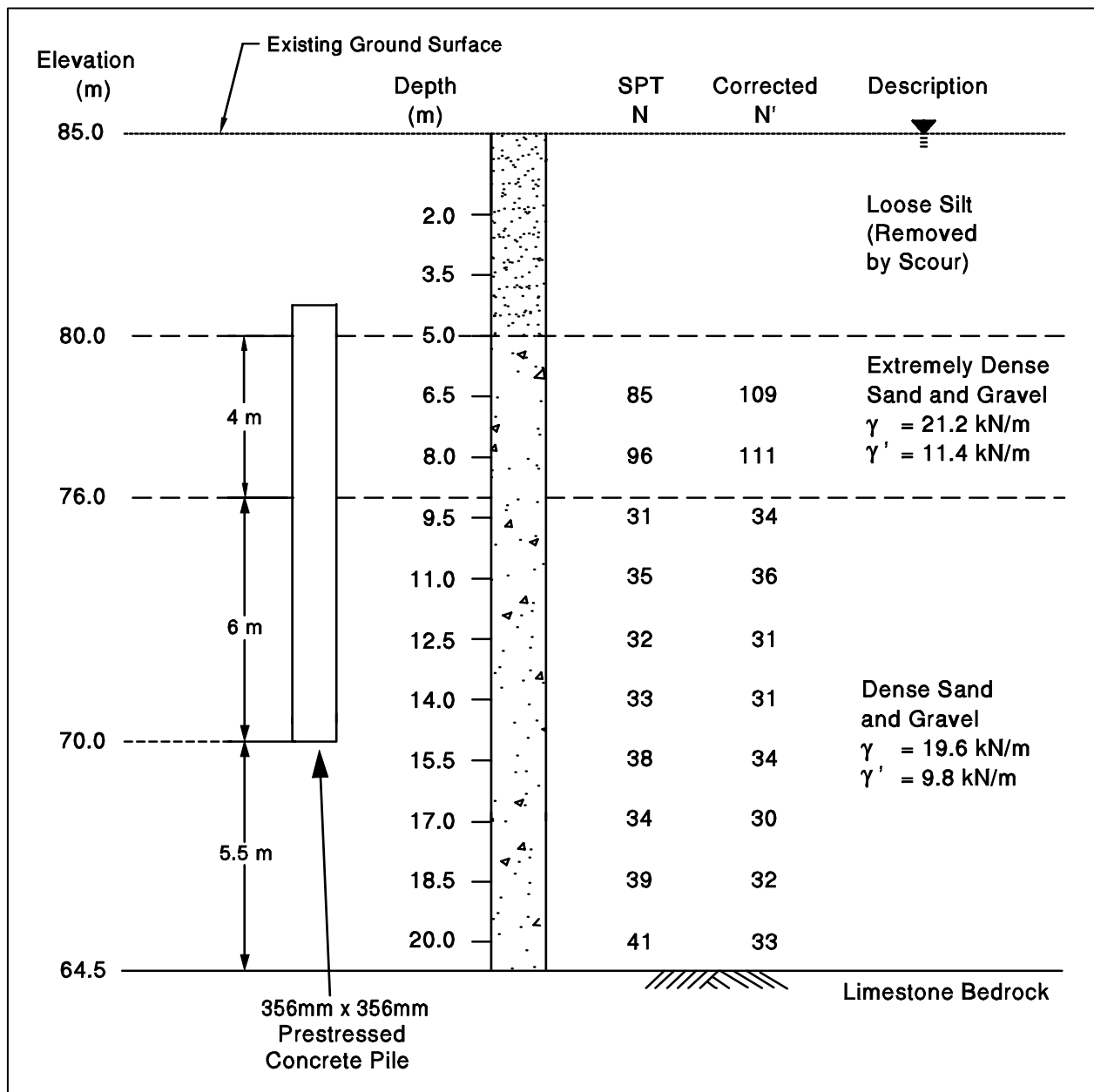


Figure F.7 Interpreted Soil Profile at Pier 2 after Scour

STEP 1 Delineate the soil profile into layers and determine the ϕ angle for each layer.

- a. Construct p_o diagram using procedure described in Section 9.4. This is completed in Figure F.6.
- b. Correct SPT field N values for overburden pressure using Figure 4.6 from Chapter 4 and obtain corrected SPT N' values. For Soil Boring S-2, this was done in the previous example (see Section F.2.2.1, Step 1).

Note: Although scour has eroded the 5 meter thick loose silt layer, the original overburden pressure (with the loose silt layer still in place) should be used when correcting the SPT field N values.

- c. Determine ϕ angle for each layer from laboratory tests or in-situ data.

Since the ϕ angle is not provided by either laboratory or in-situ data, it should be determined using the average corrected SPT N' value, \bar{N}' , as calculated below.

- d. In the absence of laboratory or in-situ test data, determine the average corrected SPT N' value, \bar{N}' , for each soil layer and estimate ϕ angle from Table 4-6 in Chapter 4.

As the example in Section F.2.2.2, the soil profile along the pile embedded length is delineated into two layers of 4, and 6 meters thick. The average corrected SPT N' value for each soil layer is as follow.

Layer 1: $\bar{N}'_1 = 110$ (Layer 1 - depth 5 to 9 m below existing ground surface; Extremely dense sand and gravel)

Layer 2: $\bar{N}'_2 = 33$ (Layer 2 - depth 9 to 15 m below existing ground surface; Dense sand and gravel)

Use the average corrected SPT N' value for each soil layer to estimate ϕ angle from Table 4-6 in Chapter 4.

STEP 1 (continued)

As discussed in Section F.2.2.2 - Step 1, a limiting friction angle should be used for the hard angular gravel of layer 1.

Layer 1: $\phi_1 = 36^\circ$ from limiting friction angle

For layer 2, the friction angle is computed from Table 4-6:

Layer 2: $\phi_2 = 35^\circ$ for $\bar{N}_2' = 33$

STEP 2 Determine δ , the friction angle between pile and soil based on displaced soil volume, V , and the soil friction angle, ϕ .

- a. Compute volume of soil displaced per unit length of pile, V .
Since this is a uniform cross section ($\omega = 0^\circ$) pile,

$$V = (0.356 \text{ m})(0.356 \text{ m})(1.0 \text{ m/m}) = 0.127 \text{ m}^3/\text{m}$$

For a non-uniform pile cross section ($\omega \neq 0^\circ$), the pile should be divided into sections and the volume for each section should be calculated.

- b. Enter Figure 9.10 with V and determine δ/ϕ ratio for pile type.

For a precast, prestressed concrete pile with $V = 0.127 \text{ m}^3/\text{m}$

$$\delta/\phi = 0.84$$

- c. Calculate δ from δ/ϕ ratio.

Layer 1: $\delta_1 = 0.84 (36^\circ) = 30.2^\circ$

Layer 2: $\delta_2 = 0.84 (35^\circ) = 29.4^\circ$

STEP 3 Determine the coefficient of lateral earth pressure, K_δ , for each ϕ angle.

- a. Determine K_δ for ϕ angle based on displaced volume, V , and pile taper angle, ω , using either Figure 9.11, 9.12, 9.13, or 9.14 and the appropriate procedure described in Step 3b, 3c, 3d, or 3e.

The pile taper angle, ω , = 0° .

For Layer 1:

$\phi_1 = 36^\circ$ and $V = 0.127 \text{ m}^3/\text{m}$, therefore use Step 3e.

A step by step procedure for determining K_δ using the linear interpolation and the log linear interpolation is presented in Section F.2.1.2 - Step 3.

For $\phi_1 = 36^\circ$, $\omega = 0^\circ$, and $V = 0.127 \text{ m}^3/\text{m}$:

$$K_{\delta 1} = 2.10$$

For Layer 2:

$\phi_2 = 35^\circ$ and $V = 0.127 \text{ m}^3/\text{m}$, therefore use Step 3d.

A step by step procedure for determining K_δ using the log linear interpolation is presented in Section F.2.1.2 - Step 3.

For $\phi_2 = 35^\circ$, $\omega = 0^\circ$, and $V = 0.127 \text{ m}^3/\text{m}$:

$$K_{\delta 2} = 1.83$$

STEP 4 Determine the correction factor, C_F , to be applied to K_δ if $\delta \neq \phi$.

Use Figure 9.15 to determine the correction factor for each K_δ . Enter figure with ϕ angle and $\delta/\phi=0.84$ to determine C_F .

Layer 1: For $\phi_1 = 36^\circ \rightarrow C_{F1} = 0.92$

Layer 2: For $\phi_2 = 35^\circ \rightarrow C_{F2} = 0.93$

STEP 5 Compute the average effective overburden pressure at the midpoint of each soil layer, p_d (kPa). (Note: a limiting value is not applied to p_d)

The effective overburden pressure at the midpoint of each layer is equal to the average effective overburden pressure of that layer. The effective overburden pressure diagram for Pier 2 after scour is presented in Figure F.8. The purpose of this example is to illustrate how scour reduces the average effective overburden pressures, and hence the pile shaft and toe resistance.

Layer 1: $p_{d1} = 22.8$ kPa (midpoint of layer 1 - at depth of 7.0 m below existing ground surface)

Layer 2: $p_{d2} = 75.0$ kPa (midpoint of layer 2 - at depth of 12.0 m below existing ground surface)

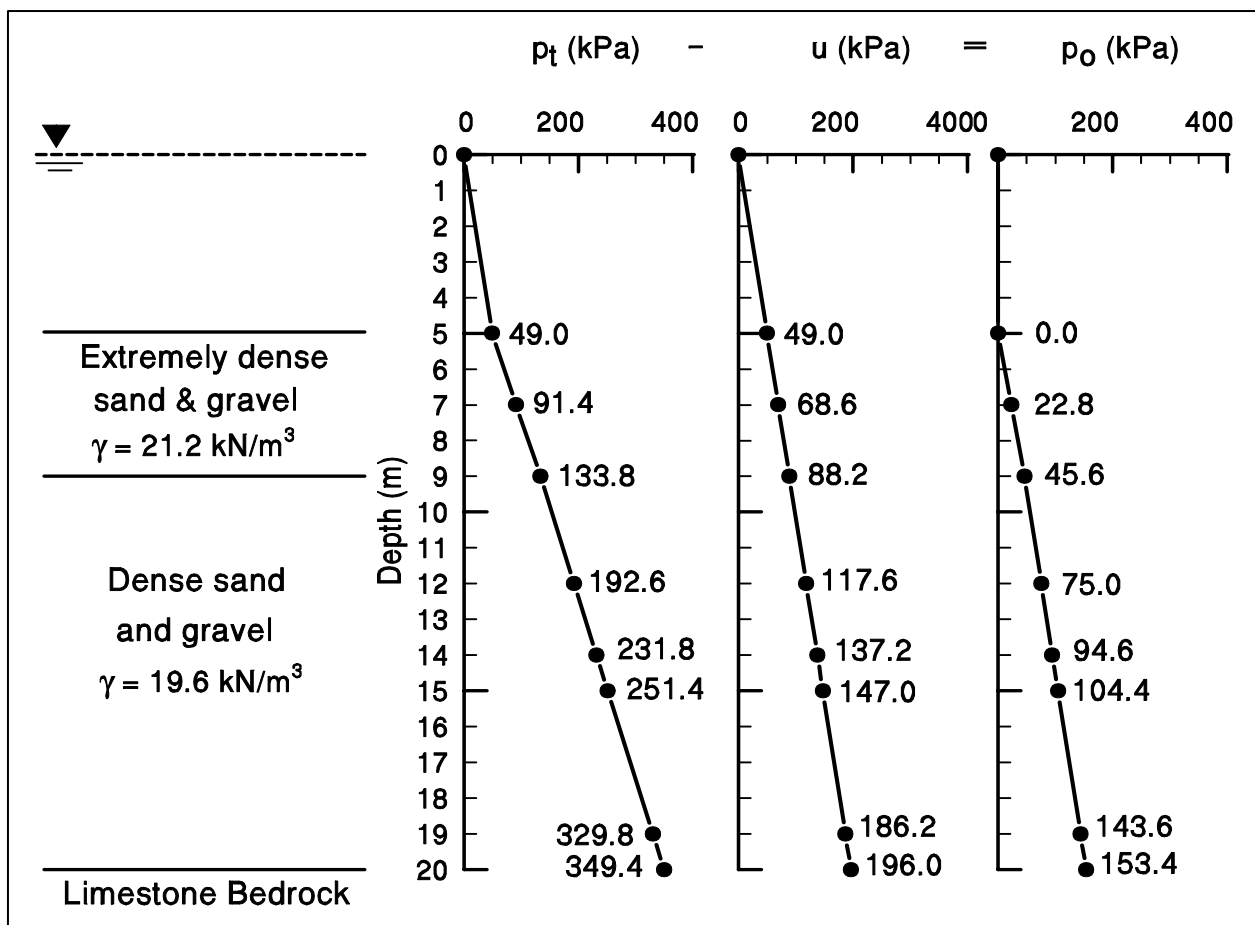


Figure F.8 Effective Overburden Pressure Design – Pier 2 after Scour

STEP 6 Compute the shaft resistance in each soil layer. Sum the shaft resistance from each soil layer to obtain the ultimate shaft resistance, R_s (kN).

$$R_s = K_\delta C_F p_d \sin \delta C_d D \quad (\text{for uniform pile cross section})$$

$$\text{where : } C_d = (4) (0.356 \text{ m}) = 1.424 \text{ m}$$

$$\begin{aligned} \text{Layer 1: } R_{s1} &= 2.10 (0.92) (22.8 \text{ kPa}) (\sin 30.2^\circ) (1.424 \text{ m}) (4 \text{ m}) \\ &= 126 \text{ kN} \end{aligned}$$

$$\begin{aligned} \text{Layer 2: } R_{s2} &= 1.83 (0.93) (75.0 \text{ kPa}) (\sin 29.4^\circ) (1.424 \text{ m}) (6 \text{ m}) \\ &= 535 \text{ kN} \end{aligned}$$

$$\begin{aligned} \text{Total: } R_s &= R_{s1} + R_{s2} = 126 \text{ kN} + 535 \text{ kN} \\ &= 661 \text{ kN} \rightarrow \text{as compared to 984 kN before scour.} \end{aligned}$$

STEP 7 Determine the α_t coefficient and the bearing capacity factor, N'_q , from the ϕ angle near the pile toe.

As in Section F.2.2.2,

$$\bar{N}'_{toe} = 34 \rightarrow \phi_{toe} = 36^\circ$$

a. Enter Figure 9.16(a) with ϕ angle near pile toe to determine α_t coefficient based on pile length to diameter ratio.

$$(D/b) = (10.0 \text{ m}) / (0.356 \text{ m}) = 28.1$$

$$\text{For } \phi_{toe} = 36^\circ \text{ and } (D/b) = 28.1 \rightarrow \alpha_t = 0.69$$

b. Enter Figure 9.16(b) with ϕ angle near pile toe to determine N'_q .

$$\text{For } \phi_{toe} = 36^\circ \rightarrow N'_q = 75$$

STEP 8 Compute the effective overburden pressure at the pile toe, p_t (kPa).

The effective overburden pressure at the pile toe should be limited to a maximum of 150 kPa.

The effective overburden pressure at the pile toe, p_t , after scour has been computed and shown in Figure F.8:

$$p_t = 104.4 \text{ kPa} < 150 \text{ kPa} \rightarrow \text{OK}$$

STEP 9 Compute the ultimate toe resistance, R_t (kN).

a. $R_t = \alpha_t N'_q A_t p_t$

$$= 0.69 (75) (0.356 \text{ m}) (0.356 \text{ m}) (104.4 \text{ kPa})$$

$$= 686 \text{ kN}$$

b. limiting $R_t = q_L A_t$

Using the estimated $\phi=36^\circ$ and Figure 9.17, the limiting unit toe resistance is:

$$q_L = 7,400 \text{ kPa}$$

Therefore,

$$R_t = 7,400 \text{ kPa} (0.356 \text{ m}) (0.356 \text{ m})$$

$$= 940 \text{ kN}$$

c. Use lesser of the two R_t values obtained in steps a and b which is:

$$R_t = 686 \text{ kN} \rightarrow \text{as compared to } 854 \text{ kN before scour.}$$

STEP 10 Compute the ultimate pile capacity, Q_u (kN).

$$Q_u = R_s + R_t$$

$$= 661 \text{ kN} + 686 \text{ kN}$$

$$= 1,347 \text{ kN} \rightarrow \text{as compared to } 1,838 \text{ kN before scour.}$$

Note: After scour has occurred, the factor of safety is only:

$$\text{Factor of Safety} = \frac{Q_u}{\text{Design Load}} = \frac{1,347 \text{ kN}}{890 \text{ kN}} = 1.51$$

F.2.2.4 Static Axial Pile Capacity Calculations by Nordlund Method (before scour at 14 m)

For the soil profile interpreted from Soil Boring S-2 as shown in Figure F.5. Perform a Nordlund method pile capacity calculation for an embedded length of 14 meters. Assume that scour has not occurred. Use the step-by-step method outlined in Section 9.7.1.1b.

STEP 1 Delineate the soil profile into layers and determine the ϕ angle for each layer.

- a. Construct p_o diagram using procedure described in Section 9.4. This is completed in Figure F.6.
- b. Correct SPT field N values for overburden pressure using Figure 4.6 from Chapter 4 and obtain corrected SPT N' values. For Soil Boring S-2, this has been done in a previous example (see Section F.2.2.1, Step 1).
- c. Determine ϕ angle for each layer from laboratory tests or in-situ data.

Since the ϕ angle is not provided by either laboratory or in-situ data, it should be determined using the average corrected SPT N' value, \bar{N}' , as calculated below.

- d. In the absence of laboratory or in-situ test data, determine the average corrected SPT N' value, \bar{N}' , for each soil layer and estimate ϕ angle from Table 4-6 in Chapter 4.

The soil profile along the pile embedded length is delineated into two layers of 4, and 10 meters thick. The average corrected SPT N' value for each soil layer is as follow.

$$\bar{N}'_1 = 110 \quad \text{(Layer 1 - depth 5 to 9 m; Extremely dense sand and gravel)}$$

$$\bar{N}'_2 = \frac{34 + 36 + 31 + 31 + 34 + 30 + 32}{7} = 33$$

(Layer 2 - depth 9 to 19 m;
Dense sand and gravel)

STEP 1 (continued)

Use the average corrected SPT N' value for each soil layer to estimate ϕ angle from Table 4-6 in Chapter 4.

As discussed in Section F.2.2.2 - Step 1, a limiting friction angle should be used for the hard angular gravel of layer 1.

Layer 1: $\phi_1 = 36^\circ$ from limiting friction angle

For layer 2, the friction angle is computed from Table 4-6:

Layer 2: $\phi_2 = 35^\circ$ for $\bar{N}_2' = 33$

STEP 2 Determine δ , the friction angle between pile and soil based on displaced soil volume, V , and the soil friction angle, ϕ .

- a. Compute volume of soil displaced per unit length of pile, V .
Since this is a uniform cross section ($\omega = 0^\circ$) pile,

$$V = (0.356 \text{ m})(0.356 \text{ m})(1.0 \text{ m/m}) = 0.127 \text{ m}^3/\text{m}$$

- b. Enter Figure 9.10 with V and determine δ/ϕ ratio for pile type.

For a precast, prestressed concrete pile with $V = 0.127 \text{ m}^3/\text{m}$

$$\delta/\phi = 0.84$$

- c. Calculate δ from δ/ϕ ratio.

Layer 1: $\delta_1 = 0.84 (36^\circ) = 30.2^\circ$

Layer 2: $\delta_2 = 0.84 (35^\circ) = 29.4^\circ$

STEP 3 Determine the coefficient of lateral earth pressure, K_δ , for each ϕ angle.

- a. Determine K_δ for ϕ angle based on displaced volume, V , and pile taper angle, ω , using either Figure 9.11, 9.12, 9.13, or 9.14 and the appropriate procedure described in Step 3b, 3c, 3d, or 3e.

The pile taper angle, ω , = 0° .

For Layer 1:

$\phi_1 = 36^\circ$ and $V = 0.127 \text{ m}^3/\text{m}$, therefore use Step 3e.

A step by step procedure for determining K_δ using the linear interpolation and the log linear interpolation is presented in Section F.2.1.2 - Step 3.

For $\phi_1 = 36^\circ$, $\omega = 0^\circ$, and $V = 0.127 \text{ m}^3/\text{m}$:

$$K_{\delta 1} = 2.10$$

For Layer 2:

$\phi_2 = 35^\circ$ and $V = 0.127 \text{ m}^3/\text{m}$, therefore use Step 3d.

A step by step procedure for determining K_δ using the log linear interpolation is presented in Section F.2.1.2 - Step 3.

For $\phi_2 = 35^\circ$, $\omega = 0^\circ$, and $V = 0.127 \text{ m}^3/\text{m}$:

$$K_{\delta 2} = 1.83$$

STEP 4 Determine the correction factor, C_F , to be applied to K_δ if $\delta \neq \phi$.

Use Figure 9.15 to determine the correction factor for each K_δ . Enter figure with ϕ angle and $\delta/\phi=0.84$ to determine C_F .

Layer 1: For $\phi_1 = 36^\circ \rightarrow C_{F1} = 0.92$

Layer 2: For $\phi_2 = 35^\circ \rightarrow C_{F2} = 0.93$

STEP 5 Compute the average effective overburden pressure at the midpoint of each soil layer, p_d (kPa). (Note: a limiting value is not applied to p_d).

The effective overburden pressure at the midpoint of each soil layer is equal to the average effective overburden pressure of that layer. The effective overburden pressure versus depth for the Pier 2 has been computed and tabulated in a previous example (see Section F.2.2.1 - Step 1). The effective overburden pressure diagram for Pier 2 is presented in Figure F.6.

Layer 1: $p_{d1} = 48.3$ kPa (midpoint of layer 1 - at depth of 7.0 m)

Layer 2: $p_{d2} = 120.1$ kPa (midpoint of layer 2 - at depth of 14.0 m)

STEP 6 Compute the shaft resistance in each soil layer. Sum the shaft resistance from each soil layer to obtain the ultimate shaft resistance, R_s (kN).

$$R_s = K_\delta C_F p_d \sin \delta C_d D \quad (\text{for uniform pile cross section})$$

$$\text{where: } C_d = (4)(0.355 \text{ m}) = 1.424 \text{ m}$$

$$\begin{aligned} \text{Layer 1: } R_{s1} &= 2.10 (0.92) (48.3 \text{ kPa}) (\sin 30.2^\circ) (1.424 \text{ m}) (4 \text{ m}) \\ &= 267 \text{ kN} \end{aligned}$$

$$\begin{aligned} \text{Layer 2: } R_{s2} &= 1.83 (0.93) (120.1 \text{ kPa}) (\sin 29.4^\circ) (1.424 \text{ m}) (10 \text{ m}) \\ &= 1,429 \text{ kN} \end{aligned}$$

$$\begin{aligned} \text{Total: } R_s &= 267 \text{ kN} + 1,429 \text{ kN} \\ &= 1,696 \text{ kN} \end{aligned}$$

STEP 7 Determine the α_t coefficient and the bearing capacity factor, N'_q , from the ϕ angle near the pile toe.

Since the ϕ angle is not provided by either laboratory tests or in-situ data, the ϕ angle can be estimated from Table 4-6 using the average corrected SPT N' value over the zone from the pile toe to 3 diameter below the pile toe (1.065 meters). The soil near the pile toe is a dense sand and gravel.

$$\bar{N}'_{toe} = 33 \quad \rightarrow \quad \phi_{toe} = 35^\circ$$

a. Enter Figure 9.16(a) with ϕ angle near pile toe to determine α_t coefficient based on pile length to diameter ratio.

$$(D/b) = (14.0 \text{ m}) / (0.356 \text{ m}) = 39.3$$

$$\text{For } \phi_{toe} = 35^\circ \text{ and } (D/b) = 39.3 \quad \rightarrow \quad \alpha_t = 0.66$$

b. Enter Figure 9.16(b) with ϕ angle near pile toe to determine N'_q .

$$\text{For } \phi_{toe} = 35^\circ \rightarrow \quad N'_q = 65$$

STEP 8 Compute the effective overburden pressure at the pile toe, p_t (kPa).

The effective overburden pressure at the pile toe should be limited to a maximum of 150 kPa.

The effective overburden pressure at the pile toe, p_t , has been computed in the previous example (Section F.2.2.1, Step 1):

$$p_t = 169.1 \text{ kPa} \quad > \quad 150 \text{ kPa} \quad \rightarrow \quad \text{so use } p_t = 150 \text{ kPa}$$

STEP 9 Compute the ultimate toe resistance, R_t (kN).

$$\begin{aligned} \text{a. } R_t &= \alpha_t N'_q A_t p_t \\ &= 0.66 (65) (0.356 \text{ m})(0.356 \text{ m})(150.0 \text{ kPa}) \\ &= 817 \text{ kN} \end{aligned}$$

$$\text{b. limiting } R_t = q_L A_t$$

Using the estimated $\phi=35^\circ$ and Figure 9.17, the limiting unit toe resistance is:

$$q_L = 5,000 \text{ kPa}$$

Therefore,

$$R_t = 5,000 \text{ kPa} (0.356 \text{ m})(0.356 \text{ m}) = 635 \text{ kN}$$

c. Use lesser of the two R_t values obtained in steps a and b which is:

$$R_t = 635 \text{ kN}$$

STEP 10 Compute the ultimate pile capacity, Q_u (kN).

$$\begin{aligned} Q_u &= R_s + R_t \\ &= 1,696 \text{ kN} + 635 \text{ kN} = 2,331 \text{ kN} \end{aligned}$$

STEP 11 Compute allowable design load, Q_a (kN).

$$Q_a = \frac{Q_u}{\text{Factor of Safety}} = \frac{2,331 \text{ kN}}{\text{Factor of Safety}}$$

Note: Factor of Safety should be selected based on the construction control method to be specified. Recommended factors of safety are described in Section 9.6.

F.2.2.5 Static Axial Pile Capacity Calculations by Nordlund Method (after scour at 14 m)

For the soil profile interpreted from Soil Boring S-2 after scour as shown in Figure F.7. Perform a Nordlund method pile capacity calculation for an embedded length of 14 meters. Assume that scour has removed the 5 meter thick loose silt layer. Use the step-by-step method outlined in Section 9.7.1.1b.

STEP 1 Delineate the soil profile into layers and determine the ϕ angle for each layer.

- a. Construct p_o diagram using procedure described in Section 9.4. This is completed in Figure F.6.
- b. Correct SPT field N values for overburden pressure using Figure 4.6 from Chapter 4 and obtain corrected SPT N' values. For Soil Boring S-2, this has been done in the previous example (see Chapter F.2.2.1 - Step 1).

Note: Although scour has eroded the 5 meter thick loose silt layer, the original overburden pressure (with the loose silt layer still in place) should be used when correcting the SPT field N values.

- c. Determine ϕ angle for each layer from laboratory tests or in-situ data.

Since the ϕ angle is not provided by either laboratory or in-situ data, it should be determined using the average corrected SPT N' value, \bar{N}' , as calculated below.

- d. In the absence of laboratory or in-situ test data, determine the average corrected SPT N' value, \bar{N}' , for each soil layer and estimate ϕ angle from Table 4-6 in Chapter 4.

The soil profile along the pile embedded length is delineated into two layers of 4, and 10 meters thick. The average corrected SPT N' value for each soil layer is as follow.

$$\bar{N}'_1 = 110$$

(Layer 1 - depth 5 to 9 m;
Extremely dense sand and gravel)

STEP 1 (continued)

$$\bar{N}_2' = \frac{34 + 36 + 31 + 31 + 34 + 30 + 32}{7} = 33$$

(Layer 2 - depth 9 to 19 m;
Dense sand and gravel)

Use the average corrected SPT N' value for each soil layer to estimate ϕ angle from Table 4-6 in Chapter 4.

As discussed in Section F.2.2.2 - Step 1, a limiting friction angle should be used for the hard angular gravel of layer 1.

Layer 1: $\phi_1 = 36^\circ$ from limiting friction angle

For layer 2, the friction angle is computed from Table 4-6:

Layer 2: $\phi_2 = 35^\circ$ for $\bar{N}_2' = 33$

STEP 2 Determine δ , the friction angle between pile and soil based on displaced soil volume, V , and the soil friction angle, ϕ .

- a. Compute volume of soil displaced per unit length of pile, V .
Since this is a uniform cross section ($\omega = 0^\circ$) pile,

$$V = (0.356 \text{ m})(0.356 \text{ m})(1.0 \text{ m/m}) = 0.127 \text{ m}^3/\text{m}$$

- b. Enter Figure 9.10 with V and determine δ/ϕ ratio for pile type.

For a precast, prestressed concrete pile with $V = 0.127 \text{ m}^3/\text{m}$

$$\delta/\phi = 0.84$$

- c. Calculate δ from δ/ϕ ratio.

Layer 1: $\delta_1 = 0.84 (36^\circ) = 30.2^\circ$

Layer 2: $\delta_2 = 0.84 (35^\circ) = 29.4^\circ$

STEP 3 Determine the coefficient of lateral earth pressure, K_δ , for each ϕ angle.

- a. Determine K_δ for ϕ angle based on displaced volume, V , and pile taper angle, ω , using either Figure 9.11, 9.12, 9.13, or 9.14 and the appropriate procedure described in Step 3b, 3c, 3d, or 3e.

The pile taper angle, ω , = 0° .

For Layer 1:

$\phi_1 = 36^\circ$ and $V = 0.127 \text{ m}^3/\text{m}$, therefore use Step 3e.

A step by step procedure for determining K_δ using the linear interpolation and the log linear interpolation is presented in Section F.2.1.2 - Step 3.

For $\phi_1 = 36^\circ$, $\omega = 0^\circ$, and $V = 0.127 \text{ m}^3/\text{m}$:

$$K_{\delta 1} = 2.10$$

For Layer 2:

$\phi_2 = 35^\circ$ and $V = 0.127 \text{ m}^3/\text{m}$, therefore use Step 3d.

A step by step procedure for determining K_δ using the log linear interpolation is presented in Section F.2.1.2 - Step 3.

For $\phi_2 = 35^\circ$, $\omega = 0^\circ$, and $V = 0.127 \text{ m}^3/\text{m}$:

$$K_{\delta 2} = 1.83$$

STEP 4 Determine the correction factor, C_F , to be applied to K_δ if $\delta \neq \phi$.

Use Figure 9.15 to determine the correction factor for each K_δ . Enter figure with ϕ angle and $\delta/\phi=0.84$ to determine C_F .

Layer 1: For $\phi_1 = 36^\circ \rightarrow C_{F1} = 0.92$

Layer 2: For $\phi_2 = 35^\circ \rightarrow C_{F2} = 0.93$

STEP 5 Compute the average effective overburden pressure at the midpoint of each soil layer, p_d (kPa). (Note: a limiting value is not applied to p_d).

The effective overburden pressure at the midpoint of each soil layer is equal to the average effective overburden pressure of that layer. The effective overburden pressure diagram for Pier 2 after scour is presented in Figure F.8.

Layer 1: $p_{d1} = 22.8 \text{ kPa}$ (midpoint of layer 1 - at depth of 7.0 m)

Layer 2: $p_{d2} = 94.6 \text{ kPa}$ (midpoint of layer 2 - at depth of 14.0 m)

STEP 6 Compute the shaft resistance in each soil layer. Sum the shaft resistance from each soil layer to obtain the ultimate shaft resistance, R_s (kN).

$$R_s = K_\delta C_F p_d \sin \delta C_d D \quad (\text{for uniform pile cross section})$$

$$\text{where : } C_d = (4) (0.356 \text{ m}) = 1.424 \text{ m}$$

$$\begin{aligned} \text{Layer 1: } R_{s1} &= 2.10 (0.92) (22.8 \text{ kPa}) (\sin 30.2^\circ) (1.424 \text{ m}) (4 \text{ m}) \\ &= 126 \text{ kN} \end{aligned}$$

$$\begin{aligned} \text{Layer 2: } R_{s2} &= 1.83 (0.93) (94.6 \text{ kPa}) (\sin 29.4^\circ) (1.424 \text{ m}) (10 \text{ m}) \\ &= 1,126 \text{ kN} \end{aligned}$$

$$\begin{aligned} \text{Total: } R_s &= R_{s1} + R_{s2} \\ &= 126 \text{ kN} + 1,126 \text{ kN} \\ &= 1,252 \text{ kN} \end{aligned}$$

STEP 7 Determine the α_t coefficient and the bearing capacity factor, N'_q , from the ϕ angle near the pile toe.

Since the ϕ angle is not provided by either laboratory tests or in-situ data, the ϕ angle can be estimated from Table 4-6 using the average corrected SPT N' value over the zone from the pile toe to 3 diameter below the pile toe (1.065 meters). The soil near the pile toe is a dense sand and gravel.

$$\bar{N}'_{toe} = 33 \quad \rightarrow \quad \phi_{toe} = 35^\circ$$

a. Enter Figure 9.16(a) with ϕ angle near pile toe to determine α_t coefficient based on pile length to diameter ratio.

$$\begin{aligned} (D/b) &= (14.0 \text{ m}) / (0.356 \text{ m}) \\ &= 39.3 \end{aligned}$$

$$\text{For } \phi_{toe} = 35^\circ \text{ and } (D/b) = 39.3 \quad \rightarrow \quad \alpha_t = 0.66$$

b. Enter Figure 9.16(b) with ϕ angle near pile toe to determine N'_q .

$$\text{For } \phi_{toe} = 35^\circ \quad \rightarrow \quad N'_q = 65$$

STEP 8 Compute the effective overburden pressure at the pile toe, p_t (kPa).

The effective overburden pressure at the pile toe should be limited to a maximum of 150 kPa.

The effective overburden pressure at the pile toe, p_t , after scour has been computed and shown in Figure F.8:

$$p_t = 143.6 \text{ kPa} < 150 \text{ kPa} \quad \rightarrow \quad \text{OK}$$

STEP 9 Compute the ultimate toe resistance, R_t (kN).

$$\begin{aligned} \text{a. } R_t &= \alpha_t N'_q A_t p_t \\ &= 0.66 (65) (0.356 \text{ m }) (0.356 \text{ m }) (143.6 \text{ kPa }) \\ &= 782 \text{ kN} \end{aligned}$$

$$\text{b. limiting } R_t = q_L A_t$$

Use the estimated $\phi=35^\circ$ and Figure 9.17, the limiting unit toe resistance is:

$$\begin{aligned} q_L &= 5,000 \text{ kPa} \\ R_t &= 5,000 \text{ kPa } (0.356 \text{ m }) (0.356 \text{ m }) \\ &= 635 \text{ kN} \end{aligned}$$

c. Use lesser of the two R_t values obtained in steps a and b which is:

$$R_t = 635 \text{ kN}$$

STEP 10 Compute the ultimate pile capacity, Q_u (kN).

$$\begin{aligned} Q_u &= R_s + R_t \\ &= 1,252 \text{ kN} + 635 \text{ kN} = 1,887 \text{ kN} \end{aligned}$$

STEP 11 Compute allowable design load, Q_a .

$$Q_a = \frac{Q_u}{\text{Factor of Safety}} = \frac{1,887 \text{ kN}}{\text{Factor of Safety}}$$

Note: Factor of Safety should be selected based on the construction control method to be specified. Recommended factors of safety are described in Section 9.6.

F.2.2.6 Static Axial Pile Capacity Calculations by Effective Stress Method (before scour)

For the soil profile interpreted from Soil Boring S-2 as shown in Figure F.5. Perform an Effective Stress method pile capacity calculation for an embedded length of 10 meters. Assuming that scour has not occurred. Use the step-by-step method outlined in Section 9.7.1.3.

STEP 1 Delineate the soil profile into layers and determine ϕ' angle for each layer.

- a. Use the procedure described in Section 9.4 to construct a p_o diagram.

For Soil Boring S-2, the p_o diagram has been constructed in Section F.2.2.1 - Step 1 and also presented in Figure F.6.

- b. Divide the soil profile throughout the pile penetration depth into layers and determine the effective overburden pressure, p_o , at the midpoint of each layer.

As for the example in Section F.2.2.1, the soil profile along the pile embedded length is delineated into two layers of 4 and 6 meters thick. The average effective overburden pressure of each layer is equal to the effective overburden pressure at the midpoint of that layer as follows.

Layer 1: $p_{o1} = 48.3 \text{ kPa}$ (midpoint of layer 1 - at depth of 7.0 m)

Layer 2: $p_{o2} = 100.5 \text{ kPa}$ (midpoint of layer 2 - at depth of 12.0 m)

- c. Determine the ϕ' angle for each soil layer from laboratory or in-situ test data.

Since the ϕ' angle is not provided by either laboratory or in-situ test data, the average corrected SPT N' value will be used to estimate the ϕ' angle.

- d. In the absence of laboratory or in-situ test data for cohesionless soil layers, determine the average corrected SPT N' value for each soil layer and estimate the ϕ' angle from Table 4-6 in Chapter 4.

STEP 1 (continued)

As in the previous example (Section F.2.2.1), the average corrected SPT N' value and the soil type for each soil layer are as follows.

Layer 1: $\bar{N}_1' = 110$ (Layer 1 - depth 5 to 9 m;
Extremely dense sand and gravel)

Layer 2: $\bar{N}_2' = 33$ (Layer 2 - depth 9 to 15 m;
Dense sand and gravel)

Use the average corrected SPT N' value for each soil layer to estimate ϕ' angle from Table 4-6 in Chapter 4.

Layer 1: $\phi_1' = 36^\circ$ (From limiting friction angle; see discussion in
Section F.2.2.2 - Step 1)

Layer 2: $\phi_2' = 35^\circ$ for $\bar{N}_2' = 33$

STEP 2 Select the β coefficient for each soil layer.

- a. Use local experience to select β coefficient for each layer.

Assume no local experience.

- b. In the absence of local experience, use Table 9-6 or Figure 9.20 to estimate β coefficient from ϕ' angle for each layer.

Use the soil type, the estimated ϕ' angle, and Table 9-6 or Figure 9.20 to estimate the β coefficient for each layer.

Layer 1: $\beta_1 = 0.42$ (For extremely dense sand and gravel
with $\phi_1' = 36^\circ$)

Layer 2: $\beta_2 = 0.39$ (For dense sand and gravel with $\phi_2' = 35^\circ$)

STEP 3 For each soil layer compute the unit shaft resistance, f_s (kPa).

$$f_s = \beta p_o$$

$$\text{Layer 1: } f_{s1} = 0.42 (48.3 \text{ kPa}) = 20.29 \text{ kPa}$$

$$\text{Layer 2: } f_{s2} = 0.39 (100.5 \text{ kPa}) = 39.20 \text{ kPa}$$

STEP 4 Compute the shaft resistance in each soil layer and the ultimate shaft resistance, R_s (kN) from the sum of the shaft resistance from each soil layer.

$$R_s = f_s A_s$$

where A_s = Pile-soil surface area from pile perimeter and length

$$\text{Layer 1: } R_{s1} = 20.29 (4) (0.356 \text{ m}) (4 \text{ m})$$

$$= 116 \text{ kN}$$

$$\text{Layer 2: } R_{s2} = 39.20 (4) (0.356 \text{ m}) (6 \text{ m})$$

$$= 335 \text{ kN}$$

$$\text{Total: } R_s = R_{s1} + R_{s2}$$

$$= 116 \text{ kN} + 335 \text{ kN}$$

$$= 451 \text{ kN}$$

STEP 5 Compute the unit toe resistance, q_t (kPa).

$$q_t = N_t p_t$$

a. Use local experience to select N_t coefficient.

Assume no local experience.

STEP 5 (continued)

- b. In the absence of local experience, estimate N_t coefficient from Table 9-6 or Figure 9.21 based on ϕ' angle.

Table 9-6 or Figure 9.21 are a function of soil type and the ϕ' angle. The soil type for each layer can be obtained from the soil boring. The ϕ' angle for each layer can be obtained from laboratory tests or in-situ data. In the absence of either laboratory or in-situ test data, the ϕ' angle should be estimated from Table 4-6 in Chapter 4 using the average corrected SPT N' value, \bar{N}' , over the zone from the pile toe to 3 diameter below the pile toe (1.065 meters). The soil near the pile toe is a dense sand and gravel.

$$\bar{N}'_{\text{toe}} = 34 \quad \rightarrow \quad \phi'_{\text{toe}} = 36^\circ$$

Use the soil type, the estimated ϕ' angle, and Table 9-6 or Figure 9.21 to estimate the N_t coefficient.

$$N_t = 70 \quad (\text{For dense sand and gravel with } \phi'_{\text{toe}} = 36^\circ)$$

- c. Calculate the effective overburden pressure at the pile toe, p_t .

The effective overburden pressure at the pile toe, p_t , has been computed in the previous example (Section F.2.2.1, Step 1):

$$p_t = 129.9 \text{ kPa}$$

The unit toe resistance, q_t is:

$$\begin{aligned} q_t &= N_t p_t \\ &= 70 (129.9 \text{ kPa}) \\ &= 9,093 \text{ kPa} \end{aligned}$$

STEP 6 Compute the ultimate toe resistance, R_t (kN).

$$\begin{aligned} R_t &= q_t A_t \\ &= 9,093 (0.356 \text{ m}) (0.356 \text{ m}) \\ &= 1,155 \text{ kN} \end{aligned}$$

STEP 7 Compute the ultimate pile capacity, Q_u (kN).

$$\begin{aligned} Q_u &= R_s + R_t \\ &= 451 \text{ kN} + 1,155 \text{ kN} \\ &= 1,606 \text{ kN} \end{aligned}$$

Note: The ultimate capacity according to the Effective Stress method is less than the required 1780 kN ultimate capacity. The Effective Stress method would require a pile penetration depth of 12.5 meters for a 1780 kN capacity.

STEP 8 Compute the allowable design load, Q_a (kN).

$$Q_a = \frac{Q_u}{\text{Factor of Safety}} = \frac{1,606 \text{ kN}}{\text{Factor of Safety}}$$

Note: Factor of Safety should be selected based on the construction control method to be specified. Recommended factors of safety are described in Section 9.6.

F.2.2.7 Static Axial Pile Capacity Calculations by Driven Computer Program (considering Scour)

Note: In the following tables, the depth corresponding to the pile tip is 15 m. The “driving strength loss (%)” factor used in Driven for Boring S-2 was selected based on Table 9-20. Because these soils are cohesionless sands and gravels, the soil set-up factor selected was 1.0. For this problem, the driving strength loss is therefore 0%. In the Driven results, the “Restrike” and “Driving” tables are the same because no strength was lost during driving to be regained when the restrike is performed. The “Ultimate” tables consider the removal of the silty upper 5 m of the soil profile due to scour.

DRIVEN 1.2
GENERAL PROJECT INFORMATION

Filename: C:\DRIVEN\S2.DVN
 Project Name: Boring S-2 Project Date: 09/11/2003
 Project Client: FHWA Manual
 Computed By: BRR
 Project Manager:

PILE INFORMATION

Pile Type: Concrete Pile
 Top of Pile: 4.99 m
 Length of Square Side: 356.00 mm

ULTIMATE CONSIDERATIONS

Water Table Depth At Time Of:	- Drilling:	0.00 m
	- Driving/Restrike	0.00 m
	- Ultimate:	0.00 m
Ultimate Considerations:	- Local Scour:	0.00 m
	- Long Term Scour:	5.00 m
	- Soft Soil:	0.00 m

ULTIMATE PROFILE

Layer	Type	Thickness	Driving Loss	Unit Weight	Strength	Ultimate Curve
1	Cohesionless	5.00 m	0.00%	14.90 kN/m ³	30.7/30.7	Nordlund
2	Cohesionless	4.00 m	0.00%	21.20 kN/m ³	36.0/36.0	Nordlund
3	Cohesionless	6.00 m	0.00%	19.60 kN/m ³	35.0/36.0	Nordlund
4	Cohesionless	5.50 m	0.00%	19.60 kN/m ³	35.0/36.0	Nordlund

RESTRIKE - SKIN FRICTION

Depth	Soil Type	Effective Stress At Midpoint	Sliding Friction Angle	Adhesion	Skin Friction
0.01 m	Cohesionless	0.00 kPa	0.00	N/A	0.00 kN
3.01 m	Cohesionless	0.00 kPa	0.00	N/A	0.00 kN
4.99 m	Cohesionless	25.47 kPa	25.83	N/A	0.00 kN
5.01 m	Cohesionless	25.55 kPa	30.32	N/A	0.45 kN
8.01 m	Cohesionless	42.65 kPa	30.32	N/A	180.11 kN
8.99 m	Cohesionless	48.23 kPa	30.32	N/A	269.98 kN
9.01 m	Cohesionless	71.14 kPa	29.48	N/A	271.82 kN
12.01 m	Cohesionless	85.83 kPa	29.48	N/A	580.23 kN
14.99 m	Cohesionless	100.43 kPa	29.48	N/A	991.08 kN
15.01 m	Cohesionless	129.93 kPa	29.48	N/A	994.18 kN
18.01 m	Cohesionless	144.63 kPa	29.48	N/A	1513.70 kN
20.49 m	Cohesionless	156.78 kPa	29.48	N/A	2022.87 kN

RESTRIKE - END BEARING

Depth	Soil Type	Effective Stress At Tip	Bearing Cap. Factor	Limiting End Bearing	End Bearing
0.01 m	Cohesionless	0.00 kPa	33.50	110.80 kN	0.00 kN
3.01 m	Cohesionless	0.00 kPa	33.50	110.80 kN	0.00 kN
4.99 m	Cohesionless	0.00 kPa	33.50	110.80 kN	0.00 kN
4.98 m	Cohesionless	0.00 kPa	33.50	110.80 kN	0.00 kN
4.99 m	Cohesionless	25.47 kPa	33.50	110.80 kN	64.36 kN
5.01 m	Cohesionless	25.61 kPa	77.60	919.89 kN	174.59 kN
8.01 m	Cohesionless	59.80 kPa	77.60	919.89 kN	407.27 kN
8.99 m	Cohesionless	70.97 kPa	77.60	919.89 kN	482.70 kN
9.01 m	Cohesionless	71.18 kPa	77.60	919.89 kN	484.13 kN
12.01 m	Cohesionless	100.58 kPa	77.60	919.89 kN	681.68 kN
14.99 m	Cohesionless	129.78 kPa	77.60	919.89 kN	877.21 kN
15.01 m	Cohesionless	129.98 kPa	77.60	919.89 kN	878.52 kN
18.01 m	Cohesionless	159.37 kPa	77.60	919.89 kN	919.89 kN
20.49 m	Cohesionless	183.67 kPa	77.60	919.89 kN	919.89 kN

RESTRIKE - SUMMARY OF CAPACITIES

Depth	Skin Friction	End Bearing	Total Capacity
0.01 m	0.00 kN	0.00 kN	0.00 kN
3.01 m	0.00 kN	0.00 kN	0.00 kN
4.99 m	0.00 kN	64.36 kN	64.36 kN
5.01 m	0.45 kN	174.59 kN	175.05 kN
8.01 m	180.11 kN	407.27 kN	587.38 kN
8.99 m	269.98 kN	482.70 kN	752.68 kN
9.01 m	271.82 kN	484.13 kN	755.95 kN
12.01 m	580.23 kN	681.68 kN	1261.91 kN
14.99 m	991.08 kN	877.21 kN	1868.29 kN
15.01 m	994.18 kN	878.52 kN	1872.71 kN
18.01 m	1513.70 kN	919.89 kN	2433.59 kN
20.49 m	2022.87 kN	919.89 kN	2942.76 kN

DRIVING - SKIN FRICTION

Depth	Soil Type	Effective Stress At Midpoint	Sliding Friction Angle	Adhesion	Skin Friction
0.01 m	Cohesionless	0.00 kPa	0.00	N/A	0.00 kN
3.01 m	Cohesionless	0.00 kPa	0.00	N/A	0.00 kN
4.99 m	Cohesionless	25.47 kPa	25.83	N/A	0.00 kN
5.01 m	Cohesionless	25.55 kPa	30.32	N/A	0.45 kN
8.01 m	Cohesionless	42.65 kPa	30.32	N/A	180.11 kN
8.99 m	Cohesionless	48.23 kPa	30.32	N/A	269.98 kN
9.01 m	Cohesionless	71.14 kPa	29.48	N/A	271.82 kN
12.01 m	Cohesionless	85.83 kPa	29.48	N/A	580.23 kN
14.99 m	Cohesionless	100.43 kPa	29.48	N/A	991.08 kN
15.01 m	Cohesionless	129.93 kPa	29.48	N/A	994.18 kN
18.01 m	Cohesionless	144.63 kPa	29.48	N/A	1513.70 kN
20.49 m	Cohesionless	156.78 kPa	29.48	N/A	2022.87 kN

DRIVING - END BEARING

Depth	Soil Type	Effective Stress At Tip	Bearing Cap. Factor	Limiting End Bearing	End Bearing
0.01 m	Cohesionless	0.00 kPa	33.50	110.80 kN	0.00 kN
3.01 m	Cohesionless	0.00 kPa	33.50	110.80 kN	0.00 kN
4.99 m	Cohesionless	25.47 kPa	33.50	110.80 kN	64.36 kN
5.01 m	Cohesionless	25.61 kPa	77.60	919.89 kN	174.59 kN
8.01 m	Cohesionless	59.80 kPa	77.60	919.89 kN	407.27 kN
8.99 m	Cohesionless	70.97 kPa	77.60	919.89 kN	482.70 kN
9.01 m	Cohesionless	71.18 kPa	77.60	919.89 kN	484.13 kN
12.01 m	Cohesionless	100.58 kPa	77.60	919.89 kN	681.68 kN
14.99 m	Cohesionless	129.78 kPa	77.60	919.89 kN	877.21 kN
15.01 m	Cohesionless	129.98 kPa	77.60	919.89 kN	878.52 kN
18.01 m	Cohesionless	159.37 kPa	77.60	919.89 kN	919.89 kN
20.49 m	Cohesionless	183.67 kPa	77.60	919.89 kN	919.89 kN

DRIVING - SUMMARY OF CAPACITIES

Depth	Skin Friction	End Bearing	Total Capacity
0.01 m	0.00 kN	0.00 kN	0.00 kN
3.01 m	0.00 kN	0.00 kN	0.00 kN
4.99 m	0.00 kN	64.36 kN	64.36 kN
5.01 m	0.45 kN	174.59 kN	175.05 kN
8.01 m	180.11 kN	407.27 kN	587.38 kN
8.99 m	269.98 kN	482.70 kN	752.68 kN
9.01 m	271.82 kN	484.13 kN	755.95 kN
12.01 m	580.23 kN	681.68 kN	1261.91 kN
14.99 m	991.08 kN	877.21 kN	1868.29 kN
15.01 m	994.18 kN	878.52 kN	1872.71 kN
18.01 m	1513.70 kN	919.89 kN	2433.59 kN
20.49 m	2022.87 kN	919.89 kN	2942.76 kN

ULTIMATE - SKIN FRICTION

Depth	Soil Type	Effective Stress At Midpoint	Sliding Friction Angle	Adhesion	Skin Friction
0.01 m	Cohesionless	0.00 kPa	0.00	N/A	0.00 kN
3.01 m	Cohesionless	0.00 kPa	0.00	N/A	0.00 kN
4.99 m	Cohesionless	0.00 kPa	0.00	N/A	0.00 kN
5.01 m	Cohesionless	0.06 kPa	30.32	N/A	0.00 kN
8.01 m	Cohesionless	17.16 kPa	30.32	N/A	72.41 kN
8.99 m	Cohesionless	22.74 kPa	30.32	N/A	127.24 kN
9.01 m	Cohesionless	45.64 kPa	29.48	N/A	128.43 kN
12.01 m	Cohesionless	60.34 kPa	29.48	N/A	345.29 kN
14.99 m	Cohesionless	74.94 kPa	29.48	N/A	665.21 kN
15.01 m	Cohesionless	104.44 kPa	29.48	N/A	667.71 kN
18.01 m	Cohesionless	119.13 kPa	29.48	N/A	1095.68 kN
20.49 m	Cohesionless	131.28 kPa	29.48	N/A	1529.18 kN

ULTIMATE - END BEARING

Depth	Soil Type	Effective Stress At Tip	Bearing Cap. Factor	Limiting End Bearing	End Bearing
0.01 m	Cohesionless	0.00 kPa	0.00	0.00 kN	0.00 kN
3.01 m	Cohesionless	0.00 kPa	0.00	0.00 kN	0.00 kN
4.99 m	Cohesionless	0.00 kPa	0.00	0.00 kN	0.00 kN
5.01 m	Cohesionless	0.11 kPa	77.60	919.89 kN	0.78 kN
8.01 m	Cohesionless	34.31 kPa	77.60	919.89 kN	233.94 kN
8.99 m	Cohesionless	45.48 kPa	77.60	919.89 kN	310.11 kN
9.01 m	Cohesionless	45.69 kPa	77.60	919.89 kN	311.55 kN
12.01 m	Cohesionless	75.09 kPa	77.60	919.89 kN	511.99 kN
14.99 m	Cohesionless	104.29 kPa	77.60	919.89 kN	708.33 kN
15.01 m	Cohesionless	104.48 kPa	77.60	919.89 kN	709.64 kN
18.01 m	Cohesionless	133.88 kPa	77.60	919.89 kN	906.55 kN
20.49 m	Cohesionless	158.18 kPa	77.60	919.89 kN	919.89 kN

ULTIMATE - SUMMARY OF CAPACITIES

Depth	Skin Friction	End Bearing	Total Capacity
0.01 m	0.00 kN	0.00 kN	0.00 kN
3.01 m	0.00 kN	0.00 kN	0.00 kN
4.99 m	0.00 kN	0.00 kN	0.00 kN
5.01 m	0.00 kN	0.78 kN	0.78 kN
8.01 m	72.41 kN	233.94 kN	306.35 kN
8.99 m	127.24 kN	310.11 kN	437.35 kN
9.01 m	128.43 kN	311.55 kN	439.98 kN
12.01 m	345.29 kN	511.99 kN	857.27 kN
14.99 m	665.21 kN	708.33 kN	1373.53 kN
15.01 m	667.71 kN	709.64 kN	1377.35 kN
18.01 m	1095.68 kN	906.55 kN	2002.23 kN
20.49 m	1529.18 kN	919.89 kN	2449.06 kN

F.2.2.8 Summary of Pier 2 Capacity Calculation Results

Summary of Pile Capacity Estimates with an Embedded Pile Length of 10.0 meters

Method Used for Estimation of Pile Capacity	Calculated Pile Shaft Resistance (kN)	Calculated Pile Toe Resistance (kN)	Calculated Ultimate Pile Capacity (kN)
Meyerhof Method - SPT Data	1,134	1,676	2,810
Nordlund Method - SPT Data	984	854	1,838
Effective Stress Method	451	1,155	1,606
Driven Program - SPT Data	994	878	1,873

Summary of Pile Length Estimates for the 1,780 kN Ultimate Pile Capacity

Method Used for Estimation of Pile Capacity	Calculated Pile Length for the 1,780 kN Ultimate Pile Capacity
Meyerhof Method - SPT Data	1.0 meters for 2,136 kN
Nordlund Method - SPT Data	10.0 meters for 1,838 kN
Effective Stress Method	12.5 meters for 1,847 kN
Driven Program - SPT Data	10.0 meters for 1,873 kN

Note: All analyses do not consider scour effects on ultimate capacity.

Summary of Pile Capacity Estimates Before and After Channel Degradation Scour
Based on Nordlund Method

Pile Embedment	Ultimate Pile Capacity	
	Before Scour	After Scour
10 meters	1,838 kN	1,347 kN
14 meters	2,331 kN	1,887 kN

Summary of Pile Capacity Estimates Before and After Channel Degradation Scour
Based on Driven Program

Pile Embedment	Ultimate Pile Capacity	
	Before Scour	After Scour
10 meters	1873 kN	1377 kN
13 meters	2433 kN	2002 kN

Similar to the North Abutment, the ultimate pile group capacity at Pier 2, may also be taken as the sum of the ultimate capacities of the individual piles in the group. The design recommendation for estimating group capacity in cohesionless soil, presented in Section 9.8.1.1, should be referred to for detail considerations.

F.2.3 Pier 3 - Soil Boring S-3 (Cohesive and Cohesionless Soil)

F.2.3.1 Static Axial Pile Capacity Calculations by Nordlund and α -Method

For the soil profile interpreted from Soil Boring S-3 as shown in Figure F.9. Perform a static pile capacity calculation using the Nordlund and α methods for an embedded length of 13 meters. Use the Nordlund method for the cohesionless soil layer and α -Method for the cohesive soil layer. Use the appropriate portions of the step-by-step methods outlined in Section 9.7.1.1b and 9.7.1.2a.

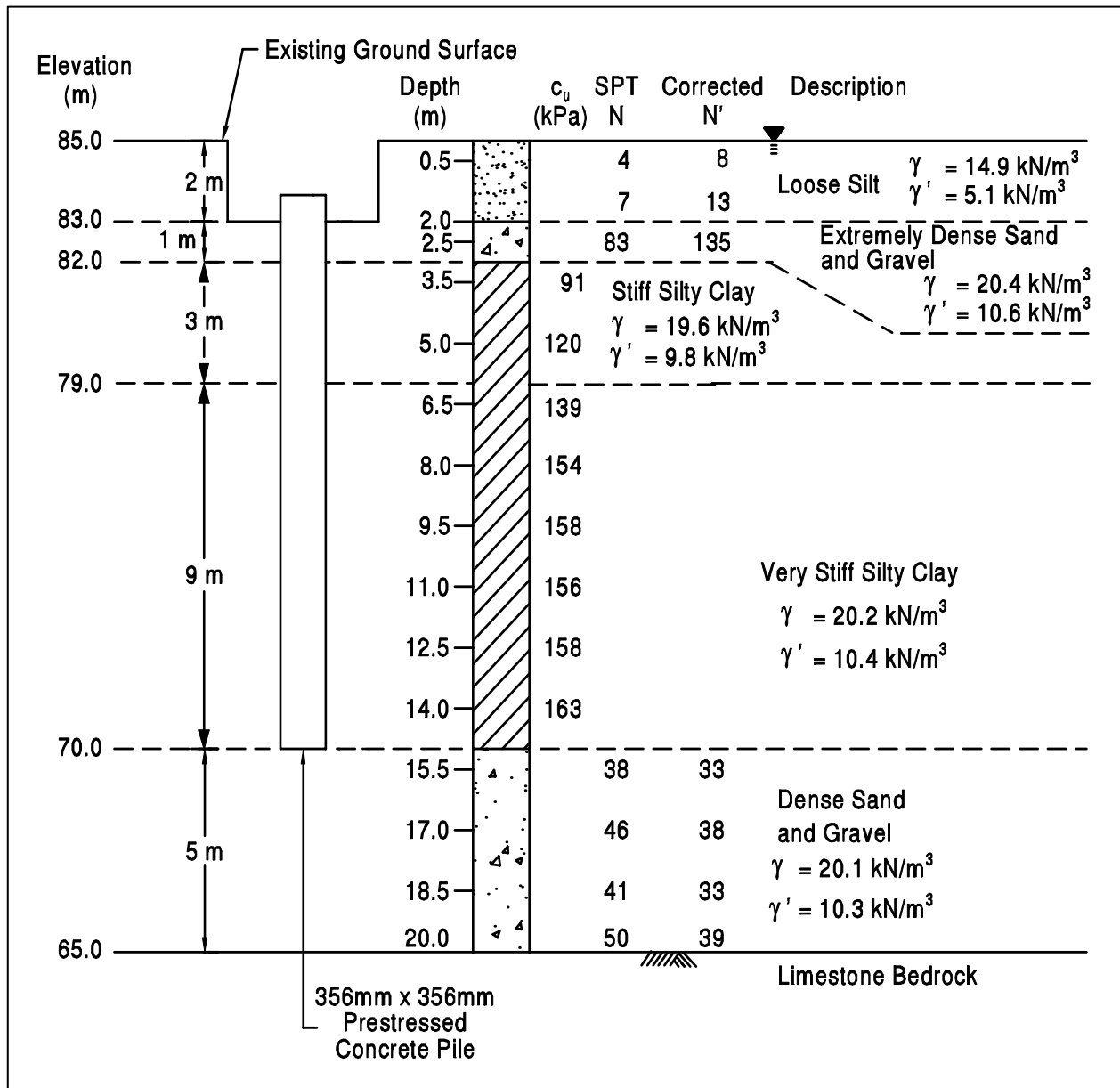


Figure F.9 Interpreted Soil Profile from Soil Boring S-3 at Pier 3

STEP 1 Delineate the soil profile into layers. Determine the ϕ angle for the cohesionless layer, and the undrained shear strength, c_u , for the cohesive layer.

a. Construct p_o diagram using procedure described in Section 9.4.

Effective overburden pressures, p_o , are needed to correct SPT field N values. The method for calculating the effective overburden pressure is explained in Section 9.4. A working example is presented in Section F.2.1.1. The effective overburden pressure diagram and soil layers are presented in Figure F.10.

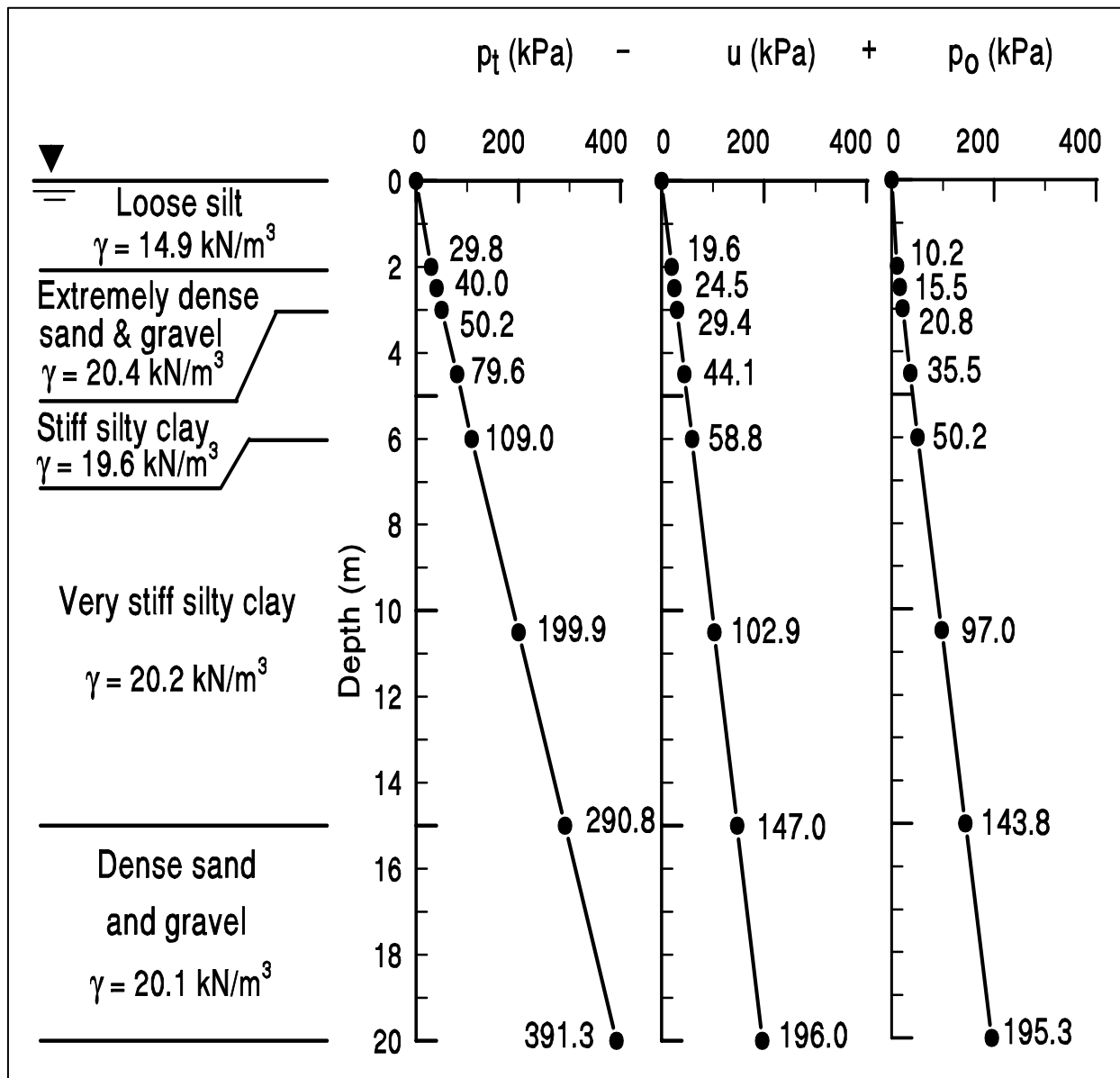


Figure F.10 Effective Overburden Pressure Diagram – Pier 3

STEP 1 (continued)

- b. Correct SPT field N values for overburden pressure using Figure 4.6 from Chapter 4 and obtain corrected SPT N' values.

Depth (m)	p_o (kPa)	Field SPT N value	Correction Factor	Corrected SPT N' (Field SPT N x Correction Factor)
2.0	10.2	7	1.80	13
2.5	15.5	83	1.63	135
15.5	149.0	38	0.87	33
17.0	164.6	46	0.83	38
18.5	180.2	41	0.80	33
20.0	195.3	50	0.77	39

Along the pile embedded length, the soil profile is delineated into three layers. Layer 1 is extremely dense sand and gravel that is 1.0 meter thick (cohesionless), layer 2 is stiff silty clay that is 3.0 meters thick (cohesive), and layer 3 is very stiff silty clay that is 9.0 meters thick (cohesive).

For the cohesionless soil layer, determine the average corrected SPT N' value, \bar{N}' , for the layer and estimate the ϕ angle from Table 4-6 in Chapter 4.

Layer 1: $\bar{N}'_1 = 135$ (Layer 1 - depth 2 to 3 m;
Extremely dense sand and Gravel)

For $N' > 50$, the ϕ angle computed by Table 4-6 can be as high as 43° . However, a limiting friction angle (as discussed in Section F.2.2.2 - Step 1) will govern for soil layer 1 since this layer contains hard angular gravel.

Layer 1: $\phi_1 = 36^\circ$ from limiting friction angle

STEP 1 (continued)

For the cohesive soil layer, determine the average undrained shear strength, c_u for each soil layer.

$$\text{Layer 2: } c_{u2} = \frac{91 + 120}{2} = 106 \text{ kPa} \quad (\text{Layer 2 - depth 3 to 6 m;} \\ \text{Stiff silty clay})$$

$$\text{Layer 3: } c_{u3} = \frac{139 + 154 + 158 + 156 + 158 + 163}{6} = 155 \text{ kPa} \\ (\text{Layer 3 - depth 6 to 15 m;} \\ \text{Very stiff silty clay})$$

STEP 2 Compute the shaft resistance at soil layer 1 (cohesionless) using Nordlund method.

a. (Nordlund - Step 2): Determine δ , the friction angle between pile and soil based on displaced soil volume, V , and the soil friction angle, ϕ .

(i) Compute volume of soil displaced per unit length of pile, V .

Since this is a uniform cross section ($\omega = 0^\circ$) pile,

$$V = (0.356 \text{ m})(0.356 \text{ m})(1.0 \text{ m/m}) = 0.127 \text{ m}^3/\text{m}$$

(ii) Enter Figure 9.10 with V and determine δ/ϕ ratio for pile type.

For a precast, prestressed concrete pile with $V = 0.127 \text{ m}^3/\text{m}$,

$$\delta/\phi = 0.84$$

(iii) Calculate δ from δ/ϕ ratio.

$$\text{Layer 1: } \delta_1 = 0.84 (36^\circ) = 30.2^\circ$$

STEP 2 (continued)

- b. (Nordlund - Step 3): Determine the coefficient of lateral earth pressure, K_δ , for each ϕ angle.

- (i) Determine K_δ for ϕ angle based on displaced volume, V , and pile taper angle, ω , using either Figure 9.11, 9.12, 9.13, or 9.14 and the appropriate procedure described in Step 3b, 3c, 3d, or 3e.

For $\phi_1 = 36^\circ$ and $V = 0.127 \text{ m}^3/\text{m}$, therefore use Step 3e.

A step by step procedure for determining K_δ using the linear interpolation and the log linear interpolation is presented in Section F.2.1.2 - Step 3.

For $\phi_1 = 36^\circ$, $\omega = 0^\circ$, and $V = 0.127 \text{ m}^3/\text{m}$:

$$K_{\delta 1} = 2.10$$

- c. (Nordlund - Step 4): Determine the correction factor, C_F , to be applied to K_δ if $\delta \neq \phi$.

Use Figure 9.15 to determine the correction factor for each K_δ . Enter figure with ϕ angle and $\delta/\phi=0.84$ to determine C_F .

Layer 1: For $\phi_1 = 36^\circ \rightarrow C_{F1} = 0.92$

- d. (Nordlund - Step 5): Compute the average effective overburden pressure at the midpoint of each soil layer, p_d (kPa). (Note: a limiting value is not applied to p_d).

The effective overburden pressure at the midpoint of the soil layer is equal to the average effective overburden pressure of that layer. The effective overburden pressure diagram for Pier 3 is presented in Figure F.10.

Layer 1: $p_{d1} = 15.5 \text{ kPa}$ (midpoint of layer 1 - at depth of 2.5 m)

STEP 2 (continued)

- e. (Nordlund - Step 6): Compute the shaft resistance in soil layer 1.

$$R_s = K_\delta C_F p_d \sin \delta C_d D \quad (\text{for uniform pile cross section})$$

$$\text{where : } C_d = (4) (0.356 \text{ m}) = 1.424 \text{ m}$$

$$\begin{aligned} \text{Layer 1: } R_{s1} &= 2.10 (0.92) (15.5 \text{ kPa}) (\sin 30.2^\circ) (1.424 \text{ m}) (1 \text{ m}) \\ &= 22 \text{ kN} \end{aligned}$$

STEP 3 Compute the shaft resistance at soil layers 2 and 3 (cohesive) using α -method.

- a. (α -Method - Steps 1 and 2): Determine the adhesion, c_a , from Figure 9.18 or adhesion factor, α , from Figure 9.19 for the cohesive soil layer.

An extremely dense sand and gravel overlying stiff silty clay of soil layer 2 agrees with the soil stratigraphy shown in Figure 9.19a. The depth to pile diameter ratio is:

$$(D/b) = (3.0 \text{ m}) / (0.356 \text{ m}) = 8.43$$

For $c_{u2} = 106 \text{ kPa}$ and $(D/b) = 8.43$, the adhesion factor interpolated from Figure 9.19a is:

$$\alpha = 1.0$$

The adhesion is:

$$\begin{aligned} c_{a2} &= \alpha c_{u2} \\ &= 1.0 (106 \text{ kPa}) = 106 \text{ kPa} \end{aligned}$$

Therefore, the unit shaft resistance of soil layer 2 is :

$$\text{Layer 2: } f_{s2} = c_{a2} = 106 \text{ kPa}$$

STEP 3 (continued)

For soil layer 3, Figure 9.19 and 9.18 should be used to compute the adhesion of the very stiff silty clay. Depending on the thickness of the extremely dense sand and gravel of soil layer 1 and the thickness of the stiff silty clay of soil layer 2, the soil stratigraphy for soil layer 3 may also agree with that of Figure 9.19a. However, it is reasonable to assume here that the pile would not be able to drag the sand and gravel far enough from soil layer 1 through the stiff silty clay of soil layer 2 to reach soil layer 3. Therefore, soil layer 3 should not be affected by the sand and gravel from soil layer 1 and hence, the adhesion should be determined from Figure 9.19c or 9.18. The depth, D , to pile diameter, b , ratio is:

$$(D/b) = (9.0 \text{ m}) / (0.356 \text{ m}) = 25.28$$

Interpolating the adhesion factor from Figure 9.19c, for $c_{u3} = 155 \text{ kPa}$ and $(D/b) = 25.28$:

$$\alpha = 0.35$$

The adhesion is therefore:

$$\begin{aligned} c_{a3} &= \alpha c_{u3} \\ &= 0.35 (155 \text{ kPa}) \\ &= 54.3 \text{ kPa} \end{aligned}$$

For comparison, using Figure 9.18 for concrete pile with $(D/b) = 25.35$ and $c_{u3} = 155 \text{ kPa}$, the adhesion obtained from the interpolation between curves is:

$$c_{a3} = 54.7 \text{ kPa} \rightarrow \text{similar to Figure 9.19c.}$$

Therefore,

$$\text{Layer 3: } f_{s3} = c_{a3} = 54.3 \text{ kPa}$$

STEP 3 (continued)

- b. (α -Method - Step 3): Compute the ultimate shaft resistance in soil layer 2 and soil layer 3.

$$\begin{aligned}\text{Layer 2: } R_{s2} &= f_{s2} A_s \\ &= 106.0 \text{ kPa } (4)(0.356 \text{ m})(3 \text{ m}) = 453 \text{ kN}\end{aligned}$$

$$\begin{aligned}\text{Layer 3: } R_{s3} &= f_{s3} A_s \\ &= 54.3 \text{ kPa } (4)(0.356 \text{ m})(9 \text{ m}) = 696 \text{ kN}\end{aligned}$$

- STEP 4 Sum the shaft resistance from each soil layer to obtain the ultimate shaft resistance, R_s (kN).

$$\begin{aligned}\text{Total: } R_s &= R_{s1} + R_{s2} + R_{s3} \\ &= 22 \text{ kN} + 453 \text{ kN} + 696 \text{ kN} = 1,171 \text{ kN}\end{aligned}$$

- STEP 5 Compute the ultimate toe resistance using Nordlund method.

Use Nordlund method, since the soil at pile toe is dense sand and gravel (cohesionless).

- (i) (Nordlund - Step 7): Determine the α_t coefficient and the bearing capacity factor, N'_q , from the ϕ angle near the pile toe.

Since the ϕ angle is not provided by either laboratory tests or in-situ data, it can be estimated from Table 4-6 using the average corrected SPT N' value over the zone from the pile toe to 3 diameter below the pile toe (1.065 meters).

$$\bar{N}'_{toe} = 33 \quad \rightarrow \quad \phi_{toe} = 35^\circ$$

STEP 5 (continued)

- a. Enter Figure 9.16(a) with ϕ angle near pile toe to determine α_t coefficient based on pile length to diameter ratio.

$$(D/b) = (13.0 \text{ m}) / (0.356 \text{ m}) = 36.52$$

$$\text{For } \phi_{\text{toe}} = 35^\circ \text{ and } (D/b) = 36.52 \rightarrow \alpha_t = 0.67$$

- b. Enter Figure 9.16(b) with ϕ angle near pile toe to determine N'_q .

$$\text{For } \phi_{\text{toe}} = 35^\circ \rightarrow N'_q = 65$$

- (ii) (Nordlund - Step 8): Compute the effective overburden pressure at the pile toe, p_t (kPa).

The effective overburden pressure at the pile toe should be limited to a maximum of 150 kPa.

The effective overburden pressure at the pile toe, p_t , has been computed in Figure F.10:

$$p_t = 143.8 \text{ kPa} < 150 \text{ kPa} \rightarrow \text{OK}$$

- (iii) (Nordlund - Step 9): Compute the ultimate toe resistance, R_t (kN).

$$\text{a. } R_t = \alpha_t N'_q A_t p_t$$

$$= 0.67 (65) (0.356 \text{ m}) (0.356 \text{ m}) (143.8 \text{ kPa}) = 795 \text{ kN}$$

$$\text{b. limiting } R_t = q_L A_t$$

Using the estimated $\phi=35^\circ$ and Figure 9.17, the limiting unit toe resistance is:

$$q_L = 5,000 \text{ kPa}$$

STEP 5 (continued)

Therefore,

$$\begin{aligned} R_t &= 5,000 \text{ kPa } (0.356 \text{ m })(0.356 \text{ m }) \\ &= 635 \text{ kN} \end{aligned}$$

c. Use lesser of the two R_t values obtained in steps a and b which is:

$$R_t = 635 \text{ kN}$$

STEP 6 Compute the ultimate pile capacity, Q_u (kN).

$$\begin{aligned} Q_u &= R_s + R_t \\ &= 1,171 \text{ kN} + 635 \text{ kN} \\ &= 1,806 \text{ kN} \end{aligned}$$

Note: In reality, the pile toe will not stop at the top of the bearing stratum. The pile toe will be driven further into the dense sand and gravel bearing stratum and therefore the ultimate toe resistance of the pile is expected to be higher than 635 kN.

STEP 7 Compute the allowable design load, Q_a (kN).

$$Q_a = \frac{Q_u}{\text{Factor of Safety}} = \frac{1,806 \text{ kN}}{\text{Factor of Safety}}$$

Note: Factor of Safety should be selected based on the construction control method to be specified. Recommended factors of safety are described in Section 9.6.

F.2.3.2 Static Axial Pile Capacity Calculations by Effective Stress Method

For the soil profile interpreted from Soil Boring S-3 as shown in Figure F.9. Perform an Effective Stress method pile capacity calculation for an embedded length of 13 meters. Use the step-by-step method outlined in Section 9.7.1.3.

STEP 1 Delineate the soil profile into layers and determine ϕ' angle for each layer.

- a. Use the procedure described in Section 9.4 to construct a p_o diagram.

For Soil Boring S-3, the p_o diagram has been constructed in Section F.2.3.1 - Step 1 and also presented in Figure F.10.

- b. Divide the soil profile throughout the pile penetration depth into layers and determine the effective overburden pressure, p_o , at the midpoint of each layer.

As the example in Section F.2.3.1, the soil profile along the pile embedded length is delineated into three layers of 1, 3, and 9 meters thick. The average effective overburden pressure of each layer is equal to the effective overburden pressure at the midpoint of that layer as follows.

Layer 1: $p_{o1} = 15.5$ kPa (midpoint of layer 1 - at depth of 2.5 m)

Layer 2: $p_{o2} = 35.5$ kPa (midpoint of layer 2 - at depth of 4.5 m)

Layer 3: $p_{o3} = 97.0$ kPa (midpoint of layer 3 - at depth of 10.5 m)

- c. Determine the ϕ' angle for each soil layer from laboratory or in-situ test data.

Since the ϕ' angle is not provided by either laboratory or in-situ test data, the average corrected SPT N' value will be used to estimate the ϕ' angle.

- d. In the absence of laboratory or in-situ test data for cohesionless soil layers, determine the average corrected SPT N' value for each soil layer and estimate the ϕ' angle from Table 4-6 in Chapter 4.

STEP 1 (continued)

For cohesionless soil layer 1, the average corrected SPT N' value and the soil type for each soil layer is as follows.

Layer 1: $\bar{N}_1' = 135$ (Layer 1 - depth 2 to 3 m;
Extremely dense sand and gravel)

Use the average corrected SPT N' value for soil layer 1 to estimate the ϕ' angle from Table 4-6 in Chapter 4.

Layer 1: $\phi_1' = 36^\circ$ (Limiting friction angle is used; See discussion in
Section F.2.2.2 - Step 1)

For the cohesive soil layers 2 and 3, the effective friction angle is obtained from from the laboratory triaxial test.

Layer 2: $\phi_2' = 27^\circ$

Layer 3: $\phi_3' = 29^\circ$

STEP 2 Select the β coefficient for each soil layer.

- a. Use local experience to select β coefficient for each layer.

Assume no local experience.

- b. In the absence of local experience, use Table 9-6 or Figure 9.20 to estimate β coefficient from ϕ' angle for each layer.

Use the soil type, the estimated ϕ' angle, and Table 9-6 or Figure 9.20 to estimate the β coefficient for each soil layer.

Layer 1: $\beta_1 = 0.40$ (For extremely dense sand and gravel
with $\phi_1' = 36^\circ$)

Layer 2: $\beta_2 = 0.29$ (For stiff silty clay with $\phi_2' = 27^\circ$)

STEP 2 (continued)

$$\text{Layer 3: } \beta_3 = 0.38 \quad (\text{For stiff silty clay with } \phi_3' = 29^\circ)$$

STEP 3 For each soil layer compute the unit shaft resistance, f_s (kPa).

$$f_s = \beta p_o$$

$$\text{Layer 1: } f_{s1} = 0.40 (15.5 \text{ kPa}) = 6.20 \text{ kPa}$$

$$\text{Layer 2: } f_{s2} = 0.29 (35.5 \text{ kPa}) = 10.30 \text{ kPa}$$

$$\text{Layer 3: } f_{s3} = 0.38 (97.0 \text{ kPa}) = 36.86 \text{ kPa}$$

STEP 4 Compute the shaft resistance in each soil layer and the ultimate shaft resistance, R_s (kN), from the sum of the shaft resistance from each soil layer.

$$R_s = f_s A_s$$

where A_s = Pile-soil surface area from pile perimeter and length

$$\begin{aligned} \text{Layer 1: } R_{s1} &= 6.20 (4) (0.356 \text{ m}) (1 \text{ m}) \\ &= 9 \text{ kN} \end{aligned}$$

$$\begin{aligned} \text{Layer 2: } R_{s2} &= 10.30 (4) (0.356 \text{ m}) (3 \text{ m}) \\ &= 44 \text{ kN} \end{aligned}$$

$$\begin{aligned} \text{Layer 3: } R_{s3} &= 36.86 (4) (0.356 \text{ m}) (9 \text{ m}) \\ &= 472 \text{ kN} \end{aligned}$$

$$\begin{aligned} \text{Total: } R_s &= R_{s1} + R_{s2} + R_{s3} \\ &= 9 \text{ kN} + 44 \text{ kN} + 472 \text{ kN} \\ &= 525 \text{ kN} \end{aligned}$$

STEP 5 Compute the unit toe resistance, q_t (kPa).

$$q_t = N_t p_t$$

- a. Use local experience to select N_t coefficient.

Assume no local experience.

- b. In the absence of local experience, estimate N_t coefficient from Table 9-6 or Figure 9.21 based on ϕ' angle.

Table 9-6 or Figure 9.21 are a function of soil type and the ϕ' angle. The soil type for each layer can be obtained from the soil boring. The ϕ' angle for each layer can be obtained from laboratory tests or in-situ data. In the absence of either laboratory or in-situ test data, the ϕ' angle should be estimated from Table 4-6 in Chapter 4 using the average corrected SPT N' value, \bar{N}' , over the zone from the pile toe to 3 diameter below the pile toe (1.065 meters). The soil near the pile toe is a dense sand and gravel.

$$\bar{N}'_{toe} = 33 \quad \rightarrow \quad \phi'_{toe} = 35^\circ$$

Use the soil type, the estimated ϕ' angle, and Table 9-6 or Figure 9.21 to estimate the N_t coefficient.

$$N_t = 58 \quad (\text{For dense sand and gravel with } \phi'_{toe} = 35^\circ)$$

- c. Calculate the effective overburden pressure at the pile toe, p_t .

The effective overburden pressure at the pile toe, p_t , has been computed in a previous example (Section F.2.3.1, Step 1):

$$p_t = 143.8 \text{ kPa}$$

STEP 5 (continued)

The unit toe resistance, q_t is:

$$\begin{aligned}q_t &= N_t p_t \\ &= 58 (143.8 \text{ kPa}) = 8,340 \text{ kPa}\end{aligned}$$

STEP 6 Compute the ultimate toe resistance, R_t (kN).

$$\begin{aligned}R_t &= q_t A_t \\ &= 8,340 (0.356 \text{ m}) (0.356 \text{ m}) = 1,059 \text{ kN}\end{aligned}$$

STEP 7 Compute the ultimate pile capacity, Q_u (kN).

$$\begin{aligned}Q_u &= R_s + R_t \\ &= 525 \text{ kN} + 1,059 \text{ kN} = 1,584 \text{ kN}\end{aligned}$$

Note: The ultimate capacity according to the Effective Stress method is less than the required 1780 kN ultimate capacity. As discussed in the Nordlund method, in reality the pile toe will not be stopped at the top of the bearing stratum. The pile toe will be driven further into the dense sand and gravel bearing stratum, and therefore, the ultimate toe resistance of the pile is expected to be higher than 1,059 kN. The Effective Stress method would require a pile penetration depth of 14.0 meters for a 1780 kN capacity.

STEP 8 Compute the allowable design load, Q_a (kN).

$$Q_a = \frac{Q_u}{\text{Factor of Safety}} = \frac{1,584 \text{ kN}}{\text{Factor of Safety}}$$

Note: Factor of Safety should be selected based on the construction control method to be specified. Recommended factors of safety are described in Section 9.6.

F.2.3.3 Static Axial Pile Capacity Calculations by Driven Computer Program

Note: In the following tables, the depth corresponding to the pile tip is 15 m. The “driving strength loss (%)” factor used in Driven for Boring S-2 was selected based on Table 9-20. For the cohesionless silts, sands and gravels, the soil set-up factor selected was 1.0, which leads to a driving strength loss of 0%. For the cohesive silty clay layers, the selected soil set-up factor selected was 2.0, which leads to a driving strength loss of 50%. In the Driven results, the “Driving” tables reflect the lost resistance in the clay layers due to driving. The “Restrike” tables reflect a time when the clay layers have regained that resistance after pore water pressure dissipation. The “Ultimate” tables consider the removal of the silty upper 2 m of the soil profile due to scour. Note the minor loss of 29 kN between the “Restrike” and “Ultimate” results due to the loss of the silty material.

DRIVEN 1.2 **GENERAL PROJECT INFORMATION**

Filename: C:\DRIVEN\S3.DVN
Project Name: BORING S-3 Project Date: 09/11/2003
Project Client: FHWA Manual
Computed By: BRR
Project Manager:

PILE INFORMATION

Pile Type: Concrete Pile
Top of Pile: 2.00 m
Length of Square Side: 356.00 mm

ULTIMATE CONSIDERATIONS

Water Table Depth At Time Of:	- Drilling:	0.00 m
	- Driving/Restrike:	0.00 m
	- Ultimate:	0.00 m
Ultimate Considerations:	- Local Scour:	0.00 m
	- Long Term Scour:	2.00 m
	- Soft Soil:	0.00 m

ULTIMATE PROFILE

Layer	Type	Thickness	Driving Loss	Unit Weight	Strength	Ultimate Curve
1	Cohesionless	2.00 m	0.00%	14.90 kN/m ³	31.0/31.0	Nordlund
2	Cohesionless	1.00 m	0.00%	20.40 kN/m ³	36.0/36.0	Nordlund
3	Cohesive	3.00 m	50.00%	19.60 kN/m ³	106.00 kPa	T-80 Sand
4	Cohesive	9.00 m	50.00%	20.20 kN/m ³	155.00 kPa	T-79 Concrete
5	Cohesionless	5.00 m	0.00%	20.10 kN/m ³	36.0/36.0	Nordlund

RESTRIKE - SKIN FRICTION

Depth	Soil Type	Effective Stress At Midpoint	Sliding Friction Angle	Adhesion	Skin Friction
0.01 m	Cohesionless	0.00 kPa	0.00	N/A	0.00 kN
1.99 m	Cohesionless	0.00 kPa	0.00	N/A	0.00 kN
2.01 m	Cohesionless	10.25 kPa	30.32	N/A	0.14 kN
2.99 m	Cohesionless	15.44 kPa	30.32	N/A	21.44 kN
3.01 m	Cohesive	N/A	N/A	106.00 kPa	23.24 kN
5.99 m	Cohesive	N/A	N/A	106.00 kPa	473.03 kN
6.01 m	Cohesive	N/A	N/A	47.10 kPa	475.21 kN
9.01 m	Cohesive	N/A	N/A	54.64 kPa	708.74 kN
12.01 m	Cohesive	N/A	N/A	62.19 kPa	1006.71 kN
14.99 m	Cohesive	N/A	N/A	67.79 kPa	1342.35 kN
15.01 m	Cohesionless	143.83 kPa	30.32	N/A	1345.34 kN
18.01 m	Cohesionless	159.28 kPa	30.32	N/A	2015.65 kN
19.99 m	Cohesionless	169.47 kPa	30.32	N/A	2529.26 kN

RESTRIKE - END BEARING

Depth	Soil Type	Effective Stress At Tip	Bearing Cap. Factor	Limiting End Bearing	End Bearing
0.01 m	Cohesionless	0.00 kPa	35.20	125.39 kN	0.00 kN
1.99 m	Cohesionless	0.00 kPa	35.20	125.39 kN	0.00 kN
2.01 m	Cohesionless	10.30 kPa	77.60	919.89 kN	70.25 kN
2.99 m	Cohesionless	20.69 kPa	77.60	919.89 kN	141.07 kN
3.01 m	Cohesive	N/A	N/A	N/A	120.90 kN
5.99 m	Cohesive	N/A	N/A	N/A	120.90 kN
6.01 m	Cohesive	N/A	N/A	N/A	176.79 kN
9.01 m	Cohesive	N/A	N/A	N/A	176.79 kN
12.01 m	Cohesive	N/A	N/A	N/A	176.79 kN
14.99 m	Cohesive	N/A	N/A	N/A	176.79 kN
15.01 m	Cohesionless	143.88 kPa	77.60	919.89 kN	919.89 kN
18.01 m	Cohesionless	174.78 kPa	77.60	919.89 kN	919.89 kN
19.99 m	Cohesionless	195.17 kPa	77.60	919.89 kN	919.89 kN

RESTRIKE - SUMMARY OF CAPACITIES

Depth	Skin Friction	End Bearing	Total Capacity
0.01 m	0.00 kN	0.00 kN	0.00 kN
1.99 m	0.00 kN	0.00 kN	0.00 kN
2.01 m	0.14 kN	70.25 kN	70.39 kN
2.99 m	21.44 kN	141.07 kN	162.51 kN
3.01 m	23.24 kN	120.90 kN	144.14 kN
5.99 m	473.03 kN	120.90 kN	593.93 kN
6.01 m	475.21 kN	176.79 kN	652.00 kN
9.01 m	708.74 kN	176.79 kN	885.53 kN
12.01 m	1006.71 kN	176.79 kN	1183.50 kN
14.99 m	1342.35 kN	176.79 kN	1519.14 kN
15.01 m	1345.34 kN	919.89 kN	2265.22 kN
18.01 m	2015.65 kN	919.89 kN	2935.54 kN
19.99 m	2529.26 kN	919.89 kN	3449.15 kN

DRIVING - SKIN FRICTION

Depth	Soil Type	Effective Stress At Midpoint	Sliding Friction Angle	Adhesion	Skin Friction
0.01 m	Cohesionless	0.00 kPa	0.00	N/A	0.00 kN
1.99 m	Cohesionless	0.00 kPa	0.00	N/A	0.00 kN
2.01 m	Cohesionless	10.25 kPa	30.32	N/A	0.14 kN
2.99 m	Cohesionless	15.44 kPa	30.32	N/A	21.44 kN
3.01 m	Cohesive	N/A	N/A	106.00 kPa	22.34 kN
5.99 m	Cohesive	N/A	N/A	106.00 kPa	247.24 kN
6.01 m	Cohesive	N/A	N/A	47.10 kPa	248.33 kN
9.01 m	Cohesive	N/A	N/A	54.64 kPa	365.09 kN
12.01 m	Cohesive	N/A	N/A	62.19 kPa	514.08 kN
14.99 m	Cohesive	N/A	N/A	67.79 kPa	681.90 kN
15.01 m	Cohesionless	143.83 kPa	30.32	N/A	684.88 kN
18.01 m	Cohesionless	159.28 kPa	30.32	N/A	1355.20 kN
19.99 m	Cohesionless	169.47 kPa	30.32	N/A	1868.81 kN

DRIVING - END BEARING

Depth	Soil Type	Effective Stress At Tip	Bearing Cap. Factor	Limiting End Bearing	End Bearing
0.01 m	Cohesionless	0.00 kPa	35.20	125.39 kN	0.00 kN
1.99 m	Cohesionless	0.00 kPa	35.20	125.39 kN	0.00 kN
2.01 m	Cohesionless	10.30 kPa	77.60	919.89 kN	70.25 kN
2.99 m	Cohesionless	20.69 kPa	77.60	919.89 kN	141.07 kN
3.01 m	Cohesive	N/A	N/A	N/A	120.90 kN
5.99 m	Cohesive	N/A	N/A	N/A	120.90 kN
6.01 m	Cohesive	N/A	N/A	N/A	176.79 kN
9.01 m	Cohesive	N/A	N/A	N/A	176.79 kN
12.01 m	Cohesive	N/A	N/A	N/A	176.79 kN
14.99 m	Cohesive	N/A	N/A	N/A	176.79 kN
15.01 m	Cohesionless	143.88 kPa	77.60	919.89 kN	919.89 kN
18.01 m	Cohesionless	174.78 kPa	77.60	919.89 kN	919.89 kN
19.99 m	Cohesionless	195.17 kPa	77.60	919.89 kN	919.89 kN

DRIVING - SUMMARY OF CAPACITIES

Depth	Skin Friction	End Bearing	Total Capacity
0.01 m	0.00 kN	0.00 kN	0.00 kN
1.99 m	0.00 kN	0.00 kN	0.00 kN
1.99 m	0.00 kN	0.00 kN	0.00 kN
2.00 m	0.00 kN	27.42 kN	27.42 kN
2.01 m	0.14 kN	70.25 kN	70.39 kN
2.99 m	21.44 kN	141.07 kN	162.51 kN
3.01 m	22.34 kN	120.90 kN	143.24 kN
5.99 m	247.24 kN	120.90 kN	368.14 kN
6.01 m	248.33 kN	176.79 kN	425.12 kN
9.01 m	365.09 kN	176.79 kN	541.88 kN
12.01 m	514.08 kN	176.79 kN	690.87 kN
14.99 m	681.90 kN	176.79 kN	858.69 kN
15.01 m	684.88 kN	919.89 kN	1604.77 kN
18.01 m	1355.20 kN	919.89 kN	2275.08 kN
19.99 m	1868.81 kN	919.89 kN	2788.69 kN

ULTIMATE - SKIN FRICTION

Depth	Soil Type	Effective Stress At Midpoint	Sliding Friction Angle	Adhesion	Skin Friction
0.01 m	Cohesionless	0.00 kPa	0.00	N/A	0.00 kN
1.99 m	Cohesionless	0.00 kPa	0.00	N/A	0.00 kN
2.01 m	Cohesionless	0.05 kPa	30.32	N/A	0.00 kN
2.99 m	Cohesionless	5.25 kPa	30.32	N/A	7.28 kN
3.01 m	Cohesive	N/A	N/A	106.00 kPa	8.94 kN
5.99 m	Cohesive	N/A	N/A	106.00 kPa	458.73 kN
6.01 m	Cohesive	N/A	N/A	47.10 kPa	460.91 kN
9.01 m	Cohesive	N/A	N/A	54.64 kPa	694.45 kN
12.01 m	Cohesive	N/A	N/A	62.19 kPa	992.41 kN
14.99 m	Cohesive	N/A	N/A	67.79 kPa	1328.05 kN
15.01 m	Cohesionless	133.63 kPa	30.32	N/A	1330.89 kN
18.01 m	Cohesionless	149.08 kPa	30.32	N/A	1958.31 kN
19.99 m	Cohesionless	159.28 kPa	30.32	N/A	2443.61 kN

ULTIMATE - END BEARING

Depth	Soil Type	Effective Stress At Tip	Bearing Cap. Factor	Limiting End Bearing	End Bearing
0.01 m	Cohesionless	0.00 kPa	0.00	0.00 kN	0.00 kN
1.99 m	Cohesionless	0.00 kPa	0.00	0.00 kN	0.00 kN
2.01 m	Cohesionless	0.11 kPa	77.60	919.89 kN	0.72 kN
2.99 m	Cohesionless	10.49 kPa	77.60	919.89 kN	71.54 kN
3.01 m	Cohesive	N/A	N/A	N/A	120.90 kN
5.99 m	Cohesive	N/A	N/A	N/A	120.90 kN
6.01 m	Cohesive	N/A	N/A	N/A	176.79 kN
9.01 m	Cohesive	N/A	N/A	N/A	176.79 kN
12.01 m	Cohesive	N/A	N/A	N/A	176.79 kN
14.99 m	Cohesive	N/A	N/A	N/A	176.79 kN
15.01 m	Cohesionless	133.69 kPa	77.60	919.89 kN	905.23 kN
18.01 m	Cohesionless	164.58 kPa	77.60	919.89 kN	919.89 kN
19.99 m	Cohesionless	184.97 kPa	77.60	919.89 kN	919.89 kN

ULTIMATE - SUMMARY OF CAPACITIES

Depth	Skin Friction	End Bearing	Total Capacity
0.01 m	0.00 kN	0.00 kN	0.00 kN
1.99 m	0.00 kN	0.00 kN	0.00 kN
2.01 m	0.00 kN	0.72 kN	0.72 kN
2.99 m	7.28 kN	71.54 kN	78.83 kN
3.01 m	8.94 kN	120.90 kN	129.84 kN
5.99 m	458.73 kN	120.90 kN	579.63 kN
6.01 m	460.91 kN	176.79 kN	637.70 kN
9.01 m	694.45 kN	176.79 kN	871.23 kN
12.01 m	992.41 kN	176.79 kN	1169.20 kN
14.99 m	1328.05 kN	176.79 kN	1504.84 kN
15.01 m	1330.89 kN	905.23 kN	2236.12 kN
18.01 m	1958.31 kN	919.89 kN	2878.20 kN
19.99 m	2443.61 kN	919.89 kN	3363.50 kN

F.2.3.4 Static Axial Pile Capacity Calculations by LPC CPT Method - Computer Program

L.P.C. CPT Method

Page 1/2

Peach Freeway CPT-3 at Pier 3 -- 356 mm-square PCPS Concrete Pile

Installation Method: 9 - Driven Prefabricated Piles (Concrete)

Depth to Water Table: 0.0 meter

Pile No.	Toe Area (m ²)	Perimeter (m)
1	0.127	1.424

Depth to Bottom of Layer (m)	Soil Type
1.9	4
3.0	7
15.0	2
20.0	7

Depth (m)	Cone Tip Resistance (kPa)
0.0	1,244.9
2.0	1,244.9
3.0	33,228.7
7.0	3,715.5
11.0	2,848.9
12.0	4,117.7
13.0	4,237.4
14.0	4,472.0
15.0	4,256.5
16.0	17,715.6
17.0	18,816.8
18.0	20,588.4
19.0	19,056.2
19.5	19,678.7
20.0	23,940.0

Peach Freeway CPT-3 at Pier 3 -- 356 mm-square PCPS Concrete Pile

Depth (m)	Unit Friction (kPa)	Toe Bearing (kPa)	Shaft Resistance (kN)	Toe Resistance (kN)	Ultimate Capacity (kN)
0.00	38.21	746.93	0.0	94.3	94.3
2.00	11.54	2508.91	105.4	317.1	422.6
3.00	70.38	2796.19	163.7	353.6	517.3
7.00	60.14	2231.21	505.7	282.0	787.7
11.00	58.03	1972.66	842.0	249.5	1091.5
12.00	61.14	2236.00	926.5	282.9	1209.4
13.00	61.43	2537.64	1013.7	320.7	1334.4
14.00	62.00	4108.10	1101.3	519.5	1621.3
15.00	61.48	6655.32	1189.4	841.1	2030.5
16.00	64.49	5860.51	1281.0	740.6	2021.6
17.00	64.93	7124.54	1373.1	900.7	2273.8
18.00	65.60	7306.49	1465.6	923.8	2389.5
19.00	65.02	7847.53	1558.6	991.9	2549.6
19.50	65.26	8062.99	1604.8	1019.5	2624.3
20.00	66.84	8259.30	1652.0	1044.4	2696.4

Note: Depth is referenced from the original ground surface.

F.2.3.5 Static Axial Pile Capacity Calculations by Schmertmann Method

Location: Peach Freeway CPT-3 at Pier 3.

Depth (m)	fs(avg) (bars)	Unit Friction (bars)	Increment Friction (kN)	Shaft Resistance (kN)	qc(avg) (bars)	qc1(min) (bars)	qc2 (bars)	Toe Resistance (kN)	Ultimate Capacity (kN)
10.00	1.99	0.80	27.77	1,050	32.87				
10.25	1.93	0.77	26.93	1,077	29.15				
10.50	2.13	0.85	29.76	1,107	31.50				
10.75	2.36	0.94	32.86	1,140	33.35				
11.00	2.24	0.90	31.29	1,171	35.10	38.88	29.68	416	1,587
11.25	2.20	0.88	30.63	1,202	42.65				
11.50	2.29	0.92	31.95	1,234	44.30	42.19	21.49	386	1,620
11.75	2.45	0.98	34.12	1,268	43.50				
12.00	2.54	1.02	35.44	1,303	41.33	42.34	33.71	461	1,764
12.25	2.22	0.89	30.91	1,334	43.35	43.86	34.25	474	1,808
12.50	2.21	0.88	30.79	1,365	45.03	44.03	35.44	482	1,847
12.75	2.17	0.87	30.20	1,395	45.00				
13.00	2.26	0.91	31.58	1,427	43.53	43.32	37.30	489	1,916
13.25	2.74	1.10	38.23	1,465	46.50				
13.50	2.84	1.14	39.67	1,504	47.27	43.39	39.34	502	2,006
13.75	2.59	1.04	36.14	1,541	47.30				
14.00	2.47	0.99	34.51	1,575	45.80	42.46	40.82	505	2,080
14.25	2.13	0.85	29.66	1,605	41.35				
14.50	2.21	0.88	30.84	1,636	43.07	44.93	41.35	523	2,159
14.75	2.21	0.88	30.84	1,666	46.80				
15.00	2.05	1.74	60.69	1,727	130.90	161.05	41.95	1231	2,958
15.25	1.62	1.37	47.88	1,775	191.20				
15.50	1.48	1.26	43.79	1,819	195.97				
15.75	1.16	0.98	34.25	1,853	180.90				
16.00	1.15	0.98	34.19	1,887	170.97				

Note: Depth is referenced from the original ground surface.

F.2.3.6 Summary of Pier 3 Capacity Calculation Results

Summary of Pile Capacity Estimates with an Embedded Pile Length of 13.0 meters

Method Used for Estimation of Pile Capacity	Calculated Pile Shaft Resistance (kN)	Calculated Pile Toe Resistance (kN)	Calculated Ultimate Pile Capacity* (kN)
Norlund and α Method - SPT Data	1,171	635	1,806
Effective Stress Method	525	1,059	1,584
Driven Program - SPT Data	1,345	920	2,265
LPC CPT Program - CPT Data	1,189	841	2,030
Schmertmann Method - CPT Data	1,727	1,231	2,958

*Scour was not included in these analysis, but the Driven analysis shows it has little effect

Summary of Pile Length Estimates for the 1,780 kN Ultimate Pile Capacity

Method Used for Estimation of Pile Capacity	Calculated Pile Length for the 1,780 kN Ultimate Pile Capacity Prior to Scour
Norlund and α Method - SPT Data	13.0 meters for 1,806 kN
Effective Stress Method	14.0 meters for 1,980 kN
Driven Program - SPT Data	13.0 meters for 2,265 kN
LPC CPT Program - CPT Data	12.5 meters for 1,826 kN
Schmertmann Method - CPT Data	10.2 meters for 1,808 kN

The ultimate pile group capacity at Pier 3 should be calculated based on Steps 1 to 3 of the design recommendations presented in Section 9.8.1.2, since most of the soil along the pile embedded length is cohesive type. One of the design recommendations for estimating the ultimate pile group capacity in cohesive soil is to calculate the ultimate pile group capacity against block failure using the procedure described in Section 9.8.1.3. The ultimate pile group capacity should be governed by the lesser of the ultimate pile group capacity calculated from steps 1 to 3 of the design recommendations presented in Section 9.8.1.3. An example calculations of the ultimate pile group capacity against block failure for the South Abutment is presented in Section F.2.4.1 - Step 8.

F.2.4 South Abutment - Soil Boring S-4 (Cohesive Soil)

F.2.4.1 Static Axial Pile Capacity Calculations by α -Method

For the soil profile interpreted from Soil Boring S-4 as shown in Figure F.11. Perform the α -method pile capacity calculation for an embedded length of 17.5 meters. Use the step-by-step method outlined in Section 9.7.1.2a.

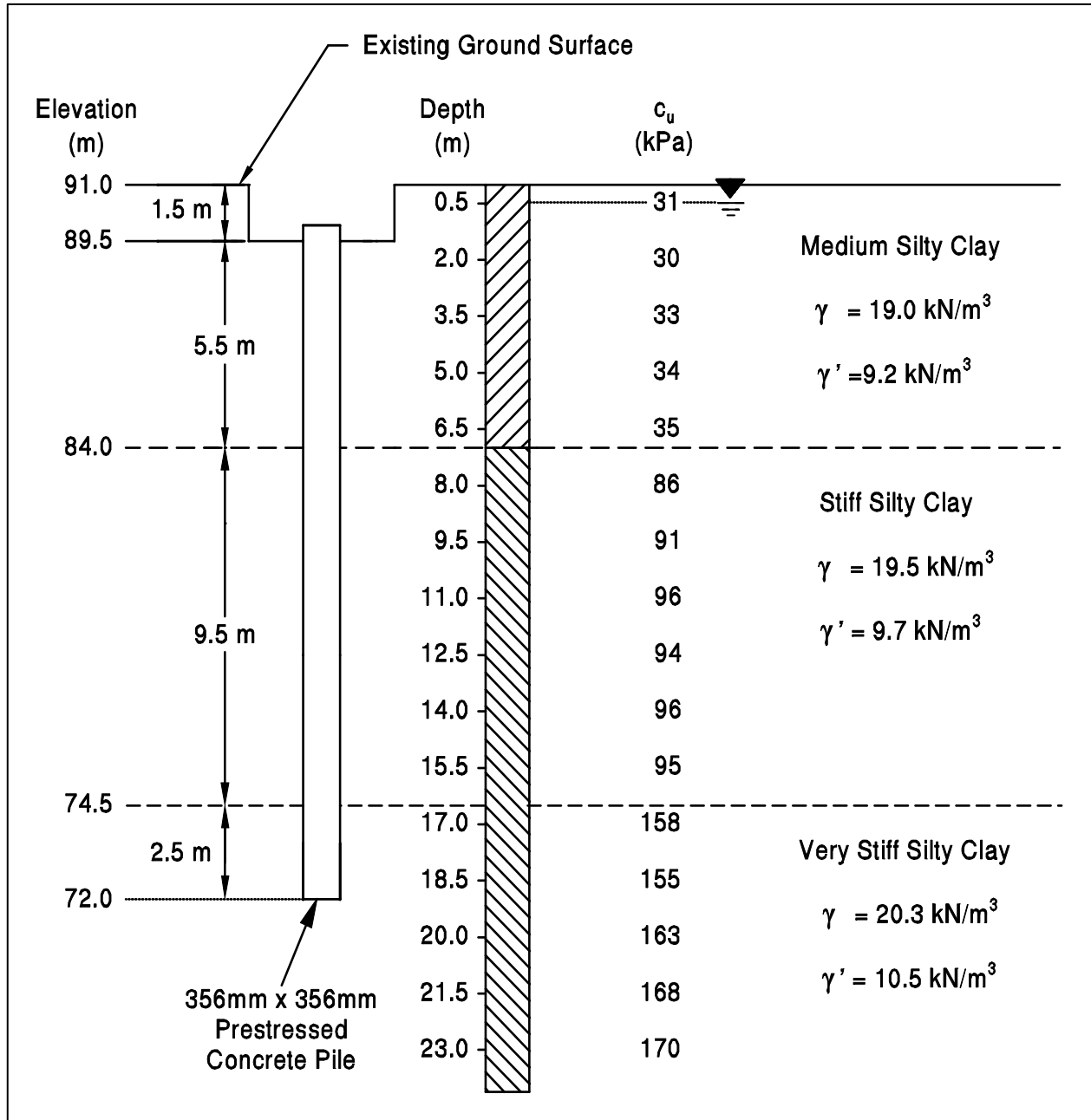


Figure F.11 Interpreted Soil Profile from Soil Boring S-4 at the South Abutment

STEP 1 Delineate the soil profile into layers and determine the adhesion, c_a from Figure 9.18 or adhesion factor, α from Figure 9.19 for each layer.

Enter appropriate figure (based on soil stratigraphy) with the undrained shear strength of the soil, c_u , and determine adhesion or adhesion factor based on the ratio of embedded pile length in clay, D , and pile diameter, b .

Along the pile embedded length, the soil profile is delineated into three layers. Layer 1 is medium silty clay that is 5.5 meters thick, layer 2 is stiff silty clay that is 9.5 meters thick, and layer 3 is very stiff silty clay that is 2.5 meters thick.

Determine the average undrained shear strength, c_u for each soil layer.

$$\text{Layer 1: } c_{u1} = \frac{31 + 30 + 33 + 34 + 35}{5} = 33 \text{ kPa}$$

(Layer 1 - depth 1.5 to 7 m;
Medium silty clay)

$$\text{Layer 2: } c_{u2} = \frac{86 + 91 + 96 + 94 + 96 + 95}{6} = 93 \text{ kPa}$$

(Layer 2 - depth 7 to 16.5 m;
Stiff silty clay)

$$\text{Layer 3: } c_{u3} = \frac{158 + 155}{2} = 157 \text{ kPa}$$

(Layer 3 - depth 16.5 to 19.0 m;
Very stiff silty clay)

The soil stratigraphy of layers 1, 2, and 3 matches that of Figures 9.19c or 9.18. In fact, for concrete piles, the adhesion obtained from Figure 9.18 should be the same as the adhesion factor from Figure 9.19c times the undrained shear strength. Figure 9.18 and the depth to pile diameter ratio, D/b , will be used here to determine the adhesion for soil layers 1, 2, and 3.

STEP 1 (continued)

For soil layer 1:

$$(D/b) = (5.5 \text{ m}) / (0.356 \text{ m}) = 15.45$$

Interpolating from Figure 9.18 for $c_{u1} = 33 \text{ kPa}$ and $(D/b) = 15.45$:

$$c_{a1} = 33 \text{ kPa}$$

For soil layer 2:

$$(D/b) = (15 \text{ m}) / (0.356 \text{ m}) = 42.13$$

Interpolating from Figure 9.18, for $c_{u2} = 93 \text{ kPa}$ and $(D/b) = 42.13$:

$$c_{a2} = 85 \text{ kPa}$$

For soil layer 3:

$$(D/b) = (17.5 \text{ m}) / (0.355 \text{ m}) = 49.16$$

Interpolating from Figure 9.18, for $c_{u3} = 157 \text{ kPa}$ and $(D/b) = 49.16$:

$$c_{a3} = 67 \text{ kPa}$$

STEP 2 For each soil layer, compute the unit shaft resistance, f_s (kPa).

$$f_s = c_a$$

Layer 1: $f_{s1} = c_{a1} = 33 \text{ kPa}$

Layer 2: $f_{s2} = c_{a2} = 85 \text{ kPa}$

Layer 3: $f_{s3} = c_{a3} = 67 \text{ kPa}$

STEP 3 Compute the shaft resistance in each soil layer and the ultimate shaft resistance, R_s (kN) from the sum of the shaft resistance from each layer.

$$R_s = f_s A_s$$

where A_s = Pile-soil surface area from perimeter and length

$$\begin{aligned} \text{Layer 1: } R_{s1} &= 33 \text{ kPa } (4)(0.356 \text{ m})(5.5 \text{ m}) \\ &= 259 \text{ kN} \end{aligned}$$

$$\begin{aligned} \text{Layer 2: } R_{s2} &= 85 \text{ kPa } (4)(0.356 \text{ m})(9.5 \text{ m}) \\ &= 1,150 \text{ kN} \end{aligned}$$

$$\begin{aligned} \text{Layer 3: } R_{s3} &= 67 \text{ kPa } (4)(0.356 \text{ m})(2.5 \text{ m}) \\ &= 239 \text{ kN} \end{aligned}$$

$$\begin{aligned} \text{Total: } R_s &= R_{s1} + R_{s2} + R_{s3} \\ &= 259 \text{ kN} + 1,150 \text{ kN} + 239 \text{ kN} = 1,648 \text{ kN} \end{aligned}$$

STEP 4 Compute the unit toe resistance, q_t (kPa).

$$q_t = 9 c_u$$

Where: c_u = undrained shear strength of soil at the pile toe.

$$\text{At the pile toe } c_u = \frac{155 + 163}{2} = 159 \text{ kPa}$$

STEP 4 (continued)

Therefore, the unit toe resistance is:

$$\begin{aligned}q_t &= 9 (159 \text{ kPa}) \\ &= 1,431 \text{ kPa}\end{aligned}$$

STEP 5 Compute the ultimate toe resistance, R_t (kN).

$$\begin{aligned}R_t &= q_t A_t \\ &= 1,431 \text{ kPa} (0.356 \text{ m})(0.356 \text{ m}) \\ &= 182 \text{ kN}\end{aligned}$$

STEP 6 Compute the ultimate pile capacity, Q_u (kN).

$$\begin{aligned}Q_u &= R_s + R_t \\ &= 1,648 \text{ kN} + 182 \text{ kN} \\ &= 1,830 \text{ kN}\end{aligned}$$

STEP 7 Compute the allowable design load, Q_a (kN).

$$Q_a = \frac{Q_u}{\text{Factor of Safety}} = \frac{1,830 \text{ kN}}{\text{Factor of Safety}}$$

Note: Factor of Safety should be selected based on the construction control method to be specified. Recommended factors of safety are described in Section 9.6.

The group capacity in a cohesive soil should be checked for block failure.

STEP 8 Investigate the possibility of a block failure of pile groups as discussed in Section 9.8.1.3.

Block failure of pile groups should be considered in the design of pile groups in soft cohesive soils or in cohesionless soils underlain by a weak cohesive layer. For a pile group in cohesive soil, the ultimate capacity of the pile group against block failure can be expressed as:

$$Q_{ug} = 2D (B+Z) c_{u1} + B Z c_{u2} N_c$$

Where:

D = embedded lengths of piles = 17.5 m.

B = width of pile group = 3.36 m.

Z = length of pile group = 10.86 m

c_{u1} = the weighted average of the undrained shear strength over the depth of pile embedment for the cohesive soils along the pile group perimeter

Layer 1: $c_{u1-1} = 33$ kPa

Layer 2: $c_{u1-2} = 93$ kPa

Layer 3: $c_{u1-3} = 157$ kPa

c_{u2} = average undrained shear strength of the cohesive soils at the base of the pile group to a depth of 2B below pile toe level

$$= \frac{155 + 162 + 168}{3} = 162 \text{ kPa}$$

N_c = bearing capacity factor = 9

STEP 8 (continued)

The group shaft resistance against block failure is $2D (B+Z) c_{u1}$:

$$\text{Layer 1: } 2 (5.5 \text{ m}) (3.36 \text{ m} + 10.86 \text{ m}) (33 \text{ kPa}) = 5,162 \text{ kN}$$

$$\text{Layer 2: } 2 (9.5 \text{ m}) (3.36 \text{ m} + 10.86 \text{ m}) (93 \text{ kPa}) = 25,127 \text{ kN}$$

$$\text{Layer 3: } 2 (2.5 \text{ m}) (3.36 \text{ m} + 10.86 \text{ m}) (157 \text{ kPa}) = 11,163 \text{ kN}$$

The group toe resistance against block failure is:

$$\begin{aligned} B Z c_{u2} N_c &= 3.36 \text{ m} (10.86 \text{ m}) (162 \text{ kPa}) (9) \\ &= 53,202 \text{ kN} \end{aligned}$$

Therefore,

$$\begin{aligned} Q_{ug} &= 5,162 \text{ kN} + 25,127 \text{ kN} + 11,163 \text{ kN} + 53,202 \text{ kN} \\ &= 94,654 \text{ kN} \end{aligned}$$

The ultimate pile group capacity in cohesive soil should be taken as the lesser of the ultimate pile group capacity calculated from Steps 1 to 4 as described in Section 9.8.1.2. Steps 1 and 2 take into account the pile center to center spacing and the undrained shear strength of the cohesive soil. For the South Abutment soil strength and pile spacing, this results in a group efficiency of 1.0. Therefore, the ultimate pile group capacity is the calculated ultimate pile capacity of 1,830 kN time the 24 piles in the group or 43,920 kN. The ultimate pile group capacity against block failure, Q_{ug} , calculated above is equal to 94,654 kN. Therefore, block failure is not a problem. The ultimate pile group capacity of 43,920 kN is in excess of the required ultimate pile group capacity of 42,720 kN.

F.2.4.2 Static Axial Pile Capacity Calculations by Effective Stress Method

For the soil profile interpreted from Soil Boring S-4 as shown in Figure F.11. Perform an Effective Stress method pile capacity calculation for an embedded length of 17.5 meters. Use the step-by-step method outlined in Section 9.7.1.3.

STEP 1 Delineate the soil profile into layers and determine ϕ' angle for each layer.

- a. Use the procedure described in Section 9.4 to construct a p_o diagram.

For Soil Boring S-4, the p_o diagram is presented below in Figure F.12.

- b. Divide the soil profile throughout the pile penetration depth into layers and determine the effective overburden pressure, p_o , at the midpoint of each layer.

As the example in Section F.2.4.1, the soil profile along the pile embedded length is delineated into three layers of 5.5, 9.5, and 2.5 meter thick. The average effective overburden pressure of each layer is equal to the effective overburden pressure at the midpoint of that layer as follows.

Layer 1: $p_{o1} = 44.0$ kPa (at depth of 4.25 meters)

Layer 2: $p_{o2} = 115.4$ kPa (at depth of 11.75 meters)

Layer 3: $p_{o3} = 174.6$ kPa (at depth of 17.75 meters)

- c. Determine the ϕ' angle for each soil layer from laboratory or in-situ test data.

The effective frictional angle for each layer was obtained from the laboratory triaxial test.

Layer 1: $\phi_1' = 27^\circ$

Layer 2: $\phi_2' = 29^\circ$

Layer 3: $\phi_3' = 30^\circ$

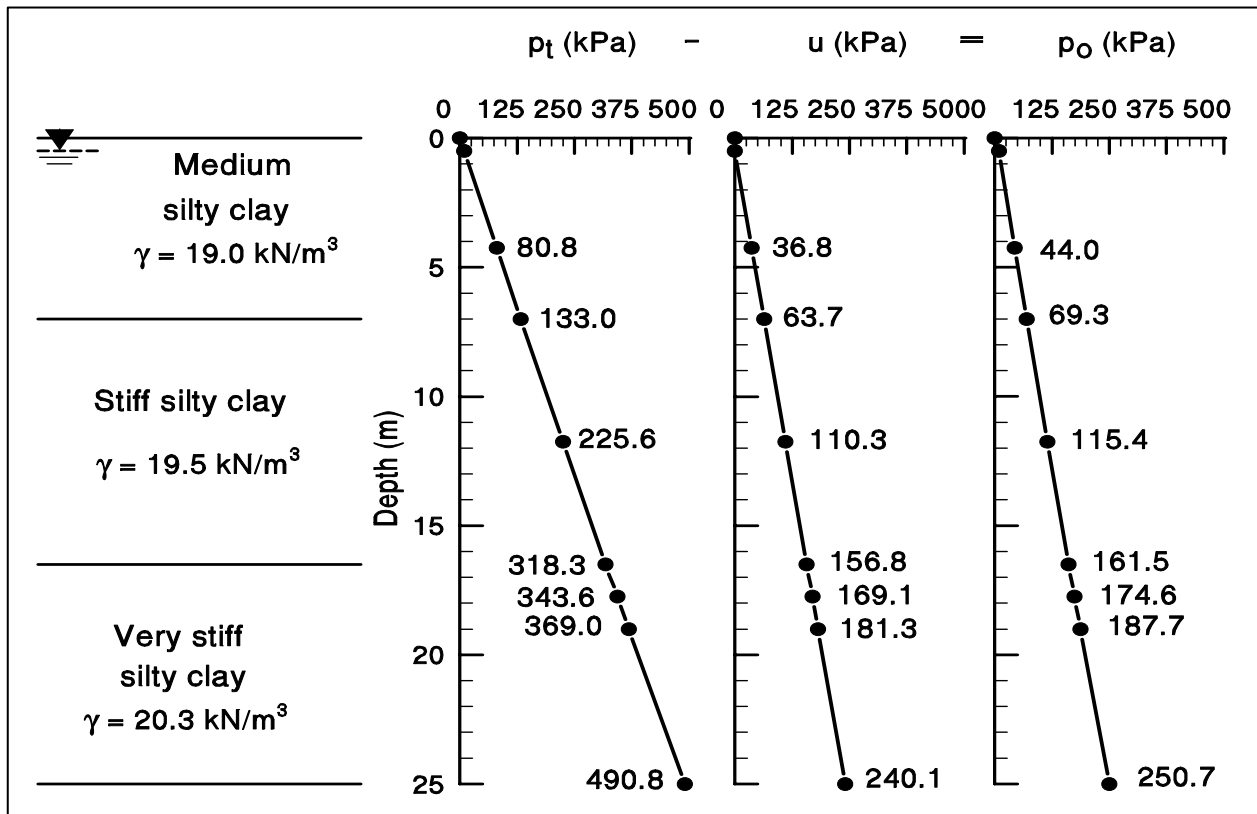


Figure F.12 Effective Overburden Pressure Diagram – South Abutment

STEP 2 Select the β coefficient for each soil layer.

- a. Use local experience to select β coefficient for each layer.

Assume no local experience.

- b. In the absence of local experience, use Table 9-6 or Figure 9.20 to estimate β coefficient from ϕ' angle for each layer.

Use the soil type, the estimated ϕ' angle, and Table 9-6 or Figure 9.20 to estimate the β coefficient for each soil layer.

Layer 1: $\beta_1 = 0.30$ (For medium silty clay with $\phi_1' = 27^\circ$)

Layer 2: $\beta_2 = 0.35$ (For stiff silty clay with $\phi_2' = 29^\circ$)

Layer 3: $\beta_3 = 0.40$ (For very stiff silty clay with $\phi_3' = 30^\circ$)

STEP 3 For each soil layer, compute the unit shaft resistance, f_s (kPa).

$$f_s = \beta p_o$$

Layer 1: $f_{s1} = 0.30 (44.0 \text{ kPa}) = 13.20 \text{ kPa}$

Layer 2: $f_{s2} = 0.35 (115.4 \text{ kPa}) = 40.39 \text{ kPa}$

Layer 3: $f_{s3} = 0.40 (174.6 \text{ kPa}) = 69.84 \text{ kPa}$

STEP 4 Compute the shaft resistance in each soil layer and the ultimate shaft resistance, R_s (kN) from the sum of the shaft resistance from each soil layer.

$$R_s = f_s A_s$$

Layer 1: $R_{s1} = 13.20 (4) (0.356 \text{ m}) (5.5 \text{ m})$
 $= 103 \text{ kN}$

Layer 2: $R_{s2} = 40.39 (4) (0.356 \text{ m}) (9.5 \text{ m})$
 $= 546 \text{ kN}$

Layer 3: $R_{s3} = 69.84 (4) (0.356 \text{ m}) (2.5 \text{ m})$
 $= 249 \text{ kN}$

Total: $R_s = R_{s1} + R_{s2} + R_{s3}$
 $= 103 \text{ kN} + 546 \text{ kN} + 249 \text{ kN}$
 $= 898 \text{ kN}$

STEP 5 Compute the unit toe resistance, q_t (kPa).

$$q_t = N_t p_t$$

- a. Use local experience to select N_t coefficient.

Assume no local experience.

- b. In the absence of local experience, estimate N_t coefficient from Table 9-6 or Figure 9.21 based on ϕ' angle.

Based on the laboratory triaxial test, the undrained frictional angle is:

$$\phi'_{\text{toe}} = 30^\circ$$

Use the soil type, the estimated ϕ' angle, and Table 9-6 or Figure 9.21 to estimate the N_t coefficient.

$$N_t = 30$$

- c. Calculate the effective overburden pressure at the pile toe, p_t .

The effective overburden pressure at the pile toe, p_t , has been computed in Figure F.12:

$$p_t = 187.7 \text{ kPa}$$

The unit toe resistance, q_t is:

$$\begin{aligned} q_t &= N_t p_t \\ &= 30 (187.7 \text{ kPa}) \\ &= 5,631 \text{ kPa} \end{aligned}$$

STEP 6 Compute the ultimate toe resistance, R_t (kN).

$$\begin{aligned} R_t &= q_t A_t \\ &= 5,631 \text{ kPa} (0.356 \text{ m}) (0.356 \text{ m}) \\ &= 715 \text{ kN} \end{aligned}$$

STEP 7 Compute the ultimate pile capacity, Q_u (kN).

$$\begin{aligned} Q_u &= R_s + R_t \\ &= 898 \text{ kN} + 715 \text{ kN} \\ &= 1,613 \text{ kN} \end{aligned}$$

STEP 8 Compute the allowable design load, Q_a (kN).

$$Q_a = \frac{Q_u}{\text{Factor of Safety}} = \frac{1,613 \text{ kN}}{\text{Factor of Safety}}$$

Note: Factor of Safety should be selected based on the construction control method to be specified. Recommended factors of safety are described in Section 9.6.

F.2.4.3 Static Axial Pile Capacity Calculations by the Driven Computer Program

Note: In the following tables, the depth corresponding to the pile tip is 15 m. The “driving strength loss (%)” factor used in Driven for Boring S-2 was selected based on Table 9-20. For the cohesive silty clay layers, the selected soil set-up factor selected was 2.0, which leads to a driving strength loss of 50%. In the Driven results, the “Driving” tables reflect the lost resistance in the clay layers due to driving. The “Restrike” and “Ultimate” tables reflect a time when the clay layers have regained that resistance after pore water pressure dissipation.

DRIVEN 1.2 **GENERAL PROJECT INFORMATION**

Filename: C:\DOCUME~1\BRENT\DESKTOP\FHWAMA~1\APPFDR~1\S4.DVN
Project Name: Boring S-4 Project Date: 09/11/2003
Project Client: FHWA Manual
Computed By: BRR
Project Manager:

PILE INFORMATION

Pile Type: Concrete Pile
Top of Pile: 1.50 m
Length of Square Side: 356.00 mm

ULTIMATE CONSIDERATIONS

Water Table Depth At Time Of:	- Drilling:	0.50 m
	- Driving/Restrike	0.50 m
	- Ultimate:	0.50 m
Ultimate Considerations:	- Local Scour:	0.00 m
	- Long Term Scour:	0.00 m
	- Soft Soil:	0.00 m

ULTIMATE PROFILE

Layer	Type	Thickness	Driving Loss	Unit Weight	Strength	Ultimate Curve
1	Cohesive	7.00 m	50.00%	19.00 kN/m ³	33.00 kPa	T-79 Concrete
2	Cohesive	9.50 m	50.00%	19.50 kN/m ³	93.00 kPa	T-79 Concrete
3	Cohesive	2.50 m	50.00%	20.30 kN/m ³	157.00 kPa	T-79 Concrete
4	Cohesive	4.00 m	50.00%	20.30 kN/m ³	167.00 kPa	T-79 Concrete

RESTRIKE - SKIN FRICTION

Depth	Soil Type	Effective Stress At Midpoint	Sliding Friction Angle	Adhesion	Skin Friction
0.01 m	Cohesive	N/A	N/A	0.00 kPa	0.00 kN
1.49 m	Cohesive	N/A	N/A	0.00 kPa	0.00 kN
1.50 m	Cohesive	N/A	N/A	32.24 kPa	0.00 kN
3.01 m	Cohesive	N/A	N/A	32.24 kPa	69.33 kN
6.01 m	Cohesive	N/A	N/A	32.31 kPa	207.51 kN
6.99 m	Cohesive	N/A	N/A	32.38 kPa	253.14 kN
7.01 m	Cohesive	N/A	N/A	71.76 kPa	254.63 kN
10.01 m	Cohesive	N/A	N/A	77.24 kPa	584.68 kN
13.01 m	Cohesive	N/A	N/A	82.73 kPa	961.57 kN
16.01 m	Cohesive	N/A	N/A	84.97 kPa	1343.80 kN
16.49 m	Cohesive	N/A	N/A	84.97 kPa	1401.88 kN
16.51 m	Cohesive	N/A	N/A	67.30 kPa	1404.05 kN
18.99 m	Cohesive	N/A	N/A	67.30 kPa	1641.71 kN
19.01 m	Cohesive	N/A	N/A	65.12 kPa	1643.60 kN
22.01 m	Cohesive	N/A	N/A	65.12 kPa	1921.76 kN
22.99 m	Cohesive	N/A	N/A	65.12 kPa	2012.63 kN

RESTRIKE - END BEARING

Depth	Soil Type	Effective Stress At Tip Factor	Bearing Cap.	Limiting End Bearing	End Bearing
0.01 m	Cohesive	N/A	N/A	N/A	0.00 kN
1.49 m	Cohesive	N/A	N/A	N/A	0.00 kN
1.50 m	Cohesive	N/A	N/A	N/A	37.64 kN
3.01 m	Cohesive	N/A	N/A	N/A	37.64 kN
6.01 m	Cohesive	N/A	N/A	N/A	37.64 kN
6.99 m	Cohesive	N/A	N/A	N/A	37.64 kN
7.01 m	Cohesive	N/A	N/A	N/A	106.07 kN
10.01 m	Cohesive	N/A	N/A	N/A	106.07 kN
13.01 m	Cohesive	N/A	N/A	N/A	106.07 kN
16.01 m	Cohesive	N/A	N/A	N/A	106.07 kN
16.49 m	Cohesive	N/A	N/A	N/A	106.07 kN
16.51 m	Cohesive	N/A	N/A	N/A	179.07 kN
18.99 m	Cohesive	N/A	N/A	N/A	179.07 kN
19.01 m	Cohesive	N/A	N/A	N/A	190.48 kN
22.01 m	Cohesive	N/A	N/A	N/A	190.48 kN
22.99 m	Cohesive	N/A	N/A	N/A	190.48 kN

RESTRIKE - SUMMARY OF CAPACITIES

Depth	Skin Friction	End Bearing	Total Capacity
0.01 m	0.00 kN	0.00 kN	0.00 kN
1.49 m	0.00 kN	0.00 kN	0.00 kN
1.50 m	0.00 kN	37.64 kN	37.64 kN
3.01 m	69.33 kN	37.64 kN	106.97 kN
6.01 m	207.51 kN	37.64 kN	245.15 kN
6.99 m	253.14 kN	37.64 kN	290.78 kN
7.01 m	254.63 kN	106.07 kN	360.70 kN
10.01 m	584.68 kN	106.07 kN	690.75 kN
13.01 m	961.57 kN	106.07 kN	1067.64 kN
16.01 m	1343.80 kN	106.07 kN	1449.87 kN
16.49 m	1401.88 kN	106.07 kN	1507.95 kN
16.51 m	1404.05 kN	179.07 kN	1583.12 kN
18.99 m	1641.71 kN	179.07 kN	1820.78 kN
19.01 m	1643.60 kN	190.48 kN	1834.07 kN
22.01 m	1921.76 kN	190.48 kN	2112.24 kN
22.99 m	2012.63 kN	190.48 kN	2203.11 kN

DRIVING - SKIN FRICTION

Depth	Soil Type	Effective Stress At Midpoint	Sliding Friction Angle	Adhesion	Skin Friction
0.01 m	Cohesive	N/A	N/A	0.00 kPa	0.00 kN
1.49 m	Cohesive	N/A	N/A	0.00 kPa	0.00 kN
1.50 m	Cohesive	N/A	N/A	32.24 kPa	0.00 kN
3.01 m	Cohesive	N/A	N/A	32.24 kPa	34.67 kN
6.01 m	Cohesive	N/A	N/A	32.31 kPa	103.75 kN
6.99 m	Cohesive	N/A	N/A	32.38 kPa	126.57 kN
7.01 m	Cohesive	N/A	N/A	71.76 kPa	127.31 kN
10.01 m	Cohesive	N/A	N/A	77.24 kPa	292.34 kN
13.01 m	Cohesive	N/A	N/A	82.73 kPa	480.78 kN
16.01 m	Cohesive	N/A	N/A	84.97 kPa	671.90 kN
16.49 m	Cohesive	N/A	N/A	84.97 kPa	700.94 kN
16.51 m	Cohesive	N/A	N/A	67.30 kPa	702.02 kN
18.99 m	Cohesive	N/A	N/A	67.30 kPa	820.86 kN
19.01 m	Cohesive	N/A	N/A	65.12 kPa	821.80 kN
22.01 m	Cohesive	N/A	N/A	65.12 kPa	960.88 kN
22.99 m	Cohesive	N/A	N/A	65.12 kPa	1006.32 kN

DRIVING - END BEARING

Depth	Soil Type	Effective Stress At Tip Factor	Bearing Cap.	Limiting End Bearing	End Bearing
0.01 m	Cohesive	N/A	N/A	N/A	0.00 kN
1.49 m	Cohesive	N/A	N/A	N/A	0.00 kN
1.50 m	Cohesive	N/A	N/A	N/A	37.64 kN
3.01 m	Cohesive	N/A	N/A	N/A	37.64 kN
6.01 m	Cohesive	N/A	N/A	N/A	37.64 kN
6.99 m	Cohesive	N/A	N/A	N/A	37.64 kN
7.01 m	Cohesive	N/A	N/A	N/A	106.07 kN
10.01 m	Cohesive	N/A	N/A	N/A	106.07 kN
13.01 m	Cohesive	N/A	N/A	N/A	106.07 kN
16.01 m	Cohesive	N/A	N/A	N/A	106.07 kN
16.49 m	Cohesive	N/A	N/A	N/A	106.07 kN
16.51 m	Cohesive	N/A	N/A	N/A	179.07 kN
18.99 m	Cohesive	N/A	N/A	N/A	179.07 kN
19.01 m	Cohesive	N/A	N/A	N/A	190.48 kN
22.01 m	Cohesive	N/A	N/A	N/A	190.48 kN
22.99 m	Cohesive	N/A	N/A	N/A	190.48 kN

DRIVING - SUMMARY OF CAPACITIES

Depth	Skin Friction	End Bearing	Total Capacity
0.01 m	0.00 kN	0.00 kN	0.00 kN
1.49 m	0.00 kN	0.00 kN	0.00 kN
1.50 m	0.00 kN	37.64 kN	37.64 kN
3.01 m	34.67 kN	37.64 kN	72.30 kN
6.01 m	103.75 kN	37.64 kN	141.39 kN
6.99 m	126.57 kN	37.64 kN	164.21 kN
7.01 m	127.31 kN	106.07 kN	233.39 kN
10.01 m	292.34 kN	106.07 kN	398.41 kN
13.01 m	480.78 kN	106.07 kN	586.86 kN
16.01 m	671.90 kN	106.07 kN	777.97 kN
16.49 m	700.94 kN	106.07 kN	807.01 kN
16.51 m	702.02 kN	179.07 kN	881.09 kN
18.99 m	820.86 kN	179.07 kN	999.93 kN
19.01 m	821.80 kN	190.48 kN	1012.27 kN
22.01 m	960.88 kN	190.48 kN	1151.36 kN
22.99 m	1006.32 kN	190.48 kN	1196.79 kN

ULTIMATE - SKIN FRICTION

Depth	Soil Type	Effective Stress At Midpoint	Sliding Friction Angle	Adhesion	Skin Friction
0.01 m	Cohesive	N/A	N/A	0.00 kPa	0.00 kN
1.49 m	Cohesive	N/A	N/A	0.00 kPa	0.00 kN
1.50 m	Cohesive	N/A	N/A	32.24 kPa	0.00 kN
3.01 m	Cohesive	N/A	N/A	32.24 kPa	69.33 kN
6.01 m	Cohesive	N/A	N/A	32.31 kPa	207.51 kN
6.99 m	Cohesive	N/A	N/A	32.38 kPa	253.14 kN
7.01 m	Cohesive	N/A	N/A	71.76 kPa	254.63 kN
10.01 m	Cohesive	N/A	N/A	77.24 kPa	584.68 kN
13.01 m	Cohesive	N/A	N/A	82.73 kPa	961.57 kN
16.01 m	Cohesive	N/A	N/A	84.97 kPa	1343.80 kN
16.49 m	Cohesive	N/A	N/A	84.97 kPa	1401.88 kN
16.51 m	Cohesive	N/A	N/A	67.30 kPa	1404.05 kN
18.99 m	Cohesive	N/A	N/A	67.30 kPa	1641.71 kN
19.01 m	Cohesive	N/A	N/A	65.12 kPa	1643.60 kN
22.01 m	Cohesive	N/A	N/A	65.12 kPa	1921.76 kN
22.99 m	Cohesive	N/A	N/A	65.12 kPa	2012.63 kN

ULTIMATE - END BEARING

Depth	Soil Type	Effective Stress At Tip	Bearing Cap. Factor	Limiting End Bearing	End Bearing
0.01 m	Cohesive	N/A	N/A	N/A	0.00 kN
1.49 m	Cohesive	N/A	N/A	N/A	0.00 kN
1.50 m	Cohesive	N/A	N/A	N/A	37.64 kN
3.01 m	Cohesive	N/A	N/A	N/A	37.64 kN
6.01 m	Cohesive	N/A	N/A	N/A	37.64 kN
6.99 m	Cohesive	N/A	N/A	N/A	37.64 kN
7.01 m	Cohesive	N/A	N/A	N/A	106.07 kN
10.01 m	Cohesive	N/A	N/A	N/A	106.07 kN
13.01 m	Cohesive	N/A	N/A	N/A	106.07 kN
16.01 m	Cohesive	N/A	N/A	N/A	106.07 kN
16.49 m	Cohesive	N/A	N/A	N/A	106.07 kN
16.51 m	Cohesive	N/A	N/A	N/A	179.07 kN
18.99 m	Cohesive	N/A	N/A	N/A	179.07 kN
19.01 m	Cohesive	N/A	N/A	N/A	190.48 kN
22.01 m	Cohesive	N/A	N/A	N/A	190.48 kN
22.99 m	Cohesive	N/A	N/A	N/A	190.48 kN

ULTIMATE - SUMMARY OF CAPACITIES

Depth	Skin Friction	End Bearing	Total Capacity
0.01 m	0.00 kN	0.00 kN	0.00 kN
1.49 m	0.00 kN	0.00 kN	0.00 kN
1.50 m	0.00 kN	37.64 kN	37.64 kN
3.01 m	69.33 kN	37.64 kN	106.97 kN
6.01 m	207.51 kN	37.64 kN	245.15 kN
6.99 m	253.14 kN	37.64 kN	290.78 kN
7.01 m	254.63 kN	106.07 kN	360.70 kN
10.01 m	584.68 kN	106.07 kN	690.75 kN
13.01 m	961.57 kN	106.07 kN	1067.64 kN
16.01 m	1343.80 kN	106.07 kN	1449.87 kN
16.49 m	1401.88 kN	106.07 kN	1507.95 kN
16.51 m	1404.05 kN	179.07 kN	1583.12 kN
18.99 m	1641.71 kN	179.07 kN	1820.78 kN
19.01 m	1643.60 kN	190.48 kN	1834.07 kN
22.01 m	1921.76 kN	190.48 kN	2112.24 kN
22.99 m	2012.63 kN	190.48 kN	2203.11 kN

F.2.4.4 Static Axial Pile Capacity Calculations by LPC CPT Method - Computer Program

L.P.C. CPT Method Page 1/2
 Peach Freeway CPT-4 at South Abutment -- 356 mm-square PCPS Concrete Pile

Installation Method: 9 - Driven Prefabricated Piles (Concrete)
 Depth to Water Table: 1.00 meter

Pile No.	Toe Area (m ²)	Perimeter (m)
1	0.127	1.424

Depth to Bottom of Layer (m)	Soil Type
7.0	1
29.0	2
30.0	8

Depth (m)	Cone Tip Resistance (kPa)
0.0	1,149.1
3.5	1,149.1
7.0	1,053.4
10.0	3,255.8
15.0	2,872.8
16.0	4,438.5
17.0	3,433.0
18.0	4,989.1
19.0	4,141.6
20.0	4,021.9
21.0	3,361.2
22.0	3,064.3
23.0	6,875.6
24.0	5,266.8
26.0	4,979.5
28.0	5,027.4
28.5	4,309.2
29.0	20,492.6
30.0	48,981.2

Depth (m)	Unit Friction (kPa)	Toe Bearing (kPa)	Shaft Resistance (kN)	Toe Resistance (kN)	Ultimate Capacity (kN)
0.00	35.81	689.47	0.0	87.2	87.2
3.50	35.81	689.47	178.4	87.2	265.6
7.00	31.22	1292.76	345.2	163.2	508.4
10.00	59.04	1953.50	596.9	246.9	843.8
5.00	58.08	2025.32	1013.3	256.2	1269.5
16.00	61.91	2164.18	1098.7	273.6	1372.2
17.00	59.47	2542.43	1185.0	321.2	1506.1
18.00	63.25	2513.70	1272.1	318.0	1590.2
19.00	61.19	2590.31	1360.6	327.8	1688.5
20.00	60.90	2312.60	1447.4	292.2	1739.6
21.00	59.28	2168.96	1532.8	274.4	1807.2
22.00	58.56	2666.92	1616.4	337.6	1954.0
23.00	67.85	3011.65	1706.3	380.8	2087.0
24.00	63.92	3385.12	1800.1	427.9	2228.0
26.00	63.20	3026.02	1981.1	382.5	2363.7
28.00	63.35	8637.55	2160.8	1092.4	3253.3
28.50	61.57	9576.00	2205.3	1210.8	3416.1
29.00	101.07	9576.00	2263.1	1210.8	3473.9
30.00	76.37	9576.00	2371.7	1210.8	3582.4

Note: Depth is referenced from the original ground surface.

F.2.4.5 Static Axial Pile Capacity Calculations by Schmertmann Method

Location: Peach Freeway CPT-4 at South Abutment.

Depth (m)	fs(avg) (bars)	Unit Friction (bars)	Increment Friction (kN)	Shaft Resistance (kN)	q _c (avg) (bars)	q _{c1} (min) (bars)	q _{c2} (bars)	Toe Resistance (kN)	Ultimate Capacity (kN)
15.00	2.24	0.90	31.22	1,191	45.20				
15.25	3.19	1.28	44.44	1,235	54.84				
15.50	2.53	1.01	35.27	1,271	44.96	33.90	20.38	29	1,599
15.75	2.41	0.96	33.57	1,304	43.12				
16.00	2.49	1.00	34.76	1,339	42.38	32.13	25.23	347	1,686
16.25	1.82	0.73	25.37	1,364	33.98				
16.50	1.29	0.58	20.26	1,385	29.10	31.80	27.41	358	1,743
16.75	1.97	0.79	27.43	1,412	34.50	40.16	28.48	416	1,828
17.00	2.35	0.94	32.78	1,445	45.82	43.94	29.55	445	1,890
17.25	3.07	1.23	42.80	1,488	55.86				
17.50	2.69	1.08	37.49	1,525	53.16	40.59	29.83	426	1,951
17.75	2.60	1.04	36.27	1,561	62.30				
18.00	2.15	0.86	29.97	1,591	37.04	34.39	28.94	383	1,975
18.25	2.26	0.91	31.56	1,623	46.56				
18.50	3.08	1.23	42.96	1,666	64.02	33.90	28.94	380	2,046
18.75	1.84	0.74	25.71	1,692	32.00				
19.00	1.77	0.72	25.26	1,717	30.44	29.32	28.94	353	2,070
19.25	1.53	0.66	22.99	1,740	28.94				
19.50	2.22	0.89	30.98	1,771	42.22	30.27	28.94	358	2,129
19.75	1.48	0.62	21.69	1,793	30.34				
20.00	1.33	0.60	20.80	1,813	27.26	29.92	27.26	346	2,160
20.25	1.94	0.78	27.10	1,841	36.50				
20.50	1.48	0.62	21.69	1,862	30.50	23.62	18.54	255	2,117
20.75	1.94	0.77	26.99	1,889	33.60				
21.00	2.35	0.94	32.73	1,922	39.78	22.78	18.54	250	2,172
21.25	1.59	0.67	23.30	1,945	27.36				
21.50	1.06	0.52	18.17	1,963	22.38	19.50	18.54	230	2,194
21.75	0.78	0.45	15.53	1,979	18.54				

Note: Depth is referenced from the original ground surface.

Location: Peach Freeway CPT-4 at South Abutment (continued).

Depth (m)	fs(avg) (bars)	Unit Friction (bars)	Increment Friction (kN)	Shaft Resistance (kN)	qc(avg) (bars)	qc1(min) (bars)	qc2 (bars)	Toe Resistance (kN)	Ultimate Capacity (kN)
22.00	2.12	0.85	29.61	2,090	46.92	47.34	18.54	399	2,407
22.25	5.48	4.65	162.21	2,171	116.78				
22.50	3.78	3.21	111.91	2,283	71.18	42.20	22.26	390	2,673
22.75	2.86	1.14	39.81	2,323	61.10				
23.00	1.96	0.78	27.35	2,350	38.18	34.17	22.38	342	2,692
23.25	1.90	0.76	26.46	2,376	33.42				
23.50	2.79	1.12	38.87	2,415	46.08	34.99	24.30	359	2,774

Note: Depth is referenced from the original ground surface.

F.2.4.6 Summary of South Abutment Capacity Calculation Results

Summary of Pile Capacity Estimates with an Embedded Pile Length of 17.5 meters

Method Used for Estimation of Pile Capacity	Calculated Pile Shaft Resistance (kN)	Calculated Pile Toe Resistance (kN)	Calculated Ultimate Pile Capacity (kN)
α Method	1,648	182	1,830
Effective Stress Method	898	715	1,613
Driven Program - SPT Data	1,644	190	1,834
LPC CPT Program - CPT Data	1,361	328	1,689
Schmertmann Method - CPT Data	1,717	353	2,070

Summary of Pile Length Estimates for the 1,780 kN Ultimate Pile Capacity

Method Used for Estimation of Pile Capacity	Calculated Pile Length for the 1,780 kN Ultimate Pile Capacity
α Method	17.5 meters for 1,830 kN
Effective Stress Method	18.7 meters for 1,800 kN
Driven Program - SPT Data	17.5 meters for 1,834 kN
LPC CPT Program - CPT Data	19.5 meters for 1,807 kN
Schmertmann Method - CPT Data	15.2 meters for 1,828 kN

The ultimate pile group capacity at the South Abutment should be calculated based on the lesser of the ultimate pile group capacity calculated from Steps 1 to 4 of the design recommendations presented in Section 9.8.1.2. The ultimate pile group capacity based on the design recommendations is equal to 43,920 kN which is in excess of the required ultimate pile group capacity of 42,720 kN.

F.3 GROUP SETTLEMENT CALCULATIONS

The substructure of the bridge is designed to be supported on a pile group having three rows of piles with 8 piles in each row. The piles are arranged at 1.5 m center to center spacing with a total pile group area of 3.36 m by 10.86 m. Piles in a group are combined with a pile cap having a dimension of 4.5 m by 12 m.

The bridge division has estimated that the maximum compression loads per substructure unit are 12,600 kN. The maximum pile group settlement should be less than 25 mm under the compression loads.

Calculations of pile group settlement will be demonstrated for pile groups embedded in both cohesionless, cohesive, and combined layers of cohesionless and cohesive soils. The pile groups at the North Abutment and Pier 2 has a cohesionless soil profile. The pile groups at Pier 3 has a combined layers of cohesionless and cohesive soils, and the pile groups at the South Abutment has a cohesive soil profile.

F.3.1 North Abutment - Meyerhof Method Based on SPT Test Data

The soil profile interpreted from Soil Boring S-1 for the pile group at the North Abutment was shown in Figure F.3. Calculate the immediate settlement of pile group using the Meyerhof method based on SPT test data for an embedded pile length of 11.5 meters. Use the method outlined in Section 9.8.2.2a.

STEP 1 Calculate total pile group settlement due to soil compression.

Meyerhof recommended that the settlement of a pile group in a homogeneous sand deposit not underlain by a more compressible soil at a greater depth may be conservatively estimated by the following expression:

STEP 1 (continued)

Where:

p_f = foundation pressure (kPa). Group load divided by group area.
Notes: settlement should be calculated for the design load to be imposed on the pile group, and not the ultimate or allowable pile group capacities.

$$= \frac{12,600 \text{ kN}}{(3.36 \text{ m})(10.86 \text{ m})} = 345 \text{ kPa}$$

B = the width of pile group = 3.36 m

\bar{N}' = average corrected SPT N' value within a depth B below pile toe level.

$$= \frac{34 + 32 + 33}{3} = 33$$

D = pile embedment depth = 11.5 m

I_f = influence factor for group embedment.

$$= 1 - [D / 8B] \geq 0.5$$

$$= 1 - [(11.5 \text{ m}) / 8(3.36 \text{ m})] = 0.572$$

Therefore,

s = estimated total pile group settlement due to soil compression.

$$= \frac{0.96(345 \text{ kPa})\sqrt{3.36(0.572)}}{33} = 10.52 \text{ mm}$$

Note: For silty sand, a different equation should be used as indicated in Section 9.8.2.2a.

STEP 2 Calculate the elastic compression of pile material under design load on each pile as described in Section 9.8.2.1.

The design load on each pile = 890 kN. The elastic compression of each pile can be calculated with the following expression:

$$\Delta = \frac{Q_a L}{A E}$$

Where:

L = Length of pile (mm) = 11,500 mm

A = Pile cross sectional area (m²) = 0.127 m²

E = Modulus of elasticity of pile material (kPa) = 27.8 x 10⁶ kPa

Q_a = Design axial load in pile (kN), as discussed below.

Because of the shaft resistance, the axial load transferred to the pile varies along the pile length. For this reason, the average axial load in each pile segment should be calculated. The pile is divided into four segments according to the number of soil layers used in shaft resistance computations presented in Section F.2.1.2 (Nordlund Method). The first segment is 1 meter length, the second is 3 meters, the third is 7 meters, and the fourth is 0.5 meters. The shaft resistance as calculated using the Nordlund method for the first, second, third, and fourth segment is 37 kN, 146 kN, 615 kN, and 100 kN, respectively. The average axial load transferred to each pile segment is equal to the axial load transferred to the mid length of each pile segment as shown in Figure F.13. The average axial load transferred is used to calculate the elastic compression of the pile segment. The total elastic compression of the pile is equal to the sum of elastic compression from each pile segment.

$$\text{Pile segment 1a: } \Delta_{1a} = \frac{(872 \text{ kN})(1000 \text{ mm})}{(0.127 \text{ m}^2)(27,800,000 \text{ kPa})} = 0.247 \text{ mm}$$

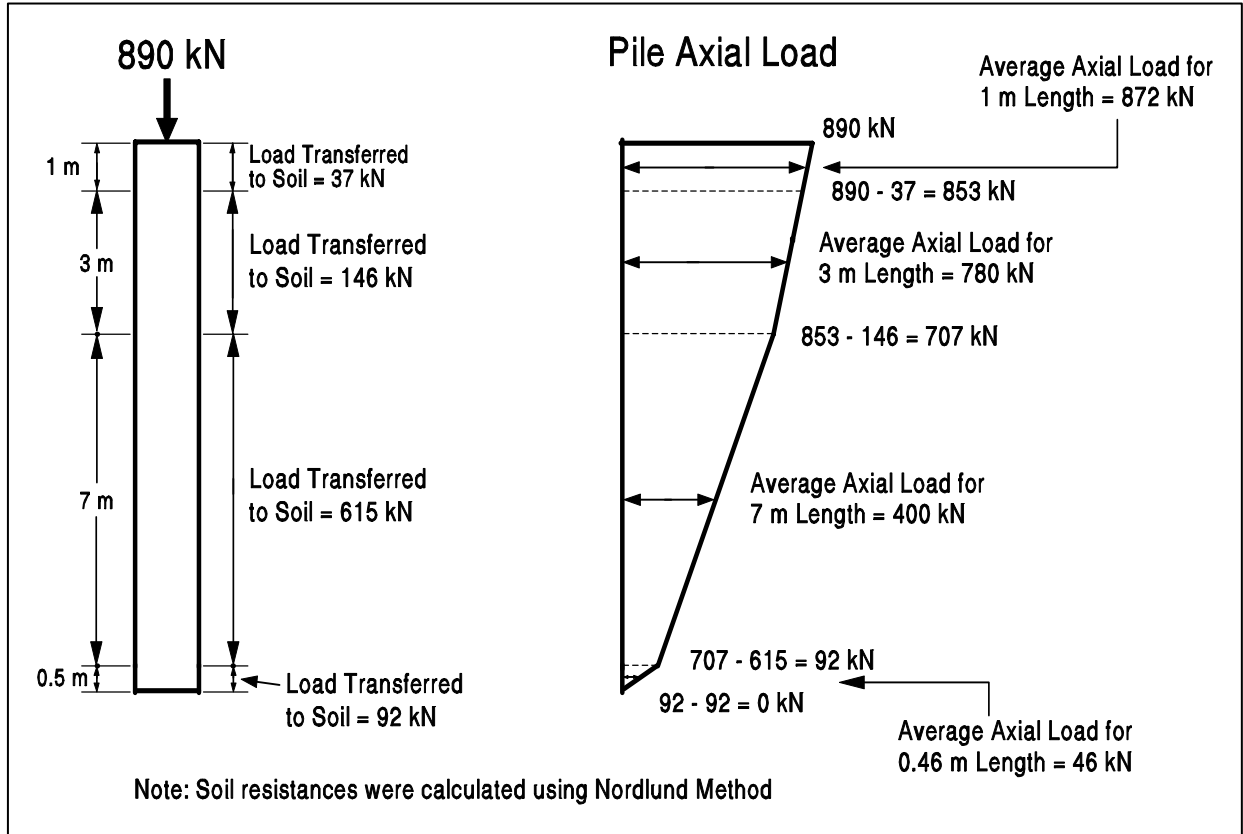


Figure F.13 Calculation of Axial Load Transfer to the Pile at the North Abutment

STEP 2 (continued)

Pile segment 1b:
$$\Delta_{1b} = \frac{(780 \text{ kN})(3000 \text{ mm})}{(0.127 \text{ m}^2)(27,800,000 \text{ kPa})} = 0.663 \text{ mm}$$

Pile segment 2:
$$\Delta_2 = \frac{(400 \text{ kN})(7000 \text{ mm})}{(0.127 \text{ m}^2)(27,800,000 \text{ kPa})} = 0.793 \text{ mm}$$

Pile segment 3:
$$\Delta_3 = \frac{(46 \text{ kN})(460 \text{ mm})}{(0.127 \text{ m}^2)(27,800,000 \text{ kPa})} = 0.006 \text{ mm}$$

Total:
$$\Delta = \Delta_{1a} + \Delta_{1b} + \Delta_2 + \Delta_3$$

$$= 0.247 \text{ mm} + 0.663 \text{ mm} + 0.793 \text{ mm} + 0.006 \text{ mm} = 1.709 \text{ mm}$$

STEP 3 Compute total pile group settlement.

$$\begin{aligned}\Delta(\text{ total }) &= \Delta (\text{ soil compression }) + \Delta (\text{ elastic pile compression }) \\ &= 10.52 \text{ mm} + 1.709 \text{ mm} \\ &= 12.23 \text{ mm} \quad \text{or} \quad 0.012 \text{ m}\end{aligned}$$

Note: Total pile group settlement is less than the maximum allowable settlement of 25 mm.

F.3.2 Pier 2 - Meyerhof Method Based on SPT Test Data

The soil profile interpreted from Soil Boring S-2 for the pile group at Pier 2 was shown in Figure F.5. Calculate the immediate settlement of pile group using the Meyerhof method based on SPT test data for an embedded pile length of 10 meters. Use the method outlined in Section 9.8.2.2a.

STEP 1 Calculate total pile group settlement due to soil compression.

Meyerhof recommended that the settlement of a pile group in a homogeneous sand deposit not underlain by a more compressible soil at a greater depth may be conservatively estimated by the following expression:

$$s = \frac{0.96 p_f \sqrt{B} l_f}{\bar{N}'}$$

Where:

p_f = foundation pressure (kPa). Group load divided by group area.
Notes: settlement should be calculated for the design load to be imposed on the pile group, and not the ultimate or allowable pile group capacities.

$$= \frac{12,600 \text{ kN}}{(3.36 \text{ m})(10.86 \text{ m})} = 345 \text{ kPa}$$

B = the width of pile group = 3.36 m

\bar{N}' = average corrected SPT N' value within a depth B below pile toe level

$$= \frac{34 + 30 + 32}{3} = 32$$

D = pile embedment depth = 10 m

STEP 1 (continued)

$$\begin{aligned} I_f &= \text{influence factor for group embedment} \\ &= 1 - [D / 8B] \geq 0.5 \\ &= 1 - [(10 \text{ m}) / 8(3.36 \text{ m})] = 0.628 \end{aligned}$$

Therefore,

$$\begin{aligned} s &= \text{estimated total pile group settlement due to soil compression} \\ &= \frac{0.96(345 \text{ kPa})\sqrt{.36}(0.628)}{32} = 11.91 \text{ mm} \end{aligned}$$

Note: For silty sand, a different equation should be used as indicated in Section 9.8.2.2a.

STEP 2 Calculate the elastic compression of pile material under design load on each pile.

The design load on each pile = 890 kN. The elastic compression of each pile can be calculated with the following expression:

$$\Delta = \frac{Q_a L}{A E}$$

Where:

$$L = \text{Length of pile (mm)} = 10,000 \text{ mm}$$

$$A = \text{Pile cross sectional area (m}^2\text{)} = 0.127 \text{ m}^2$$

$$E = \text{Modulus of elasticity of pile material (kPa)} = 27.8 \times 10^6 \text{ kPa}$$

$$Q_a = \text{Design axial load in pile (kN), as discussed below.}$$

Because of the shaft resistance, the axial load transferred to the pile varies along the pile length. For this reason, the average axial load in each pile segment should be calculated. The pile is divided into two segments according to the number of soil layers presented in Figure F.5. The first segment is 4

STEP 2 (continued)

meters length and the second is 6 meters. The shaft resistance as calculated using the Nordlund method (as presented in Section F.2.2.2) for the first and second segment is 267 kN and 717 kN, respectively. The average axial load transferred to each pile segment is equal to the axial load transferred to the mid length of each pile segment as described earlier in Section F.3.1 and shown in Figure F.14. The average axial load transferred is used to calculate the elastic compression of the pile segment. The total elastic compression of the pile is equal to the sum of elastic compression from each pile segment.

$$\text{Pile segment 1: } \Delta_1 = \frac{(757 \text{ kN})(4000 \text{ mm})}{(0.127 \text{ m}^2)(27,800,000 \text{ kPa})} = 0.858 \text{ mm}$$

$$\text{Pile segment 2: } \Delta_2 = \frac{(312 \text{ kN})(5213 \text{ mm})}{(0.127 \text{ m}^2)(27,800,000 \text{ kPa})} = 0.461 \text{ mm}$$

$$\begin{aligned} \text{Total: } \quad \Delta &= \Delta_1 + \Delta_2 \\ &= 0.858 \text{ mm} + 0.461 \text{ mm} = 1.319 \text{ mm} \end{aligned}$$

STEP 3 Compute total pile group settlement.

$$\begin{aligned} \Delta (\text{ total }) &= \Delta (\text{ soil compression }) + \Delta (\text{ elastic pile compression }) \\ &= 11.91 \text{ mm} + 1.319 \text{ mm} \\ &= 13.23 \text{ mm} \quad \text{or} \quad 0.013 \text{ m} \end{aligned}$$

Note: Total pile group settlement is less than the maximum allowable settlement of 25 mm.

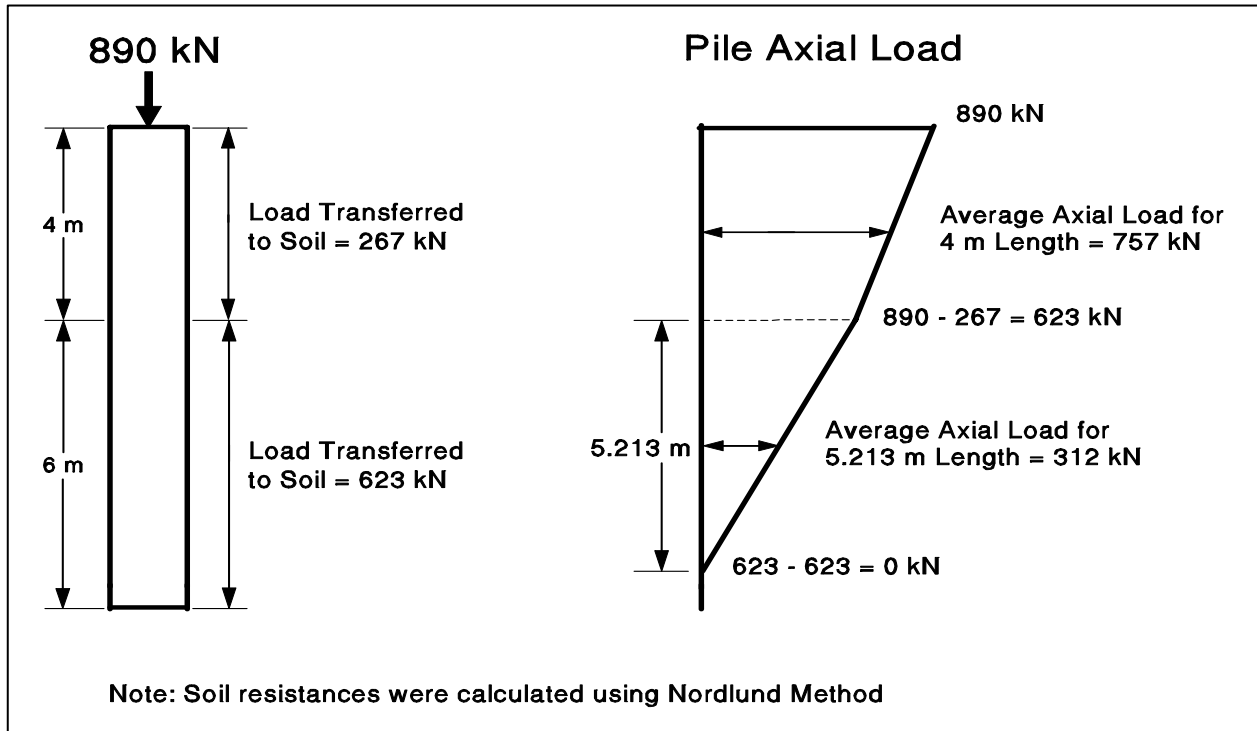


Figure F.14 Calculation of Axial Load Transfer to the Pile at Pier 2

F.3.3 Pier 3 - Equivalent Footing Method for Layered Soils

For the pile group at Pier 3 and the soil profile interpreted from Soil Boring S-3 as shown in Figure F.9. Calculate the immediate settlements of pile groups using the equivalent footing method for layered soils for an embedded pile length of 13 meters. Use the step-by-step method outlined in Section 9.8.2.5.

STEP 1 Determine the new load imposed on soil by the pile group.

- a. Determine the location of the equivalent footing.

The location of the equivalent footing is based on the shaft and toe resistance condition and the soil profile. Figure 9.62 should be used to determine the location of the equivalent footing and the pressure distribution. The soil profile for Soil Boring S-3, and the shaft and toe resistance combination match that in Figure 9.62(d), and therefore the equivalent footing is placed at depth of $\frac{2}{3} D$ from the bottom of the pile cap as shown in the figure.

STEP 1 (continued)

Depth of Equivalent Footing:

- below the pile cap $= \frac{2}{3} (13.0 \text{ m}) = 8.67 \text{ m}$
- or below the existing ground $= 8.67 \text{ m} + 2.0 \text{ m} = 10.67 \text{ m}$

b. Determine the dimensions of the equivalent footing.

All the piles in the pile group are vertical, and the pile group has a dimension of 3.36 meters by 10.86 meters. To account for load transfer, the equivalent footing has a modified dimension that spreads as a pyramid with a side slope of 1H:4V, as shown in Figure 9.44(d). Since the equivalent footing is 8.67 meters below the pile cap, the equivalent footing dimensions are:

$$\begin{aligned} \text{The width of the equivalent footing, } B_1 &= 3.36 \text{ m} + 2 \left(\frac{8.67 \text{ m}}{4} \right) \\ &= 7.70 \text{ m} \end{aligned}$$

$$\begin{aligned} \text{The length of the equivalent footing, } Z_1 &= 10.86 \text{ m} + 2 \left(\frac{8.67 \text{ m}}{4} \right) \\ &= 15.20 \text{ m} \end{aligned}$$

c. Determine the pressure distribution to soil layers below the equivalent footing up to the depth at which the pressure increase from the equivalent footing is less than 10% of existing effective overburden pressure at that depth.

The pressure distribution diagram below the equivalent footing is presented in Figure F.15. Note, the pressure distribution area increases with depth below the equivalent footing which results in a pressure reduction with depth below the equivalent footing. The dimension of the pressure distribution surface also spreads as a pyramid with depth but with a side slope of 1H:2V.

For example, at depth of 0.67 meter below the equivalent footing (or 11.34 meters below the existing ground surface), the pressure distribution surface has the following dimensions:

STEP 1 (continued)

$$\text{Width of pressure distribution surface, } B_2 = 7.70 \text{ m} + 2 \left(\frac{0.67 \text{ m}}{2} \right) = 8.37 \text{ m}$$

$$\text{Length of pressure distribution surface, } Z_2 = 15.20 \text{ m} + 2 \left(\frac{0.67 \text{ m}}{2} \right) = 15.87 \text{ m}$$

$$\begin{aligned} \text{Area of pressure distribution surface, } A_2 &= (B_2) (Z_2) = (8.37 \text{ m}) (15.87 \text{ m}) \\ &= 132.8 \text{ m}^2 \end{aligned}$$

Therefore, at depth of 0.67 meter below the equivalent footing the pressure increase due to the imposed design load is:

$$\Delta p = \left(\frac{12,600 \text{ kN}}{132.8 \text{ m}^2} \right) = 94.88 \text{ kPa}$$

The pressure increase at other locations below the equivalent footing is summarized in Table F-1. The limestone bedrock was reached before the imposed pressure increase becomes less than 10% of existing effective overburden pressure. Therefore for settlement calculation, the total soil thickness up to the bedrock will be used.

- d. Divide the cohesive soil layers in the affected pressure increase zone into several thinner layers of 1.5 to 3 meter thickness. The thickness of each layer is the thickness H for the settlement computation for that layer.

For this example, the soil is divided into 1.5 meter thick layers as presented in column 3 of Table F-2. The soil layer boundaries are presented in column 2 of Table F-2.

- e. Determine the existing effective overburden pressure, p_o , at the midpoint of each layer.

The midpoint location of each soil layer below the existing ground is presented in column 4 of Table F-2. The effective overburden pressure, p_o , at the midpoint of each layer is presented in column 5 of Table F-2.

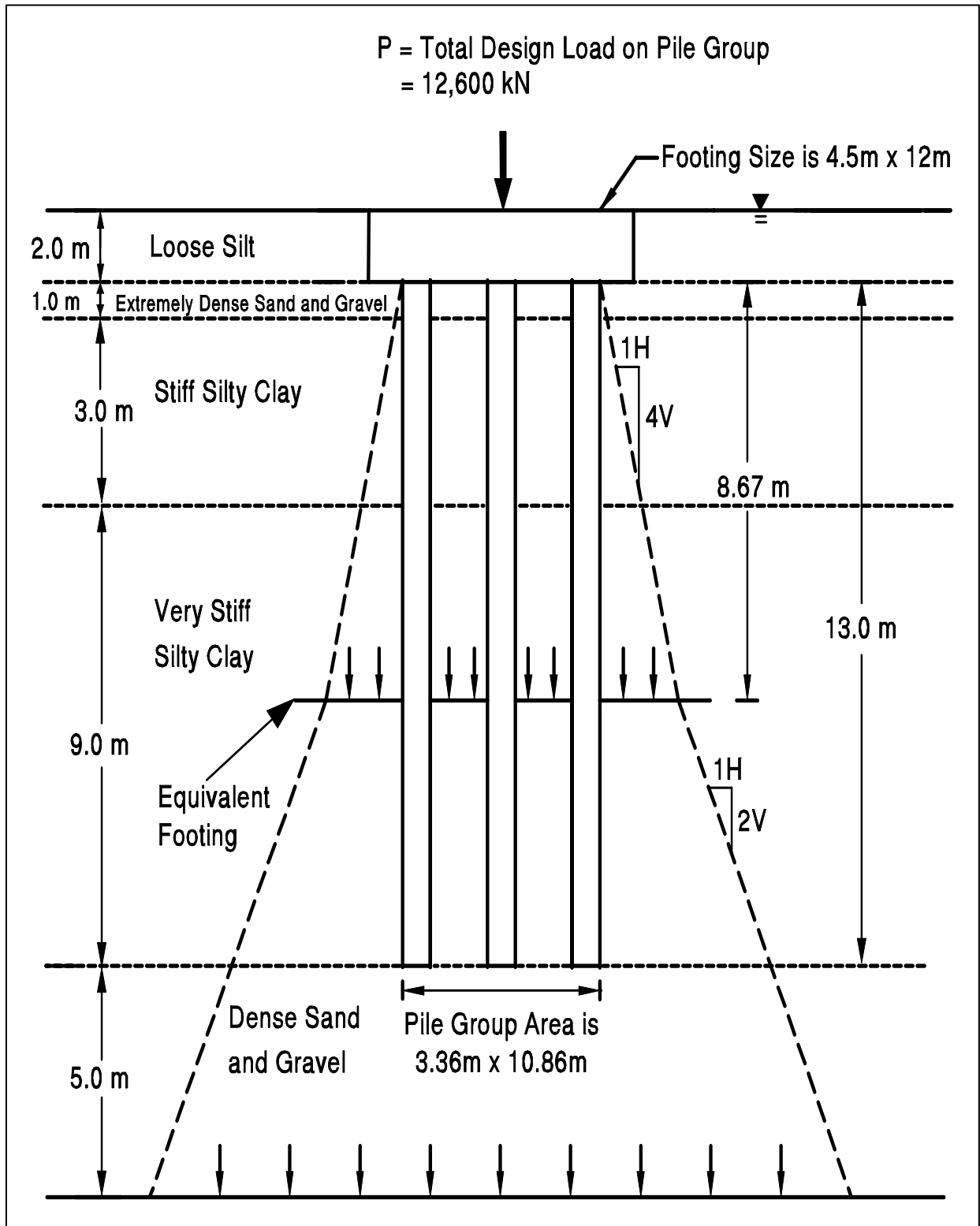


Figure F.15 Pressure Distribution Below Equivalent Footing for Pile Group at Pier 3

Table F-1 Summary of Pressure Distribution Below Equivalent Footing							
Depth Below Existing Ground (m)	Depth Below Equivalent Footing (m)	Load Distribution Surface			Imposed Pressure Increase Δp (kPa)	Effective Overburden Pressure p_o (kPa)	$\left(\frac{\Delta p}{p_o}\right) 100\%$ (%)
		Width B_2 (m)	Length Z_2 (m)	Area $(B_2)(Z_2)$ (m^2)			
10.67	0.00	7.70	15.20	117.0	107.66	98.77	109.0
11.34	0.67	8.37	15.87	132.8	94.88	105.74	89.7
12.75	2.08	9.78	17.28	169.0	74.56	120.40	61.9
14.25	3.58	11.28	18.78	211.8	59.48	136.00	43.7
15.75	5.08	12.78	20.28	259.2	48.62	151.53	32.1
17.25	6.58	14.28	21.78	311.0	40.51	166.98	24.3
18.75	8.08	15.78	23.28	367.4	34.30	182.43	18.8
19.75	9.08	16.78	24.28	407.4	30.93	192.73	16.1

Note: Equivalent Footing is at 10.67 meters below existing ground.

STEP 1 (continued)

- f. Determine the imposed pressure increase, Δp , at the midpoint of each affected soil layer based on the appropriate pressure distribution surface.

The imposed pressure increase, Δp , at the midpoint of each affected soil layer is presented in column 6 of Table F-2. Calculations of the imposed pressure increase based on the pressure distribution area were presented earlier in Step 1c.

STEP 2 Determine consolidation test parameters for the cohesive soil layer.

The laboratory consolidation test results on the undisturbed samples of stiff silty clay from layer 2 and very stiff silty clay from layer 3 were plotted on the "log pressure, p versus void ratio, e " (similar to Figure 9.43).

Table F-2 Settlement Calculations							
1 Soil Type	2 Soil Layer Below Existing Ground (m)	3 Soil Layer Thickness (m)	4 Depth of Midpoint Below Existing Ground (m)	5 Effective Overburden Pressure at Midpoint p_o (kPa)	6 Imposed Pressure Increase at Midpoint Δp (kPa)	7 $(p_o + \Delta p)$ (kPa)	8 Layer Settlement (m)
Layer 3 $p_c=297$ kPa; $e_0=0.54$ $C_c=0.20$; $C_{cr}=0.020$	10.67 - 1.00	1.33	11.34	105.74	94.88	200.62	0.0048
	12.00 - 1.50	1.50	12.75	120.40	74.56	194.96	0.0041
	13.50 - 5.00	1.50	14.25	136.00	59.48	195.48	0.0031
Layer 4 $\bar{N}'=33$; $C'=146$ $\bar{N}'=38$; $C'=173$ $\bar{N}'=33$; $C'=146$ $\bar{N}'=39$; $C'=180$							
	15.00 - 16.50	1.50	15.75	151.53	48.62	200.15	0.0012
	16.50 - 1.00	1.50	17.25	166.98	40.51	207.49	0.0008
	18.00 - 9.50	1.50	18.75	182.43	34.30	216.73	0.0008
	19.50 - 2.00	0.50	19.75	192.73	30.93	223.66	0.0002
Total Settlement =							0.0150

STEP 2 (continued)

The following consolidation test parameters were obtained from the plot.

Soil Layer 3 (very stiff silty clay):

Preconsolidation pressure, p_c	=	297 kPa
Initial void ratio, e_0	=	0.54
Compression index, C_c	=	0.20
Recompression index, C_{cr}	=	0.020

STEP 3 Determine bearing capacity index for each cohesionless layer.

Determine the average corrected SPT N' value, \bar{N}' , for each cohesionless layer.

Use \bar{N}' for the appropriate SPT hammer type in Figure 9.63 to obtain the bearing capacity index for each layer.

Soil Layer 4:

Layer 15.0 - 16.5:	$\bar{N}'=33$ from Safety Hammer; $C'=146$ from Figure 9.63
Layer 16.5 - 18.0:	$\bar{N}'=38$ from Safety Hammer; $C'=173$ from Figure 9.63
Layer 18.0 - 19.5:	$\bar{N}'=33$ from Safety Hammer; $C'=146$ from Figure 9.63
Layer 19.5 - 20.0:	$\bar{N}'=39$ from Safety Hammer; $C'=180$ from Figure 9.63

STEP 4 Compute settlement due to soil compression.

Compute settlement of each cohesive soil layer using the following equations:

$$s = H \left[\frac{C_{cr}}{1 + e_0} \log \frac{p_o + \Delta p}{p_o} \right] \quad \text{when } p_o + \Delta p \leq p_c$$
$$= H \left[\frac{C_{cr}}{1 + e_0} \log \frac{p_c}{p_o} \right] + H \left[\frac{C_c}{1 + e_0} \log \frac{p_o + \Delta p}{p_o} \right] \quad \text{when } p_o + \Delta p > p_c$$

For example, the soil layer increment 10.67 m to 12.00 m corresponds to:

$$(p_o + \Delta p) = 200.62 \text{ kPa} < p_c = 297 \text{ kPa}$$

STEP 4 (continued)

Therefore, layer settlement as shown in column 8 of settlement calculations table:

$$\begin{aligned} s &= H \left[\frac{C_{cr}}{1 + e_0} \log \frac{p_o + \Delta p}{p_o} \right] \\ &= 1.33 \left[\frac{0.020}{(1 + 0.54)} \log \left(\frac{200.62}{105.74} \right) \right] = 0.0048 \text{ m} \end{aligned}$$

Compute settlement of each cohesionless soil layer using the following equations:

$$s = H \left[\frac{1}{C'} \log \frac{p_o + \Delta p}{p_o} \right]$$

For the soil layer increment 15.0 m to 16.5 m corresponds to soil layer 3:

Therefore, the settlement for the soil layer increment as shown in column 8 of Table F-2 is:

$$s = 1.50 \left[\frac{1}{146} \log \left(\frac{200.15}{151.53} \right) \right] = 0.0012 \text{ m}$$

Following similar procedures, the total estimated pile group settlement due to soil compression is equal to the sum of settlements of all layers, or the sum of column 8 of Table F-2 and is equal to 0.0150 meter or 15.0 mm.

STEP 5 Calculate the elastic compression of pile material under design load on each pile. (See Section 9.8.2.1)

Note, for elastic compression calculations, it is assumed that all piles in the group are loaded with the 890 kN design load. This assumption is conservative because piles in the middle and rear rows have smaller loads. The elastic compression of each pile can be calculated with the following expression:

$$\Delta = \frac{Q_a L}{A E}$$

STEP 5 (continued)

Where:

L = Length of pile (mm) = 13,000 mm

A = Pile cross sectional area (m²) = 0.127 m²

E = Modulus of elasticity of pile material (kPa) = 27.8 x 10⁶ kPa

Q_a = Design axial load in pile (kN), as discussed below.

Because of shaft resistances, the axial load transferred to the pile varies along the length of the pile. Therefore, for elastic compression calculations the pile should be divided into segments with the average axial load in each segment calculated. For this example, the pile is divided into three segments based on the soil layers presented in Figure F.9. The first segment is 1.0 meter length, the second is 3.0 meters, and the third is 9.0 meters. The shaft resistance as calculated using the Nordlund method for the cohesionless soil layer and the α -method for the cohesive soil layer (as presented in Section F.2.3.1) for the first, second, and third segment is 22 kN, 453 kN, and 696 kN, respectively.

The average axial load transferred to each pile segment is equal to the axial load transferred to the mid-length of the segment, as shown in Figure F.16. The average axial load is used to calculate the elastic compression of each pile segment. Figure F.16 also shows that there is 868 kN to be transferred to soil layer 2, and 415 kN to be transferred to soil layer 3 which is capable of supporting up to 696 kN over the 9.0 meter layer thickness. Therefore, the 415 kN load will be fully transferred to the soil at depth of (415 kN / 696 kN) times (9.0 meters), or 5.366 meters below the top of layer 3, or the 890 kN total load will be fully transferred to the soil at depth of 9.366 meters below the pile cap. In other words, the lower 3.634 meters of the pile will not be subjected to any load or elastic compression.

$$\text{Pile segment 1: } \Delta_1 = \frac{(879 \text{ kN})(1,000 \text{ mm})}{(0.127 \text{ m}^2)(27,800,000 \text{ kPa})} = 0.249 \text{ mm}$$

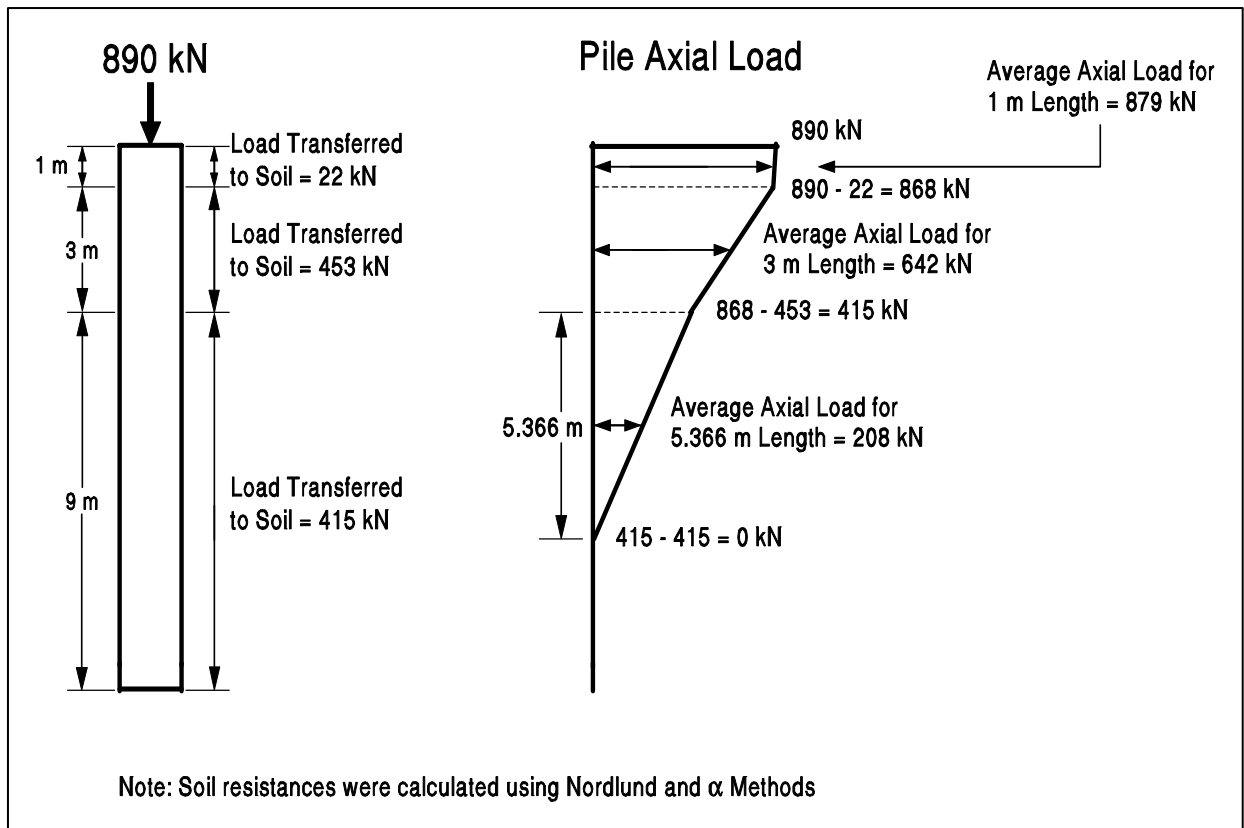


Figure F.16 Calculation of Axial Load Transfer to the Pile at Pier 3

STEP 5 (continued)

$$\text{Pile segment 2: } \Delta_2 = \frac{(642 \text{ kN})(3,000 \text{ mm})}{(0.127 \text{ m}^2)(27,800,000 \text{ kPa})} = 0.546 \text{ mm}$$

$$\text{Pile segment 3: } \Delta_3 = \frac{(208 \text{ kN})(5,366 \text{ mm})}{(0.127 \text{ m}^2)(27,800,000 \text{ kPa})} = 0.316 \text{ mm}$$

$$\begin{aligned} \text{Total: } \Delta &= \Delta_1 + \Delta_2 + \Delta_3 \\ &= 0.249 \text{ mm} + 0.546 \text{ mm} + 0.316 = 1.111 \text{ mm} \end{aligned}$$

Note: The elastic pile compression is small relative to the soil compression (15.0 mm), and therefore it is usually ignored.

STEP 6 Compute total pile group settlement.

$$\begin{aligned}\Delta(\text{ total }) &= \Delta(\text{ soil compression }) + \Delta(\text{ elastic pile compression }) \\ &= 15.0 \text{ mm} + 1.111 \text{ mm} = 16.111 \text{ mm or } 0.016 \text{ m}\end{aligned}$$

The total pile group settlement is smaller than the maximum allowable pile group settlement of 25 mm.

The Meyerhof method for settlement calculations based on SPT test data (Section 9.8.2.2a) will be performed on the following to compare with settlement calculated above.

STEP 1 Calculate total pile group settlement due to soil compression.

Meyerhof recommended that the settlement of a pile group in a homogeneous sand deposit not underlain by a more compressible soil at greater depth may be conservatively estimated by the following expression:

$$s = \frac{0.96 p_f \sqrt{B} I_f}{\bar{N}'}$$

Where:

p_f = foundation pressure (kPa). Group load divided by group area.
Notes: settlement should be calculated for the design load to be imposed on the pile group, and not the ultimate or allowable pile group capacities.

$$= \frac{12,600 \text{ kN}}{(3.36 \text{ m})(10.86 \text{ m})} = 345 \text{ kPa}$$

B = the width of pile group = 3.36 m

\bar{N}' = average corrected SPT N' value within a depth B below pile toe level

$$= \frac{33 + 38 + 33}{3} = 35$$

STEP 1 (continued)

$$D = \text{pile embedment depth} = 13 \text{ m}$$

$$I_f = \text{influence factor for group embedment}$$

$$= 1 - [D / 8B] \geq 0.5$$

$$= 1 - [(13 \text{ m}) / 8(3.36 \text{ m})] = 0.516$$

Therefore,

$$s = \text{estimated total pile group settlement due to soil compression}$$

$$= \frac{0.96(345 \text{ kPa})\sqrt{.36(0.516)}}{35} = 8.95 \text{ mm}$$

The settlement estimated using the Meyerhof method (8.95 mm) is less than the settlement calculated based on the equivalent method (15.2 mm). In this soil profile, the equivalent footing method calculates most of the foundation settlement (12 mm) to occur in the clay layer with minimal settlement of the underlying sand layer in which the piles are founded. It is unlikely that the magnitude of settlement calculated in the clay layer would occur due to the lack of strain compatibility between the layers. Therefore, the Meyerhof method is a better estimate of group settlement in this profile.

F.3.4 South Abutment - Equivalent Footing Method

For the pile group at the South Abutment and the soil profile interpreted from Soil Boring S-4 as shown in Figure F.11. Calculate the immediate settlements of pile groups using the equivalent footing method for an embedded pile length of 17.5 meters. Use the step-by-step method outlined in Section 9.8.2.3.

STEP 1 Determine the new load imposed on soil by the pile group.

- a. Determine the location of the equivalent footing.

The location of the equivalent footing is based on the shaft and toe resistance condition and the soil profile. Figure 9.62 should be used to determine the location of the equivalent footing and the pressure distribution. The soil profile for Soil Boring S-4 matches Figure 9.62(b), and therefore the equivalent footing is placed at depth of $\frac{2}{3}$ D from the bottom of the pile cap as shown in the figure.

Depth of Equivalent Footing:

- below the pile cap $= \frac{2}{3} (17.5 \text{ m}) = 11.67 \text{ m}$
- or below the existing ground $= 11.67 \text{ m} + 1.50 \text{ m} = 13.17 \text{ m}$

- b. Determine the dimensions of the equivalent footing.

All the piles in the pile group are vertical, and the pile group has a dimension of 3.36 meters by 10.86 meters. To account for load transfer, the equivalent footing has a modified dimension that spreads as a pyramid with a side slope of 1H:4V, as shown in Figure 9.62(b). Since the equivalent footing is 11.67 meters below the pile cap, the equivalent footing dimensions are:

$$\begin{aligned} \text{The width of the equivalent footing, } B_1 &= 3.36 \text{ m} + 2 \left(\frac{11.67 \text{ m}}{4} \right) \\ &= 9.20 \text{ m} \end{aligned}$$

STEP 1 (continued)

$$\begin{aligned}\text{The length of the equivalent footing, } Z_1 &= 10.86 \text{ m} + 2 \left(\frac{11.67 \text{ m}}{4} \right) \\ &= 16.70 \text{ m}\end{aligned}$$

- c. Determine the pressure distribution to soil layers below the equivalent footing up to the depth at which the pressure increase from the equivalent footing is less than 10% of existing effective overburden pressure at that depth.

The pressure distribution diagram below the equivalent footing is presented in Figure F.17. Note, the pressure distribution area increases with depth below the equivalent footing which results in a pressure reduction with depth below the equivalent footing. The dimension of the pressure distribution surface also spreads as a pyramid with depth but with a side slope of 1H:2V.

For example, at depth of 0.17 meter below the equivalent footing (or 13.34 meters below the existing ground surface), the pressure distribution surface has the following dimensions:

$$\text{Width of pressure distribution surface, } B_2 = 9.20 \text{ m} + 2 \left(\frac{0.17 \text{ m}}{2} \right) = 9.37 \text{ m}$$

$$\text{Length of pressure distribution surface, } Z_2 = 16.70 \text{ m} + 2 \left(\frac{0.17 \text{ m}}{2} \right) = 16.87 \text{ m}$$

$$\begin{aligned}\text{Area of pressure distribution surface, } A_2 &= (B_2) (Z_2) = (9.37 \text{ m}) (16.87 \text{ m}) \\ &= 158.1 \text{ m}^2\end{aligned}$$

Therefore, at depth of 0.17 meter below the equivalent footing the pressure increase due to the imposed design load is:

$$\Delta p = \left(\frac{12,600 \text{ kN}}{158.1 \text{ m}^2} \right) = 79.71 \text{ kPa}$$

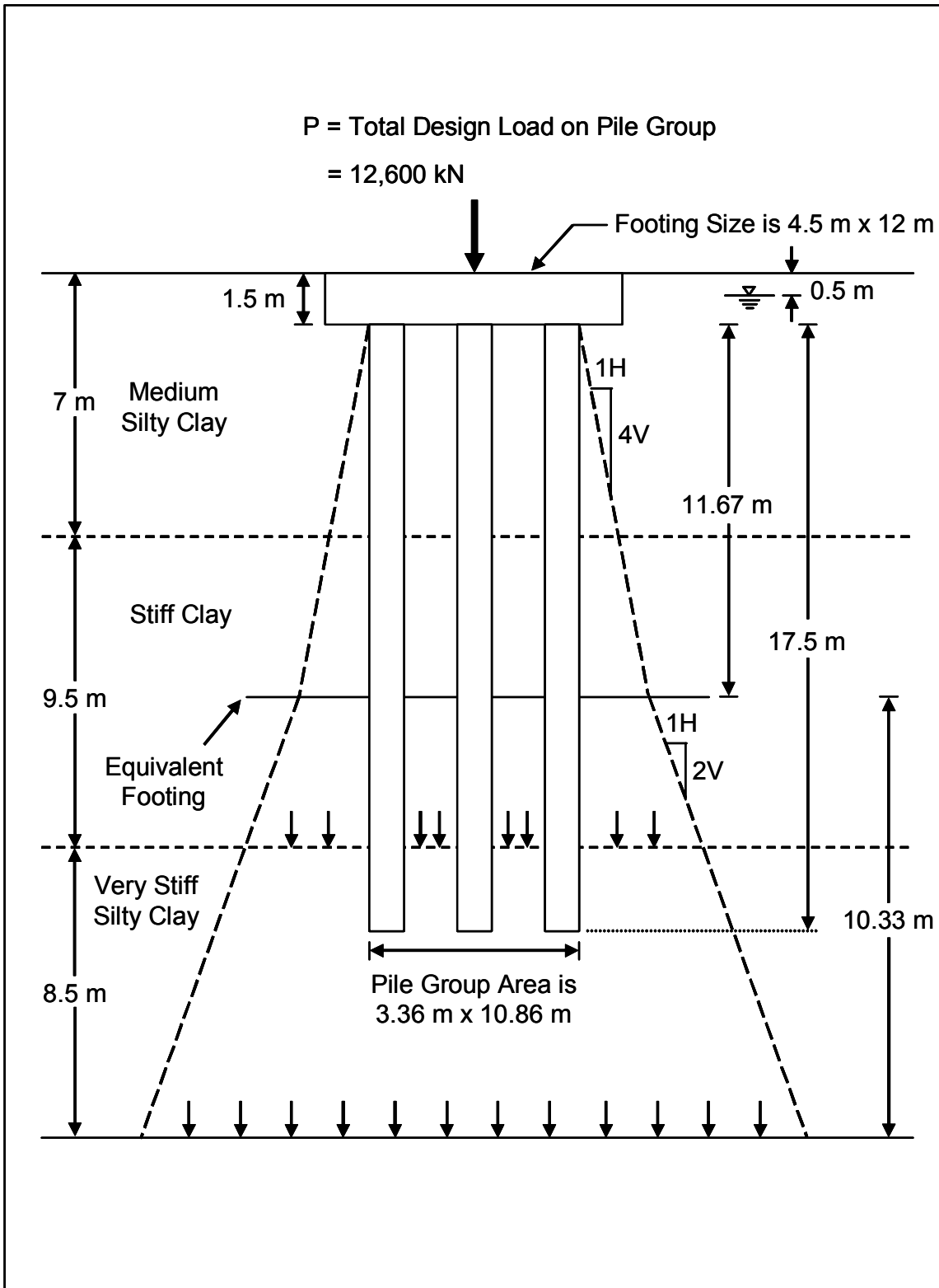


Figure F.17 Pressure Distribution Below Equivalent Footing for Pile Group at the South Abutment

STEP 1 (continued)

The pressure increase at other locations below the equivalent footing is summarized in Table F-3. The imposed pressure increase becomes less than 10% of existing effective overburden pressure at depth of 11.58 meters below the equivalent footing or 24.75 meters below the existing ground.

- d. Divide the cohesive soil layers in the affected pressure increase zone into several thinner layers of 1.5 to 3 meter thickness. The thickness of each layer is the thickness H for the settlement computation for that layer.

For this example, the soil is divided into 1.5 meter thick layers as presented in column 3 of Table F-4. The soil layer boundaries are presented in column 2 of Table F-4.

- e. Determine the existing effective overburden pressure, p_o , at the midpoint of each layer.

The midpoint location of each soil layer below the existing ground is presented in column 4 of Table F-4. The effective overburden pressure, p_o , at the midpoint of each layer is presented in column 5 of Table F-4.

- f. Determine the imposed pressure increase, Δp , at the midpoint of each affected soil layer based on the appropriate pressure distribution surface.

The imposed pressure increase, Δp , at the midpoint of each affected soil layer is presented in column 6 of Table F-4. Calculations of the imposed pressure increase based on the pressure distribution area were presented earlier in Step 1c.

Table F-3 Summary of Pressure Distribution Below Equivalent Footing							
Depth Below Existing Ground (m)	Depth Below Equivalent Footing (m)	Load Distribution Surface			Imposed Pressure Increase Δp (kPa)	Effective Overburden Pressure p_o (kPa)	$\left(\frac{\Delta p}{p_o}\right) 100\%$ (%)
		Width B_2 (m)	Length Z_2 (m)	Area $(B_2)(Z_2)$ (m ²)			
13.17	0.00	9.20	16.70	153.5	82.08	129.15	63.6
13.34	0.17	9.37	16.87	158.1	79.71	130.80	60.9
14.25	1.08	10.28	17.78	182.8	68.94	139.63	49.4
15.75	2.58	11.78	19.28	227.1	55.48	154.18	36.0
17.25	4.08	13.28	20.78	276.0	45.66	169.33	27.0
8.75	5.58	14.78	22.28	329.3	38.26	185.08	20.7
20.25	7.08	16.28	23.78	387.1	32.55	200.83	16.2
21.75	8.58	17.78	25.28	449.5	28.03	216.58	12.9
23.25	10.08	19.28	26.78	516.3	24.40	232.33	10.5
24.75	11.58	20.78	28.28	587.7	21.44	248.08	8.6

Note: Equivalent Footing is at 13.17 meters below existing ground.

STEP 2 Determine consolidation test parameters.

The laboratory consolidation test results on the undisturbed samples of stiff silty clay from layer 2 and very stiff silty clay from layer 3 were plotted on the "log pressure, p versus void ratio, e " (similar to Figure 9.61). The following consolidation test parameters were obtained from the plot.

Soil Layer 2:

Preconsolidation pressure, $p_c = 200$ kPa

Initial void ratio, $e_0 = 0.80$

Compression index, $C_c = 0.30$

Recompression index, $C_{cr} = 0.030$

Table F-4 Settlement Calculations							
1 Soil Type	2 Soil Layer Below Existing Ground (m)	3 Soil Layer Thickness (m)	4 Depth of Midpoint Below Existing Ground (m)	5 Effective Overburden Pressure at Midpoint p_o (kPa)	6 Imposed Pressure Increase at Midpoint Δp (kPa)	7 $(p_o + \Delta p)$ (kPa)	8 Layer Settlement (m)
Layer 2 $p_c=200$ kPa; $e_0=0.80$ $C_c=0.30$; $C_{cr}=0.030$	13.17 - 11.50	0.33	13.34	130.80	79.71	210.51	0.0022
	13.50 - 11.00	1.50	14.25	139.63	68.94	208.57	0.0085
	15.00 - 16.50	1.50	15.75	154.18	55.48	209.66	0.0079
Layer 3 $p_c=297$ kPa $e_0=0.54$ $C_c=0.20$ $C_{cr}=0.020$	16.50 - 18.00	1.50	17.25	169.33	45.66	214.99	0.0020
	18.00 - 19.50	1.50	18.75	185.08	38.26	223.34	0.0016
	19.50 - 21.00	1.50	20.25	200.83	32.55	233.38	0.0013
	21.00 - 22.50	1.50	21.75	216.58	28.03	244.61	0.0010
	22.50 - 24.00	1.50	23.25	232.33	24.40	256.73	0.0008
	24.00 - 25.50	1.50	24.75	248.08	21.44	269.52	0.0007
Total Settlement =							0.0260

STEP 2 (continued)

Soil Layer 3:

Preconsolidation pressure, $p_c = 297$ kPa

Initial void ratio, $e_0 = 0.54$

Compression index, $C_c = 0.20$

Recompression index, $C_{cr} = 0.020$

STEP 3 Compute settlement due to soil compression.

Compute settlement of each soil layer using the following equations:

$$s = H \left[\frac{C_{cr}}{1+e_0} \log \frac{p_o + \Delta p}{p} \right] \quad \text{when } p_o + \Delta p \leq p_c$$

$$= H \left[\frac{C_{cr}}{1+e_0} \log \frac{p_c}{p_o} \right] + H \left[\frac{C_c}{1+e_0} \log \frac{p_o + \Delta p}{p_c} \right] \quad \text{when } p_o + \Delta p > p_c$$

For example, the soil layer increment 13.17 m to 13.50 m corresponds to:

$$(p_o + \Delta p) = 210.51 \text{ kPa} > p_c = 200 \text{ kPa}$$

Therefore, layer settlement as shown in column 8 of settlement calculations table:

$$\begin{aligned} s &= H \left[\frac{C_{cr}}{1+e_0} \log \frac{p_c}{p_o} \right] + H \left[\frac{C_c}{1+e_0} \log \frac{p_o + \Delta p}{p_c} \right] \\ &= 0.33 \left[\frac{0.030}{(1+0.80)} \log \left(\frac{200}{130.80} \right) \right] + 0.33 \left[\frac{0.30}{(1+0.80)} \log \left(\frac{210.51}{200} \right) \right] = 0.0022\text{m} \end{aligned}$$

For the soil layer increment 16.50 m to 18.00 m corresponds to soil layer 3:

$$(p_o + \Delta p) = 214.99 \text{ kPa} < p_c = 297 \text{ kPa}$$

STEP 3 (continued)

Therefore, the settlement for the soil layer increment as shown in column 8 of Table F-4 is:

$$\begin{aligned} s &= H \left[\frac{C_{cr}}{1+e_0} \log \frac{p_o + \Delta p}{p_o} \right] \\ &= 1.5\text{m} \left[\frac{0.020}{(1+0.54)} \log \left(\frac{214.99}{169.33} \right) \right] = 0.0020\text{m} \end{aligned}$$

Following similar procedures, the total estimated pile group settlement due to soil compression is equal to the sum of settlements of all layers, or the sum of column 8 of Table F-4 and is equal to 0.0260 meter or 26.0 mm.

STEP 4 Calculate the elastic compression of pile material under design load on each pile as described in Section 9.8.2.1a.

Note, for elastic compression calculations, it is assumed that all piles in the group are loaded with the 890 kN design load. This assumption is conservative because piles in the middle and rear rows have smaller loads. The elastic compression of each pile can be calculated with the following expression:

$$\Delta = \frac{Q_a L}{A E}$$

Where:

L = Length of pile (mm) = 17,500 mm

A = Pile cross sectional area (m²) = 0.127 m²

E = Modulus of elasticity of pile material (kPa) = 27.8 x 10⁶ kPa

Q_a = Design axial load in pile (kN), as discussed below.

STEP 4 (continued)

Because of shaft resistances, the axial load transferred to the pile varies along the length of the pile. Therefore, for elastic compression calculations the pile should be divided into segments with the average axial load in each segment calculated. For this example, the pile is divided into three segments based on the soil layers presented in Figure F.11. The first segment is 5.5 meters length, the second is 9.5 meters, and the third is 2.5 meters. The shaft resistance as calculated using the α -method (as presented in Section F.2.4.1) for the first, second, and third segment is 259 kN, 1,150 kN, and 239 kN, respectively.

The average axial load transferred to each pile segment is equal to the axial load transferred to the mid-length of the segment, as shown in Figure F.18. The average axial load is used to calculate the elastic compression of each pile segment. Figure F.18 also shows that there is 631 kN to be transferred to soil layer 2 which is capable of supporting up to 1,150 kN over the 9.5 meter layer thickness. Therefore, the 631 kN load will be fully transferred to the soil at depth of $(631 \text{ kN} / 1,150 \text{ kN})$ times (9.5 meters) , or 5.213 meters below the top of layer 2, or the 890 kN total load will be fully transferred to the soil at depth of 10.713 meters below the pile cap. In other words, the lower 6.787 meters of the pile will not be subjected to any load or elastic compression.

$$\text{Pile segment 1: } \Delta_1 = \frac{(761 \text{ kN})(5,500 \text{ mm})}{(0.127 \text{ m}^2)(27,800,000 \text{ kPa})} = 1.186 \text{ mm}$$

$$\text{Pile segment 2: } \Delta_2 = \frac{(316 \text{ kN})(5,213 \text{ mm})}{(0.127 \text{ m}^2)(27,800,000 \text{ kPa})} = 0.467 \text{ mm}$$

$$\begin{aligned} \text{Total: } \quad \Delta &= \Delta_1 + \Delta_2 \\ &= 1.186 \text{ mm} + 0.467 \text{ mm} = 1.653 \text{ mm} \end{aligned}$$

Note: The elastic pile compression is small relative to the soil compression (26.0 mm), and therefore it is usually ignored.

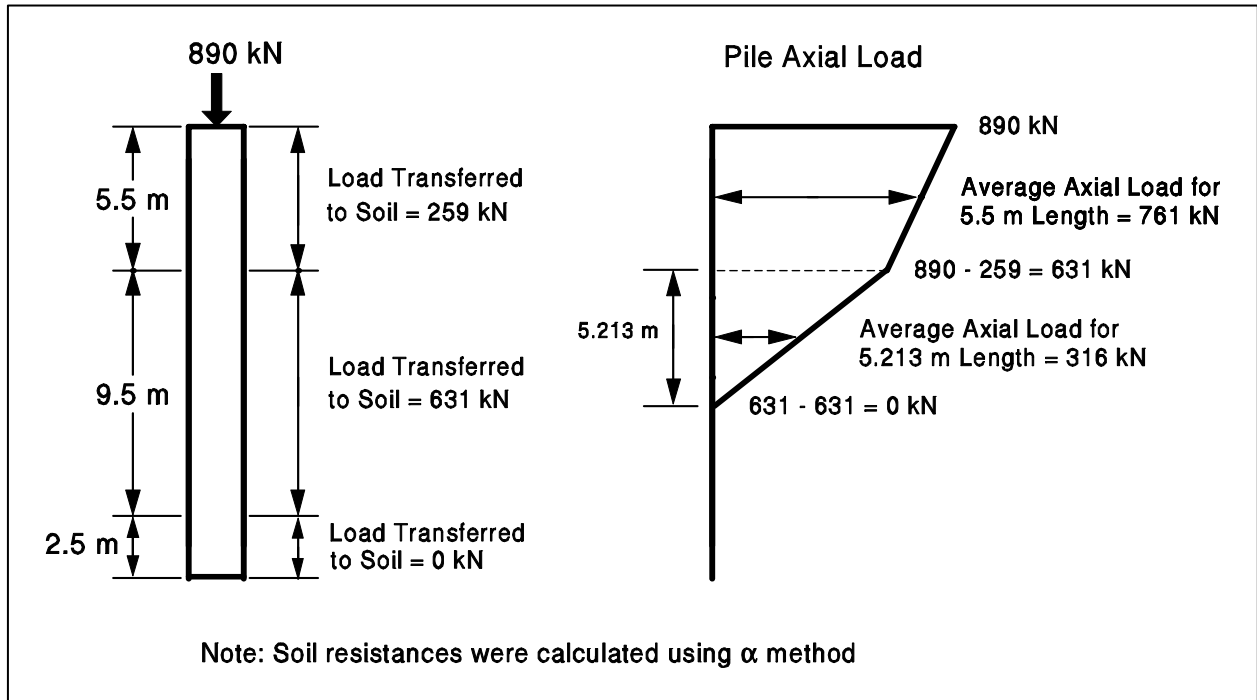


Figure F.18 Calculation of Axial Load Transfer to the Pile at South Abutment

STEP 5 Compute total pile group settlement.

$$\begin{aligned}
 \Delta(\text{total}) &= \Delta(\text{soil compression}) + \Delta(\text{elastic pile compression}) \\
 &= 26.0 \text{ mm} + 1.653 \text{ mm} \\
 &= 27.653 \text{ mm} \quad \text{or} \quad 0.028 \text{ m}
 \end{aligned}$$

The total pile group settlement is larger than the maximum allowable pile group settlement of 25 mm. The total settlement will even be larger after the placement of the approach embankment fill materials behind the abutment wall, as discussed in Section F.6. Therefore, preloading of the South Abutment should be performed prior to pile installation. The interaction of the approach embankment fill with the South Abutment foundation is discussed in greater detail in Section F.6.

F.4 LATERAL PILE CAPACITY ANALYSIS

The bridge division estimated that the group lateral loads range from 600 kN at the interior pile groups to 900 kN at the abutment pile groups. The maximum lateral load per pile is limited to 40 kN. A horizontal deflection of up to 10 mm is permissible under lateral loading.

F.4.1 Broms' Method - North Abutment

Perform a lateral pile capacity analysis for a pile at the North Abutment using Soil Boring S-1 as shown in Figure F.3. Perform the analysis based on an embedded pile length of 11.5 meters. Use the step by step procedure for the Broms' method outlined in Section 9.7.3.2.

STEP 1 Determine the general soil type within the critical depth below ground surface (about 4 or 5 pile diameters).

For pile diameter of 0.356 meter, the critical depth below the ground surface is about 1.42 to 1.78 meters. Based on the soil conditions for the North Abutment shown in Figure F.3, the general soil type within the critical depth below the ground surface is a loose silty fine sand cohesionless soil.

STEP 2 Determine the coefficient of horizontal subgrade reaction, K_h , within the critical depth based on cohesive or cohesionless soils.

For cohesionless soils, choose the K_h from Table 9-14 based on soil density and ground water table. For a loose silty fine sand, K_h is either 1,086 or 1,900 kN/m³ depending on whether the ground water table is below or above the critical depth, respectively. When the ground water table is within the critical depth region, a linear interpolation between these two values should be used to calculate K_h .

Assuming the critical depth is at 1.60 meters depth below the bottom of the excavation. Based on Figure F.3, the ground water table is at 1.0 meter below the bottom of the excavation. Therefore, using a linear interpolation, the coefficient of horizontal subgrade reaction, K_h , is:

STEP 2 (continued)

$$K_h = 1,086 + \frac{1.00}{1.60} (1,900 - 1,086) = 1,595 \text{ kN/ m}^3$$

STEP 3 Adjust K_h for loading and soil conditions.

Assuming that a cyclic loading exists at the site. For cyclic loading in loose cohesionless soils:

$$\begin{aligned} K_h &= \frac{1}{4} K_h \\ &= \frac{1}{4} (1,595) = 399 \text{ kN/m}^3 \end{aligned}$$

STEP 4 Determine pile parameters.

- a. Modulus of elasticity, E = 27,800 MPa
- b. Moment of inertia, I = $1.32 \times 10^{-3} \text{ m}^4$
- c. Section modulus, S = $7.46 \times 10^{-3} \text{ m}^3$
- d. Ultimate compressive strength, f_c = 34.5 MPa
- e. Embedded pile length, D = 11.5 m
- f. Pile width, b = 0.356 m
- g. Eccentricity of applied load, e_c = 0 for fixed-headed pile
- h. Dimensionless shape factor, C_s , applied only to steel piles.
- i. Resisting moment of pile, M_y = $f_c S$ for concrete piles
= 34.5 MPa ($7.46 \times 10^{-3} \text{ m}^3$)
= 257.4 kN-m

STEP 5 Determine η for cohesionless soils.

$$\begin{aligned}\eta &= \sqrt[5]{K_h/EI} = \sqrt[5]{\frac{399 \text{ kN/m}^3}{(27.8 \times 10^6 \text{ kN/m}^2) (1.32 \times 10^{-3} \text{ m}^4)}} \\ &= 0.405 \text{ m}^{-1}\end{aligned}$$

STEP 6 Determine the dimensionless length factor for cohesionless soil.

$$\eta D = 0.405 \text{ m}^{-1} (11.5 \text{ m}) = 4.66$$

STEP 7 Determine if pile is long or short according to the cohesionless soil criteria.

Since $\eta D = 4.66$ is greater than 4.0, the pile is long.

STEP 8 Determine other soil parameters.

a. Rankine passive pressure coefficient for cohesionless soil, K_p , is:

$$K_p = \tan^2 (45 + \phi/2)$$

where ϕ is the average soil friction angle along the embedded pile length.

As shown in Figure F.3, the soil profile along the embedded pile length is divided into three layers. As discussed in Section F.2.1.2, the soil friction angle, ϕ , from each layer is calculated using the corrected SPT N' value and Table 4-6.

$$\text{Layer 1 (4 m depth): } \bar{N}_1' = 8 \quad \rightarrow \quad \phi_1 = 29^\circ$$

$$\text{Layer 2 (7 m depth): } \bar{N}_2' = 14 \quad \rightarrow \quad \phi_2 = 31^\circ$$

$$\text{Layer 3 (0.5 m depth): } \bar{N}_3' = 34 \quad \rightarrow \quad \phi_3 = 36^\circ$$

The average ϕ angle is calculated from the weighted ϕ angle based on the thickness of each layer.

STEP 8 (continued)

The average ϕ angle is:

$$\phi = \frac{29^\circ (4 \text{ m}) + 31^\circ (7 \text{ m}) + 36^\circ (0.5 \text{ m})}{11.5 \text{ m}} = 30.5^\circ$$

Therefore, the Rankine passive pressure coefficient, K_p , is:

$$\begin{aligned} K_p &= \tan^2 (45 + \phi/2) \\ &= \tan^2 (45 + 30.5/2) = 3.06 \end{aligned}$$

b. Average effective soil unit weight over embedded length of pile, γ (kN/m^3).

The average effective soil unit weight, γ , will also be calculated from the weighted γ of each layer based on the thickness of each layer.

$$\begin{aligned} \gamma &= \frac{16.5 \text{ kN/m}^3 (1 \text{ m}) + 6.7 \text{ kN/m}^3 (3 \text{ m}) + 7.8 \text{ kN/m}^3 (7 \text{ m}) + 9.8 \text{ kN/m}^3 (0.5 \text{ m})}{11.5 \text{ m}} \\ &= 8.36 \text{ kN/m}^3 \end{aligned}$$

STEP 9 Determine the ultimate (failure) lateral load, Q_u , for a single pile.

The pile will be used in a group under a pile cap, therefore it is considered a fixed headed pile. For a long fixed headed pile in a cohesionless soil, Figure 9.40 should be used to calculate the ultimate load. First $M_y / (b^4 \gamma K_p)$ must be calculated.

$$\frac{M_y}{b^4 \gamma K_p} = \frac{257.4 \text{ kN-m}}{(0.356 \text{ m})^4 (8.36 \text{ kN/m}^3) (3.06)} = 626$$

Enter Figure 9.40 with this value to the fixed head curve to obtain $Q_u / K_p b^3 \gamma = 190$.

STEP 9 (continued)

So,

$$\begin{aligned} Q_u &= 190 K_p b^3 \gamma \\ &= 190 (3.06) (0.356 \text{ m})^3 (8.36 \text{ kN/m}^3) \\ &= 219 \text{ kN} \end{aligned}$$

STEP 10 Calculate the maximum allowable working load for a single pile, Q_m , from the ultimate load, Q_u , determined in Step 9, as shown in Figure 9.41.

$$Q_m = \frac{Q_u}{2.5} = \frac{219 \text{ kN}}{2.5} = 88 \text{ kN}$$

STEP 11 Calculate the deflection, y , corresponding to the desired design load, Q_a of 40 kN.

For fixed headed pile in cohesionless soil, enter Figure 9.43 with $\eta D = 4.66$ to obtain $y(EI)^{3/5} K_h^{2/5} / Q_a D$. This results in

$$y(EI)^{3/5} K_h^{2/5} / Q_a D = 0.21$$

The calculated deflection y is:

$$\begin{aligned} y &= 0.21 Q_a D / (EI)^{3/5} K_h^{2/5} \\ &= 0.21(40 \text{ kN})(11.5 \text{ m}) / (27.8 \times 10^6 \text{ kN/m}^2)^{3/5} (1.32 \times 10^{-3} \text{ m}^4)^{3/5} (399 \text{ kN/m}^3)^{2/5} \\ &= 0.016 \text{ m} \quad \text{or} \quad 16 \text{ mm} \end{aligned}$$

Therefore, the desired design load of 40 kN will cause the pile head to deflect 16 mm at the ground surface which exceeds the bridge division's allowable deflection of 10 mm. Therefore, the maximum design load that will not exceed the 10 mm deflection should be determined.

STEP 11 (continued)

$$y = 0.21 Q_a D / (EI)^{3/5} K_n^{2/5}$$

$$.01 = 0.21 (Q_a) (11.5 \text{ m}) / (21 \times 10^6 \text{ kN/m}^2)^{3/5} (1.32 \times 10^{-3} \text{ m}^4)^{3/5} (399 \text{ kN/m}^3)^{2/5}$$

$$Q_a = 0.01 (27.8 \times 10^6 \text{ kN/m}^2)^{3/5} (1.32 \times 10^{-3} \text{ m}^4)^{3/5} (399 \text{ kN/m}^3)^{2/5} / (0.21)(11.5 \text{ m})$$
$$= 24.9 \text{ kN}$$

STEP 12 Compare the design load Q_a , and design deflection, y , with the maximum allowable working load, Q_m , and deflection, y_m .

The maximum design load of 24.9 kN determined from the design deflection is less than the maximum allowable working load of 87 kN.

STEP 13 Reduce the maximum allowable load to account for group effects and method of installation.

a. Group effects.

The center to center pile spacing, z , is designed to be 1.5 meters.

$$(z/b) = (1.5 \text{ m}) / (0.356 \text{ m}) = 4.21$$

Using the reduction factor table and linear interpolation:

$$\text{reduction factor} = 0.532$$

$$\text{So, } Q_m = 0.532 Q_m = 0.532 (88 \text{ kN}) = 47 \text{ kN}$$

b. Method of installation.

No reduction is required for driven piles. So, $Q_m = 47 \text{ kN}$.

STEP 14 Compute the total lateral load capacity of the pile group.

The total lateral load capacity of the pile group is equal to the adjusted allowable load per pile from Step 13b times the number of piles.

$$\text{Total Pile Group Lateral Load Capacity} = 24 (47 \text{ kN}) = 1,128 \text{ kN}$$

However, this group lateral load cannot be achieved at the deflection limit required by the bridge division and therefore a lower group load must be used.

To meet the 10 mm deflection requirements, a design lateral load of 25 kN per pile must be used. This lateral load is less than desired. Therefore, the group capacity of 600 kN (24 piles at 25 kN/pile) is insufficient, and more piles would be required.

F.4.2 LPILE Analysis - North Abutment

A LPILE analysis was performed to evaluate the lateral load capacity of the 356 mm square prestressed concrete pile at the North Abutment. The concrete pile was driven 11.5 m into the dense sand and gravel stratum as depicted in Figure F.3.

The North Abutment concrete pile was analyzed considering full fixity at the base of the pile cap. The geometric and elastic properties of the pile were input along with the relevant soil properties and stratigraphic information. Soil input parameters were obtained from Table 9-12. Moment-dependent flexural rigidity (concrete cracking effects) are included explicitly in the analyses. In order to rigorously evaluate the moment-stiffness relationship, the longitudinal reinforcement (4 No. 8 bars) was also characterized with respect to cross-section geometry and steel properties using LPILE analysis type 4 – “Computation of Ultimate Bending Moment and Pile Response with User Specified EI.” The p-y curves were generated by the program assuming cyclic loading conditions were applied. The program calculated internally the flexural rigidity along the pile as a function of bending moment and axial force (assumed full 890 kN compression load) for each applied lateral load level. Ten equal 20 kN increments of load were applied to a maximum of 200 kN. The graphical output contains all ten increments; the numeric summaries are abridged.

An echo print of the input file is presented on the following page. LPILE generated summaries of the problem input and output are provided including nonlinear bending stiffness calculations. For selected lateral loads, Figures F.19 to F.22 provide graphical presentations of deflection, movement, shear, and soil reaction versus depth.

The LPILE solutions for the North abutment indicate the pile deflection under the 40 kN design load will be 3.2 mm. The corresponding maximum moment and shear stress are - 54.2 m-kN and 14,500 kN/m², respectively. The deflection, moment and shear stress under the design load are acceptable. Hence, the more rigorous LPILE analysis indicates a 40 kN design lateral load could be used whereas the Broms' method indicated only a 24.9 kN design load. Additional LPILE analyses should be performed to evaluate group response using the p-multiplier approach described in Section 9.8.4.

LPILEP4

FWA North Abut. - 355 mm-sq PSC Fixed-Head/Cyclic/Crack Modeled

2	3	0	0	0	0
100	2	0	11.5	0	
0	0.355	0.0013		0.126	27800000
11.5	0.355	0.0013		0.126	27800000
4	8	8	0	0	
4	0	1	6790	6790	
4	1	4	5430	5430	
4	4	11	16300	16300	
4	11	11.5	33900	33900	
0	16.5				
1	16.5				
1	6.7				
4	6.7				
4	7.8				
11	7.8				
11	9.8				
11.5	9.8				
0	0	29	0	0	
1	0	29	0	0	
1	0	29	0	0	
4	0	29	0	0	
4	0	30	0	0	
11	0	30	0	0	
11	0	36	0	0	
11.5	0	36	0	0	
0	0	20			
10					
2	20	0	890		
2	40	0	890		
2	60	0	890		
2	80	0	890		
2	100	0	890		
2	120	0	890		
2	140	0	890		
2	160	0	890		
2	180	0	890		
2	200	0	890		
0					
1	1	0			
100	1E-6	1			
1	1				
890					
41370	262000		413685.52	2.0685E8	
0.355	0.355	0	0	0	
0.0005		4	2	0.0762	
0.102	0.0006				
-0.102		0.0006			

North Abutment - Echo of Input File

=====

LPILE Plus for Windows, Version 4.0 (4.0.7)

Analysis of Individual Piles and Drilled Shafts
Subjected to Lateral Loading Using the p-y Method

(c) Copyright ENSOFT, Inc., 1985-2003
All Rights Reserved

=====

Program Options

Units Used in Computations - SI Units, meters, kilopascals

Basic Program Options:

Analysis Type 4:

- Computation of Nonlinear Bending Stiffness and Ultimate Bending Moment Capacity with Pile Response Using User-specified Constant EI

Computation Options:

- Only internally-generated p-y curves used in analysis
- Analysis does not use p-y multipliers (individual pile or shaft action only)
- Analysis assumes no shear resistance at pile tip
- Analysis for fixed-length pile or shaft only
- No computation of foundation stiffness matrix elements
- Output pile response for full length of pile
- Analysis assumes no soil movements acting on pile
- No additional p-y curves to be computed at user-specified depths

Solution Control Parameters:

- Number of pile increments = 100
- Maximum number of iterations allowed = 100
- Deflection tolerance for convergence = 10.000E-06 m
- Maximum allowable deflection = 1.0000E+00 m

Printing Options:

- Values of pile-head deflection, bending moment, shear force, and soil reaction are printed for full length of pile.
- Printing Increment (spacing of output points) = 1

 File Structural Properties and Geometry

Pile Length = 11.50 m
 Depth of ground surface below top of pile = .00 m
 Slope angle of ground surface = .00 deg.

Structural properties of pile defined using 2 points

Point	Depth X m	Pile Diameter m	Moment of Inertia m**4	Pile Area Sq. m	Modulus of Elasticity kN/Sq. m
1	0.0000	.35500000	.001300	.1260	27800000.000
2	11.5000	.35500000	.001300	.1260	27800000.000

Please note that because this analysis makes computations of ultimate moment capacity and pile response using nonlinear bending stiffness that the above values of moment of inertia and modulus of are not used for any computations other than total stress due to combined axial loading and bending.

 Soil and Rock Layering Information

The soil profile is modelled using 4 layers

Layer 1 is sand, p-y criteria by Reese et al., 1974

Distance from top of pile to top of layer = .000 m
 Distance from top of pile to bottom of layer = 1.000 m
 p-y subgrade modulus k for top of soil layer = 6790.000 kN/ m**3
 p-y subgrade modulus k for bottom of layer = 6790.000 kN/ m**3

Layer 2 is sand, p-y criteria by Reese et al., 1974

Distance from top of pile to top of layer = 1.000 m
 Distance from top of pile to bottom of layer = 4.000 m
 p-y subgrade modulus k for top of soil layer = 5430.000 kN/ m**3
 p-y subgrade modulus k for bottom of layer = 5430.000 kN/ m**3

Layer 3 is sand, p-y criteria by Reese et al., 1974

Distance from top of pile to top of layer = 4.000 m
 Distance from top of pile to bottom of layer = 11.000 m
 p-y subgrade modulus k for top of soil layer = 16300.000 kN/ m**3
 p-y subgrade modulus k for bottom of layer = 16300.000 kN/ m**3

Layer 4 is sand, p-y criteria by Reese et al., 1974

Distance from top of pile to top of layer = 11.000 m
 Distance from top of pile to bottom of layer = 11.500 m
 p-y subgrade modulus k for top of soil layer = 33900.000 kN/ m**3
 p-y subgrade modulus k for bottom of layer = 33900.000 kN/ m**3

(Depth of lowest layer extends .00 m below pile tip)

 Effective Unit Weight of Soil vs. Depth

Distribution of effective unit weight of soil with depth
 is defined using 8 points

Point No.	Depth X m	Eff. Unit Weight kN/ m**3
1	.00	16.50000
2	1.00	16.50000
3	1.00	6.70000
4	4.00	6.70000
5	4.00	7.80000
6	11.00	7.80000
7	11.00	9.80000
8	11.50	9.80000

 Shear Strength of Soils

Distribution of shear strength parameters with depth
 defined using 8 points

Point No.	Depth X m	Cohesion c kN/ m**2	Angle of Friction Deg.	E50 or k_rm	RQD %
1	.000	.00000	29.00	-----	-----
2	1.000	.00000	29.00	-----	-----
3	1.000	.00000	29.00	-----	-----
4	4.000	.00000	29.00	-----	-----
5	4.000	.00000	30.00	-----	-----
6	11.000	.00000	30.00	-----	-----
7	11.000	.00000	36.00	-----	-----
8	11.500	.00000	36.00	-----	-----

Notes:

- (1) Cohesion = uniaxial compressive strength for rock materials.
- (2) Values of E50 are reported for clay strata.
- (3) Default values will be generated for E50 when input values are 0.
- (4) RQD and k_rm are reported only for weak rock strata.

 Loading Type

Cyclic loading criteria was used for computation of p-y curves

Number of cycles of loading = 20.

 Pile-head Loading and Pile-head Fixity Conditions

Number of loads specified = 10

Load Case Number 1

Pile-head boundary conditions are Shear and Slope (BC Type 2)

Shear force at pile head = 20.000 kN
 Slope at pile head = .000 m/ m
 Axial load at pile head = 890.000 kN

(Zero slope for this load indicates fixed-head condition)

.
 . [Abridged]

.
 Load Case Number 10

Pile-head boundary conditions are Shear and Slope (BC Type 2)

Shear force at pile head = 200.000 kN
 Slope at pile head = .000 m/ m
 Axial load at pile head = 890.000 kN

(Zero slope for this load indicates fixed-head condition)

 Computations of Ultimate Moment Capacity and Nonlinear Bending Stiffness

Pile Description:

The pile shape is a rectangular solid pile.

Width = .355 m
 Depth = .355 m

Material Properties:

Compressive Strength of Concrete = 41370.000 kN/ m**2
 Yield Stress of Reinforcement = 262000. kN/ m**2
 Modulus of Elasticity of Reinforcement = 206850000. kN/ m**2
 Number of Reinforcing Bars = 4
 Area of Single Bar = .00050 m**2
 Number of Rows of Reinforcing Bars = 2
 Cover Thickness (edge to bar center) = .076 m

Ultimate Axial Squash Load Capacity = 4703.81 kN

Distribution and Area of Steel Reinforcement

Row Number	Area of Reinforcement m**2	Distance to Centroidal Axis m
1	.000600	.1020
2	.000600	-.1020

Axial Thrust Force = 890.00 kN

Bending Moment kN-m	Bending Stiffness kN-m2	Bending Curvature rad/m	Maximum Strain m/m	Neutral Axis Position m
1.54295127	39190.962	.00003937	.00023366	5.93486814
7.71444547	39189.382	.00019685	.00026170	1.32942587
13.885	39185.750	.00035433	.00028986	.81803677
20.053	39179.988	.00051181	.00031813	.62158314
26.218	39172.157	.00066929	.00034653	.51775257
32.378	39162.188	.00082677	.00037504	.45362225
38.534	39150.185	.00098425	.00040367	.41013020
44.683	39136.085	.00114173	.00043242	.37873943
50.825	39119.844	.00129921	.00046129	.35505146
56.988	39121.516	.00145669	.00049033	.33660160
63.049	39059.507	.00161417	.00051931	.32172146
69.110	39008.681	.00177165	.00054844	.30956600
75.155	38958.023	.00192913	.00057769	.29945812
81.088	38861.083	.00208661	.00060684	.29082363
81.088	36133.990	.00224409	.00061495	.27403133
81.088	33764.548	.00240157	.00063793	.26562977
81.469	31835.639	.00255906	.00066017	.25797573
83.923	30893.279	.00271654	.00068196	.25104214
86.229	30003.115	.00287402	.00070333	.24472065
88.411	29164.014	.00303150	.00072433	.23893543
90.481	28372.973	.00318898	.00074498	.23361065
92.458	27628.502	.00334646	.00076533	.22869755
94.358	26929.177	.00350394	.00078544	.22415821
96.109	26249.199	.00366142	.00080493	.21984097
97.855	25623.877	.00381890	.00082447	.21589207
99.561	25038.090	.00397638	.00084391	.21223026
110.590	21442.569	.00515748	.00098201	.19040569
120.077	18943.856	.00633858	.00111351	.17567181
128.620	17104.480	.00751969	.00124079	.16500599
136.481	15686.050	.00870079	.00136470	.15684818
143.755	14547.283	.00988189	.00148690	.15046711
145.817	13180.644	.01106299	.00158671	.14342518
147.540	12049.856	.01224409	.00168395	.13753162
148.999	11098.438	.01342520	.00177927	.13253185
150.255	10286.974	.01460630	.00187345	.12826336
151.236	9579.525	.01578740	.00196414	.12441196
152.156	8966.965	.01696850	.00205603	.12116726
153.062	8433.379	.01814961	.00214772	.11833424
153.569	7944.317	.01933071	.00223691	.11571789
154.075	7511.548	.02051181	.00232536	.11336697
154.597	7126.607	.02169291	.00242001	.11155773
154.870	6770.554	.02287402	.00250841	.10966183
155.085	6447.050	.02405512	.00259871	.10803135
155.264	6152.428	.02523622	.00269049	.10661213
155.477	5885.409	.02641732	.00278965	.10559917
155.534	5635.593	.02759843	.00288088	.10438580
155.547	5404.764	.02877953	.00297346	.10331867
155.550	5191.809	.02996063	.00306693	.10236530
155.550	4994.901	.03114173	.00316169	.10152569
155.550	4812.383	.03232283	.00325744	.10077816
155.550	4642.734	.03350394	.00336721	.10050190
155.550	4484.639	.03468504	.00346243	.09982479
155.550	4336.956	.03586614	.00355857	.09921810
155.550	4198.689	.03704724	.00365529	.09866558
155.550	4068.967	.03822835	.00375256	.09816181
155.550	3947.020	.03940945	.00418210	.10611919
Ultimate Moment Capacity at a Concrete Strain of 0.003 =				155.548 m- kN

 Computed Values of Load Distribution and Deflection
 for Lateral Loading for Load Case Number 1

Pile-head boundary conditions are Shear and Slope (BC Type 2)
 Specified shear force at pile head = 20.000 kN
 Specified slope at pile head = 0.000E+00 m/ m
 Specified axial load at pile head = 890.000 kN

(Zero slope for this load indicates fixed-head conditions)

Depth X m	Deflect. y m	Moment M kN- m	Shear V kN	Slope S Rad.	Total Stress kN/ m**2	Flx. Rig. EI kN- m**2	Soil Res p kN/ m
0.000	.001561	-26.8503	20.0000	1.60E-17	1.07E+04	36140.000	0.000
.115	.001556	-24.5459	19.9447	-8.18E-05	1.04E+04	36140.000	-.962181
.230	.001542	-22.2463	19.7509	-1.56E-04	1.01E+04	36140.000	-2.408
.345	.001520	-19.9712	19.4077	-2.23E-04	9790.3	36140.000	-3.560
.460	.001491	-17.7368	18.9353	-2.83E-04	9485.2	36140.000	-4.656
.575	.001455	-15.5581	18.3410	-3.36E-04	9187.8	36140.000	-5.680
.690	.001413	-13.4495	17.6338	-3.83E-04	8899.9	36140.000	-6.621
.805	.001367	-11.4241	16.8235	-4.22E-04	8623.3	36140.000	-7.470
.920	.001316	-9.4937	15.9212	-4.55E-04	8359.7	36140.000	-8.221
1.035	.001262	-7.6690	15.0394	-4.83E-04	8110.6	36140.000	-7.115
.
. [ABRIDGED]							
.
11.040	-4.48E-08	3.34E-03	-1.23E-02	-2.50E-07	7063.9	36140.000	.011567
11.155	-7.28E-08	2.03E-03	-1.05E-02	-2.41E-07	7063.8	36140.000	.019107
11.270	-1.00E-07	9.65E-04	-7.91E-03	-2.36E-07	7063.6	36140.000	.026670
11.385	-1.27E-07	2.55E-04	-4.40E-03	-2.34E-07	7063.5	36140.000	.034350
11.500	-1.54E-07	0.0	0.0	-2.34E-07	7063.5	36140.000	.042215

Please note that because this analysis makes computations of ultimate moment capacity and pile response using nonlinear bending stiffness that the above values of total stress due to combined axial stress and bending may not be representative of actual conditions.

Output Verification:

Computed forces and moments are within specified convergence limits.

Output Summary for Load Case No. 1:

Pile-head deflection = .00156072 m
 Computed slope at pile head = 1.60273E-17
 Maximum bending moment = -26.850 kN- m
 Maximum shear force = 20.000 kN
 Depth of maximum bending moment = 0.000 m
 Depth of maximum shear force = 0.000 m
 Number of iterations = 5
 Number of zero deflection points = 3

[ABRIDGED—ADDITIONAL LOAD CASES OMITTED]

 Summary of Pile-head Response

Definition of symbols for pile-head boundary conditions:

y = pile-head displacement, m
 M = pile-head moment, kN- m
 V = pile-head shear force, kN
 S = pile-head slope, radians
 R = rotational stiffness of pile-head, m- kN/rad

BC Type	Boundary Condition 1	Boundary Condition 2	Axial Load kN	Pile Head Deflection m	Maximum Moment m- kN	Maximum Shear kN
2	V= 20.000	S= 0.000	890.0000	.001561	-26.8503	20.0000
2	V= 40.000	S= 0.000	890.0000	.003153	-54.1631	40.0000
2	V= 60.000	S= 0.000	890.0000	.004853	-82.7732	60.0000
2	V= 80.000	S= 0.000	890.0000	.006807	-113.7237	80.0000
2	V= 100.000	S= 0.000	890.0000	.009130	-147.3525	100.0000
2	V= 120.000	S= 0.000	890.0000	.011611	-181.8318	120.0000
2	V= 140.000	S= 0.000	890.0000	.014199	-216.8237	140.0000
2	V= 160.000	S= 0.000	890.0000	.017001	-253.3626	160.0000
2	V= 180.000	S= 0.000	890.0000	.020117	-291.9951	180.0000
2	V= 200.000	S= 0.000	890.0000	.023611	-332.8377	200.0000

The analysis ended normally.

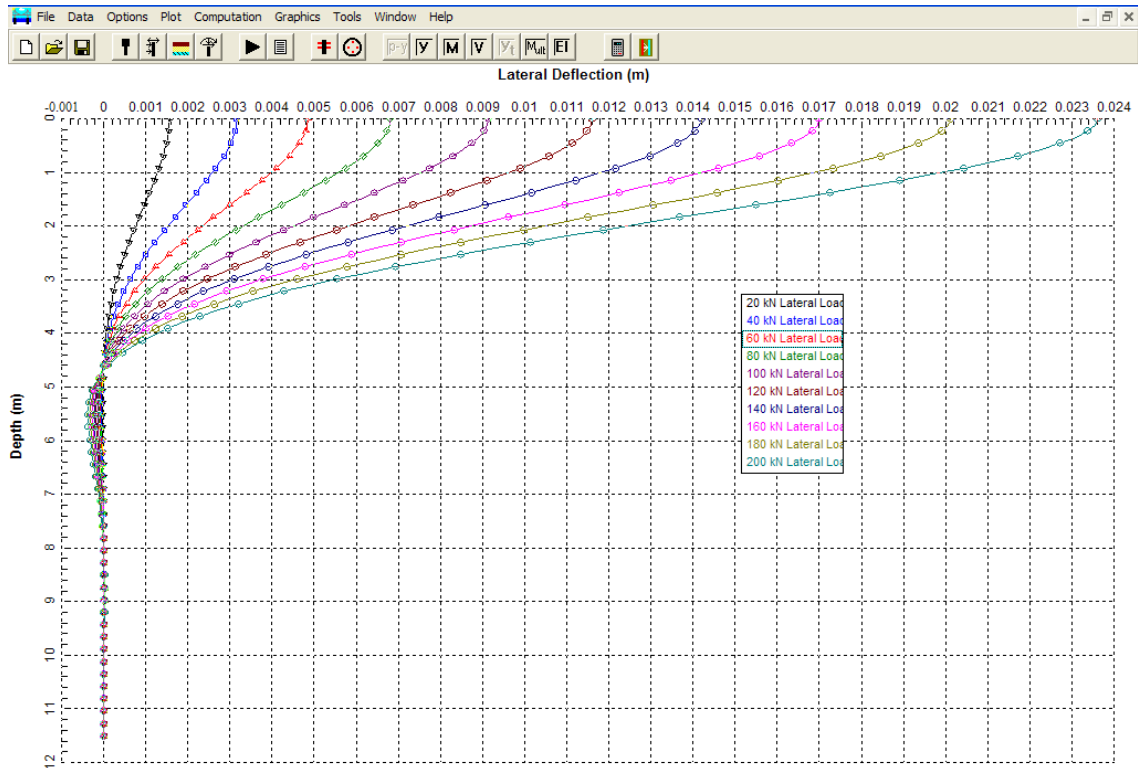


Figure F.19: North Abutment - Plot of Deflection vs. Depth as a Function of Lateral Load

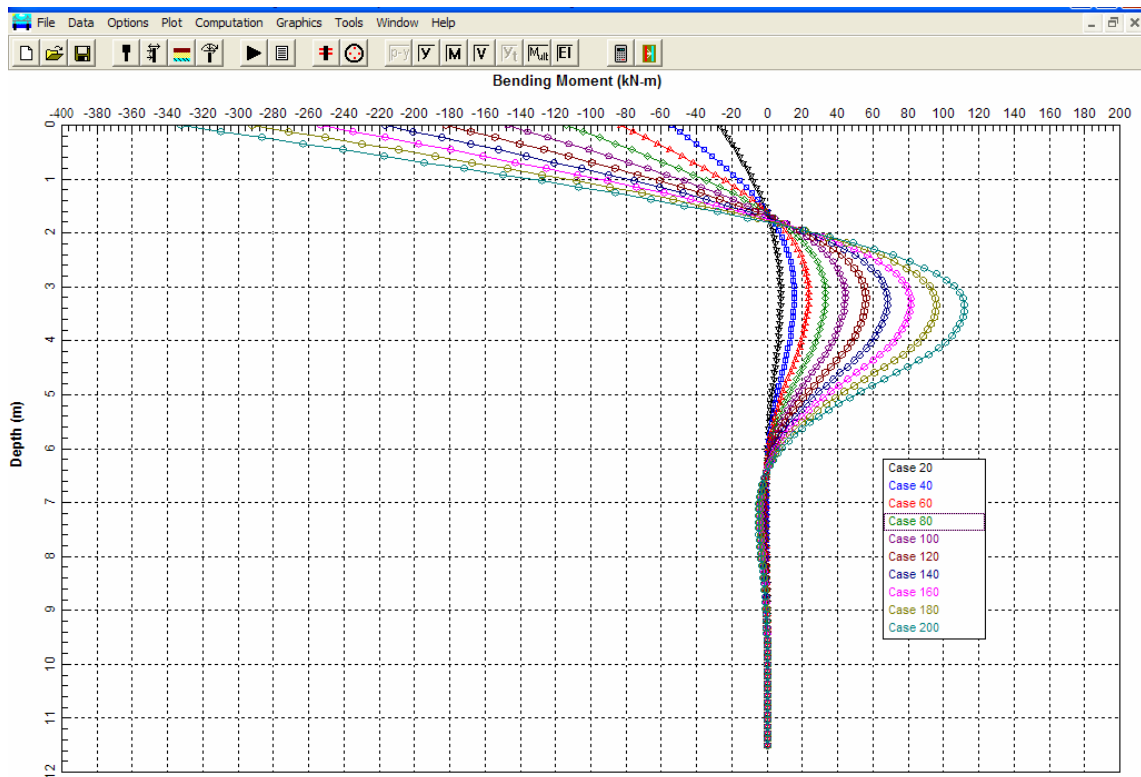


Figure F.20: North Abutment – Plot of Moment *versus* Depth as a Function of Lateral Load

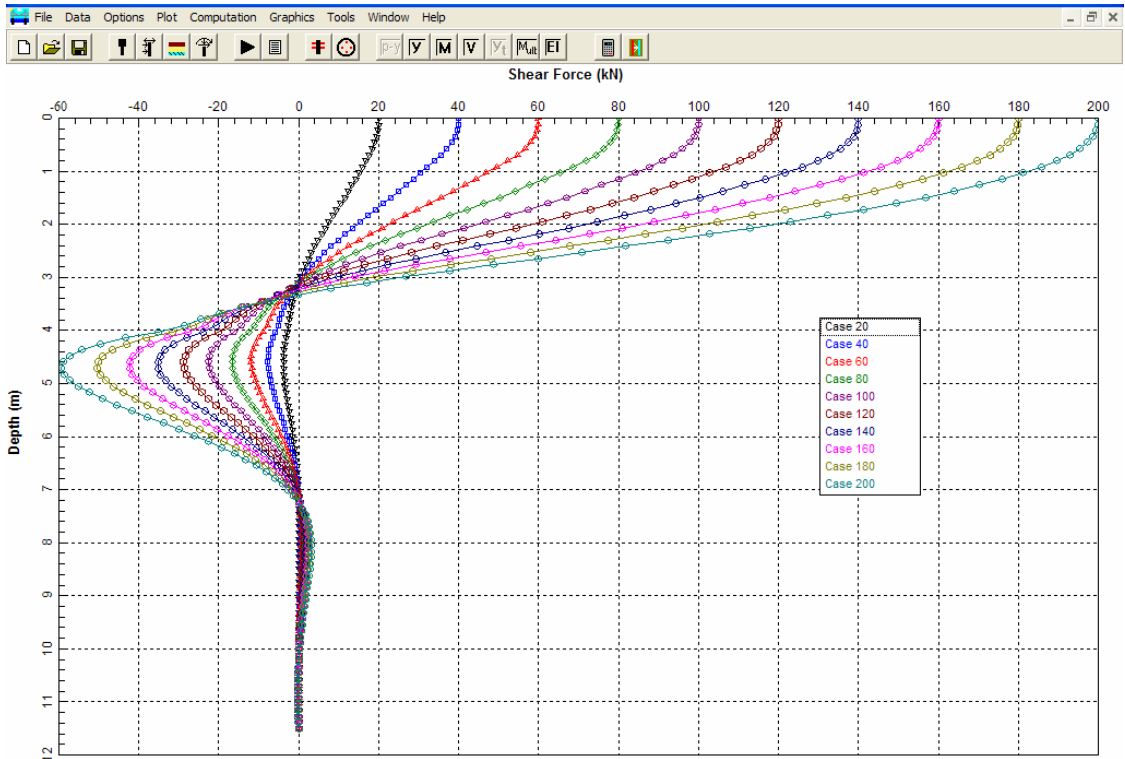


Figure F.21: North Abutment – Plot of Shear *versus* Depth as a Function of Lateral Load

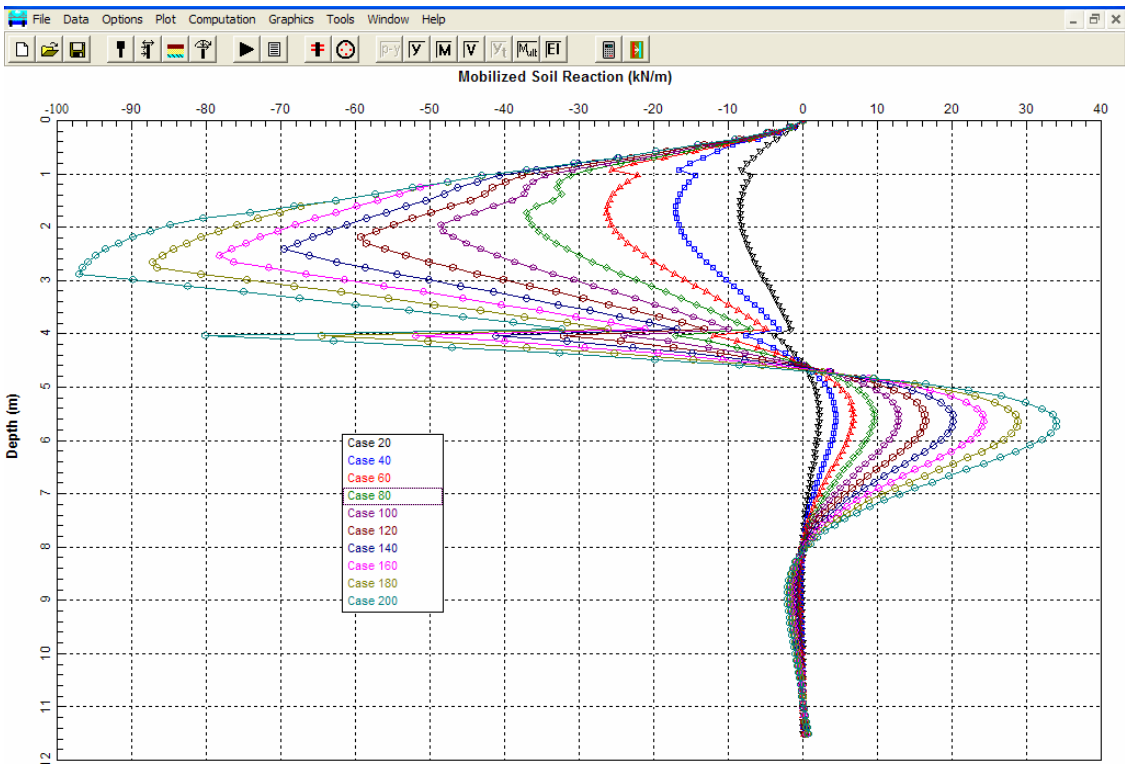


Figure F.22: North Abutment - Plot of Soil Reaction vs. Depth as a Function of Lateral Load

F.4.3 LPILE - Pier 2 H-pile, X-X Axis and Y-Y Axis

As discussed in Chapter 12, wave equation driveability analyses at the internal piers indicated a potential driveability problem for 356 mm concrete piles. Therefore, low displacement HP 360x152 H-piles were chosen for the pile foundations at the interior piers.

For the selected H-pile section at Pier 2, LPILE solutions for lateral loading in the major (X-X) and minor (Y-Y) axis directions were obtained. These analyses again assumed full fixity at the base of the pier. At Pier 2, it was assumed that near-surface scour protection prevented removal of materials below the pier base in this case. In the full design process a number of other variables such as partial rotational constraint or extreme scour depth could be evaluated. The presence of the extremely dense sand and gravel stratum in the upper 4 m of the soil profile introduced a considerably stiffer soil response in comparison with that modeled at the North Abutment. Table 9-16 only has dense sand, therefore the slope of soil modulus for this extremely dense sand and gravel was assumed to be 50,000 kN/m³. As in the previous example, the detailed results were saved only for every other lateral load increment up to the maximum lateral load evaluated of 220 kN.

LPILE analysis of lateral loading in the X-X and Y-Y axis are presented on the following pages. The analysis output includes an echo print of the input file followed by the LPILE generated summaries of the problem input and output. The output includes a summary table of deflection, moment, shear, and soil reaction versus lateral load. For selected lateral loads in the X-X axis, Figures F.23 to F.26 provide graphical presentations of deflection, moment, shear, and soil reaction versus depth. These graphical presentations for loads in the Y-Y axis are presented in Figure F.27 to F.30.

The LPILE analyses indicate the performance of the H-pile is acceptable when laterally loaded in either axis. The maximum deflection under the 40 kN design load is less than 2 mm.

Additional LPILE analyses should be performed to evaluate group response using the p-multiplier approach described in Section 9.8.4.


```

LPILEP4
FHWA Pier 2, HP360x152 X-X Axis/Fixed-Head Cyclic
2 1 0 0 0 0
100 2 0 14 0
0 0.3565 0.0004 0.0194 2.1E8
14 0.3565 0.0004 0.0194 2.1E8
2 4 4 0 0
4 0 4 50000 50000
4 4 14 33900 33900
0 11.4
4 11.4
4 9.8
14 9.8
0 0 36 0 0
4 0 36 0 0
4 0 35 0 0
14 0 35 0 0
0 0 20
10
2 40 0 890
2 60 0 890
2 80 0 890
2 100 0 890
2 120 0 890
2 140 0 890
2 160 0 890
2 180 0 890
2 200 0 890
2 220 0 890
0
1 1 0
100 1E-5 2

```

Pier 2 X-X Axis - Echo of Input File

=====

LPILE Plus for Windows, Version 4.0 (4.0.7)

Analysis of Individual Piles and Drilled Shafts
 Subjected to Lateral Loading Using the p-y Method

(c) Copyright ENSOFT, Inc., 1985-2003
 All Rights Reserved

Program Options

Units Used in Computations - SI Units, meters, kilopascals

Basic Program Options:

Analysis Type 1:

- Computation of Lateral Pile Response Using User-specified Constant EI

Computation Options:

- Only internally-generated p-y curves used in analysis
- Analysis does not use p-y multipliers (individual pile or shaft action only)
- Analysis assumes no shear resistance at pile tip
- Analysis for fixed-length pile or shaft only
- No computation of foundation stiffness matrix elements
- Output pile response for full length of pile
- Analysis assumes no soil movements acting on pile
- No additional p-y curves to be computed at user-specified depths

Solution Control Parameters:

- Number of pile increments = 100
- Maximum number of iterations allowed = 100
- Deflection tolerance for convergence = 1.0000E-05 m
- Maximum allowable deflection = 2.0000E+00 m

Printing Options:

- Values of pile-head deflection, bending moment, shear force, and soil reaction are printed for full length of pile.
- Printing Increment (spacing of output points) = 5

Pile Structural Properties and Geometry

Pile Length = 14.00 m
 Depth of ground surface below top of pile = .00 m
 Slope angle of ground surface = .00 deg.

Structural properties of pile defined using 2 points

Point	Depth X m	Pile Diameter m	Moment of Inertia m**4	Pile Area Sq. m	Modulus of Elasticity kN/Sq. m
1	0.0000	.35650000	4.00000E-04	.019400	210000000.000
2	14.0000	.35650000	4.00000E-04	.019400	210000000.000

Soil and Rock Layering Information

The soil profile is modelled using 2 layers

Layer 1 is sand, p-y criteria by Reese et al., 1974

Distance from top of pile to top of layer = .000 m
Distance from top of pile to bottom of layer = 4.000 m
p-y subgrade modulus k for top of soil layer = 50000.000 kN/ m**3
p-y subgrade modulus k for bottom of layer = 50000.000 kN/ m**3

Layer 2 is sand, p-y criteria by Reese et al., 1974

Distance from top of pile to top of layer = 4.000 m
Distance from top of pile to bottom of layer = 14.000 m
p-y subgrade modulus k for top of soil layer = 33900.000 kN/ m**3
p-y subgrade modulus k for bottom of layer = 33900.000 kN/ m**3

(Depth of lowest layer extends .00 m below pile tip)

Effective Unit Weight of Soil vs. Depth

Distribution of effective unit weight of soil with depth
is defined using 4 points

Point No.	Depth X m	Eff. Unit Weight kN/ m**3
1	.00	11.40000
2	4.00	11.40000
3	4.00	9.80000
4	14.00	9.80000

Shear Strength of Soils

Distribution of shear strength parameters with depth
defined using 4 points

Point No.	Depth X m	Cohesion c kN/ m**2	Angle of Friction Deg.	E50 or k_rm	RQD %
1	.000	.00000	36.00	-----	-----
2	4.000	.00000	36.00	-----	-----
3	4.000	.00000	35.00	-----	-----
4	14.000	.00000	35.00	-----	-----

Notes:

- (1) Cohesion = uniaxial compressive strength for rock materials.
- (2) Values of E50 are reported for clay strata.
- (3) Default values will be generated for E50 when input values are 0.
- (4) RQD and k_rm are reported only for weak rock strata.

Loading Type

Cyclic loading criteria was used for computation of p-y curves

Number of cycles of loading = 20.

Pile-head Loading and Pile-head Fixity Conditions

Number of loads specified = 10

Load Case Number 1

Pile-head boundary conditions are Shear and Slope (BC Type 2)
Shear force at pile head = 40.000 kN
Slope at pile head = .000 m/ m
Axial load at pile head = 890.000 kN

(Zero slope for this load indicates fixed-head condition)

.

.

[ABRIDGED]

.

.

Load Case Number 10

Pile-head boundary conditions are Shear and Slope (BC Type 2)
Shear force at pile head = 220.000 kN
Slope at pile head = .000 m/ m
Axial load at pile head = 890.000 kN

(Zero slope for this load indicates fixed-head condition)

 Computed Values of Load Distribution and Deflection
 for Lateral Loading for Load Case Number 1

Pile-head boundary conditions are Shear and Slope (BC Type 2)

Specified shear force at pile head = 40.000 kN
 Specified slope at pile head = 0.000E+00 m/ m
 Specified axial load at pile head = 890.000 kN

(Zero slope for this load indicates fixed-head conditions)

Depth X m	Deflect. Y m	Moment M kN- m	Shear V kN	Slope S Rad.	Total Stress kN/ m**2	Soil Res p kN/ m
0.000	8.14E-04	-47.1053	40.0000	3.872E-18	66867.5983	0.0000
.700	7.02E-04	-19.7659	35.8968	-2.770E-04	54684.4589	-15.0633
1.400	4.72E-04	.9085	22.5879	-3.490E-04	46281.1434	-15.2146
2.100	2.44E-04	12.5820	9.0945	-2.864E-04	51483.1390	-23.1076
2.800	8.34E-05	14.0092	-3.8300	-1.695E-04	52119.1374	-11.6742
3.500	2.11E-06	9.5302	-7.7446	-6.956E-05	50123.1883	-.3700
4.200	-2.37E-05	4.5520	-6.0892	-1.173E-05	47904.7646	3.4722
4.900	-2.22E-05	1.2138	-3.4091	1.103E-05	46417.1981	3.7781
5.600	-1.28E-05	-.3423	-1.1795	1.362E-05	46028.8109	2.4745
6.300	-4.75E-06	-.6881	.029271	8.762E-06	46182.9277	1.0342
7.000	-5.14E-07	-.5017	.3994	3.635E-06	46099.8680	.1241
7.700	8.31E-07	-.2293	.3395	6.193E-07	45978.4487	-.2201
8.400	7.90E-07	-.050297	.1710	-4.656E-07	45898.7024	-.2283
9.100	4.05E-07	.021177	.045222	-5.281E-07	45885.7257	-.1267
9.800	1.15E-07	.029767	-.010279	-2.901E-07	45889.5534	-.038599
10.500	-1.14E-08	.017431	-.019934	-8.921E-08	45884.0563	.004092
11.200	-3.52E-08	.005695	-.012507	3.540E-09	45878.8264	.013493
11.900	-2.27E-08	2.281E-05	-.004217	2.346E-08	45876.2988	.009270
12.600	-8.09E-09	-.001152	1.660E-04	1.672E-08	45876.8019	.003489
13.300	6.64E-10	-5.244E-04	.001173	9.275E-09	45876.5223	-3.022E-04
14.000	6.30E-09	0.0000	0.0000	7.638E-09	45876.2887	-.003015

Output Verification:

Computed forces and moments are within specified convergence limits.

Output Summary for Load Case No. 1:

Pile-head deflection = .00081352 m
 Computed slope at pile head = 3.87215E-18
 Maximum bending moment = -47.105 kN- m
 Maximum shear force = 40.000 kN
 Depth of maximum bending moment = 0.000 m
 Depth of maximum shear force = 0.000 m
 Number of iterations = 6
 Number of zero deflection points = 4

.

[ABRIDGED]

.

.

 Summary of Pile-head Response

Definition of symbols for pile-head boundary conditions:

y = pile-head displacement, m
 M = pile-head moment, kN- m
 V = pile-head shear force, kN
 S = pile-head slope, radians
 R = rotational stiffness of pile-head, m- kN/rad

BC Type	Boundary Condition 1	Boundary Condition 2	Axial Load kN	Pile Head Deflection m	Maximum Moment m- kN	Maximum Shear kN
2	V= 40.000	S= 0.000	890.0000	8.135E-04	-47.1053	40.0000
2	V= 60.000	S= 0.000	890.0000	.001507	-77.1836	60.0000
2	V= 80.000	S= 0.000	890.0000	.002311	-108.9651	80.0000
2	V= 100.000	S= 0.000	890.0000	.003214	-142.1167	100.0000
2	V= 120.000	S= 0.000	890.0000	.004192	-176.2173	120.0000
2	V= 140.000	S= 0.000	890.0000	.005244	-211.2150	140.0000
2	V= 160.000	S= 0.000	890.0000	.006356	-246.8856	160.0000
2	V= 180.000	S= 0.000	890.0000	.007523	-283.1503	180.0000
2	V= 200.000	S= 0.000	890.0000	.008739	-319.8726	200.0000
2	V= 220.000	S= 0.000	890.0000	.009996	-356.9209	220.0000

The analysis ended normally.

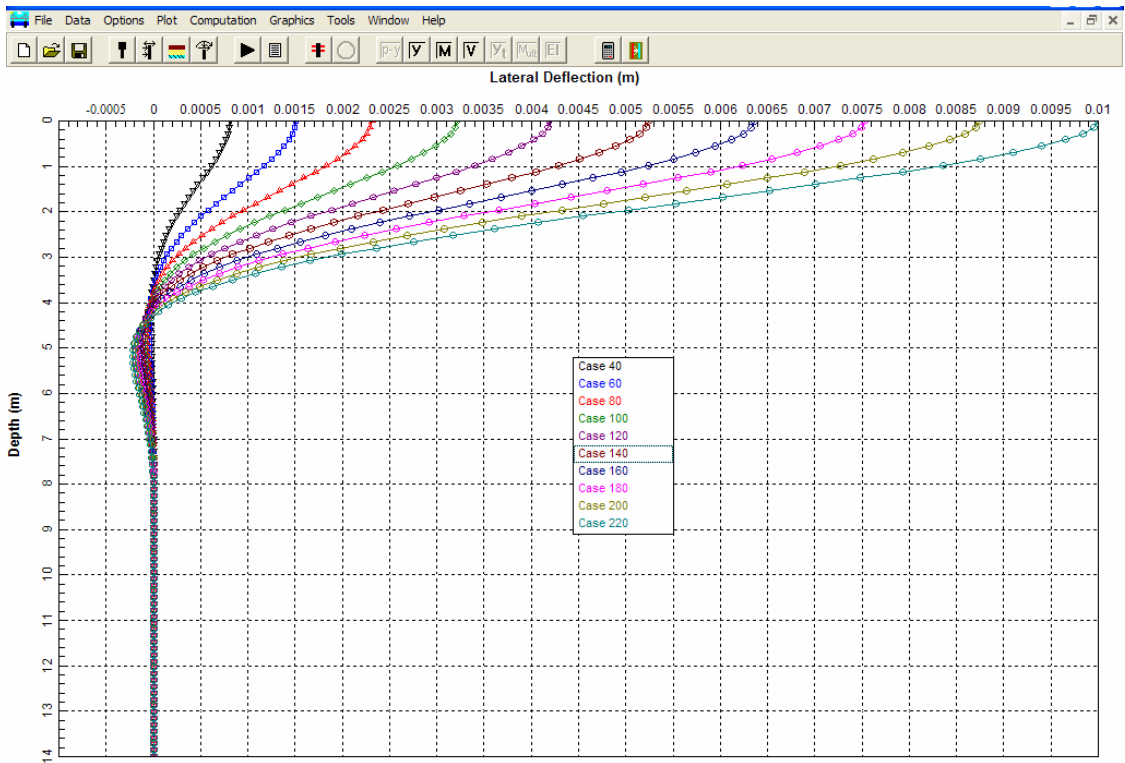


Figure F.23: Pier 2 – Plot of Deflection *versus* Depth as a Function on Lateral Load on X-X Axis

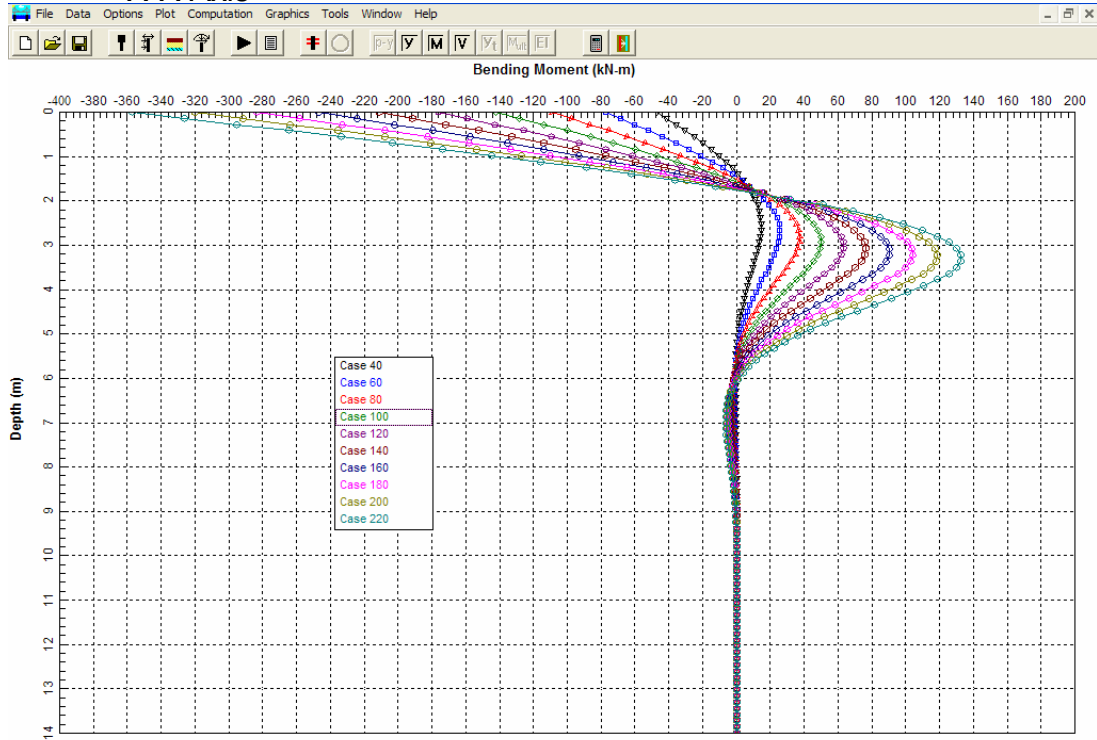


Figure F.24: Pier 2 – Plot of Moment *versus* Depth as a Function of Lateral Load on X-X Axis

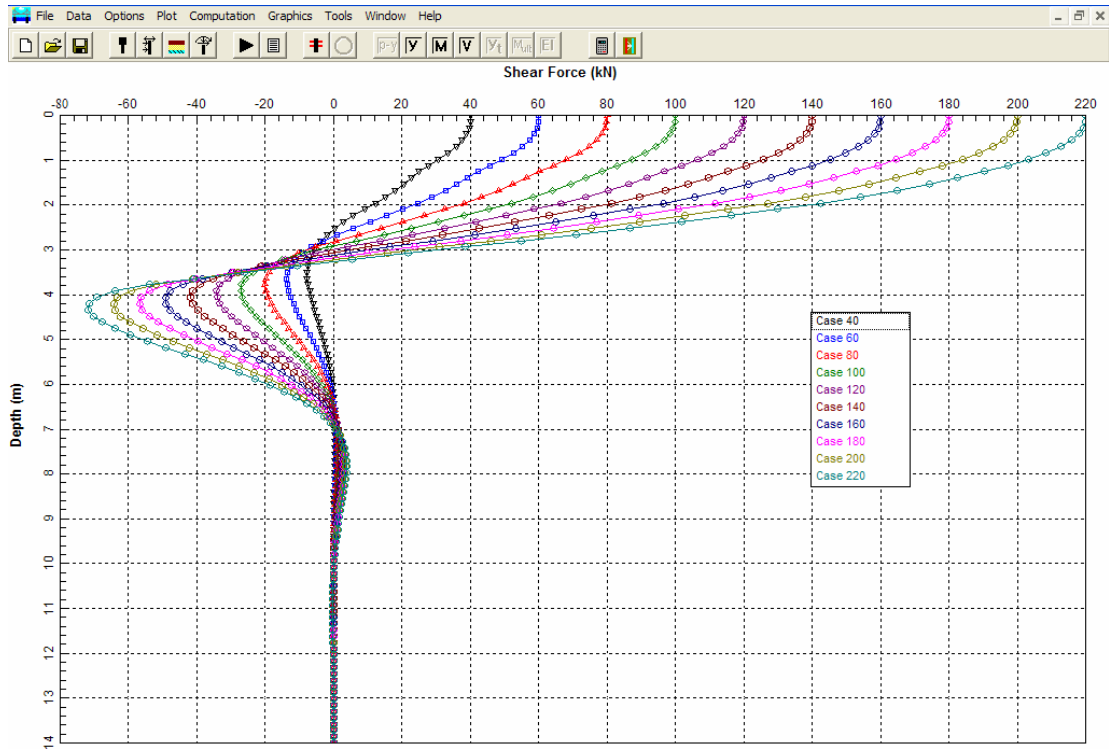


Figure F.25: Pier 2 – Plot of Shear *versus* Depth as a Function of Lateral Load on X-X Axis

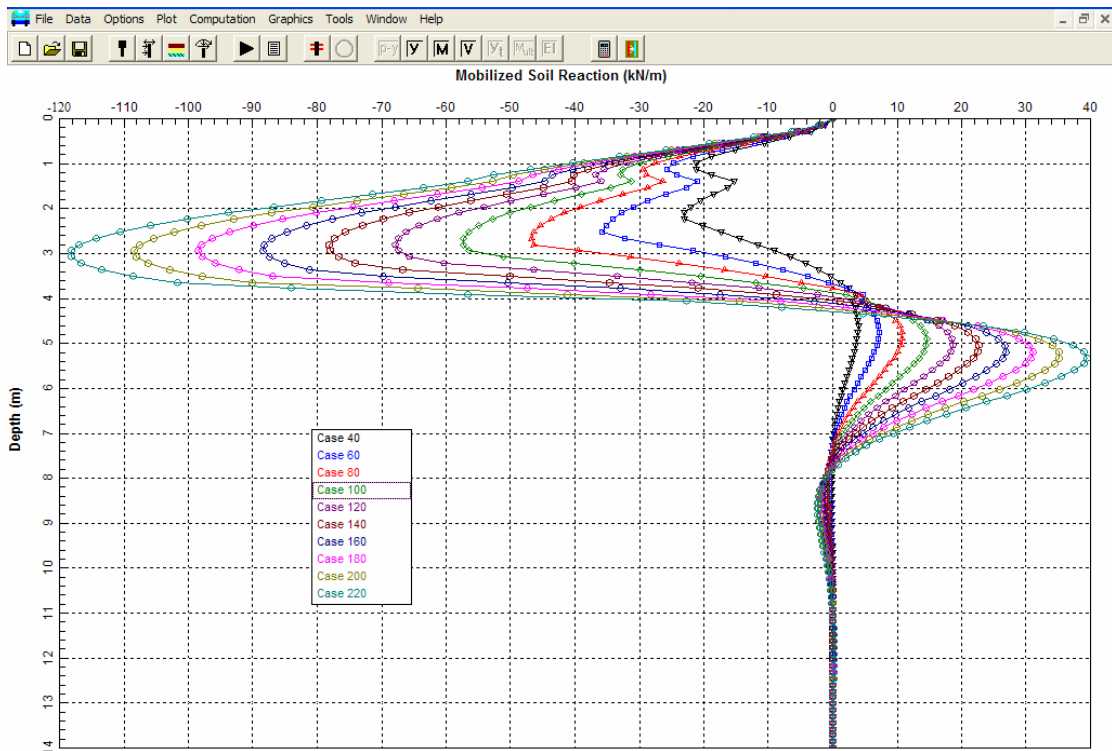


Figure F.26: Pier 2 – Plot of Soil Reaction *versus* Depth as a Function of Lateral Load on X-X Axis


```

LPILEP4
FHWA Pier 2, HP360x152 Y-Y Axis/Fixed-Head Cyclic
2 1 0 0 0 0
100 2 0 14 0
0 0.376 0.0002 0.0194 2.1E8
14 0.376 0.0002 0.0194 2.1E8
2 4 4 0 0
4 0 4 50000 50000
4 4 14 33900 33900
0 11.4
4 11.4
4 9.8
14 9.8
0 0 36 0 0
4 0 36 0 0
4 0 35 0 0
14 0 35 0 0
0 0 20
10
2 40 0 890
2 60 0 890
2 80 0 890
2 100 0 890
2 120 0 890
2 140 0 890
2 160 0 890
2 180 0 890
2 200 0 890
2 220 0 890
0
1 1 0
100 1E-5 2

```

Pier 2 Y-Y Axis - Echo of Input File

=====

LPILE Plus for Windows, Version 4.0 (4.0.7)

Analysis of Individual Piles and Drilled Shafts
 Subjected to Lateral Loading Using the p-y Method

(c) Copyright ENSOFT, Inc., 1985-2003
 All Rights Reserved

Program Options

Units Used in Computations - SI Units, meters, kilopascals

Basic Program Options:

Analysis Type 1:

- Computation of Lateral Pile Response Using User-specified Constant EI

Computation Options:

- Only internally-generated p-y curves used in analysis
- Analysis does not use p-y multipliers (individual pile or shaft action only)
- Analysis assumes no shear resistance at pile tip
- Analysis for fixed-length pile or shaft only
- No computation of foundation stiffness matrix elements
- Output pile response for full length of pile
- Analysis assumes no soil movements acting on pile
- No additional p-y curves to be computed at user-specified depths

Solution Control Parameters:

- Number of pile increments = 100
- Maximum number of iterations allowed = 100
- Deflection tolerance for convergence = 1.0000E-05 m
- Maximum allowable deflection = 2.0000E+00 m

Printing Options:

- Values of pile-head deflection, bending moment, shear force, and soil reaction are printed for full length of pile.
- Printing Increment (spacing of output points) = 5

Pile Structural Properties and Geometry

Pile Length = 14.00 m
 Depth of ground surface below top of pile = .00 m
 Slope angle of ground surface = .00 deg.

Structural properties of pile defined using 2 points

Point	Depth X m	Pile Diameter m	Moment of Inertia m**4	Pile Area Sq. m	Modulus of Elasticity kN/Sq. m
1	0.0000	.37600000	2.00000E-04	.019400	210000000.000
2	14.0000	.37600000	2.00000E-04	.019400	210000000.000

Soil and Rock Layering Information

The soil profile is modelled using 2 layers

Layer 1 is sand, p-y criteria by Reese et al., 1974
Distance from top of pile to top of layer = .000 m
Distance from top of pile to bottom of layer = 4.000 m
p-y subgrade modulus k for top of soil layer = 50000.000 kN/ m**3
p-y subgrade modulus k for bottom of layer = 50000.000 kN/ m**3

Layer 2 is sand, p-y criteria by Reese et al., 1974
Distance from top of pile to top of layer = 4.000 m
Distance from top of pile to bottom of layer = 14.000 m
p-y subgrade modulus k for top of soil layer = 33900.000 kN/ m**3
p-y subgrade modulus k for bottom of layer = 33900.000 kN/ m**3

(Depth of lowest layer extends .00 m below pile tip)

Effective Unit Weight of Soil vs. Depth

Distribution of effective unit weight of soil with depth
is defined using 4 points

Point No.	Depth X m	Eff. Unit Weight kN/ m**3
1	.00	11.40000
2	4.00	11.40000
3	4.00	9.80000
4	14.00	9.80000

Shear Strength of Soils

Distribution of shear strength parameters with depth
defined using 4 points

Point No.	Depth X m	Cohesion c kN/ m**2	Angle of Friction Deg.	E50 or k_rm	RQD %
1	.000	.00000	36.00	-----	-----
2	4.000	.00000	36.00	-----	-----
3	4.000	.00000	35.00	-----	-----
4	14.000	.00000	35.00	-----	-----

Notes:

- (1) Cohesion = uniaxial compressive strength for rock materials.
- (2) Values of E50 are reported for clay strata.
- (3) Default values will be generated for E50 when input values are 0.
- (4) RQD and k_rm are reported only for weak rock strata.

Loading Type

Cyclic loading criteria was used for computation of p-y curves

Number of cycles of loading = 20.

 Pile-head Loading and Pile-head Fixity Conditions

Number of loads specified = 10

Load Case Number 1

Pile-head boundary conditions are Shear and Slope (BC Type 2)

Shear force at pile head = 40.000 kN
 Slope at pile head = .000 m/ m
 Axial load at pile head = 890.000 kN

(Zero slope for this load indicates fixed-head condition)

. [ABRIDGED]

Load Case Number 10

Pile-head boundary conditions are Shear and Slope (BC Type 2)

Shear force at pile head = 220.000 kN
 Slope at pile head = .000 m/ m
 Axial load at pile head = 890.000 kN

(Zero slope for this load indicates fixed-head condition)

 Computed Values of Load Distribution and Deflection
 for Lateral Loading for Load Case Number 1

Pile-head boundary conditions are Shear and Slope (BC Type 2)

Specified shear force at pile head = 40.000 kN
 Specified slope at pile head = 0.000E+00 m/ m
 Specified axial load at pile head = 890.000 kN

(Zero slope for this load indicates fixed-head conditions)

Depth X m	Deflect. y m	Moment M kN- m	Shear V kN	Slope S Rad.	Total Stress kN/ m**2	Soil Res p kN/ m
0.000	.001216	-43.1920	40.0000	-6.970E-18	86476.7805	0.0000
.700	.001016	-15.8536	35.4883	-4.886E-04	60778.6640	-16.3858
1.400	6.24E-04	3.9838	19.6133	-5.719E-04	49621.0522	-20.6143
2.100	2.69E-04	13.1367	4.9083	-4.155E-04	58224.7945	-23.8423
2.800	5.65E-05	11.7234	-7.2107	-1.967E-04	56896.3012	-7.9139
3.500	-2.32E-05	5.9570	-7.9588	-4.867E-05	51475.8564	4.0609
4.200	-3.18E-05	1.6998	-4.2171	1.145E-05	47474.0619	4.6506
4.900	-1.83E-05	-.2112	-1.4064	2.121E-05	46074.8505	3.1201
5.600	-5.95E-06	-.6057	.061142	1.303E-05	46445.6693	1.1540
6.300	-8.76E-08	-.3937	.4168	4.381E-06	46246.3472	.019053
7.000	1.21E-06	-.1352	.2868	1.014E-07	46003.3342	-.2915
7.700	7.99E-07	-.002966	.1004	-8.736E-07	45879.0767	-.2119
8.400	2.60E-07	.027293	.002072	-5.794E-07	45901.9443	-.075033
9.100	3.31E-09	.017820	-.020495	-1.832E-07	45893.0391	-.001035
9.800	-4.67E-08	.005368	-.013161	2.693E-09	45881.3345	.015703
10.500	-2.72E-08	-3.015E-04	-.003765	3.604E-08	45876.5720	.009803
11.200	-6.80E-09	-.001184	3.805E-04	1.983E-08	45877.4020	.002608
11.900	1.08E-09	-6.030E-04	9.201E-04	4.479E-09	45876.8555	-4.405E-04
12.600	1.76E-09	-1.242E-04	4.126E-04	-1.087E-09	45876.4054	-7.605E-04
13.300	6.60E-10	1.115E-05	3.019E-05	-1.669E-09	45876.2991	-3.003E-04
14.000	-4.51E-10	0.0000	0.0000	-1.548E-09	45876.2887	2.157E-04

Output Verification:

Computed forces and moments are within specified convergence limits.

Output Summary for Load Case No. 1:

File-head deflection = .00121631 m
 Computed slope at pile head = -6.96987E-18
 Maximum bending moment = -43.192 kN- m
 Maximum shear force = 40.000 kN
 Depth of maximum bending moment = 0.000 m
 Depth of maximum shear force = 0.000 m
 Number of iterations = 7
 Number of zero deflection points = 5

.
 .
 .[ABRIDGED]
 .
 .

 Summary of Pile-head Response

Definition of symbols for pile-head boundary conditions:

y = pile-head displacement, m
 M = pile-head moment, kN- m
 V = pile-head shear force, kN
 S = pile-head slope, radians
 R = rotational stiffness of pile-head, m- kN/rad

BC Type	Boundary Condition 1	Boundary Condition 2	Axial Load kN	Pile Head Deflection m	Maximum Moment m- kN	Maximum Shear kN
2	V= 40.000	S= 0.000	890.0000	.001216	-43.1920	40.0000
2	V= 60.000	S= 0.000	890.0000	.002322	-71.2590	60.0000
2	V= 80.000	S= 0.000	890.0000	.003623	-101.0843	80.0000
2	V= 100.000	S= 0.000	890.0000	.005082	-132.1560	100.0000
2	V= 120.000	S= 0.000	890.0000	.006679	-164.2676	120.0000
2	V= 140.000	S= 0.000	890.0000	.008387	-197.1322	140.0000
2	V= 160.000	S= 0.000	890.0000	.010186	-230.5318	160.0000
2	V= 180.000	S= 0.000	890.0000	.012058	-264.2880	180.0000
2	V= 200.000	S= 0.000	890.0000	.013984	-298.2736	200.0000
2	V= 220.000	S= 0.000	890.0000	.015974	-332.7162	220.0000

The analysis ended normally.

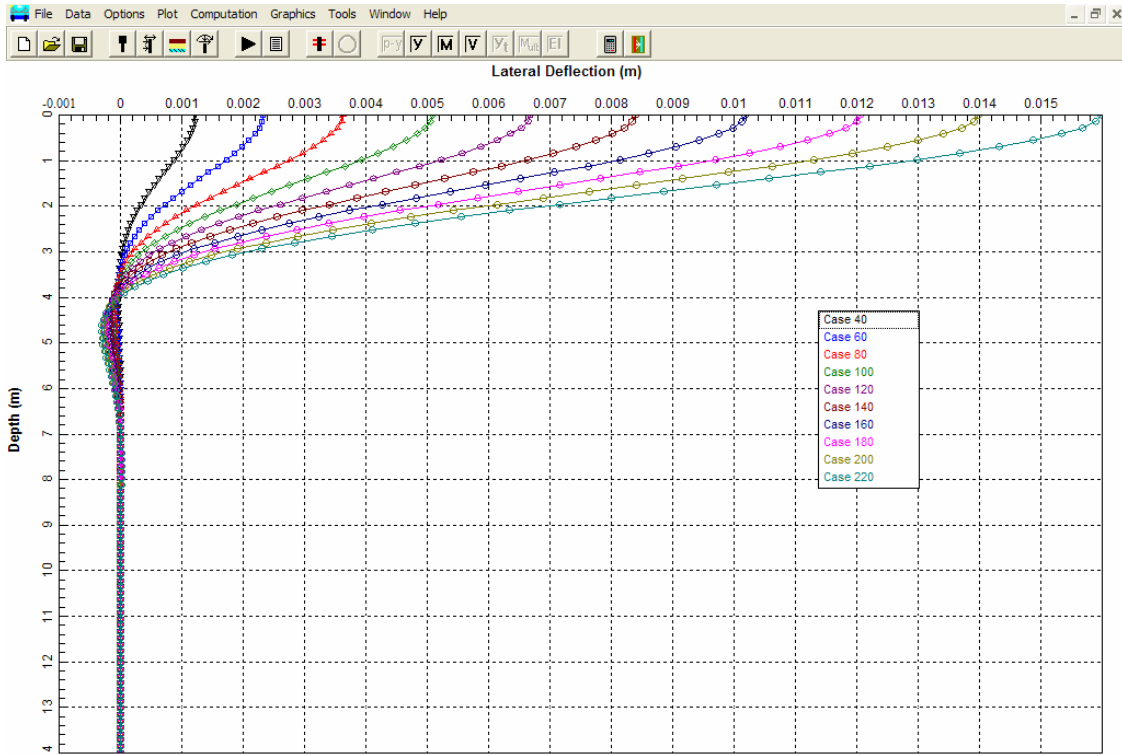


Figure F.27: Pier 2 – Plot of Deflection *versus* Depth as a Function of Lateral Load on Y-Y Axis

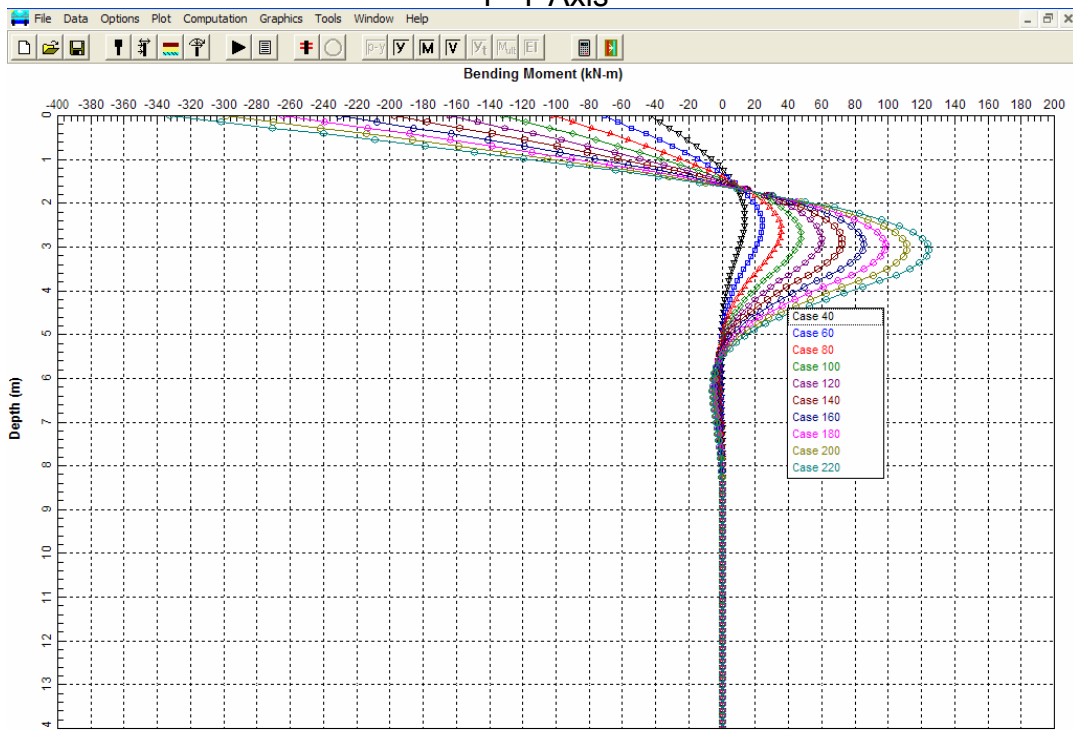


Figure F.28: Pier 2 – Plot of Moment *versus* Depth as a Function of Lateral Load on Y-Y Axis

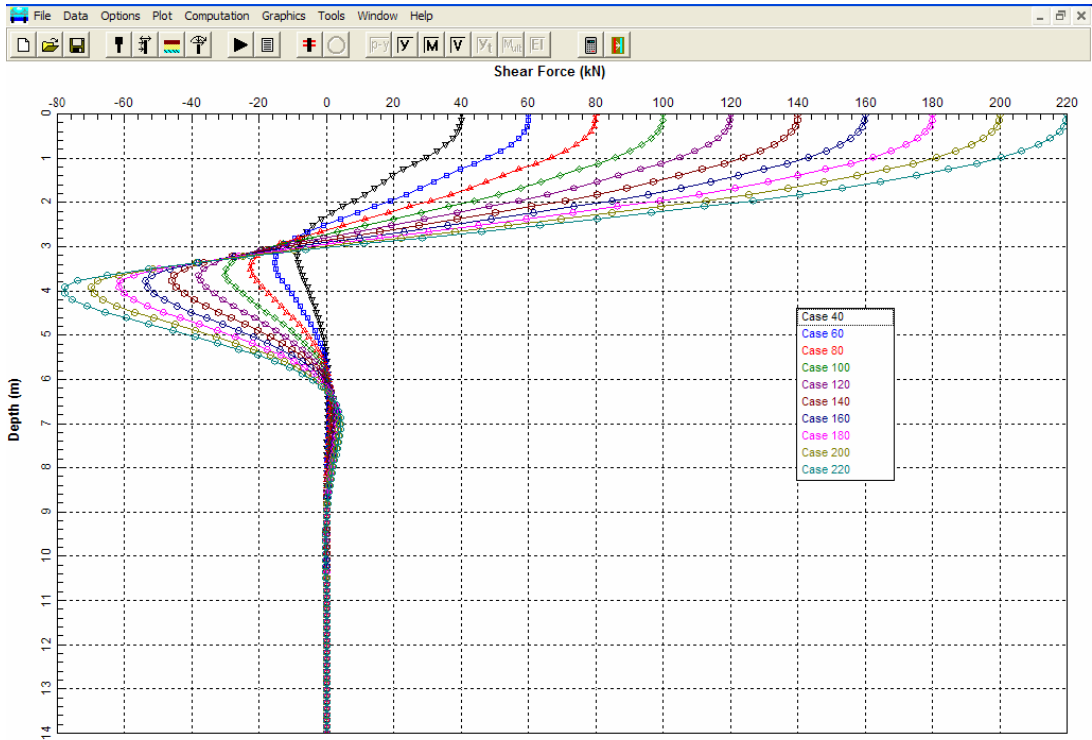


Figure F.29: Pier 2 – Plot of Shear *versus* Depth as a Function of Lateral Load on Y-Y Axis

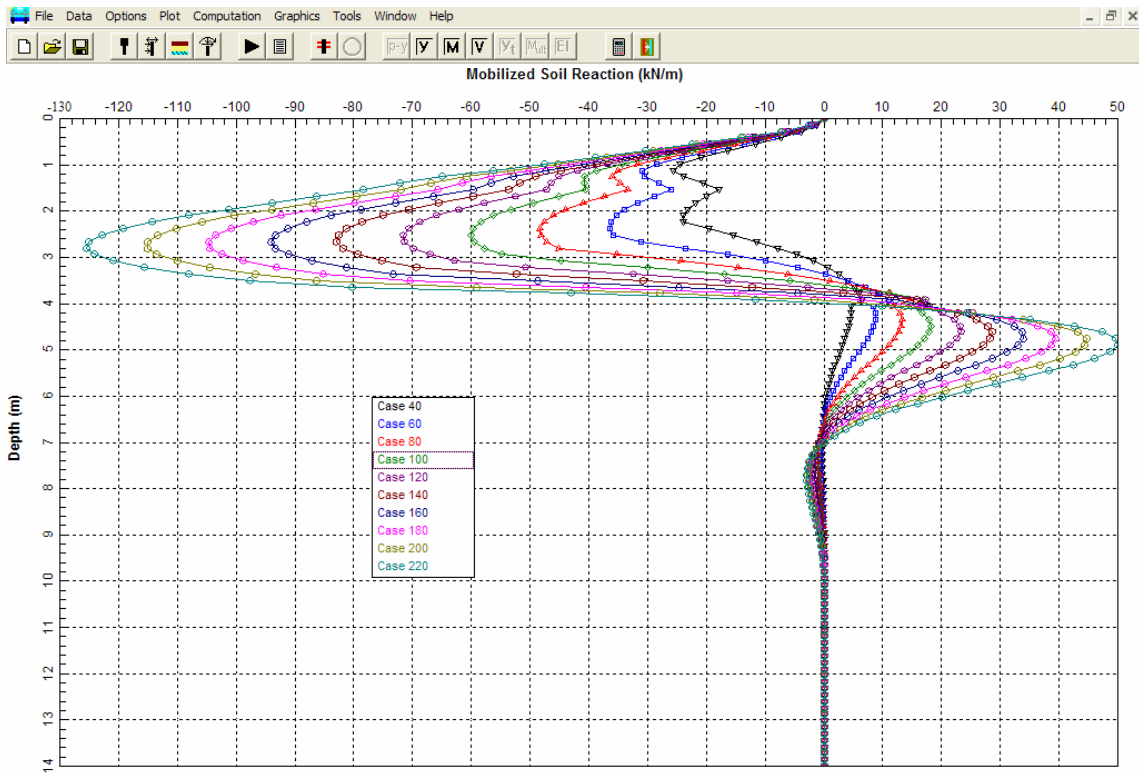


Figure F.30: Pier 2 – Plot of Soil Reaction *versus* Depth as a Function of Lateral Load on Y-Y Axis

F.4.4 LPILE - Pier 3 H-pile, X-X Axis and Y-Y Axis

As discussed in Chapter 12, wave equation driveability analyses at the internal piers indicated a potential driveability problem for 356 mm concrete piles. Therefore, low displacement HP 360x152 H-piles were chosen for the pile foundations at the interior piers.

LPILE solutions for lateral loading of the selected H-pile section at Pier 3 in both the major (X-X) and minor (Y-Y) axes directions were also obtained. The same assumptions used for Pier 2 also apply to Pier 3. The four meter extremely dense sand and gravel layer at Pier 2 decreases to one meter at Pier 3 location. The same assumed slope soil modulus (50,000 kN/m³) was used for the extremely dense sand and gravel layer. Soil parameters for the cohesive soil layers were obtained from Tables 9-15 and 9-16.

LPILE analysis of lateral loading in the X-X and Y-Y axes are presented on the following pages. The analysis output includes an echo print of the input file followed by the LPILE generated summaries of the problem input and output. The output includes a summary table of deflection, moment, shear, and soil reaction versus lateral load. For selected lateral loads in the X-X axis, Figures F.31 to F.34 provide graphical presentations of deflection, moment, shear, and soil reaction versus depth. These graphical presentations for loads in the Y-Y axis are presented in Figure F.35 to F.38.

The LPILE analyses indicate the performance of the H-pile subjected to lateral loading is acceptable in either axis. The maximum deflection under the 40 kN design load is less than 1 mm.

Additional LPILE analyses should be performed to evaluate group response using the p-multiplier approach described in Section 9.8.4.


```

LPILEP4
FHWA Pier 3, HP360x152 X-X Axis/Fixed-Head Cyclic
2 1 0 0 0 0
100 2 0 13 0
0 0.3565 0.0004 0.0194 2.1E8
14 0.3565 0.0004 0.0194 2.1E8
3 6 6 0 0
4 0 1 50000 50000
3 1 4 54300 54300
3 4 13 108500 108500
0 10.6
1 10.6
1 9.8
4 9.8
4 10.4
13 10.4
0 0 36 0 0
1 0 36 0 0
1 106 0 0.005 0
4 106 0 0.005 0
4 155 0 0.005 0
13 155 0 0.005 0
0 0 20
10
2 40 0 890
2 60 0 890
2 80 0 890
2 100 0 890
2 120 0 890
2 140 0 890
2 160 0 890
2 180 0 890
2 200 0 890
2 220 0 890
0
1 1 0
100 1E-5 2

```

Pier 3 X-X Axis - Echo of Input File

=====

LPILE Plus for Windows, Version 4.0 (4.0.7)

Analysis of Individual Piles and Drilled Shafts
 Subjected to Lateral Loading Using the p-y Method

(c) Copyright ENSOFT, Inc., 1985-2003
 All Rights Reserved

Program Options

Units Used in Computations - SI Units, meters, kilopascals

Basic Program Options:

Analysis Type 1:

- Computation of Lateral Pile Response Using User-specified Constant EI

Computation Options:

- Only internally-generated p-y curves used in analysis
- Analysis does not use p-y multipliers (individual pile or shaft action only)
- Analysis assumes no shear resistance at pile tip
- Analysis for fixed-length pile or shaft only
- No computation of foundation stiffness matrix elements
- Output pile response for full length of pile
- Analysis assumes no soil movements acting on pile
- No additional p-y curves to be computed at user-specified depths

Solution Control Parameters:

- Number of pile increments = 100
- Maximum number of iterations allowed = 100
- Deflection tolerance for convergence = 1.0000E-05 m
- Maximum allowable deflection = 2.0000E+00 m

Printing Options:

- Values of pile-head deflection, bending moment, shear force, and soil reaction are printed for full length of pile.
- Printing Increment (spacing of output points) = 5

Pile Structural Properties and Geometry

Pile Length = 13.00 m
 Depth of ground surface below top of pile = .00 m
 Slope angle of ground surface = .00 deg.

Structural properties of pile defined using 2 points

Point	Depth X m	Pile Diameter m	Moment of Inertia m**4	Pile Area Sq. m	Modulus of Elasticity kN/Sq. m
1	0.0000	.35650000	4.00000E-04	.019400	210000000.000
2	14.0000	.35650000	4.00000E-04	.019400	210000000.000

Soil and Rock Layering Information

The soil profile is modelled using 3 layers

Layer 1 is sand, p-y criteria by Reese et al., 1974

Distance from top of pile to top of layer = .000 m
 Distance from top of pile to bottom of layer = 1.000 m
 p-y subgrade modulus k for top of soil layer = 50000.000 kN/ m**3
 p-y subgrade modulus k for bottom of layer = 50000.000 kN/ m**3

Layer 2 is stiff clay without free water

Distance from top of pile to top of layer = 1.000 m
 Distance from top of pile to bottom of layer = 4.000 m
 p-y subgrade modulus k for top of soil layer = 54300.000 kN/ m**3
 p-y subgrade modulus k for bottom of layer = 54300.000 kN/ m**3

Layer 3 is stiff clay without free water

Distance from top of pile to top of layer = 4.000 m
 Distance from top of pile to bottom of layer = 13.000 m
 p-y subgrade modulus k for top of soil layer = 108500.000 kN/ m**3
 p-y subgrade modulus k for bottom of layer = 108500.000 kN/ m**3

(Depth of lowest layer extends .00 m below pile tip)

Effective Unit Weight of Soil vs. Depth

Distribution of effective unit weight of soil with depth is defined using 6 points

Point No.	Depth X m	Eff. Unit Weight kN/ m**3
1	.00	10.60000
2	1.00	10.60000
3	1.00	9.80000
4	4.00	9.80000
5	4.00	10.40000
6	13.00	10.40000

Shear Strength of Soils

Distribution of shear strength parameters with depth defined using 6 points

Point No.	Depth X m	Cohesion c kN/ m**2	Angle of Friction Deg.	E50 or k_rm	RQD %
1	.000	.00000	36.00	-----	-----
2	1.000	.00000	36.00	-----	-----
3	1.000	106.00000	.00	.00500	.0
4	4.000	106.00000	.00	.00500	.0
5	4.000	155.00000	.00	.00500	.0
6	13.000	155.00000	.00	.00500	.0

Notes:

- (1) Cohesion = uniaxial compressive strength for rock materials.
- (2) Values of E50 are reported for clay strata.
- (3) Default values will be generated for E50 when input values are 0.
- (4) RQD and k_rm are reported only for weak rock strata.

Loading Type

Cyclic loading criteria was used for computation of p-y curves

Number of cycles of loading = 20.

Pile-head Loading and Pile-head Fixity Conditions

Number of loads specified = 10

Load Case Number 1

Pile-head boundary conditions are Shear and Slope (BC Type 2)
Shear force at pile head = 40.000 kN
Slope at pile head = .000 m/ m
Axial load at pile head = 890.000 kN

(Zero slope for this load indicates fixed-head condition)

.
.[**ABRIDGED**]

.
Load Case Number 10

Pile-head boundary conditions are Shear and Slope (BC Type 2)
Shear force at pile head = 220.000 kN
Slope at pile head = .000 m/ m
Axial load at pile head = 890.000 kN

(Zero slope for this load indicates fixed-head condition)

 Computed Values of Load Distribution and Deflection
 for Lateral Loading for Load Case Number 1

File-head boundary conditions are Shear and Slope (BC Type 2)

Specified shear force at pile head = 40.000 kN
 Specified slope at pile head = 0.000E+00 m/ m
 Specified axial load at pile head = 890.000 kN

(Zero slope for this load indicates fixed-head conditions)

Depth X m	Deflect. Y m	Moment M kN- m	Shear V kN	Slope S Rad.	Total Stress kN/ m**2	Soil Res p kN/ m
0.000	4.82E-04	-41.4026	40.0000	-4.170E-19	64326.3147	0.0000
.650	3.99E-04	-15.7980	37.2719	-2.204E-04	52916.2782	-10.7758
1.300	2.34E-04	5.0149	23.7742	-2.566E-04	48111.0717	-28.4179
1.950	9.01E-05	14.5288	5.1555	-1.734E-04	52350.6850	-27.9604
2.600	1.44E-05	12.4030	-11.0138	-6.262E-05	51403.3740	-20.2403
3.250	-2.32E-06	3.0988	-11.7209	-2.124E-06	47257.1964	19.4326
3.900	-4.41E-07	-.7026	-.7681	2.671E-06	46189.3708	12.4916
4.550	2.19E-09	.019768	.1542	-3.208E-08	45885.0978	-3.4451
5.200	1.42E-18	7.313E-09	2.526E-06	-5.670E-15	45876.2887	-3.972E-05
5.850	0.000	7.528E-22	-2.804E-18	0.0000	45876.2887	4.305E-17
6.500	0.000	0.0000	0.0000	0.0000	45876.2887	0.0000
7.150	0.000	0.0000	0.0000	0.0000	45876.2887	0.0000
7.800	0.000	0.0000	0.0000	0.0000	45876.2887	0.0000
8.450	0.000	0.0000	0.0000	0.0000	45876.2887	0.0000
9.100	0.000	0.0000	0.0000	0.0000	45876.2887	0.0000
9.750	0.000	0.0000	0.0000	0.0000	45876.2887	0.0000
10.400	0.000	0.0000	0.0000	0.0000	45876.2887	0.0000
11.050	0.000	0.0000	0.0000	0.0000	45876.2887	0.0000
11.700	0.000	0.0000	0.0000	0.0000	45876.2887	0.0000
12.350	0.000	0.0000	0.0000	0.0000	45876.2887	0.0000
13.000	0.000	0.0000	0.0000	0.0000	45876.2887	0.0000

Output Verification:

Computed forces and moments are within specified convergence limits.

Output Summary for Load Case No. 1:

File-head deflection = .00048191 m
 Computed slope at pile head = -4.17001E-19
 Maximum bending moment = -41.403 kN- m
 Maximum shear force = 40.000 kN
 Depth of maximum bending moment = 0.000 m
 Depth of maximum shear force = 0.000 m
 Number of iterations = 6
 Number of zero deflection points = 35

 Summary of Pile-head Response

Definition of symbols for pile-head boundary conditions:

- y = pile-head displacement, m
- M = pile-head moment, kN- m
- V = pile-head shear force, kN
- S = pile-head slope, radians
- R = rotational stiffness of pile-head, m- kN/rad

BC Type	Boundary Condition 1	Boundary Condition 2	Axial Load kN	Pile Head Deflection m	Maximum Moment m- kN	Maximum Shear kN
2	V= 40.000	S= 0.000	890.0000	4.819E-04	-41.4026	40.0000
2	V= 60.000	S= 0.000	890.0000	9.860E-04	-68.6692	60.0000
2	V= 80.000	S= 0.000	890.0000	.001653	-98.6945	80.0000
2	V= 100.000	S= 0.000	890.0000	.002501	-131.2477	100.0000
2	V= 120.000	S= 0.000	890.0000	.003507	-165.6023	120.0000
2	V= 140.000	S= 0.000	890.0000	.004670	-201.7577	140.0000
2	V= 160.000	S= 0.000	890.0000	.005986	-239.3866	160.0000
2	V= 180.000	S= 0.000	890.0000	.007455	-278.4169	180.0000
2	V= 200.000	S= 0.000	890.0000	.009050	-318.4934	200.0000
2	V= 220.000	S= 0.000	890.0000	.010785	-359.6486	220.0000

The analysis ended normally.

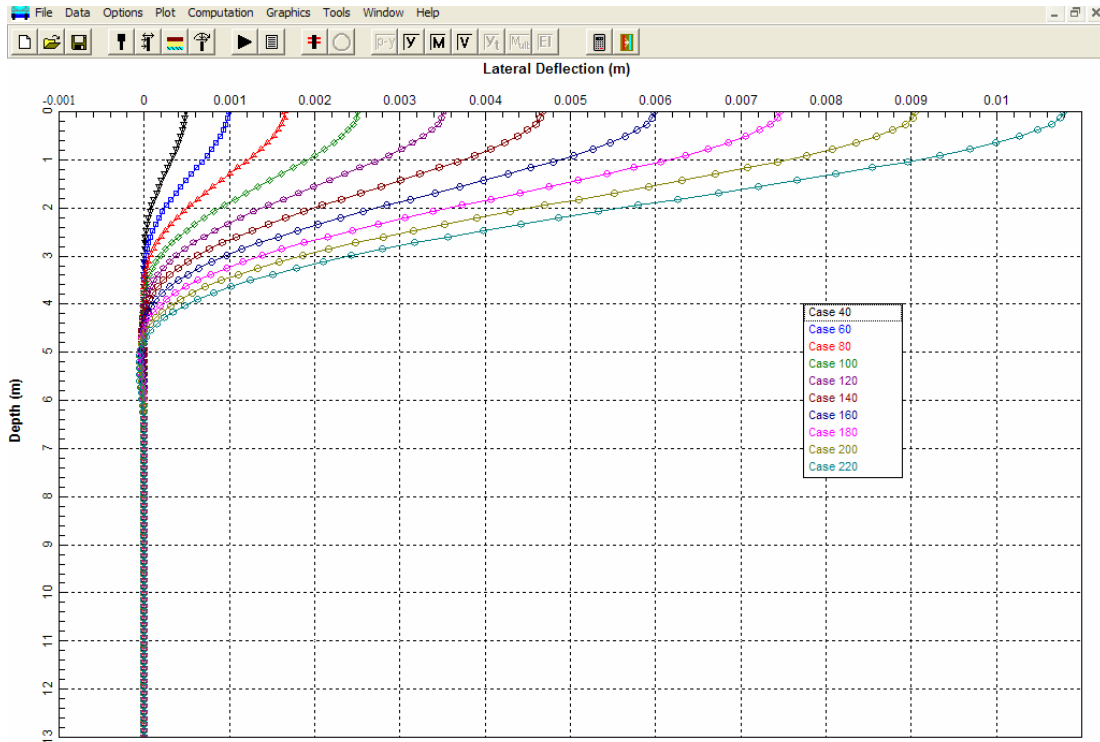


Figure F.31: Pier 3 – Plot Deflection *versus* Depth as a Function on Lateral Load on X-X Axis

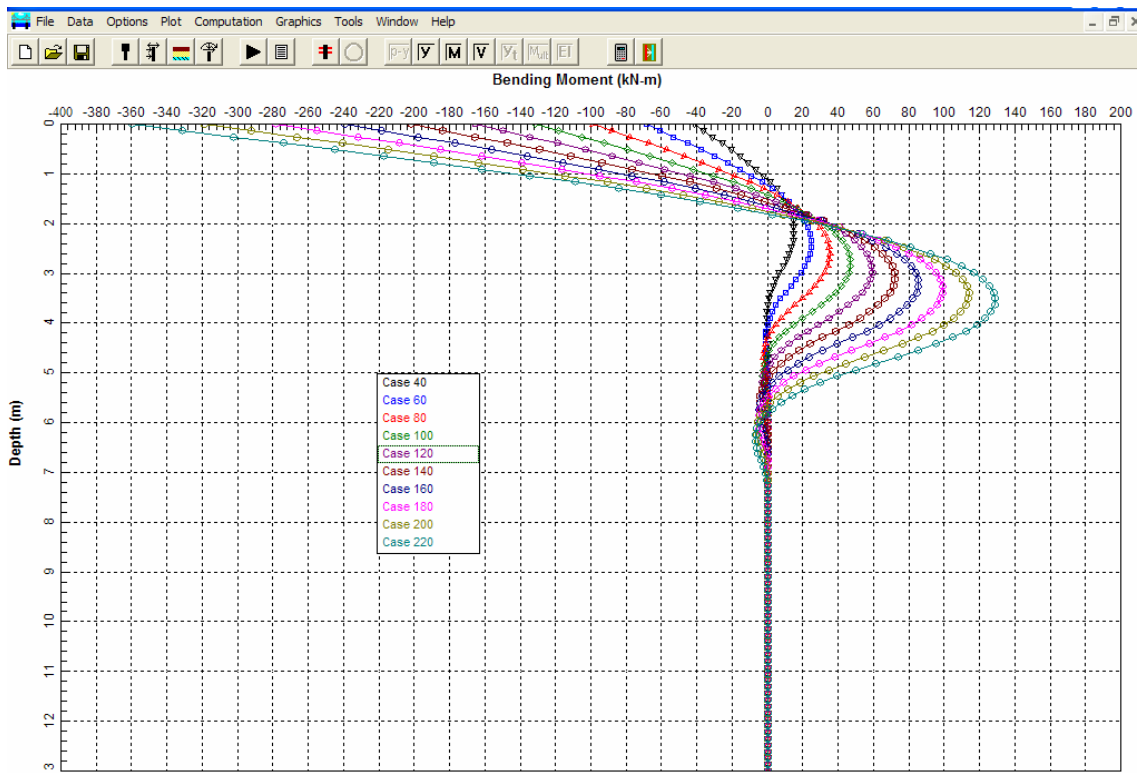


Figure F.32: Pier 3 – Plot of Moment *versus* Depth as a Function of Lateral Load on X-X Axis

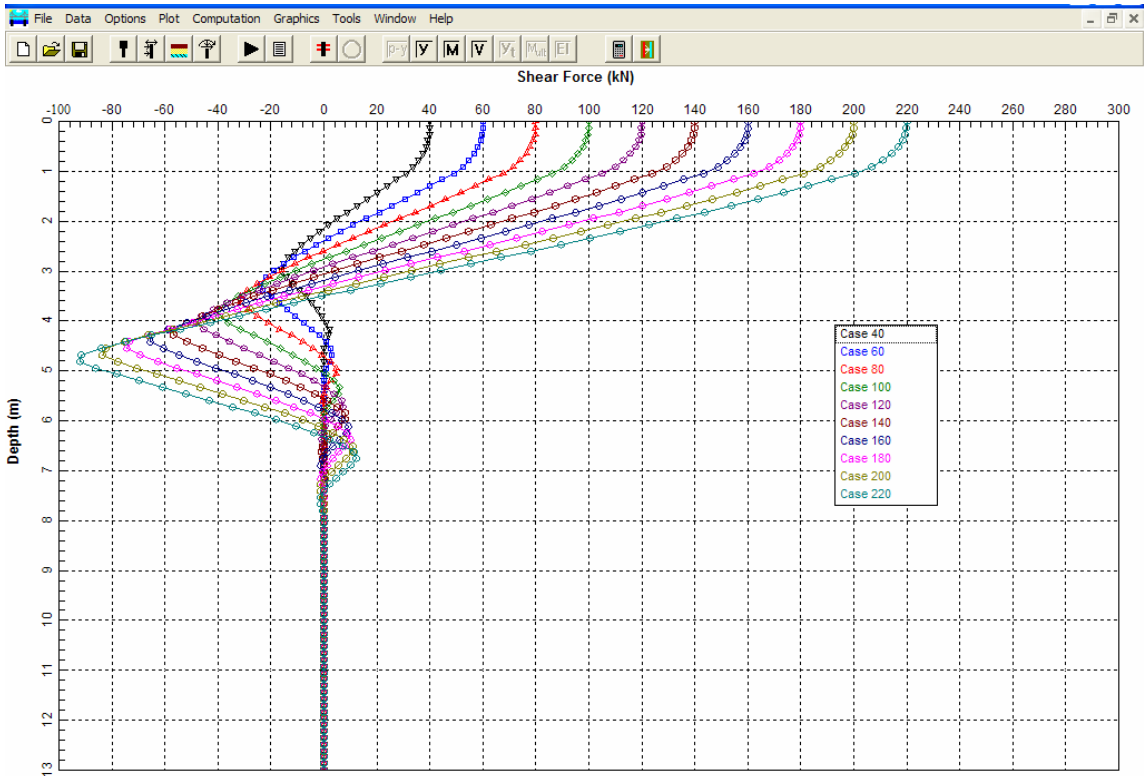


Figure F.33: Pier 3 – Plot of Shear *versus* Depth as a Function of Lateral Load on X-X Axis

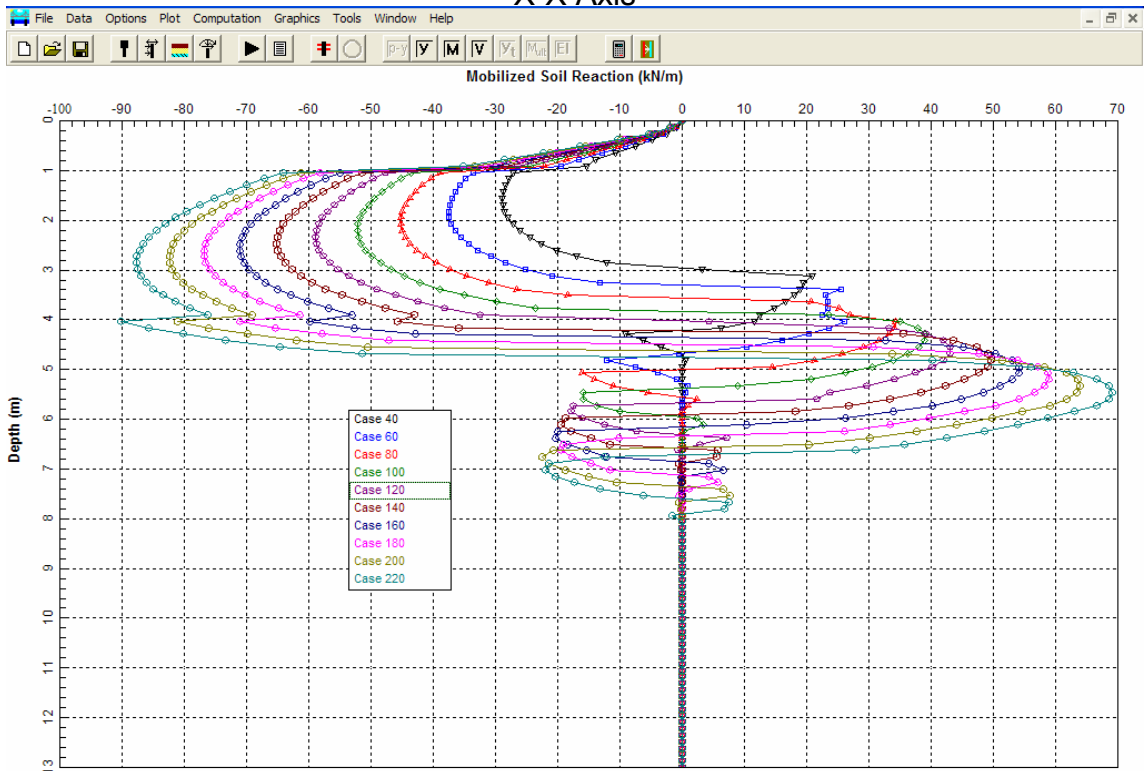


Figure F.34: Pier 3 – Plot of Soil Reaction *versus* Depth as a Function of Lateral Load on X-X Axis


```

LPILEP4
FHWA Pier 3, HP360x152 Y-Y Axis/Fixed-Head Cyclic
2 1 0 0 0 0
100 2 0 13 0
0 0.3755 0.0002 0.0194 2.1E8
14 0.3755 0.0002 0.0194 2.1E8
3 6 6 0 0
4 0 1 50000 50000
3 1 4 54300 54300
3 4 13 108500 108500
0 10.6
1 10.6
1 9.8
4 9.8
4 10.4
13 10.4
0 0 36 0 0
1 0 36 0 0
1 106 0 0.005 0
4 106 0 0.005 0
4 155 0 0.005 0
13 155 0 0.005 0
0 0 20
10
2 40 0 890
2 60 0 890
2 80 0 890
2 100 0 890
2 120 0 890
2 140 0 890
2 160 0 890
2 180 0 890
2 200 0 890
2 220 0 890
0
5 1 0
100 1E-5 2

```

Pier 3 Y-Y Axis - Echo of Input File

=====

LPILE Plus for Windows, Version 4.0 (4.0.7)

Analysis of Individual Piles and Drilled Shafts
 Subjected to Lateral Loading Using the p-y Method

(c) Copyright ENSOFT, Inc., 1985-2003
 All Rights Reserved

Program Options

Units Used in Computations - SI Units, meters, kilopascals

Basic Program Options:

Analysis Type 1:

- Computation of Lateral Pile Response Using User-specified Constant EI

Computation Options:

- Only internally-generated p-y curves used in analysis
- Analysis does not use p-y multipliers (individual pile or shaft action only)
- Analysis assumes no shear resistance at pile tip
- Analysis for fixed-length pile or shaft only
- No computation of foundation stiffness matrix elements
- Output pile response for full length of pile
- Analysis assumes no soil movements acting on pile
- No additional p-y curves to be computed at user-specified depths

Solution Control Parameters:

- Number of pile increments = 100
- Maximum number of iterations allowed = 100
- Deflection tolerance for convergence = 1.0000E-05 m
- Maximum allowable deflection = 2.0000E+00 m

Printing Options:

- Values of pile-head deflection, bending moment, shear force, and soil reaction are printed for full length of pile.
- Printing Increment (spacing of output points) = 5

Pile Structural Properties and Geometry

Pile Length = 13.00 m
 Depth of ground surface below top of pile = .00 m
 Slope angle of ground surface = .00 deg.

Structural properties of pile defined using 2 points

Point	Depth X m	Pile Diameter m	Moment of Inertia m**4	Pile Area Sq. m	Modulus of Elasticity kN/Sq. m
1	0.0000	.37550000	2.00000E-04	.019400	210000000.000
2	14.0000	.37550000	2.00000E-04	.019400	210000000.000

Soil and Rock Layering Information

The soil profile is modelled using 3 layers

Layer 1 is sand, p-y criteria by Reese et al., 1974

Distance from top of pile to top of layer = .000 m
 Distance from top of pile to bottom of layer = 1.000 m
 p-y subgrade modulus k for top of soil layer = 50000.000 kN/ m**3
 p-y subgrade modulus k for bottom of layer = 50000.000 kN/ m**3

Layer 2 is stiff clay without free water

Distance from top of pile to top of layer = 1.000 m
 Distance from top of pile to bottom of layer = 4.000 m
 p-y subgrade modulus k for top of soil layer = 54300.000 kN/ m**3
 p-y subgrade modulus k for bottom of layer = 54300.000 kN/ m**3

Layer 3 is stiff clay without free water

Distance from top of pile to top of layer = 4.000 m
 Distance from top of pile to bottom of layer = 13.000 m
 p-y subgrade modulus k for top of soil layer = 108500.000 kN/ m**3
 p-y subgrade modulus k for bottom of layer = 108500.000 kN/ m**3

(Depth of lowest layer extends .00 m below pile tip)

Effective Unit Weight of Soil vs. Depth

Distribution of effective unit weight of soil with depth is defined using 6 points

Point No.	Depth X m	Eff. Unit Weight kN/ m**3
1	.00	10.60000
2	1.00	10.60000
3	1.00	9.80000
4	4.00	9.80000
5	4.00	10.40000
6	13.00	10.40000

Shear Strength of Soils

Distribution of shear strength parameters with depth defined using 6 points

Point No.	Depth X m	Cohesion c kN/ m**2	Angle of Friction Deg.	E50 or k_rm	RQD %
1	.000	.00000	36.00	-----	-----
2	1.000	.00000	36.00	-----	-----
3	1.000	106.00000	.00	.00500	.0
4	4.000	106.00000	.00	.00500	.0
5	4.000	155.00000	.00	.00500	.0
6	13.000	155.00000	.00	.00500	.0

Notes:

- (1) Cohesion = uniaxial compressive strength for rock materials.
- (2) Values of E50 are reported for clay strata.
- (3) Default values will be generated for E50 when input values are 0.
- (4) RQD and k_rm are reported only for weak rock strata.

Loading Type

Cyclic loading criteria was used for computation of p-y curves
 Number of cycles of loading = 20.

File-head Loading and File-head Fixity Conditions

Number of loads specified = 10

Load Case Number 1

Pile-head boundary conditions are Shear and Slope (BC Type 2)

Shear force at pile head = 40.000 kN
 Slope at pile head = .000 m/ m
 Axial load at pile head = 890.000 kN

(Zero slope for this load indicates fixed-head condition)

.[ABRIDGED]

Load Case Number 10

Pile-head boundary conditions are Shear and Slope (BC Type 2)

Shear force at pile head = 220.000 kN
 Slope at pile head = .000 m/ m
 Axial load at pile head = 890.000 kN

(Zero slope for this load indicates fixed-head condition)

Computed Values of Load Distribution and Deflection
 for Lateral Loading for Load Case Number 1

Pile-head boundary conditions are Shear and Slope (BC Type 2)

Specified shear force at pile head = 40.000 kN
 Specified slope at pile head = 0.000E+00 m/ m
 Specified axial load at pile head = 890.000 kN

(Zero slope for this load indicates fixed-head conditions)

Depth X m	Deflect. y m	Moment M kN- m	Shear V kN	Slope S Rad.	Total Stress kN/ m**2	Soil Res p kN/ m
0.000	7.76E-04	-38.7573	40.0000	-1.251E-18	82259.6833	0.0000
.650	6.23E-04	-13.1536	36.9218	-3.997E-04	58224.2592	-12.0373
1.300	3.33E-04	6.9774	21.3244	-4.347E-04	52426.2873	-32.3114
1.950	1.03E-04	14.2468	.6777	-2.536E-04	59250.4846	-30.0090
2.600	5.75E-06	9.0549	-15.3582	-5.998E-05	54376.5658	-16.0991
3.250	-3.82E-06	.7024	-6.9571	6.951E-06	46535.6511	18.8813
3.900	-8.27E-08	-.4808	1.7088	1.465E-06	46327.6789	4.9423
4.550	-1.17E-10	.002128	-.049741	-2.468E-09	45878.2865	.4849
5.200	-1.97E-20	-1.959E-10	-2.093E-09	3.033E-16	45876.2887	5.537E-08
5.850	0.000	-1.458E-24	2.344E-20	0.0000	45876.2887	-3.604E-19
6.500	0.000	0.0000	0.0000	0.0000	45876.2887	0.0000
7.150	0.000	0.0000	0.0000	0.0000	45876.2887	0.0000
7.800	0.000	0.0000	0.0000	0.0000	45876.2887	0.0000
8.450	0.000	0.0000	0.0000	0.0000	45876.2887	0.0000
9.100	0.000	0.0000	0.0000	0.0000	45876.2887	0.0000
9.750	0.000	0.0000	0.0000	0.0000	45876.2887	0.0000
10.400	0.000	0.0000	0.0000	0.0000	45876.2887	0.0000
11.050	0.000	0.0000	0.0000	0.0000	45876.2887	0.0000
11.700	0.000	0.0000	0.0000	0.0000	45876.2887	0.0000
12.350	0.000	0.0000	0.0000	0.0000	45876.2887	0.0000
13.000	0.000	0.0000	0.0000	0.0000	45876.2887	0.0000

Output Verification:

Computed forces and moments are within specified convergence limits.

Output Summary for Load Case No. 1:

Pile-head deflection = .00077584 m
 Computed slope at pile head = -1.25100E-18
 Maximum bending moment = -38.757 kN- m
 Maximum shear force = 40.000 kN
 Depth of maximum bending moment = 0.000 m
 Depth of maximum shear force = 0.000 m
 Number of iterations = 5
 Number of zero deflection points = 36

.
 .
 .[ABRIDGED]
 .
 .

 Summary of Pile-head Response

Definition of symbols for pile-head boundary conditions:

y = pile-head displacement, m
 M = pile-head moment, kN- m
 V = pile-head shear force, kN
 S = pile-head slope, radians
 R = rotational stiffness of pile-head, m- kN/rad

BC Type	Boundary Condition 1	Boundary Condition 2	Axial Load kN	Pile Head Deflection m	Maximum Moment m- kN	Maximum Shear kN
2	V= 40.000	S= 0.000	890.0000	7.758E-04	-38.7573	40.0000
2	V= 60.000	S= 0.000	890.0000	.001595	-64.4761	60.0000
2	V= 80.000	S= 0.000	890.0000	.002701	-92.8759	80.0000
2	V= 100.000	S= 0.000	890.0000	.004081	-123.4155	100.0000
2	V= 120.000	S= 0.000	890.0000	.005726	-155.7800	120.0000
2	V= 140.000	S= 0.000	890.0000	.007628	-189.7682	140.0000
2	V= 160.000	S= 0.000	890.0000	.009763	-225.0271	160.0000
2	V= 180.000	S= 0.000	890.0000	.012132	-261.4188	180.0000
2	V= 200.000	S= 0.000	890.0000	.014712	-298.8351	200.0000
2	V= 220.000	S= 0.000	890.0000	.017626	-338.3204	220.0000

The analysis ended normally.

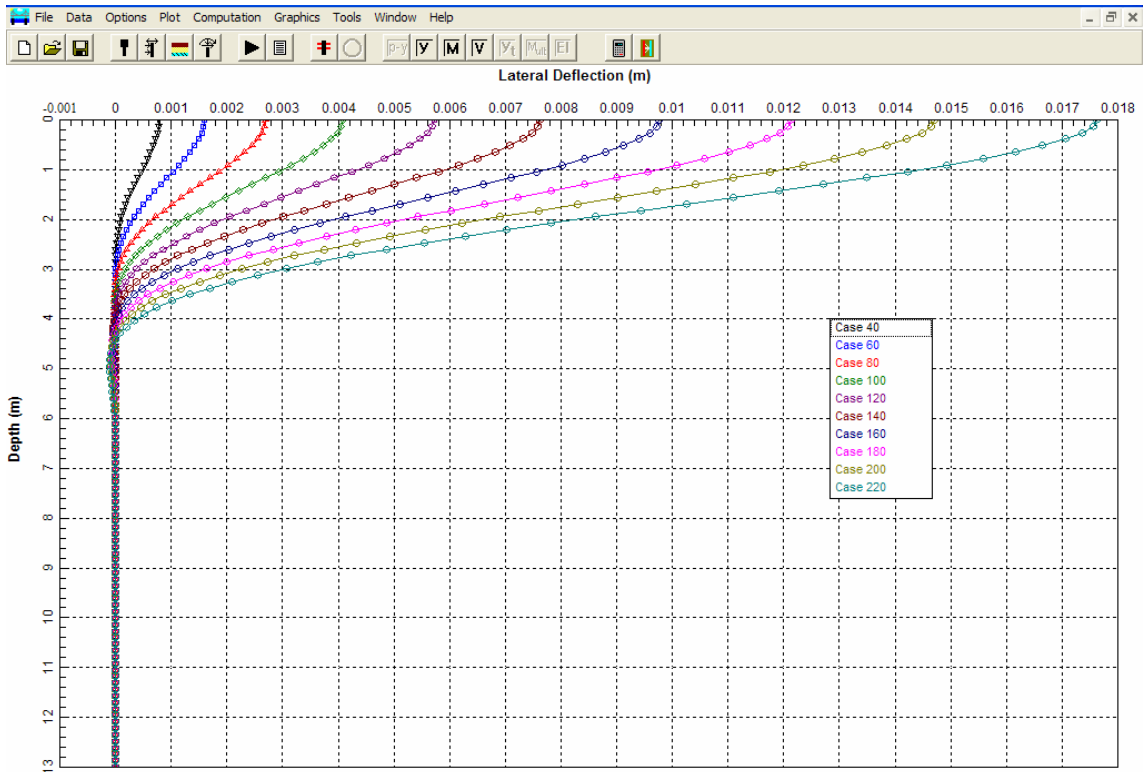


Figure F.35: Pier 3 – Plot of Deflection *versus* Depth as a Function of Lateral Load on Y-Y Axis

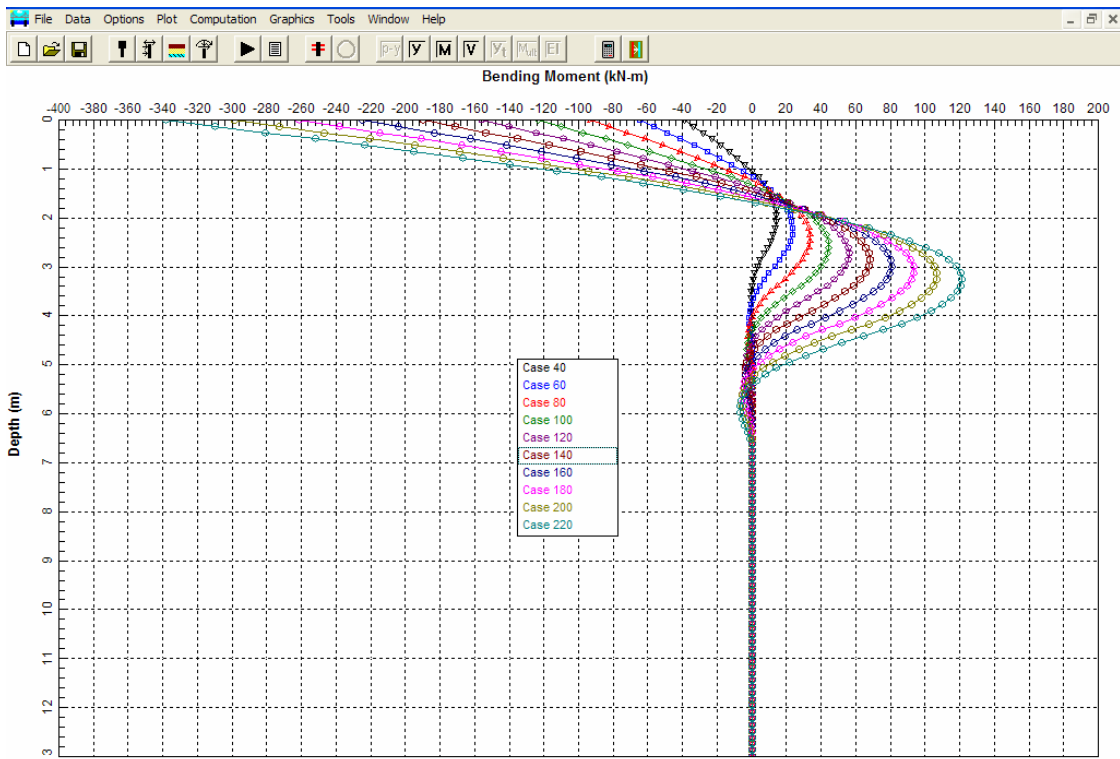


Figure F.36: Pier 3 – Plot of Moment *versus* Depth as a Function of Lateral Load on Y-Y Axis

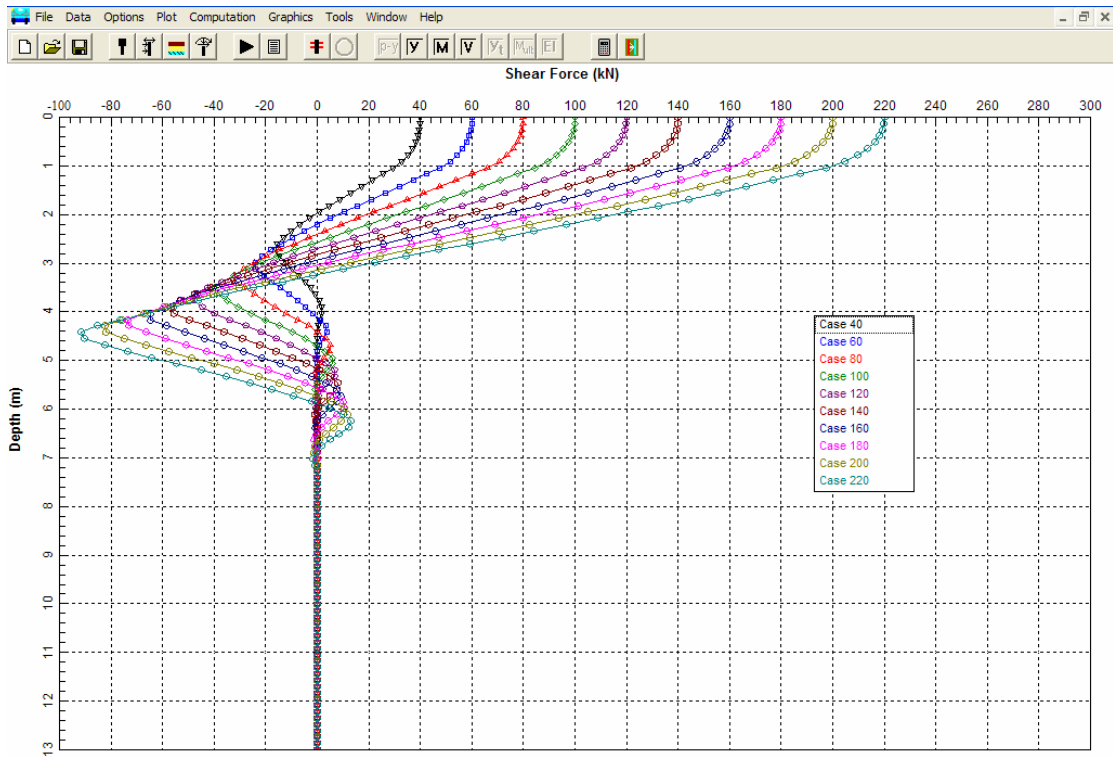


Figure F.37: Pier 3 – Plot of Shear *versus* Depth as a Function of Lateral Load on Y-Y Axis

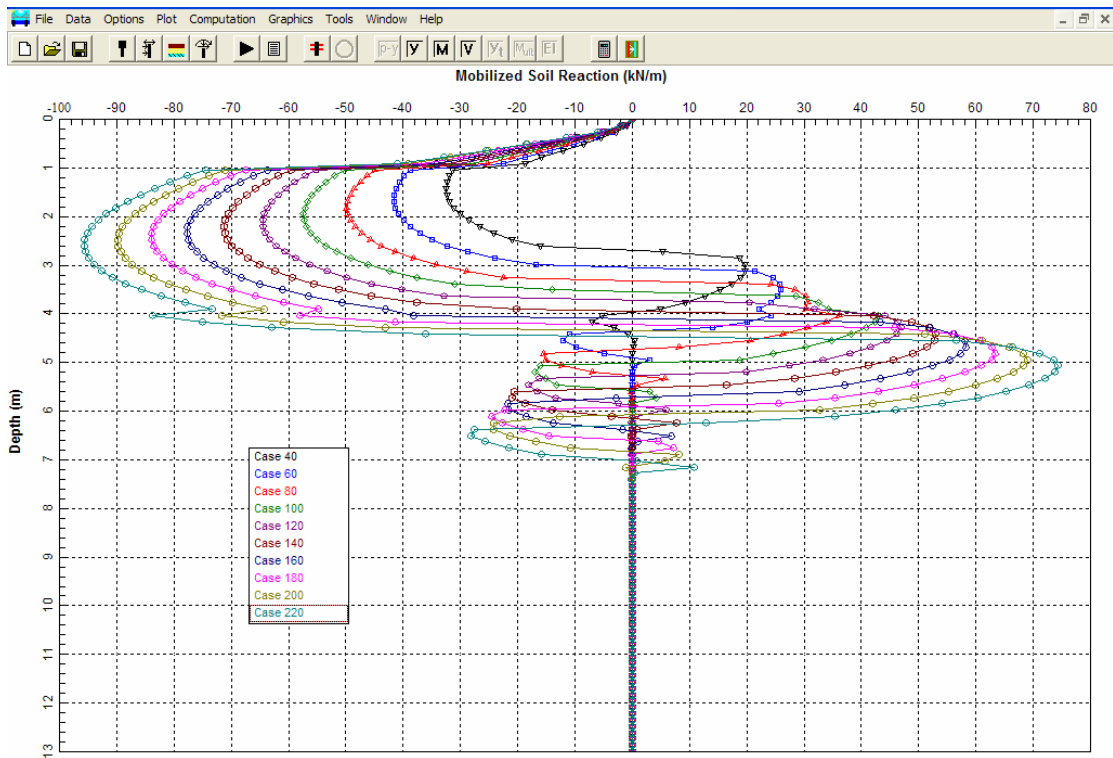


Figure F.38: Pier 3 – Plot of Soil Reaction *versus* Depth as a Function of Lateral Load on Y-Y Axis

F.4.5 LPILE Analysis - South Abutment

A LPILE analysis was performed to evaluate the performance of the 356 mm square prestressed concrete pile under lateral load at the South abutment. Unlike the North Abutment, the soil at the South abutment consists of only cohesive type. Again, soil parameters were obtained from Tables 9-15 and 9-16.

The same assumptions and analysis options as the North abutment were used. Ten lateral loads were analyzed from 20 to 200 kN in 20 kN increments.

An echo print of the input file is presented on the following page. LPILE generated summaries of the problem input and output are provided. For selected lateral loads, Figures F.39 to F.42 provide graphical presentations of deflection, movement, shear, and soil reaction versus depth.

The LPILE solutions for the South abutment indicate the pile deflection under the 40 kN design load will be 1.9 mm. The corresponding maximum moment and shear stress are -44.4 m-kN and 13,100 kN/m², respectively. The deflection, moment and shear stress under the design load are acceptable.

Additional LPILE analyses should be performed to evaluate group response using the p-multiplier approach described in Section 9.8.4.


```

LPILEP4
FWA South Abut. - 355 mm-sq PSC Fixed-Head/Cyclic/Crack Modeled
2 3 0 0 0 0
100 2 0 21 0
0 0.355 0.0013 0.126 27800000
21 0.355 0.0013 0.126 27800000
3 6 6 0 0
1 0 5.5 0 0
3 5.5 15 54300 54300
3 15 21 108500 108500
0 9.2
5.5 9.2
5.5 9.7
15 9.7
15 10.5
21 10.5
0 33 0 0.01 0
5.5 33 0 0.01 0
5.5 93 0 0.007 0
15 93 0 0.007 0
15 161 0 0.005 0
21 161 0 0.005 0
0 0 20
10
2 20 0 890
2 40 0 890
2 60 0 890
2 80 0 890
2 100 0 890
2 120 0 890
2 140 0 890
2 160 0 890
2 180 0 890
2 200 0 890
0
1 1 0
100 1E-6 1
1 1
890
41370 248220 413685.52 2.0685E8
0.355 0.355 0 0 0
0.0005 4 2 0.0762
0.102 0.0006
-0.102 0.0006

```

South Abutment - Echo of Input File

=====

LPILE Plus for Windows, Version 4.0 (4.0.7)

Analysis of Individual Piles and Drilled Shafts
 Subjected to Lateral Loading Using the p-y Method

(c) Copyright ENSOFT, Inc., 1985-2003
 All Rights Reserved

Program Options

Units Used in Computations - SI Units, meters, kilopascals

Basic Program Options:

Analysis Type 4:

- Computation of Nonlinear Bending Stiffness and Ultimate Bending Moment Capacity with Pile Response Using User-specified Constant EI

Computation Options:

- Only internally-generated p-y curves used in analysis
- Analysis does not use p-y multipliers (individual pile or shaft action only)
- Analysis assumes no shear resistance at pile tip
- Analysis for fixed-length pile or shaft only
- No computation of foundation stiffness matrix elements
- Output pile response for full length of pile
- Analysis assumes no soil movements acting on pile
- No additional p-y curves to be computed at user-specified depths

Solution Control Parameters:

- Number of pile increments = 100
- Maximum number of iterations allowed = 100
- Deflection tolerance for convergence = 10.000E-06 m
- Maximum allowable deflection = 1.0000E+00 m

Printing Options:

- Values of pile-head deflection, bending moment, shear force, and soil reaction are printed for full length of pile.
- Printing Increment (spacing of output points) = 1

Pile Structural Properties and Geometry

Pile Length = 21.00 m
 Depth of ground surface below top of pile = .00 m
 Slope angle of ground surface = .00 deg.

Structural properties of pile defined using 2 points

Point	Depth X m	Pile Diameter m	Moment of Inertia m**4	Pile Area Sq. m	Modulus of Elasticity kN/Sq. m
1	0.0000	.35500000	.001300	.1260	27800000.000
2	21.0000	.35500000	.001300	.1260	27800000.000

Please note that because this analysis makes computations of ultimate moment capacity and pile response using nonlinear bending stiffness that the above values of moment of inertia and modulus of are not used for any computations other than total stress due to combined axial loading and bending.

Soil and Rock Layering Information

The soil profile is modelled using 3 layers

Layer 1 is soft clay, p-y criteria by Matlock, 1970

Distance from top of pile to top of layer = .000 m
 Distance from top of pile to bottom of layer = 5.500 m

Layer 2 is stiff clay without free water

Distance from top of pile to top of layer = 5.500 m
 Distance from top of pile to bottom of layer = 15.000 m
 p-y subgrade modulus k for top of soil layer = 54300.000 kN/ m**3
 p-y subgrade modulus k for bottom of layer = 54300.000 kN/ m**3

Layer 3 is stiff clay without free water

Distance from top of pile to top of layer = 15.000 m
 Distance from top of pile to bottom of layer = 21.000 m
 p-y subgrade modulus k for top of soil layer = 108500.000 kN/ m**3
 p-y subgrade modulus k for bottom of layer = 108500.000 kN/ m**3

(Depth of lowest layer extends .00 m below pile tip)

Effective Unit Weight of Soil vs. Depth

Distribution of effective unit weight of soil with depth is defined using 6 points

Point No.	Depth X m	Eff. Unit Weight kN/ m**3
1	.00	9.20000
2	5.50	9.20000
3	5.50	9.70000
4	15.00	9.70000
5	15.00	10.50000
6	21.00	10.50000

Shear Strength of Soils

Distribution of shear strength parameters with depth defined using 6 points

Point No.	Depth X m	Cohesion c kN/ m**2	Angle of Friction Deg.	E50 or k_rm	RQD %
1	.000	33.00000	.00	.01000	.0
2	5.500	33.00000	.00	.01000	.0
3	5.500	93.00000	.00	.00700	.0
4	15.000	93.00000	.00	.00700	.0
5	15.000	161.00000	.00	.00500	.0
6	21.000	161.00000	.00	.00500	.0

Notes:

- (1) Cohesion = uniaxial compressive strength for rock materials.
- (2) Values of E50 are reported for clay strata.
- (3) Default values will be generated for E50 when input values are 0.
- (4) RQD and k_rm are reported only for weak rock strata.

Loading Type

Cyclic loading criteria was used for computation of p-y curves

Number of cycles of loading = 20.

Pile-head Loading and Pile-head Fixity Conditions

Number of loads specified = 10

Load Case Number 1

Pile-head boundary conditions are Shear and Slope (BC Type 2)

Shear force at pile head = 20.000 kN
Slope at pile head = .000 m/ m
Axial load at pile head = 890.000 kN

(Zero slope for this load indicates fixed-head condition)

.[ABRIDGED]

Load Case Number 10

Pile-head boundary conditions are Shear and Slope (BC Type 2)

Shear force at pile head = 200.000 kN
Slope at pile head = .000 m/ m
Axial load at pile head = 890.000 kN

(Zero slope for this load indicates fixed-head condition)

Computations of Ultimate Moment Capacity and Nonlinear Bending Stiffness

File Description:

The pile shape is a rectangular solid pile.

Width = .355 m
Depth = .355 m

Material Properties:

Compressive Strength of Concrete = 41370.000 kN/ m**2
Yield Stress of Reinforcement = 248220. kN/ m**2
Modulus of Elasticity of Reinforcement = 206850000. kN/ m**2
Number of Reinforcing Bars = 4
Area of Single Bar = .00050 m**2
Number of Rows of Reinforcing Bars = 2
Cover Thickness (edge to bar center) = .076 m

Ultimate Axial Squash Load Capacity = 4687.27 kN

Distribution and Area of Steel Reinforcement

Row Number	Area of Reinforcement m**2	Distance to Centroidal Axis m
1	.000600	.1020
2	.000600	-.1020

Axial Thrust Force = 890.00 kN

Bending Moment kN-m	Bending Stiffness kN-m ²	Bending Curvature rad/m	Maximum Strain m/m	Neutral Axis Position m
1.54295127	39190.962	.00003937	.00023366	5.93486814
7.71444547	39189.382	.00019685	.00026170	1.32942587
13.885	39185.750	.00035433	.00028986	.81803677
20.053	39179.988	.00051181	.00031813	.62158314
26.218	39172.157	.00066929	.00034653	.51775257
32.378	39162.188	.00082677	.00037504	.45362225
38.534	39150.185	.00098425	.00040367	.41013020
44.683	39136.085	.00114173	.00043242	.37873943
50.825	39119.844	.00129921	.00046129	.35505146
56.988	39121.516	.00145669	.00049033	.33660160
63.049	39059.507	.00161417	.00051931	.32172146
69.110	39008.681	.00177165	.00054844	.30956600
75.155	38958.023	.00192913	.00057769	.29945812
81.088	38861.083	.00208661	.00060684	.29082363
81.088	36133.990	.00224409	.00061495	.27403133
81.088	33764.548	.00240157	.00063793	.26562977
81.469	31835.639	.00255906	.00066017	.25797573
83.923	30893.279	.00271654	.00068196	.25104214
86.229	30003.115	.00287402	.00070333	.24472065
88.411	29164.014	.00303150	.00072433	.23893543
90.481	28372.973	.00318898	.00074498	.23361065
92.458	27628.502	.00334646	.00076533	.22869755
94.358	26929.177	.00350394	.00078544	.22415821
96.109	26249.199	.00366142	.00080493	.21984097
97.855	25623.877	.00381890	.00082447	.21589207
99.561	25038.090	.00397638	.00084391	.21223026
110.590	21442.569	.00515748	.00098201	.19040569
120.077	18943.856	.00633858	.00111351	.17567181
128.620	17104.480	.00751969	.00124079	.16500599
136.481	15686.050	.00870079	.00136470	.15684818
142.143	14384.225	.00988189	.00148005	.14977375
144.188	13033.330	.01106299	.00157940	.14276432
145.892	11915.286	.01224409	.00167612	.13689243
147.331	10974.243	.01342520	.00177083	.13190350
148.579	10172.279	.01460630	.00186443	.12764584
149.683	9481.177	.01578740	.00195798	.12402195
150.467	8867.434	.01696850	.00204601	.12057682
151.314	8337.066	.01814961	.00213887	.11784672
151.873	7856.558	.01933071	.00222570	.11513828
152.385	7429.115	.02051181	.00231392	.11280903
152.897	7048.226	.02169291	.00240709	.11096188
153.186	6696.962	.02287402	.00249515	.10908222
153.411	6377.467	.02405512	.00258529	.10747341
153.715	6091.050	.02523622	.00268420	.10636295
153.799	5821.896	.02641732	.00277391	.10500332
153.865	5575.122	.02759843	.00286459	.10379536
153.883	5346.955	.02877953	.00295694	.10274448
153.894	5136.551	.02996063	.00305021	.10180737
153.894	4941.739	.03114173	.00314448	.10097317
153.894	4761.164	.03232283	.00325113	.10058315
153.894	4593.320	.03350394	.00334652	.09988438
153.894	4436.907	.03468504	.00344120	.09921268
153.894	4290.796	.03586614	.00353701	.09861683
153.894	4154.001	.03704724	.00363341	.09807514
153.894	4025.660	.03822835	.00373041	.09758221
153.894	3905.010	.03940945	.00415798	.10550709

Ultimate Moment Capacity at a Concrete Strain of 0.003 = 153.888 m- kN

 Computed Values of Load Distribution and Deflection
 for Lateral Loading for Load Case Number 1

File-head boundary conditions are Shear and Slope (BC Type 2)
 Specified shear force at pile head = 20.000 kN
 Specified slope at pile head = 0.000E+00 m/ m
 Specified axial load at pile head = 890.000 kN

(Zero slope for this load indicates fixed-head conditions)

Depth X m	Deflect. Y m	Moment M kN- m	Shear V kN	Slope S Rad.	Total Stress kN/ m**2	Flx. Rig. EI kN- m**2	Soil Res p kN/ m
0.000	5.22E-04	-18.0043	20.0000	-5.16E-19	9521.8	36140.000	-6.843
.210	5.11E-04	-13.9454	18.4837	-9.28E-05	8967.6	36140.000	-7.598
.420	4.83E-04	-10.2065	16.8203	-1.63E-04	8457.1	36140.000	-8.244
.630	4.43E-04	-6.8200	15.0334	-2.12E-04	7994.7	36140.000	-8.773
.840	3.94E-04	-3.8130	13.1488	-2.43E-04	7584.1	36140.000	-9.175
1.050	3.41E-04	-1.2066	11.1938	-2.58E-04	7228.2	36140.000	-9.443
1.260	2.86E-04	.9848	9.1977	-2.59E-04	7198.0	36140.000	-9.568
1.470	2.32E-04	2.7531	7.1907	-2.48E-04	7439.4	36140.000	-9.546
1.680	1.82E-04	4.0975	5.2045	-2.28E-04	7623.0	36140.000	-9.370
1.890	1.36E-04	5.0242	3.2720	-2.01E-04	7749.5	36140.000	-9.035
2.100	9.73E-05	5.5470	1.4272	-1.71E-04	7820.9	36140.000	-8.535
2.310	6.48E-05	5.6874	-.2945	-1.38E-04	7840.0	36140.000	-7.862
2.520	3.93E-05	5.4749	-1.8551	-1.06E-04	7811.0	36140.000	-7.001
2.730	2.05E-05	4.9477	-3.2110	-7.53E-05	7739.0	36140.000	-5.913
2.940	7.73E-06	4.1544	-4.3014	-4.88E-05	7630.7	36140.000	-4.471
3.150	1.07E-08	3.1593	-4.8212	-2.76E-05	7494.9	36140.000	-.479385
3.360	-3.85E-06	2.1397	-4.4661	-1.22E-05	7355.6	36140.000	3.862
3.570	-5.10E-06	1.2881	-3.5982	-2.21E-06	7239.4	36140.000	4.404
3.780	-4.78E-06	.6293	-2.6832	3.36E-06	7149.4	36140.000	4.310
3.990	-3.69E-06	.1599	-1.8154	5.66E-06	7085.3	36140.000	3.955
4.200	-2.40E-06	-.1352	-1.0398	5.73E-06	7082.0	36140.000	3.431
4.410	-1.28E-06	-.2789	-.3870	4.53E-06	7101.6	36140.000	2.787
4.620	-4.99E-07	-.2995	.1202	2.85E-06	7104.4	36140.000	2.044
4.830	-8.46E-08	-.2295	.4558	1.31E-06	7094.8	36140.000	1.152
5.040	5.01E-08	-.1085	.4794	3.26E-07	7078.3	36140.000	-.927970
5.250	5.25E-08	-2.83E-02	.2814	-7.10E-08	7067.4	36140.000	-.957485
5.460	2.03E-08	9.71E-03	.1069	-1.25E-07	7064.8	36140.000	-.704314
5.670	5.60E-12	1.66E-02	-2.31E-02	-4.84E-08	7065.8	36140.000	-.534327
5.880	-1.56E-12	7.14E-06	-3.96E-02	-1.33E-11	7063.5	36140.000	.377189
6.090	-1.50E-17	-1.27E-06	-1.70E-05	3.70E-12	7063.5	36140.000	2.20E-04
6.300	1.89E-18	-1.54E-11	3.03E-06	3.56E-17	7063.5	36140.000	-2.89E-05
6.510	2.64E-23	1.55E-12	3.66E-11	-4.51E-18	7063.5	36140.000	-4.19E-10
6.720	-2.14E-24	2.52E-17	-3.70E-12	-6.30E-23	7063.5	36140.000	3.52E-11
6.930	0.000	-1.76E-18	-6.00E-17	5.10E-24	7063.5	36140.000	6.51E-16
7.140	0.000	-3.58E-23	4.18E-18	0.000	7063.5	36140.000	-3.98E-17
7.350	0.000	1.95E-24	8.51E-23	0.000	7063.5	36140.000	-8.99E-22
7.560	0.000	0.0	-4.64E-24	0.000	7063.5	36140.000	4.42E-23
7.770	0.000	0.0	0.0	0.000	7063.5	36140.000	0.000
7.980	0.000	0.0	0.0	0.000	7063.5	36140.000	0.000
8.190	0.000	0.0	0.0	0.000	7063.5	36140.000	0.000
8.400	0.000	0.0	0.0	0.000	7063.5	36140.000	0.000
8.610	0.000	0.0	0.0	0.000	7063.5	36140.000	0.000
8.820	0.000	0.0	0.0	0.000	7063.5	36140.000	0.000
9.030	0.000	0.0	0.0	0.000	7063.5	36140.000	0.000
9.240	0.000	0.0	0.0	0.000	7063.5	36140.000	0.000
9.450	0.000	0.0	0.0	0.000	7063.5	36140.000	0.000
9.660	0.000	0.0	0.0	0.000	7063.5	36140.000	0.000
9.870	0.000	0.0	0.0	0.000	7063.5	36140.000	0.000
10.080	0.000	0.0	0.0	0.000	7063.5	36140.000	0.000
10.290	0.000	0.0	0.0	0.000	7063.5	36140.000	0.000
10.500	0.000	0.0	0.0	0.000	7063.5	36140.000	0.000
10.710	0.000	0.0	0.0	0.000	7063.5	36140.000	0.000
10.920	0.000	0.0	0.0	0.000	7063.5	36140.000	0.000

11.130	0.000	0.0	0.0	0.000	7063.5	36140.000	0.000
11.340	0.000	0.0	0.0	0.000	7063.5	36140.000	0.000
11.550	0.000	0.0	0.0	0.000	7063.5	36140.000	0.000
11.760	0.000	0.0	0.0	0.000	7063.5	36140.000	0.000
11.970	0.000	0.0	0.0	0.000	7063.5	36140.000	0.000
12.180	0.000	0.0	0.0	0.000	7063.5	36140.000	0.000
12.390	0.000	0.0	0.0	0.000	7063.5	36140.000	0.000
12.600	0.000	0.0	0.0	0.000	7063.5	36140.000	0.000
12.810	0.000	0.0	0.0	0.000	7063.5	36140.000	0.000
13.020	0.000	0.0	0.0	0.000	7063.5	36140.000	0.000
13.230	0.000	0.0	0.0	0.000	7063.5	36140.000	0.000
13.440	0.000	0.0	0.0	0.000	7063.5	36140.000	0.000
13.650	0.000	0.0	0.0	0.000	7063.5	36140.000	0.000
13.860	0.000	0.0	0.0	0.000	7063.5	36140.000	0.000
14.070	0.000	0.0	0.0	0.000	7063.5	36140.000	0.000
14.280	0.000	0.0	0.0	0.000	7063.5	36140.000	0.000
14.490	0.000	0.0	0.0	0.000	7063.5	36140.000	0.000
14.700	0.000	0.0	0.0	0.000	7063.5	36140.000	0.000
14.910	0.000	0.0	0.0	0.000	7063.5	36140.000	0.000
15.120	0.000	0.0	0.0	0.000	7063.5	36140.000	0.000
15.330	0.000	0.0	0.0	0.000	7063.5	36140.000	0.000
15.540	0.000	0.0	0.0	0.000	7063.5	36140.000	0.000
15.750	0.000	0.0	0.0	0.000	7063.5	36140.000	0.000
15.960	0.000	0.0	0.0	0.000	7063.5	36140.000	0.000
16.170	0.000	0.0	0.0	0.000	7063.5	36140.000	0.000
16.380	0.000	0.0	0.0	0.000	7063.5	36140.000	0.000
16.590	0.000	0.0	0.0	0.000	7063.5	36140.000	0.000
16.800	0.000	0.0	0.0	0.000	7063.5	36140.000	0.000
17.010	0.000	0.0	0.0	0.000	7063.5	36140.000	0.000
17.220	0.000	0.0	0.0	0.000	7063.5	36140.000	0.000
17.430	0.000	0.0	0.0	0.000	7063.5	36140.000	0.000
17.640	0.000	0.0	0.0	0.000	7063.5	36140.000	0.000
17.850	0.000	0.0	0.0	0.000	7063.5	36140.000	0.000
18.060	0.000	0.0	0.0	0.000	7063.5	36140.000	0.000
18.270	0.000	0.0	0.0	0.000	7063.5	36140.000	0.000
18.480	0.000	0.0	0.0	0.000	7063.5	36140.000	0.000
18.690	0.000	0.0	0.0	0.000	7063.5	36140.000	0.000
18.900	0.000	0.0	0.0	0.000	7063.5	36140.000	0.000
19.110	0.000	0.0	0.0	0.000	7063.5	36140.000	0.000
19.320	0.000	0.0	0.0	0.000	7063.5	36140.000	0.000
19.530	0.000	0.0	0.0	0.000	7063.5	36140.000	0.000
19.740	0.000	0.0	0.0	0.000	7063.5	36140.000	0.000
19.950	0.000	0.0	0.0	0.000	7063.5	36140.000	0.000
20.160	0.000	0.0	0.0	0.000	7063.5	36140.000	0.000
20.370	0.000	0.0	0.0	0.000	7063.5	36140.000	0.000
20.580	0.000	0.0	0.0	0.000	7063.5	36140.000	0.000
20.790	0.000	0.0	0.0	0.000	7063.5	36140.000	0.000
21.000	0.000	0.0	0.0	0.000	7063.5	36140.000	0.000

Please note that because this analysis makes computations of ultimate moment capacity and pile response using nonlinear bending stiffness that the above values of total stress due to combined axial stress and bending may not be representative of actual conditions.

Output Verification:

Computed forces and moments are within specified convergence limits.

Output Summary for Load Case No. 1:

Pile-head deflection	=	.00052244	m
Computed slope at pile head	=	-5.16287E-19	
Maximum bending moment	=	-18.004	kN- m
Maximum shear force	=	20.000	kN
Depth of maximum bending moment	=	0.000	m
Depth of maximum shear force	=	0.000	m
Number of iterations	=	10	
Number of zero deflection points	=	39	

 Summary of Pile-head Response

Definition of symbols for pile-head boundary conditions:

y = pile-head displacement, m
 M = pile-head moment, kN- m
 V = pile-head shear force, kN
 S = pile-head slope, radians
 R = rotational stiffness of pile-head, m- kN/rad

BC Type	Boundary Condition 1	Boundary Condition 2	Axial Load kN	Pile Head Deflection m	Maximum Moment m- kN	Maximum Shear kN
2	V= 20.000	S= 0.000	890.0000	5.224E-04	-18.0043	20.0000
2	V= 40.000	S= 0.000	890.0000	.001897	-44.4270	40.0000
2	V= 60.000	S= 0.000	890.0000	.004016	-75.2557	60.0000
2	V= 80.000	S= 0.000	890.0000	.006833	-109.3218	80.0000
2	V= 100.000	S= 0.000	890.0000	.010330	-146.0260	100.0000
2	V= 120.000	S= 0.000	890.0000	.014498	-185.0004	120.0000
2	V= 140.000	S= 0.000	890.0000	.019306	-226.0812	140.0000
2	V= 160.000	S= 0.000	890.0000	.024733	-269.0181	160.0000
2	V= 180.000	S= 0.000	890.0000	.031494	-318.1544	180.0000
2	V= 200.000	S= 0.000	890.0000	.041557	-381.1517	200.0000

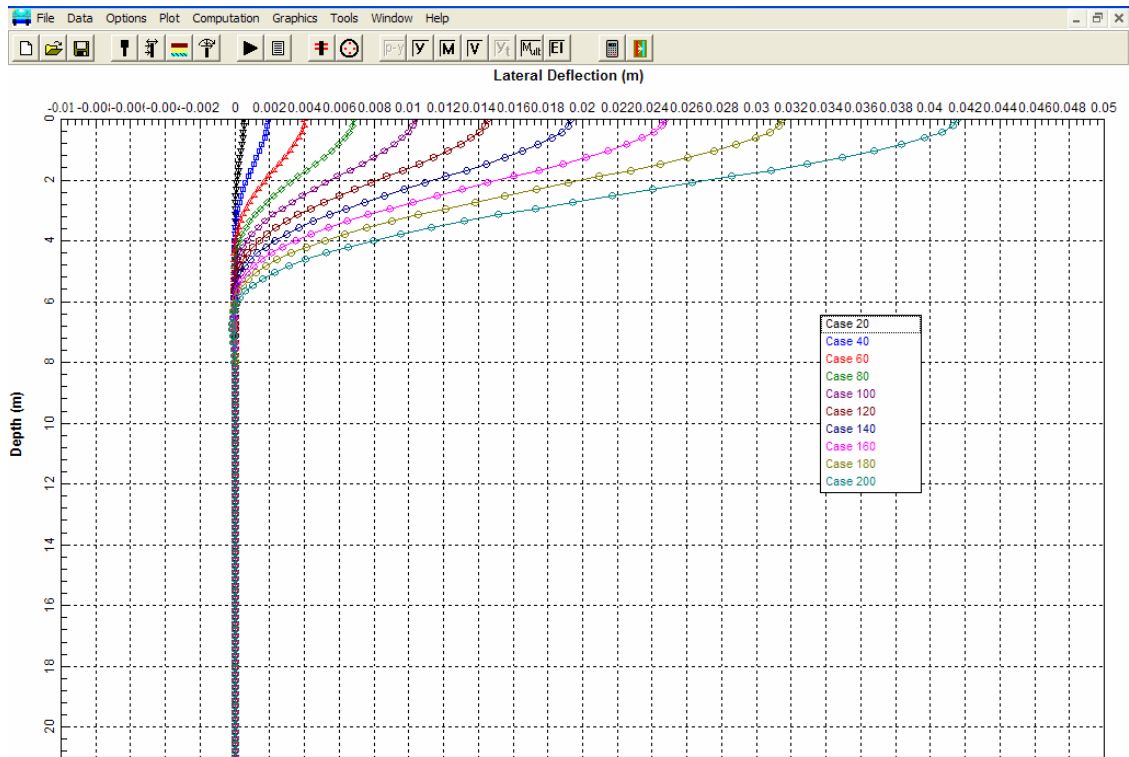


Figure F.39: South Abutment – Plot of Deflection *versus* Depth as a Function of Lateral Load

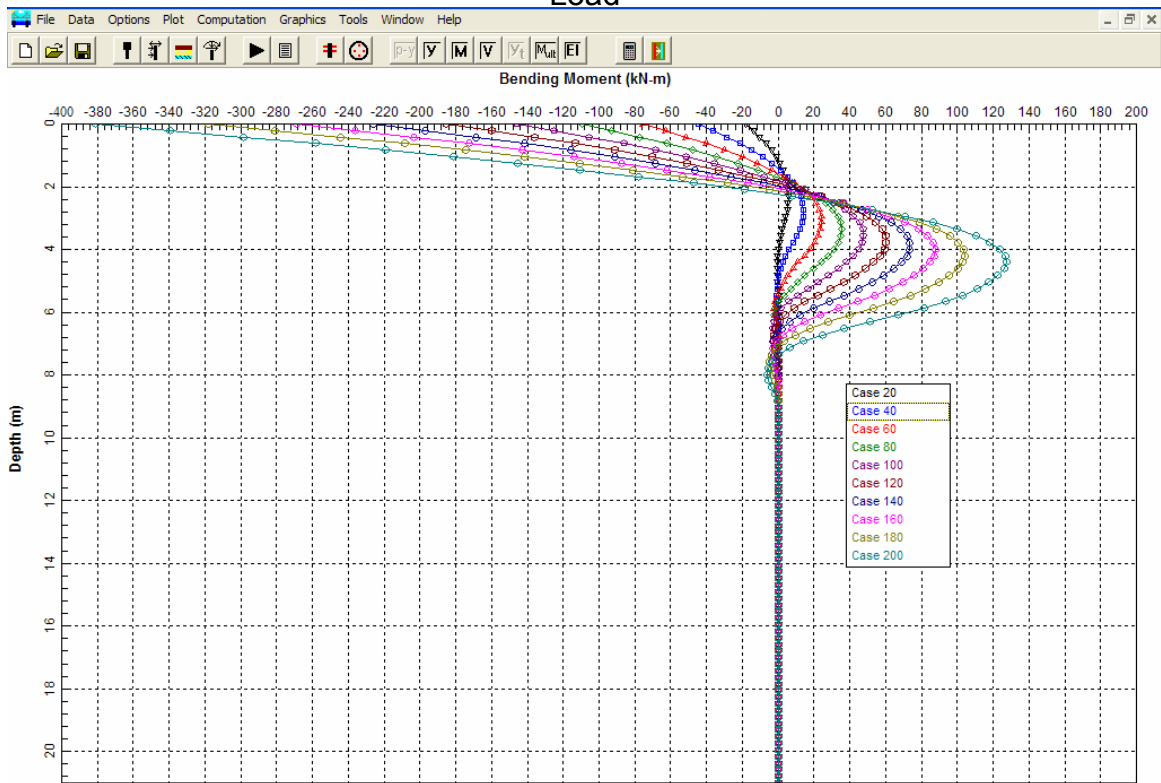


Figure F.40: South Abutment – Plot of Moment *versus* Depth as a Function of Lateral Load

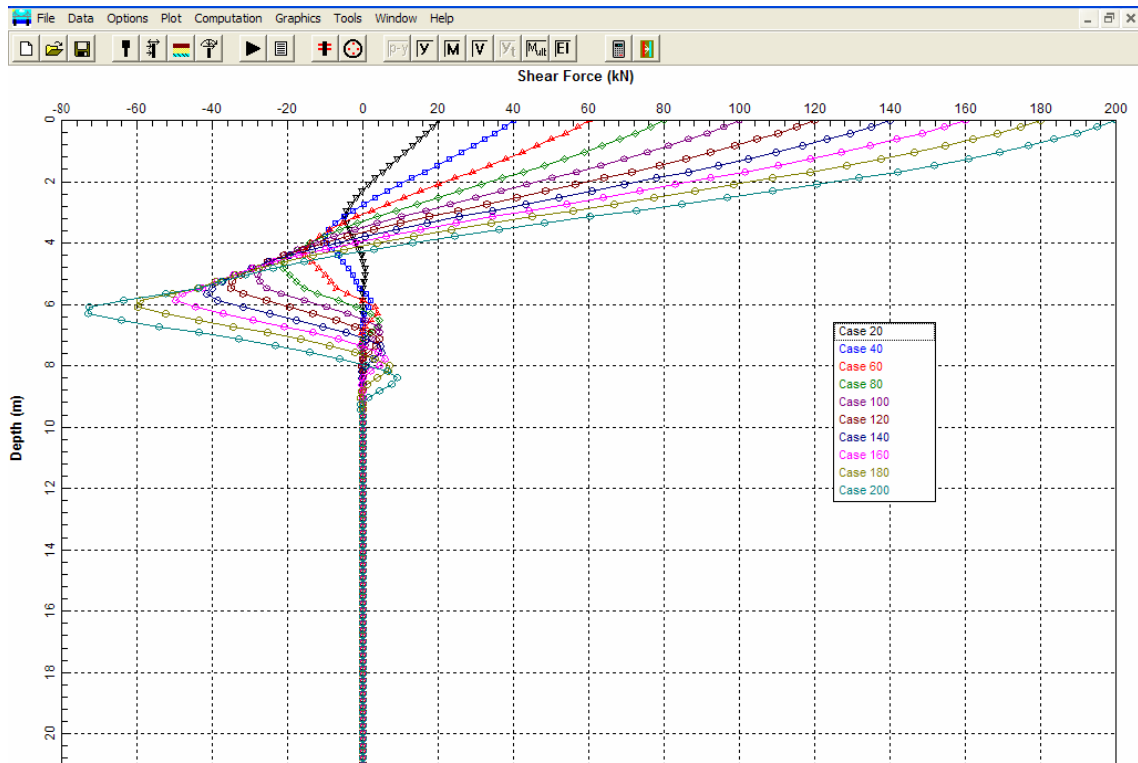


Figure F.41: South Abutment – Plot of Shear *versus* Depth as a Function of Lateral Load

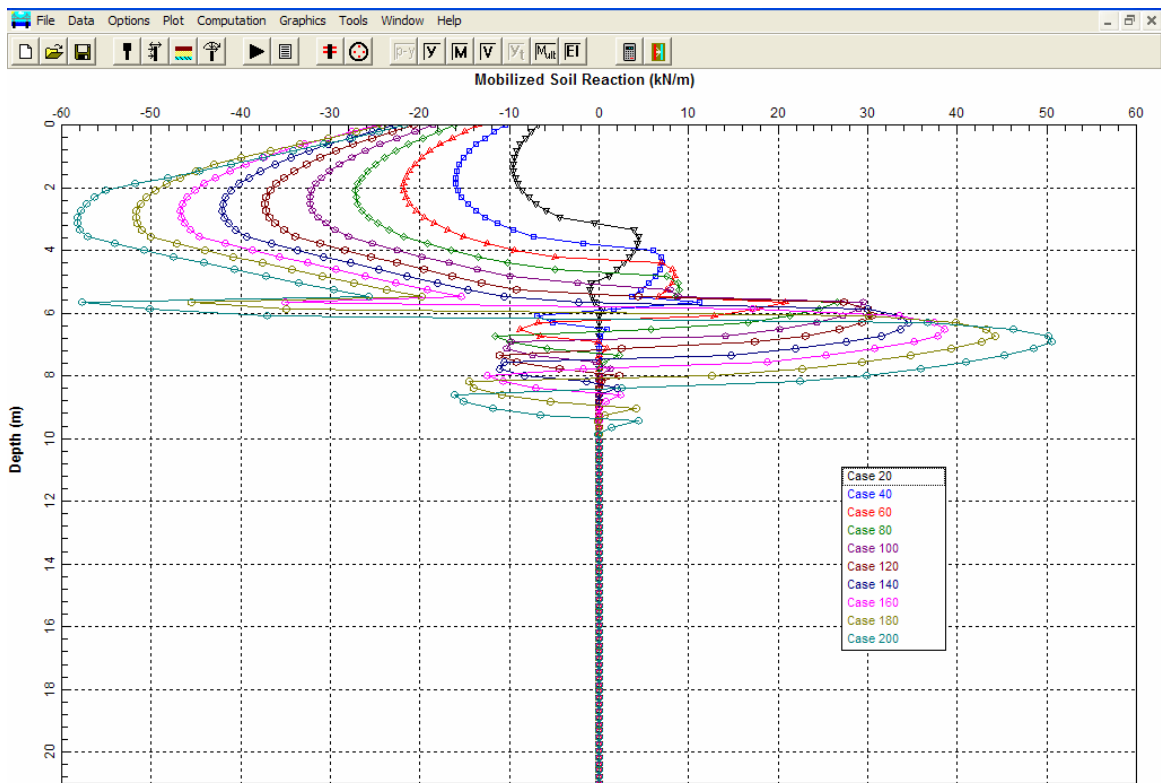


Figure F.42: South Abutment – Plot of Soil Reaction *versus* Depth as a Function of Lateral Load

F.5 GROUP UPLIFT LOAD CALCULATIONS

The maximum uplift load on a pile group is estimated to be 1,800 kN with a maximum uplift load per pile of 100 kN.

F.5.1 North Abutment - AASHTO Code (2002)

For the pile group at the North Abutment and the soil profile interpreted from Soil Boring S-1 as shown in Figure F.3. Perform an uplift capacity calculations based on the AASHTO Code for service load design. Use the method outlined in Section 9.8.3.1.

According to AASHTO specifications (2002), the uplift capacity of a pile group should be limited to the lesser value determined from any of the following.

1. The design uplift capacity of a single pile times the number of piles in a pile group. The design uplift capacity of a single pile is specified as $\frac{1}{3}$ the ultimate shaft resistance calculated in a static analysis method or $\frac{1}{2}$ the failure load determined from an uplift load test.

The ultimate shaft resistance for a single pile as calculated from a static analysis using the Nordlund method is 898 kN. The design uplift capacity is:

$$= \frac{1}{3} \text{ (ultimate shaft resistance)}$$

$$= \frac{1}{3} \text{ (898 kN)}$$

$$= 299 \text{ kN}$$

The design group uplift capacity based on criterion 1 is:

$$= \text{(uplift capacity of a single pile) (number of piles in a group)}$$

$$= 299 \text{ kN (24)}$$

$$= 7,176 \text{ kN}$$

North Abutment - AASHTO Code (2002) (continued)

2. Two-thirds ($\frac{2}{3}$) of the effective weight of the pile group and the soil contained within a block defined by the perimeter of the pile group and the embedded length of the piles.

$$\text{Buoyant unit weight of concrete} = 24 \text{ kN/m}^3 - 9.8 \text{ kN/m}^3 = 14.2 \text{ kN/m}^3$$

Effective weight of pile group (24 piles):

$$\begin{aligned} &= 24 (0.356 \text{ m}) (0.356 \text{ m}) (11.5 \text{ m}) (24 \text{ kN/m}^3 - 9.8 \text{ kN/m}^3) \\ &= 497 \text{ kN} \end{aligned}$$

Effective weight of soil:

$$\begin{aligned} &= (\text{Layer 1} + \text{Layer 2} + \text{Layer 3}) (\text{Gross Area of Pile Group} - \text{Pile Area}) \\ &= [16.5 \text{ kN/m}^3 (1.0 \text{ m}) + 6.7 \text{ kN/m}^3 (3.0 \text{ m}) + 7.8 \text{ kN/m}^3 (7.0 \text{ m}) + \\ &\quad 9.8 \text{ kN/m}^3 (0.5 \text{ m})] \{ (3.36 \text{ m}) (10.86 \text{ m}) - 24 (0.356 \text{ m}) (0.356 \text{ m}) \} \\ &= [16.5 \text{ kN/m}^2 + 20.1 \text{ kN/m}^2 + 54.6 \text{ kN/m}^2 + 4.9 \text{ kN/m}^2] \{ 36.49 \text{ m}^2 - 3.04 \text{ m}^2 \} \\ &= [96.1 \text{ kN/m}^2] \{ 33.45 \text{ m}^2 \} = 3,215 \text{ kN} \end{aligned}$$

The effective weight of the pile group and the soil contained within a block defined by the perimeter of the pile group and the embedded length of the pile is equal to 497 kN plus 3,215 kN, or 3,712 kN.

The design group uplift capacity based on criterion 2 is:

$$\begin{aligned} &= \frac{2}{3} (3,712 \text{ kN}) \\ &= 2,475 \text{ kN} \end{aligned}$$

North Abutment - AASHTO Code (2002) (continued)

3. One-half ($\frac{1}{2}$) the effective weight of the pile group and the soil contained within a block defined by the perimeter of the pile group and the embedded pile length plus $\frac{1}{2}$ the total soil shear resistance on the peripheral surface of the pile group.

The effective weight of the pile group and the soil contained within a block defined by the perimeter of the pile group, as calculated in criteria 2 above, is equal to 3,712 kN.

The total soil shear resistance on the peripheral surface of the pile group is calculated from the following equation.

$$\text{Unit shear resistance of cohesionless soil} = p_d \tan \phi$$

Where:

p_d is the effective overburden stress at depth d , and

ϕ is the friction angle of the soil.

Note: $p_d \tan \phi$ is used for a soil-to-soil failure.

As calculated in Section F.2.1.2:

Layer 1a: $p_{d1a} = 57.8 \text{ kPa}$ (midpoint of layer 1a - 1 m thick)

$$\phi_{1a} = 29^\circ$$

Layer 1b: $p_{d1b} = 76.1 \text{ kPa}$ (midpoint of layer 1b - 3 m thick)

$$\phi_{1b} = 29^\circ$$

Layer 2: $p_{d2} = 113.4 \text{ kPa}$ (midpoint of layer 2 - 7 m thick)

$$\phi_2 = 31^\circ$$

North Abutment - AASHTO Code (2002) (continued)

$$\text{Layer 3: } p_{d3} = 143.1 \text{ kPa (midpoint of layer 3 - 0.5 m thick)}$$

$$\phi_3 = 36^\circ$$

Thus,

$$\begin{aligned} \text{Layer 1a: } R_{s1a} &= 57.8 \text{ kPa (tan } 29^\circ) (3.36 \text{ m} + 10.86 \text{ m}) (1 \text{ m}) (2) \\ &= 911 \text{ kN} \end{aligned}$$

$$\begin{aligned} \text{Layer 1b: } R_{s1a} &= 76.1 \text{ kPa (tan } 29^\circ) (3.36 \text{ m} + 10.86 \text{ m}) (3 \text{ m}) (2) \\ &= 3,599 \text{ kN} \end{aligned}$$

$$\begin{aligned} \text{Layer 2: } R_{s2} &= 113.4 \text{ kPa (tan } 31^\circ) (3.36 \text{ m} + 10.86 \text{ m}) (7 \text{ m}) (2) \\ &= 13,565 \text{ kN} \end{aligned}$$

$$\begin{aligned} \text{Layer 3: } R_{s3} &= 143.1 \text{ kPa (tan } 36^\circ) (3.36 \text{ m} + 10.86 \text{ m}) (0.5 \text{ m}) (2) \\ &= 1,478 \text{ kN} \end{aligned}$$

$$\begin{aligned} \text{Total soil shear resistance} &= R_{s1a} + R_{s1b} + R_{s2} + R_{s3} \\ &= 911 \text{ kN} + 3,599 \text{ kN} + 13,565 \text{ kN} + 1,478 \text{ kN} \\ &= 19,553 \text{ kN} \end{aligned}$$

The design group uplift capacity based on criterion 3 is:

$$\begin{aligned} &= \frac{1}{2} (3,712 \text{ kN}) + \frac{1}{2} (19,553 \text{ kN}) \\ &= 1,856 \text{ kN} + 9,777 \text{ kN} = 11,633 \text{ kN} \end{aligned}$$

According to AASHTO specifications (2002), the uplift capacity of this pile group is limited to 2,475 kN. This is greater than the maximum uplift load in the pile group of 1,800 kN.

F.5.2 Pier 2 - AASHTO Code (2002)

For the pile group at Pier 2 and the soil profile interpreted from Soil Boring S-2 as shown in Figure F.5. Perform an uplift capacity calculations based on the AASHTO Code for service load design. Use the method outlined in Section 9.8.3.1.

According to AASHTO specifications (2002), the uplift capacity of a pile group should be limited to the lesser value determined from any of the following.

1. The design uplift capacity of a single pile times the number of piles in a pile group. The design uplift capacity of a single pile is specified as $\frac{1}{3}$ the ultimate shaft resistance calculated in a static analysis method or $\frac{1}{2}$ the failure load determined from an uplift load test.

The ultimate shaft resistance for a single pile as calculated from a static analysis using the Nordlund method is 984 kN. The design uplift capacity is:

$$= \frac{1}{3} \text{ (ultimate shaft resistance)}$$

$$= \frac{1}{3} \text{ (984 kN)}$$

$$= 328 \text{ kN}$$

The design group uplift capacity based on criterion 1 is:

$$= \text{(uplift capacity of a single pile) (number of piles in a group)}$$

$$= 328 \text{ kN (24)}$$

$$= 7,872 \text{ kN}$$

Pier 2 - AASHTO Code (2002)(continued)

2. Two-thirds ($\frac{2}{3}$) of the effective weight of the pile group and the soil contained within a block defined by the perimeter of the pile group and the embedded length of the piles.

Effective weight of pile group (24 piles):

$$\begin{aligned} &= 24 (0.356 \text{ m}) (0.356 \text{ m}) (10.0 \text{ m}) (24 \text{ kN/m}^3 - 9.8 \text{ kN/m}^3) \\ &= 432 \text{ kN} \end{aligned}$$

Effective weight of soil:

$$\begin{aligned} &= (\text{Layer 1} + \text{Layer 2}) (\text{Gross Area of Pile Group} - \text{Pile Area}) \\ &= [11.4 \text{ kN/m}^3 (4.0 \text{ m}) + 9.8 \text{ kN/m}^3 (6.0 \text{ m})] \\ &\quad \{ (3.36 \text{ m}) (10.86 \text{ m}) - 24 (0.356 \text{ m}) (0.356 \text{ m}) \} \\ &= [45.6 \text{ kN/m}^2 + 58.8 \text{ kN/m}^2] \{ 36.49 \text{ m}^2 - 3.04 \text{ m}^2 \} \\ &= [104.4 \text{ kN/m}^2] \{ 33.45 \text{ m}^2 \} \\ &= 3,492 \text{ kN} \end{aligned}$$

The effective weight of the pile group and the soil contained within a block defined by the perimeter of the pile group and the embedded length of the pile is equal to 432 kN plus 3,492 kN, or 3,924 kN.

The design group uplift capacity based on criterion 2 is:

$$\begin{aligned} &= \frac{2}{3} (3,924 \text{ kN}) \\ &= 2,616 \text{ kN} \end{aligned}$$

Pier 2 - AASHTO Code (2002)(continued)

3. One-half ($\frac{1}{2}$) the effective weight of the pile group and the soil contained within a block defined by the perimeter of the pile group and the embedded pile length plus $\frac{1}{2}$ the total soil shear resistance on the peripheral surface of the pile group.

The effective weight of the pile group and the soil contained within a block defined by the perimeter of the pile group, as calculated in criteria 2 above, is equal to 3,924 kN.

The total soil shear resistance on the peripheral surface of the pile group is calculated from the following equation.

$$\text{Unit shear resistance of cohesionless soil} = p_d \tan \phi$$

Where:

p_d is the effective overburden stress at depth d , and

ϕ is the friction angle of the soil.

Note: $p_d \tan \phi$ is used for a soil-to-soil failure.

As calculated in Section F.2.2.2:

$$\text{Layer 1: } p_{d1} = 48.3 \text{ kPa} \quad (\text{midpoint of layer 1 - 4 m thick})$$

$$\phi_1 = 36^\circ$$

$$\text{Layer 2: } p_{d2} = 100.5 \text{ kPa} \quad (\text{midpoint of layer 2 - 6 m thick})$$

$$\phi_2 = 35^\circ$$

Pier 2 - AASHTO Code (2002)(continued)

Thus,

$$\begin{aligned}\text{Layer 1: } R_{s1} &= 48.3 \text{ kPa } (\tan 36^\circ) (3.36 \text{ m} + 10.86 \text{ m}) (4 \text{ m}) (2) \\ &= 3,992 \text{ kN}\end{aligned}$$

$$\begin{aligned}\text{Layer 2: } R_{s2} &= 100.5 \text{ kPa } (\tan 35^\circ) (3.36 \text{ m} + 10.86 \text{ m}) (6 \text{ m}) (2) \\ &= 12,008 \text{ kN}\end{aligned}$$

$$\begin{aligned}\text{Total soil shear resistance} &= R_{s1} + R_{s2} \\ &= 3,992 \text{ kN} + 12,008 \text{ kN} \\ &= 16,000 \text{ kN}\end{aligned}$$

The design group uplift capacity based on criterion 3 is:

$$\begin{aligned}&= \frac{1}{2} (3,924 \text{ kN}) + \frac{1}{2} (16,000 \text{ kN}) \\ &= 9,962 \text{ kN}\end{aligned}$$

According to AASHTO specifications (2002), the uplift capacity of this pile group is limited to 2,616 kN. This is greater than the maximum uplift load in the pile group of 1,800 kN.

F.5.3 Pier 3 - AASHTO Code (2002)

For the pile group at Pier 3 and the soil profile interpreted from Soil Boring S-3 as shown in Figure F.9. Perform an uplift capacity calculations based on the AASHTO Code for service load design. Use the method outlined in Section 9.8.3.1.

According to AASHTO specifications (2002), the uplift capacity of a pile group should be limited to the lesser value determined from any of the following.

1. The design uplift capacity of a single pile times the number of piles in a pile group. The design uplift capacity of a single pile is specified as $\frac{1}{3}$ the ultimate shaft resistance calculated in a static analysis method or $\frac{1}{2}$ the failure load determined from an uplift load test.

The ultimate shaft resistance for a single pile as calculated from a static analysis using the Nordlund method and α -Method is 1,171 kN. The design uplift capacity is:

$$= \frac{1}{3} \text{ (ultimate shaft resistance)}$$

$$= \frac{1}{3} \text{ (1,171 kN)}$$

$$= 390 \text{ kN}$$

The design group uplift capacity based on criterion 1 is:

$$= \text{(uplift capacity of a single pile) (number of piles in a group)}$$

$$= 390 \text{ kN (24)}$$

$$= 9,360 \text{ kN}$$

Pier 3 - AASHTO Code (2002)(continued)

2. Two-thirds ($\frac{2}{3}$) of the effective weight of the pile group and the soil contained within a block defined by the perimeter of the pile group and the embedded length of the piles.

Effective weight of pile group (24 piles):

$$\begin{aligned} &= 24 (0.356 \text{ m}) (0.356 \text{ m}) (13.0 \text{ m}) (24 \text{ kN/m}^3 - 9.8 \text{ kN/m}^3) \\ &= 562 \text{ kN} \end{aligned}$$

Effective weight of soil:

$$\begin{aligned} &= (\text{Layer 1} + \text{Layer 2} + \text{Layer 3}) (\text{Gross Area of Pile Group} - \text{Pile Area}) \\ &= [10.6 \text{ kN/m}^3 (1.0 \text{ m}) + 9.8 \text{ kN/m}^3 (3.0 \text{ m}) + 10.4 \text{ kN/m}^3 (9.0 \text{ m})] \\ &\quad \{ (3.36 \text{ m}) (10.86 \text{ m}) - 24 (0.356 \text{ m}) (0.356 \text{ m}) \} \\ &= [10.6 \text{ kN/m}^2 + 29.4 \text{ kN/m}^2 + 93.6 \text{ kN/m}^2] \{ 36.49 \text{ m}^2 - 3.04 \text{ m}^2 \} \\ &= [133.6 \text{ kN/m}^2] \{ 33.45 \text{ m}^2 \} \\ &= 4,469 \text{ kN} \end{aligned}$$

The effective weight of the pile group and the soil contained within a block defined by the perimeter of the pile group and the embedded length of the pile is equal to 562 kN plus 4,469 kN, or 5,031 kN.

The design group uplift capacity based on criterion 2 is:

$$\begin{aligned} &= \frac{2}{3} (5,031 \text{ kN}) \\ &= 3,354 \text{ kN} \end{aligned}$$

Pier 3 - AASHTO Code (2002)(continued)

- 3 One-half ($\frac{1}{2}$) the effective weight of the pile group and the soil contained within a block defined by the perimeter of the pile group and the embedded pile length plus $\frac{1}{2}$ the total soil shear resistance on the peripheral surface of the pile group.

The effective weight of the pile group and the soil contained within a block defined by the perimeter of the pile group, as calculated in criteria 2 above, is equal to 5,031 kN.

The total soil shear resistance on the peripheral surface of the pile group is calculated from the following equation.

$$\text{Unit shear resistance of cohesionless soil} = p_d \tan \phi$$

$$\text{Unit shear resistance of cohesive soil} = c_u$$

Where:

p_d is the effective overburden stress at depth d ,

ϕ is the friction angle of the soil, and

c_u is the average undrained shear strength of the soil.

Note: $p_d \tan \phi$ is used for a soil-to-soil failure.

As calculated in Section F.2.3.1:

$$\text{Layer 1: } p_{d1} = 15.5 \text{ kPa} \quad (\text{midpoint of layer 1 - 1 m thick})$$

$$\phi_1 = 36^\circ$$

$$\text{Layer 2: } c_{u2} = 106 \text{ kPa} \quad (\text{layer 2 - 3 m thick})$$

$$\text{Layer 3: } c_{u3} = 155 \text{ kPa} \quad (\text{layer 3 - 9 m thick})$$

Pier 3 - AASHTO Code (2002)(continued)

Thus,

$$\begin{aligned}\text{Layer 1: } R_{s1} &= 15.5 \text{ kPa } (\tan 36^\circ) (3.36 \text{ m} + 10.86 \text{ m}) (1 \text{ m}) (2) \\ &= 320 \text{ kN}\end{aligned}$$

$$\begin{aligned}\text{Layer 2: } R_{s2} &= 106 \text{ kPa } (3.36 \text{ m}) (10.86 \text{ m}) (3 \text{ m}) (2) \\ &= 9,044 \text{ kN}\end{aligned}$$

$$\begin{aligned}\text{Layer 3: } R_{s3} &= 155 \text{ kPa } (3.36 \text{ m}) (10.86 \text{ m}) (9 \text{ m}) (2) \\ &= 39,674 \text{ kN}\end{aligned}$$

$$\begin{aligned}\text{Total soil shear resistance} &= R_{s1} + R_{s2} + R_{s3} \\ &= 320 \text{ kN} + 9,044 \text{ kN} + 39,674 \text{ kN} \\ &= 49,038 \text{ kN}\end{aligned}$$

The design group uplift capacity based on criterion 3 is:

$$\begin{aligned}&= \frac{1}{2} (5,031 \text{ kN}) + \frac{1}{2} (49,038 \text{ kN}) \\ &= 27,035 \text{ kN}\end{aligned}$$

According to AASHTO specifications (2002), the uplift capacity of this pile group is limited to 3,354 kN. This is greater than the maximum uplift load in the pile group of 1,800 kN.

F.5.4 South Abutment - AASHTO Code (2002)

For the pile group at the South Abutment and the soil profile interpreted from Soil Boring S-4 as shown in Figure F.11. Perform an uplift capacity calculations based on the AASHTO Code for service load design. Use the method outlined in Section 9.8.3.1.

According to AASHTO specifications (2002), the uplift capacity of a pile group should be limited to the lesser value determined from any of the following.

1. The design uplift capacity of a single pile times the number of piles in a pile group. The design uplift capacity of a single pile is specified as $\frac{1}{3}$ the ultimate shaft resistance calculated in a static analysis method or $\frac{1}{2}$ the failure load determined from an uplift load test.

The ultimate shaft resistance for a single pile as calculated from a static analysis using the α -Method is 1,648 kN. The design uplift capacity is:

$$= \frac{1}{3} \text{ (ultimate shaft resistance)}$$

$$= \frac{1}{3} \text{ (1,648 kN)}$$

$$= 549 \text{ kN}$$

The design group uplift capacity based on criterion 1 is:

$$= \text{(uplift capacity of a single pile) (number of piles in a group)}$$

$$= 549 \text{ kN (24)}$$

$$= 13,176 \text{ kN}$$

South Abutment - AASHTO Code (2002) (continued)

2. Two-thirds ($\frac{2}{3}$) of the effective weight of the pile group and the soil contained within a block defined by the perimeter of the pile group and the embedded length of the piles.

Effective weight of pile group (24 piles):

$$\begin{aligned} &= 24 (0.356 \text{ m}) (0.356 \text{ m}) (17.5 \text{ m}) (24 \text{ kN/m}^3 - 9.8 \text{ kN/m}^3) \\ &= 756 \text{ kN} \end{aligned}$$

Effective weight of soil:

$$\begin{aligned} &= (\text{Layer 1} + \text{Layer 2} + \text{Layer 3}) (\text{Gross Area of Pile Group} - \text{Pile Area}) \\ &= [9.2 \text{ kN/m}^3 (5.5 \text{ m}) + 9.7 \text{ kN/m}^3 (9.5 \text{ m}) + 10.5 \text{ kN/m}^3 (2.5 \text{ m})] \\ &\quad \{ (3.36 \text{ m}) (10.86 \text{ m}) - 24 (0.356 \text{ m}) (0.356 \text{ m}) \} \\ &= [50.6 \text{ kN/m}^2 + 92.2 \text{ kN/m}^2 + 26.3 \text{ kN/m}^2] \{ 36.49 \text{ m}^2 - 3.04 \text{ m}^2 \} \\ &= [169.1 \text{ kN/m}^2] \{ 33.45 \text{ m}^2 \} \\ &= 5,656 \text{ kN} \end{aligned}$$

The effective weight of the pile group and the soil contained within a block defined by the perimeter of the pile group and the embedded length of the pile is equal to 756 kN plus 5,656 kN, or 6,412 kN.

The design group uplift capacity based on criterion 2 is:

$$\begin{aligned} &= \frac{2}{3} (6,412 \text{ kN}) \\ &= 4,275 \text{ kN} \end{aligned}$$

South Abutment - AASHTO Code (2002) (continued)

3. One-half ($\frac{1}{2}$) the effective weight of the pile group and the soil contained within a block defined by the perimeter of the pile group and the embedded pile length plus $\frac{1}{2}$ the total soil shear resistance on the peripheral surface of the pile group.

The effective weight of the pile group and the soil contained within a block defined by the perimeter of the pile group, as calculated in criteria 2 above, is equal to 6,412 kN.

The total soil shear resistance on the peripheral surface of the pile group is calculated from the following equation.

$$\text{Unit shear resistance of cohesive soil} = c_u$$

Where: c_u is the average undrained shear strength of the soil.

As calculated in Section F.2.4.1:

$$\text{Layer 1: } c_{u1} = 33 \text{ kPa} \quad (\text{layer 1 - 5.5 m thick})$$

$$\text{Layer 2: } c_{u2} = 93 \text{ kPa} \quad (\text{layer 2 - 9.5 m thick})$$

$$\text{Layer 3: } c_{u3} = 157 \text{ kPa} \quad (\text{layer 3 - 2.5 m thick})$$

Thus,

$$\begin{aligned} \text{Layer 1: } R_{s1} &= 33 \text{ kPa} (3.36 \text{ m} + 10.86 \text{ m}) (5.5 \text{ m}) (2) \\ &= 5,162 \text{ kN} \end{aligned}$$

$$\begin{aligned} \text{Layer 2: } R_{s2} &= 93 \text{ kPa} (3.36 \text{ m} + 10.86 \text{ m}) (9.5 \text{ m}) (2) \\ &= 25,127 \text{ kN} \end{aligned}$$

South Abutment - AASHTO Code (2002) (continued)

$$\begin{aligned}\text{Layer 3: } R_{s3} &= 157 \text{ kPa } (3.36 \text{ m} + 10.86 \text{ m}) (2.5 \text{ m}) (2) \\ &= 11,163 \text{ kN}\end{aligned}$$

$$\begin{aligned}\text{Total soil shear resistance} &= R_{s1} + R_{s2} + R_{s3} \\ &= 5,162 \text{ kN} + 25,127 \text{ kN} + 11,163 \text{ kN} \\ &= 41,452 \text{ kN}\end{aligned}$$

The design group uplift capacity based on criterion 3 is:

$$\begin{aligned}&= \frac{1}{2} (6,412 \text{ kN}) + \frac{1}{2} (41,452 \text{ kN}) \\ &= 23,932 \text{ kN}\end{aligned}$$

According to AASHTO specifications (2002), the uplift capacity of this pile group is limited to 4,275 kN. This is greater than the maximum uplift load in the pile group of 1,800 kN.

F.6 NEGATIVE SHAFT RESISTANCE CALCULATIONS

F.6.1 South Abutment – α -Method

Piles at the South Abutment will be subjected to negative shaft resistance due to soil settlement following the placement of 10 m of approach embankment material behind the abutment after pile installation. This settlement needs to be estimated prior to determining the location of the negative and positive shaft resistances along the pile. The α -method is used to estimate both the positive and negative shaft resistance components. The step-by-step procedure for the analysis of downdrag loading is outlined in Section 9.9.1.1a. The soil profile for the South Abutment interpreted from Soil Boring S-4 is presented in Figure F.11.

STEP 1 Establish the simplified soil profile and soil properties for computing settlement.

Schematic of the South Abutment showing the approach embankment backfill material and the soil profile is presented in Figure F.43.

STEP 2 Determine the overburden pressure increase, Δp , due to the approach embankment fill placed behind the abutment.

The overburden pressure increase, Δp , is calculated using the pressure coefficient, K_f , determined from the pressure distribution chart presented in Figure F.44. The pressure distribution chart calculates the pressure coefficient, K_f , at various depths below the bottom of the fill (x_{b_f}), and also at various distances from the centerline of the fill. The depth below the bottom of the fill is given as a multiple of “ b_f ”, where b_f is the distance from the centerline of the fill to the midpoint of the fill slope, as shown in Figure F.44. Given:

The top width of the fill = 12 m

Side slope of the fill = 2H:1V

The height of the fill, h_f = 10 m

$$\text{Thus, } b_f = \left(\frac{12 \text{ m}}{2} \right) + \left(\frac{10 \text{ m}}{2} \right) 2 = 16 \text{ m}$$

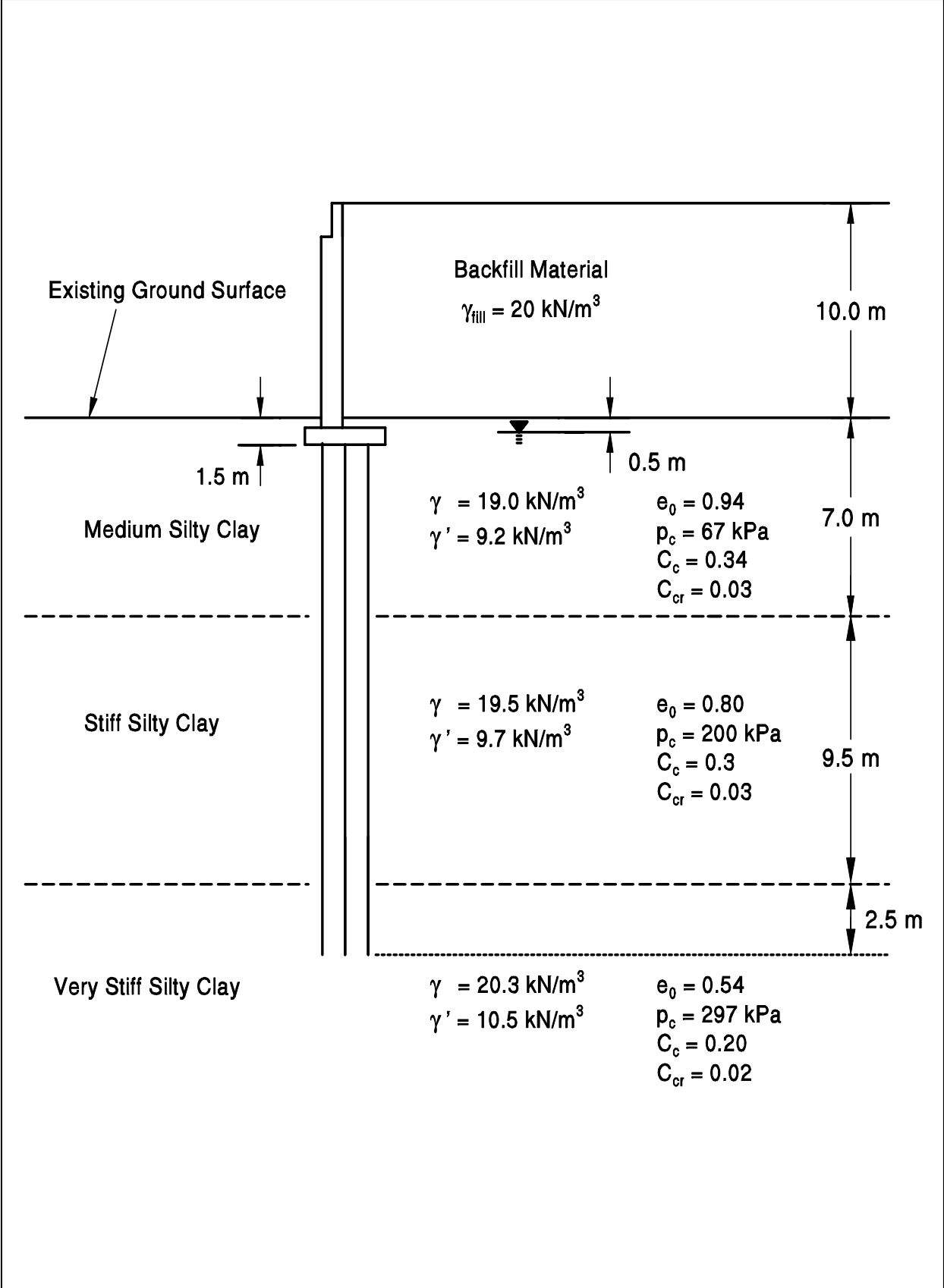


Figure F.43: Schematic of South Abutment Showing the Backfill Material and Soil Profile

Pressure Distribution Chart

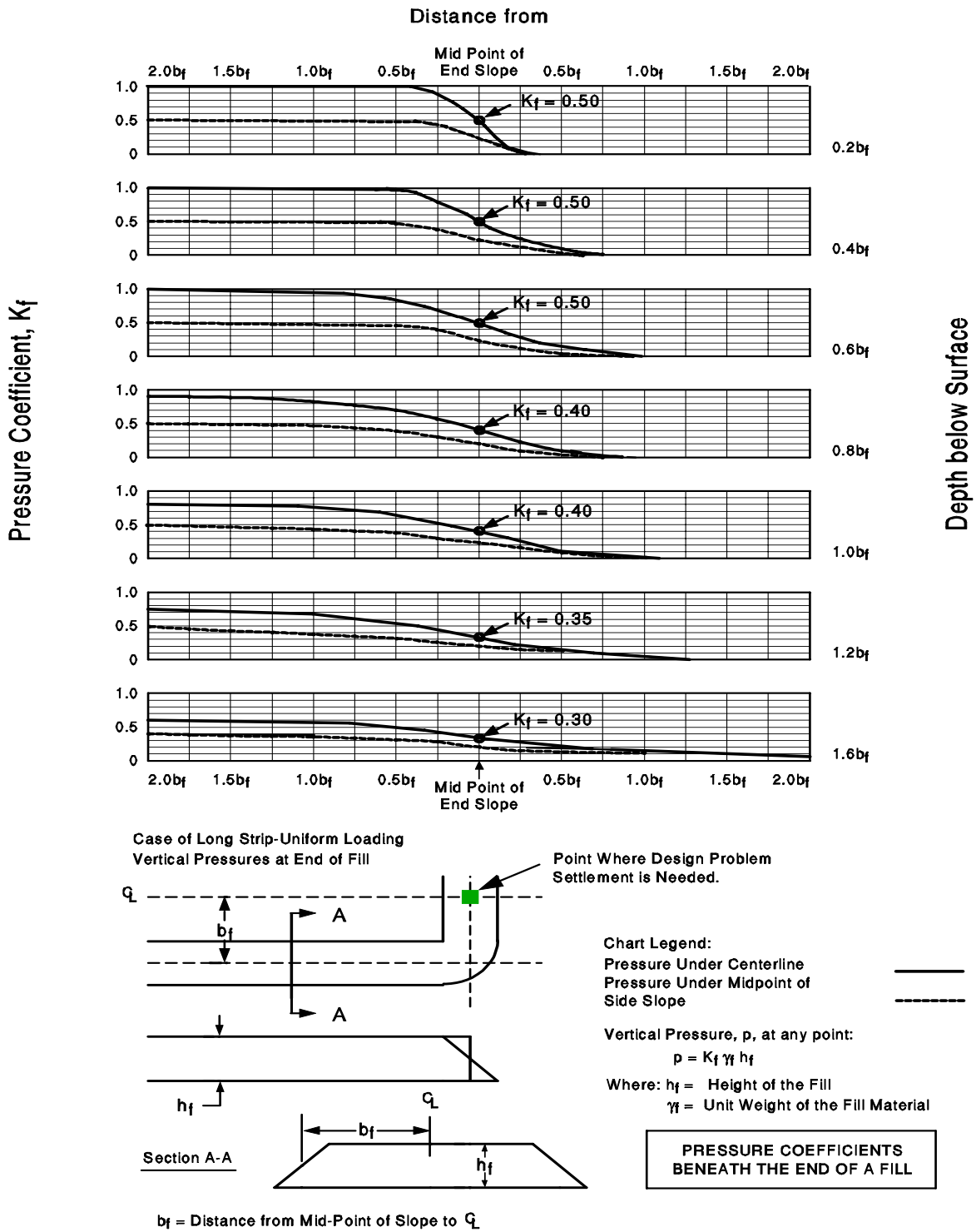


Figure F.44: Pressure Distribution Chart

STEP 2 (continued)

For settlement calculations, the overburden pressure increase, Δp , at various depths beneath the centerline of the fill needs to be calculated. The overburden pressure increase is equal to the pressure coefficient, K_f , multiplied by the unit weight of the fill, γ_f , and the height of the fill, h_f . The unit weight of the fill, γ_f , is 20 kN/m^3 . The height of the fill, h_f , is 10 meters. Table F-5 shows the overburden pressure increase, Δp , at various depths beneath the bottom of the fill. The effective overburden pressure diagram in Figure F.45 shows the effective overburden pressure, p_o , before the backfill is placed, and the effective pressure, $p_o + \Delta p$, after the backfill placement.

For example at depth 3.2 meters below existing ground, the overburden pressure increase, Δp , is equal to:

$$\Delta p = 0.5 (20 \text{ kN/m}^3) (10 \text{ m}) = 100 \text{ kPa}$$

Table F-5 Overburden Pressure Increase Computations - South Abutment		
Depth Below Existing Ground (m)	Pressure Coefficient K_f	$\Delta p = K_f \gamma_f h_f$ (kPa)
Existing Ground Surface = 0	0.50	100.0
$0.2b_f = 3.2 \text{ m}$	0.50	100.0
$0.4b_f = 6.4 \text{ m}$	0.50	100.0
$0.6b_f = 9.6 \text{ m}$	0.50	100.0
$0.8b_f = 12.8 \text{ m}$	0.40	80.0
$1.0b_f = 16.0 \text{ m}$	0.40	80.0
$1.2b_f = 19.2 \text{ m}$	0.35	70.0
$1.6b_f = 25.6 \text{ m}$	0.30	60.0

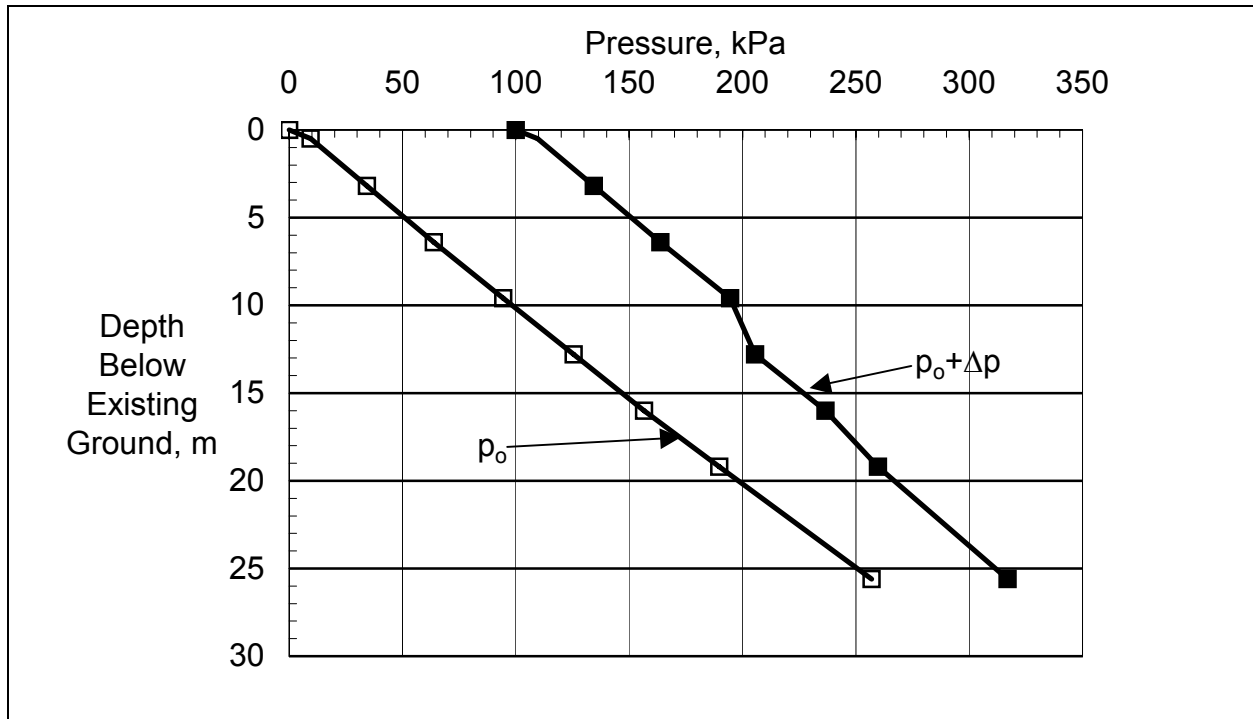


Figure F.45 Effective Overburden Diagram – Original and Original + Increase

STEP 3 Perform settlement computations for the soil layers along the embedded pile length.

- a. Determine consolidation test parameters for each soil layer from laboratory consolidation test results.

The laboratory consolidation test results on the undisturbed samples were plotted on the "log pressure, p versus void ratio, e " (similar to Figure 9.61). The following consolidation test parameters were obtained from the plot.

Soil Layer 1: Preconsolidation pressure, $p_c = 67$ kPa
 Initial void ratio, $e_0 = 0.94$
 Compression index, $C_c = 0.34$
 Recompression index, $C_{cr} = 0.030$

Soil Layer 2: Preconsolidation pressure, $p_c = 200$ kPa
 Initial void ratio, $e_0 = 0.80$
 Compression index, $C_c = 0.30$
 Recompression index, $C_{cr} = 0.030$

STEP 3 (continued)

Soil Layer 3: Preconsolidation pressure, $p_c = 297$ kPa
 Initial void ratio, $e_0 = 0.54$
 Compression index, $C_c = 0.20$
 Recompression index, $C_{cr} = 0.020$

- b. Compute settlement of each soil layer using the appropriate settlement equation provided in Section 9.8.2.3 for cohesive layers or Section 9.8.2.5 for cohesionless layers.

The following equations apply to cohesive layers (see Section 9.8.2.3):

$$s = H \left[\frac{C_{cr}}{1 + e_0} \right] \log \frac{p_o + \Delta p}{p_o} \quad \text{when } p_o + \Delta p \leq p_c$$

$$= H \left[\frac{C_{cr}}{1 + e_0} \log \frac{p_c}{p_o} \right] + H \left[\frac{C_c}{1 + e_0} \log \frac{p_o + \Delta p}{p_c} \right] \quad \text{when } p_o + \Delta p > p_c$$

The settlement of each layer is summarized in the settlement computations in Table F-6. An example of settlement calculation has been presented earlier in Section F.3.

- b. Compute the total settlement over the embedded pile length which is equal to the sum of the settlement from each soil layer.

Based on the settlement calculation table, the calculated settlement is 0.499 meters. Because the total long term settlement of the clay is very high (0.499 m), it is assumed that preloading of soil will be performed by placing additional temporary surcharge for the necessary time period prior to pile installation. It is also assumed that 90% consolidation of clay will be achieved prior to pile installation. Therefore, after installation, the piles will only be subjected to the 10% consolidation settlement left as shown in column 9 of the settlement calculation table, or a total settlement of 0.0499 meter or 49.9 mm.

Table F-6: Settlement Calculations Table - South Abutment

1	2	3	4	5	6	7	8	9	10	11
Soil Type	Soil Layer Below Existing Ground (m)	Soil Layer Thickness (m)	Depth of Midpoint Below Existing Ground (m)	Effective Overburden Pressure at Midpoint p_o (kPa)	Imposed Pressure Increase at Midpoint Δp (kPa)	$(p_o + \Delta p)$ (kPa)	Layer Settlement (m)	10% of Layer Settlement (m)	Depth Below Existing Ground (m)	Relative Soil Movement due to 10% Settlement (m)
Layer 1 $p_c=67\text{kPa}$; $e_0=0.94$ $C_c=0.34$; $C_{cr}=0.030$									0.0	0.0499
	0.0 - 3.0	3.0	1.50	18.7	100.0	118.7	0.156	0.0156	3.0	0.0343
	3.0 - 7.0	4.0	5.00	50.9	100.0	150.9	0.255	0.0255	7.0	0.0088
Layer 2 $p_c=200\text{kPa}$; $e_0=0.80$ $C_c=0.30$; $C_{cr}=0.030$	7.0 - 10.5	3.5	7.75	76.6	100.0	176.6	0.021	0.0021	10.5	0.0067
	10.5 - 13.5	3.0	12.00	117.8	85.0	202.8	0.015	0.0015	13.5	0.0052
	13.5 - 16.5	3.0	15.00	146.9	80.0	226.9	0.034	0.0034	16.5	0.0018
Layer 3 $p_c=297\text{kPa}$; $e_0=0.54$ $C_c=0.20$; $C_{cr}=0.020$	16.5 - 19.5	3.0	18.00	177.2	73.8	251.0	0.006	0.0006	19.5	0.0012
	19.5 - 22.5	3.0	21.00	208.7	67.2	275.9	0.005	0.0005	22.5	0.0007
	22.5 - 25.5	3.0	24.00	240.2	62.5	302.7	0.007	0.0007	25.5	0.0000
Total Settlement =								0.499	0.0499	

STEP 4 Determine the pile length that will experience negative shaft resistance.

Negative shaft resistance occurs due to the settlement between soil and pile. The amount of settlement between soil and pile necessary to mobilize the negative shaft resistance is about 10 mm. Therefore, negative shaft resistance will occur on the pile shaft in each soil layer or portion of a soil layer with a settlement greater than 10 mm.

Column 11 of Table F-6 presents the settlement between soil and pile due to the 10% consolidation settlement at various locations along the pile embedded length. The existing ground surface will experience a total consolidation settlement of 0.0499 meter. At a depth of 3 meters below the existing ground surface, a lesser total settlement will occur which is equal to the total settlement at the existing ground surface minus the consolidation settlement of the top 3 meter soil layer, or 0.0343 meter, as shown in column 11 of the table.

The table also shows that the settlement between soil and pile due the 10% consolidation settlement at 7 meters depth below existing ground is already less than 10 mm which is the minimum required to mobilized the negative shaft resistance. The 7 meter depth also happens to be the end of soil layer 1. Therefore, the pile segment above the 7 meter depth will be subjected to the negative shaft resistances (downdrag) from soil layer 1 while the pile segment below the 7 meter depth will provide the positive shaft resistances (or capacity) to sustain loads from the structure and the negative shaft resistances (downdrag).

STEP 5 Determine magnitude of negative shaft resistance, Q_s^- .

The method used to calculate the ultimate negative shaft resistance over the pile length determined in Step 4 should be the same method used to calculate the ultimate positive shaft resistance, except that it will act in the opposite direction.

As calculated in Step 4 above, the negative shaft resistance will be caused by soil layer 1 which is a medium silty clay. The pile length in soil layer 1 is 5.5 meters. The ultimate positive shaft resistance in soil layer 1 has been calculated with the α -method in Section F.2.4.1 and is equal to:

$$R_{s1} = 259 \text{ kN}$$

STEP 5 (continued)

Therefore, the ultimate negative shaft resistance is equal to:

$$Q_s^- = 259 \text{ kN}$$

STEP 6 Calculate the ultimate pile capacity provided by the positive shaft resistance and the toe resistance, Q_u^+ .

Positive shaft and toe resistances will develop below the depth where the relative pile-soil movements are less than 10 mm. The positive soil resistances can be calculated on the pile length remaining below the negative shaft resistance depth from Step 4 using an appropriate static analysis method for the soil type.

The ultimate pile capacity will be provided by the shaft resistance from soil layers 2 and 3, and the toe resistance, as calculated in Section F.2.4.1. The shaft resistance provided by each of soil layer and the ultimate positive shaft resistance is as follows:

$$\text{Layer 2: } R_{s2}^+ = 1,150 \text{ kN}$$

$$\text{Layer 3: } R_{s3}^+ = 239 \text{ kN}$$

$$\begin{aligned} \text{Total: } R_s^+ &= R_{s2}^+ + R_{s3}^+ \\ &= 1,150 \text{ kN} + 239 \text{ kN} \\ &= 1,389 \text{ kN} \end{aligned}$$

Also as calculated in Section F.2.4.1, the ultimate toe resistance is equal to:

$$R_t = 182 \text{ kN}$$

STEP 6 (continued)

Hence, the ultimate pile capacity is equal to:

$$\begin{aligned} Q_u^+ &= R_s^+ + R_t \\ &= 1,389 \text{ kN} + 182 \text{ kN} = 1,571 \text{ kN} \end{aligned}$$

STEP 7 Calculate the net ultimate pile capacity, Q_u^{NET} , available to resist imposed loads.

$$\begin{aligned} Q_u^{\text{NET}} &= Q_u^+ - Q_s^- \\ &= 1,571 \text{ kN} - 259 \text{ kN} = 1,312 \text{ kN} \end{aligned}$$

The net ultimate pile capacity is smaller than the required ultimate pile capacity of 1780 kN. Therefore, alternatives to obtain higher pile capacities must be considered.

STEP 8 Consider alternatives to obtain higher net ultimate pile capacity.

Alternatives are described in Section 9.9.1.2 and include use of preloading or wick drains to reduce settlements prior to pile installation, use of lightweight fills to reduce settlements that cause downdrag loads, use of friction reducers to reduce downdrag loads, use of higher allowable material stress, and isolation of pile from consolidating soil.

Three alternatives will be further investigated on the following.

Alternate 1: Use bitumen coating on piles to reduce negative shaft resistance.

According to Goudreault and Fellenius (2002), the maximum pile adhesion, c_a , used in the static pile capacity calculation should be limited to 10 kPa when the pile is coated with bitumen.

STEP 8 (continued)

According to the α -method presented in Section F.2.4.1, the pile adhesion from soil layer 1, c_{a1} , is equal to 33 kPa. If the 5.5 m pile length in layer 1 is coated with bitumen, the pile adhesion will become 10 kPa, and therefore the positive or negative shaft resistance is equal to:

$$\begin{aligned} R_{s1}^+ &= Q_s^- = 10 \text{ kPa} (4) (0.356 \text{ m}) (5.5 \text{ m}) \\ &= 78 \text{ kN} \end{aligned}$$

The net ultimate pile capacity available to resist imposed loads is equal to:

$$\begin{aligned} Q_u^{\text{NET}} &= Q_u^+ - Q_s^- \\ &= 1,571 \text{ kN} - 78 \text{ kN} = 1,493 \text{ kN} \end{aligned}$$

This is still less than the required ultimate bearing capacity (1780 kN).

- Notes: 1. Bitumen coating should be applied only to the top 5.5 m of the pile.
2. Batter piles should be avoided if possible.

Alternate 2: Use longer piles driven to a stiffer or denser noncompressible layer.

Try an extra pile embedded length of 3.5 meters or a total pile embedded length of 21.0 meters. This extra pile embedded length will increase the shaft resistance from soil layer 3 and the toe resistance.

The average undrained shear strength of soil layer 3 is equal to:

$$c_{u3} = \frac{158 + 155 + 163 + 168}{4} = 161 \text{ kPa}$$

$$(D/b) = (20.5 \text{ m}) / (0.356 \text{ m}) = 57.58$$

STEP 8 (continued)

Using Figure 9.18 and for $c_{u3} = 161$ kPa and $(D/b) = 57.58$, the pile adhesion is:

$$c_{a3} = 66 \text{ kPa} \quad \text{and therefore } f_{s3} = 66 \text{ kPa}$$

Hence,

$$\begin{aligned} R_{s3} &= 66 \text{ kPa} (4) (0.356 \text{ m}) (6.0 \text{ m}) \\ &= 564 \text{ kN} \end{aligned}$$

The ultimate positive shaft resistance:

$$\begin{aligned} R_s^+ &= R_{s2}^+ + R_{s3}^+ \\ &= 1,150 \text{ kN} + 564 \text{ kN} \\ &= 1,714 \text{ kN} \end{aligned}$$

The average undrained shear strength of soil at the pile toe is equal 170 kPa. The unit toe resistance, q_t , is:

$$\begin{aligned} q_t &= 9 c_u \\ &= 9 (170 \text{ kPa}) = 1,530 \text{ kPa} \end{aligned}$$

The ultimate toe resistance, R_t , is equal to:

$$\begin{aligned} R_t &= 1,530 \text{ kPa} (0.356 \text{ m}) (0.356 \text{ m}) \\ &= 194 \text{ kN} \end{aligned}$$

STEP 8 (continued)

The ultimate pile capacity is equal to:

$$\begin{aligned} Q_u^+ &= R_s^+ + R_t \\ &= 1,714 \text{ kN} + 194 \text{ kN} \\ &= 1,908 \text{ kN} \end{aligned}$$

The net ultimate pile capacity available to resist imposed loads, with an increased pile length to 20.5 meters and a bitumen coating on the top 5.5 meter of the pile:

$$\begin{aligned} Q_u^{\text{NET}} &= Q_u^+ - Q_s^- \\ &= 1,908 \text{ kN} - 78 \text{ kN} \\ &= 1,830 \text{ kN} \end{aligned}$$

This alternate provides the required ultimate capacity, but a cost analysis of alternatives 1 and 2 and a combination of both alternatives should be performed before making the selection.

Alternate 3: A stub abutment instead of a full height abutment may be a better choice for the south abutment. The stub abutment could be supported on a spread footing with specified embankment material and density control in the foundation area. A stub abutment with pile foundation is another alternative available for consideration.

This design problem illustrates the difficulties encountered in designing pile foundations in clay where substantial settlements occur and large downdrag loads are encountered by piles.

F.7 LATERAL SQUEEZE CALCULATIONS

F.7.1 South Abutment - Investigation of Lateral Squeeze

Use the guidelines presented in Section 9.9.3 of Chapter 9.

STEP 1 Determine if abutment tilting can occur.

The backfill material properties:

$$\gamma_f = 20 \text{ kN/m}^3.$$

$$h_f = 10 \text{ meters.}$$

Any tilting which may occur will take place on the top soil layer which is the medium silty clay. The average undrained shear strength, c_u , of the medium silty clay layer is 33 kPa.

Abutment tilting will occur if the following condition govern:

$$\gamma_f h_f > 3 c_u$$

$$20 \text{ kN/m}^3 (10 \text{ m}) > 3 (33 \text{ kPa})$$

$$200 \text{ kPa} > 99 \text{ kPa}$$

Hence, abutment tilting can occur.

STEP 2 Determine the magnitude of horizontal movement.

Two cases will be investigated on the following.

Case 1: If piles are placed before any soil compression occurs.

The computations performed previously for negative shaft resistance indicated the vertical fill settlement is equal to 0.495 meter.

Estimated horizontal movement = $0.25 (0.495 \text{ m}) = 0.124 \text{ m}$

This horizontal movement is not tolerable as it is greater than the 10 mm allowable by the bridge division.

Case 2: If piles are driven after 90% of vertical settlement has occurred.

Estimated vertical fill settlement after 90% settlement has occurred is 0.0495 meter.

Estimated horizontal movement = $0.25 (0.0495 \text{ m}) = 0.0124 \text{ m}$

This movement is also larger than the 10 mm allowed by the bridge division. Because the estimated movement is close, provisions can be made in the bridge shoe and expansion joint design so this movement is tolerable.

F.8 LATERALLY LOADED PILE GROUP CALCULATIONS

As noted in section F.4, the bridge division estimated that group lateral loads range from 600 kN at the interior pile groups to 900 kN at the abutment pile groups. The maximum lateral load per pile is limited to 40kN.

F.8.1 Laterally Loaded Pile Group, North Abutment Example Calculation

Perform a lateral pile group capacity analysis for the 24 pile layout at the North Abutment using the single pile LPILE analyses from section F.4.2 as a starting point. The piles will be laid out in three rows of eight piles (see Figure F.2), with the lateral loading acting along the three pile axis. Prestressed concrete piles, 356 mm square are planned and will be spaced 1.5 meters on center. Piles are embedded 11.5 meters. Use the step by step procedure outlined in Section 9.8.4.

STEP 1 Develop p-y curves for a single pile.

In section F.4.2, p-y curves were assumed based on general soil type used in the LPILE program.

STEP 2 Perform LPILE analyses.

- a. Using the LPILE analysis for the North Abutment in F.4.2 (with nonlinear flexural rigidity effects), edit the input file and use the P_m value for the first row to develop load-deflection and load-moment data. Section 9.8.4 suggests using P_m values of 0.8 for the first row. The p-multiplier can be entered by clicking the Options menu, then selecting "Include p-y Modification Factors." p-multipliers can then be entered by clicking the Data menu, then selecting "Modification Factors for p-y Curves" option. In this screen, p-multipliers can be varied by depth. The input file and abridged numerical output follows.

LPILEP4

FHWA North Abut. - 355 mm-sq PSC - Group lateral, Row 1

```
2 3 0 0 0 0
100 2 0 11.5 0
0 0.355 0.0013 0.126 27800000
11.5 0.355 0.0013 0.126 27800000
4 8 8 0 2
4 0 1 6790 6790
4 1 4 5430 5430
4 4 11 16300 16300
4 11 11.5 33900 33900
0 16.5
1 16.5
1 6.7
4 6.7
4 7.8
11 7.8
11 9.8
11.5 9.8
0 0 29 0 0
1 0 29 0 0
1 0 29 0 0
4 0 29 0 0
4 0 30 0 0
11 0 30 0 0
11 0 36 0 0
11.5 0 36 0 0
0 0.8 1
11.5 0.8 1
0 0 20
10
2 20 0 890
2 40 0 890
2 60 0 890
2 80 0 890
2 100 0 890
2 120 0 890
2 140 0 890
2 160 0 890
2 180 0 890
2 200 0 890
0
1 1 0
100 1E-6 1
1 1
890
41370 262000 413685.52 2.0685E8
0.355 0.355 0 0 0
0.0005 4 2 0.0762
0.102 0.0006
-0.102 0.0006
```

North Abutment, Front Row Lateral Analysis-Echo Input

=====
LPILE Plus for Windows, Version 4.0 (4.0.7)
Analysis of Individual Piles and Drilled Shafts
Subjected to Lateral Loading Using the p-y Method

(c) Copyright ENSOFT, Inc., 1985-2003
All Rights Reserved

=====

Problem Title

FHWA North Abut. - 355 mm-sq PSC - Group lateral, Row 1

Program Options

Units Used in Computations - SI Units, meters, kilopascals

Basic Program Options:

Analysis Type 4:

- Computation of Nonlinear Bending Stiffness and Ultimate Bending Moment Capacity with Pile Response Using User-specified Constant EI

Computation Options:

- Only internally-generated p-y curves used in analysis
- Analysis uses p-y multipliers for group action
- Analysis assumes no shear resistance at pile tip
- Analysis for fixed-length pile or shaft only
- No computation of foundation stiffness matrix elements
- Output pile response for full length of pile
- Analysis assumes no soil movements acting on pile
- No additional p-y curves to be computed at user-specified depths

Solution Control Parameters:

- Number of pile increments = 100
- Maximum number of iterations allowed = 100
- Deflection tolerance for convergence = 10.000E-06 m
- Maximum allowable deflection = 1.0000E+00 m

Printing Options:

- Values of pile-head deflection, bending moment, shear force, and soil reaction are printed for full length of pile.
- Printing Increment (spacing of output points) = 5

 File Structural Properties and Geometry

Pile Length = 11.50 m
 Depth of ground surface below top of pile = .00 m
 Slope angle of ground surface = .00 deg.

Structural properties of pile defined using 2 points

Point	Depth X m	Pile Diameter m	Moment of Inertia m**4	Pile Area Sq. m	Modulus of Elasticity kN/Sq. m
1	0.0000	.35500000	.001300	.1260	27800000.000
2	11.5000	.35500000	.001300	.1260	27800000.000

Please note that because this analysis makes computations of ultimate moment capacity and pile response using nonlinear bending stiffness that the above values of moment of inertia and modulus of are not used for any computations other than total stress due to combined axial loading and bending.

 Soil and Rock Layering Information

The soil profile is modelled using 4 layers

Layer 1 is sand, p-y criteria by Reese et al., 1974

Distance from top of pile to top of layer = .000 m
 Distance from top of pile to bottom of layer = 1.000 m
 p-y subgrade modulus k for top of soil layer = 6790.000 kN/ m**3
 p-y subgrade modulus k for bottom of layer = 6790.000 kN/ m**3

Layer 2 is sand, p-y criteria by Reese et al., 1974

Distance from top of pile to top of layer = 1.000 m
 Distance from top of pile to bottom of layer = 4.000 m
 p-y subgrade modulus k for top of soil layer = 5430.000 kN/ m**3
 p-y subgrade modulus k for bottom of layer = 5430.000 kN/ m**3

Layer 3 is sand, p-y criteria by Reese et al., 1974

Distance from top of pile to top of layer = 4.000 m
 Distance from top of pile to bottom of layer = 11.000 m
 p-y subgrade modulus k for top of soil layer = 16300.000 kN/ m**3
 p-y subgrade modulus k for bottom of layer = 16300.000 kN/ m**3

Layer 4 is sand, p-y criteria by Reese et al., 1974

Distance from top of pile to top of layer = 11.000 m
 Distance from top of pile to bottom of layer = 11.500 m
 p-y subgrade modulus k for top of soil layer = 33900.000 kN/ m**3
 p-y subgrade modulus k for bottom of layer = 33900.000 kN/ m**3

(Depth of lowest layer extends .00 m below pile tip)

 Effective Unit Weight of Soil vs. Depth

Distribution of effective unit weight of soil with depth
 is defined using 8 points

Point No.	Depth X m	Eff. Unit Weight kN/ m**3
1	.00	16.50000
2	1.00	16.50000
3	1.00	6.70000
4	4.00	6.70000
5	4.00	7.80000
6	11.00	7.80000
7	11.00	9.80000
8	11.50	9.80000

 Shear Strength of Soils

Distribution of shear strength parameters with depth
 defined using 8 points

Point No.	Depth X m	Cohesion c kN/ m**2	Angle of Friction Deg.	E50 or k_rm	RQD %
1	.000	.00000	29.00	-----	-----
2	1.000	.00000	29.00	-----	-----
3	1.000	.00000	29.00	-----	-----
4	4.000	.00000	29.00	-----	-----
5	4.000	.00000	30.00	-----	-----
6	11.000	.00000	30.00	-----	-----
7	11.000	.00000	36.00	-----	-----
8	11.500	.00000	36.00	-----	-----

Notes:

- (1) Cohesion = uniaxial compressive strength for rock materials.
- (2) Values of E50 are reported for clay strata.
- (3) Default values will be generated for E50 when input values are 0.
- (4) RQD and k_rm are reported only for weak rock strata.

 p-y Modification Factors

Distribution of p-y multipliers with depth defined using 2 points

Point No.	Depth X m	p-mult	y-mult
1	.000	.8000	1.0000
2	11.500	.8000	1.0000

Loading Type

Cyclic loading criteria was used for computation of p-y curves

Number of cycles of loading = 20.

Pile-head Loading and Pile-head Fixity Conditions

Number of loads specified = 10

Load Case Number 1

Pile-head boundary conditions are Shear and Slope (BC Type 2)

Shear force at pile head = 20.000 kN
Slope at pile head = .000 m/ m
Axial load at pile head = 890.000 kN

(Zero slope for this load indicates fixed-head condition)

Load Case Number 2

Pile-head boundary conditions are Shear and Slope (BC Type 2)

Shear force at pile head = 40.000 kN
Slope at pile head = .000 m/ m
Axial load at pile head = 890.000 kN

(Zero slope for this load indicates fixed-head condition)

.
.[ABRIDGED]

.
Load Case Number 10

Pile-head boundary conditions are Shear and Slope (BC Type 2)

Shear force at pile head = 200.000 kN
Slope at pile head = .000 m/ m
Axial load at pile head = 890.000 kN

(Zero slope for this load indicates fixed-head condition)

 Computations of Ultimate Moment Capacity and Nonlinear Bending Stiffness

File Description:

The pile shape is a rectangular solid pile.

Width = .355 m
 Depth = .355 m

Material Properties:

Compressive Strength of Concrete = 41370.000 kN/ m**2
 Yield Stress of Reinforcement = 262000. kN/ m**2
 Modulus of Elasticity of Reinforcement = 206850000. kN/ m**2
 Number of Reinforcing Bars = 4
 Area of Single Bar = .00050 m**2
 Number of Rows of Reinforcing Bars = 2
 Cover Thickness (edge to bar center) = .076 m

Ultimate Axial Squash Load Capacity = 4703.81 kN

Distribution and Area of Steel Reinforcement

Row Number	Area of Reinforcement m**2	Distance to Centroidal Axis m
1	.000600	.1020
2	.000600	-.1020

Axial Thrust Force = 890.00 kN

Bending Moment kN-m	Bending Stiffness kN-m2	Bending Curvature rad/m	Maximum Strain m/m	Neutral Axis Position m
1.54295127	39190.962	.00003937	.00023366	5.93486814
7.71444547	39189.382	.00019685	.00026170	1.32942587
13.885	39185.750	.00035433	.00028986	.81803677
20.053	39179.988	.00051181	.00031813	.62158314
26.218	39172.157	.00066929	.00034653	.51775257
32.378	39162.188	.00082677	.00037504	.45362225
38.534	39150.185	.00098425	.00040367	.41013020
44.683	39136.085	.00114173	.00043242	.37873943
50.825	39119.844	.00129921	.00046129	.35505146
56.988	39121.516	.00145669	.00049033	.33660160
63.049	39059.507	.00161417	.00051931	.32172146
69.110	39008.681	.00177165	.00054844	.30956600
75.155	38958.023	.00192913	.00057769	.29945812
81.088	38861.083	.00208661	.00060684	.29082363
81.088	36133.990	.00224409	.00061495	.27403133
81.088	33764.548	.00240157	.00063793	.26562977
81.469	31835.639	.00255906	.00066017	.25797573
83.923	30893.279	.00271654	.00068196	.25104214
86.229	30003.115	.00287402	.00070333	.24472065
88.411	29164.014	.00303150	.00072433	.23893543
90.481	28372.973	.00318898	.00074498	.23361065

92.458	27628.502	.00334646	.00076533	.22869755
94.358	26929.177	.00350394	.00078544	.22415821
96.109	26249.199	.00366142	.00080493	.21984097
97.855	25623.877	.00381890	.00082447	.21589207
99.561	25038.090	.00397638	.00084391	.21223026
110.590	21442.569	.00515748	.00098201	.19040569
120.077	18943.856	.00633858	.00111351	.17567181
128.620	17104.480	.00751969	.00124079	.16500599
136.481	15686.050	.00870079	.00136470	.15684818
143.755	14547.283	.00988189	.00148690	.15046711
145.817	13180.644	.01106299	.00158671	.14342518
147.540	12049.856	.01224409	.00168395	.13753162
148.999	11098.438	.01342520	.00177927	.13253185
150.255	10286.974	.01460630	.00187345	.12826336
151.236	9579.525	.01578740	.00196414	.12441196
152.156	8966.965	.01696850	.00205603	.12116726
153.062	8433.379	.01814961	.00214772	.11833424
153.569	7944.317	.01933071	.00223691	.11571789
154.075	7511.548	.02051181	.00232536	.11336697
154.597	7126.607	.02169291	.00242001	.11155773
154.870	6770.554	.02287402	.00250841	.10966183
155.085	6447.050	.02405512	.00259871	.10803135
155.264	6152.428	.02523622	.00269049	.10661213
155.477	5885.409	.02641732	.00278965	.10559917
155.534	5635.593	.02759843	.00288088	.10438580
155.547	5404.764	.02877953	.00297346	.10331867
155.550	5191.809	.02996063	.00306693	.10236530
155.550	4994.901	.03114173	.00316169	.10152569
155.550	4812.383	.03232283	.00325744	.10077816
155.550	4642.734	.03350394	.00336721	.10050190
155.550	4484.639	.03468504	.00346243	.09982479
155.550	4336.956	.03586614	.00355857	.09921810
155.550	4198.689	.03704724	.00365529	.09866558
155.550	4068.967	.03822835	.00375256	.09816181
155.550	3947.020	.03940945	.00418210	.10611919

Ultimate Moment Capacity at a Concrete Strain of 0.003 = 155.548 m- kN

 Computed Values of Load Distribution and Deflection
 for Lateral Loading for Load Case Number 1

Pile-head boundary conditions are Shear and Slope (BC Type 2)
 Specified shear force at pile head = 20.000 kN
 Specified slope at pile head = 0.000E+00 m/ m
 Specified axial load at pile head = 890.000 kN

(Zero slope for this load indicates fixed-head conditions)

Depth X m	Deflect. y m	Moment M kN- m	Shear V kN	Slope S Rad.	Total Stress kN/ m**2	Flx. Rig. EI kN- m**2	Soil Res p kN/ m
0.000	.001791	-28.2073	20.0000	1.70E-17	1.09E+04	36140.000	0.000
.575	.001678	-16.8808	18.4825	-3.58E-04	9368.4	36140.000	-5.242
1.150	.001411	-7.0773	14.6306	-5.46E-04	8029.8	36140.000	-7.067
1.725	.001076	.3865	10.1909	-5.96E-04	7116.3	36140.000	-8.081
2.300	7.44E-04	5.2214	5.6633	-5.48E-04	7776.4	36140.000	-7.441
2.875	4.57E-04	7.5841	1.8469	-4.43E-04	8099.0	36140.000	-5.714
3.450	2.38E-04	8.0079	-.8275	-3.17E-04	8156.9	36140.000	-3.574
4.025	9.18E-05	7.1809	-2.4876	-1.95E-04	8044.0	36140.000	-4.901
4.600	1.02E-05	5.2666	-3.9801	-9.47E-05	7782.6	36140.000	-.621689
5.175	-2.34E-05	3.0487	-3.6091	-2.88E-05	7479.8	36140.000	1.602
5.750	-2.88E-05	1.2915	-2.4598	4.94E-06	7239.8	36140.000	2.187
6.325	-2.19E-05	.2216	-1.2787	1.61E-05	7093.7	36140.000	1.825
6.900	-1.25E-05	-.2555	-.4235	1.52E-05	7098.4	36140.000	1.135
7.475	-5.16E-06	-.3534	4.07E-02	1.00E-05	7111.7	36140.000	.507519
8.050	-9.29E-07	-.2747	.2039	4.92E-06	7101.0	36140.000	.098348
8.625	8.16E-07	-.1554	.1969	1.50E-06	7084.7	36140.000	-.092513
9.200	1.12E-06	-6.14E-02	.1264	-1.74E-07	7071.9	36140.000	-.135321
9.775	8.29E-07	-9.87E-03	5.51E-02	-6.89E-07	7064.8	36140.000	-.106451
10.350	4.23E-07	7.09E-03	7.75E-03	-6.76E-07	7064.5	36140.000	-.057485
10.925	6.78E-08	4.93E-03	-1.14E-02	-5.67E-07	7064.2	36140.000	-.009720
11.500	-2.45E-07	0.0	0.0	-5.35E-07	7063.5	36140.000	.053636

Please note that because this analysis makes computations of ultimate moment capacity and pile response using nonlinear bending stiffness that the above values of total stress due to combined axial stress and bending may not be representative of actual conditions.

Output Verification:

Computed forces and moments are within specified convergence limits.

Output Summary for Load Case No. 1:

Pile-head deflection = .00179060 m
 Computed slope at pile head = 1.69701E-17
 Maximum bending moment = -28.207 kN- m
 Maximum shear force = 20.000 kN
 Depth of maximum bending moment = 0.000 m
 Depth of maximum shear force = 0.000 m
 Number of iterations = 5
 Number of zero deflection points = 3

 Computed Values of Load Distribution and Deflection
 for Lateral Loading for Load Case Number 3

Pile-head boundary conditions are Shear and Slope (BC Type 2)
 Specified shear force at pile head = 60.000 kN
 Specified slope at pile head = 0.000E+00 m/ m
 Specified axial load at pile head = 890.000 kN

(Zero slope for this load indicates fixed-head conditions)

Depth X m	Deflect. Y m	Moment M kN- m	Shear V kN	Slope S Rad.	Total Stress kN/ m**2	Flx. Rig. EI kN- m**2	Soil Res p kN/ m
0.000	.005659	-87.8505	60.0000	-1.89E-17	1.91E+04	36140.000	0.000
.575	.005308	-53.4721	57.2204	-.001123	1.44E+04	36140.000	-12.004
1.150	.004465	-22.6370	46.3629	-.001721	1.02E+04	36140.000	-22.368
1.725	.003410	1.0387	32.3826	-.001882	7205.3	36140.000	-25.597
2.300	.002357	16.4098	18.0357	-.001733	9304.1	36140.000	-23.587
2.875	.001450	23.9456	5.9335	-.001403	1.03E+04	36140.000	-18.127
3.450	7.57E-04	25.3316	-2.5545	-.001004	1.05E+04	36140.000	-11.350
4.025	2.92E-04	22.7462	-7.8311	-6.18E-04	1.02E+04	36140.000	-15.597
4.600	3.31E-05	16.7006	-12.5925	-3.01E-04	9343.8	36140.000	-2.015
5.175	-7.39E-05	9.6778	-11.4364	-9.17E-05	8384.9	36140.000	5.052
5.750	-9.13E-05	4.1071	-7.8031	1.53E-05	7624.3	36140.000	6.923
6.325	-6.94E-05	.7112	-4.0612	5.09E-05	7160.6	36140.000	5.786
6.900	-3.97E-05	-.8053	-1.3491	4.82E-05	7173.4	36140.000	3.603
7.475	-1.64E-05	-1.1186	.1249	3.18E-05	7216.2	36140.000	1.613
8.050	-2.98E-06	-.8707	.6445	1.56E-05	7182.4	36140.000	.314985
8.625	2.57E-06	-.4931	.6237	4.78E-06	7130.8	36140.000	-.291558
9.200	3.54E-06	-.1953	.4011	-5.38E-07	7090.2	36140.000	-.428395
9.775	2.63E-06	-3.17E-02	.1750	-2.18E-06	7067.8	36140.000	-.337492
10.350	1.34E-06	2.23E-02	2.49E-02	-2.14E-06	7066.5	36140.000	-.182478
10.925	2.17E-07	1.56E-02	-3.60E-02	-1.80E-06	7065.6	36140.000	-.031051
11.500	-7.75E-07	0.0	0.0	-1.70E-06	7063.5	36140.000	.169800

Please note that because this analysis makes computations of ultimate moment capacity and pile response using nonlinear bending stiffness that the above values of total stress due to combined axial stress and bending may not be representative of actual conditions.

Output Verification:

Computed forces and moments are within specified convergence limits.

Output Summary for Load Case No. 3:

Pile-head deflection = .00565918 m
 Computed slope at pile head = -1.88557E-17
 Maximum bending moment = -87.850 kN- m
 Maximum shear force = 60.000 kN
 Depth of maximum bending moment = 0.000 m
 Depth of maximum shear force = 0.000 m
 Number of iterations = 6
 Number of zero deflection points = 3

 Summary of Pile-head Response

Definition of symbols for pile-head boundary conditions:

- y = pile-head displacement, m
- M = pile-head moment, kN- m
- V = pile-head shear force, kN
- S = pile-head slope, radians
- R = rotational stiffness of pile-head, m- kN/rad

BC Type	Boundary Condition 1	Boundary Condition 2	Axial Load kN	Pile Head Deflection m	Maximum Moment m- kN	Maximum Shear kN
2	V= 20.000	S= 0.000	890.0000	.001791	-28.2073	20.0000
2	V= 40.000	S= 0.000	890.0000	.003632	-57.0762	40.0000
2	V= 60.000	S= 0.000	890.0000	.005659	-87.8505	60.0000
2	V= 80.000	S= 0.000	890.0000	.008105	-121.7768	80.0000
2	V= 100.000	S= 0.000	890.0000	.010847	-157.4910	100.0000
2	V= 120.000	S= 0.000	890.0000	.013734	-193.8464	120.0000
2	V= 140.000	S= 0.000	890.0000	.016845	-231.7067	140.0000
2	V= 160.000	S= 0.000	890.0000	.020361	-272.0828	160.0000
2	V= 180.000	S= 0.000	890.0000	.024357	-314.9833	180.0000
2	V= 200.000	S= 0.000	890.0000	.028850	-360.1588	200.0000

The analysis ended normally.

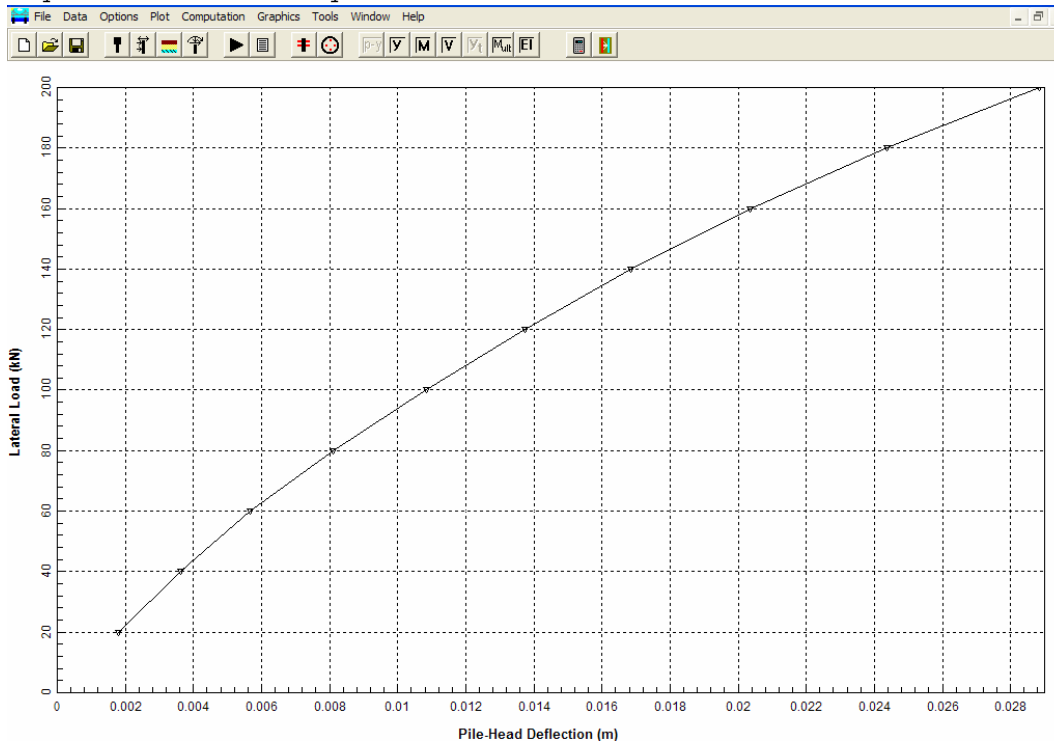


Figure F.46 North Abutment LPILE analysis—Front Row Lateral Load vs Pile Head Deflection

STEP 2 (cont.)

- b. Adjust the LPILE analysis for the first row, using the P_m value for the second row to develop load-deflection and load-moment data. Section 9.8.4 suggests using P_m values of 0.4 for the second row. The input file and abridged numerical output follows.

```
LPILEP4
FHWA North Abut. - 355 mm-sq PSC - Group lateral, Row 2
2 3 0 0 0 0
100 2 0 11.5 0
0 0.355 0.0013 0.126 27800000
11.5 0.355 0.0013 0.126 27800000
4 8 8 0 2
4 0 1 6790 6790
4 1 4 5430 5430
4 4 11 16300 16300
4 11 11.5 33900 33900
0 16.5
1 16.5
1 6.7
4 6.7
4 7.8
11 7.8
11 9.8
11.5 9.8
0 0 29 0 0
1 0 29 0 0
1 0 29 0 0
4 0 29 0 0
4 0 30 0 0
11 0 30 0 0
11 0 36 0 0
11.5 0 36 0 0
0 0.4 1
11.5 0.4 1
0 0 20
10
2 20 0 890
2 40 0 890
2 60 0 890
2 80 0 890
2 100 0 890
2 120 0 890
2 140 0 890
2 160 0 890
2 180 0 890
2 200 0 890
0
1 1 0
100 1E-6 1
1 1
890
41370 262000 413685.52 2.0685E8
0.355 0.355 0 0 0
0.0005 4 2 0.0762
0.102 0.0006
-0.102 0.0006
```

=====

LPPILE Plus for Windows, Version 4.0 (4.0.7)

Analysis of Individual Piles and Drilled Shafts
Subjected to Lateral Loading Using the p-y Method

(c) Copyright ENSOFT, Inc., 1985-2003
All Rights Reserved

=====

Problem Title

FHWA North Abut. - 355 mm-sq PSC - Group lateral, Row 2

Program Options

Units Used in Computations - SI Units, meters, kilopascals

Basic Program Options:

Analysis Type 4:

- Computation of Nonlinear Bending Stiffness and Ultimate Bending Moment Capacity with Pile Response Using User-specified Constant EI

Computation Options:

- Only internally-generated p-y curves used in analysis
- Analysis uses p-y multipliers for group action
- Analysis assumes no shear resistance at pile tip
- Analysis for fixed-length pile or shaft only
- No computation of foundation stiffness matrix elements
- Output pile response for full length of pile
- Analysis assumes no soil movements acting on pile
- No additional p-y curves to be computed at user-specified depths

Solution Control Parameters:

- Number of pile increments = 100
- Maximum number of iterations allowed = 100
- Deflection tolerance for convergence = 10.000E-06 m
- Maximum allowable deflection = 1.0000E+00 m

Printing Options:

- Values of pile-head deflection, bending moment, shear force, and soil reaction are printed for full length of pile.
- Printing Increment (spacing of output points) = 5

 File Structural Properties and Geometry

Pile Length = 11.50 m
 Depth of ground surface below top of pile = .00 m
 Slope angle of ground surface = .00 deg.

Structural properties of pile defined using 2 points

Point	Depth X m	Pile Diameter m	Moment of Inertia m**4	Pile Area Sq. m	Modulus of Elasticity kN/Sq. m
1	0.0000	.35500000	.001300	.1260	27800000.000
2	11.5000	.35500000	.001300	.1260	27800000.000

Please note that because this analysis makes computations of ultimate moment capacity and pile response using nonlinear bending stiffness that the above values of moment of inertia and modulus of are not used for any computations other than total stress due to combined axial loading and bending.

 Soil and Rock Layering Information

The soil profile is modelled using 4 layers

Layer 1 is sand, p-y criteria by Reese et al., 1974

Distance from top of pile to top of layer = .000 m
 Distance from top of pile to bottom of layer = 1.000 m
 p-y subgrade modulus k for top of soil layer = 6790.000 kN/ m**3
 p-y subgrade modulus k for bottom of layer = 6790.000 kN/ m**3

Layer 2 is sand, p-y criteria by Reese et al., 1974

Distance from top of pile to top of layer = 1.000 m
 Distance from top of pile to bottom of layer = 4.000 m
 p-y subgrade modulus k for top of soil layer = 5430.000 kN/ m**3
 p-y subgrade modulus k for bottom of layer = 5430.000 kN/ m**3

Layer 3 is sand, p-y criteria by Reese et al., 1974

Distance from top of pile to top of layer = 4.000 m
 Distance from top of pile to bottom of layer = 11.000 m
 p-y subgrade modulus k for top of soil layer = 16300.000 kN/ m**3
 p-y subgrade modulus k for bottom of layer = 16300.000 kN/ m**3

Layer 4 is sand, p-y criteria by Reese et al., 1974

Distance from top of pile to top of layer = 11.000 m
 Distance from top of pile to bottom of layer = 11.500 m
 p-y subgrade modulus k for top of soil layer = 33900.000 kN/ m**3
 p-y subgrade modulus k for bottom of layer = 33900.000 kN/ m**3

(Depth of lowest layer extends .00 m below pile tip)

 Effective Unit Weight of Soil vs. Depth

Distribution of effective unit weight of soil with depth
 is defined using 8 points

Point No.	Depth X m	Eff. Unit Weight kN/ m**3
1	.00	16.50000
2	1.00	16.50000
3	1.00	6.70000
4	4.00	6.70000
5	4.00	7.80000
6	11.00	7.80000
7	11.00	9.80000
8	11.50	9.80000

 Shear Strength of Soils

Distribution of shear strength parameters with depth
 defined using 8 points

Point No.	Depth X m	Cohesion c kN/ m**2	Angle of Friction Deg.	E50 or k_rm	RQD %
1	.000	.00000	29.00	-----	-----
2	1.000	.00000	29.00	-----	-----
3	1.000	.00000	29.00	-----	-----
4	4.000	.00000	29.00	-----	-----
5	4.000	.00000	30.00	-----	-----
6	11.000	.00000	30.00	-----	-----
7	11.000	.00000	36.00	-----	-----
8	11.500	.00000	36.00	-----	-----

Notes:

- (1) Cohesion = uniaxial compressive strength for rock materials.
- (2) Values of E50 are reported for clay strata.
- (3) Default values will be generated for E50 when input values are 0.
- (4) RQD and k_rm are reported only for weak rock strata.

 p-y Modification Factors

Distribution of p-y multipliers with depth defined using 2 points

Point No.	Depth X m	p-mult	y-mult
1	.000	.4000	1.0000
2	11.500	.4000	1.0000

Loading Type

Cyclic loading criteria was used for computation of p-y curves

Number of cycles of loading = 20.

Pile-head Loading and Pile-head Fixity Conditions

Number of loads specified = 10

Load Case Number 1

Pile-head boundary conditions are Shear and Slope (BC Type 2)

Shear force at pile head = 20.000 kN
Slope at pile head = .000 m/ m
Axial load at pile head = 890.000 kN

(Zero slope for this load indicates fixed-head condition)

.
.[ABRIDGED]
.

Load Case Number 10

Pile-head boundary conditions are Shear and Slope (BC Type 2)

Shear force at pile head = 200.000 kN
Slope at pile head = .000 m/ m
Axial load at pile head = 890.000 kN

(Zero slope for this load indicates fixed-head condition)

Computations of Ultimate Moment Capacity and Nonlinear Bending Stiffness

Pile Description:

The pile shape is a rectangular solid pile.

Width = .355 m
Depth = .355 m

Material Properties:

Compressive Strength of Concrete = 41370.000 kN/ m**2
Yield Stress of Reinforcement = 262000. kN/ m**2
Modulus of Elasticity of Reinforcement = 206850000. kN/ m**2
Number of Reinforcing Bars = 4
Area of Single Bar = .00050 m**2
Number of Rows of Reinforcing Bars = 2
Cover Thickness (edge to bar center) = .076 m
Ultimate Axial Squash Load Capacity = 4703.81 kN

Distribution and Area of Steel Reinforcement

Row Number	Area of Reinforcement m**2	Distance to Centroidal Axis m
1	.000600	.1020
2	.000600	-.1020

Axial Thrust Force = 890.00 kN

Bending Moment kN-m	Bending Stiffness kN-m2	Bending Curvature rad/m	Maximum Strain m/m	Neutral Axis Position m
1.54295127	39190.962	.00003937	.00023366	5.93486814
7.71444547	39189.382	.00019685	.00026170	1.32942587
13.885	39185.750	.00035433	.00028986	.81803677
20.053	39179.988	.00051181	.00031813	.62158314
26.218	39172.157	.00066929	.00034653	.51775257
32.378	39162.188	.00082677	.00037504	.45362225
38.534	39150.185	.00098425	.00040367	.41013020
44.683	39136.085	.00114173	.00043242	.37873943
50.825	39119.844	.00129921	.00046129	.35505146
56.988	39121.516	.00145669	.00049033	.33660160
63.049	39059.507	.00161417	.00051931	.32172146
69.110	39008.681	.00177165	.00054844	.30956600
75.155	38958.023	.00192913	.00057769	.29945812
81.088	38861.083	.00208661	.00060684	.29082363
81.088	36133.990	.00224409	.00061495	.27403133
81.088	33764.548	.00240157	.00063793	.26562977
81.469	31835.639	.00255906	.00066017	.25797573
83.923	30893.279	.00271654	.00068196	.25104214
86.229	30003.115	.00287402	.00070333	.24472065
88.411	29164.014	.00303150	.00072433	.23893543
90.481	28372.973	.00318898	.00074498	.23361065
92.458	27628.502	.00334646	.00076533	.22869755
94.358	26929.177	.00350394	.00078544	.22415821
96.109	26249.199	.00366142	.00080493	.21984097
97.855	25623.877	.00381890	.00082447	.21589207
99.561	25038.090	.00397638	.00084391	.21223026
110.590	21442.569	.00515748	.00098201	.19040569
120.077	18943.856	.00633858	.00111351	.17567181
128.620	17104.480	.00751969	.00124079	.16500599
136.481	15686.050	.00870079	.00136470	.15684818
143.755	14547.283	.00988189	.00148690	.15046711
145.817	13180.644	.01106299	.00158671	.14342518
147.540	12049.856	.01224409	.00168395	.13753162
148.999	11098.438	.01342520	.00177927	.13253185
150.255	10286.974	.01460630	.00187345	.12826336
151.236	9579.525	.01578740	.00196414	.12441196
152.156	8966.965	.01696850	.00205603	.12116726
153.062	8433.379	.01814961	.00214772	.11833424
153.569	7944.317	.01933071	.00223691	.11571789
154.075	7511.548	.02051181	.00232536	.11336697
154.597	7126.607	.02169291	.00242001	.11155773
154.870	6770.554	.02287402	.00250841	.10966183
155.085	6447.050	.02405512	.00259871	.10803135
155.264	6152.428	.02523622	.00269049	.10661213

155.477	5885.409	.02641732	.00278965	.10559917
155.534	5635.593	.02759843	.00288088	.10438580
155.547	5404.764	.02877953	.00297346	.10331867
155.550	5191.809	.02996063	.00306693	.10236530
155.550	4994.901	.03114173	.00316169	.10152569
155.550	4812.383	.03232283	.00325744	.10077816
155.550	4642.734	.03350394	.00336721	.10050190
155.550	4484.639	.03468504	.00346243	.09982479
155.550	4336.956	.03586614	.00355857	.09921810
155.550	4198.689	.03704724	.00365529	.09866558
155.550	4068.967	.03822835	.00375256	.09816181
155.550	3947.020	.03940945	.00418210	.10611919

Ultimate Moment Capacity at a Concrete Strain of 0.003 = 155.548 m- kN

 Computed Values of Load Distribution and Deflection
 for Lateral Loading for Load Case Number 1

Pile-head boundary conditions are Shear and Slope (BC Type 2)
 Specified shear force at pile head = 20.000 kN
 Specified slope at pile head = 0.000E+00 m/ m
 Specified axial load at pile head = 890.000 kN

(Zero slope for this load indicates fixed-head conditions)

Depth X m	Deflect. y m	Moment M kN- m	Shear V kN	Slope S Rad.	Total Stress kN/ m**2	Flx. Rig. EI kN- m**2	Soil Res p kN/ m
0.000	.002734	-33.0244	20.0000	1.89E-18	1.16E+04	36140.000	0.000
.575	.002600	-21.5836	18.9224	-4.34E-04	1.00E+04	36140.000	-4.060
1.150	.002267	-11.2392	15.8860	-6.93E-04	8598.1	36140.000	-5.680
1.725	.001831	-2.7351	12.2183	-8.01E-04	7436.9	36140.000	-6.872
2.300	.001367	3.5533	8.2239	-7.92E-04	7548.7	36140.000	-6.841
2.875	9.35E-04	7.5783	4.5408	-7.01E-04	8098.2	36140.000	-5.845
3.450	5.70E-04	9.6255	1.6140	-5.62E-04	8377.7	36140.000	-4.278
4.025	2.93E-04	10.1847	-.6518	-4.02E-04	8454.1	36140.000	-7.811
4.600	1.07E-04	8.9405	-3.7787	-2.48E-04	8284.2	36140.000	-3.250
5.175	1.79E-06	6.5126	-4.6611	-1.24E-04	7952.7	36140.000	-.061164
5.750	-4.37E-05	3.9721	-4.1388	-4.12E-05	7605.8	36140.000	1.658
6.325	-5.25E-05	1.9153	-2.9883	4.78E-06	7325.0	36140.000	2.187
6.900	-4.32E-05	.5457	-1.7704	2.35E-05	7138.0	36140.000	1.964
7.475	-2.85E-05	-.1881	-.7952	2.56E-05	7089.2	36140.000	1.402
8.050	-1.52E-05	-.4580	-.1642	2.00E-05	7126.0	36140.000	.803476
8.625	-5.84E-06	-.4551	.1542	1.25E-05	7125.6	36140.000	.330933
9.200	-5.76E-07	-.3344	.2513	6.15E-06	7109.1	36140.000	.034826
9.775	1.64E-06	-.1953	.2249	1.95E-06	7090.2	36140.000	-.105163
10.350	2.04E-06	-8.66E-02	.1511	-2.35E-07	7075.3	36140.000	-.138800
10.925	1.62E-06	-2.15E-02	7.62E-02	-1.04E-06	7066.4	36140.000	-.116361
11.500	9.75E-07	0.0	0.0	-1.15E-06	7063.5	36140.000	-.106891

Please note that because this analysis makes computations of ultimate moment capacity and pile response using nonlinear bending stiffness that the above values of total stress due to combined axial stress and bending may not be representative of actual conditions.

Output Verification:

Computed forces and moments are within specified convergence limits.

Output Summary for Load Case No. 1:

Pile-head deflection = .00273403 m
 Computed slope at pile head = 1.88557E-18
 Maximum bending moment = -33.024 kN- m
 Maximum shear force = 20.000 kN
 Depth of maximum bending moment = 0.000 m
 Depth of maximum shear force = 0.000 m
 Number of iterations = 5
 Number of zero deflection points = 2

 Computed Values of Load Distribution and Deflection
 for Lateral Loading for Load Case Number 2

Pile-head boundary conditions are Shear and Slope (BC Type 2)

Specified shear force at pile head = 40.000 kN
 Specified slope at pile head = 0.000E+00 m/ m
 Specified axial load at pile head = 890.000 kN

(Zero slope for this load indicates fixed-head conditions)

Depth X m	Deflect. y m	Moment M kN- m	Shear V kN	Slope S Rad.	Total Stress kN/ m**2	Flx. Rig. EI kN- m**2	Soil Res p kN/ m
0.000	.005698	-68.0143	40.0000	-2.26E-17	1.64E+04	36140.000	0.000
.575	.005421	-44.9851	38.6053	-8.99E-04	1.32E+04	36140.000	-6.030
1.150	.004731	-23.5969	33.0520	-.001440	1.03E+04	36140.000	-11.850
1.725	.003822	-5.8593	25.5797	-.001669	7863.5	36140.000	-14.347
2.300	.002856	7.3083	17.2380	-.001652	8061.4	36140.000	-14.290
2.875	.001954	15.7486	9.5423	-.001463	9213.8	36140.000	-12.216
3.450	.001193	20.0561	3.4233	-.001173	9801.9	36140.000	-8.947
4.025	6.13E-04	21.2525	-1.3176	-8.41E-04	9965.3	36140.000	-16.352
4.600	2.24E-04	18.6733	-7.8684	-5.19E-04	9613.1	36140.000	-6.819
5.175	4.36E-06	13.6119	-9.7263	-2.60E-04	8922.0	36140.000	-.148874
5.750	-9.10E-05	8.3082	-8.6447	-8.66E-05	8197.9	36140.000	3.450
6.325	-1.10E-04	4.0107	-6.2462	9.73E-06	7611.1	36140.000	4.564
6.900	-9.03E-05	1.1472	-3.7036	4.89E-05	7220.1	36140.000	4.102
7.475	-5.96E-05	-.3888	-1.6658	5.35E-05	7116.6	36140.000	2.931
8.050	-3.18E-05	-.9547	-.3463	4.18E-05	7193.8	36140.000	1.681
8.625	-1.22E-05	-.9502	.3203	2.61E-05	7193.2	36140.000	.693609
9.200	-1.23E-06	-.6988	.5242	1.29E-05	7158.9	36140.000	.074330
9.775	3.41E-06	-.4084	.4699	4.10E-06	7119.3	36140.000	-.218832
10.350	4.26E-06	-.1812	.3160	-4.77E-07	7088.2	36140.000	-.289682
10.925	3.39E-06	-4.51E-02	.1594	-2.16E-06	7069.7	36140.000	-.243269
11.500	2.05E-06	0.0	0.0	-2.40E-06	7063.5	36140.000	-.224200

Please note that because this analysis makes computations of ultimate moment capacity and pile response using nonlinear bending stiffness that the above values of total stress due to combined axial stress and bending may not be representative of actual conditions.

Output Verification:

Computed forces and moments are within specified convergence limits.

Output Summary for Load Case No. 2:

Pile-head deflection = .00569808 m
 Computed slope at pile head = -2.26268E-17
 Maximum bending moment = -68.014 kN- m
 Maximum shear force = 40.000 kN
 Depth of maximum bending moment = 0.000 m
 Depth of maximum shear force = 0.000 m
 Number of iterations = 6
 Number of zero deflection points = 2

.[ABRIDGED]

 Summary of Pile-head Response

Definition of symbols for pile-head boundary conditions:

y = pile-head displacement, m
 M = pile-head moment, kN- m
 V = pile-head shear force, kN
 S = pile-head slope, radians
 R = rotational stiffness of pile-head, m- kN/rad

BC Type	Boundary Condition 1	Boundary Condition 2	Axial Load kN	Pile Head Deflection m	Maximum Moment m- kN	Maximum Shear kN
2	V= 20.000	S= 0.000	890.0000	.002734	-33.0244	20.0000
2	V= 40.000	S= 0.000	890.0000	.005698	-68.0143	40.0000
2	V= 60.000	S= 0.000	890.0000	.009400	-107.5652	60.0000
2	V= 80.000	S= 0.000	890.0000	.013487	-148.7898	80.0000
2	V= 100.000	S= 0.000	890.0000	.018066	-192.3571	100.0000
2	V= 120.000	S= 0.000	890.0000	.023574	-240.1437	120.0000
2	V= 140.000	S= 0.000	890.0000	.030126	-291.7676	140.0000
2	V= 160.000	S= 0.000	890.0000	.037798	-346.9042	160.0000
2	V= 180.000	S= 0.000	890.0000	.046752	-405.5691	180.0000
2	V= 200.000	S= 0.000	890.0000	.057086	-467.6713	200.0000

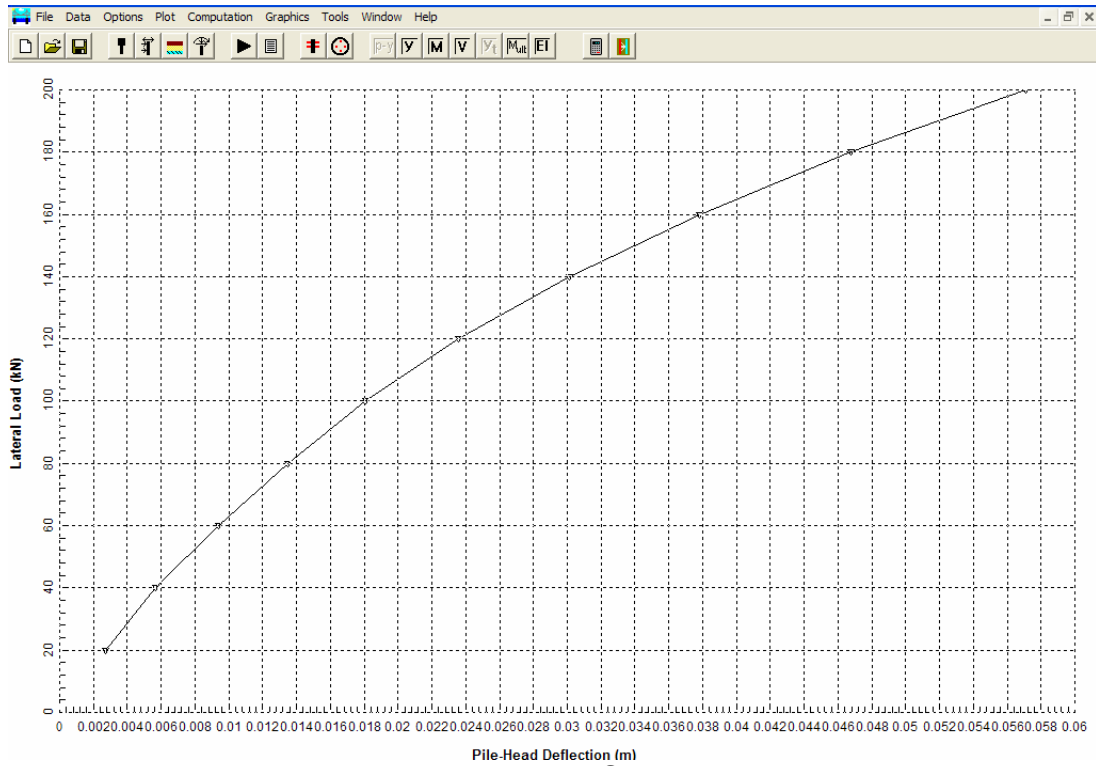


Figure F.47 North Abutment LPILE analysis—Second Row Lateral Load vs Pile Head Deflection

STEP 2 (cont.)

- c. Using the LPILE analysis for second row as a starting point, edit the input file using the P_m value for the third row to develop load-deflection and load-moment data. Section 9.8.4 suggests using P_m values of 0.3 for the third row. The input file and abridged numerical output follows.

```

LPILEP4
FHWA North Abut. - 355 mm-sq PSC - Group lateral, Row 3
2 3 0 0 0 0
100 2 0 11.5 0
0 0.355 0.0013 0.126 27800000
11.5 0.355 0.0013 0.126 27800000
4 8 8 0 2
4 0 1 6790 6790
4 1 4 5430 5430
4 4 11 16300 16300
4 11 11.5 33900 33900
0 16.5
1 16.5
1 6.7
4 6.7
4 7.8
11 7.8
11 9.8
11.5 9.8
0 0 29 0 0
1 0 29 0 0
1 0 29 0 0
4 0 29 0 0
4 0 30 0 0
11 0 30 0 0
11 0 36 0 0
11.5 0 36 0 0
0 0.3 1
11.5 0.3 1
0 0 20
10
2 20 0 890
2 40 0 890
2 60 0 890
2 80 0 890
2 100 0 890
2 120 0 890
2 140 0 890
2 160 0 890
2 180 0 890
2 200 0 890
0
1 1 0
100 1E-6 1
1 1
890
41370 262000 413685.52 2.0685E8
0.355 0.355 0 0 0
0.0005 4 2 0.0762
0.102 0.0006
-0.102 0.0006

```

Row 3 Group Lateral Analysis-LPILE Echo Input

=====

LPPILE Plus for Windows, Version 4.0 (4.0.7)

Analysis of Individual Piles and Drilled Shafts
Subjected to Lateral Loading Using the p-y Method

(c) Copyright ENSOFT, Inc., 1985-2003
All Rights Reserved

=====

Problem Title

FHWA North Abut. - 355 mm-sq PSC - Group lateral, Row 3

Program Options

Units Used in Computations - SI Units, meters, kilopascals

Basic Program Options:

Analysis Type 4:

- Computation of Nonlinear Bending Stiffness and Ultimate Bending Moment Capacity with Pile Response Using User-specified Constant EI

Computation Options:

- Only internally-generated p-y curves used in analysis
- Analysis uses p-y multipliers for group action
- Analysis assumes no shear resistance at pile tip
- Analysis for fixed-length pile or shaft only
- No computation of foundation stiffness matrix elements
- Output pile response for full length of pile
- Analysis assumes no soil movements acting on pile
- No additional p-y curves to be computed at user-specified depths

Solution Control Parameters:

- Number of pile increments = 100
- Maximum number of iterations allowed = 100
- Deflection tolerance for convergence = 10.000E-06 m
- Maximum allowable deflection = 1.0000E+00 m

Printing Options:

- Values of pile-head deflection, bending moment, shear force, and soil reaction are printed for full length of pile.
- Printing Increment (spacing of output points) = 5

 File Structural Properties and Geometry

Pile Length = 11.50 m
 Depth of ground surface below top of pile = .00 m
 Slope angle of ground surface = .00 deg.

Structural properties of pile defined using 2 points

Point	Depth X m	Pile Diameter m	Moment of Inertia m**4	Pile Area Sq. m	Modulus of Elasticity kN/Sq. m
1	0.0000	.35500000	.001300	.1260	27800000.000
2	11.5000	.35500000	.001300	.1260	27800000.000

Please note that because this analysis makes computations of ultimate moment capacity and pile response using nonlinear bending stiffness that the above values of moment of inertia and modulus of are not used for any computations other than total stress due to combined axial loading and bending.

 Soil and Rock Layering Information

The soil profile is modelled using 4 layers

Layer 1 is sand, p-y criteria by Reese et al., 1974

Distance from top of pile to top of layer = .000 m
 Distance from top of pile to bottom of layer = 1.000 m
 p-y subgrade modulus k for top of soil layer = 6790.000 kN/ m**3
 p-y subgrade modulus k for bottom of layer = 6790.000 kN/ m**3

Layer 2 is sand, p-y criteria by Reese et al., 1974

Distance from top of pile to top of layer = 1.000 m
 Distance from top of pile to bottom of layer = 4.000 m
 p-y subgrade modulus k for top of soil layer = 5430.000 kN/ m**3
 p-y subgrade modulus k for bottom of layer = 5430.000 kN/ m**3

Layer 3 is sand, p-y criteria by Reese et al., 1974

Distance from top of pile to top of layer = 4.000 m
 Distance from top of pile to bottom of layer = 11.000 m
 p-y subgrade modulus k for top of soil layer = 16300.000 kN/ m**3
 p-y subgrade modulus k for bottom of layer = 16300.000 kN/ m**3

Layer 4 is sand, p-y criteria by Reese et al., 1974

Distance from top of pile to top of layer = 11.000 m
 Distance from top of pile to bottom of layer = 11.500 m
 p-y subgrade modulus k for top of soil layer = 33900.000 kN/ m**3
 p-y subgrade modulus k for bottom of layer = 33900.000 kN/ m**3

(Depth of lowest layer extends .00 m below pile tip)

 Effective Unit Weight of Soil vs. Depth

Distribution of effective unit weight of soil with depth
 is defined using 8 points

Point No.	Depth X m	Eff. Unit Weight kN/ m**3
1	.00	16.50000
2	1.00	16.50000
3	1.00	6.70000
4	4.00	6.70000
5	4.00	7.80000
6	11.00	7.80000
7	11.00	9.80000
8	11.50	9.80000

 Shear Strength of Soils

Distribution of shear strength parameters with depth
 defined using 8 points

Point No.	Depth X m	Cohesion c kN/ m**2	Angle of Friction Deg.	E50 or k_rm	RQD %
1	.000	.00000	29.00	-----	-----
2	1.000	.00000	29.00	-----	-----
3	1.000	.00000	29.00	-----	-----
4	4.000	.00000	29.00	-----	-----
5	4.000	.00000	30.00	-----	-----
6	11.000	.00000	30.00	-----	-----
7	11.000	.00000	36.00	-----	-----
8	11.500	.00000	36.00	-----	-----

Notes:

- (1) Cohesion = uniaxial compressive strength for rock materials.
- (2) Values of E50 are reported for clay strata.
- (3) Default values will be generated for E50 when input values are 0.
- (4) RQD and k_rm are reported only for weak rock strata.

 p-y Modification Factors

Distribution of p-y multipliers with depth defined using 2 points

Point No.	Depth X m	p-mult	y-mult
1	.000	.3000	1.0000
2	11.500	.3000	1.0000

Loading Type

Cyclic loading criteria was used for computation of p-y curves

Number of cycles of loading = 20.

Pile-head Loading and Pile-head Fixity Conditions

Number of loads specified = 10

Load Case Number 1

Pile-head boundary conditions are Shear and Slope (BC Type 2)

Shear force at pile head = 20.000 kN
Slope at pile head = .000 m/ m
Axial load at pile head = 890.000 kN

(Zero slope for this load indicates fixed-head condition)

.
[ABRIDGED]
.

Load Case Number 10

Pile-head boundary conditions are Shear and Slope (BC Type 2)

Shear force at pile head = 200.000 kN
Slope at pile head = .000 m/ m
Axial load at pile head = 890.000 kN

(Zero slope for this load indicates fixed-head condition)

Computations of Ultimate Moment Capacity and Nonlinear Bending Stiffness

File Description:

The pile shape is a rectangular solid pile.

Width = .355 m
Depth = .355 m

Material Properties:

Compressive Strength of Concrete = 41370.000 kN/ m**2
Yield Stress of Reinforcement = 262000. kN/ m**2
Modulus of Elasticity of Reinforcement = 206850000. kN/ m**2
Number of Reinforcing Bars = 4
Area of Single Bar = .00050 m**2
Number of Rows of Reinforcing Bars = 2

Cover Thickness (edge to bar center) = .076 m

Ultimate Axial Squash Load Capacity = 4703.81 kN

Distribution and Area of Steel Reinforcement

Row Number	Area of Reinforcement m**2	Distance to Centroidal Axis m
1	.000600	.1020
2	.000600	-.1020

Axial Thrust Force = 890.00 kN

Bending Moment kN-m	Bending Stiffness kN-m2	Bending Curvature rad/m	Maximum Strain m/m	Neutral Axis Position m
1.54295127	39190.962	.00003937	.00023366	5.93486814
7.71444547	39189.382	.00019685	.00026170	1.32942587
13.885	39185.750	.00035433	.00028986	.81803677
20.053	39179.988	.00051181	.00031813	.62158314
26.218	39172.157	.00066929	.00034653	.51775257
32.378	39162.188	.00082677	.00037504	.45362225
38.534	39150.185	.00098425	.00040367	.41013020
44.683	39136.085	.00114173	.00043242	.37873943
50.825	39119.844	.00129921	.00046129	.35505146
56.988	39121.516	.00145669	.00049033	.33660160
63.049	39059.507	.00161417	.00051931	.32172146
69.110	39008.681	.00177165	.00054844	.30956600
75.155	38958.023	.00192913	.00057769	.29945812
81.088	38861.083	.00208661	.00060684	.29082363
81.088	36133.990	.00224409	.00061495	.27403133
81.088	33764.548	.00240157	.00063793	.26562977
81.469	31835.639	.00255906	.00066017	.25797573
83.923	30893.279	.00271654	.00068196	.25104214
86.229	30003.115	.00287402	.00070333	.24472065
88.411	29164.014	.00303150	.00072433	.23893543
90.481	28372.973	.00318898	.00074498	.23361065
92.458	27628.502	.00334646	.00076533	.22869755
94.358	26929.177	.00350394	.00078544	.22415821
96.109	26249.199	.00366142	.00080493	.21984097
97.855	25623.877	.00381890	.00082447	.21589207
99.561	25038.090	.00397638	.00084391	.21223026
110.590	21442.569	.00515748	.00098201	.19040569
120.077	18943.856	.00633858	.00111351	.17567181
128.620	17104.480	.00751969	.00124079	.16500599
136.481	15686.050	.00870079	.00136470	.15684818
143.755	14547.283	.00988189	.00148690	.15046711
145.817	13180.644	.01106299	.00158671	.14342518
147.540	12049.856	.01224409	.00168395	.13753162
148.999	11098.438	.01342520	.00177927	.13253185
150.255	10286.974	.01460630	.00187345	.12826336
151.236	9579.525	.01578740	.00196414	.12441196
152.156	8966.965	.01696850	.00205603	.12116726
153.062	8433.379	.01814961	.00214772	.11833424
153.569	7944.317	.01933071	.00223691	.11571789
154.075	7511.548	.02051181	.00232536	.11336697
154.597	7126.607	.02169291	.00242001	.11155773

154.870	6770.554	.02287402	.00250841	.10966183
155.085	6447.050	.02405512	.00259871	.10803135
155.264	6152.428	.02523622	.00269049	.10661213
155.477	5885.409	.02641732	.00278965	.10559917
155.534	5635.593	.02759843	.00288088	.10438580
155.547	5404.764	.02877953	.00297346	.10331867
155.550	5191.809	.02996063	.00306693	.10236530
155.550	4994.901	.03114173	.00316169	.10152569
155.550	4812.383	.03232283	.00325744	.10077816
155.550	4642.734	.03350394	.00336721	.10050190
155.550	4484.639	.03468504	.00346243	.09982479
155.550	4336.956	.03586614	.00355857	.09921810
155.550	4198.689	.03704724	.00365529	.09866558
155.550	4068.967	.03822835	.00375256	.09816181
155.550	3947.020	.03940945	.00418210	.10611919

Ultimate Moment Capacity at a Concrete Strain of 0.003 = 155.548 m- kN

 Computed Values of Load Distribution and Deflection
 for Lateral Loading for Load Case Number 1

Pile-head boundary conditions are Shear and Slope (BC Type 2)
 Specified shear force at pile head = 20.000 kN
 Specified slope at pile head = 0.000E+00 m/ m
 Specified axial load at pile head = 890.000 kN

(Zero slope for this load indicates fixed-head conditions)

Depth X m	Deflect. y m	Moment M kN- m	Shear V kN	Slope S Rad.	Total Stress kN/ m**2	Flx. Rig. EI kN- m**2	Soil Res p kN/ m
0.000	.003250	-35.2968	20.0000	-4.34E-17	1.19E+04	36140.000	0.000
.575	.003105	-23.8112	19.1013	-4.70E-04	1.03E+04	36140.000	-3.637
1.150	.002742	-13.2527	16.3651	-7.63E-04	8873.0	36140.000	-5.151
1.725	.002256	-4.3402	13.0075	-9.00E-04	7656.1	36140.000	-6.353
2.300	.001730	2.5372	9.2691	-9.12E-04	7409.9	36140.000	-6.490
2.875	.001225	7.2732	5.7183	-8.31E-04	8056.6	36140.000	-5.741
3.450	7.84E-04	10.0685	2.7802	-6.91E-04	8438.2	36140.000	-4.413
4.025	4.35E-04	11.3297	.3509	-5.19E-04	8610.4	36140.000	-8.714
4.600	1.88E-04	10.5547	-3.3539	-3.42E-04	8504.6	36140.000	-4.300
5.175	3.68E-05	8.2444	-4.8036	-1.92E-04	8189.2	36140.000	-.942768
5.750	-3.97E-05	5.5210	-4.6914	-8.22E-05	7817.3	36140.000	1.129
6.325	-6.54E-05	3.0951	-3.7318	-1.43E-05	7486.1	36140.000	2.046
6.900	-6.24E-05	1.2977	-2.5025	1.98E-05	7240.7	36140.000	2.126
7.475	-4.70E-05	.1798	-1.3792	3.07E-05	7088.0	36140.000	1.733
8.050	-2.95E-05	-.3714	-.5423	2.86E-05	7114.2	36140.000	1.171
8.625	-1.51E-05	-.5317	-2.56E-02	2.10E-05	7136.1	36140.000	.642715
9.200	-5.45E-06	-.4717	.2232	1.28E-05	7127.9	36140.000	.247101
9.775	-3.63E-08	-.3222	.2882	6.45E-06	7107.5	36140.000	.001749
10.350	2.44E-06	-.1663	.2487	2.59E-06	7086.2	36140.000	-.124069
10.925	3.36E-06	-4.82E-02	.1591	9.52E-07	7070.1	36140.000	-.180467
11.500	3.79E-06	0.0	0.0	6.87E-07	7063.5	36140.000	-.311409

Please note that because this analysis makes computations of ultimate moment capacity and pile response using nonlinear bending stiffness that the above values of total stress due to combined axial stress and bending may not be representative of actual conditions.

Output Verification:

Computed forces and moments are within specified convergence limits.

Output Summary for Load Case No. 1:

Pile-head deflection = .00324962 m
 Computed slope at pile head = -4.33681E-17
 Maximum bending moment = -35.297 kN- m
 Maximum shear force = 20.000 kN
 Depth of maximum bending moment = 0.000 m
 Depth of maximum shear force = 0.000 m
 Number of iterations = 5
 Number of zero deflection points = 2

 Computed Values of Load Distribution and Deflection
 for Lateral Loading for Load Case Number 2

Pile-head boundary conditions are Shear and Slope (BC Type 2)

Specified shear force at pile head = 40.000 kN
 Specified slope at pile head = 0.000E+00 m/ m
 Specified axial load at pile head = 890.000 kN

(Zero slope for this load indicates fixed-head conditions)

Depth X m	Deflect. y m	Moment M kN- m	Shear V kN	Slope S Rad.	Total Stress kN/ m**2	Flx. Rig. EI kN- m**2	Soil Res p kN/ m
0.000	.006955	-73.7808	40.0000	2.64E-17	1.71E+04	36140.000	0.000
.575	.006651	-50.6821	38.9019	-9.90E-04	1.40E+04	36140.000	-4.743
1.150	.005883	-28.7626	34.3624	-.001619	1.10E+04	36140.000	-10.163
1.725	.004850	-9.8239	28.0662	-.001922	8404.8	36140.000	-12.580
2.300	.003723	5.0753	20.1427	-.001954	7756.5	36140.000	-13.970
2.875	.002640	15.3748	12.4934	-.001785	9162.7	36140.000	-12.378
3.450	.001694	21.4927	6.1543	-.001487	9998.1	36140.000	-9.530
4.025	9.43E-04	24.3000	.9020	-.001119	1.04E+04	36140.000	-18.861
4.600	4.10E-04	22.7003	-7.1296	-7.39E-04	1.02E+04	36140.000	-9.348
5.175	8.19E-05	17.7659	-10.2970	-4.15E-04	9489.2	36140.000	-2.099
5.750	-8.39E-05	11.9193	-10.0883	-1.79E-04	8690.9	36140.000	2.387
6.325	-1.40E-04	6.6980	-8.0415	-3.20E-05	7978.0	36140.000	4.382
6.900	-1.34E-04	2.8221	-5.4030	4.18E-05	7448.8	36140.000	4.570
7.475	-1.01E-04	.4063	-2.9853	6.58E-05	7119.0	36140.000	3.733
8.050	-6.37E-05	-.7887	-1.1804	6.14E-05	7171.2	36140.000	2.528
8.625	-3.27E-05	-1.1400	-6.35E-02	4.52E-05	7219.2	36140.000	1.391
9.200	-1.19E-05	-1.0146	.4762	2.77E-05	7202.0	36140.000	.538343
9.775	-1.65E-07	-.6943	.6193	1.40E-05	7158.3	36140.000	.007951
10.350	5.21E-06	-.3589	.5359	5.66E-06	7112.5	36140.000	-.265151
10.925	7.23E-06	-.1042	.3436	2.12E-06	7077.7	36140.000	-.388693
11.500	8.20E-06	0.0	0.0	1.55E-06	7063.5	36140.000	-.673827

Please note that because this analysis makes computations of ultimate moment capacity and pile response using nonlinear bending stiffness that the above values of total stress due to combined axial stress and bending may not be representative of actual conditions.

Output Verification:

Computed forces and moments are within specified convergence limits.

Output Summary for Load Case No. 2:

Pile-head deflection = .00695511 m
 Computed slope at pile head = 2.63980E-17
 Maximum bending moment = -73.781 kN- m
 Maximum shear force = 40.000 kN
 Depth of maximum bending moment = 0.000 m
 Depth of maximum shear force = 0.000 m
 Number of iterations = 7
 Number of zero deflection points = 2

. [ABRIDGED]

 Summary of Pile-head Response

Definition of symbols for pile-head boundary conditions:

y = pile-head displacement, m
 M = pile-head moment, kN- m
 V = pile-head shear force, kN
 S = pile-head slope, radians
 R = rotational stiffness of pile-head, m- kN/rad

BC Type	Boundary Condition 1	Boundary Condition 2	Axial Load kN	Pile Head Deflection m	Maximum Moment m- kN	Maximum Shear kN
2	V= 20.000	S= 0.000	890.0000	.003250	-35.2968	20.0000
2	V= 40.000	S= 0.000	890.0000	.006955	-73.7808	40.0000
2	V= 60.000	S= 0.000	890.0000	.011498	-116.6035	60.0000
2	V= 80.000	S= 0.000	890.0000	.016553	-161.2939	80.0000
2	V= 100.000	S= 0.000	890.0000	.022735	-210.8144	100.0000
2	V= 120.000	S= 0.000	890.0000	.030344	-265.1962	120.0000
2	V= 140.000	S= 0.000	890.0000	.039597	-324.1805	140.0000
2	V= 160.000	S= 0.000	890.0000	.050707	-387.6993	160.0000
2	V= 180.000	S= 0.000	890.0000	.063563	-455.0322	180.0000
2	V= 200.000	S= 0.000	890.0000	.078336	-526.1806	200.0000

The analysis ended normally.

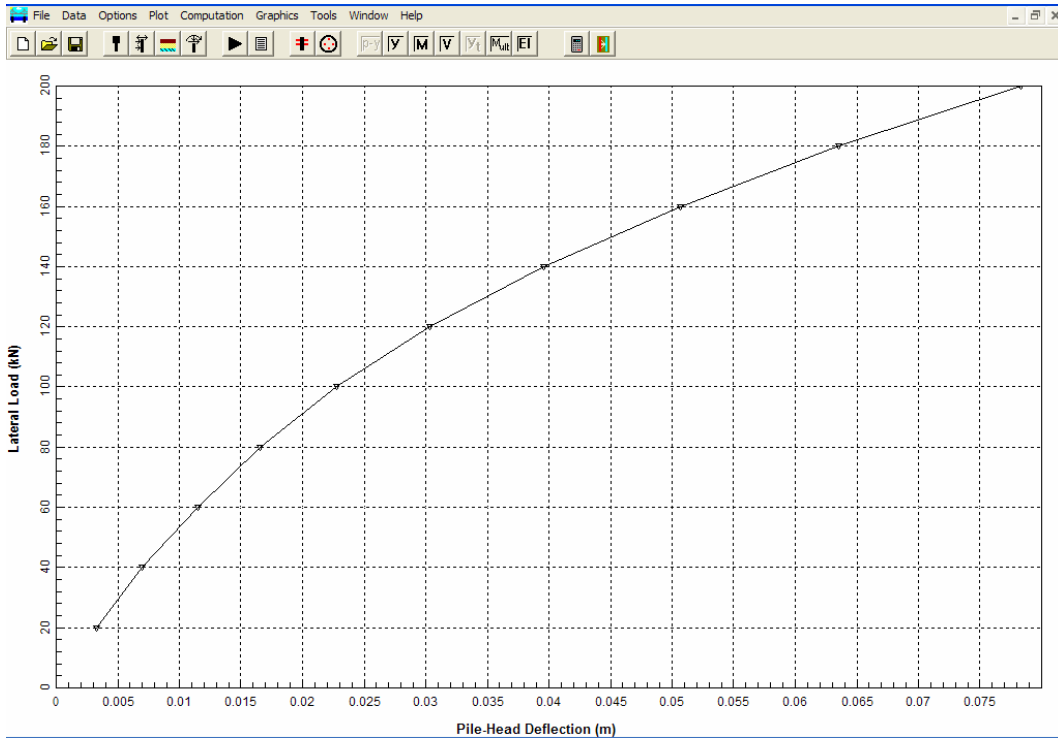


Figure F.48 North Abutment LPILE analysis—Third Row Lateral Load vs Pile Head Deflection

STEP 3 Estimate group deflection under lateral load.

- a. Plot the Lateral Load vs. Pile Head Deflection Curves for each Row (shown in Figures F.46, F.47 and F.48) on the same plot. Average the loads for a given deflection to determine the average group response to a lateral load as shown in Figure F.49.
- b. Divide the lateral load to be resisted (900 kN) by number of piles (24) to determine the average lateral load resisted per pile. Estimate the group deflection from the average group deflection curve at this load. From Figure F.49, the average group deflection for an approximately 40 kN per pile lateral load is 5.4 mm.

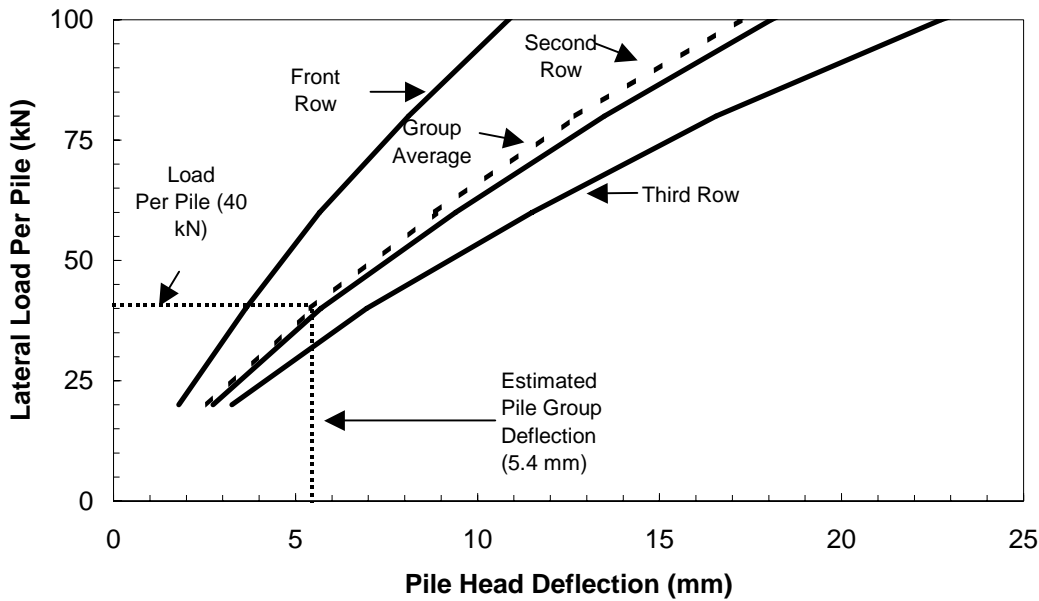


Figure F.49 Average Group Deflection vs. Lateral Load Curves

STEP 4. Evaluate pile structural acceptability.

- a. Plot the maximum bending moment versus deflection for each row of piles as shown in Figure F.50. This plot can be constructed from the “Summary of Pile Head Response” tables shown in the LPILE numeric summaries.
- b. Check the structural adequacy for each row of piles. Using the 5.4 mm estimated group deflection, determine the maximum bending moment. In this example, the graphs show maximum bending moments of 84, 64 and 58 kN-m for the front, second and third rows, respectively.
- c. In the LPILE “Load Case Number...” output tables, find the maximum bending moment and determine the maximum pile stress associated with it. For the North abutment, maximum bending moments of 84, 64 and 58 kN-m in rows 1, 2 and 3, respectively, correspond to Total Stresses of 19,000; 16,000; and 14,500 kPa.
- d. Compare maximum pile stresses to the pile yield stress. Assuming a 34,500 kPa compressive strength and a prestress level of 6,900 kPa, the maximum total stress of 19,000 kPa is within normally recommended limits.

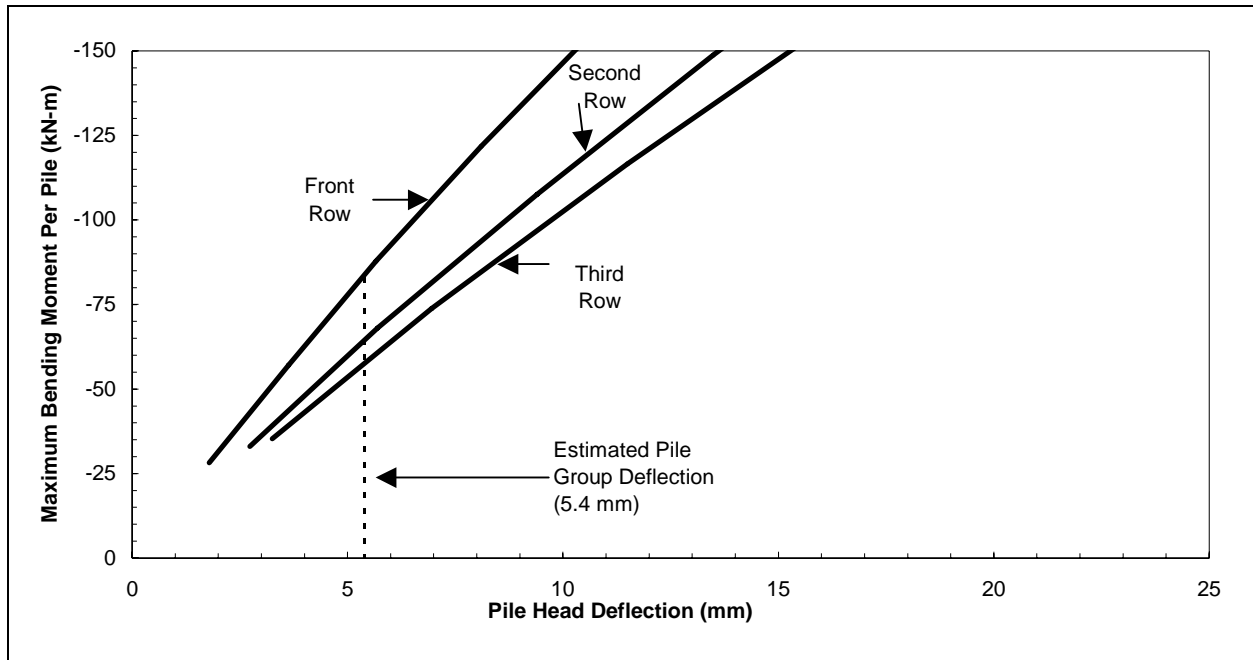


Figure F.50 Maximum Bending Moment vs Pile Head Deflection

- STEP 5 Perform refined pile group evaluation that considers superstructure-substructure interaction. These analyses are not shown here, but can be performed with FBPIER or other methods.
- STEP 6 Repeat for each Pier and the South Abutment. These analyses are not included in this discussion.

F.9 PRECONSTRUCTION DRIVEABILITY ANALYSES WITH GRLWEAP

As noted in Chapter 12.11, the proposed pile sections and minimum pile penetrations should be evaluated by using a wave equation program to ensure the piles can be safely installed. Using the static soil analyses calculated by Driven in sections F.2.1.4, F.2.2.7, F.2.3.3, and F.2.4.3., GRLWEAP driveability files are generated. The hammer and driving system data is input, the depths to be analyzed are refined, and the analysis is run. The input and output results will be summarized here.

For each soil profile, the following hammer was selected based on local availability. It is used to evaluate installation penetration resistance and stresses with a “typical” hammer; once a contractor is selected, further wave equation studies should be performed or submitted to check the hammer that will actually be used to install the piles on the site.

Hammer	Conmaco 140 (single acting air) 56.9 kJ rated energy; 62.2 kN ram, 0.91 m stroke
Hammer Cushion	152 mm Blue Nylon
Helmet	18.09 kN
Pile Cushion	254 mm Plywood (Concrete Piles only)

F.9.1 North Abutment Preconstruction Driveability

This analysis was initially generated from the Soil Boring S-1 file in Driven. Driven created a GRLWEAP input file that included the general pile properties, a detailed soil resistance distribution and soil damping, quake and set-up parameters based on the soil type. The hammer and driving system parameters were entered, the gain/loss factor was selected as 1.0 for both shaft and toe (per Table 9-20), and the depths for analysis were set every 0.5 m to the pile penetration. The analysis was run, and the results follow. In this case, penetration resistance is greater than 25 blows per 0.25 m, and the pile compressive and tensile stresses are with FHWA limits for typical prestressed concrete piles.

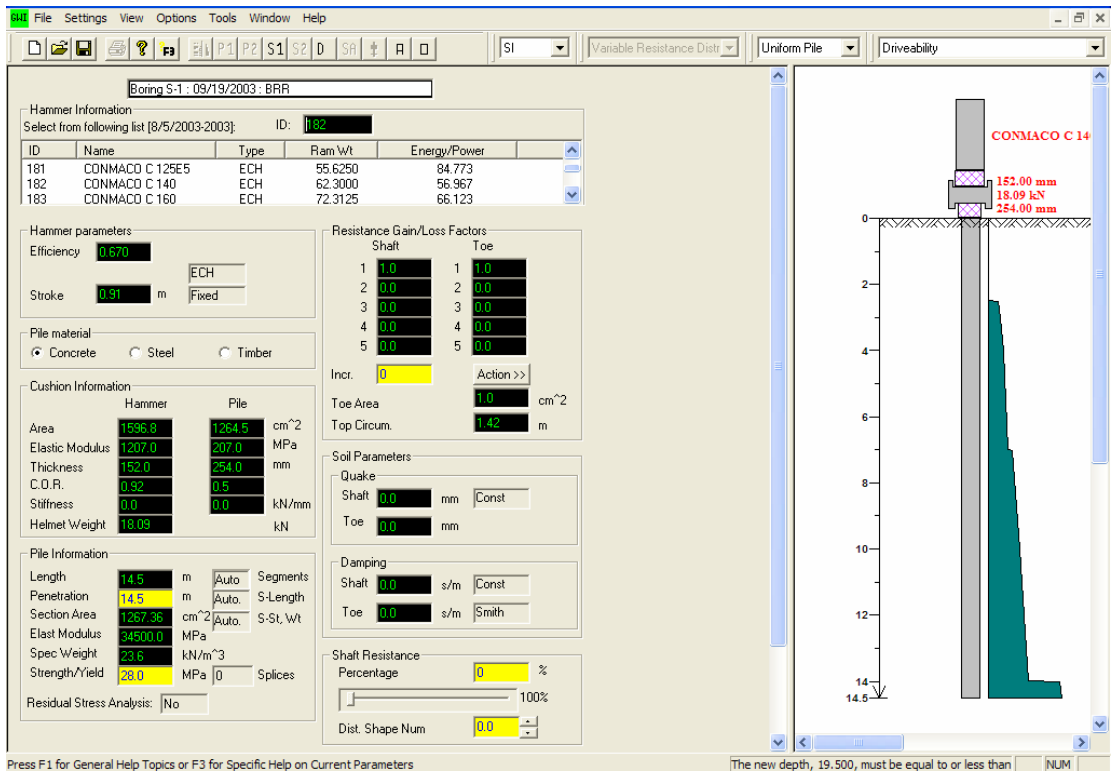


Figure F 51 GRLWEAP Main Input Screen

Input File Contents

```

Boring S-1 : 09/19/2003 : BRR
OUT OSG HAM STR FUL PEL N SPL N-U P-D %SK ISM 0 PHI RSA ITR H-D MXT DEx
-100 0 182 0 0 0 0 0 0 3 0 0 0 0 0 0 0 0.000
  File g Hammer g
  9.810 9.810
    W Cp A Cp E Cp T Cp CoR ROut StCp
  18.090 1596.800 1207.0 152.000 0.920 3.000 0.0
    A Cu E Cu T Cu CoR ROut StCu
  1264.500 207.0 254.000 0.500 3.000 0.0
    LPle APle EPle WPle Circ Strg CoR ROut
  14.500 1267.360 34500.000 23.600 1.420 28.000 1.000 0.010
  Manufac Hmr Name HmrType No Seg-s
  CONMACO C 140 3 1
    Ram Wt Ram L Ram Dia MaxStrk RtdStrk Effic
  62.30 1397.00 612.65 0.91 0.91 0.67
  No. Assmbly Segs
  2
<---- Assembly Masses ----><----Assembly Stiffnesses---->
  37.291 37.291 0.000 12540.6 12540.6 0.0
  Stroke Effic. Pressure R-Weight T-Delay Exp-Coeff Eps-Str
  0.9100 0.6700 0.0000 0.0000 0.0000 0.0000 0.0100 0.0000
    Qs Qt Js Jt Qx Jx Rati Dept
  0.000 0.000 0.000 0.000 0.000 0.000 0.000 0.000
  Research Soil Model: Atoe, Plug, Gap, Q-fac
  0.000 0.000 0.000 0.000
  Research Soil Model: RD-skn: m, d, toe: m, d
  0.000 0.000 0.000 0.000
  Res. Distribution
  Dpth Rskn Rtoe Qs Qt Js Jt SU F RelE SU T
  0.01 0.00 0.00 2.54 2.97 0.16 0.50 1.00 0.00 0.00
  2.49 0.00 0.00 2.54 2.97 0.16 0.50 1.00 0.00 0.00
  2.50 18.34 77.01 2.54 2.97 0.16 0.50 1.00 0.00 0.00
  3.01 22.08 80.82 2.54 2.97 0.16 0.50 1.00 0.00 0.00
  3.99 29.28 80.82 2.54 2.97 0.16 0.50 1.00 0.00 0.00
  4.01 29.38 80.82 2.54 2.97 0.16 0.50 1.00 0.00 0.00
  6.99 38.26 80.82 2.54 2.97 0.16 0.50 1.00 0.00 0.00
  7.01 47.44 125.39 2.54 2.97 0.16 0.50 1.00 0.00 0.00
  10.01 60.33 125.39 2.54 2.97 0.16 0.50 1.00 0.00 0.00
  13.01 73.21 125.39 2.54 2.97 0.16 0.50 1.00 0.00 0.00
  13.99 77.41 125.39 2.54 2.97 0.16 0.50 1.00 0.00 0.00
  14.01 138.65 919.89 2.54 2.97 0.16 0.50 1.00 0.00 0.00
  14.49 143.29 919.89 2.54 2.97 0.16 0.50 1.00 0.00 0.00
  14.51 143.48 919.89 2.54 2.97 0.16 0.50 1.00 0.00 0.00
  Gain/Loss factors: shaft and toe
  1.00000 0.00000 0.00000 0.00000 0.00000
  1.00000 0.00000 0.00000 0.00000 0.00000
    Dpth L Wait Strk Pmx% Eff. Stff CoR
  0.50 14.50 0.00 0.000 0.000 0.000 0.000 0.000
  1.00 14.50 0.00 0.000 0.000 0.000 0.000 0.000
  1.50 14.50 0.00 0.000 0.000 0.000 0.000 0.000
  2.00 14.50 0.00 0.000 0.000 0.000 0.000 0.000
  2.50 14.50 0.00 0.000 0.000 0.000 0.000 0.000
  3.00 14.50 0.00 0.000 0.000 0.000 0.000 0.000
  3.50 14.50 0.00 0.000 0.000 0.000 0.000 0.000
  4.00 14.50 0.00 0.000 0.000 0.000 0.000 0.000
  .
  .[ABRIDGED]
  .
  10.00 14.50 0.00 0.000 0.000 0.000 0.000 0.000
  10.50 14.50 0.00 0.000 0.000 0.000 0.000 0.000
  11.00 14.50 0.00 0.000 0.000 0.000 0.000 0.000
  11.50 14.50 0.00 0.000 0.000 0.000 0.000 0.000
  12.00 14.50 0.00 0.000 0.000 0.000 0.000 0.000
  12.50 14.50 0.00 0.000 0.000 0.000 0.000 0.000
  13.00 14.50 0.00 0.000 0.000 0.000 0.000 0.000
  13.50 14.50 0.00 0.000 0.000 0.000 0.000 0.000
  14.00 14.50 0.00 0.000 0.000 0.000 0.000 0.000
  14.50 14.50 0.00 0.000 0.000 0.000 0.000 0.000
  0.00 0.00 0.00 0.000 0.000 0.000 0.000 0.000

```

GRLWEAP: WAVE EQUATION ANALYSIS OF PILE FOUNDATIONS
Version 2003
SI Units

Boring S-1 : 09/19/2003 : BRR

Hammer Model:	C 140	Made by:	CONMACO		
No.	Weight kN	Stiffn kN/mm	CoR	C-Slk mm	Dampg kN/m/s
1	62.300				
Helmet	18.090	1231.0	0.920	3.0000	111.8
Cushion		103.1	0.500	3.0000	
Combined Pile Top		100.8			
Assembly	Weight kN	Stiffn kN/mm	CoR	C-Slk mm	
1	37.291	12540.6			
2	37.291	12540.6	0.800	3.0480	

HAMMER OPTIONS:

Hammer File ID No.	182	Hammer Type	Ext.Comb.
--------------------	-----	-------------	-----------

HAMMER DATA:

Ram Weight	(kN)	62.30	Ram Length	(mm)	1397.00
Maximum (Eq) Stroke	(m)	0.91	Actual (Eq) Stroke	(m)	0.91
Efficiency		0.670			

Rated Energy	(kJ)	56.97	Potential Energy	(kJ)	56.69
Kinetic Energy	(kJ)	37.98	Impact Velocity	(m/s)	3.46

HAMMER CUSHION

Cross Sect. Area	(cm2)	1596.80	PILE CUSHION Cross Sect. Area	(cm2)	1264.50
Elastic-Modulus	(MPa)	1207.0	Elastic-Modulus	(MPa)	207.0
Thickness	(mm)	152.00	Thickness	(mm)	254.00
Coeff of Restitution		0.920	Coeff of Restitution		0.500
RoundOut	(mm)	3.0	RoundOut	(mm)	3.0
Stiffness	(kN/mm)	1268.0	Stiffness	(kN/mm)	103.1

Depth (m) 0.5
 Shaft Gain/Loss Factor 1.000 Toe Gain/Loss Factor 1.000

PILE PROFILE:

L b Top	Area	E-Mod	Spec Wt	Circmf	Strength	Wave Sp	EA/c
m	cm2	MPa	kN/m3	m	MPa	m/s	kN/m/s
0.00	1267.4	34500.	23.60	1.420	28.00	3787.	1154.60
14.50	1267.4	34500.	23.60	1.420	28.00	3787.	1154.60

Wave Travel Time 2L/c (ms) 7.658

Pile and Soil Model						Total Capacity Rut (kN)				0.0	
No.	Weight	Stiffn	C-Slk	T-Slk	CoR	Soil-S	Soil-D	Quake	LbTop	Circm	Area
	kN	kN/mm	mm	mm		kN	s/m	mm	m	m	cm2
1	2.891	4523.	3.000	0.000	1.00	0.0	0.000	2.54	0.97	1.4	1267.4
2	2.891	4523.	0.000	0.000	1.00	0.0	0.000	2.54	1.93	1.4	1267.4
15	2.891	4523.	0.000	0.000	1.00	0.0	0.160	2.54	14.50	1.4	1267.4
Toe						0.0	0.500	2.97			

PILE, SOIL, ANALYSIS OPTIONS:

Uniform pile
 No. of Slacks/Splices 0
 File Segments: Automatic
 Pile Damping (%) 3
 Pile Damping Fact.(kN/m/s) 69.276

Driveability Analysis

Soil Damping Option Smith
 Max No Analysis Iterations 0 Time Increment/Critical 160
 Output Time Interval 1 Analysis Time-Input (ms) 0
 Output Level: Normal
 Gravity Mass, Pile, Hammer: 9.810 9.810 9.810
 Output Segment Generation: Automatic

Depth	Stroke	Efficy	PileC.St.	PileC.CoR
m	m		kN/mm	
0.50	0.91	0.670	103.	0.500

INITIAL STATIC ANALYSIS: Total Wt, Sum(R) 136.0 0.0
 Hammer+Pile Weight > Rult: Pile Runs

The remainder of the output file was omitted.

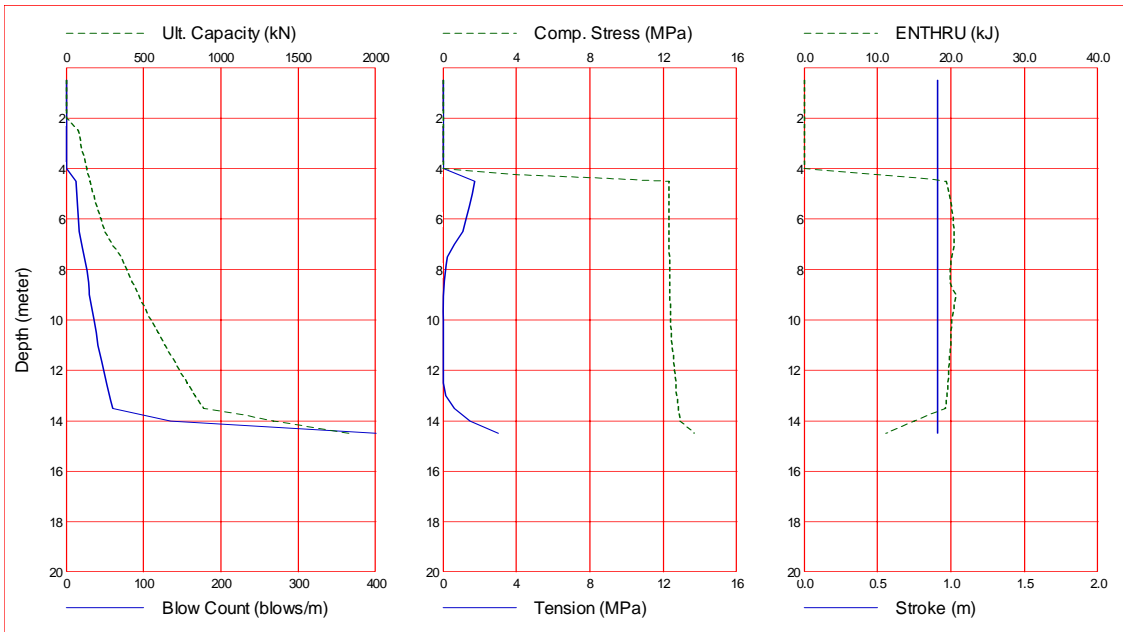


Figure F 52 North Abutment Graphical Driveability Results

Gain/Loss 1 at Shaft and Toe 1.000 / 1.000

Depth m	Ultimate Capacity kN	Friction kN	End Bearing kN	Blow Count blows/m	Comp. Stress MPa	Tension Stress MPa	Stroke m	ENTHRU kJ
0.5	0.0	0.0	0.0	0.0	0.000	0.000	0.91	0.0
1.0	0.0	0.0	0.0	0.0	0.000	0.000	0.91	0.0
1.5	0.0	0.0	0.0	0.0	0.000	0.000	0.91	0.0
2.0	0.0	0.0	0.0	0.0	0.000	0.000	0.91	0.0
2.5	77.1	0.1	77.0	0.0	0.000	0.000	0.91	0.0
3.0	95.2	14.5	80.7	0.0	0.000	0.000	0.91	0.0
3.5	112.2	31.4	80.8	0.0	0.000	0.000	0.91	0.0
4.0	131.7	50.9	80.8	0.0	0.000	0.000	0.91	0.0
4.5	153.1	72.3	80.8	13.0	12.316	-1.725	0.91	19.4
5.0	175.5	94.7	80.8	13.8	12.316	-1.587	0.91	19.8
5.5	199.0	118.2	80.8	14.6	12.317	-1.439	0.91	20.1
6.0	223.6	142.7	80.8	15.5	12.319	-1.272	0.91	20.3
6.5	249.1	168.3	80.8	16.5	12.321	-1.087	0.91	20.4
7.0	298.1	195.0	103.1	19.4	12.325	-0.625	0.91	20.4
7.5	354.8	229.4	125.4	23.7	12.332	-0.222	0.91	20.1
8.0	390.7	265.3	125.4	26.4	12.341	-0.139	0.91	19.9
8.5	428.2	302.8	125.4	28.7	12.350	-0.054	0.91	19.9
9.0	467.2	341.8	125.4	29.9	12.363	-0.003	0.91	20.6
9.5	507.7	382.3	125.4	33.0	12.379	0.000	0.91	20.4
10.0	549.7	424.3	125.4	36.0	12.413	-0.005	0.91	20.1
10.5	593.3	467.9	125.4	38.7	12.454	-0.010	0.91	20.0
11.0	638.4	513.0	125.4	41.5	12.501	-0.015	0.91	20.0
11.5	685.0	559.6	125.4	44.6	12.550	-0.023	0.91	19.8
12.0	733.1	607.7	125.4	48.2	12.606	0.000	0.91	19.7
12.5	782.8	657.4	125.4	52.0	12.672	0.000	0.91	19.6
13.0	834.0	708.6	125.4	55.9	12.740	-0.136	0.91	19.5
13.5	886.7	761.3	125.4	59.9	12.807	-0.637	0.91	19.3
14.0	1338.3	815.7	522.5	135.0	12.910	-1.460	0.91	15.0
14.5	1835.5	915.6	919.9	445.4	13.671	-3.005	0.91	11.1

Total Number of Blows: 487

Driving Time (min): 16 12 9 8 6 6 5 4 4 4

@Blow Rate (b/min): 30 40 50 60 70 80 90 100 110 120

Driving Time for continuously running hammer; any wait times not included

Table F.7 North Abutment Driveability Results

F.9.2 Pier 2 Preconstruction Driveability Analyses

The analyses performed for Pier 2 were discussed in detail in Chapter 16, Example 5 (Section 16.5.5). The input and output files are printed here.

F.9.2.1 Pier 2, Single Concrete Pile Example

Hammer Information
Select from following list [8/5/2003-2003]: ID: 182

ID	Name	Type	Ram Wt	Energy/Power
181	CONMACO C 125E5	ECH	55.625	84.773
182	CONMACO C 140	ECH	62.300	56.967
183	CONMACO C 160	ECH	72.313	66.123

Hammer parameters
Efficiency: 0.670
Stroke: 0.91 m
Type: ECH Fixed

Resistance Gain/Loss Factors

1	1.0	1	1.0
2	0.0	2	0.0
3	0.0	3	0.0
4	0.0	4	0.0
5	0.0	5	0.0

Incr.: 0
Action >>

Soil Parameters

Quake
Shaft: 2.5 mm Const
Toe: 2.5 mm

Damping
Shaft: 0.15 s/m Const
Toe: 0.5 s/m Smith

Shaft Resistance
Percentage: 0 %
Dist. Shape Num: 0.0

Diagram Labels:
CONMACO C 140
152.00 mm
18.09 kN
254.00 mm

Output the result for current input
The new depth, 19.500, must be equal to or less than NUM

Figure F 53 GRLWEAP Main Input Screen, Pier 2 Single Concrete

Input File Contents

```

FHWA - GRLWEAP EXAMPLE #5 - First Pile
OUT OSG HAM STR FUL PEL N SPL N-U P-D %SK ISM 0 PHI RSA ITR H-D MXT Dex
0 0 182 0 0 0 0 0 0 0 3 0 1 0 0 0 0 0 0 0.000
File g Hammer g
9.810 9.810
W Cp A Cp E Cp T Cp CoR ROut StCp
18.090 1596.800 1207.0 152.000 0.920 3.000 0.0
A Cu E Cu T Cu CoR ROut StCu
1264.500 207.0 254.000 0.500 3.000 0.0
LPle APle EPle WPle Circ Strg CoR ROut
14.500 1260.300 40000.000 24.000 1.420 0.000 0.850 3.000
Manufac Hmr Name HmrType No Seg-s
CONMACO C 140 3 1
Ram Wt Ram L Ram Dia MaxStrk RtdStrk Effic
62.30 1397.00 612.65 0.91 0.91 0.67
No. Assmby Segs
2
<---- Assembly Masses <----><----Assembly Stiffnesses<---->
37.291 37.291 0.000 12540.6 12540.6 0.0
Stroke Effic. Pressure R-Weight T-Delay Exp-Coeff Eps-Str
0.9100 0.6700 0.0000 0.0000 0.0000 0.0000 0.0100 0.0000
Qs Qt Js Jt Qx Jx Rati Dept
2.500 2.500 0.150 0.500 0.000 0.000 0.000 0.000
Research Soil Model: Atoe, Plug, Gap, Q-fac
0.000 0.000 0.000 0.000
Research Soil Model: RD-skn: m, d, toe: m, d
0.000 0.000 0.000 0.000
Res. Distribution
Dpth Rskn Rtoe Qs Qt Js Jt SU F RelE SU T
0.00 0.00 0.00 0.00 0.00 0.00 0.00 0.00 0.00 0.00
0.50 28.17 954.00 0.00 0.00 0.00 0.00 0.00 0.00 0.00
3.50 44.87 1995.00 0.00 0.00 0.00 0.00 0.00 0.00 0.00
4.00 47.71 570.00 0.00 0.00 0.00 0.00 0.00 0.00 0.00
6.00 68.18 838.00 0.00 0.00 0.00 0.00 0.00 0.00 0.00
7.50 74.47 769.00 0.00 0.00 0.00 0.00 0.00 0.00 0.00
9.00 80.57 864.00 0.00 0.00 0.00 0.00 0.00 0.00 0.00
10.50 86.77 1147.00 0.00 0.00 0.00 0.00 0.00 0.00 0.00
12.00 92.97 844.00 0.00 0.00 0.00 0.00 0.00 0.00 0.00
13.50 99.21 1060.00 0.00 0.00 0.00 0.00 0.00 0.00 0.00
15.00 105.41 1127.00 0.00 0.00 0.00 0.00 0.00 0.00 0.00
Gain/Loss factors: shaft and toe
1.00000 0.00000 0.00000 0.00000 0.00000
1.00000 0.00000 0.00000 0.00000 0.00000
Dpth L Wait Strk Pmx% Eff. Stfff CoR
0.50 0.00 0.00 0.000 0.000 0.000 1.000 0.000
1.00 0.00 0.00 0.000 0.000 0.000 1.500 0.000
1.50 0.00 0.00 0.000 0.000 0.000 2.500 0.000
2.00 0.00 0.00 0.000 0.000 0.000 2.750 0.000
2.50 0.00 0.00 0.000 0.000 0.000 3.000 0.000
2.75 0.00 0.00 0.000 0.000 0.000 3.250 0.000
3.00 0.00 0.00 0.000 0.000 0.000 3.500 0.000
3.25 0.00 0.00 0.000 0.000 0.000 3.600 0.000
3.50 0.00 0.00 0.000 0.000 0.000 3.600 0.000
3.60 0.00 0.00 0.000 0.000 0.000 3.700 0.000
3.75 0.00 0.00 0.000 0.000 0.000 3.700 0.000
3.80 0.00 0.00 0.000 0.000 0.000 3.700 0.000
4.00 0.00 0.00 0.000 0.000 0.000 3.700 0.000
4.25 0.00 0.00 0.000 0.000 0.000 3.750 0.000
.
.[ABRIDGED]
.
10.00 0.00 0.00 0.000 0.000 0.000 3.960 0.000
10.50 0.00 0.00 0.000 0.000 0.000 3.970 0.000
11.00 0.00 0.00 0.000 0.000 0.000 3.970 0.000
11.50 0.00 0.00 0.000 0.000 0.000 3.980 0.000
12.00 0.00 0.00 0.000 0.000 0.000 3.980 0.000
12.50 0.00 0.00 0.000 0.000 0.000 4.000 0.000
13.00 0.00 0.00 0.000 0.000 0.000 3.990 0.000
13.50 0.00 0.00 0.000 0.000 0.000 4.000 0.000
14.00 0.00 0.00 0.000 0.000 0.000 4.000 0.000

```

GRLWEAP: WAVE EQUATION ANALYSIS OF PILE FOUNDATIONS
Version 2003
SI Units

FHWA - GRLWEAP EXAMPLE #5 - First Pile

Hammer Model:	C 140	Made by:	CONMACO		
No.	Weight kN	Stiffn kN/mm	CoR	C-Slk mm	Dampg kN/m/s
1	62.300				
Helmet	18.090	1231.0	0.920	3.0000	111.8
Cushion		103.1	0.500	3.0000	
Combined Pile Top		101.1			
Assembly	Weight kN	Stiffn kN/mm	CoR	C-Slk mm	
1	37.291	12540.6			
2	37.291	12540.6	0.800	3.0480	

HAMMER OPTIONS:

Hammer File ID No.	182	Hammer Type	Ext.Comb.
--------------------	-----	-------------	-----------

HAMMER DATA:

Ram Weight	(kN)	62.30	Ram Length	(mm)	1397.00
Maximum (Eq) Stroke	(m)	0.91	Actual (Eq) Stroke	(m)	0.91
Efficiency		0.670			

Rated Energy	(kJ)	56.97	Potential Energy	(kJ)	56.69
Kinetic Energy	(kJ)	37.98	Impact Velocity	(m/s)	3.46

HAMMER CUSHION

Cross Sect. Area	(cm ²)	1596.80	PILE CUSHION Cross Sect. Area	(cm ²)	1264.50
Elastic-Modulus	(MPa)	1207.0	Elastic-Modulus	(MPa)	207.0
Thickness	(mm)	152.00	Thickness	(mm)	254.00
Coeff of Restitution		0.920	Coeff of Restitution		0.500
RoundOut	(mm)	3.0	RoundOut	(mm)	3.0
Stiffness	(kN/mm)	1268.0	Stiffness	(kN/mm)	103.1

Depth (m) 0.5
 Shaft Gain/Loss Factor 1.000 Toe Gain/Loss Factor 1.000

PILE PROFILE:

L b Top	Area	E-Mod	Spec Wt	Circmf	Strength	Wave Sp	EA/c
m	cm2	MPa	kN/m3	m	MPa	m/s	kN/m/s
0.00	1260.3	40000.	24.00	1.420	1.00	4044.	1246.74
14.50	1260.3	40000.	24.00	1.420	1.00	4044.	1246.74

Wave Travel Time 2L/c (ms) 7.172

Pile and Soil Model						Total Capacity Rut (kN)				964.0	
No.	Weight	Stiffn	C-Slk	T-Slk	CoR	Soil-S	Soil-D	Quake	LbTop	Circm	Area
	kN	kN/mm	mm	mm		kN	s/m	mm	m	m	cm2
1	2.924	5215.	3.000	0.000	0.85	0.0	0.000	2.50	0.97	1.4	1260.3
2	2.924	5215.	0.000	0.000	1.00	0.0	0.000	2.50	1.93	1.4	1260.3
15	2.924	5215.	0.000	0.000	1.00	10.0	0.150	2.50	14.50	1.4	1260.3
Toe						954.0	0.500	2.50			

PILE, SOIL, ANALYSIS OPTIONS:

Uniform pile
 No. of Slacks/Splices 0
 Pile Segments: Automatic
 Pile Damping (%) 3
 Pile Damping Fact. (kN/m/s) 74.804

Driveability Analysis

Soil Damping Option Smith
 Max No Analysis Iterations 0 Time Increment/Critical 160
 Output Time Interval 1 Analysis Time-Input (ms) 0
 Output Level: Normal
 Gravity Mass, Pile, Hammer: 9.810 9.810 9.810
 Output Segment Generation: Automatic

Depth	Stroke	Efficy	PileC.St.	PileC.CoR
m	m		kN/mm	
0.50	0.91	0.670	103.	0.500

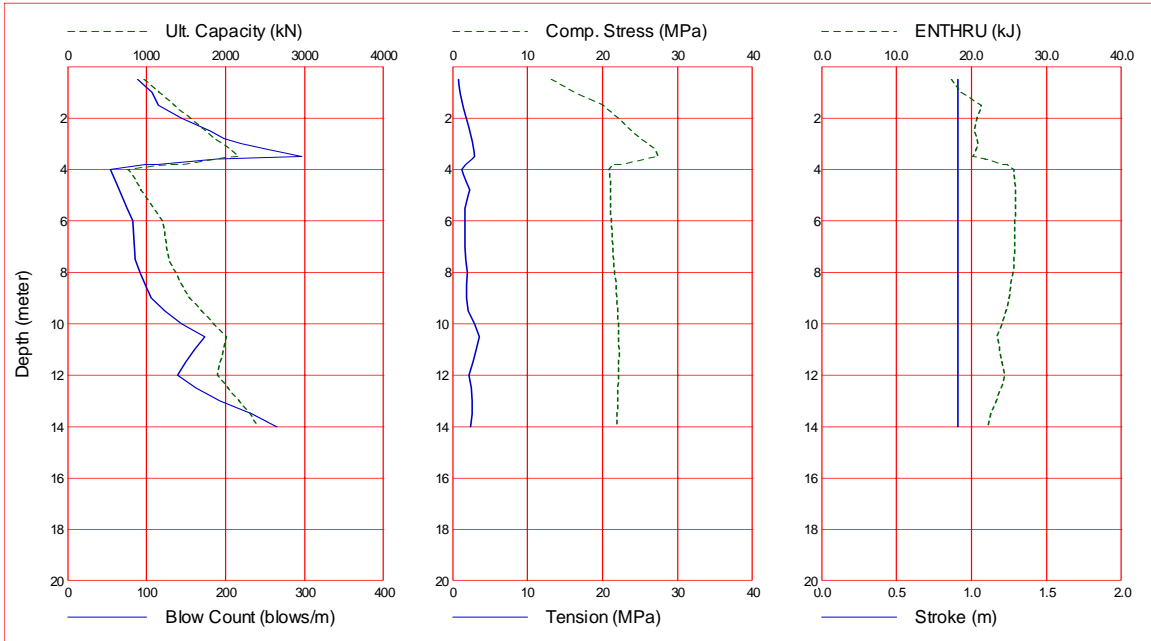


Figure F 54 GRLWEAP Driveability Results, Pier 2 Single Concrete

Gain/Loss 1 at Shaft and Toe 1.000 / 1.000

Depth m	Ultimate Capacity kN	Friction kN	End Bearing kN	Blow Count blows/m	Comp. Stress MPa	Tension Stress MPa	Stroke m	ENTHRU kJ
0.5	964.0	10.0	954.0	88.3	13.205	-0.832	0.91	17.3
1.0	1158.5	31.0	1127.5	106.8	16.253	-1.027	0.91	18.6
1.5	1355.0	54.0	1301.0	114.9	20.154	-1.343	0.91	21.3
2.0	1553.4	78.9	1474.5	143.9	22.142	-1.857	0.91	20.7
2.5	1753.8	105.8	1648.0	180.6	23.981	-2.302	0.91	20.4
2.8	1854.8	120.0	1734.7	198.0	25.085	-2.506	0.91	20.7
3.0	1956.2	134.7	1821.5	219.0	26.124	-2.672	0.91	20.9
3.2	2058.1	149.9	1908.2	251.1	26.922	-2.793	0.91	20.6
3.5	2160.6	165.6	1995.0	296.7	27.458	-2.891	0.91	20.2
3.6	1882.0	172.0	1710.0	189.0	25.658	-2.646	0.91	21.8
3.8	1464.3	181.8	1282.5	114.2	22.496	-1.796	0.91	23.9
3.8	1325.1	185.1	1140.0	98.8	21.264	-1.762	0.91	24.7
4.0	768.4	198.4	570.0	53.9	20.828	-1.183	0.91	25.6
4.2	819.3	215.8	603.5	57.5	20.924	-1.439	0.91	25.7
4.5	871.1	234.1	637.0	61.4	21.017	-1.881	0.91	25.8
4.8	923.8	253.3	670.5	65.1	21.023	-2.258	0.91	25.9
5.0	977.5	273.5	704.0	68.3	21.031	-2.099	0.91	25.9
5.5	1087.4	316.4	771.0	75.1	21.041	-1.605	0.91	25.9
6.0	1201.0	363.0	838.0	82.7	21.157	-1.618	0.91	25.8
6.5	1227.2	412.2	815.0	83.5	21.301	-1.664	0.91	25.8
7.0	1254.8	462.8	792.0	84.5	21.364	-1.655	0.91	25.8
7.5	1283.9	514.9	769.0	85.7	21.476	-1.764	0.91	25.7
8.0	1369.2	568.5	800.7	91.9	21.611	-1.993	0.91	25.5
8.5	1455.9	623.6	832.3	98.5	21.849	-1.873	0.91	25.2
9.0	1544.0	680.0	864.0	106.2	21.959	-1.898	0.91	25.0
9.5	1696.3	738.0	958.3	123.0	22.060	-2.117	0.91	24.6
10.0	1850.1	797.4	1052.7	144.8	22.160	-2.884	0.91	24.0
10.5	2005.3	858.3	1147.0	173.3	22.129	-3.564	0.91	23.4
11.0	1966.6	920.6	1046.0	160.5	22.193	-3.172	0.91	23.7
11.5	1929.4	984.4	945.0	149.3	22.133	-2.707	0.91	24.1
12.0	1893.7	1049.7	844.0	139.1	22.126	-2.190	0.91	24.4
12.5	2032.4	1116.4	916.0	162.3	22.073	-2.540	0.91	23.9
13.0	2172.7	1184.7	988.0	192.8	22.035	-2.631	0.91	23.3
13.5	2314.4	1254.4	1060.0	233.2	21.948	-2.599	0.91	22.6
14.0	2407.9	1325.5	1082.3	264.4	21.912	-2.404	0.91	22.2

Total Number of Blows: 1802

Driving Time (min): 60 45 36 30 25 22 20 18 16 15
 @Blow Rate (b/min): 30 40 50 60 70 80 90 100 110 120

Driving Time for continuously running hammer; any wait times not included

Table F.8 GRLWEAP Driveability Results, Pier 2 Single Concrete

F.9.2.2 Pier 2, Concrete Pile Example Considering Soil Densification

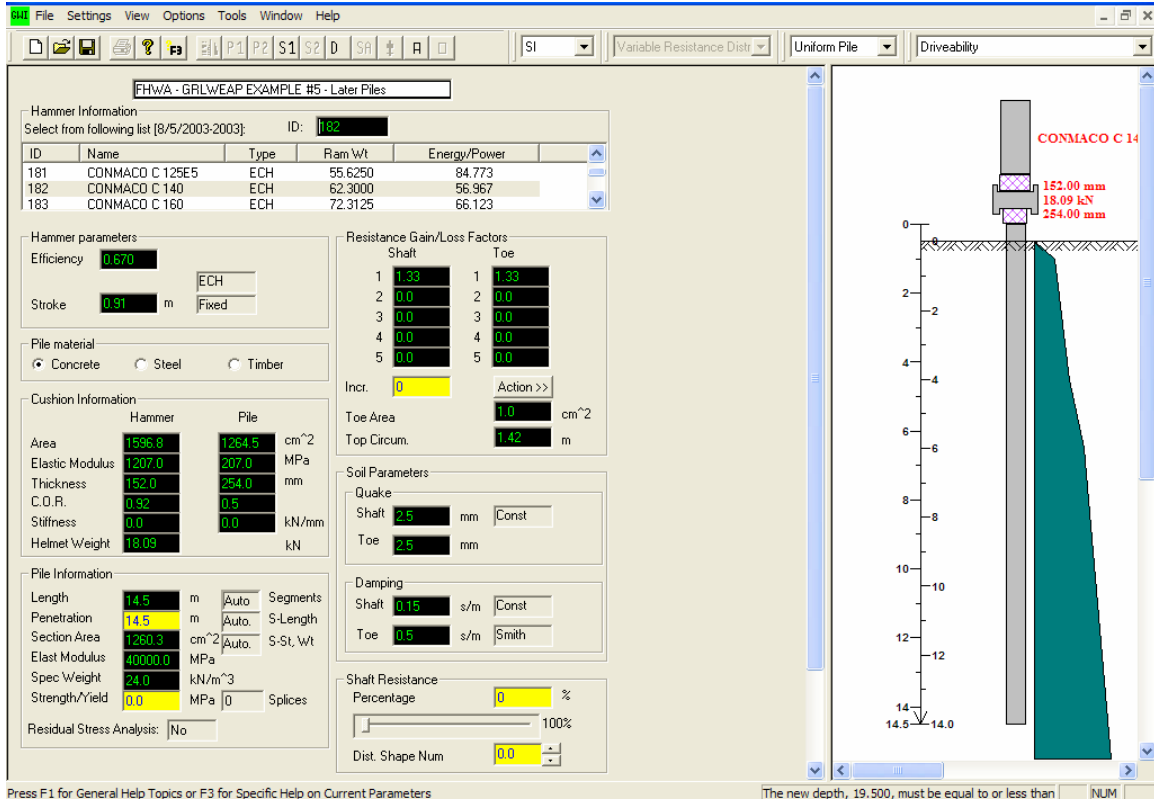


Figure F 55 GRLWEAP Driveability Input, Pier 2 with Soil Densification

Input File Contents

```

FHWA - GRLWEAP EXAMPLE #5 - Later Piles
OUT OSG HAM STR FUL PEL N SPL N-U P-D %SK ISM 0 PHI RSA ITR H-D MXT DEx
0 0 182 0 0 0 0 0 0 3 0 0 0 0 0 0 0 0.000
  File g Hammer g
  9.810 9.810
    W Cp A Cp E Cp T Cp CoR ROut StCp
    18.090 1596.800 1207.0 152.000 0.920 3.000 0.0
    A Cu E Cu T Cu CoR ROut StCu
    1264.500 207.0 254.000 0.500 3.000 0.0
    LPle APle EPle WPle Circ Strg CoR ROut
    14.500 1260.300 40000.000 24.000 1.420 0.000 0.850 3.000
  Manufac Hmr Name HmrType No Seg-s
  CONMACO C 140 3 1
    Ram Wt Ram L Ram Dia MaxStrk RtdStrk Effic
    62.30 1397.00 612.65 0.91 0.91 0.67
    No. Assmbly Segs
    2
<---- Assembly Masses ----><----Assembly Stiffnesses---->
37.291 37.291 0.000 12540.6 12540.6 0.0
Stroke Effic. Pressure R-Weight T-Delay Exp-Coeff Eps-Str
0.9100 0.6700 0.0000 0.0000 0.0000 0.0000 0.0100 0.0000
  Qs Qt Js Jt Qx Jx Rati Dept
  2.500 2.500 0.150 0.500 0.000 0.000 0.000 0.000
Research Soil Model: Atoe, Plug, Gap, Q-fac
0.000 0.000 0.000 0.000
Research Soil Model: RD-skn: m, d, toe: m, d
0.000 0.000 0.000 0.000
Res. Distribution
  Dpth Rskn Rtoe Qs Qt Js Jt SU F RelE SU T
  0.00 0.00 0.00 0.00 0.00 0.00 0.00 0.00 0.00 0.00
  0.50 28.17 954.00 0.00 0.00 0.00 0.00 0.00 0.00 0.00
  3.50 44.87 1995.00 0.00 0.00 0.00 0.00 0.00 0.00 0.00
  4.00 47.71 570.00 0.00 0.00 0.00 0.00 0.00 0.00 0.00
  6.00 68.18 838.00 0.00 0.00 0.00 0.00 0.00 0.00 0.00
  7.50 74.47 769.00 0.00 0.00 0.00 0.00 0.00 0.00 0.00
  9.00 80.57 864.00 0.00 0.00 0.00 0.00 0.00 0.00 0.00
  10.50 86.77 1147.00 0.00 0.00 0.00 0.00 0.00 0.00 0.00
  12.00 92.97 844.00 0.00 0.00 0.00 0.00 0.00 0.00 0.00
  13.50 99.21 1060.00 0.00 0.00 0.00 0.00 0.00 0.00 0.00
  15.00 105.41 1127.00 0.00 0.00 0.00 0.00 0.00 0.00 0.00
Gain/Loss factors: shaft and toe
1.33000 0.00000 0.00000 0.00000 0.00000
1.33000 0.00000 0.00000 0.00000 0.00000
  Dpth L Wait Strk Pmx% Eff. Stff CoR
  0.50 0.00 0.00 0.000 0.000 0.000 1.000 0.000
  1.00 0.00 0.00 0.000 0.000 0.000 1.500 0.000
  1.50 0.00 0.00 0.000 0.000 0.000 2.500 0.000
  2.00 0.00 0.00 0.000 0.000 0.000 2.750 0.000
  2.50 0.00 0.00 0.000 0.000 0.000 3.000 0.000
  2.75 0.00 0.00 0.000 0.000 0.000 3.250 0.000
  3.00 0.00 0.00 0.000 0.000 0.000 3.500 0.000
  3.25 0.00 0.00 0.000 0.000 0.000 3.600 0.000
  3.50 0.00 0.00 0.000 0.000 0.000 3.600 0.000
  3.60 0.00 0.00 0.000 0.000 0.000 3.700 0.000
  3.75 0.00 0.00 0.000 0.000 0.000 3.700 0.000
  3.80 0.00 0.00 0.000 0.000 0.000 3.700 0.000
.
. [ABRIDGED]
.
  9.50 0.00 0.00 0.000 0.000 0.000 3.960 0.000
  10.00 0.00 0.00 0.000 0.000 0.000 3.960 0.000
  10.50 0.00 0.00 0.000 0.000 0.000 3.970 0.000
  11.00 0.00 0.00 0.000 0.000 0.000 3.970 0.000
  11.50 0.00 0.00 0.000 0.000 0.000 3.980 0.000
  12.00 0.00 0.00 0.000 0.000 0.000 3.980 0.000
  12.50 0.00 0.00 0.000 0.000 0.000 4.000 0.000
  13.00 0.00 0.00 0.000 0.000 0.000 3.990 0.000
  13.50 0.00 0.00 0.000 0.000 0.000 4.000 0.000
  14.00 0.00 0.00 0.000 0.000 0.000 4.000 0.000

```

GRLWEAP: WAVE EQUATION ANALYSIS OF PILE FOUNDATIONS
Version 2003
SI Units

FHWA - GRLWEAP EXAMPLE #5 - Later Piles

Hammer Model:	C 140	Made by:	CONMACO		
No.	Weight kN	Stiffn kN/mm	CoR	C-Slk mm	Dampg kN/m/s
1	62.300				
Helmet	18.090	1231.0	0.920	3.0000	111.8
Cushion		103.1	0.500	3.0000	
Combined Pile Top		101.1			
Assembly	Weight kN	Stiffn kN/mm	CoR	C-Slk mm	
1	37.291	12540.6			
2	37.291	12540.6	0.800	3.0480	

HAMMER OPTIONS:

Hammer File ID No.	182	Hammer Type	Ext.Comb.
--------------------	-----	-------------	-----------

HAMMER DATA:

Ram Weight	(kN)	62.30	Ram Length	(mm)	1397.00
Maximum (Eq) Stroke	(m)	0.91	Actual (Eq) Stroke	(m)	0.91
Efficiency		0.670			

Rated Energy	(kJ)	56.97	Potential Energy	(kJ)	56.69
Kinetic Energy	(kJ)	37.98	Impact Velocity	(m/s)	3.46

HAMMER CUSHION

Cross Sect. Area	(cm ²)	1596.80	PILE CUSHION Cross Sect. Area	(cm ²)	1264.50
Elastic-Modulus	(MPa)	1207.0	Elastic-Modulus	(MPa)	207.0
Thickness	(mm)	152.00	Thickness	(mm)	254.00
Coeff of Restitution		0.920	Coeff of Restitution		0.500
RoundOut	(mm)	3.0	RoundOut	(mm)	3.0
Stiffness	(kN/mm)	1268.0	Stiffness	(kN/mm)	103.1

Depth (m) 0.5
 Shaft Gain/Loss Factor 1.330 Toe Gain/Loss Factor 1.330

PILE PROFILE:

L b Top	Area	E-Mod	Spec Wt	Circmf	Strength	Wave Sp	EA/c
m	cm ²	MPa	kN/m ³	m	MPa	m/s	kN/m/s
0.00	1260.3	40000.	24.00	1.420	1.00	4044.	1246.74
14.50	1260.3	40000.	24.00	1.420	1.00	4044.	1246.74

Wave Travel Time 2L/c (ms) 7.172

Pile and Soil Model						Total Capacity Rut (kN)				1282.1	
No.	Weight	Stiffn	C-Slk	T-Slk	CoR	Soil-S	Soil-D	Quake	LbTop	Circm	Area
	kN	kN/mm	mm	mm		kN	s/m	mm	m	m	cm ²
1	2.924	5215.	3.000	0.000	0.85	0.0	0.000	2.50	0.97	1.4	1260.3
2	2.924	5215.	0.000	0.000	1.00	0.0	0.000	2.50	1.93	1.4	1260.3
15	2.924	5215.	0.000	0.000	1.00	13.3	0.150	2.50	14.50	1.4	1260.3
Toe						1268.8	0.500	2.50			

PILE, SOIL, ANALYSIS OPTIONS:

Uniform pile
 No. of Slacks/Splices 0
 Pile Segments: Automatic
 Pile Damping (%) 3
 Pile Damping Fact. (kN/m/s) 74.804

Driveability Analysis

Soil Damping Option Smith
 Max No Analysis Iterations 0 Time Increment/Critical 160
 Output Time Interval 1 Analysis Time-Input (ms) 0
 Output Level: Normal
 Gravity Mass, Pile, Hammer: 9.810 9.810 9.810
 Output Segment Generation: Automatic

Depth	Stroke	Efficy	PileC.St.	PileC.CoR
m	m		kN/mm	
0.50	0.91	0.670	103.	0.500

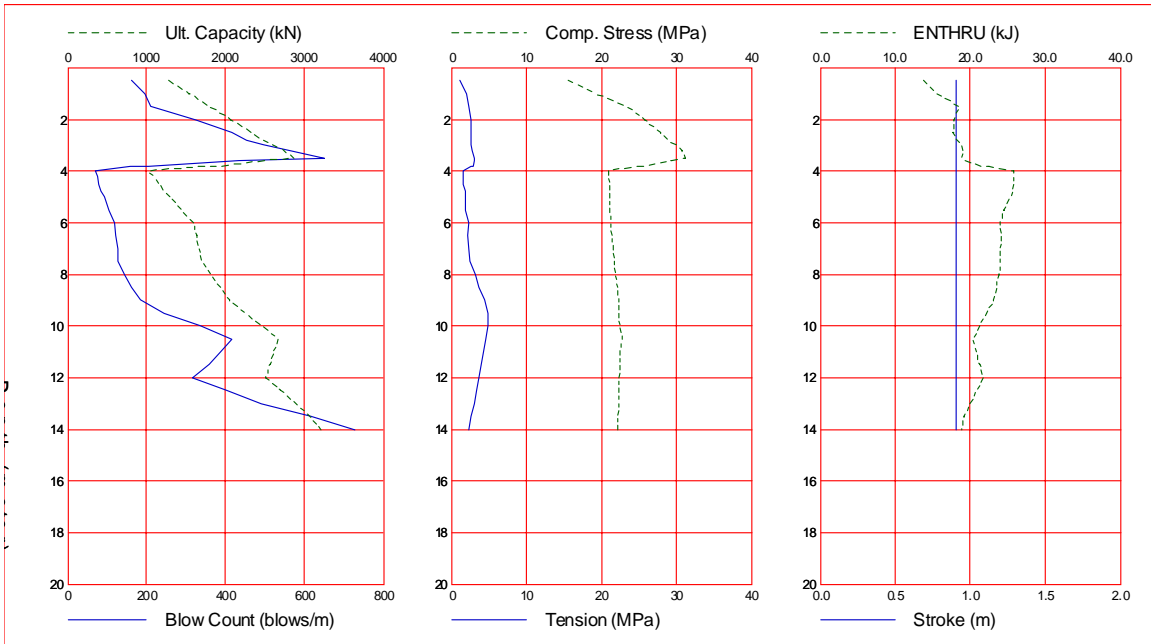


Figure F 56 GRLWEAP Driveability Results, Pier 2 with Soil Densification

Gain/Loss 1 at Shaft and Toe 1.330 / 1.330

Depth m	Ultimate Capacity kN	Friction kN	End Bearing kN	Blow Count blows/m	Comp. Stress MPa	Tension Stress MPa	Stroke m	ENTHRU kJ
0.5	1282.1	13.3	1268.8	161.5	15.522	-1.120	0.91	13.8
1.0	1540.8	41.2	1499.6	196.3	19.038	-1.979	0.91	15.5
1.5	1802.1	71.8	1730.3	212.0	23.447	-2.309	0.91	18.6
2.0	2066.0	104.9	1961.1	324.4	25.779	-2.538	0.91	17.9
2.5	2332.6	140.7	2191.8	416.0	27.766	-2.476	0.91	17.7
2.8	2466.8	159.6	2307.2	454.4	28.898	-2.555	0.91	18.3
3.0	2601.8	179.2	2422.6	497.8	29.973	-2.657	0.91	18.8
3.2	2737.3	199.4	2538.0	561.8	30.690	-2.755	0.91	19.0
3.5	2873.6	220.2	2653.3	650.6	31.142	-2.888	0.91	18.9
3.6	2503.1	228.7	2274.3	432.8	29.393	-3.028	0.91	19.4
3.8	1947.5	241.7	1705.7	203.6	25.779	-2.873	0.91	21.6
3.8	1762.3	246.1	1516.2	158.7	24.536	-2.645	0.91	22.6
4.0	1022.0	263.9	758.1	71.7	20.831	-1.539	0.91	25.8
4.2	1089.7	287.1	802.7	76.0	20.929	-1.495	0.91	25.8
4.5	1158.6	311.4	847.2	80.6	21.031	-1.496	0.91	25.8
4.8	1228.7	336.9	891.8	85.8	21.035	-1.742	0.91	25.6
5.0	1300.0	363.7	936.3	91.5	21.037	-1.822	0.91	25.3
5.5	1446.3	420.8	1025.4	104.7	21.072	-1.763	0.91	24.5
6.0	1597.3	482.8	1114.5	120.9	21.323	-2.141	0.91	24.1
6.5	1632.1	548.2	1084.0	122.9	21.385	-2.075	0.91	24.2
7.0	1668.9	615.5	1053.4	125.7	21.517	-2.256	0.91	24.1
7.5	1707.6	684.9	1022.8	128.6	21.676	-2.420	0.91	24.1
8.0	1821.0	756.1	1064.9	144.1	21.844	-3.132	0.91	23.8
8.5	1936.3	829.3	1107.0	162.3	22.133	-3.688	0.91	23.5
9.0	2053.6	904.5	1149.1	185.7	22.281	-4.282	0.91	23.1
9.5	2256.1	981.5	1274.6	244.9	22.336	-4.739	0.91	22.2
10.0	2460.6	1060.5	1400.0	336.1	22.484	-4.716	0.91	21.3
10.5	2667.0	1141.5	1525.5	416.4	22.635	-4.540	0.91	20.4
11.0	2615.6	1224.4	1391.2	387.6	22.496	-4.210	0.91	20.8
11.5	2566.1	1309.3	1256.9	359.5	22.410	-3.921	0.91	21.3
12.0	2518.6	1396.1	1122.5	317.8	22.399	-3.549	0.91	21.7
12.5	2703.1	1484.9	1218.3	401.4	22.319	-3.214	0.91	20.9
13.0	2889.6	1575.6	1314.0	491.5	22.261	-2.914	0.91	20.0
13.5	3078.1	1668.3	1409.8	616.9	22.152	-2.562	0.91	19.2
14.0	3202.5	1763.0	1439.5	729.0	22.107	-2.154	0.91	18.9

Total Number of Blows: 3815

Driving Time (min): 127 95 76 63 54 47 42 38 34 31
 @Blow Rate (b/min): 30 40 50 60 70 80 90 100 110 120

Driving Time for continuously running hammer; any wait times not included

Table F 9 GRLWEAP Driveability Results, Pier 2 with Soil Densification

F.9.2.3 Pier 2, H-Pile Example

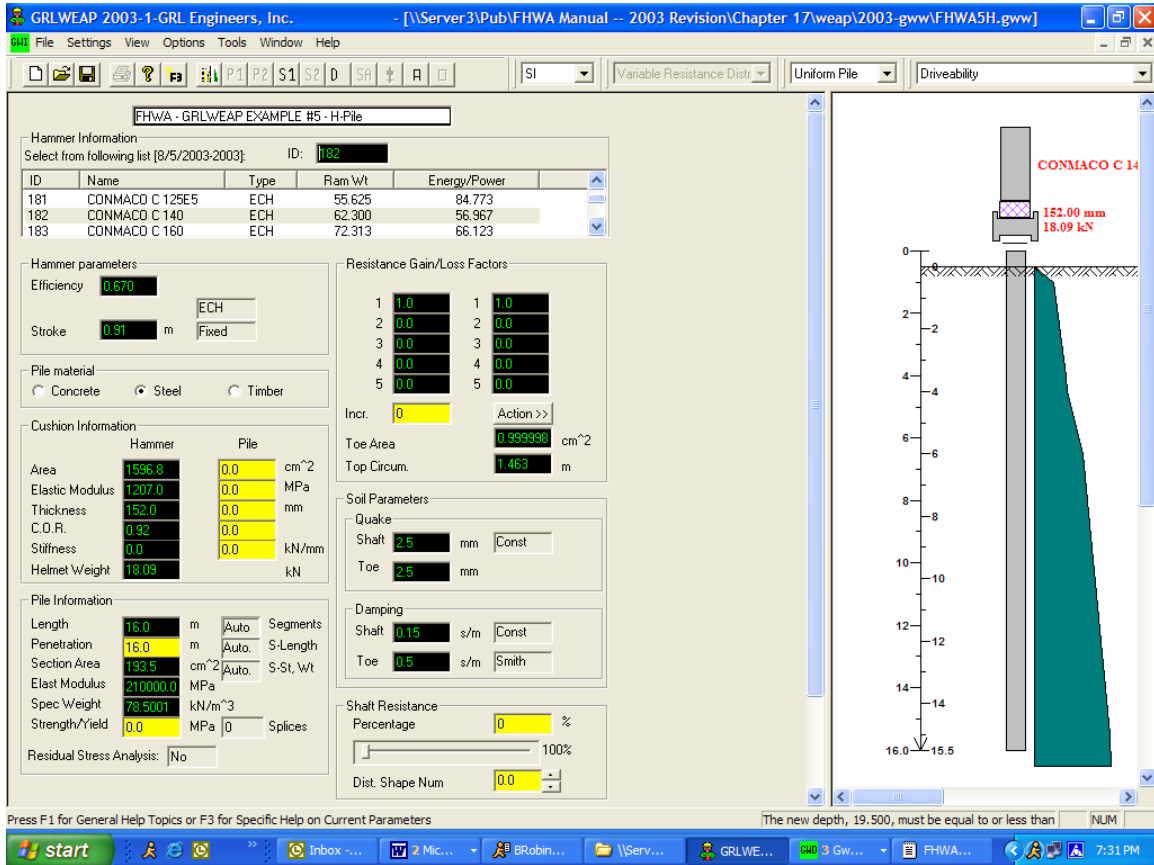


Figure F 57 GRLWEAP Driveability Results, Pier 2 H-Pile

Input File Contents

```

FHWA - GRLWEAP EXAMPLE #5 - H-Pile
OUT OSG HAM STR FUL PEL N SPL N-U P-D %SK ISM 0 PHI RSA ITR H-D MXT DEX
0 0 182 0 0 0 0 0 0 0 1 0 0 0 0 0 0 0 0.000
  Pile g Hammer g
  9.810 9.810
  W Cp A Cp E Cp T Cp CoR ROut StCp
  18.090 1596.800 1207.0 152.000 0.920 3.000 0.0
  A Cu E Cu T Cu CoR ROut StCu
  0.000 0.0 0.000 0.000 0.000 0.0
  LPle APle EPle WPle Circ Strg CoR ROut
  16.000 193.500210000.000 78.500 1.463 0.000 0.850 3.000
Manufac Hmr Name HmrType No Seg-s
CONMACO C 140 3 1
  Ram Wt Ram L Ram Dia MaxStrk RtdStrk Effic
  62.30 1397.00 612.65 0.91 0.91 0.67
  No. Assmby Segs
  2
<---- Assembly Masses ----><----Assembly Stiffnesses---->
  37.291 37.291 0.000 12540.6 12540.6 0.0
  Stroke Effic. Pressure R-Weight T-Delay Exp-Coeff Eps-Str
  0.9100 0.6700 0.0000 0.0000 0.0000 0.0000 0.0100 0.0000
  Qs Qt Js Jt Qx Jx Rati Dept
  2.500 2.500 0.150 0.500 0.000 0.000 0.000 0.000
Research Soil Model: Atoe, Plug, Gap, Q-fac
  0.000 0.000 0.000 0.000
Research Soil Model: RD-skn: m, d, toe: m, d
  0.000 0.000 0.000 0.000
Res. Distribution
  Dpth Rskn Rtoe Qs Qt Js Jt SU F ReLE SU T
  0.00 0.00 0.00 0.00 0.00 0.00 0.00 0.00 0.00 0.00
  0.50 20.36 681.00 0.00 0.00 0.00 0.00 0.00 0.00 0.00
  3.50 32.42 1425.00 0.00 0.00 0.00 0.00 0.00 0.00 0.00
  4.00 34.44 407.00 0.00 0.00 0.00 0.00 0.00 0.00 0.00
  6.00 50.59 598.00 0.00 0.00 0.00 0.00 0.00 0.00 0.00
  7.50 55.19 550.00 0.00 0.00 0.00 0.00 0.00 0.00 0.00
  9.00 59.79 617.00 0.00 0.00 0.00 0.00 0.00 0.00 0.00
  10.50 64.39 820.00 0.00 0.00 0.00 0.00 0.00 0.00 0.00
  12.00 68.99 603.00 0.00 0.00 0.00 0.00 0.00 0.00 0.00
  13.50 73.63 757.00 0.00 0.00 0.00 0.00 0.00 0.00 0.00
  15.00 78.23 805.00 0.00 0.00 0.00 0.00 0.00 0.00 0.00
  16.00 79.7620000.00 0.00 0.00 0.00 0.00 0.00 0.00 0.00
Gain/Loss factors: shaft and toe
  1.00000 0.00000 0.00000 0.00000 0.00000
  1.00000 0.00000 0.00000 0.00000 0.00000
  Dpth L Wait Strk Pmx% Eff. Stff CoR
  0.50 0.00 0.00 0.000 0.000 0.000 0.000 0.000
  1.00 0.00 0.00 0.000 0.000 0.000 0.000 0.000
  1.50 0.00 0.00 0.000 0.000 0.000 0.000 0.000
  2.00 0.00 0.00 0.000 0.000 0.000 0.000 0.000
  2.50 0.00 0.00 0.000 0.000 0.000 0.000 0.000
  2.75 0.00 0.00 0.000 0.000 0.000 0.000 0.000
  3.00 0.00 0.00 0.000 0.000 0.000 0.000 0.000
  3.25 0.00 0.00 0.000 0.000 0.000 0.000 0.000
  3.50 0.00 0.00 0.000 0.000 0.000 0.000 0.000
  3.60 0.00 0.00 0.000 0.000 0.000 0.000 0.000
  3.75 0.00 0.00 0.000 0.000 0.000 0.000 0.000
  3.80 0.00 0.00 0.000 0.000 0.000 0.000 0.000
  4.00 0.00 0.00 0.000 0.000 0.000 0.000 0.000
  4.25 0.00 0.00 0.000 0.000 0.000 0.000 0.000
  4.50 0.00 0.00 0.000 0.000 0.000 0.000 0.000
.
. [ABRIDGED]
.
  13.50 0.00 0.00 0.000 0.000 0.000 0.000 0.000
  14.00 0.00 0.00 0.000 0.000 0.000 0.000 0.000
  14.50 0.00 0.00 0.000 0.000 0.000 0.000 0.000
  15.00 0.00 0.00 0.000 0.000 0.000 0.000 0.000
  15.50 0.00 0.00 0.000 0.000 0.000 0.000 0.000

```

GRLWEAP: WAVE EQUATION ANALYSIS OF PILE FOUNDATIONS
Version 2003
SI Units

FHWA - GRLWEAP EXAMPLE #5 - H-Pile

Hammer Model:	C 140	Made by:	CONMACO		
No.	Weight kN	Stiffn kN/mm	CoR	C-Slk mm	Dampg kN/m/s
1	62.300				
Helmet	18.090	1231.0	0.920	3.0000	111.8
Combined Pile Top		4063.5			
Assembly	Weight kN	Stiffn kN/mm	CoR	C-Slk mm	
1	37.291	12540.6			
2	37.291	12540.6	0.800	3.0480	

HAMMER OPTIONS:

Hammer File ID No.	182	Hammer Type	Ext.Comb.
--------------------	-----	-------------	-----------

HAMMER DATA:

Ram Weight	(kN)	62.30	Ram Length	(mm)	1397.00
Maximum (Eq) Stroke	(m)	0.91	Actual (Eq) Stroke	(m)	0.91
Efficiency		0.670			

Rated Energy	(kJ)	56.97	Potential Energy	(kJ)	56.69
Kinetic Energy	(kJ)	37.98	Impact Velocity	(m/s)	3.46

HAMMER CUSHION

Cross Sect. Area	(cm2)	1596.80	PILE CUSHION Cross Sect. Area	(cm2)	0.00
Elastic-Modulus	(MPa)	1207.0	Elastic-Modulus	(MPa)	0.0
Thickness	(mm)	152.00	Thickness	(mm)	0.00
Coeff of Restitution		0.920	Coeff of Restitution		1.000
RoundOut	(mm)	3.0	RoundOut	(mm)	0.0
Stiffness	(kN/mm)	1268.0	Stiffness	(kN/mm)	0.0

Depth (m) 0.5
 Shaft Gain/Loss Factor 1.000 Toe Gain/Loss Factor 1.000

PILE PROFILE:

L b Top	Area	E-Mod	Spec Wt	Circmf	Strength	Wave Sp	EA/c
m	cm ²	MPa	kN/m ³	m	MPa	m/s	kN/m/s
0.00	193.5	210000.	78.50	1.463	1.00	5123.	793.21
16.00	193.5	210000.	78.50	1.463	1.00	5123.	793.21

Wave Travel Time 2L/c (ms) 6.247

Pile and Soil Model						Total Capacity Rut (kN)			688.4		
No.	Weight	Stiffn	C-Slk	T-Slk	CoR	Soil-S	Soil-D	Quake	LbTop	Circm	Area
	kN	kN/mm	mm	mm		kN	s/m	mm	m	m	cm ²
1	1.519	4063.	3.000	0.000	0.85	0.0	0.000	2.50	1.00	1.5	193.5
2	1.519	4063.	0.000	0.000	1.00	0.0	0.000	2.50	2.00	1.5	193.5
16	1.519	4063.	0.000	0.000	1.00	7.4	0.150	2.50	16.00	1.5	193.5
Toe						681.0	0.500	2.50			

PILE, SOIL, ANALYSIS OPTIONS:

Uniform pile
 No. of Slacks/Splices 0
 File Segments: Automatic
 Pile Damping (%) 1
 Pile Damping Fact. (kN/m/s) 15.864

Driveability Analysis

Soil Damping Option Smith
 Max No Analysis Iterations 0 Time Increment/Critical 160
 Output Time Interval 1 Analysis Time-Input (ms) 0
 Output Level: Normal
 Gravity Mass, Pile, Hammer: 9.810 9.810 9.810
 Output Segment Generation: Automatic

Depth Stroke Efficcy
 m m
 0.50 0.91 0.670

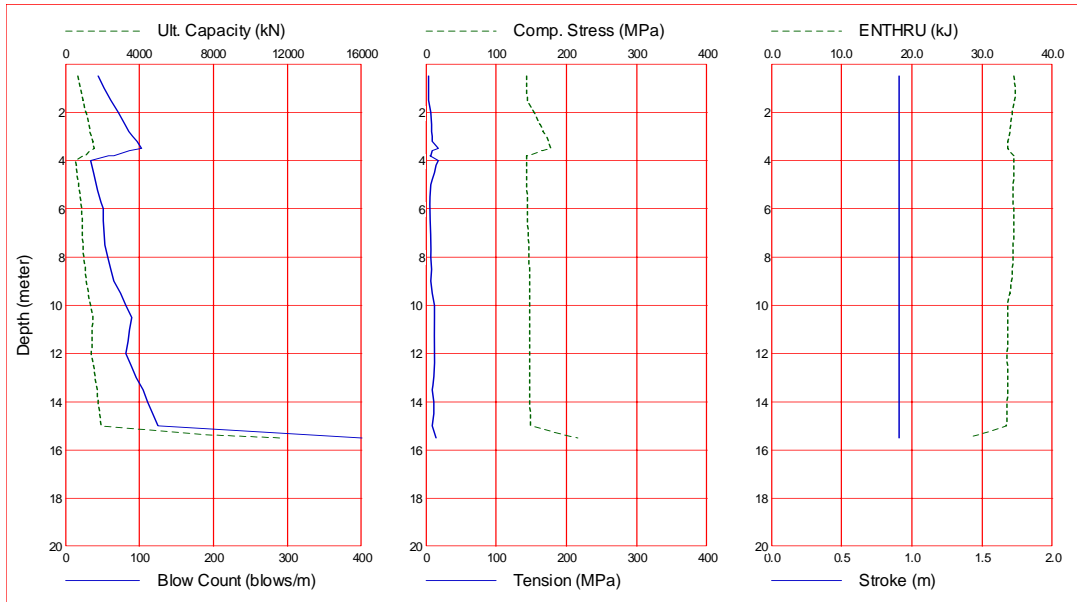


Figure F 58 GRLWEAP Driveability Results, Pier 2 H-Piles

Gain/Loss 1 at Shaft and Toe 1.000 / 1.000

Depth m	Ultimate Capacity kN	Friction kN	End Bearing kN	Blow Count blows/m	Comp. Stress MPa	Tension Stress MPa	Stroke m	ENTHRU kJ
0.5	688.4	7.4	681.0	44.2	143.839	-4.233	0.91	34.5
1.0	828.1	23.1	805.0	52.4	143.841	-3.504	0.91	34.7
1.5	969.2	40.2	929.0	61.4	144.000	-4.140	0.91	34.6
2.0	1111.7	58.7	1053.0	71.0	154.053	-6.587	0.91	34.3
2.5	1255.8	78.8	1177.0	80.5	163.144	-8.007	0.91	34.1
2.8	1328.4	89.4	1239.0	85.5	166.754	-8.432	0.91	34.0
3.0	1401.3	100.3	1301.0	90.9	170.902	-8.858	0.91	33.9
3.2	1474.6	111.6	1363.0	96.7	174.264	-9.574	0.91	33.7
3.5	1548.3	123.3	1425.0	102.9	177.535	-17.974	0.91	33.6
3.6	1349.4	128.0	1221.4	86.5	165.496	-9.311	0.91	33.9
3.8	1051.3	135.3	916.0	65.6	145.174	-6.976	0.91	34.5
3.8	952.0	137.8	814.2	58.6	143.851	-5.952	0.91	34.6
4.0	554.7	147.7	407.0	33.7	143.849	-17.499	0.91	34.5
4.2	591.6	160.7	430.9	35.8	143.854	-14.533	0.91	34.5
4.5	629.1	174.4	454.8	37.6	143.885	-11.832	0.91	34.5
4.8	667.5	188.8	478.6	39.5	143.920	-9.151	0.91	34.5
5.0	706.5	204.0	502.5	41.5	143.957	-6.460	0.91	34.4
5.5	786.8	236.6	550.2	46.2	144.086	-5.429	0.91	34.4
6.0	870.1	272.1	598.0	50.8	144.462	-5.989	0.91	34.5
6.5	891.7	309.7	582.0	51.6	144.987	-6.248	0.91	34.5
7.0	914.4	348.4	566.0	52.5	145.634	-6.867	0.91	34.5
7.5	938.2	388.2	550.0	53.5	146.332	-7.181	0.91	34.4
8.0	1001.5	429.1	572.3	57.2	147.090	-7.172	0.91	34.4
8.5	1065.8	471.2	594.7	61.3	147.332	-7.586	0.91	34.3
9.0	1131.4	514.4	617.0	65.7	147.690	-7.398	0.91	34.2
9.5	1243.3	558.7	684.7	74.0	147.974	-9.159	0.91	34.0
10.0	1356.4	604.1	752.3	81.5	147.831	-12.000	0.91	33.7
10.5	1470.6	650.6	820.0	89.3	148.113	-12.746	0.91	33.6
11.0	1445.9	698.3	747.7	86.7	147.823	-12.558	0.91	33.6
11.5	1422.4	747.1	675.3	84.1	148.097	-12.331	0.91	33.6
12.0	1400.0	797.0	603.0	81.5	147.814	-12.131	0.91	33.5
12.5	1502.3	848.0	654.3	88.5	148.095	-11.902	0.91	33.6
13.0	1605.8	900.2	705.7	96.2	147.852	-10.705	0.91	33.7
13.5	1710.5	953.5	757.0	104.9	148.186	-8.599	0.91	33.6
14.0	1780.9	1007.9	773.0	110.9	148.077	-11.058	0.91	33.5
14.5	1852.4	1063.4	789.0	117.5	148.577	-11.363	0.91	33.5
15.0	1925.1	1120.1	805.0	124.8	148.659	-9.243	0.91	33.4
15.5	11580.1	1177.6	10402.5	9999.0	215.986	-14.843	0.91	28.0

Refusal occurred; no driving time output possible

Table F 10 GRLWEAP Driveability Results, Pier 2 H-Piles

F.9.3.1 Pier 3 H-Pile Preconstruction Driveability Analysis

This analysis was initially generated from the Soil Boring S-3 file in Driven. Driven created a GRLWEAP input file that included the general pile properties, a detailed soil resistance distribution and soil damping, quake and set-up parameters based on the soil type. The hammer and driving system parameters were entered, the gain/loss factor was selected as 0.5 and 1.0 for the shaft (per cohesive soils in Table 9-20), and the depths for analysis were set every 0.5 m to the pile penetration. The analysis was run, and the results follow.

In this case, penetration resistance is less than 25 blows per 0.25 m when the hammer is run at full stroke. If the stroke can be reduced on this hammer, the analysis should be re-run at a lower stroke. The resulting penetration resistance will be higher and the stresses lower. The pile compressive and tensile stresses are with FHWA limits for steel piles.

Hammer Information
 Select from following list [8/5/2003-2003]: ID: 182

ID	Name	Type	Ram Wt	Energy/Power
181	CONMACO C 125E5	ECH	55.625	84.773
182	CONMACO C 140	ECH	62.300	56.967
183	CONMACO C 160	ECH	72.313	66.123

Hammer parameters
 Efficiency: 0.670
 Stroke: 0.91 m
 Pile material: Steel Timber

Resistance Gain/Loss Factors

Shaft	Toe
1 0.5	1 1.0
2 1.0	2 1.0
3 0.0	3 0.0
4 0.0	4 0.0
5 0.0	5 0.0

Incr: 0
 Action >>
 Toe Area: 1.0 cm²
 Top Circum: 1.42 m

Cushion Information

	Hammer	Pile	
Area	1596.8	0.0	cm ²
Elastic Modulus	1207.0	0.0	MPa
Thickness	152.0	0.0	mm
C.O.R.	0.92	0.0	
Stiffness	0.0	0.0	kN/mm
Helmet Weight	18.09		kN

Soil Parameters
 -Quake
 Shaft: 0.0 mm Const
 Toe: 0.0 mm

Damping
 Shaft: 0.0 s/m Const
 Toe: 0.0 s/m Smith

Pile Information
 Length: 15.0 m Auto Segments
 Penetration: 15.0 m Auto S-Length
 Section Area: 193.5 cm² Auto S-St, Wt
 Elast Modulus: 210000.0 MPa
 Spec Weight: 77.5 kN/m³
 Strength/Yield: 248.0 MPa 0 Splices
 Residual Stress Analysis: No

Shaft Resistance
 Percentage: 0 %
 Dist. Shape Num: 0.0

Press F1 for General Help Topics or F3 for Specific Help on Current Parameters

The new depth, 19.500, must be equal to or less than NUM

Input File Contents

```

BORING S-3 --H-Pile
OUT OSG HAM STR FUL PEL N SPL N-U P-D %SK ISM 0 PHI RSA ITR H-D MXT DEx
-100 0 182 0 0 0 0 0 0 1 0 0 0 0 0 0 0 0.000
  Pile g Hammer g
  9.810 9.810
    W Cp A Cp E Cp T Cp CoR ROut StCp
  18.090 1596.800 1207.0 152.000 0.920 3.000 0.0
    A Cu E Cu T Cu CoR ROut StCu
  0.000 0.0 0.000 0.000 0.000 0.0
    LPle APle EPle WPle Circ Strg CoR ROut
  15.000 193.500210000.000 77.500 1.420 248.000 0.850 0.010
  Manufac Hmr Name HmrType No Seg-s
  CONMACO C 140 3 1
    Ram Wt Ram L Ram Dia MaxStrk RtdStrk Effic
  62.30 1397.00 612.65 0.91 0.91 0.67
  No. Assmbly Segs
  2
<---- Assembly Masses ----><----Assembly Stiffnesses---->
  37.291 37.291 0.000 12540.6 12540.6 0.0
  Stroke Effic. Pressure R-Weight T-Delay Exp-Coeff Eps-Str
  0.9100 0.6700 0.0000 0.0000 0.0000 0.0000 0.0100 0.0000
    Qs Qt Js Jt Qx Jx Rati Dept
  0.000 0.000 0.000 0.000 0.000 0.000 0.000 0.000
  Research Soil Model: Atoe, Plug, Gap, Q-fac
  0.000 0.000 0.000 0.000
  Research Soil Model: RD-skn: m, d, toe: m, d
  0.000 0.000 0.000 0.000
  Res. Distribution
  Dpth Rskn Rtoe Qs Qt Js Jt SU F RelE SU T
  0.01 0.00 0.00 2.54 2.97 0.16 0.50 1.00 0.00 0.00
  1.99 0.00 0.00 2.54 2.97 0.16 0.50 1.00 0.00 0.00
  1.99 0.00 0.00 2.54 2.97 0.16 0.50 1.00 0.00 0.00
  2.00 5.61 27.42 2.54 2.97 0.16 0.50 1.00 0.00 0.00
  2.01 10.15 70.25 2.54 2.97 0.16 0.50 1.00 0.00 0.00
  2.99 20.38 141.00 2.54 2.97 0.16 0.50 1.00 0.00 0.00
  3.01 106.00 120.90 2.54 2.97 0.65 0.50 2.00 0.00 0.00
  5.99 106.00 120.90 2.54 2.97 0.65 0.50 2.00 0.00 0.00
  6.01 47.10 176.79 2.54 2.97 0.65 0.50 2.00 0.00 0.00
  9.01 54.64 176.79 2.54 2.97 0.65 0.50 2.00 0.00 0.00
  12.01 62.19 176.79 2.54 2.97 0.65 0.50 2.00 0.00 0.00
  14.99 67.79 176.79 2.54 2.97 0.65 0.50 2.00 0.00 0.00
  15.01 141.70 919.89 2.54 2.97 0.16 0.50 1.00 0.00 0.00
  Gain/Loss factors: shaft and toe
  0.50000 1.00000 0.00000 0.00000 0.00000
  1.00000 1.00000 0.00000 0.00000 0.00000
  Dpth L Wait Strk Pmx% Eff. Stff CoR
  0.50 15.00 0.00 0.000 0.000 0.000 0.000 0.000
  1.00 15.00 0.00 0.000 0.000 0.000 0.000 0.000
  1.50 15.00 0.00 0.000 0.000 0.000 0.000 0.000
  2.00 15.00 0.00 0.000 0.000 0.000 0.000 0.000
  2.50 15.00 0.00 0.000 0.000 0.000 0.000 0.000
  3.00 15.00 0.00 0.000 0.000 0.000 0.000 0.000
  3.50 15.00 0.00 0.000 0.000 0.000 0.000 0.000
  4.00 15.00 0.00 0.000 0.000 0.000 0.000 0.000
  4.50 15.00 0.00 0.000 0.000 0.000 0.000 0.000
  5.00 15.00 0.00 0.000 0.000 0.000 0.000 0.000
  5.50 15.00 0.00 0.000 0.000 0.000 0.000 0.000
  6.00 15.00 0.00 0.000 0.000 0.000 0.000 0.000
  .
  . [ABRIDGED]
  .
  13.50 15.00 0.00 0.000 0.000 0.000 0.000 0.000
  14.00 15.00 0.00 0.000 0.000 0.000 0.000 0.000
  14.50 15.00 0.00 0.000 0.000 0.000 0.000 0.000
  15.00 15.00 0.00 0.000 0.000 0.000 0.000 0.000

```

GRLWEAP: WAVE EQUATION ANALYSIS OF PILE FOUNDATIONS
Version 2003
SI Units

BORING S-3 --H-Pile

Hammer Model:	C 140	Made by:	CONMACO		
No.	Weight kN	Stiffn kN/mm	CoR	C-Slk mm	Dampg kN/m/s
1	62.300				
Helmet	18.090	1231.0	0.920	3.0000	111.8
Combined Pile Top		4063.5			
Assembly	Weight kN	Stiffn kN/mm	CoR	C-Slk mm	
1	37.291	12540.6			
2	37.291	12540.6	0.800	3.0480	

HAMMER OPTIONS:

Hammer File ID No.	182	Hammer Type	Ext.Comb.
--------------------	-----	-------------	-----------

HAMMER DATA:

Ram Weight	(kN)	62.30	Ram Length	(mm)	1397.00
Maximum (Eq) Stroke	(m)	0.91	Actual (Eq) Stroke	(m)	0.91
Efficiency		0.670			

Rated Energy	(kJ)	56.97	Potential Energy	(kJ)	56.69
Kinetic Energy	(kJ)	37.98	Impact Velocity	(m/s)	3.46

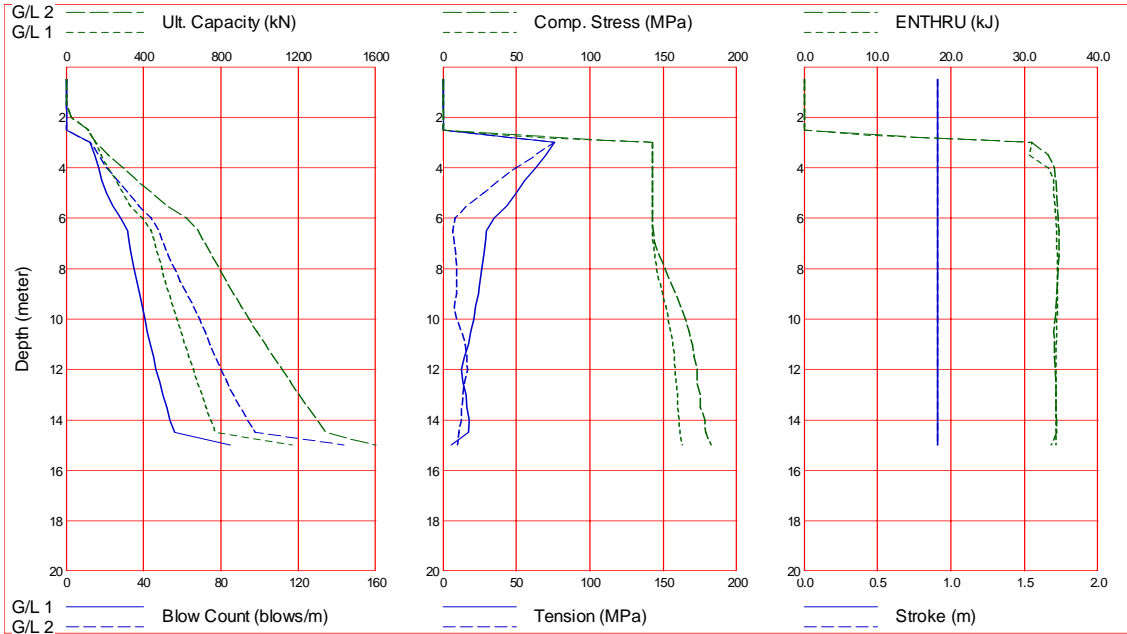
HAMMER CUSHION

Cross Sect. Area	(cm2)	1596.80	PILE CUSHION		
Elastic-Modulus	(MPa)	1207.0	Cross Sect. Area	(cm2)	0.00
Thickness	(mm)	152.00	Elastic-Modulus	(MPa)	0.0
Coeff of Restitution		0.920	Thickness	(mm)	0.00
RoundOut	(mm)	3.0	Coeff of Restitution		1.000
Stiffness	(kN/mm)	1268.0	RoundOut	(mm)	0.0
			Stiffness	(kN/mm)	0.0

BORING S-3 --H-Pile

Gain/Loss 1 at Shaft and Toe 0.500 / 1.000
 Gain/Loss 2 at Shaft and Toe 1.000 / 1.000

GRLWEAP(TM) Version 2003



Gain/Loss 1 at Shaft and Toe 0.500 / 1.000

Depth m	Ultimate Capacity kN	Friction kN	End Bearing kN	Blow Count blows/m	Comp. Stress MPa	Tension Stress MPa	Stroke m	ENTHRU kJ
0.5	0.0	0.0	0.0	0.0	0.000	0.000	0.91	0.0
1.0	0.0	0.0	0.0	0.0	0.000	0.000	0.91	0.0
1.5	0.0	0.0	0.0	0.0	0.000	0.000	0.91	0.0
2.0	27.5	0.0	27.4	0.0	0.000	0.000	0.91	0.0
2.5	114.6	9.0	105.6	0.0	0.000	0.000	0.91	0.0
3.0	152.9	21.9	130.9	12.3	142.675	-76.224	0.91	31.0
3.5	180.5	59.6	120.9	14.7	142.676	-69.887	0.91	30.7
4.0	218.1	97.2	120.9	16.9	142.677	-63.117	0.91	33.2
4.5	255.8	134.9	120.9	18.6	142.680	-55.726	0.91	34.0
5.0	293.3	172.4	120.9	21.0	142.683	-50.084	0.91	34.0
5.5	331.0	210.1	120.9	24.0	142.707	-43.651	0.91	34.2
6.0	396.4	247.6	148.8	28.2	142.750	-34.911	0.91	34.3
6.5	441.5	264.7	176.8	31.6	142.908	-29.849	0.91	34.4
7.0	458.8	282.0	176.8	32.6	143.298	-28.832	0.91	34.4
7.5	476.7	299.9	176.8	34.0	144.224	-27.440	0.91	34.5
8.0	494.9	318.1	176.8	35.2	145.499	-26.440	0.91	34.5
8.5	513.7	336.9	176.8	36.7	147.693	-25.158	0.91	34.5
9.0	532.8	356.0	176.8	37.9	149.569	-24.177	0.91	34.5
9.5	552.5	375.7	176.8	39.5	151.736	-22.348	0.91	34.5
10.0	572.5	395.7	176.8	40.7	153.518	-20.979	0.91	34.4
10.5	593.0	416.2	176.8	42.1	154.832	-19.062	0.91	34.4
11.0	613.9	437.1	176.8	43.4	156.377	-17.394	0.91	34.3
11.5	635.4	458.6	176.8	45.0	157.613	-14.711	0.91	34.3
12.0	657.1	480.4	176.8	46.5	158.176	-12.457	0.91	34.3
12.5	679.5	502.7	176.8	48.3	158.828	-13.766	0.91	34.3
13.0	702.0	525.2	176.8	49.9	159.549	-15.769	0.91	34.3
13.5	724.9	548.1	176.8	51.9	159.924	-16.370	0.91	34.3
14.0	748.1	571.3	176.8	53.7	160.872	-18.042	0.91	34.3
14.5	771.7	595.0	176.8	55.9	161.529	-17.233	0.91	34.3
15.0	1167.4	619.1	548.3	84.8	162.863	-5.707	0.91	34.3

Total Number of Blows: 451

Driving Time (min): 15 11 9 7 6 5 5 4 4 3
 @Blow Rate (b/min): 30 40 50 60 70 80 90 100 110 120

Driving Time for continuously running hammer; any wait times not included

Gain/Loss 2 at Shaft and Toe 1.000 / 1.000

Depth m	Ultimate Capacity kN	Friction kN	End Bearing kN	Blow Count blows/m	Comp. Stress MPa	Tension Stress MPa	Stroke m	ENTHRU kJ
0.5	0.0	0.0	0.0	0.0	0.000	0.000	0.91	0.0
1.0	0.0	0.0	0.0	0.0	0.000	0.000	0.91	0.0
1.5	0.0	0.0	0.0	0.0	0.000	0.000	0.91	0.0
2.0	27.5	0.0	27.4	0.0	0.000	0.000	0.91	0.0
2.5	114.6	9.0	105.6	0.0	0.000	0.000	0.91	0.0
3.0	152.9	22.0	130.9	12.4	142.675	-76.217	0.91	31.0
3.5	217.8	96.9	120.9	16.9	142.677	-63.209	0.91	33.2
4.0	293.1	172.2	120.9	21.0	142.679	-49.650	0.91	34.1
4.5	368.4	247.5	120.9	26.4	142.683	-37.880	0.91	34.3
5.0	443.6	322.7	120.9	32.0	142.687	-27.211	0.91	34.4
5.5	518.9	398.0	120.9	37.5	142.731	-16.424	0.91	34.5
6.0	621.9	473.0	148.8	43.8	142.793	-8.516	0.91	34.6
6.5	683.9	507.1	176.8	47.8	143.322	-6.929	0.91	34.7
7.0	718.7	541.9	176.8	50.3	144.259	-7.491	0.91	34.7
7.5	754.3	577.5	176.8	53.0	147.346	-8.902	0.91	34.7
8.0	790.9	614.1	176.8	55.9	151.032	-9.133	0.91	34.6
8.5	828.3	651.5	176.8	59.0	154.961	-9.500	0.91	34.5
9.0	866.6	689.8	176.8	62.4	158.810	-9.166	0.91	34.4
9.5	905.9	729.1	176.8	66.0	161.663	-7.739	0.91	34.3
10.0	946.0	769.2	176.8	69.2	165.110	-9.465	0.91	34.2
10.5	987.0	810.2	176.8	71.7	167.670	-12.443	0.91	34.0
11.0	1028.9	852.1	176.8	74.3	169.994	-15.204	0.91	34.1
11.5	1071.7	894.9	176.8	77.1	171.142	-16.379	0.91	34.1
12.0	1115.4	938.6	176.8	80.0	173.189	-16.563	0.91	34.2
12.5	1159.8	983.1	176.8	83.2	173.156	-14.500	0.91	34.3
13.0	1205.0	1028.2	176.8	86.5	175.406	-13.689	0.91	34.3
13.5	1250.8	1074.0	176.8	90.1	175.406	-12.761	0.91	34.3
14.0	1297.3	1120.5	176.8	93.8	178.310	-12.610	0.91	34.4
14.5	1344.4	1167.6	176.8	97.9	179.132	-10.871	0.91	34.4
15.0	1764.0	1215.7	548.3	143.4	182.879	-9.694	0.91	33.7

Total Number of Blows: 738

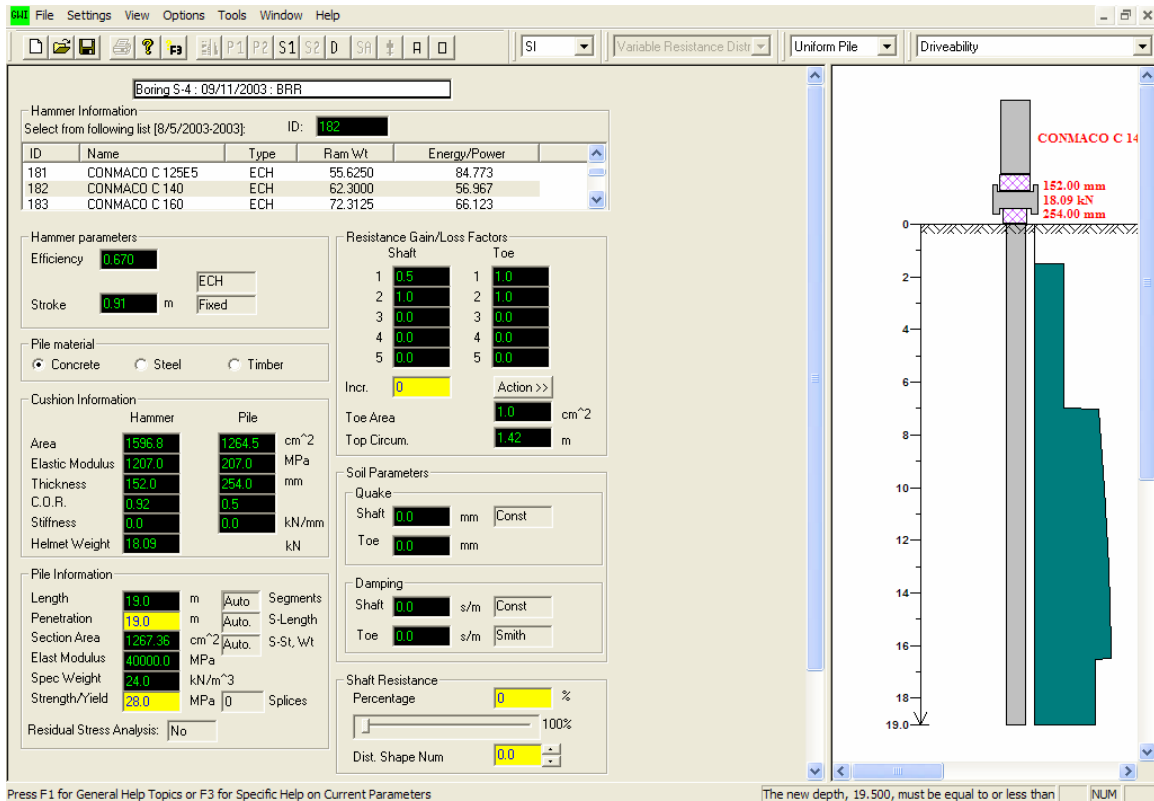
Driving Time (min):	24	18	14	12	10	9	8	7	6	6
@Blow Rate (b/min):	30	40	50	60	70	80	90	100	110	120

Driving Time for continuously running hammer; any wait times not included

F.9.4.1 South Abutment, Concrete Pile

This analysis was initially generated from the Soil Boring S-4 file in Driven. Driven created a GRLWEAP input file that included the general pile properties, a detailed soil resistance distribution and soil damping, quake and set-up parameters based on the soil type. The hammer and driving system parameters were entered, the gain/loss factor was selected as 0.5 and 1.0 for the shaft (per cohesive soils in Table 9-20) and 1.0 for the toe. The depths for analysis were set every 0.5 m to the pile penetration. The analysis was run, and the results follow.

In this case, penetration resistance is less than 25 blows per 0.25 m when the hammer is run at full stroke. If the stroke can be reduced on this hammer, the analysis should be re-run at a lower stroke. The resulting penetration resistance will be higher and the stresses lower. The pile compressive and tensile stresses are with FHWA limits for typical prestressed concrete piles.



Input File Contents

Boring S-4 : 09/11/2003 : BRR

OUT	OSG	HAM	STR	FUL	PEL	N	SPL	N-U	P-D	%SK	ISM	0	PHI	RSA	ITR	H-D	MXT	DEx
-100	0	182	0	0	0	0	0	0	3	0	0	0	0	0	0	0	0	0.000

File g Hammer g
 9.810 9.810

W Cp	A Cp	E Cp	T Cp	CoR	ROut	StCp
18.090	1596.800	1207.0	152.000	0.920	3.000	0.0

A Cu	E Cu	T Cu	CoR	ROut	StCu
1264.500	207.0	254.000	0.500	3.000	0.0

LPle	APle	EPle	WPle	Circ	Strg	CoR	ROut
19.000	1267.360	40000.000	24.000	1.420	28.000	1.000	0.010

Manufac Hmr Name HmrType No Seg-s
 CONMACO C 140 3 1

Ram Wt	Ram L	Ram Dia	MaxStrk	RtdStrk	Efficy
62.30	1397.00	612.65	0.91	0.91	0.67

No. Assmbly Segs
 2

<---- Assembly Masses ----><----Assembly Stiffnesses---->

Stroke	Effic.	Pressure	R-Weight	T-Delay	Exp-Coeff	Eps-Str	Eps-Str
37.291	37.291	0.000	12540.6	12540.6	0.0	0.0100	0.0000

Qs	Qt	Js	Jt	Qx	Jx	Rati	Dept
0.000	0.000	0.000	0.000	0.000	0.000	0.000	0.000

Research Soil Model: Atoe, Plug, Gap, Q-fac
 0.000 0.000 0.000 0.000

Research Soil Model: RD-skn: m, d, toe: m, d
 0.000 0.000 0.000 0.000

Res. Distribution

Dpth	Rskn	Rtoe	Qs	Qt	Js	Jt	SU F	RelE	SU T
0.01	0.00	0.00	2.54	2.97	0.65	0.50	2.00	0.00	0.00
1.49	0.00	0.00	2.54	2.97	0.65	0.50	2.00	0.00	0.00
1.50	32.24	37.64	2.54	2.97	0.65	0.50	2.00	0.00	0.00
3.01	32.24	37.64	2.54	2.97	0.65	0.50	2.00	0.00	0.00
6.01	32.31	37.64	2.54	2.97	0.65	0.50	2.00	0.00	0.00
6.99	32.38	37.64	2.54	2.97	0.65	0.50	2.00	0.00	0.00
7.01	71.76	106.07	2.54	2.97	0.65	0.50	2.00	0.00	0.00
10.01	77.24	106.07	2.54	2.97	0.65	0.50	2.00	0.00	0.00
13.01	82.73	106.07	2.54	2.97	0.65	0.50	2.00	0.00	0.00
16.01	84.97	106.07	2.54	2.97	0.65	0.50	2.00	0.00	0.00
16.49	84.97	106.07	2.54	2.97	0.65	0.50	2.00	0.00	0.00
16.51	67.30	179.07	2.54	2.97	0.65	0.50	2.00	0.00	0.00
18.99	67.30	179.07	2.54	2.97	0.65	0.50	2.00	0.00	0.00
19.01	65.12	190.48	2.54	2.97	0.65	0.50	2.00	0.00	0.00

Gain/Loss factors: shaft and toe

Dpth	L	Wait	Strk	Pmx%	Eff.	Stff	CoR
0.50	19.00	0.00	0.000	0.000	0.000	0.000	0.000
1.00	19.00	0.00	0.000	0.000	0.000	0.000	0.000
1.50	19.00	0.00	0.000	0.000	0.000	0.000	0.000
2.00	19.00	0.00	0.000	0.000	0.000	0.000	0.000
2.50	19.00	0.00	0.000	0.000	0.000	0.000	0.000
3.00	19.00	0.00	0.000	0.000	0.000	0.000	0.000
3.50	19.00	0.00	0.000	0.000	0.000	0.000	0.000
4.00	19.00	0.00	0.000	0.000	0.000	0.000	0.000
4.50	19.00	0.00	0.000	0.000	0.000	0.000	0.000
5.00	19.00	0.00	0.000	0.000	0.000	0.000	0.000
5.50	19.00	0.00	0.000	0.000	0.000	0.000	0.000

. [ABRIDGED]

Dpth	L	Wait	Strk	Pmx%	Eff.	Stff	CoR
14.00	19.00	0.00	0.000	0.000	0.000	0.000	0.000
14.50	19.00	0.00	0.000	0.000	0.000	0.000	0.000
15.00	19.00	0.00	0.000	0.000	0.000	0.000	0.000
15.50	19.00	0.00	0.000	0.000	0.000	0.000	0.000
16.00	19.00	0.00	0.000	0.000	0.000	0.000	0.000
16.50	19.00	0.00	0.000	0.000	0.000	0.000	0.000
17.00	19.00	0.00	0.000	0.000	0.000	0.000	0.000
17.50	19.00	0.00	0.000	0.000	0.000	0.000	0.000
18.00	19.00	0.00	0.000	0.000	0.000	0.000	0.000

18.50	19.00	0.00	0.000	0.000	0.000	0.000	0.000
19.00	19.00	0.00	0.000	0.000	0.000	0.000	0.000
0.00	0.00	0.00	0.000	0.000	0.000	0.000	0.000

GRLWEAP: WAVE EQUATION ANALYSIS OF PILE FOUNDATIONS
Version 2003
SI Units

Boring S-4 : 09/11/2003 : BRR

Hammer Model:	C 140	Made by:	CONMACO		
No.	Weight kN	Stiffn kN/mm	CoR	C-Slk mm	Dampg kN/m/s
1	62.300				
Helmet	18.090	1231.0	0.920	3.0000	111.8
Cushion		103.1	0.500	3.0000	
Combined Pile Top		101.0			
Assembly	Weight kN	Stiffn kN/mm	CoR	C-Slk mm	
1	37.291	12540.6			
2	37.291	12540.6	0.800	3.0480	

HAMMER OPTIONS:

Hammer File ID No.	182	Hammer Type	Ext.Comb.
--------------------	-----	-------------	-----------

HAMMER DATA:

Ram Weight	(kN)	62.30	Ram Length	(mm)	1397.00
Maximum (Eq) Stroke	(m)	0.91	Actual (Eq) Stroke	(m)	0.91
Efficiency		0.670			

Rated Energy	(kJ)	56.97	Potential Energy	(kJ)	56.69
Kinetic Energy	(kJ)	37.98	Impact Velocity	(m/s)	3.46

HAMMER CUSHION

Cross Sect. Area	(cm2)	1596.80	PILE CUSHION	Cross Sect. Area	(cm2)	1264.50
Elastic-Modulus	(MPa)	1207.0	Elastic-Modulus	(MPa)	207.0	
Thickness	(mm)	152.00	Thickness	(mm)	254.00	
Coeff of Restitution		0.920	Coeff of Restitution		0.500	
RoundOut	(mm)	3.0	RoundOut	(mm)	3.0	
Stiffness	(kN/mm)	1268.0	Stiffness	(kN/mm)	103.1	

Boring S-4 : 09/11/2003 : BRR
 GRL Engineers, Inc.

2003/09/24
 GRLWEAP(TM) Version 2003

Depth (m) 0.5
 Shaft Gain/Loss Factor 0.500 Toe Gain/Loss Factor 1.000

PILE PROFILE:

L b Top	Area	E-Mod	Spec Wt	Circmf	Strength	Wave Sp	EA/c
m	cm2	MPa	kN/m3	m	MPa	m/s	kN/m/s
0.00	1267.4	40000.	24.00	1.420	28.00	4044.	1253.72
19.00	1267.4	40000.	24.00	1.420	28.00	4044.	1253.72

Wave Travel Time 2L/c (ms) 9.398

Pile and Soil Model						Total Capacity Rut (kN)				0.0	
No.	Weight	Stiffn	C-Slk	T-Slk	CoR	Soil-S	Soil-D	Quake	LbTop	Circm	Area
	kN	kN/mm	mm	mm		kN	s/m	mm	m	m	cm2
1	3.042	5069.	3.000	0.000	1.00	0.0	0.000	2.54	1.00	1.4	1267.4
2	3.042	5069.	0.000	0.000	1.00	0.0	0.000	2.54	2.00	1.4	1267.4
19	3.042	5069.	0.000	0.000	1.00	0.0	0.650	2.54	19.00	1.4	1267.4
Toe						0.0	0.500	2.97			

PILE, SOIL, ANALYSIS OPTIONS:

Uniform pile
 No. of Slacks/Splices 0
 Pile Segments: Automatic
 Pile Damping (%) 3
 Pile Damping Fact. (kN/m/s) 75.223

Driveability Analysis

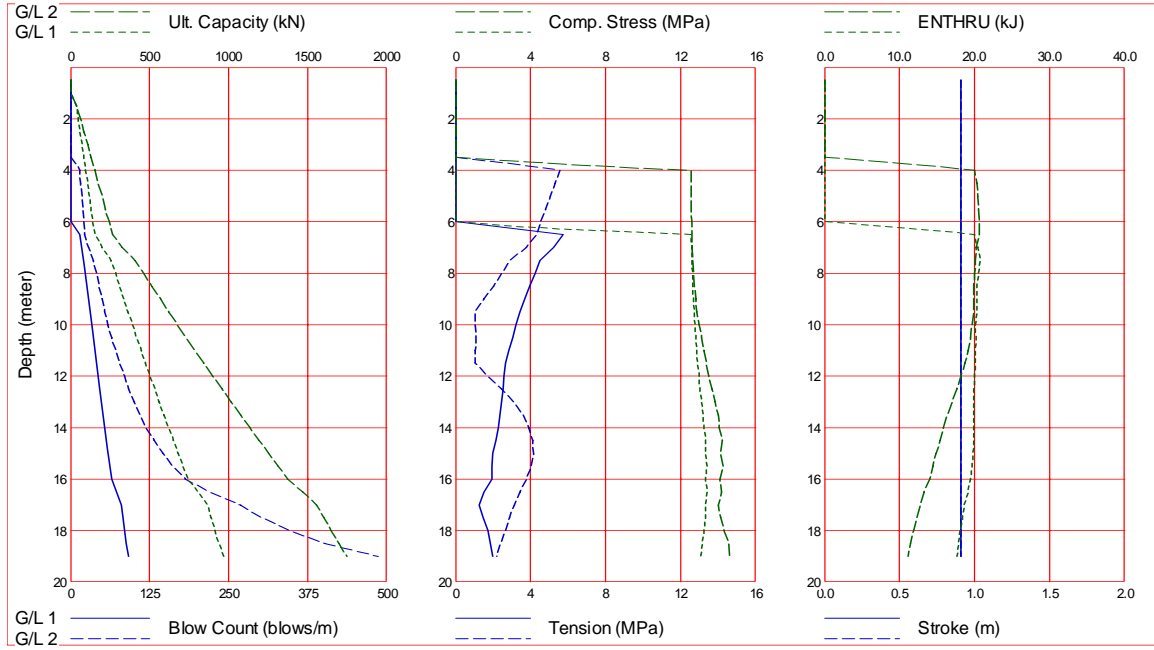
Soil Damping Option Smith
 Max No Analysis Iterations 0 Time Increment/Critical 160
 Output Time Interval 1 Analysis Time-Input (ms) 0
 Output Level: Normal
 Gravity Mass, Pile, Hammer: 9.810 9.810 9.810
 Output Segment Generation: Automatic

Depth	Stroke	Efficy	PileC.St.	PileC.CoR
m	m		kN/mm	
0.50	0.91	0.670	103.	0.500

Boring S-4 : 09/11/2003 : BRR

Gain/Loss 1 at Shaft and Toe 0.500 / 1.000
Gain/Loss 2 at Shaft and Toe 1.000 / 1.000

GRLWEAP(TM) Version 2003



Gain/Loss 1 at Shaft and Toe 0.500 / 1.000

Depth m	Ultimate Capacity kN	Friction kN	End Bearing kN	Blow Count blows/m	Comp. Stress MPa	Tension Stress MPa	Stroke m	ENTHRU kJ
0.5	0.0	0.0	0.0	0.0	0.000	0.000	0.91	0.0
1.0	0.0	0.0	0.0	0.0	0.000	0.000	0.91	0.0
1.5	37.8	0.1	37.6	0.0	0.000	0.000	0.91	0.0
2.0	49.2	11.6	37.6	0.0	0.000	0.000	0.91	0.0
2.5	60.6	23.0	37.6	0.0	0.000	0.000	0.91	0.0
3.0	72.1	34.5	37.6	0.0	0.000	0.000	0.91	0.0
3.5	83.5	45.9	37.6	0.0	0.000	0.000	0.91	0.0
4.0	95.0	57.4	37.6	0.0	0.000	0.000	0.91	0.0
4.5	106.5	68.8	37.6	0.0	0.000	0.000	0.91	0.0
5.0	117.9	80.3	37.6	0.0	0.000	0.000	0.91	0.0
5.5	129.4	91.7	37.6	0.0	0.000	0.000	0.91	0.0
6.0	140.8	103.2	37.6	0.0	0.000	0.000	0.91	0.0
6.5	152.3	114.7	37.6	15.0	12.583	-5.741	0.91	20.0
7.0	198.1	126.2	71.9	17.5	12.600	-5.241	0.91	20.4
7.5	257.9	151.8	106.1	20.8	12.609	-4.509	0.91	20.7
8.0	283.8	177.8	106.1	23.2	12.630	-4.224	0.91	20.5
8.5	310.1	204.0	106.1	26.0	12.650	-3.948	0.91	20.3
9.0	336.7	230.6	106.1	28.9	12.682	-3.687	0.91	20.3
9.5	363.6	257.6	106.1	31.3	12.716	-3.442	0.91	20.3
10.0	390.9	284.8	106.1	34.1	12.759	-3.224	0.91	20.1
10.5	418.5	312.4	106.1	36.5	12.805	-3.031	0.91	20.2
11.0	446.4	340.3	106.1	39.2	12.854	-2.846	0.91	20.1
11.5	474.6	368.5	106.1	41.7	12.913	-2.679	0.91	20.1
12.0	503.2	397.1	106.1	44.2	12.974	-2.584	0.91	20.0
12.5	532.0	426.0	106.1	46.5	13.045	-2.544	0.91	19.9
13.0	561.2	455.2	106.1	48.9	13.112	-2.472	0.91	19.9
13.5	590.7	484.6	106.1	51.3	13.193	-2.382	0.91	19.9
14.0	620.2	514.2	106.1	53.9	13.267	-2.269	0.91	19.9
14.5	649.9	543.9	106.1	56.5	13.354	-2.138	0.91	19.9
15.0	679.8	573.7	106.1	59.3	13.353	-1.981	0.91	19.8
15.5	709.7	603.6	106.1	62.3	13.430	-1.961	0.91	19.7
16.0	739.8	633.7	106.1	65.4	13.351	-1.934	0.91	19.5
16.5	806.4	663.9	142.6	72.9	13.407	-1.518	0.91	19.1
17.0	866.9	687.8	179.1	79.8	13.327	-1.260	0.91	18.6
17.5	890.8	711.7	179.1	82.4	13.313	-1.481	0.91	18.4
18.0	914.7	735.6	179.1	85.2	13.231	-1.723	0.91	18.1
18.5	938.5	759.5	179.1	88.1	13.178	-1.860	0.91	17.9
19.0	968.1	783.4	184.8	91.9	13.089	-1.997	0.91	17.6

Total Number of Blows: 629

Driving Time (min): 20 15 12 10 8 7 6 6 5 5
 @Blow Rate (b/min): 30 40 50 60 70 80 90 100 110 120

Driving Time for continuously running hammer; any wait times not included

Gain/Loss 2 at Shaft and Toe 1.000 / 1.000

Depth m	Ultimate Capacity kN	Friction kN	End Bearing kN	Blow Count blows/m	Comp. Stress MPa	Tension Stress MPa	Stroke m	ENTHRU kJ
0.5	0.0	0.0	0.0	0.0	0.000	0.000	0.91	0.0
1.0	0.0	0.0	0.0	0.0	0.000	0.000	0.91	0.0
1.5	37.9	0.2	37.6	0.0	0.000	0.000	0.91	0.0
2.0	60.8	23.1	37.6	0.0	0.000	0.000	0.91	0.0
2.5	83.7	46.0	37.6	0.0	0.000	0.000	0.91	0.0
3.0	106.6	68.9	37.6	0.0	0.000	0.000	0.91	0.0
3.5	129.4	91.8	37.6	0.0	0.000	0.000	0.91	0.0
4.0	152.4	114.7	37.6	15.1	12.569	-5.585	0.91	20.0
4.5	175.3	137.6	37.6	16.4	12.573	-5.310	0.91	20.3
5.0	198.2	160.5	37.6	17.8	12.578	-5.051	0.91	20.4
5.5	221.1	183.5	37.6	19.3	12.582	-4.792	0.91	20.5
6.0	244.1	206.4	37.6	20.7	12.592	-4.564	0.91	20.6
6.5	267.0	229.4	37.6	22.1	12.604	-4.339	0.91	20.6
7.0	324.3	252.5	71.9	27.9	12.628	-3.757	0.91	20.2
7.5	409.7	303.6	106.1	35.9	12.649	-2.888	0.91	20.1
8.0	461.6	355.5	106.1	40.8	12.692	-2.455	0.91	20.0
8.5	514.2	408.1	106.1	45.3	12.731	-2.006	0.91	19.9
9.0	567.4	461.3	106.1	49.6	12.804	-1.505	0.91	19.9
9.5	621.2	515.1	106.1	54.2	12.885	-1.060	0.91	19.9
10.0	675.7	569.7	106.1	59.3	12.989	-1.046	0.91	19.7
10.5	730.9	624.8	106.1	64.9	13.106	-1.083	0.91	19.5
11.0	786.7	680.6	106.1	71.2	13.227	-1.042	0.91	19.1
11.5	843.1	737.1	106.1	78.3	13.367	-1.049	0.91	18.7
12.0	900.2	794.2	106.1	85.1	13.513	-1.686	0.91	18.2
12.5	958.0	851.9	106.1	92.3	13.677	-2.468	0.91	17.6
13.0	1016.4	910.3	106.1	100.5	13.831	-3.079	0.91	17.0
13.5	1075.2	969.2	106.1	109.7	14.005	-3.590	0.91	16.4
14.0	1134.4	1028.3	106.1	120.2	14.072	-3.885	0.91	15.8
14.5	1193.8	1087.7	106.1	132.0	14.232	-4.100	0.91	15.4
15.0	1253.4	1147.4	106.1	145.9	14.151	-4.146	0.91	14.9
15.5	1313.4	1207.3	106.1	161.9	14.288	-4.034	0.91	14.5
16.0	1373.6	1267.5	106.1	181.1	14.117	-3.784	0.91	14.0
16.5	1470.3	1327.8	142.6	220.7	14.192	-3.435	0.91	13.3
17.0	1554.7	1375.6	179.1	268.6	14.023	-3.122	0.91	12.7
17.5	1602.5	1423.4	179.1	303.0	14.153	-2.884	0.91	12.3
18.0	1650.2	1471.2	179.1	346.4	14.330	-2.657	0.91	11.9
18.5	1698.0	1519.0	179.1	401.9	14.585	-2.429	0.91	11.5
19.0	1751.5	1566.7	184.8	486.4	14.621	-2.202	0.91	11.1

Total Number of Blows: 1775

Driving Time (min): 59 44 35 29 25 22 19 17 16 14
 @Blow Rate (b/min): 30 40 50 60 70 80 90 100 110 120

Driving Time for continuously running hammer; any wait times not included

APPENDIX G

Driven Pile Foundation Design by LRFD

	Page
G.1 Introduction.....	G-3
G.2 ASIC Concepts of ASD and LRFD.....	G-3
G.3 Calibration of Probability Based LRFD.....	G-7
G.4 LRFD Details.....	G-11
G.5 The Design Process.....	G-14
G.6 A Simple Example.....	G-14
G.6.1 ASD.....	G-17
G.6.2 LRFD.....	G-17
G.6.3 Comments.....	G-18
References.....	G-19

APPENDIX G

DRIVEN PILE FOUNDATION DESIGN BY LRFD

G.1 INTRODUCTION

In 1994, the AASHTO Subcommittee on Bridges adopted a Bridge Design Specification based on the use of the Load and Resistance Factor (LRFD) method (AASHTO, 1994). The geotechnical parts of the new specification had been developed by an NCHRP Research Project (Barker et al). The driven pile part of the 1994 version of the specification was then extensively edited in the Second Edition of 1998 (AASHTO, 1998). In general, the new specification has generated considerable resistance to its implementation from many parts of bridge design community including the driven pile part. A very few States implemented it immediately while many still have made little progress in its implementation (2005). The purpose here is to provide the necessary basis for preparing the deep foundation designer to use this new method in driven pile design.

The geotechnical portion of the specification has proven to be one of the most difficult to implement. This includes shallow and deep foundations, and earth retaining systems. Considerable effort has been spent, since the adoption in 1994, to modify the document to satisfy the concerns of the users. In the driven pile area, it was extensively modified in the Second Edition (AASHTO 1998), but those modifications failed to satisfy many of the criticisms. This Appendix is being written using that Second Edition version of the Code. Basic concepts of LRFD will be presented, the application to driven pile design will be discussed and examples will be solved using the requirements of that Code with the application of some imagination.

G.2 BASIC CONCEPTS OF ASD AND LRFD

In order for the designer to understand and appreciate LRFD for the design of driven pile foundations, it is necessary to briefly summarize the fundamental basis for allowable stress design (ASD) and then to review the history of the development of the LRFD and its early implementation. The history of the development of LRFD is particularly interesting in view of what has happened recently and, in addition, it places the changes wrought by LRFD in proper perspective.

Allowable Stress Design (ASD) grew out of the development of methods of structural analysis during the nineteenth century. These methods were based on the assumption that the structure behaved elastically and they produced a rational evaluation of structural behavior that satisfied both equilibrium and compatibility. Prior to these developments, structures were designed based entirely on experience and sets of rules. But, the analyses only explained structural behavior. It was desirable that a rational design approach be developed and it was logical to limit the calculated stresses in a structure to some fraction of the structural material strength. Gradually, structural loads appropriate for design were defined and then codified. So, if member stresses could be calculated it was logical to limit those stresses and values of allowable stresses were gradually accepted based on the experience that the structure did not fail. These limiting stress values became known “design stresses” or “allowable stresses.” For instance, the allowable stresses in steel beams in bending have been limited to between about 0.4 and 0.66 times the steel yield strength.

But, linear elastic behavior is not universally observed in all structural elements. For example, the failure strength of a column is related the slenderness ratio of the member and methods are available to calculate the failure load with considerable confidence. Similar considerations affect the design of other structural elements. The approach that came to be used in some applications during the development of ASD was to apply a “safety factor” to the calculated ultimate member capacity.

Geotechnical engineering has the universal problem that a linear elastic analysis will not represent the strength of a soil structure. Therefore, the use of factors of safety applied to the strength is universal in geotechnical design. So, in ASD foundation design the superstructure is analyzed using an elastic analysis. From this analysis, the element forces including the foundations are determined. Then the elements are selected so that they will carry the elastically calculated loads with the required factor of safety.

Factors of safety were selected so that failures were very unlikely, based on experience, but the magnitudes of the factors of safety were based only on experience. The geotechnical engineer should understand that he does not “own” all of the factor of safety. It must be adequate to deal with the variability of the loads and the inadequacy of the analysis in addition to the strength variability.

Until 1956, the analysis of a concrete section subject to bending was performed assuming that the compression stress in the concrete was linearly distributed on the cross section with the further assumption that concrete could carry no tension. Designs were limited by placing limits on the calculated stress in both the concrete in compression and in the steel in both tension and compression (if compression steel was present). In other words, the element strength was treated as if the materials were elastic and, to perform the analysis, the steel was then “transformed” into concrete based on the relative moduli of the two materials. The result of these assumptions produced quite conservative results, particularly if compression reinforcement was present as is always the case with columns. The time dependent deformation of concrete subjected to compression causes its effective modulus to be time dependent. Extensive research was performed in the first half of the twentieth century to understand what the actual stress distribution was and how it could be used in design.

These fundamental problems with the use of ASD caused the American Concrete Institute (ACI) in 1956 to adopt a new edition of their Building Code for the design of concrete structures and in that code an Appendix was included that used a strength design approach (ACI 1956) to replace the allowable stress method described above. The ultimate strength of the element in bending was calculated using a prescribed, nonlinear concrete stress distribution on the section at failure. The computational procedure was quite simple and the result was element strength not stress. The Appendix of ACI 318-56 achieved little use.

The ACI Committee that prepared this method then took another major step. Instead of selecting a factor of safety for particular failure modes they broke the factor of safety into parts. They realized that the limiting value of ultimate load should depend on the variability of the particular load types. So they specified different “load factors” for the various types of loads and, indirectly, they applied an additional multiplier to provide structural safety for the strength variability of member types and failure modes.

ACI 318-63, adopted in 1963, made extensive changes from the 1956 Code and the result had the form that we now know as LRFD (ACI 1963).

$$\sum \gamma_{ij} Q_{ij} \leq \phi_k R_{nk} \quad (1)$$

Where, γ is the load factor, Q is the load effect (this refers the element load calculated from the applied loads by a linear elastic structural analysis. The subscripts i and j refer

to the load condition (dead, live, wind, etc.) and the load combination, respectively. ϕ is the resistance factor for a given limit state (failure mode), R_{nk} is the nominal resistance in the k^{th} limit state. The term nominal resistance was adopted to define the element strength determined by some specified method. (It should be noted that in the AASHTO LRFD Code the term nominal resistance is used instead of nominal strength.) The summation on the left side of Expression (1) is known as the factored load. A generally used name for the right side of the expression has not been accepted. The term factored resistance will be used here.

The version of Expression (1) used in the AASHTO LRFD Design Specification is somewhat different. It has the form

$$\sum \eta \gamma_{ij} Q_{ij} \leq \phi_k R_{nk} \quad (2)$$

where η is a factor related to the ductility, redundancy and operational importance.

When ACI 318-63 was adopted the load and resistance factors were generated based on judgment followed by extensive comparative designs. By 1965, the designers of concrete structures in the private sector had almost universally adopted the ACI LRFD Code. There were a few minor changes in the load factors in the next edition of the Code in 1968 (ACI 1968) and the ASD section was dropped completely. The ACI LRFD Building Code was then essentially unchanged until 2002 (ACI 2002) when extensive changes were made primarily to the load and resistance factors. During this entire development period the design method was known as “Ultimate Strength Design”.

The LRFD procedure adopted by ACI 318-63 was applicable to structural concrete elements for buildings only. It did not apply to the geotechnical aspects of foundation design. This produced a considerable anomaly for reinforced concrete building designers. For example, in the design process the geotechnical engineer recommended an allowable bearing pressure for a spread footing. The structural designer then had to size the footing using allowable loads – and that implied the use of a different set of loads - but perform the structural design of the reinforced concrete footing with factored loads.

Driven pile cap design was even more absurd. The geotechnical engineer selected an ultimate pile capacity based on subsurface conditions. Most of the methods that are used to establish pile capacity produce ultimate capacity. Those methods include wave

equation analysis, dynamic testing or static load testing. The one exception is the use of a dynamic formula and most formulas usually give allowable loads. The Gates Formula is an exception in that it produces a predicted ultimate load. The geotechnical engineer then selected a factor of safety to arrive at an allowable load. Again, the structural engineer had to use allowable loads to do the pile group selection and layout but then factored loads to design the pile cap. Private sector designers have been dealing with this inconsistency for forty years.

In 1969, Cornell published a paper in the ACI Journal (Cornell 1969) showing that the load and resistance factors could be determined rationally using a probabilistic analysis. As input to that analysis the variability of both the loads and the resistance was required. The National Bureau of Standards (NBS) completed a research project to collect the necessary information for buildings and they generated the associated factors (Ellingwood et al 1980). At that time the only LRFD Design Code in use was the ACI Code and the NBS factors were quite different than those contained in the ACI Code. These differences continued until 2002.

Today, LRFD design specifications are available for both steel and concrete buildings. Beginning with the 2002 ACI Building Code the load factors for both steel and concrete structures became the same. All concrete buildings are designed using LRFD but in the case of steel buildings the implementation of LRFD is not complete and an ASD design specification is still available and widely used for steel structures.

G.3 CALIBRATION OF PROBABILITY BASED LRFD

The original work of Cornell (1969) produced a major research effort to develop a probabilistic approach to structural design based on the load and resistance factor concept. The fundamental concept held that, since neither the loads nor the resistance are deterministic, it is appropriate to treat both load and resistance as random variables and to develop an approach to the design of structures based on probability theory. The concept is illustrated in Figure G.1 where probability density functions are shown for both the load effect, Q , and the resistance, R . The area under the resistance curve between a and b represents the probability of the resistance being between a and b . The region where the two curves overlap represents cases of "failure." Probability-based design is founded on the concept that the design be selected so that the probability of failure is equal to, or less than, some prescribed value. The limiting failure probability was originally established from laboratory test data on structural elements.

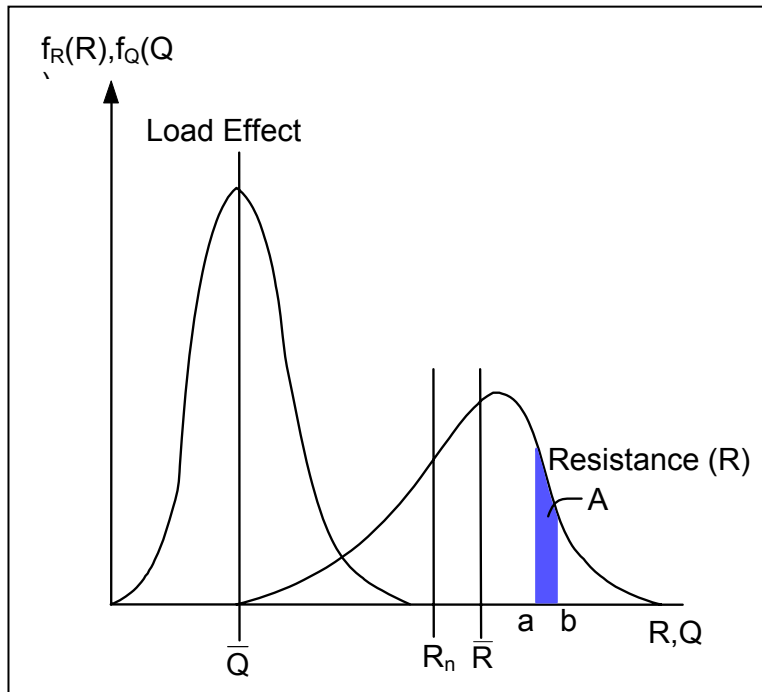


Figure G.1: Example of Probability Density Functions for both Load and Resistance

The load effect in Figure G.1 has been shown much narrower than the resistance for illustrative purposes, indicating that, in this case, the load has less variability than the resistance. The variability is defined by the standard deviation of the distribution. (The standard deviations are not shown in Figure G.1.) In Figure G.1, the mean values are denoted by \bar{Q} and \bar{R} . The nominal resistance, R_n is not necessarily the same as the mean resistance as illustrated in Figure G.1, but is the resistance that would be determined by the specified analysis method.

If distributions are available for both the load effect and the resistance, then the probability of failure can be determined. One approach that has been used is to consider the combined probability density function for $R-Q$ and this is illustrated in Figure G.2. Failure is defined when $R-Q$ is less than zero and the region is shaded in Figure G.2. The probability of failure is the area of the shaded portion under the curve. The basis for design is to require that the mean of that distribution, $\overline{R-Q}$, be greater than the value of $R-Q = 0$. The distance of that mean above zero is taken as a multiple, β , of the standard deviation of the distribution. β is known as the safety index or

reliability index. There are other approaches to establishing a measure of safety. A more detailed discussion of probabilistic code calibration has been presented by Kulicki (1998).

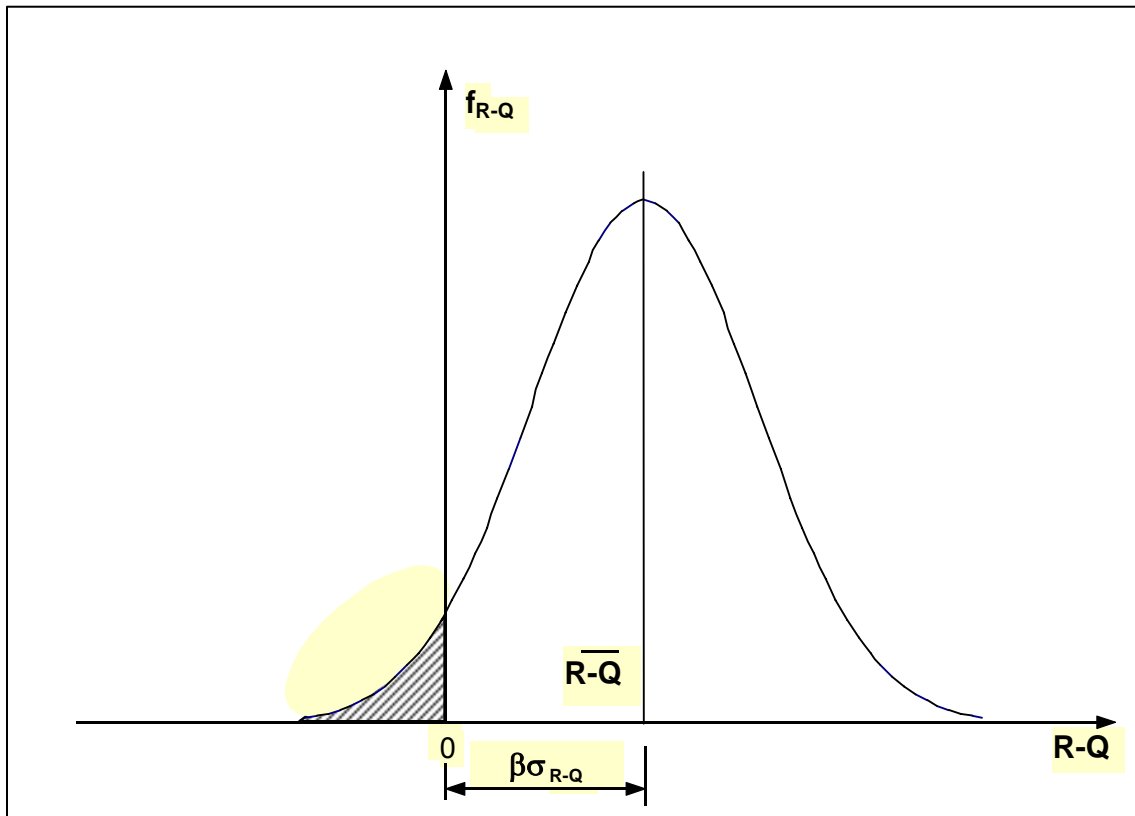


Figure G.2: Probability Density Function for R-Q

Existing structures that have performed satisfactorily have been analyzed to determine safety indices and from these analyses recommended values have been determined. Then, with knowledge of the load and the strength variabilities it is possible to select load and resistance factors to produce the required safety index. Structural engineers have established load factors for the various load types in the AASHTO Bridge Code and most of these values are probably not subject to change today. So the geotechnical resistance factors must be selected to achieve the required appropriate safety index.

Geotechnical strength measurement is very difficult to describe statistically due to the lack of standardized procedures for material characterization of soils. But, load and resistance factors can be calibrated based on a direct comparison with existing design practice. Load factors have been selected for the AASHTO LRFD Bridge Code so resistance factors can be directly determined to produce designs similar to those obtained in current ASD practice. For example, the AASHTO Strength I case is considered since it is commonly critical in design. The equality condition is used to obtain a unique and limiting expression. The expression can be stated in a simplified fashion as

$$\gamma_D Q_D + \gamma_L Q_L = \phi_k R_{nk} \quad (3)$$

where the subscript D refers to dead load and L refers to live load. Values are available for the dead and live load factors for Strength I in the AASHTO LRFD Bridge Code and Expression (3) becomes

$$1.25 Q_D + 1.75 Q_L = \phi_k R_{nk} \quad (4)$$

The equivalent ASD relationship can be stated

$$(Q_D + Q_L) FS = R_{nk} \quad (5)$$

where FS is the ASD factor of safety. For the equality condition, R_{nk} can be eliminated from Expressions (4) and (5) and this results in a single relationship for ϕ_k , in terms of FS and the Q_L/Q_D ratio.

$$\phi_k = \frac{FS(1 + Q_L / Q_D)}{(1.25 + 1.75 Q_L / Q_D)} \quad (6)$$

Figure G.3 shows resistance factors for various factors of safety as a function of Q_L/Q_D ratio for the AASHTO LRFD Code. Regardless of the source of resistance factors they must be checked against existing ASD practice. For example, if the probability analysis produced smaller resistance factors than the equivalent ASD factors of safety this would imply an unnecessary increase in conservatism in the design.

The factor η in Expression (2) has been ignored in the above discussion. The primary concern with η in foundation design comes when only a very few deep foundation

elements are used so that the foundation is non-redundant. While it is not so clear how redundancy can be determined since it is to some degree controlled by the superstructure geometry it can be critical and must be evaluated. Certainly a single deep foundation element will be non-redundant. Of course, most driven pile foundations will have enough piles to be redundant.

G.4 LRFD DETAILS

Now let us look at what we have to do to verify the safety of an LRFD-based design. We will consider the issue, “Does the structural element (pile) have adequate axial strength.” We have spoken at some length about the fundamental concepts on which LRFD is based. Now, how do we actually use this concept that has often been presented as a radical new approach? It is best to consider the details. First, consider the determination of the loads that would be used in bridge design. There are five strength limit states, two extreme event limit states, four serviceability limit states and one fatigue limit state given in Table 3.4.1-1 of the AASHTO LRFD Bridge Code. We will consider only the strength limit states here. The factored loads for those five cases are

Strength I

$$\gamma_p D + 1.75 L + 1.0 WA + 1.0 FR$$

Strength II

$$\gamma_p D + 1.35 L + 1.0 WA + 1.0 FR$$

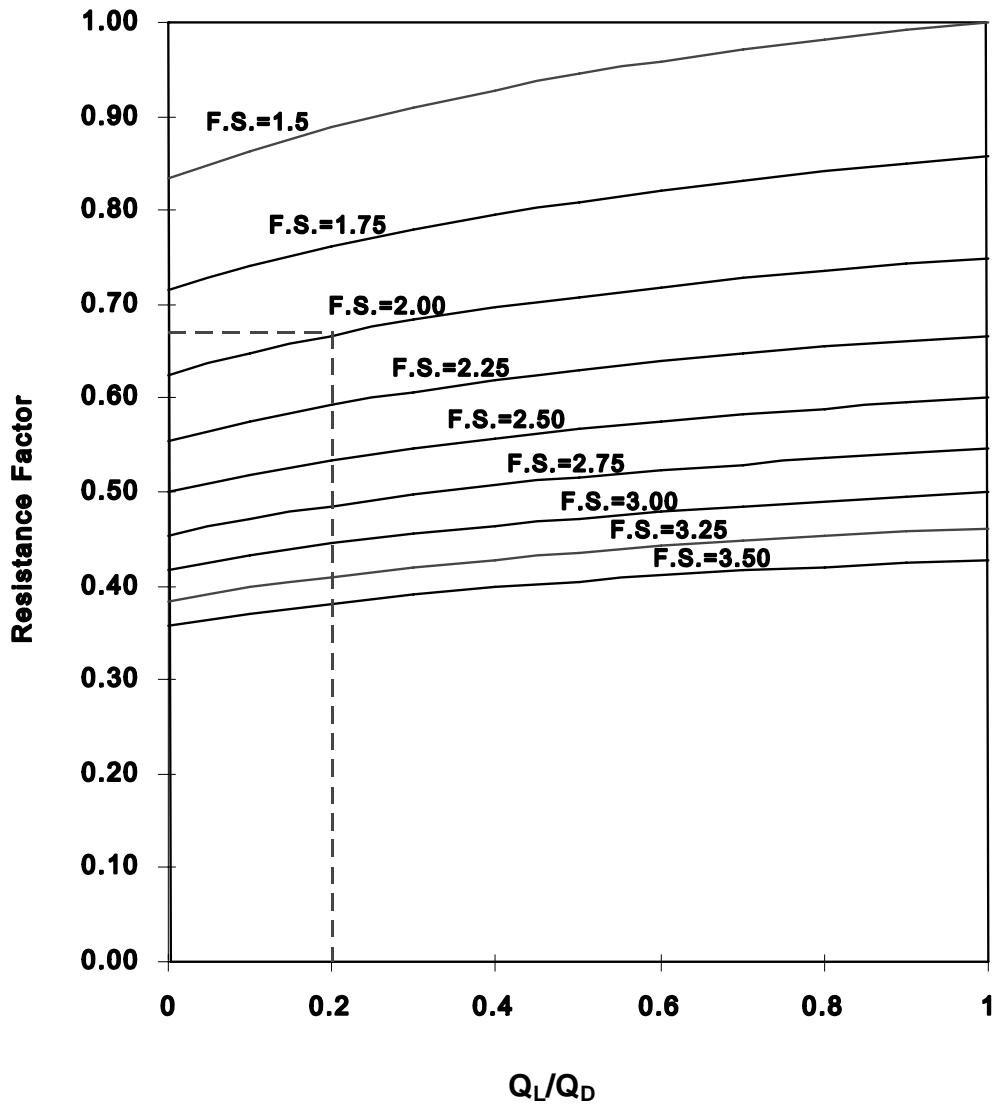


Figure G.3: Resistance Factor as a Function of Q_L/Q_D for Various Factors of Safety for the AASHTO LRFD Bridge Code

Strength III

$$\gamma_p D + 1.0 WA + 1.4 WS + 1.0 FR$$

Strength IV

$$\gamma_p D + 1.0 WA + 1.0 FR$$

but for dead load due to structural components only

$$1.5 D$$

Strength V

$$\gamma_p D + 1.35 L + 1.0 WA + 0.4 WS + 1.0 WL + 1.0 FR$$

These load combinations have been somewhat simplified for this discussion. The notation can be defined as follows:

γ_p – load factor for the various types of dead load. For the superstructure dead load γ_p is 1.25, but other values are specified for other types of dead load.

D – dead load.

L – live load

WA – water and stream load

FR – friction load

WS – wind load on the structure

WL – wind load on the live load

Since the load combinations have been somewhat simplified, the reader is encouraged to review Sections 3.3 through 3.6 of the AASHTO LRFD Bridge Design Specifications. Probably geotechnical engineers that are responsible for driven pile design will not be required to determine the factored loads, but a general understanding of those loads provides a better understanding of the entire design process. While the above loads and load combinations have differences from that of previous AASHTO Specifications the general structure of the loads is unchanged. Since there may be several different sets of loads (for instance, maximum and minimum) for each of the strength limit states the final set of factored loads will usually be larger than the five given above and sometimes much larger, particularly if extreme event conditions must be considered.

So now, in the foundation design process, the factored loads will be determined by the structural designer and with the exception of the downdrag case it is unlikely that these loads or load combinations will change in future AASHTO Codes. We have now completed a review of the left side of Expression (2).

The right side of Expression (2) is of greater concern for the geotechnical foundation designer. He must determine values of ϕ_k , the resistance factor, and R_{nk} , the nominal

strength. Values for ϕ_k must be defined by code. It has often been implied that resistance factors may be determined in the design process using a probability analysis. This is not realistic and certainly not necessary for driven pile design. At the present, the resistance factors contained in the AASHTO Bridge Code are poorly defined and not always unique. They will not be discussed here since the entire document may soon be replaced. However, it is quite clear what resistance factors are needed, only their values are not clearly defined. Methods must be available to determine the nominal strength, R_{nk} .

G.5 THE DESIGN PROCESS

The design process for LRFD will now be reviewed. The Flow Chart for LRFD-based design is given in Figure G.4. This flow chart is very similar to that given in Figure 2.1 to show the process for ASD-based design. All of the Blocks are similar through Block 7. Requirements must be determined and the subsurface must be investigated and evaluated to obtain the necessary geotechnical design quantities. A driven pile type is selected. Then in Block 8 the factored loads are determined. In Blocks 10 or 12 the resistance factor is selected based on the capacity verification procedure and the quality control method that has been selected. In the ASD method, a factor of safety is selected based on the information in Table 4.5.6.2.1A of the AASHTO Standard Specification. The resistance factor for LRFD is given in the Table 10.5.5-2 of the AASHTO LRFD Specification. Selection of the proper value for resistance factor from the LRFD Specification will not be discussed here.

The rest of the Design Flow chart is similar to the one for ASD. It can be seen that there is little difference in the design process for LRFD compared to ASD.

G.6 A SIMPLE EXAMPLE

A very simple numerical design example will be solved to illustrate the differences between ASD and LRFD. Only strength will be considered since those limitations are the only ones that are different for the two methods. The example uses the soil of Example 1, of Chapter 16, Section 16.5.1 of this manual. The soil

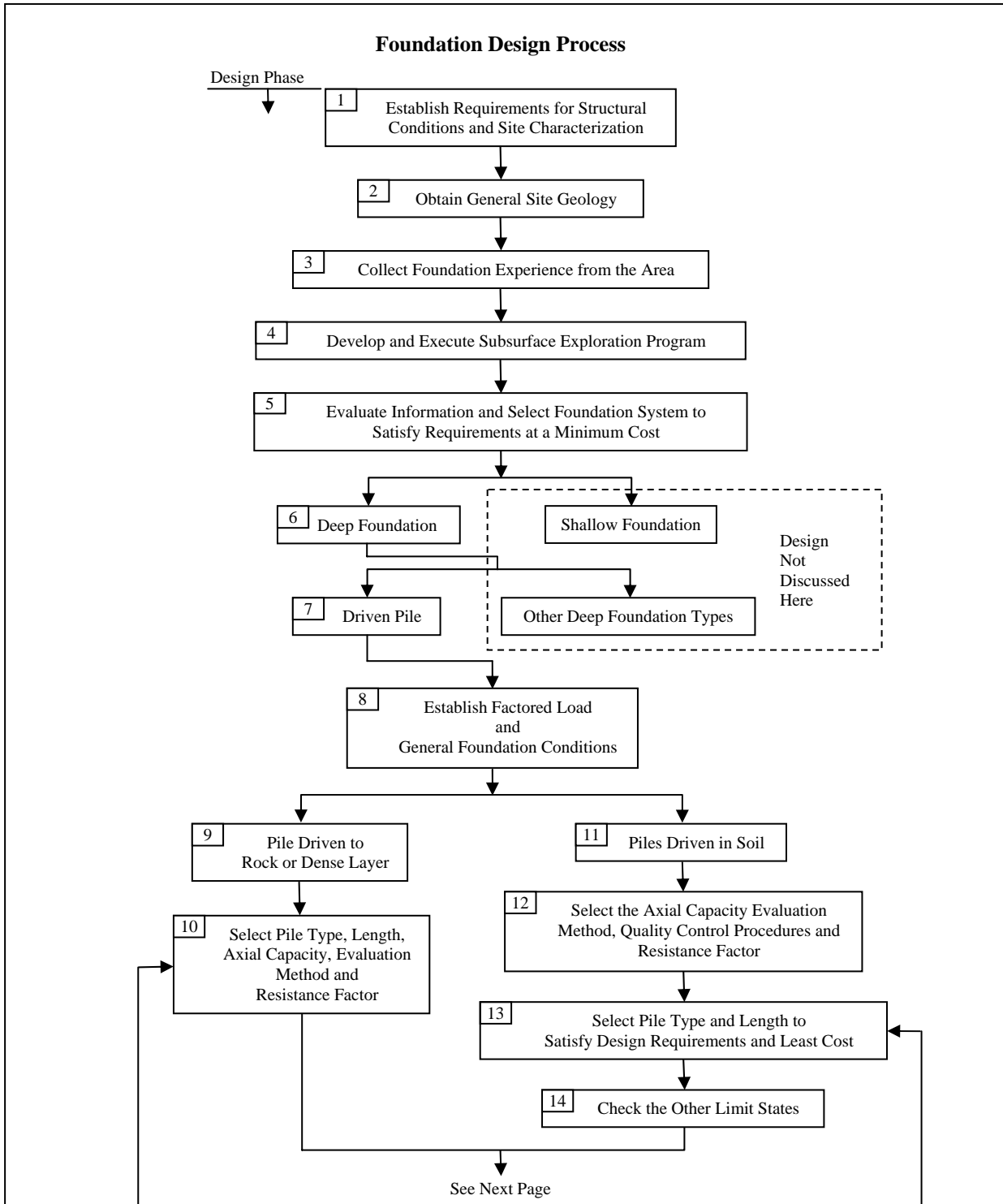


Figure G.4: Driven Pile Design and Construction Process by LRFD

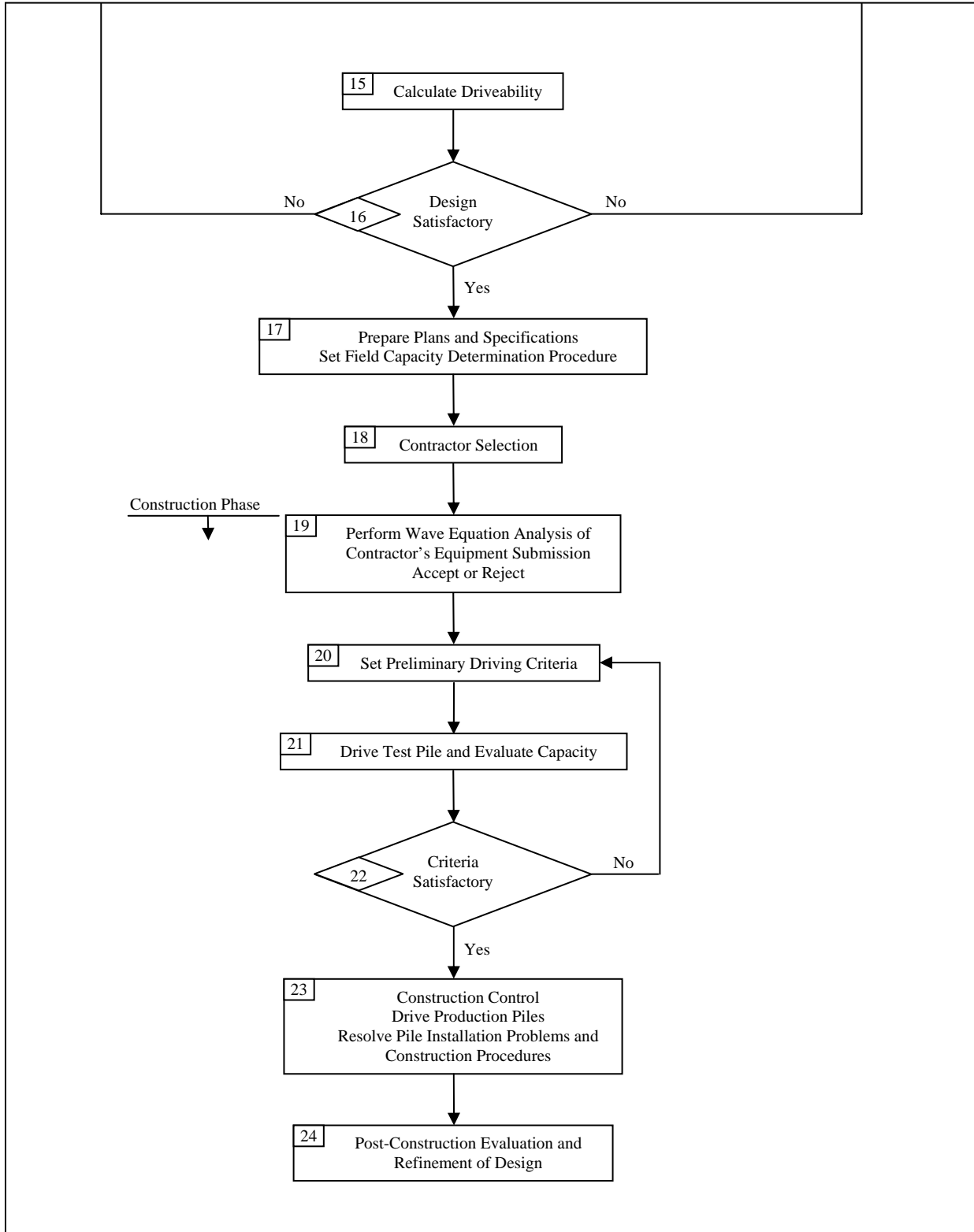


Figure G.5: Driven Pile Design and Construction Process by LRFD (Continued)

is a medium dense sand with an adjusted N-value of 20 and a friction angle of 33 degrees. In this trial design, a closed end steel pile having a length of 20 m (66.7 feet) and a cross section 356 mm x 8 mm (14 inches x 5/16 inches) has been selected and a geotechnical analysis indicates a nominal resistance of 1480 kN (330 kips). The working load on the foundation will be taken as 2225 kN (500 kips) dead load and 3560 kN (800 kips) live load including impact.

G.6.1 ASD

According to Table 3.22.1A of the Standard Bridge Code for the service load Case I, the design load is

$$2225 + 3560 = 5785 \text{ kN (1300 k)}$$

First, assume that a static load test will be used in addition to a drivability analysis by wave equation with subsurface investigation and static analysis to verify the driving criteria. Therefore, the factor of safety specified in Table 4.5.6.2A is 2.0 and the required nominal axial resistance is 11,570 kN (2600 k). Now if the pile nominal resistance is 1480 kN (333 k), then the total required number of piles will be

$$11,570/1480 = 7.8 \text{ piles, 8 piles}$$

If dynamic measurement and analysis is used the specified factor of safety is 2.25, giving a required ultimate axial resistance of 13,016 kN (2924 k). In this case the required number of piles will be

$$13,016/1480 = 8.8 \text{ piles, 9 piles}$$

G.6.2 LRFD

First, determine the factored load. In this very simple example, only Strength I of Table 3.4.1-1 of the LRFD Bridge Code will be considered.

$$1.25 \times 2250 + 1.75 \times 3560 = 9,042 \text{ kN (2032 k)}$$

The specified resistance factor to be used with a static load test is given in Table 10.5.5-2. It is interpreted to be $0.8\lambda_v$ for static load test. The value of λ_v with a wave equation analysis used in the field is 0.85. The resistance factor is.

$$0.80 \times 0.85 = 0.68$$

The required nominal resistance is

$$9,042/0.68 = 13,297 \text{ kN (2988 k)}$$

The required number of piles is

$$13,297/1480 = 9.0 \text{ piles}$$

The required value of resistance factor for the case of dynamic measurement and analysis cannot be interpreted from the current AASHTO LRFD Specification.

G.6.3 Comments

This very simple example illustrates the difference between ASD and LRFD. Of course, only one failure mode limit state was considered. In a real design problem, several load combinations would be included, the loads would include overturning loads and all aspects of the problem would be much more complex. This simple example illustrates the total difference between ASD and LRFD clearly and simply. No conclusions should be made regarding the fact that the LRFD design was more conservative in this case. However, the importance of live-dead load ratio becomes clear. For short span bridges the live load may be much larger than the dead load which is the case here while for very long spans structures the live loads can be almost inconsequential. In the latter case, Condition Strength IV would become critical and fewer piles would be required.

REFERENCES

- American Association of State Highway and Transportation Officials, 1994. *AASHTO LRFD Bridge Design Specifications*, 1st ed. AASHTO, Washington, D.C.
- American Association of State Highway and Transportation Officials, 1998. *AASHTO LRFD Bridge Design Specifications*, 2nd ed. AASHTO, Washington, D.C.
- American Concrete Institute, 1956. *Building Code Requirements for Reinforced Concrete*, ACI 318-56. Detroit, Michigan.
- American Concrete Institute, 1963. *Building Code Requirements for Reinforced Concrete*, ACI 318-68. Detroit, Michigan.
- American Concrete Institute, 1968. *Building Code Requirements for Reinforced Concrete*, ACI 318-63. Detroit, Michigan.
- American Concrete Institute, 2002. *Building Code Requirements for Structural Concrete*, ACI 318-02. Detroit, Michigan.
- Barker, R.M., J.M. Duncan, K.B. Rojiani, P.S.K. Ooi, C.K. Tan and S.G. Kim, 1991. *NCHRP Report 343: Manuals for the Design of Bridge Foundations*. Transportation Research Board, National Research Council, Washington, D.C.
- Cornell, C.A., 1969. "A Probability-Based Structural Code," *ACI Journal*, December, pp. 974-985.
- Ellingwood, B., T.V. Galambos, J.G. MacGregor and C.A. Cornell, 1980. "Development of a Probability Based Load Criteria for American National Standard A-58, Building Code Requirements for Minimum Design Loads in Buildings and Other Structures," National Bureau of Standards, Washington, D.C.
- Kulicki, J.M., 1998. *NCHRP Research Results Digest 198: Development of Comprehensive Bridge Specifications and Commentary*, May.



U.S. Department of Transportation
Federal Highway Administration

Publication No. FHWA NHI-05-043
April 2006

NHI Courses No. 132021 and 132022 **Design and Construction of Driven Pile Foundations**

Reference Manual – Volume II



National Highway Institute

NOTICE

The contents of this report reflect the views of the authors, who are responsible for the facts and the accuracy of the data presented herein. The contents do not necessarily reflect policy of the Department of Transportation. This report does not constitute a standard, specification, or regulation. The United States Government does not endorse products or manufacturers. Trade or manufacturer's names appear herein only because they are considered essential to the objective of this document.

1. REPORT NO. FHWA-NHI-05-043	2. GOVERNMENT ACCESSION NO.	3. RECIPIENT'S CATALOG NO.	
4. TITLE AND SUBTITLE Design and Construction of Driven Pile Foundations – Volume II		5. REPORT DATE April 2006	
		6. PERFORMING ORGANIZATION CODE	
7. AUTHOR(S) P.J. Hannigan, G.G. Goble, G.E. Likins, and F. Rausche		8. PERFORMING ORGANIZATION REPORT NO.	
9. PERFORMING ORGANIZATION NAME AND ADDRESS Ryan R. Berg & Associates, Inc. 2190 Leyland Alcove Woodbury, MN 55125		10. WORK UNIT NO.	
		11. CONTRACT OR GRANT NO. DTFH61-02-T-63020	
12. SPONSORING AGENCY NAME AND ADDRESS National Highway Institute Federal Highway Administration U.S. Department of Transportation Washington, D.C.		13. TYPE OF REPORT & PERIOD COVERED Final Report	
		14. SPONSORING AGENCY CODE	
15. SUPPLEMENTARY NOTES FHWA Technical Consultants: J.A. DiMaggio, P.E. and C. Dumas, P.E. COTR - L. Jones <i>This manual is an update and revision of FHWA-HI-97-021 prepared by Goble Rausche Likins and Associates, Inc. Authors: P.J. Hannigan, G.G. Goble, G. Thendean, G.E. Likins and F. Rausche</i> FHWA Technical Consultant: J.A. DiMaggio			
16. ABSTRACT This manual is the reference text used for the FHWA NHI course Nos. 130221 Driven Pile Foundations – Design and Construction and 130222 Driven Pile Foundations – Construction Monitoring and reflects the current practice for pile foundations. The manual is also intended to serve as the FHWA's primary reference of recommended practice for driven pile foundations. The Design and Construction of Driven Pile Foundations manual is directed to geotechnical, structural, and construction engineers involved in the design and construction of pile supported structures. This manual is intended to serve as a practical reference of driven pile foundations. Volume I of the manual addresses design aspects including subsurface exploration, laboratory testing, static analyses, as well as specifications and foundation report preparation. Volume II covers construction aspects including dynamic formulas, wave equation analysis, dynamic pile testing, static load testing, Statnamic testing, Osterberg cell testing, as well as pile driving equipment, pile driving accessories, and pile installation inspection. Step by step procedures are included to facilitate use of most analysis procedures.			
17. KEY WORDS pile foundations, foundation deign, static analysis, foundation construction inspection		18. DISTRIBUTION STATEMENT No restrictions.	
19. SECURITY CLASSIF. Unclassified	20. SECURITY CLASSIF. Unclassified	21. NO. OF PAGES 486	22. PRICE

U.S. - SI Conversion Factors

From English	To SI	Multiply by	Quantity	From SI	To English	Multiply by
ft	m	0.3048	Length	m	ft	3.2808
inch	mm	25.40		mm	inch	0.039
ft ²	m ²	0.0929	Area	m ²	ft ²	10.764
inch ²	mm ²	645.2		mm ²	in ²	0.0015
ft ³	m ³	0.028	Volume	m ³	ft ³	35.714
inch ³	mm ³	16387		mm ³	inch ³	61x10 ⁻⁶
ft ⁴	m ⁴	0.0086	Second Moment of Area	m ⁴	ft ⁴	115.856
inch ⁴	mm ⁴	416231		mm ⁴	inch ⁴	2x10 ⁻⁶
lbm	kg	0.4536	Mass	kg	lbm	2.2046
lbm/ft ³	kg/m ³	16.02	Mass Density	kg/m ³	lbm/ft ³	0.062
lb	N	4.448	Force	N	lb	0.2248
kip	kN	4.448		kN	kip	0.2248
lbs/ft	N/m	14.59	Force/Unit- Length	N/m	lbs/ft	0.0685
kips/ft	kN/m	14.59		kN/m	kips/ft	0.0685
lbs/in ²	kPa	6.895	Force/Unit- Area; Stress; Pressure; Elastic Mod.	kPa	lbs/in ²	0.145
kips/in ²	MPa	6.895		MPa	kips/in ²	0.145
lbs/ft ²	Pa	47.88		Pa	lbs/ft ²	0.021
kips/ft ²	kPa	47.88		kPa	kips/ft ²	0.021

U.S. - SI Conversion Factors (continued)

From	To	Multiply by	Quantity	From	To	Multiply by
English	SI			SI	English	
lbs/ft ³	N/m ³	157.1	Force/Unit- Volume	N/m ³	lbs/ft ³	0.0064
kip/ft ³	kN/m ³	157.1		kN/m ³	kip/ft ³	0.0064
lb-inch	N-mm	112.98	Moment; or Energy	N-mm	lb-inch	0.0089
kip-inch	kN-mm	112.98		kN-mm	kip-inch	0.0089
lb-ft	N-m	1.356		N-m	lb-ft	0.7375
kip-ft	kN-m	1.356		kN-m	kip-ft	0.7375
ft-lb	Joule	1.356		Joule	ft-lb	0.7375
ft-kip	kJoule	1.356		kJoule	ft-kip	0.7375
s/ft	s/m	3.2808	Damping	s/m	s/ft	0.3048
blows/ft	blows/m	3.2808	Blow count	blows/m	blows/ft	0.3048

PREFACE

Engineers and contractors have been designing and installing pile foundations for many years. During the past three decades this industry has experienced several major improvements including newer and more accurate methods of predicting capacities, highly specialized and sophisticated equipment for pile driving, and improved methods of construction control.

In order to take advantage of these new developments, the FHWA developed a manual in connection with Demonstration Project No. 66, Design and Construction of Driven Pile Foundations. The primary purpose of the 1985 Manual was to support educational programs conducted by FHWA for transportation agencies. These programs consisted of (1) a workshop for geotechnical, structural, and construction engineers, and (2) field demonstrations of static and dynamic load testing equipment. Technical assistance on construction projects in areas covered by this Demonstration Project was provided to transportation agencies on request. A second purpose of equal importance was to serve as the FHWA's standard reference for highway projects involving driven pile foundations.

The original Manual was written by Suneel N. Vanikar with review and comment from Messrs. Ronald Chassie, Jerry DiMaggio, and Richard Cheney.

1996 Edition

After a decade of use, the Manual was updated in 1996. The manual was modified to include new developments that had taken place in the intervening years and to take advantage of the experience gained in using the Manual in the many workshops that were presented by Demonstration Project 66. The 1996 version of the Manual was prepared by Goble, Rausche, Likins, and Associates, Inc. under contract with the FHWA.

The authors' recognize the efforts of the project technical manager, Mr. Jerry DiMaggio, FHWA Principal Geotechnical Engineer, who provided invaluable guidance and input for the new manual. The authors' also acknowledge the additional contributions of the following technical review panel members of the 1996 manual listed in alphabetical order:

Mr. Chien-Tan Chang - FHWA
Mr. Tom Cleary - New Hampshire DOT
Mr. Chris Dumas - FHWA
Mr. Sam Holder - FHWA
Mr. Paul Passe - Florida DOT
Mr. Suneel Vanikar - FHWA

Mr. Richard Cheney - FHWA
Mr. Kerry Cook - FHWA
Mr. Carl Ealy - FHWA
Mr. Paul Macklin - Colorado DOT
Mr. Jan Six - Oregon DOT

The following individuals of the author's internal peer review team are also acknowledged for their technical advice and contributions in preparing the 1996 version of the manual.

Dr. Joseph Caliendo - Utah State University
Dr. D. Michael Holloway - InSituTech
Mr. Robert Lukas - Ground Engineering Consultants

Lastly, the authors' wish to thank the following Goble, Rausche, Likins, and Associates, Inc. employees for their vital contributions and significant effort in preparing the manual: Ms. Barbara Strader, Ms. Beth Richardson, Mr. Scott Webster, Mr. Neil Harnar, Mr. Jay Berger and Mr. Joe Beno.

2006 Edition

The 2006 version of the Manual is the third major version of the manual and was prepared by GRL Engineers, Inc. under contract with Ryan R Berg & Associates, Inc. The 2006 version of the Manual was once again updated to include new developments that had taken place since 1996 and to again serve a dual purpose. First, as a workshop participant's manual for the FHWA's National Highway Institute Courses on Driven Pile Foundations, and second to serve as FHWA's primary reference of recommended practice for driven pile foundations.

The authors' again recognize the efforts of the FHWA project technical manager Mr. Chris Dumas, and of Mr. Jerry DiMaggio, FHWA Principal Bridge Engineer - Geotechnical.

The manual is presented in two volumes. Volume I addresses design aspects and Volume II presents topics related to driven pile installation, monitoring, and inspection.

Design and Construction of Driven Pile Foundations- Volume II

		Page
Table of Contents		
14	INTRODUCTION TO CONSTRUCTION MONITORING	
14.1The Role of Construction Monitoring	14-1
14.2Selection of Factor of Safety	14-3
14.3Driving Criteria... ..	14-4
14.4Communication.. ..	14-5
	References..... ..	14-7
15	DYNAMIC FORMULAS FOR STATIC CAPACITY DETERMINATION	15-1
15.1Accuracy of Dynamic Formulas	15-1
15.2Problems with Dynamic Formulas	15-5
15.3Dynamic Formulas.....	15-6
15.4Alternatives to Use of Dynamic Formulas.....	15-8
15.5Dynamic Formula Case Histories	15-8
	15.5.1 Case History 1.....	15-8
	15.5.2 Case History 2.....	15-9
	15.5.3 Case History 3.....	15-10
	References..... ..	15-11
16	DYNAMIC ANALYSIS BY WAVE EQUATION	16-1
16.1 Introduction..... ..	16-1
16.2 Wave Propagation.....	16-2
16.3 Wave Equation Methodology	16-2
16.4 Wave Equation Applications	16-6
16.5 Wave Equation Examples.....	16-9
	16.5.1 Example 1 – General Bearing Graph	16-9
	16.5.2 Example 2 – Constant Capacity / Variable Stroke Option ..	16-13
	16.5.3 Example 3 – Tension and Compression Stress Control	16-16
	16.5.4 Example 4 – Use of Soil Setup.....	16-20
	16.5.5 Example 5 – Driveability Studies	16-23
	16.5.6 Example 6 – Driving System Characteristics.....	16-28
	16.5.7 Example 7 – Assessment of Pile Damage	16-32
	16.5.8 Example 8 – Selection of Wall Thickness.....	16-37
	16.5.9 Example 9 – Evaluation of Vibratory Driving	16-41
16.6 Analysis Decisions for Wave Equation Problems	16-45
	16.6.1 Selecting the Proper Approach	16-45

Table of Contents		Page
16.6.2	Hammer Data Input, External Combustion Hammers	16-46
16.6.3	Hammer Data Input, Diesel Hammers.....	16-47
16.6.4	Cushion Input.....	16-48
16.6.5	Soil Parameter Selection.....	16-49
16.6.6	Comparison with Dynamic Measurements	16-51
16.7....	Wave Equation Input Parameters	16-53
16.7.1	Other GRLWEAP Options	16-72
16.8....	GRLWEAP Output.....	16-79
16.9....	Plotting of GRLWEAP Results.....	16-85
16.10...	Suggestions for Problem Solving	16-85
	References.....	16-91
17	DYNAMIC PILE TESTING AND ANALYSIS.....	17-1
17.1....	Background.....	17-1
17.2....	Applications for Dynamic Testing Methods.....	17-2
17.2.1	Static Pile Capacity	17-2
17.2.2	Hammer and Driving System Performance	17-3
17.2.3	Driving Stresses and Pile Integrity	17-3
17.3....	Dynamic Testing Equipment.....	17-4
17.4....	Basic Wave Mechanics.....	17-8
17.5....	Dynamic Testing Methodology.....	17-16
17.5.1	Case Method Capacity	17-17
17.5.2	Energy Transfer	17-20
17.5.3	Driving Stresses and Integrity	17-20
17.5.4	The CAPWAP Method (<u>C</u> Ase <u>P</u> ile <u>W</u> ave <u>A</u> nalysis Program)	17-24
17.6....	Usage of Dynamic Testing Methods.....	17-31
17.7....	Presentation and Interpretation of Dynamic Testing Results	17-33
17.8....	Advantages.....	17-46
17.9....	Disadvantages.....	17-47
17.10...	Case History	17-47
17.11...	Low Strain Integrity Testing Methods.....	17-49
17.11.1	Pulse Echo Method	17-50
17.11.2	Transient Response Method (TRM)	17-52
17.11.3	Low Strain Applications to Unknown Foundations.....	17-53
17.11.4	Limitations and Conclusions of Low Strain Methods	17-53
	References.....	17-55

Table of Contents		Page
18	STATIC PILE LOAD TESTING.....	18-1
	18.1 Reasons for Load Testing	18-1
	18.2 Prerequisites for Load Testing	18-1
	18.3 Developing a Static Load Test Program.....	18-2
	18.4 Advantages of Static Load Testing.....	18-3
	18.5 When to Load Test.....	18-4
	18.6 Effective use of Load Tests	18-5
	18.6.1 Design State.....	18-5
	18.6.2 Construction Stage.....	18-6
	18.7.... Compression Load Tests	18-6
	18.7.1 Compression Test Equipment	18-8
	18.7.2 Recommended Compression Test Loading Method	18-11
	18.7.3 Presentation and Interpretation of Compression Test Results	18-13
	18.7.4 Plotting the Load-Movement Curve.....	18-15
	18.7.5 Determination of the Ultimate Load.....	18-15
	18.7.6 Determination of the Allowable Load.....	18-16
	18.7.7 Load Transfer Evaluations	18-16
	18.7.8 Limitations of Compression Load Tests	18-18
	18.8.... Tensile Load Tests	18-20
	18.8.1 Tension Test Equipment	18-20
	18.8.2 Tension Test Loading Methods	18-21
	18.8.3 Presentation and Interpretation of Tension Test Results....	18-22
	18.9.... Lateral Load Tests	18-23
	18.9.1 Lateral Load Test Equipment	18-23
	18.9.2 Lateral Test Loading Methods.....	18-24
	18.9.3 Presentation and Interpretation of Lateral Test Results	18-27
	References.....	18-29
19	THE OSTERBERG CELL METHOD	19-1
	19.1 Osterberg Cell Background.....	19-1
	19.2 Test Equipment	19-3
	19.3 Interpretation of Test Results	19-7
	19.4 Applications.....	19-8
	19.5 Advantages	19-9
	19.6 Disadvantages	19-10
	19.7 Case Histories.....	19-11
	References.....	19-17

Table of Contents		Page
20	THE STATNAMIC METHOD.....	20-1
	20.1 Statnamic Background.....	20-1
	20.2 Test Equipment.....	20-2
	20.3 Test Interpretation.....	20-6
	20.3.1 Unloading Point Method.....	20-6
	20.3.2 Modified Unloading Point Method.....	20-10
	20.3.3 Segmental Unloading Point Method.....	20-10
	20.3.4 Loading Rate Reduction Factors.....	20-11
	20.4 Applications.....	20-11
	20.5 Case History.....	20-13
	20.6 Advantages.....	20-14
	20.7 Disadvantages.....	20-14
	References.....	20-16
21	PILE DRIVING EQUIPMENT	21-1
	21.1.... Leads.....	21-1
	21.2.... Templates.....	21-8
	21.3.... Helmets.....	21-9
	21.4.... Hammer Cushions.....	21-10
	21.5.... Pile Cushions.....	21-12
	21.6.... Hammers.....	21-13
	21.6.1 Hammer Energy Concepts.....	21-14
	21.7... Drop Hammers	21-18
	21.8... Single Acting Air/Steam Hammers.....	21-19
	21.9... Double Acting Air/Steam Hammers.....	21-22
	21.10.. Differential Acting Air/Steam Hammers.....	21-24
	21.11.. Single Acting (Open End) Diesel Hammers.....	21-26
	21.12.. Double Acting (Closed End) Diesel Hammer.....	21-29
	21.13.. Hydraulic Hammers.....	21-31
	21.14.. Vibratory Hammers.....	21-34
	21.15.. Hammer Size Selection.....	21-34
	21.16.. Hammer Kinetic Energy Monitoring.....	21-36
	21.17.. Noise Suppression Equipment.....	21-40
	21.18.. Followers.....	21-41
	21.19.. Jetting.....	21-42
	21.20.. Predrilling.....	21-44
	21.21.. Spudding.....	21-45
	21.22.. Bubble Curtains.....	21-45

Table of Contents		Page
21.23..	Representative List of U.S.A. Hammer Manufacturers and Suppliers	21-47
21.24..	Useful Hammer Information Web Addresses	21-53
	References.....	21-55
22	ACCESSORIES FOR PILE INSTALLATION.....	22-1
22.1....	Timber Piles.....	22-1
22.1.1	Pile Toe Attachments	22-1
22.1.2	Attachment at Pile Head.....	22-3
22.1.3	Splices... ..	22-3
22.2....	Steel H-Piles	22-5
22.2.1	Pile Toe Attachments	22-5
22.2.2	Splices... ..	22-7
22.3....	Accessories for Steel Pipe Piles	22-7
22.3.1	Pile Toe Attachments	22-7
22.3.2	Splices... ..	22-10
22.4....	Precast Concrete Piles	22-10
22.4.1	Pile Toe Attachments	22-10
22.4.2	Splices... ..	22-13
22.5....	A List of Manufacturers and Suppliers of Pile Accessories.....	22-17
	References.....	22-19
23	INSPECTION OF PILE INSTALLATION	23-1
23.1....	Items to be Inspected	23-2
23.2....	Review of Project Plans and Specifications.....	23-2
23.3....	Inspector's Tools.....	23-4
23.4....	Inspection of Piles Prior to and During Installation.....	23-5
23.4.1	Timber Piles	23-5
23.4.2	Precast Concrete Piles.....	23-5
23.4.3	Steel H-Piles	23-7
23.4.4	Steel Pipe Piles	23-8
23.5....	Inspection of Driving Equipment	23-8
23.6....	Inspection of Driving Equipment During Installation.....	23-12
23.6.1	Drop Hammers.....	23-13
23.6.2	Single Acting Air/Steam Hammers	23-14
23.6.3	Double Acting or Differential Air/Steam Hammers	23-17
23.6.4	Single Acting Diesel Hammers.....	23-20
23.6.5	Double Acting Diesel Hammers	23-27
23.6.6	Hydraulic Hammers.....	23-30

Table of Contents	Page
23.6.7 Vibratory Hammers	23-36
23.7.... Inspection of Test or Indicator Piles.....	23-36
23.8.... Inspection of Production Piles.....	23-39
23.9.... Driving Records and Reports.....	23-48
23.10... Safety	23-53
References.....	23-54

List of Appendices

APPENDIX A... List of FHWA Pile Foundation Design and Construction References	A-1
APPENDIX B... List of ASTM Pile Design and Testing Specifications.....	B-1
APPENDIX C-1 Information and Data on Various Pile Types, Metric Units.....	C1-1
APPENDIX C-2 Information and Data on Various Pile Types, U.S. Units.....	C2-1
APPENDIX D .. Pile Hammer Information	D-1

List of Tables Page

Table 14-1	Responsibilities of Design and Construction Engineers.....	14-2
Table 14-2	Recommended Factor of Safety Based on Construction Control	14-3
Table 15-1	Mean Values and Coefficients of Variation for Various Methods	15-4
Table 16-1	Example 6 Proposed Hammer and Driving Systems	16-29
Table 16-2	Example 8 Stress and Blow Count Results.....	16-40
Table 16-3	Soil Parameters in ST Analysis for Granular Soil Types.....	16-64
Table 16-4	Soil Parameters in ST Analysis for Cohesive Soil Types	16-64
Table 16-5	Suggested Use of the Wave Equation to Solve Field Problems	16-86
Table 16-6	Wave Equation Analysis Problems	16-89
Table 17-1	Summary of Case Damping Factors for RSP Equation	17-18
Table 17-2	Pile Damage Guidelines (Rausche and Goble, 1979).....	17-24
Table 17-3	Descriptions of PDA Output Codes.....	17-36
Table 17-4	Typical Tabular Presentation of Dynamic Testing.....	17-44
Table 21-1	Typical Pile Hammer Characteristics and Uses	21-16
Table 21-2	Preliminary Hammer Energy Requirements.....	21-36
Table 22-1	Summary of Precast Concrete Pile Splices	22-14
Table 23-1	Common Problems and Problem Indicators for Air/Steam Hammers (from Williams Earth Sciences, 1995).....	23-16
Table 23-2	Common Problems and Problem Indicators for Single Acting Diesel Hammers (from Williams Earth Sciences, 1995) .	23-25
Table 23-3	Common Problems and Problem Indicators for Double Acting Diesel Hammers (from Williams Earth Sciences, 1995) .	23-30
Table 23-4	Common Problems and Problem Indicators for Hydraulic Hammers (from Williams Earth Sciences, 1995).....	23-34
Table 23-5	Common Pile Installation Problems & Possible Solutions.....	23-44

List of Figures		Page
Figure 15.1	Log Normal Probability Density Function for Four Capacity Prediction Methods (after Rausche, et al., 1996)	15-4
Figure 16.1	Wave Propagation in a Pile (adapted from Cheney and Chassie, 2000)	16-3
Figure 16.2	Typical Wave Equation Models.....	16-5
Figure 16.3	Example 1 Problem Profile	16-10
Figure 16.4	Example 1 Typical Bearing Graph – SI and US Units	16-12
Figure 16.5	Example 2 Constant Capacity Analysis – SI and US Units	16-15
Figure 16.6	Example 3 Problem Profile	16-16
Figure 16.7	Example 3 Bearing Graph for Easy Driving Condition – Two Pile Cushion Thicknesses.....	16-18
Figure 16.8	Example 3 Bearing Graph for End of Driving Condition.....	16-20
Figure 16.9	Example 4 Problem Profile	16-21
Figure 16.10	Using a Bearing Graph with Soil Setup.....	16-23
Figure 16.11	Example 5 Using a Problem Profile	16-24
Figure 16.12	Example 5 Driveability Results for First Driven 356 mm (14 inch) Concrete Pile without Densification.....	16-26
Figure 16.13	Example 5 Driveability Results for Later Driven 356 mm (14 inch) Concrete Piles with Densification	16-27
Figure 16.14	Example 5 Driveability Results for H-Pile.....	16-27
Figure 16.15	Example 6 Problem Profile	16-29
Figure 16.16a	Example 6 Bearing Graph – for Two Hammers with Equivalent Potential Energy and High Toe Quake	16-30
Figure 16.16b	Example 6 Bearing Graph for Two Hammers with Equivalent Potential Energy and Low Toe Quake.....	16-32
Figure 16.17	Example 7 Problem Profile	16-33
Figure 16.18	Example 7 Wave Equation Bearing Graph for Proposed Driving System.....	16-34
Figure 16.19	Example 7 Comparison of Wave Equation Bearing Graphs for Damaged and Undamaged Pile.....	16-37
Figure 16.20	Example 8 Problem Profile	16-38
Figure 16.21	Example 8 Bearing Graphs for 6.3 and 7.1 mm Wall Pipe Piles.....	16-39
Figure 16.22	Example Bearing Graph for 7.9 and 9.5 mm Wall Pipe Piles....	16-40
Figure 16.23(a)	Example 9 Soil Resistance Information for Vibratory Sheet Pile Driving.....	16-42
Figure 16.23(b)	Example 9 Vibratory Hammer Model	16-43
Figure 16.23(c)	Example 9 Pile Profile.....	16-44
Figure 16.23(d)	Example 9 Summary over Depths	16-44
Figure 16.24	Pile and Driving Equipment Data Form.....	16-55
Figure 16.25	GRLWEAP Help Window for Main Input Form.....	16-56

List of Figures		Page
Figure 16.26	Job Information Window	16-57
Figure 16.27	Select Hammer Window	16-57
Figure 16.28	Analysis Type Window	16-58
Figure 16.29a	Pile Input Window	16-59
Figure 16.29b	Area Calculator Window	16-60
Figure 16.30	Hammer Cushion Window	16-62
Figure 16.31a & Figure 16.31b	Soil Profile Input Window for Soil Type Based Static Soil Analysis and Soil Parameter Input Window for Bearing Graph Analysis	16-65
Figure 16.32a	Ultimate Capacity Window for Bearing Graph and Inspector's Chart Analyses	16-66
Figure 16.32b	Resistance Gain/Loss Factors Window for Driveability Analyses	16-67
Figure 16.33	SI Form	16-68
Figure 16.34a	Static Analysis General Information	16-70
Figure 16.34b	Profile/Resistance for Static Analysis	16-70
Figure 16.35	Depths, Modifiers Input Form	16-71
Figure 16.36	Completed Main Input for a Simple Bearing Graph	16-72
Figure 16.37	Slack/Splice Information Input Window	16-75
Figure 16.38	Data Entry Screen for Non-Uniform Piles	16-76
Figure 16.39	Numeric Options Window	16-77
Figure 16.40	Damping Options Window	16-77
Figure 16.41	Stroke Options Window for Diesel Hammers	16-78
Figure 16.42	Output Options Window	16-80
Figure 16.43	Hammer Model, Hammer Options, and Driving System Output	16-81
Figure 16.44	Pile, Soil, and Analysis Options	16-83
Figure 16.45	Extrema Table Output	16-84
Figure 16.46	Final Summary for Bearing Graph Analysis	16-84
Figure 17.1	Pile Preparation for Dynamic Testing	17-5
Figure 17.2	Pile Positioned for Driving and Gage Attachment	17-5
Figure 17.3	Strain Transducer and Accelerometer Bolted to Pipe Pile	17-6
Figure 17.4	Pile Driving Analyzer – Model PAK (courtesy of Pile Dynamics, Inc.)	17-6
Figure 17.5	Pile Driving Analyzer – Model PAL-R (courtesy of Pile Dynamics, Inc.	17-7
Figure 17.6	Free End Wave Mechanics	17-9

List of Figures		Page
Figure 17.7	Force and Velocity Measurements versus Time for Free End Condition	17-10
Figure 17.8	Fixed End Wave Mechanics	17-11
Figure 17.9	Force and Velocity Measurements versus Time for Fixed End Condition	17-12
Figure 17.10	Soil Resistance Effects on Force and Velocity Records (after Hannigan, 1990)	17-13
Figure 17.11	Typical Force and Velocity Records for Various Soil Resistance Conditions (after Hannigan, 1990)	17-15
Figure 17.12	Standard, RSP and Maximum, RMX, Case Method Capacity Estimates	17-19
Figure 17.13	Energy Transfer Computation (after Hannigan, 1990)	17-21
Figure 17.14	Example of Tension and Compression Stress Computations ...	17-23
Figure 17.15	Schematic of CAPWAP Analysis Method	17-25
Figure 17.16	Factors Most Influencing CAPWAP Force Wave Matching (after Hannigan, 1990)	17-26
Figure 17.17	CAPWAP Iteration Matching Process (after Hannigan, 1990).....	17-28
Figure 17.18	CAPWAP Final Results Table.....	17-29
Figure 17.19	CAPWAP EXTREMA and Case Method Tables	17-30
Figure 17.20	APPLE Drop Weight System (courtesy of GRL Engineers, Inc.)	17-32
Figure 17.21	Typical Screen Display for Pile Driving Analyzer – DOS System.....	17-34
Figure 17.22	Typical Screen for Pile Driving Analyzer – Windows System....	17-34
Figure 17.23	Energy Transfer Ratios for Select Hammer and Pile Combinations.....	17-38
Figure 17.24(a)	Histograms of Energy Transfer Ratio for Diesel Hammers on Steel Piles (top graph) and Concrete/Timber Piles (bottom graph)	17-39
Figure 17.24(b)	Histograms of Energy Transfer Ratio for Single Acting Air/Steam Hammers on Steel Piles (top) and Concrete/Timber Piles (bottom)	17-40
Figure 17.25	Force and Velocity Records Indicating Pile Damage	17-42
Figure 17.26	Photographs of Extracted Damaged Pile from Figure 17.25.....	17-42
Figure 17.27	Force and Velocity Record for Pile with Splice Failures.....	17-43
Figure 17.28	Force and Velocity Record for H-pile to Rock.....	17-43
Figure 17.29	Typical Graphical Presentation of Dynamic Testing Results versus Depth.....	17-45
Figure 17.30	Pulse Echo Velocity versus Time Record for Undamaged Pile.	17-51
Figure 17.31	Pulse Echo Velocity versus Time for Damaged Pile	17-51
Figure 17.32	Typical response Curve from a TRM Test	17-52

	List of Figures	Page
Figure 18.1	Basic Mechanism of a Pile Load Test.....	18-7
Figure 18.2	Typical Arrangement for Applying Load in an Axial Compressive Test (Kyfor, et al., 1992)	18-9
Figure 18.3	Load Test Load Application and Monitoring Components.....	18-10
Figure 18.4	Load Test Movement Monitoring Components	18-11
Figure 18.5	Typical Compression Load Test Arrangement with Reaction Piles.....	18-12
Figure 18.6	Typical Compression Load Test Arrangement using a Weighted Platform	18-13
Figure 18.7	Presentation of Typical Static Pile Load-Movement Results.....	18-14
Figure 18.8	Example of Residual Load Effects on Load Transfer Evaluation	18-18
Figure 18.9	Sister Bar Vibrating Wire Gages for Concrete Embedment	18-19
Figure 18.10	Arc-weldable Vibrating Wire Strain Gage Attached to H-pile ...	18-19
Figure 18.11	Tension Load Test Arrangement on Batter Pile (courtesy of Florida DOT)	18-21
Figure 18.12	Typical Tension Load Test Load-Movement Curve	18-22
Figure 18.13	Typical Lateral Load Test Arrangement (courtesy of WKG2)....	18-24
Figure 18.14	Jack for Lateral Load Test (courtesy of WKG2)	18-25
Figure 18.15	Spherical Bearing Plate and Load Cell for Lateral Load Test ...	18-25
Figure 18.16	Multiple Inclinator String Components for Lateral Load Test	18-26
Figure 18.17	Typical Lateral Load Test Pile Head Load-Deflection Curve.....	18-27
Figure 18.18	Comparison of Measured and COM624P Predicted Load- Deflection Behavior versus Depth (after Kyfor, et al, 1992)	18-28
Figure 19.1	Schematic Comparison between Osterberg Cell and Conventional Tests	19-2
Figure 19.2	Osterberg Cell and Related Equipment Used for Static Pile Tests.....	19-4
Figure 19.3	Osterberg Cell Ready for Placement in Concrete Pile Form (courtesy of Loadtest, Inc.)	19-5
Figure 19.4	Osterberg Test in Progress on a 457 mm Concrete Pile (courtesy of Loadtest, Inc.)	19-6
Figure 19.5	Summary of Subsurface Profile and Test Results at Pines River Bridge, MA.....	19-13
Figure 19.6	Test Results from Pines River Bridge, MA.....	19-14
Figure 19.7	Equivalent Pile Head Load-Movement Curve from Pines River Bridge, MA.....	19-14
Figure 19.8	Summary of Subsurface Profile and Test Results at Aucilla River Bridge, FL.....	19-15
Figure 19.9	Test Results from Aucilla River Bridge, FL	19-16
Figure 19.10	Equivalent Pile Head Load-Movement Curve from Aucilla	

	List of Figures	Page
	River Bridge, FL.....	19-16
Figure 20.1	Statnamic Concept (courtesy of Berminghammer Foundation Equipment)	20-2
Figure 20.2	4,400 kN (1000 kip) Hydraulic Catch Device on Prestressed Concrete Pile (courtesy of Applied Foundation Testing).....	20-3
Figure 20.3	Statnamic Test in Progress with Gravel Catch Mechanism 40,000 kN (9,000 kip) Device (courtesy of Applied Foundation Testing).....	20-4
Figure 20.4	Statnamic Signals (courtesy of Berminghammer Foundation Equipment).....	20-5
Figure 20.5	Statnamic Load versus Displacement (courtesy of Berminghammer Foundation Equipment)	20-5
Figure 20.6	Free Body Diagram of Pile Forces in a Statnamic Test (after Middendorp et al., 1992).....	20-8
Figure 20.7	Five Stages of a Statnamic Test (after Middendorp et al., 1992).....	20-8
Figure 20.8	Derived Statnamic Load Displacement Curve with Rate Effects (courtesy of Berminghammer Foundation Equipment)	20-11
Figure 20.9	Lateral Statnamic Test on Nine Pile Group (courtesy of Utah State University)	20-12
Figure 20.10	Statnamic Test Result (courtesy off Minnesota Department of Transportation)	20-13
Figure 21.1	Swinging Lead Systems (after D.F.I. Publication, 1981).....	21-2
Figure 21.2	Fixed Lead Systems (after D.F.I. Publication, 1981).....	21-3
Figure 21.3	Lead Configurations for Batter Piles (after D.F.I. Publication, 1981)	21-4
Figure 21.4	Typical Offshore Lead Configuration	21-5
Figure 21.5	Typical Lead Types (after D.F.I. Publication, 1981)	21-6
Figure 21.6	Typical Template Arrangement.....	21-8
Figure 21.7	Template Elevation Effects on Batter Piles (after Passe, 1994).....	21-9
Figure 21.8	Helmet Components (after D.F.I. Publication, 1981)	21-10
Figure 21.9	Helmet on H-pile	21-11
Figure 21.10	Typical Hammer Cushion Materials	21-12
Figure 21.11	Plywood Pile Cushion	21-13
Figure 21.12	Pile Hammer Classification	21-15
Figure 21.13	Typical Drop Hammer	21-19
Figure 21.14	Schematic of Single Acting Air/Steam Hammer.....	21-20

List of Figures		Page
Figure 21.15	Single Acting Air Hammer	21-21
Figure 21.16	Double Acting Air Hammer	21-21
Figure 21.17	Schematic of Double Acting Air/Steam Hammer	21-23
Figure 21.18	Schematic of Differential Air/Steam Hammer.....	21-25
Figure 21.19	Schematic of Single Acting Diesel Hammer.....	21-27
Figure 21.20	Single Acting Diesel Hammer (courtesy of Pileco).....	21-29
Figure 21.21	Double Acting Diesel Hammer.....	21-29
Figure 21.22	Schematic of Double Acting Diesel Hammer	21-30
Figure 21.23	Schematics of Single and Double Acting Hydraulic Hammers..	21-32
Figure 21.24	Single Acting Hydraulic Hammer	21-33
Figure 21.25	Double Acting Hydraulic Hammer	21-33
Figure 21.26	Vibratory Hammer.....	21-35
Figure 21.27	IHC Hydraulic Hammer Kinetic Energy Readout Panel	21-37
Figure 21.28	Proximity Switches Attachment for a Berminghammer Diesel Hammer	21-38
Figure 21.29	Proximity Switches, Readout Device, and Driving Log Trigger Switch for Berminghammer Diesel Hammer	21-38
Figure 21.30	Proximity Switches and Transmitter on Retrofitted Diesel Hammer	21-39
Figure 21.31	E-Saximeter Wireless Kinetic Energy Readout Device	21-39
Figure 21.32	Noise Shroud for IHC Hydraulic Hammer	21-40
Figure 21.33	Follower Used for Driving H-Piles	21-41
Figure 21.34	Dual Jet System Mounted on a Concrete Pile (courtesy of Florida DOT)	21-43
Figure 21.35	Jet/Punch System (courtesy of Florida DOT).....	21-43
Figure 21.36	Solid Flight Auger Predrilling System (courtesy of Florida DOT)	21-44
Figure 21.37	Bubble Ring with Containment Device.....	21-46
Figure 22.1	Timber Pile Toe Attachments.....	22-2
Figure 22.2	Banded Timber Pile Head.....	22-3
Figure 22.3	Splices for Timber Piles	22-4
Figure 22.4	Damaged H-piles without Pile Toe Protection.....	22-6
Figure 22.5	Driving Shoes for Protection of H-pile	22-6
Figure 22.6	Typical H-pile Splicer	22-8
Figure 22.7	Pile Toe Attachments for Pipe Piles.....	22-9
Figure 22.8	Splices for Pipe Piles	22-11
Figure 22.9	Splicer for Pipe Pile.....	22-11
Figure 22.10	Pile Toe Attachments for Precast Concrete Piles	22-12
Figure 22.11	Steel H-pile Tip for Precast Concrete Pile.....	22-12
Figure 22.12	Commonly used Prestressed Concrete Pile Splices (after PCI, 1993).....	22-15

	List of Figures	Page
Figure 22.13	Cement-Dowel Splice (after Bruce and Herbert, 1974).....	22-16
Figure 23.1	Pile Inspection Flow Chart	23-3
Figure 23.2	Hammer Cushion Check.....	23-10
Figure 23.3	Damaged Hammer Cushion	23-10
Figure 23.4	Pile Cushion Replacement.....	23-10
Figure 23.5	Air Compressor Display Panel.....	23-15
Figure 23.6	Inspection Form for Single and Differential Acting Air/Steam Hammers	23-18
Figure 23.7	Inspection Form for Enclosed Double Acting Air/Steam Hammers	23-21
Figure 23.8	Fixed Four Step Fuel Pump on Delmag Hammer	23-23
Figure 23.9	APE Variable Fuel Pump on Hammer (courtesy APE).....	23-23
Figure 23.10	Adjustable Pressure Pump for Fuel Setting on ICE Hammer....	23-23
Figure 23.11	Inspection form for Single Acting Diesel Hammers.....	23-26
Figure 23.12	Typical External Bounce Chamber Pressure Gauge.....	23-28
Figure 23.13	Inspection Form for Double Acting Diesel Hammers	23-31
Figure 23.14	IHC Hydraulic Hammer Read-Out Panel (courtesy of L.B. Foster Co.).....	23-33
Figure 23.15	Inspection Form for Hydraulic Hammers.....	23-35
Figure 23.16	Driving Sequence of Displacement Pile Groups (after Passe, 1994).....	23-42
Figure 23.17a	Pile Driving Log (SI Version).....	23-49
Figure 23.17b	Pile Driving Log (US Version)	23-50
Figure 23.18	Daily Inspection Report.....	23-52

LIST OF SYMBOLS

- A - Pile cross sectional area.
- A_g - Pile area at gage location.
- A_{np} - Net area of piston.
- a - Acceleration.
- a_m - Measured acceleration.
- b - Pile diameter.
- C - Wave speed of pile material.
- C_4 - Statnamic damping constant.
- D_w - Wave length.
- E - Modulus of elasticity of pile material.
- E_p - Energy transferred to pile.
- E_d - Dynamic stiffness.
- E_r - Manufacturers rated hammer energy.
- F - Force.
- F_a - Statnamic inertia force.
- F_p - Statnamic pore water pressure force.
- F_u - Statnamic static soil resistance force.
- F_v - Statnamic dynamic soil resistance force.
- F_{stn} - Statnamic induced force.
- $F(t)$ - Force measured at gage location.

LIST OF SYMBOLS (continued)

- Δf - Change in frequency.
- h - Hammer stroke.
- J - Soil damping factor.
- J_c - Dimensionless Case damping factor.
- L - Total pile length.
- ΔL - Length of pile between two measuring points under no load conditions.
- L_g - Pile length below gage location.
- m - Mass.
- N_b - The number of hammer blows per 25 mm.
- N_w - Wave number.
- p_h - Pressure at hammer.
- Q - Load.
- Q_a - Allowable design load of a pile.
- Q_{avg} - Average load in the pile.
- Q_f - Failure load.
- Q_h - Applied pile head load.
- Q_o - Osterberg cell load.
- Q_r - Load from reaction system.
- Q_u - Ultimate bearing capacity of a pile.
- q - Soil quake.

LIST OF SYMBOLS (continued)

- R - Soil resistance.
- R_1 - Deflection reading at upper of two measuring points.
- R_2 - Deflection reading at lower of two measuring points.
- R_s - Ultimate pile shaft resistance.
- R_t - Ultimate pile toe resistance.
- R_u - Ultimate soil resistance.
- s_b - Set per blow.
- s_f - Settlement at failure.
- T_L - Load duration.
- t_1 - Time of initial impact.
- t_2 - Time of reflection of initial impact from pile toe (t_1+2L/c).
- t_4 - Time at Statnamic stage 4.
- t_{umax} - Time of maximum displacement.
- U - Displacement.
- $V(t)$ - Velocity measured at gage location.
- v_i - Impact velocity.
- W - Ram weight.
- WD - Downward traveling wave, wave down.
- WU - Upward traveling wave, wave up.
- Δ - Elastic compression.

LIST OF SYMBOLS (continued)

ε - Strain.

ϕ - Angle of internal friction of soil.

LIST OF SYMBOLS (continued)

Chapter 14

INTRODUCTION TO CONSTRUCTION MONITORING

Volume II of the Manual on Design and Construction of Driven Pile Foundations focuses on the construction aspects of driven pile foundations. Following this introductory chapter are chapters on pile capacity evaluation using dynamic formulas (Chapter 15), wave equation analysis (Chapter 16), dynamic testing and analysis (Chapter 17), static load testing (Chapter 18), the Osterberg load cell device (Chapter 19) and the Statnamic method (Chapter 20). These chapters on pile testing methods are followed by chapters detailing pile driving equipment (Chapter 21), driven pile accessories (Chapter 22), and pile inspection (Chapter 23).

14.1 THE ROLE OF CONSTRUCTION MONITORING

Proper pile installation is as important as rational pile design in obtaining a cost effective and safe foundation. Driven piles must develop the required capacity without sustaining structural damage during installation. Construction monitoring of driven piles is much more difficult than for spread footings where the footing excavation and footing construction can be visually observed to assure quality. Since piles cannot be seen after their installation, direct quality control of the finished product is impossible. Therefore substantial control must be exercised over the pile installation process to obtain the desired end product.

It is essential that all pile installation limitations be considered during the project design stage so that the piles shown on the plans can be installed as designed. For example, consideration should be given to how new construction may affect existing structures and how limitations on construction equipment access, size, operational area, or environmental issues may dictate the pile type that can be most cost effectively installed.

Construction monitoring should be exercised in three areas: pile materials, installation equipment, and the estimation of static capacity. These areas are interrelated since changes in one affects the others. Table 14-1 highlights the items to be included in the plans and specifications that are the design engineer's responsibility, and the items to be checked for quality assurance that are the construction engineer's responsibility.

TABLE 14-1 RESPONSIBILITIES OF DESIGN AND CONSTRUCTION ENGINEERS

Item	Design Engineer's Responsibilities	Construction Engineer's Responsibilities
Pile Details	Include in plans and specifications: <ol style="list-style-type: none"> a. Material and strength: concrete, steel, or timber. b. Cross section: diameter, tapered or straight, and wall thickness. c. Special coatings for corrosion or downdrag. d. Splices, toe protection, <i>etc.</i> e. Estimated pile tip elevation. f. Estimated pile length. g. Pile design load and ultimate capacity. h. Allowable driving stresses. 	Quality control testing or certification of materials.
Soils Data	Include in plans and specifications: <ol style="list-style-type: none"> a. Subsurface profile. b. Soil resistance to be overcome to reach estimated length. c. Minimum pile penetration requirements. d. Special notes: boulders, artesian pressure, buried obstructions, time delays for embankment fills, <i>etc.</i> 	Report major discrepancies in soil profile to the designer.
Installation	Include in plans and specifications: <ol style="list-style-type: none"> a. Method of hammer approval. b. Method of determining ultimate pile capacity. c. Compression, tension, and lateral load test requirements (as needed) including specification for tests and the method of interpretation of test results. d. Dynamic testing requirements (as needed). f. Limitations on vibrations, noise, fish kill, and head room. g. Special notes: spudding, predrilling, jetting, set-up period, <i>etc.</i> 	<ol style="list-style-type: none"> a. Confirm that the hammer and driving system components agree with the contractor's approved submittal. b. Confirm that the hammer is maintained in good working order and the hammer and pile cushions are replaced regularly. c. Determination of the final pile length from driving resistance, estimated lengths and subsurface conditions. d. Pile driving stress control. e. Conduct pile load tests. f. Documentation of field operations. g. Ensure quality control of pile splices, coatings, alignment and driving equipment.

14.2 SELECTION OF FACTOR OF SAFETY

In the design stage, a design load is selected for the pile section as a result of static analyses and consideration of the allowable stresses in the pile material. A factor of safety is applied to the design load depending upon the confidence in the static analysis method, the quality of the subsurface exploration program, and the construction control method specified. Static analyses yield the estimated pile length, based on the penetration depth in suitable soils required to develop the design load times the factor of safety. Soil resistance from unsuitable support layers, or layers subject to scour, are not included in determining the required pile penetration depth.

During construction, the ultimate pile capacity to be obtained is the sum of the design load, times a factor of safety, plus the soil resistance from unsuitable layers not counted on for long term support or subject to scour. The plans and specifications should state the ultimate pile capacity to be obtained in conjunction with the construction control method to be used for determination of the ultimate pile capacity.

The factor of safety used should be based on the quality of the subsurface exploration information and the construction control method used for capacity verification. There are several capacity verification methods that can be used for construction control which are described in subsequent chapters. The factor of safety applied to the design load should increase with the increasing unreliability of the method used for determining ultimate pile capacity during construction. The recommended factor of safety on the design load for various construction control methods from Cheney and Chassie (2000) and/or AASHTO (2002) are in Table 14-2. The factor of safety for other test methods not included in Table 14-2 should be determined by the individual designer.

Table 14-2. Recommended Factor of Safety Based on Construction Control	
Construction Control Method	Factor of Safety
Static Load Test (ASTM D-1143)	2.00
Dynamic Measurements (ASTM D-4945) and Signal Matching Analysis coupled with Wave Equation Analysis	2.25
Indicator Piles coupled with Wave Equation Analysis	2.50
Wave Equation Analysis	2.75
Modified Gates Dynamic Formula	3.50
Engineering News Formula	Not a Recommended Method

Consider a pile with a design load of 700 kN (157 kips). If no unsuitable soil layers exist, and a static load test will be performed for construction control, then an ultimate pile capacity of 1400 kN (314 kips) would be specified. For this same example, an ultimate pile capacity of 1925 kN (432 kips) would be required when construction control is by wave equation analysis. Hence, the higher ultimate capacity would require piles to be driven harder and deeper thereby increasing the foundation cost and completion time. These factors should be considered when selecting the method of construction control.

If unsuitable or scour susceptible layers exist, the resistance from these layers should be added to the required ultimate pile capacity. For a pile with a design load of 700 kN (157 kips) in a soil profile with 250 kN (56 kips) of soil resistance from unsuitable soils, or soils subject to scour, an ultimate pile capacity of 1650 kN (370 kips) would be required for construction control with a static load test. For this case, an ultimate pile capacity of 2175 kN (488 kips) would be specified for construction control by wave equation analysis.

14.3 DRIVING CRITERIA

The foundation designer should specify the method to be used for determination of the driving criteria. Construction personnel should clearly understand the method being used and its proper implementation on the project. A driving criteria usually consists of a specified penetration resistance at a given hammer stroke and, in some cases, a minimum pile penetration depth.

The driving criteria should consider time dependent changes in pile capacity as discussed in Section 9.10.1. In soils exhibiting set-up, penetration resistances at the end of driving less than that required for the ultimate capacity may be acceptable. Conversely in soils exhibiting relaxation, penetration resistances at the end of driving higher than that required for the ultimate capacity may be required. Restrike tests are typically performed in soils with time dependent soil strength changes to confirm the expected change in pile capacity. The driving criteria should be substantiated by static load tests whenever possible. In cases where time dependent soil strength changes are anticipated, load tests should also be delayed an appropriate waiting period until the anticipated soil strength changes have occurred. Approximate waiting periods for various soil types were discussed in Sections 9.10.1.1 and 9.10.1.2 of Chapter 9.

In the past, dynamic formulas were the primary means of establishing driving criteria. As discussed elsewhere in this manual, dynamic formulas do not provide information on pile

driving stresses and, in many circumstances, have proven unreliable in determining pile capacity. Therefore, their continued use is not recommended on significant projects.

Wave equation analysis offers a rational means of establishing a relationship between the static capacity of a driven pile and the number of blows per 0.25 meter (blows per foot) from a particular hammer in a given soil situation. Wave equation analysis also provide information on compression and tension stresses versus penetration resistance. Driving criteria established from wave equation analysis should be substantiated by static load tests whenever practical.

Dynamic testing and analysis of indicator or test piles allows an assessment of the static pile capacity and pile stresses during driving. This is also an appropriate means of establishing a driving criterion. Restrike dynamic tests are typically performed in soils with time dependent soil strength changes to determine the ultimate pile capacity after an appropriate waiting time. The driving criteria established by dynamic testing and analysis should also be substantiated by static load tests whenever practical.

Driving criteria should not be established that require excessive amounts of driving beyond refusal driving conditions. Practical refusal is typically defined as 20 blows per 25 mm of penetration (20 blows per inch) with the hammer operated at its maximum fuel or energy setting, or at a reduced fuel or energy setting recommended by the Engineer based on pile installation stress control. In no case should driving continue for more than 75 mm (3 inches) at practical refusal driving conditions.

Absolute refusal is typically defined as a penetration resistance 50% greater than that of practical refusal, i.e. 30 blows per 25 mm (30 blows per inch). Driving should be terminated immediately once absolute refusal driving conditions are encountered.

14.4 COMMUNICATION

Proper construction monitoring of pile driving requires good communication between design and construction engineers. Such communication cannot always follow traditional lines and still be effective. Information is needed in a short time to minimize expensive contractor down time or to prevent pile driving from continuing in an unacceptable fashion.

Good communication should begin with a pre-construction meeting of the foundation designer and the construction engineer on all projects with significant piling items. Prior to

the meeting, the construction engineer should review the project foundation report and be fully aware of any construction concerns. At the meeting, the designer should briefly explain the design and point out uncertainties and potential problem areas. The primary objective of this meeting is to establish a direct line of communication.

During construction, the construction engineer should initiate communication with the designer if proposed pile installation methods or results differ from the plans and specifications. The designer should advise the construction engineer on the design aspects of the field problems. The construction engineer should provide feedback on construction monitoring data to the design engineer.

The ultimate decision making authority should follow along the traditional lines of communication established by the state transportation agency. However, informal interaction between design offices and the field should be encouraged and will simplify and expedite decisions.

REFERENCES

- American Association of State Highway and Transportation Officials [AASHTO], (2002). Standard Specifications for Highway Bridges. Seventeenth Edition, AASHTO Highway Subcommittee on Bridges and Structures, Washington, D.C.
- Cheney, R.S. and Chassie, R.G. (2000). Soils and Foundations Workshop Reference Manual. Publication No. FHWA-HI-00-045, U.S. Department of Transportation, Federal Highway Administration and the National Highway Institute, Washington, D.C., 358.

Chapter 15

DYNAMIC FORMULAS FOR STATIC CAPACITY DETERMINATION

Ever since engineers began using piles to support structures, they have attempted to find rational methods for determining the pile's load carrying capacity. Methods for predicting capacities were proposed, using pile penetration observations obtained during driving. The only realistic measurement that could be obtained during driving was the pile set per blow. Thus energy concepts equating the kinetic energy of the hammer to the resistance on the pile as it penetrates the soil were developed to determine pile capacity. In equation form this can be expressed as:

$$Wh = R s_b$$

Where: W = Ram weight.
 h = Ram stroke.
 R = Soil resistance.
 s_b = Set per blow.

These types of expressions are known as dynamic formulas. Because of their simplicity, dynamic formulas have been widely used for many years. More comprehensive dynamic formulas include consideration of pile weight, energy losses in drive system components, and other factors. Whether simple or more comprehensive dynamic formulas are used, pile capacities determined from dynamic formulas have shown poor correlations and wide scatter when statistically compared with static load test result. Therefore, except where well supported empirical correlations under a given set of physical and geological conditions are available or where a site specific correlation has been obtained for a hammer-pile-soil system with a static load test result, dynamic formulas should not be used.

15.1 ACCURACY OF DYNAMIC FORMULAS

Wellington proposed the popular Engineering News formula in 1893. It was developed for evaluating the capacity of timber piles driven primarily with drop hammers in sands. Concrete and steel piles were unknown at that time as were many of the pile hammer types and sizes used today. Therefore, it should be of little surprise that the formula performs poorly in predicted capacities of modern pile foundations.

The inadequacies of dynamic formulas have been known for a long time. In 1941, an ASCE committee on pile foundations assembled the results of numerous pile load tests along with the predicted capacities from several dynamic formulas, including the Engineering News, Hiley, and Pacific Coast formulas. The mean failure load of the load test data base was 91 tons. After reviewing the data base, Peck (1942) proposed that a new and simple dynamic formula could be used that stated the capacity of every pile was 91 tons. Peck concluded that the use of this new formula would result in a prediction statistically closer to the actual pile capacity than that obtained by using any of the dynamic formulas contained in the 1941 study.

More recently, Chellis (1961) noted that the actual factor of safety obtained by using the Engineering News formula varied from as low as $\frac{1}{2}$ to as high as 16. Sowers (1979) reported that the safety factor from the Engineering News formula varied from as low as $\frac{2}{3}$ to as high as 20. Fragasny *et al.* (1988) in the Washington State DOT study entitled "Comparison of Methods for Estimating Pile Capacity" found that the Hiley, Gates, Janbu, and Pacific Coast Uniform Building code formulas all provide relatively more dependable results than the Engineering News formula. Unfortunately, many transportation departments continue to use the Engineering News formula, which also remains the dynamic formula contained in current AASHTO Standard Specifications for Highway Bridges (2002).

As part of a FHWA research project, Rausche *et al.* (1996) compiled a data base of static load test piles that included pile capacity predictions using the FHWA recommended static analysis methods, preconstruction and refined wave equations, as well as dynamic measurements coupled with CAPWAP analysis. The reliability of the various capacity prediction methods were then compared with the results of the static loading tests. The results of these comparisons are presented in Figure 15.1 in the form of probability density function curves versus the ratio of predicted load over the static load test result. The mean values and coefficients of variation for the methods studied are presented in Table 15-1. The closer the mean value of the ratio of the predicted/static load test result is to 1.0 and the smaller the coefficient of variation (COV) the more reliable the method. Prediction method performance using driving observations of blow count and hammer stroke are identified as EOD for end of driving observations or BOR for beginning of restrike.

The data base compiled by Rausche *et al.* (1996) has been modified to include capacity predictions from the Engineering News and Modified Gates dynamic formulas at both the end of driving and beginning of restrike. The data base for the dynamic formulas has also been expanded, and includes additional data sets. For evaluation of dynamic

formula performance, the allowable load determined using the Engineering News formula was compared to one half of the ultimate capacity determined from the static load test. The ultimate capacity from the Modified Gates formula was compared directly to the ultimate capacity determined from the static load test. The correlation results of the dynamic formulas are included in Table 15-1.

Based on the end of driving data, the Engineering News formula had a mean value of 1.22 and a coefficient of variation of 0.74, while the Modified Gates had a mean value of 0.96 with a coefficient of variation of 0.41. The coefficient of variation is the standard deviation divided by the mean value. Hence, the greater a method's mean value is from 1.0 the lower the accuracy of the method, and the larger the coefficient of variation the less reliable the method. Table 15-1 clearly shows the Engineering News formula has a tendency to overpredict pile capacity. The higher coefficient of variation also suggests that the Engineering News formula is significantly less reliable than the Modified Gates formula.

Table 15-1 illustrates that evaluation of pile capacity, by either Gates or Engineering News dynamic formula from restrike set and energy observations, has a significant tendency to overpredict pile capacity. The Engineering News formula capacity results, from restrike observations, had a mean value of 1.89 and a coefficient of variation of 0.46. The Modified Gates formula capacity results, from restrike observations, had a mean value of 1.33 and a coefficient of variations of 0.48

If the static load test failure loads are divided by the Engineering News allowable design loads, the data base indicates an average factor of safety of 2.3 as compared to the factor of safety of 6.0 theoretically included in the formula. More important, the actual factor of safety from the Engineering News formula ranged from 0.6 to 13.1. This lack of reliability causes the Engineering News formula to be ineffective as a tool for estimating pile capacity. The fact that 12% of the data base has a factor of safety of 1.0 or less is also significant. However, complete failure of a bridge due to inadequate pile capacity determined by Engineering News formula is unusual. The problem usually is indicated by long term damaging settlements which occur after construction when the maximum load is intermittently applied.

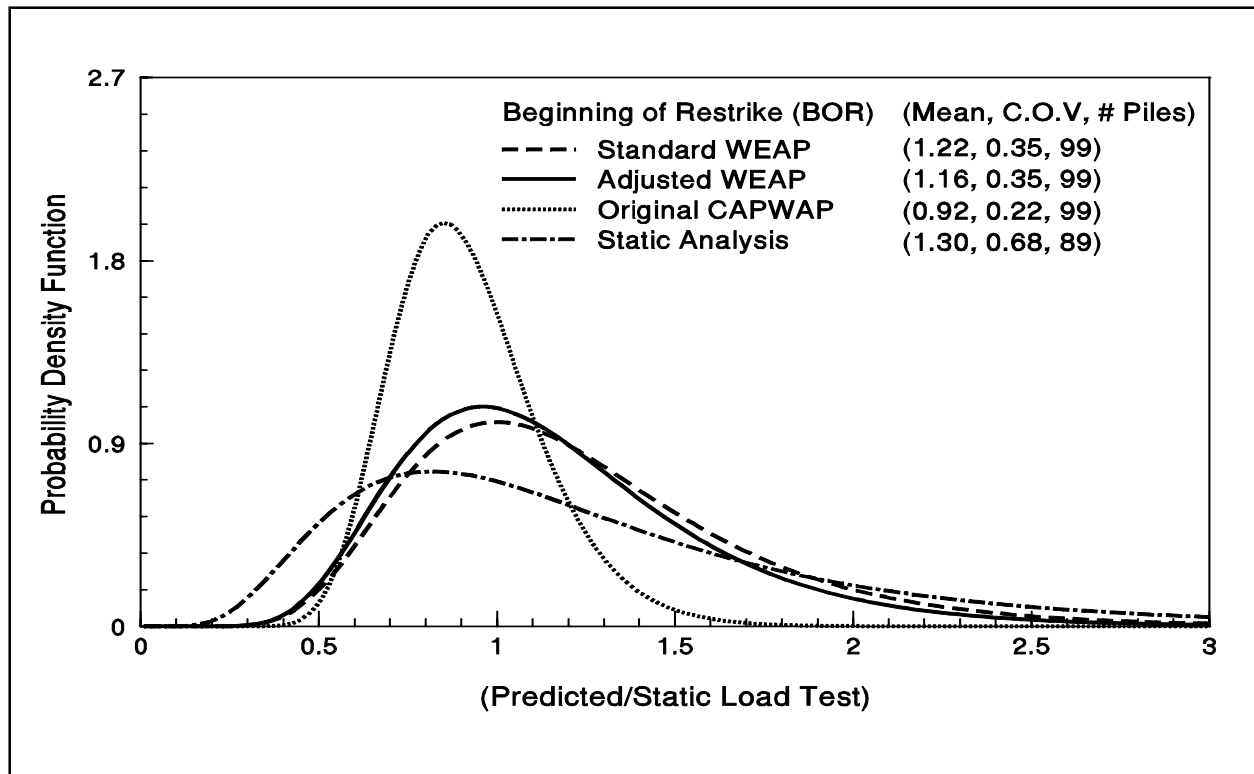


Figure 15.1 Log Normal Probability Density Function for Four Capacity Prediction
(after Rausche *et al.* 1996)

TABLE 15-1 MEAN VALUES AND COEFFICIENTS OF VARIATION FOR VARIOUS METHODS				
Prediction Method	Status	Mean	C.O.V.	# Piles
Standard WEAP*	BOR	1.22	0.35	99
Hammer Performance Adjusted WEAP*	BOR	1.16	0.35	99
CAPWAP*	BOR	0.92	0.22	99
Static Analysis*	-	1.30	0.68	89
Engineering News Formula	EOD	1.22	0.74	139
Engineering News Formula	BOR	1.89	0.46	122
Modified Gates Formula	EOD	0.96	0.41	139
Modified Gates Formula	BOR	1.33	0.48	122

* From Rausche *et al.* (1996)

EOD = End of Driving, BOR = Beginning of Restrike

15.2 PROBLEMS WITH DYNAMIC FORMULAS

Dynamic formulas are fundamentally incorrect. The problems associated with pile driving formulas can be traced to the modeling of each component within the pile driving process: the driving system, the soil, and the pile. Dynamic formulas offer a poor representation of the driving system and the energy losses of drive system components. Dynamic formulas also assume a rigid pile, thus neglecting pile axial stiffness effects on driveability, and further assume that the soil resistance is constant and instantaneous to the impact force. A more detailed discussion of these problems is presented below.

First, the derivation of most formulas is not based on a realistic treatment of the driving system. Most formulas only consider the kinetic energy of the driving system. The variability of equipment performance is typically not considered. Driving systems include many elements in addition to the ram, such as the anvil for a diesel hammer, the helmet, the hammer cushion, and for a concrete pile, the pile cushion. These components affect the distribution of the hammer energy with time, both at and after impact, which influences the magnitude and duration of peak force. The peak force and its duration determine the ability of the driving system to advance the pile into the soil.

Second, the soil resistance is very crudely treated by assuming that it is a constant force. This assumption neglects even the most obvious characteristics of real soil behavior. The dynamic soil resistance is the resistance of the soil to rapid pile penetration produced by a hammer blow. This resistance is by no means identical with the static soil resistance. However, most dynamic formulas consider the resistance during driving equal to the static resistance or pile capacity. The rapid penetration of the pile into the soil during driving is resisted not only by static friction and cohesion, but also by the soil viscosity, which is comparable to the viscous resistance of liquids against rapid displacement under an applied force. The net effect is that the driving process creates dynamic resistance forces along the pile shaft and at the pile toe, due to the high shear rate. The soil resistance during driving, from the combination of dynamic soil resistance and available static soil resistance, is generally not equal to the static soil resistance or pile capacity under static loads.

Third, the pile is assumed to be rigid and its length is not considered. This assumption completely neglects the pile's flexibility, which affects its ability to penetrate the soil. The energy delivered by the hammer sets up time-dependent stresses and displacements in the helmet, in the pile, and in the surrounding soil. In addition, the pile behaves, not as a concentrated mass, but as a long elastic rod in which stresses travel

longitudinally as waves. Compressive waves which travel to the pile toe are responsible for advancing the pile into the ground.

15.3 DYNAMIC FORMULAS

As noted in Section 15.1, the Engineering News formula is generally recognized to be one of the least accurate and least consistent of dynamic formulas. Due to the overall poor correlations documented between pile capacities determined from this method and static load test results, the use of the Engineering News formula is not recommended.

For small projects where a dynamic formula is used, statistics indicate that the FHWA Modified Gates formula is preferable, since it correlates better with static load test results. The Modified Gates formula presented below has been revised to reflect the ultimate pile capacity in kilonewtons and includes the 80 percent efficiency factor on the rated energy, E_r , recommended by Gates. It should be noted that the US and SI versions of the Modified Gates Formula may yield slightly different results due to a refinement of the formula by FHWA when it was soft converted from US to SI units.

Modified Gates Formula in SI Units

$$R_u = [6.7\sqrt{E_r} \log(10 N_b)] - 445$$

Where: R_u = the ultimate pile capacity (kN).

E_r = the manufacturer's rated hammer energy (Joules) at the **field observed ram stroke**.

$\log(10N_b)$ = logarithm to the base 10 of the quantity 10 multiplied by N_b , the number of hammer blows per 25 mm at final penetration.

The number of hammer blows per 0.25 meter of pile penetration required to obtain the ultimate pile capacity shall be calculated as follows:

$$N_{qm} = 10(10^x)$$

Where: $x = [(R_u + 445) / (6.7\sqrt{E_r})] - 1$

Modified Gates Formula in US Units

$$R_u = [1.75\sqrt{E_r} \log(10 N_b)] - 100$$

Where: R_u = the ultimate pile capacity (kips).

E_r = the manufacturer's rated hammer energy (ft-lbs) at the **field observed ram stroke**.

$\log(10N_b)$ = logarithm to the base 10 of the quantity 10 multiplied by N_b , the number of hammer blows per 1 inch at final penetration.

The number of hammer blows per foot of pile penetration required to obtain the ultimate pile capacity shall be calculated as follows:

$$N_{ft} = 12 (10^x)$$

Where: $x = [(R_u + 100)/1.75\sqrt{E_r}] - 1$

Most dynamic formulas are in terms of ultimate pile capacity, rather than allowable design load. For ultimate pile capacity formulas, the design load should be multiplied by a factor of safety to obtain the ultimate pile capacity that is input into the formula to determine the "set", or amount of pile penetration per blow required. A factor of safety of 3.5 is recommended when using the Gates formula. For example, if a design load of 890 kN (200 kips) is required in the bearing layer, then an ultimate pile capacity of 3115 kN (700 kips) should be used in the Gates formula to determine the necessary driving resistance.

Highway agencies should establish long term correlations between pile capacity prediction from dynamic formulas and static load test results to failure.

15.4 ALTERNATIVES TO USE OF DYNAMIC FORMULAS

Most shortcomings of dynamic formulas can be overcome by a more realistic analysis of the pile driving process. The one-dimensional wave equation analysis discussed in Chapter 16 is a more realistic method. However as little as twenty years ago, wave equation analyses were primarily performed on main frame computers. Therefore, wave equation analysis was often viewed as a tool for special projects and not routine use. With the widespread use of fast personal computers in every day practice, wave equation analysis can now be easily performed in a relatively short amount of time.

As indicated in Table 15-1, ultimate pile capacity estimates from standard wave equation analysis using restrike driving resistance observations had a mean value of 1.22 and a coefficient of variation of 0.35. The performance of the wave equation capacity predictions improved when the hammer efficiency was adjusted to agree with the measured drive system performance from dynamic measurements.

Dynamic testing and analysis is another tool which is superior to use of dynamic formulas. This topic will be discussed in greater detail in Chapter 17. Table 15-1 illustrates that dynamic measurement with CAPWAP analysis performed better than either the Engineering News or Modified Gates dynamic formulas. Ultimate pile capacity estimates from restrike dynamic measurements with CAPWAP analysis had a mean value of 0.92 and a coefficient of variation of 0.22.

Modern dynamic methods of wave equation analysis, as well as dynamic testing and analysis, are superior to traditional dynamic formulas. Modern methods should be used in conjunction with static pile load tests whenever possible, and the use of dynamic formulas should be discontinued.

15.5 DYNAMIC FORMULA CASE HISTORIES

To illustrate the variable performance of dynamic formulas compared to modern methods, three case histories will be briefly discussed. The case histories were selected to include a range of pile types and sizes, hammer types, and soil conditions.

15.5.1 Case History 1

Case History 1 involves a 610 mm (24 inch) square prestressed concrete pile with a 305 mm (12 inch) diameter circular void at the pile center. The concrete pile was driven

through loose to medium dense clayey sands to a dense clayey sand layer. A Vulcan 520 single acting air hammer operated at a reduced stroke of 0.9 m (3 ft) and corresponding rated energy of 81 kJ (60 ft-kips) was used to drive the pile. The pile was driven to a final penetration resistance of 34 blows per 0.25 meter (42 blows per foot). When restruck 13 days after initial driving, the pile had a penetration resistance of 118 blows per 0.25 meter (144 blows per foot). This pile was then statically load tested.

Using end of driving set observations, the Engineering News formula predicted an allowable design load of 1360 kN (306 kips) and the Modified Gates formula predicted an ultimate pile capacity of 2476 kN. (557 kips) Modern dynamic methods of the wave equation and dynamic testing with CAPWAP analysis gave restrike ultimate pile capacities of 4561 and 4111 kN (1026 and 925 kips), respectively. The static load test pile had a Davisson failure load of 4223 kN (950 kips). Hence, the Engineering News and Modified Gates dynamic formulas significantly underpredicted the allowable and ultimate pile capacity, respectively. Dynamic test data indicated the restrike capacity was 2.5 times the capacity at the end of initial driving. This high setup condition most likely caused the underpredictions by the dynamic formulas.

15.5.2 Case History 2

Case History 2 involves a 356 mm (14 inch) O.D. closed end pipe pile driven into a dense to very dense sand and gravel. The pile had a design load of 620 kN (140 kips) and a required ultimate capacity of 1550 kN (349 kips), which included an anticipated capacity loss due to scour. An IHC S-70 hydraulic hammer with a maximum rated energy of 69 kJ (51 ft-kips) was used to install the pile. The IHC hydraulic hammers can be operated over a wide energy range and include a readout panel that indicates for each blow the hammer kinetic energy prior to impact. The static load test pile was driven to a final penetration resistance of 26 blows per 0.25 m (32 blows per foot) at a readout panel energy of 28 kJ (20.7 ft-kips). Restrike tests at the site indicated minimal changes in pile capacity with time.

Based on end of driving set observations, the Engineering News formula predicted an allowable design load of 387 kN (87 kips) and the Modified Gates formula predicted an ultimate pile capacity of 1142 kN (257 kips). The preconstruction wave equation analysis predicted an ultimate pile capacity of 1333 kN (300 kips). Restrike dynamic testing with CAPWAP analysis predicted an ultimate pile capacity of 1605 kN (361 kips). The static load test pile had a Davisson failure load of 1627 kN (366 kips). Hence, both the Engineering News and Modified Gates dynamic formulas significantly underpredicted the allowable and ultimate pile capacity, respectively. In this particular

case, the poor performance of the dynamic formulas is most likely attributed to the high energy transfer efficiency of the IHC type hydraulic hammer relative to its kinetic energy rating based on the readout panel.

15.5.3 Case History 3

In Case History 3, a 356 mm (14 inch) O.D. closed end pipe pile was driven through loose to medium dense sands to toe bearing in a very dense sand. The pipe pile had a design load of 980 kN (220 kips) and a required ultimate pile capacity of 1960 kN (440 kips). An ICE 42-S single acting diesel hammer with a rated energy of 57 kJ (42 ft-kips) was used to drive the load test pile to a final driving resistance of 148 blows per 0.25 m (180 blows per foot) at a hammer stroke of 3 m (9.8 ft).

Using the end of driving set observations, the Engineering News formula predicted an allowable design load of 2180 kN (490 kips) and the Modified Gates formula predicted an ultimate pile capacity of 2988 kN (672 kips). Dynamic testing with CAPWAP analysis indicated an ultimate pile capacity of 2037 kN (458 kips) at the end of initial driving, that decreased to an ultimate capacity of 1824 kN (410 kips) during restrike. The static load test pile had a Davisson failure load of 1868 kN (420 kips). Assuming a safety factor of 2, the allowable pile capacity would be 934 kN (210 kips). Hence, the Engineering News formula overpredicted the allowable design load by more than 230% and the Modified Gates formula overpredicted the ultimate pile capacity by 60%.

The magnitude of the overprediction by the dynamic formulas is at least partially attributed to the soil relaxation (capacity at end of driving higher than some time later) that occurred at the site. Pile capacities determined from dynamic formulas are routinely calculated from initial driving observations. Therefore, the time dependent decrease in pile capacity would not likely have been detected if only dynamic formulas had been used for pile driving control on this project.

The case histories above illustrate that different methods often result in a range of predicted capacities at a given site. The magnitude of pile capacity changes with time. Both hammer performance characteristics and soil behavior can be different from those than typically assumed. The three case histories presented illustrate that pile capacity evaluations with modern dynamic methods handle these variations better than traditional dynamic formulas.

REFERENCES

- American Association of State Highway and Transportation Officials [AASHTO], (2002). Standard Specifications for Highway Bridges, 17th Edition, Division II, AASHTO Highway Subcommittee on Bridges and Structures, Washington, D.C.
- Chellis R.D. (1961). Pile Foundations. Second Edition, McGraw-Hill Book Company, New York, 21-23.
- Fragasny, R.J., Higgins, J.D. and Argo, D.E. (1988). Comparison of Methods for Estimating Pile Capacity. Report No. WA-RD 163.1, Washington State Department of Transportation, 62.
- Peck, R.B. (1942). Discussion: Pile Driving Formulas. Proceedings of the American Society of Civil Engineers, Vol. 68, No. 2, 905-909.
- Rausche, F., Thendean, G., Abou-matar, H., Likins, G.E. and Goble, G.G. (1996). Determination of Pile Driveability and Capacity from Penetration Tests. Final Report, U.S. Department of Transportation, Federal Highway Administration Research Contract DTFH61-91-C-00047.
- Sowers, G.F. (1979). Introductory Soil Mechanics and Foundations. Fourth Edition, Macmillan Publishing Co., Inc., New York, 531-533.

Chapter 16

DYNAMIC ANALYSIS BY WAVE EQUATION

16.1 INTRODUCTION

As discussed in previous chapters, dynamic formulas, together with observed penetration resistances, do not yield acceptably accurate predictions of actual pile capacities. Moreover, they do not provide information on stresses in the piles during driving. The so-called “wave equation analysis” of pile driving has eliminated many shortcomings associated with dynamic formulas by realistically simulating the hammer impacts and pile penetration process. For most engineers, the term wave equation refers to a partial differential equation. However, for the foundation specialist, it means a complete approach to the mathematical representation of a system consisting of hammer, cushions, helmet, pile and soil and an associated computer program for the convenient calculation of the dynamic motions and forces in this system after ram impact.

The approach was developed by E.A.L. Smith (1960), and after the rationality of the approach had been recognized, several researchers developed a number of computer programs. For example, the Texas Department of Highways supported research at the Texas Transportation Institute (TTI) in an attempt to determine driving stresses and reduce concrete pile damage using a realistic analysis method. FHWA sponsored the development of both the TTI program (Hirsch *et al.*, 1976) and the WEAP program (Goble and Rausche, 1976). FHWA supported the WEAP development to obtain analysis results backed by measurements taken on construction piles during installation for a variety of hammer models. The WEAP program was updated several times under FHWA sponsorship, until 1986 (Goble and Rausche, 1986). Later, additional options, improved data files, refined mathematical representations and modern user conveniences were added to this program on a proprietary basis, and the program is now known as GRLWEAP (Pile Dynamics, Inc. 2005). Similar computer programs based on the method of characteristics have been developed such as PDPWAVE (Bielefeld and Middendorp, 1992).

The wave equation approach has been subjected to a number of checks and correlation studies. Studies on the performance of WEAP have produced publications demonstrating that program's performance and utility (*e.g.* Blendy 1979, Soares *et al.* 1984, Rausche *et al.*, 2004). A documentation of the most recent version of this program, GRLWEAP 2005, has been prepared by Pile Dynamics, Inc. (2005).

This chapter will explain what a wave equation analysis is, how it works, and what problems it can solve. Example problems, highlighting program applications, will be demonstrated. Also, basic program usage and application of program results will be presented. While GRLWEAP is used for these example and application purposes, this should not be construed as a promotion or endorsement.

16.2 WAVE PROPAGATION

Input preparation for wave equation analyses is often very simple, requiring only very basic driving system and pile parameters in addition to a few soil parameters for which standard recommendations are given. Thus, a wave equation program can be run with minimal specialized knowledge. However, interpretation of calculated results is facilitated, and errors in result application may be avoided, by a knowledge of the mechanics of stress wave propagation and familiarity with the particular project's design requirements and constraints.

In the first moment, after a hammer has struck the pile top, only the pile particles near the ram-pile interface are compressed. This compressed zone, or force pulse, as shown in Figure 16.1, expands into the pile toward the pile toe at a constant wave speed, C , which depends on the pile's elastic modulus and mass density (or specific weight). When the force pulse reaches the embedded portion of the pile, its amplitude is reduced by the action of static and dynamic soil resistance forces. Depending on the magnitude of the soil resistances along the pile shaft and at the pile toe, the force pulse will reflect from the pile toe either as a tensile or a compressive force pulse, which travels back to the pile head. Both incident and reflected force pulses will cause a pile toe motion and produce a permanent pile set if their combined energy and force are sufficient to overcome the static and dynamic resistance effects of the soil.

16.3 WAVE EQUATION METHODOLOGY

In a Smith-type wave equation analysis, the hammer, helmet, and pile are modeled by a series of segments each consisting of a concentrated mass and a weightless spring. The hammer and pile segments are approximately one meter in length. Shorter segments

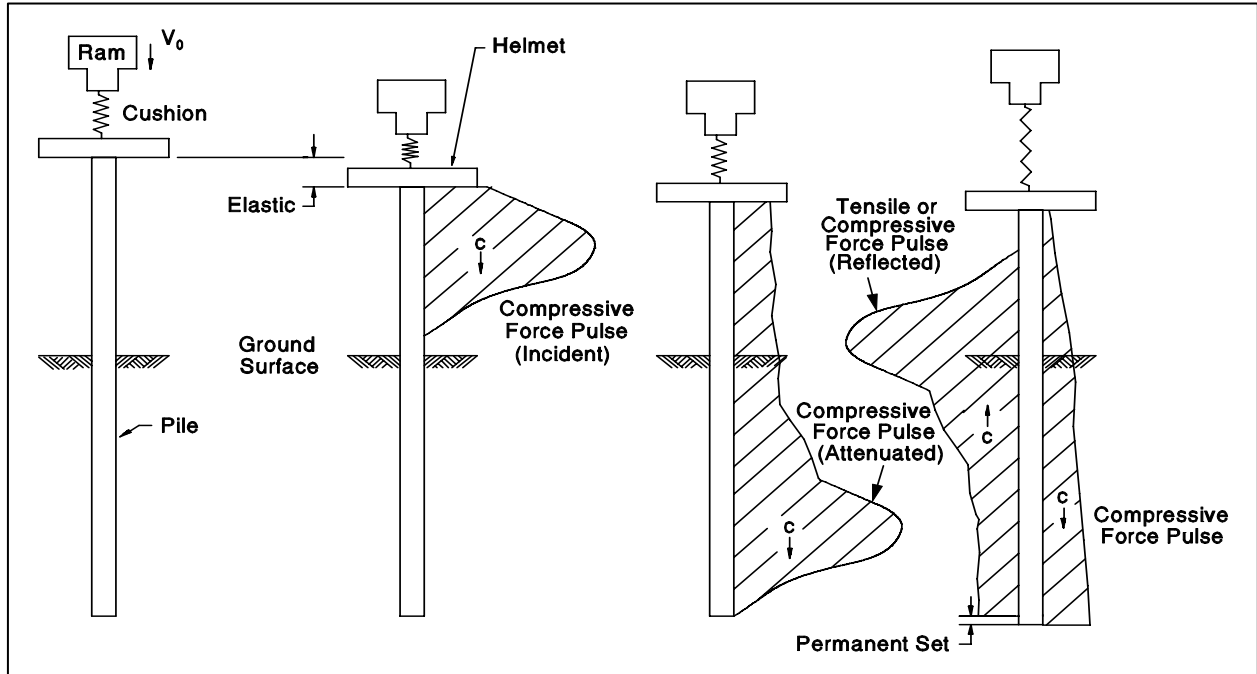


Figure 16.1 Wave Propagation in a Pile (adapted from Cheney and Chassie, 2000)

occasionally improve the accuracy of the numerical solution at the expense of longer computer run times (Rausche et. al., 2004). Spring stiffness and mass values are calculated from the cross sectional area, modulus of elasticity, and specific weight of the corresponding pile section. Hammer and pile cushions are represented by additional springs whose stiffnesses are calculated from area, modulus of elasticity, and thickness of the cushion materials. In addition, coefficients of restitution (COR) are usually specified to model energy losses in cushion materials, and in all segments, which can separate from their neighboring segments by a certain slack distance. The COR is equal to one for a perfectly elastic collision which preserves all energy and is equal to zero for a perfectly plastic condition which loses all deformation energy. The usual condition of partially elastic collisions is modeled with an intermediate COR value.

The soil resistance along the embedded portion of the pile and at the pile toe is represented by both static and dynamic components. Therefore, both a static and a dynamic soil resistance force acts on every embedded pile segment. The static soil resistance forces are modeled by elasto-plastic springs and the dynamic soil resistance by dashpots. The displacement at which the soil changes from elastic to plastic behavior is referred to as the soil "quake". In the Smith damping model, the dynamic soil resistance is proportional to a damping factor times the pile velocity times the assigned static soil resistance. A schematic of the wave equation hammer-pile-soil model is presented in Figure 16.2.

As the analysis commences, a calculated or assumed ultimate capacity, R_{ut} , from user specified values is distributed along the shaft and toe according to user input or program calculation among the elasto-plastic springs. Similarly, user specified damping factors are assigned to shaft and toe to represent the dynamic soil resistance. The analysis then proceeds by calculating a ram velocity based on hammer efficiency and stroke inputs. The ram movement causes displacements of helmet and pile head springs, and therefore compressions (or extensions) and related forces acting at the top and bottom of the segments. Furthermore, the movement of a pile segment causes both static and dynamic soil resistance forces. A summation of all forces acting on a segment, divided by its mass, yields the acceleration of the segment. The product of acceleration and time step summed over time is the segment velocity. The velocity multiplied by the time step yields a change of segment displacement which then results in new spring forces. These spring forces divided by the pile cross sectional area at the corresponding section equal the stress at that point.

Similar calculations are made for each segment until the accelerations, velocities and displacements of all segments have been calculated during the time step. The analysis then repeats for the next time step using the updated motion of the segments from the previous time step. From this process, the accelerations, velocities, displacements, forces, and stresses of each segment are computed over time. Additional time steps are analyzed until the pile toe begins to rebound.

The permanent set in mm (inch) of the pile toe is calculated by subtracting a weighted average of the shaft and toe quakes from the maximum pile toe displacement. The inverse of the permanent set is the penetration resistance (blow count) in blows per meter (blows per foot) that corresponds to the input ultimate capacity. By performing wave equation analyses over a wide range of ultimate capacities, a curve or "bearing graph" can be plotted which relates ultimate capacity to penetration resistance.

A wave equation bearing graph is substantially different from a similar graph generated from a dynamic formula. The wave equation bearing graph is associated with a single driving system, hammer stroke, pile type, soil profile, and a particular pile length. If any one of the above items is changed, the bearing graph will also change. Furthermore, wave equation bearing graphs also include the maxima of calculated compression and tension stresses.

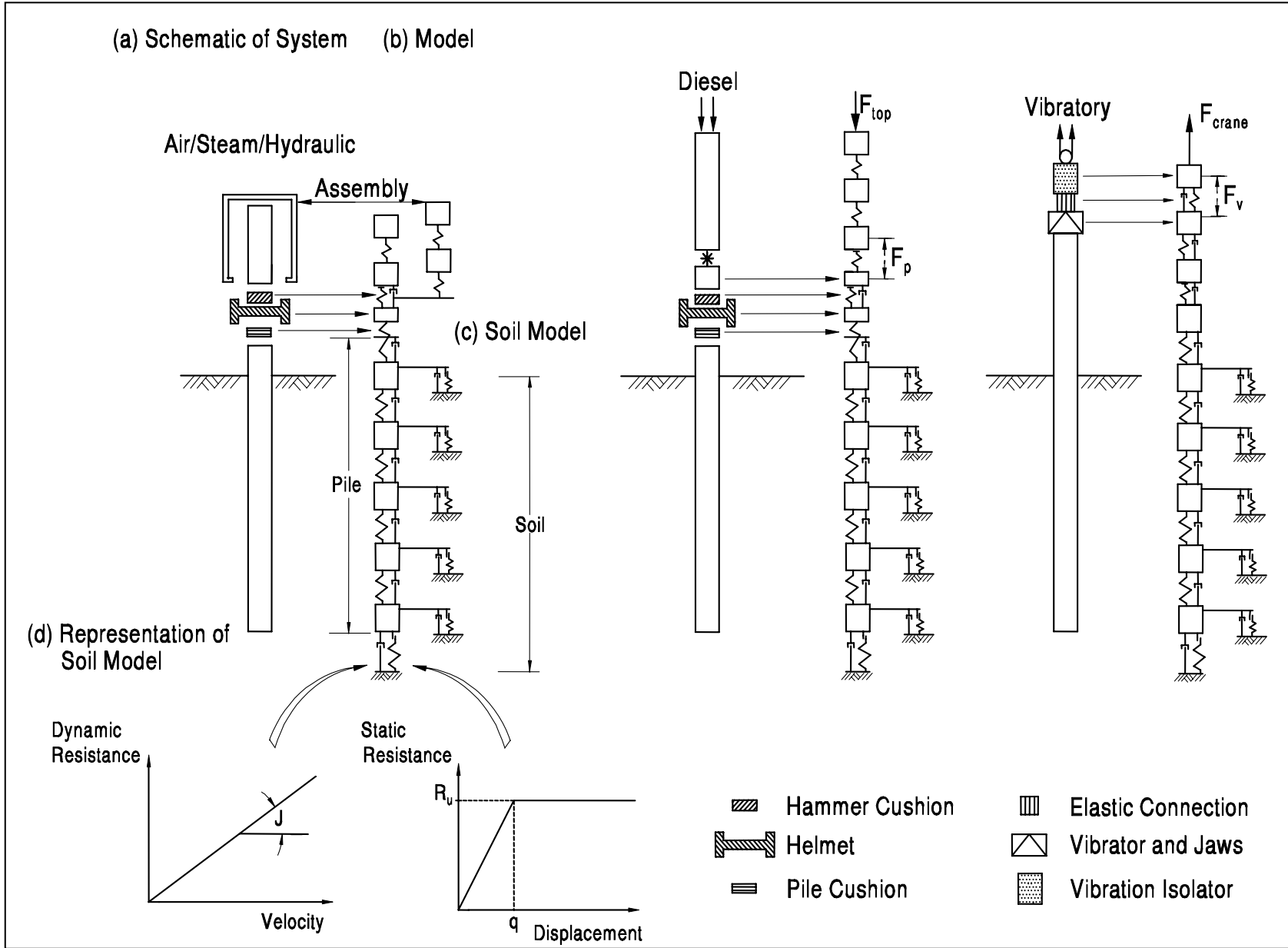


Figure 16.2 Typical Wave Equation Models

In addition to the bearing graph, GRLWEAP provides options for two alternative results, the constant capacity analysis, or "inspector's chart", and the "driveability analysis." The inspector's chart establishes a relationship between variable hammer energy or stroke and penetration resistance for one particular, user specified, ultimate capacity value. Associated stress maxima are also included in the chart, enabling the user to select a practical hammer energy or stroke range both for reasonable penetration resistances and driving stress control. This analysis option is described in greater detail in Section 16.5.2.

The driveability analysis calculates penetration resistances and stresses from user input shaft and toe resistance values at up to 100 user selected pile penetrations. The calculated results can then be plotted together with the capacity values versus pile penetration. The resulting plot would depict those pile penetrations where refusal might be expected or where dangerously high driving stress levels could develop. In addition, a crude estimate of pure driving time (not counting interruptions) is provided by this analysis option. The driveability option is described in greater detail in Section 16.5.5.

16.4 WAVE EQUATION APPLICATIONS

A bearing graph provides the wave equation analyst with two types of information:

1. It establishes a relationship between ultimate capacity and penetration resistance. From the user's input data of the resistance values along shaft and at the toe, the wave equation analysis estimates the permanent set in mm (inch) under one hammer blow. Specifying up to ten ultimate capacity values yields a relationship between ultimate capacity and penetration resistance (or blow count) in blows per 0.25 meters (blows/ft).
2. The analysis also relates driving stresses in the pile to pile penetration resistance.
3. The analysis also relates hammer stroke or hammer energy to pile penetration resistance for a given ultimate capacity.

The user usually develops a bearing graph or an inspector's chart for different pile lengths and uses these graphs in the field, with the observed penetration resistance, to determine when the pile has been driven to the required ultimate capacity.

In the design stage, the foundation engineer should select typical pile types and driving equipment known to be locally available. Then by performing the wave equation analysis with various equipment and pile size combinations, it becomes possible to rationally:

1. Design the pile section for driveability to the required depth and/or capacity.

For example, scour considerations or consolidation of lower soft layers may make it necessary to drive a pile through hard layers whose penetration resistance exceeds the resistance expected at final penetration. A thin walled pipe pile may have been initially chosen during design. However, when this section is checked for driveability, the wave equation analysis may indicate that even the largest hammers will not be able to drive the pipe pile to the required depth, because it is too flexible (its impedance is too low). Therefore, a wall thickness greater than necessary to carry the design load, has to be chosen for driveability considerations. (Switching to an H-pile or predrilling may be other alternatives).

2. Aid in the selection of pile material properties to be specified based on probable driving stresses in reaching penetration and/or capacity requirements.

Suppose that it would be possible to drive a thinner walled pipe pile or lower weight H-pile section to the desired depth, but with excessive driving stresses. More cushioning or a reduced hammer energy would lower the stresses, but would result in a refusal penetration resistance. Choosing a high strength steel grade for the pipe or H-section could solve this problem. For concrete piles, higher concrete strength and/or higher prestress levels may provide acceptable solutions.

3. Support the decision for a new penetration depth, design load, and/or different number of piles.

In the above example, after it has been determined that the pile section or its material strength had to be increased to satisfy pile penetration requirements, it may have become feasible to increase the design load of each pile and to reduce the total number of piles. Obviously, these considerations would require revisiting geotechnical and/or structural considerations.

Once the project has reached the construction stage, additional wave equation analyses should be performed on the actual driving equipment by:

1. Construction engineers - for hammer approval and cushion design.

Once the pile type, material, and pile penetration requirements have been selected by the foundation designer, the hammer size and hammer type must be selected. These parameters may have a decisive influence on driving stresses. For example, a hammer with adjustable stroke or fuel pump setting may have the ability to drive a concrete pile

through a hard layer while allowing for reduced stroke heights and increased tension stress control when penetrating soft soil layers.

Cushions are often chosen to reduce driving stresses. However, softer cushions absorb and dissipate greater amounts of energy thereby increasing the penetration resistance. Since it is both safer (reducing fatigue effects) and more economical to limit the number of blows applied to a pile, softer cushions cannot always be chosen to maintain acceptable driving stresses. Also, experience has shown that the addition of hammer cushion material is relatively ineffective for limiting driving stresses.

Hammer size, energy setting, and cushion materials should always be chosen such that the maximum expected penetration resistance is less than 98 blows/0.25m (120 blows/ft). Exceptions to this upper limit are end-of-driving blow counts of pure end bearing piles where the limit may be raised to 200 blows/0.25m (240 blows/ft). The final penetration resistance should also be greater than 25 blows/0.25m (30 blows/ft) for a reasonably accurate driving criterion. This is required, because (a) the relative error of an inaccurate blow count measurement is greater for lower penetration resistances and (b) the dynamic methods of pile capacity assessment tend to over-predict when driving is very easy. Of course, adjustable hammers may be accepted based on their lower energy settings. Exceptions should also be made when the accuracy of the blow count measurement is irrelevant. Such situations arise when the pile has to be driven to depth at expected capacities above the required minimum or because a large component of the pile bearing capacity is derived from soil setup.

2. Contractors - to select an economical driving system to minimize installation cost.

While the construction engineer is interested in the safest installation method, contractors would like to minimize driving time for cost considerations. Light weight, simple, and rugged hammers which have a high blow rate are obviously preferred. The wave equation analysis can be used to roughly estimate the anticipated number of hammer blows and the time of driving. This information is particularly useful for a relative evaluation of the economy of driving systems.

Additional considerations might include the cost of pile cushions, which are usually discarded after a pile has been installed. Thus, thick plywood pile cushions may produce a considerable cost over time.

Near refusal penetration resistances are particularly time-consuming and since it is known that stiffer piles drive faster with lower risk of damage, the contractor may even

choose to upgrade the wall thickness of a pipe pile or the section of an H-pile for improved overall economy.

16.5 WAVE EQUATION EXAMPLES

This section presents several examples that illustrate the application of the wave equation analysis for the solution of design and construction problems. The factor of safety applied to the design load in the following examples is 2. This assumes that a static pile load test was subsequently performed on each project to confirm the wave equation result. As noted in Chapter 14, a factor of safety of 2.5 to 2.75 should be applied to the design load in wave equation analyses if static load testing or dynamic testing is not included in the project. The ultimate capacity in a wave equation analysis should consist of the factor of safety, times the design load, plus the sum of the ultimate resistances from any overlying layers unsuitable for or not present during long term support.

Note: The figures illustrating the following examples were generated from the proprietary program GRLWEAP. These figures are not intended as endorsements of Pile Dynamics, Inc. (PDI) or its products.

16.5.1 Example 1 - General Bearing Graph

A generally primary application of a wave equation analysis is to develop a bearing graph relating the ultimate pile capacity to the pile penetration resistance. For a desired ultimate pile capacity, the required penetration resistance can be found easily from this graph. Consider the soil profile in Figure 16.3. In this example, a 20 m (66 ft) long, 356 mm (14 inch) by 8 mm (0.315 inch) wall, closed end pipe pile with a steel yield strength of 241 MPa (35 ksi) is to be driven into a deep deposit of medium sands.

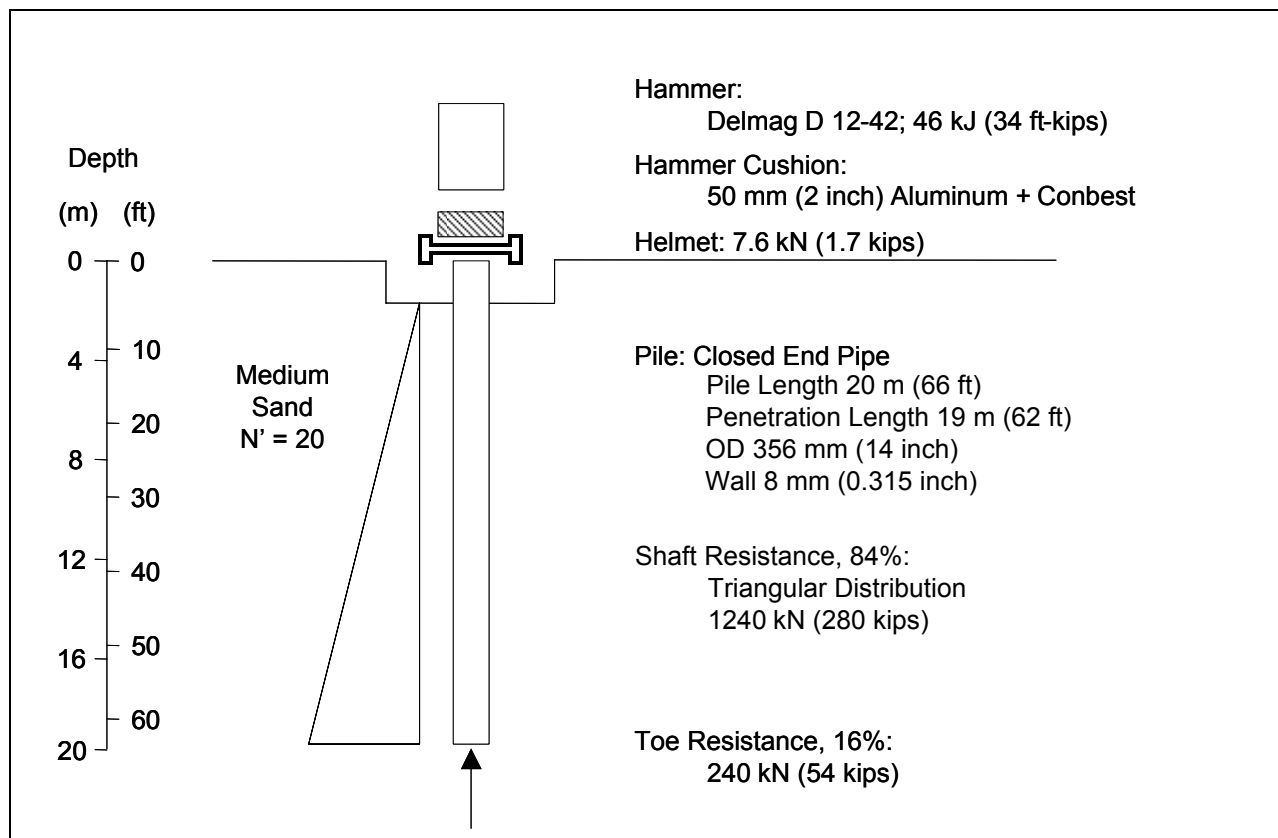


Figure 16.3 Example 1 Problem Profile

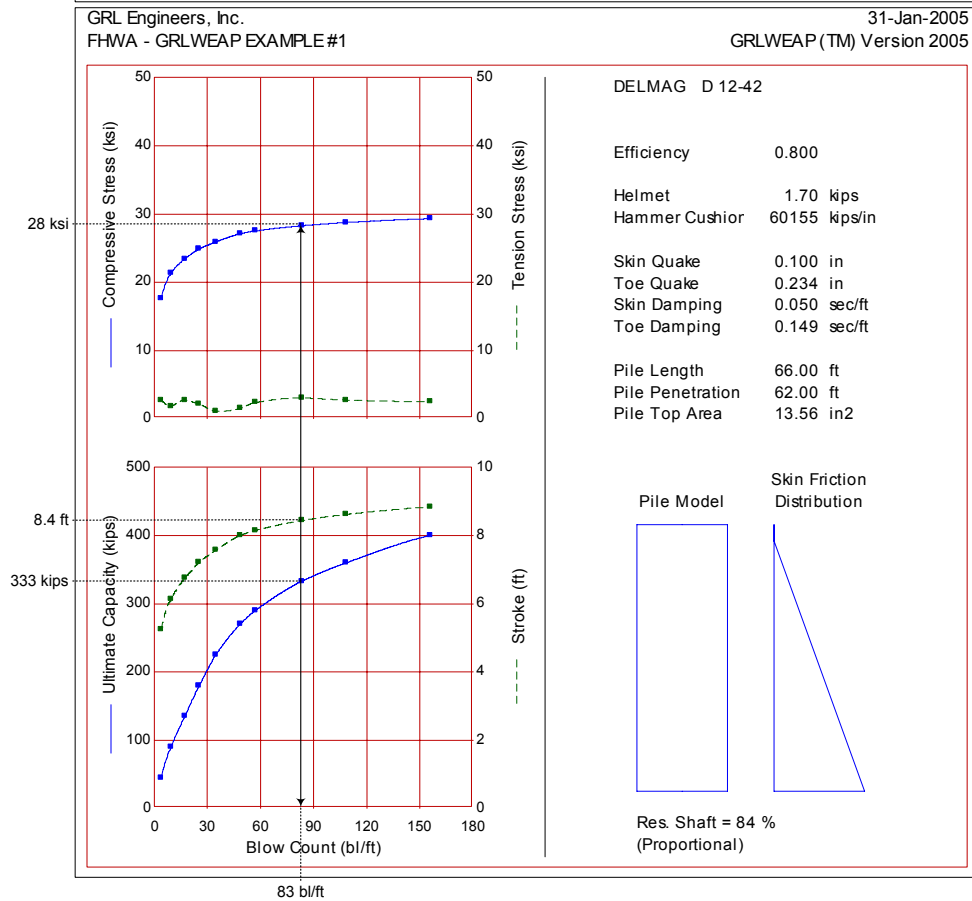
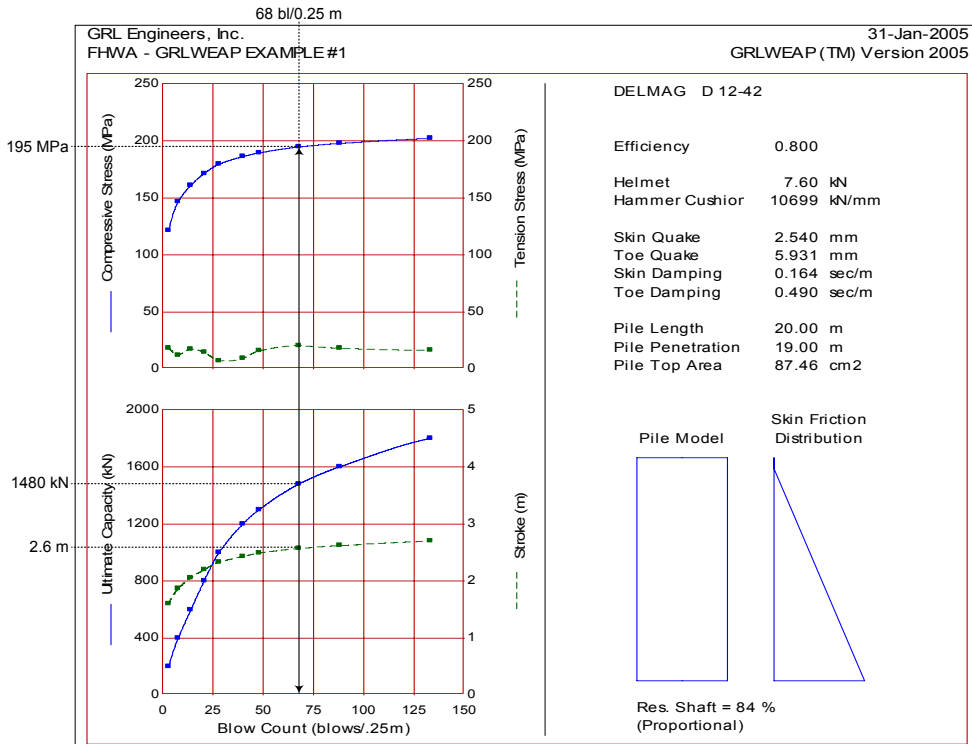
As a first step in any wave equation analysis, a static soil analysis must be performed. For uniform piles, GRLWEAP offers the ST (Soil Type) option which calculates the necessary input based on simple soil type classifications for bearing graphs (see also Section 16.7). The ST option is not intended to replace a traditional static analysis but to allow simple bearing graph analyses to be performed when more accurate soil information and static analysis method results are not available. In the present example, a static analysis was performed by means of the DRIVEN program, which indicates that an ultimate pile capacity of 1480 kN (333 kips) can be obtained for the proposed pile type at a penetration depth of 19 m (62 ft). This calculated ultimate pile capacity is the expected long term capacity and because the soil type is sand it can be expected that the resistance during driving will be essentially equal to the long term capacity. Depending on the anticipated effort to be expended on testing (static load test, dynamic testing or only blow count observation with wave equation analysis), the ultimate capacity must be divided by the appropriate factor of safety (see Section 9.6) to yield the maximum design load that the pile can support.

The static analysis also indicates that the ultimate capacity is distributed as 84% shaft resistance and 16% toe bearing resistance with a triangular shaft resistance distribution along the pile shaft.

The contractor selected a Delmag D 12-42 single acting diesel hammer for driving the pipe piles. The contractor's hammer submittal indicates that the hammer cushion will consist of 25 mm (1 inch) of aluminum and 25 mm (1 inch) of Conbest with a cross sectional area of 1464 cm² (227 inch²). A helmet weight of 7.6 kN (1.7 kips) is reported.

Based on this information, a wave equation analysis can be performed. The ultimate pile capacity of 1480 kN (333 kips) is input along with selected additional ultimate capacities. The wave equation analysis calculates the net permanent set of the pile toe for each input ultimate capacity. The inverse of the set is the penetration resistance for the given ultimate capacity expressed in blows per 0.25 meters (blows/ft). By plotting calculated penetration resistances versus the corresponding input ultimate capacities, a bearing graph is developed. The results of such a calculation are shown in Figure 16.4 for this example.

In the bottom half of each bearing graph, the ultimate pile capacity versus penetration resistance in blows/0.25 m (blows/ft) is represented by the solid line. This graph shows that for an ultimate pile capacity of 1480 kN (333 kips) a penetration resistance of 68 blows/0.25m (83 blows/ft) is required. (This requirement is equivalent to approximately 35 mm (1.4 inch) for 10 blows). This is a reasonable blow count requirement being neither excessively high, which would demand extreme driving efforts, nor very low and, therefore, inaccurate (see recommended limits on driving resistance in Chapter 11). Also in the bottom half of each bearing graph, the corresponding hammer stroke versus penetration resistance is represented by the dashed line. This curve is important for variable stroke hammers as a check on hammer performance when the driving criterion is applied. In this case, the penetration resistance of 68 blows/0.25 m (83 blows/ft) for the 1480 kN (333 kips) capacity is based upon a hammer stroke of 2.6 m (8.4 ft). Should field observations indicate significantly (say more than 10% difference) higher or lower strokes, then a lower or higher penetration resistance would be necessary for the same capacity, because the hammer energy would be higher or lower. Hammer stroke information is therefore essential for field evaluation and control of the pile installation process. An inspector's chart analysis (see example 2) provides this information determining blow count as a function of hammer stroke. For significantly differing hammer field performance, new wave equation analyses would be necessary with a modified maximum combustion pressure or a fixed input stroke.



Figures 16.4 Example 1 Typical Bearing Graph – SI and US Units

In the upper half of each graph of Figure 16.4, maximum compression and tension driving stresses are also plotted as a function of penetration resistance. Of primary interest for a steel pile is the compression driving stress, which is represented by the solid line. This curve shows that, at the penetration resistance of 68 blows/0.25 m (83 blows/ft) associated with the required ultimate pile capacity, the maximum compression stress calculated in the pile is 195 MPa (28 ksi), which is less than 90% of the yield strength of 241 (35 ksi) or 217 MPa (31.5 ksi), and therefore acceptable according to AASHTO specifications (Chapter 10). Note, however, that any non-uniform stress components (such as from bending which may be caused by poor hammer-pile alignment or pile-toe contact with sloping rock) are not included in the wave equation results and would be additional. Yet in any case, the 90% yield limit applies to the stress averaged over the pile cross section.

Though the analysis was conducted for an estimated penetration of 19 m (62 ft), in the field the required penetration resistance may be reached at a lesser or greater depth. The static analysis only serves as an initial estimate of the required penetration depth. The actual driving behavior and construction monitoring will confirm whether or not the static calculation was adequate. If the actual driving behavior is significantly different from the analyzed situation (say the required blow count is already reached at 15 m (50 ft) penetration), an additional analysis should be performed to better match field observations. In general, the capacity versus driving resistance relationship is relatively insensitive to changes in penetration and, therefore, to the distribution of the resistance along the pile, unless there is a significant change in the soil profile. Of course, if either hammer and driving system performance or unexpected soil properties appear to cause the difference, then it would be prudent to check the equipment performance and soil resistance by monitoring with a Pile Driving Analyzer. Higher penetration resistances from penetrating embankment fills or scour susceptible material, *etc.*, should also be considered in this assessment.

16.5.2 Example 2 - Constant Capacity / Variable Stroke Option

The hammer-pile-soil information used in Example 1 will be reused for a constant capacity (or inspector's chart) analysis in Example 2. In this example, the penetration resistance required for the 1480 kN (333 kip) ultimate capacity is evaluated at hammer strokes other than the predicted 2.6 m (8.4 ft) value. The resulting graph would be helpful for field personnel in determining when pile driving can be terminated if the field observed hammer stroke varies from that predicted by the wave equation.

In the constant capacity/variable stroke option, a single ultimate capacity (usually the required ultimate capacity) is chosen and the hammer stroke is varied from a user selected lowest value to the manufacturer's maximum stroke. The necessary penetration resistance at each hammer stroke is then calculated for the input ultimate capacity. Figure 16.5 shows the resulting inspector's charts in SI and US units. The lower half of either graph in Figure 16.5 presents these results for an ultimate pile capacity of 1480 kN (333 kips). Where the point of intersection of the observed stroke and penetration resistance plots below the curve, the ultimate pile capacity has not been obtained. Any combination of stroke and penetration resistance plotting above the curve indicates that the required ultimate pile capacity has been reached. For example, any stroke greater than 2.5 m (8.2 ft) at a penetration resistance of 74 blows/0.25 m (90 blows/ft) is acceptable. The upper half of either graph shows the stress maxima associated with a particular driving resistance. Hence, the inspector's chart analysis aids the inspection personnel in field control.

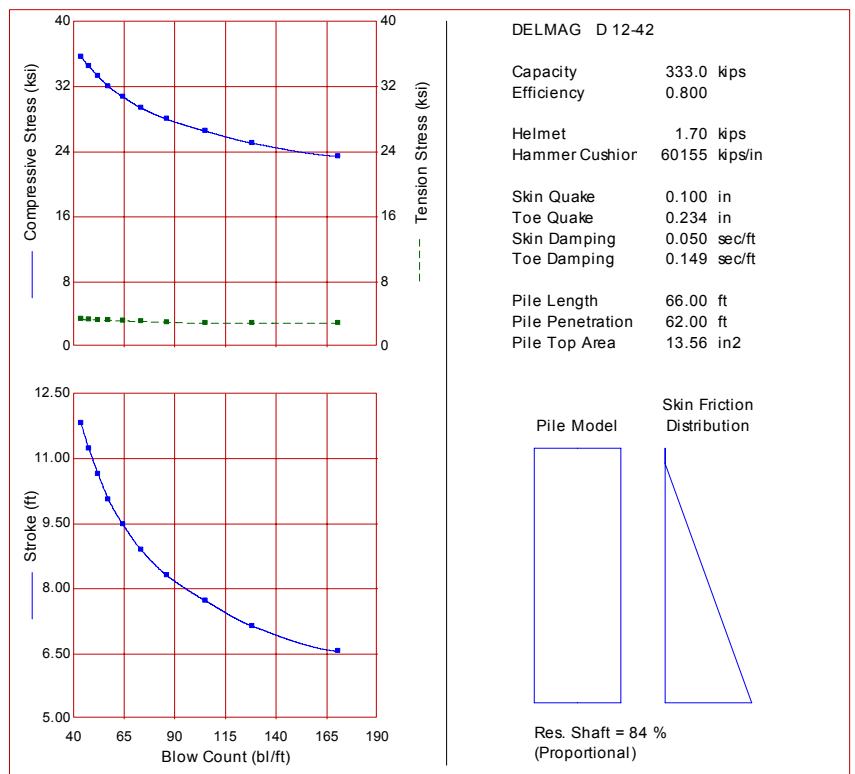
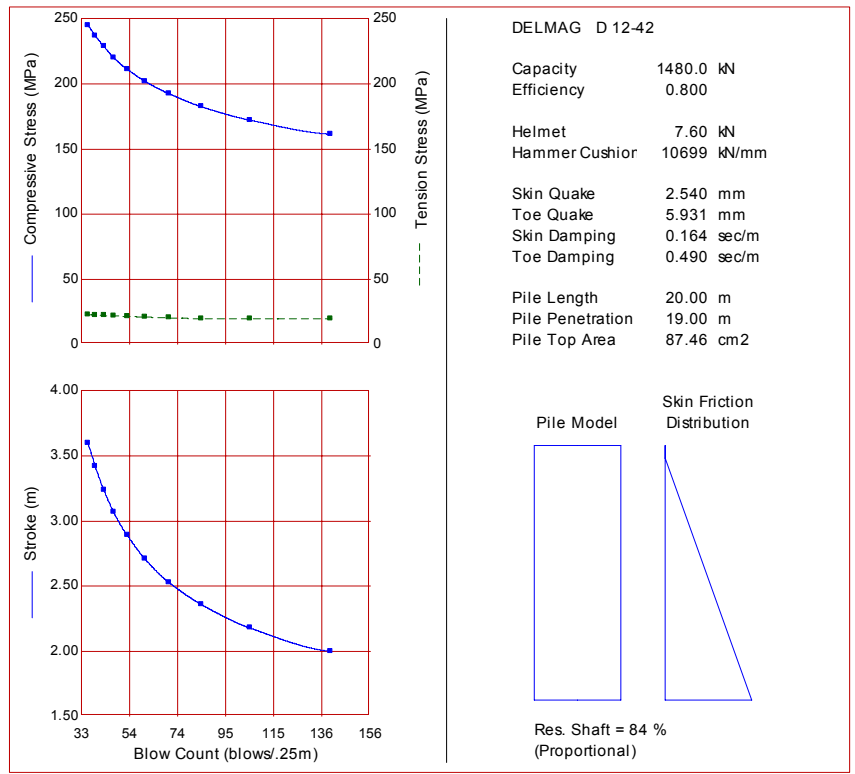


Figure 16.5 Example 2 Constant Capacity Analysis – SI and US Units

16.5.3 Example 3 - Tension and Compression Stress Control

Example 3 illustrates the use of the wave equation for the control of tension stresses in concrete piles. The Peach Freeway design problem presented in Chapter 12 will be used for this example problem. For the North Abutment, static calculations performed using DRIVEN indicate that a 12 m (40 ft), 356 mm (14 inch) square prestressed concrete pile driven through 4 m (13 ft) of loose silty fine sand, 7 m (23 ft) of medium dense silty fine sand, and 0.5 m (1.6 ft) into a dense sand and gravel deposit could develop an ultimate pile capacity of 1807 kN (406 kips), which is slightly more than the 1780 kN (400 kips) required. The static analysis also indicates that the ultimate capacity is distributed as 48% shaft resistance and 52% toe resistance with a variable shaft resistance distribution along the pile shaft. The soil profile for this problem is presented in Figure 16.6.

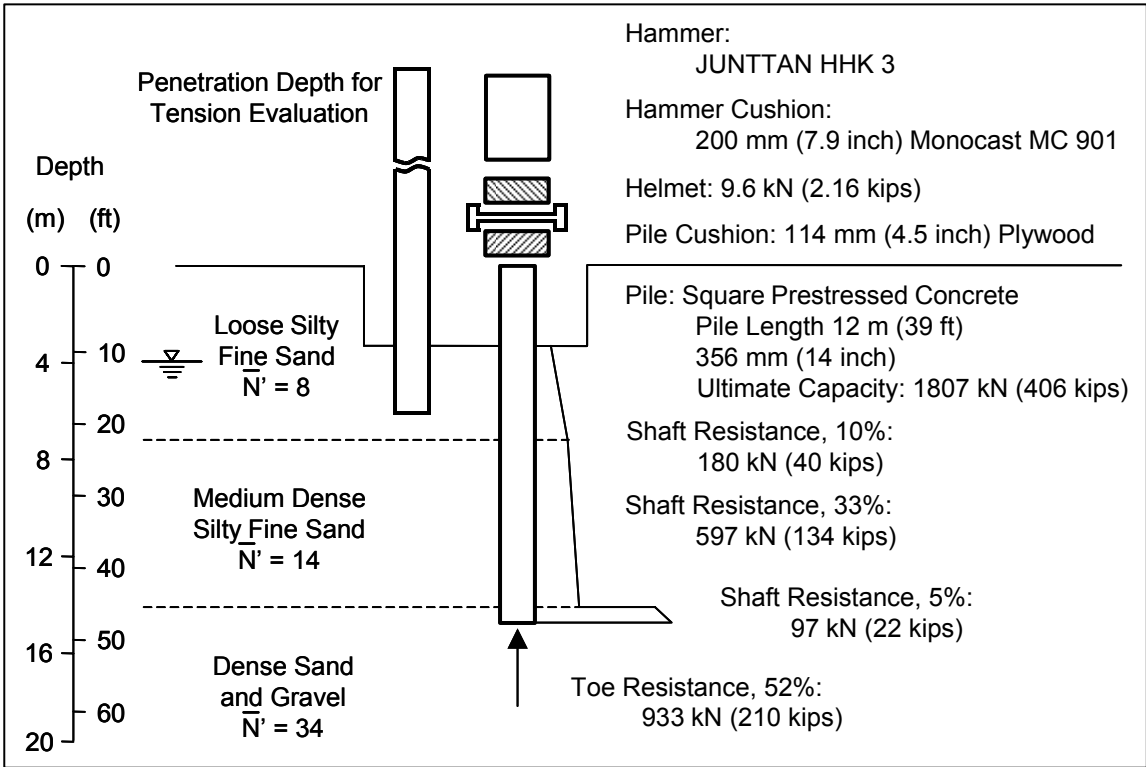


Figure 16.6 Example 3 Problem Profile

The contractor selected a Junttan HHK 3 hydraulic hammer for driving the prestressed concrete piles. The contractor’s hammer submittal indicates that the hammer cushion will consist of 200 mm (7.9 inch) of Monocast MC 901 with a cross sectional area of 1590 cm² (247 inch²). A helmet weight of 9.6 kN (2.16 kips) is owned by the contractor and will, therefore, be utilized for the driving system. The pile will have a concrete compression strength of 37.9 MPa (5.5 ksi) and an effective prestress after losses of 4.8 MPa (0.70 ksi).

Using the AASHTO driving stress recommendations from Chapter 10, this results in a maximum recommended compression stress of 28.1 MPa (4.1 ksi) and a maximum tension driving stress of 6.3 MPa (0.92 ksi).

One of the main concerns with concrete piles is the possibility of developing high tension stresses during easy driving conditions when the soil provides little or no toe resistance. Therefore, the wave equation should be used to evaluate the contractor's proposed driving system during both low and high resistance conditions.

First, evaluation of tension stresses during easy driving is presented. The weight of the pile and driving system is anticipated to be on the order of 100 kN (22 kips). Hence, the pile penetration depth for the wave equation analysis should be selected below the depth to which the pile will likely penetrate or "run" under the weight of the pile and driving system, or approximately 3.5 m (10 ft). At this depth, the pile is still within the loose silty fine sand stratum and tension driving stresses are anticipated to be near their peak. Although not strictly correct, for the first low resistance analysis of 100 kN (22.5 kips) it is accurate enough to assume the same shaft resistance percentage (48%) as indicated in Figure 16.6. For a complete bearing graph not only the 100 kN (22.5 kips) capacity but also other higher values are input into the wave equation analysis and analyzed.

The contractor submitted a plywood pile cushion design comprised of six 19 mm (3/4 inch) sheets with a total thickness of 114 mm (4.5 inch). Pile cushion stiffness significantly affects tension driving stresses; therefore, it is necessary to determine whether or not the contractor's proposed pile cushion thickness is sufficient to maintain tension stress levels below specified limits. In the first trial, the 114 mm (4.5 inches) pile cushion is assumed to possess the properties of new plywood. Thus, the original pile cushion thickness of 114 mm (4.5 inches) and the new cushion elastic modulus of 207 MPa (30 ksi) are input.

Based on this information, the wave equation analysis indicates for the 100 kN (22.5 kips) capacity a maximum tension stress of 8.7 MPa (1.26 ksi). The magnitude of the calculated tension stress therefore exceeds the allowable driving stress limitation of 6.3 MPa (0.92 ksi) and another analysis should be performed with an increased pile cushion thickness.

■ FHWA - GRLWEAP EXAMPLE #3, 114mm @ 3.5m
 * FHWA - GRLWEAP EXAMPLE #3, 209mm @ 3.5m

GRLWEAP (TM) Version 2005

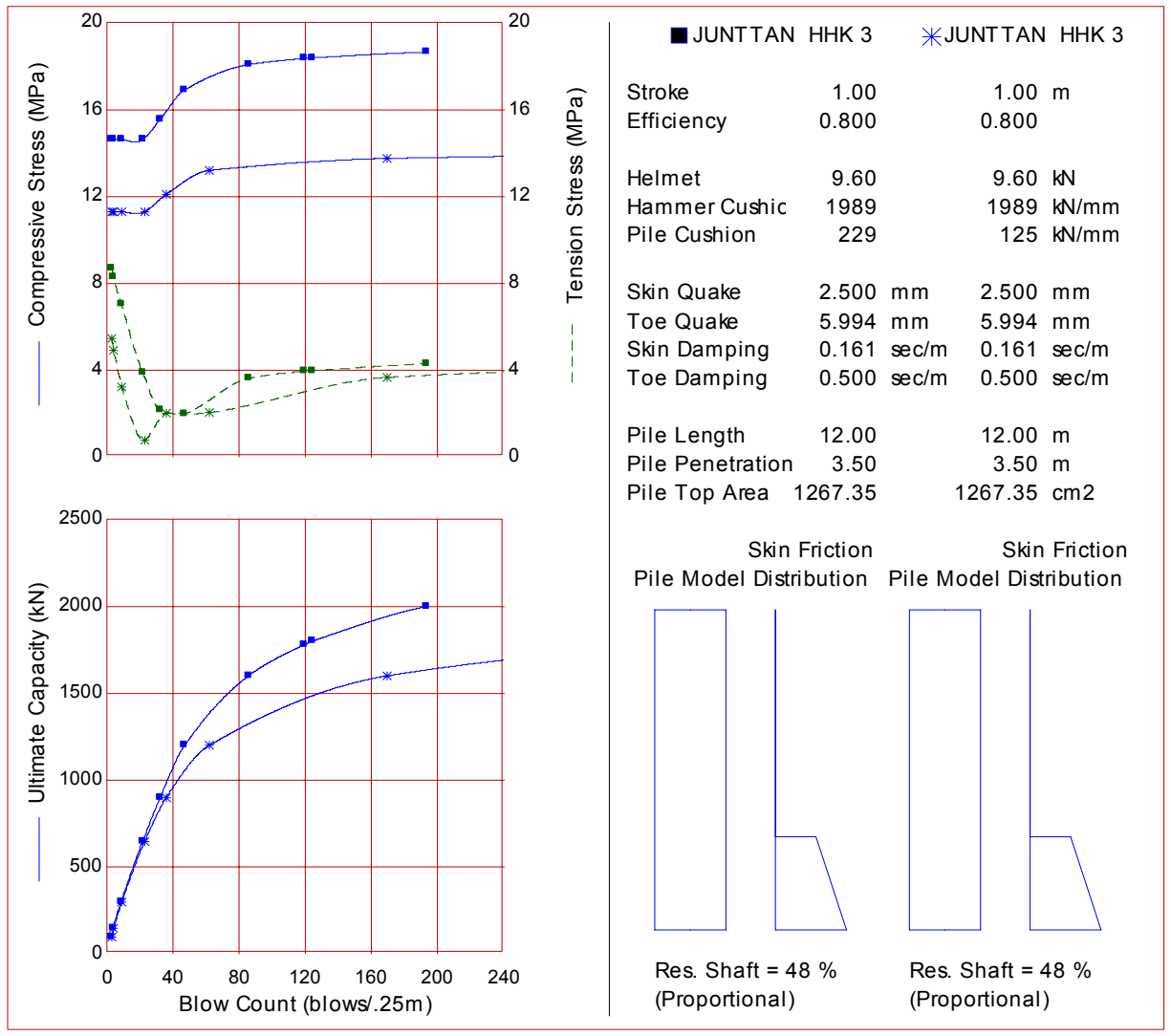


Figure 16.7 Example 3 Bearing Graph for Easy Driving Condition – Two Pile Cushion Thicknesses

In the second trial run, eleven sheets of 19 mm (3/4 inch) thick plywood with a total thickness of 209 mm (8.2 inches) are input for the pile cushion thickness. Again the assumption is made for early driving that new cushion properties, in particular an elastic modulus of 207 MPa (30 ksi), apply. The result of the second wave equation analysis produces a reduced maximum tension stress of 5.5 MPa (0.8 ksi), which is less than the specification limits. A comparison of the driving stresses from the two analyses with different pile cushion thicknesses can be made in the standard bearing graphs presented in Figure 16.7.

Next, the driving stresses and penetration resistance at final driving for the required 1780 kN (400 kips) ultimate pile capacity must be checked. In this analysis, it is assumed that the additional hammer blows required to achieve the final pile penetration depth have resulted in additional compression of the pile cushion material. Based on Rausche et al., 2004, the documentation of GRLWEAP program recommends that end-of-driving situations of concrete piles be analyzed with an increased modulus of elasticity of the pile cushion of 517 MPa (75 ksi) and the nominal (i.e., uncompressed) cushion thickness.

The analysis result indicates a final penetration resistance of 96 blows/0.25 m (117 blows/ft) for a 1780 kN (400 kip) ultimate capacity which should result in a reasonably efficient driving time. Figure 16.8 also shows that the maximum compression stresses of 18 MPa (2.6 ksi) at final driving are within the allowable limit of 27.0 MPa (3.9 ksi) while tension stresses will only be less than allowable after the driving resistance has increased above 15 blows/0.25 m (18 blows/ft). However, it is not expected that the low driving resistances will materialize until after the cushion has significantly compressed. Therefore, the 209 mm (8.2 inch) pile cushion is recommended for control of both tension stresses during easy driving and compression stresses at final driving. Note that this hammer model can also be operated with reduced energy levels. Indeed, it would be more economical to reduce the energy in early driving rather than using heavy pile cushioning. The final driving would also be at lower driving resistances and therefore more economical if a thinner pile cushion were employed.

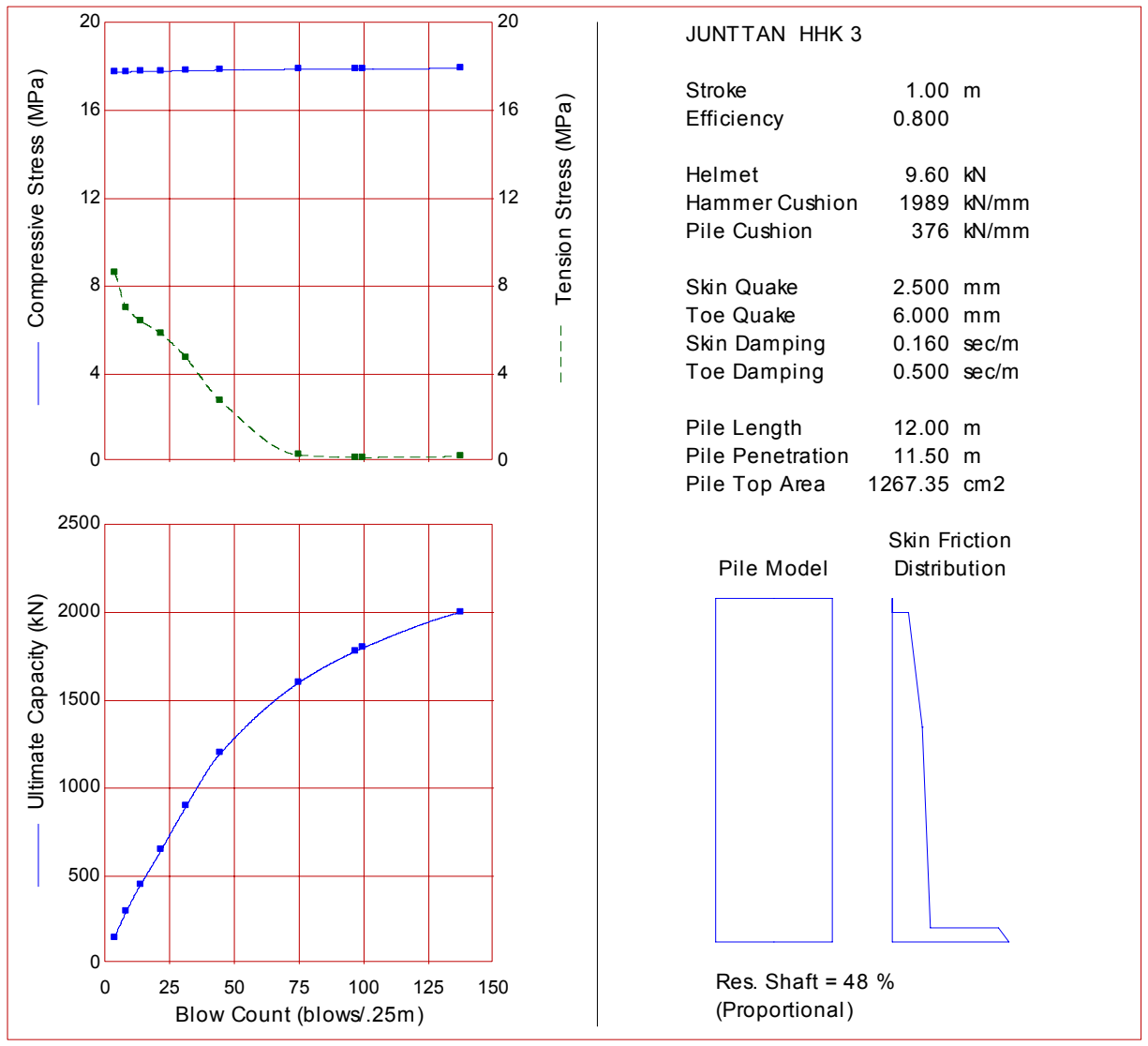


Figure 16.8 Example 3 Bearing Graph for End of Driving Condition

16.5.4 Example 4 - Use of Soil Setup

Consider the soil profile in Figure 16.9. In this example, a 305 mm (12 inch) square, prestressed concrete pile is to be driven into a thick deposit of stiff clay. The stiff clay has an average shear strength of 70 kPa (1.47 ksf). Based on field vane shear tests, it is estimated that the remolded shear strength at the time of driving will be 52.5 kPa (1.10 ksf), resulting in an expected soil setup factor of 1.33. A static analysis performed using the DRIVEN program indicates that an ultimate pile capacity of 1340 kN (300 kips) after setup can be obtained for the proposed pile type at a penetration depth of 15 m (49.2 ft). The

static analysis also indicates that the ultimate capacity is distributed as 92% shaft resistance and 8% toe bearing resistance, with the shaft resistance being distributed uniformly along the pile shaft.

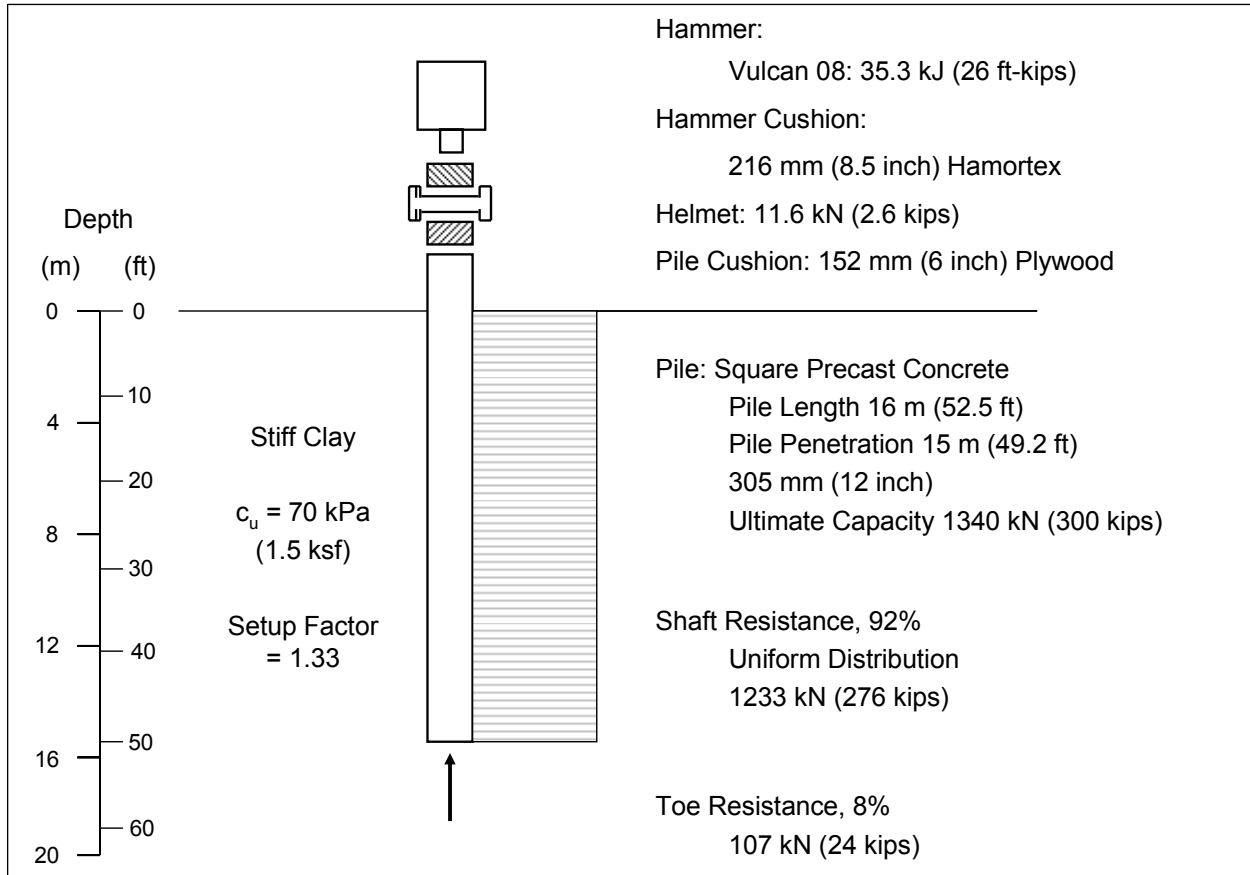
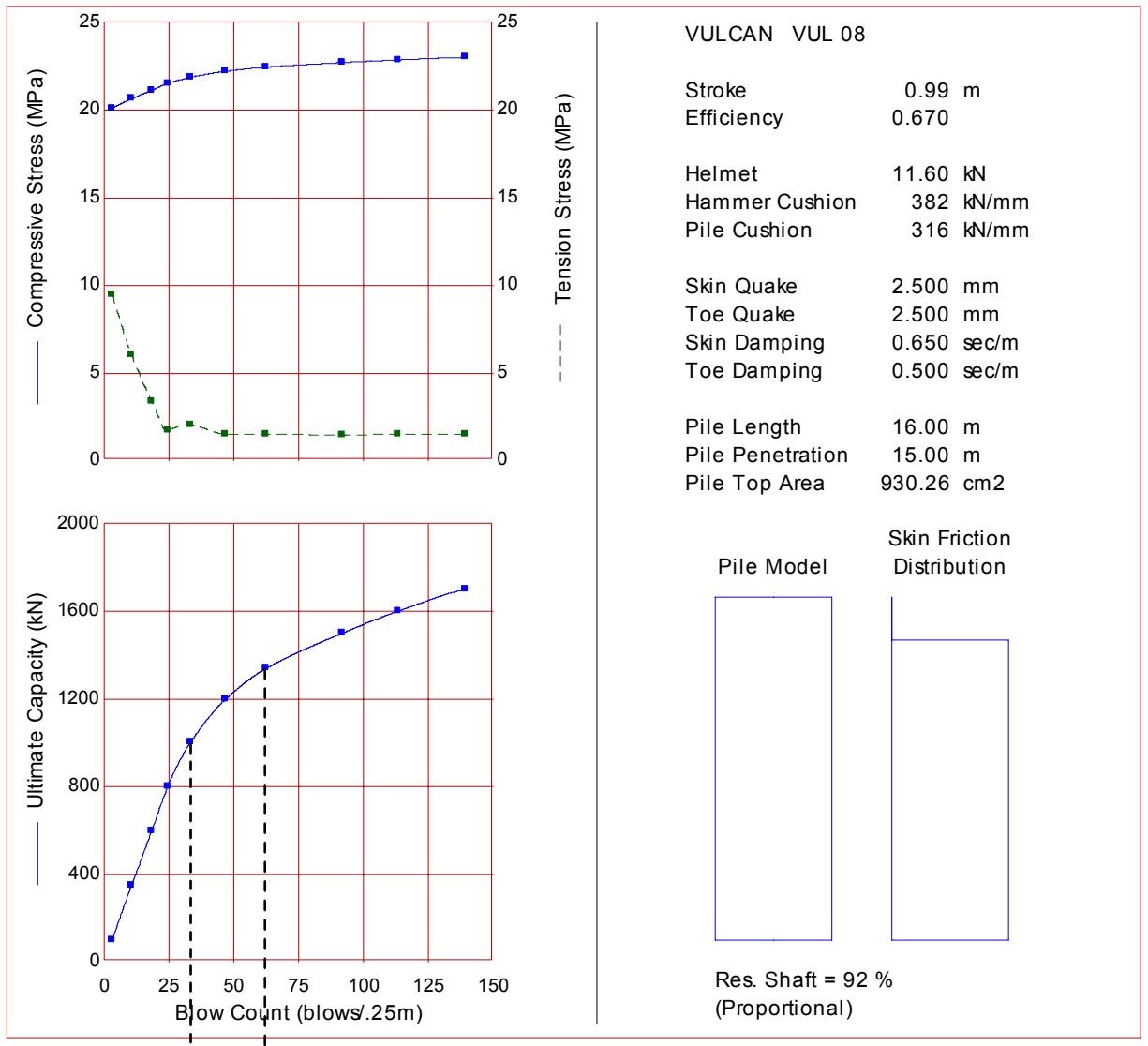


Figure 16.9 Example 4 Problem Profile

The contractor selected a Vulcan 08 single acting air hammer for driving the prestressed concrete piles. The contractor's hammer submittal indicates that the hammer cushion will consist of 216 mm (8.5 inch) of Hamortex with a cross sectional area of 958 cm^2 (148 inch^2). The pile cushion will consist of eight 19 mm (3/4 inch) sheets of plywood with a total thickness of 152 mm (6.0 inch). It is anticipated that the pile cushion will compress and stiffen during driving similar to that described in Example 3. The contractor's submittal indicates that the helmet weighs 11.6 kN (2.6 kips). For an easy driving analysis, the assumption of a new pile cushion with the elastic modulus of 207 MPa (30 ksi) would apply. For the late driving scenario, a compressed cushion modulus of 517 MPa (75 ksi) should be considered.

Based upon the reported soil type and setup behavior, a 33% increase in pile capacity with time is expected at this site. Therefore, piles could be driven to a reduced capacity, or static resistance to driving (SRD), of 1005 kN (225 kips) instead of the ultimate capacity of 1340 kN (300 kips) with the remaining 335 kN (75 kips) of capacity expected from soil setup. As noted in Section 16.5 of this chapter, a static load test will be performed on the project to confirm the expected pile capacity.

The wave equation results presented in Figure 16.10 indicate a final penetration resistance of 34 blows/0.25m (41 blows/ft) could be used as the driving criteria for a 1005 kN (225 kip) capacity. This is significantly less than the 62 blows/0.25 m (76 blows/ft) required for an ultimate pile capacity of 1340 kN (300 kips). Hence, significant pile length and driving effort may be saved by driving the piles to the lower 1005 kN (225 kips) capacity instead of the required 1340 kN (300 kip) ultimate pile capacity, subject to confirmation of the anticipated soil setup. This would require a restrike test or a static load test some time after pile installation; the waiting time period is soil type dependent as discussed in Section 17.6.



← 62 blows/0.25 m with anticipated soil
← 34 blows/0.25 m without soil setup

Figure 16.10 Using a Bearing Graph with Soil Setup

16.5.5 Example 5 - Driveability Studies

The effect of scour and seismic design considerations on pile foundations often result in increased pile penetration requirements. Therefore, the ability of a given pile to be driven to the depth required by static analysis should be evaluated in the design stage by wave equation driveability study, as presented in this example.

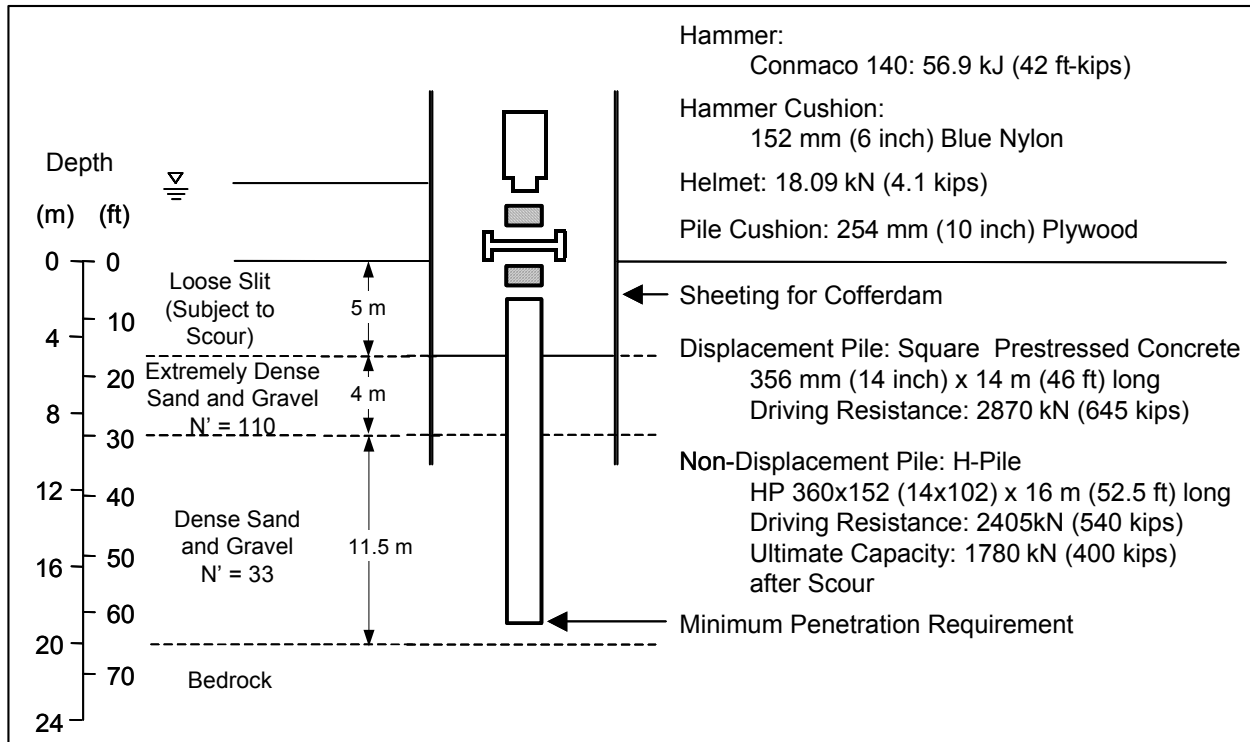


Figure 16.11 Example 5 Problem Profile

Figure 16.11 illustrates the installation conditions at interior Pier 2 of the Peach Freeway design problem from Chapter 12. A cofferdam will be required for pier construction. The interior of the cofferdam will be excavated 5 m (16.5 ft) below original grade prior to pile installation. The extremely dense sand and gravel layer was estimated to have a soil friction angle, ϕ , of 43° . This ϕ angle was used in the static calculations of toe resistance. However, the ϕ angle was limited to 36° for the hard angular gravel when calculating shaft resistance, as discussed in Section 9.5.

During construction, the silt soils will be removed from within the cofferdam area. However, the silt soils outside the cofferdam will still be present at the time of construction. Therefore, the soil resistance to pile driving should be calculated with consideration for the overburden pressure from these materials. However, hydraulic experts predict that the 5 m (16.5 ft) of loose silt may erode completely due to channel degradation scour. Thus, for long term pile capacity, static calculations should ignore the effective weight of the silt layer. As a result, a higher soil resistance than required to meet the static load requirements must be anticipated during pile installation.

Initial static analysis indicates that a 356 mm (14 inch) square prestressed concrete pile would develop the ultimate capacity of 1780 kN (400 kips), primarily through toe bearing, at a depth of 3 m (10 ft) below the cofferdam excavation level. However, when considering

the reduction in the effective overburden pressure from the removal of the silt layer, the pile would have an ultimate capacity of only 924 kN (208 kips) at the 3 m (10 ft) depth. Additional static capacity calculations were performed at increased pile penetration depths for the pre-scour profile. These analyses show that when punching through the upper, very dense sand layer the capacity would at first be lower in the dense sand and gravel but would again reach a 1780 kN (400 kip) ultimate capacity at a depth of almost 10 m (30.5 ft) below cofferdam excavation level.

After scour, the ultimate pile capacity would reduce to only 1320 kN (300 kips) at the 10 m depth, requiring an additional 4m (13 ft) of penetration to obtain the desired 1780 kN (400 kip) ultimate pile capacity after scour. The pre-scour analysis at the 14 m (46 ft) depth shows that the pile will have a capacity of 2400 kN (517 kips) and this is the soil resistance that must be overcome during driving.

Next, the static pile capacity calculations, including the silt overburden, versus depth were input into a wave equation driveability study. The soil profile primarily indicates sandy materials and it is, therefore, not necessary to consider setup or relaxation effects for the driveability analysis. Thus, gain/loss factors for both shaft and toe were set to 1.0. Since the study is conducted in the design stage, the use of a locally available single acting air hammer driving system was assumed. The driveability analysis result (Figure 16.12) indicated that the 356 mm (14 inch) concrete pile would encounter a maximum penetration resistance of 74 blows/0.25 m (90 blows/ft) in the upper extremely dense sand and gravel deposit and a final penetration resistance of 66 blows/0.25 m (80 blows/ft) at 14 m (46 ft) depth.

The calculated driving resistance values would support the conclusion that the 356 mm (14 inch) concrete pile could be driven to the required penetration depth of 14 m (46 ft). This might be an erroneous conclusion. Although the static analysis would likely provide an adequate assessment of soil resistance for the first pile driven, an increase in the ϕ angle from group densification could significantly affect the resistance to driving of additional displacement piles, particularly within the added confinement of the cofferdam. Also, dense deposits tend to develop negative pore pressures during shear, resulting in temporary increases in soil resistance. If it is assumed that these factors cause a 33% increase in both shaft and toe resistances during the driving of subsequent piles, a second driveability analysis would indicate that the later piles practically refuse at a penetration depth of 3.5 m (11.5 ft) with a penetration resistance of 162 blows/0.25 m (198 bl/ft). A corresponding soil resistance of 2870 kN (645 kips) must also be overcome to reach the 14 m (46 ft) depth. The computed maximum compression driving stresses approach 31 MPa (4.5 ksi), discouraging use of a larger hammer. If displacement piles were used, predrilling or jetting

would likely be required to advance the piles through the upper stratum. A low displacement pile, i.e., an H-pile or open end pipe pile, which would cause a lower or no densification, presents a more attractive foundation solution.

The wave equation driveability results for the first and later driven 356 mm (14 inch) concrete piles appear in Figures 16.12 and 16.13, respectively. Wave equation driveability results for the low displacement HP 360x152 (14x102) H-pile are displayed in Figure 16.14. Note that the penetration depths in these figures correspond to the depth below cofferdam excavation level. The maximum penetration resistance calculated for the H-pile to penetrate the extremely dense sand and gravel stratum is only 26 blows/0.25m (32 blows/ft). Corresponding compression driving stresses do not exceed 216 MPa (32 ksi) and are, therefore, within the recommended limits for H-piles given in Chapter 10. Based on the driveability study results, the low displacement H-pile would be a preferable foundation option. The results also indicate that the H-pile could be driven to bedrock and, therefore, increase design loads and reduce the number of piles, providing for a more cost effective design.

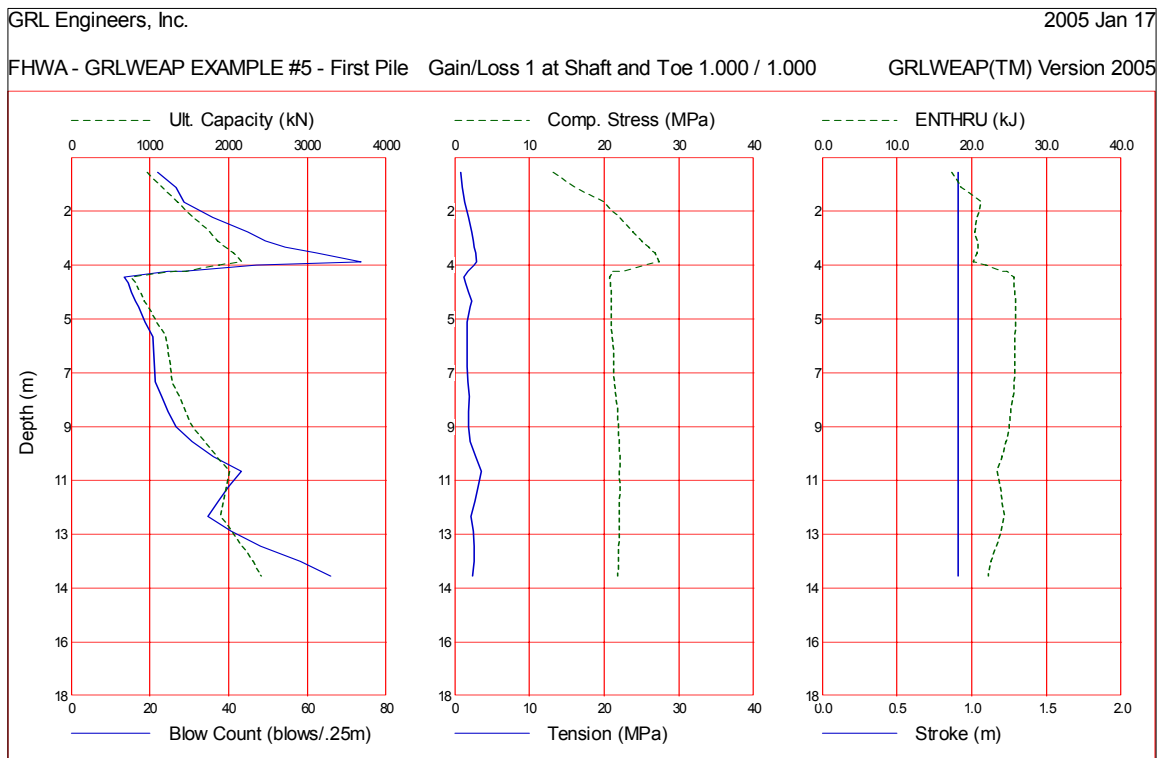


Figure 16.12 Example 5 Driveability Results for First Driven 356 mm (14 inch) Concrete Pile without Densification

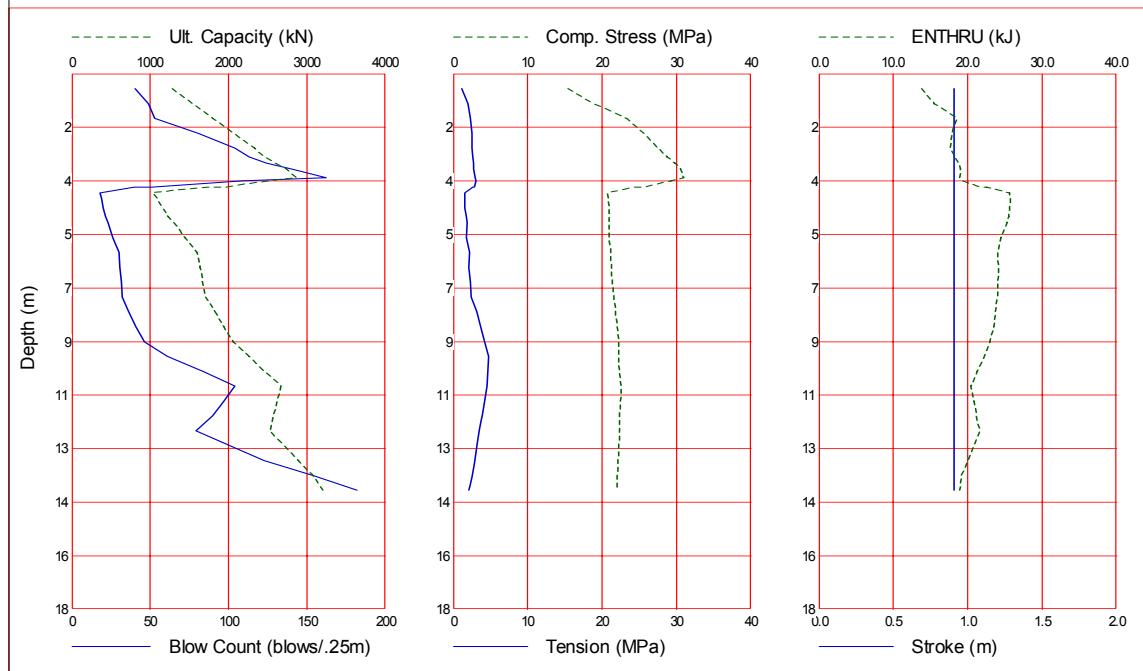


Figure 16.13 Example 5 Driveability Results for Later Driven 356 mm (14 inch) Concrete Piles with Densification

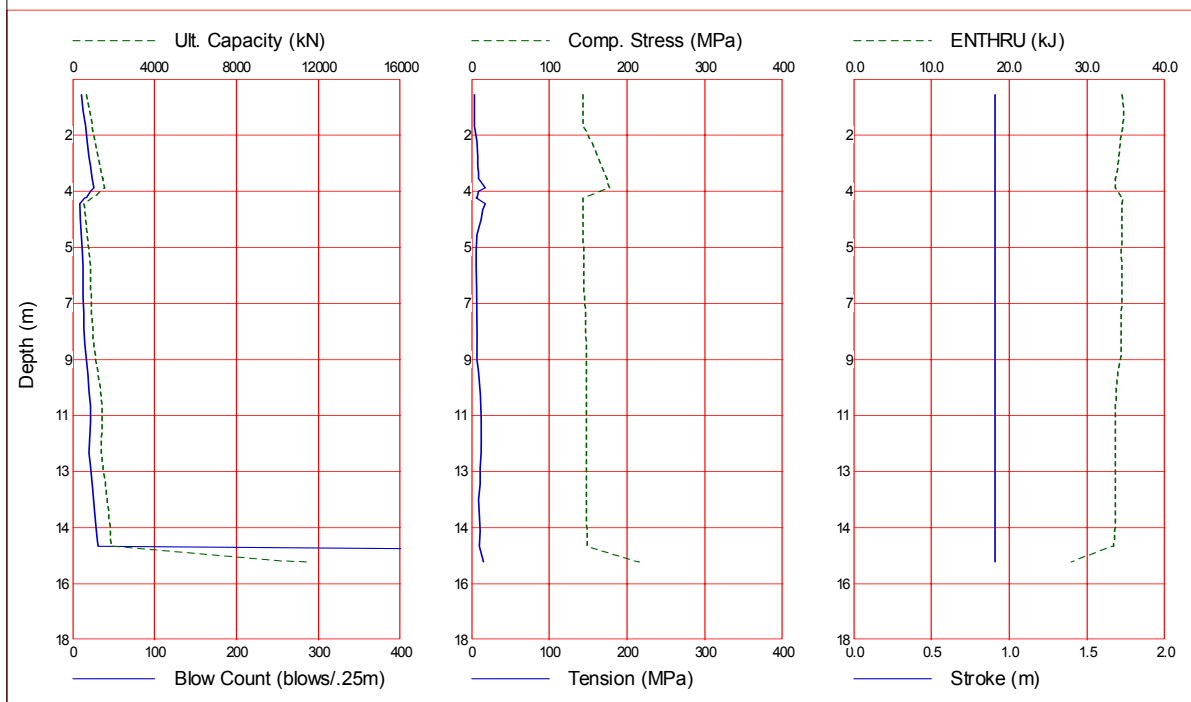


Figure 16.14 Example 5 Driveability Results for H-Pile

16.5.6 Example 6 - Driving System Characteristics

Example 6 presents a wave equation comparison of two hammers having the same potential energy. Both the Engineering News and the Modified Gates dynamic formulas consider only the potential energy of the driving system; therefore, the penetration resistance required for a specific capacity by either of these formulas would be the same for both hammers provided that the hammers had the same potential energy. The penetration resistances predicted by the wave equation for the two hammers in the same pile-soil condition is, however, quite different.

In this example problem, a 356 mm by 9.5 mm (14 x 0.375 inch) wall closed end pipe pile is to be driven to an ultimate pile capacity of 1800 kN (405 kips). The pile has a furnished length of 20 m (66 ft) and an embedded length of 16 m (52.5 ft). A static analysis indicates that the soil resistance distribution will be 30% shaft resistance and 70% toe resistance. The shaft resistance will be distributed triangularly along the embedded portion of the pile shaft. The example problem's soil profile is presented in Figure 16.15. With a very dense dry soil at the pile toe, the normal GRLWEAP recommendation for the quake at the pile toe is $D/120$ or 3 mm (0.12 inch). However, actual measurements showed that the silty fine sand at this site is highly elastic and has a larger than normal toe quake of 10 mm (0.4 inch).

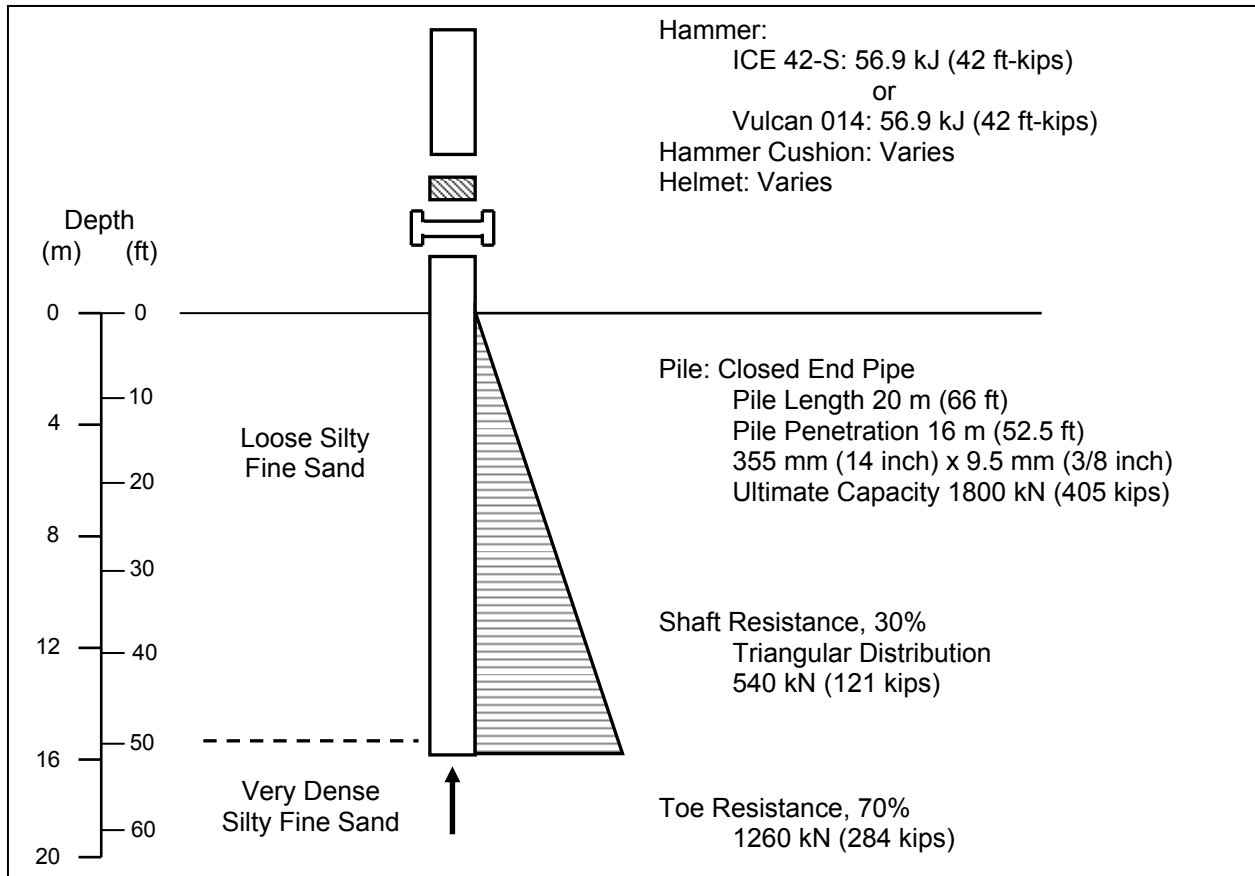


Figure 16.15 Example 6 Problem Profile

The contractor is considering using either a Vulcan 014 air hammer or an ICE 42-S open end diesel hammer to drive the piles. Both hammers are rated with the same energy, however, the ram of the Vulcan 014 is roughly 3.5 times heavier than the ram of the ICE hammer. Details of these hammers and their associated proposed driving systems are summarized in Table 16-1.

Table 16-1 Example 6 Proposed Hammer and Driving Systems						
Hammer			Vulcan 014		ICE 42-S	
Unit System	SI	English	SI	English	SI	English
Ram Weight	kN	kips	62.3	14	18.2	4.09
Rated Energy	kJ	ft-kips	57	42	57	42
Rated Stroke	m	ft	0.91	3.0	3.13	10.3
Helmet Weight	kN	kips	7.45	1.67	9.12	2.05
H. Cushion Material			Nycast		Blue Nylon	
H. Cushion E-Mod	MPa	ksi	1428	208	1207	175
H. Cushion Area	cm ²	inch ²	1508	234	2568	398
H. Cushion Thickn.	mm	inch	152	6.0	51	2.0

Wave equation results for the two hammers are plotted on the same bearing graph in Figures 16.16a and 16.16b for the 10 and 3 mm (0.4 and 0.12 inch) toe quakes, respectively. For the high quake case, GRLWEAP calculates for the Vulcan 014 (Hy Ram) a penetration resistance of 79 blows/0.25 m (96 blows/ft) to achieve an 1800 kN (405 kip) ultimate pile capacity, whereas the ICE 42-S (Lt Ram) requires a penetration resistance of 150 blows/0.25 m (181 blows/ft). For the standard toe quake, the Hy Ram (air hammer) requires a penetration resistance of 47 blows/0.25 m (57 blows/ft), while the Lt Ram (diesel hammer) requires 75 blows/0.25 m (91 blows/ft). Hence, even though both hammers have the same potential energy, the required penetration resistance for the 1800 kN (405 kip) ultimate pile capacity is quite different.

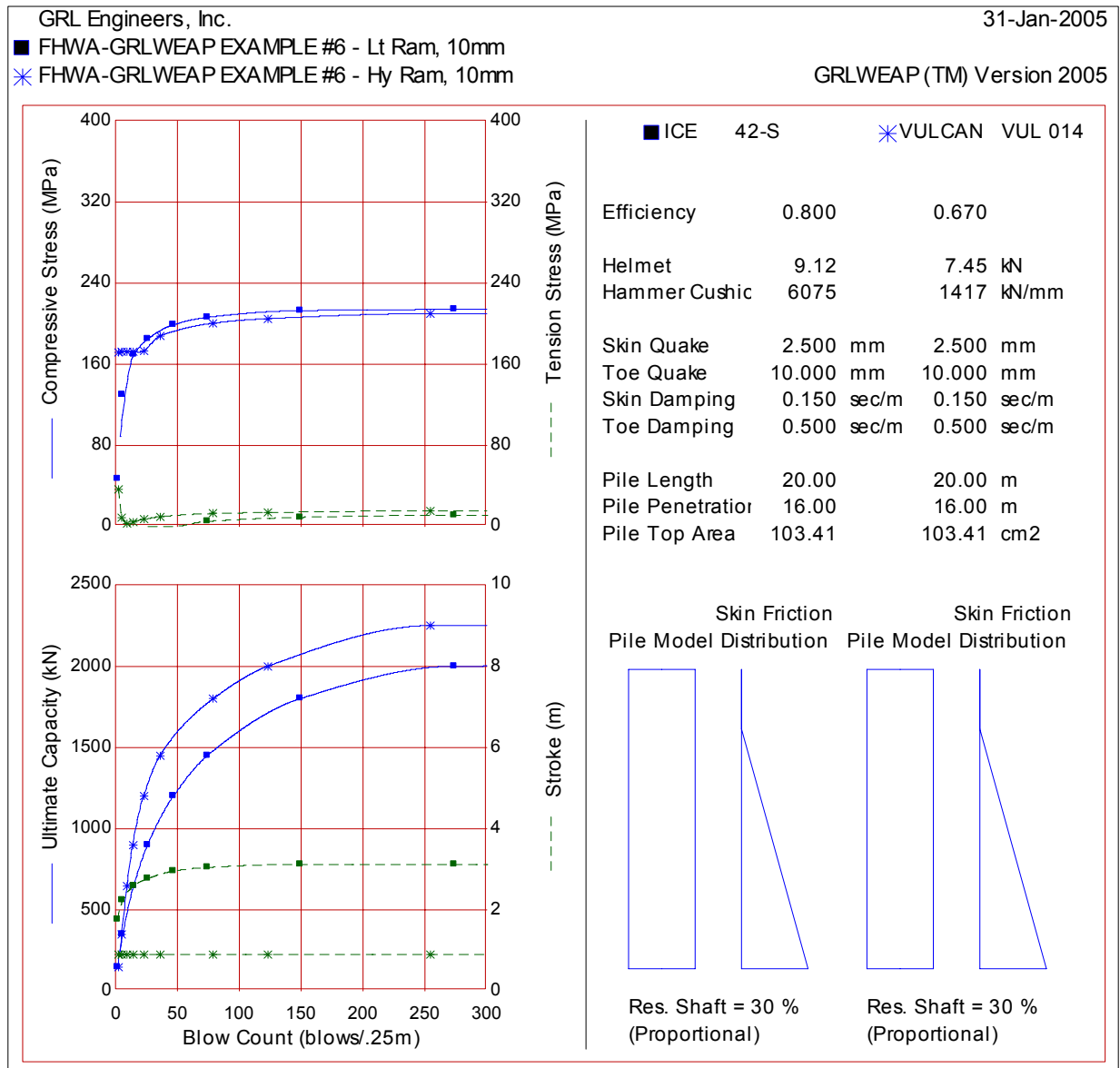


Figure 16.16a Example 6 Bearing Graph – for Two Hammers with Equivalent Potential Energy and High Toe Quake

Even though the Vulcan 014 requires a lower penetration resistance for the same capacity and has a lower efficiency (0.67 vs. 0.80 for the diesel hammer), it transfers roughly 20% more energy into the pile. This is in part because, first, the diesel hammer uses part of its energy to compress the gasses prior to impact. Second, the lower impact velocity of the heavy hammer is associated with lower energy losses. And last, the duration of the air hammer's impact is longer and consequently more effective at driving into a soil with a large quake. It is, however, interesting to note that for the smaller quake (Figure 16.16b) the lighter ram's blow counts improve relative to the heavier hammer at high capacities and driving resistances. This phenomenon can be explained with the diesel hammer's higher stroke and, therefore, higher impact force during hard driving. At the higher resistance levels, energy is not as important as force to overcome the soil resistance.

This example illustrates the dynamic complexities of hammer-pile-soil interaction. Clearly, the potential energy alone, which is the sole hammer input in dynamic formulas, does not adequately assess pile driveability.

■ FHWA-GRLWEAP EXAMPLE #6 - Lt Ram, 3.0mm
 * FHWA-GRLWEAP EXAMPLE #6 - Hy Ram, 3.0mm

GRLWEAP (TM) Version 2005

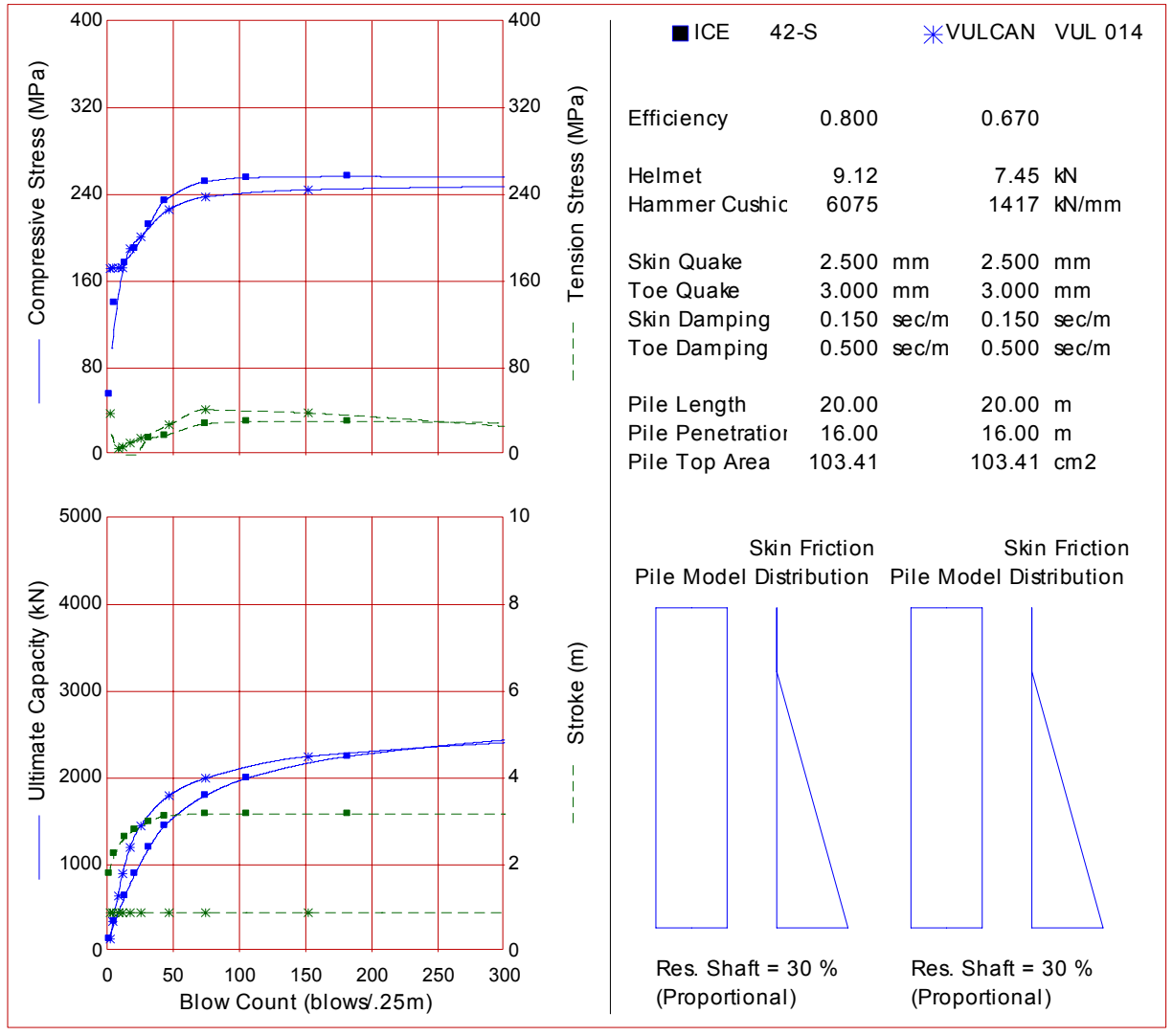


Figure 16.16b Example 6 Bearing Graph for Two Hammers with Equivalent Potential Energy and Low Toe Quake

16.5.7 Example 7 - Assessment of Pile Damage

Another pile driving construction concern is pile damage. Although it is frequently assumed that steel H-piles can be driven through boulders and fill materials containing numerous obstructions, investigations reveal that this assumption is invalid. H-piles without commercially manufactured pile toe reinforcement present one of the most commonly damaged pile types. The damage occurs because of the ease with which flanges can be

curled, rolled, and torn. Pile damage has detrimental effects on both penetration resistance and ultimate capacity.

This example illustrates how the wave equation can be used to obtain insight into a driving situation involving pile damage. The project conditions are shown in Figure 16.17. The HP 310x79 (12x53) H-piles were 10.5 m (34.4 ft) in length with a design load of 845 kN (190 kips) and an ultimate pile capacity of 1690 kN (380 kips). The soil profile consisted of 4.5 (14.8 ft) to 5.0 m (16.4 ft) of miscellaneous fill, including some bricks and concrete. Below the fill, 4.5 m (14.8 ft) of silty clay overlaid bedrock which was encountered at a depth of about 10 m (32.8 ft).

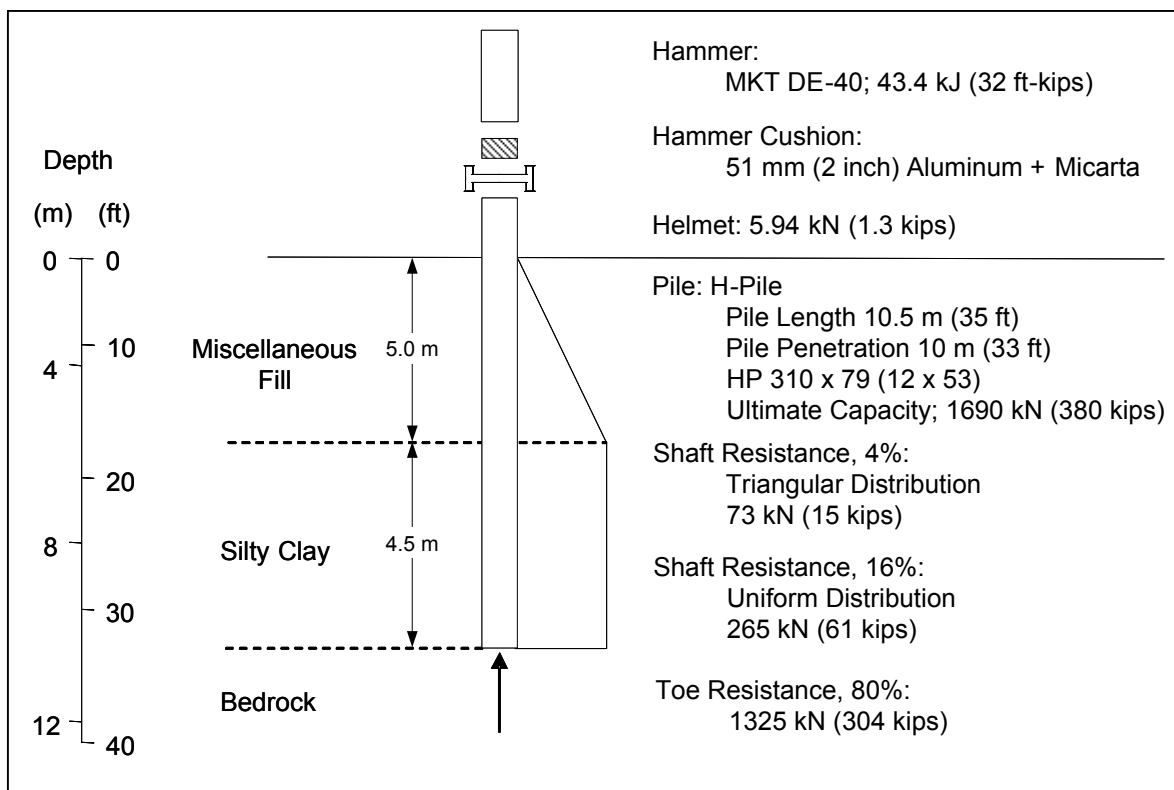


Figure 16.17 Example 7 Problem Profile

The contractor selected an MKT DE-40 single acting diesel hammer with a rated energy of 43.4 kJ (31.9 ft-kips) to drive the piles. Using the Engineering News (EN) formula specified in the contract documents, the required penetration resistance was 42 blows/0.25 m (51 blows/ft) for this hammer. Figure 16.18 presents the wave equation results indicating a pile capacity of 1170 kN (263 kips) at the EN blow count of 42 blows/0.25 m (51 blows/ft), well below the 1690 kN (380 kips) required ultimate capacity. On the other hand, the wave equation also showed that the maximum compressive stresses at the pile toe would reach

255 MPa (37 ksi) when the required ultimate capacity was reached at 81 blows/0.25 m (98 blows/ft). While most H-pile sections are lately made of steel with a 345 MPa (50 ksi) yield strength, in the given case, the yield strength was only 248 MPa (36 ksi) and the allowable driving stress, therefore, 223 MPa (32.4 ksi).

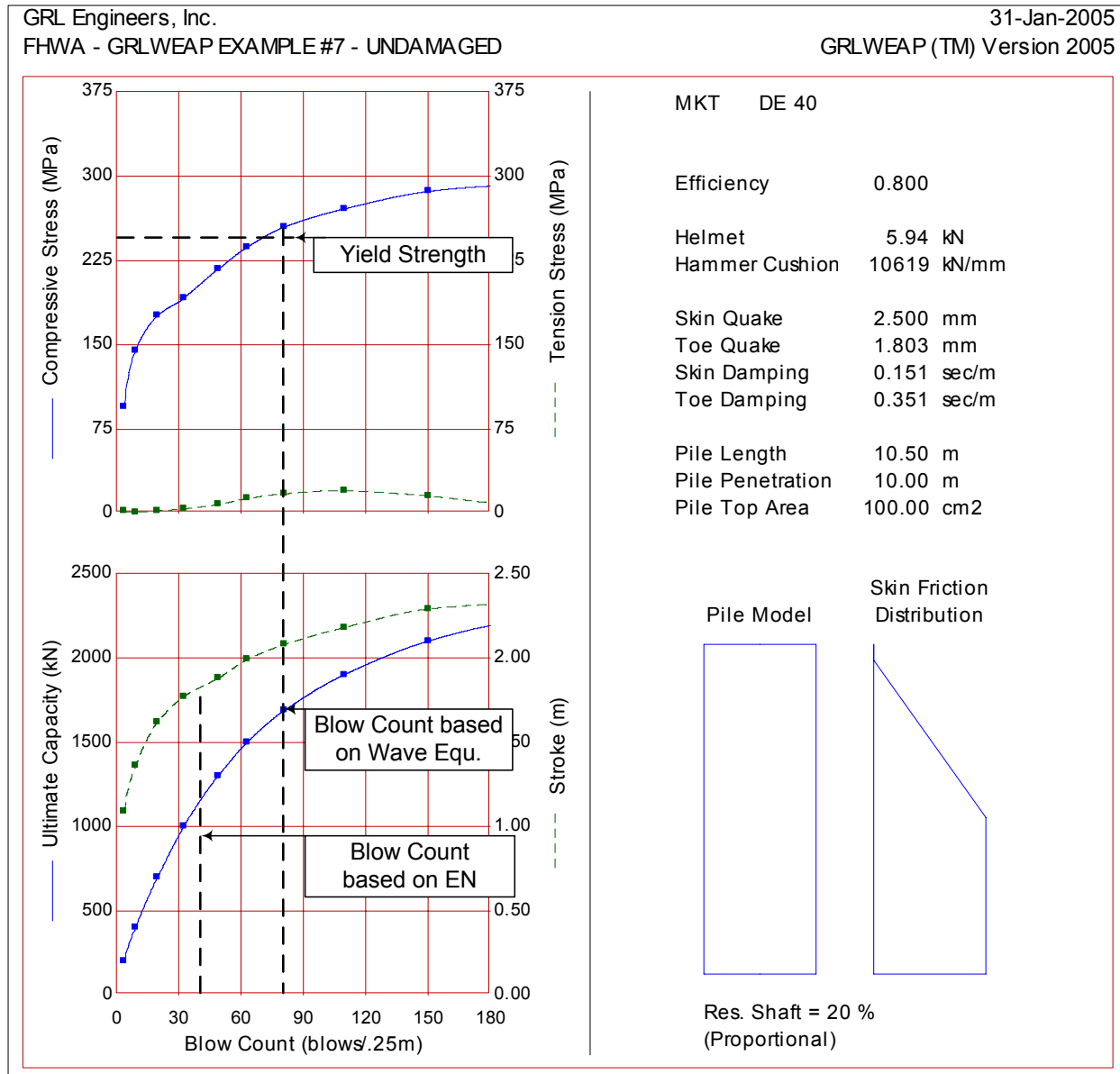


Figure 16.18 Example 7 Wave Equation Bearing Graph for Proposed Driving System

In accordance with the contract requirement, several static load tests were conducted. In all cases, the piles failed to carry the 1690 kN (380 kip) ultimate capacity in spite of the fact that several of the piles were eventually driven to a penetration resistance exceeding 200 blows/0.25 m (243 blows/ft) with no indication of damage at the pile head. Because of the

high penetration resistances, to which several piles were driven, it was apparent that even harder driving would not result in a higher pile bearing capacity. Consequently, the contractor was requested to pull several of the piles to check for possible damage. Upon extraction, it was noted that the piles were severely damaged. The flanges were separated and rolled up from the web. While the damage probably occurred as the unprotected piles were driven through the miscellaneous rubble fill, it is also obvious from Figure 16.18 that the refusal blow count would generate dynamic steel pile stresses in excess of 290 MPa (42 ksi) and therefore in excess of the yield strength. The highest stresses would occur at the pile toe according to the numerical wave equation results.

The effect of the damage on the pile driveability can be evaluated with a wave equation analysis. Since static load tests indicate that piles driven as hard as 200 blows/0.25 m (243 blows/ft) did not support the 1690 kN (380 kips) one pair of ultimate capacity and penetration resistance values is available as a reference point on the wave equation bearing graph. For the damaged pile scenario, the bearing graph may be determined by adjusting the stiffness, simply modeled by a reduction of the elastic modulus, of the lower pile segment until results agree with the penetration resistance and capacity observations. The resulting toe segment stiffness is roughly only 10% of that of the undamaged pile.

Figure 16.19 presents wave equation results for both the undamaged and the damaged pile scenarios. The results indicate that the ultimate load of 1690 kN (380 kips) could not be obtained for the damaged pile, regardless of the penetration resistance. Essentially, the damaged pile section "cushioned" the hammer blow and attenuated the hammer energy. Once damaged, the soil resistance at the pile tip could not be overcome, and therefore, the pile tip would not advance. The above illustrates that driving stresses also may limit the driveability of a pile to the required ultimate capacity.

The potential for pile damage on this project could have been greatly reduced if a wave equation had been performed during the design stage or had been specified for construction control. As pointed out earlier, the wave equation bearing graph in Figure 16.18 illustrates that the ultimate capacity of 1690 kN (380 kips) could only be obtained by the contractor's driving system at a penetration resistance of 81 blows/0.25 m (98 blows/ft) or more with an associated pile toe stress of 255 MPa (37 ksi), a stress in excess of the steel yield strength of 248 MPa (36 ksi). Considering that the stresses calculated by the wave equation are averages over the cross section, a non-uniform distribution of the soil or rock resistance could have added significant additional bending stresses in the steel pile near its toe. Hence, the potential damage would have been clearly apparent at the time of the contractor's hammer submittal had a wave equation analysis been performed. Additional wave equation analyses of the contractor's driving system could have been

performed at the same time to determine if driving stress levels could be acceptably reduced by using reduced fuel settings and shorter hammer strokes. If driving stresses could not be controlled in this manner, approval of the proposed driving system should not have been obtained, and either alternate hammers should have been evaluated or a higher yield strength required.

In any event, where H-piles have to be driven through materials that could include obstructions or where piles have to be driven to rock, it is always strongly recommended to protect the pile toe with a so-called driving shoe. Commercially available driving shoes (see Section 22.2) may be steel castings which can be welded to the pile toe. They tend to centralize the toe resistance force and/or reinforce the flanges.

■ FHWA - GRLWEAP EXAMPLE #7 - UNDAMAGED
 * FHWA - GRLWEAP EXAMPLE #7 - DAMAGED

GRLWEAP (TM) Version 2005

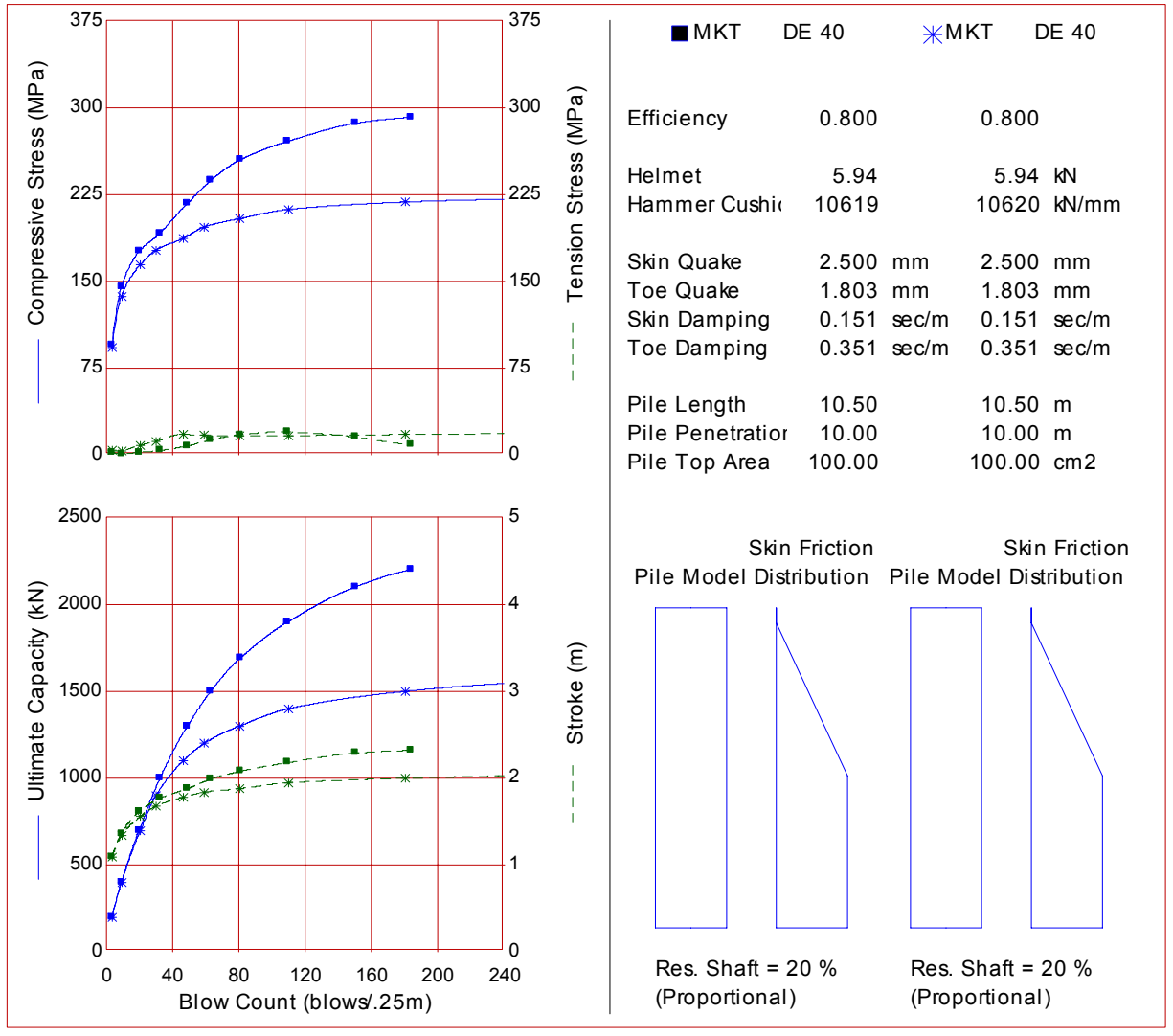


Figure 16.19 Example 7 Comparison of Wave Equation Bearing Graphs For Damaged and Undamaged Pile

16.5.8 Example 8 – Selection of Wall Thickness

This wave equation example demonstrates the selection process for the required wall thickness of a pipe pile. Consider the soil and problem profile presented in Figure 16.20. Based upon static analysis and structural loading conditions, a 324 mm (12.75 inch) outside diameter closed end pipe pile with a design load of 665 kN (150 kips) is selected as the pile foundation type. Static analysis indicates that the overlying, unsuitable layers provide 140 kN (31 kips) of resistance. With a specified factor of safety of 2.0, the required ultimate pile

capacity is therefore $2 \times 665 + 140 = 1470 \text{ kN}$ (330 kips). The pile length is 15 m (49 ft), and the calculated embedded pile length for this ultimate capacity is 14 m (46 ft).

Being a design stage issue, actual hammer and driving system configuration is unknown. Therefore, a typical hammer size and driving system configuration must be assumed with consideration of typical, locally available equipment as well as the calculated soil resistance at the time of driving. Table 21-2 suggests a minimum hammer energy of 39 kJ (28.8 ft-kips) for ultimate pile capacities of 1351 to 1850 kN (301 to 415 kips). A Berminghammer B 2005 single acting diesel hammer with a rated energy of 32.7 kJ (24 ft-kips) is routinely available in the area but is slightly smaller than the recommended size for the 1470 kN (330 kip) ultimate capacity.

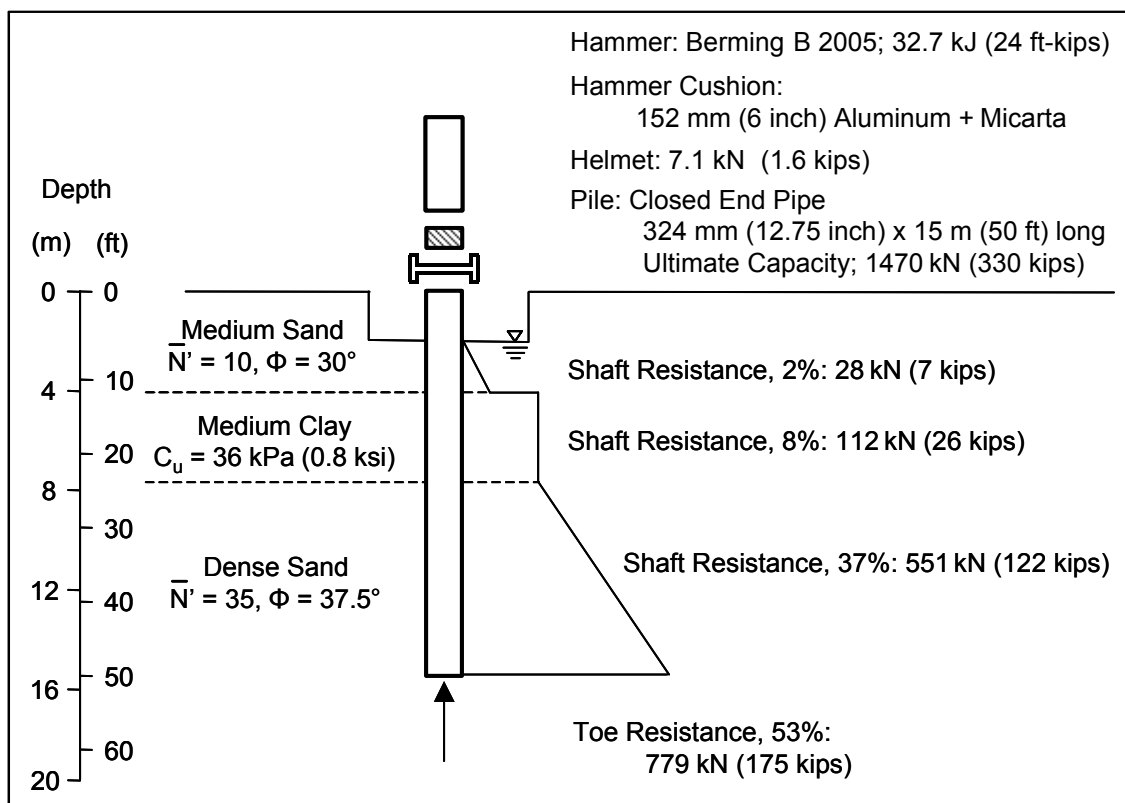


Figure 16.20 Example 8 Problem Profile

Wave equation analyses were performed for a 324 mm (12-3/4 inch) outside diameter pipe pile with the four different wall thicknesses of 6.3, 7.1, 7.9 and 9.5 mm (0.25, 0.281, 0.312, and 0.375 inch).

Figures 16.21 and 16.22 present the results of these analyses in the form of bearing graphs and Table 16-2 summarizes stress and blow count results. While stresses would always be less than 90% of yield for a Grade 3 pipe with a yield strength of 310 MPa (45 ksi), only the 9.5 mm (0.375 inch) thickness would provide suitable driveability to the required capacity. As discussed in Chapter 11, suitable driveability is a penetration resistance between 30 and 98 blows per 0.25 m (36 and 120 blows/ft). Higher calculated blow counts contain the risk of near refusal conditions in the field if hammer efficiency, driving system performance, or soil parameters are even slightly less favorable than predicted. In the present example, therefore, the 9.5 mm (0.375 inch) wall thickness pipe has the suitable driveability for the required capacity and is an acceptable selection for the foundation design. However, driving stresses are low enough and blow counts high enough that a larger hammer closer to the minimum suggested size such as a Berminghammer B2505 should also be evaluated.

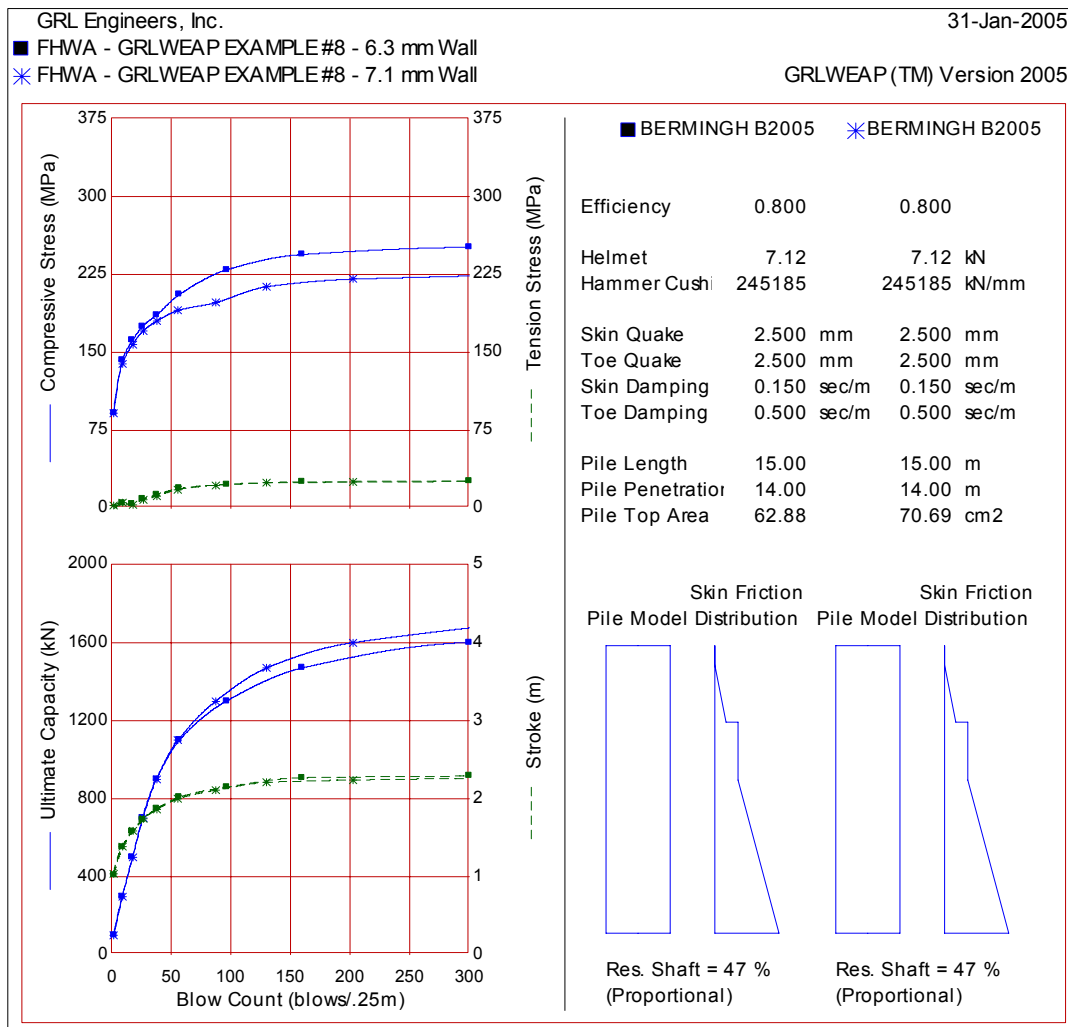


Figure 16.21 Example 8 Bearing Graphs for 6.3 and 7.1 mm Wall Pipe Piles

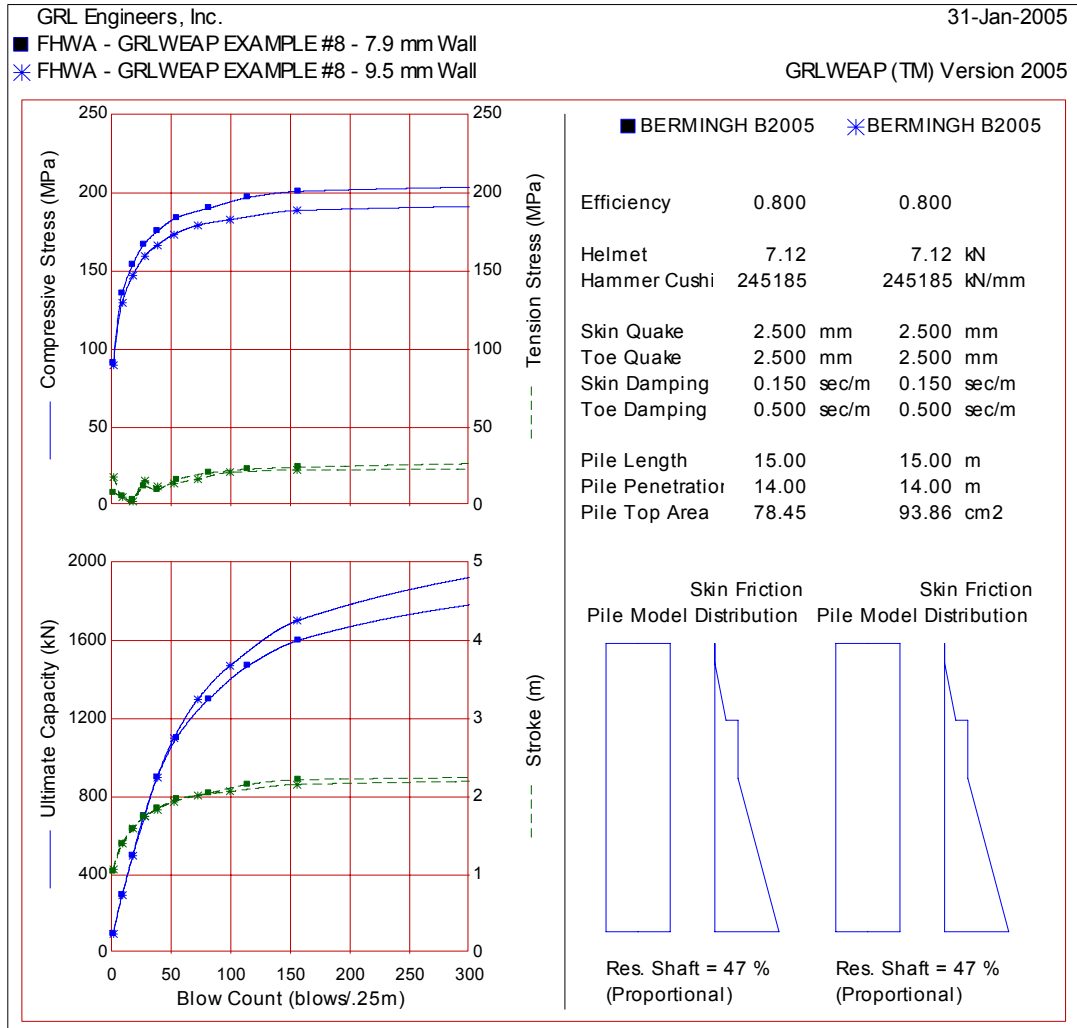


Figure 16.22 Example Bearing Graph for 7.9 and 9.5 mm Wall Pipe Piles

Table 16-2 Example 8 Stress and Blow Count Results					
Wall Thickness		Compressive Stress		Blow Count	
Mm	inch	MPa	ksi	Blows/0.25 m	Blows/ft
6.3	0.25	244	35.4	160	195
7.1	0.281	213	30.9	130	158
7.9	0.312	197	28.6	115	140
9.5	0.375	183	26.5	99.6	120

16.5.9 Example 9 - Evaluation of Vibratory Driving

This example illustrates the use of a wave equation analysis for evaluating vibratory hammer installation of the sheet piles required for the cofferdam construction in Example 5. The sheet piles of Example 5 must be installed using a vibratory hammer. The contractor has an ICE 815 hammer available and intends to drive pairs of AZ18 sheet piles whose combined cross sectional area is 190 cm^2 (29.5 inch^2). These are Z-section sheets, each with a width of 630 mm (24.8 inch), a depth of 380 mm (15 inch), and a thickness of 9.5 mm (0.37 inch). At the time of sheet pile installation, the soil within the cofferdam is not excavated and the piles are, therefore, driven from mudline to an estimated depth of 10 m (32.8 ft) below mudline. The sheet pile length is 15 m (49.2 ft).

For the non-excavated condition, the sheet piles must first penetrate a 5 m (16.4 ft) thick layer of soft silt, followed by the extremely dense sand and then the dense sand and gravel layers. Using the soil profile given in Example 5, the static resistance values were calculated in the **SA** routine of the GRLWEAP 2005 program, based on an SPT value of 5 for the silt, 60 (maximum) for the extremely dense sand and gravel, and 33 for the dense sand and gravel. As is reasonable for submerged coarse grained soils subjected to vibratory driving, a gain/loss factor of 0.25 was input for the shaft resistance (Note that it is not recommendable to use such a low gain/loss factor for either vibratory pile driving in a clay or for impact driving in a sand). The gain/loss factor for the end bearing was conservatively left at the 1.0 default value. The static resistance calculated by the **SA** method and reduced by the gain/loss factors yields the static resistance to driving (SRD). For vibratory pile driving, the SRD is often much lower than the long term SRD in submerged coarse grained soils. As per GRLWEAP recommendations, damping factors and quakes were set to twice the values assumed for impact driving, i.e., a shaft damping of 0.33 s/m (0.1 s/ft) in the sand and gravel layers and a quake of 5 mm (0.2 inch) for both shaft and toe. The calculated soil resistance and the associated dynamic soil parameters are shown in Figure 16.23(a).

Depth	Skin Frictn	End Bearing	Skin Quake	Toe Quake	Skin Damping	Toe Damping
m	kPa	kN	mm	mm	s/m	s/m
0.00	0.0	0.0	5.00	5.00	0.660	1.000
5.00	13.5	20.5	5.00	5.00	0.660	1.000
5.00	21.3	228.0	5.00	5.00	0.330	1.000
9.00	60.4	228.0	5.00	5.00	0.330	1.000
9.00	24.0	125.4	5.00	5.00	0.330	1.000
15.00	45.4	125.4	5.00	5.00	0.330	1.000
ft	ksf	kips	inch	inch	s/ft	s/ft
0.0	0.00	0.0	0.20	0.20	0.20	0.31
16.4	0.28	4.6	0.20	0.20	0.20	0.31
16.4	0.45	51.3	0.20	0.20	0.10	0.31
29.5	1.26	51.3	0.20	0.20	0.10	0.31
29.5	0.50	28.2	0.20	0.20	0.10	0.31
49.2	0.95	28.2	0.20	0.20	0.10	0.31

Figure 16.23(a) Example 9 Soil Resistance Information for Vibratory Sheet Pile Driving

Figure 16.23(b) lists the hammer model, which consists of two masses and an elastomer connection modeled by a spring with 1.1 kN/mm (6 kips/inch) spring stiffness. The bottom mass (oscillator) of the vibratory hammer includes the clamp weight. The product of the listed eccentric weight and the eccentric radius equals the hammer's rated moment. As per input, the frequency is 20 Hz (1200 RPM) even though the hammer is capable of running at 26 Hz (1560 RPM). Efficiency and start-up time (the time necessary for the hammer to reach full frequency) are left at their 1.0 and 0.0 default values. Another input is a 25 kN (5.6 kips) line pull, or upward directed crane force, which may be needed to maintain hammer-pile system stability. Often during harder driving, the operator will let the line slacken which will allow for a greater downward force and therefore an increase in the speed of pile penetration. An upward directed (positive) line force is therefore a conservative input.

GRLWEAP: WAVE EQUATION ANALYSIS OF PILE FOUNDATIONS
Version 2005
SI Units

Vibratory ICE 815; 2 AZ18 Sheet Piles

Hammer Model:	815		Made by:	ICE	
No.	Weight kN	Stiffn kN/mm	CoR	C-Slk mm	Dampg kN/m/s
1	24.475				
Bottom+Clamp	46.045	1.1	1.000	3.0480	102.4
Top Weight	(kN)	24.47	Bottom Weight+Clamp	(kN)	46.05
Connect. Stiffness	(kN/mm)	1.05	Connect. Dashpot	(kN/m/s)	102.4
Eccenter Moment	(kN-m)	0.499			
Maximum Frequency	(1/s)	26.70	Actual Target Frequ.	(1/s)	20.00
Efficiency		1.0000	Rated Power	(kW)	375.0
Line Pull	(kN)	25.0000	Start-Up Time	(s)	0.000

Figure 16.23(b) Example 9 Vibratory Hammer Model

Analyses were performed for pile penetration depths between 5 and 10 m (16.4 and 32.8 ft) at 0.5 m (1.6 ft) increments. Figure 16.23(c) shows the pile and soil model for the final depth of 10 m (32.8 ft). At that point, the SRD is 316 kN (71 kips) with 125 kN (28 kips) acting at the sheet pile toe (the steel area of the pile). The difference of 191 kN (43 kips), between the SRD and toe resistance, is 25% of the long term shaft resistance calculated by the **SA** routine.

For the first analyzed depth of 5 m (16.4 ft), the static capacity is smaller than all of the applied weights (hammer weight plus clamp weight plus pile weight minus line pull) causing the sheet pile to “run” as indicated in the final result table in Figure 16.23(d) by the zero (0) penetration time. After the pile penetrates into the extremely dense sand layer, the required penetration time sharply increases to values around 75 s/m (23 s/ft), but reduces to much more comfortable values as the sheet pile toe enters the dense sand and gravel. The final penetration time is 13 s/m (4.0 s/ft). Vibratory hammer refusal has occasionally been specified as low as 25 mm/min (1 inch/min) corresponding to penetration times of 2400 s/m (720 s/ft), and the results, therefore, suggest that the sheet pile installation should be possible with the 815 hammer. However, the accuracy of the wave equation prediction strongly depends on the realism of the relatively crudely estimated static resistance to driving (SRD). Furthermore, a good alignment of the sheet piles and thus no excessive interlock friction is another condition for a successful installation.

Vibratory ICE 815; 2 AZ18 Sheet Piles							2005/01/27				
GRL Engineers, Inc.							GRLWEAP(TM) Version 2005				
Depth	(m)	10.0									
Shaft Gain/Loss Factor		0.250	Toe Gain/Loss Factor	1.000							
PILE PROFILE:											
Toe Area	(cm ²)	190.000	Pile Type	Sheet Pile							
Pile Size	(cm)	0.000									
L b Top	Area	E-Mod	Spec Wt	Perim	Strength	Wave Sp	EA/c				
m	cm ²	MPa	kN/m ³	m	MPa	m/s	kN/m/s				
0.00	190.0	210000.	77.50	3.420	248.00	5156.	773.89				
15.00	190.0	210000.	77.50	3.420	248.00	5156.	773.89				
Wave Travel Time 2L/c (ms)			5.819								
Pile and Soil Model											
No.	Weight	Stiffn	C-Slk	T-Slk	CoR	Soil-S	Soil-D	Quake	Rut	(kN)	316.1
	kN	kN/mm	mm	mm		kN	s/m	mm	LbTop	Perim	Area
									m	m	cm ²
1	1.472	3990.	3.000	0.000	0.85	0.0	0.000	5.00	1.00	3.4	190.0
2	1.472	3990.	0.000	0.000	1.00	0.0	0.000	5.00	2.00	3.4	190.0
6	1.472	3990.	0.000	0.000	1.00	1.2	0.659	5.00	6.00	3.4	190.0
7	1.472	3990.	0.000	0.000	1.00	3.5	0.659	5.00	7.00	3.4	190.0
8	1.472	3990.	0.000	0.000	1.00	5.8	0.659	5.00	8.00	3.4	190.0
9	1.472	3990.	0.000	0.000	1.00	8.1	0.659	5.00	9.00	3.4	190.0
10	1.472	3990.	0.000	0.000	1.00	10.4	0.659	5.00	10.00	3.4	190.0
11	1.472	3990.	0.000	0.000	1.00	22.4	0.331	5.00	11.00	3.4	190.0
12	1.472	3990.	0.000	0.000	1.00	30.8	0.331	5.00	12.00	3.4	190.0
13	1.472	3990.	0.000	0.000	1.00	39.1	0.331	5.00	13.00	3.4	190.0
14	1.472	3990.	0.000	0.000	1.00	47.5	0.331	5.00	14.00	3.4	190.0
15	1.472	3990.	0.000	0.000	1.00	22.0	0.331	5.00	15.00	3.4	190.0
Toe						125.4	1.001	5.00			
22.087 kN total unreduced pile weight (g= 9.81 m/s ²)											
22.087 kN total reduced pile weight (g= 9.81 m/s ²)											

Figure 16.23(c) Example 9 Pile Profile

SUMMARY OVER DEPTHS								
G/L at Shaft and Toe: 0.250 1.000								
Depth	Rut	Frictn	End Bg	PenTime	CompStr	Ten Str	Power	
m	kN	kN	kN	s/m	MPa	MPa	kW	
5.0	49.3	28.8	20.5	0.0	0.000	0.000	0.0	
5.5	267.0	39.0	228.0	72.7	16.876	-16.784	128.8	
6.0	279.2	51.2	228.0	72.5	17.291	-17.381	135.5	
6.5	293.6	65.6	228.0	73.1	17.885	-18.124	143.7	
7.0	310.0	82.0	228.0	73.5	18.371	-18.932	152.3	
7.5	328.5	100.5	228.0	73.6	19.002	-19.924	163.7	
8.0	349.2	121.2	228.0	74.2	19.965	-21.034	175.6	
8.5	371.9	143.9	228.0	75.3	21.067	-22.322	189.7	
9.0	396.7	168.7	228.0	76.4	22.739	-23.778	205.4	
9.5	304.7	179.3	125.4	12.8	19.902	-15.881	159.2	
10.0	316.1	190.7	125.4	13.1	20.446	-16.657	166.9	
Total Driving Time			5 minutes					

Figure 16.23(d) Example 9 Summary over Depths

16.6. ANALYSIS DECISIONS FOR WAVE EQUATION PROBLEMS

16.6.1 Selecting the Proper Approach

Even though the wave equation analysis is an invaluable tool for the pile design process, it should not be confused with a static geotechnical analysis, granted certain wave equation programs, such as GRLWEAP, provide for some simplified static analysis. The basic wave equation approach does not determine the capacity of a pile based on soil boring data. The wave equation calculates a penetration resistance for an assumed ultimate capacity, or conversely, it assigns an estimated ultimate capacity to a pile based on a field observed penetration resistance. It is one thing to perform a wave equation bearing graph for an expected capacity at a particular pile penetration and a totally different matter to actually realize that capacity at that depth. The greatest disappointments happen when pile lengths required during construction vary significantly from those estimated during design by a static analysis. To avoid such disappointments, it is absolutely imperative that a static analysis, as described in Chapter 9, precede the wave equation analysis. The static analysis will yield an approximate pile penetration for a desired capacity or a capacity for a certain depth. The static analysis can also generate a plot of estimated pile capacity as a function of depth. As a preparation for the wave equation analysis, it is important that the static analysis evaluate the soil resistance in the driving situation (*e.g.* remolded soil strengths, before excavation, before scour, before fill placement, *etc.*). For the assessment of long term static conditions, the static analysis must consider the critical situations of soil setup or relaxation, additional change due to excavation, water table variations, and scour, etc.

After completion of the static analysis, a wave equation analysis may follow leading to either a bearing graph or a driveability analysis of penetration resistances and stresses versus depth. Sometimes both analyses are performed. The validity of the bearing graph depends on the proximity of the analyzed soil profile and the site variability of the soil properties. The driveability analysis calculates penetration resistances and stresses for a number of penetration depths and, therefore, provides a more complete result. However, there is a very basic difference between these two approaches. The bearing graph approach allows the engineer to assess pile capacity given a penetration resistance at a certain depth. The driveability analysis points out certain problems that might occur during driving prior to reaching the target penetration. If the pile actually drives differently from the wave equation predictions, a reanalysis with different soil resistance parameters would be needed to match the observed behavior.

Even if an accurate static analysis and a wave equation analysis have been performed with realistic soil parameters, the experienced foundation engineer would not be surprised if the penetration resistance during pile installation were to differ substantially from the predicted one. Most likely, the observed penetration resistance would be lower than calculated. As an example, suppose that a 500 kN (112 kip) pile had to be driven into a clay. With a factor of safety of 2.5, the required ultimate capacity would be 1250 kN (280 kips). The static soil analysis indicates that the pile has to be 25 m (82 ft) long for this ultimate capacity. There would be negligible toe resistance, and based upon remolded soil strength parameters, the soil may exhibit only 50% of its long term strength during driving (setup factor = 2). It is therefore only necessary to drive the pile to a capacity of 625 kN (140 kips), which should be achieved at the 25 m (82 ft) depth. The expected end of installation penetration resistance would then correspond to 625 kN (140 kips). A restrike test, performed 7 days after installation would include setup effects and might show the 1250 kN (280 kip) capacity and, therefore, a much higher penetration resistance than at the end of driving.

The above discussion points out one major reason for differences between analysis and reality. However, as with all mathematical simulations of complex situations, agreement of wave equation results with actual pile performance depends on the realism of the method itself and on the accuracy of the model parameters. The accuracy of the wave equation analysis will be poor when either soil model or soil parameters inaccurately reflect the actual soil behavior and when the driving system parameters do not represent the state of maintenance of hammer or cushions. The pile behavior is satisfactorily represented by the wave equation approach in the majority of cases. A review of potential wave equation error sources follows.

16.6.2 Hammer Data Input, External Combustion Hammers

The most important wave equation input quantity is the hammer efficiency. It is defined as that portion of the potential ram energy that is available in the form of kinetic ram energy immediately preceding the time of impact. Many sources of energy loss are usually lumped into this one number. If the hammer efficiency is set too high, an optimistically low penetration resistance would be predicted. This in turn could lead to a dangerous overprediction of ultimate pile capacity. If the efficiency is set very low, for conservative pile capacity assessments, the stresses may be underpredicted, leading to possible pile damage during installation.

Hammer efficiency should be reduced for inclined (battered) pile driving. The efficiency reduction depends on the hammer type and batter angle. For hammers with internal ram energy measurements, no reductions are required to cover losses due to inclined pile driving. Modern hydraulic hammers often allow for a continuously adjustable ram kinetic energy which is measured and displayed on the control panel. In this case, the hammer efficiency need not cover friction losses of the descending ram but only losses that occur during the impact (e.g. due to improper ram-pile alignment), and it may therefore be relatively high (say 0.95). For such hammers, the wave equation analysis can select the proper energy level for control of driving stresses and economical penetration resistances by trying various energy (stroke) values that are lower than the rated value.

Similarly, a number of air/steam hammers can be fitted with equipment that allows for variable strokes. The wave equation analysis can help to find the penetration resistance at which the stroke can be safely increased to maximum. It is important, however, to realize that the reduced stroke is often exceeded and the maximum stroke not fully reached. Corresponding increases and decreases of efficiency for the low and high stroke, respectively, may, therefore, be investigated.

16.6.3 Hammer Data Input, Diesel Hammers

The diesel hammer stroke increases when the soil resistance, and therefore penetration resistance, increases. Certain wave equation programs, such as GRLWEAP, simulate this behavior by trying a down stroke and, when the calculated up stroke is different, repeating the analysis with the new value for the down stroke until the strokes converge. The accuracy of the resulting stroke is therefore dependent on the realism of the complete hammer-pile-soil model and should be checked in the field by comparison with the actual stroke. The consequences of an inaccurate stroke could be varied. For example, an optimistic assumption of combustion pressure could lead to high stroke predictions and, therefore, non-conservative predictions of ultimate pile capacity while stress estimates would be conservatively high (which may lead to a hammer rejection).

Stroke and energy transferred into the pile appear to be closely related, and large differences (say more than 10%) between stroke predictions and observations should be explained. Unfortunately, higher strokes do not always mean higher transferred energy values. When a diesel hammer preignites, probably because of poor maintenance, the gases combusting before impact slow the speed of the descending ram and cushion its impact. As a result, only a small part of the ram energy is transferred to the pile. A larger part of the ram energy remains in the hammer producing a high stroke. If, in this case, the combustion pressure would be calculated by matching the computed with the observed

stroke under the assumption of a normally performing hammer, the calculated transferred energy would be much higher than the measured one, and the calculated penetration resistances (blow counts) would be non-conservatively low. It is, therefore, recommended that hammer problems are corrected as soon as detected on the construction site. If this is not possible, several diesel stroke or pressure options should be tried when matching wave equation results with field observations, and the most conservative results should be selected. Section 16.7.1.1 discusses the available diesel hammer stroke options in greater detail.

Generally the hammer data file of wave equation programs contain reduced combustion pressures for those hammers which have stepwise adjustable fuel pumps. Note that decreasing combustion pressures may be associated with program input fuel pump settings that have increasing numbers. For example, Delmag hammers' fuel pump settings of 4 (maximum), 3, 2, and 1 (minimum) roughly correspond to combustion pressures of 100, 90, 81 and 73 percent of that associated with the hammer's rated energy. Other diesel hammers may have continuously adjustable fuel pumps; for stroke control of such diesel hammers, a reduced combustion pressure may be chosen as a percentage of the data file value which corresponds to the hammer's rated energy. However, for construction control, the hammer stroke has to be measured, e.g., calculating it from the hammer's speed of operation in blows per minute using a so-called Saximeter, and adjustments of the fuel amount have to be made by the operator until the desired, analyzed stroke is achieved.

16.6.4 Cushion Input

Cushions are subjected to destructive stresses during their service and, therefore, continuously change properties. Pile cushions experience a particularly pronounced increase in their stiffness because they are generally made of soft wood with its grain perpendicular to the load. Typically, the effectiveness of wood cushions in transferring energy increases until they start to burn. Then they quickly deteriorate; this happens after approximately 1500 hammer blows. For conservative stress predictions, the harder, used cushion could be modeled by an increased elastic modulus and reduced thickness. However, according to Rausche, et al. (2004), improved agreement with measurements can be achieved if used plywood cushions, i.e. for the end of driving condition, are analyzed with an elastic modulus of 75 MPa (520 ksi) and the nominal (uncompressed) thickness. For conservative capacity predictions, a less effective pile cushion may be represented by a somewhat lower, approximately 50% lower than normally recommended, input of both elastic modulus and coefficient of restitution. Wood chips as a hammer cushion are totally unpredictable and therefore should never be allowed.

In recent years, uncushioned hammers have been used with increasing frequency. For the wave equation analysis, since there is no hammer cushion, the stiffness of the spring between hammer and helmet is derived from the elastic properties of either ram or impact block (diesels). This stiffness is very high, much higher than the stiffness values of most other components within the system, and for numerical reasons, may lead to inaccurate stress predictions. Analyses with different numbers of pile segments would show the sensitivity of the numerical solution. In general, the greater the number of pile segments, the more accurate the stress calculation.

16.6.5 Soil Parameter Selection

The greatest errors in ultimate capacity predictions are usually observed when the soil resistance has been improperly considered. A very common error is the confusion of design loads with the wave equation's ultimate capacity. Note that the wave equation capacity always must be divided by a factor of safety to yield the allowable design load. Factors of safety suggested by FHWA and AASHTO are discussed in Chapter 14.

Since the soil is disturbed at the end of driving, it then often has a lower capacity (occasionally also a higher one) than at a later time. For this reason, a restrike test should be conducted to assess the ultimate pile capacity after time dependent soil strength changes have occurred. However, restrike testing is not always easy. The hammer is often not warmed up and only slowly starts to deliver the expected energy while at the same time the bearing capacity of the soil deteriorates. Depending on the sensitivity of the soil, the penetration resistance may be taken from the first 75 mm (3 inch) of pile penetration even though this may be conservative for some sensitive soils. For construction control, rather than restrike testing many piles, it is more reasonable to develop a site specific setup factor in a preconstruction test program. As long as the hammer is powerful enough to move the pile during restrike and mobilize the soil resistance, restrike tests with dynamic measurements are an excellent tool to calculate setup factors. For the production pile installation criterion, the required end of driving capacity is then the required ultimate capacity divided by the setup factor. From the wave equation calculated bearing graph and with the reduced end of driving capacity, the required end of driving penetration resistance is found.

Although the proper consideration of static resistance at the time of driving or restriking is of major importance for accurate results, dynamic soil resistance parameters sometimes play an equally important role. Damping factors have been observed to vary with waiting times after driving. Thus, damping factors higher than recommended in the GRLWEAP Manual (say twice as high) may have to be chosen for analyses modeling restrike situations.

Studies on this subject are still continuing. In any event, damping factors are not a constant for a given soil type. For soft soils, these factors may be much higher than recommended, and on hard rock they may be much lower. Choosing a low damping factor may produce non-conservative capacity predictions.

Shaft quakes are usually satisfactory as recommended at 2.5 mm (0.1 inch). However, toe quakes can vary widely and reach values well in excess of the GRLWEAP recommended range of 1/60 and 1/120 of pile diameter or pile width, particularly when the soil is in saturated soils and rather sensitive to dynamic effects. Only dynamic measurements can reveal more accurate soil quakes. However, short of such measurements, conservative assumptions must sometimes be made to protect against unforeseen problems. Fortunately, toe quakes have a relatively insignificant effect on the wave equation results of piles having most of their resistance acting along the shaft. For end bearing piles, however, large toe quakes often develop during driving in saturated soils causing the toe resistance to build up only very slowly during the hammer blow. As a consequence, at the first instant of stress wave arrival at the pile toe, little resistance exists and damaging tension stress reflections can develop in concrete piles even if the penetration resistance is high. At the same time, large toe quakes dissipate an unusually large amount of energy and therefore cause high penetration resistances. Thus, more cushioning or lower hammer strokes may not be a possible alternative for stress reductions. Instead, in extreme cases, hammers with heavier rams and lower strokes should be chosen to reduce the detrimental effects of large toe quakes. Example 6 in Section 16.5.6 illustrates the effect of a large toe quake.

Stress predictions, particularly tension stresses, are also sensitive to the input of the resistance distribution and to the percentage of toe resistance. If the soil resistance distribution is based on a static analysis, chances are that the shaft resistance is set too high because of the loss of shaft resistance during driving. It is therefore recommended that driveability analyses be performed with shaft resistances reduced by estimated setup factors, which will adjust the statically calculated capacity to match the conditions occurring during driving.

Residual stress wave equation analyses are superior to normal analyses in basic concept and probably also in results. Unfortunately, not enough correlation work has been performed to empirically determine dynamic soil constants (quake and damping values) that should be used with residual stress analyses. However, for long slender piles with significant shaft resistance components, residual stress analyses should be performed (maybe in addition to standard analyses) to assess potentially damaging stress conditions and the possibility of ultimate capacities which could be much higher than indicated by the standard wave equation analysis. Note that residual stress analyses may not be meaningful

for representation of early restrike situations in which energies increase from blow to blow while, in sensitive soils, capacities successively decrease. The residual stress analysis assumes that hammer energy and pile capacity are constant under several hammer blows.

16.6.6 Comparison With Dynamic Measurements

Often, wave equation predicted stresses and capacity values initially appear to agree quite well with results from field dynamic measurements, described in Chapter 17. However, there are additional observations and measurements that should be compared, such as stroke or bounce chamber pressure and transferred energy. Often transferred energy values are somewhat lower than calculated, and adjustment of hammer efficiency alone may improve energy agreement but produce problems with driving stress and capacity agreement. Thus, instead of adjusting hammer efficiency, the cushion stiffness or coefficient of restitution may require reduction. Sometimes matching of measured values can be very frustrating and difficult, and the task should be done with reason. Matching stresses and transferred energies within 10% of the observed or measured quantities may be accurate enough.

Note: The wave equation maximum stresses in the final summary table can occur anywhere along the length of the pile and therefore at a location different from where the field measurements were taken. It is therefore important to check the maximum driving stresses in the Extrema Tables for the pile segment that corresponds to the measurement location when comparing GRLWEAP and field measurement results.

The following procedure requires that wave equation input parameters for hammer, driving system, and soil resistance are adjusted and then wave equation analyses are run for the CAPWAP calculated capacity. The following data preparation steps and successive input parameter adjustments generally lead to an acceptable solution. The correlation procedure may differ for other wave equation and/or signal matching programs depending upon the hammer, pile, and soil models used in those programs.

- a. Set up a table with the observed stroke or bounce chamber pressure for diesel hammers, and measured values of compressive stresses and transferred energy, both at the measurement location. Include in this table for concrete piles the PDA calculated maximum tension stresses. These values should be averages over several consistent blows of pile installation or the earliest consistent blows of restrike testing. Additional matching quantities are CAPWAP calculated capacity and penetration resistance.

- b. Set up a wave equation model to run bearing graphs for the actual hammer, pile, and driving system with total capacity, resistance distribution, quake, and damping from CAPWAP.
- c. Run wave equation analyses and compare results with table values from step a. Adjust hammer efficiency (for diesel hammers, also maximum combustion pressure) until agreement between measured and wave equation computed compressive stress and transferred energy (for diesel hammers, also stroke) is within 10%. For steel piles, occasionally the hammer cushion stiffness, and for concrete piles modifications of the pile cushion stiffness, may also be needed. In rare cases, it is necessary to change the cushion coefficients of restitution.
- d. After an initial agreement has been achieved for transferred energy and pile top compressive stress, compare calculated penetration resistance for CAPWAP capacity and associated maximum tension stresses. For steel piles, adjust hammer cushion stiffness and coefficient of restitution, and for concrete piles, adjust the equivalent pile cushion parameters, together with efficiency, to improve agreement of penetration resistance and tension stresses within the 10% tolerance.
- e. Adjust the hammer efficiency to values not greater than 0.95 and not less than 50% of the standard recommended hammer efficiency values for that hammer type. The exceptions are hammers whose stroke input is based on measured impact velocity. Efficiency values greater than 0.95 are then possible. Adjust cushion coefficients of restitution between 0.25 and 1.0.
- f. If penetration resistance and stresses cannot be simultaneously matched by adjusting hammer and driving system parameters, change the shaft and toe damping and the toe quake simultaneously and proportionately to achieve agreement between measured and computed penetration resistance. Under certain conditions, it may also be necessary to change the wave equation damping model from Smith to Smith-Viscous.

Perfect agreement should not be expected between wave equation results and field observations plus CAPWAP calculated quantities. The reason is primarily a difference between the measured pile top force and velocity and the corresponding quantities obtained by the wave equation driving system model. Also, there are some differences in the pile model and in the soil model for CAPWAP which has a wider range of soil resistance parameters than the very basic Smith model. Plots of wave equation calculated and PDA measured pile top variables can be easily generated and can sometimes explain the differences between observed and calculated values.

16.7 WAVE EQUATION INPUT PARAMETERS

As described in the previous sections, the input for a wave equation analysis consists of information about the soil, pile, hammer, cushions, helmet, splices, and any other devices which participate in the transfer of energy from hammer to soil. This input information is usually gathered from contract plans, the contractor's completed Pile and Driving Equipment Data Form (Figure 16.24), soil boring, and a static pile capacity analysis. In a case where the contractor proposes using a follower as part of the driving system, detailed drawings of the follower should also be obtained. Helpful information can also be found in the "Help" display (function key F3) of the GRLWEAP input. These tables are correct only for ideal situations but may yield valuable data before a specific driving system has been identified. In general, contractors tend to assemble equipment from a variety of sources, not all of them of a standard type. It is therefore important to check and confirm the equipment that the contractor has actually included in the driving system on the job.

The following sections explain the most important input quantities needed to run the GRLWEAP program. For a more detailed explanation of input quantities, reference is made to the program's Help Section (function key **F1** or **F3** or click on Help).

The second topic of the Help Menu (**F1** or click on Help) explains the Main Input screen and all of its menus, data entry fields, and information indicators. Figure 16.25 shows this Help Window as it first appears and subdivides the Main Input screen into 10 major sections:

- A Standard Window Menus
- B Icons for standard Windows Operations
- C Icons for GRLWEAP displays and operations
- D GRLWEAP Drop-Down Menus
- E Input fields for Title and Hammer Selection
- F Hammer Parameters and Pile Material Selection
- G Hammer and Pile Cushion Input
- H Pile Data Input
- I Ultimate Capacity Input or Resistance Gain/Loss Factors
- J Soil Parameters

Although a simple bearing graph analysis only requires input in the GRLWEAP Main Input Screen, it is recommended to utilize the step-by-step input requests generated after clicking on the "New Document" icon (or New in the File Menu).

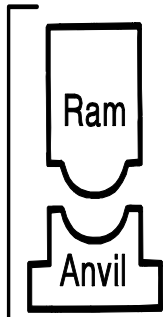
The **Job Information** window shown in Figure 16.26 will display first, accepting input of a title of up to 40 characters and the assignment of a file name and directory. **Browse** may be used to navigate the user's computer and assign the desired directory.

Clicking on **Next** will open up the **Select Hammer** window shown in Figure 16.27. The GRLWEAP program includes a hammer data file in which the major mechanical properties of approximately 1000 hammers are stored. By selecting an identification (**ID**) number and/or corresponding hammer name in the List of Hammers window, the user prompts the program to automatically input the selected hammer's properties. Note that the automatic hammer input assumes use of a well maintained and unmodified hammer. Appendix D includes a complete listing of the GRLWEAP pile hammer information.

Contract No.: _____ Structure Name and/or No.: _____
 Project: _____ Pile Driving Contractor or Subcontractor: _____
 County: _____

(Piles driven by)

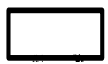
Hammer Components



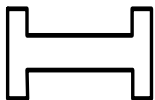
Hammer
 Manufacturer: _____ Model No.: _____
 Hammer Type: _____ Serial No.: _____
 Manufacturers Maximum Rated Energy: _____ (Joules) (ft-k)
 Stroke at Maximum Rated Energy: _____ (meters) (ft)
 Range in Operating Energy: _____ to _____ (Joules) (ft-k)
 Range in Operating Stroke: _____ to _____ (meters) (ft)
 Ram Weight: _____ (kN) (kips)
 Modifications: _____



Striker Plate
 Weight: _____ (kN) (kips) Diameter: _____ (mm) (in)
 Thickness: _____ (mm) (in)



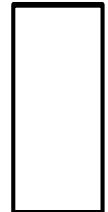
Hammer Cushion
 Material #1 Material #2
 (for Composite Cushion)
 Name: _____ Name: _____
 Area: _____ (cm²) (in²) Area: _____ (cm²) (in²)
 Thickness/Plate: _____ (mm) (in) Thickness/Plate: _____ (mm) (in)
 No. of Plates: _____ No. of Plates: _____
 Total Thickness of Hammer Cushion: _____ (mm) (in)



Helmet (Drive Head)
 Weight: _____ including inserts (kN) (kips)



Pile Cushion
 Material: _____
 Area: _____ (cm²) (in²) Thickness/Sheet: _____ (mm) (in)
 No. of Sheets: _____
 Total Thickness of Pile Cushion: _____ (mm) (in)



Pile
 Pile Type: _____
 Wall Thickness: _____ (mm) (in) Taper: _____
 Cross Sectional Area: _____ (cm²) (in²) Weight/Meter: _____
 Ordered Length: _____ (m) (ft)
 Design Load: _____ (kN) (kips)
 Ultimate Pile Capacity: _____ (kN) (kips)
 Description of Splice: _____
 Driving Shoe/Closure Plate Description: _____
 Submitted By: _____ Date: _____
 Telephone No.: _____ Fax No.: _____

Figure 16.24 Pile Driving and Equipment Data Form

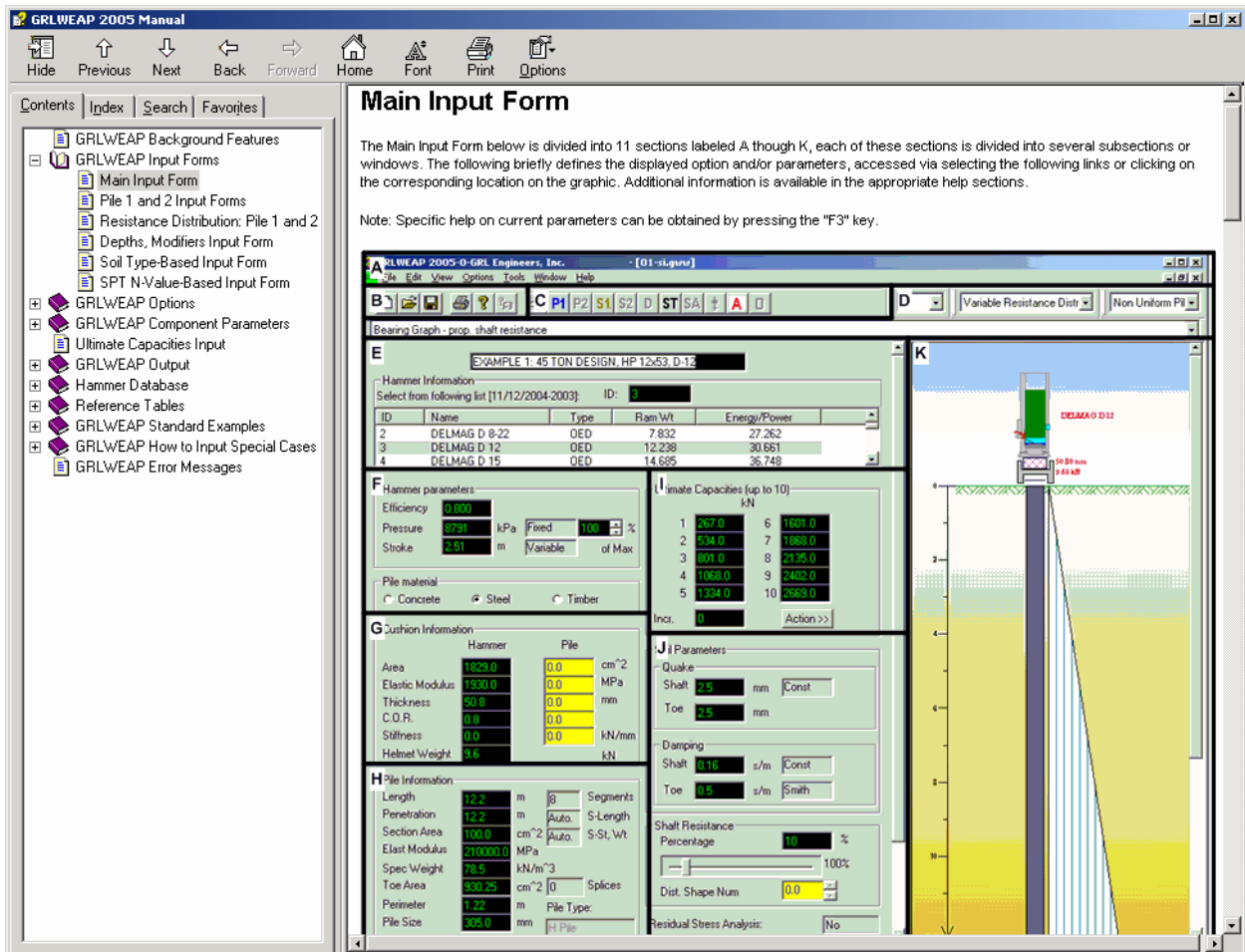


Figure 16.25 GRLWEAP Help Window for Main Input Form

While initially all hammers are displayed in the order of hammer ID number, the display may be reorganized by certain hammer types or manufacturers. Hammer types are OED (Open End Diesels), CED (Closed End Diesels), ECH (External Combustion Hammers, including the air, steam, hydraulic and drop hammer categories), and VIB (Vibratory Hammers). The user can also organize the contents in the List of Hammers window by hammer **Name**, **Type**, **Ram Weight** or **Rated Energy** by clicking on the column heading.

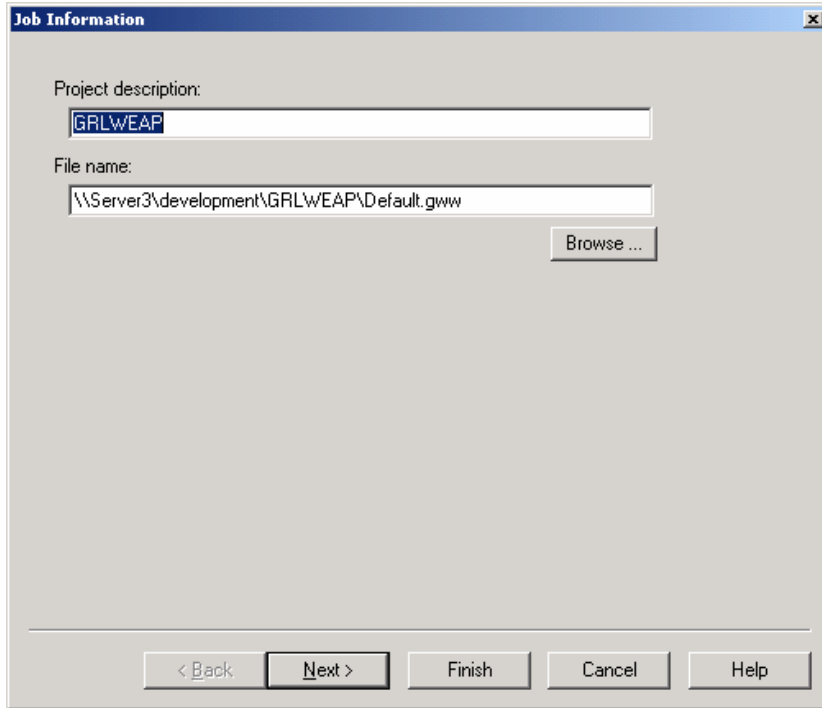


Figure 16.26 Job Information Window

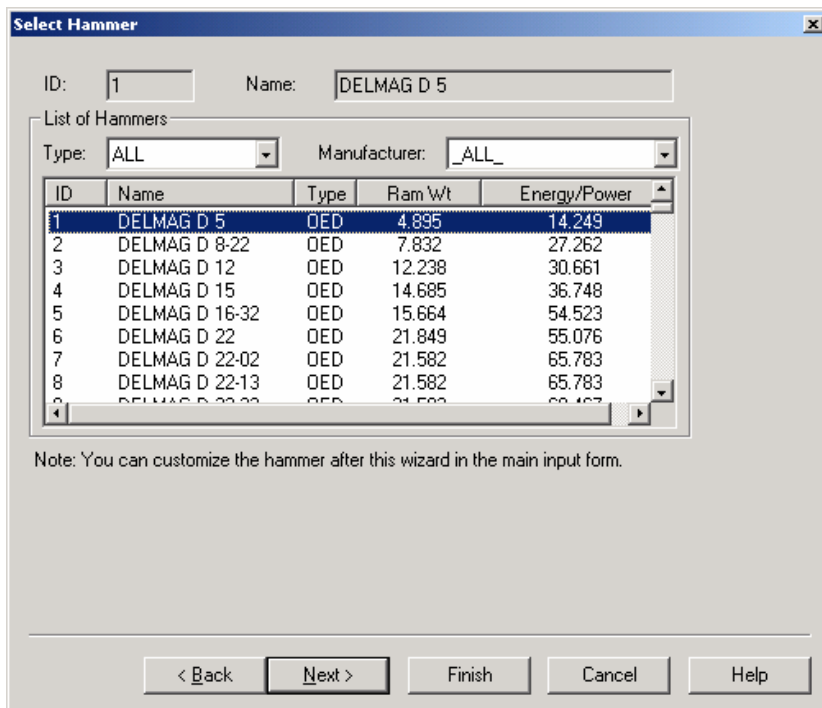


Figure 16.27 Select Hammer Window

The next section involves the **Analysis Type** window, displayed in Figure 16.28.

For a simple **Bearing Graph**, the **Proportional Shaft Resistance** option is the default. It assumes constant percentages of shaft resistance and end bearing for all capacity values to be analyzed. The alternate bearing graph options analyze the various ultimate capacity values either assuming a **Constant Shaft Resistance** or a **Constant End Bearing**.

A modified Bearing Graph approach, the **Inspector's Chart** provides the possibility of analysis with an increasing stroke (or hammer energy values) for a single ultimate capacity value. This option is useful for diesel hammers, whose stroke can vary and/or be adjusted by different fuel settings, and for hydraulic hammers, whose energy level can be selected on the hammers' control panel.

The user may also choose the Driveability option. It requires as an input the shaft resistance and end bearing as a function of pile penetration and, therefore, requires an accurate static soil analysis. The resulting output will show the corresponding ultimate capacity together with calculated blow count, pile stress maxima, and other quantities and, thus, indicates the complete, expected driving behavior.

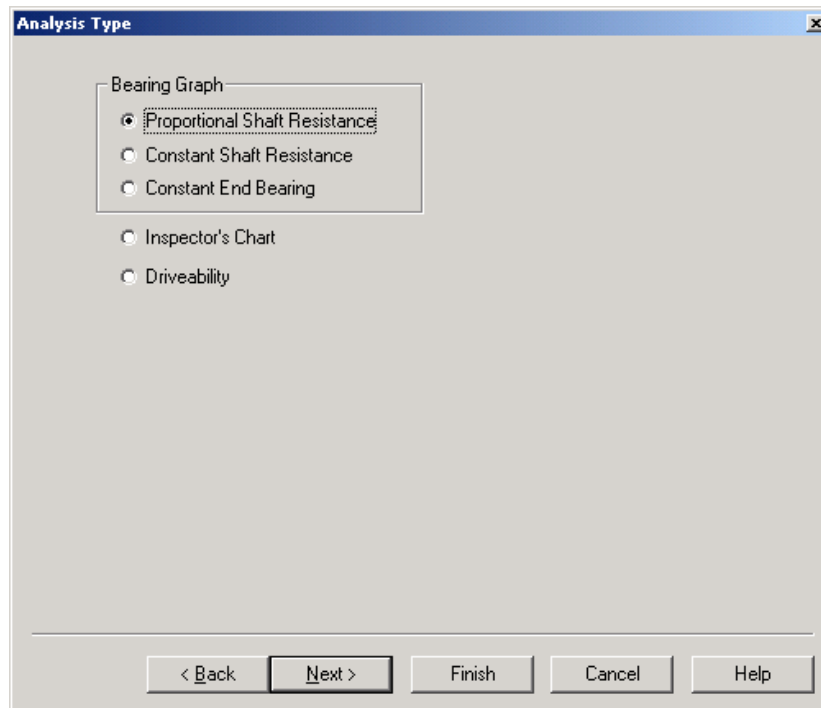


Figure 16.28 Analysis Type Window

Clicking on **Next** brings up the **Pile Input** window, illustrated in Figure 16.29a. After selection of the pile material, i.e. **Concrete**, **Steel**, or **Timber**, the program inputs default values for pile top elastic modulus, coefficient of restitution, and specific weight in the corresponding fields and also, for concrete pile material, activates the pile cushion input section. As with the hammer cushion, described below, the user may utilize the **Area Calculator** and the **Cushion Material Properties** Help by pressing the **F3** function key or directly input a stiffness. Additionally, selection of the pile material will automatically select the pile damping parameter which is accessible through **Options, General Options, Damping**. The user may adjust the aforementioned defaults but must enter the initial inputs for the **Pile Length** and cross **Section Area**. For the latter, the user may again employ the **Area Calculator**, shown in Figure 16.29b, which also provides the **Pile Size**, **Perimeter** and **Toe Area** based on pile type and pile dimensional information.

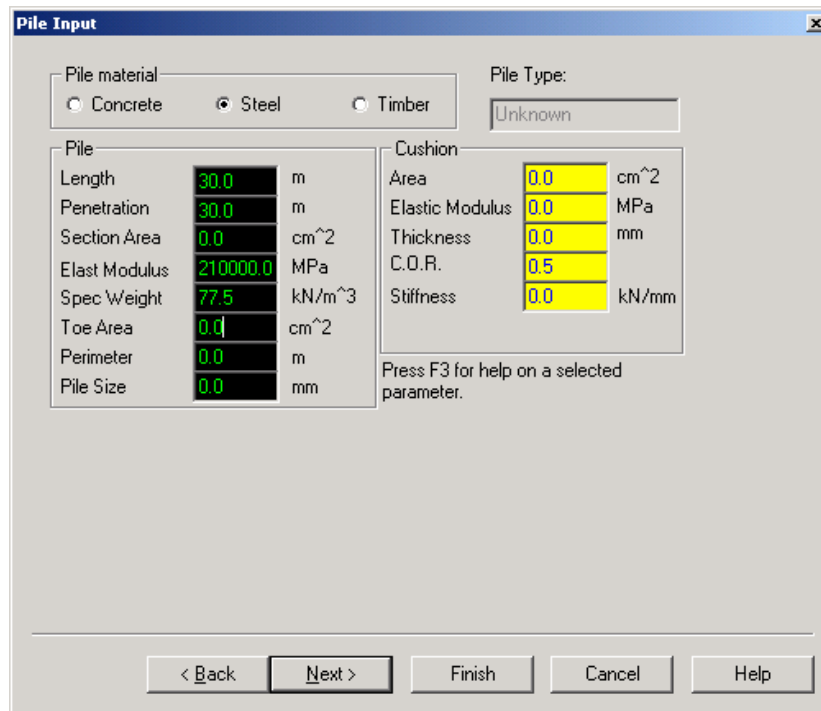


Figure 16.29a: Pile Input Window

It is important to note that for non-uniform piles the input quantities in this window only refer to the pile top. Once the data entry wizard has been finished, the non-uniform quantities must be entered in the **P1** window, accessible after clicking on the pile type drop-down menu. The default values for pile elastic modulus and specific weight may or may not be correct and must be reviewed by the program user. For example, for concrete or timber piles, measurements could indicate other values. Pressing **F3** with the cursor on the

Elastic Modulus or **Specific Weight** input field brings up added Help information. The following information is required for the pile top.

Length is the total pile length in the leads in m (ft). For example, if plans require a pile of 15 m (49 ft) in length but the contractor is driving 18 m (59 ft) long piles, the proper analysis length would be the full 18 m (59 ft). If pile sections are spliced together to form a longer pile, an analysis before and after splicing may be of interest. In such cases, the **Length** may be either the length of a single section before splicing or the combined length after splicing.

Penetration is a required input for Bearing Graph and Inspector's Chart analyses and refers to the analyzed pile toe penetration below grade in m (ft). This measurement must use the same soil grade reference as that of the soil resistance distribution.

Section Area is the pile cross section area at the pile head in cm^2 (inch^2).

Elast Modulus is the elastic modulus of the pile material at the pile head in MPa (ksi).

Spec Weight is the weight per unit volume of the pile material at the pile head in kN/m^3 (lbs/ft^3).

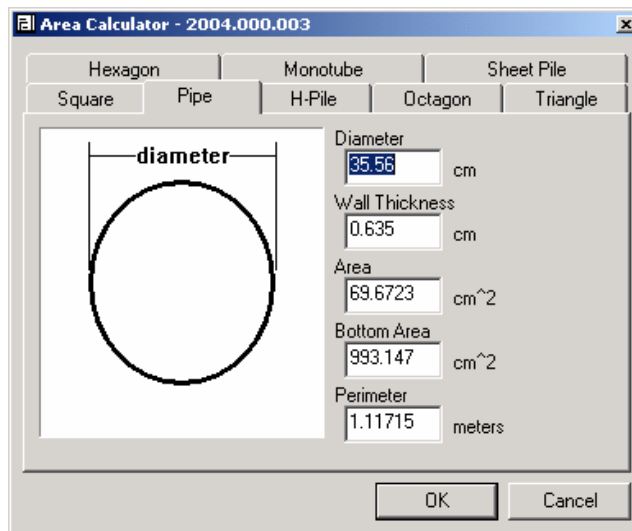


Figure 16.29b: Area Calculator Window

After the pile input is done, clicking on **Next** will open up the **Hammer Cushion** window, as shown in Figure 16.30. GRLWEAP offers an extensive data file for those situations in which the contractor's available equipment is unknown. The data file has been made possible courtesy of the various manufacturers and dealers whose products are listed. Please note that this file is neither complete nor necessarily appropriate for all situations, as the contractor may not follow the manufacturer's recommendations. The required information consists of:

Area is the area of the hammer cushion perpendicular to the load in cm^2 (in^2).

Elastic Modulus is the elastic modulus of the hammer cushion material in MPa (ksi).

Thickness of the hammer cushion. For sandwiched cushions, this is the thickness of the cushion material that corresponds to the elastic modulus in mm (inches). If the entire stack thickness is entered, the combined elastic modulus of the sandwich and the striker plate is not included. If no hammer cushion exists, leave this value and the stiffness value at zero.

C.O.R. is the Coefficient of Restitution of the hammer cushion material.

Stiffness of the hammer cushion in kN/mm (kips/inch). Use of this optional input will override the inputs for area, elastic modulus, and thickness.

Helmet Weight, consisting of the combined weight of the helmet, hammer cushion, striker plate, inserts, and all other components located between the hammer and pile in kN (kips). The input may be zero if there is no helmet mass.

Ideally, the contractor would provide the above drive system data for his actual hammer system; however, if not available, the required hammer cushion data may be selected using one of three different methods:

1. The hammer cushion **Stiffness** and **Coefficient of Restitution** may be known from other analyses and can be input directly into the appropriate fields. In such cases, hammer cushion area, elastic modulus, and thickness are not needed.
2. If some or all of the driving system data is to be retrieved from the program data file, merely pressing **F3** while the cursor is on one of the associated input fields and then clicking on **Manufacturer's Recommended Driving System** opens a listing of the recommended input. The user may transfer the suggestions in whole or part to the input sheet.

3. If the cushion material **area**, **thickness**, and type are known but **modulus of elasticity** and **Coefficient of Restitution** are not, pressing **F3** while the cursor is on the elastic modulus field and then selecting **Cushion Material Properties** brings up a list of frequently used cushion materials and their properties. These values can be transferred directly to the hammer cushion data input fields.

The screenshot shows a software window titled "Hammer Cushion". It is divided into two main sections: "Info. for Selected Hammer" and "Cushion".

Info. for Selected Hammer	
ID:	1
Name:	DELMAG D 5
Type:	OED
Ram Wt.:	4.895 kN
Energy/Power:	14.249 kJ

Cushion	
Area	0.0 cm ²
Elastic Modulus	0.0 MPa
Thickness	0.0 mm
C.O.R.	0.8
Stiffness	0.0 kN/mm
Helmet Weight	0.0 kN

Below the input fields, there is a text prompt: "Press F3 for help on a selected parameter."

At the bottom of the window, there are five buttons: "< Back", "Next >", "Finish", "Cancel", and "Help".

Figure 16.30 Hammer Cushion Window

The **Next** input sections for bearing graph or inspector's chart analyses may be done in the dynamic soil parameters window on the **Main Input Form** or **Soil Profile Input** window, displayed in Figure 16.31. (For Driveability analyses, the **S1 Form** is opened as later discussed.) The most convenient input is through the **ST** analysis in the **Soil Profile Input** window. There, the user first specifies the:

Number of Soil Layers. It is recommended to divide the soil into layers of not more than 3 m (10 ft) thickness for improved accuracy.

Final Penetration Depth is the distance from grade to that depth to which data is to be given in m (ft). The window will at first display the value entered under the pile information. However, it may be changed here with the exception that it cannot be greater than the pile length.

Water Table is the distance from grade in m (ft) where the water table begins. If grade is underwater, enter zero.

Effective Overburden at Grade is the intensity of any overburden pressure in kPa (ksf). For example, in the case of an excavation of limited extent, the depth of excavation times the soil unit weight equals the effective overburden.

For each layer, the analyst then enters:

Either the **Layer Bottom Depth** or the **Layer Thickness** in m (ft).

The layer soil type as either **Granular** (non-cohesive soil for primarily sandy or other coarse grained soils) or **Cohesive** (for clays and silts) and selects as sub types the density or consistency of the layer. For intermediate soil types or non-cohesive silts, it may be conservative to choose “cohesive”, since soil damping is then assigned a higher value. However, under all circumstances, the analyst should review the results obtained from this very simplified analysis.

After clicking **Update**, the program will display an ultimate capacity (**Ru**) and an ultimate shaft resistance (**Rs**) value. These two results pertain to the **Final penetration Depth**, where the ratio **Rs/Ru** is the percentage of shaft resistance and one of the soil resistance inputs generated by the routine. Under no circumstances should these values be used for pile design purposes. The results are based on the following two Methods:

For Non-Cohesive Soils

Using the Effective Stress Method, the unit shaft resistance is $R_s = \beta p_o$, with β being the Bjerrum-Burland beta coefficient as tabulated in Table 16-3 and p_o being the effective vertical stress in a soil layer. The unit toe resistance is $R_t = N_t P_t$, where N_t is a toe bearing capacity coefficient (see Table 16-3) and P_t is the effective overburden pressure at the pile toe. Both **Rs** and R_t are subjected to certain specified limits.

Table 16-3 Soil Parameters in ST Analysis for Granular Soil Types									
Soil Type	SPT N	Friction Angle	Unit Weight	B	N _t	Limit			
		degrees	kN/m ³			R _s		R _t	
						kPa	ksf	kPa	ksf
Very loose	2	25 - 30	13.5	0.203	12.1	24	0.5	2400	50
Loose	7	27 - 32	16.0	0.242	18.1	48	1.0	4800	100
Medium	20	30 - 35	18.5	0.313	33.2	72	1.5	7200	150
Dense	40	35 - 40	19.5	0.483	86.0	96	2.0	9600	200
Very Dense	50+	38 - 43	22.0	0.627	147	190	4.0	19000	400

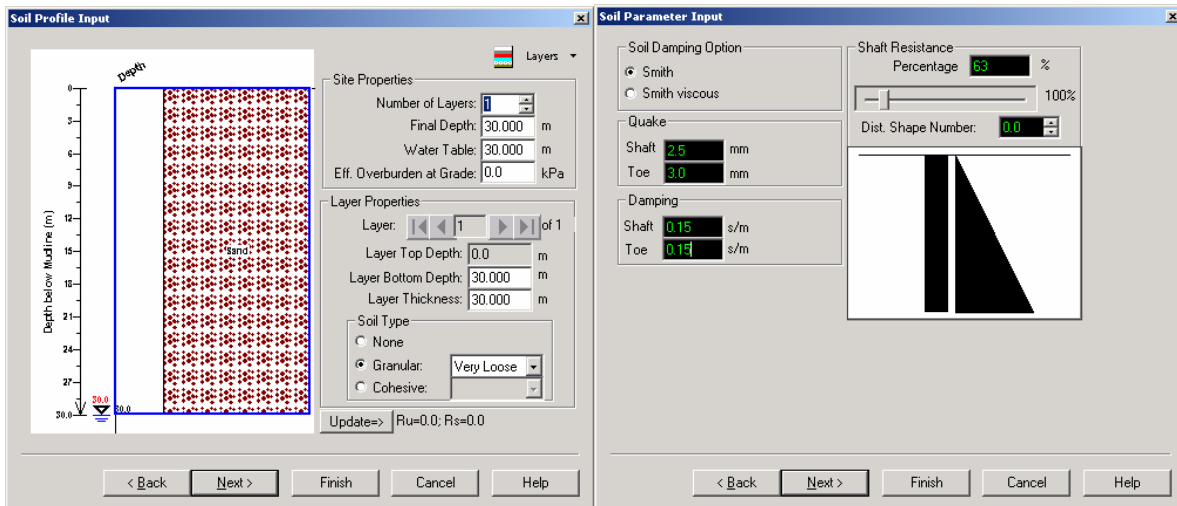
For Cohesive Soils

For cohesive soils, **ST** applies a modified α -method, also called the total stress method, and relies on the unconfined compressive strength (q_u) of the soil layer. The q_u -value and, based on it, the unit shaft resistance and end bearing values are shown as a function of both soil type and a representative N-value in Table 16-4.

Table 16-4 Soil Parameters in ST Analysis for Cohesive Soil Types								
Soil Type	SPT N	Unconfined Compressive Strength		Unit Weight	R _s		R _t	
		kPa	psi	kN/m ³	kPa	ksf	kPa	ksf
Very soft	1	12	1.7	17.5	3.5	0.07	54	1.1
Soft	3	36	5.2	17.5	11	0.23	160	3.3
Medium	6	72	10	18.5	19	0.40	320	6.7
Stiff	12	144	21	20.5	39	0.81	650	14
Very stiff	24	288	42	20.5	64	1.3	1300	27
Hard	32+	384+	56+	19 – 22	77	1.6	1730	36

After the soil types of all layers have been entered, the program computes the percentage and distribution of shaft resistance, the average shaft damping parameter, and the toe quake. These wave equation input values are based on pile penetration, pile size, pile perimeter, and pile toe area. Again, this analysis is not applicable to non-uniform piles. Note that shaft quake and toe damping values are always left at their default values.

It is very important that the user carefully reviews the wave equation input parameters resulting from this very simplified static soil analysis, possible in the Soil Parameters Input window (see Figure 16.31b). Particular attention should be paid to the pile toe area because the shaft resistance percentage and toe quake directly depend on its magnitude. Also, it is recommended to perform comparative analyses, for example, when the soil type does not clearly fall into either the cohesive or granular categories. In such cases, results for both soil types should be obtained and compared. The **ST** generated input parameters should be reviewed once the input wizard has been finished and the main screen is displayed.



Figures 16.31a and b Soil Profile Input Window for Soil Type Based Static Soil Analysis and Soil Parameter Input Window for Bearing Graph Analysis

Help pertaining to both soil type input and soil quakes and damping appears in the program Help Menu under **GRLWEAP Input Forms, Soil Type-Based Input Form** and **GRLWEAP Component Parameters, Soil Parameters**, respectively. It is also recommended that the user carefully review both the PDI Procedures and Models (2005) report and the program Help.

For Bearing Graphs or Inspector's Charts, the user must input between one and ten ultimate capacity values in the **Ultimate Capacity** window shown in Figure 16.32a. Several options are available including values spaced at constant increments (**Incr.**), generated by pressing **Interpolate** to interpolate between the first and last entries, and **Automatic Capacities**, based on the pile cross section properties. It is recommended to analyze capacities that will provide a meaningful bearing graph for both easy and hard driving conditions. The input wizard is now finished. The completed **Main Input** screen should resemble that shown in Figure 16.36. To perform a more complex analysis, additional

inputs may be made by specifying a **Non Uniform Pile** or a more detailed soil resistance distribution in **Variable Resistance Distribution**.

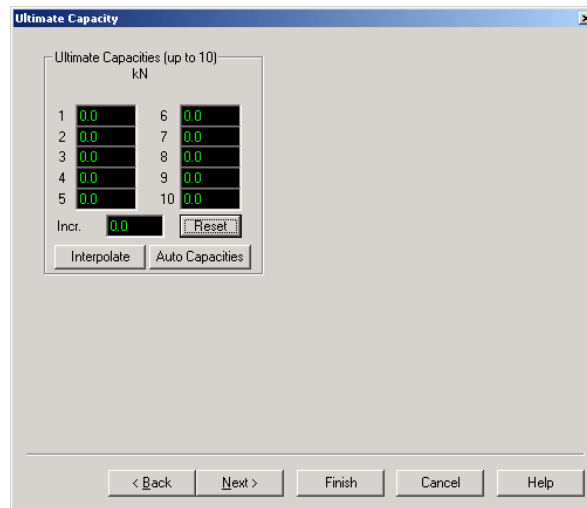


Figure 16.32a Ultimate Capacity Window for Bearing Graph and Inspector's Chart Analyses

For Driveability, instead of Ultimate Capacity values, the analyst must input **Resistance Gain/Loss Factors**. Figure 16.32b shows the related window. The analyst may perform at most 5 analyses at each specified depth and provide at most five associated gain/loss factors for both the pile shaft and toe. These factors are related to the soil resistance parameters to be entered in the **S1 Form**, discussed below. A factor of 1.0 implies no change in soil strength during driving and thus that no resistance gain or loss will be analyzed. A factor less than 1.0 proportionally reduces the resistance values under consideration of their relative setup factors and thus reflects that the soil resistance is lower during driving and increases after pile installation, i.e., soil setup. A factor greater than 1.0 proportionally increases the resistance values and thus reflects the soil relaxation scenario, i.e., the soil resistance is greatest during driving. In most cases, it is sufficient to enter two values for the shaft analysis. The first **Shaft 1**, marked **1**, would be the inverse of the highest soil setup factor entered in the **S1 Form** and would represent the greatest resistance loss during driving along the shaft. The associated end bearing factor, **Toe 1**, would be set to 1.0 to indicate neither gain nor loss of toe resistance during driving. For the second analysis, **Shaft 2** and the associated factor **Toe 2** would be set to 1.0. This

latter input reflects the absence of both gain and loss during driving at each depth analyzed (see Figure 16.32b).

Resistance Gain/Loss Factors	
Shaft	Toe
1 1.0	1 1.0
2 0.0	2 0.0
3 0.0	3 0.0
4 0.0	4 0.0
5 0.0	5 0.0

Incr. 0.0 Reset

Interpolate Auto Capacities

< Back Next > Finish Cancel Help

Figure 16.32b Resistance Gain/Loss Factors Window for Driveability Analyses

Next for Driveability analyses, the GRLWEAP program requires input in the **S1 Form** (see Figure 16.33). Important inputs for each soil layer are (refer also to descriptions for the equivalent bearing graph inputs):

Depth is the soil layer distance below grade or mudline in m (ft).

Unit Shaft Resistance in kPa (ksf) is determined by static geotechnical analysis (e.g., the DRIVEN program or the GRLWEAP **SA** routine). GRLWEAP multiplies this input by the pile perimeter, the segment length, and a soil layer specific gain/loss factor to yield the shaft resistance at the segment.

Toe Resistance in kN (kips) equals the unit end bearing determined by static geotechnical analysis multiplied with the pile effective bottom area.

Skin quake is the shaft quake in mm (inch), usually left at the default value of 2.5 mm (0.1 inch).

Toe quake in mm (inch) is per the Soil Parameter Help.

Skin damping is the shaft damping in s/m (s/ft) as per the Soil Parameter Help.

Toe damping is in s/m (s/ft), usually left at the default value of 0.5 s/m (0.15 s/ft).

Setup factor is based on site specific knowledge and, in conjunction with the resistance gain/loss factor, determines for each soil layer the soil resistance to driving.

The parameters of **Limit Distance** and **Setup Time** allow for a qualitative evaluation of soil strength change during driving interruptions, providing for more detailed analyses of splice time interruptions. These parameters have no influence on results as long as entered **Wait Times** in the **Depths, Modifiers Input Form** (see Figure 16.35) are zero.

Enter Project Title Here
Resistance Distribution Input for Pile 1

General Information
 Pile Length: 30.0 m
 Depths are below ground surface

Add Row Insert Row Delete Row

Depth	Unit Shaft Resist	Toe Resist	Skin Quake	Toe Quake	Skin Damping	Toe Damping	Setup Factor	Limit Distance	Setup Time
m	kPa	kN	mm	mm	s/m	s/m		m	hours
0.000	0.000	0.000	0.000	0.000	0.000	0.000	0.0	0.000	0.0
0.000	0.000	0.000	0.000	0.000	0.000	0.000	0.0	0.000	0.0
30.000	1.000	0.000	0.000	0.000	0.000	0.000	0.0	0.000	0.0

Figure 16.33 S1 Form

Should the user utilize the static analysis (**SA**) routine that is built into the GRLWEAP program to complete the **S1 Form**, clicking the **SA** icon will open the Figure 16.34b window. First, selection of Profile and **New** allows specification of the following quantities in the **Static Analysis General Information** window (refer to Figure 16.34a):

The **Total Number of Soil Layers** to be included between grade and a depth equal to the total pile length in m (ft).

The depth of the **Water Table** in m (ft).

Overburden Pressure in kPa (ksf); see also **ST** above for an explanation of these inputs.

After closing the **Profile** window, the soil layer specific input can be made in the SA window. The following information should be provided:

Layer Bottom Depth or **Layer Thickness** is in m (ft).

If the SPT N-value is known, choose from **Gravel, Sand** (with sub types indicating **Grading** and **Grain Size**), **Silt, Clay**, or **Rock**. Then enter the SPT N-value (not greater than 60), and the program will calculate a unit resistance and a unit weight for the soil layer.

If the SPT N-value is unknown, choose **Other** and either **Cohesive** or **Cohesionless** and then provide the **Unit Weight** in kN/m^3 (kips/ft^3) and the Unit Shaft Resistance (**Friction**) and Unit **End Bearing**, both in kPa (ksf). The program will reduce the input unit weight value below the water table to yield an effective overburden.

Upon user request, the **SA** routine will also fill in the **Other** Parameters, i.e., the input values for quake, damping, setup factor, limit distance and setup time columns. Oftentimes these values do not differ from the default values specified earlier and then can be left at zero. Again, the user should carefully review the automatically generated input values prior to performing the actual wave equation analysis.

The **SA** routine is basically an effective stress method with different approaches for sand, silt and clay. This method is described in detail in the Background Report of the GRLWEAP program (PDI, 2005) and that description should be reviewed prior to using this approach. It differs from the DRIVEN approach, is only applicable to piles with straight sections (not applicable to tapered piles) and should never serve as the sole static soil analysis method for a pile design. In fact, it is always prudent to compare several static analysis methods for an assessment of the range of possible results.

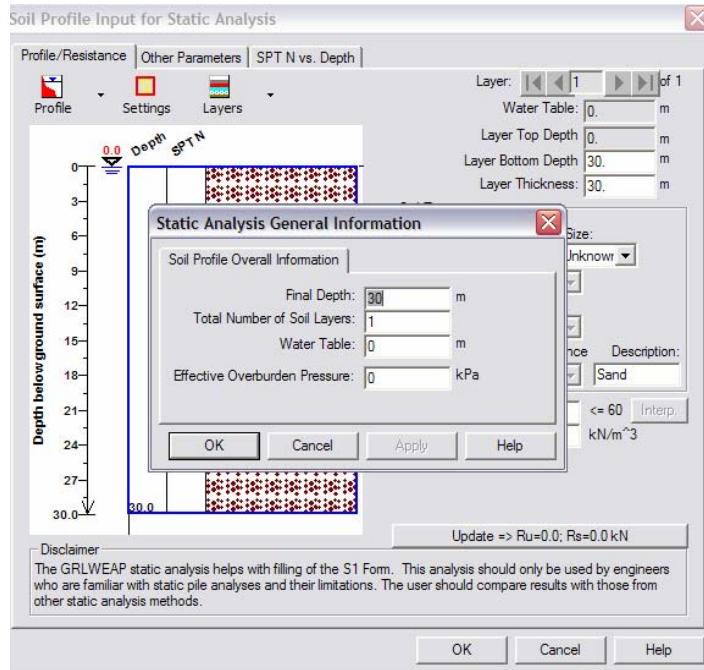


Figure 16.34a Static Analysis General Information

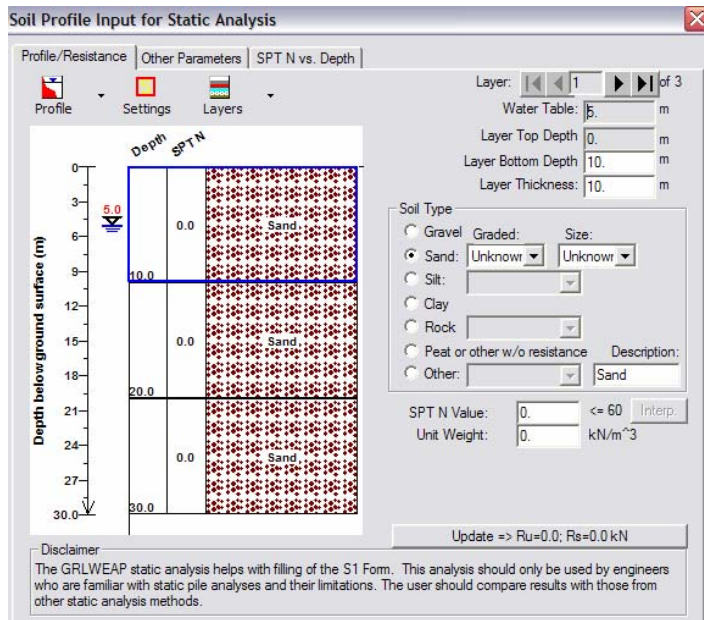


Figure 16.34b Profile/Resistance for Static Analysis

In a Driveability analysis, another required input is found in the **Depths, Modifiers Input Form**, accessible after clicking the **D** icon (see Figure 16.35). This form provides for the input of:

Depth to be analyzed in m (ft) is a required input for at least two different depth values.

The pile **Temporary Length** in m (ft) may be less than or equal to the length value given as the final length input and allows for consideration of a reduced pile length prior to splicing.

Wait Time in hr, which would be applicable if driving were to be interrupted, for example, for splicing operations. This input is only useful for a qualitative assessment of setup effects during the driving interruption, which, in turn, is a function of the **Limit Distance** and the **Setup Time**. (As mentioned, this is rarely needed for highway construction projects.)

Stroke and **Efficiency** allow for variation of these hammer parameters as a function of depth. If not specified, the values input previously will be considered. See also Section 16.7.1.1.

Diesel Pressure input allows for a modification of the hammer setting and/or stroke.

Pile Cushion Coefficient Of Restitution or **Stiffness Factor** can also be varied as a function of depth. For example, and considering the recommendations for new and used pile cushion parameters, the **Stiffness Factor** may be gradually increased from 1.0 to 2.5 if the cushion elastic modulus was specified earlier with the “New” elastic modulus.

Enter Project Parameters
Depth_Driving System Modifications

General Information
File Length: 30.0 m Depth Inc. 2.0 m
Depths are below ground surface

Add Row Insert Row Delete Row Reset

Depth	Temp	Wait	Diesel	Efficiency	Pile Cushion	
	Length	Time			Pressure	Stiffness
m	m	hr	m	%	Factor	
3	0	0	0	0	0	0
6	0	0	0	0	0	0
9	0	0	0	0	0	0
12	0	0	0	0	0	0
15	0	0	0	0	0	0
18	0	0	0	0	0	0
21	0	0	0	0	0	0

Figure 16.35 Depths, Modifiers Input Form

16.7.1 Other GRLWEAP Options

A variety of options exist in the GRLWEAP program for non-standard input, analyses, and out put. The setting of important options is indicated on the Main Input screen (see Figure 16.36). Please refer to the program Help Menu for additional, less frequently used options.

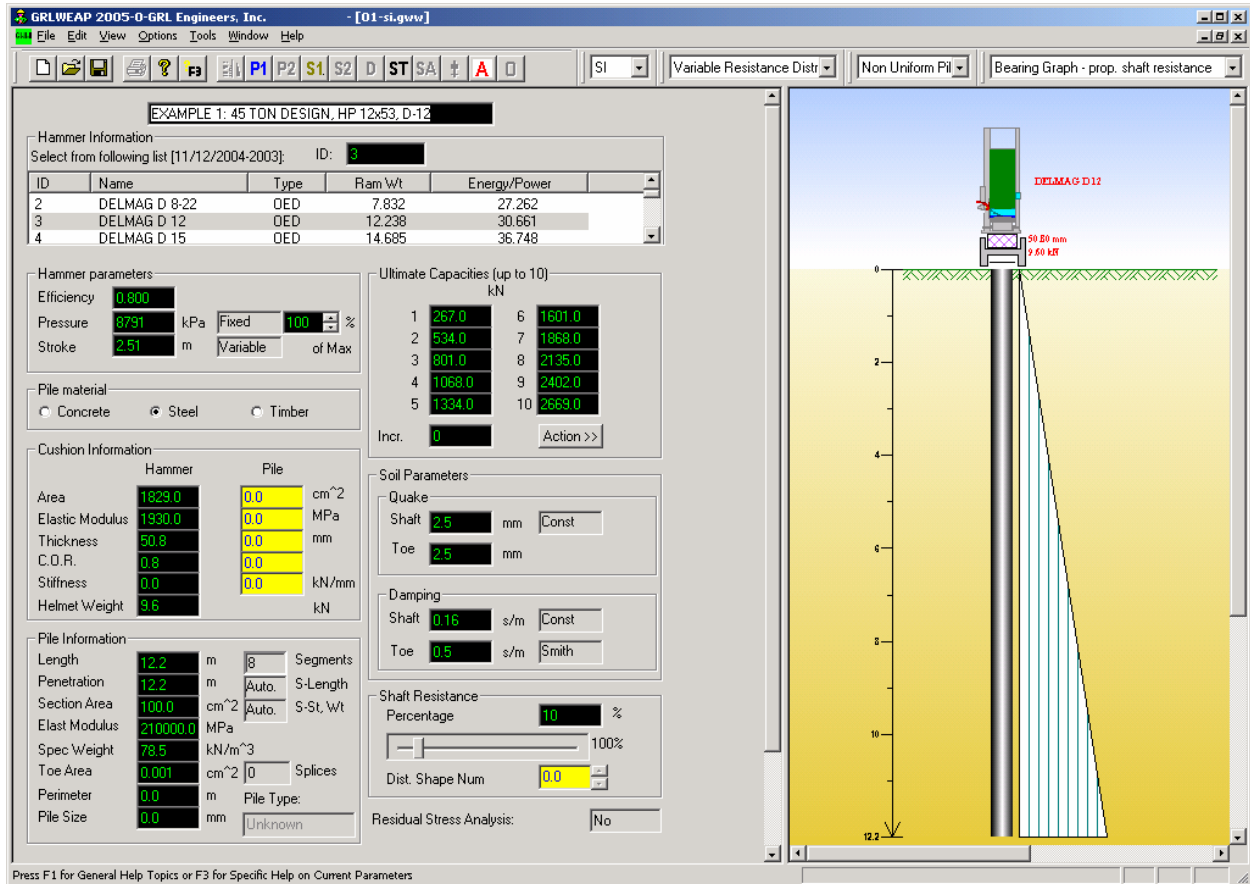


Figure 16.36 Completed Main Input for a Simple Bearing Graph

Important options pertain to the modification of certain hammer parameter, pile model, and soil resistance input. These options are generally accessible by clicking **Options, General Options, or Hammer Parameters, or Pile Parameters, or Soil Parameters.** For proper hammer modeling, the **Efficiency** and **Stroke** values contained in the hammer data file must often be modified. This modification can be done on the Main Input screen below the Hammer Information window. Alternatively, these and other hammer details may be modified by clicking on **Options, Hammer Parameters.** Relevant quantities are explained in the GRLWEAP Help Menu and will not be further discussed here.

Efficiency is one of the most important hammer parameters. The efficiency values in the hammer data file were selected according to the observed average behavior of all hammers of the same type. However, depending on a particular hammer's make or state of maintenance, the hammer may perform differently than assumed, and its parameters should be adjusted accordingly. Furthermore, because of uncertainties in actual hammer performance, greater and lesser efficiency values should be analyzed for conservative stresses and blow counts, respectively. Finally, efficiency should be adjusted for an inclined pile (refer to the Help Menu for recommended efficiency reductions for battered pile driving).

Stroke in m (ft) is a useful performance parameter for single acting diesel hammers whose ram is visible and whose stroke is not equal to the rated value. For other hammers, energy level may be known, but since stroke is equal to energy divided by ram weight, stroke serves as an input for an adjusted hammer energy setting.

Pressure in kPa (psi) is important for diesel hammers when the calculated and observed hammer strokes differ. A new pressure value may be tried for better agreement. Also, if the hammer is physically run at a reduced fuel setting, this value should be reduced in the program.

Several options for **Pile Parameters** are available in GRLWEAP primarily for the purpose of flexibility in pile model generation. The status of many of these options is indicated under the Pile top Information on the Main Input Form.

The **Number of Pile Segments** may either be automatically set based on segment lengths of 1 m (3.3 ft), or the user may use a different number by clicking on **Options, Pile Parameters, Pile Segment Option**. Usually the program default of 1 m (3.3 ft) segment lengths yields satisfactory accuracy. To avoid loss of this computational accuracy, only segments smaller than the default value should be entered. In the Pile Segment Option, the user can also modify the relative length of the segments (the information field marked **S-Length** would then be set to Man. for manual) and enter the segment stiffness and mass values. In the latter case, the information field marked **S-ST, Wt** would be set to manual.

Some piles are spliced with devices that allow for slippage during extension or compression. In **Options, Pile Parameters, Splices**, the user can choose the **Number of Splices** to be modeled and, after clicking on **Update**, edit the entry fields shown in Figure 16.37. For each splice, the user enters the **Distance** in m (ft) of the splice location referenced from the pile top, the **Tension Slack** in mm (ft), i.e. the distance that the splice can extend without transmitting a tension force, the **C.O.R.** or coefficient of restitution for the spring representing the spliced section, and the **Compressive Slack** in mm (ft), i.e., the distance that the splice can compress without transmitting a compressive force. The Main Input Form indicates the selected number of splices; the visual of the hammer, driving system, pile, and soil model on the Main Input Form also indicates a splice with a slight gap in the pile representation. Note that neither an uncracked welded splice of a steel pile nor a well performing epoxy splice of a concrete pile requires slack modeling. These splices do not allow for slippage and, therefore, should be modeled as a uniform pile section and not as a splice with a slack.

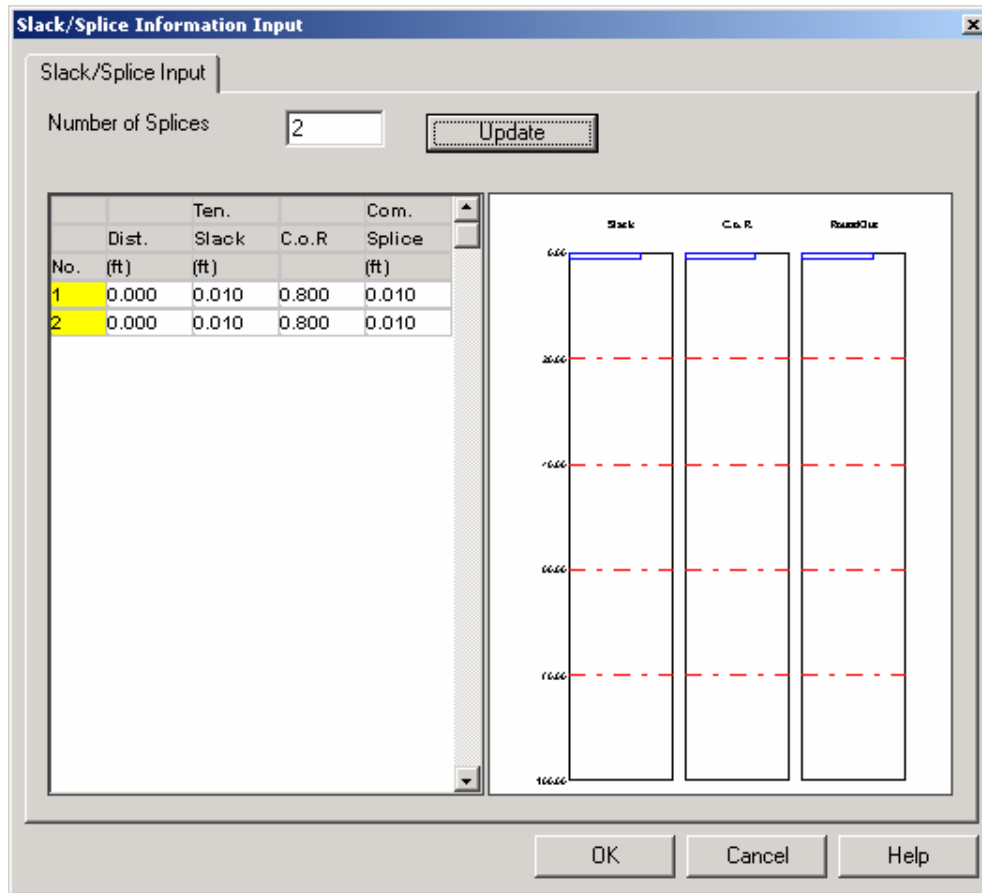


Figure 16.37 Slack/Splice Information Input Window

Non-Uniform Piles are modeled by selecting **Non-Uniform Pile** from the Pile Type drop-down menu and activating the **P1** window. The user should complete the necessary information by specifying pile variations and adding the necessary number of rows immediately above and below a change of cross sectional area (**X-Area**), elastic modulus (**E. Modulus**), specific weight (**Spec. Wt.**), **Perimeter**, and **Strength** (see Figure 16.38). Note that **Perimeter** is needed for the computation of total shaft resistance in Driveability analyses. The **Strength** input is needed for the listing of critical rather than absolute maximum stresses in the result summary for piles consisting of materials of different strengths. Critical stress is defined as one which has the highest stress to strength ratio. Note that entry of strength information will not generate warnings when the stresses exceed the strength levels.

A somewhat different pile option, and alternate type of analysis, is the **Residual Stress Analysis (RSA)**. This option can be set in **Options, General Options, Numeric** (see Figure 16.39). The input number indicates the maximum number of repeat analyses allowed, with a "1" representing the absolute limit of 100 cycles.

Potentially important for large piles is the input of an adjusted **Hammer** and **Pile Gravity** (see Figure 16.39). The default gravitational constant is 9.81 m/s^2 (32.17 ft/s^2). The default value would represent a vertically driven pile above the water table. If the static weight is less due to either pile inclination or buoyancy, this value should be reduced using **Options, General Options, Numeric**. Note that the hammer and pile mass magnitudes will not be affected by this change of gravitational constant.

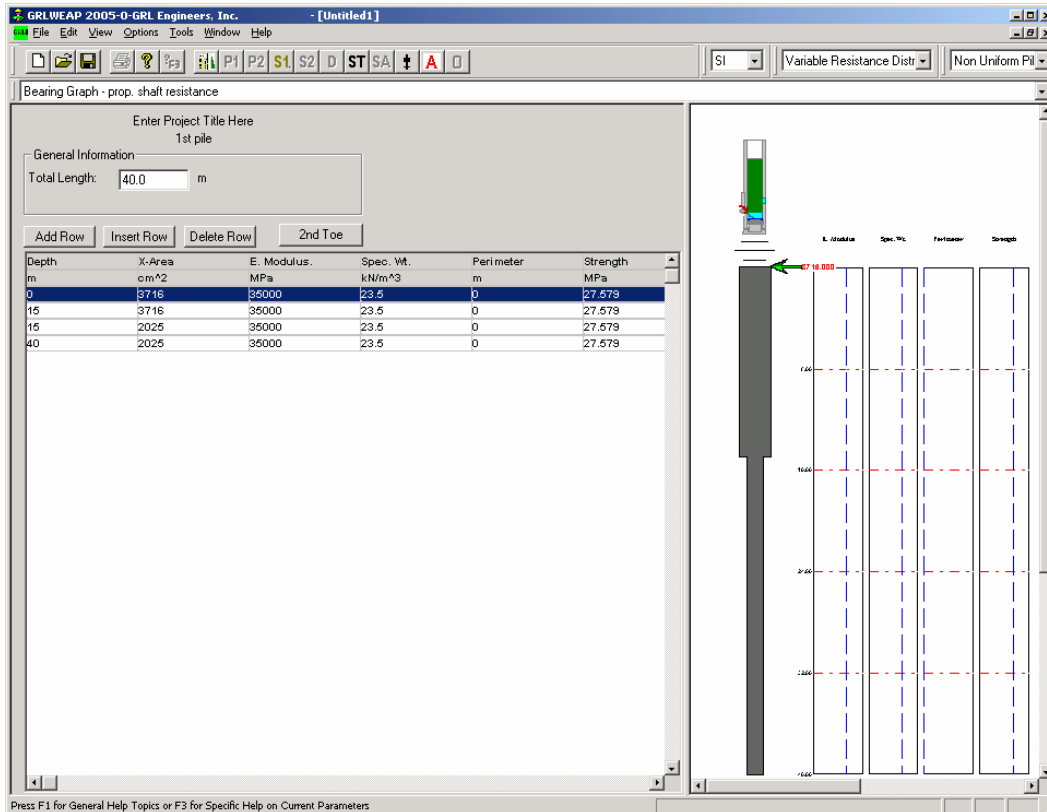


Figure 16.38 Data Entry Screen for Non-Uniform Piles

Soil parameter options, like pile options, allow for increased input flexibility. Under **Options, Soil Parameters**, it is possible to enter individual ultimate capacity, damping, and quake values for each pile segment. Use of these options causes the corresponding field labels in the soil input section of the Main Input Form to read “Variable”.

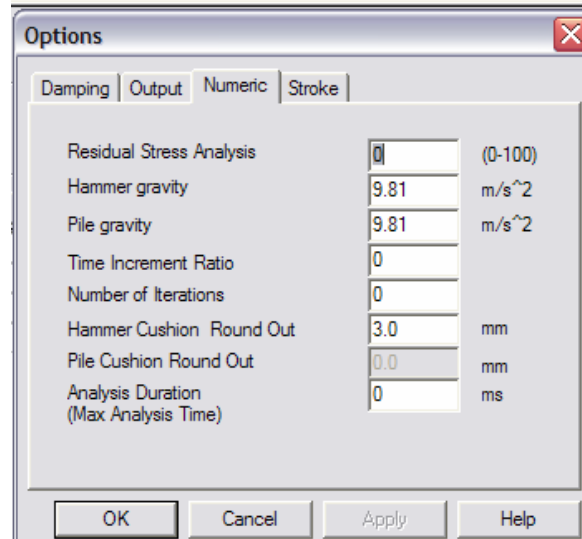


Figure 16.39 Numeric Options Window

The **Damping Option**, accessible in **Options, General Options, Damping** (Figure 16.40), is rarely used for routine applications and is more useful for the researcher. In general, the **Soil Damping** is set to **Smith** damping, and only if the **Residual Stress Analysis** option is invoked should **Smith viscous** damping be chosen. **Hammer Damping** and **Pile Damping Options** have been preset to a percentage of the impedance of the ram and hammer cushion and the pile, respectively, though the preset values may be replaced with small nonnegative integers. Given a negative input, the program will read a zero value. For the pile material, the program automatically chooses values of 1, 2 and 5 for steel, concrete and wood, respectively. Another pile material (e.g., plastic piles) may require other, possibly higher inputs. Although not enough is known about these parameters, their effect on the computed results is relatively insignificant.

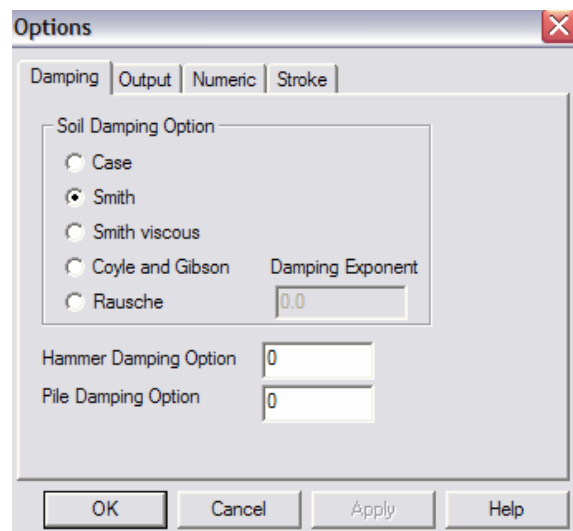


Figure 16.40 Damping Options Window

The **Stroke Option**, important for diesel hammers, is accessible in **Options, General Options, Stroke** (see Figure 16.41). For any diesel hammer, the stroke is a function of fuel settings, pile mass and stiffness, and soil resistance. The stroke option allows the user to control whether the program will analyze a fixed stroke or calculate the stroke (default) based on the combustion pressure provided in either the hammer database or the user modified input. A fixed stroke can either be analyzed with an iteratively adjusted combustion pressure, such that upstroke equals down stroke, or with a single impact whose upstroke is then potentially different from its down stroke. On the Main Input Form below the Hammer Information window, this selected stroke option is identified. The selection of the Stroke Option is particularly important for Inspector's Chart analyses, and the reading of the associated Help is strongly recommended.

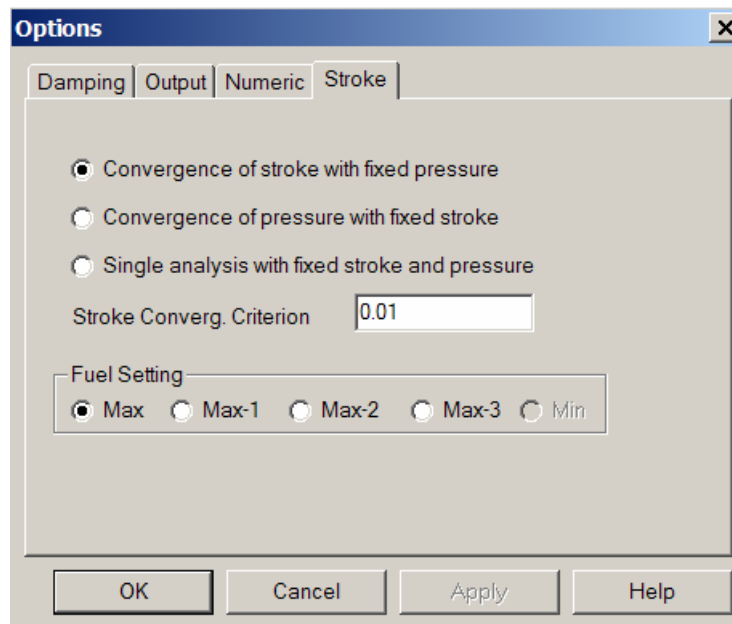


Figure 16.41 Stroke Options Window for Diesel Hammers

The Stroke Options window also allows for a selection of Fuel Settings for those diesel hammers that have stepwise adjustable fuel pumps. Alternatively, the corresponding fractions of the maximum combustion pressures can be selected on the Main Input Form. As noted in Section 16.6.3, analyzing a hammer with a high combustion pressure, even if the high stroke is the result of pre-ignition, may lead to high calculated transferred energies and, therefore, non-conservative capacity predictions and conservative stress predictions. On the other hand, if the observed hammer stroke is relatively low and friction (which should be modeled with a reduced hammer efficiency) has been eliminated as a reason for the low stroke, a reduced combustion pressure presents a reasonable analysis option. Because of the potential for a capacity overprediction due to excessive pressure adjustment, the inspector's chart option does not increase the combustion pressure above the value in the hammer data

file despite the presence of any values for high stroke analyses in the **”Convergence of pressure with fixed stroke.”**

16.8 GRLWEAP OUTPUT

The GRLWEAP program offers several output options that may be invoked or modified using **Options, General Options, Output** as displayed in Figure 16.42. The box labeled **Type** allows for selection of certain variables (e.g., force, velocity, stress) at a number of different segments. The user may opt to plot these variables as a function of time or create a table for transfer to other programs. Of particular interest is the plotting of pile top force and proportional velocity vs. time for comparison with PDA measurements.

The Numerical box underneath allows for the control of the numerical output in one of three means. Choosing **Minimum** (default for driveability analyses) will exclude the extrema tables that are included in the **Normal** output selection. The extrema tables are very helpful when investigating the location of maximum stress values, and even though they may make the output very long, it is often desirable to revert to the **Normal** option, even for driveability analyses. Another worthy candidate for the normal output is the multimaterial pile. The final numerical option, **Debug** generates so much numerical output that it is rarely needed for real applications.

After an analysis has been run, clicking the **O** (Output) icon transfers control to the output program in which several output modes (depending on output and analysis options) of the **Project Summary** (containing several important parameters and title components) become available: **Bearing Graph or Driveability, Variables vs. Time** and **Numeric results**.

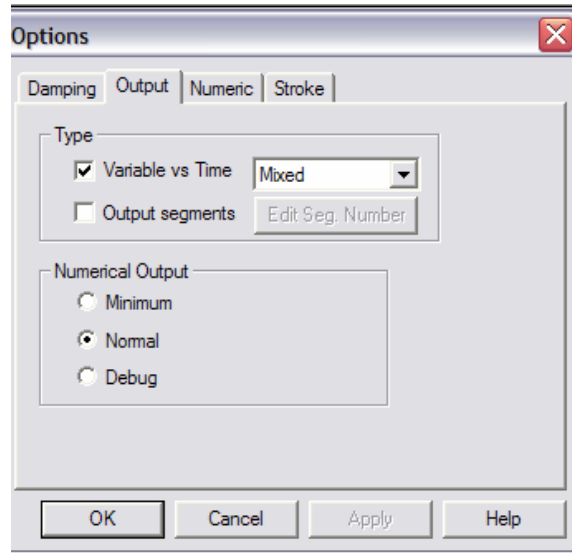


Figure 16.42 Output Options Window

The Numerical GRLWEAP Output, or Numeric results, is the most important output. It begins with a listing of file names used for input and the input file (*.GWW). There follows a disclaimer pointing out some of the uncertainties associated with wave equation analyses. The user is urged to check that the correct data file is used and consider the disclaimer when drawing conclusions from analysis results.

GRLWEAP: WAVE EQUATION ANALYSIS OF PILE FOUNDATIONS

Version 2005					
SI Units					
FHWA - GRLWEAP EXAMPLE #1					
Hammer Model:		D 12-42		Made by: DELMAG	
No.	Weight kN	Stiffn kN/mm	CoR	C-Slk mm	Dampg kN/m/s
1	3.137				
2	3.137	21506.7	1.000	3.0480	
3	3.137	21506.7	1.000	3.0480	
4	3.137	21506.7	1.000	3.0480	
Imp Block	2.746	11046.8	0.900	3.0400	
Helmet	7.600	10699.5	0.800	3.0000	75.2
Combined Pile Top		1836.7			
HAMMER OPTIONS:					
Hammer File ID No.	38		Hammer Type	OE Diesel	
Stroke Option	FxdP-VarS		Stroke Convergence Crit.	0.010	
Fuel Pump Setting	Maximum				
HAMMER DATA:					
Ram Weight	(kN)	12.55	Ram Length	(mm)	2628.90
Maximum (Eq) Stroke	(m)	3.60			
Rated (Eq) Stroke	(m)	3.60	Efficiency	0.800	
Maximum Pressure	(kPa)	11311.92	Actual Pressure	(kPa)	11307.00
Compression Exponent		1.350	Expansion Exponent	1.250	
Ram Diameter	(mm)	299.97			
Combustion Delay	(s)	0.00200	Ignition Duration	(s)	0.00200
The Hammer Data Includes Estimated (NON-MEASURED) Quantities					
HAMMER CUSHION			PILE CUSHION		
Cross Sect. Area	(cm ²)	1464.00	Cross Sect. Area	(cm ²)	0.00
Elastic-Modulus	(MPa)	3654.2	Elastic-Modulus	(MPa)	0.0
Thickness	(mm)	50.00	Thickness	(mm)	0.00
Coeff of Restitution		0.800	Coeff of Restitution	0.000	
RoundOut	(mm)	3.0	RoundOut	(mm)	0.0
Stiffness	(kN/mm)	10699.5	Stiffness	(kN/mm)	0.0

Figure 16.43 Hammer Model, Hammer Options, and Driving System Output

The first page of output, shown in Figure 16.43, lists the hammer and drive system components used in the analysis. Hence hammer model, stroke, and efficiency, helmet weight, and hammer and pile cushion properties including thickness, area, elastic modulus, and coefficient of restitution are but a few of the input details printed on this page.

The second page of output, presented in Figure 16.44, summarizes the pile and soil model used in the analysis. A brief summary of the pile profile is provided at the top of the page and includes the pile length, area, modulus of elasticity, specific weight, perimeter, material strength (normally 0 for uniform piles), wave speed, and pile impedance (EA/c). A detailed summary of the pile and soil model follows the pile profile. The detailed pile model includes the number of pile segments, their weight and stiffness, and any compression slacks (C-Slk) or tension slacks (T-Slk) with associated coefficient of restitution (C.O.R.). The listing also shows segment bottom depth (LbTop) and the averages of both segment circumference and cross sectional area.

The summarized soil model includes the soil static soil resistance distribution (Soil-S), the soil damping parameters (Soil-D) along the shaft and at the pile toe, as well as the soil shakes along the shaft and at the pile toe. Additional pile and soil modeling options, including the percent shaft resistance, are summarized below in Figure 16.44.

On the third page, shown in Figure 16.45, an extrema table is printed for each pile segment number. This extrema output is printed for each analyzed ultimate capacity and includes:

No	the pile segment number
mxTForce	the maximum tension (negative) force in kN (kips)
mxCForce	the maximum compression force in kN (kips)
mxTStrss	the maximum tension (negative) stress in MPa (ksi)
mxCStrss	the maximum compression stress in MPa (ksi)
max V	the maximum velocity in m/s (ft/s)
max D	the maximum displacement in mm (inch)
max Et	the maximum transferred energy in kJ (kip-ft)

The "t" values following the extreme values are times in milliseconds relative to hammer impact. Note that tension is shown as a negative in these tables. For the analysis of diesel hammers, the iteration on hammer stroke is indicated beneath the extrema table information followed by the maximum combustion pressure analyzed in kPa (psi).

For bearing graph analyses, GRLWEAP concludes by printing a summary table for all input ultimate capacities after the extrema table listing for the final ultimate capacity analysis. The summary table is illustrated in Figure 16.46 and includes the analyzed ultimate capacity, R_{ut} , and corresponding penetration resistance (BI Ct), analyzed hammer stroke (for diesel hammers, both the down stroke and the rebound stroke), maximum tension stress (negative, Ten Str), maximum compression stress (Comp Str), maximum transferred energy (ENTHRU), and, for diesel hammers, hammer operating speed (BI Rt). The indicators "i t" locate where (pile segment number) and when (time after impact in ms) the extreme stress values occur.

PILE PROFILE:

Toe Area (cm2) 995.382 Pile Type Pipe
 Pile Size (cm) 35.600

L b Top	Area	E-Mod	Spec Wt	Perim	Strength	Wave Sp	EA/c
m	cm2	MPa	kN/m3	m	MPa	m/s	kN/m/s
0.00	87.5	210000.	78.50	1.118	0.00	5123.	358.52
20.00	87.5	210000.	78.50	1.118	0.00	5123.	358.52

Wave Travel Time 2L/c (ms) 7.808

File and Soil Model						Total Capacity Rut			200.0		
No.	Weight	Stiffn	C-Slk	T-Slk	CoR	Soil-S	Soil-D	Quake	LbTop	Perim	Area
	kN	kN/mm	mm	mm		kN	s/m	mm	m	m	cm2
1	0.687	1837.	3.000	0.000	0.85	0.0	0.164	2.54	1.00	1.1	87.5
2	0.687	1837.	0.000	0.000	1.00	0.5	0.164	2.54	2.00	1.1	87.5
3	0.687	1837.	0.000	0.000	1.00	1.4	0.164	2.54	3.00	1.1	87.5
4	0.687	1837.	0.000	0.000	1.00	2.3	0.164	2.54	4.00	1.1	87.5
5	0.687	1837.	0.000	0.000	1.00	3.3	0.164	2.54	5.00	1.1	87.5
6	0.687	1837.	0.000	0.000	1.00	4.2	0.164	2.54	6.00	1.1	87.5
7	0.687	1837.	0.000	0.000	1.00	5.1	0.164	2.54	7.00	1.1	87.5
8	0.687	1837.	0.000	0.000	1.00	6.0	0.164	2.54	8.00	1.1	87.5
9	0.687	1837.	0.000	0.000	1.00	7.0	0.164	2.54	9.00	1.1	87.5
10	0.687	1837.	0.000	0.000	1.00	7.9	0.164	2.54	10.00	1.1	87.5
11	0.687	1837.	0.000	0.000	1.00	8.8	0.164	2.54	11.00	1.1	87.5
12	0.687	1837.	0.000	0.000	1.00	9.8	0.164	2.54	12.00	1.1	87.5
13	0.687	1837.	0.000	0.000	1.00	10.7	0.164	2.54	13.00	1.1	87.5
14	0.687	1837.	0.000	0.000	1.00	11.6	0.164	2.54	14.00	1.1	87.5
15	0.687	1837.	0.000	0.000	1.00	12.6	0.164	2.54	15.00	1.1	87.5
16	0.687	1837.	0.000	0.000	1.00	13.5	0.164	2.54	16.00	1.1	87.5
17	0.687	1837.	0.000	0.000	1.00	14.4	0.164	2.54	17.00	1.1	87.5
18	0.687	1837.	0.000	0.000	1.00	15.4	0.164	2.54	18.00	1.1	87.5
19	0.687	1837.	0.000	0.000	1.00	16.3	0.164	2.54	19.00	1.1	87.5
20	0.687	1837.	0.000	0.000	1.00	17.2	0.164	2.54	20.00	1.1	87.5
Toe						32.0	0.490	5.93			

13.731 kN total unreduced pile weight (g= 9.81 m/s2)
 13.731 kN total reduced pile weight (g= 9.81 m/s2)

PILE, SOIL, ANALYSIS OPTIONS:

Uniform pile Pile Segments: Automatic
 No. of Slacks/Splices 0 Pile Damping (%) 1
 Pile Penetration (m) 19.00 Pile Damping Fact.(kN/m/s) 7.170
 % Shaft Resistance 84
 Soil Damping Option Smith
 Max No Analysis Iterations 0 Time Increment/Critical 160
 Output Time Interval 1 Analysis Time-Input (ms) 0
 Output Level: Normal
 Gravity Mass, Pile, Hammer: 9.810 9.810 9.810
 Output Segment Generation: Automatic

Figure 16.44 Pile, Soil, and Analysis Options

GRL Engineers, Inc. GRLWEAP(TM) Version 2005

Rut= 200.0, Rtoe = 32.0 kN, Time Inc. =0.076 ms

No	mxTForce kN	t ms	mxCForce kN	t ms	mxTStrss MPa	t ms	mxCStrss MPa	t ms	max V m/s	t ms	max D mm	t ms	max Et kJ
1	0.	0	1050.	2	0.0	0	120.1	2	3.71	10	76.7	52	20.87
2	-128.	10	1054.	2	-14.6	10	120.5	2	3.43	10	76.7	47	20.88
3	-160.	9	1057.	2	-18.3	9	120.8	2	3.32	9	76.7	47	20.84
4	-148.	9	1060.	2	-16.9	9	121.2	2	3.38	9	76.6	47	20.70
5	-131.	9	1061.	3	-14.9	9	121.3	3	3.44	9	76.6	47	20.47
6	-117.	9	1059.	3	-13.3	9	121.1	3	3.49	9	76.6	47	20.15
7	-105.	9	1058.	3	-12.1	9	121.0	3	3.54	9	76.6	47	19.74
8	-94.	9	1054.	3	-10.8	9	120.5	3	3.60	8	76.5	47	19.25
9	-81.	8	1048.	3	-9.3	8	119.8	3	3.67	8	76.5	47	18.66
10	-66.	8	1042.	4	-7.5	8	119.1	4	3.73	8	76.5	47	17.98
11	-59.	8	1032.	4	-6.8	8	118.0	4	3.77	8	76.4	47	17.20
12	-63.	8	1020.	4	-7.2	8	116.7	4	3.80	8	76.4	48	16.33
13	-65.	7	1007.	4	-7.4	7	115.2	4	3.85	7	76.4	48	15.36
14	-62.	7	990.	4	-7.1	7	113.2	4	3.91	7	76.4	48	14.29
15	-59.	7	970.	5	-6.7	7	110.9	5	3.95	7	76.4	48	13.13
16	-69.	7	945.	5	-7.9	7	108.0	5	3.97	7	76.4	48	11.87
17	-83.	7	907.	5	-9.4	7	103.8	5	4.03	6	76.4	48	10.51
18	-75.	7	826.	5	-8.6	7	94.5	5	4.21	6	76.4	48	9.05
19	-65.	14	662.	5	-7.5	14	75.7	5	4.47	6	76.4	48	7.49
20	-22.	14	395.	5	-2.5	14	45.2	5	4.77	6	76.4	48	6.68

(Eq) Strokes Analyzed and Last Return (m):
 3.60 1.23 1.74 1.56 1.61 1.60 1.60

Max. Combustion Pressure 11307.0 kPa

Figure 16.45 Extrema Table Output

Rut kN	Bl Ct b/m	Stroke down	(m) up	Ten Str MPa	i	t	Comp Str MPa	i	t	ENTHRU kJ	Bl Rt b/min
200.0	13.6	1.60	1.60	-18.26	3	9	121.27	5	3	20.9	51.8
400.0	31.9	1.87	1.86	-12.48	8	41	146.64	6	3	18.7	47.9
600.0	57.2	2.06	2.07	-17.71	9	30	161.07	5	3	17.8	45.5
800.0	83.9	2.20	2.21	-14.78	6	29	170.98	5	3	17.2	44.1
1000.0	113.4	2.33	2.31	-7.55	6	23	179.59	5	2	17.3	43.0
1200.0	160.3	2.43	2.41	-9.43	4	18	186.19	5	2	17.8	42.0
1300.0	192.4	2.49	2.47	-16.11	4	18	189.45	5	2	18.0	41.6
1480.0	271.7	2.57	2.56	-20.57	5	18	194.61	4	2	18.3	40.9
1600.0	352.0	2.62	2.61	-18.29	6	17	197.72	4	2	18.5	40.5
1800.0	531.6	2.69	2.69	-16.48	5	18	202.06	4	2	18.9	39.9

Figure 16.46 Final Summary for Bearing Graph Analysis

Review of the "printed output" can be accomplished on the computer screen before printing. This review is extremely important as it can point out inadvertent omissions or erroneous input data. The reviewer should carefully check ram weight, stroke, efficiency, cushion

stiffness, pile mass and stiffness values, soil parameters, *etc.* Furthermore, any error messages or warnings issued by the program should be checked for relevance to the results.

16.9 PLOTTING OF GRLWEAP RESULTS

The summary table results are usually presented in the form of a bearing graph relating the ultimate capacity to penetration resistance. Maximum compression and tension stresses versus penetration resistance are also plotted in the bearing graph. A typical GRLWEAP bearing graph was presented in Figure 16.4 as part of Example 1.

The wave equation bearing graph or inspector's chart should be provided for the resident construction engineer, pile inspector, and the contractor.

16.10 SUGGESTIONS FOR PROBLEM SOLVING

Table 16-5 summarizes some of the field problems that can be solved through use of wave equation analysis. Field problems may arise due to soil, hammer, driving system, and pile conditions that are not as anticipated or unknown. Of course, all possibilities cannot be treated in this summary. Sometimes, the performance of the wave equation program may produce an unexpected or apparently useless result and a corrective action may be required. A number of such problems together with suggested solutions are listed in Table 16-6. Further information may also be found in PDI, 2005 and in the program's Help Menu.

TABLE 16-5 SUGGESTED USE OF THE WAVE EQUATION TO SOLVE FIELD PROBLEMS	
Problem	Solution
Concrete pile spalling or slabbing near pile head.	Perform wave equation analysis; find pile head stress for observed blow count and compare with allowable stresses. If high calculated stress, add pile cushioning. If low calculated stress, investigate pile quality, hammer performance, hammer-pile alignment.
Concrete piles develop complete horizontal cracks in easy driving.	Perform wave equation analysis; check tension stresses along pile (extrema tables) for observed blow counts. If high calculated tension stresses, add cushioning or reduce stroke. If low calculated tension stresses, check hammer performance and/or perform measurements.
Concrete piles develop complete horizontal cracks in hard driving.	Perform wave equation analysis; check tension stresses along pile (extrema table). If high calculated tension stresses, consider heavier ram. If low calculated tension stresses, take measurements and determine quakes, which are probably higher than anticipated.
Concrete piles develop partial horizontal cracks in easy driving.	Check hammer-pile alignment since bending may be the problem. If alignment appears to be normal, tension and bending combined may be too high; solution as for complete cracks.

TABLE 16-5 SUGGESTED USE OF THE WAVE EQUATION TO SOLVE FIELD PROBLEMS (CONTINUED)	
Problem	Solution
Steel pile head deforms, timber pile top mushrooms.	Check helmet size/shape; check steel strength; check evenness of pile head, banding of timber pile head. If okay, perform wave equation and determine pile head stress. If calculated stress is high, reduce hammer energy (stroke) for low blow counts; for high blow counts different hammer or pile type may be required.
Unexpectedly low blow counts during pile driving.	Investigate soil borings; if soil borings do not indicate soft layers, pile may be damaged below grade. Perform wave equation and investigate both tensile stresses along pile and compressive stresses at toe. If calculated stresses are acceptable, investigate possibility of obstructions / uneven toe contact on hard layer or other reasons for pile toe damage.
Higher blow count than expected.	Review wave equation analysis and check that all parameters were reasonably considered. Check hammer and driving system. If no obvious defects are found in driving system, field measurements should be taken. Problem could be pre-ignition, preadmission, low hammer efficiency, soft cushion, large quakes, high damping, greater soil strengths, or temporarily increased soil resistance with later relaxation (perform restrike tests to check).
Lower blow count than expected.	Probably soil resistance is lower than anticipated. Perform wave equation and assess soil resistance. Perform restrike testing (soil resistance may have been lost due to pile driving), establish setup factor and drive to lower capacity. Hammer performance may also be better than anticipated, check by measurement.

TABLE 16-5 SUGGESTED USE OF THE WAVE EQUATION TO SOLVE FIELD PROBLEMS (CONTINUED)

Problem	Solution
<p>Diesel hammer stroke (bounce chamber pressure) is higher than calculated.</p>	<p>The field observed stroke exceeds the wave equation calculated stroke by more than 10%. Compare calculated and observed blow counts. If observed are higher, soil resistance is probably higher than anticipated. If blow counts are comparable, reanalyze with higher combustion pressure to match observed stroke <u>and</u> assure that pre-ignition is not a problem, e.g., by measurements.</p>
<p>Diesel hammer stroke (bounce chamber pressure) is lower than calculated.</p>	<p>The field observed stroke is less than 90% of the stroke calculated by the wave equation. Check that ram friction is not a problem (ram surface should have well lubricated appearance). Compare calculated and observed blow count. If observed one is lower, soil resistance is probably lower than anticipated. If blow counts are comparable, reanalyze with lower combustion pressure to match observed hammer stroke.</p>

TABLE 16-6 WAVE EQUATION ANALYSIS PROBLEMS

Problem	Solution
Cannot find hammer in data file.	Contact the hammer manufacturer or the author(s) of the wave equation program. Pile Dynamics, Inc., for example, regularly updates and posts its hammer data file on its web page. Alternatively, the user may utilize a hammer of same type and of similar ram weight and energy rating and modify its data to match the unlisted hammer's specifications as closely as possible.
Cannot find an acceptable hammer to drive pile within driving stress and penetration resistance limits.	Both calculated stresses and blow counts are too high. Increase pile impedance or material strength or redesign for lower capacities. Alternatively, check whether soil has potential for setup. If soil is fine grained or known to exhibit setup gains after driving, then end of driving capacity may be chosen lower than required. Capacity should be confirmed by restrrike testing or static load testing.
Diesel hammer analysis with low or zero transferred energies.	Probably soil resistance too low for hammer to run. Try higher capacities.
Unknown hammer energy setting.	Perform analyses until the cushion thickness/hammer energy setting combination yields acceptable stresses with minimum cushion thickness. Specify that the corresponding cushion thickness and hammer fuel setting be used in the field and their effectiveness verified by measurements.
Cannot find a suggested set of driving system data.	Contact contractor, equipment manufacturer, or use data for similar systems.
Unknown pile cushion thickness.	Perform analyses until cushion thickness/hammer energy setting combination is found that yields acceptable stresses with minimum cushion thickness. Specify that this thickness be used in the field and its effectiveness verified by measurements.

TABLE 16-6 WAVE EQUATION ANALYSIS PROBLEMS (CONTINUED)

Problem	Solution
Calculated pile cushion thickness is uneconomical.	In order to limit stresses, an unusually thick pile cushion was needed for pile protection. Try to analyze with reduced energy settings. For tension stress problems, energy settings often can be increased after pile reaches sufficient soil resistance.
Calculated driving times are unrealistically high or low.	The calculation of driving times is very sensitive, particularly at high blow counts. Use extreme caution when using these results for cost estimation. Also, no interruption times are included and the estimate is only applicable to non-refusal driving.
Wave equation calculated energy and/or forces are difficult to match with field measurements.	In general, it is often difficult to make all measured quantities agree with their calculated equivalents. A 10% agreement should be sufficient. Parameters to be varied include hammer efficiency, diesel hammer combustion pressure, external combustion hammer stroke, coefficients of restitution, hammer cushion properties for steel piles, pile cushion properties for concrete piles, and pile top properties for timber piles.

REFERENCES

- American Association of State Highway and Transportation Officials, [AASHTO] (2002). Standard Specifications for Highway Bridges, Seventeenth Edition, Washington, D.C.
- Bielefeld, M.W. and Middendorp, P. (1992). Improved Pile Driving Prediction for Impact and Vibratory Hammers, Proceedings of the 4th International Conference on the Application of Stresswave Theory to Piles, The Hague, A.A. Balkema Publishers.
- Blendy, M.M. (1979). Rational Approach to Pile Foundations. Symposium on Deep Foundations, ASCE National Convention.
- Cheney, R.S. and Chassie, R.G. (2000). Soils and Foundations Workshop Reference Manual. Publication No. FHWA H1-00-045, U.S. Department of Transportation, National Highway Institute Federal Highway Administration, Washington, D.C., 358.
- Goble, G.G. and Rausche, F. (1976). Wave Equation Analysis of Pile Driving – WEAP Program, U.S. Department of Transportation, Federal Highway Administration, Office of Research and Development, Washington, D.C., Volumes I-IV.
- Goble, G.G. and Rausche, F. (1986). Wave Equation Analysis of Pile Driving –WEAP86 Program, U.S. Department of Transportation, Federal Highway Administration, Implementation Division, McLean, Volumes I-IV.
- Hirsch, T.J., Carr, L. and Lowery, L.L. (1976). Pile Driving Analysis. TTI Program, U.S. Department of Transportation, Federal Highway Administration, Offices of Research and Development, IP-76-13, Washington, D.C., Volumes I-IV.
- PDI, Pile Dynamics, Inc. (2005). GRLWEAP Procedures and Models, Version 2005. 4535 Renaissance Parkway, Cleveland, OH.
- Reiding, F.J., Middendorp, P., Schoenmaker, R.P., Middendorp, F.M., and Bielefeld, M.W., (1988). FPDS-2, A New Generation of Foundation Diagnostic Equipment, Proc. of the Third International Conference on the Application of Stress Wave Theory to Piles, Ottawa, B.H. Fellenius, Ed., BiTech Publishers, 123-134.

Rausche, F., Liang, L., Allin, R., and Rancman, D. (2004). Applications and Correlations of the Wave Equation Analysis Program GRLWEAP. Proceedings of the 7th International Conference on the Application of Stresswave Theory to Piles, Petaling Jaya, Selangor, Malaysia, 2004.

Soares, M., de Mello, J. and de Matos, S. (1984). Pile Driveability Studies, Pile Driving Measurements. Proceedings of the Second International Conference on the Application of Stress-Wave Theory to Piles, Stockholm, 64-71.

Smith, E.A.L. (1960). Pile Driving Analysis by the Wave Equation. American Society of Civil Engineers, Journal of the Soil Mechanics and Foundations Division, 86(4), 35-61.

U.S. Army Corps of Engineers, Department of the Army (1993). Engineering Manual EM 110-2-2906, reprinted by American Society of Civil Engineers in Design of Pile Foundations, 345 East 47th Street, New York, NY.

Chapter 17

DYNAMIC PILE TESTING AND ANALYSIS

Dynamic test methods use measurements of strain and acceleration taken near the pile head as a pile is driven or restruck with a pile driving hammer. These dynamic measurements can be used to evaluate the performance of the pile driving system, calculate pile installation stresses, determine pile integrity, and estimate static pile capacity.

Dynamic test results can be further evaluated using signal matching techniques to determine the relative soil resistance distribution on the pile, as well as representative dynamic soil properties for use in wave equation analyses. This chapter provides a brief discussion of the equipment and methods of analysis associated with dynamic measurements. Additional information on dynamic testing equipment and methods may be found at www.pile.com.

17.1 BACKGROUND

Work on the development of the dynamic pile testing techniques that have become known as the Case Method started with a Master thesis project at Case Institute of Technology. This work was done by Eiber (1958) at the suggestion and under the direction of Professor H.R. Nara. In this first project, a laboratory study was performed in which a rod was driven into dry sand. The Ohio Department of Transportation (ODOT) and the Federal Highway Administration subsequently funded a project with HPR funds at Case Institute of Technology beginning in 1964. This project was directed by Professors R.H. Scanlan and G.G. Goble. At the end of the first two year phase, Professor Scanlan moved to Princeton University. The research work at Case Institute of Technology under the direction of Professor Goble continued to be funded by ODOT and FHWA, as well as several other public and private organizations until 1976.

Four principal directions were explored during the 12 year period that the funded research project was active. There was a continuous effort to develop improved transducers for the measurement of force and acceleration during pile driving. Field equipment for recording and data processing was also continually improved. Model piles were driven and tested both statically and dynamically at sites in Ohio. Full scale piles driven and statically tested by ODOT, and later other DOT's, were also tested dynamically to obtain capacity correlations. Finally, analysis method improvements

were developed, including both field solutions (Case Method) and a rigorous numerical modeling technique (Case Pile Wave Analysis Program or CAPWAP). Additional information on the research project and its results may be found in Goble and Rausche (1970), Rausche *et al.* (1972) and Goble *et al.* (1975).

ODOT began to apply the results of this research to their construction projects in about 1968. Commercial use of the methods began in 1972 when the Pile Driving Analyzer and CAPWAP became practical for use in routine field testing by a trained engineer. There have been continual improvements in the hardware and software since 1972, making the equipment more reliable and easier to use. Further implementation of dynamic testing methods resulted from FHWA Demonstration Project 66, in which additional correlation data was collected, and the method benefits were demonstrated on real projects throughout the US. Other dynamic testing and analysis systems have subsequently been developed, primarily in Europe, such as the FPDS equipment and its associated signal matching technique, TNOWAVE, Reiding *et al.* (1988). However, based on the current state of practice in the United States, this manual will focus on the Pile Driving Analyzer and CAPWAP. This is not intended as an endorsement of Pile Dynamics, Inc. (PDI) or its products.

17.2 APPLICATIONS FOR DYNAMIC TESTING METHODS

Cheney and Chassie (2000) note that dynamic testing costs much less and requires less time than static pile load testing. They also note that important information can be obtained regarding the behavior of the pile driving system and pile-soil response that is not available from a static pile load test. Determination of driving stresses and pile integrity with dynamic test methods has facilitated the use of fewer, high capacity piles in foundations through better pile installation control. Some of the applications of dynamic pile testing are discussed below.

17.2.1 Static Pile Capacity

- a. Evaluation of static pile capacity at the time of testing. Soil setup or relaxation potential can be also assessed by restriking several piles and comparing restrike capacities with end-of-initial driving capacities.
- b. Assessments of static pile capacity versus pile penetration depth can be obtained by testing from the start to the end of driving. This can be helpful in profiling the depth to the bearing strata and thus the required pile lengths.

- c. CAPWAP analysis can provide refined estimates of static capacity, assessment of soil resistance distribution, and soil quake and damping parameters for wave equation input.

17.2.2 Hammer and Driving System Performance

- a. Calculation of energy transferred to the pile for comparison with the manufacturer's rated energy and wave equation predictions which indicate hammer and drive system performance. Energy transfer can also be used to determine effects of changes in hammer cushion or pile cushion materials on pile driving resistance.
- b. Determination of drive system performance under different operating pressures, strokes or batters, or changes in hammer maintenance by comparative testing of hammers or of a single hammer over an extended period of use.
- c. Identification of hammer performance problems, such as preignition problems with diesel hammers or preadmission in air/steam hammers.
- d. Determination of whether soil behavior or hammer performance is responsible for changes in observed driving resistances.

17.2.3 Driving Stresses and Pile Integrity

- a. Calculation of compression and tension driving stresses. In cases with driving stress problems, this information can be helpful when evaluating adjustments to pile installation procedures. Calculated stresses can also be compared to specified driving stress limits.
- b. Determination of the extent and location of pile structural damage, Rausche and Goble (1979). Thus, costly extraction may not be necessary to confirm or quantify damage suspected from driving records.
- c. CAPWAP analysis for stress distribution throughout pile.

17.3 DYNAMIC TESTING EQUIPMENT

A typical dynamic testing system consists of a minimum of two strain transducers and two accelerometers bolted to diametrically opposite sides of the pile to monitor strain and acceleration and account for nonuniform hammer impacts and pile bending. Because of nonuniform impacts and bending, the use of two diametrically opposite mounted strain transducers is essential for a valid test. The reusable strain transducers and accelerometers are generally attached two to three diameters below the pile head. Almost any driven pile type (concrete, steel pipe, H, Monotube, timber, *etc.*) can be tested with the pile preparation for each pile type slightly varying.

Figures 17.1 and 17.2 illustrate the typical pile preparation procedures required for dynamic testing. In Figure 17.1, a prestressed concrete pile is being prepared for gage attachment by drilling and then installing concrete anchors. In Figure 17.2, the concrete pile to be tested during driving has been positioned in the leads for driving. A member of the pile crew climbs the leads and then bolts the gages to the pile at this time. Piles to be tested during restrike can be instrumented at any convenient location and the climbing of the leads is usually not necessary. Pile preparation and gage attachment typically requires 10 to 20 minutes per pile tested. After the gages are attached, the driving or restrike process continues following usual procedures. Most restrike tests are only 50 blows or less as described in Chapter 11.

A close up view of a strain transducer and an accelerometer bolted to a steel pipe pile is shown in Figure 17.3. The individual cables from each gage are combined into a single main cable which in turn relays the signals from each hammer blow to the data acquisition system on the ground. The data acquisition system, such as the Pile Driving Analyzer shown in Figure 17.4, conditions and converts the strain and acceleration signals to force and velocity records versus time. The force is computed from the measured strain, ϵ , times the product of the pile elastic modulus, E , and cross sectional area, A , or: $F(t) = E A \epsilon (t)$. The velocity is obtained by integrating the measured acceleration record, a , or: $V(t) = \int a(t) dt$.

Older dynamic testing systems required multiple components for processing, recording, and display of dynamic test signals. In newer dynamic testing systems, these components have been combined into one PC computer based system. During driving, the Pile Driving Analyzer performs integrations and all other required computations to analyze the dynamic records for transferred energy, driving stresses, structural integrity, and pile capacity. Numerical results for each blow for up to nine dynamic quantities are



Figure 17.1 Pile Preparation for Dynamic Testing



Figure 17.2 Pile Positioned for Driving and Gage Attachment



Figure 17.3 Strain Transducer and Accelerometer Bolted to Pipe Pile



Figure 17.4 Pile Driving Analyzer – Model PAK (courtesy of Pile Dynamics, Inc.)

electronically stored in a file which can be later used to produce graphical and numeric summary outputs. In this system, force and velocity records are also viewed on a graphic LCD computer screen during pile driving to evaluate data quality, soil resistance distribution, and pile integrity. Complete force and velocity versus time records from each gage are also digitally stored for later reprocessing and analysis by CAPWAP.

Data quality is automatically evaluated by the Pile Driving Analyzer and if any problem is detected, then a warning is given to the test engineer. Other precautionary advice is also displayed to assist the engineer in collecting data. The capabilities discussed in the remainder of this chapter are those included in these newer systems.

The latest generation of dynamic test equipment, the PAL-R Pile Driving Analyzer is illustrated in Figure 17.5. This unit can be operated remotely (off site) by the test engineer via a cell phone connection. In a remote test, basic pile information is entered into the unit by on-site personnel and then the unit is connected to the test engineer's location. For sites where cell phone service is not available the data can be stored and later sent over a telephone line. Remote testing can be particularly cost effective on remote construction sites or when large numbers of production piles are to be tested.

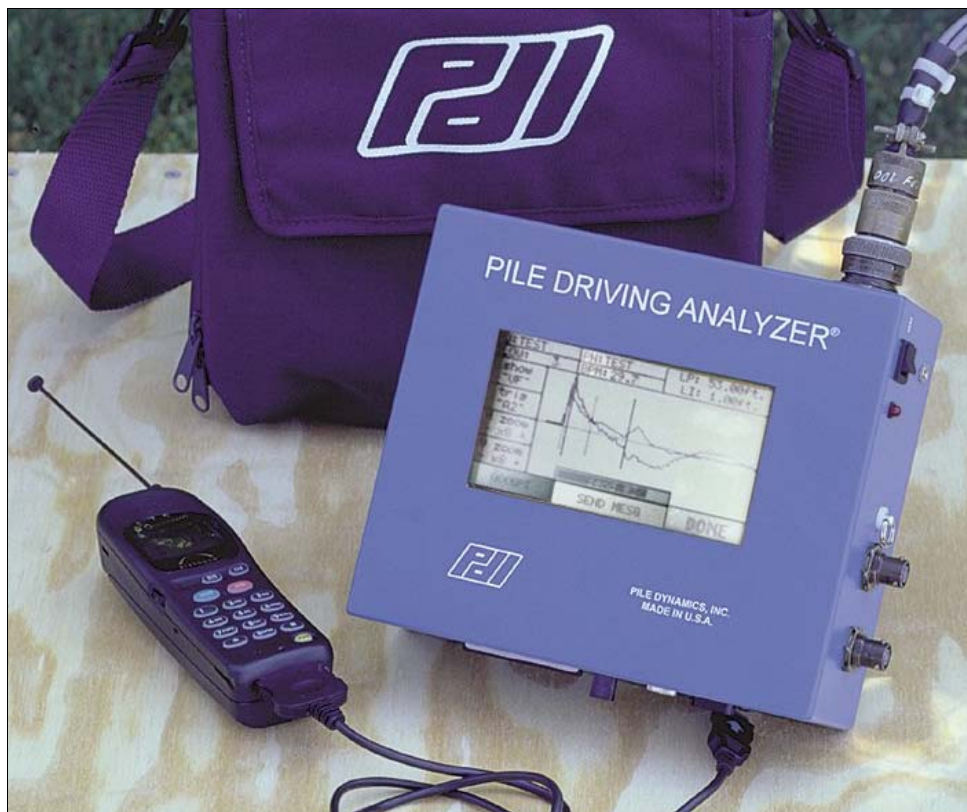


Figure 17.5 Pile Driving Analyzer – Model PAL-R (courtesy of Pile Dynamics, Inc)

Additional information on the equipment requirements for dynamic testing are detailed in ASTM D-4945, Standard Test Method for High Strain Dynamic Testing of Piles and in AASHTO T-298-33, Standard Method of Test for High Strain Dynamic Testing of Piles.

17.4 BASIC WAVE MECHANICS

This section is intended to summarize wave mechanics principles applicable to pile driving. Through this general overview, an understanding of how dynamic testing functions and how test results can be qualitatively interpreted can be obtained.

When a uniform elastic rod of cross sectional area, A , elastic modulus, E , and wave speed, C , is struck by a mass, then a force, F , is generated at the impact surface of the rod. This force compresses the adjacent part of the rod. Since the adjacent material is compressed, it also experiences an acceleration and attains a particle velocity, V . As long as there are no resistance effects on the uniform rod, the force in the rod will be equal to the particle velocity times the rod impedance, EA/C .

Figure 17.6(a) illustrates a uniform rod of length, L , with no resistance effects, that is struck at one end by a mass. Force and velocity (particle velocity) waves will be created in the rod, as shown in Figure 17.6(b). These waves will then travel down the rod at the material wave speed, C . At time L/C , the waves will arrive at the end of the rod, as shown in Figures 17.6(c) and 17.6(d). Since there are no resistance effects acting on the rod, a free end condition exists, and a tensile wave reflection occurs, which doubles the pile velocity at the free end and the net force becomes zero. The wave then travels up the rod with force of the same magnitude as the initial input, except in tension, and the velocity of the same magnitude and same sign.

Consider now that the rod is a pile with no resistance effects, and that force and velocity measurements are made near the pile head. Typical force and velocity measurements versus time for this "free end" condition are presented in Figure 17.7. The toe response in the records occurs at time $2L/C$. This is the time required for the waves to travel to the pile toe and back to the measurement location, divided by the wave speed. Since there are no resistance effects acting on the pile shaft, the force and velocity records are equal until the reflection from the free end condition arrives at the measurement location. At time $2L/C$, the force wave goes to zero and the velocity wave doubles in magnitude. Note the repetitive pattern in the records at $2L/C$ intervals generated as the waves continue to travel down and up the pile. This illustration is typical of an easy driving situation where the pile "runs" under the hammer blow.

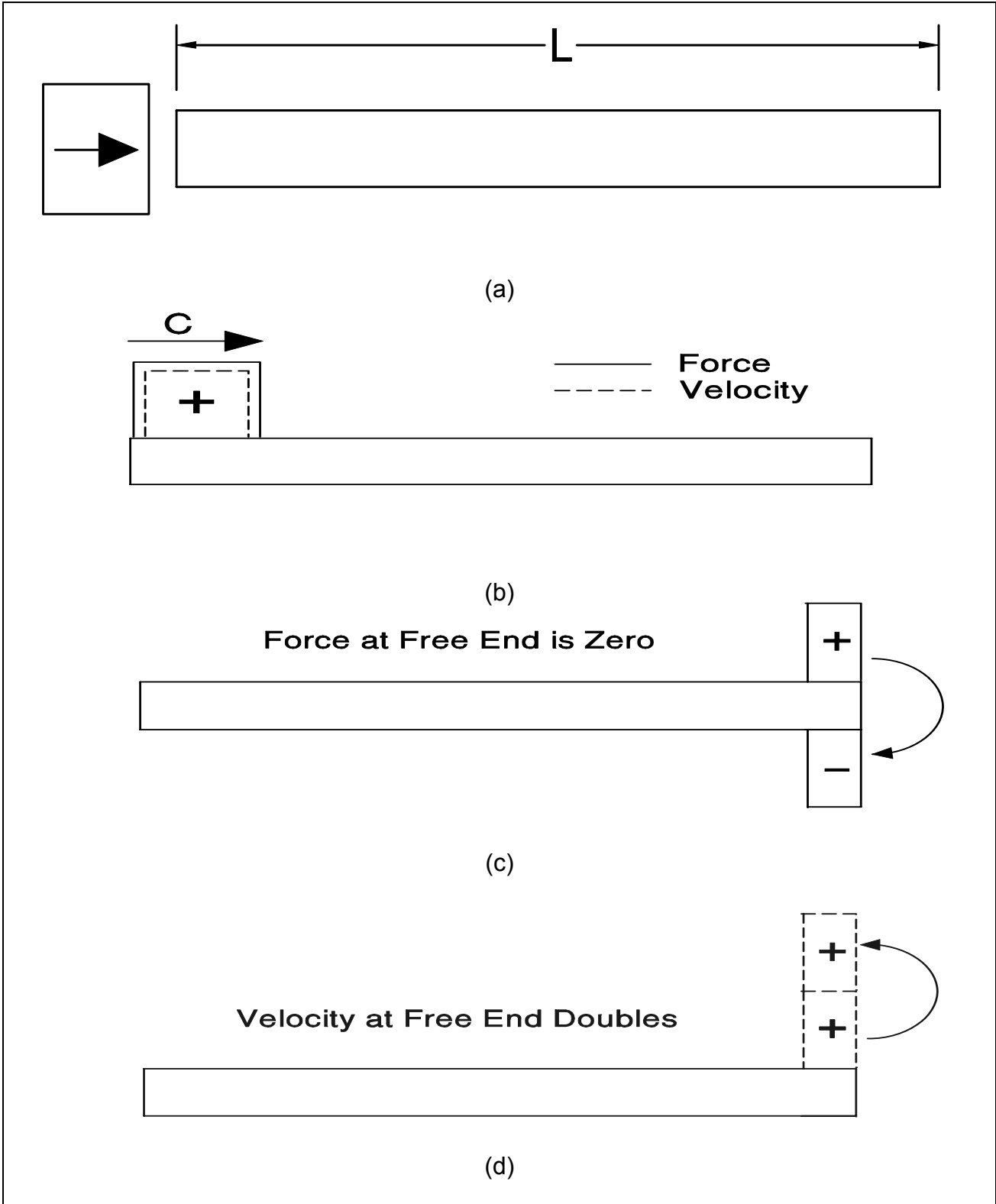


Figure 17.6 Free End Wave Mechanics

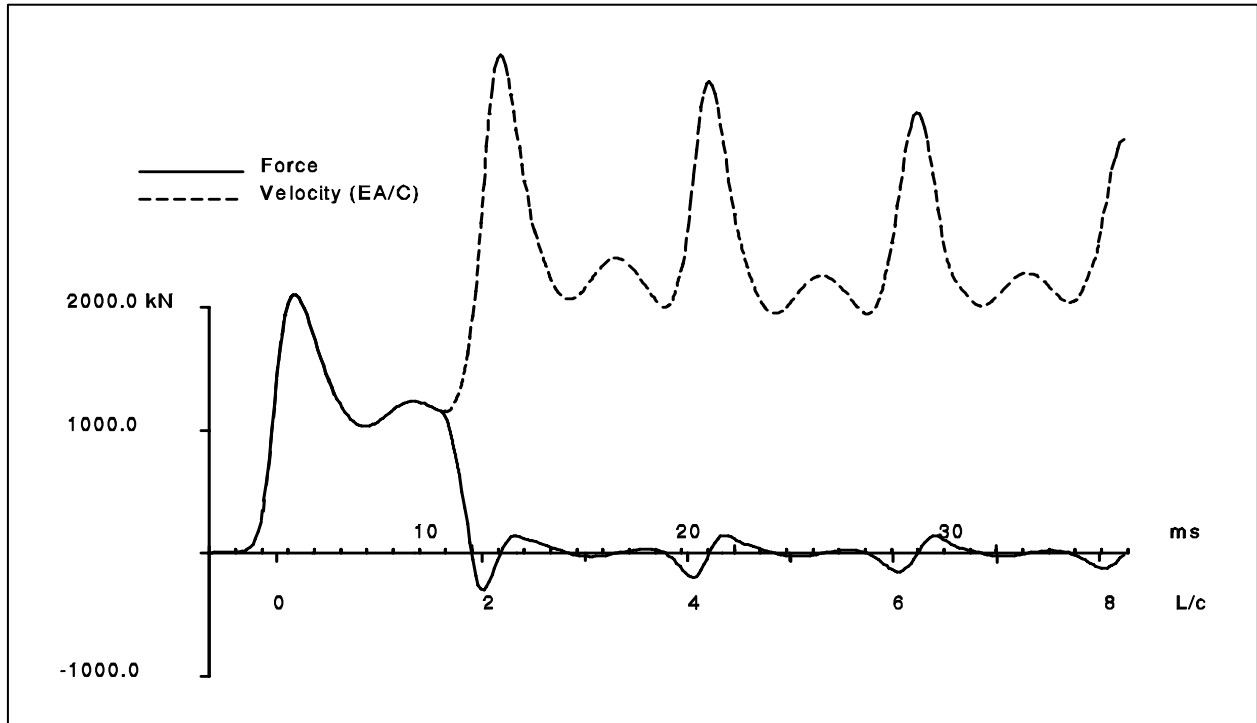


Figure 17.7 Force and Velocity Measurements versus Time for Free End Condition

Figure 17.8(a) illustrates a uniform rod of length, L , that is struck by a mass. Again there are no resistance effects along the rod length, but the pile end is fixed, *i.e.*, it is prevented by some mechanism from moving in such a manner that the particle velocity must be zero material wave speed, C . At time L/C , the waves will arrive at the end of the rod as shown in Figures 17.8(c) and 17.8(d). There the fixed end condition will cause a compression wave reflection and therefore the force at the fixed end doubles in magnitude and the pile velocity becomes zero. A compression wave then travels up the rod.

Consider now that the rod is a pile with a fixed end condition and that force and velocity measurements are again made near the pile head. The force and velocity measurements versus time for this condition are presented in Figure 17.9. Since there are no resistance effects acting on the pile shaft, the force and velocity records are equal until the reflection from the fixed end condition arrives at the measurement location. At time $2L/C$, the force wave increases in magnitude and the velocity wave goes to zero. This illustration is typical of a hard driving situation where the pile is driven to rock.

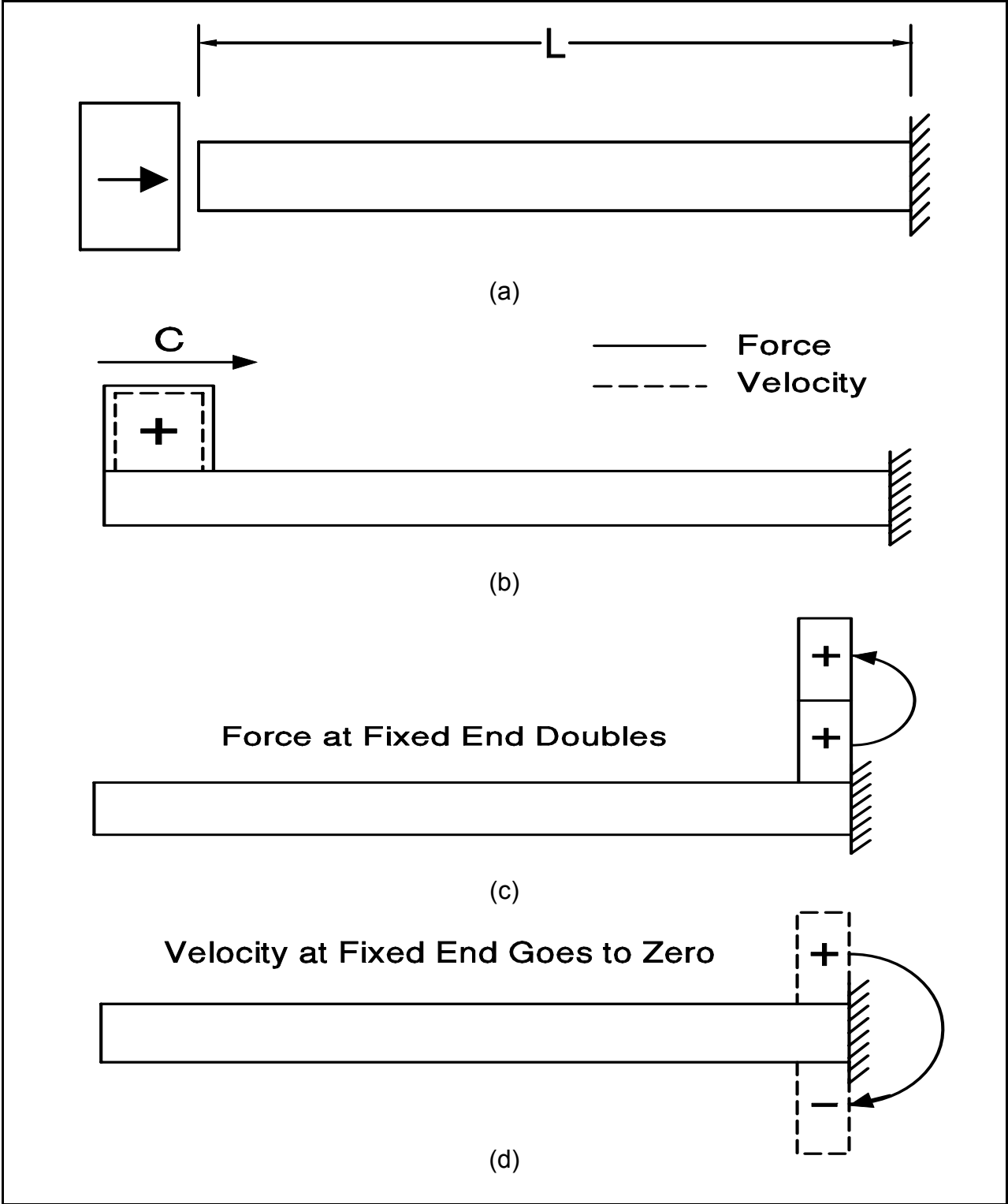


Figure 17.8 Fixed End Wave Mechanics

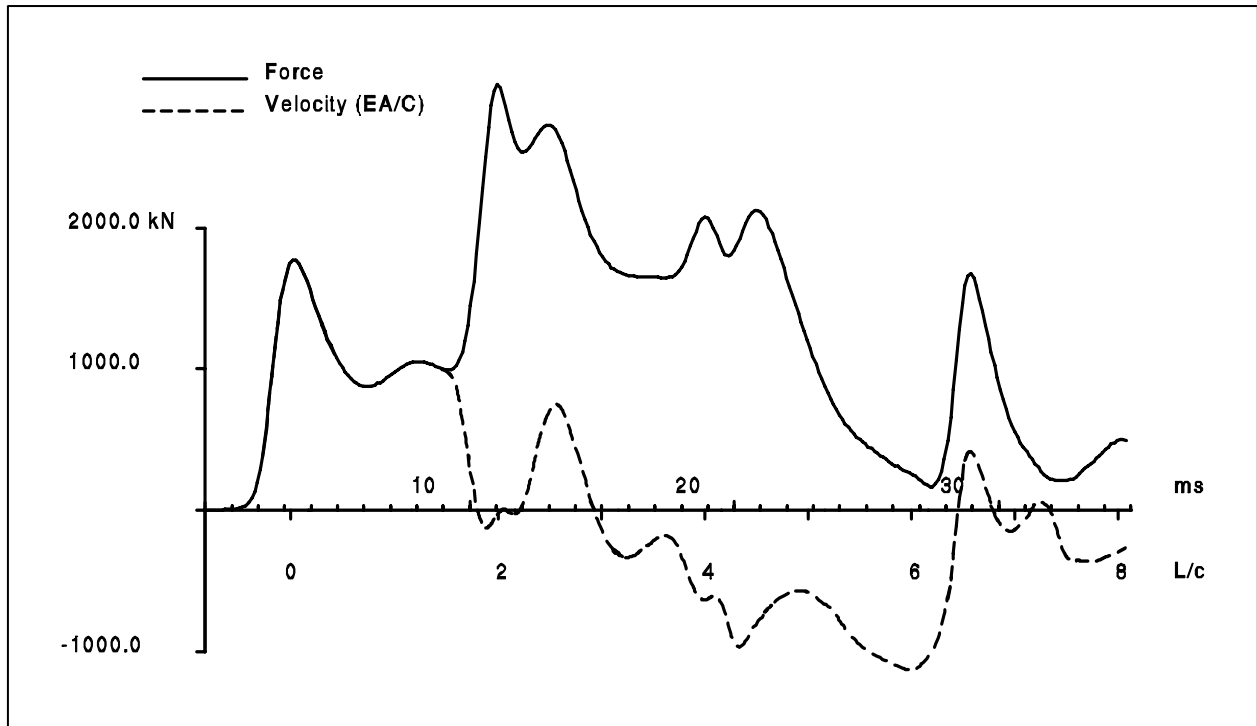


Figure 17.9 Force and Velocity Measurements versus Time for Fixed End Condition

As discussed above, the force and velocity records versus time are equal or proportional at impact and remain proportional thereafter until affected by soil resistance or cross sectional changes. Reflections from either effect will arrive at the measurement location at time $2X/C$ where X is the distance to the soil resistance or cross section change. Both soil resistance effects and cross sectional increases will cause an increase in the force record and a proportional decrease in the velocity record. Conversely, cross sectional reductions, such as those caused by pile damage, will cause a decrease in the force record and an increase in the velocity record.

The concept of soil resistance effects on force and velocity records can be further understood by reviewing the theoretical soil resistance example presented in Figure 17.10. In this case, the soil resistance on a pile consists only of a small resistance located at a depth, A , below the measurement location, and a larger soil resistance at depth B . No other resistance effects act on the pile, so a free end condition is present at the pile toe. The force and velocity records versus time for this example will be proportional until time $2A/C$, when the reflection from the small soil resistance effect arrives at the measurement location. This soil resistance reflection will then cause a small increase in the force record and a small decrease in the velocity record.

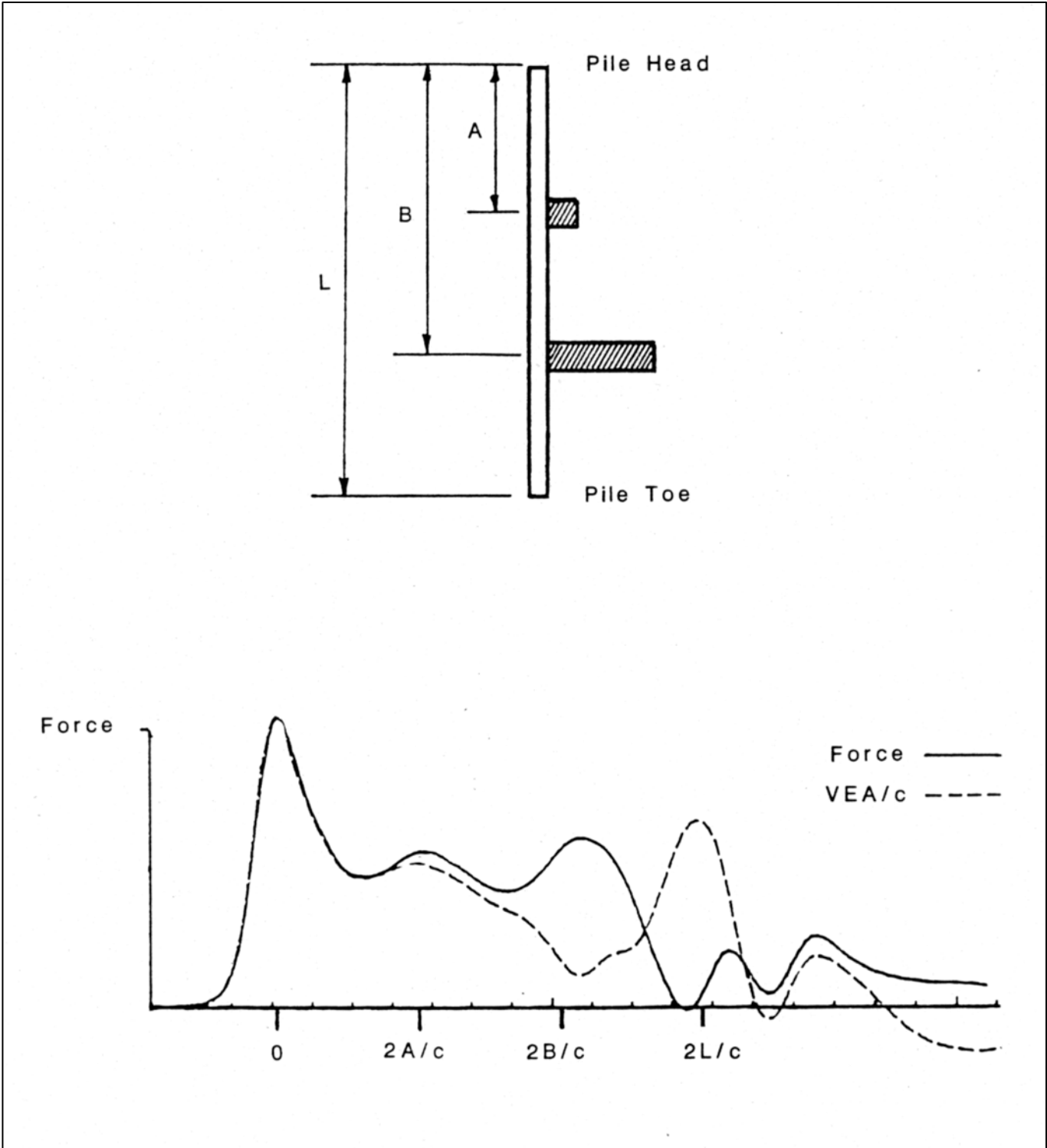


Figure 17.10 Soil Resistance Effects on Force and Velocity Records (after Hannigan, 1990)

No additional soil resistance effects act on the pile between times $2A/C$ and $2B/C$. Therefore, the force and velocity records will remain parallel over this time interval with no additional separation. At time $2B/C$, the reflection from the large soil resistance effect will arrive at the measurement location. This large soil resistance reflection will then cause a large increase in the force record and a large decrease in the velocity record. No additional soil resistance effects act on the pile between times $2B/C$ and $2L/C$. Therefore, the force and velocity records will again remain parallel over this time interval with no additional separation between the records.

At time $2L/C$, the reflection from the pile toe will arrive at the measurement location. Since no resistance is present at the pile toe, a free end condition exists and a tensile wave will be reflected. Hence, an increase in the velocity record and a decrease in the force record will occur.

These basic interpretation concepts of force and velocity records versus time can be used to qualitatively evaluate the soil resistance effects on a pile. In Figure 17.11(a), minimal separation occurs between the force and velocity records between time 0, or the time of impact, and time $2L/C$. In addition, a large increase in the velocity record and corresponding decrease in the force record occurs at time $2L/C$. Hence, this record indicates minimal shaft and toe resistance on the pile.

In Figure 17.11(b), minimal separation again occurs between the force and velocity records between time 0 and time $2L/C$. However in this example, a large increase in the force record and corresponding decrease in the velocity record occurs at time $2L/C$. Therefore, this force and velocity record indicates minimal shaft and a large toe resistance on the pile.

In Figure 17.11(c), a large separation between the force and velocity records occurs between time 0 and time $2L/C$. This force and velocity record indicates a large shaft resistance on the pile.

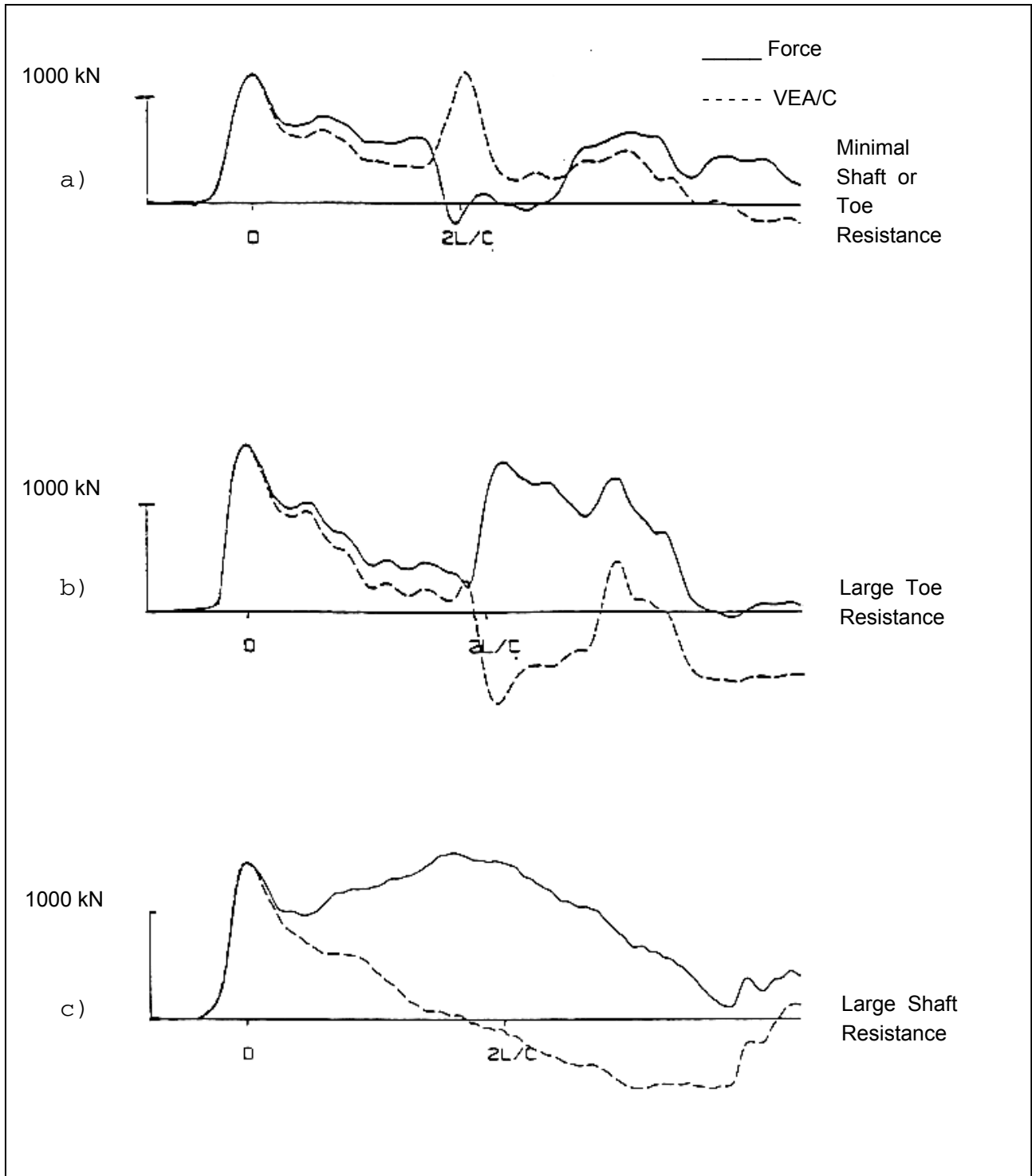


Figure 17.11 Typical Force and Velocity Records for Various Soil Resistance Conditions (after Hannigan, 1990)

17.5 DYNAMIC TESTING METHODOLOGY

As introduced in Section 17.1, two methods have developed for analyzing dynamic measurement data, the Case Method and CAPWAP. These methods along with the wave equation analysis method described in Chapter 16 are sometimes confused so it is useful to briefly review all of these methods and their usage.

The wave equation is a computer program that is typically performed prior to field work. The program inputs require the engineer to make assumptions on the hammer performance and soil response. A refined wave equation analysis is also often performed after test piles are driven. In a refined analysis, the engineer uses hammer performance and soil response information from dynamic measurements to “calibrate” the wave equation to the field conditions. This process was described in Section 16.6.6 of Chapter 16. The wave equation provides a relationship between the ultimate static pile capacity and the pile penetration resistance or blow count, and is therefore often used in establishing the driving criteria or in assessing the ultimate capacity of a pile based on it’s observed penetration resistance.

During pile driving in the field, the Pile Driving Analyzer uses the Case Method capacity equations for estimates of the ultimate static pile capacity. Case Method capacity results are calculated in real time from the measured force and velocity records obtained for each hammer blow. Correlating Case Method capacity results with pile penetration resistance information is another means of establishing the driving criteria. The Case Method capacity equations are described in detail in Section 17.5.1 of this chapter. Additional Case Method equations are used for calculation of driving stresses and pile integrity, as well as computation of transferred hammer energy. These additional Case Method equations are also described in this chapter.

The CAPWAP analysis method is a more rigorous numerical analysis procedure that uses the measured force and velocity records (PDA data) from one hammer blow. The CAPWAP program uses the dynamic measurement data along with wave equation type pile and soil modeling to calculate the ultimate static pile capacity, the relative soil resistance distribution, the dynamic soil properties of quake and damping, and the driving stresses throughout the pile. CAPWAP capacity results are considered a more accurate assessment of the ultimate static pile capacity than Case Method results. The CAPWAP determined soil information along with the PDA data on driving system performance are often used in the development of a refined wave equation analysis. This is the best use of all the three methods for driving criteria determination. CAPWAP is described in greater detail in Section 17.5.4 of this chapter.

17.5.1 Case Method Capacity

Research conducted at Case Western Reserve University in Cleveland, Ohio, resulted in a method which uses electronic measurements taken during pile driving to predict static pile capacity. Assuming the pile is linearly elastic and has constant cross section, the total static and dynamic resistance on a pile during driving, RTL, can be expressed using the following equation, which was derived from a closed form solution to the one dimensional wave propagation theory:

$$RTL = 1/2 [F(t_1) + F(t_2)] + 1/2 [V(t_1) - V(t_2)] EA/C$$

Where: F = Force measured at gage location.
V = Velocity measured at gage location.
t₁ = Time of initial impact.
t₂ = Time of reflection of initial impact from pile toe (t₁ + 2L/C).
E = Pile modulus of elasticity.
C = Wave speed of pile material.
A = Pile area at gage location.
L = Pile length below gage location.

To obtain the static pile capacity, the dynamic resistance (damping) must be subtracted from the above equation. Goble *et al.* (1975) found that the dynamic resistance component could be approximated as a linear function of a damping factor times the pile toe velocity, and that the pile toe velocity could be estimated from dynamic measurements at the pile head. This led to the standard Case Method capacity equation, RSP, expressed below:

$$RSP = RTL - J [V(t_1)EA/C + F(t_1) - RTL]$$

Where: J = Dimensionless damping factor based on soil type near the pile toe.

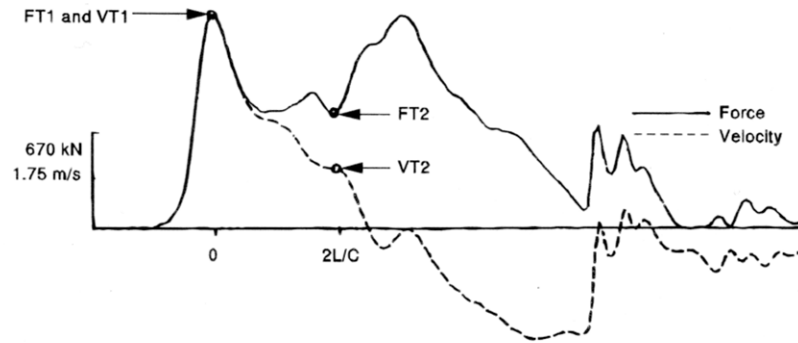
Typical damping factors versus soil type at the pile toe were determined by finding the range in the Case damping factor, J, for a soil type that provided a correlation of the RSP static capacity within 20% of the static load test failure load, determined using the Davisson (1972) offset limit method. The original range in Case damping factor versus soil type from this correlation study, Goble *et al.* (1975), as well as typical ranges in

Case damping factor for the RSP equation based on subsequent experience, Pile Dynamics, Inc. (2004), are presented in Table 17-1. While use of these values with the RSP equation may provide good initial capacity estimates, site specific damping correlations should be developed based upon static load test results or CAPWAP analysis. It should also be noted that Case damping is a non-dimensional damping factor and is not the same as the Smith damping discussed in Chapter 17 for wave equation analysis.

TABLE 17-1 SUMMARY OF CASE DAMPING FACTORS FOR RSP EQUATION		
Soil Type at Pile Toe	Original Case Damping Correlation Range Goble <i>et al.</i> (1975)	Updated Case Damping Ranges Pile Dynamics (2004)
Clean Sand	0.05 to 0.20	0.10 to 0.15
Silty Sand, Sand Silt	0.15 to 0.30	0.15 to 0.25
Silt	0.20 to 0.45	0.25 to 0.40
Silty Clay, Clayey Silt	0.40 to 0.70	0.40 to 0.70
Clay	0.60 to 1.10	0.70 or higher

The RSP or standard Case Method equation is best used to evaluate the capacity of low displacement piles, and piles with large shaft resistances. For piles with large toe resistances and for displacement piles driven in soils with large toe quakes, the toe resistance is often delayed in time. This condition can be identified from the force and velocity records. In these instances, the standard Case Method equation may indicate a relatively low pile capacity and the maximum Case Method equation, RMX, should be used. The maximum Case Method equation searches for the t_1 time in the force and velocity records which results in the maximum capacity. An example of this technique is presented in Figure 17.12. When using the maximum Case Method equation, experience has shown that the Case damping factor should be at least 0.4, and on the order of 0.2 higher than that used for the standard Case Method capacity equation, RSP.

The RMX and RSP Case Method equations are the two most commonly used solutions for field evaluation of pile capacity. Additional automatic Case Method solutions are available that do not require selection of a Case damping factor. These automatic

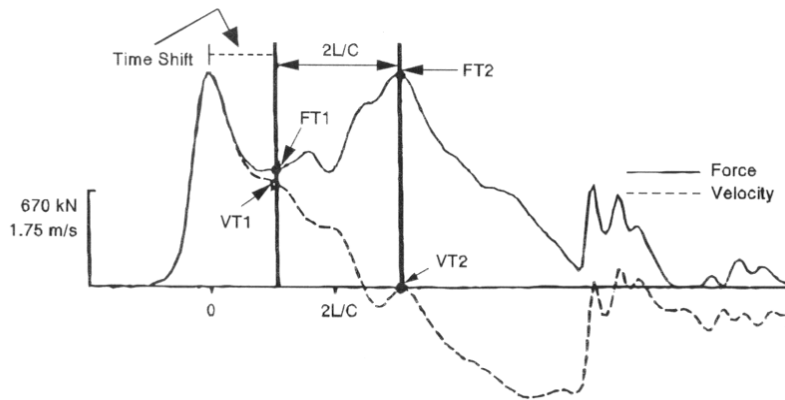


TOTAL RESISTANCE

$$\begin{aligned}
 RTL &= 1/2 (FT1 + FT2) + 1/2 (VT1 - VT2) (EA/C) \\
 &= 1/2 (1486 + 819) + 1/2 (3.93 - 1.07) 381 \\
 &= 1153 + 545 = 1698 \text{ kN.}
 \end{aligned}$$

STATIC RESISTANCE

$$\begin{aligned}
 RSP &= RTL - J[VT1 (EA/C) + FT1 - RTL] \\
 &= 1698 - 0.4 [3.93 (381) + 1486 - 1698] \\
 &= 1698 - 514 = 1184 \text{ kN.}
 \end{aligned}$$



TOTAL RESISTANCE

$$\begin{aligned}
 RTL &= 1/2 (FT1 + FT2) + 1/2 (VT1 - VT2) (EA/C) \\
 &= 1/2 (819 + 1486) + 1/2 (1.92 - 0.0) 381 \\
 &= 1153 + 366 = 1519 \text{ kN.}
 \end{aligned}$$

STATIC RESISTANCE

$$\begin{aligned}
 RMX &= RTL - J[VT1 (EA/C) + FT1 - RTL] \\
 &= 1519 - 0.7 [1.92 (381) + 819 - 1519] \\
 &= 1519 - 22 = 1497 \text{ kN.}
 \end{aligned}$$

Figure 17.12 Standard, RSP and Maximum, RMX, Case Method Capacity Estimates

methods, referred to as RAU and RA2, search for the time when the pile toe velocity is zero and hence damping is minimal. The RAU method may be applicable for piles with minimal shaft resistance and the RA2 method may be applicable to piles with toe resistance plus moderate shaft resistance. It is recommended that these automatic methods be used as supplemental indicators of pile capacity where appropriate with the more traditional standard or maximum Case Method equations primarily used to evaluate pile capacity.

17.5.2 Energy Transfer

The energy transferred to the pile head can be computed from the strain and acceleration measurements. As described in Section 17.3, the acceleration signal is integrated to obtain velocity and the strain measurement is converted to force. Transferred energy is equal to the work done which can be computed from the integral of the force and velocity records over time as given below:

$$E_p(t) = \int_0^t F(t) V(t) dt$$

Where: E_p = The energy at the gage location expressed as a function of time.
 F = The force at the gage location expressed as a function of time.
 V = The velocity at the gage location expressed as a function of time.

This procedure is illustrated in Figure 17.13. The maximum energy transferred to the pile head corresponds to the maximum value of $E_p(t)$. The Pile Driving Analyzer output quantity EMX is the maximum value of $E_p(t)$ and can be used to evaluate the performance of the hammer and driving system as described in Section 17.7.

17.5.3 Driving Stresses and Integrity

The Pile Driving Analyzer calculates the compression stress at the gage location using the measured strain and pile modulus of elasticity. However, the maximum compression stress in the pile may be greater than the compression stress calculated at the gage location, such as in the case of a pile driven through soft soils to rock. In these cases CAPWAP or wave equation analysis may be used to evaluate the maximum compression stress in the pile.

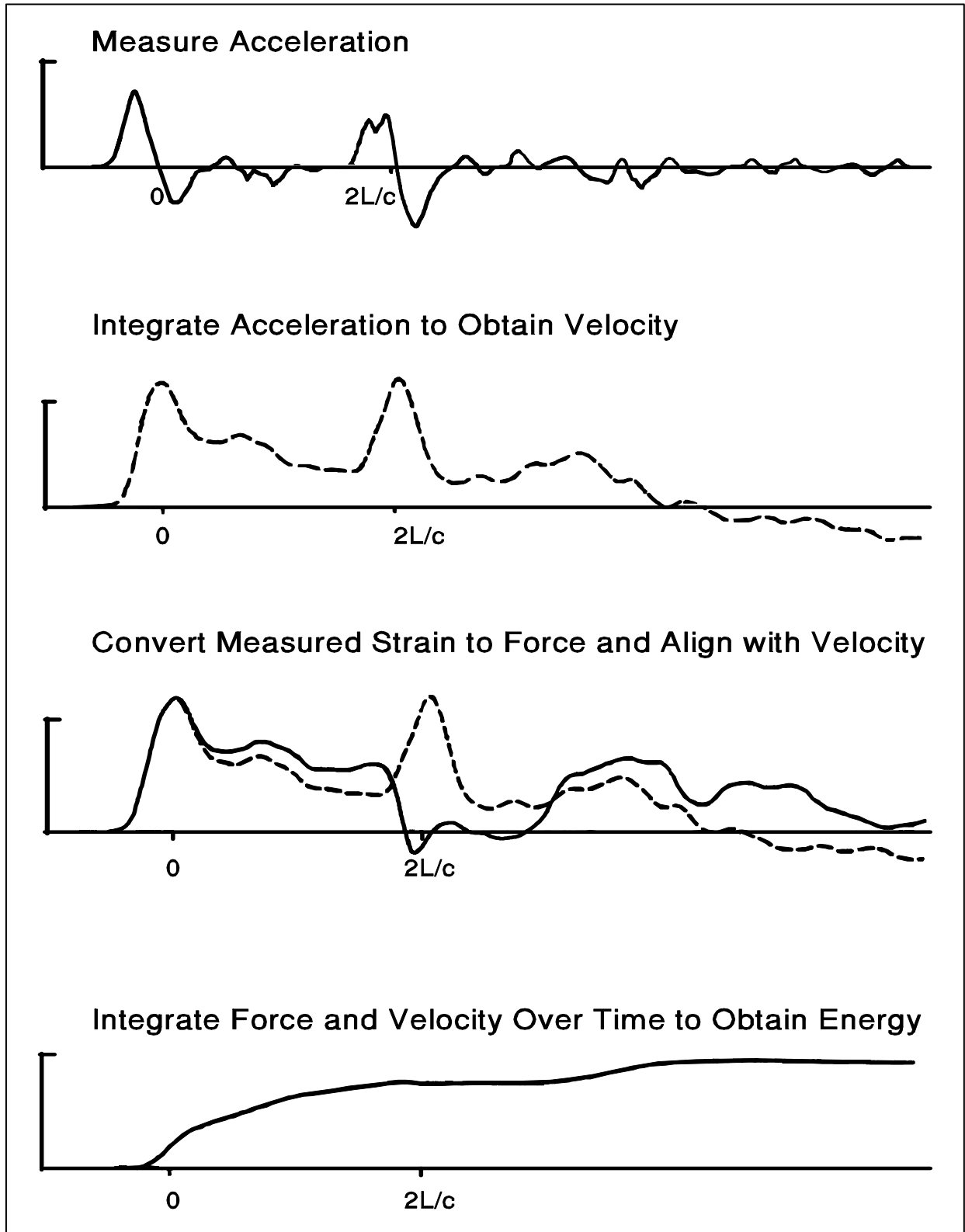


Figure 17.13 Energy Transfer Computation (after Hannigan, 1990)

Figure 17.14 illustrates the computation process for compression and tension stresses. Force and velocity records for a 457 mm (18 in) square prestressed concrete pile with a large toe resistance are presented in the top half of the figure. The penetration resistance associated with this record is 282 blows per 0.25 m (29 blows per inch). The vertical scale between the zero axis and the top of the box is identified as 6000 kN. Point A identifies the maximum compression force at the gage location of 3537 kN (795 kips). The maximum compression stress at the gage location, CSX, is then this force divided by the pile cross section area of 2090.3 cm² (324 in²) or 16.9 MPa (2.45 ksi).

Computed tension stresses are based upon the superposition of the upward and downward traveling waves calculated by the Pile Driving Analyzer. The downward traveling wave, wave down, and the upward traveling wave, wave up are presented in the lower half of Figure 17.14. The vertical scale between the zero axis and the top of the lower box is once again 6000 kN. The value of wave down, WD, at time (t) is computed from the measured force and velocity records according to:

$$WD(t) = \frac{1}{2} [F(t) + V(t)(EA/C)]$$

The value of wave up, WU, at time (t) is computed from the measured force and velocity records according to:

$$WU(t) = \frac{1}{2} [F(t) - V(t)(EA/C)]$$

In Figure 17.14, the PDA computes the tension in the pile from the superposition of the maximum upward tension force in wave up at time $2L/C \pm 20\%$ identified by point B, and the minimum downward compression force in wave down between time 0 and time $2L/C$ identified by point C. For the example presented, these values are -274 kN (-62 kips) for point B and 199 kN (45 kips). The computed net tension force is -75 kN (-17 kips) which corresponds to a tension stress of 0.4 MPa (0.05 ksi). The computation described above is the maximum tension stress from the upward traveling wave and would be identified by the three letter PDA code CTX. This low tension stress in the upward traveling wave agrees with the hard driving conditions.

The PDA also computes the maximum tension stress from the downward traveling. In the example given, the maximum tension force in wave down occurs at point D and has a value of 1084 kN (-244 kips). The minimum compression force in wave up within a $2L/C$ window of this maximum tension force is identified by point E and has a value of 219 kN (49 kips). The computed net tension force is -865 kN (-195 kips) which corresponds to a tension stress of 4.1 MPa (0.60 ksi). The maximum computed tension stress in either the upward or downward traveling wave is identified by the

three letter PDA code TSX. Hence, the maximum PDA computed tension stress in this example occurs in the downward traveling wave and a tension stress value of 4.1 MPa would be reported. The example records illustrate that high tension stresses can also occur in hard driving cases in the downward traveling wave. This occurs when the reflected compression wave from a fixed toe condition reaches the free end at the pile head and reflects down the pile as a tension wave.

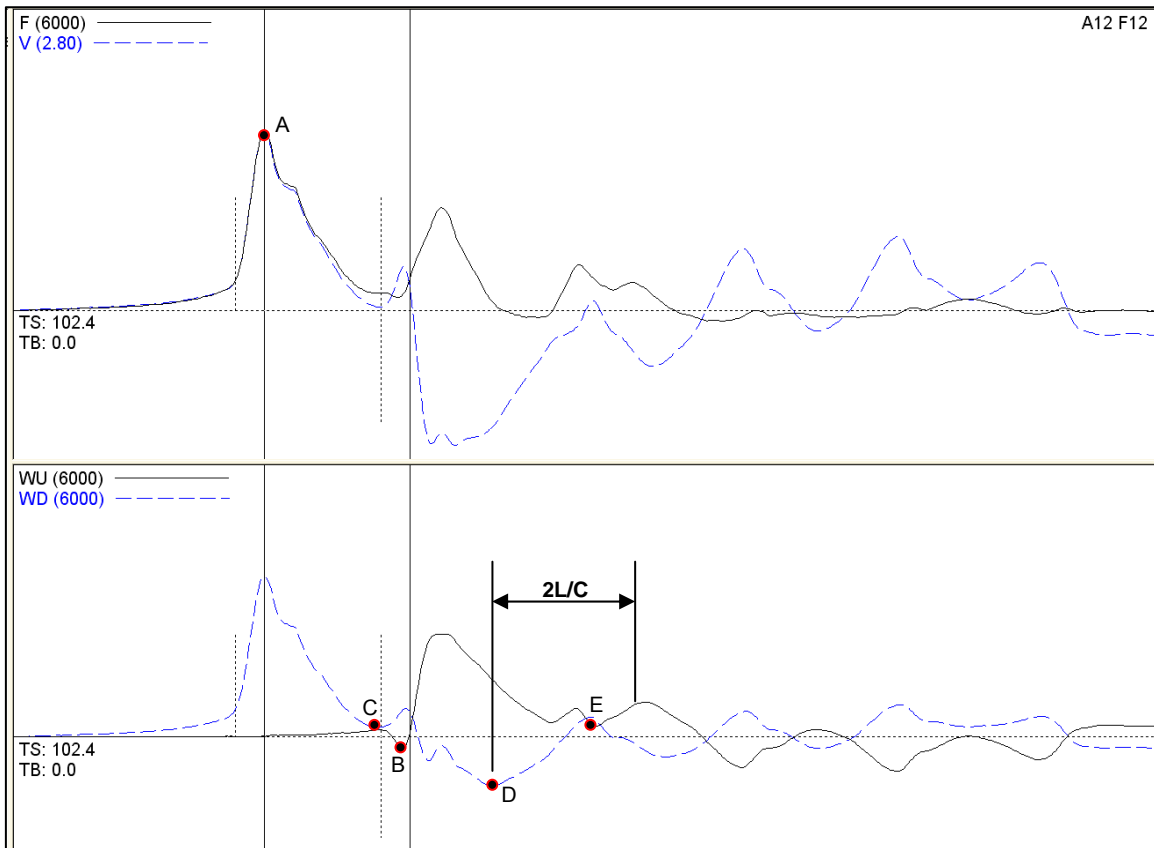


Figure 17.4. Example of Tension and Compression Stress Computations

The basic concepts of wave mechanics were presented in Section 17.4. Convergence between the force and velocity records prior to the toe response at time $2L/C$ indicates an impedance (EA/C) reduction in the pile. For uniform cross section piles an impedance reduction is therefore pile damage. The degree of convergence between the force and velocity records is termed BTA, which can be used to evaluate pile damage following the guidelines presented in Rausche and Goble, (1979). These guidelines are provided in Table 17-2. Piles with BTA values below 80% correspond to damaged or broken piles.

TABLE 17-2 PILE DAMAGE GUIDELINES (Rausche and Goble, 1979)	
BTA	Severity of Damage
1.0	Undamaged
0.8 - 1.0	Slightly Damaged
0.6 - 0.8	Damaged
Below 0.6	Broken

17.5.4 The CAPWAP Method (Case Pile Wave Analysis Program)

CAPWAP is a computer program for a more rigorous evaluation of static pile capacity, the relative soil resistance distribution, and soil quake and damping characteristics. A CAPWAP analysis is performed on an individual hammer blow that is usually selected from the end of driving or beginning of restrike. As such, a CAPWAP analysis refines the Case Method dynamic test results at a particular penetration depth or time. CAPWAP uses wave equation type pile and soil models; the Pile Driving Analyzer measured force and velocity records are used as the head boundary condition, replacing the hammer model.

In the CAPWAP method depicted in Figure 17.15, the pile is modeled by a series of continuous pile segments and the soil resistance modeled by elasto-plastic springs (static resistance) and dashpots (dynamic resistance). The force and acceleration data from the Pile Driving Analyzer are used to quantify pile force and pile motion, which are

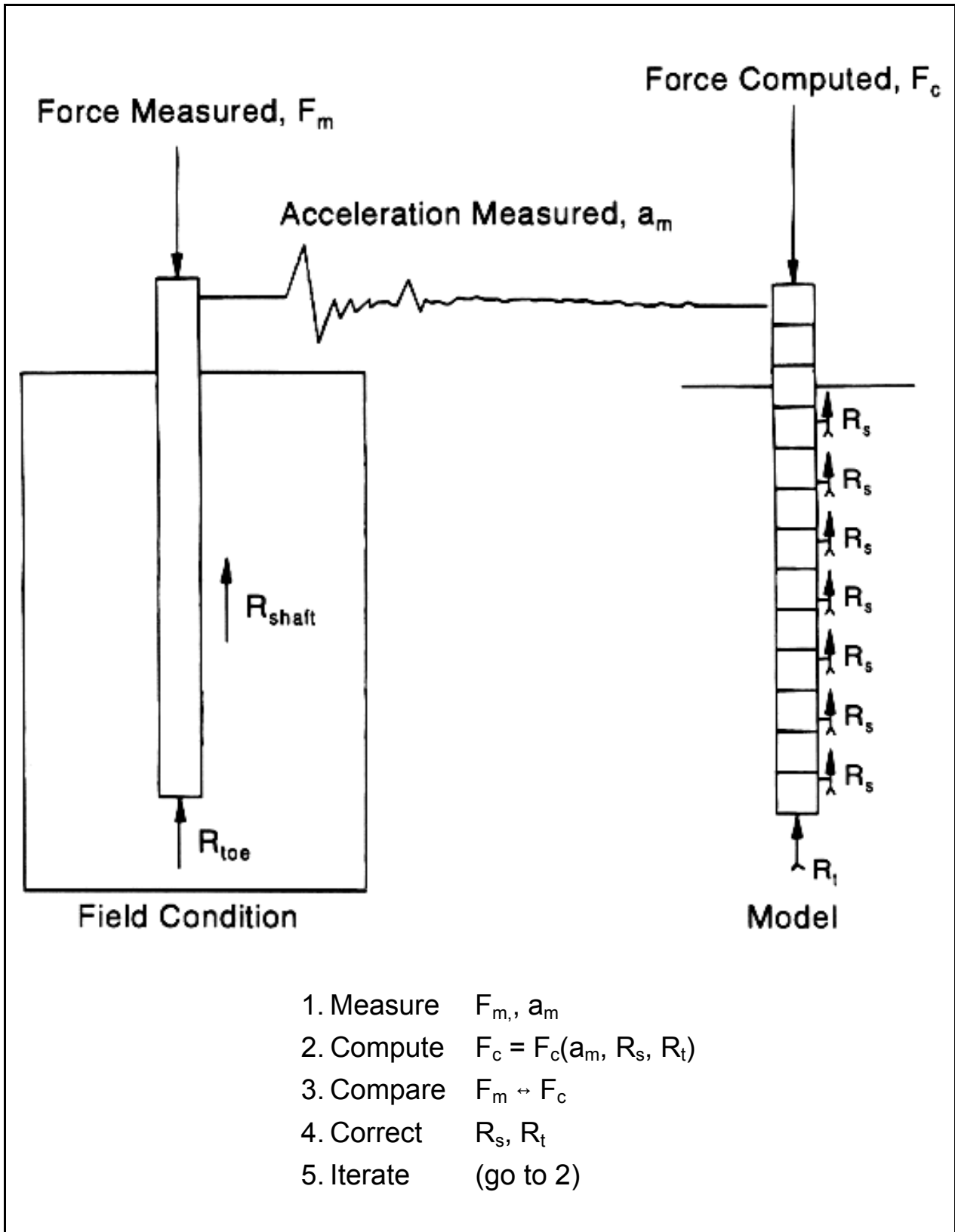


Figure 17.15 Schematic of CAPWAP Analysis Method

two of the three unknowns. The remaining unknown is the boundary conditions, which are defined by the soil model. First, reasonable estimates of the soil resistance distribution and quake and damping parameters are made. Then, the measured acceleration is used to set the pile model in motion. The program then computes the equilibrium pile head force, which can be compared to the Pile Driving Analyzer determined force. Initially, the computed and measured pile head forces will not agree with each other. Adjustments are made to the soil model assumptions and the calculation process repeated.

In the CAPWAP matching process, the ability to match the measured and computed waves at various times is controlled by different factors. Figure 17.16 illustrates the factors that most influence match quality in a particular zone. The assumed shaft resistance distribution has the dominant influence on match quality beginning with the rise of the record at time t_r before impact and continuing for a time duration of $2L/C$ thereafter. This is identified as Zone 1 in Figure 17.16.

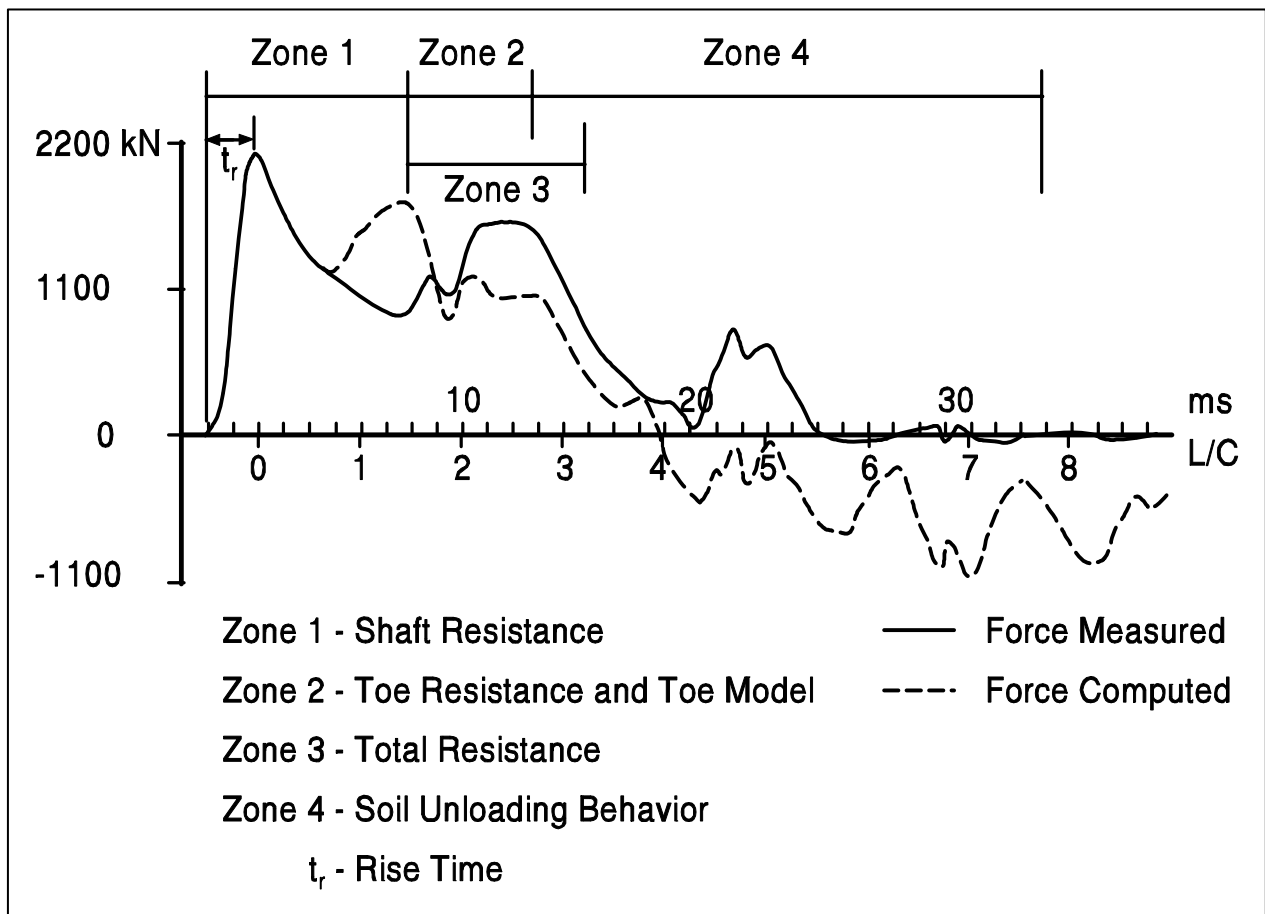


Figure 17.16 Factors Most Influencing CAPWAP Force Wave Matching (after Hannigan, 1990)

In Zone 2, the toe resistance and toe model (toe damping, toe quake and toe gap) most influence the wave match. Zone 2 begins where Zone 1 ends and continues for a time duration equal to the rise time, t_r plus 3 ms. During Zone 3, which begins where Zone 1 ends and continues for a time duration of the rise time t_r plus 5 ms, the overall capacity controls the match quality. A good wave match in Zone 3 is essential for accurate capacity assessments. Zone 4 begins at the end of Zone 2 and continues for a duration of 20 ms. The unloading behavior of the soil most influences match quality in this zone.

With each analysis, the program evaluates the match quality by summing the absolute values of the relative differences between the measured and computed waves. The program computes a match quality number for each analysis that is the sum of the individual match quality numbers for each of these four zones. An illustration of the CAPWAP iteration process is presented in Figure 17.17.

Through this trial and error iteration adjustment process to the soil model as illustrated in Figure 17.15, the soil model is refined until no further agreement can be obtained between the measured and computed pile head forces. The resulting soil model is then considered the best estimate of the static pile capacity, the soil resistance distribution, and the soil quake and damping characteristics. An example of the final CAPWAP result summary is presented in Figure 17.18. For each soil segment, this table lists the depth below grade and the corresponding soil resistance force, R_u .

Two additional CAPWAP output tables are illustrated in Figure 17.19. The top table, labeled the "EXTREMA TABLE", summarizes the stress distribution throughout the pile. This table is important because it indicates if higher compression stresses are present in the pile below the PDA gage location at pile segment number 1. The lower part of Figure 17.19 includes the "CASE METHOD" summary table. This table can be used to determine which Case Method capacity equation and damping factor correlates best with the more rigorous CAPWAP capacity. Hence, this table helps determine which Case Method equation and what damping factor should be used for similar piles that will not be analyzed by CAPWAP. For the data in Figure 17.19, the RMX Case Method equation with a damping factor of 0.60 to 0.65 would likely be selected. A CAPWAP analysis also includes a simulated static load-set graph based on the CAPWAP calculated static resistance parameters and the elastic compression characteristics of the pile at the time of testing.

CAPWAP is a proprietary program of Pile Dynamics, Inc. and the software is available from the developer. Alternatively, analysis of dynamic test data can be obtained from the developer or other consulting engineers who have acquired program licenses.

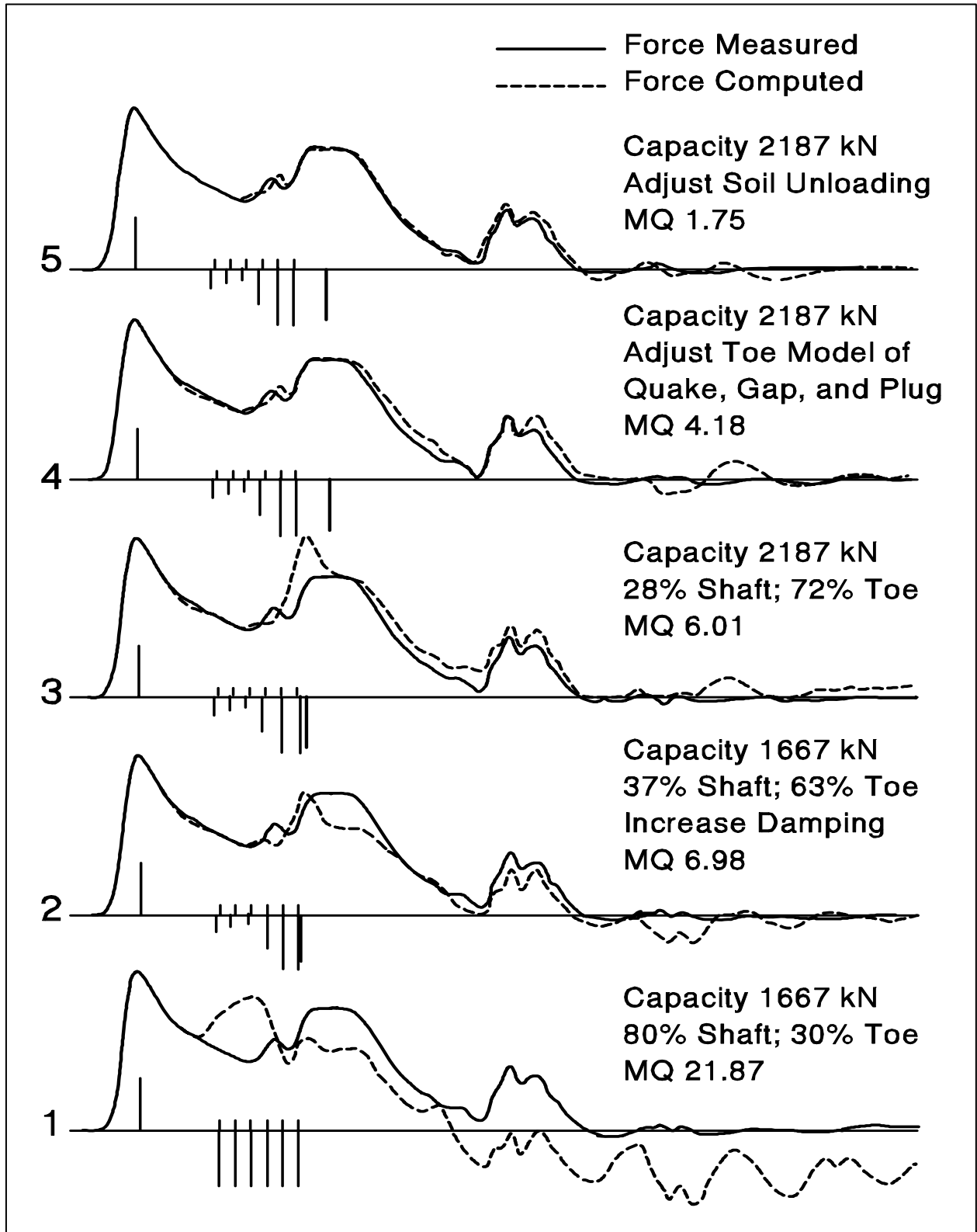


Figure 17.17 CAPWAP Iteration Matching Process (after Hannigan, 1990)

River Bridge; Pile: Test Pile #1, EOID
 Delmag D-30-32, HP 14x89; Blow: 1437
 GRL Engineers, Inc.

Test: 01-May-2003
 CAPWAP® Ver. 2000-3
 OP: GRL

CAPWAP FINAL RESULTS

Total CAPWAP Capacity: 3215.9; along Shaft 555.9; at Toe 2660.0 kN

Soil Sgmnt No.	Dist. Below Gages m	Depth Below Grade m	Ru kN	Force in Pile kN	Sum of Ru kN	Unit Resist. (Depth) kN/m	Unit Resist. (Area) kPa	Smith Damping Factor s/m	Quake mm
				3215.9					
1	7.1	1.6	8.9	3207.0	8.9	4.40	3.09	0.755	1.520
2	9.1	3.6	13.3	3193.7	22.2	6.58	4.62	0.755	1.519
3	11.1	5.7	17.8	3175.9	40.0	8.81	6.19	0.755	1.519
4	13.1	7.7	17.8	3158.1	57.8	8.81	6.19	0.755	1.519
5	15.2	9.7	17.8	3140.3	75.6	8.81	6.19	0.755	1.519
6	17.2	11.7	22.2	3118.1	97.8	10.99	7.72	0.755	1.519
7	19.2	13.7	26.7	3091.4	124.5	13.21	9.28	0.755	1.519
8	21.2	15.8	31.1	3060.3	155.6	15.39	10.81	0.755	1.519
9	23.2	17.8	31.1	3029.2	186.7	15.39	10.81	0.755	1.519
10	25.3	19.8	37.8	2991.4	224.5	18.71	13.14	0.755	1.519
11	27.3	21.8	40.0	2951.4	264.5	19.80	13.91	0.755	1.519
12	29.3	23.8	40.0	2911.4	304.5	19.80	13.91	0.755	1.519
13	31.3	25.9	35.6	2875.8	340.1	17.62	12.38	0.755	1.519
14	33.3	27.9	35.6	2840.2	375.7	17.62	12.38	0.755	1.519
15	35.4	29.9	44.5	2795.7	420.2	22.02	15.47	0.755	1.519
16	37.4	31.9	44.5	2751.2	464.7	22.02	15.47	0.755	1.519
17	39.4	33.9	44.5	2706.7	509.2	22.02	15.47	0.755	1.519
18	41.4	36.0	46.7	2660.0	555.9	23.11	16.24	0.755	1.519
Avg. Skin			30.9			15.46	10.74	0.755	1.519
Toe			2660.0				21035.76	0.279	4.570

Soil Model Parameters/Extensions

	Skin	Toe	
Case Damping Factor	0.617	1.091	Smith Type
Unloading Quake	(% of loading quake)	100	26
Reloading Level	(% of Ru)	100	100
Unloading Level	(% of Ru)	90	

CAPWAP match quality: 1.78(Wave Up Match)
 Observed: final set = 2.540 mm; blow count = 394 b/m
 Computed: final set = 2.455 mm; blow count = 407 b/m

Figure 17.18 CAPWAP Final Results Table

River Bridge; File: Test Pile #1, EOID
 Delmag D-30-32, HP 14x89; Blow: 1437
 GRL Engineers, Inc.

Test: 01-May-2003
 CAPWAP® Ver. 2000-3
 OP: GRL

EXTREMA TABLE

Pile Sgmt No.	Dist. Below Gages m	max. Force kN	min. Force kN	max. Comp. Stress MPa	max. Tens. Stress MPa	max. Trnsfd. Energy kJ	max. Veloc. m/s	max. Displ. mm
1	1.0	3270.0	-198.2	194.194	-11.769	45.10	4.6	23.359
2	2.0	3274.9	-202.7	194.487	-12.039	44.95	4.6	23.074
4	4.0	3284.6	-209.4	195.065	-12.433	44.65	4.6	22.490
6	6.1	3308.3	-209.9	196.473	-12.464	44.33	4.5	21.885
8	8.1	3299.7	-202.7	195.957	-12.040	43.45	4.5	21.261
10	10.1	3278.1	-188.8	194.676	-11.211	42.42	4.4	20.772
12	12.1	3240.4	-174.1	192.438	-10.339	41.17	4.4	20.239
14	14.1	3204.2	-183.0	190.287	-10.868	39.90	4.3	19.656
16	16.2	3174.8	-228.2	188.543	-13.550	38.63	4.2	19.031
18	18.2	3153.9	-249.3	187.298	-14.807	37.10	4.1	18.336
20	20.2	3080.7	-268.0	182.956	-15.913	35.36	4.1	17.596
22	22.2	3014.6	-287.1	179.031	-17.052	33.36	4.0	16.759
24	24.2	2956.9	-299.8	175.603	-17.802	31.32	3.9	15.853
26	26.3	2879.9	-304.7	171.027	-18.096	29.05	3.8	14.924
28	28.3	2796.1	-306.4	166.052	-18.196	26.60	3.7	13.858
30	30.3	2710.4	-310.3	160.962	-18.425	24.20	3.6	12.772
32	32.3	2646.2	-303.3	157.149	-18.014	21.80	3.5	11.561
34	34.4	2601.0	-244.7	154.464	-14.534	19.21	3.4	10.217
36	36.4	2547.6	-212.2	151.294	-12.603	16.45	3.2	8.837
38	38.4	2824.0	-167.4	167.711	-9.943	13.39	3.6	7.273
40	40.4	2883.3	-66.6	171.228	-3.956	10.39	3.8	5.662
41	41.4	3188.0	-51.1	189.326	-3.033	9.87	3.2	4.865
Absolute	7.1 31.3			197.253			(T = (T =	22.1 ms) 51.1 ms)

CASE METHOD

J =	0.0	0.1	0.2	0.3	0.4	0.5	0.6	0.7	0.8	0.9
RS1	3745.5	3467.0	3188.5	2910.0	2631.6	2353.1	2074.6	1796.1	1517.7	1239.2
RMX	4187.0	4009.0	3830.9	3652.8	3514.8	3378.6	3242.4	3106.2	2990.5	2889.2
RSU	3779.8	3504.7	3229.7	2954.7	2679.6	2404.6	2129.5	1854.5	1579.4	1304.4

RAU= 439.8 (kN); RA2= 1932.0 (kN)

Current CAPWAP Ru= 3215.9 (kN); Corresponding J(Rs)= 0.19; J(Rx)=0.62

VMX	VFN	VT1*Z	FT1	FMX	DMX	DFN	EMX	RLT
m/s	m/s	kN	kN	kN	mm	mm	kJ	kN
4.62	0.00	3139.5	3390.7	3390.7	23.485	2.524	45.5	3501.8

Figure 17.19 CAPWAP EXTREMA and Case Method Tables

17.6 USAGE OF DYNAMIC TESTING METHODS

Dynamic testing is specified in many ways, depending upon the information desired or purpose of the testing. For example, a number of test piles driven at preselected locations may be specified. In this application, the test piles are usually driven in advance of, or at the start of, production driving so that the information obtained can be used to establish driving criteria and/or pile order lengths for each substructure unit. Alternatively, or in addition to a test pile program, testing of production piles on a regular interval may be specified. Production pile testing is usually performed for quality assurance checks on hammer performance, driving stress compliance, pile integrity, and ultimate capacity. Lastly, dynamic testing can be used on projects where it was not specified to troubleshoot problems that arise during construction.

The number of piles that should be dynamically tested on the project depends upon the project size, variability of the subsurface conditions, the availability of static load test information, and the reasons for performing the dynamic tests. A higher percentage of piles should be tested, for example, where there are difficult subsurface conditions with an increased risk of pile damage, or where time dependent soil strength changes are being relied upon for a significant portion of the ultimate pile capacity.

On small projects, a minimum of two dynamic tests is recommended. On larger projects and small projects with anticipated installation difficulties or significant time dependent capacity issues, a greater number of piles should be tested. Dynamically testing one or two piles per substructure location is not unusual in these situations. Regardless of the project size, specifications should allow the engineer to adjust the number and locations of dynamically tested piles based on design or construction issues that arise.

Restrike dynamic tests should be performed whenever pile capacity is being evaluated by dynamic test methods. Restrikes are commonly specified 24 hours after initial driving. However, in fine grained soils, longer time periods are generally required for the full time dependent capacity changes to occur. Therefore, longer restrike times should be specified in these soil conditions whenever possible. On small projects, long restrike durations can present significant construction sequencing problems. Even so, at least one longer term restrike should be performed in these cases. The longer term restrike should be specified 2 to 6 days after the initial 24 hour restrike, depending upon the soil type. A warmed up hammer (from driving or restriking a non-test pile) should be used whenever restrike tests are performed.

In soils that exhibit large setup, it may not be possible to activate all the soil resistance available at the time of restrike with the pile hammer used for original pile installation. A drop hammer system, such as the 140 kN (31 kip) ram shown in Figure 17.20, can be used to effectively evaluate restrike pile capacities in these situations. Typically, a ram weight of approximately 2% of the desired ultimate pile capacity is required.



Figure 17.20 APPLE Drop Weight System (courtesy GRL Engineers, Inc.)

When dynamic testing is performed by a consultant, the requirements for CAPWAP analyses should be specifically addressed in the dynamic testing specification. On larger projects, CAPWAP analyses are typically performed on 20 to 40% of the dynamic

test data obtained from both initial driving and restrike dynamic tests. This percentage typically increases on smaller projects with only a few test piles, or on projects with highly variable subsurface conditions.

It is often contractually convenient to specify that the general contractor retain the services of the dynamic testing firm. However, this can create potential problems since the contractor is then responsible for the agency's quality assurance program. Some agencies have contracted directly with the dynamic testing firm to avoid this potential conflict and many large public owners have purchased the equipment and perform the tests with their own staff.

17.7 PRESENTATION AND INTERPRETATION OF DYNAMIC TESTING RESULTS

The results of dynamic pile tests should be summarized in a formal report that is sent to both the construction engineer and foundation designer. The construction engineer should understand the information available from the dynamic testing and its role in the project construction. As discussed in Chapter 9, numerous factors are considered in a pile foundation design. Therefore, the foundation designer should interpret the dynamic test results since many other factors; (downdrag, scour, uplift, lateral loading, settlement, *etc.*) may be involved in the overall design and construction requirements.

Construction personnel are often presented with dynamic testing results with minimal guidance on how to interpret or use the information. Therefore, it may be helpful to both construction personnel and foundation designers to familiarize themselves with the typical screen display and information available during a dynamic test. Figure 17.21 presents a typical Pile Driving Analyzer display for a PDA using a DOS operating system and the display for a Windows based PDA is presented in Figure 17.22.

In both systems, the main Pile Driving Analyzer input quantities are displayed near the upper left corner of the screen and include the pile length below gages, LE; the pile cross sectional area at the gages, AR; the pile elastic modulus, EM; the unit weight of the pile material, SP; the pile wave speed, WS; as well as the Case damping factor, JC.

In the DOS unit, construction personnel reviewing field results should note the units indicator, UN, on the screen. The force units are noted to be in "kN * 10" or kilonewtons times 10. This means any forces (but not stresses), capacity, or energy results displayed in the numerical results must be multiplied by 10. In the Windows unit, a unit multiplier is not used and numerical results therefore do not need to be adjusted.

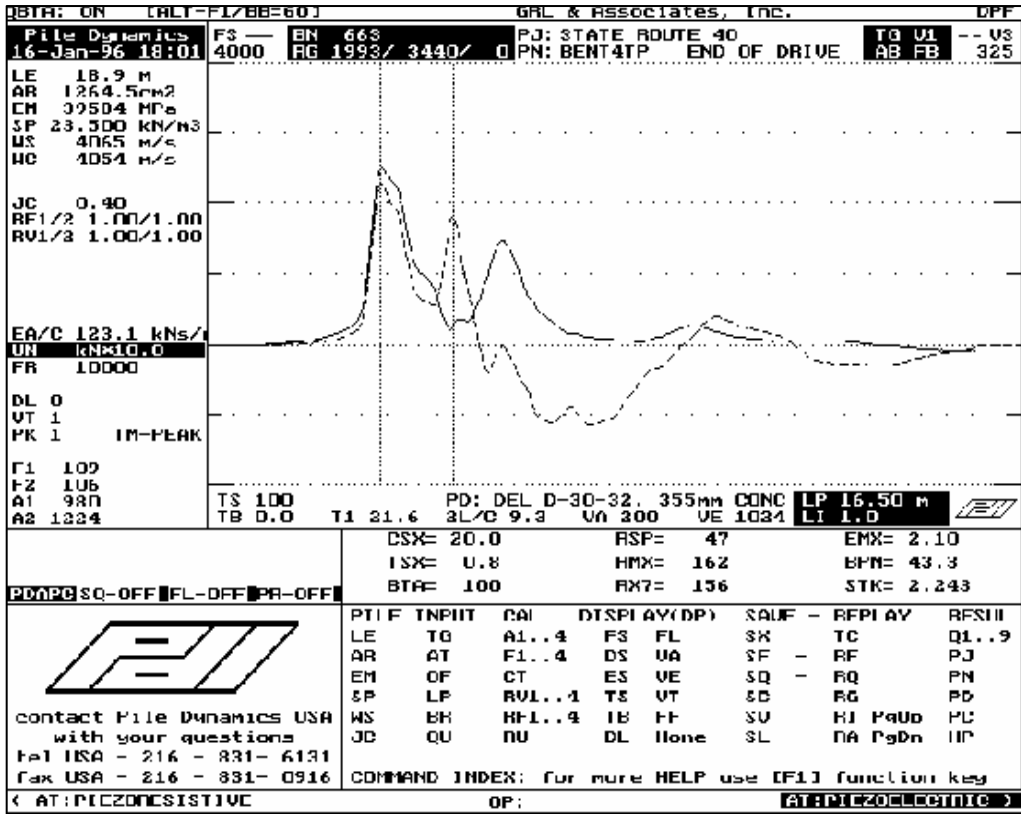


Figure 17.21 Typical Screen Display for Pile Driving Analyzer – DOS System

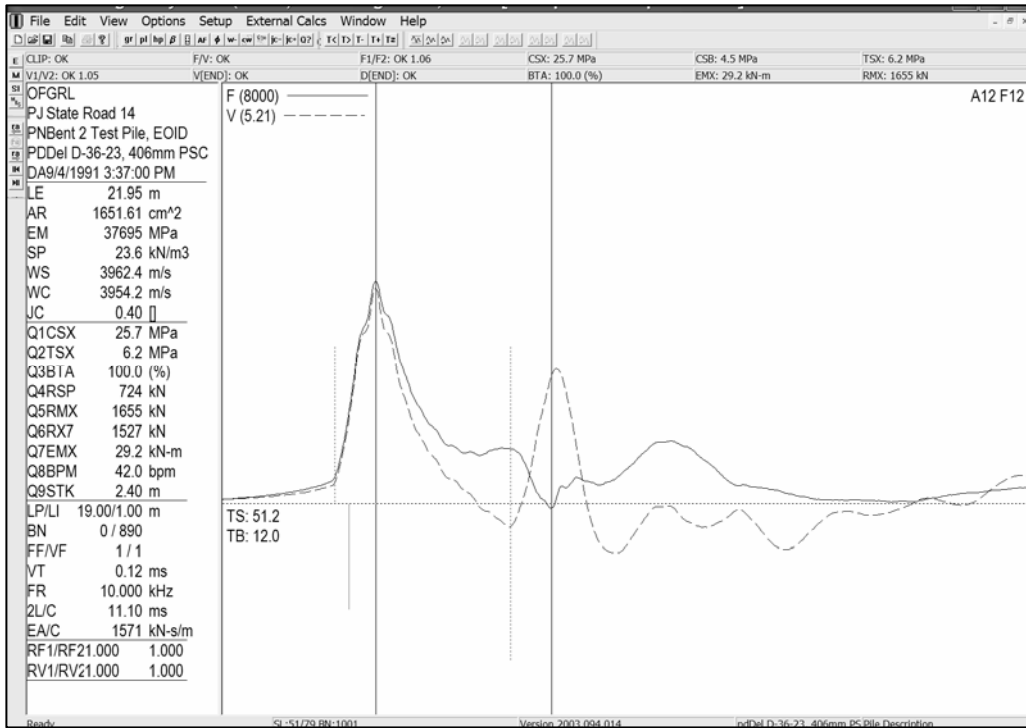


Figure 17.22 Typical Screen Display for Pile Driving Analyzer – Windows System

In both operating systems, the screen is dominated by the graphical display of force (solid line) and velocity (dashed line) records versus time. This display will change for each hammer blow. The first vertical line represents time t_1 in the Case Method calculations and corresponds to the time of impact as the waves pass the gage location near the pile head. The second vertical line represents time t_2 in the Case Method calculations and corresponds to the time when the input waves have traveled to the pile toe and returned to the gage location or time $2L/C$. (Note in the Windows PDA the t_1 and t_2 times are the full length vertical lines.)

An experienced test engineer can visually interpret these signals for data quality, soil resistance distribution and pile integrity. As discussed earlier, soil resistance forces cause a relative increase in the force wave and a corresponding relative decrease in the velocity wave. Therefore on a pile with a uniform cross section, the separation between the force and velocity records between times t_1 and t_2 indicates the shaft resistance. The magnitude of separation is also indicative of the magnitude of the soil resistance at that depth. Toe resistance is indicated by the separation between these records near and after time t_2 .

The Pile Driving Analyzer searches for convergence between the force and velocity records beginning at the time of the sharp rise in the records prior to time t_1 and continuing for a time interval of $2L/C$ thereafter. If convergence between the force and velocity records occurs prior to the rise in the velocity record preceding time t_2 , a cross sectional reduction or pile damage is indicated. The degree of convergence between the force and velocity records is expressed by the BTA integrity value as a percentage of the approximate reduced cross sectional area.

Numerical results from Case Method computations are identified by three letter codes displayed below the graphical records in a DOS PDA unit and to the left of the graphical records in a Windows PDA unit. A summary of the most commonly computed quantities and their corresponding three letter code is presented in Table 17-3. In the example given in Figure 17.22, the first three output quantities Q1, Q2, and Q3 provide information on the driving stresses and pile integrity. The compression stress at the gage location near the pile head, CSX, is 25.7 MPa (3.73 ksi) and the calculated tension stress, TSX, is 6.2 MPa (0.90 ksi). Recommended driving stress limits for piles are presented in Chapter 10. For a prestressed concrete pile with a 28 day concrete strength of 34.5 MPa (5 ksi) and an effective prestress after losses of 5 MPa (0.7 ksi), the maximum recommended compression and tension driving stresses would be 24.3 (3.52 ksi) and 6.5 MPa (0.94 ksi). Hence, the compression stress would exceed the

TABLE 17-3 DESCRIPTIONS OF PDA OUTPUT CODES		
Output Information	PDA 3 Letter Code	Output Quantity Description
Pile Stresses & Integrity	CSX	Maximum Compression Stress at Gage Location.
	CSI	Maximum Compression Stress from One Gage.
	CSB	Maximum Computed Compression Stress at Pile Toe.
	TSX	Maximum Computed Tension Stress.
	BTA	Pile Integrity Factor.
	LTD	Length to Pile Damage.
Drive System Performance	EMX	Maximum Energy Transfer to Gages.
	ETR	Energy Transfer Ratio (EMX / E rated).
	STK	Computed Hammer Stroke.
	BPM	Hammer Operating Rate.
Static Pile Capacity	RMX	Maximum Case Method (requires damping factor, J).
	RSP	Standard Case Method (requires damping factor, J).
	RSU	Case Method with Unloading Correction (requires J).
	RAU	Automatic Case Method – End Bearing. No Friction.
	RA2	Automatic Case Method - Moderate Friction.

driving stress limit and the tension stress is approaching the limit. Pile integrity, BTA, is calculated as 100%, indicating that no damage is present.

The middle three output quantities Q4, Q5, and Q6 include computations for the standard Case Method capacity, RSP, and maximum Case Method capacity, RMX, both calculated with the input Case damping factor, JC, of 0.4. These results are 724 (163 kips) and 1655 kN (372 kips) respectively. As noted earlier, a damping factor at least 0.2 higher is usually used with the maximum Case Method as compared to the standard Case Method. Therefore, the capacity using the RMX equation with a damping factor of 0.7 labeled RX7 was calculated and indicated a capacity of 1527 kN (343 kips). From the force and velocity records in the example, the experienced test engineer would note that the resistance is delayed in time, based upon the separation between the force and velocity records occurring after time t_2 . Therefore, the maximum Case Method equation

should be used for capacity evaluation, and from the capacity results noted above, a Case Method capacity of 1527 kN (343 kips) would be chosen.

The final three output quantities Q7, Q8, and Q9 include the maximum transferred hammer energy, EMX, which is 29 kJ (21 ft-kips); the hammer operating speed in blows per minute, BPM, which is 42.0; and the calculated hammer stroke for the single acting diesel hammer, STK which is 2.40 m (7.9 ft).

Depending upon the hammer-pile combination, average transferred energies as a percentage of the rated energy range from about 26% for a diesel hammer on a concrete pile to 55% for an air hammer on a steel pile. Hence, the transferred energy of 29 kJ (21 ft-kips) is 24% of the rated energy and is therefore slightly below average.

The performance of a hammer and driving system can be evaluated from a driving system's energy transfer ratio, which is defined as the energy transferred to the pile head divided by the manufacturer's rated hammer energy. Figure 17.23 presents energy transfer ratios for selected hammer and pile type combinations expressed as a percentile. In this graph, the average transfer efficiency for a given hammer-pile combination can be found by noting where that graph intersects the 50 percentile. Histograms of the transfer efficiencies for each of these hammer and pile types are also presented in Figure 17.24. The histograms may be useful in assessing drive system performance as they provided the distribution and standard deviation of drive system performance for a given hammer-pile combination at the end of drive condition. It should be noted that numerous factors affect the transferred energy including the pile impedance, pile length, soil resistance, dynamic soil properties, helmet weight, hammer and pile cushions, and the hammer efficiency.

In the field, construction personnel should check that the calculated driving stresses, CSX and TSX, are maintained within specification limits. Drive system performance indicated by the transferred energy, EMX, should be within a reasonable range of that predicted by wave equation analysis or recorded on previous tests at the site. If significant variations in energy are noted, the reasons for the discrepancy should be evaluated. The recorded hammer speed should be compared to the manufacturer's specifications. Capacity estimates should be compared with the required ultimate pile capacity. In soils with time dependent changes in capacity, this comparison should be based on restrrike tests and not end-of-initial driving results.

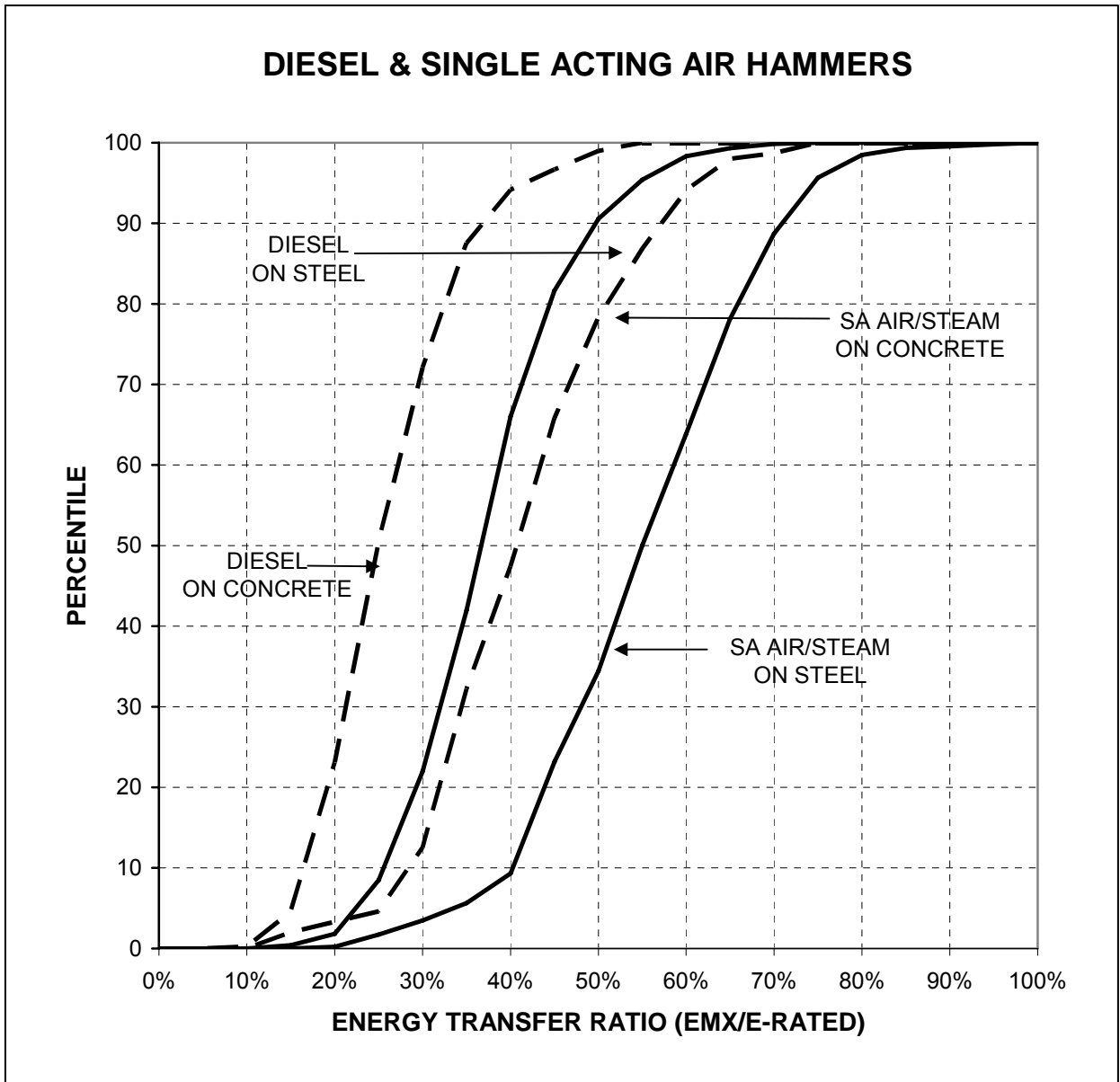


Figure 17.23. Energy Transfer Ratios for Select Hammer and Pile Combinations

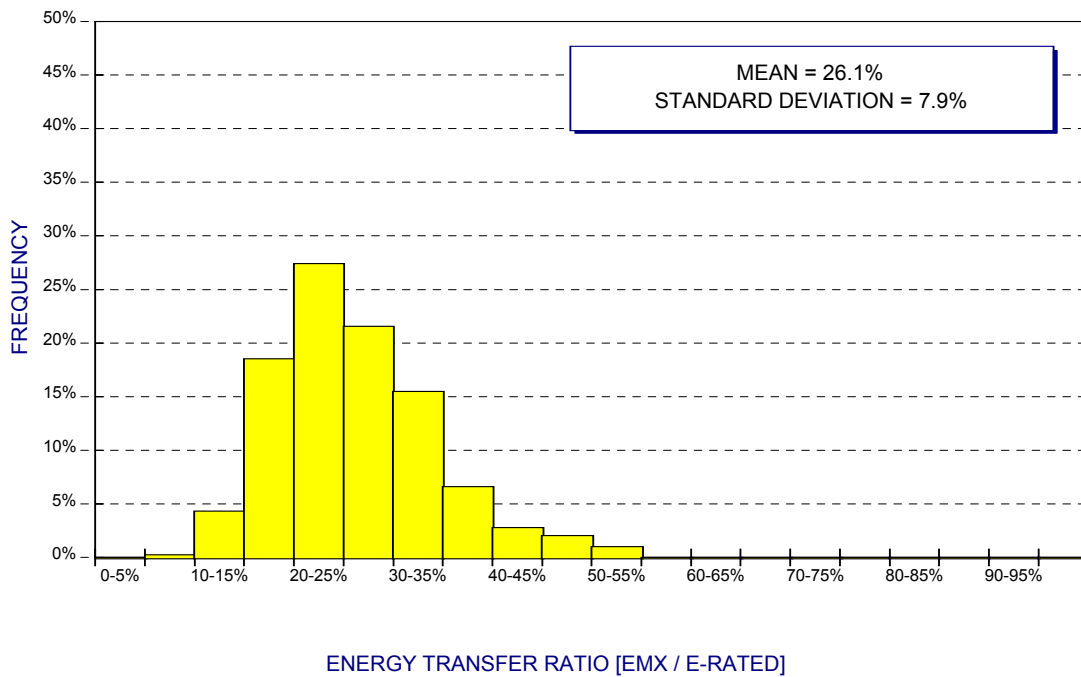
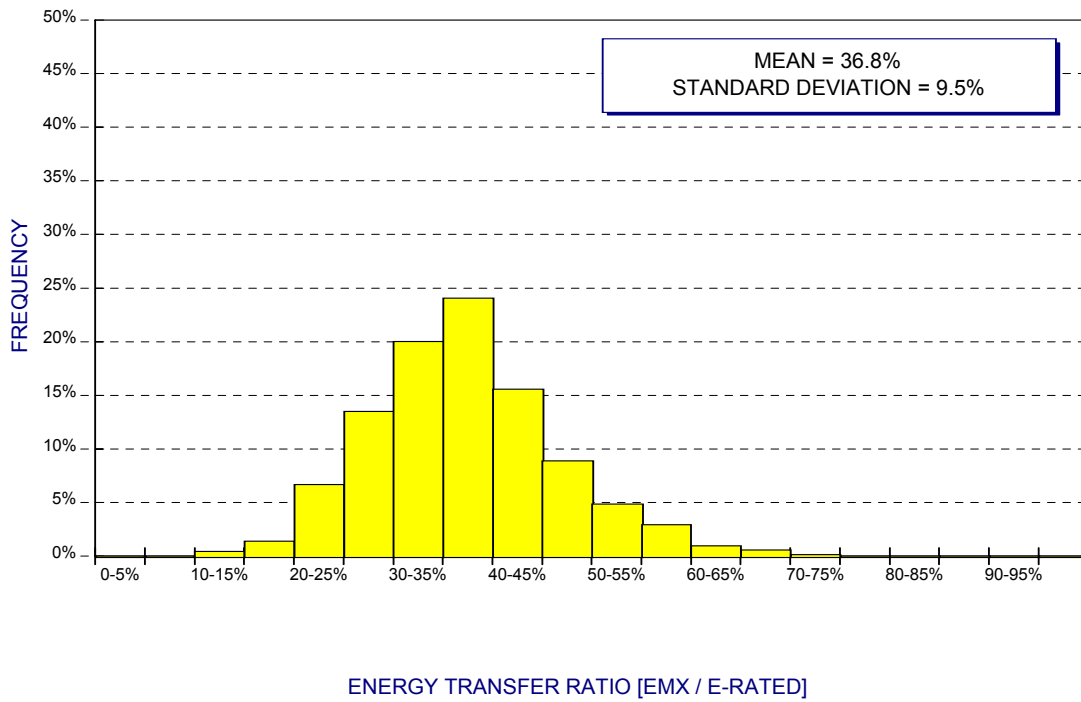


Figure 17.24(a) Histograms of Energy Transfer Ratio for Diesel Hammers on Steel Piles (top) and Concrete/Timber Piles (bottom).

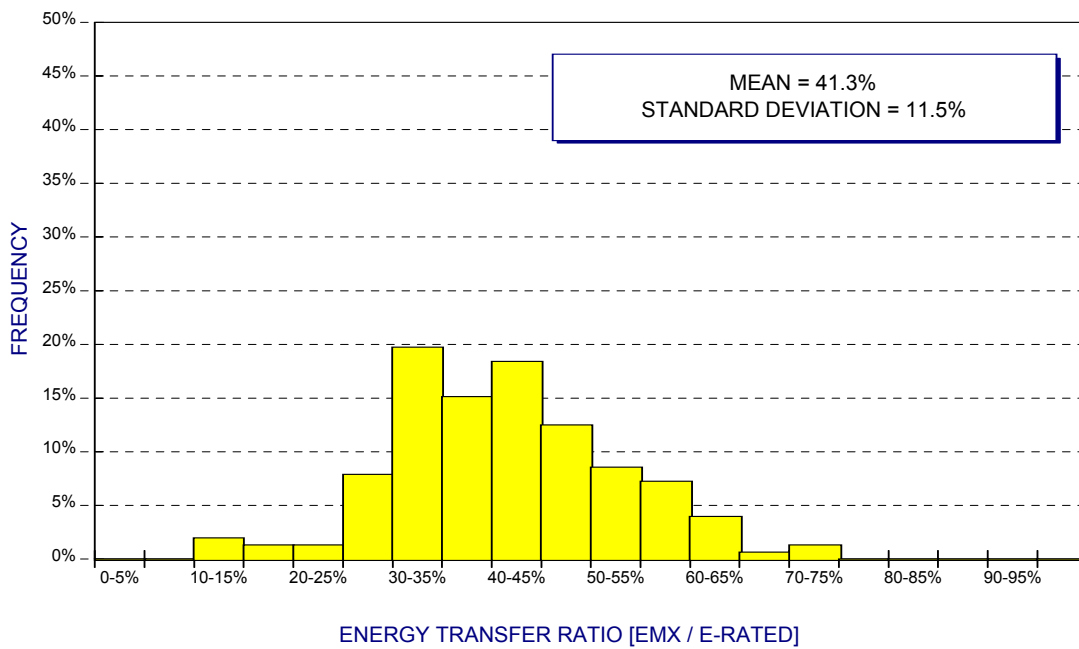
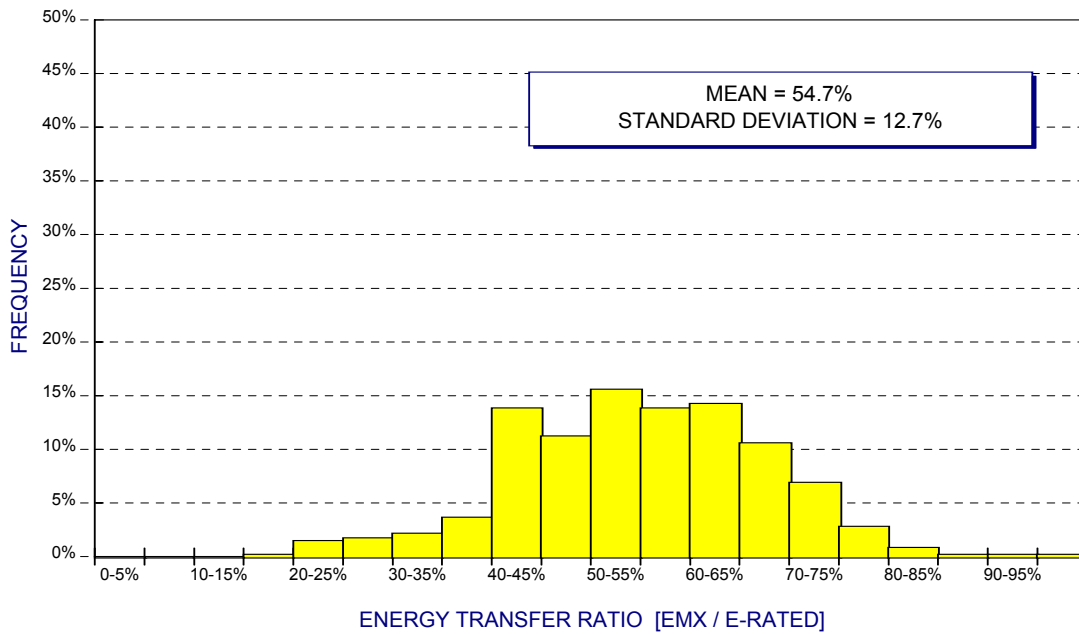


Figure 17.24(b) Histograms of Energy Transfer Ratio for Single Acting Air/Steam Hammers on Steel Piles (top) and Concrete/Timber Piles (bottom).

A force and velocity record for a HP 360 x 174 (HP 14x117) H-pile is presented in Figure 17.25. As can be seen from the input properties, the H-pile is 26.9 meters (88 ft) long below gages. A visual interpretation of the signal would indicate the pile has developed moderate shaft resistance over the lower portion of the pile with a significant amount of the pile capacity due to toe resistance. Note that a dash and dotted vertical line has also appeared between the two solid vertical lines corresponding to the pile head, t_1 , and pile toe, t_2 . Convergence between the force and velocity records before time $2L/C$, as noted by the dash and dotted line, indicates a pile impedance reduction or damage. The BTA warning box near the top of the screen has also turned black and indicates a calculated BTA value of 81%. For the example shown, damage was occurring at a depth of 24.3 meters (80 ft) below gages due to the H-pile buckling and bending at this location. The pile was extracted to confirm the PDA indicated damage. Photographs of the extracted pile are presented in Figure 17.26.

Records for a 63.8 m (209 ft) long pile with multiple failing welded splices is depicted in Figure 17.27. Significant cross section reductions are indicated in the record for the welded splices located 34.8 m and 45.1 m below the gage location. The PDA computed BTA values for these two splices are 77% and 39%, respectively. While a Case Method capacity is calculated for the record, this capacity should not be used since the pile is no longer of uniform cross section. A pile with this severity of damage should be abandoned and a replacement pile or piles installed.

In Figure 17.28, a force and velocity record for a HP 360 x 132 H-pile driven to rock is presented. Note the strong separation in the force and velocity records at time $2L/C$ (second full length vertical line). The compression stress at the gage location, CSX, is 224 MPa (32.5 ksi). This is slightly above the recommended driving stress limit of 223 MPa (32.4 ksi) for A-36 steel given in Chapter 10. The Pile Driving Analyzer can also compute an estimate of the compression stress at the pile toe, CSB. This quantity may be helpful in driving stress control for piles to rock. For the record shown, CSB is calculated to be 241 MPa (34.9 ksi) which is above the recommended driving stress limit. Therefore, a slight reduction in hammer stroke at final driving may be necessary. The CSB quantity is an approximate value. A better assessment of the compression stresses at the pile toe could be gained from CAPWAP or wave equation analyses.

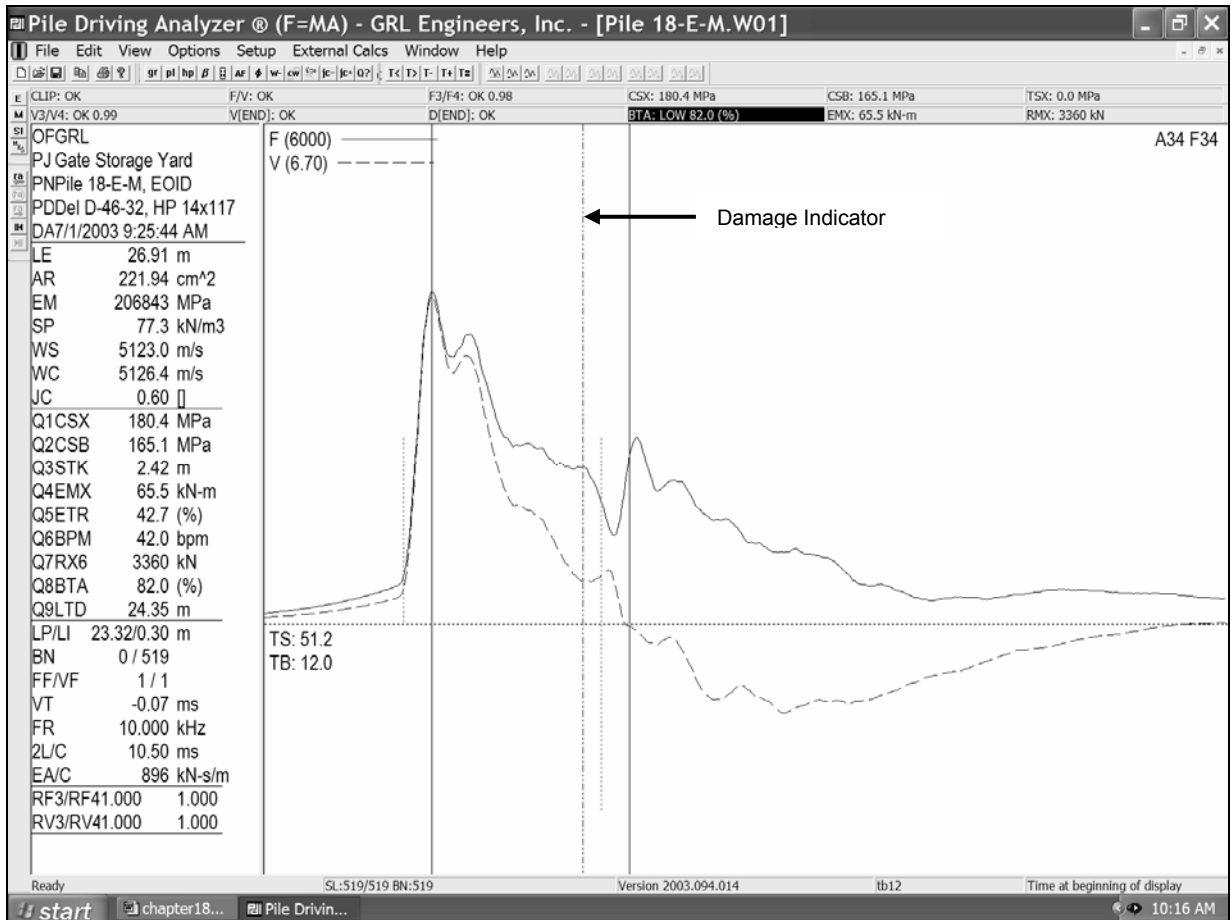


Figure 17.25 Force and Velocity Records Indicating Pile Damage



Figure 17.26 Photographs of Extracted Damaged Pile From Figure 17.25

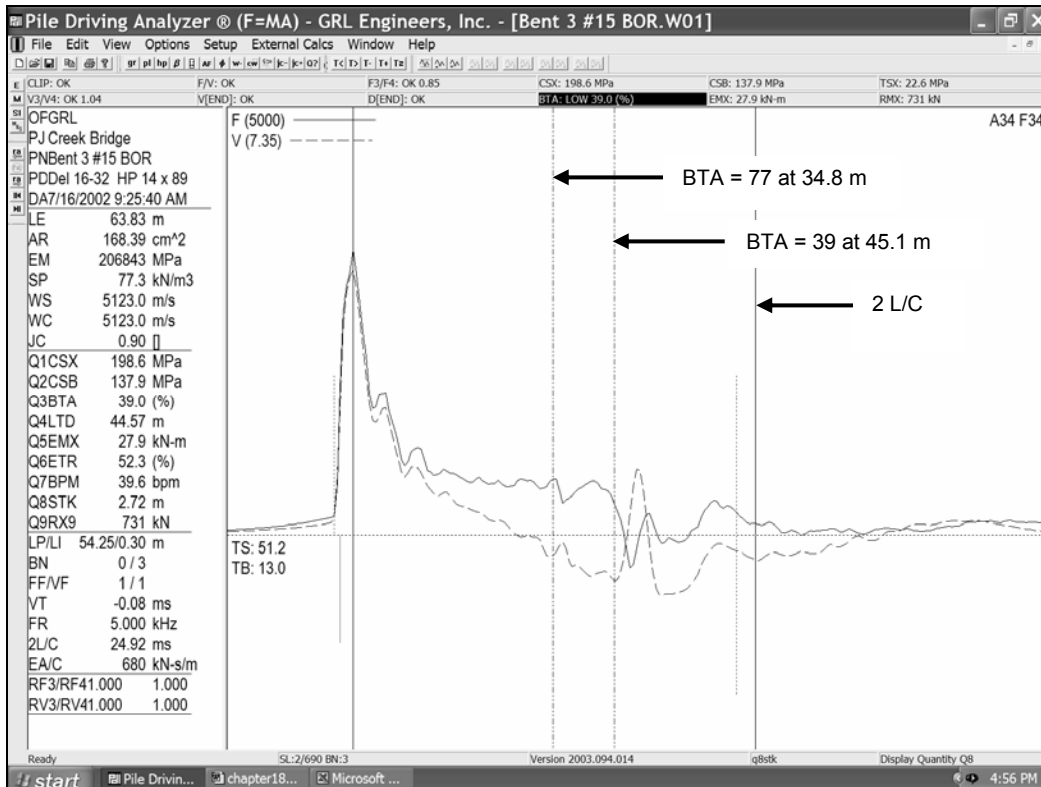


Figure 17.27 Force and Velocity Record for Pile With Splice Failures

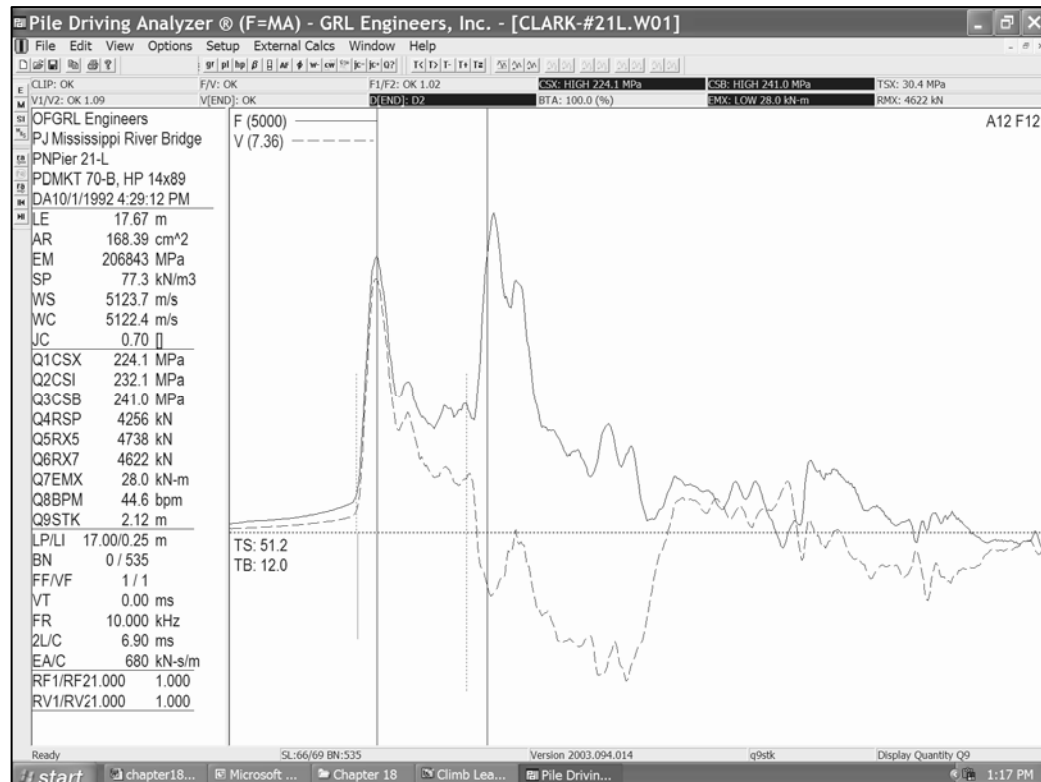


Figure 17.28 Force and Velocity Record for H-pile to Rock

Additional insight into the pile and soil behavior during driving can be obtained by comparing the dynamic test numerical results versus pile penetration depth and corresponding driving resistance. Dynamic testing systems typically assign a sequential blow number to each hammer blow. By comparing the pile driving records with these blow numbers, numerical and graphical summaries of the dynamic testing results versus pile penetration depth and driving resistance can be prepared.

An example of a numerical summary of the dynamic testing results versus depth for a 610 mm (24 inch) octagonal concrete pile is presented in Table 17-4 with accompanying graphical results presented in Figure 17.29. Specification should require that the dynamic test data for each pile tested be processed in this manner. These numerical and graphical results can easily be compared to project requirements by construction personnel.

TABLE 17-4 TYPICAL TABLUAR PRESENTATION OF DYNAMIC TESTING

Proj: PDAPLOT EXAMPLE		Increment = (depth)		Pg1						
File: PRESTRESSED CONCRETE		FileName = FGCTP5.MDF								
Desc: DIESEL HAMMER		BL# 2 to 1349		31-Oct-94						

CSX: Max Measured C-Stress		RMX: Capacity - RMX								
TSX: Max Computed T-Stress		BPM: Blows Per Minute								
EMX: Max Transferred Energy		STK: Stroke (O.E.Diesels)								

BL#	depth	TYPE	#Bls	CSX	TSX	EMX	RMX	BPM	STK	
end	bl/m	m		MPa	MPa	kN-m	kN	bl/min	m	
11	18	8.00	AVG	6	8.48	2.05	18.85	285	56.1	1.439
34	23	9.00	AVG	9	12.04	2.92	27.03	584	49.6	1.696
64	30	10.00	AVG	23	14.67	3.63	27.40	1107	47.6	1.845
92	28	11.00	AVG	12	15.25	3.43	27.98	1210	47.5	1.846
123	31	12.00	AVG	15	15.62	4.08	28.03	1059	47.6	1.843
166	43	13.00	AVG	14	15.93	5.33	30.79	577	48.1	1.801
199	33	14.00	AVG	11	17.29	3.92	30.55	1143	47.1	1.882
225	26	15.00	AVG	8	17.62	4.96	33.44	875	47.5	1.850
245	20	16.00	AVG	7	18.29	6.23	33.91	586	47.4	1.857
266	21	17.00	AVG	6	18.03	6.47	33.83	340	48.1	1.802
289	23	18.00	AVG	8	18.09	6.65	35.90	284	48.0	1.808
322	33	19.00	AVG	16	18.25	6.14	36.47	529	47.1	1.880
370	48	20.00	AVG	24	20.80	5.75	39.59	1104	45.9	1.989
409	39	21.00	AVG	20	25.14	7.97	45.27	1137	45.3	2.045
453	44	22.00	AVG	22	26.33	7.91	45.81	1124	45.5	2.026
493	40	23.00	AVG	20	26.31	8.10	46.87	1003	45.6	2.014
568	75	24.00	AVG	30	15.65	1.52	33.30	1040	47.3	1.863
609	41	25.00	AVG	13	16.63	3.56	34.01	931	47.8	1.824
641	32	26.00	AVG	15	17.01	4.48	32.45	893	48.3	1.780
668	27	27.00	AVG	14	18.19	5.50	33.36	857	48.2	1.793
696	28	28.00	AVG	14	19.54	6.30	36.02	864	47.5	1.847
730	34	29.00	AVG	16	19.88	6.67	35.87	816	48.2	1.794
759	29	30.00	AVG	14	20.50	6.51	39.53	870	47.1	1.876
785	26	31.00	AVG	13	23.97	8.49	44.45	868	46.9	1.896
820	35	32.00	AVG	18	25.61	9.52	45.19	761	47.2	1.868
857	37	33.00	AVG	18	27.16	9.16	48.37	861	46.4	1.939
893	36	34.00	AVG	18	28.13	8.13	51.74	1056	45.8	1.994
933	40	35.00	AVG	20	27.48	9.15	49.39	868	46.5	1.933
971	38	36.00	AVG	19	26.64	9.04	45.58	767	47.3	1.867
1012	41	37.00	AVG	41	25.49	7.91	38.45	899	48.9	1.739
1050	38	38.00	AVG	38	24.55	9.00	36.31	796	49.4	1.699
1078	28	39.00	AVG	14	24.27	9.75	36.11	671	49.5	1.692
1106	28	40.00	AVG	10	22.62	8.52	35.04	596	49.6	1.689
1199	93	41.00	AVG	49	15.60	1.67	28.10	948	49.4	1.703
1235	144	41.25	AVG	18	17.01	0.60	31.84	1672	47.6	1.839
1275	160	41.50	AVG	18	16.88	1.16	30.38	2072	47.7	1.835
1329	216	41.75	AVG	26	19.70	1.50	40.17	2434	44.7	2.115
1349	200	41.85	AVG	9	33.30	6.11	67.31	2623	41.5	2.451

31-Oct-94

GRL & ASSOC, INC.

PDAPLOT EXAMPLE, PRESTRESSED CONCRETE, DIESEL HAMMER

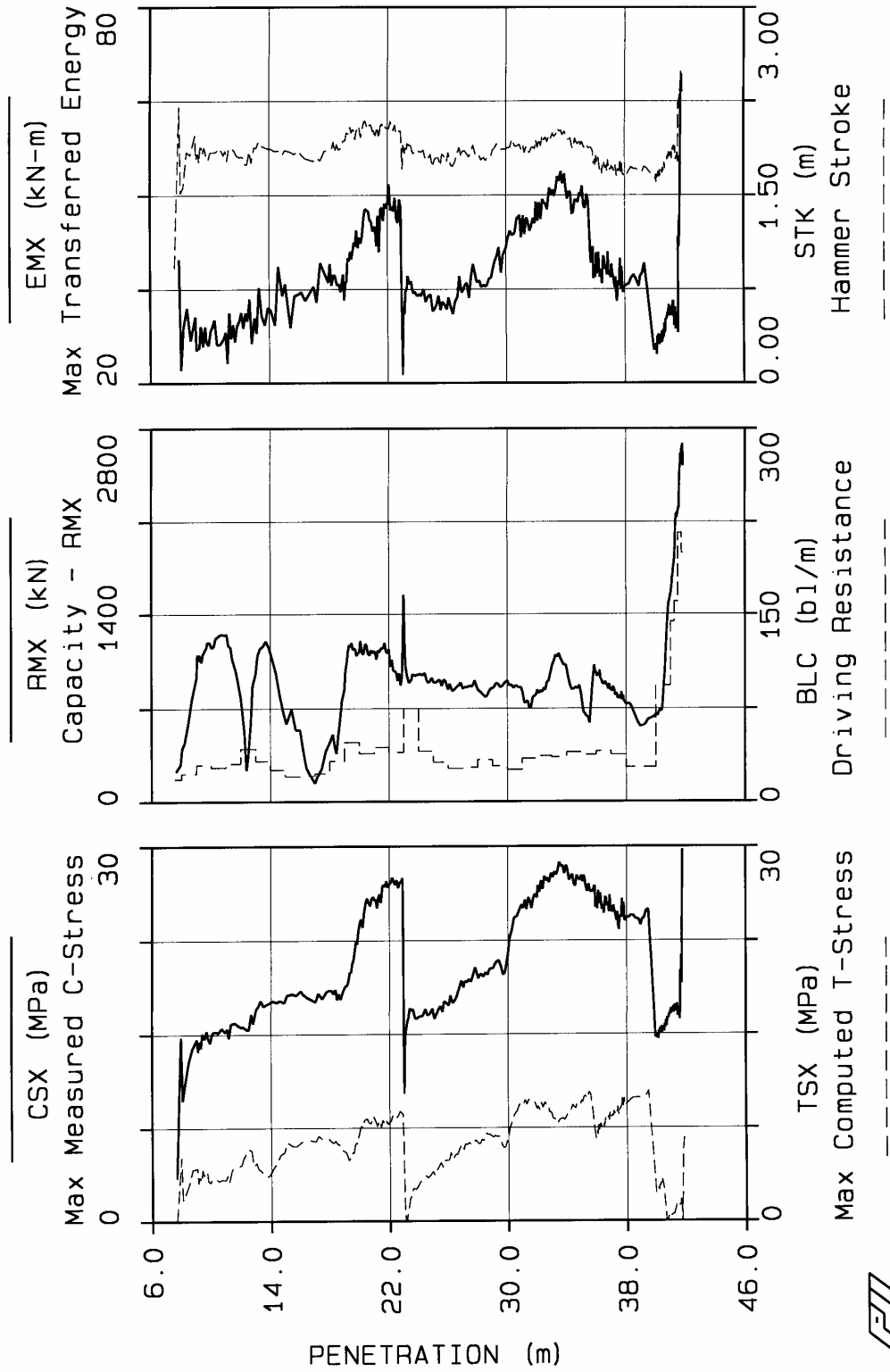


Figure 17.29 Typical Graphical Presentation of Dynamic Testing Results versus Depth

17.8 ADVANTAGES

Dynamic tests provide information on the complete pile installation process. Test results can be used to estimate pile capacity, to check hammer and drive system performance, to monitor driving stresses, and to assess pile structural integrity.

Many piles can be tested during initial driving or during restrike in one day. This makes dynamic testing an economical and quick testing method. Results are generally available immediately after each hammer blow.

On large projects, dynamic testing can be used to supplement static pile load tests or reduce the overall number of static tests to be performed. Since dynamic tests are more economical than static tests, additional coverage can also be obtained across a project at reduced costs. On small projects where static load tests may be difficult to justify economically, dynamic tests offer a viable construction control method.

Dynamic tests can provide information on pile capacity versus depth, capacity variations between locations, and capacity variations with time after installation through restrike tests. This information can be helpful in augmenting the foundation design, when available from design stage test pile programs, or in optimizing pile lengths when used early in construction test programs.

When used as a construction monitoring and quality control tool, dynamic testing can assist in early detection of pile installation problems such as poor hammer performance or high driving stresses. Test results can then facilitate the evaluation and solution of these installation problems.

On projects where dynamic testing was not specified and unexpected or erratic driving behavior or pile damage problems develop, dynamic testing offers a quick and economical method of troubleshooting.

Results from dynamic testing and analysis can be used for driving criteria development including wave equation input parameter selection and refinement of wave equation results as described in Section 16.6.6.

17.9 DISADVANTAGES

Dynamic testing to determine the ultimate static pile capacity requires that the driving system mobilize all the soil resistance acting on the pile. Shaft resistance can generally be mobilized at a fraction of the movement required to mobilize the toe resistance. However, when pile penetration resistances approach 100 blows per quarter meter (10 blows per inch), the soil resistance may not be fully mobilized at and near the pile toe. In these circumstances, dynamic test capacities tend to produce lower bound capacity estimates. At times, a larger pile hammer or higher hammer stroke can be used to increase the pile net penetration per blow.

Dynamic testing estimates of static pile capacity indicate the capacity at the time of testing. Since increases and decreases in the pile capacity with time typically occur due to soil setup/relaxation, restrike tests after an appropriate waiting period are usually required for a better indication of long term pile capacity. This may require an additional move of the pile driving rig for restrike testing.

Larger diameter open ended pipe piles or H-piles which do not bear on rock may behave differently under dynamic and static loading conditions. This is particularly true if a soil plug does not form during driving. In these cases, limited toe bearing resistance develops during the dynamic test. However, under slower static loading conditions, these open section piles may develop a soil plug and therefore a higher pile capacity under static loading conditions. Interpretation of test results by experienced personnel is important in these situations.

17.10 CASE HISTORY

The following case history illustrates how dynamic pile testing and analysis was used on a small single span bridge constructed in a remote area. The subsurface exploration for the project found a 30 m (98 ft) deposit of moderately clean, medium dense to dense sands with SPT N values ranging from 17 to 50. Based upon these conditions, the foundation report recommended 324 mm (12.75 inch) O.D. closed end pipe piles be used for the bridge abutment foundations. The pipe piles had an estimated length of 12 m (39 ft) for an ultimate pile capacity of 1450 kN (326 kips). The foundation report recommended wave equation analysis be used for construction control. Dynamic testing of one test pile at each abutment was also specified with the test pile information to be used by the engineer to provide the contractor pile order lengths.

The Case Method was used to evaluate pile capacity versus penetration depth during the test pile driving. More rigorous CAPWAP analyses were also performed on the dynamic test data to check the Case Method results at selected pile penetration depths. During initial driving at Abutment 1, the 324 mm (12.75 inch) pipe pile drove beyond the estimated pile penetration depth without developing the required ultimate capacity. The pile was driven to a depth of 23 m (75 ft) and had an end of drive ultimate capacity of 1044 kN (235 kips). A restrike dynamic test performed one day after initial driving indicated the pile capacity increased slightly to 1089 kN (245 kips).

While the test pile information from Abutment 1 was being evaluated, three additional test piles were driven at Abutment 2. First, dynamic testing of a 406 mm (16 inch) O.D. closed end pipe pile was performed to determine if a larger diameter pipe pile could develop the required ultimate pile capacity and, if so what pile penetration depth was necessary. The 406 mm (16 inch) pile was driven to a depth of 27 m (89 ft) and had an end of drive ultimate capacity of 989 kN (222 kips). A one day restrike test on this pile indicated an ultimate capacity of 1245 kN (280 kips). The 406 mm (16 inch) pile was driven deeper following the restrike test to a final penetration depth of 34 m (112 ft). With the additional driving, the end of redrive ultimate capacity decreased to 1067 kN (240 kips).

Approximately two weeks later, a 324 mm (12.75 inch) O.D. closed end pipe pile and a 356 mm (14 inch) diameter Monotube pile with a 7.6 m (25 ft) tapered lower section were driven at Abutment 2. The 324 mm (12.75 inch) pipe pile was driven to a penetration depth of 29 m (95 ft) with an end of drive ultimate capacity of 778 kN (175 kips). The Monotube pile was driven to a depth of 13 m (43 ft) and had an end of drive ultimate capacity of 845 kN (190 kips). One day restrike tests on both piles indicated a slight increase in ultimate capacity to 800 kN (180 kips) and 911 kN (205 kips), respectively. During this same site visit, a 16 day restrike test was performed on the 406 mm (16 inch) pipe pile. The long term restrike ultimate capacity for the 406 mm (16 inch) pipe pile was 1778 kN (400 kips).

The dynamic testing results from both abutments indicated that the desired ultimate pile capacity could not be obtained at or near the estimated pile penetration depth with the 324 mm (12.75 inch) pipe piles. However, two foundation solutions were indicated by the dynamic testing results. If a reduced ultimate capacity were chosen, the test results indicated a Monotube pile driven to a significantly shorter penetration depth could develop about the same ultimate pile capacity as could be developed by the 324 mm (12.75 inch) pipe piles. Alternatively, if the original ultimate pile capacity was desired, 406 mm (16 inch) pipe piles could be driven on the order of 28 m (92 ft) below grade.

Although not originally planned, two static load tests were performed to confirm the ultimate pile capacities that could be developed at the site. The 324 mm (12.75 inch) pipe and the 356 mm (14 inch) Monotube piles at Abutment 2 were selected for testing. The static load test results indicated the 324 mm (12.75 inch) pipe pile with a pile penetration depth of 29 m (95 ft) had an ultimate capacity of 1022 kN (230 kips) and the Monotube pile with a pile penetration depth of 13 m (43 ft) had an ultimate capacity of 978 kN (220 kips). The dynamic test restrike capacities were in good agreement with these static load tests results particularly when the additional time between the dynamic restrike tests and static load tests is considered.

Based on the required pile lengths and capacities determined from the dynamic and static load testing, a cost evaluation of the foundation alternatives was performed. The cost analysis indicated that the Monotube piles would be the most economical pile foundation type. This case study illustrates how the routine application of dynamic testing on a small project helped facilitate the solution to an unexpected foundation problem.

17.11 LOW STRAIN INTEGRITY TESTING METHODS

The previous sections of the chapter described high strain dynamic testing methods and their applications. This section will discuss low strain integrity testing methods which can be used on driven pile foundations. These low strain methods may be used to evaluate pile length or integrity of piles with a high impedance (EA/C), such as solid concrete piles or concrete filled pipe piles. Additional details on low strain methods including equipment requirements and analysis of measurements may be found in ASTM D-5882 Standard Test Method for Low Strain Integrity Testing of Piles. Low strain integrity methods are not applicable to steel H-piles or unconcreted pipe piles.

17.11.1 Pulse Echo Method

Pulse echo pile testing consists of applying a low strain impact to the head of a pile, and monitoring the resulting pile head response. A small 0.5 to 4.5 kg (1.0 to 10 lb) hand-held hammer is employed to deliver a clean impact to the pile head. An accelerometer, temporarily attached to the pile head, records pile head response as the generated low strain stress wave propagates down the pile length. Any changes in pile impedance (determined by the cross sectional area, the elastic modulus of the pile material and the stress wave speed of the pile material) along the pile shaft will generate a partial reflection of the downward travelling stress wave, thus identifying pile damage. At the pile toe a significant change in impedance would also occur, therefore allowing determination of pile length. The accelerometer records the magnitude and arrival time of the reflected waves. For undamaged piles, if a toe reflection is apparent, then it is possible to reasonably estimate an unknown pile length based upon an assumed wave speed.

The returning analog signals are captured and digitized by a portable high accuracy analog to digital data acquisition system. A display panel presents the record of one or more (averaged) blows for review and interpretation. Typically, the acceleration versus time data is integrated to a velocity versus time record to facilitate record evaluation.

This test method can also be used in cases where the pile length is known but the pile integrity is in question. In this application, a clearly indicated toe signal, together with a fairly steady velocity trace between the impact time and toe reflection, are signs of a sound pile. Strong velocity reflections before the expected toe signal are the result of changes in pile cross section and indicate pile damage.

Pulse echo integrity records of velocity versus time are presented in Figures 17.30 and 17.31 for two 305 mm (12 inch) square prestressed concrete piles. These records were obtained after a slope failure occurred during construction and the integrity of the driven piles was questioned. Figure 17.30 shows an amplified record for an undamaged 16.3 m (53 ft) long pile. Note the record drops below the origin at a depth 5 m (16 ft) which corresponds to soil resistance effects. A clear toe signal is apparent in the record at a depth of 16.3 m (53 ft).

In Figure 17.31, an amplified pulse echo record on a nearby pile is presented. This pile has a clear indication of damage due to the slope movements based on the positive velocity reflection starting at a depth of 4 m (13 ft).

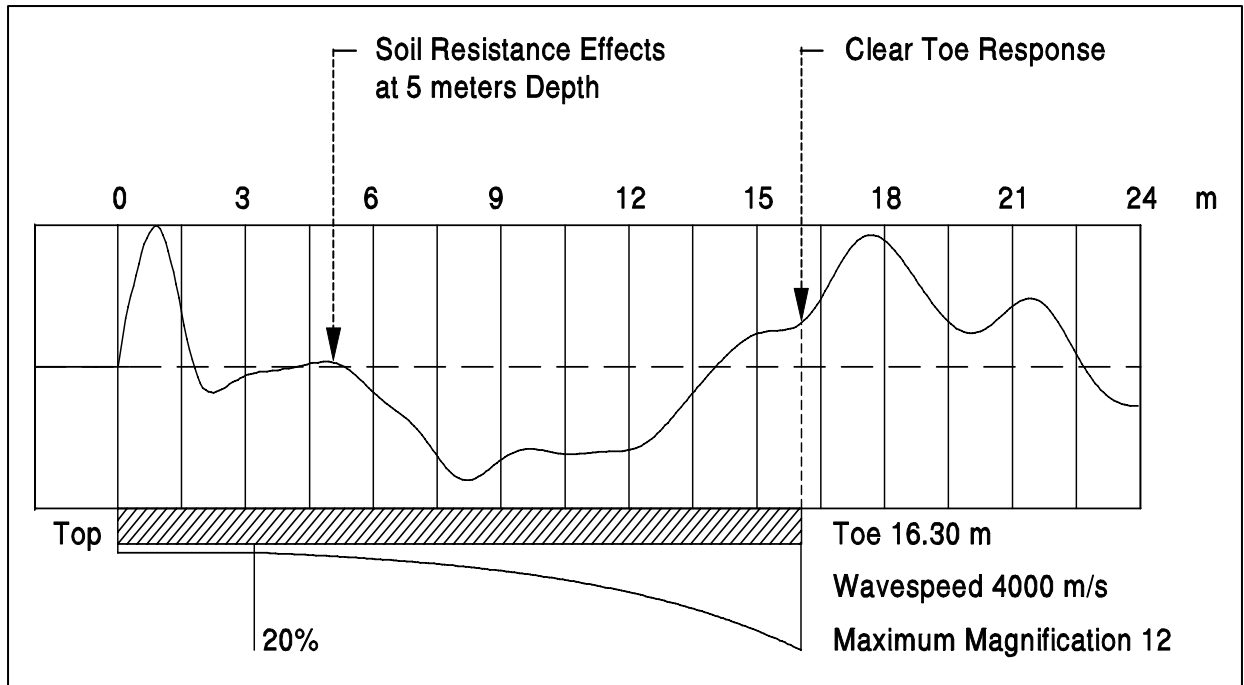


Figure 17.30 Pulse Echo Velocity versus Time Record for Undamaged Pile

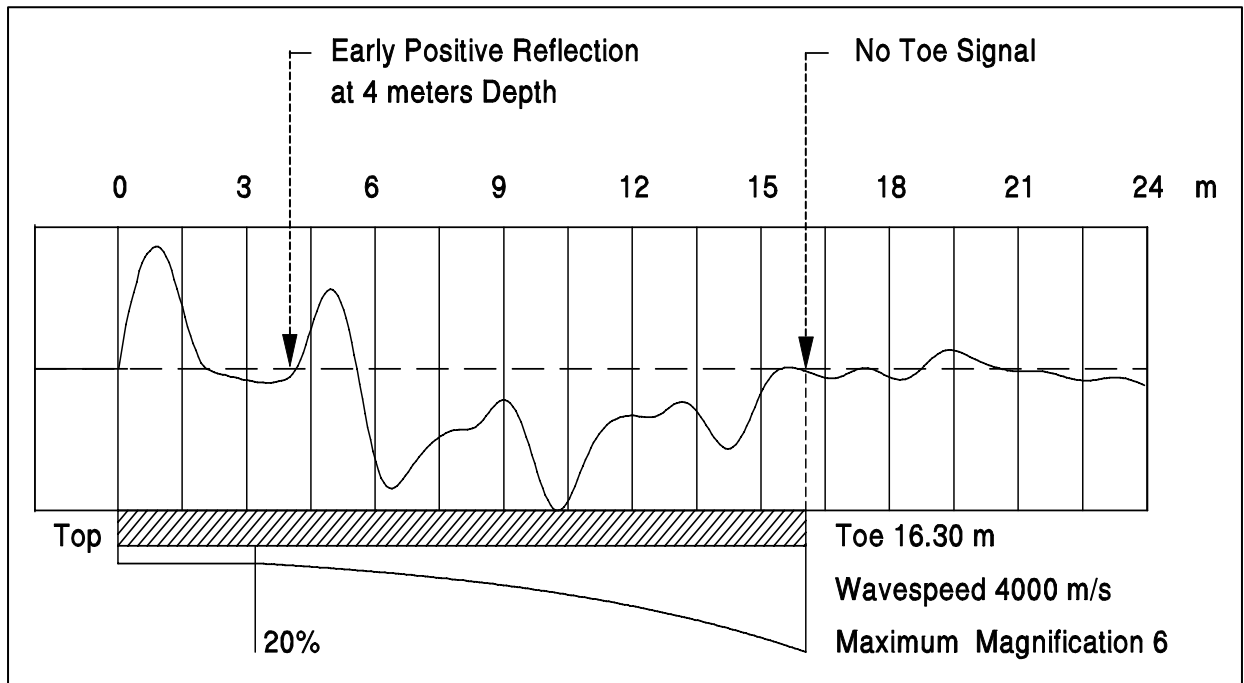


Figure 17.31 Pulse Echo Velocity versus Time Record for Damaged Pile

17.11.2 Transient Response Method (TRM)

In the TRM method, both the pile head response and the impact force are measured. A simple hand held hammer can adequately produce the frequency components necessary to test both well constructed and defective piles with TRM. The standard TRM plot of the ratio of the frequency velocity spectrum to force spectrum is called "mobility", and is an indication of the pile's velocity response to a particular excitation force at a certain frequency. Figure 17.32 depicts a typical response curve for a TRM test.

A mobility peak occurs at a frequency indicative of the time when the velocity changes due to a reflection from the pile toe or an intermediate impedance reduction or defect. Mobility peaks occurring at regular intervals are indicative of a dominant frequency Δf . The corresponding length to the pile toe or to a major defect at which the change in frequency occurs is calculated from:

$$L = C / 2 \Delta f$$

Where: C = Wave speed.
L = Pile length.
 Δf = Change in frequency.

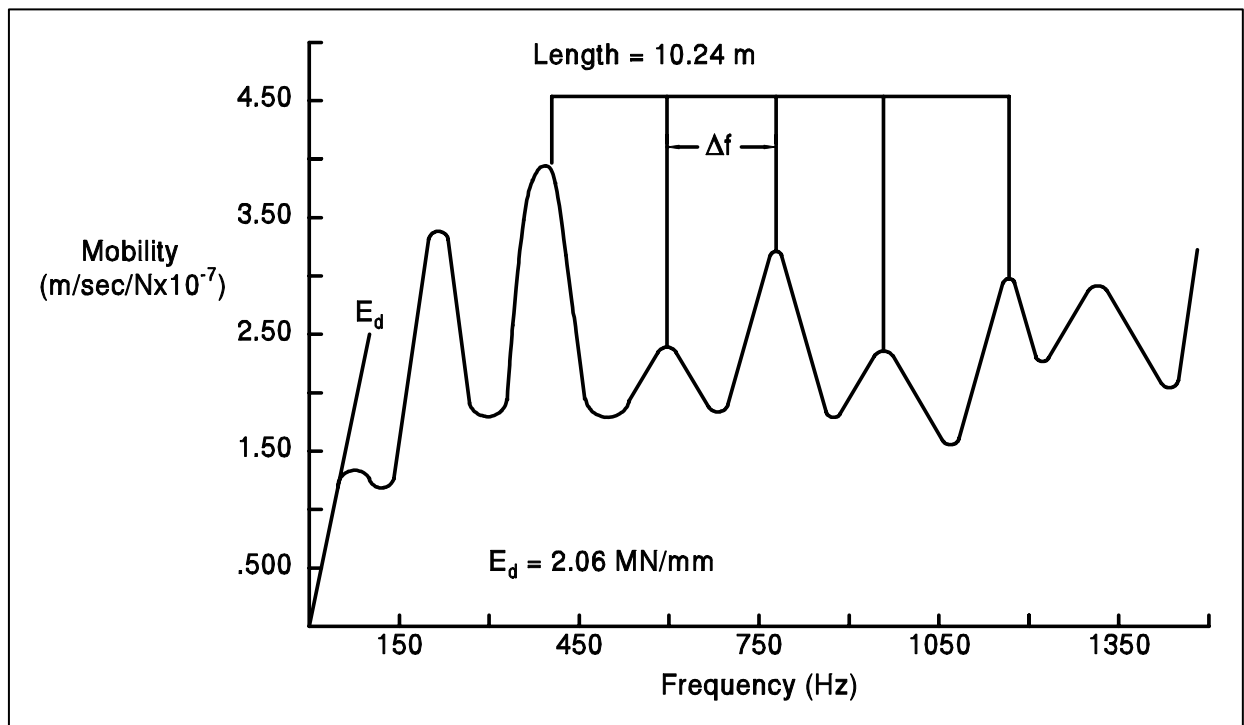


Figure 17.32 Typical Response Curve from a TRM Test

In practice, low frequency (*i.e.* near static) values are divided by the associated mobility yielding a so-called dynamic stiffness, E_d . This quantity increases with decreasing pile toe response. A low pile toe response is often the result of high soil resistance. A low pile toe resistance may also be caused by highly variable pile properties of internal pile damping, and is therefore only indirectly related to pile capacity. However, E_d is calculated, since it does provide a quantitative result for the evaluation of pile quality. Generally, higher stiffness values (for piles on the same site and of comparable length) indicate piles of higher strength (structural and soil) while lower stiffnesses indicate piles with potential defects or lower soil strength. The physical basis for the method, and the principles of data analysis, were first described by Davis and Dunn (1974).

17.11.3 Low Strain Applications to Unknown Foundations

Design or construction records on many older bridges are not available. In some cases, the foundation supporting these structures is unknown and therefore the performance of these structures under extreme events such as scour is uncertain. An NCHRP research effort by Olson (1996) on the application of non-destructive testing methods to the evaluation of unknown foundations found the pulse echo and transient response methods fair to excellent in their ability to identify the depth of exposed piles and poor to good in their ability to determine the depth of footing or pile cap. These techniques are most applicable when the bridge is supported on a columnar substructure rather than a pier or abutment. Access to the bridge substructure is also generally required for implementation of these techniques. FHWA Geotechnical Guideline No. 16 (1998) provides a summary of this NCHRP study.

17.11.4 Limitations and Conclusions of Low Strain Methods

The low strain methods can typically be used for integrity or length assessments of pile foundations where the length to diameter ratio does not exceed about 30. For piles with severe cracks or manufactured mechanical joints, the stress wave will generally not be transmitted below the gap. Therefore, the pile integrity or length below this gap cannot be evaluated. Records from piles with multiple or varying (*i.e.* tapered piles) cross sectional areas can also be difficult to interpret. For piles of low impedance (H-piles and unfilled pipe piles) low strain methods are generally not suitable. When used for pile length determinations, the length information obtained from a toe signal (or a governing frequency) is only as accurate as the wave speed value assumed in the processing of the records. Wave speed variations of approximately 10% are not uncommon. Some defects can also have secondary and tertiary wave reflections. For example, if an

impedance reduction occurs in the middle of the pile, then what may appear to be the pile toe response may actually be a secondary reflection of the mid-pile defect.

The additional force measurement obtained during TRM testing provides supplemental information of cross sectional changes near the pile head, *i.e.* within the distance corresponding to the impact signal. The minor additional expense of the force measurements is therefore worthwhile whenever questions arise as to the integrity of upper (1.5 m) pile portion.

Using low strain methods, many piles can be tested for integrity in a typical day. Therefore, low strain methods are a relatively economical test method and can provide valuable information when used in the proper application such as illustrated in the case study discussed in Section 17.11.1. Low strain testing has been used to assist in evaluating integrity questions on high impedance piles due to construction equipment or vessel impact, pulling on out of position piles, and storm damage.

REFERENCES

- American Association of State Highway and Transportation Offices (AASHTO). Standard Method of Test for High Strain Dynamic Testing of Piles, AASHTO Designation T-298-33.
- American Society for Testing and Materials, ASTM (2004). Annual Book of Standards, ASTM D-4945, Standard Test Method for High-Strain Dynamic Testing of Piles.
- American Society for Testing and Materials, ASTM (2004). Annual Book of Standards, ASTM D-5882, Standard Test Method for Low-Strain Dynamic Testing of Piles.
- Cheney, R.S. and Chassie, R.G. (2000). Soils and Foundations Workshop Manual. Second Edition, Publication No. FHWA NHI-00-045, Federal Highway Administration, National Highway Institute, Washington, D.C., 353-362.
- Davis, A.G. and Dunn, C.S. (1974). From Theory to Experience with the Nondestructive Vibration Testing of Piles. Proceedings of the Institution of Civil Engineers, Part 2, Volume 57, Paper 7764, London, 571-593.
- Davisson, M.T. (1972). High Capacity Piles. Proceedings of the Soil Mechanics Lecture Series on Innovations in Foundation Construction, American Society of Civil Engineers, ASCE, Illinois Section, 81-112.
- Eiber, R.J. (1958). A Preliminary Laboratory Investigation of the Prediction of Static Pile Resistances in Sand. Master's Thesis, Department of Civil Engineering, Case Institute of Technology, Cleveland, OH.
- Federal Highway Administration (1998). Geotechnical Guideline No. 16, Geotechnical Engineering Notebook, U.S. Department of Transportation, Washington D.C., 69.
- Goble, G.G., Likins, G.E. and Rausche, F. (1975). Bearing Capacity of Piles from Dynamic Measurements. Final Report, Department of Civil Engineering, Case Western Reserve University, Cleveland, OH.
- Goble, G.G. and Rausche, F. (1970). Pile Load Test by Impact Driving. Highway Research Record, Highway Research Board, No. 333, Washington, DC.

- Goble, G.G., Rausche, F. and Likins, G.E. (1980). The Analysis of Pile Driving - A State-of-the-Art. Proceedings of the 1st International Seminar on the Application of Stress-Wave Theory on Piles, Stockholm, H. Bredenberg, Editor, A.A. Balkema Publishers, 131-161.
- Hannigan, P.J. (1990). Dynamic Monitoring and Analysis of Pile Foundation Installations. Deep Foundations Institute Short Course Text, First Edition, 69.
- Olson, L.D. (1996). Non-Destructive Testing of Unknown Subsurface Bridge Foundations Results of NCHRP Project 21-5, National Cooperative Highway Research Program, Transportation Research Board, Washington, D.C., 42.
- Pile Dynamics, Inc. (2004). Pile Driving Analyzer Manual; Model PAK, Cleveland, OH.
- Rausche, F., Goble, G.G. and Likins, G.E. (1985b). Dynamic Determination of Pile Capacity. American Society of Civil Engineers, ASCE, Journal of the Geotechnical Engineering Division, Vol 111, No. 3, 367-383.
- Rausche, F. and Goble, G.G. (1979). Determination of Pile Damage by Top Measurements. Behavior of Deep Foundations. American Society for Testing and Materials, ASTM STP 670, R. Lundgren, Editor, 500-506.
- Rausche, F., Likins, G.E., Goble, G.G. and Miner, R. (1985a). The Performance of Pile Driving Systems. Main Report, U.S. Department of Transportation, Federal Highway Administration, Office of Research and Development, Washington, D.C., Volumes I-IV.
- Rausche, F., Moses, F., and Goble, G.G. (1972). Soil Resistance Predictions from Pile Dynamics. Journal of the Soil Mechanics and Foundations Division, ASCE, Vol. 98, No. SM9.
- Reiding, F.J., Middendorp, P., Schoenmaker, R.P., Middendorp, F.M. and Bielefeld, M.W. (1988). FPDS-2, A New Generation of Foundation Diagnostic Equipment, Proceeding of the 3rd International Conference on the Application of Stress Wave Theory to Piles, Ottawa, B.H. Fellenius, Editor, BiTech Publishers, 123-134.

Chapter 18

STATIC PILE LOAD TESTING

Static load testing of piles is the most accurate method of determining load capacity. Depending upon the size of the project, static load tests may be performed either during the design stage or construction stage. Conventional load test types include the axial compression, axial tension and lateral load tests.

The purpose of this chapter is to provide an overview of static testing and its importance as well as to describe the basic test methods and interpretation techniques. For additional details on pile load testing, reference should be made to FHWA publication FHWA-SA-91-042, "Static Testing of Deep Foundation" by Kyfor *et al.* (1992) as well as the other publications listed at the end of this chapter.

18.1 REASONS FOR LOAD TESTING

1. Load tests are performed to develop information for use in the design and/or construction of a pile foundation.
2. Load tests are performed to confirm the suitability of the pile-soil system to support the pile design load with an appropriate factor of safety.
3. Implementation of new static or dynamic analysis methods or procedures.
4. LRFD calibration.

18.2 PREREQUISITES FOR LOAD TESTING

In order to adequately plan and implement a static load testing program, the following information should be obtained or developed.

1. A detailed subsurface exploration program at the test location. A load test is not a substitute for a subsurface exploration program.
2. Well defined subsurface stratigraphy including engineering properties of soil materials and identification of groundwater conditions.

3. Static pile capacity analyses to select pile type(s) and length(s) as well as to select appropriate location(s) for load test(s).

18.3 DEVELOPING A STATIC LOAD TEST PROGRAM

The goal of a static load test program should be clearly established. The type and frequency of tests should be selected to provide the required knowledge for final design purposes or construction verification. A significantly different level of effort and instrumentation is required if the goal of the load test program is simply to confirm the ultimate pile capacity or if detailed load-transfer information is desired for final design. The following items should be considered during the test program planning so that the program provides the desired information.

1. The capacity of the loading apparatus (reaction system and jack) should be specified so that the test pile(s) may be loaded to plunging failure. A loading apparatus designed to load a pile to only twice the design load is usually insufficient to obtain plunging failure. Hence, the true factor of safety on the design load cannot be determined, and the full benefit from performing the static test is not realized.
2. Specifications should require use of a load cell and spherical bearing plate as well as dial gages with sufficient travel to allow accurate measurements of load and movement at the pile head. (Where possible, deformation measurements should also be made at the pile toe and at intermediate points to allow for an evaluation of shaft and toe bearing resistance).
3. The load test program should be supervised by a person experienced in this field of work.
4. A test pile installation record should be maintained with installation details appropriately noted. Too often, only the hammer model and driving resistance are recorded on a test pile log. Additional items such as hammer stroke (particularly at final driving), fuel setting, accurately determined final set, installation aids used and depths such as predrilling, driving times, stops for splicing, *etc.*, should be recorded.
5. Use of dynamic monitoring equipment on the load test pile is recommended for estimates of pile capacity at the time of driving, evaluation of drive system performance, calculation of driving stresses, and subsequent refinement of soil parameters for wave equation analysis.

18.4 ADVANTAGES OF STATIC LOAD TESTING

The advantages of performing static load tests are summarized below.

1. A static load test allows a more rational design. Confirmation of pile-soil capacity through static load testing is considerably more reliable than capacity estimates from static capacity analyses and dynamic formulas.
2. An improved knowledge of pile-soil behavior is obtained that may allow a reduction in pile lengths or an increase in the pile design load, either of which may result in potential savings in foundation costs.
3. With the improved knowledge of pile-soil behavior, a lower factor of safety may be used on the pile design load. A factor of safety of 2.0 is generally applied to design loads confirmed by load tests as compared to a factor of safety of 3.5 used on design loads in the Modified Gates dynamic formula. Hence, a cost savings potential again exists.
4. The ultimate pile capacity determined from load testing allows confirmation that the design load may be adequately supported at the planned pile penetration depth.

Engineers are sometimes hesitant to recommend a static load test because of cost concerns or potential time delays in design or construction. While the cost of performing a static load test should be weighed against the anticipated benefits, cost alone should not be the determining factor.

Delays to a project in the design or construction stage usually occur when the decision to perform static load tests is added late in the project. During a design stage program, delays can be minimized by determining early in the project whether a static load test program should be performed. In the construction stage, delays can be minimized by clearly specifying the number and locations of static load test to be performed as well as the time necessary for the engineer to review the results. In addition, the specifications should state that the static test must be performed prior to ordering pile lengths or commencing production driving. In this way, the test results are available to the design and construction engineer early in the project so that the maximum benefits can be obtained. At the same time the contractor is also aware of the test requirements and analysis duration and can schedule the project accordingly.

18.5 WHEN TO LOAD TEST

The following criteria, adapted and modified from FHWA-SA-91-042 by Kyfor *et al.* (1992), summarize conditions when pile load testing can be effectively utilized:

1. When substantial cost savings can be realized. This is often the case on large projects either involving friction piles (to prove that lengths can be reduced) or end bearing piles (to prove that the design load can be increased). Testing can also be justified if the savings obtained by using a lower factor of safety equals or exceeds the testing cost.
2. When a safe design load is uncertain due to limitations of an engineer's experience base or due to unusual site or project conditions.
3. When subsurface conditions vary considerably across the project, but can be delineated into zones of similar conditions. Static tests can then be performed in representative areas to delineate foundation variation.
4. When a significantly higher design load is contemplated relative to typical design loads and practice.
5. When time dependent changes in pile capacity are anticipated as a result of soil setup or relaxation.
6. Verification of new design or testing methods.
7. When new, unproven pile types and/or pile installation procedures are utilized.
8. When existing piles will be reused to support a new structure with heavier design loads.
9. When a reliable assessment of pile uplift capacity or lateral behavior is important.
10. When, during construction, the estimated ultimate capacity using dynamic formulas or dynamic analysis methods differs from the estimated capacity at that depth determined by static analysis. For example, H-piles that "run" when driven into loose to medium dense sands and gravels.

11. LRFD calibrations.

Experience has also shown that load tests will typically confirm that pile lengths can be reduced at least 15 percent versus the lengths that would be required by the Engineering News formula on projects where piles are supported predominantly by shaft resistance. This 15 percent pile length reduction was used to establish the following rule of thumb formula to compute the total estimated pile length which the project must have to make the load test cost effective based purely on material savings alone.

$$\text{Total estimate pile length in meters on project} \geq \frac{\text{cost of load test}}{(0.15) (\text{cost / meter of pile})}$$

18.6 EFFECTIVE USE OF LOAD TESTS

18.6.1 Design Stage

The best information for design of a pile foundation is provided by the results of a load testing program conducted during the design phase. The number of static tests, types of piles to be tested, method of driving and test load requirements should be selected by the geotechnical and structural engineers responsible for design. A cooperative effort between the two is necessary. The following are the advantages of load testing during the design stage.

- a. Allows load testing of several different pile types and lengths resulting in the design selection of the most economical pile foundation.
- b. Confirm driveability to minimum penetration requirements and suitability of foundation capacity at estimated pile penetration depths.
- c. Establishes preliminary driving criteria for production piles.
- d. Pile driving information released to bidders should reduce their bid "contingency."
- e. Reduces potential for claims related to pile driving problems.
- f. Allows the results of load test program to be reflected in the final design and specifications.

18.6.2 Construction Stage

Load testing at the start of construction may be the only practical time for testing on smaller projects that can not justify the cost of a design stage program. Construction stage static tests are invaluable to confirm that the design loads are appropriate and that the pile installation procedure is satisfactory. Driving of test piles and load testing is frequently done to determine the pile order length at the beginning of construction. These results refine the estimated pile lengths shown on the plans and establish minimum pile penetration requirements.

18.7 COMPRESSION LOAD TESTS

Piles are most often tested in compression, but they can also be tested in tension or for lateral load capacity. Figure 18.1 illustrates the basic mechanism of performing a compression pile load test. This mechanism normally includes the following steps:

1. The pile is loaded incrementally from the pile head using some predetermined loading sequence, or it can be loaded at a continuous, constant rate.
2. Measurements of load, time, and movement at the pile head and at various points along the pile shaft are recorded during the test.
3. A load movement curve is plotted.
4. The failure load and the movement at the failure load are determined by one of the several methods of interpretation.
5. The movement is usually measured only at the pile head. However, the pile can be instrumented to determine movement anywhere along the pile. Telltales (solid rods protected by tubes) shown in Figure 18.1 or strain gages may be used to obtain this information.

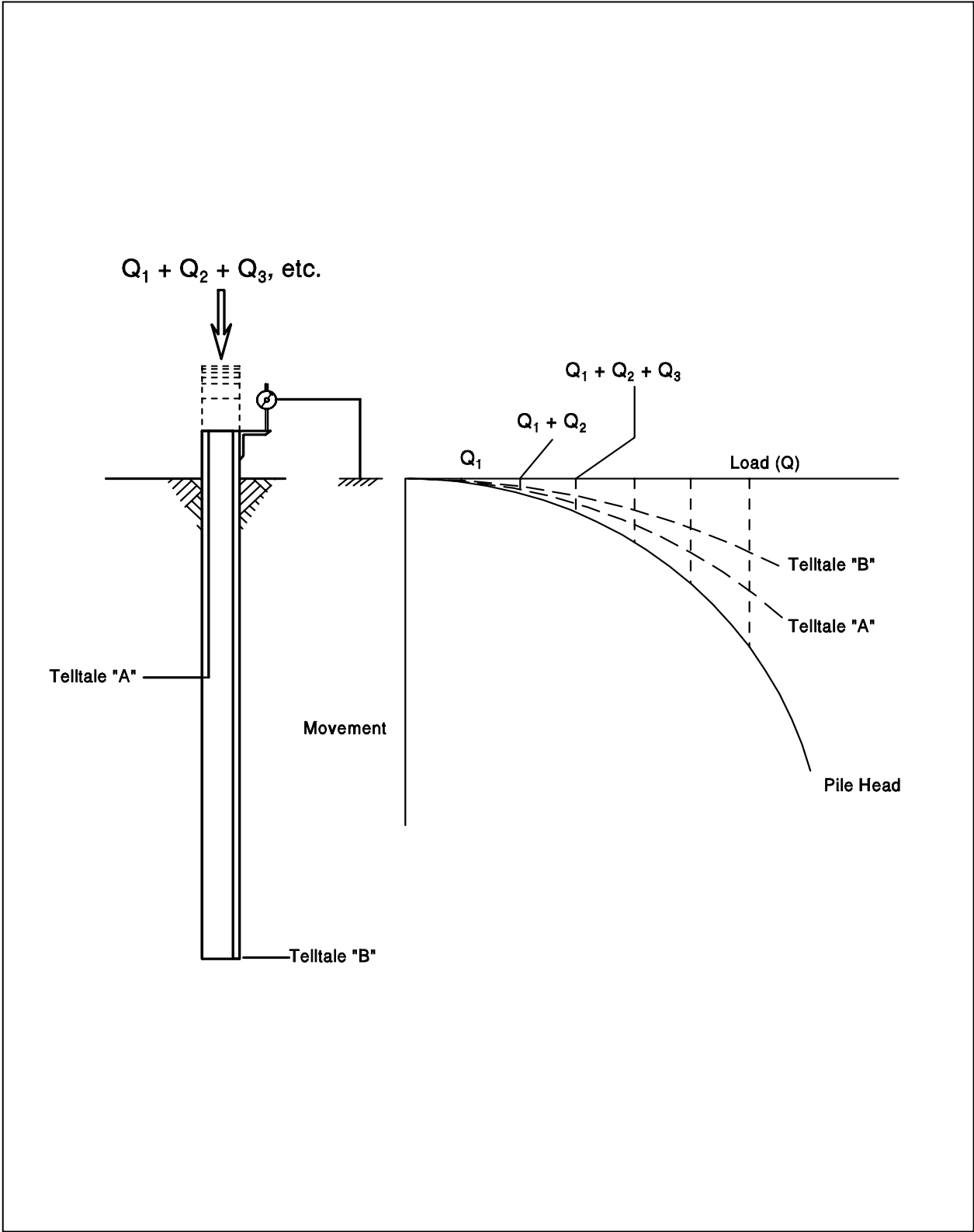


Figure 18.1 Basic Mechanism of a Pile Load Test

18.7.1 Compression Test Equipment

ASTM D-1143-81 (re-approved 1994) recommends several alternative systems for (1) applying compressive load to the pile, and (2) measuring movements. Most often, compressive loads are applied by hydraulically jacking against a beam that is anchored by piles or ground anchors, or by jacking against a weighted platform. The primary means of measuring the load applied to the pile should be with a calibrated load cell. The jack load should also be recorded from a calibrated pressure gage. To minimize eccentricities in the applied load, a spherical bearing plate should be included in the load application arrangement.

Axial pile head movements are usually measured by dial gages or LVDT's that measure movement between the pile head and an independently supported reference beam. ASTM requires the dial gages or LVDT's have a minimum of 50 mm (2 inches) of travel and a precision of at least 0.25 mm (0.01 inches). It is preferable to have gages with a minimum travel of 75 mm (3 inches) particularly for long piles with large elastic deformations under load and with a precision of 0.025 mm (0.001 inches). A minimum of two dial gages or LVDT's mounted equidistant from the center of the pile and diametrically opposite should be used. Two backup systems consisting of a scale, mirror, and wire system should be provided with a scale precision of 0.25 mm (0.01 inches). The backup systems should also be mounted on diametrically opposite pile faces. Both the reference beams and backup wire systems are to be independently supported with a clear distance of not less than 2.5 m (8 ft) between supports and the test pile. A remote backup system consisting of a survey level should also be used in case reference beams or wire systems are disturbed during the test.

ASTM specifies that the clear distance between a test pile and reaction piles be at least 5 times the maximum diameter of the reaction pile or test pile (whichever has the greater diameter if not the same pile type) but not less than 2 meters (7 ft). If a weighted platform is used, ASTM requires the clear distance between cribbing supporting the weighted platform and the test pile exceed 1.5 meters (5 ft).

A schematic of a typical compression load test setup is presented in Figure 18.2 and photographs of the load application and movement monitoring components are presented in Figures 18.3 and 18.4. A typical compression load test arrangement using reaction piles is presented in Figure 18.5 and a weighted platform arrangement is shown in Figure 18.6. Additional details on load application as well as pile head load and movement measurements may be found in ASTM D-1143 as well as in FHWA-SA-91-042 by Kyfor *et al.* (1992).

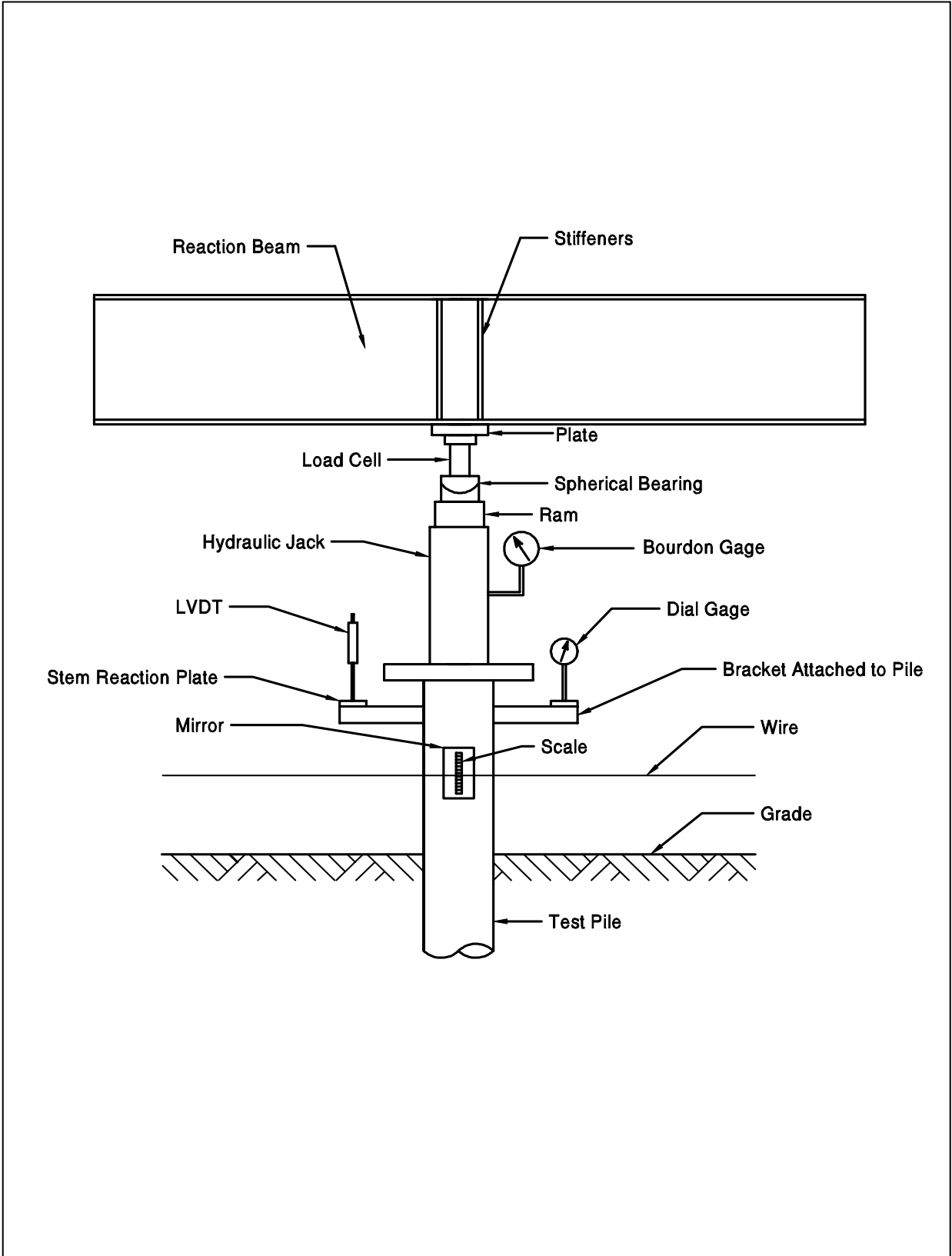


Figure 18.2 Typical Arrangement for Applying Load in an Axial Compressive Test (Kyfor *et al.* 1892)

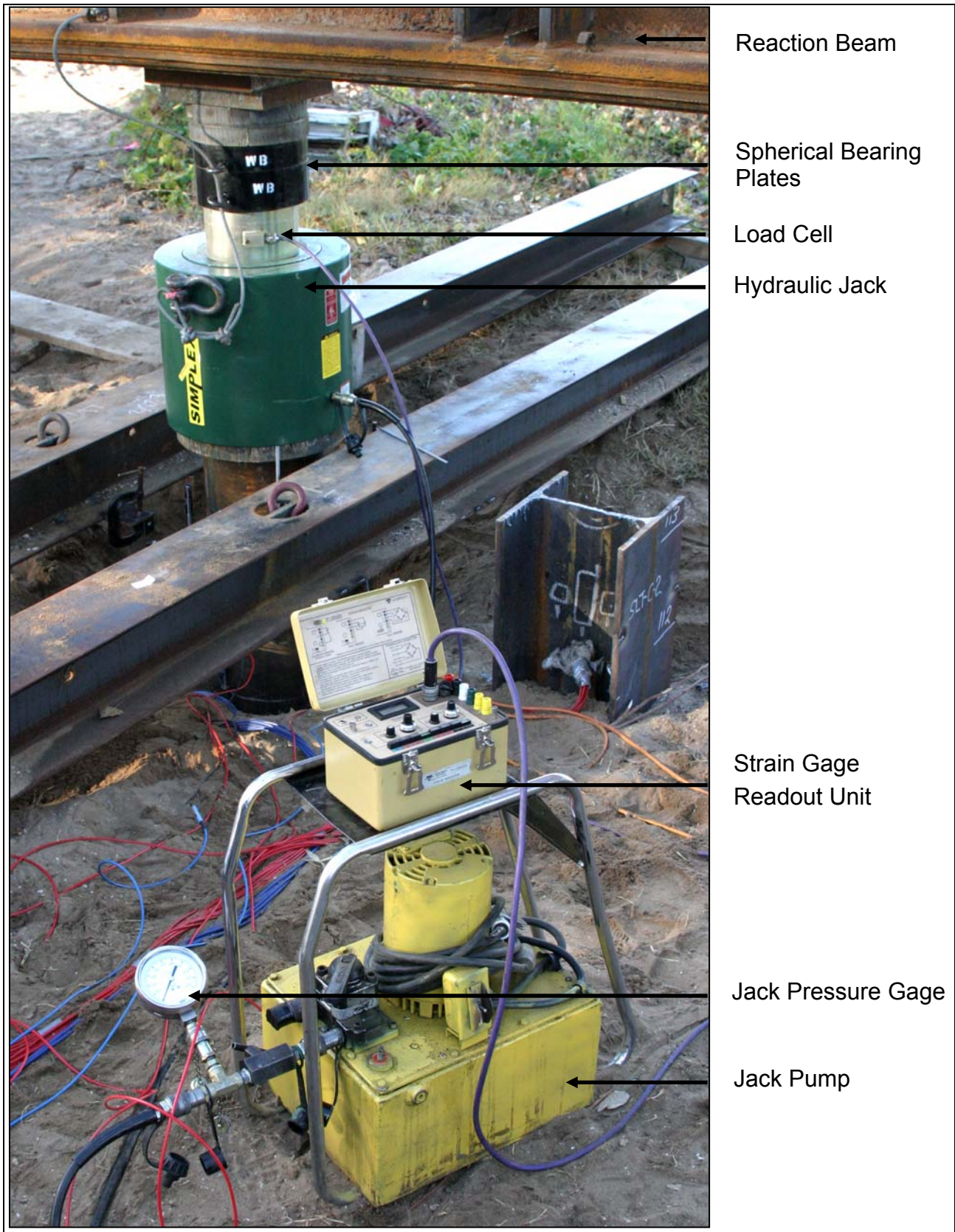


Figure 18.3 Load Test Load Application and Monitoring Components

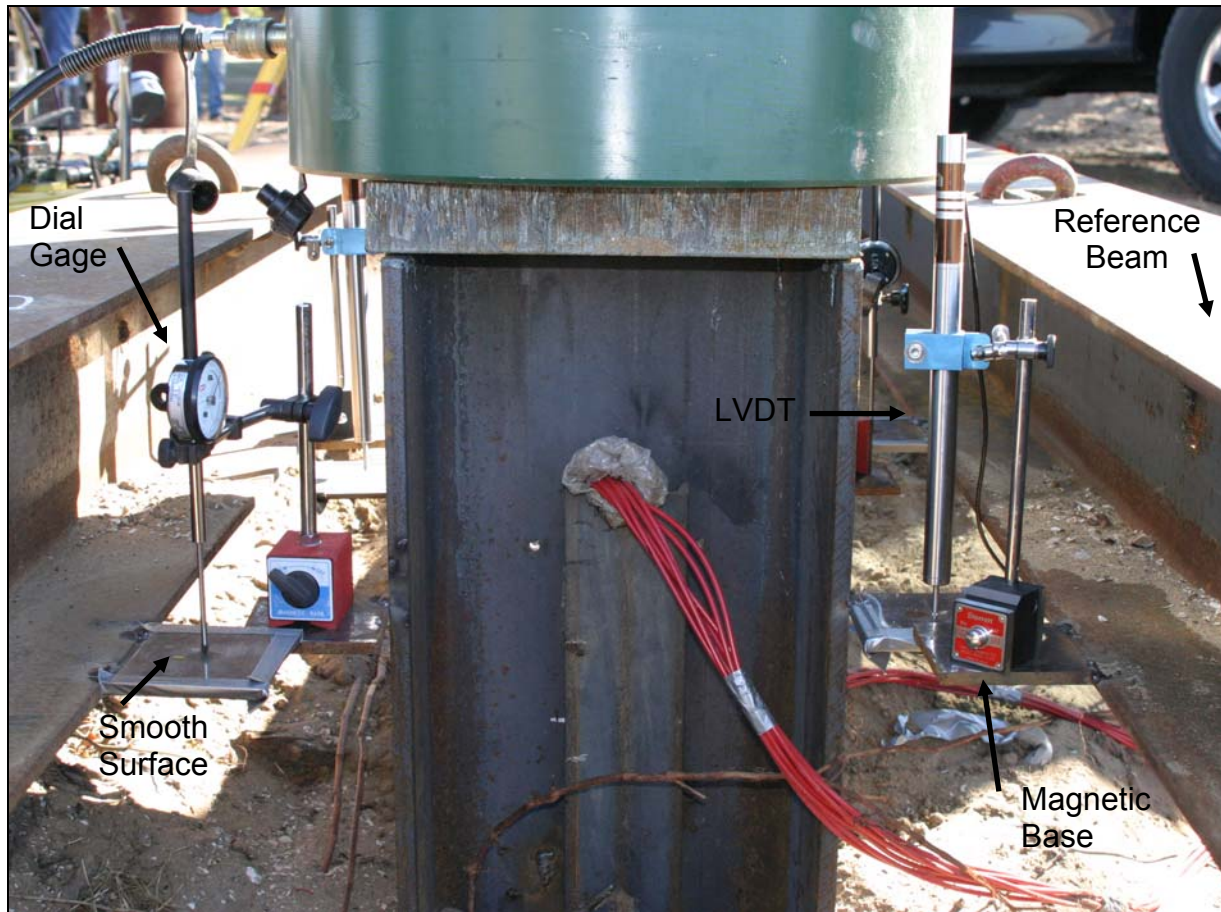


Figure 18.4 Load Test Movement Monitoring Components

18.7.2 Recommended Compression Test Loading Method

It is extremely important that standardized load testing procedures are followed. Several loading procedures are detailed in ASTM D-1143, Standard Test Method for Piles Under Static Axial Compressive Load. The quick load test method is recommended. This method replaces traditional methods where each load increment was held for extended periods of time. The quick test method requires that load be applied in increments of 10 to 15% of the pile design load with a constant time interval of 2½ minutes or as otherwise specified between load increments. Readings of time, load, and gross movement are to be recorded immediately before and after the addition of each load increment. This procedure is to continue until continuous jacking is required to maintain the test load or the capacity of

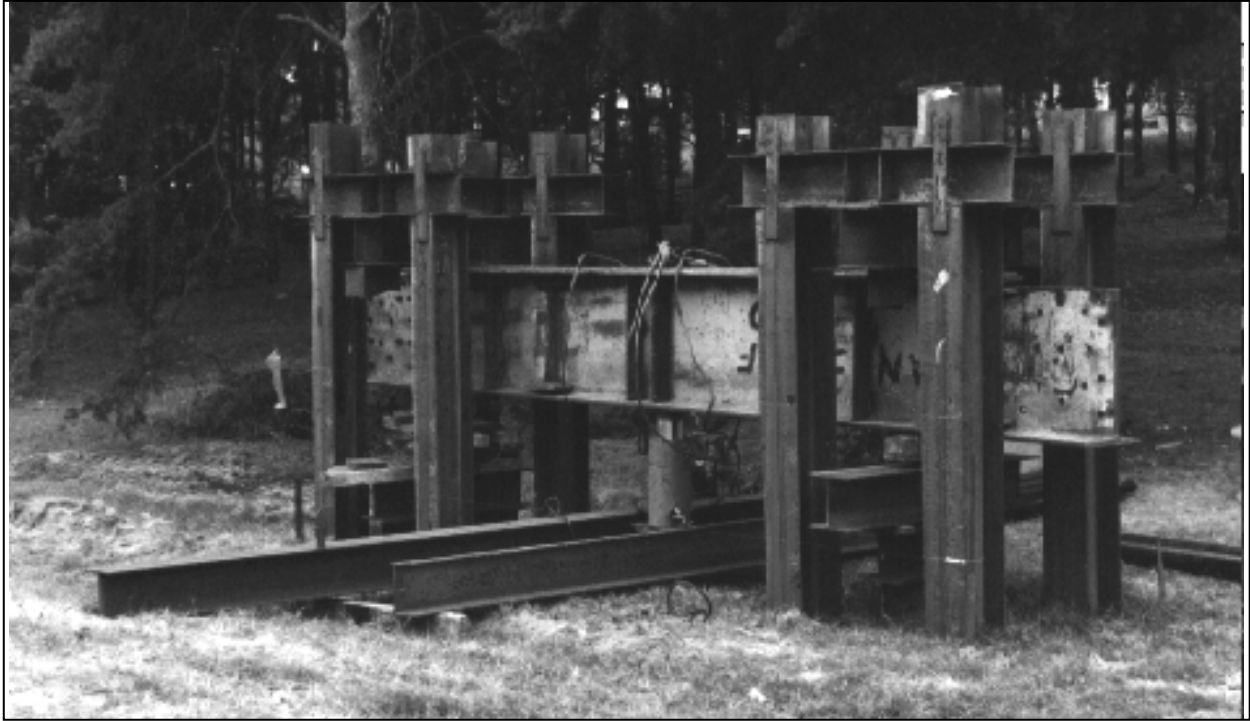


Figure 18.5 Typical Compression Load Test Arrangement with Reaction Piles

the loading apparatus is reached, whichever occurs first. Upon reaching and holding the maximum load for 5 minutes, the pile is unloaded in four equal load decrements which are each held for 5 minutes. Readings of time, load, and gross movement are once again recorded immediately after, 2½ minutes after, and 5 minutes after each load reduction, including the zero load.



Figure 18.6 Typical Compression Load Test Arrangement using a Weighted Platform

18.7.3 Presentation and Interpretation of Compression Test Results

The results of load tests should be presented in a report conforming to the requirements of ASTM D-1143. A load-movement curve similar to the one shown in Figure 18.7 should be plotted for interpretation of test results.

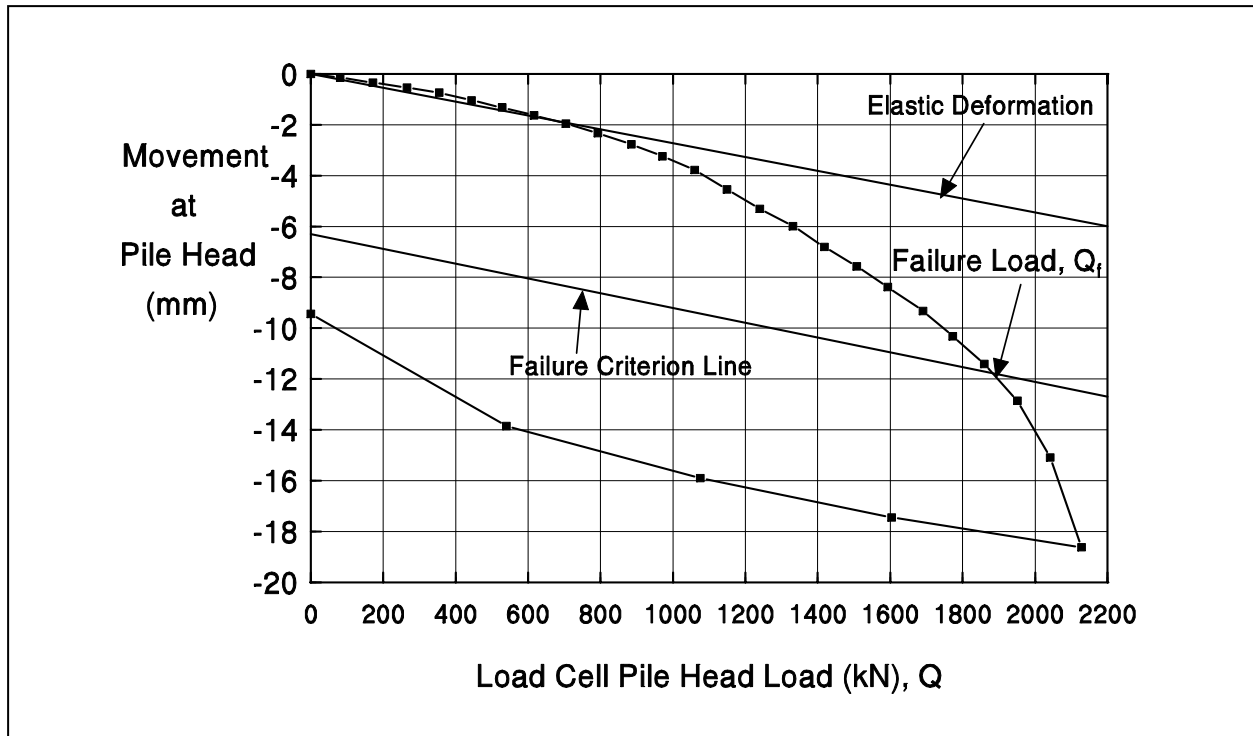


Figure 18.7 Presentation of Typical Static Pile Load-Movement Results

The literature abounds with different methods of defining the failure load from static load tests. Methods of interpretation based on maximum allowable gross movements, which do not take into account the elastic deformation of the pile shaft, are not recommended. These methods overestimate the allowable capacities of short piles and underestimate the allowable capacities of long piles. The methods which account for elastic deformation and are based on failure criterion provide a better understanding of pile performance and provide more accurate results.

AASHTO (2002) and FHWA SA-91-042, Kyfor *et al.* (1992) recommend compression test results be evaluated using an offset limit method as proposed by Davisson (1972). This method is described in the following section and is applicable for load tests in which the increment of load is held for not more than 1 hour.

18.7.4 Plotting the Load-Movement Curve

Figure 18.7 shows the load-movement curve from a pile load test. To facilitate the interpretation of the test results, the scales for the loads and movements are selected so that the line representing the elastic deformation Δ of the pile is inclined at an angle of about 20° from the load axis. The elastic deformation Δ is computed from:

$$\Delta = \frac{QL}{AE}$$

Where: Δ = Elastic deformation in mm (inches).
Q = Test load in kN (kips).
L = Pile length in mm (inches).
A = Cross sectional area of the pile in m^2 (in^2)
E = Modulus of elasticity of the pile material in kPa (ksi).

18.7.5 Determination of the Ultimate Load

The ultimate or failure load Q_f of a pile is that load which produces a movement of the pile head equal to:

$$\text{In SI units} \quad s_f = \Delta + (4.0 + 0.008b)$$

$$\text{In US Units} \quad s_f = \Delta + (0.15 + 0.008b)$$

Where: s_f = Settlement at failure in mm (inches).
b = Pile diameter or width in mm (inches).
 Δ = Elastic deformation of total pile length in mm (inches).

A failure criterion line parallel to the elastic deformation line is plotted as shown in Figure 18.7. The point at which the observed load-movement curve intersects the failure criterion is by definition the failure load. If the load-movement curve does not intersect the failure criterion line, the pile has an ultimate capacity in excess of the maximum applied test load.

For large diameter piles (diameter greater than 610 mm or 24 inches), additional pile toe movement is necessary to develop the toe resistance. For large diameter piles, the failure load can be defined as the load which produces at movement at the pile head equal to:

$$s_f = \Delta + (b / 30)$$

18.7.6 Determination of the Allowable Load

The allowable design load is usually determined by dividing the ultimate load, Q_f , by a suitable factor of safety. A factor of safety of 2.0 is recommended in AASHTO code (2002) and is often used. However, larger factors of safety may be appropriate under the following conditions:

- a. Where soil conditions are highly variable.
- b. Where a limited number of load tests are specified.
- c. For friction piles in clay, where group settlement may control the allowable load.
- d. Where the total movement that can be tolerated by the structure is exceeded.
- e. For piles installed by means other than impact driving, such as vibratory driving or jetting.

18.7.7 Load Transfer Evaluations

Kyfor *et al.* (1992) provides a method for evaluation of the soil resistance distribution from telltales embedded in a load test pile. The average load in the pile, Q_{avg} , between two measuring points can be determined as follows:

$$Q_{avg} = A E \frac{R_1 - R_2}{\Delta L}$$

Where: ΔL = Length of pile between two measuring points under no load condition.
 A = Cross sectional area of the pile.
 E = Modulus of elasticity of the pile.
 R_1 = Deflection readings at upper of two measuring points.
 R_2 = Deflection readings at lower of two measuring points.

If the R_1 and R_2 readings correspond to the pile head and the pile toe respectively, then an estimate of the shaft and toe resistances may be computed. For a pile with an assumed constant soil resistance distribution (uniform), Fellenius (1990) states that an estimate of the toe resistance, R_t , can be computed from the applied pile head load, Q_h . The applied pile head load, Q_h , is chosen as close to the failure load as possible.

$$R_t = 2Q_{avg} - Q_h$$

For a pile with an assumed linearly increasing soil resistance distribution (triangular), the estimated toe resistance may be calculated using:

$$R_t = 3Q_{avg} - 2Q_h$$

The estimated shaft resistance can then be calculated from the applied pile head load minus the toe resistance.

During driving, residual loads can be locked into a pile that does not completely rebound after a hammer blow (*i.e.* return to a condition of zero stress along its entire length). This is particularly true for flexible piles, piles with large frictional resistances, and piles with large toe quakes. Load transfer evaluations using telltale measurements described above assume that no residual loads are locked in the pile during driving. Therefore, the load distribution calculated from the above equations would not include residual loads. If measuring points R_1 and R_2 correspond to the pile head and pile toe of a pile that has locked-in residual loads, the calculated average pile load would also include the residual loads. This would result in a lower toe resistance being calculated than actually exists as depicted in Figure 18.8. Additional details on telltale load transfer evaluation, including residual load considerations, may be found in Fellenius (1990).

When detailed load transfer data is desired, telltale measurements alone are insufficient, since residual loads can not be directly accounted for. Dunnicliff (1988) suggests that weldable vibrating wire strain gages be used on steel piles and sister bars with vibrating wire strain gages be embedded in concrete piles for detailed load transfer evaluations. A geotechnical instrumentation specialist should be used to select the appropriate instrumentation to withstand pile handling and installation, to determine the redundancy required in the instrumentation system, to determine the appropriate data acquisition system, and to reduce and report the data acquired from the instrumentation program.

A sister bar vibrating wire strain gage for embedment in concrete or concrete filled pile piles is shown in Figure 18.9 and an arc-weldable vibrating wire strain gage attached to a steel H-pile is presented in Figure 18.10. When detailed load transfer data is desired, a data acquisition system should be used.

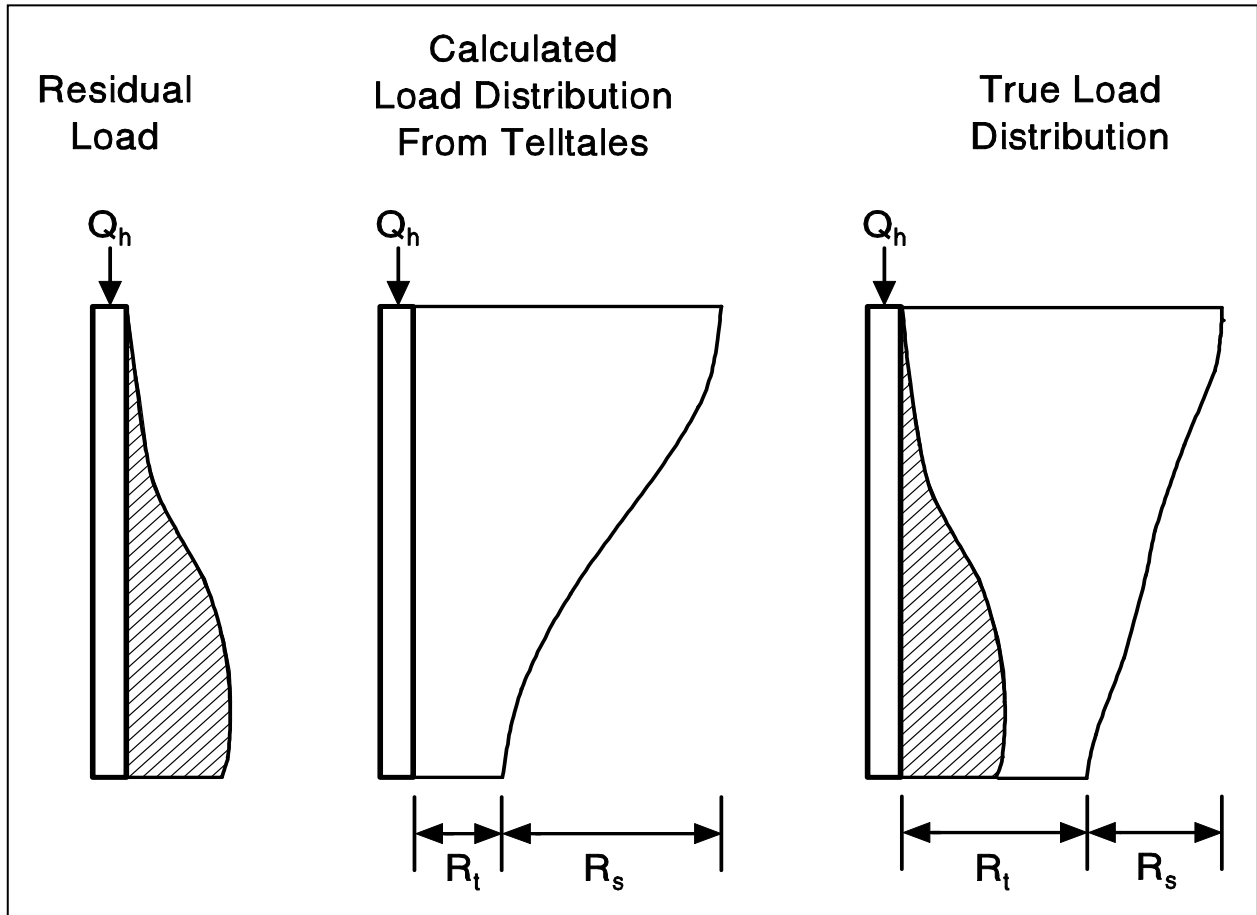


Figure 18.8 Example of Residual Load Effects on Load Transfer Evaluation

18.7.8 Limitations of Compression Load Tests

Compression load tests can provide a wealth of information for design and construction of pile foundations and are the most accurate method of determining pile capacity. However, static load test results cannot be used to account for long-term settlement, downdrag from consolidating and settling soils, or to adequately represent pile group action. Other shortcomings of static load tests include test cost, the time required to setup and complete a test, and the minimal information obtained on driving stresses or extent of pile damage (if any). Static load test results can also be misleading on projects with highly variable soil conditions.



Figure 18.9 Sister Bar Vibrating Wire Gages for Concrete Embedment



Figure 18.10 Arc-weldable Vibrating Wire Strain Gage Attached to H-pile. (Note: Protective Channel Cover Shown on Left)

18.8 TENSILE LOAD TESTS

Tensile load tests are performed to determine axial tensile (uplift) load capacities of piles. The uplift capacity of piles is important for pile groups subjected to large overturning moments. Hence, the importance of determining pile uplift capacity has greatly increased in recent years, particularly with regard to seismic design issues. The basic mechanics of the test are similar to compression load testing, except the pile is loaded in tension.

18.8.1 Tension Test Equipment

ASTM D-3689-90 (re-approved 1995) describes The Standard Method of Testing Individual Piles Under Static Axial Tensile Load by the American Society of Testing Materials. Several alternative systems for (1) applying tensile load to the pile, and (2) measuring movements are provided in this standard. Most often, tensile loads are applied by centering a hydraulic jack on top of a test beam(s) and jacking against a reaction frame connected to the pile to be tested. The test beam in turn is supported by piles or cribbing. When a high degree of accuracy is required, the primary means of measuring the load applied to the pile should be from a calibrated load cell with the jack load recorded from a calibrated pressure gage as backup. A spherical bearing plate should be included in the load application arrangement.

Axial pile head movements are usually measured by dial gages or LVDT's that measure movement between the pile head and an independently supported reference beam. For tensile load testing, ASTM requires a longer travel length and higher precision for movement measuring devices than in a compression load test. For tensile testing, ASTM requires that the dial gages or LVDT's have a minimum of 75 mm (3 inches) of travel and a precision of at least 0.025 mm (0.001 inches). A minimum of two dial gages or LVDT's mounted equidistant from the center of the pile and diametrically opposite should be used. Two backup systems consisting of a scale, mirror, and wire system should also be provided with a scale precision of 0.25 mm (0.01 inches). The backup systems should be mounted on diametrically opposite pile faces and be independently supported systems. Additional details on load application, and pile head load and movement measurements may be found in ASTM D-3689. A photograph of a typical tension load test arrangement is presented in Figure 18.11.

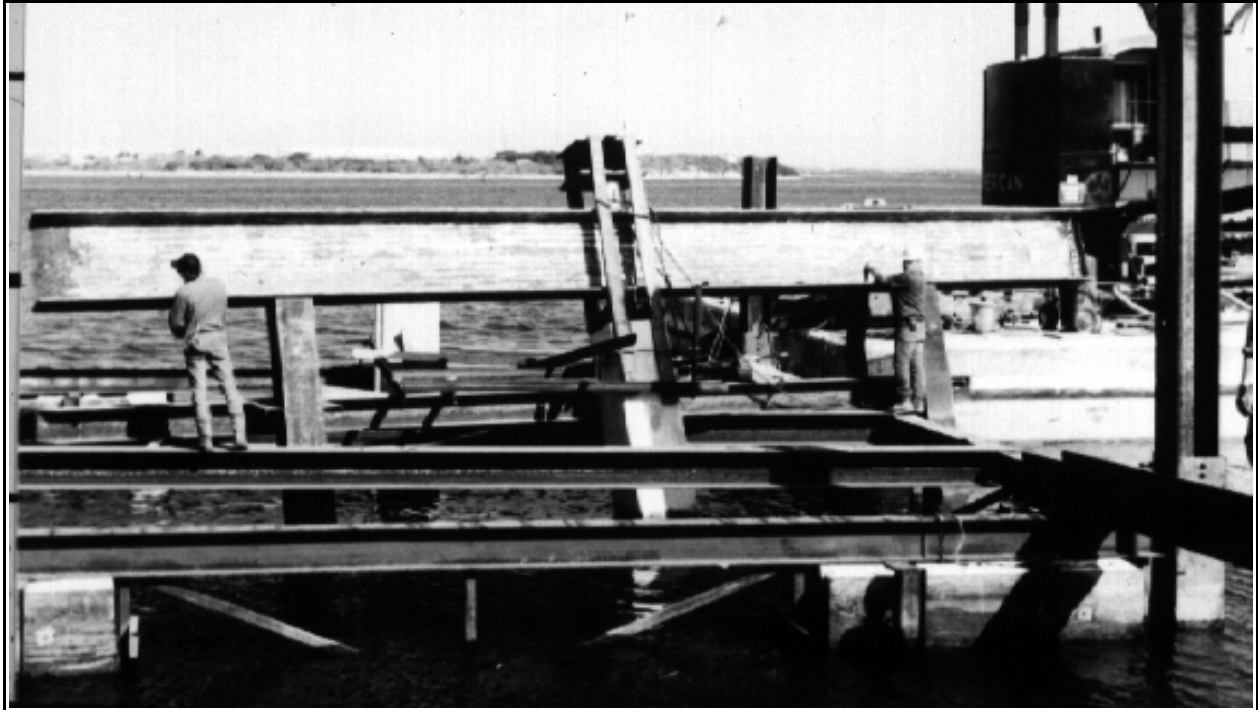


Figure 18.11 Tension Load Test Arrangement on Batter Pile (courtesy of Florida DOT)

18.8.2 Tension Test Loading Methods

Several loading procedures are detailed in ASTM D-3689. The quick loading procedure is recommended. This procedure requires that load be applied in increments of 10 to 15% of the pile design load with a constant time interval of 2½ minutes, or as otherwise specified between load increments. Readings of time, load, and gross movement are to be recorded immediately before and after the addition of each load increment. This procedure is to continue until continuous jacking is required to maintain the test load, or the capacity of the loading apparatus is reached, whichever occurs first. Upon reaching and holding the maximum load for 5 minutes, the pile is unloaded in four equal load decrements which are each held for 5 minutes. Readings of time, load, and gross movement are once again recorded immediately after, 2½ minutes after, and 5 minutes after each load reduction including the zero load. Additional optional loading procedures are detailed in ASTM D-3689.

It is generally desirable to test a pile in tensile loading to failure, particularly during a design stage test program. If construction stage tensile tests are performed on production piles, the piles should be redriven to the original pile toe elevation and the previous driving resistance upon completion of the testing.

18.8.3 Presentation and Interpretation of Tension Test Results

The results of tensile load tests should be presented in a report conforming to the requirements of ASTM D-3689. A load-movement curve similar to the one shown in Figure 18.12 should be plotted for interpretation of tensile load test results.

A widely accepted method for determining the ultimate pile capacity in uplift loading has not been published. Fuller (1983) reported that acceptance criteria for uplift tests have included a limit on the gross or net upward movement of the pile head, the slope of the load movement curve, or an offset limit method that accounts for the elastic lengthening of the pile plus an offset.

Due to the increased importance of tensile load testing, it is recommended that the elastic lengthening of the pile plus an offset limit be used for interpretation of test results. For tensile loading, the suggested offset is 4.0 mm (0.15 inches). The load at which the load movement curve intersects the elastic lengthening plus 4.0 mm (0.15 inches) is then defined as the tensile failure load. The uplift design load may be chosen between $\frac{1}{2}$ to $\frac{2}{3}$ of this failure load.

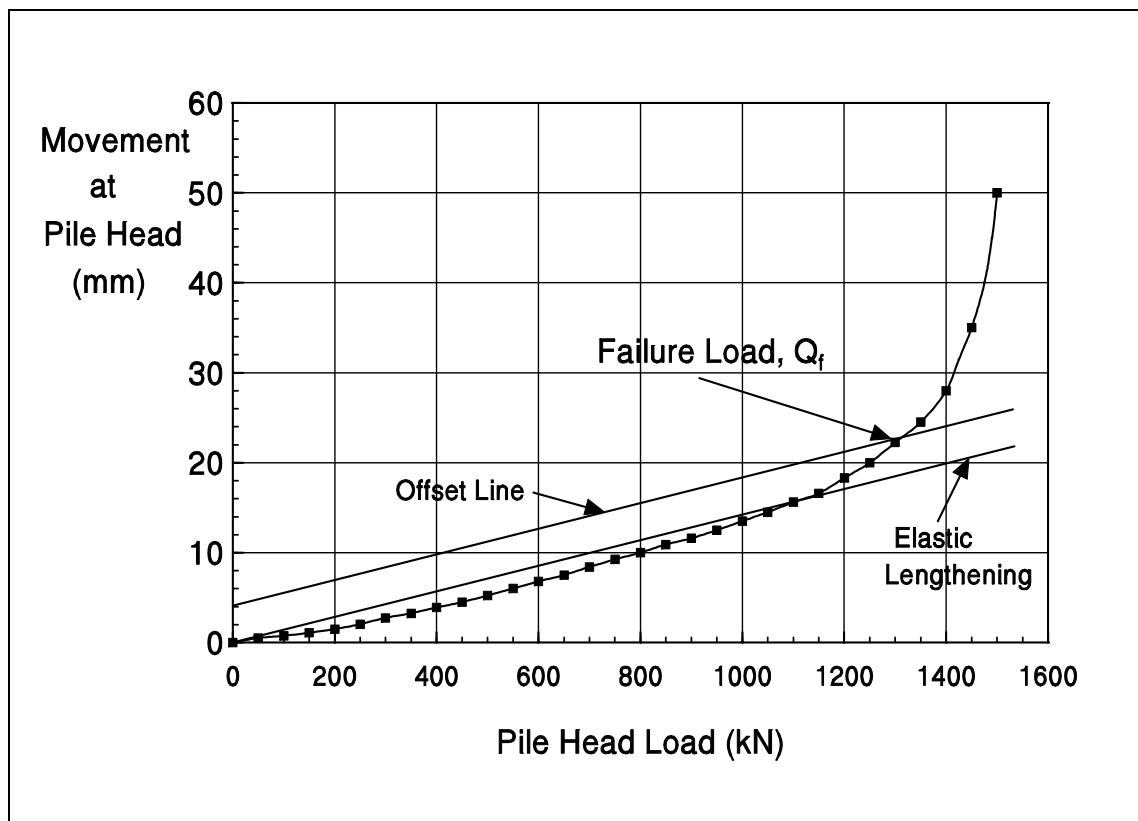


Figure 18.12 Typical Tension Load Test Load-Movement Curve

18.9 LATERAL LOAD TESTS

Lateral load tests are performed on projects where piles are subjected to significant lateral loads. The importance of determining pile response to lateral loading has greatly increased in recent years, particularly with regard to special design events such as seismic and vessel impact. This need has also increased due to the greater use of noise walls and large overhead signs. The primary purpose of lateral load testing is to determine the p-y curves to be used in the design or to verify the appropriateness of the p-y curves on which the design is based.

18.9.1 Lateral Load Test Equipment

ASTM D-3966-90 (re-approved 1995) describes The Standard Method of Testing Piles Under Lateral Load by the American Society of Testing Materials. Several alternative systems for (1) applying the lateral load to the pile, and (2) measuring movements are provided in this standard. Most often, lateral loads are applied by a hydraulic jack acting against a reaction system (piles, deadman, or weighted platform), or by a hydraulic jack acting between two piles. The primary means of measuring the load applied to the pile(s) should be from a calibrated load cell with the jack load recorded from a calibrated pressure gage as backup. ASTM requires a spherical bearing plate(s) be included in the load application arrangement unless the load is applied by pulling.

Lateral pile head movements are usually measured by dial gages or LVDT's that measure movement between the pile head and an independently supported reference beam mounted perpendicular to the direction of movement. For lateral load testing, ASTM requires the dial gages or LVDT's have a minimum of 75 mm (3 inches) of travel and a precision of at least 0.25 mm (0.01 inches). For tests on a single pile, one dial gage or LVDT is mounted on the side of the test pile opposite the point of load application. A backup system consisting of a scale, mirror, and wire system should be provided with a scale precision of 0.25 mm (0.01 inches). The backup system is mounted on the top center of the test pile or on a bracket mounted along the line of load application.

It is strongly recommended that lateral deflection measurements versus depth also be obtained during a lateral load test. This can be accomplished by installing an inclinometer casing on or in the test pile to a depth of 10 to 20 pile diameters and recording inclinometer readings immediately after application or removal of a load increment held for a duration of 30 minutes or longer. Kyfor *et al.* (1992) noted that lateral load tests in which only the lateral deflection of the pile head is measured are seldom justifiable. Additional details on load application, and pile head load and movement measurements may be found in ASTM

D-3966 and FHWA-SA-91-042. A photograph of a typical lateral load test arrangement is presented in Figure 18.13. This figure shows a 356 mm and 406 mm (14 and 16 inch) O.D. concrete filled pipe pile being pushed apart. The jack is located adjacent to the right pile and the load cell and spherical bearing plate are located adjacent to the left pile. Figures 18.14 and 18.15 present close-ups of these devices. Both piles were also equipped with a string of inclinometers for prompt readout of the deflected pile shape with each load increment. A photograph of the multiple inclinometer string components is presented in Figure 18.16



Figure 18.13 Typical Lateral Load Test Arrangement (courtesy of WKG2)

18.9.2 Lateral Test Loading Methods

Several loading procedures are detailed in ASTM D-3966. The standard loading procedure requires that the total test load be 200% of the proposed lateral design load. Variable load increments are applied with the magnitude of load increment decreasing with applied load.



Figure 18.14 Jack for Lateral Load Test (courtesy WKG2)



Figure 18.15 Spherical Bearing Plate and Load Cell for Lateral Load Test



Figure 18.16 Multiple Incliner String Components for Lateral Load Test

The load duration is also variable, increasing from 10 minutes early in the test to 60 minutes at the maximum load. Upon completing the maximum test load, the pile is unloaded in four load decrements equal to 25% of the maximum load with 1 hour between load decrements.

A modified lateral loading schedule was proposed by Kyfor *et al.* in FHWA-SA-91-042. The recommended loading increment is 12.5% of the total test load with each load increment held for 30 minutes. Upon reaching and holding the maximum load for 60 minutes, the pile is unloaded and held for 30 minutes at 75, 50, 25 and 5% of the test load.

Readings of time, load, and gross movement are recorded immediately after each change in load. Additional readings are taken at 1, 2, 4, 8, 15 and 30 minutes. This procedure is followed during both the loading and unloading cycle.

18.9.3 Presentation and Interpretation of Lateral Test Results

The results of lateral load tests should be presented in a report conforming to the requirements of ASTM D-3966. The interpretation and analysis of lateral load test results is much more complicated than those for compression and tensile load testing. Figure 18.17 presents a typical lateral load test pile head load-movement curve. A lateral deflection versus depth curve similar to the one shown in Figure 18.18 should also be plotted for interpretation of lateral load test results that include lateral deflection measurements versus depth. The measured lateral load test results should then be plotted and compared with the calculated result as indicated in Figure 18.18.

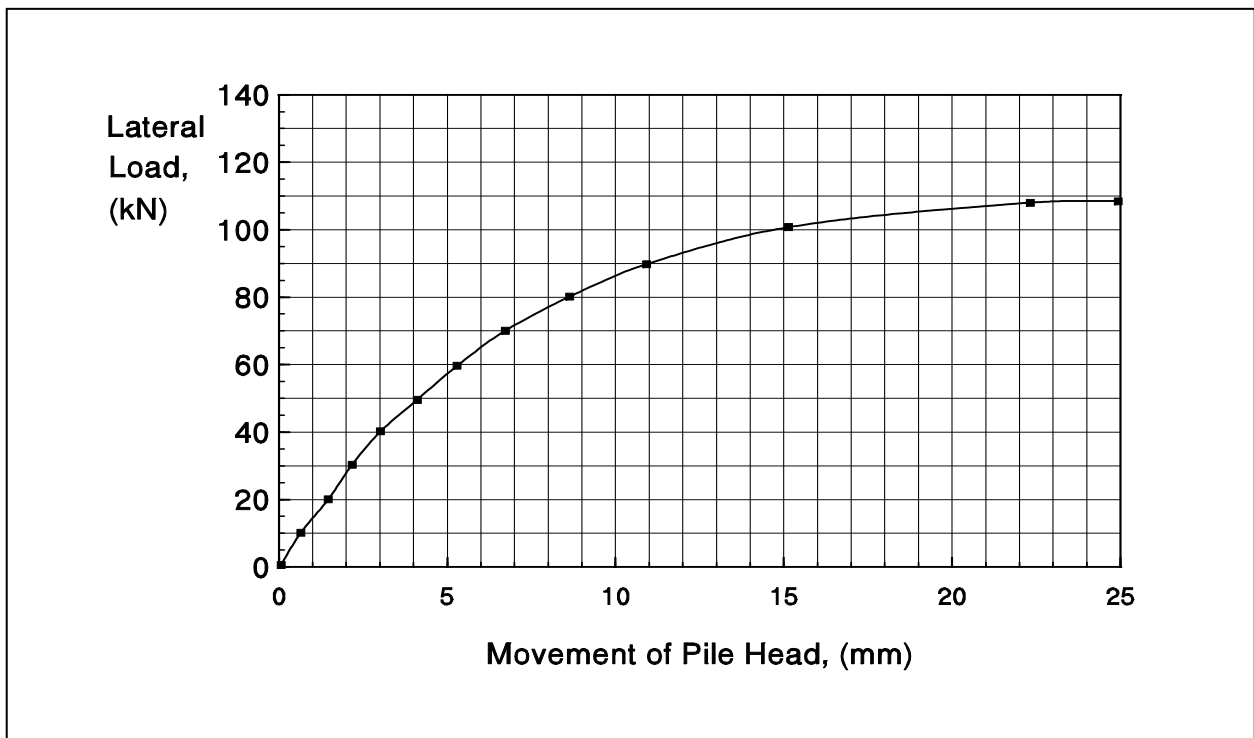


Figure 18.17 Typical Lateral Load Test Pile Head Load-Deflection Curve

Based upon the comparison of measured and predicted results, the p-y curves to be used for design (design stage tests), or the validity of the p-y curves on which the design was based (construction stage tests) can be determined.

Refer to FHWA-IP-84-11, Handbook on Design of Piles and Drilled Shafts Under Lateral Load by Reese (1984) as well as FHWA-SA-91-042, Static Testing of Deep Foundation by Kyfor *et al.* (1992) for additional information on methods of analysis and interpretation of lateral load test results.

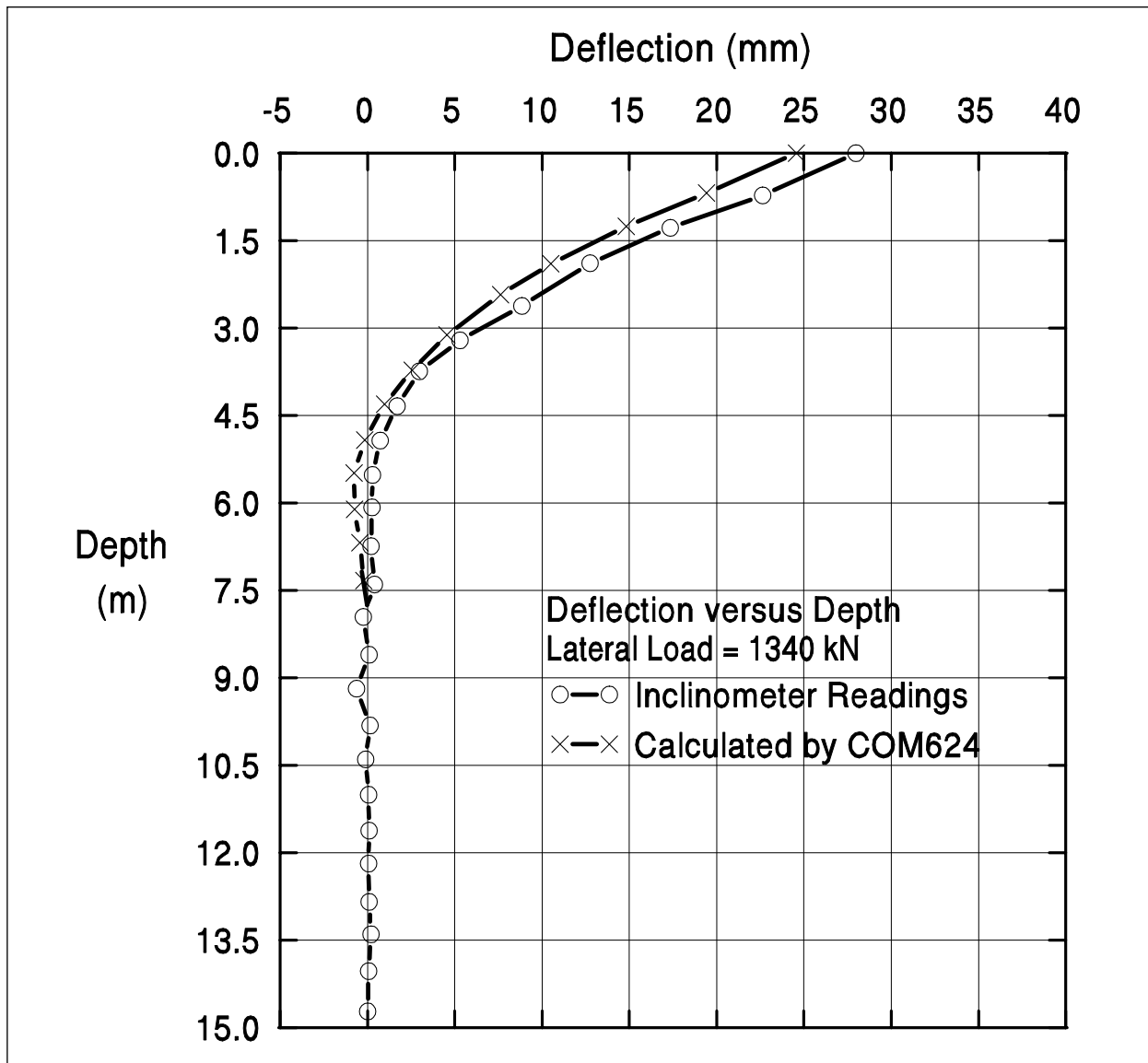


Figure 18.18 Comparison of Measured and COM624P Predicted Load-Deflection Behavior versus Depth (after Kyfor *et al.* 1992)

REFERENCES

- American Association of State Highway and Transportation Officials [AASHTO], (2002). Standard Specifications for Highway Bridges. Division 2, Washington, D.C.
- American Society for Testing and Materials, ASTM (2004). Annual Book of Standards, ASTM D-1143-81, Standard Test Method for Piles Under Static Axial Compressive Load.
- American Society for Testing and Materials, ASTM (2004). Annual Book of Standards, ASTM D-3689-90, The Standard Method of Testing Individual Piles Under Static Axial Tensile Load.
- American Society for Testing and Materials, ASTM (2004). Annual Book of Standards, ASTM D-3966-90, The Standard Method of Testing Piles Under Lateral Load.
- Cheney, R.S. and Chassie, R.G. (2000). Soils and Foundations Workshop Reference Manual. Publication No. FHWA HI-00-045, Federal Highway Administration, National Highway Institute, Washington, D.C., 358.
- Crowther, C.L. (1988). Load Testing of Deep Foundations: the Planning, Design, and Conduct of Pile Load Tests. John Wiley & Sons, New York, 233.
- Davisson, M.T. (1972). High Capacity Piles, Proceedings, Soil Mechanics Lecture Series on Innovations in Foundation Construction. American Society of Civil Engineers, ASCE, Illinois Section, Chicago, 81-112.
- Dunnicliff, J. (1988). Geotechnical Instrumentation for Monitoring Field Performance. John Wiley & Sons, New York, 467-479.
- Fellenius, B.H. (1990). Guidelines for the Interpretation of the Static Loading Test. Deep Foundations Institute Short Course Text, First Edition, 44.
- Fuller, F.M. (1983). Engineering of Pile Installations. McGraw-Hill, New York, 286.

Kyfor, Z.G., Schnore, A.S., Carlo, T.A. and Bailey, P.F. (1992). Static Testing of Deep Foundations. Report No. FHWA-SA-91-042, U.S. Department of Transportation, Federal Highway Administration, Office of Technology Applications, Washington, D.C., 174.

Reese, L.C. (1984). Handbook on Design of Piles and Drilled Shafts Under Lateral Load. Report No. FHWA-IP-84-11, U.S. Department of Transportation, Federal Highway Administration, Office of Implementation, McLean, 386.

Chapter 19

THE OSTERBERG CELL METHOD

An alternate and innovative method for evaluation of driven pile capacity utilizes the Osterberg Cell or O-cell[®]. This device provides a simple, efficient and economical method of performing a static test on a deep foundation. The O-cell is a sacrificial loading device which is generally attached to the toe of a driven pile before driving.

The Osterberg Cell test can be easily applied to driven, displacement piles such as closed - end pipe piles and prestressed concrete piles. The O-cell cannot be employed with H-piles, sheet piles or timber piles. Closed end pipe piles and concrete piles require cell installation prior to driving, and thus additional prior planning is needed. For open end pipe piles and mandrel driven piles, the cell may be installed after driving is complete.

Testing a driven pile with an O-cell eliminates the need for a reaction system and can provide significant cost and time savings. The Osterberg Cell has many applications and provides the engineer with a cost effective and versatile tool for the static testing of driven piles. The Osterberg Cell Method is not standardized by AASHTO or ASTM and is nationally licensed to a single source. Additional information about the Osterberg Cell may be found in FHWA publication FHWA-SA-94-035 by Osterberg (1995) or at the supplier's web site: www.loadtest.com.

19.1 OSTERBERG CELL BACKGROUND

Dr. Jorj Osterberg, Professor Emeritus at Northwestern University, developed and patented the test method and device which now carries his name. The device was first used in an experimental drilled shaft in 1984. Following this successful prototype test, the O-cell evolved from a bellows type expansion cell to the current design, which is very similar to the piston type jack commonly used for conventional top down load tests.

The first O-cell test on a driven pile occurred in 1987. In this initial driven pile application, a 457 mm (18 inch) diameter O-cell was welded to the toe of a 457 mm (18 inch) diameter, closed end, steel pipe pile. In 1994, the first O-cell tests were performed on 457 mm (18 inch) square, prestressed concrete piles. For these piles, the O-cell was cast into the pile toe.

Figure 19.1 presents a schematic of the difference between a conventional static load test and an O-cell test. A conventional static test loads the pile in compression from the pile head using an overhead reaction system or dead load. The pile shaft and toe resistances are opposed by the applied pile head load. The pile shaft and toe resistances can be separated by analysis of strain gage or telltale measurements.

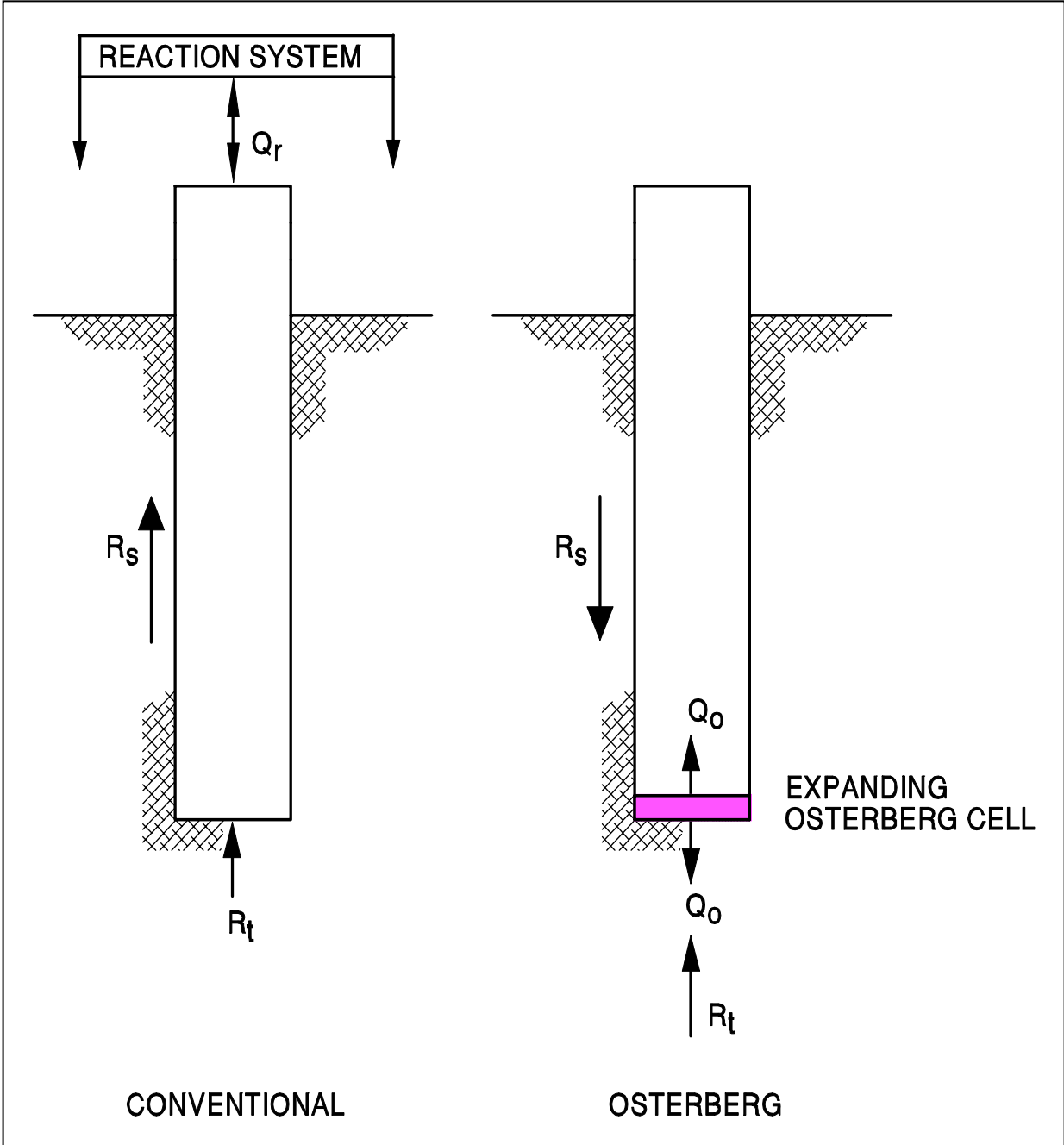


Figure 19.1 Schematic Comparison Between Osterberg Cell and Conventional Tests

In an O-cell test, the pile is also loaded in compression, but the load is applied at, or near, the pile toe instead of the pile head. As the cell expands, the toe resistance provides reaction for the shaft resistance, and visa-versa. The test is complete when either the ultimate shaft or toe resistance is reached, or the cell reaches its load capacity or nominal stroke.

An O-cell test automatically separates the shaft and toe resistance components. When one of the components fails at an O-cell load, Q_o , the conventional pile head load, Q_r , required to fail both the shaft resistance and toe resistance would have to exceed $2Q_o$. Thus, an O-cell test load placed at the pile toe is always twice as effective as the same load placed at the pile head.

19.2 TEST EQUIPMENT

The O-cell in its current design is capable of developing an internal pressure of 69 MPa (10 ksi). Typical cell capacities for driven piles of up to 8000 kN (1800 kips) have been used. For large diameter drilled shafts, a maximum test load of 279,000 kN (62,700 kips) has been achieved by utilizing a group of O-cells. The cell consists of a piston and cylinder with input and output ports connected to embedded hoses that extend to the ground surface. The total nominal expansion of a standard O-cell is 150 mm (6 inches). Specially built O-cells with greater expansion are available in some cases. Figure 19.2 shows a typical cross section of a concrete pile and the setup for an O-cell test.

Tests performed using the O-cell usually follow the quick loading method described in ASTM D-1143, Standard Test Method for Piles Under Static Axial Compressive Load. However, other methods are not precluded. The instrumentation used to measure load and movement is similar to that used for conventional load tests. The O-cell is designed so that driving forces are transmitted through the cell without damage to the cell or the pile. An O-cell ready for placement in a 457 mm (18 inch) prestressed concrete pile is shown in Figure 19.3. After this pile was cast, the only visible parts of the O-cell were the bottom plates.

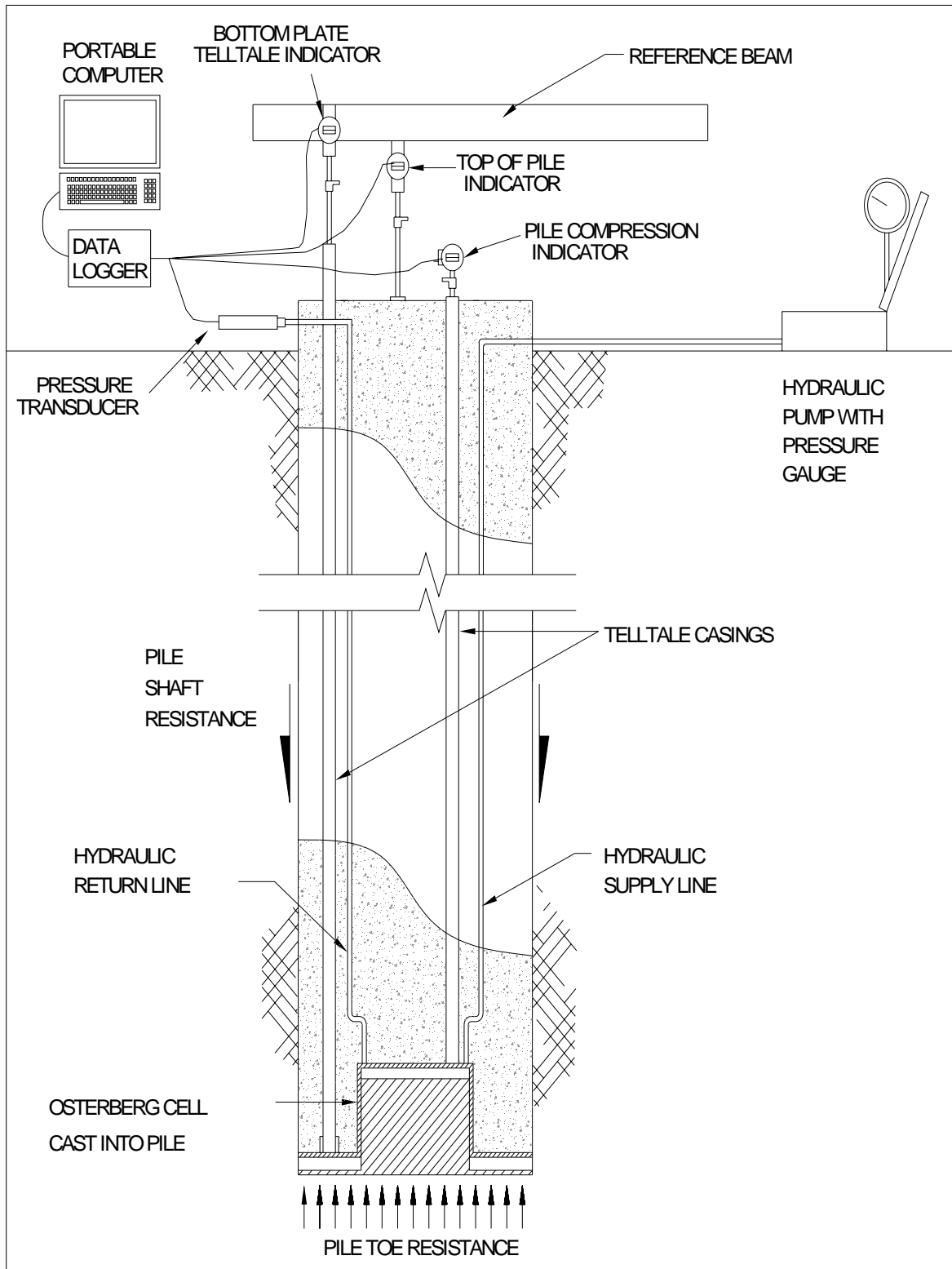


Figure 19.2 Osterberg Cell and Related Equipment Used for Static Pile Tests



Figure 19.3 Osterberg Cell Ready for Placement in Concrete Pile Form (courtesy of Loadtest, Inc.)

After the pile is driven, a hand pump or small automatic pump (electric or air driven) is connected to a central pipe which provides a pressure conduit to the O-cell. The load applied by an O-cell is calibrated versus hydraulic pressure before installation and the pressure applied to the cell is measured using a Bourdon gage or pressure transducer. The O-cell seals typically limit internal friction to less than 2% of the applied load. In Figure 19.4, both a vibrating wire piezometer and a test gage are being used to measure the cell pressure, which is applied with a hand pump.



Figure 19.4 Osterberg Test in Progress on a 457 mm Concrete Pile (courtesy of Loadtest, Inc.)

The cell and instrumentation are normally installed in concrete piles during casting of the pile. For closed end pipe piles, the cell must be attached to the pile toe prior to driving. For open end pipe piles and concrete cylinder piles, the cell and instrumentation have been placed as a combined unit after the pile is driven, internally cleaned out to the O-cell depth, and then concreted in place.

Movements during an O-cell test are typically measured using mechanical or electronic gages. The cell expansion (less any pile compression) is directly indicated by steel telltales that extend to the bottom of the cell. The telltales are placed in pairs, one each in a pair of preinstalled steel pipes, 180 degrees opposed. The telltale movement is measured with respect to the top of pile. Additional telltales, indicating compression of the pile, are similarly installed in pairs and extend to the top of the O-cell. The upward movement of the pile is measured by gages attached to a reference beam and checked by an independent measurement such as a survey level.

When an O-cell test is performed on a production pile it will usually be necessary to grout the O-cell and the space outside the O-cell after completing the test. This is accomplished by pumping grout through the hydraulic hoses and bottom plate telltale pipes respectively.

19.3 INTERPRETATION OF TEST RESULTS

The Osterberg Cell loads the test pile in compression similar to a conventional static load test. Data from an Osterberg test is therefore analyzed much the same as conventional static test data. The only significant difference is that the O-cell provides two load-movement curves, one for the pile shaft resistance and one for the pile toe resistance. The upper pile shaft movement (upward top of O-cell movement) is computed by adding the measured pile compression to the measured top of pile movement. The pile toe movement (downward bottom of O-cell movement) is computed by subtracting the top of pile movement from the bottom plate telltale measurement. The failure load for each component may be determined from these curves using a failure criteria similar to that recommended for conventional load tests. To determine the pile shaft resistance, the buoyant weight of the pile must be subtracted from the upward O-cell load.

The engineer may further utilize the component curves to construct an equivalent pile head load-movement curve and investigate the overall pile capacity. Construction of the equivalent pile head load-movement curve begins by determining the pile shaft resistance at an arbitrary movement point on the shaft resistance-movement curve. If the pile is assumed rigid, the pile head and toe move together and have the same movement at this load. By adding the pile shaft resistance to the mobilized toe resistance at the chosen movement, a single point on the equivalent pile head load-movement curve is determined. Additional points may then be calculated to develop the curve up to the maximum movement (or maximum extrapolated movement) of the component that did not fail. Points beyond the maximum movement of the non-failing component may also be obtained by conservatively assuming that at greater movements the load remains constant. Once this rigid curve is developed an additional correction can be made to account for the fact that

additional elastic compression may have occurred had the pile been loaded from the top. Example results using this method are included with the case history data below.

As noted by Osterberg (1994), the above construction makes three basic assumptions:

1. The shaft resistance load-movement curve resulting from the upward movement of the top of the O-cell is the same as developed by the downward pile head movement of a conventional compression load test.
2. The toe resistance load-movement curve resulting from the downward movement of the bottom of the O-cell is the same as developed by the downward pile toe movement of a conventional load test.
3. The compression of the pile is considered negligible, i.e. a rigid pile.

The first of these assumptions highlights a significant difference between the O-cell test and a conventional compression load test, namely the change in direction of the mobilized shaft resistance from downward to upward. Researchers at the University of Florida have investigated the effect of this direction reversal using the finite element method. Their results indicate that the O-cell produces slightly lower shaft resistance than a conventional load test, but that in general the effect is small and may be ignored. Several full scale field tests tend to confirm these findings. Note that the shaft resistance direction in an O-cell test matches that in a conventional tension or uplift test.

Lower confining stresses due to the gap induced around the expanding cell may also cause the O-cell to measure a slightly lower toe resistance, but this effect is conservative and also seems negligible. In general, the above assumptions seem to produce conservative and reasonable results.

19.4 APPLICATIONS

Although its use is not feasible for all pile types, the O-cell test has many potential applications with common driven piles. Its versatility also provides additional options. A partial list of applications follows:

1. Displacement Piles: The O-cell may be installed prior to driving solid concrete piles and closed end pipe piles.

2. Mandrel Driven Piles: Mandrel driven piles can be tested by grouting the O-cell into the pile toe after removing the mandrel.
3. Open Ended Pipe Piles: The O-cell may be installed in open ended pipe piles and voided concrete piles by removing the soil plug after driving.
4. Batter Piles: Conventional static load tests to evaluate the axial capacity of batter piles can be very difficult to perform. For applicable pile types in these situations, the O-cell test offers an alternate test method that is easier to perform.
5. Testing Over Water or at Constricted Sites: Because the O-cell test requires no overhead reaction, the surface test setup is minimized. Tests over water require only a work platform. Sites with poor access, limited headroom or confined work area are ideal applications for an O-cell test.
6. Proof Tests: Because of the simplicity and usually lower cost of O-cell tests compared to conventional static load tests, several piles can be economically proof tested as a check of pile capacity.
7. Repetitive Tests: Multiple static tests on the same pile may be performed with the O-cell to investigate the effect of time on pile capacity. Use of the O-cell minimizes the mobilization required for each static test.
8. Exploratory Testing: With the proper design, it is possible to use the O-cell to test the same pile at different pile penetration depths. After each test, the pile is driven deeper and retested. This method also develops the shaft resistance distribution incrementally.

19.5 ADVANTAGES

Osterberg (1994) and Schmertmann (1993) summarized a number of potential advantages vs. conventional testing that may be realized by using the Osterberg Cell. These include:

1. Economy: The O-cell method becomes more economical as loads increase, unlike top-down static tests.
2. Automation / Static Creep Effects: The O-cell test is a static maintained load test and uses automatic data acquisition techniques and load maintenance for accurate,

efficient data processing and creep measurements.

3. Design: Excellent tool for value engineering.
4. Improved Safety: No reaction system is required at ground level and the test energy is safely buried well below ground.
5. Reduced Work Area: Required work area (overhead and laterally) is greatly reduced vs. any other static load testing system. Testing has been performed inside buildings, under overpasses, in narrow interstate/highway median strips and offshore.
6. Accuracy: Since there are no anchors, reaction piles or a reaction mass required, the influence of these devices on test pile performance are eliminated.
7. Shaft / Toe Resistance Components: O-cell tests are designed to separate test piles into 2 or 3 pile sections; thus automatically measuring the reaction of each component.
8. Soil Setup: The O-cell provides a convenient method to obtain additional tests on the same pile at selected time intervals after driving allowing soil setup effects to be quantified.
9. Production Piles: Post-test grouting techniques allow for testing of production piles;
10. Offshore: The O-cell test method particularly excels in offshore testing environments due to the advantages listed above.

19.6 DISADVANTAGES

The O-cell has some disadvantages or limitations compared to conventional tests as discussed below:

1. Not Suitable for Certain Types of Piles: The O-cell cannot be used to test H-piles. Installation of an O-cell on a timber pile would be difficult. Installation in open end pipe piles is feasible, but requires internal pile cleanout after driving for cell placement

and subsequent concrete or grout placement above the installed cell. In tapered piles, the equivalent shaft resistance of a tapered pile loaded in compression will not be developed since the effects of the taper will be lost when loaded upward from the pile toe in an O-cell test.

2. Need for Planning: With closed end and solid displacement piles, the O-cell must be installed prior to driving. For these pile types, an O-cell test cannot be chosen after installation.
3. Limited Capacity: An O-cell test reaches the ultimate load in only one of the two resistance components. The pile capacity demonstrated by the O-cell test is limited to two times the failed component. Also, once installed, the cell capacity cannot be increased if inadequate. To use the cell efficiently, the engineer should first analyze the expected shaft and toe resistances, and then attempt to balance the two or ensure a failure in the preferred component.
4. Equivalent Pile Head Load-Movement Curve: Although the equivalent static load-movement curve can be constructed from O-cell test data, it is not a direct measurement and may be too conservative.
5. Lack of Redundancy to Check Load Calibration: The O-Cell load is based only on pressure readings. There is no load cell for redundancy as exists in a conventional static test.

19.7 CASE HISTORIES

To date, only closed end pipe piles and prestressed concrete driven piles have been tested using the O-cell. Examples of case studies for both pile types are presented below.

In 1987, a 457 mm (18 inch) diameter steel pipe pile with an O-cell of the same diameter welded to the pile toe was driven at the Pines River Bridge in Saugus, MA. As shown in Figure 19.5, this pile was driven through soft clay and a layer of glacial till, then founded in weathered Argillite rock at a depth of 36 m (118 ft) below the ground surface. It was driven to practical refusal with a Delmag D 36-13 diesel hammer with a rated energy 112.7 kJ (83.1 ft-kips). The final driving resistance was 10 blows for the last 13 mm (0.5 inches). As indicated by the shaft and toe resistance load-movement curves shown in Figure 19.6, the Pines River pile failed in shaft resistance at a cell load of 1910 kN (429 kips). The small upward movement evident during the initial portion of the test is due to pressure effects on

the central pipe and has little effect on the capacity results. After subtracting the pile weight to get shaft resistance, the minimum ultimate capacity of this pile was estimated as 3740 kN (841 kips). An equivalent pile head load-movement curve constructed from the test data is included in Figure 19.7. The maximum toe resistance of 1910 kN (429 kips) was used at movements greater than 1.0 mm (0.04 inches). For reference, the numbered pile head load-movement points were calculated at movements corresponding to the numbered points on the shaft resistance curve. Thompson *et al.* (1989) provides additional details on this case history.

O-cell tests can also be useful for special investigations. For example, O-cells were recently cast into four 457 mm (18 inch) square, prestressed concrete piles which were then driven and tested as part of a research project by the University of Florida (UF). This research project is investigating long term shaft resistance changes. The O-cell is being used in this application to perform repeated tests over a period of at least two years after the piles are driven. To allow the prestressed pile manufacturer to cast ordinary production piles along with the research piles, the O-cell used for the UF research is designed to fit within the standard prestressed cable pattern. The strands were then pulled through holes drilled in the load plates of the cell. These cells have a 229 mm (9 inch) diameter piston and a maximum stroke of 152 mm (6 inches). They provide a capacity of 2700 kN (600 kips) at a pressure of 69 MPa (10 ksi). To prevent damage during driving extra lateral reinforcement was added at the pile toe. Longitudinal reinforcement was also added above the O-cell to insure good load transfer during testing and driving. Otherwise, the research piles followed a standard Florida DOT design and were cast as part of a full production bed of piles.

The pile driven at Aucilla River is 22 m (72 ft) long and has been tested four times over a 2 month period. Its shaft resistance has increased 64% over this time period to 1490 kN (335 kips), and indications are that it will continue to increase in capacity with additional time. As shown in Figure 19.8, this pile was driven to bearing on limerock at 16 blows for the final 25 mm (1 inch) using a Fairchild 32 air hammer with a rated energy of 43.4 kJ (32 ft-kips). Figures 19.9 and 19.10 show the component and equivalent pile head load-movement curves for the most recent test. The maximum toe resistance of 1560 kN (351 kips) was used at deflections greater than 2.3 mm (0.09 inches). Repeated tests have influenced the toe resistance, which now shows some disturbance effects in the early loads. Otherwise this test is representative of the research results.

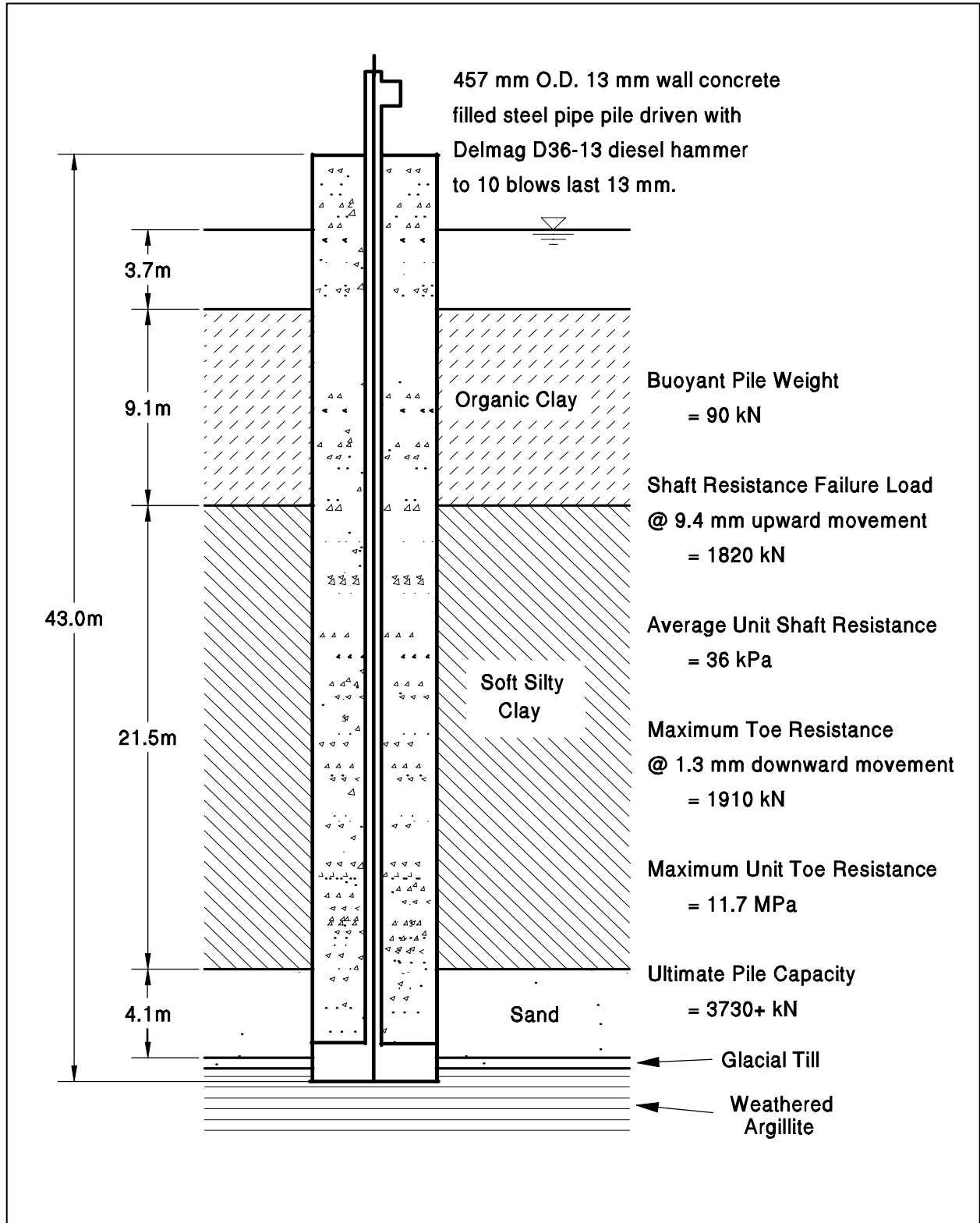


Figure 19.5 Summary of Subsurface Profile and Test Results at Pines River Bridge, MA

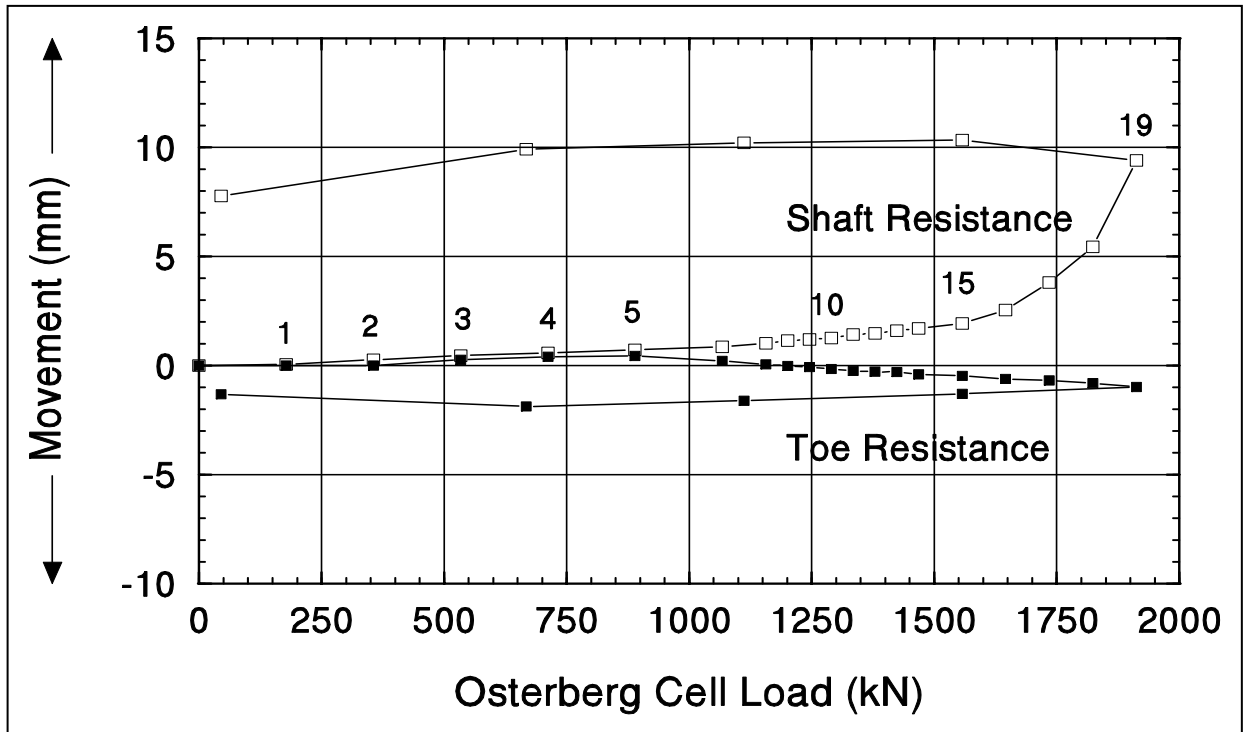


Figure 19.6 Test Results from Pines River Bridge, MA

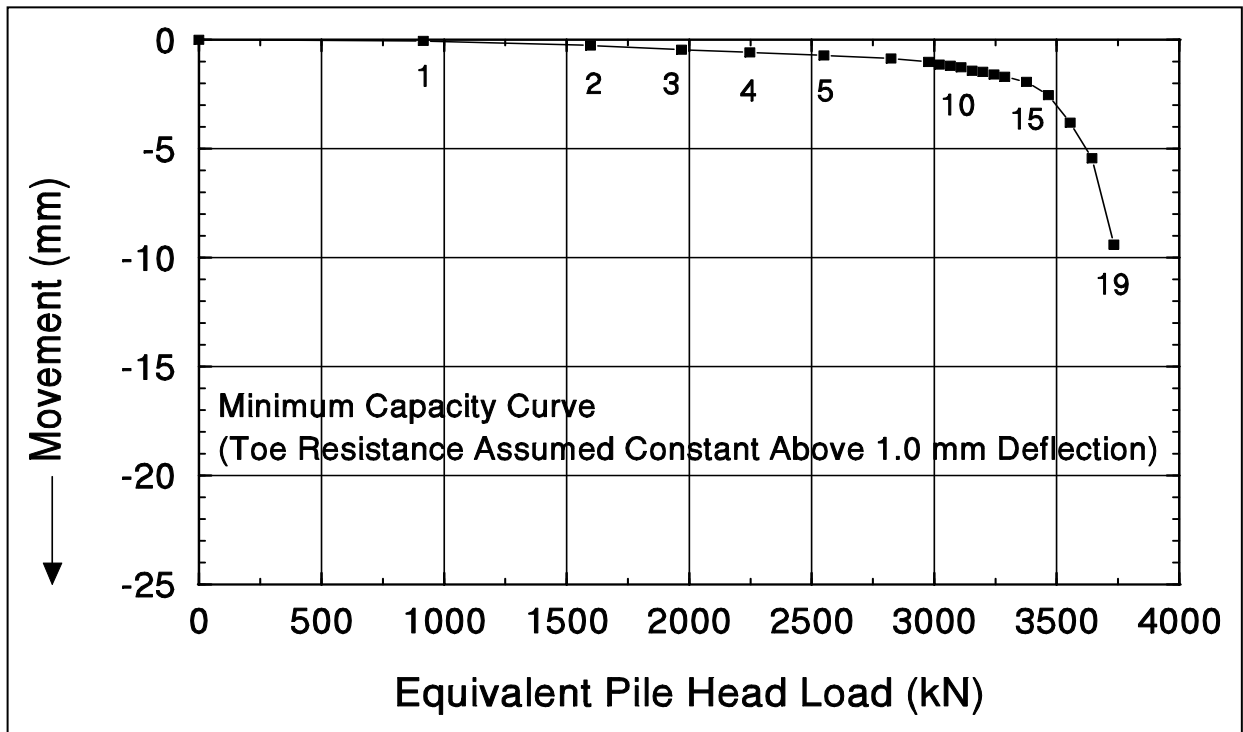


Figure 19.7 Equivalent Pile Head Load-Movement Curve from Pines River Bridge, MA

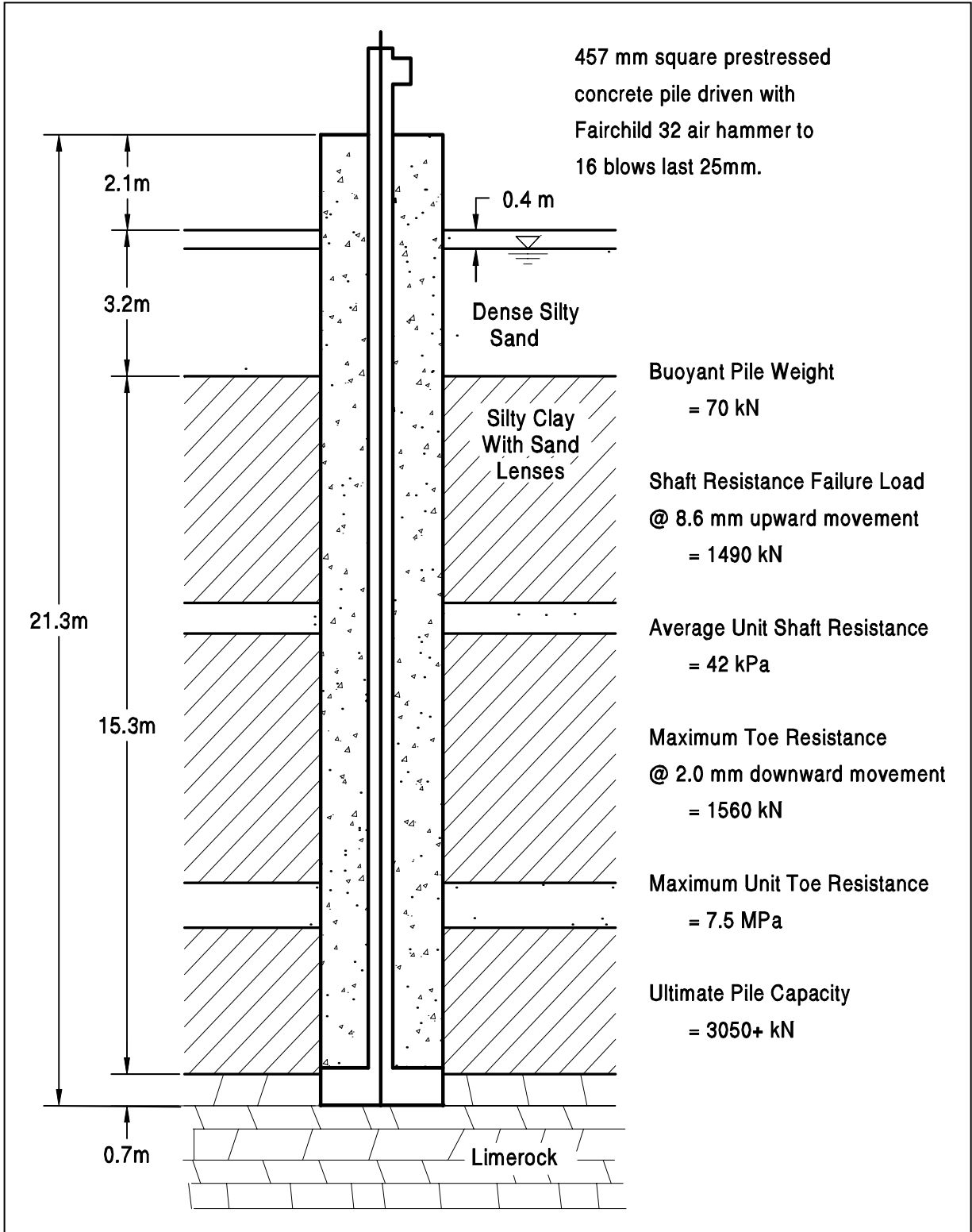


Figure 19.8 Summary of Subsurface Profile and Test Results at Aucilla River Bridge, FL

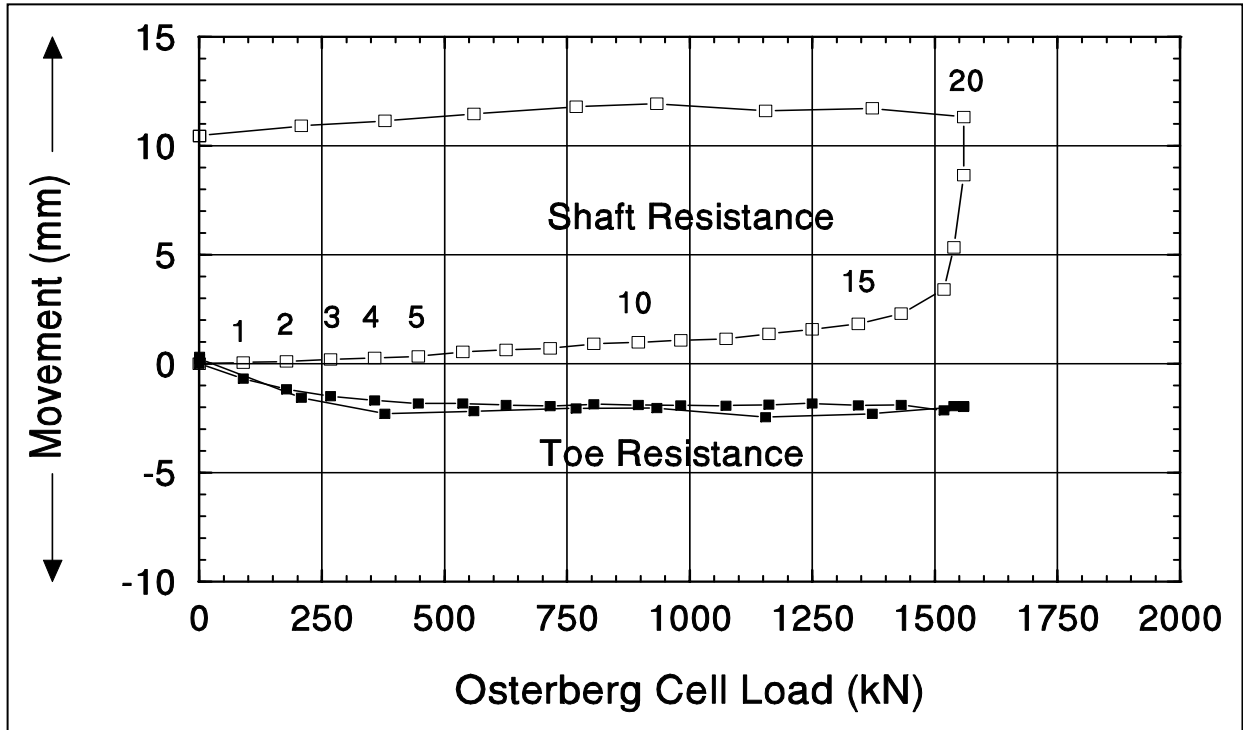


Figure 19.9 Test Results from Aucilla River Bridge, FL

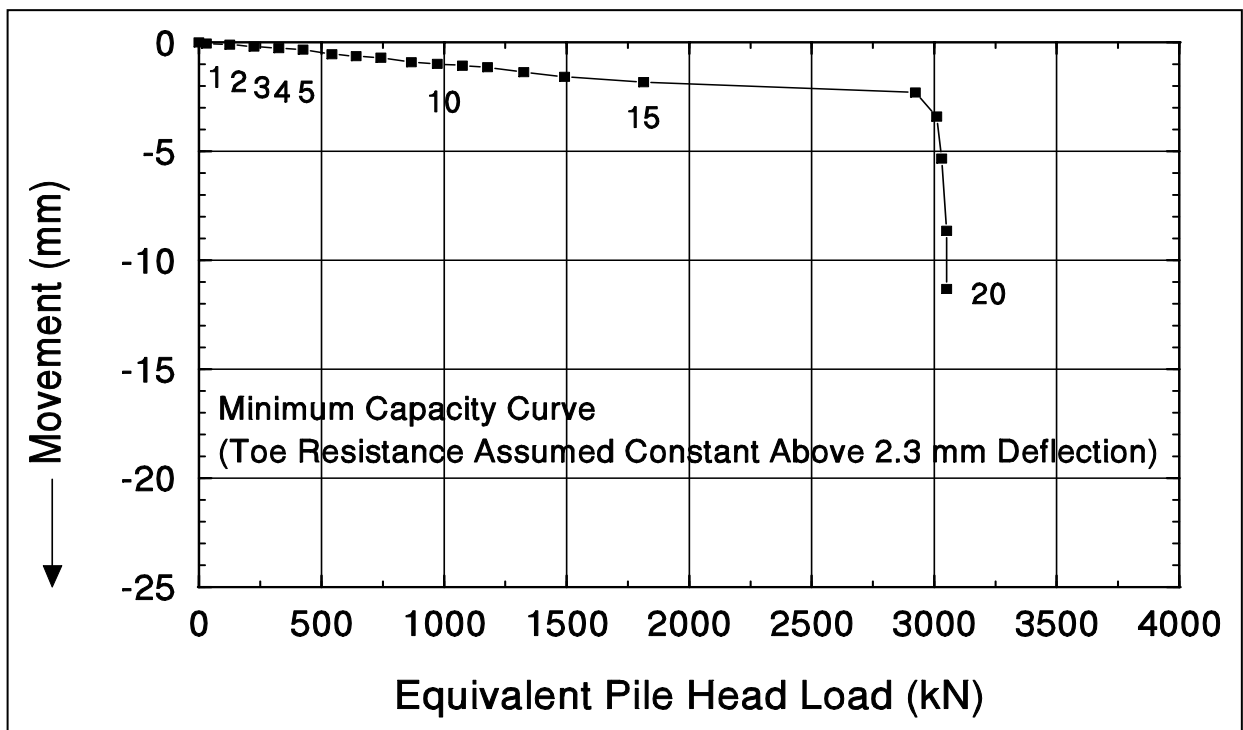


Figure 19.10 Equivalent Pile Head Load-Movement Curve from Aucilla River Bridge, FL

REFERENCES

- American Society for Testing and Materials [ASTM], (1994). Annual Book of Standards. ASTM D-1143, Standard Test Method for Piles Under Axial Compressive Load, Vol. 4.08, Philadelphia, PA.
- Goodwin, J.W. (1993). Bi-Directional Load Testing of Shafts to 6000 tons. Design and Performance of Deep Foundations: Piles and Piers in Soil and Soft Rock, ASCE, NY, NY, 204-217.
- Osterberg, J.O. (1984). A New Simplified Method for Load Testing Drilled Shafts. Foundation Drilling, ADSC, Dallas, TX, Vol. 23, No. 6, 9-11.
- Osterberg, J.O. (1994). Recent Advances in Load Testing Driven Piles and Drilled Shafts using the Osterberg Load Cell Method. Geotechnical Lecture Series, Geotechnical Division of the Illinois Section, ASCE, Chicago, IL.
- Osterberg, J.O. (1995). The Osterberg Cell for Load Testing Drilled Shafts and Driven Piles. Report No. FHWA-SA-94-035, U.S. Department of Transportation, Federal Highway Administration, Office of Technology Applications, Washington, D.C., 92.
- Schmertmann, J.H. (1993). The Bottom-up, Osterberg Cell Method for Static Testing of Shafts and Piles. Progress in Geotechnical Engineering Practice Proceedings, Hershey PA, Central Pennsylvania ASCE, Harrisburg, PA, 7.
- Thompson, D.E., Erikson, C.M. and Smith, J.E. (1989). Load Testing of Deep Foundations Using the Osterberg Cell. Proceedings of the 14th Annual Members Conference, Deep Foundations Institute, Sparta, NJ, 31-44.

Chapter 20

THE STATNAMIC METHOD

An alternate and innovative method for evaluation of driven pile capacity is the Statnamic Method. The Statnamic method can be applied to all driven pile types on land or over water. The test method can provide cost and time savings where high loads are required or access is difficult.

The Statnamic testing method was developed in 1988 by Berminghammer Foundation Equipment and TNO, the Dutch governmental organization for applied scientific research. The method uses solid fuel burned within a pressure chamber to rapidly accelerate upward the reaction mass positioned on the pile head. As the gas pressure increases, an upward force is exerted on the reaction mass, while an equal and opposite force pushes downward on the pile. Loading increases to a maximum and then unloads by a venting of the gas pressure. A load cell and accelerometers measure load and acceleration. At the time of this publication, the Statnamic test method is not yet standardized by AASHTO or ASTM and is nationally licensed to a single source. Additional information on the Statnamic test can be obtained from the developer at: www.berminghammer.com or from the single source supplier at www.testpile.com.

20.1 STATNAMIC BACKGROUND

The principles of Statnamic can be described by Newton's Laws of Motion:

1. A body will continue in a state of rest or uniform motion unless compelled to change by an external force.
2. A body subjected to an external force accelerates in the direction of the external force and the acceleration is proportional to the force magnitude ($F = ma$).
3. For every action there is an opposite and equal reaction ($F_{12} = -F_{21}$).

In the Statnamic test, a reaction mass is placed on top of the pile to be tested. The ignition and burning of the solid fuel creates a gas pressure force, F , that causes the reaction mass, m , to be propelled upward so that the acceleration amounts to about 20 g's ($F=ma$). An equivalent downward force is applied to the foundation element, ($F_{12} = -F_{21}$). The Statnamic concept is illustrated in Figure 20.1.

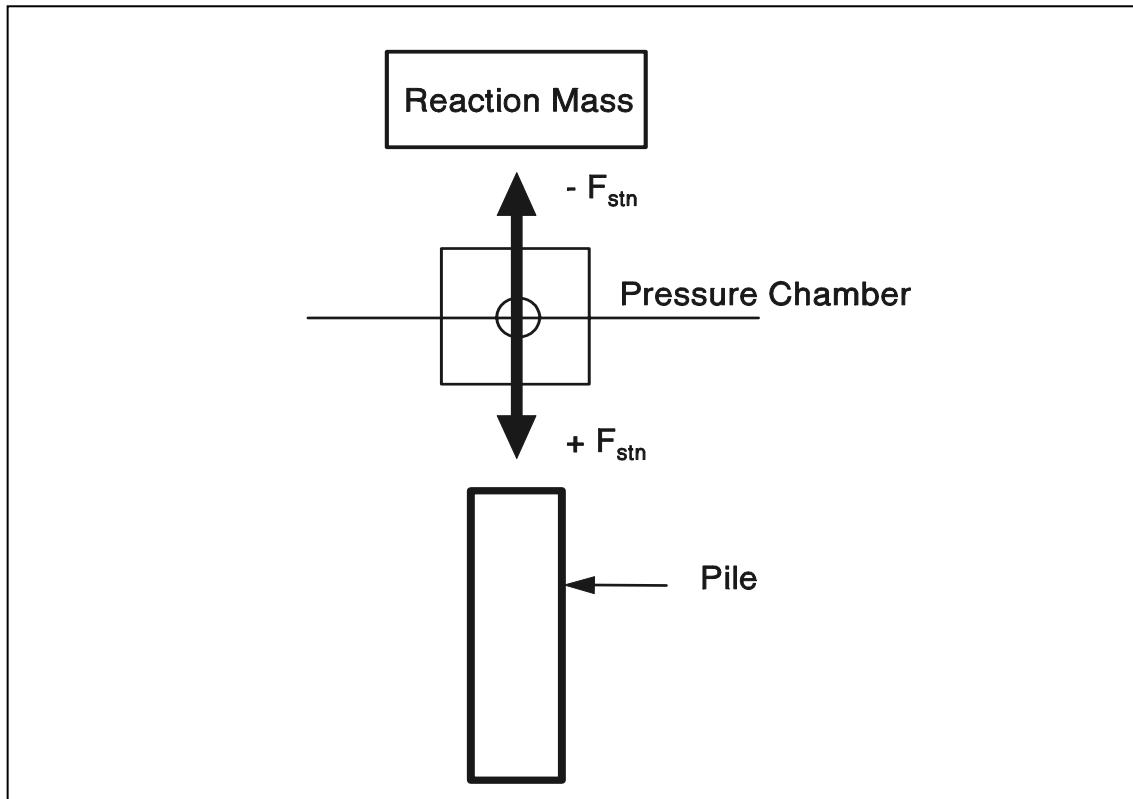


Figure 20.1 Statnamic Concept (courtesy of Berminghammer Foundation Equipment)

20.2 TEST EQUIPMENT

Development began in 1988 with a Statnamic device capable of a 100 kN (22 kips) test load. From 1988 through 1992, the test load capability was incrementally increased to 16,000 kN (3600 kips). In 1994, a 30,000 kN (6800 kips) testing device was introduced. In 1998, a hydraulic catch mechanism illustrated in Figure 20.2 was developed. The maximum test capacity was increased to 40,000 kN (9000 kips) in 2005.

A base plate is attached to the pile head. The load cell, accelerometer, and piston base are positioned on top of the base plate. Next, the launching cylinder is placed on top of the piston base, thus enclosing the pressure chamber and propellant material. The segmental reaction mass is then stacked on the launching cylinder and a catching mechanism is placed around the reaction mass.

Depending upon the test load, a hydraulic catch, mechanical catch, or gravel retention structure is used to catch the reaction mass. The hydraulic catch system shown in Figure 20.2 is used for test loads of 4,400 kN (1000 kips). A mechanical catch system is used for test loads of up to 19,500 kN (4,400 kips) and a gravel retention structure as shown in Figure 20.3 is used for loads of up to 40,000 kN (9,000 kips). For the gravel retention

structure, gravel backfill is placed in the annulus between the reaction mass and the retention structure. After propellant ignition and reaction mass launch, the granular backfill slumps into the remaining void to cushion the reaction mass fall.



Figure 20.2. 4,400 kN (1000 kip) hydraulic catch device on prestressed concrete pile. (courtesy of Applied Foundation Testing)



Figure 20.3. STATNOMIC test in progress with gravel catch mechanism 40,000 kN (9,000 kip) device. (courtesy of Applied Foundation Testing)

The magnitude and duration of the applied load and the loading rate are controlled by the selection of piston and cylinder size, the fuel mass, the fuel type, the reaction mass, and the gas venting technique. The force applied to the pile is measured by the load cell. The acceleration of the pile head is monitored by the accelerometer and is integrated once to obtain pile head velocity and again to obtain displacement. Load and displacement data from the load cell and accelerometers are recorded, digitized, and displayed immediately in the field. Typical raw signals of the load and displacement records are given in Figure 20.4.

These signals can then be converted into a raw load - displacement curve as given in Figure 20.5, which requires interpretation to derive the static pile capacity.

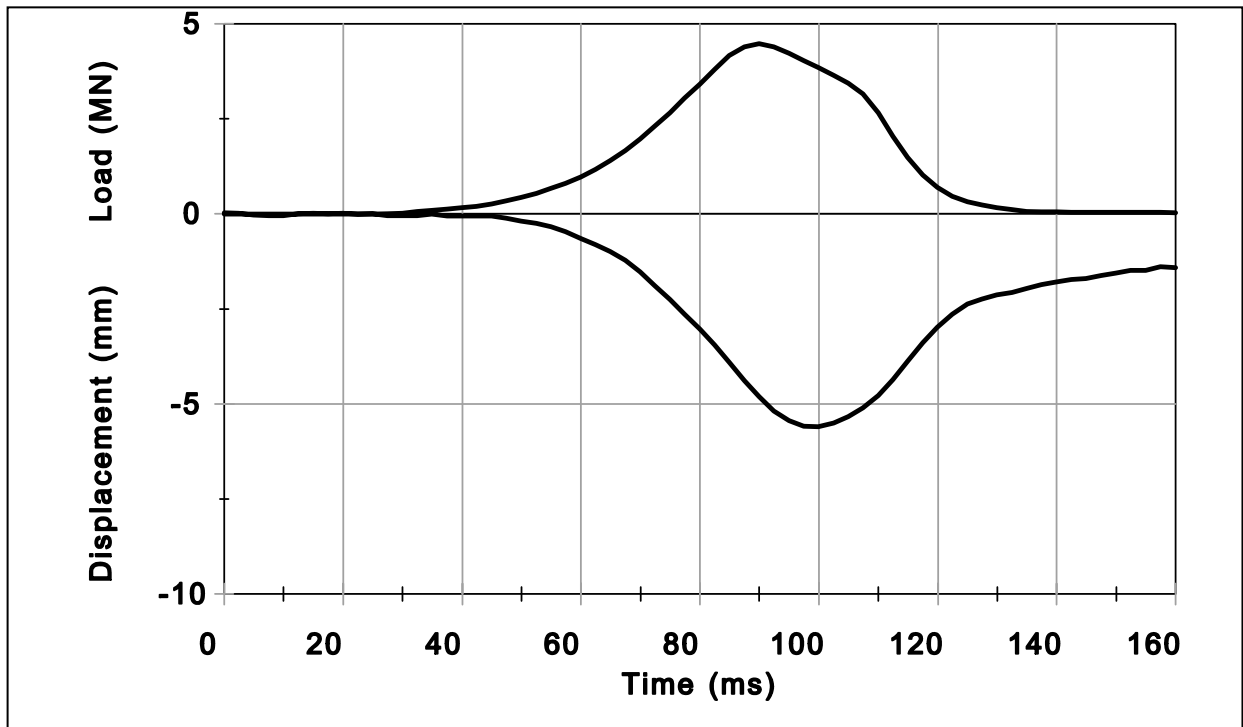


Figure 20.4 Statnamic Signals (courtesy of Berminghammer Foundation Equipment)

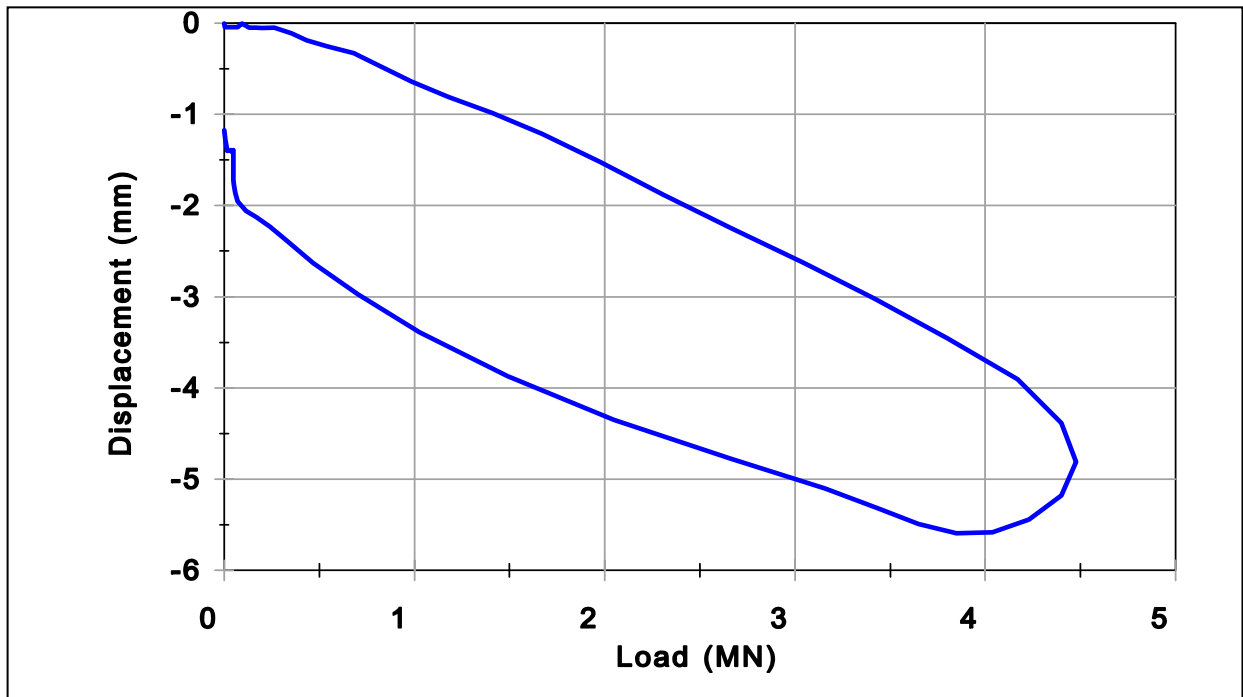


Figure 20.5 Statnamic Load versus Displacement (courtesy of Berminghammer Foundation Equipment)

20.3 TEST INTERPRETATION

Initial correlations of Statnamic tests with static load tests for toe bearing piles founded in till and rock showed good agreement without adjustment of the Statnamic load - displacement results, Janes *et al.* (1991). However, some later tests found that Statnamic overpredicted the ultimate pile capacity in some soils due to the dynamic loading rate effects. Over time, various analysis procedures have been developed to derive the static capacity from Statnamic test results depending upon pile length and pile response and to adjust the derived static capacity by a rate effect factor. These analysis procedures include the Unloading Point Method (UPM), the Modified Unloading Point Method (MUP), and the Segmental Unloading Point Method (SUP). These methods are described later in this section. NCHRP 21-08 on Innovative Load Testing Systems developed and recommended loading rate reduction factors for Statnamic test results analyzed with these methods as a function of soil type, Paikowsky (2002). These loading rate reduction factors are also discussed later in this section.

Middendorp and Bielefeld (1995) proposed the wave number, N_w , as a guide for determining whether the Statnamic test was influenced by stress wave behavior and to determine the analysis procedure to be used. The wave number considers the foundation length, the wave speed of the pile material, and the duration of loading and is calculated from:

$$N_w = D_w/L = CT_L/L$$

D_w is the wave length, L is the total pile length in m (ft), C is the wave speed of the pile material in m/s (ft/s), and T_L is the load duration in seconds. The wave length, D_w , is calculated by multiplying the wave speed by the load duration.

20.3.1 Unloading Point Method

The first widely used analysis method to adjust the raw Statnamic load - displacement results for dynamic loading rate effects was the Unloading Point Method (UPM) proposed by Middendorp *et al.* (1992).

Because the duration of loading in a Statnamic test is about 100 ms or 0.1 s, all elements of the pile move in the same direction and with almost the same velocity. According to the developers, this allows the pile to be treated as a rigid body undergoing translation as long as the pile has a wave number greater than 12. The forces acting on the pile during a

Statnamic test include the Statnamic induced load, F_{stn} , the pile inertia force, F_a , and the soil resistance forces which include the static soil resistance, F_u , the dynamic soil resistance, F_v , and the resistance from pore water pressure, F_p . A free body diagram of the forces acting on a pile during a Statnamic test is presented in Figure 20.6. The soil resistance forces shown in the free body diagram are distributed along the pile shaft as well as at the pile toe.

In mathematical terms, the force equilibrium on the pile may be described as follows:

$$F_{stn}(t) = F_a(t) + F_u(t) + F_v(t) + F_p(t)$$

This equation may be rewritten in terms of static soil resistance as follows:

$$F_u(t) = F_{stn}(t) - F_a(t) - F_v(t) - F_p(t)$$

A simplifying assumption is made that the pore water pressure resistance, F_p , can be treated as part of the damping resistance, F_v . This simplifies the above equation to:

$$F_u(t) = F_{stn}(t) - F_a(t) - F_v(t)$$

Consider the Statnamic load - displacement data presented in Figure 20.7. The Statnamic load - displacement data can be separated into five stages. Stage 1 includes the assembling of the Statnamic piston and reaction mass and thus is a static loading phase. The reaction mass is launched and Stage 2 therefore provides the initial loading of the dynamic event. The soil resistance is treated as linearly elastic. Pile acceleration and velocity are small, resulting in low inertia and damping forces on the pile.

Stage 3 is the basic load application portion of the cycle with fuel burning and pressure in the combustion chamber. In Stage 3, significant nonlinear soil behavior occurs as the pile and soil experience high acceleration and velocity. Thus the highest inertia and damping forces are generated in this stage. The maximum Statnamic applied load is reached at the end of Stage 3.

In Stage 4, pressure in the combustion chamber is allowed to vent. Pile downward velocity and displacement continue but decrease throughout Stage 4. While the maximum Statnamic load is reached at the end of Stage 3, the maximum displacement occurs at the end of Stage 4. This is often due to the pile inertia force or significant dynamic resistance

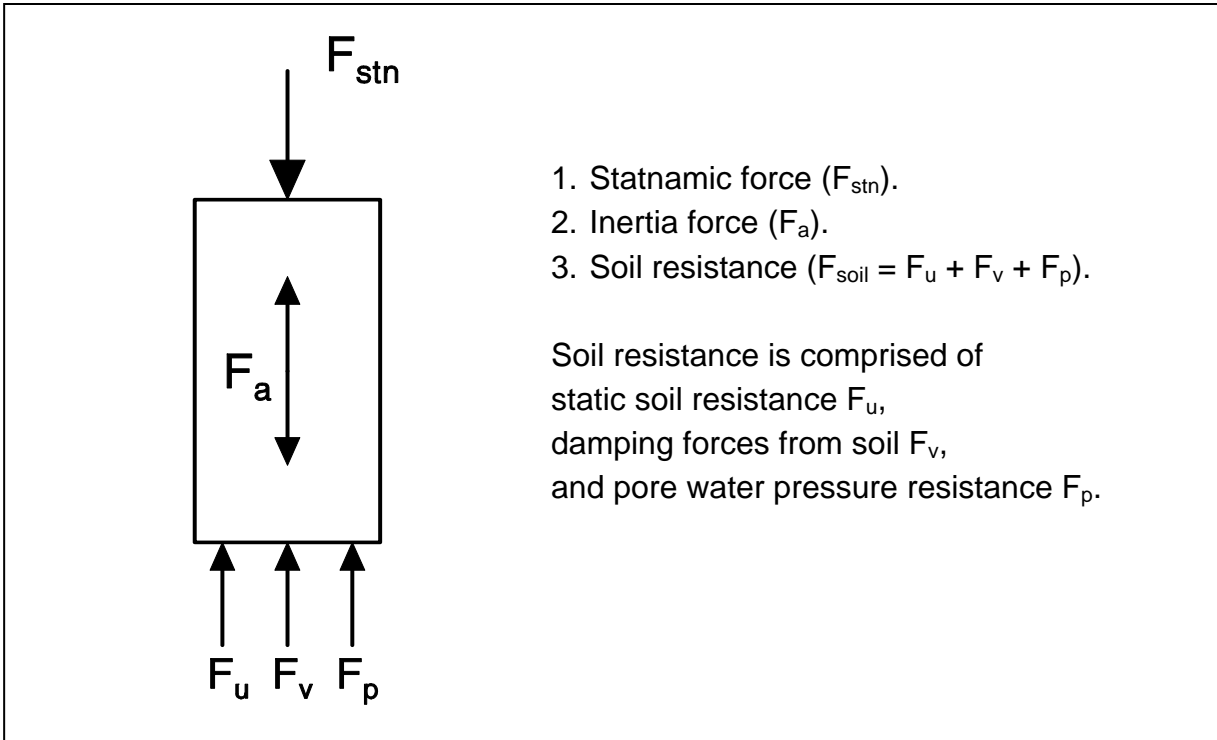


Figure 20.6 Free Body Diagram of Pile Forces in a Statnamic Test (after Middendorp *et al.* 1992)

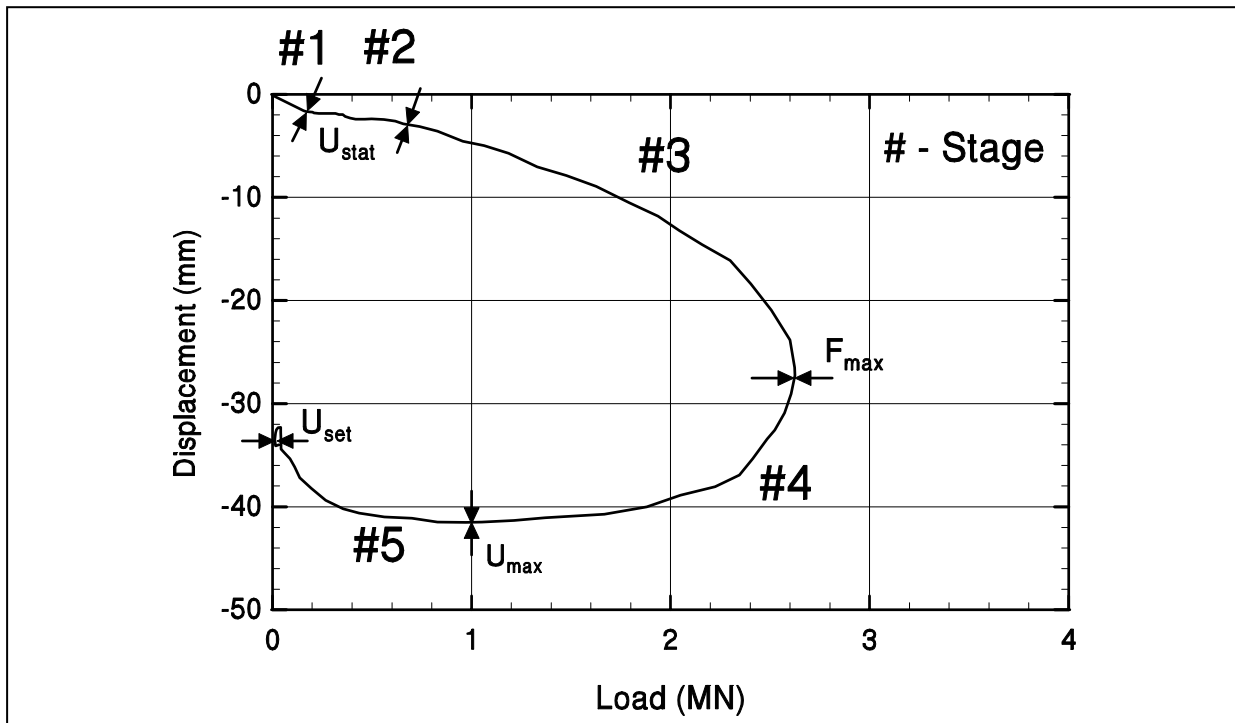


Figure 20.7 Five Stages of a Statnamic Test (after Middendorp *et al.* 1992)

forces, $F_v(t)$, but may also occur in soils with strain softening (the residual soil resistance is significantly lower than the peak resistance). Since the pile velocity is zero at the point of maximum displacement, $t_{u\max}$, the viscous damping, $F_v(t)$, on the pile is also zero at the end of Stage 4 and the static pile capacity may be expressed only at that time as:

$$F_u(t_{u\max}) = F_{stn}(t_{u\max}) - F_a(t_{u\max})$$

In Stage 5, the soil rebounds from the loading event and to achieve final equilibrium the pile unloads and rebounds as load and movement cease. The displacement at the end of Stage 5 is the permanent displacement or set experienced under the test event.

The data processing system records the applied Statnamic load and pile head acceleration and displacement throughout the test. The ultimate static soil resistance, F_u , can then be calculated from the Statnamic load at the point of maximum displacement, $F_{stn}(t_{u\max})$, minus the pile inertia force. This ultimate static soil resistance yields one point on the derived static load - displacement curve and may occur at a large displacement. If a limiting movement criterion such as described in Section 18.7.5 is used for load test interpretation, the ultimate pile capacity may be less than this ultimate static soil resistance.

To obtain the remaining points on the derived static load - displacement curve, the damping resistance, F_v , at other load - displacement points must be determined. Assuming all damping is viscous (e.g., linear), then the damping resistance force can be expressed in terms of a damping constant, C_4 , times the pile velocity at the corresponding time $v(t)$. The pile velocity is obtained by differentiating the measured pile head displacement.

If the maximum applied Statnamic load is greater than the ultimate pile capacity, then the soil resistance at the beginning of Stage 4 through the point of maximum displacement at the end of Stage 4 will be a constant and will be equal to $F_u(t_{u\max})$, assuming the soil is perfectly plastic and does not exhibit strain hardening. The damping constant, C_4 , may be calculated from the maximum Statnamic load at the beginning of Stage 4, t_4 . This may be expressed as:

$$C_4 = [F_{stn}(t_4) - F_u(t_{u\max}) - ma(t_4)] / v(t_4)$$

Assuming the damping constant, C_4 , is constant throughout the Statnamic loading event, the derived static load may be calculated at any point in time from:

$$F_u(t) = F_{stn}(t) - ma(t) - C_4v(t)$$

The derived Statnamic load - displacement curve is then constructed using the above equation and corresponding pile head displacement. An example of the derived load-displacement curve with the Unloading Point Method illustrating how the dynamic rate effects are subtracted from the Statnamic results is presented in Figure 20.8.

20.3.2 Modified Unloading Point Method

The Unloading Point Method rigid body assumption is not applicable for piles with a high toe resistance. On these piles, the pile head response (acceleration, velocity, and displacement) is significantly different than that at the pile toe. Because of the shortcomings of the UPM in this condition, the Modified Unloading Point Method (MUP) was developed by Justason (1997). The MUP method requires adding an additional accelerometer at the pile toe to define the toe behavior. The MUP method still assumes the pile to be a single mass but the acceleration of the mass is defined from the average of the pile head and toe displacement. The MUP method then uses the previously described UPM analysis procedure using the applied Statnamic force and the average accelerations and velocities.

20.3.3 Segmental Unloading Point Method

Analytical studies by Brown (1995) have shown that the rigid body assumption used in the Unloading Point Method can result in overpredictions of capacity and is not appropriate for long slender piles. Analysis of relatively long piles with a wave number less than 10 was also problematic with the averaging techniques used in the Modified Unloading Point Method because of the time delay between the movement of the pile head and the movement of the pile toe and the resulting phase shift of the signals. To address this condition, the Segmental Unloading Point (SUP) Method was developed, Mullins *et al.* (2001). The SUP method separates the pile into discrete segments of shorter length. Strain gages are used to define the segments, and to calculate the force, acceleration, velocity and displacement of each segment. Details of the computation procedures may be found in Mullins *et al.* (2001), and in NCHRP 21-08, Paikowsky (2002).

The maximum number of segments is controlled by the number of strain gages. However, each strain gage level does not constitute a segment. Segments are defined by the length required to maintain the wave number greater than 12. Strain gage placement is usually determined by soil stratification considerations.

The SUP method performs MUP analyses for each segment. The pile head derived static capacity is then calculated by summing the derived static response of each pile segment.

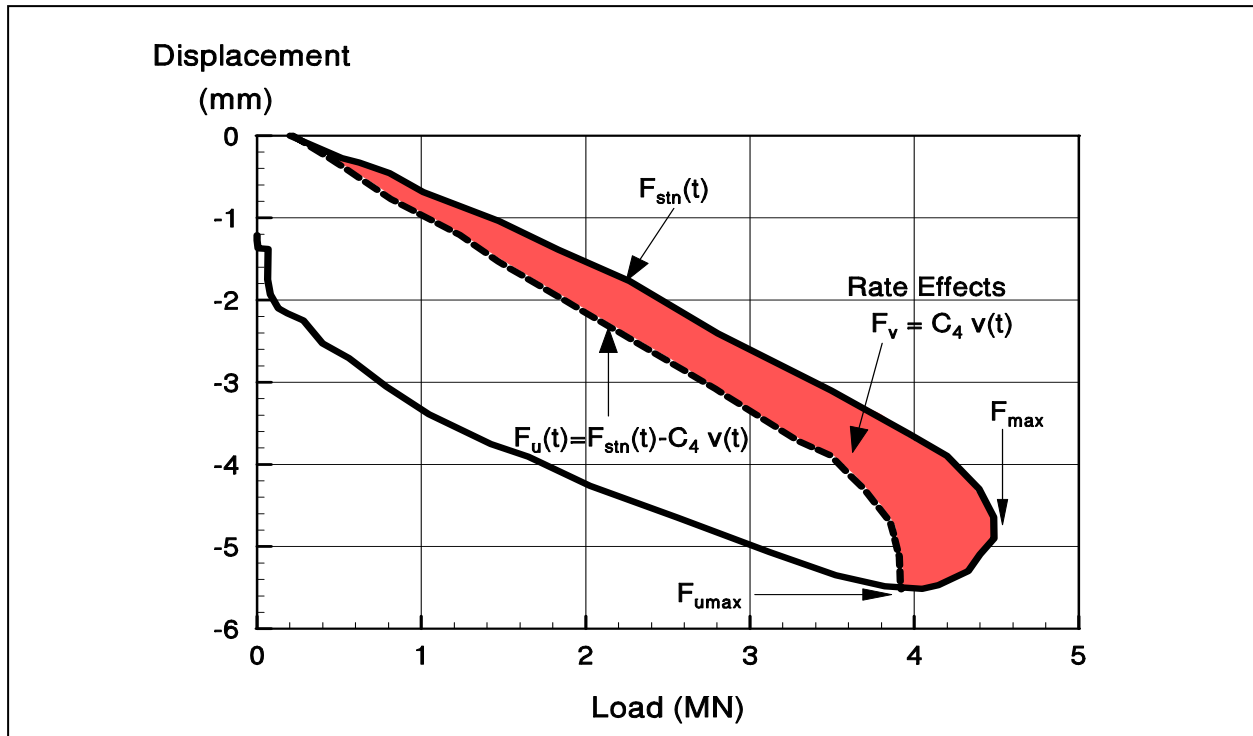


Figure 20.8 Derived Statnamic Load Displacement Curve With Rate Effects (courtesy of Berminghammer Foundation Equipment)

20.3.4 Loading Rate Reduction Factors

In NCHRP 21-08, Innovative load Testing Systems, Paikowsky (2002) studied the correlation of 34 Statnamic test results with static load test results. The correlation data base included driven H-piles, pipe piles and concrete piles as well as drilled shafts. Paikowsky developed a loading rate reduction factor to be applied to a Statnamic derived static load-movement curve to account for over-predictions associated with the loading rate. Loading rate reduction factors of 0.96, 0.91, 0.69, and 0.65 were developed and recommended for rock, sand, silt, and clay, respectively. Paikowsky recommended the loading rate reduction factors be used with UPM, MUP, and SUP analyses of Statnamic test results. With the loading rate reduction factor applied, a factor of safety of 2.0 was recommended on the Statnamic test results.

20.4 APPLICATIONS

Statnamic tests for evaluation of static pile capacity have been performed on steel, concrete and timber piles. Individual piles or pile groups with a combined static and dynamic resistance less than 40,000 kN (9,000 kips) can be tested. Axial compressive

capacity tests have been conducted on both vertical and battered piles. The test method has been used on land and over water.

Use of the Statnamic test for lateral load application was also studied in NCHRP Report 461, Static and Dynamic Lateral Loading of Pile Groups by Brown *et al.* (2001). A lateral Statnamic test on a nine pile group is shown in Figure 20.9. The maximum lateral load applied to date in a Statnamic test is 12,000 kN (2,700 kips). However, this is not a limit of the Statnamic test device but rather of the pile group response.

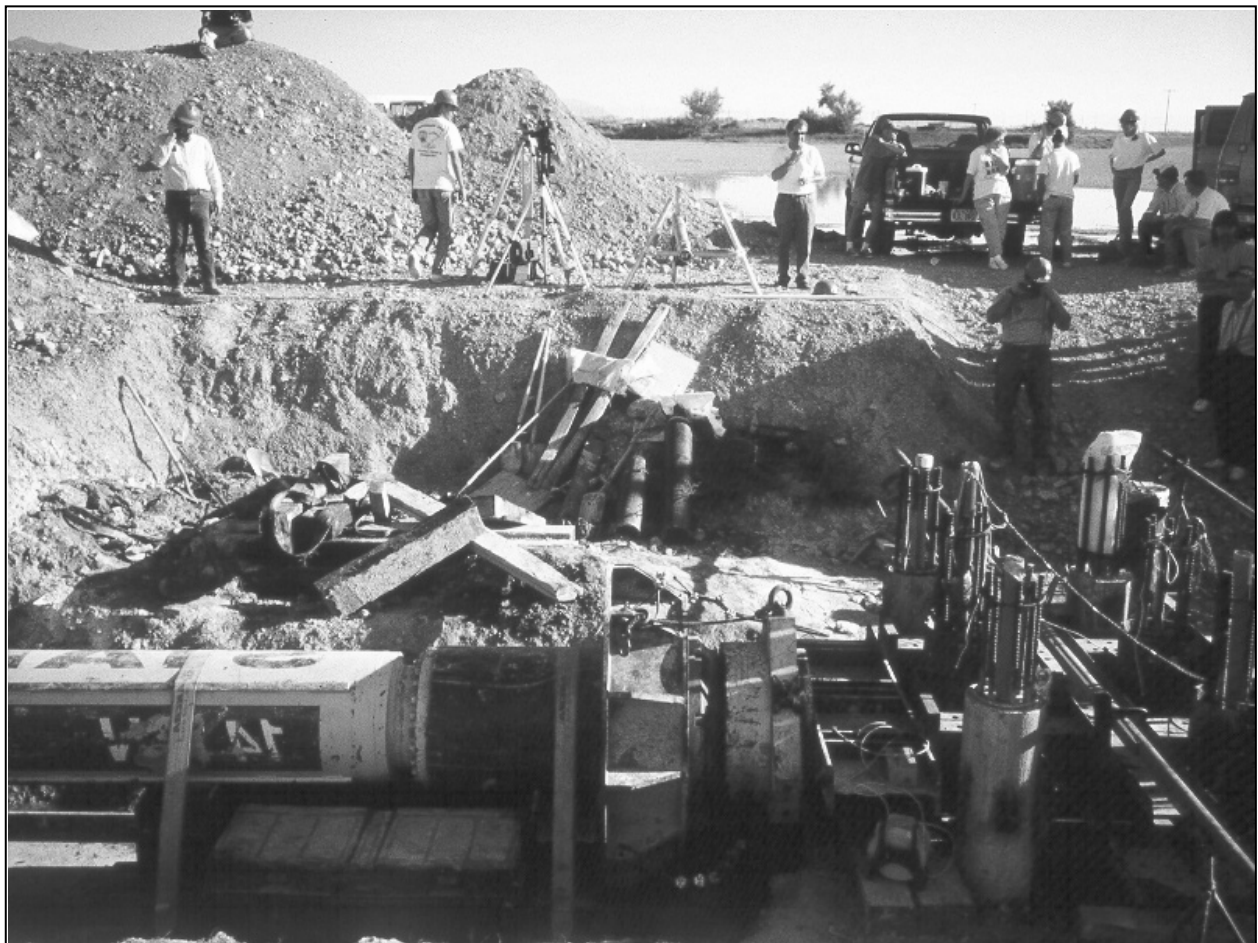


Figure 20.9 Lateral Statnamic Test on Nine Pile Group
(courtesy of Utah State University)

20.5 CASE HISTORY

In 2004, a Statnamic test was conducted on a 33.7 m (111 ft) long, 1067 mm O.D. x 19 mm wall (42 in. O.D. x 0.75 in.), open end pipe pile. The Statnamic load-displacement plot for this test is presented in Figure 20.10. The soil conditions at the site were generally described as clay with interbedded layers of sands and silts over the upper 14 m (46 ft) underlain by sands to a depth of 29 m (95 ft). From 29 to 36 m (95 to 118 ft), interbedded layers of sands and clayey silts were reported.

The Statnamic test apparatus had a maximum capacity of 19,000 kN (4270 kips) and applied a load of 17,080 kN (3840 kips). The Modified Unloading Point Method was used to evaluate the Statnamic test result. The pile was driven without anticipating that a Statnamic test would be later conducted so it was not equipped with a pile toe accelerometer. Therefore, the testing firm assumed that the pile toe acceleration was one half of the measured pile head acceleration, and the average of the measured and assumed acceleration was then used to conduct the MUP analysis. A rate reduction factor of 0.856 (weighted for the site stratigraphy) was also applied to the test result. The Statnamic derived static load-displacement curve was then evaluated according to the FHWA recommended static load test interpretation criterion for large piles in use at that time. That criterion defined failure as the sum of the elastic deflection plus the ratio of the pile diameter over 30. The assigned failure load following this approach was 11,040 kN.

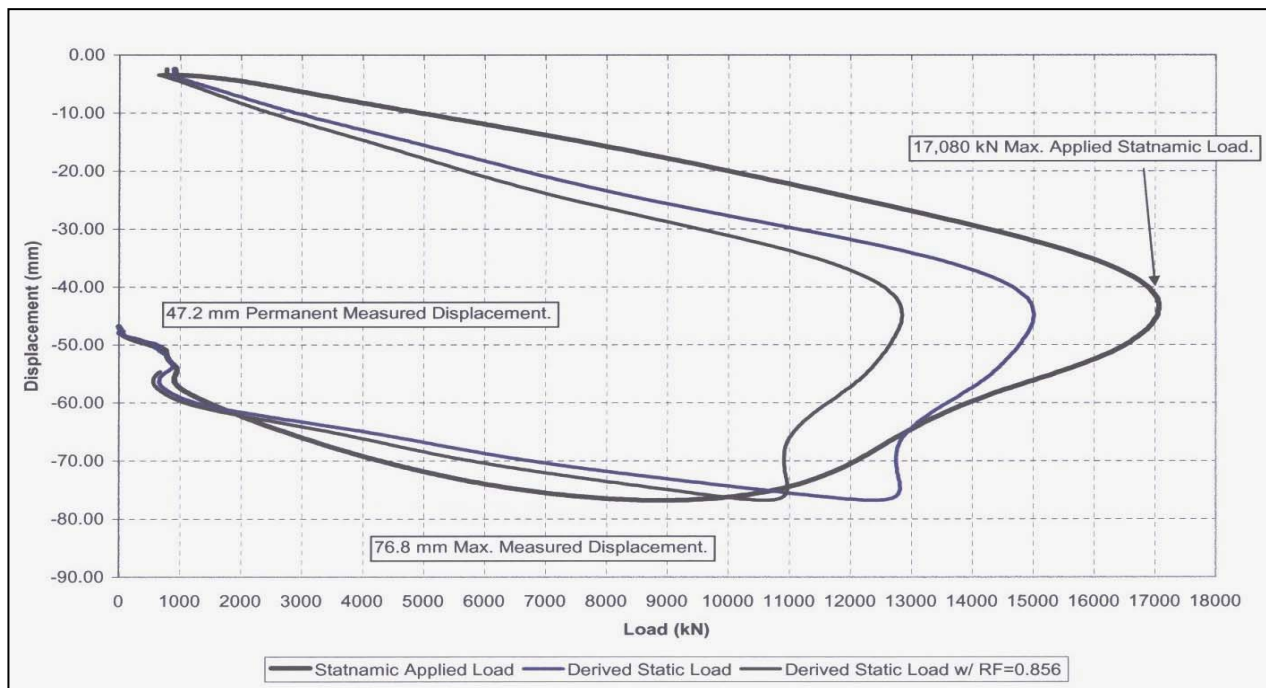


Figure 20.10 Statnamic Test Result (courtesy Minnesota Department of Transportation)

20.6 ADVANTAGES

Advantages of Statnamic testing include lower cost, shorter test time, and mobility. Depending upon the magnitude of load, the site location, and labor costs, the cost of a Statnamic test is on the order of one quarter to one half the cost of an equivalent capacity static load test. Savings may increase for higher pile capacities or for multiple tests performed.

Once Statnamic is mobilized to a site, one or two tests can typically be performed in one day using the gravel catch structure. The hydraulic or mechanical catch mechanisms, permit a higher number of tests to be conducted per day. The mechanical catch mechanism is typically used with Statnamic devices of up to 19,500 kN (4400 kips), above this test load the gravel catch structure is usually used.

The design of a segmental reaction mass allows assembly with relatively small hoisting equipment. In addition, since the reaction mass is typically 5 to 10 percent of the applied load, movement around a site for multiple tests is easier than for a static test using dead weight.

Applied pile head load is measured by load cell and displacement computed from measured acceleration. The load and acceleration readings are digitized at 4000 samples per second.

The Statnamic method is a simple concept governed by Newtonian principles.

20.7 DISADVANTAGES

A disadvantage of the Statnamic test is the fact that loading rate effects need special attention in all soils. Correlations with conventional static tests are still being obtained to address this issue.

To assure that the ultimate pile capacity has been achieved, the applied Statnamic force must be larger than the combined ultimate static and dynamic soil resistances. In the case history presented, the Statnamic applied load was 55% greater than the derived static capacity and the Statnamic applied stress was 278 MPa (40.3 ksi).

The interpretation method is sufficiently complicated that it is difficult to independently check the result.

Tests conducted without pile strain gage information lack the redundant check available in a conventional static load test (load cell and pressure gage) to check the load calibration accuracy.

REFERENCES

- Bermingham, P. and Janes, M. (1989). An Innovative Approach to Load Testing of High Capacity Piles. Proceedings of the International Conference on Piling and Deep Foundations, Volume 1, J.B. Burland and J.M. Mitchell Editors, A.A. Balkema Publishers, Rotterdam, 409-413.
- Bermingham Corporation, Ltd. (1994). Statnamic Newsletter, Volume 2, Number 1.
- Brown, D.A. (1995). Closure – Evaluation of Static Capacity of Deep Foundations from Statnamic Testing. ASTM, Geotechnical Testing Journal, GTJODJ, Vol. 18, No. 4, 495-498.
- Brown, D.A., O'Neill, M.W., Hoit, M., McVay, M., El Naggar, M.H., and Chakraborty, S. (2001). Static and Dynamic Lateral Loading of Pile Groups, NCHRP Report 461, National Cooperative Highway Research Program, Transportation Research Program, Washington, D.C.
- Janes, M., Sy, A. and Campanella, R.G. (1994). A Comparison of Statnamic and Static Load Tests on Steel Pipe Piles in the Fraser Delta. Deep Foundations. Proceedings of the 8th Annual Vancouver Geotechnical Society Symposium, Vancouver, 1-17.
- Janes, M., Bermingham, P. and Horvath, B. (1991). Pile Load Test Results Using the Statnamic Method. Proceedings of the 4th International Conference on Piling and Deep Foundations, Vol. 1, Deep Foundations Institute, Editor, A.A Balkema Publishers, Rotterdam, 481-489.
- Janes, M. (1995). Statnamic Load Testing of Bridge Pier Foundations in North America. Proceedings of the 31st First Symposium on Engineering Geology and Geotechnical Engineers, Utah State University, Logan, Utah.
- Justason, M.D. (1997). Report of Load Testing at the Taipei Municipality Incinerator Expansion Project, Taipei City, Taiwan.

Middendorp, P., Bermingham, P. and Kuiper, B. (1992). Statnamic Load Testing of Foundation Piles. Proceedings of the 4th International Conference on the Application of Stress-Wave Theory to Piles, A.A. Balkema Publishers, Rotterdam, 581-588.

Middendorp, P., and Bielefeld, M.W., (1995). Statnamic Load Testing and the Influence of Stress Wave Phenomena, Proceeding of the First International Statnamic Seminar, Vancouver, 207-220.

Mullins, G., Lewis, C.L., and Justason, M.D. (2001). Advancements in Statnamic Data Regression Techniques, ASCE Conference, Orlando, Florida.

Paikowsky, S. (2002). Innovative Load Testing Systems, Preliminary Draft Final Report, NCHRP 21-08, National Cooperative Highway Research Program, Transportation Research Program, Washington, D.C.

Chapter 21

PILE DRIVING EQUIPMENT

The task of successfully installing piles involves selecting the most cost-effective equipment to drive each pile to its specified depth without damage in the least amount of time. The pile driving system is also used as a measuring instrument to evaluate driving resistance. Therefore, the challenge to both the engineer and the pile contractor becomes one of knowing, or learning about, the most suitable equipment for a given set of site conditions, and then confirming that the driving system is operating properly.

Figures 21.1 and 21.2 show the components of a typical driving system. The crane, leads, hammer and helmet are the primary components of any driving system. Followers and equipment for jetting, predrilling, and spudding, may be permitted under certain circumstances for successful pile driving. This chapter presents a basic description of each component of a driving system. For additional guidance, readers are referred to pile driving equipment manufacturers and suppliers.

21.1 LEADS

The function of a set of leads is to maintain alignment of the hammer-pile system so that a truly concentric blow is delivered to the pile for each impact. Figures 21.1 through 21.4 shows several lead systems used for pile driving. Figure 21.5 shows various lead types. The box lead is the most versatile lead and its use allows all the configurations shown in Figures 21.1 through 21.4.

Swinging leads, illustrated in Figure 21.1, are widely used because of their simplicity, lightness and low cost. The most common arrangement is shown in Figure 21.1(b) where the lead and hammer are held by separate crane lines. The leads can also be hung from the boom with hanger straps as illustrated in Figure 21.1(a) with the hammer held by a crane line. Swinging leads are free to rotate sufficiently to align the hammer and the head of the pile without precise alignment of the crane with the pile head. Because the weight of the leads is low, this type of lead generally permits the largest crane operating radius, providing more site coverage from one crane position.

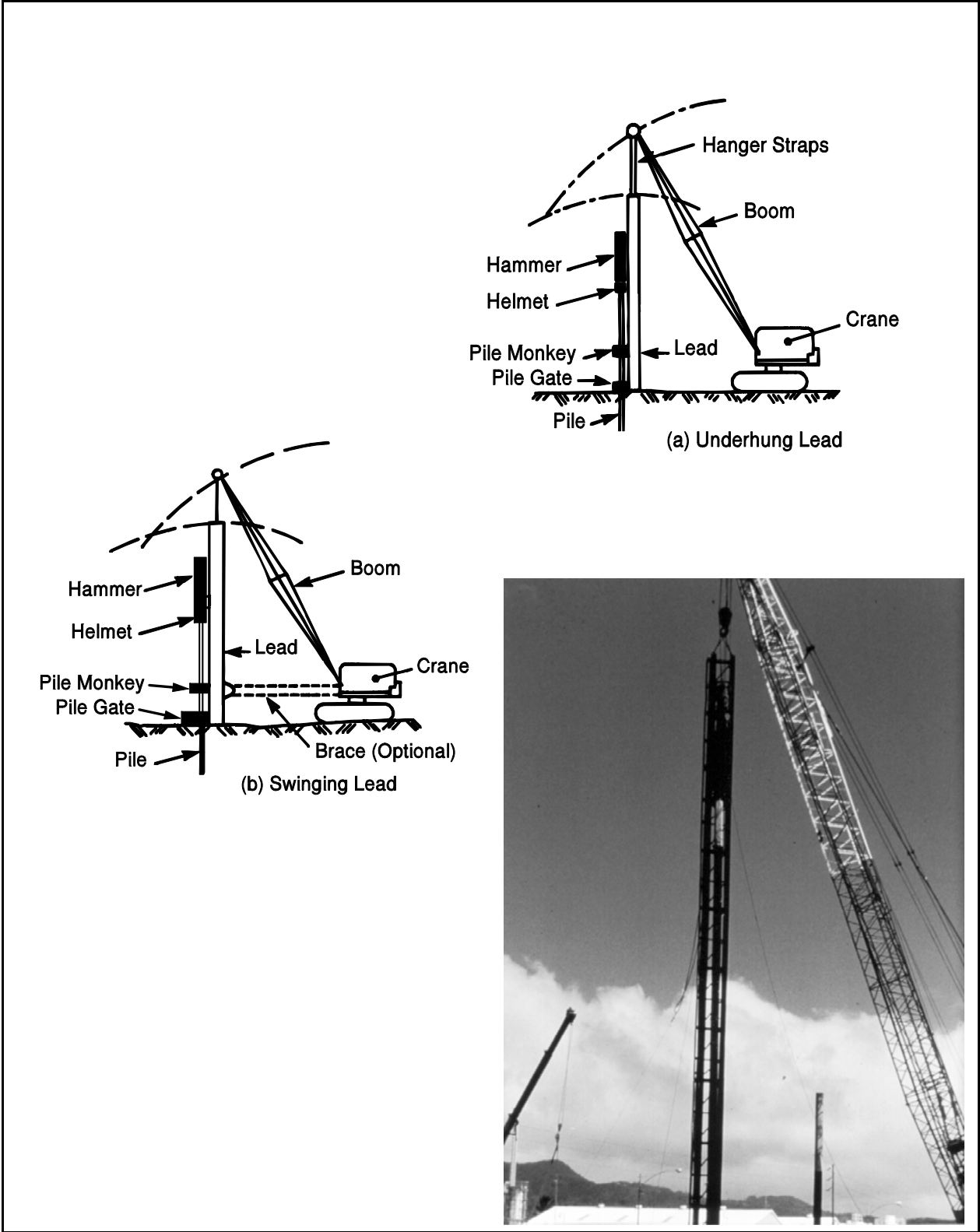


Figure 21.1 Swinging Lead Systems (after D.F.I. Publication 1981)

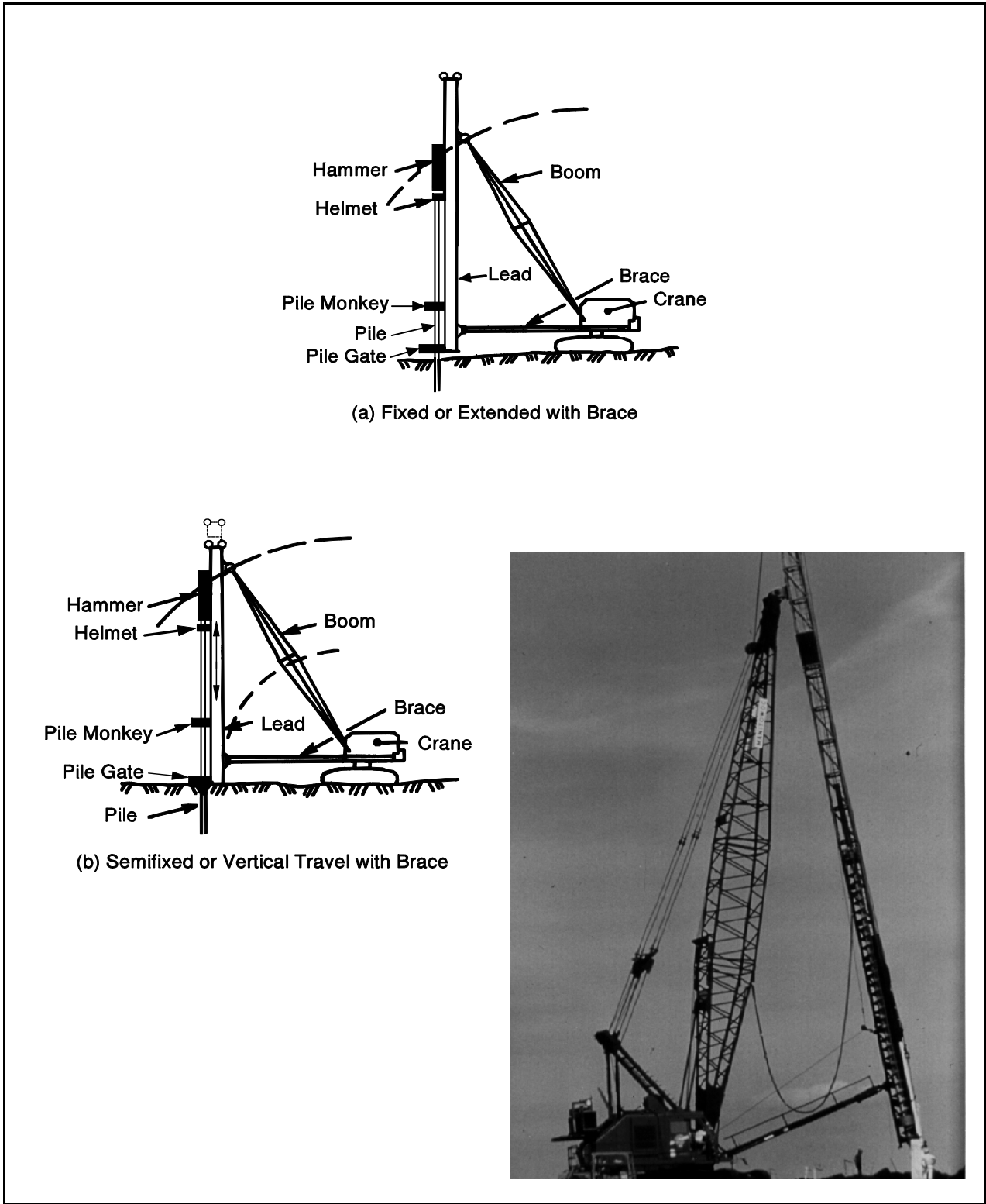
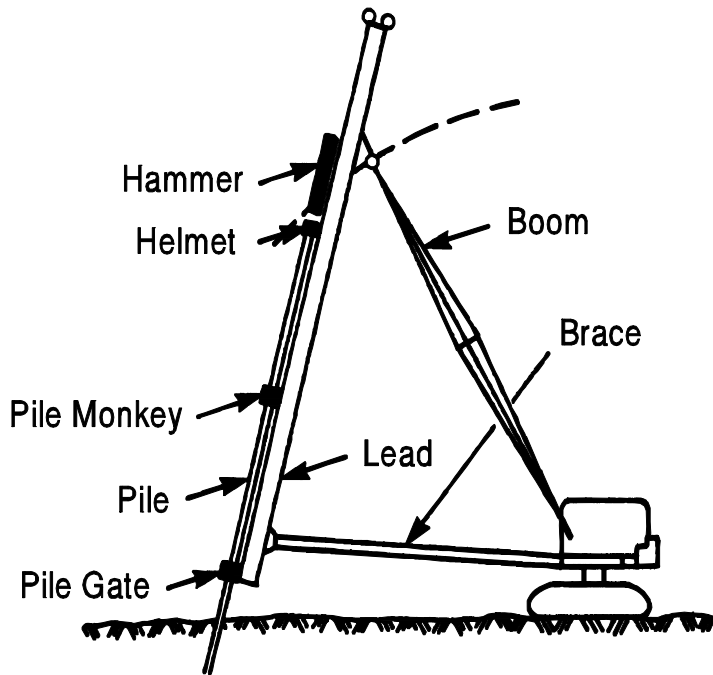
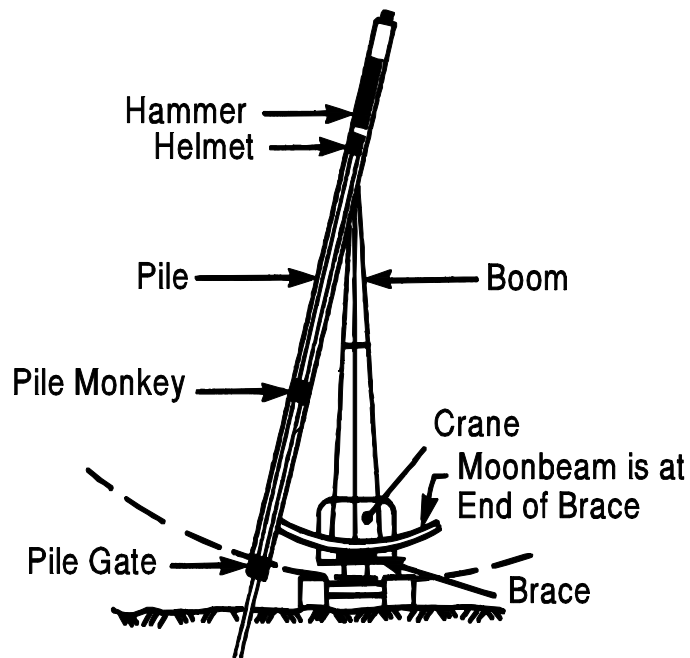


Figure 21.2 Fixed Lead Systems (after D.F.I. Publication, 1981)



(a) Fore (Positive) Batter



(b) Side Batter by Moonbeam

Figure 21.3 Lead Configurations for Batter Piles (after D.F.I. Publication, 1981)

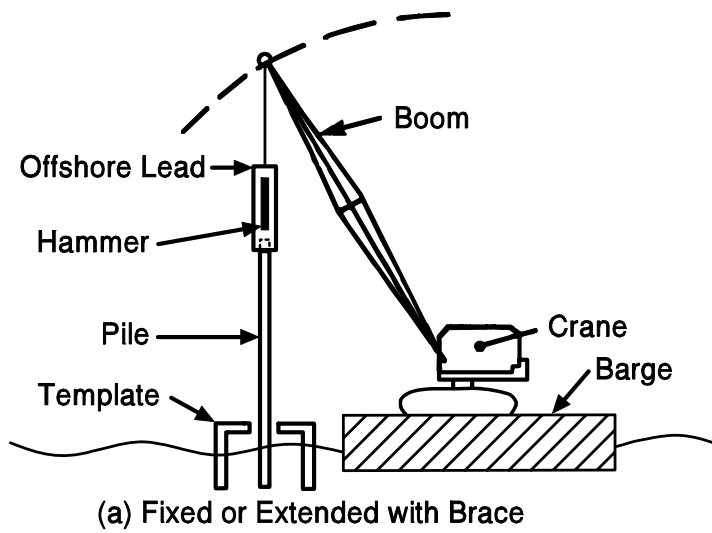


Figure 21.4 Typical Offshore Lead Configuration

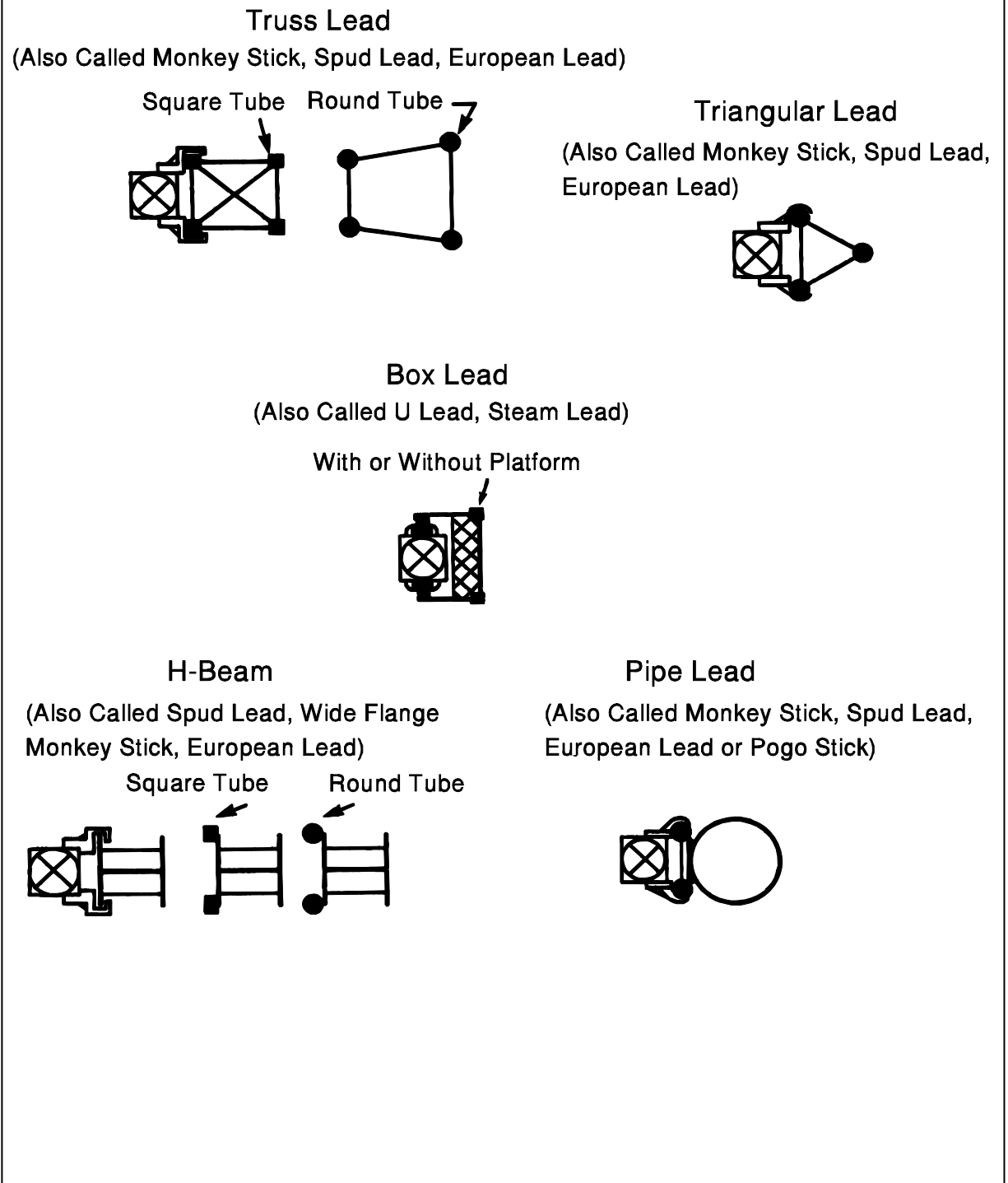


Figure 21.5 Typical Lead Types (after D.F.I. Publication, 1981)

Standard fixed leads shown in Figure 21.2 are slung from the boom point with a brace running from the bottom of the leads to the crane cab frame. A schematic of a typical fixed lead system is depicted in Figure 21.2(a). A variation of a fixed lead system is a semi-fixed or vertical travel lead as shown in Figure 21.2(b). The semi-fixed lead allows vertical lead movement at the lead connection points to the boom and brace which the standard fixed lead system does not. Figure 21.3(a) illustrates that a fixed lead is limited to plumb piles or batter piles in line with the leads and crane boom. To drive side batter piles, a moonbeam must be attached at the end of the brace as depicted in Figure 21.3(b). A fixed lead attempts to hold the pile in true alignment while driving but may require more set up time.

Offshore leads shown in Figure 21.4 are similar to swinging leads in that they are free to rotate sufficiently to align the hammer and head of the pile without precise alignment of the crane with the pile head. They generally consist of a short lead section of sufficient length to hold the hammer and axially align the hammer with the pile head. Offshore leads are used with a template that holds the pile in place.

Pile driving specifications have historically penalized or prohibited swinging leads. This general attitude is not justified based on currently available equipment. In fact, there are many cases where swinging leads are more desirable than fixed leads. For example, swinging leads are preferable for pile installation in excavations or over water. The function of a lead is to hold the pile in good alignment with the driving system in order to prevent damage, and to hold the pile in its proper position for driving. If a swinging lead is long enough so that the bottom is firmly embedded in the ground, and if the bottom of the lead is equipped with a gate, then bottom alignment of the pile will be maintained. In this situation, if the pile begins to move out of position during driving, it must move the bottom of the lead with it. Swinging leads should be of sufficient length so that the free line between the boom tip and the top of the leads is short, thus holding the top of the lead in good alignment. When batter piles are driven, pile alignment is more difficult to set with swinging leads. This problem is accentuated for diesel hammers since the hammer starting operation will tend to pull the pile out of line.

Regardless of lead type chosen, the pile must be kept in good alignment with the hammer to avoid eccentric impacts which could cause local stress concentrations and pile damage. The hammer and helmet, centered in the leads and on the pile head, keep the pile head in alignment. A pile gate at the bottom of the leads should be used to keep the lower portion of the pile centered in the leads.

21.2 TEMPLATES

Templates are required to hold piles in proper position and alignment when an offshore type or swinging lead system is used over water. The top of the template should be located within 1.5 m (5 ft) of the pile cutoff elevation or the water elevation, whichever is lower. The preferred elevation of the template is at or below the pile cutoff elevation so that final driving can occur without stopping for template removal. A photograph of a typical template is presented in Figure 21.6.

When positioning templates that include batter piles, it must be remembered that the correct template position of batter piles will vary depending upon the template elevation relative to the pile cutoff elevation. For example, consider a template located 1.5 m (5 ft) above pile cutoff elevation. If the plan pile locations at cutoff are used at the template elevation, a 1H:4V batter pile would be 375 mm (15 inches) out of location at the pile cutoff elevation. This problem is illustrated in Figure 21.7. Template construction should also allow the pile to pass freely through the template without binding. Templates with rollers are preferable, particularly for batter piles.



Figure 21.6 Typical Template Arrangement

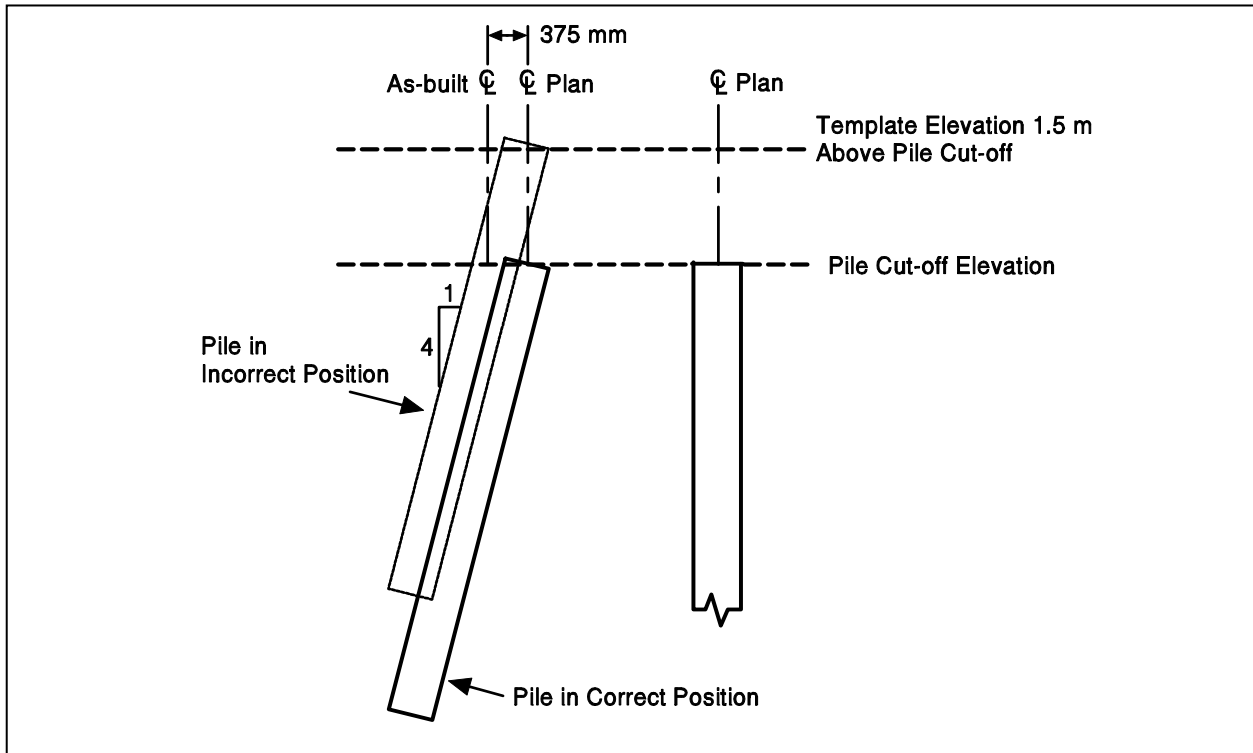


Figure 21.7 Template Elevation Effects on Batter Piles (after Passe 1994)

21.3 HELMETS

Figure 21.8 shows the components of a typical helmet (also called a drive cap) and the nomenclature used for these components. The helmet configuration and size used depends upon the lead type, pile type and the type of hammer used for driving. Details on the proper helmet for a particular hammer can be obtained from hammer manufacturers, suppliers and contractors. To avoid the transmission of torsion or bending forces, the helmet should fit loosely, but not so loosely as to prevent the proper alignment of hammer and pile. Helmets should be approximately 2 to 5 mm (0.1 to 0.2 inches) larger than the pile diameter. Proper hammer-pile alignment is particularly critical for precast concrete piles. Figure 21.9 shows a helmet for a steel H-pile.

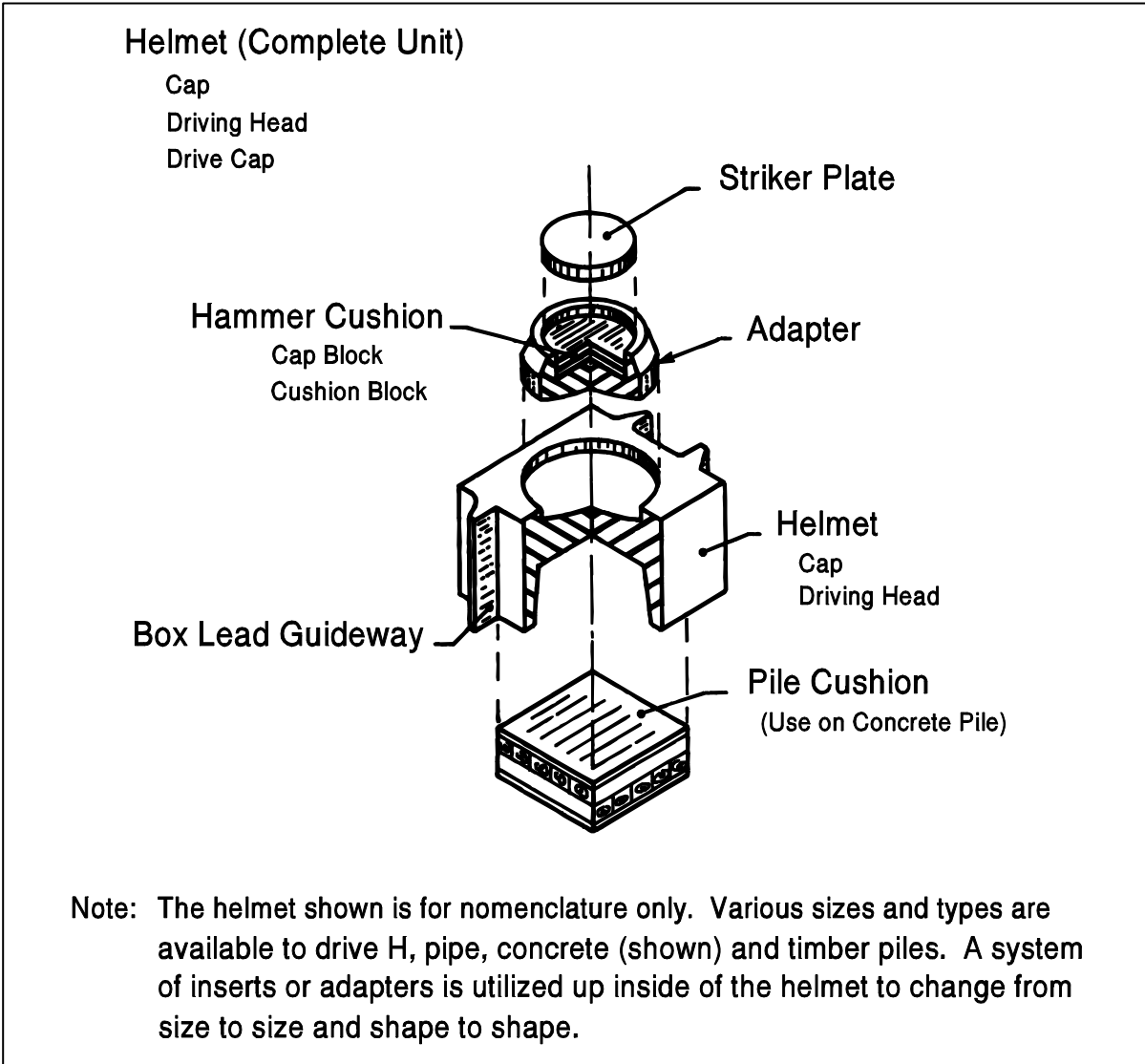


Figure 21.8 Helmet Components (after D.F.I. Publication, 1981)

21.4 HAMMER CUSHIONS

Most hammers use a hammer cushion between the hammer and the helmet to relieve the impact shock, thus protecting the pile hammer. However, some hammer models exist that do not require a hammer cushion, or utilize a direct drive option where the hammer cushion is replaced by a steel striker plate. Ineffective hammer cushions in hammers requiring a cushion can cause damage to hammer striking parts, anvil, helmet or pile. All cushion materials become compressed and stiffen as additional hammer impacts are applied. Therefore, hammer cushions eventually become ineffective, or may result in significant



Figure 21.9 Helmet on H-pile

reduction in transferred energy or increased bending stress. Hammer cushion materials are usually proprietary man-made materials such as micarta, nylon, urethane or other polymers. In the past, a commonly used hammer cushion was made of hardwood (one piece), approximately 150 mm (6 inches) thick, with the wood grain parallel to the pile axis. This type of cushioning has the disadvantage of quickly becoming crushed and burned as well as having variable elastic properties during driving. With the widespread availability of manufactured hammer cushion materials, hardwood hammer cushions are no longer recommended.

Proprietary man-made hammer cushion materials have better energy transmission characteristics than a hardwood block, maintain more nearly constant elastic properties, and have a relatively long life. Their use results in more consistent transmission of hammer energy to the pile and more uniform driving. Since laminated cushioning materials have a long life, up to 200 hours of pile driving for some materials, it is often sufficient to inspect the cushion material only once before the driving operation begins for smaller projects. Periodic inspections of hammer cushion wear and thickness should be performed on larger projects. Many hammers require a specific cushion thickness for proper hammer timing. In these hammers, improper cushion thickness will result in poor hammer performance. Some man-made hammer cushions are laminated, such as aluminum and micarta, for

example. The aluminum is used to transfer the heat generated during impact out of the cushion, thus prolonging its useful life. Hammer cushions consisting of small pieces of wood, coils or chunks of wire rope, or other highly elastic material should not be permitted. Cushion materials containing asbestos are not acceptable because of health hazards. Common proprietary hammer cushion materials are illustrated in Figure 21.10.



Figure 21.10 Typical Hammer Cushion Materials

21.5 PILE CUSHIONS

To avoid damage to the head of a concrete pile as a result of direct impact from the helmet, a pile cushion should be placed between the helmet and the pile head. Typical pile cushions are made of compressible material such as plywood, hardwood, plywood and hardwood composites or other man made materials. Wood pile cushions should have a minimum thickness of 100 mm (4 inches). Pile cushions should be checked periodically for damage and replaced before excessive compression or charring takes place. After replacing a cushion during driving, the blow count from the first 100 blows should not be used for pile acceptance as the cushion is still rapidly absorbing energy. The blow count

will only be reliable after 100 blows of full energy application. The total number of blows which can be applied to a wood cushion is generally between 1000 and 2000. For wood pile cushions, it is recommended that a new, dry cushion be used for each pile. Old or water soaked cushions do not have good energy transfer, and will often deteriorate quickly. A photograph of a typical plywood pile cushion is presented in Figure 21.11.



Figure 21.11 Plywood Pile Cushion

21.6 HAMMERS

Pile hammers can be categorized in two main types: impact hammers and vibratory hammers. There are numerous types of impact hammers having variations in the types of power source, configurations, and rated energies. Figure 21.12 shows a classification of hammers based on motivation and configuration factors. Table 21-1 presents characteristics and uses of several types of hammers. A discussion of various types of hammers follows in this chapter. Additional detailed descriptions of the operation of each hammer type and inspection guides are given in Chapter 23 of this manual, in Rausche *et al.* (1986), and in the Deep Foundation Institute Pile Inspector's Guide to Hammers (1995). Appendix D includes information on a majority of the currently available pile hammers.

21.6.1 Hammer Energy Concepts

Before the advent of computers and the availability of the wave equation to evaluate pile driving, driving criteria for a certain pile capacity was evaluated by concepts of work or energy. Work is done when the hammer forces the pile into the ground a certain distance. The hammer energy was equated with the work required, defined as the pile resistance times the final set. This simple idea led engineers to calculate energy ratings for pile hammers and resulted in numerous dynamic formulas which ranged from very simple to very complex. Dynamic formulas have since been widely discredited and replaced by the more accurate wave equation analysis. However, the energy rating legacy for pile hammers remains.

The energy rating of hammers operating by gravity principles only (drop, single acting air/steam or hydraulic hammers) was assigned based on their potential energy at full stroke (ram weight times stroke, h). Although single acting (open end) diesel hammers could also be rated this way, some manufacturers have used other principles for energy rating. Historically, these hammers have usually been rated by the manufacturer's rating, while the actual observed stroke was often ignored in using the dynamic formula. In current practice, the stroke is often measured electronically from the blow rate, which is an improvement over past practice. In the case of all double acting hammers (air/steam, hydraulic, or diesel), the net effect of the downward pressure on the ram during the downstroke is to increase the equivalent stroke and reduce time required per blow cycle. The equivalent stroke is defined as the stroke of the equivalent single acting hammer yielding the same impact velocity. The manufacturers generally calculate the potential energy equivalent for double acting hammers.

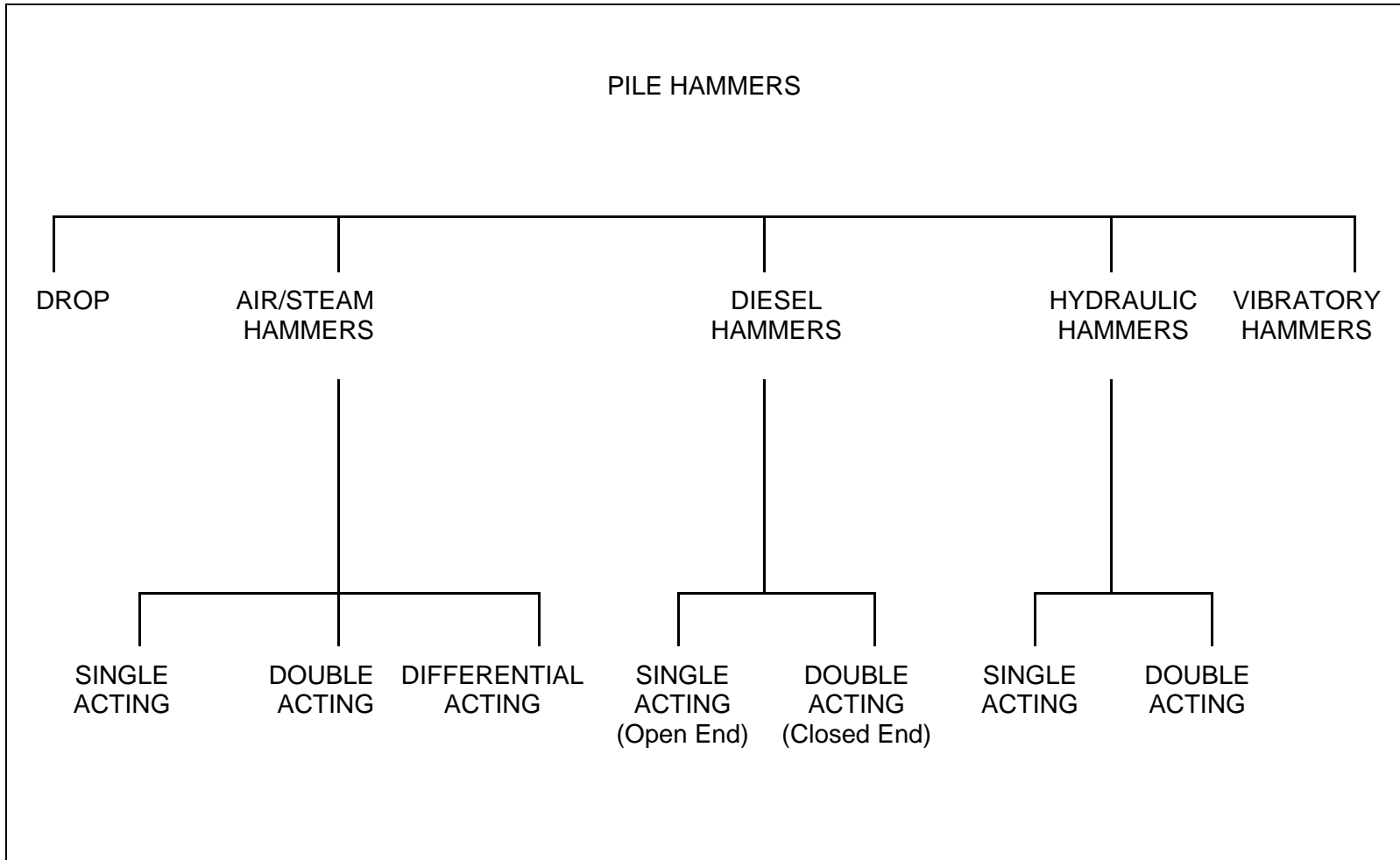


Figure 21.12 Pile Hammer Classification

TABLE 21-1 TYPICAL PILE HAMMER CHARACTERISTICS AND USES									
Hammer Type	Drop	Steam or Air			Diesel		Hydraulic		Vibratory
		Single Acting	Double Acting	Differential	Single Acting (open end)	Double Acting (closed end)	Single Acting	Double Acting	
Rated energy range	9 to 81 kJ (7 to 60 ft-kips)	10 to 2440 kJ (7 to 1800 ft-kips)	1 to 29 kJ (1 to 21 ft-kips)	20 to 68 kJ (15 to 50 ft-kips)	12 to 667 kJ (9 to 492 ft-kips)	11 to 98 (5 to 73 ft-kips)	35 to 2932 (25 to 2162 ft-kips)	35 to 2945 (25 to 2172 ft-kips)	----
Impact velocity (m/sec)	7 to 10	2.5 to 5	4.5 to 6	4 to 4.5	3 to 5	2.5 to 5	1.5 to 5.5	1.5 to 7	----
Blows/minute	4 to 8	35 to 60	95 to 300	98 to 303	40 to 60	80 to 105	30 to 50	40 to 90	750 to 2,000 pulses/minute
Energy (per blow)	Ram weight x height of fall.	Ram weight x ram stroke.	(Ram weight + effective piston head area x effective fluid pressure) x stroke.		Ram weight x stroke.	(Ram weight + chamber pressure) x stroke.	Ram weight x stroke.	(Ram weight + effective piston head area x effective fluid pressure) x stroke.	----
Lifting power	Provided by hoisting engine or a crane.	Steam or air.	Steam or air.		Provided by the explosion of injected diesel fluid.		Hydraulic	Hydraulic	Electricity or hydraulic power.
Maintenance	Simple	More complex than for drop hammer.	More complex than for single acting.		More complex than most air impact hammers.		More complex than other impact hammers.	More complex than other impact hammers.	Highest maintenance cost.
Hammer suitability for types of piles	All types except concrete piles.	Versatile for any pile, particularly large concrete and steel pipe.	Timber, steel H and pipe piles.		All types of piles.		All types of piles.	All types of piles.	Steel H and pipe end bearing piles. Very effective in granular soils.
Major advantages	Lowest initial cost equipment.	Relatively simple and moderate cost.	Fully enclosed and permit underwater operation. More productive than single acting. Generate lower dynamic forces. Differential hammer uses less volume of air or steam than double acting and has lower impact velocity.		Carry their own fuel from which power is internally generated. Stroke is a function of pile resistance.		Fully variable energy can be delivered.	Energy is variable over a wide range. Can be used for underwater driving.	Can be used for pulling or driving. Fastest operating installation tool.
Major disadvantages	Very high dynamic forces and danger of pile damage. Lowest pile productivity.	Need air compressor or steam plant. Heavy compared with most diesel hammers.	Costs more than single acting. Need air compressor or steam plant. Heavy compared to diesel hammer.		Pollutes air with diesel exhaust. Higher cost hammer. Low blows per minute at higher strokes for single acting.		Higher initial cost.	Higher initial cost.	High investment and maintenance. Not recommend for friction pile installations.
Remarks	Becoming obsolete.	----	Ram accelerates downward under pressure.		Stroke variable in single acting diesel hammer. Very popular hammer type. Biodiesel models available.		Newer hammer type and may require additional field inspection and/or testing.	Newer hammer type and may require additional field inspection and/or testing.	----

Ideally, the impact velocity, v_i , could be directly computed using basic laws of physics from the equivalent maximum stroke

$$v_i = \sqrt{2gh}$$

Where: g = Acceleration due to gravity, m/s^2 (ft/s^2).
 h = Hammer stroke, m (ft).

The kinetic energy could be computed from the equation

$$K.E. = \frac{1}{2} m v_i^2$$

Where: m = Ram mass.

If there were no losses, the kinetic energy would equal the potential energy. In reality however, energy losses occur due to a variety of factors (friction, residual air pressures, preadmission, gas compression in the diesel combustion cylinder, preignition, *etc.*) which result in the kinetic energy being less than the potential energy. It is the inspector's task to minimize these losses when and where possible, or to at least identify and try to correct situations where losses are excessive. Some hammers, such as modern hydraulic hammers, measure the velocity near impact and hence can calculate the actual kinetic energy available.

Further losses occur in the transmission of energy to the pile. The hammer cushion, helmet, and pile cushion all have kinetic energy and store some strain energy. The pile head also has inelastic collision losses. The hammer transfers its energy to the pile with time. The energy delivered to the pile can be calculated from the work done as the integral of the product of force and velocity with time and is referred to as the transferred energy or ENTHRU.

The pile length, stiffness and capacity influence the energy delivered to the pile. The actual stroke (or potential energy) of diesel hammers depends on the pile resistance and the net transferred energy is also a variable. The stroke of single acting air/steam hammers is also somewhat dependent upon the pile capacity and rebound. The stroke of all double acting hammers is even more dependent on pile capacity due to lift-off considerations. Actually the transferred energy increases only when both the force and velocity are positive (compression forces; downward velocity). As resistance increases and/or the pile becomes shorter, the rebound or upward velocity occurs earlier and the pile then transfers energy back to the driving system. In fact, the energy returning to the hammer may occur before all the energy has been transferred into the pile.

21.7 DROP HAMMERS

The most rudimentary pile hammer still in use today is the drop hammer as shown in Figure 21.13. These hammers consist of a hoisting engine having a friction clutch, a hoist line, and a drop weight. The hammer stroke is widely variable and often not very precisely controlled. The hammer is operated by engaging the hoist clutch to raise the drop weight or ram. The hoist clutch is then disengaged, allowing the drop weight to fall as the hoist line pays out. The fall may not be very efficient since the ram attached by cable to the hoist must also overcome the rotational inertia of the hoist. Ideally, the crane operator engages the clutch immediately after impact to prevent excessive cable spooling. If the operator prematurely engages the clutch, or it is partially engaged during spooling, then the fall efficiency and hence impact energy is further reduced.

The hammer operating speed (blows per minute) depends upon the skill of the operator and the height of fall being used, but is generally very slow. One of the greatest risks in using a drop hammer is overstressing and damaging the pile. Pile stresses are generally increased with an increase in the impact velocity (hammer stroke) of the striking weight. Therefore, the maximum stroke should be limited to those strokes where pile damage is not expected to occur. In general, drop hammers are not as efficient as other impact hammers but are inexpensive and simple to operate and maintain. Current use of these hammers is generally limited to sheet pile installations where pile capacity is not an issue. Because of the uncertainties described above, drop hammers are not recommended for foundation piles.

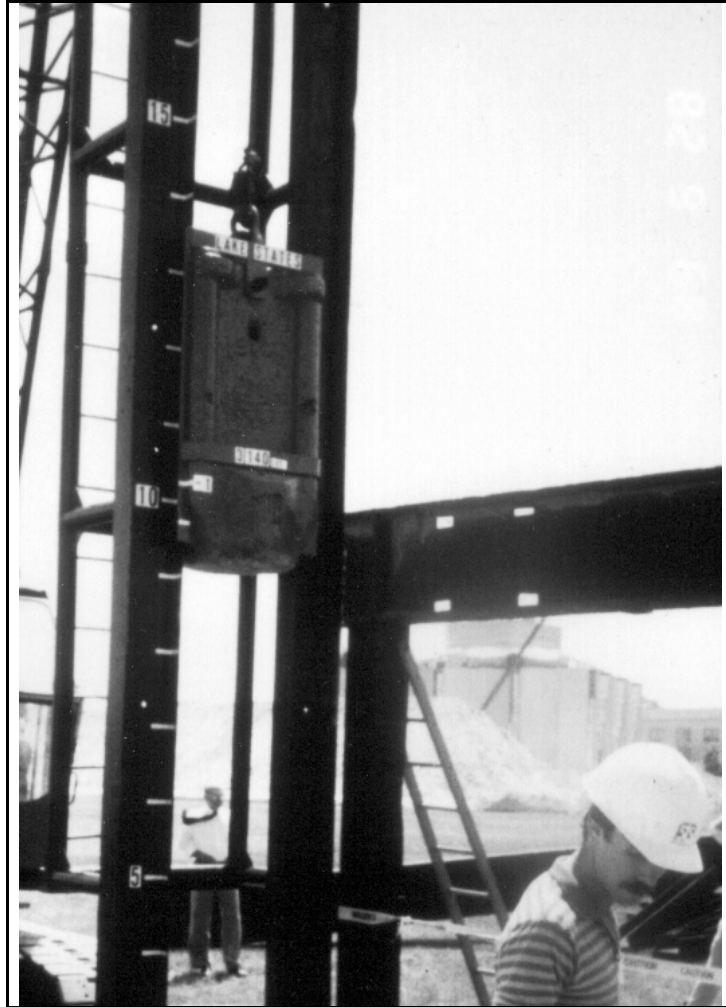


Figure 21.13 Typical Drop Hammer

21.8 SINGLE ACTING AIR/STEAM HAMMERS

Single acting air/steam hammers are essentially gravity, or drop hammers, for which the hoist line has been replaced by a pressurized medium, being either steam or air. While originally developed for steam power, most of these hammers today operate on compressed air. To lift the ram weight with motive pressure, a simple one-cylinder steam engine principle is used. The ram consists of a compact block with a so-called ram point attached at its base. The ram point strikes against a striker plate as illustrated in Figure 21.14. A photograph of a typical single acting air/steam hammer is presented in Figure 21.15.

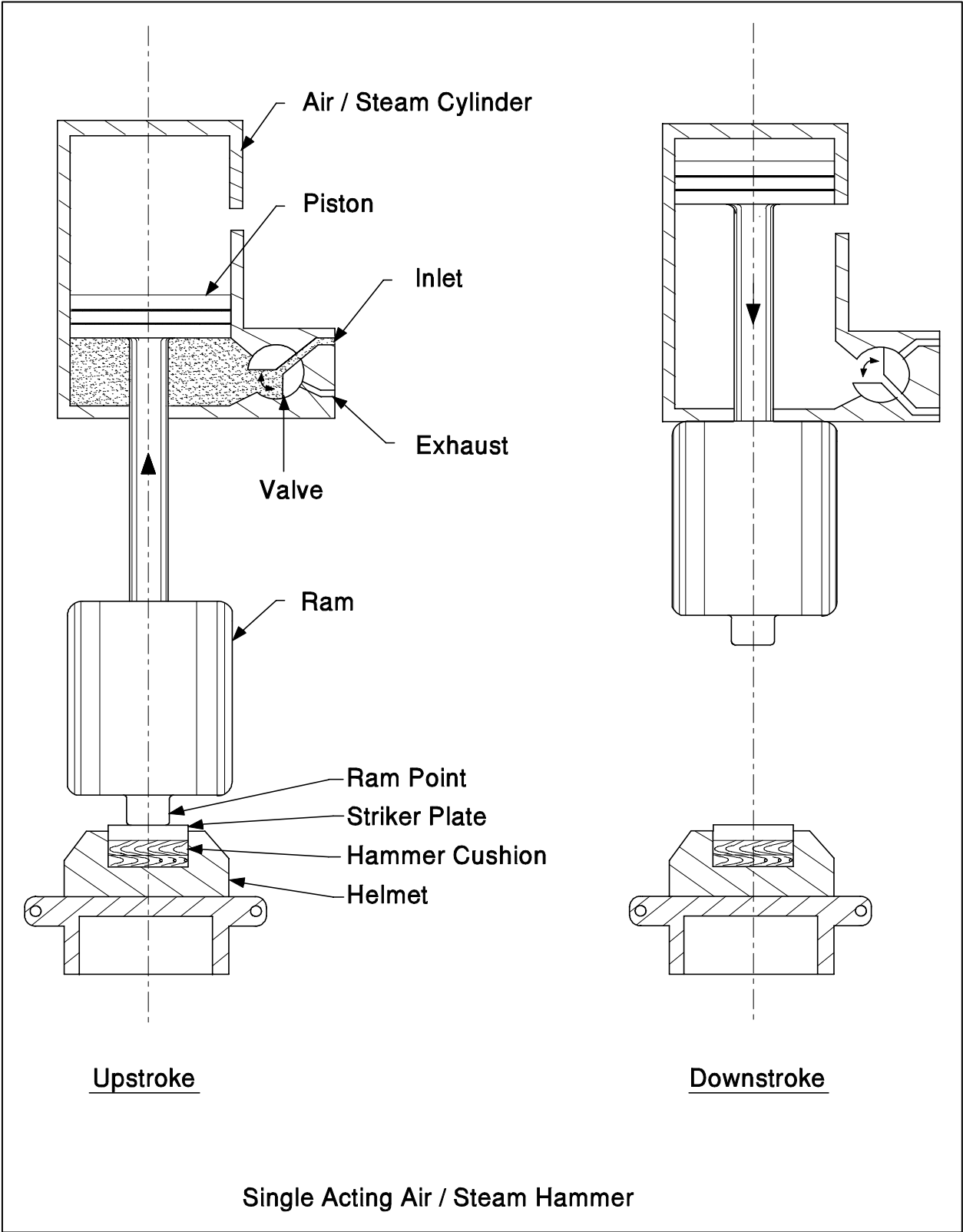


Figure 21.14 Schematic of Single Acting Air/Steam Hammer



Figure 21.15 Single Acting Air Hammer



Figure 21.16 Double Acting Air Hammer

During the upstroke cycle, the ram is raised by externally produced air or steam pressure acting against a piston housed in the hammer cylinder. The piston in turn is connected to the ram by a rod. Once the ram is raised a certain distance, a valve is activated and the pressure in the chamber is released. At that time, the ram has some remaining upward velocity that depends upon the pile rebound, inlet air pressure, and volume of air within the hammer cylinder. Against the action of gravity and friction, the ram then "coasts" up to the maximum height (stroke). The maximum stroke, and hence hammer potential energy, is therefore not constant and depends upon the pressure and volume of air or steam supplied, as well as the amount of pile rebound due to pile resistance effects. During the downstroke cycle, the ram falls by gravity (less friction) to impact the striker plate and hammer cushion. Just before impact, the pressure valve is activated and pressure again enters the cylinder. This occurs approximately 50 mm (2 in) before impact, but depends on having the correct hammer cushion thickness. If the hammer cushion height is too low, then the pressure is introduced too early, reducing the impact energy of the ram. This is referred to as "preadmission".

The dynamic forces exerted on a pile by a single acting air/steam hammer are of the same short-time duration as those exerted by a drop hammer. Because operating strokes are generally shorter, the accelerations generated by single acting air/steam hammers do not reach the magnitude of drop hammers. Some hammers may be equipped with two nominal strokes, one full stroke and another of lesser height. The hammer operator can switch between the two to better match the driving conditions and limit driving resistance or control tension driving stresses as needed. The maximum stroke of single acting air/steam hammers generally ranges from 0.9 to 1.5 meters (3 to 5 ft). The weights of single acting air/steam hammer rams are usually considerably higher than drop hammer weights. Single acting air/steam hammers have the advantages of moderate cost and relatively simple operation and maintenance. They are versatile for many pile types, particularly large concrete and steel pipe piles.

21.9 DOUBLE ACTING AIR/STEAM HAMMERS

A photograph of an enclosed double acting air hammer is presented in Figure 21.16 and the working principle of a double acting hammer is illustrated in Figure 21.17. The ram of a double acting hammer is raised by pressurized steam or air during the upstroke. As the ram nears the maximum up stroke, the lower air valve opens, allowing the lower cylinder chamber to release the pressurized air. Once the ram reaches full stroke, the upper valve changes to admit pressurized steam or air to the upper cylinder. Gravity and the upper cylinder pressure accelerate the ram through its downward fall. As with the single acting hammer, the stroke is again not constant, due to variable lift pressure and volume as well as differing pile rebound. During hard driving with high pile rebound, the pressure may need to be reduced to prevent lift-off, with the hammer actually lifting up away from the pile. Since the maximum stroke is limited and the same lifting pressure is applied during downstroke, a pressure reduction may cause the kinetic energy at impact to be reduced during these hard driving situations. Just before impact, the valve positions are reversed and the cycle repeats.

The correct cushion thickness is extremely important for the proper operation of the hammer. If the hammer timing is off significantly, it is possible for the hammer to run with the ram moving properly, but with little or no impact force delivered to the pile. The kinetic energy of the ram at impact depends on the ram weight and stroke as well as the motive pressure effects. The overall result is that a properly operating double acting hammer with its shorter stroke delivers comparable impact energy per blow at up to about two times the blow rate of a single acting hammer of the same ram weight.

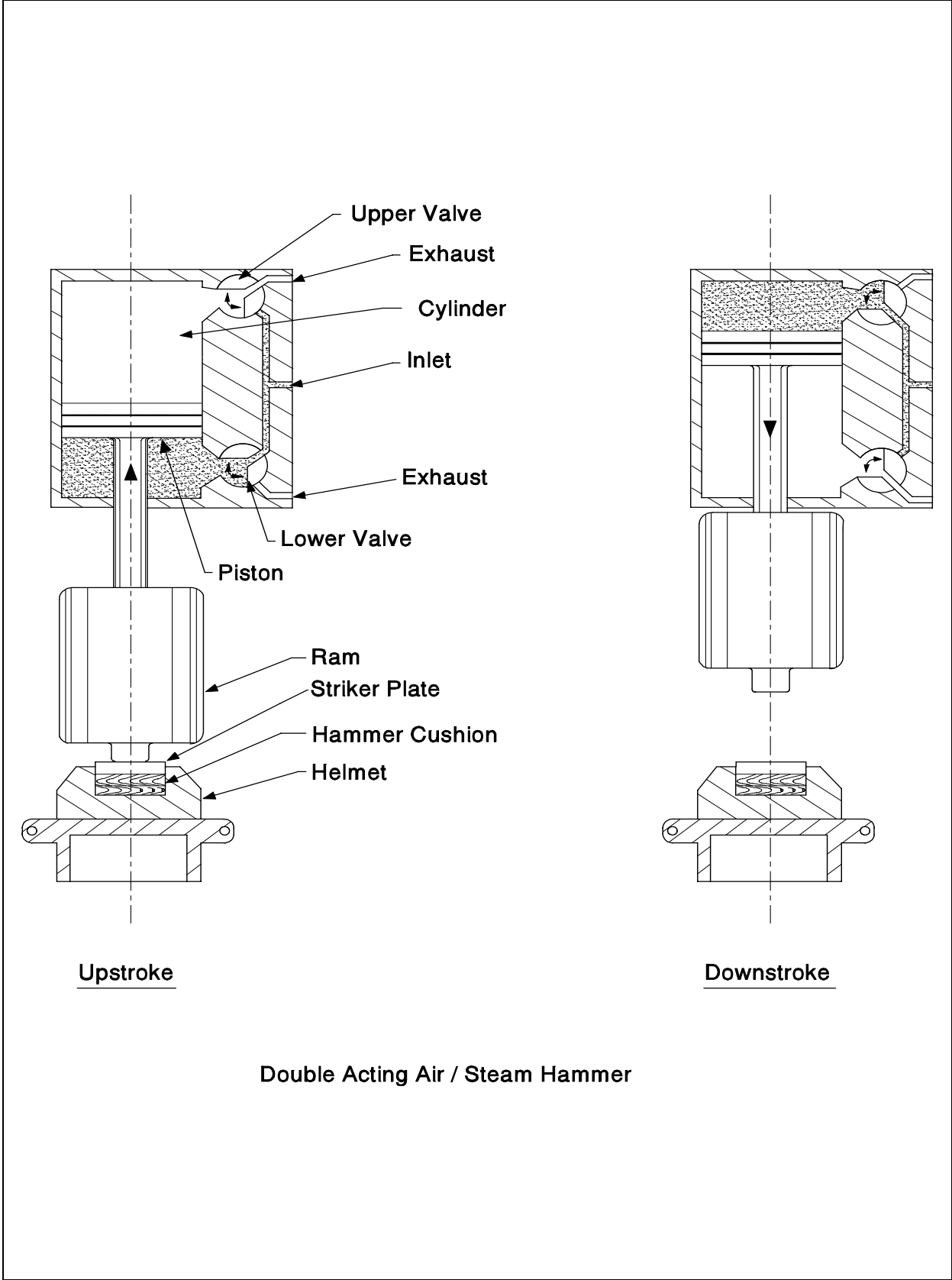


Figure 21.17 Schematic of Double Acting Air/Steam Hammer

Some double acting air/steam hammers are fully enclosed and can be operated underwater such as the one shown in Figure 21.16. They may be more productive than single acting hammers, but are more dependent upon the air pressure. Experience has shown that on average, they are slightly less efficient than equivalently rated single acting hammers. Double acting hammers generally cost more than single acting hammers and require additional maintenance. Similar to single acting air/steam hammers, they require an air compressor or a steam plant. However, double acting air/steam hammers consume more air and require greater air pressures than equivalent single acting hammers.

21.10 DIFFERENTIAL ACTING AIR/STEAM HAMMERS

A differential acting air/steam hammer is another type of double acting hammer with relatively short stroke and fast blow rates. The working principle of a differential hammer is illustrated in Figure 21.18. Operation is achieved by pressure acting on two different diameter pistons connected to the ram. At the start of the cycle, the single valve is positioned so that the upper chamber is open to atmospheric pressure only and the lower chamber is pressurized with the motive fluid. The pressure between the two pistons has a net upward effect due to the differing areas, thus raising the ram. The ram has an upward velocity when the valve position changes and applies air pressure into the upper chamber, causing the net force to change to the downward direction. Thus air pressure along with gravity and friction slows the ram, and after attaining the maximum stroke of the cycle, assists gravity during the downstroke to speed the ram.

As with the double acting hammers, the kinetic energy at impact may need to be reduced during hard driving since the pressure, which assists gravity during downstroke, must be reduced to prevent hammer lift-off. As with the other air/steam hammers, when the ram attains its maximum kinetic energy just before impact, the valve position is reversed and the cycle begins again. Therefore, the hammer cushion must be of the proper thickness to prevent preadmission which could cause reduced transferred energy. Very high air pressures between 820 and 970 kPa (120 and 140 psi) at the hammer inlet are required for proper operation. However, most air compressors only produce pressures of about 820 to 900 kPa (120 to 130 psi) at the compressor. As with the double acting hammer, the efficiency of a differential hammer is somewhat lower than the equivalent single acting air/steam hammer. The heavier ram of the differential acting hammer is lifted and driven downward with a lower volume of air or steam than is used by a double acting hammer.

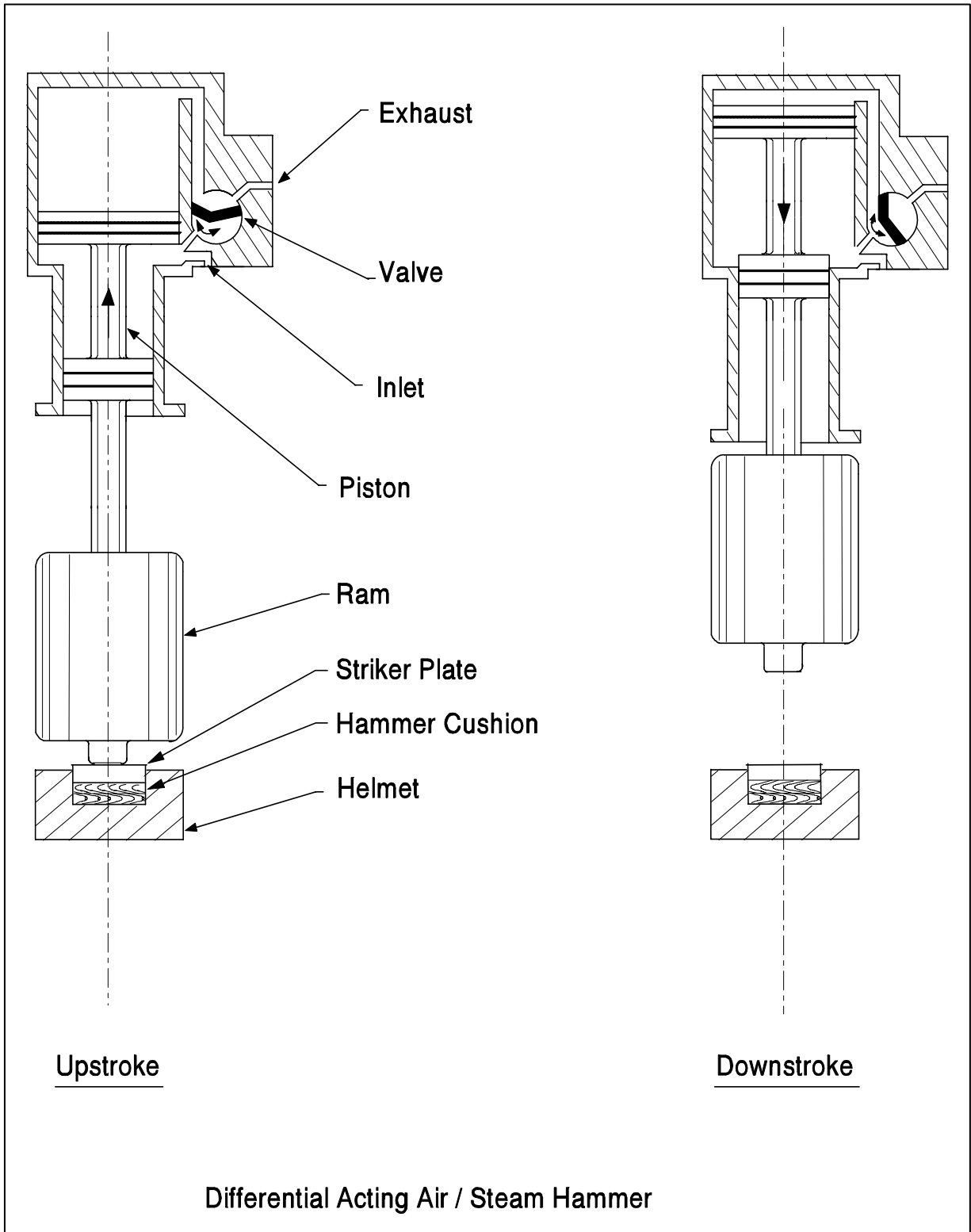


Figure 21.18 Schematic of Differential Air/Steam Hammer

21.11 SINGLE ACTING (OPEN END) DIESEL HAMMER

The basic distinction between all diesel hammers and all air/steam hammers is that, whereas air/steam hammers are one-cylinder engines requiring motive power from an external source, diesel hammers carry their own fuel from which they generate power internally. Figure 21.19 shows the working principle of a single acting diesel hammer. The initial power to lift the ram must be furnished by a hoist line or other source to lift the ram upward on a trip block. After the trip mechanism is released, the ram guided by the outer hammer cylinder falls under gravity. As the ram falls, diesel fuel is injected into the cylinder below the air/exhaust ports. Once the ram passes the air/exhaust ports the diesel fuel is compressed and heats the entrapped air. As the ram impacts the anvil the fuel explodes, increasing the gas pressure. In some hammers the fuel is injected in liquid form as shown in Figure 21.19(b), while in other hammers the fuel is atomized and injected later in the cycle and just prior to impact. In either case, the combination of ram impact and fuel explosion drives the pile downward, and the gas pressure and pile rebound propels the ram upward in the cylinder. On the upstroke, the ram passes the air ports and the spent gases are exhausted. Since the ram has a velocity at that time, the ram continues upward against gravity, and fresh air is pulled into the cylinder. The cycle then repeats until the fuel input is interrupted.

There is no consensus by the various hammer manufacturers on how a single acting diesel hammer should be rated. Many manufacturers use the maximum potential energy computed simply from maximum stroke times the ram weight. The actual hammer stroke achieved is a function of fuel charge, condition of piston rings containing the compressed gases, recoil dampener thickness, driving resistance, and pile length and stiffness. Therefore, the hammer stroke cannot be fully controlled. A set of conditions will generate a certain stroke which can only be adjusted within a certain range by the fuel charge. It may not be possible to achieve the manufacturer's maximum rated stroke under normal conditions. In normal conditions, part of the available potential energy is used to compress the gases as the ram proceeds downward after passing the air ports. The gases ignite when they attain a certain combination of pressure and temperature. Under continued operation, when the hammer's temperature increases due to the burning of the gases, the hammer fuel may ignite prematurely. This condition, called "preignition", reduces the effectiveness of the hammer, as the pressure increases dramatically before impact, causing the ram to do more work compressing the gases and leaving less energy available to be transferred into the pile.

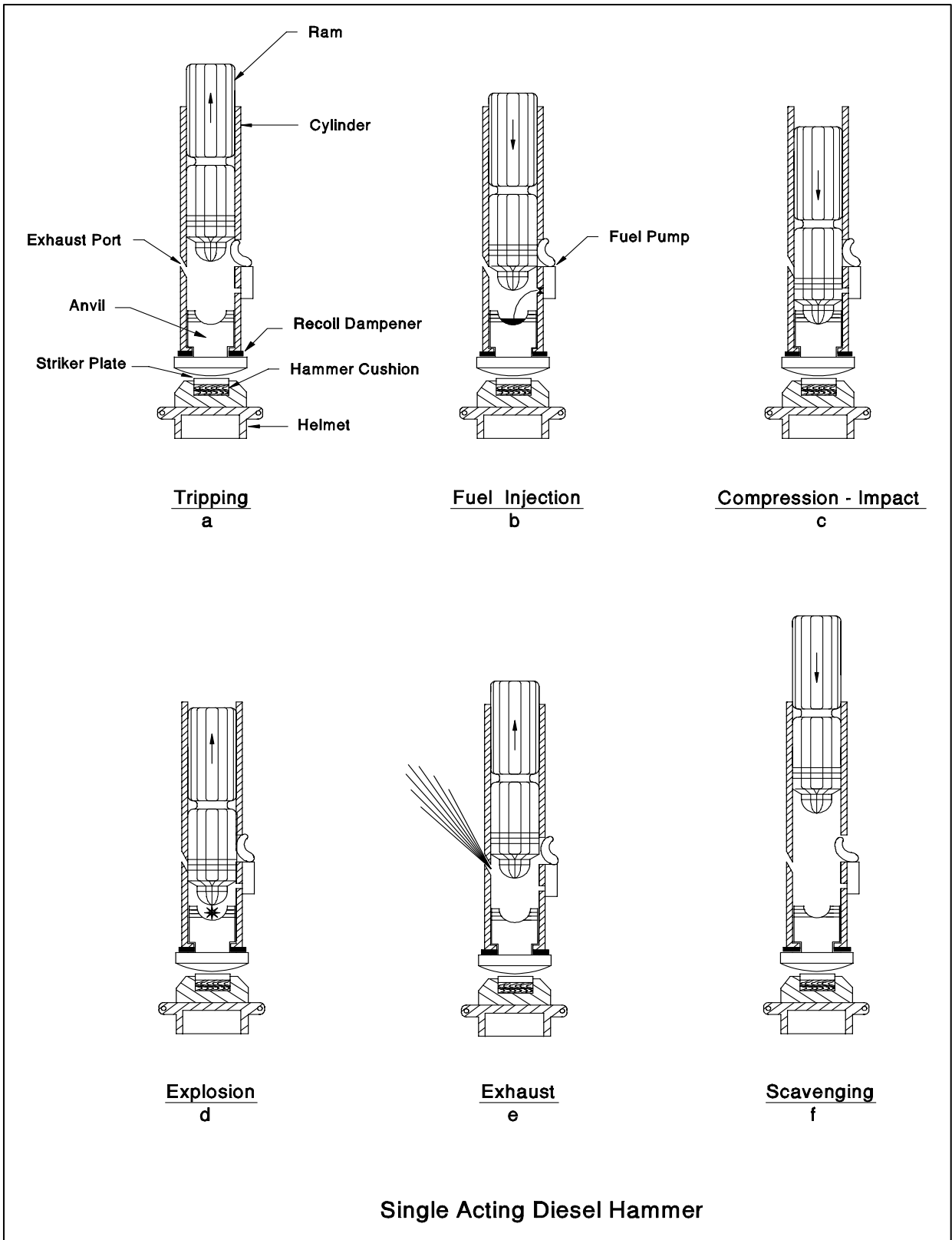


Figure 21.19 Schematic of Single Acting Diesel Hammer

When driving resistance is very low, the upward ram stroke may be insufficient to scavenge (or suction) the air into the cylinder and the hammer may not continue to operate. Thus, the ram must be manually lifted repeatedly until resistance increases. The stroke can be reduced for most hammers by reducing the amount of fuel injected. Some hammers have stepped fuel settings while others have continuously variable throttles. Other hammers use pressure to maintain fuel flow by connecting a hand operated fuel pump to the hammer, which is operated at the ground. By adjusting the fuel pump pressure, hammer strokes may be reduced. Using the hammer on reduced fuel can be useful for limiting driving stresses. For single acting diesel hammers, the stroke is also a function of pile resistance, which also helps in limiting driving stresses. This feature is very useful in controlling tensile stresses in concrete piles during easy driving conditions. The actual stroke can and should be monitored. The stroke of a single acting diesel hammer can be calculated from the following formula:

Stroke in SI Units

$$h = [4400/[bpm^2]] - 0.09$$

Stroke in US Units

$$h = [4.01 [60/bpm]^2] - 0.3$$

Where: h = Hammer stroke in meters (SI units) or feet (US units).
bpm = Blows per minute.

NOTE: These formulas are only applicable for calculating the stroke of single acting diesel hammers and not correct for other hammer types.

Diesel hammers may be expensive and their maintenance more complex. Concerns over air pollution from the hammer exhaust have also arisen, causing some areas to require a switch to kerosene fuel. However, it should be noted that diesel hammers burn far less fuel to operate than the air compressor required for an air/steam hammer. To address environmental concerns, some diesel hammers can be operated using biodiesel fuel and non-petroleum lubricants. One manufacturer has also developed a smokeless diesel hammer. Diesel hammers are also considerably lighter than air/steam hammers with similar energy ratings, allowing a larger crane operating radius and/or a lighter crane to be used. A photograph of a typical single acting diesel hammer is shown in Figure 21.20.

21.12 DOUBLE ACTING (CLOSED END) DIESEL HAMMER

The double acting diesel hammer works very much in principle like the single acting diesel hammer. The main change consists of a closed cylinder top. When the ram moves upward, air is being compressed at the top of the ram in the so called "bounce chamber" which causes a shorter stroke and therefore a higher blow rate. A photograph of a typical double acting diesel hammer is provided in Figure 21.21.



Figure 21.20 Single Acting Diesel Hammer
(courtesy of Pileco)



Figure 21.21 Double Acting Diesel
Hammer

The bounce chamber has ports so that atmospheric pressure exists as long as the ram top is below these ports, as shown in Figure 21.22. Operationally, as the ram passes the bounce chamber port and moves toward the cylinder top, it creates a pressure which effectively reduces the stroke and stores energy, which in turn will be used on the downstroke. Like the single acting hammer, the actual stroke depends on fuel charge, pile length and stiffness, soil resistance, and condition of piston rings. As the stroke increases, the chamber pressure also increases until the total upward force is in balance with the weight of the cylinder itself. Further compression beyond this maximum stroke is not

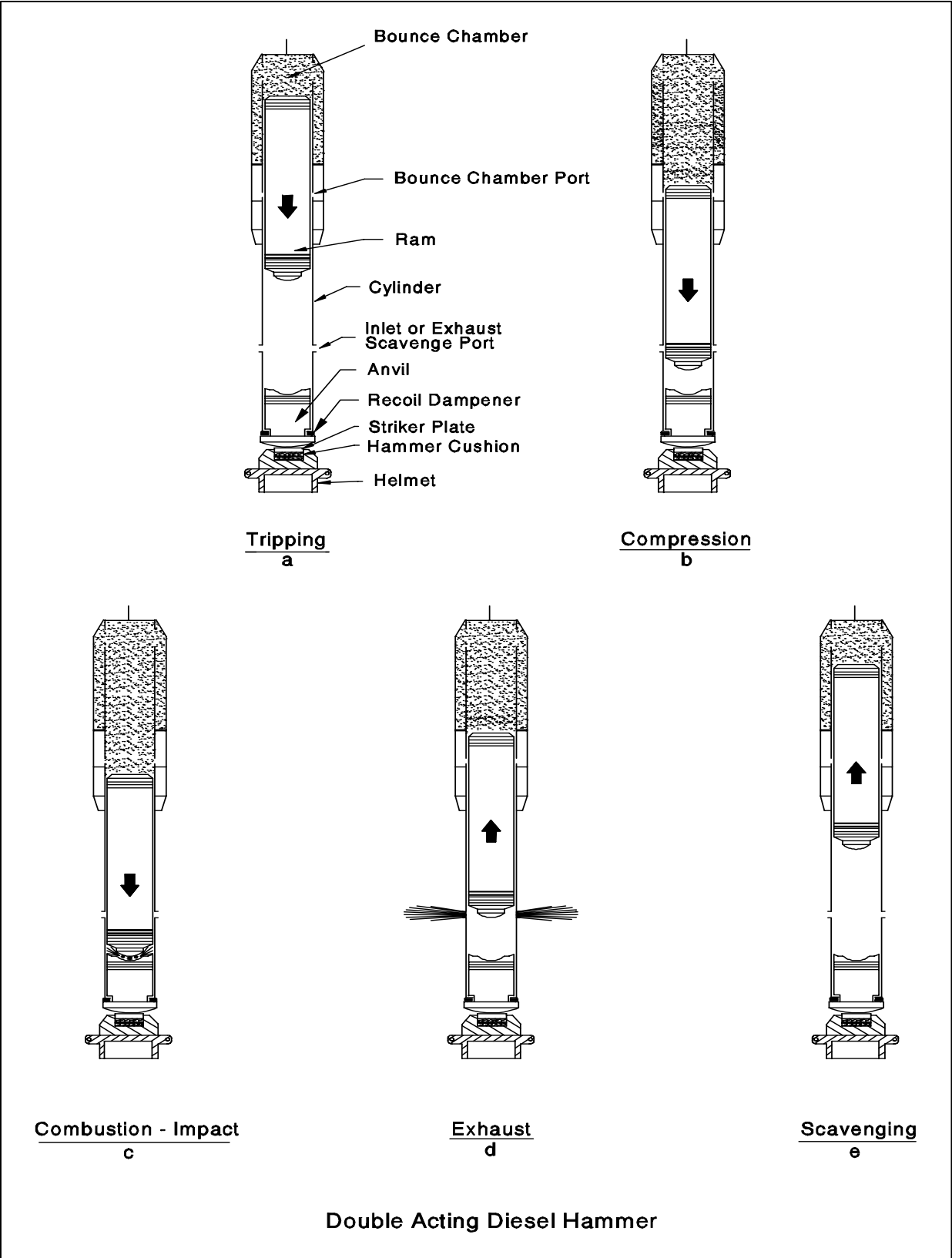


Figure 21.22 Schematic of Double Acting Diesel Hammer

possible, and if the ram still has an upward velocity, uplift of the hammer will result. This uplift should be avoided as it can lead both to an unstable driving condition and to hammer damage. For this reason, the fuel amount, and hence maximum combustion chamber pressure, has to be reduced so that there is only a very slight lift-off or none at all. Most of these hammers have hand held fuel pumps connected by rubber hose to control the fuel flow. Hammer strokes, and therefore hammer energy, may be increased or decreased by the fuel pump pressure.

To determine the energy provided by the hammer, the peak bounce chamber pressure in the hammer is read from a bounce chamber pressure gage. The hammer manufacturer should supply a chart which correlates the bounce chamber pressure gage reading as a function of hose length with the energy provided by the hammer.

21.13 HYDRAULIC HAMMERS

There are many different types of hydraulic hammers. However, all hydraulic hammers use an external hydraulic power source to lift the ram, as illustrated in Figure 21.23. The ram drop may be due to gravity only, or may be hydraulically assisted. They can be perhaps thought of as a modern, although more complicated, version of air/steam hammers in that the ram weights and maximum strokes are similar in sizes and the ram is lifted by an external power source. The simplest version lifts the ram with hydraulic cylinders which then retract quickly, fully releasing the ram, which then falls under gravity. The ram impacts the striker plate and hammer cushion located in the helmet. The hydraulic cylinder then lifts the ram again and the cycle is repeated. Other models employ hydraulic accumulators during the downstroke to store a volume of hydraulic fluid used to speed up the ram lifting operation after impact. Similar to air/steam hammers, hydraulic hammers are also made in both single and double acting versions. The above models with hydraulic accumulators often have a relatively small double acting component. Other more complicated models have nitrogen charged accumulator systems, which store significant energy allowing a shortened stroke and increased blow rate. Photographs of single acting and double acting hydraulic hammers are provided in Figures 21.24 and 21.25, respectively.

All hydraulic hammers allow the ram stroke to be continuously variable and controlled to adapt to the driving conditions. Very short strokes for easy driving may be used to prevent pile run or to minimize tension stresses in concrete piles. Higher strokes are available for hard driving conditions. On many hydraulic hammers, the stroke can be visually estimated.

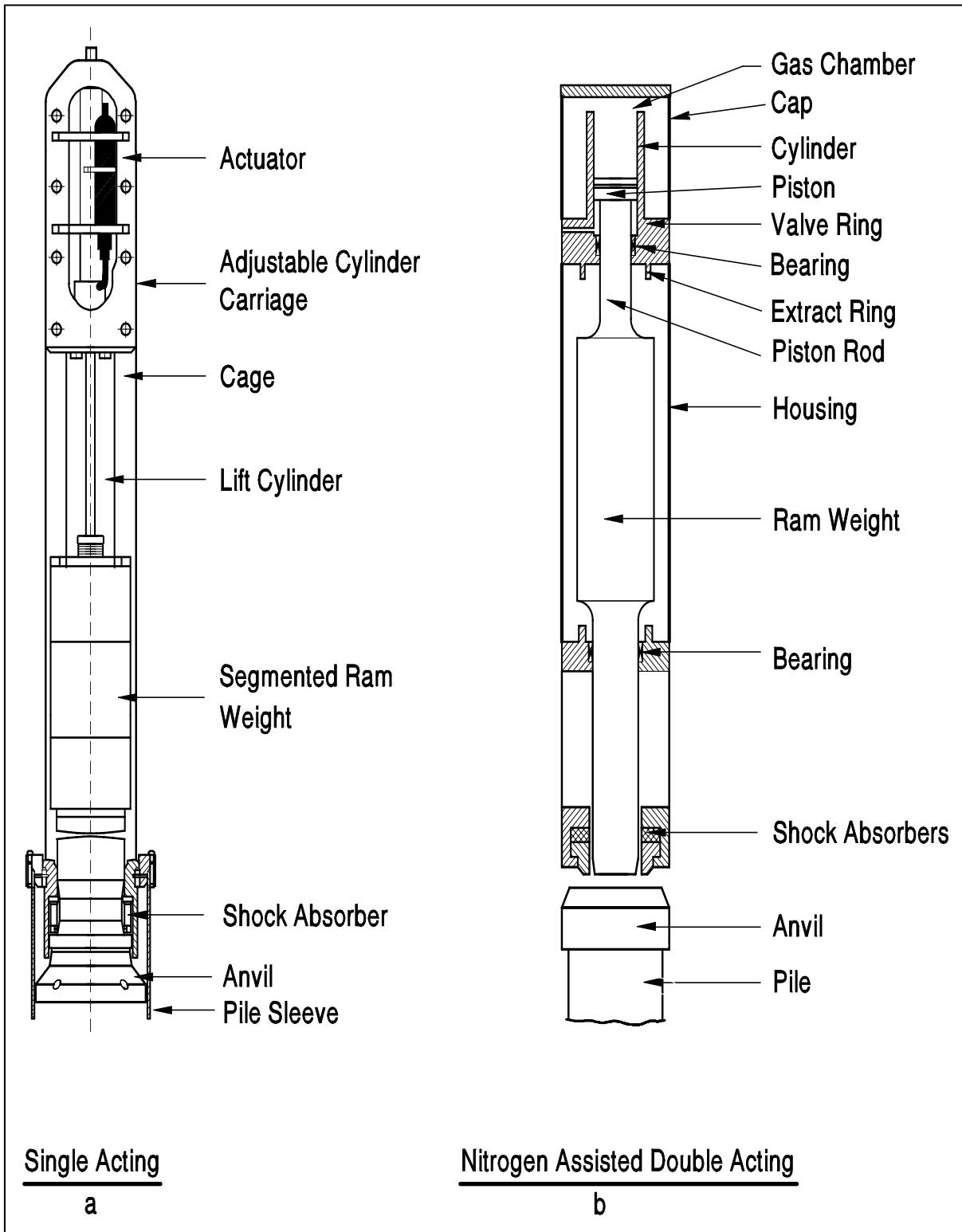


Figure 21.23 Schematics of Single and Double Acting Hydraulic Hammers



Figure 21.24
Single Acting Hydraulic Hammer

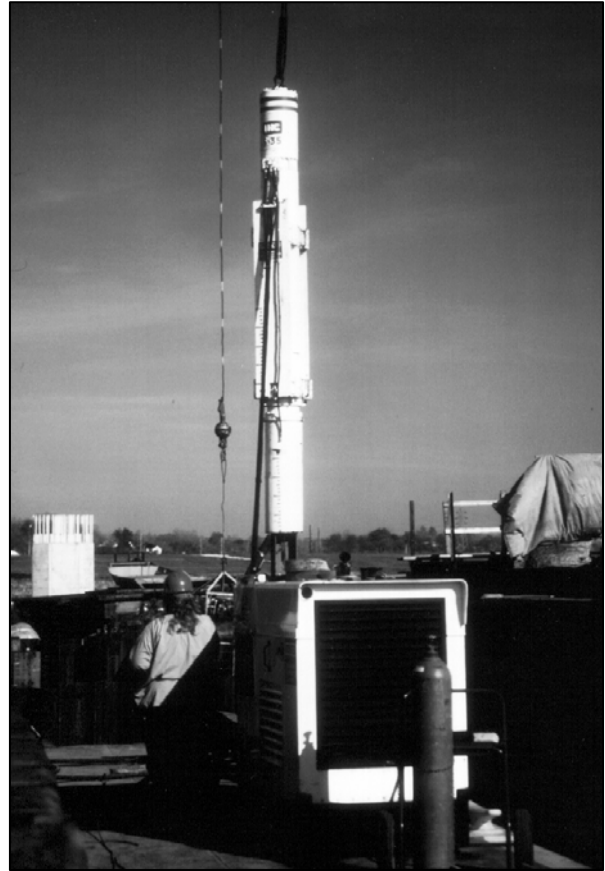


Figure 21.25
Double Acting Hydraulic Hammer

However, most hydraulic hammers include a built-in monitoring system which determines the ram velocity just before impact. The ram velocity can be converted to kinetic energy or equivalent stroke. Because of the variability of stroke, this hammer monitor should be required as part of the hammer system. The monitor results should be observed during pile driving with appropriate hammer performance notes recorded on the driving log.

Some hydraulic hammers can be equipped with extra noise abatement panels. A significant advantage of some hydraulic hammers is that they are fully enclosed and can operate underwater. This allows piles to be driven without using a follower or extra length pile. Some hydraulic hammers do not have hammer cushions and thus generate steel to steel impacts with high hammer efficiencies. Therefore, hydraulic hammers are often not used at their full energy potential. Hydraulic hammers require a dedicated hydraulic power pack, and can be more complex to operate and maintain compared to other hammers.

21.14 VIBRATORY HAMMERS

Vibratory hammers use paired counter-rotating eccentric weights to impart a sinusoidal vibrating axial force to the pile (the horizontal components of the paired eccentors cancel). A schematic of a vibratory hammer is presented in Figure 21.26(a) and a photograph is included in Figure 21.26(b). Most common hammers operate at about 1000 Hz. These hammers are rigidly connected by hydraulic clamps to the pile head and may be used for either pile installation or extraction. These hammers typically do not require leads, although templates are often required for sheet pile cells. Vibratory hammers are not rated by impact energy delivered per blow, but instead are classified by energy developed per second and/or by the driving force they deliver to the pile. The power source to operate a vibratory hammer is usually a hydraulic power pack.

Vibratory hammers are commonly used for driving/extracting sheet piles and can also be used for installing non-displacement H-piles and open end pipe piles. However, it is often difficult to install closed end pipes and other displacement piles due to difficulty in displacing the soil laterally at the toe. Vibratory hammers should not be used for precast concrete piles because of possible pile damage due to tensile and bending stress considerations. Vibratory hammers are most effective in granular soils, particularly if submerged. They also may work in silty or softer clays, but most experience suggests they are less effective in stiff to hard clays.

Some wave equation analysis programs can simulate vibratory driving. Dynamic measurements have also been made on vibratory hammer installed piles. However, a reliable technique for estimating pile capacity during vibratory hammer installation has not yet been developed. Hence, if a vibratory hammer is used for installation, a confirmation test of pile capacity by some method is still necessary.

21.15 HAMMER SIZE SELECTION

It is important that the contractor and the engineer choose the proper hammer for efficient use on a given project. A hammer which is too small may not be able to drive the pile to the required capacity, or may require an excessive number of blows. On the other hand, a hammer which is too large may damage the pile. The use of empirical dynamic pile formulas to select a hammer energy should be discontinued because this approach incorrectly assumes these formulas result in the desired pile capacities. Results from these formulas become progressively worse as the complexity of the hammers increase.

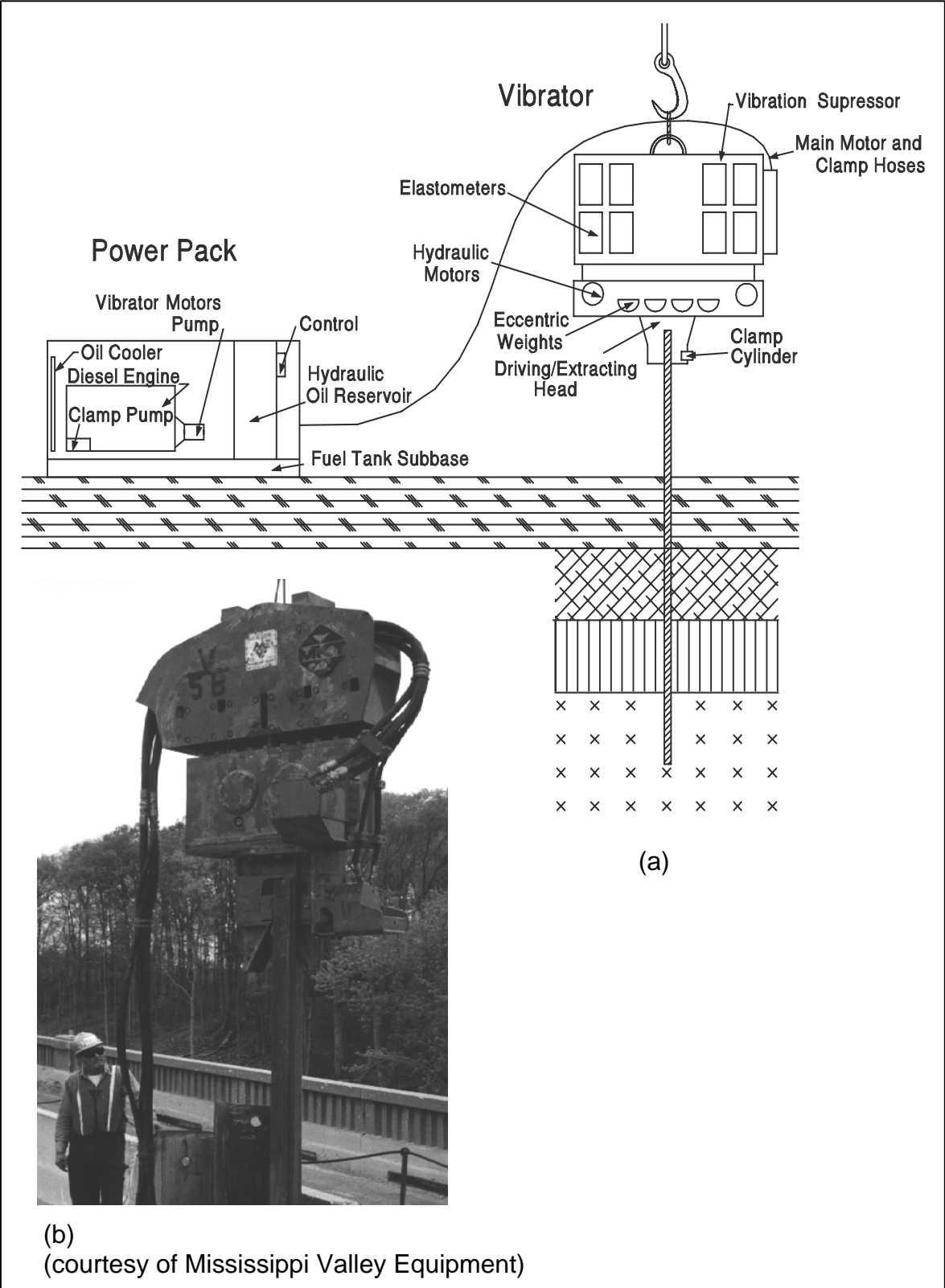


Figure 21.26 Vibratory Hammer

A wave equation analysis, which considers the hammer cushion-pile-soil system, is the recommended method to determine the optimum hammer size. For preliminary equipment evaluation, Table 21-2 provides approximate minimum hammer energy sizes for ranges of ultimate pile capacities. This is a generalization of equipment size requirements that should be modified based on pile type, pile loads, pile lengths, and local soil conditions. In some cases, such as short piles to rock, a smaller hammer than indicated may be more suitable to control driving stresses. This generalized table should not be used in a specification. Guidance on developing a minimum energy table for use in a specification is provided in Chapter 11.

TABLE 21-2 PRELIMINARY HAMMER ENERGY REQUIREMENTS			
Ultimate Pile Capacity (kN)	Minimum Manufacturer's Rated Energy (Joules)	Ultimate Pile Capacity (kips)	Minimum Manufacturer's Rated Energy (ft-lbs)
800 and under	16,500	180 and under	12,000
800 to 1350	28,500	181 to 300	21,000
1351 to 1850	39,000	301 to 415	28,800
1851 to 2400	51,000	416 to 540	37,600
2401 to 2650	57,000	540 to 600	42,000

21.16 HAMMER KINETIC ENERGY MONITORING

Several hammers can now be obtained from their manufacturers with kinetic energy readout devices. These devices typically monitor hard wired proximity switches built into the hammer body. The impact velocity and hammer kinetic energy are calculated based on the time it takes the ram to travel the distance between the proximity switches. These devices also typically provide the hammer blow rate, and for open end diesel hammers, the hammer stroke. Examples of hammer manufacturer provided devices are presented in Figure 21.27 for an IHC hydraulic hammer and Figure 21.28 and 21.29 for a Berminghammer diesel hammer.

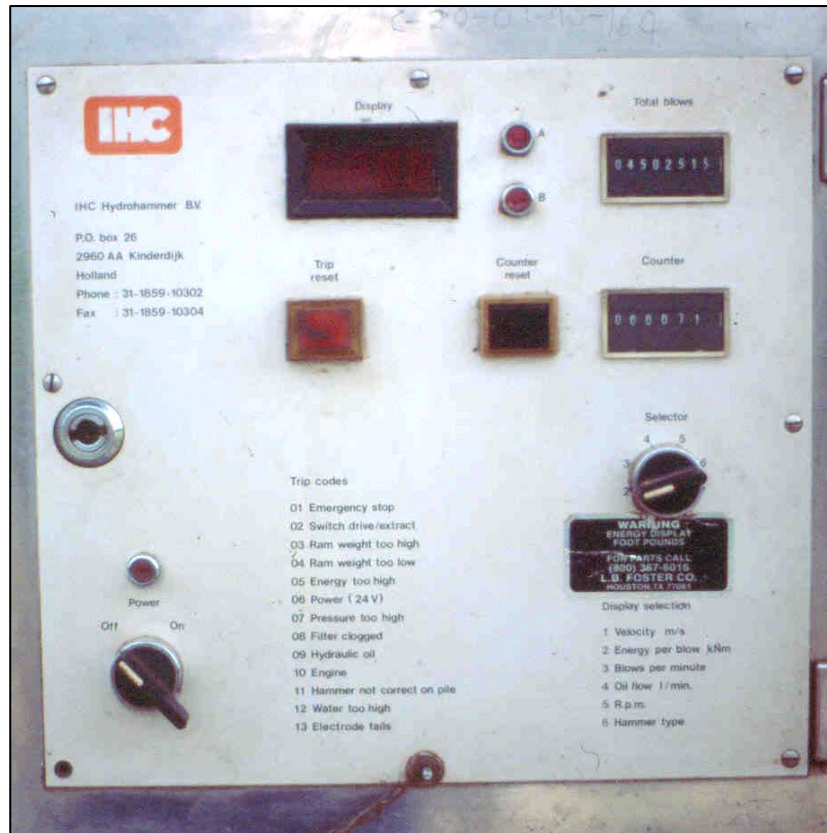


Figure 21.27 IHC Hydraulic Hammer Kinetic Energy Readout Panel

Any existing hammer can also be retrofitted for these measurements by attaching proximity switches to the hammer body. Attachment procedures vary depending upon the hammer model. For a diesel hammer, proximity switches are set into two 30 mm diameter (1.2 in) smooth bore drill holes in the cylinder wall above the combustion chamber. For air/steam or single acting hydraulic hammers, the proximity switches are attached to the hammer body. The proximity switches are connected to a transmitter mounted on the hammer that sends the impact velocity and kinetic energy to a wireless hand held unit. This hand held unit, called an E-Saximeter, can also be used to keep a pile driving log if the inspector presses the enter key with each passing pile driving increment. For single acting diesel hammers, the hammer stroke can also be calculated and displayed. A photograph of a diesel hammer retrofitted for kinetic energy measurements is presented in Figure 21.30 and the readout device is in Figure 21.31.

Hammers equipped with kinetic energy readout devices provide improved quality control and are particularly attractive on large projects or on projects using high capacity piles. These devices can detect changes in hammer performance over time that may necessitate adjustment to the pile installation criterion.

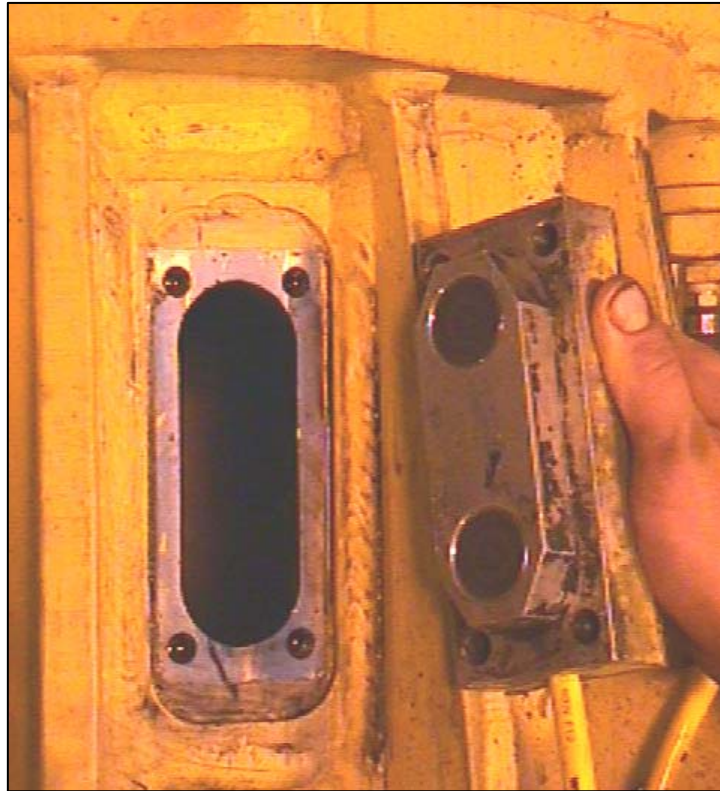


Figure 21.28 Proximity Switches Attachment for a Berminghammer Diesel Hammer



Figure 21.29 Proximity Switches, Readout Device, and Driving Log Trigger Switch for Berminghammer Diesel Hammer

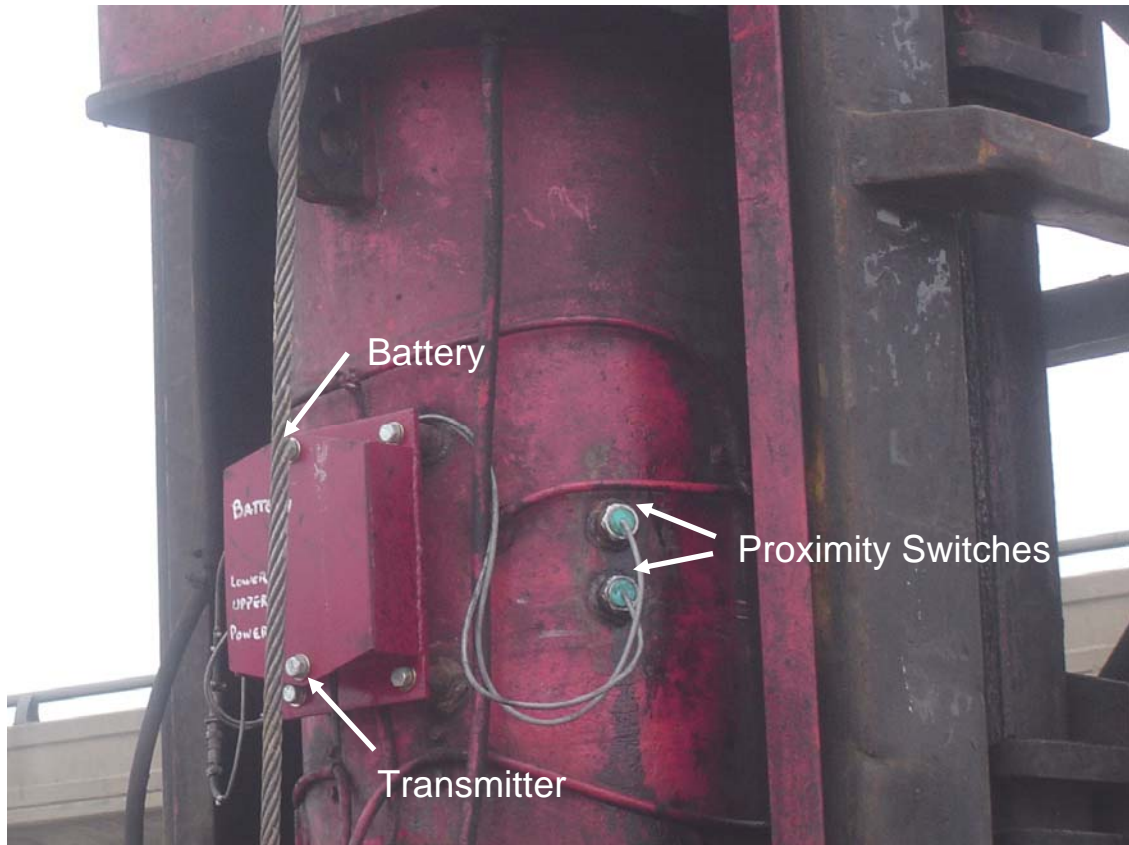


Figure 21.30 Proximity Switches and Transmitter on Retrofitted Diesel Hammer



Figure 21.31 E-Saximeter Wireless Kinetic Energy Readout Device

21.17 NOISE SUPPRESSION EQUIPMENT

Depending upon the hammer and pile type used, noise from impact pile driving operations can range from around 80 to 130 dBA. Local ordinances or specification may place limits on noise levels that may influence equipment selection or may dictate that pile driving noise shrouds be used in order to meet the specified noise limits. Manufacturer's of a few diesel and hydraulic hammers can provide optional noise suppression devices that may reduce the pile driving generated noise by about 10 dBA. Independent noise shield devices have also been produced. An example of a noise shroud produced by a hammer manufacturer is presented in Figures 21.32.



Figure 21.32 Noise Shroud for IHC Hydraulic Hammer

Greater reductions in pile driving noise have been obtained by combining noise abatement techniques on a project. A 20 to 25 dBA reduction was obtained through the combined use of shock absorbing cushion material, a hammer exhaust noise shroud, application of damping compound to the steel piles, and use of a noise shroud around the hammer-pile impact area. Hammer and pile type selection can also influence the pile driving generated noise and should be considered in the design stage of projects in noise sensitive areas.

The Pile Driving Contractor's Association (PDCA) is developing a national database on pile driving noise and vibrations.

21.18 FOLLOWERS

A follower is a structural member interposed between the pile hammer and the pile, to transmit hammer blows to the pile head when the pile head is below the reach of the hammer. This occurs when the pile head is below the bottom of leads. Followers are sometimes used for driving piles below the deck of existing bridges, for driving piles underwater, or for driving the pile head below grade. Maintaining pile alignment, particularly for batter piles, is a problem when a follower is used while driving below the bottom of the leads. The use of a follower is accompanied by a loss of effective energy delivered to the pile due to compression of the follower and losses in the connection. This loss of effective energy delivered to the pile affects the necessary driving resistance for the



Figure 21.33 Follower used for Driving H-piles

ultimate pile capacity. These losses can be estimated by an extensive and thorough wave equation analysis, or field evaluated by dynamic measurements. A properly designed follower should have about the same stiffness (per unit length) as the equivalent length of pile to be driven. Followers with significantly less stiffness should be avoided. Followers often require considerable maintenance. In view of the difficulties that can be associated with followers, their use should be avoided when possible. For piles to be driven underwater, one alternative is to use a hammer suitable for underwater driving. A photograph of a follower for driving steel H-piles underwater is presented in Figure 21.33.

21.19 JETTING

Jetting is the use of water or air to facilitate pile penetration by displacing the soil. In some cases, a high pressure air jet may be used in combination with water. Jets may be used to create a pilot hole prior to or simultaneously with pile placement. Jetting pipes may be located either inside or outside the pile. Jetting is usually most effective in loose to medium dense granular soils.

Jetting is not recommended for friction piles because the frictional resistance is reduced by jetting. Jetting should also be avoided if the piles are designed to provide substantial lateral resistance. For end bearing piles, the final required resistance must be obtained by driving (without jetting). Backfilling should be required if the jetted hole remains open after the pile installation. A separate pay item for jetting should be included in the contract documents when jetting is anticipated. Alternatives to jetting include predrilling and spudding.

The use of jetting has been greatly reduced due to environmental restrictions. Hence, jetting is rarely used unless containment of the jetted materials can be provided. Photographs of a dual jet system mounted on a concrete pile and a jet/punch system are presented in Figures 21.34 and 21.35, respectively.



Figure 21.34 Dual Jet System Mounted on a Concrete Pile (courtesy of Florida DOT)

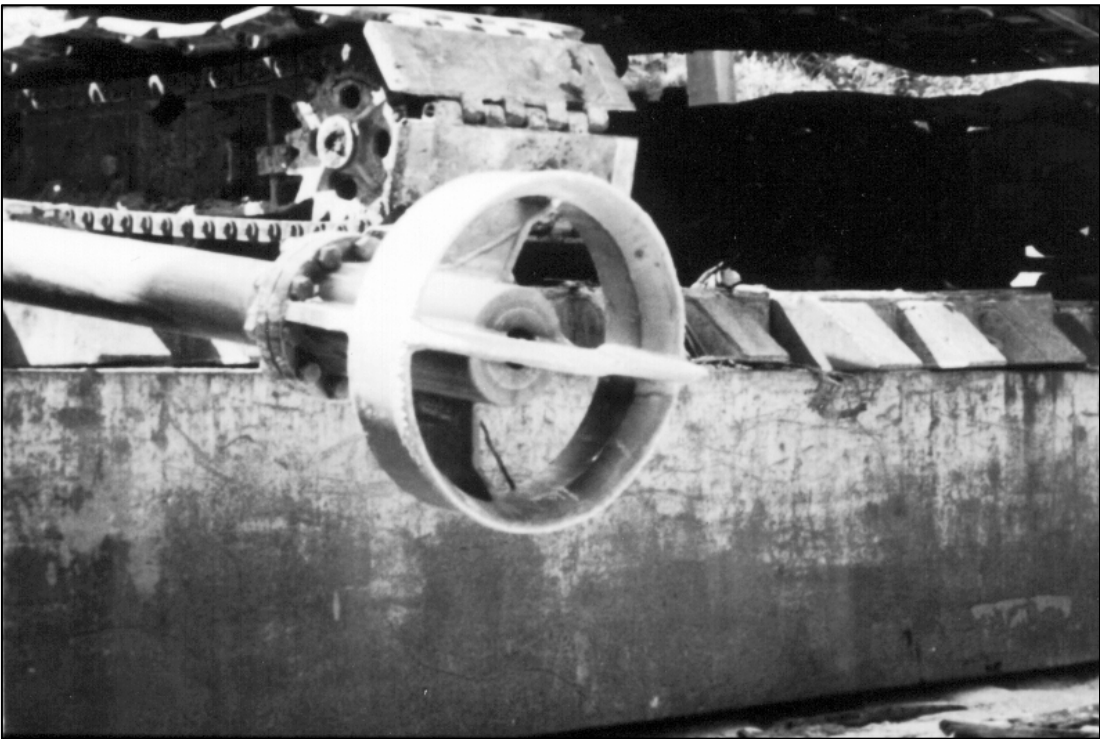


Figure 21.35 Jet/Punch System (courtesy of Florida DOT)

21.20 PREDRILLING

Soil augers or drills may sometimes be used where jetting is inappropriate. Predrilling is sometimes necessary to install a pile through soils with obstructions, such as old timbers, boulders, and riprap. Predrilling is also frequently used for pile placement through soil embankments and may be helpful to reduce pile heave when displacement piles are driven at close spacings.

The predrilled hole diameter depends upon the size and shape of the pile, and soil conditions. The hole should be large enough to permit driving but small enough so the pile will be supported against lateral movement. Under most conditions, the predrilled hole diameter should be 100 mm (4 in) less than the diagonal of square or steel-H piling, and 25 mm (1 in) less than the diameter of round piling. Where piles must penetrate into or through very hard material, it is usually necessary to use a diameter equal to the diagonal width or diameter of the piling. A separate pay item for predrilling should be included in the contract documents when predrilling is anticipated. A photograph of a solid flight auger predrilling system is presented in Figure 21.36.



Figure 21.36 Solid Flight Auger Predrilling System (courtesy of Florida DOT)

21.21 SPUDDING

Spudding is the act of opening a hole through dense material by driving or dropping a short and strong member and then removing it. The contractor may resort to spudding in lieu of jetting or predrilling when the upper soils consist of miscellaneous fill and debris. A potential difficulty of spudding is that a spud may not be able to be pulled when driven too deep. However, an advantage of spudding is that soil cuttings and groundwater are not brought to the ground surface, which could then require disposal due to environmental concerns.

21.22 BUBBLE CURTAINS

Bubble curtains are sometimes required when driving piles through water to reduce underwater sound waves, shock waves and overpressures that impact marine mammals and fish. In general, overpressure levels greater than 30 kPa (4.4 psi) have been found to be detrimental. However, the detrimental overpressure level will vary depending upon the species of fish, their size, and their maturity level.

Bubble curtain devices use air bubbles to attenuate the pile driving induced pressure wave. Bubble curtains can be categorized as bubble rings or bubble walls. A bubble ring is typically used around a single pile and typically consists of a high volume air compressor a primary feed line, a primary distribution manifold, medium volume secondary feed lines, and secondary distribution manifolds. Bubble walls combine the features of bubble rings with a sound damping curtain that encapsulates the air bubbles. Bubble walls are typically placed around a complete substructure location rather than an individual pile.

For a bubble curtain to be effective, the bubble curtain must completely surround the pile driving activity. This can sometimes be difficult to accomplish with a bubble ring in areas with tides and currents, or when the foundation design includes batter piles. Bubble rings are sometimes used in conjunction with containment devices such as a large diameter pile sleeve, a turbidity curtain, or a cofferdam in these situations. A bubble wall system may be more attractive in areas where a bubble ring system requires containment devices. A photograph of a pile driven inside bubble ring used in conjunction with a containment device is presented in Figure 21.37.



Figure 21.37 Bubble Ring with Containment Device (courtesy WSDOT)

Longmuir and Lively (2001) presented a case history where use of a bubble ring reduced overpressures during pile driving from in excess of 152 kPa (22 psi) with no mitigation to less than 21 kPa (3 psi).

21.23 REPRESENTATIVE LIST OF U.S.A. HAMMER MANUFACTURERS AND SUPPLIERS

At the time of final printing of this manual, the following manufacturers or suppliers of commonly used pile hammers were identified:

American Equipment & Fabricating Corp.
100 Water St.
East Providence, RI 02914
Ph: 401-438-2626
Fax: 401-438-0764
www.american-equipment.com

Supplier:
Berminghammer Diesel Hammers
Dawson Hydraulic Hammers
H&M Vibratory Hammers
PTC Vibratory Hammers

American Piledriving Equipment, Inc.
7032 South 196th
Kent, WA 98032
Ph: 253-872-1041 or 800-248-8498
Fax: 253-872-8710
www.apevibro.com

Manufacturer:
APE Diesel Hammers Hammers
APE Hydraulic Hammers
APE Vibratory Hammers
Supplier:
Junttan Hydraulic Hammers

Berminghammer Foundation Equipment
Wellington Street Marine Terminal
Hamilton, Ontario L8L 4Z9
Ph: 905-528-0425 or 800-668-9432
Fax: 905-528-6187
www.berminghammer.com

Manufacturer:
Berminghammer Diesel Hammers

Bay Machinery Corp.
543 58th Street
Richmond, CA 94802
Ph: 510-236-9000
Fax: 510-236-7212
www.baymachinery.com

Supplier:
Berminghammer Diesel Hammers
Dawson Hydraulic Hammers
HPSI Vibratory Hammers

Continental Machine Co., Inc.
1602 Engineers Road
Belle Chasse, LA 70037
Ph: 504-394-7330
Fax: 504-393-8715
www.conmaco.com

Manufacturer:
Conmaco Air Hammers
Supplier:
Berminghammer Diesel Hammers
HPSI Hydraulic Hammers
HPSI Vibratory Hammers
PTC Vibratory Hammers

Drive-Con, Inc.
P.O. Box 1307
8225 Washington Blvd.
Jessup, MD 20794
Ph: 410-799-8963 or 800-255-8963
or 410-799-8964 or 410-799-8971
Fax: 410-799-5264
www.drive-con.com

Supplier:
APE Diesel Hammers
J&M Hydraulic Hammers
J&M Vibratory Hammers

Equipment Corporation of America
P.O. Box 306
Coraopolis, PA 15108-0306
Ph: 412-264-4480
Fax: 412-264-1158
www.ecanet.com

Supplier:
Delmag Diesel Hammers
Dawson Hydraulic Hammers
HPSI Vibratory Hammers
IHC Hydraulic Hammers
Vulcan Air Hammers

Geoquip, Inc.
1111 Cavalier Blvd.
Chesapeake, VA 23323
Ph: 757-485-2500
Fax: 757-485-5631

Supplier:
Delmag Diesel Hammers
HPSI Hydraulic Hammers
HPSI Vibratory Hammers
Menck Hydraulic Hammers
Vulcan Air Hammers

Hammer and Steel, Inc.
11912 Missouri Bottom Road
St. Louis, MO 63042
Ph: 314-895-4600 or 800-325-7453
Fax: 314-895-4070
www.hammersteel.com

Supplier:
APE Vibratory Hammers
Dawson Hydraulic Hammers
Delmag Diesel Hammers
HPSI Vibratory Hammers
PVE Vibratory Hammers

HMC Foundation Equipment
Mid-America-Foundation Supply, Inc.
P.O. Box 5198
3101 New Haven Avenue
Fort Wayne, IN 46803
Ph: 260-424-0405 or 800-348-1890
Fax: 260-422-2040
www.hmc-us.com

Supplier:
Delmag Diesel Hammers
HMC Hydraulic Hammers
HMC Diesel Hammers
Vulcan Air Hammers
HMC Vibratory Hammers

Hydraulic Power Systems, Inc.
1203 Ozark
North Kansas City, MO 64116
Ph: 816-221-4774
Fax: 816-221-4591
www.hpsi-worldwide.com

Manufacturer:
HPSI Hydraulic Hammers
HPSI Vibratory Hammers

International Construction Equipment, Inc.
301 Warehouse Drive
Matthews, NC 28104
Ph: 704-821-8200 or 888-423-8721
Fax: 704-821-6448
www.iceusa.com

Manufacturer:
ICE Diesel Hammers
ICE Hydraulic Hammers
ICE Vibratory Hammers

J&M Foundation Equipment, LLC
1601 Banksville Road
Pittsburgh, PA 15216
Ph: 412-341-8190 or 866-462-7278
Fax: 412-341-8192
www.jandm-usa.com

Manufacturer
J&M Hydraulic Hammers
J&M Vibratory Hammers
Supplier:
APE Diesel Hammers

M.D. Moody & Sons, Inc.
P.O. Box 5350
Jacksonville, FL 32207
4600 Phillips Highway
Jacksonville, FL 32207
Ph: 800-869-4401 or 904-737-4401
Fax: 904-636-0532
www.mdmoodys.com

Supplier:
ICE Diesel Hammers
Pilemer Hydraulic Hammers

Midwest Vibro Inc.
3715 28th Street S.W.
P.O. Box 224
Grandville, MI 49468-0224
Ph: 616-532-7670 or 800-648-3403
Fax: 616-532-8505
www.hmvibro.com

Supplier:
H&M Vibratory Hammers
Dawson Vibratory Hammers
(Dawson for Michigan only)

Mississippi River Equipment
P.O. Box 249
520 Good Hope Street
Norco, LA 70079
Ph: 985-764-1194
Fax: 785-764-1196
www.mreco.com

Supplier
Dawson Hydraulic Hammers
MKT Air Hammers
MKT Diesel Hammers
MKT Vibratory Hammers
Vulcan Air Hammers

MKT Manufacturing, Inc.
1198 Pershall Road
St. Louis, MO 63137
Ph: 314-388-2254
Fax: 314-388-1218
www.mktpileman.com

Manufacturer:
MKT Air Hammers
MKT Diesel Hammers
MKT Vibratory Hammers

New England Construction Products, Inc.
22 Fifth Street - Rear
Taunton, MA 02780
Ph: 508-821-4450
Fax: 508-821-4438

Supplier:
Vulcan Air Hammers
Delmag Diesel Hammers
HPSI Hydraulic Hammers
HPSI Vibratory Hammers
IHC Hydraulic Hammers

Pacific American Commercial Company
7400 Second Avenue South
P.O. Box 3742
Seattle, WA 98124
Ph: 206-762-3550 or 800-678-6379
Fax: 206-763-4232
www.pacoequip.com

Supplier:
Dawson Hydraulic Hammers
Dawson Vibratory Hammers
Delmag Diesel Hammers
HPSI Hydraulic Hammers
HPSI Vibratory Hammers
MKT Vibratory Hammers
Vulcan Vibratory Hammers

Pile Equipment, Inc.
1058 Roland Avenue
Green Cove Springs, FL 32043
Ph: 904-284-1779
Fax: 904-284-2588
www.pile-eqp.net

Supplier:
Delmag Diesel Hammers
Berrminghammer Diesel Hammers
Dawson Hydraulic Hammers
HPSI Hydraulic Hammers
Vulcan Air Hammers

Pileco, Inc.
P.O. Box 16099
Houston, TX 77222
Ph: 713-691-3000
Fax: 713-691-0089
www.pileco.com

Manufacturer:
Pileco Diesel Hammers
Supplier:
IHC Hydraulic Hammers
Tunkers Vibratory Hammers

Seaboard Steel Corporation
P.O. Drawer 3408
Sarasota, FL 34230-3408
Ph: 941-355-9773 or 800-533-2736
Fax: 941-351-7064
www.seaboardsteel.com

Supplier:
MKT Air Hammers
MKT Diesel Hammers
MKT Vibratory Hammers

Sunbelt Rentals
1337 Hundred Oaks Drive
Charlotte, NC 28217
Ph: 866-786-2358
Fax: 704-348-2676
www.sunbeltrentals.com

Vulcan Iron Works
P.O. Box 5402
2909 Riverside Dr.
Chattanooga, TN 37406
Ph: 423-698-1581
Fax: 423-698-1587
www.vulcanhammer.com

Supplier:
Berminghammer Diesel Hammers
PVE Vibratory Hammers

Manufacturer:
Vulcan Air Hammers
Supplier:
IHC Hydraulic Hammers

21.24 USEFUL HAMMER INFORMATION WEB ADDRESSES

General Hammer Information.	www.pilehammerspecs.com
APE Hammers.	www.apevibro.com
Banut Hammers.	www.banut.com
Berminghammer Hammers.	www.berminghammer.com
BSP Hammers.	www.bsp-if.co.uk
Conmaco Hammers.	www.conmaco.com
Dawson Hammers.	www.dcpuk.com
Delmag Hammers.	www.delmag.com
DKH Pilemer Hammers.	www.dkh.co.kr/e
Fambo Hammers.	www.fambo.se
HERA Hammers.	www.hera-hammers.com
HMC Hammers.	www.hmc-us.com
HPSI Hammers.	www.hpsi-worldwide.com
ICE Hammers.	www.iceusa.com
IHC Hammers.	www.ihcfe.com
Junttan Hammers.	www.junttan.com
MAIT Hammers.	www.mait.it
Menck Hammers.	www.menck.com
MGF Hammers.	www.mgf.info
MKT Hammers.	www.mktpileman.com
Müller Hammers.	www.krupp-gft-tiefbautechnik.com

Pileco Hammers. www.pileco.com
PTC Vibratory Hammers. www.ptc.fr
PVE Hammers. www.pve-equipment.com
Twinwood Hammers. www.twindyno.com.sg
Vulcan Hammers. www.vulcanhammer.com

REFERENCES

- Associated Pile and Fitting Corporation. Design and Installation of Driven Pile Foundations.
- Chellis, R.D. (1961). Pile Foundations. McGraw-Hill Book Company.
- Compton, G.R. (1977). Piletalk Panel on Hammers and Equipment, APF Piletalk Seminar, San Francisco.
- Davisson, M.T. (1975). Pile Load Capacity. Design, Construction and Performance of Deep Foundations, ASCE and University of California, Berkeley.
- Davisson, M.T. (1980). Pile Hammer Selection. Presentation at the APF Piletalk Seminar in Carlsbad, California.
- Deep Foundations Institute (1981). A Pile Inspector's Guide to Hammers, First Edition, Deep Foundations Institute.
- Deep Foundations Institute (1995). A Pile Inspector's Guide to Hammers. Second Edition, Deep Foundations Institute.
- Fuller, F.M. (1983). Engineering of Pile Installations. McGraw-Hill Book Company.
- Goble, G.G. and Rausche F. (1981). WEAP Program, Vol. I Background. Implementation Package Prepared for the Federal Highway Administration.
- Longmuir, C. and Lively, T. (2001). Bubble Curtain Systems Help Protect the Marine Environment. Pile Driving Contractors Association Summer Newsletter, pp 11-16, www.piledrivers.org.
- Passe, Paul D. (1994). Pile Driving Inspector's Manual. State of Florida Department of Transportation.

Rausche, F., Likins, G.E., Goble, G.G. and Hussein, M. (1986). The Performance of Pile Driving Systems. Inspection Report, FHWA/RD-86/160, U.S. Department of Transportation, Federal Highway Administration, Office of Research and Development, Washington, D.C., 92.

Chapter 22

ACCESSORIES FOR PILE INSTALLATION

Pile accessories are sometimes used for pile toe protection and for splicing. Accessories available for driven piles can make installation easier and faster. They can also reduce the possibility of pile damage and help provide a more dependable permanent support for any structure. Heavier loading on piles, pile installation in sloping rock surfaces or into soils with obstructions, and longer pile length, are project situations where the use of pile shoes and splice accessories are often cost effective and sometimes necessary for a successful installation. However, pile accessories may add significant cost to the project and should not be used unless specifically needed. Pile toe attachments and splices for timber, steel, concrete and composite piles are discussed in this chapter. A list of the manufacturers and suppliers of pile accessories is provided at the end of this chapter.

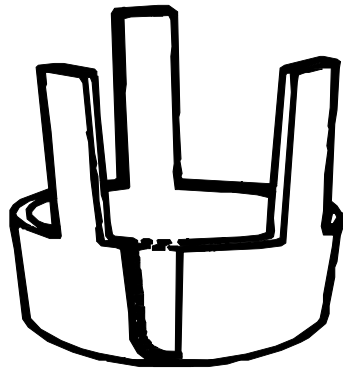
During driving and in service, pile toe attachments and splices should develop the required strength in compression, bending, tension, shear, and torsion at the point of the toe attachment or splice. The current AASHTO Bridge Specifications require that a splice must provide the full strength of a pile. Some of the manufactured splices do not satisfy this AASHTO requirement.

22.1 TIMBER PILES

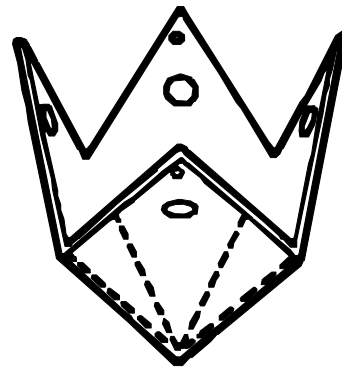
The potential problems associated with driving timber piles are splitting and brooming of the pile toe and pile head, splitting or bowing of the pile body, and breaking of the pile during driving. Protective attachments at the pile toe and at the pile head can minimize these problems.

22.1.1 Pile Toe Attachments

A timber pile toe can be protected by a metal boot or a point. The trend toward heavier hammers and heavier design loading may result in greater risk of damage for timber piles if obstructions are encountered. The pile toe attachment shown in Figure 22.1(a) and (c) covers the entire pile toe without the need for trimming. Figure 22.1(b) shows another type of pile toe protection attachment, which requires trimming of the pile toe.



(a)



(b)



(c)

Figure 22.1 Timber Pile Toe Attachments

22.1.2 Attachment at Pile Head

The American Wood Preservers Institute (AWPI) recommends banding timber piles with heavy metal strapping at the pile head prior to driving to prevent splitting. A photograph of a banded timber pile head is shown in Figure 22.2.

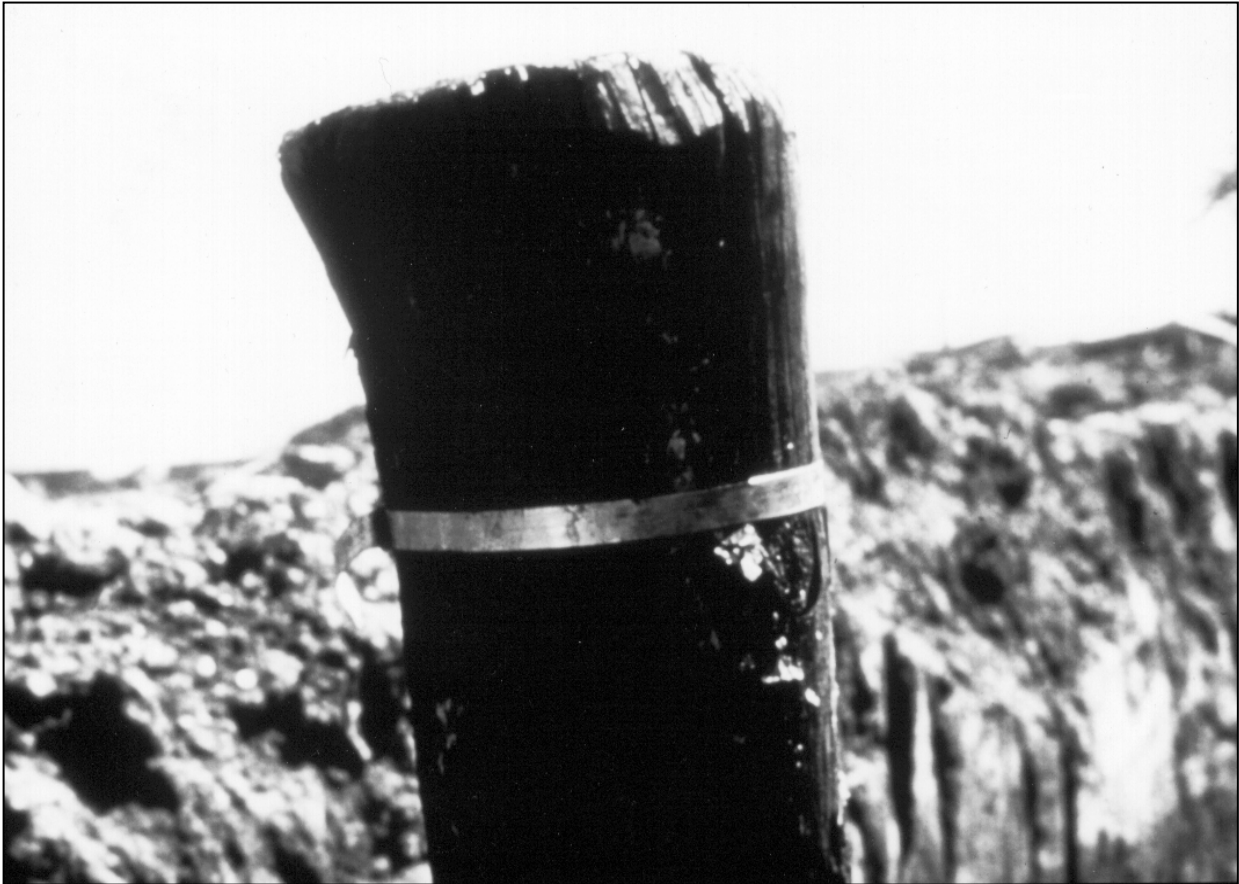


Figure 22.2 Banded Timber Pile Head

22.1.3 Splices

Timber pile splices are undesirable. It is virtually impossible to develop the full bending strength of the piling through simple splices such as those shown in Figure 22.3(a through c). In order to develop full bending strength, a detail similar to that shown in Figure 22.3(d) is required.

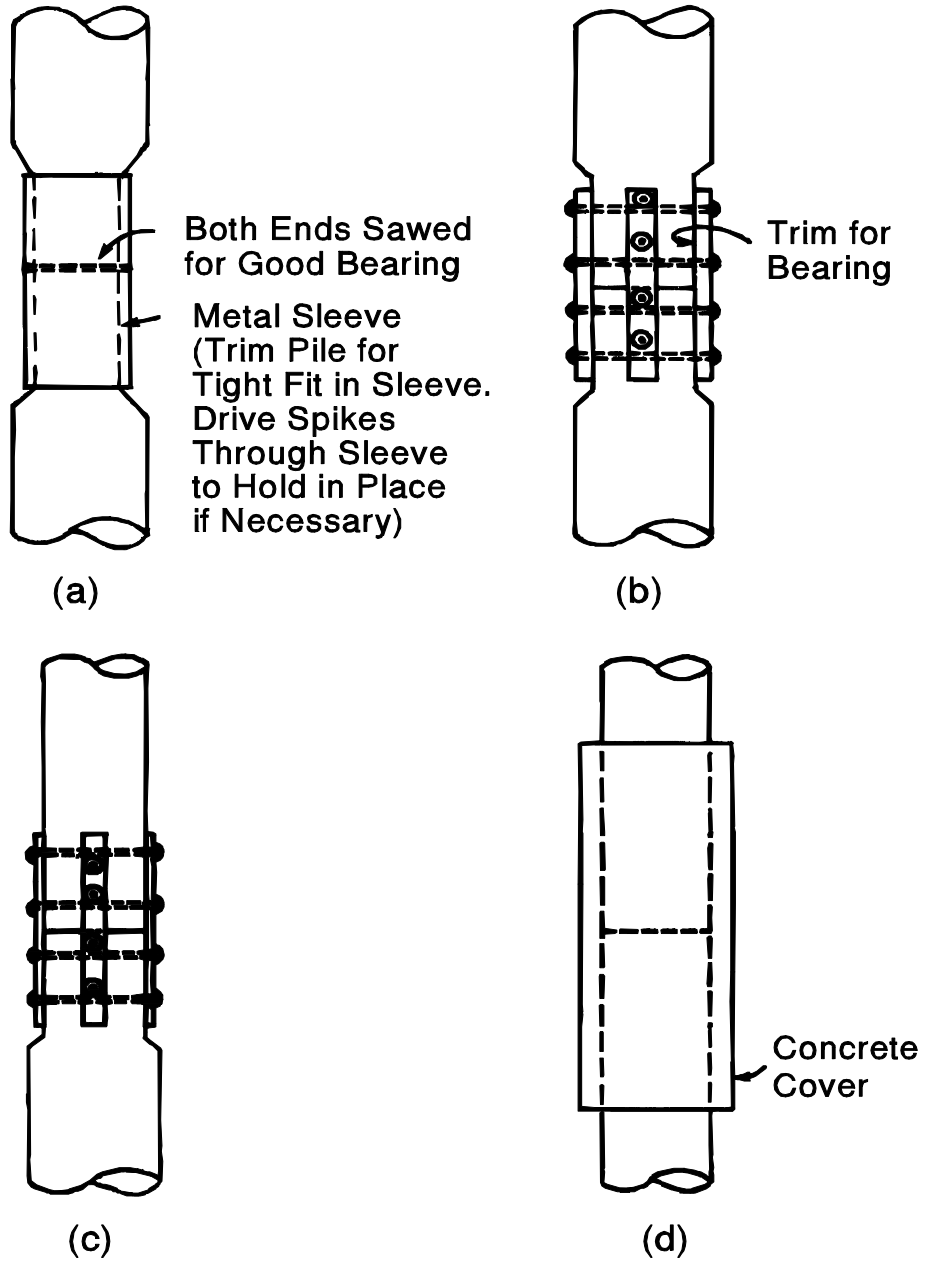


Figure 22.3 Splices for Timber Piles

22.2 STEEL H-PILES

22.2.1 Pile Toe Attachments

Steel H-piles are generally easy to install due to the non-displacement character of the pile. Problems arise when driving H-piles through man-made fills, very dense gravel or deposits containing boulders. If left unprotected under these conditions, the pile toe may deform to an unacceptable extent and separation of the flanges and web may occur (Figure 22.4). Pile toe attachments can help prevent these problems. Such attachments are also desirable for H-piles driven to rock, particularly on sloping rock surfaces.

Pile toe reinforcement consisting of steel plates welded to the flanges and web are not recommended because the reinforcement provides neither protection nor increased strength at the critical area of the flange-to-web connection. Several manufactured driving shoes are available, as shown in Figure 22.5(a through d). These shoes are attached to the H-piles with fillet welds along the outside of each flange. Pile shoes fabricated from cast steel (ASTM A 27) are recommended because of their strength and durability.

Prefabricated H-pile shoes come in various shapes and sizes. Manufacturers also recommend different shapes for various applications. It is recommended that for a given set of subsurface conditions, pile shoes from different manufacturers should be considered as equivalent if they are manufactured from similar materials and by similar fabrication techniques. Minor variations in configuration should be given minimum importance, except in specific subsurface conditions where a certain shape would give a definite advantage.



Figure 22.4 Damaged H-piles without Pile Toe Protection

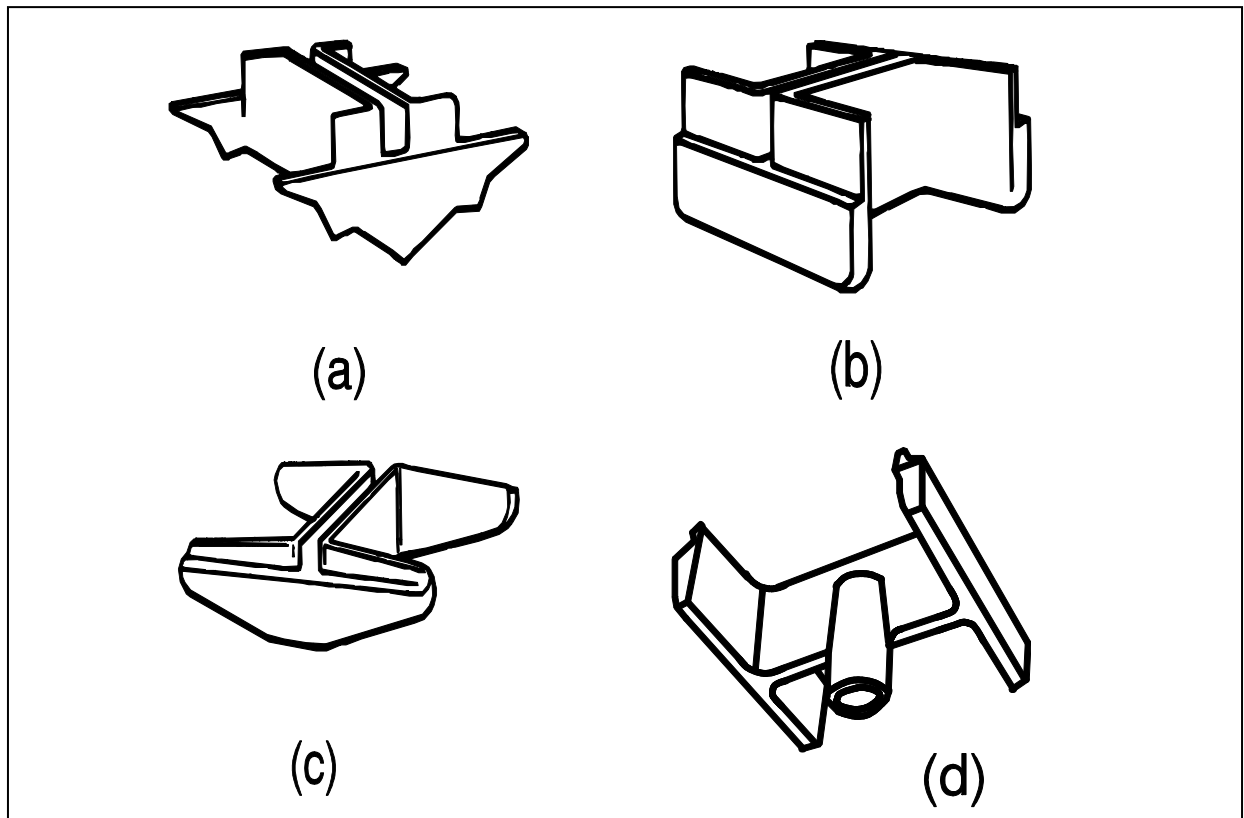


Figure 22.5 Driving Shoes for Protection of H-pile

22.2.2 Splices

H-pile splices are routinely made by full penetration groove welding along the web and both flanges, or with manufactured splicers such as the ones shown in Figures 22.6(a) and 22.6(b). For the manufactured splicer shown, a notch is cut into the web of the driven section of pile and the splicer is slipped over the pile. Short welds are then made to the flanges near the corners of the splicer. The top section must have the flanges chamfered to achieve effective welding. Typically the section of pile to be added is positioned and held while welds across flanges are made. H-pile splicers are fabricated from ASTM A 36 steel.

These splicers have been tested in the laboratory and the results have shown they provide full strength in bending as required by the AASHTO Bridge Specifications.

22.3 ACCESSORIES FOR STEEL PIPE PILES

22.3.1 Pile Toe Attachments

Problems during installation of closed end pipe piles arise when driving through materials containing obstructions. In this case, piles may deflect and deviate from their design alignment to an unacceptable extent. In case of driving open end pipe piles through or into very dense materials, the toe of the pile may be deformed. Pile toe attachments on closed end and open end piles are used to reduce the possibilities of damage and excessive deflection.

When pipe piles are installed with a closed end, a 12 to 25 mm (0.5 to 1 inch) thick flat plate is usually used as a form of toe protection. Conical toe attachments as shown in Figures 22.7(a) and 22.7(b) are also available as end-closures for pipe piles, although they generally cost more than flat plate type protection.

Generally, conical attachments have sixty degree configurations and are available with either an inside flange connection as shown in Figure 22.7(b) or outside flange connection as illustrated in Figure 22.7(a). The outside flange attachment can be driven with a press fit, so welding is not required. This additional benefit can save time and money.

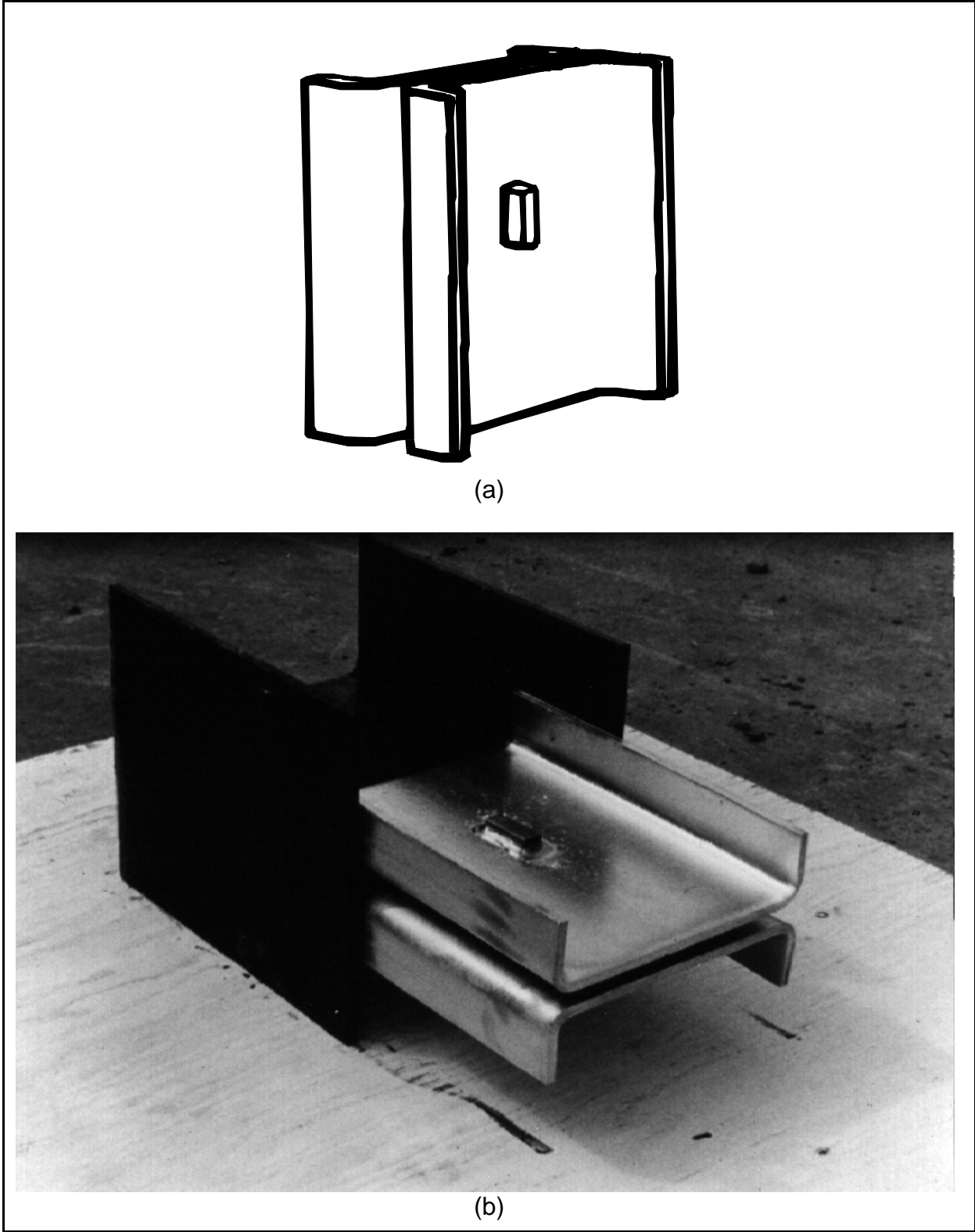


Figure 22.6 Typical H-pile Splicer

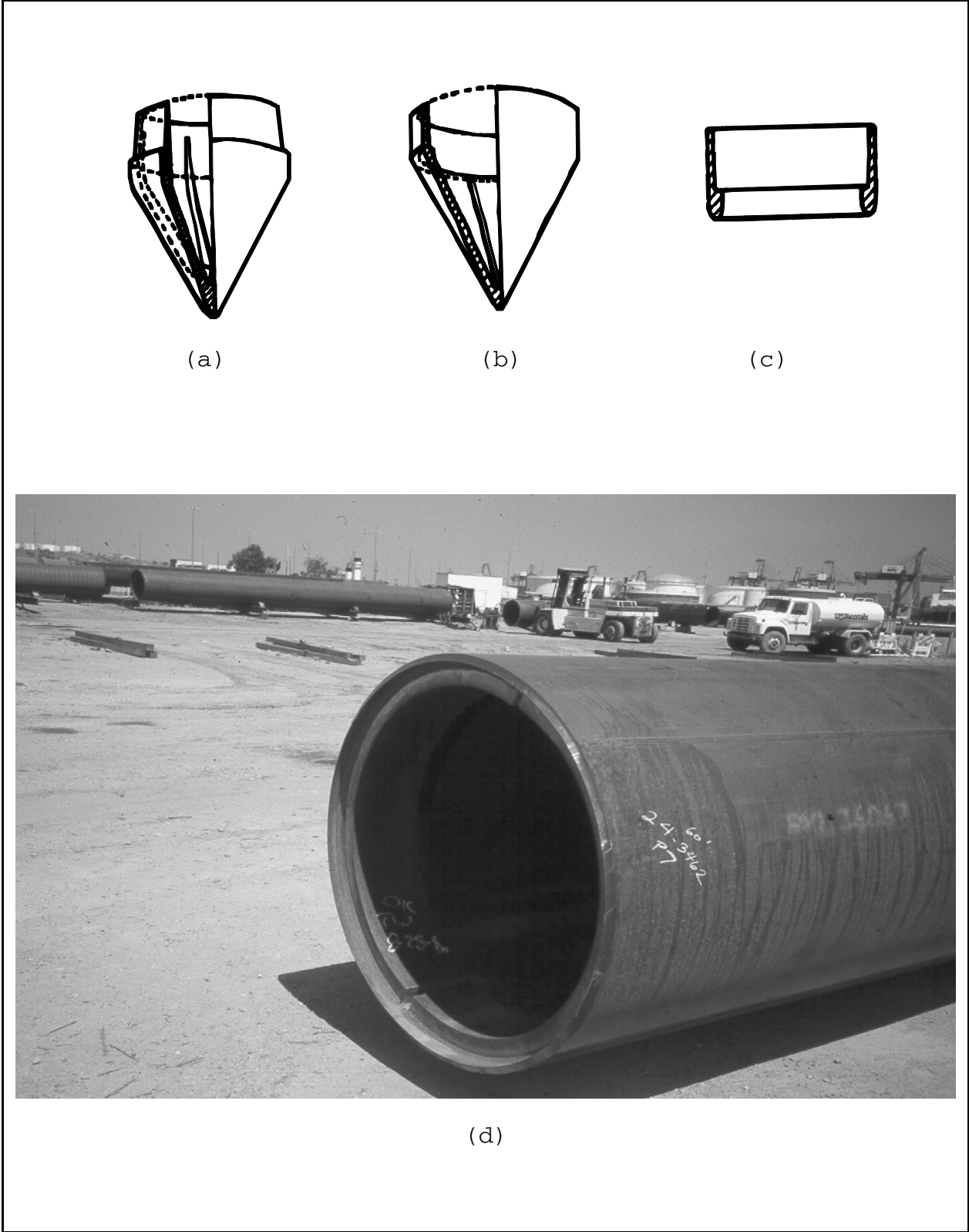


Figure 22.7 Pile Toe Attachments for Pipe Piles

When installing open end piles in dense gravel or to rock, the use of cutting shoes will help protect the piles and may make it possible to use thinner wall pipe. Cutting shoes are made from cast steel with a ridge for pile shoe bearing, as shown in Figure 22.7(c and d). Cutting shoes are welded to piles.

22.3.2 Splices

Full penetration groove welds or fillet welds as shown in Figure 22.8 are commonly used for splicing pipe piles. Pipe piles can also be spliced with manufactured splicers similar to the one shown in Figure 22.9. This splicer is fabricated from ASTM A 36 steel and is designed with a taper for a drive fit without welding so no advance preparation is required. Unless the drive fit or friction splicer is fillet welded to the pile, the splice will not provide full strength in bending.

22.4 PRECAST CONCRETE PILES

22.4.1 Pile Toe Attachments

The toe of precast concrete piles may be crushed in compression under hard driving. For hard driving conditions, or for end bearing on rock, special steel toe attachments can be used. Cast iron or steel shoes as depicted in Figure 22.10(a), or "Oslo Point" shown in Figure 22.10(b), are also used for toe protection. The characteristics of the Oslo Point are such that it can be chiseled into any type of rock to ensure proper seating. All toe attachments to precast concrete piles must be attached during casting of the piles and not in the field.

Another common type of toe attachment to increase concrete pile penetration depths in hard materials is a structural H sectional embedded in the pile, as shown in Figure 22.11. The H section extension is most often used to obtain additional penetration when uplift and scour are a concern. The H section should be proportionately sized to the concrete section to prevent overstressing and must be embedded sufficiently far for proper bonding and to develop bending strength. The H section should be protected by a H-pile toe attachment as discussed previously.

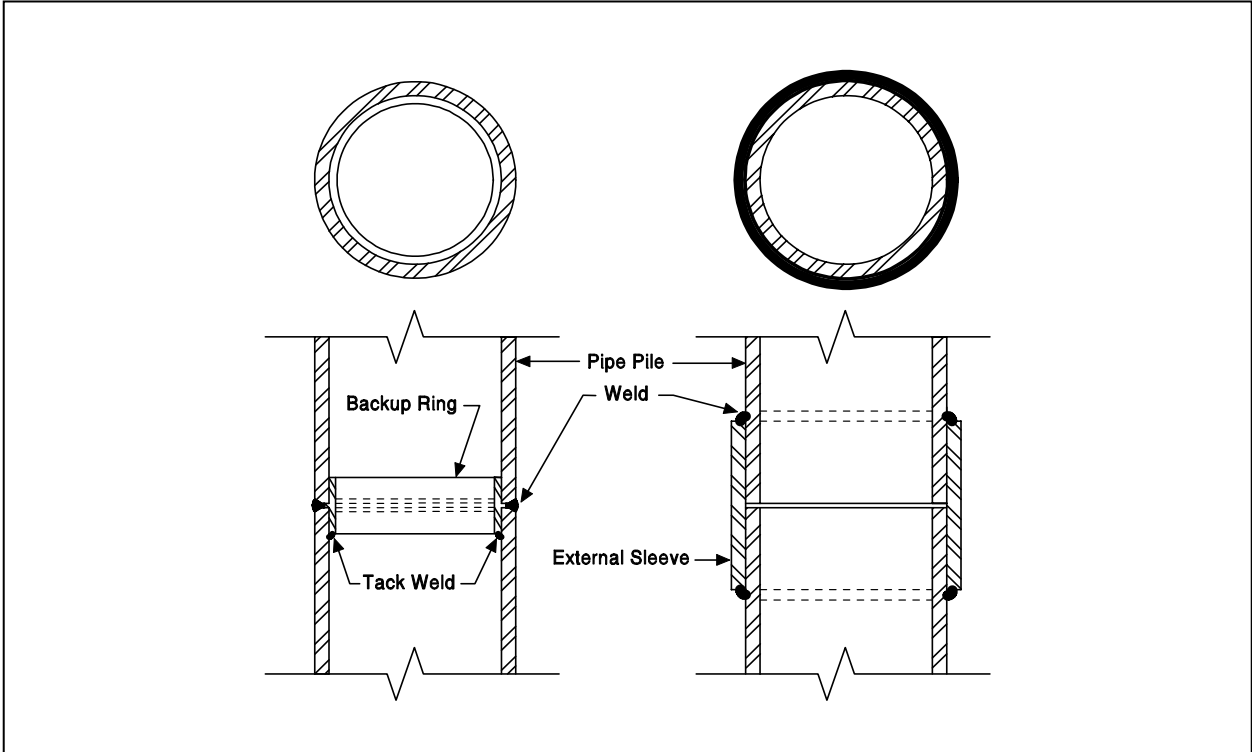


Figure 22.8 Splices for Pipe Piles

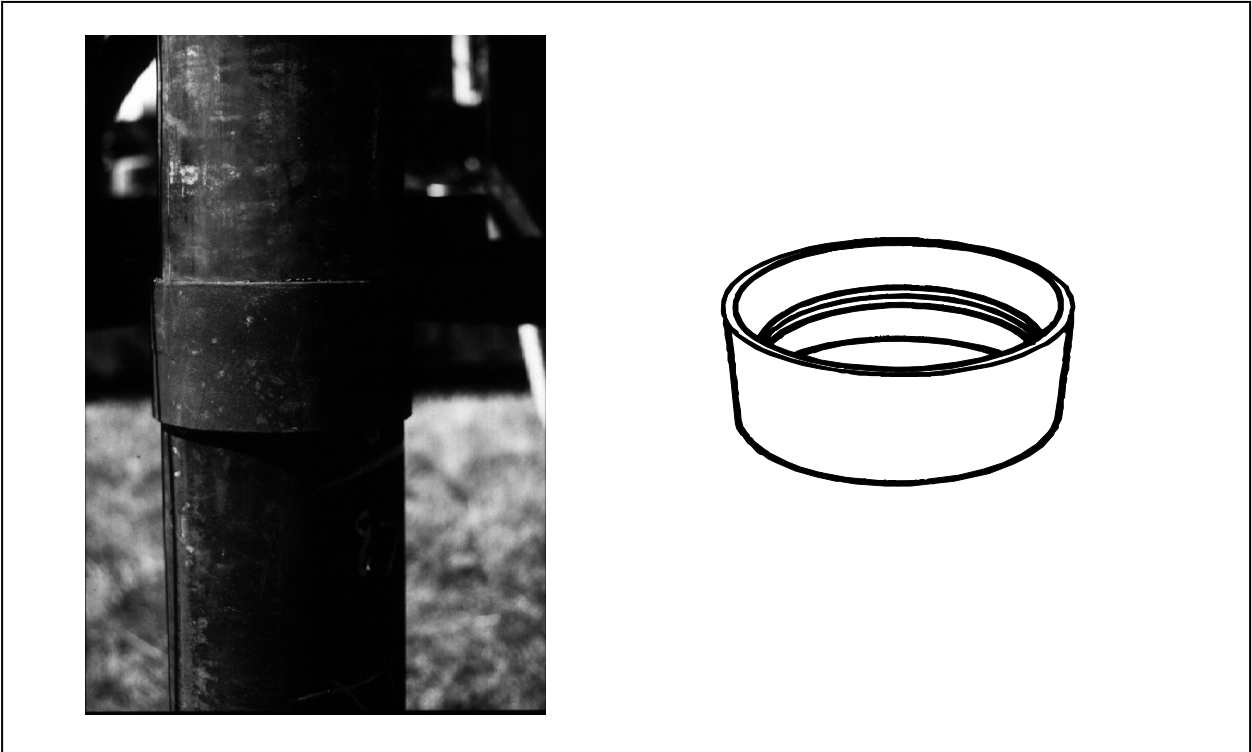


Figure 22.9 Splicer for Pipe Pile

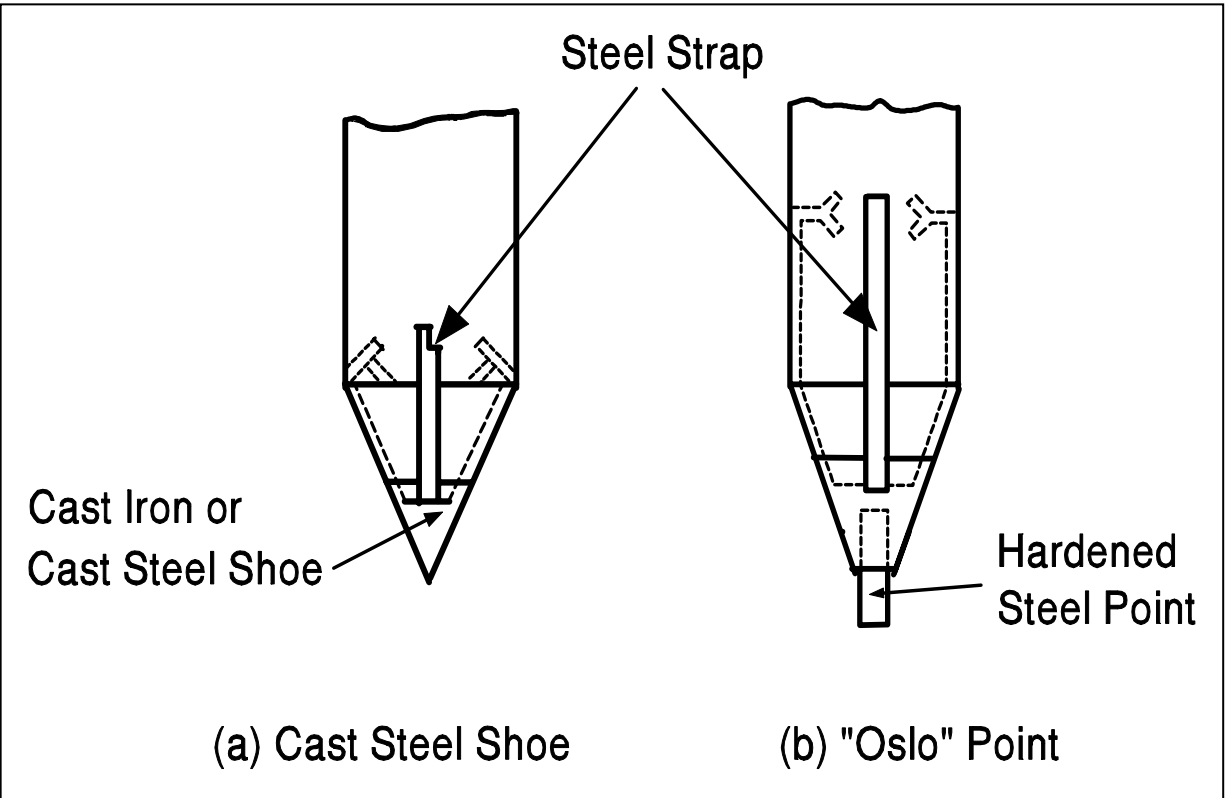


Figure 22.10 Pile Toe Attachments for Precast Concrete Piles

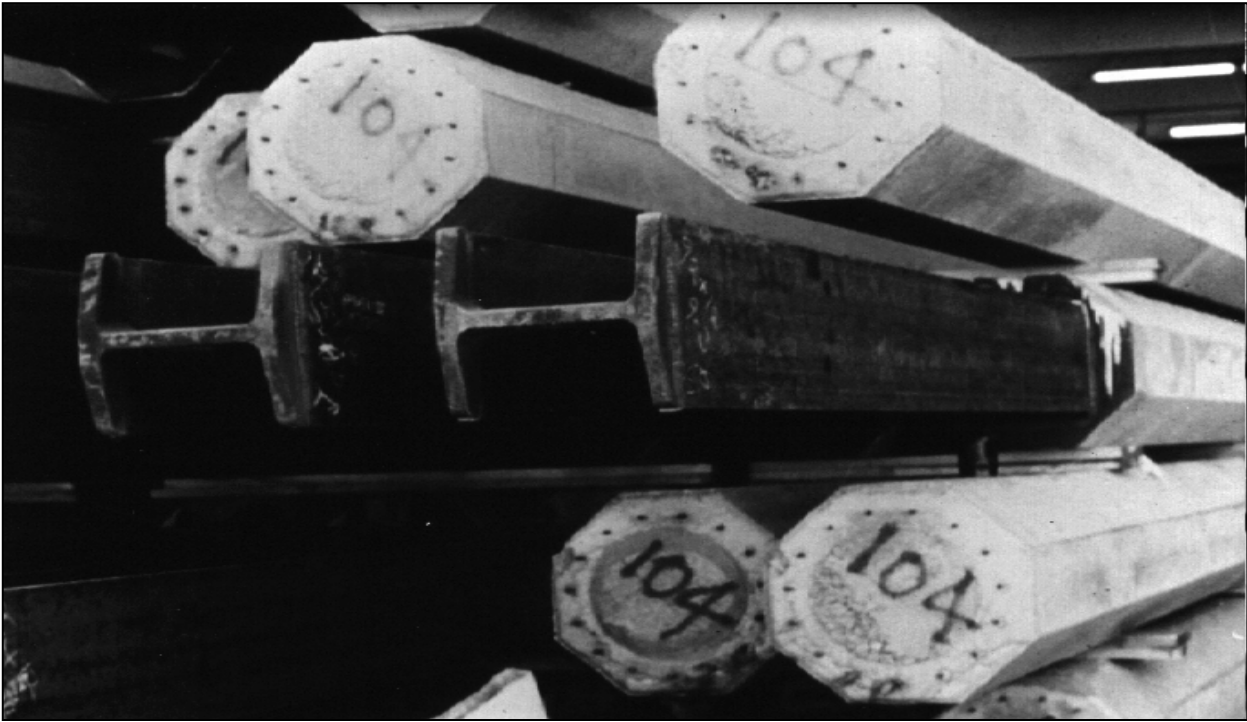


Figure 22.11 Steel H-pile Tip for Precast Concrete Pile

22.4.2 Splices

Most concrete piles driven in the United States are prestressed to minimize potential problems associated with handling and tension stresses during driving. However, the ends of prestressed concrete piles are not effectively prestressed due to development length, and thus special precautions must be taken when splicing prestressed concrete piles.

Table 22-1 from Bruce and Hebert (1974) shows a summary of splices for precast concrete piles. While this information is 20 years old, it still adequately summarizes the state of concrete pile splices. The table also provides guidelines concerning the compressive, tensile and flexural strength of the splice mechanisms. However, the actual performance of this and other splices should be evaluated on a project by project basis.

Whenever possible, concrete piles should be ordered with sufficient length to avoid splicing. However, if splicing is required, the splices available can be divided into four types: Dowel, Welded, Mechanical, and Sleeve. An overview of these splice types is given in Figure 22.12.

The generic epoxy dowel splice shown in Figure 22.13 can be used on prestressed and conventionally reinforced concrete piles. The bottom pile section to be spliced has holes which receive the dowels. These holes may be cast into the pile when splicing is planned, or drilled in the field when splicing is needed, but was unexpected. The bottom section is driven with no special consideration and the top section is cast with the dowel bars in the end of the pile. When spliced together in the field, the top section with the protruding dowels is guided and set in position and a thin sheet metal form is placed around the splice. Epoxy is then poured, filling the holes of the bottom section and the small space between the piles. The form can be removed after 15 minutes and driving resumed after curing of the epoxy. Dowel splices may be time consuming but are comparatively inexpensive. These splices have been proven reliable if dowel bars are of sufficient length and strength, and if proper application of the epoxy is provided. The number, length, and location of the dowel holes, as well as the dowel bar size, must be designed.

TABLE 22-1 SUMMARY OF PRECAST CONCRETE PILE SPLICES*							
Name of Splice	Type	Origin	Approximate Size Range (mm)	Approximate Field Time minutes	Strength		
					Percent Compressive	Percent Tensile	Percent Flexural Cracking
Marrier	Mechanical	Canada	254-330	30	100	100	100
Herkules	Mechanical	Sweden	254-508	20	100	100	100
ABB	Mechanical	Sweden	254-305	20	100	100	100
NCS	Welded	Japan	305-1195	60	100	100	100
Tokyu	Welded	Japan	305-1195	60	100	100	100
Raymond cyl. Bolognesi-Mor.	Welded	USA	914-1372	90	100	100	100
Japanese bolted	Welded	Argentina	Varied	60	100	55	100
Brunsplice	Bolted	Japan	Varied	30	100	90	90
Anderson	Connect-ring	USA	305-355	20	100	20	50
Fuentes	Sleeve	USA	Varied	20	100	0	100
Hamilton form	Weld-sleeve	Puerto Rico	254-305	30	100	100	100
Cement dowel	Sleeve	USA	Varied	90	100	75	100
Macalloy	Dowel	USA	Varied	45	100	40	65
Mouton	Post-tension	England	Varied	120	100	100	100
Raymond wedge	Combination	USA	254-355	20	100	40	100
Pile coupler	Welded wedge	USA	Varied	40	100	100	100
Nilsson	Connect-ring	USA	305-1372	20	100	100	100
Wennstrom	Mechanical	Sweden	Varied	20	100	100	100
Pogonowski	Wedge	Sweden	Varied	20	100	100	100
	Mechanical	USA	Varied	20	100	100	100

* (after Bruce and Herbert, 1974)

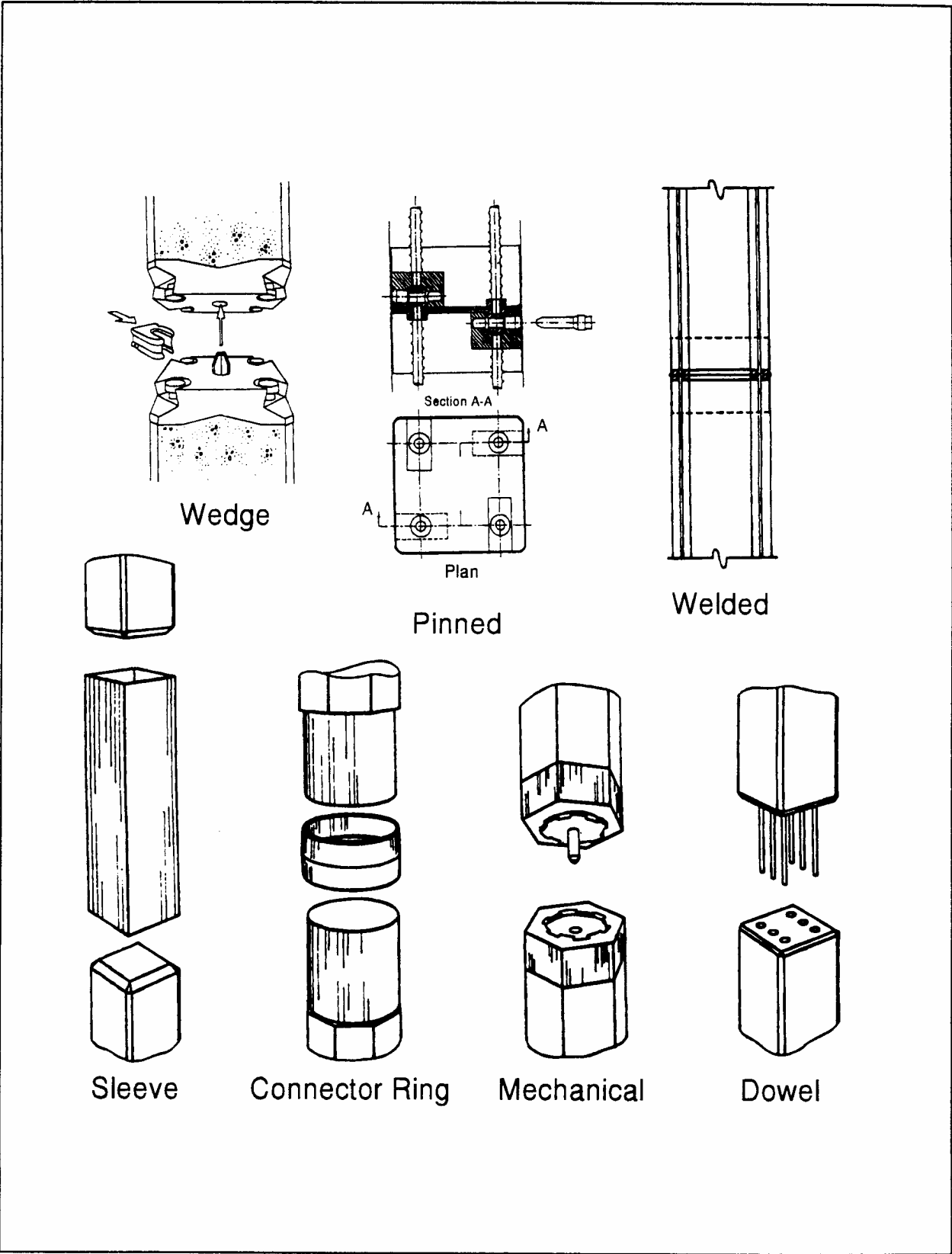


Figure 22.12 Commonly used Prestressed Concrete Pile Splices (after PCI, 1993)

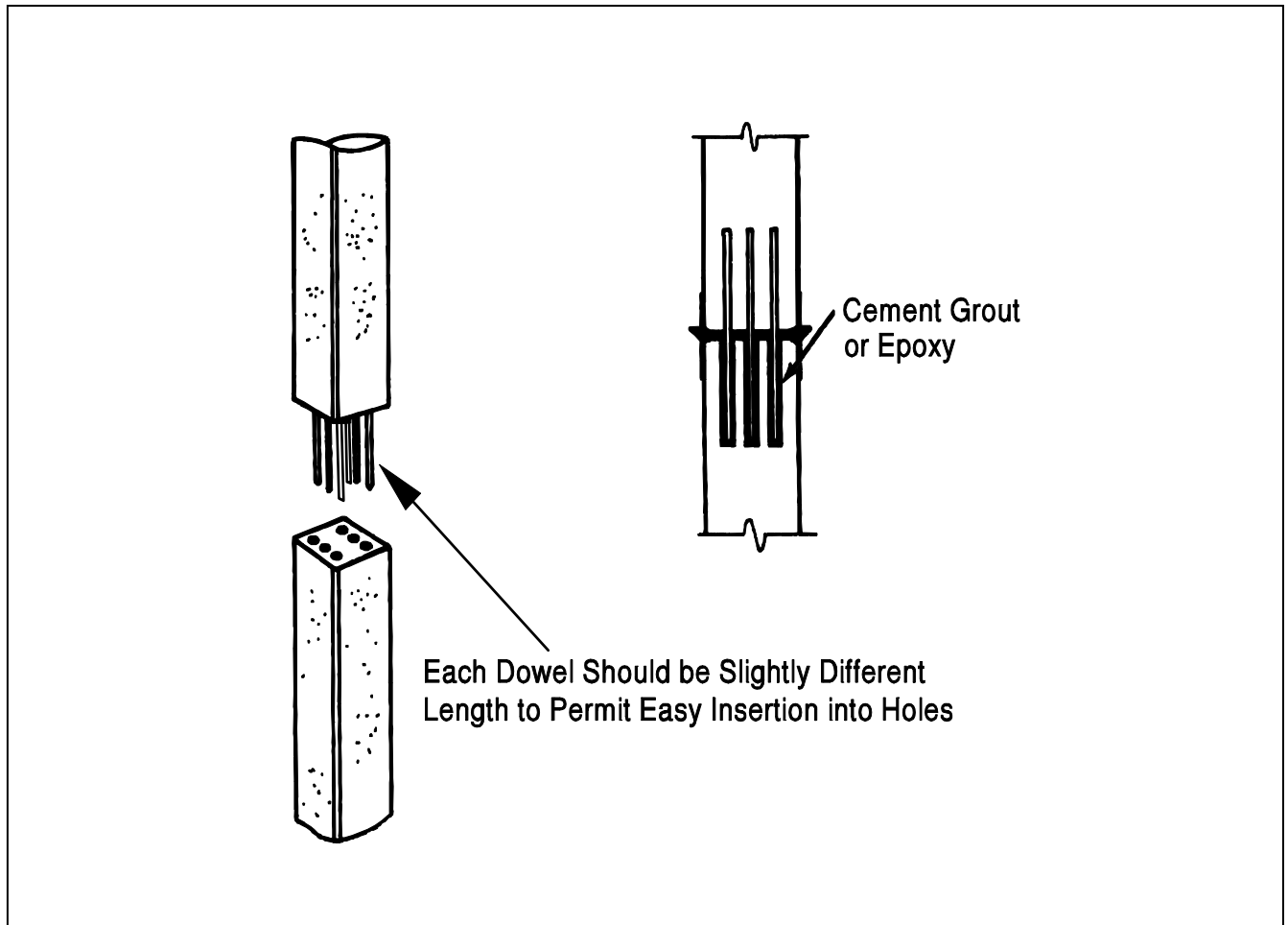


Figure 22.13 Cement-Dowel Splice (after Bruce and Herbert, 1974)

Welded splices require steel fittings be cast at the end of the sections to be spliced. The two sections are then welded around the entire perimeter. Most mechanical splices, such as the Herkules, Harddrive, Sure Lock, ABB, and Dyn-A-Splice, among others, are made of steel castings and are available for square, octagonal, hexagonal, and/or round sectional shapes. They can be used either for reinforced or prestressed concrete piles and are cast into the pile at the time of manufacture. The Herkules splice requires mating both male and female castings, while most other mechanical splices are gender neutral. All mechanical splices are then locked by inserting wedges, pins, keys, or other mechanical connections after aligning the sections. Although mechanical splices can be expensive, they do save considerable time and they have been designed to properly account for all loading conditions, including tension.

Sleeve type concrete splices can also be rapidly applied and are very effective in reducing tension driving stresses, but they cannot be used where static uplift loading will be required. The sleeve must have sufficient length and strength if lateral or bending loads are anticipated. The shorter connector ring design has limited tensile and flexural strength and is generally not recommended.

If a specific splice is specified based on previous experience, then an option for substituting some other concrete splice should not be allowed unless the substitute splicer is field tested. The alternative splice should be required to have equivalent compressive, tensile, and flexural strength to the originally specified splice. The substitute splicer can be tested by driving a number of spliced test piles and observing the performance.

22.5 A LIST OF MANUFACTURERS AND SUPPLIERS OF PILE ACCESSORIES

1. A-Joint Corporation (concrete splices)
P.O. Box 1247
Marlton, NJ 08053
Ph: 856-767-0609; Fax: 856-767-7458

2. Associated Pile and Fitting Corporation (shoes and splices)
P.O. Box 1048
Clifton, NJ 07014-1048
Ph: 800-526-9047, 973-773-8400; Fax: 973-773-8442
www.associatedpile.com

3. Dougherty Foundation Products (shoes and splicers)
P.O. Box 688
Franklin Lakes, NJ 07417
Ph: 201-337-5748; Fax: 201-337-9022
www.pilelineonline.com

4. DPNicoli (shoes and splices)
19600 S.W. Cipole Road
Tualatin, OR 97062
Ph: 800-695-5006; Fax: 503-692-1799
www.dpnicoli.com

5. Gulf Coast Pre-stress, Inc. (concrete splices)
P.O. Box 825
Pass Christian, MS 39571
Ph: 228-452-9486; Fax: 228-452-9495
www.gcprestress.com

6. HMC Foundation Equipment (shoes and splices)
P.O. Box 5198
Fort Wayne, IN 46895
Ph: 800-348-1890, 219-424-0405; Fax: 219-422-2040
www.hmc-us.com

7. International Pipe Products
P.O. Box 546
Ambridge, PA 15003
Ph: 412-266-8110; Fax: 412-266-4766

8. National Ventures, Inc. (concrete splices)
264 Cazneau Avenue
Saussalito, CA 94965
Ph: 415-331-7260; Fax: 415-331-7261
www.pilesplices.com

9. Versabite Piling Accessories (shoes and splices)
1704 Tower Industrial Drive
Monroe, NC 28110
Pn. 800-280-9950; Fax: 704-225-1567

REFERENCES

- American Wood Preservers Institute (1981). Splicing Treated Timber Piling. AWPI Technical Guidelines for Pressure Treated Wood, 2.
- American Wood Preservers Institute (1981). Specification for Strapping Timber Piling, PH.
- Bruce, R.N. and Hebert, D.C. (1974). Splicing of Precast Prestressed Concrete Piles, Parts I and II, PCI Journal, Volume 19, No. 5 and 6, September-October and November-December, 1974.
- Dougherty, J.J. (1978). Accessories for Pile Installation. Presentation made at the ASCE Metropolitan Section Seminar on Pile Driving and Installation.
- PCI (1993). Precast/Prestressed Concrete Institute Journal. Volume 38, No. 2, March-April, 1993.

Chapter 23 INSPECTION OF PILE INSTALLATION

Knowledgeable supervision and inspection play a very important role in the proper installation of pile foundations. The present trend in pile foundation design and construction is to use larger piles with higher load capacities, installed by larger equipment to achieve cost savings, made possible by advances in the state-of-the-art of design and construction methods. The inspection of these higher capacity pile installations becomes critical because of less redundancy (fewer piles required), and the smaller tolerances and factors of safety.

Inspection is only as good as the knowledge, experience and qualifications of the inspector. The inspector must understand the operation of the hammer and its accessories, the pile behavior, the soil conditions, and how these three components interact. Most pile installation problems are avoidable if a competent inspector uses systematic inspection procedures coupled with good communication and cooperation with the contractor. The inspector must be more than just a "blow counter". The inspector is the "eyes and ears" for the engineer and the owner. Timely observations, suggestions, reporting, and correction advice can ultimately assure the success of the project. **The earlier a problem or unusual condition is detected and reported by the inspector, the earlier a solution or correction in procedures can be applied, and hence a potentially negative situation can be limited to a manageable size.** If the same problem is left unattended, the number of piles affected increases, as do the cost of remediation and the potential for claims or project delays. Thus, early detection and reporting of any problem may be critical to keep the project on schedule and within budget.

An outline of inspection procedures and maintenance of pile driving records is provided in this chapter. Procedures and record keeping methods should be refined periodically as more experience is gathered by those responsible for construction operations.

23.1 ITEMS TO BE INSPECTED

There are several items to be checked by the inspector on every pile foundation project for test piles and/or production piles. Test piles may be driven for establishing order lengths or for load testing. Each of these items can be grouped under one of the following areas:

1. Review of the foundation design report, project plans and specifications prior to the arrival at the project site.
2. Inspection of piles prior to installation.
3. Inspection of pile driving equipment both before and during operation.
4. Inspection of test or indicator piles.
5. Inspection during production pile driving and maintenance of driving records.

A flow chart identifying the key components of the pile inspection process is presented in Figure 23.1.

23.2 REVIEW OF PROJECT PLANS AND SPECIFICATIONS

The first task of an inspector is to thoroughly review the project plans and specifications as they pertain to pile foundations. All equipment and procedures specified, including any indicator or test program of static and/or dynamic testing, should be clearly understood. If questions arise, clarification should be obtained from the originator of the specifications. The preliminary driving criteria should be known, as well as methods for using the test program results to adjust this criteria to site specific hammer performance and soil conditions. At this stage, the pile inspector should also determine the responsibility of his/her organization and should have answers to the following questions:

1. Is the inspector on the project in an observational capacity reporting to the foundation designer?, or

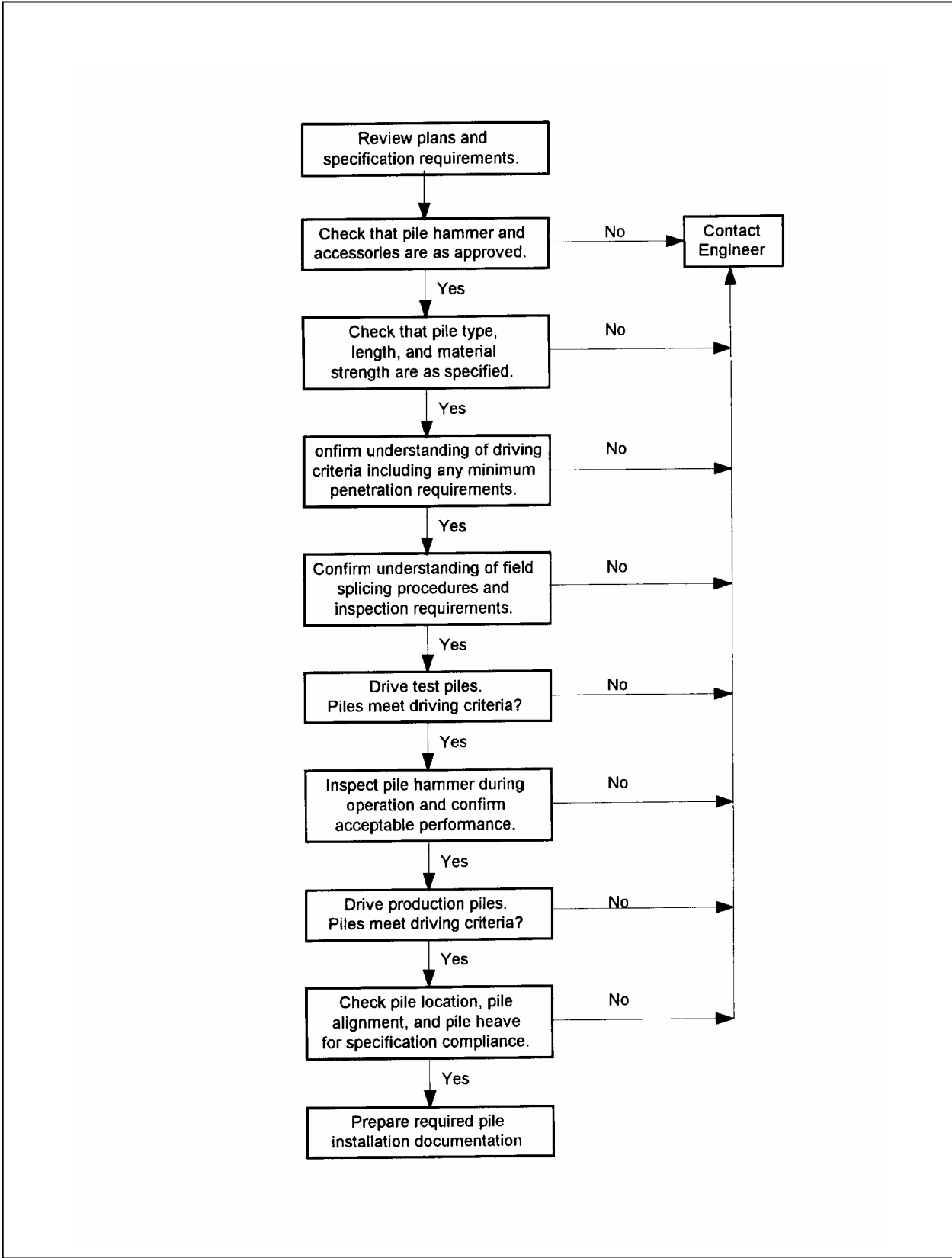


Figure 23.1 Pile Inspection Flow Chart

2. Does his/her organization have the direct responsibility to make decisions during driving of the test pile(s) and/or the production piles?

The inspector should also know:

1. Whom to contact if something goes wrong, and/or where to seek advice.
2. Whom to send copies of driving records and daily inspection reports.
3. What is required in the report during driving and at the completion of the project.

23.3 INSPECTOR'S TOOLS

The following check list, modified from Williams Earth Science (1995) summarizes the tools a pile inspector should have readily available to perform their job.

Approved Job Information

- Project Plans and Specifications with Revisions
- Special Provisions
- Pile Installation Plan
- Driving Criteria
- Casting/Ordered Lengths
- Approved Splice Detail

Daily Essentials

- Hard Hat
- Boots
- Ear Protection
- Pen/Pencil (and spare)
- Scale
- Measuring Tape
- Builder's Square
- Level
- Watch
- Calculator
- Camera

Indexed Notebook of Driven Piles

- Test Pile Program
- Production
- Construction Daily

Blank Forms

- Pile Driving Log
- Daily Inspection Reports
- Personal Diary

References

- State Standard Specifications
- Design and Construction of Driven Pile Foundations (Vol. II)
- Performance of Pile Driving Systems Inspectors Manual (FHWA/RD-86/160)

23.4 INSPECTION OF PILES PRIOR TO AND DURING INSTALLATION

The inspection check list will be different for each type of pile, but some items will be the same. A certificate of compliance for the piles is generally required by the specifications. The inspector should obtain this certificate from the contractor and compare the specification requirements with the information provided on the certificate. The following sections contain specific guidance for each major pile type.

23.4.1 Timber Piles

Physical details for round timber piles are sometimes referred to in the ASTM pile specification, ASTM D25. Regardless of the referenced specifications, the following items should be checked for compliance:

- a. The timber should be of the specified species.
- b. The piles should have the specified minimum length, and have the correct pile toe and butt sizes. The pile butt must be cut squarely with the pile axis.
- c. The twist of spiral grain and the number and distribution of knots should be acceptable.
- d. The piles should be acceptably straight.
- e. The piles must be pressure treated as specified.
- f. The pile butts and/or toe may require banding as detailed in Chapter 22.
- g. Steel shoes which may be specified must be properly attached. Details are provided in Chapter 22.
- h. Pile splices, if allowed by plans and specifications, must meet the project requirements.

23.4.2 Precast Concrete Piles

On many projects, inspection and supervision of casting operations for precast concrete piles is provided by the State transportation department. Frequently, in lieu of this

inspection, a certificate of compliance is required from the contractor. The following checklist provides items to be inspected at the casting yard (when applicable):

- a. Geometry and other characteristics of the forms.
- b. Dimensions, quantity, and quality of spiral reinforcing and prestressing steel strands, including a certificate indicating that the prestressing steel meets specifications.
- c. If the pile is to have mechanical or welded splices, or embedded toe protection, the splice or toe protection connection details including number, size and lengths of dowel bars should be checked for compliance with the approved details and for the required alignment tolerance. They should be cast within tolerance of the true axial alignment.
- d. Quality of the concrete (mix, slump, strength, *etc.*) and curing conditions.
- e. Prestressing forces and procedures, including time of release of tension, which is related to concrete strength at time of transfer.
- f. Handling and storage procedures, including minimum curing time for concrete strength before removal of piles from forms.

The following is a list of items for prestressed concrete piles to be inspected at the construction site:

- a. The piles should be of the specified length and section. Many specifications require a minimum waiting period after casting before driving is allowed. Alternatively, the inspector must be assured that a minimum concrete strength has been obtained. If the piles are to be spliced on the site, the splices should meet the specified requirements (type, alignment, *etc.*).
- b. There should be no evidence that any pile has been damaged during shipping to the site, or during unloading of piles at the site. Lifting hooks are generally cast into the piling at pick-up points. Piles should be unloaded by properly sized and tensioned slings attached to each lifting hook. Piles should be inspected for cracks or spalling.

- c. The piles should be stored properly. When piles are being placed in storage, they should be stored above ground on adequate blocking in a manner which keeps them straight and prevents undue bending stresses.
- d. The contractor should lift the piles into the leads properly and safely. Cables looped around the pile are satisfactory for lifting. Chain slings should never be permitted. Cables should be of sufficient strength and be in good condition. Frayed cables are unacceptable and should be replaced. For shorter piles, a single pick-up point may be acceptable. The pick-up point locations should be as specified by the casting yard. For longer piles, two or more pick-up points at designated locations may be required.
- e. The pile should be free to twist and move laterally in the helmet.
- f. Piles should have no noticeable cracks when placed in leads or during installation. Spalling of the concrete at the top or near splices should not be evident.

23.4.3 Steel H-Piles

The following should be inspected at the construction site:

- a. The piles should be of the specified steel grade, length, or section/weight.
- b. Pile shoes, if required for pile toe protection, should be as specified. Pile shoe details are provided in Chapter 22.
- c. Splices should be either proprietary splices or full penetration groove welds as specified. The top and bottom pile sections should be in good alignment before splicing. Pile splice details are discussed in Chapter 22.
- d. Pile shoe attachments and splices must be welded properly.
- e. The piles being driven must be oriented with flanges in the correct direction as shown on the plans. Because the lateral resistance to bending of H-piles is considerably more in the direction perpendicular to flanges, the correct orientation of H-piles is very important.

- f. There should be no observable pile damage, including deformations at the pile head.

23.4.4 Steel Pipe Piles

The following should be inspected at the construction site:

- a. The piles should be of specified steel grade, length, or minimum section/weight (wall thickness) and either seamless or spiral welded as specified.
- b. Piles should be driven either open-ended or closed-ended. Closed-ended pipe piles should have bottom closure plates or conical points of the correct size (diameter and thickness) and be welded on properly, as specified. Open end pipe piles should have cutting shoes that are welded on properly.
- c. The top and bottom pile sections should be in good alignment before splicing. Splices or full penetration groove welds should be installed as specified. Pile splice details are discussed in Chapter 22.
- d. There should be no observable pile damage, including deformations at the pile head. After installation, closed-end pipes should be visually inspected for damage or water prior to filling with concrete.

23.5 INSPECTION OF DRIVING EQUIPMENT

A typical driving system consists of crane, leads, hammer, hammer cushion, helmet, and in the case of concrete piles, a pile cushion. As discussed in Chapter 21, each component of the drive system has a specific function and plays an important role in the pile installation. The project plans and specifications may specify or restrict certain items of driving equipment. The inspector must check the contractor's driving equipment and obtain necessary information to determine conformity with the plans and specifications prior to the commencement of installation operations.

The following checklist will be useful in the inspection of driving equipment before driving:

1. The pile driving hammer should be the specified type/size.

Usually the specifications require certain hammer types and/or specify minimum and/or maximum energy ratings. A listing of hammer energy ratings is provided in Appendix D. The inspector should make sure for single acting air/steam or hydraulic hammers that the contractor uses the proper size external power source and that, for adjustable stroke hammers, the stroke necessary for the required energy be obtained.

For double acting or differential air/steam or hydraulic hammers, the contractor must again obtain the proper size external power source and the operating pressure and volume must meet the hammer manufacturer's specification. For open end diesel hammers, the inspector should obtain a chart for determining stroke from visual observation, or alternatively have available a device for electronically estimating the stroke from the blow rate. For closed end diesel hammers, the contractor should supply the inspector with a calibration certificate for the bounce chamber pressure gauge and a chart which correlates the bounce chamber pressure with the energy developed by the hammer. The bounce chamber pressure gauge should be provided by the contractor.

2. The hammer cushion being used should be checked to confirm it is of the approved material type, size and thickness.

The main function of the hammer cushion is to protect the hammer itself from fatigue and high frequency accelerations which would result from steel to steel impact with the helmet and/or pile. The hammer cushion should have the proper material and same shape/area to snugly fit inside the helmet (drive cap). If the cushion diameter is too small, the cushion will break or badly deform during hammer blows and become ineffective. The hammer cushion must not be excessively deformed or compressed. Some air/steam hammers rely upon a certain total thickness (of cushion plus striker plate) for proper valve timing. Hammers with incorrect hammer cushion thickness may not operate, or will have improper kinetic energy at impact. Since it is difficult to inspect this item once the driving operation begins, it should be checked before the contractor starts pile driving on a project as well as periodically during production driving on larger projects. A photograph of a hammer cushion check is presented in Figure 23.2.



Figure 23.2 Hammer Cushion Check



Figure 23.3 Damaged Hammer Cushion



Figure 23.4 Pile Cushion Replacement

The hammer cushion material disks are shown in the lower right corner of the photograph. A damaged hammer cushion detected by a hammer cushion check is shown in Figure 23.3.

3. The helmet (drive cap) should properly fit the pile.

The purpose of the helmet is to hold the pile head in alignment and transfer the impact concentrically from the hammer to the pile. The helmet also houses the hammer cushion, and must accommodate the pile cushion thickness for concrete piles. The helmet should fit loosely to avoid transmission of torsion or bending forces, but not so loosely as to prevent the proper alignment of hammer and pile. Helmets should ideally be of roughly similar size to the pile diameter. Although generally discouraged, spacers may be used to adapt an oversize helmet, provided the pile will still be held concentrically with the hammer. A properly fitting helmet is important for all pile types, but is particularly critical for precast concrete piles. A poorly fitting helmet often results in pile head damage. Check and record the helmet weight for conformance to wave equation analysis or for future wave equation analysis. Larger weights will reduce the energy transfer to the pile.

4. The pile cushion should be of correct type material and thickness for concrete piles.

The purpose of the pile cushion is to reduce high compression stresses, to evenly distribute the applied forces to protect the concrete pile head from damage, and to reduce the tension stresses in easy driving. Pile cushions for concrete piles should have the required thickness determined from a wave equation analysis but not less than 100 mm (4 inches). A new plywood, hardwood, or composite wood pile cushion, which is not water soaked, should be used for every pile. The cushion material should be checked periodically for damage and replaced before excessive compression (more than half the original thickness), burning, or charring occurs. Wood cushions may take only about 1,000 to 2,000 blows before they deteriorate. During hard driving, more than one cushion may be necessary for a single pile. Longer piles or piles driven with larger hammers may require thicker pile cushions. A photograph of a pile cushion being replaced is presented in Figure 23.4.

5. Predrilling, jetting or spudding equipment, if specified or permitted, should be available for use and meet the requirements. The depth of predrilling, jetting or spudding should be very carefully controlled so that it does not exceed the allowable

limits. Predrilling, jetting, or spudding below the allowed depths will generally result in a reduced pile capacity, and the pile acceptance may become questionable. Additional details on predrilling, jetting, and spudding are presented in Chapter 21.

6. The lead system being used must conform to the requirements, if any, in the specifications. Lead system details are presented in Chapter 21.

The leads perform the very important function of holding the hammer and pile in good alignment with each other. Poor alignment reduces energy transfer as some energy is then imparted into horizontal motion. Poor alignment also generally results in higher bending stresses and higher local contact stresses which can cause pile damage. This is particularly important at end of driving when penetration resistance is highest and driving stresses are generally increased. Sometimes the specifications do not allow certain lead systems or may require a certain type system. A pile gate at the lead bottom which properly centers the pile should be required, as it helps maintain good alignment.

Note: On most projects, a wave equation analysis is used to determine preliminary driving criteria for design and/or construction control. The contractor is usually required to provide a pile and driving equipment data form similar to Figure 16.3 and obtain prior approval from the State transportation agency. Even if wave equation analysis is not required, this form should be included in the project files so a wave equation analysis could be performed in the future. This form can also function as a check list for the inspector to compare the proposed equipment with the actual equipment on-site.

23.6 INSPECTION OF DRIVING EQUIPMENT DURING INSTALLATION

The main purpose of inspection is to assure that piles are installed so that they meet the driving criteria and the pile remains undamaged. The driving criteria is often defined as a minimum penetration resistance as measured by the blow count in blows per 0.25 meter (blows per foot). The driving criteria is to assure that piles have the desired capacity. However, the penetration resistance is also dependent upon the performance of the pile driving hammer. The penetration resistance will generally be lower when the hammer imparts higher energy and force to the pile, and the penetration resistance will be higher if the hammer imparts lower energy and force to the pile. High penetration resistances can be due either to soil resistance or to a poorly performing hammer. Thus, for the inspector

to assure that the minimum driving criteria has been met and therefore the capacity is adequate, the inspector must evaluate if the hammer is performing properly.

Each hammer has its own operating characteristics; the inspector should not blindly assume that the hammer on the project is in good working condition. In fact, two different types of hammers with identical energy rating will not drive the same pile in the same soil with the same penetration resistance. In fact, two supposedly identical hammers (same make and model) may not have similar driving capability due to several factors including differing friction losses, valve timing, air supply hose type-length-condition, fuel type and intake amount, and other maintenance status items. The inspector should become familiar with the proper operation of the hammer(s) used on site. The inspector may wish to contact the hammer manufacturer or supplier who generally will welcome the opportunity to supply further information. The inspector should review the operating characteristics for the hammer which are included in Chapter 21. The following checklists briefly summarize key hammer inspection issues.

23.6.1 Drop Hammers

- a. Determine/confirm the ram weight. Ram weight can be calculated from the ram volume and steel density of 78.5 kN/m^3 (492 lbs/ft^3) if necessary.
- b. The leads should have sufficient tolerance and/or the guides greased to allow the ram to fall without obstruction or binding.
- c. Make sure the desired stroke is maintained. Low strokes will reduce energy. Excessively high strokes increase pile stresses and could cause pile damage.
- d. Make sure the helmet stays properly seated on the pile and that the hammer and pile maintain alignment during operation.
- e. Make sure the hammer hoist line is spooling out freely during the drop and at impact. If the hoist line drags, less energy will be delivered. If the crane operator catches the ram too early, not only is less energy delivered, but energy is transmitted into the hoist line, crane boom, and hoist, which could cause maintenance and/or safety problems.

23.6.2 Single Acting Air/Steam Hammers

- a. Determine/confirm the ram weight. Ram weight can be calculated from the ram volume and steel density of 78.5 kN/m^3 (492 lbs/ft^3) if necessary. Check for and record any identifying labels as to hammer make, model and serial number.
- b. Check the air or steam supply and confirm it is of adequate capacity to provide the required pressure and flow volume. Also check the number, length, diameter, and condition of the air/steam hoses. Manufacturers provide guidelines for proper compressors and supply hoses. Air should be blown through the hose before attaching it to the hammer. The motive fluid lubricator should occasionally be filled with the appropriate lubricant as specified by the manufacturer. During operation, check that the pressure at the compressor or boiler is equal to the rated pressure plus hose losses. The pressure should not vary significantly during driving. The photograph of an air compressor display panel in Figure 23.5 illustrates the discharge pressure dial that should be checked.
- c. Visually inspect the slide bar and its cams for excessive wear. Some hammers can be equipped with a slide bar with dual set of cams to offer two different strokes. The stroke can be changed with a valve, usually operated from the ground. Measure the stroke being attained and confirm it meets specification.
- d. Check that the columns or ram guides, piston rod, and slide bar are well greased.
- e. For most air/steam hammers, the total thickness of hammer cushion and striker plate must match the hammer manufacturer's recommendation and the hammer cushion cavity in the helmet for proper valve timing and hammer operation. This thickness must be maintained and should be checked before placing the helmet into the leads, and thereafter by comparison of cam to valve position and/or gap between ram and hammer base when the ram is at rest on the pile top.
- f. Make sure the helmet stays properly seated on the pile and that the hammer and pile maintain alignment during operation.
- g. The ram and column keys used to fasten together hammer components should all be tight.

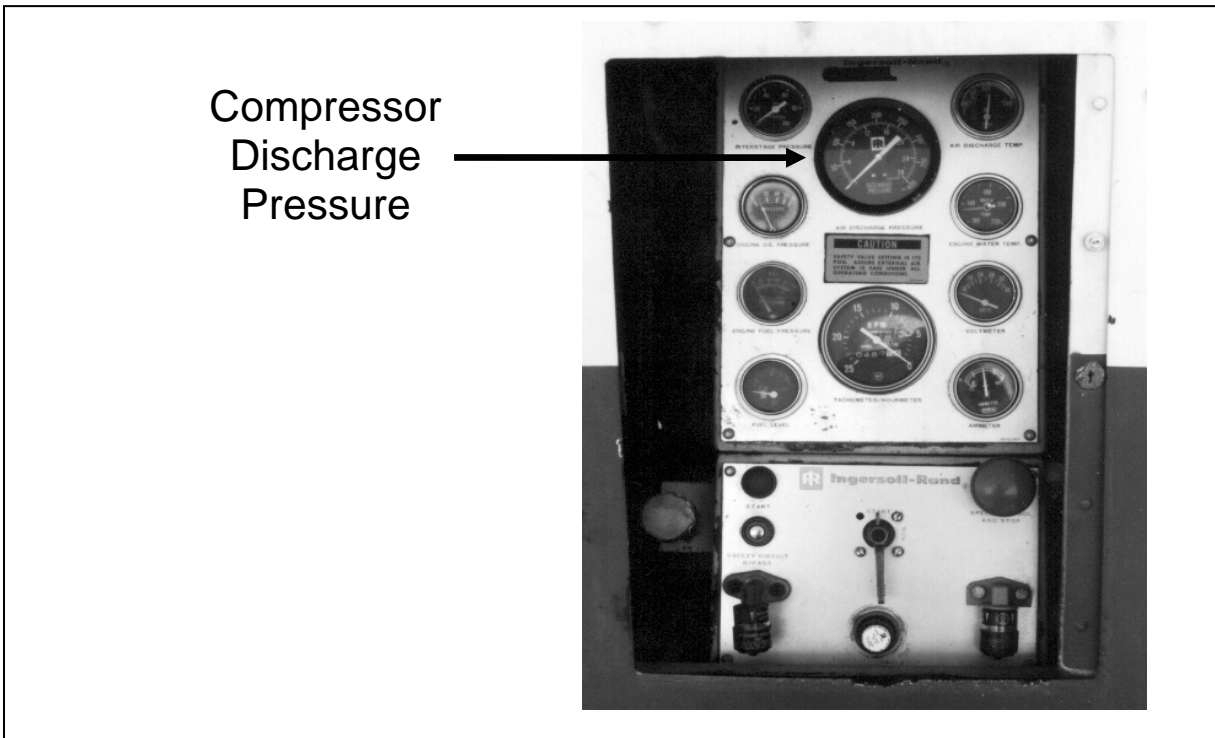


Figure 23.5 Air Compressor Display Panel

- h. The hammer hoist line should always be slack, with the hammer's weight fully carried by the pile. Excessive tension in the hammer hoist line is a safety hazard and will reduce energy to the pile. Leads should always be used.
- i. Compare the observed hammer speed in blows per minute near end of driving with the manufacturer's specifications. Blows per minute can be timed with a stopwatch or a saximeter. Slower operating rates may imply a short stroke (from inadequate pressure or volume, restricted or undersized hose, or inadequate lubrication) or improper valve timing (possibly from incorrect cushion thickness or worn parts). Erratic hammer operation, such as skipping blows, can result from improper cushion thickness, poor lubrication, foreign material in a valve, faulty valve/cam system, or loose hammer fasteners or keys.
- j. As the penetration resistance increases, the ram stroke may also increase, causing it to strike the upper hammer assembly and lifting the hammer ("racking") from the pile. If this behavior is detected, the air pressure flow should be reduced gradually until racking stops. The flow should not be overly restricted so that the stroke is reduced.

- k. Some manufacturers void their warranty if the hammer is consistently operated above 100 blows per 250 mm (10 blows per inch) of penetration beyond short periods such as required when toe bearing piles are driven to rock. Therefore, in prolonged hard driving situations, it may be more desirable to use a larger hammer or stiffer pile section.

- l. Common problems and problem indicators for air/steam hammers are summarized in Table 23-1.

TABLE 23-1 COMMON PROBLEMS AND PROBLEM INDICATORS FOR AIR/STEAM HAMMERS (from Williams Earth Sciences, 1995)	
Common Problems	Indicators
Air trip mechanism on hammer malfunctioning.	Erratic operation rates or air valve sticking open or close.
Cushion stack height not correct (affects timing of trip mechanism air valve).	Erratic operation rates.
Compressor not supplying correct pressure and volume of air to hammer.	Blows per minute rate is varying either faster or slower than the manufacturer specified.
Air supply line kinked or tangled in leads, boom or other.	Visually evident.
Moisture in air ices up hammer.	Ice crystals exiting exhaust ports of hammer.
Lack of lubricant in air supply lines.	Erratic operation rates.
Packing around air chest worn, allowing air blow by.	Ram raises slowly - blows per minute rate slower than manufacturer specifications - air leaking around piston shaft and air chest.
Nylon slide bar worn.	Visually evident.
Ram columns not sufficiently greased.	Visually evident.

An inspection form for single and differential acting air/steam hammers is provided in Figure 23.6. The primary feature of this form is the three column area in the middle of the form. The left column illustrates the key objects of the driving system. The middle column contains the manufacturer's requirements for key objects and the right column is used to record the observed condition of those objects. This format allows the inspector to quickly identify potential problems and an immediate correction may be possible. The hammer inspection form is intended to be used periodically during the course of the project as a complement to the pile driving log.

The bottom portion of the hammer inspection form contains an area where observations at final driving should be recorded. This information may be particularly interesting to an engineer who has performed a wave equation analysis as the actual situation can then be compared to the analyzed one. Therefore, it is recommended that a copy of the completed hammer inspection form be provided to appropriate design and construction personnel.

23.6.3 Double Acting or Differential Air/Steam Hammers

- a. Determine/confirm the ram weight. Ram weight can be calculated from the ram volume and steel density of 78.5 kN/m^3 (492 lbs/ft^3) if necessary. Check for and record any identifying labels as to hammer make, model and serial number.
- b. Check the air or steam supply and confirm it is of adequate capacity to provide the required pressure and flow volume. This is extremely important since approximately half the rated energy comes from the pressure on the ram during the downstroke. Check also the number, length, diameter, and condition of the air/steam hoses. Manufacturers provide guidelines for proper compressors and supply hoses. Air should be blown through the hose before attaching it to the hammer. The motive fluid lubricator should occasionally be filled with the appropriate lubricant as specified by the manufacturer. During operation, check that the pressure at the compressor or boiler is equal to the rated pressure plus hose losses. The pressure should not vary significantly during driving. Record the pressure at the beginning of driving.

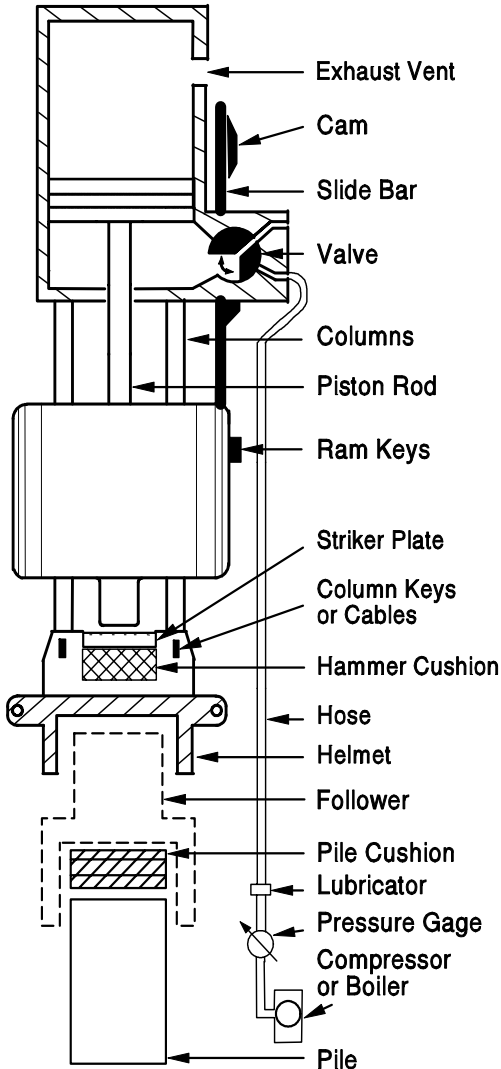
Project/Pile: _____
 Date: _____
 Conditions: _____

Hammer Name: _____
 Serial No: _____

OBJECT

REQUIREMENTS

OBSERVATIONS



Slide Bars / Cams	Yes / No
Greased? Tight?	Remarks _____
Columns Greased?	Yes / No
Ram Keys Tight?	Yes / No
Column Keys or Cables Tight?	Yes / No
Striker Plate	t = _____ D = _____
Hammer Cushion	t = _____ D = _____
	Material _____
	How long in use? _____
Helmet	Type or Weight? _____
Follower	Yes / No; Type _____
Pile Cushion	Material _____
	t = _____ Size _____
	How long in use? _____
Pile	Material _____
	Length _____ Size _____
	Batter _____
Hose	I.D. Size _____ Length _____
	Leaks? _____ Obstructions? _____
Lubricator Filled?	Yes / No
Pressure at Hammer	Measured _____ kPa (psi) at _____ m (ft) from Hammer
	_____ kPa (psi)
Fluctuating during Driving?	Yes / No; How much? _____ kPa (psi)
Check Compressor and Boiler?	Size _____ m ³ /min (ft ³ /min)
	Make _____

MANUFACTURER'S HAMMER DATA

Ram Weight _____
 Max. Stroke _____
 Rated Energy _____
 Blows/min in Hard Driving _____

ATTACHED SAXIMETER PRINTOUT

OBSERVATION WHEN BEARING IS CONFIRMED

Full Ram Stroke Yes/No, _____ %
 Blows/min _____; Blows/0.25m (blows/ft) _____
 High Pile Rebound; Pile Whipping Yes/No; Yes/No
 Pile-Hammer Alignment Front/Back _____ Sides _____
 Crane Size and Make _____
 Lead Type _____
 Hammer Lead Guides Lubricated Yes/No
 Piston Rod Lubricated _____
 Exhaust Description: Freezing? _____ Condensing? _____
 Lubricant Apparent? _____

Figure 23.6 Inspection Form for Single and Differential Acting Air/Steam Hammers

- c. Visually inspect the slide bar and its cams for excessive wear. Measure the stroke being attained and confirm that it meets specification.
- d. Check that the columns or ram guides, piston rod, and slide bar are well greased.
- e. For most air/steam hammers, the total thickness of hammer cushion and striker plate must match the hammer manufacturer's recommendation and the hammer cushion cavity in the helmet for proper valve timing and hammer operation. This thickness must be maintained, and can be checked before assembly of the helmet into the leads, and thereafter by comparison of cam to valve position and/or gap between ram and hammer base when the ram is at rest on the pile.
- f. Make sure the helmet stays properly seated on the pile and that the hammer and pile maintain alignment during operation.
- g. The ram and column keys used to fasten together hammer components should all be tight.
- h. The hammer hoist line should always be slack with the hammer's weight and be fully carried by the pile. Excessive tension in the hammer hoist line is a safety hazard and will reduce energy to the pile. Leads should always be used.
- i. Compare the observed hammer speed in blows per minute near end of driving with the manufacturer's specifications. Blows per minute can be timed with a stopwatch or a saximeter. Slower operating rates may imply a short stroke (from inadequate pressure or volume, restricted or undersized hose, or inadequate lubrication) or improper valve timing (possibly from incorrect cushion thickness or worn parts). Erratic hammer operation, such as skipping blows, can result from improper cushion thickness, poor lubrication, foreign material in a valve, faulty valve/cam system, or loose hammer fasteners or keys.
- j. As the penetration resistance increases, the ram stroke may also increase, causing it to strike the upper hammer assembly and lifting the hammer (racking) from the pile. If this behavior is detected, the pressure flow should be reduced gradually until racking stops. This will result in a reduction in energy since the pressure also acts during the downstroke, thereby contributing to the rated energy. Record the final pressure. The flow should not be overly restricted so that the stroke is also reduced, causing a further reduction in energy. For optimum

performance, the pressure flow should be kept as full as possible so that the hammer lift-off is imminent.

- k. Some manufacturers void their warranty if the hammer is consistently operated above 100 blows per 250 mm (10 blows per inch) of penetration beyond short periods such as required when toe bearing piles are driven to rock. Therefore, in prolonged hard driving situations, it may be more desirable to use a larger hammer or stiffer pile section.
- l. Record the final pressure and compare with manufacturer's energy rating at this pressure.
- m. Common problems and problem indicators for air/steam hammers are summarized in Table 23-1.

An inspection form for enclosed double acting air/steam hammers is provided in Figure 23.7. The primary feature of this form is the three column area in the middle of the form. The left column identifies key objects of the driving system. The middle column contains the manufacturer's requirements for key objects and the right column is used to record the observed condition of those objects. This format allows the inspector to quickly identify potential problems and an immediate correction may be possible. The hammer inspection form is intended to be used periodically during the course of a project as a complement to the pile driving log.

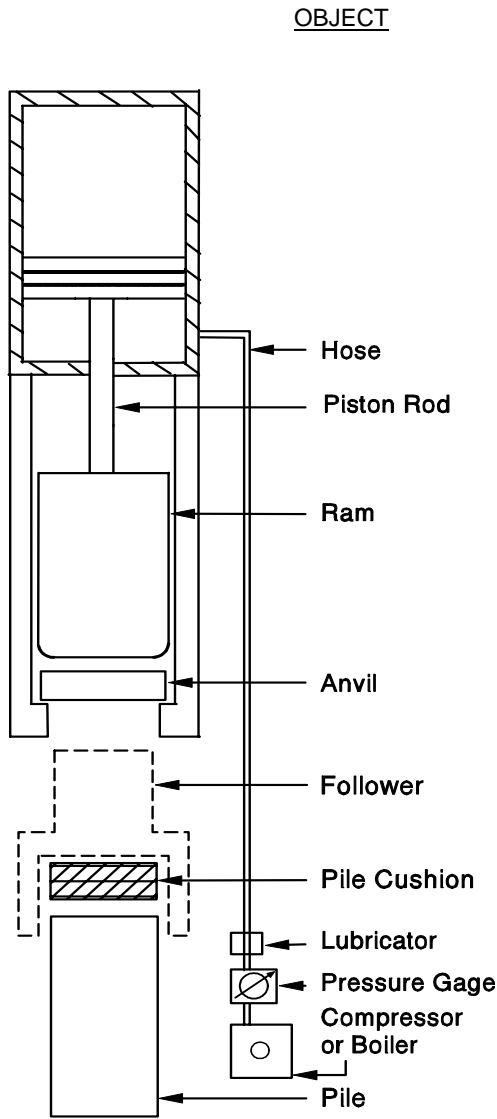
The bottom portion of the hammer inspection form contains an area where observations at final driving should be recorded. This information may be particularly interesting to an engineer who has performed a wave equation analysis as the actual situation can then be compared to the analyzed one. Therefore, it is recommended that a copy of the completed hammer inspection form be provided to appropriate design and construction personnel.

23.6.4 Single Acting Diesel Hammers

- a. Determine/confirm that the hammer is the correct make and model. Check for and record any identifying labels as to hammer make, model and serial number.
- b. Make sure all exhaust ports are open with all plugs removed.

Project/Pile: _____
 Date: _____
 Conditions: _____

Hammer Name: _____
 Serial No: _____



REQUIREMENTS	OBSERVATIONS
Follower	Yes/ No; Type _____
Pile Cushion	Material _____ t = _____ Size _____ How long in use? _____
Pile	Material _____ Length _____ Size _____ Batter _____
Hose Size?	I.D. Size _____ Length _____ Leaks? _____ Obstructions? _____
Lubricator Filled?	Yes / No
Pressure at Hammer _____ kPa (psi)	Measured _____ kPa (psi) at _____ m (ft) from Hammer
Fluctuating during Driving?	Yes / No; How much? _____
Check Compressor and Boiler?	Size _____ m ³ / min (ft ³ /min) Make _____

MANUFACTURER'S HAMMER DATA
 Ram Weight _____
 Max. Stroke _____
 Rated Energy _____
 Blows/min in Hard Driving _____
 ATTACHED SAXIMETER PRINTOUT

OBSERVATION WHEN BEARING IS CONFIRMED
 Full Ram Stroke Yes/No, _____ %
 Blows/min _____ Blows/0.25m (blows/ft) _____
 High Pile Rebound; Pile Whipping Yes/No; Yes/No
 Pile-Hammer Alignment Front/Back _____ Sides _____
 Crane Size and Make _____
 Lead Type _____
 Hammer Lead Guides Lubricated Yes/No
 Piston Rod Lubricated _____
 Exhaust Description: Freezing? _____ Condensing? _____
 Lubricant Apparent? _____

Figure 23.7 Inspection Form for Enclosed Double Acting Air/Steam Hammers

- c. Inspect the recoil dampener for condition and thickness. If excessively worn or improper thickness (consult manufacturer) it should be replaced. If the recoil dampener is too thin, the stroke will be reduced. If it is too thick, or if cylinder does not rest on dampener between blows, the ram could blow out the hammer top and become a safety hazard.
- d. Check that lubrication of all grease nipples is regularly made. Most manufacturers recommend the impact block be greased every half hour of operation.
- e. As the ram is visible between blows, check the ram for signs of uniform lubrication and ram rotation. Poor lubrication will increase friction and reduce energy to the pile.
- f. Determine the hammer stroke, especially at end of driving or beginning of restrrike. A "jump stick" attached to the cylinder is a safety hazard and should not be used. The stroke can be determined by a saximeter which measures the time between blows and then calculates the stroke. The hammer stroke height, h, can also be calculated from this formula using the number of blows per minute (bpm).recorded.

$$h \text{ [meters]} = [4400/[\text{bpm}^2]] - 0.09$$

$$h \text{ [feet]} = 4.01[60/\text{bpm}]^2 - 0.3$$

The calculated stroke may require correction for batter or inclined piles. The inspector should always observe the ram rings and visually estimate the stroke using the manufacturer's chart.

- g. As the penetration resistance increases, the stroke should also increase. At the end of driving, if the ram fails to achieve the correct stroke (part of the driving criteria from a wave equation analysis), the cause could be lack of fuel. Most hammers have adjustable fuel pumps. Some have distinct fuel settings as shown in Figure 23.8, others are continuously variable as shown in Figure 23.9, and some use a pressure pump as shown in Figure 23.10. Make sure the pump is on the correct fuel setting or pressure necessary to develop the required stroke. The fuel and fuel line should be free of dirt or other contaminants. A clogged or defective fuel injector will also reduce the stroke and should be replaced if needed.



Figure 23.8 Fixed Four Step Fuel Pump on Delmag Hammer



Figure 23.9 APE Variable Fuel Pump on Hammer (courtesy APE)



Figure 23.10 Adjustable Pressure Pump for Fuel Setting on ICE Hammer

- h. Low strokes could be due to poor compression caused by worn or defective piston or anvil rings. Check compression by raising the ram, and with the fuel turned off, allowing the ram to fall. The ram should bounce several times if the piston and anvil rings are satisfactory.
- i. Watch for signs of preignition. When a hammer preignites, the fuel burns before impact, requiring extra energy to compress gas and leaving less energy to transfer to the pile. In long sustained periods of driving, or if the wrong fuel with a low flash point is used, the hammer could overheat and preignite. When preignition occurs, less energy is transferred and the penetration resistance rises, giving a false indication of high pile capacity. If piles driven with a cold hammer drive deeper or with less hammer blows, or if the penetration resistances decrease after short breaks, preignition could be the cause and should be investigated. Dynamic testing is the preferable method to check for preignition.
- j. For some diesel hammers, the total thickness of hammer cushion and striker plate must match the hammer manufacturer's recommendation and the hammer cushion cavity in the helmet for proper fuel injection and hammer operation. This total thickness must be maintained.
- k. Make sure the helmet stays properly seated on the pile and that the hammer and pile maintain alignment during operation.
- l. The hammer hoist line should always be slack, with the hammer's weight fully carried by the pile. Excessive tension in the hammer hoist line is a safety hazard and will reduce energy to the pile. Leads should always be used.
- m. Some manufacturers void their warranty if the hammer is consistently operated above 100 blows per 250 mm (10 blows per inch) of penetration beyond short periods, such as those required when toe bearing piles are driven to rock. Therefore, in prolonged hard driving situations, it may be more desirable to use a larger hammer or stiffer pile section.
- n. Common problems and problem indicators for single acting diesel hammers are presented in Table 23-2.

TABLE 23-2 COMMON PROBLEMS AND PROBLEM INDICATORS FOR SINGLE ACTING DIESEL HAMMERS (from Williams Earth Sciences, 1995)	
Common Problems	Indicators
Water in fuel.	Hollow sound, white smoke.
Fuel lines clogged.	No smoke or little gray smoke.
Fuel pump malfunctioning.	Inconsistent ram strokes, little gray smoke or black smoke.
Fuel injectors malfunctioning.	Inconsistent ram strokes, little gray smoke or black smoke.
Oil low.	Blows per minute rate is lower than specified.
Oil pump malfunctioning.	Blows per minute rate is lower than specified.
Water in combustion chamber.	Hollow sound, white smoke.
Piston rings worn.	Low strokes.
Tripping device broken.	Pawl or pin used to lift piston does not engage piston. Pawl engages but does not lift piston.
Over heating.	Paint and oil on cooling fins start to burn/sound changes.

An inspection form for single acting diesel hammers is provided in Figure 23.11. The primary feature of this form is the three column area in the middle of the form. The left column identifies key objects of the driving system, the middle column contains the manufacturer's requirements for that object and the right column is used to record the observed condition of that object. This format allows the inspector to quickly identify potential problems and an immediate correction may be possible. The hammer inspection form is intended to be used periodically during the course of a project as a complement to the pile driving log.

The bottom portion of the hammer inspection form contains an area where observations at final driving should be recorded. This information may be particularly interesting to an engineer who has performed a wave equation analysis as the actual situation can then be compared to the analyzed one. Therefore, it is recommended that a copy of the completed hammer inspection form be provided to appropriate design and construction personnel.

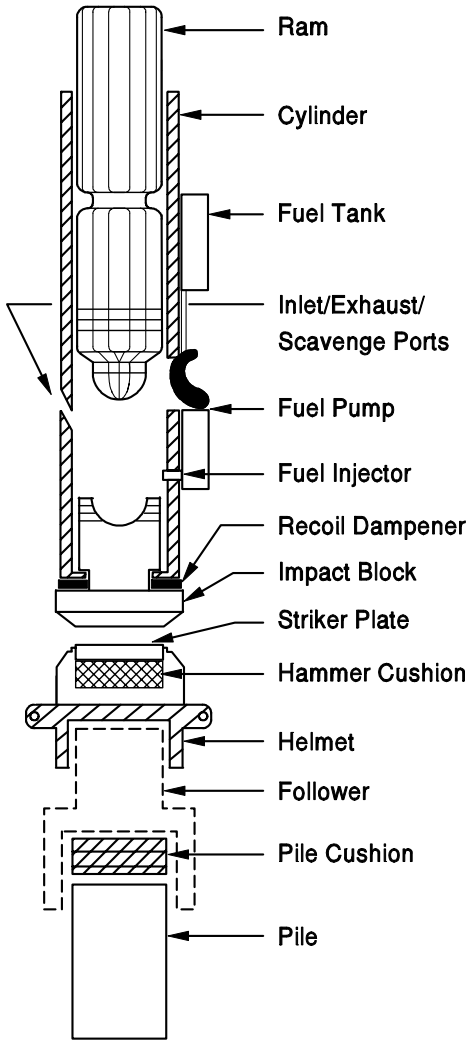
Project/Pile: _____

Hammer Name: _____

Date: _____

Serial No: _____

Conditions: _____



REQUIREMENTS

OBJECT OBSERVATIONS

Ram Lubricated?	Yes / No
Fuel Tank Filled with Type II Diesel?	Yes / No
Exhaust Ports Open?	Yes / No
Fuel Pump	Hammer Setting _____
Recoil Dampener Undamaged?	Yes / No
Impact Block Lubricated?	Yes / No
Striker Plate	t = _____ D = _____
Hammer Cushion	t = _____ D = _____
	Material _____
	How long in use? _____
Helmet	Type or Weight? _____
Follower	Yes / No; Type _____
Pile Cushion	Material _____
	t = _____ Size _____
	How long in use? _____
Pile	Material _____
	Length _____ Size _____
	Batter _____

MANUFACTURER'S HAMMER DATA

Ram Weight _____

Hammer Setting	Rated Energy kJ (ft-k)	Rated Stroke m (ft)
min.		
max.		

OBSERVATION WHEN BEARING IS CONFIRMED

Excessive Cylinder Rebound	Yes/No
High Pile Rebound	Yes/No
Pile Whipping	Yes/No
Pile-Hammer Alignment	Front/Back _____ Sides _____
Crane Size and Make	_____
Lead Type	_____
Hammer Lead Guides Lubricated	Yes/No
Color of Smoke	_____
Steel to Steel Impact Sound	_____

ATTACHED SAXIMETER PRINTOUT

Figure 23.11 Inspection Form for Single Acting Diesel Hammers

23.6.5 Double Acting Diesel Hammers

- a. Determine/confirm that the hammer is the correct make and model. Check for and record any identifying labels as to hammer make, model and serial number.
- b. Make sure all exhaust ports are open with all plugs removed.
- c. Inspect the recoil dampener for condition and thickness. If excessively worn or of improper thickness (consult manufacturer), it should be replaced. If it is too thin, the stroke will be reduced. If it is too thick or if cylinder does not rest on dampener between blows, the ram will cause hammer lift-off.
- d. Check that lubrication of all grease nipples is regularly made. Most manufacturers recommend the impact block be greased every half hour of operation.
- e. After the hammer is stopped, check the ram for signs of lubrication by looking into the exhaust port or trip slot. Poor lubrication increases friction, thus reducing energy to the pile.
- f. Always measure the bounce chamber pressure, especially at end of driving or restrike. This indirectly measures the equivalent stroke or energy. All double acting diesels have a gauge. On most hammers an external gauge is connected by a hose to the bounce chamber. A photograph of a typical external bounce chamber pressure gauge is presented in Figure 23.12. The manufacturer should supply a chart relating the bounce chamber pressure for a specific hose size/length to the rated energy. The inspector should compare measured bounce chamber pressure with the manufacturer's chart to estimate the energy. The bounce chamber pressure measured may require correction for batter or inclined piles.
- g. As the penetration resistance increases, the stroke and bounce chamber pressure should also increase. At the end of driving, if the ram fails to achieve the correct stroke or bounce chamber pressure (part of the driving criteria from a wave equation analysis), the cause could be lack of fuel. All these hammers have continuously variable fuel pumps. Check that the fuel pump is on the correct fuel setting. The fuel should be free of dirt or other contaminants. A clogged or defective fuel injector reduces the stroke.



Figure 23.12 Typical External Bounce Chamber Pressure Gauge

- h. In hard driving, high strokes cause high bounce chamber pressures. If the cylinder weight cannot balance the bounce chamber pressure, the hammer will lift-off of the pile, and the operator must reduce the fuel to prevent this unstable racking behavior. Ideally it is set and maintained so that lift-off is imminent. The bounce chamber pressure gauge reading should correspond to the hammer's maximum bounce chamber pressure for the hose length used when lift-off is imminent. If not, then the bounce chamber pressure gauge is out of calibration and should be replaced, or the bounce chamber pressure tank needs to be drained.
- i. Low strokes indicated by a low bounce chamber pressure could be due to poor compression caused by worn or defective piston or anvil rings. Check compression with the fuel turned off by allowing the ram to fall. The ram should bounce several times if the piston and anvil rings are satisfactory.
- j. Watch for preignition. When a hammer preignites, the fuel burns before impact requiring extra energy to compress the gas and reducing energy transferred to the pile. When preignition occurs, the pile penetration resistance increases giving a

false indication of high pile capacity. In long sustained periods of driving or if low flash point fuel is used, the hammer could overheat and preignite. If piles driven with a cold hammer drive deeper or with fewer hammer blows, or if the penetration resistance decreases after short breaks, investigate for preignition, preferably with dynamic testing.

- k. For some diesel hammers, the total thickness of the hammer cushion and striker plate must match the manufacturer's recommendation for proper fuel injection timing and hammer operation. This total thickness must be maintained.
- l. Make sure the helmet stays properly seated on the pile and that the hammer and pile maintain alignment during operation.
- m. The hammer hoist line should always be slack, with the hammer's weight fully carried by the pile. Excessive tension in the hammer hoist line is a safety hazard and will reduce energy to the pile. Leads should always be used.
- n. Some manufacturers void their warranty if the hammer is consistently operated above 100 blows per 250 mm (10 blows per inch) of penetration beyond short periods such as those required when toe bearing piles are driven to rock. Therefore, in prolonged hard driving situations, it may be more desirable to use a larger hammer or stiffer pile section.
- o. Common problems and problem indicators for double acting diesel hammers are presented in Table 23-3.

An inspection form for double acting diesel hammers is provided in Figure 23.13. The primary feature of this form is the three column area in the middle of the form. The left column identifies key objects of the driving system, the middle column contains the manufacturer's requirements for that object and the right column is used to record the observed condition of that object. This format allows the inspector to quickly identify potential problems and an immediate correction may be possible. The hammer inspection form is intended to be used periodically during the course of a project as a complement to the pile driving log.

TABLE 23-3 COMMON PROBLEMS AND PROBLEM INDICATORS FOR DOUBLE ACTING DIESEL HAMMERS (from Williams Earth Sciences, 1995)	
Common Problems	Indicators
Water in fuel.	Hollow sound, white smoke.
Fuel lines clogged.	No smoke or little gray smoke.
Fuel pump malfunctioning.	Inconsistent ram strokes, little gray smoke or black smoke.
Fuel injectors malfunctioning.	Inconsistent ram strokes, little gray smoke or black smoke.
Oil low.	Blows per minute rate is lower than specified.
Oil pump malfunctioning.	Blows per minute rate is lower than specified.
Build-up of oil in bounce chamber.	Not visible from exterior.
Water in combustion chamber.	Hollow sound, white smoke.
Piston rings worn.	Low strokes.
Tripping device broken.	Pawl or pin used to lift piston does not engage piston. Pawl engages but does not lift piston.
Over heating.	Paint and oil on cooling fins start to burn/ sound changes.

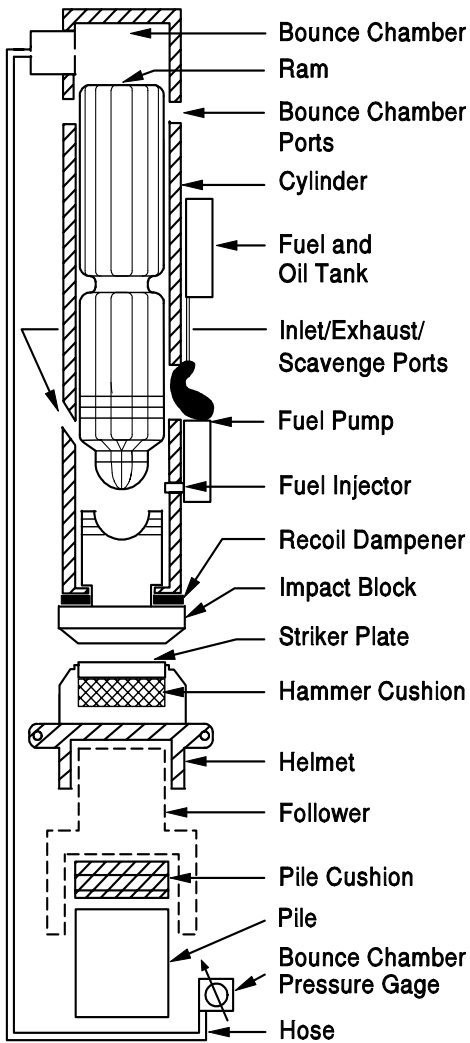
The bottom portion of the hammer inspection form contains an area where observations at final driving should be recorded. This information may be particularly interesting to an engineer who has performed a wave equation analysis as the actual situation can then be compared to the analyzed one. Therefore, it is recommended that a copy of the completed hammer inspection form be provided to appropriate design and construction personnel.

23.6.6 Hydraulic Hammers

- a. Determine/confirm the ram weight. If necessary, the ram weight can be calculated from the ram volume and steel density of 78.5 kN/m^3 (492 lbs/ft^3) although some rams may be hollow or filled with lead. There may also be identifying labels as to hammer make, model, and serial number which should be recorded.

Project/Pile: _____
 Date: _____
 Conditions: _____

Hammer Name: _____
 Serial No: _____



REQUIREMENTS	OBJECT OBSERVATIONS
Ram Lubricated?	Yes / No
Fuel Tank Filled with Type II Diesel?	Yes / No
Exhaust Ports Open?	Yes / No
Fuel Pump	Hammer Setting _____
Recoil Dampener Undamaged?	Yes / No
Impact Block Lubricated?	Yes / No
Striker Plate	t = _____ D = _____
Hammer Cushion	t = _____ D = _____ Material _____ How long in use? _____
Helmet	Type or Weight? _____
Follower	Yes / No; Type _____
Pile Cushion	Material _____ t = _____ Size _____ How long in use? _____
Pile	Material _____ Length _____ Size _____ Batter _____
Bounce Chamber Hose	Length _____

MANUFACTURER'S HAMMER DATA

Ram Weight _____
 Max. Stroke _____

Bounce Chamber Pressure, kPa (psi)	Rated Energy kJ (ft-kips)

ATTACHED SAXIMETER PRINTOUT

OBSERVATION WHEN BEARING IS CONFIRMED

Bounce Chamber Pressure _____
 Cylinder Lift-off _____ Time or Depth _____
 Excessive Cylinder Rebound Yes/No
 High Pile Rebound Yes/No
 Pile Whipping Yes/No
 Pile-Hammer Alignment Front/Back _____ Sides _____
 Crane Size and Make _____
 Lead Type _____
 Hammer Lead Guides Lubricated Yes/No
 Color of Smoke _____
 Steel to Steel Impact Sound _____

Figure 23.13 Inspection Form for Double Acting Diesel Hammers

- b. Check the power supply and confirm it has adequate capacity to provide the required pressure and flow volume. Also, check the number, length, diameter, and condition of the hoses (no leaks in hoses or connections). Manufacturers provide guidelines for power supplies and supply hoses. Hoses bent to a radius less than recommended could adversely affect hammer operation or cause hose failure.
- c. Hydraulic hammers must be kept clean and free from dirt and water. Check the hydraulic filter for blocked elements. Most units have a built in warning or diagnostic system.
- d. Check that the hydraulic power supply is operating at the correct speed and pressure. Check and record the pre-charge pressures or accumulators for double acting hammers. Allow the hammer to warm up before operation, and do not turn off power pack immediately after driving.
- e. Most hydraulic hammers have built in sensors to determine the ram velocity just prior to impact. This result may be converted to kinetic energy or equivalent stroke. The inspector should verify that the correct ram weight is entered in the hammer's "computer". **This monitored velocity, stroke, or energy result should be constantly monitored and recorded. Some hammers have, or can be equipped with, a printout device to record that particular hammer's performance information with pile penetration depth and/or pile penetration resistance.** This is the most important hammer check that the inspector can and should make for these hammers. A photograph of a hydraulic hammer readout panel is presented in Figure 23.14.
- f. For hydraulic hammers with observable rams, measure the stroke being attained and confirm that it meets specification. For hammers with enclosed rams, it is impossible to observe the ram and estimate the stroke.
- g. Check that the ram guides and piston rod are well greased.
- h. Where applicable, the total thickness of hammer cushion and striker plate must be maintained to match the manufacturer's recommendation for proper valve timing and hammer operation.

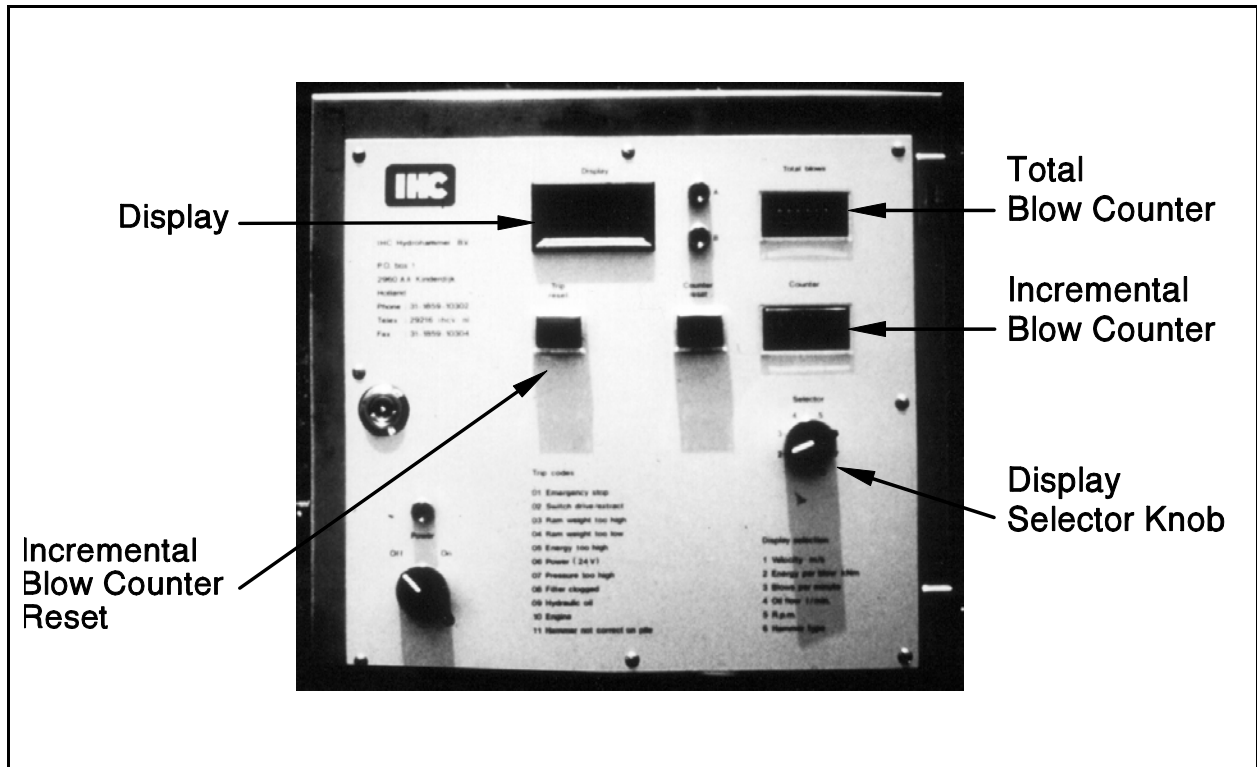


Figure 23.14 IHC Hydraulic Hammer Read-Out Panel (courtesy of L.B. Foster Co.)

- i. Make sure the helmet stays properly seated on the pile and that the hammer and pile maintain alignment during operation.
- j. The hammer hoist line should always be slack, with the hammer's weight fully carried by the pile. Excessive tension in the hammer hoist line is a safety hazard and will reduce energy to the pile. Leads should always be used.
- k. Compare the observed hammer speed in blows per minute from near end of driving with the manufacturer's specifications. Blows per minute can be timed with a stopwatch or a saximeter. Slower operating rates at full stroke may imply excessive friction, or incorrect hydraulic power supply.
- l. As the penetration resistance increases, the ram stroke may also increase, causing the ram to strike the upper hammer assembly and lifting the hammer from the pile (racking). If this behavior is detected, the pressure flow should be reduced gradually until racking stops. Many of these hammers have sensors, and if they detect this condition, the hammer will automatically shut down. The flow should not be overly restricted so that the correct stroke is maintained.

- m. Some manufacturers void their warranty if the hammer is consistently operated above 100 blows per 250 mm (10 blows per inch) of penetration beyond short periods such as those required when toe bearing piles are driven to rock. Therefore, in prolonged hard driving situations, it may be more desirable to use a larger hammer or stiffer pile section.
- n. Common problems and problem indicators for hydraulic hammers are summarized in Table 23-4.

TABLE 23-4 COMMON PROBLEMS AND PROBLEM INDICATORS FOR HYDRAULIC HAMMERS (from Williams Earth Sciences, 1995)	
Common Problems	Indicators
Hoses getting caught in leads.	Visually evident.
Fittings leaking.	Hydraulic fluid dripping.
Electrical connections.	Erratic performance.
Sensors.	Erratic performance.

An inspection form for hydraulic hammers is provided in Figure 23.15. The primary feature of this form is the three column area in the middle of the form. The left column identifies key objects of the driving system and the right column is used to record the observed condition of that object. The hammer inspection form is intended to be used periodically during the course of a project as a complement to the pile driving log.

The bottom portion of the hammer inspection form contains an area where observations at final driving should be recorded. This information may be particularly interesting to an engineer who has performed a wave equation analysis as the actual situation can then be compared to the analyzed one. Therefore, it is recommended that a copy of the completed hammer inspection form be provided to appropriate design and construction personnel.

Project/Pile: _____
 Date: _____
 Conditions: _____

Hammer Name: _____
 Serial No: _____

OBJECT	REQUIREMENTS	OBSERVATIONS
	Ram Visible?	Yes / No Observed Ram Stroke _____ m (ft)
	Ram Downward Pressure Provided ?	Yes / No Hyd. Pressure, Rated _____ kPa (psi) Hyd. Pressure, Actual _____ kPa (psi)
	Impact Velocity Measurement ?	Yes / No
	If Without Velocity Measurement Then ?	Free Fall? _____ Observed Fall Height _____ m (ft) Pressure under ram during fall _____ Preadmission Possible? _____
	Striker Plate	t = _____ D = _____
	Hammer Cushion	t = _____ D = _____ Material _____ How long in use? _____
	Helmet	Type or Weight? _____
	Follower	Yes / No; Type _____
	Pile Cushion	Material _____ t = _____ Size _____ How long in use? _____
	Hydraulic Power Pack	Make _____ Model _____
	Pressure Gage ?	Yes / No Reading _____
	Computer Readout ?	Yes / No Reading _____
	Pile	Material _____ Length _____ Size _____ Batter _____

MANUFACTURER'S HAMMER DATA

Ram Weight _____
 Max. Stroke _____
 Min. Stroke _____
 Max. Energy _____
 Min. Energy _____

ATTACH SAXIMETER PRINTOUT

OBSERVATION WHEN BEARING IS COMPLETED

Hammer Uplifting Yes/No
 Reduced Pressure Yes/No
 Blows/Minute _____
 Blow Count _____ Blows/m (Blows/ft)
 High Pile Rebound Yes/No
 Pile Whipping Yes/No
 Pile-Hammer Alignment Front/Back _____ Sides _____
 Crane Size and Make _____
 Lead Type _____
 Lead Guides Lubricated Yes/No

Figure 23.15 Inspection Form for Hydraulic Hammers

23.6.7 Vibratory Hammers

- a. Confirm that the hammer make and model meets specifications. There may also be identifying labels as to hammer make, model and serial number which should be recorded.
- b. Check the power supply to confirm adequate capacity to provide the required pressure and flow volume. Check also the number, length, diameter, and condition of the hoses (no leaks in hoses or connections). Manufacturers provide guidelines for proper power supplies and supply hoses. Hoses bent to a smaller radius than recommended could affect hammer operation or cause hose failure.
- c. Vibratory hammers must be kept clean, free from dirt and water. Check the hydraulic filter for blocked elements. Most units have a built in warning or diagnostic system.
- d. Check and record that the hydraulic power supply is operating at the correct speed and pressure. Allow the hammer to warm up before operation, and do not turn off the power pack immediately after driving.
- e. Record, if available, the vibrating frequency.
- f. Make sure the hydraulic clamps for attachment to the pile are in good working order and effective.
- g. The hammer hoist line should always be slack enough to allow penetration with the hammer's weight primarily carried by the pile. Excessive tension in the hammer hoist line will retard penetration. If used for extraction, the hoist line should be tight at all times. Leads are rarely used.

23.7 INSPECTION OF TEST OR INDICATOR PILES

Most specifications call for preconstruction verification of the foundation design through the testing of some selected piles. The size of the foundation and relative costs of testing often dictate the type and amount, if any, of confirmation testing. The inspector may be responsible for coordinating the test pile program with the contractor, other state personnel, and/or outside testing agencies.

Small foundations with few piles may be designed conservatively with high safety factors and oversized pile length and no further tests are required. All piles are then production piles and the entire pile foundation is usually installed in one or two days.

The piles, hammers, and other observations are recorded by the inspector and information appropriately passed on or filed. Inspection should be thorough as it is the only assurance of a good foundation. If any problems are observed, such as very low blow counts, refusal driving above scour depths, or excessive pile lengths, the problems and all pertinent observations must be reported quickly so that immediate corrective action can be taken.

On most projects, some additional verification is specified. Smaller projects may have only a single static test (Chapter 18) on one pile at a specific depth, or there may be a few dynamic test piles (Chapter 17). The dynamic tests may include either testing during driving to assess hammer performance and driving stresses, or testing during restrrike to assess capacity, or both. The static or dynamic tests should be performed by state department of transportation personnel having appropriate knowledge of test procedures, or engineering consultants. Generally, tests are done on some of the first piles driven to verify or adjust the driving criteria which will then be used for subsequent production piles. This further verification provides rational basis for changes to the driving criteria, if necessary, which should be applied to subsequent production pile driving.

On larger projects, multiple test piles distributed across the site are often required to verify or adjust the driving criteria. The goal is to determine a driving criteria which will lead to a safe, but economical, foundation. Such tests could be primarily done at one time at the beginning of the construction. For example, so-called indicator piles are driven in selected locations across the project site to establish order lengths for concrete piles. Such selected piles are generally statically and/or dynamically tested. Alternatively, testing could be performed as the construction progresses with some test(s) establishing the driving criteria for piles in close proximity to the test pile(s), followed by production pile driving, and then repeating the process in stages across the site.

The test piles are often the most critical part of the foundation installation. The procedures and driving criteria established during this phase will be applied to all subsequent production piles. The largest savings are often found at this time. For example, test results may determine that the design pile length results in a greater pile capacity than required and that the piles could be made substantially shorter. Alternatively, problems with the test piles are usually followed by the same problems with production piles. Since problems are in themselves costly, and if left unresolved may eventually escalate, determination of the best solution as quickly as possible should be accomplished. It is the inspector's responsibility to be observant and communicate significant observations precisely and in a timely manner to the state design and testing teams.

The answers to the following questions should be known before driving test piles. Usually the inspector has the responsibility and the decision making authority regarding these items, although advice from various agency personnel and/or outside consultants may be necessary or desirable.

1. Who determines test pile locations?
2. Who determines the test pile driving criteria?
3. Who stops the driving when the driving criteria is met?
4. Who decides at what depth to stop the indicator/test piles?
5. Who checks cutoff elevations?
6. Who checks for heave?
7. Who determines if static test and/or dynamic test results indicate an acceptable test pile?
8. Who determines if additional tests are required?
9. Who determines if modifications to procedures or equipment are required?
10. Who has authority to allow production pile installation? When is this approval to proceed to production granted?
11. Who produces what documentation?

23.8 INSPECTION OF PRODUCTION PILES

During the production pile driving operations, the inspector's function is to apply the knowledge gained from the test program to each and every production pile. Quality assurance measures for the pile quality and splices; hammer operation and cushion replacement; overall evaluation of pile integrity; procedures for completing the piles (e.g. filling pipe piles with concrete); and unusual or unexpected occurrences need to be addressed. Complete documentation for each and every pile must be obtained, and then passed on to the appropriate destination in a timely manner.

The following items should be checked frequently (e.g. for each production pile):

1. Does the pile meet specifications of type, size, length, and strength?
2. Is the pile installed in the correct location, within acceptable tolerances, and with the correct orientation?
3. Are splices, if applicable, made to specification?
4. Is pile toe protection required and properly attached?
5. Is the pile acceptably plumb?
6. Is the hammer working correctly?
7. Is the hammer cushion the correct type and thickness?
8. Is the pile cushion the correct type and thickness? Is it being replaced regularly?
9. Did the pile meet the driving criteria as expected?
10. Did the pile have unusual driving conditions and therefore potential problems?
11. Is there any indication of pile heave?
12. Is the pile cutoff at the correct elevation?
13. Is there any visual damage?

14. If appropriate, has the pipe pile been visually inspected prior to concrete filling? Has it been filled with the specified strength concrete? Were concrete samples taken?
15. Are piles which are to be filled with concrete, such as open ended pipes and prestressed concrete piles with center voids, being cleaned properly after driving is completed?
16. If there is any question about pile integrity, has the issue been resolved? Is the pile acceptable, or does it need remediation or replacement?
17. Is the documentation for this pile complete, including driving log? Has it been submitted on a timely basis to the appropriate authority?

Many of the above questions are self explanatory and need no further explanation. Every previous section of this chapter has material which will relate to inspection of production piles and offer the detailed answers to other questions raised above. Although the inspector has now had the experience of test pile installation, a few additional details and concerns are perhaps appropriate.

Counting the number of hammer blows per minute and comparing it to the manufacturer's specification will provide a good indication of whether or not the hammer is working properly. The stroke of the hammer for most single and double acting air/steam hammers can be observed. Check the stroke of a single acting diesel hammer with a saximeter or by computation from the blows per minute. Check the bounce chamber pressure for double acting diesel hammers. Most hydraulic hammers have built-in energy monitors, and this information should be recorded for each pile. The hammer inspection form presented earlier in this chapter should be completed for the hammer type being used.

A hammer cushion of manufactured material usually lasts for many hours of pile driving, (as much as 200 hours for some manufactured materials) so it is usually sufficient to check before the pile driving begins and periodically thereafter. Pile cushions (usually made of plywood) need frequent changing because of excessive compression or charring and have a typical life of about 1000 to 2000 hammer blows. Pile cushions should preferably be replaced as soon as they compress to one half of the original thickness, or if they begin to burn. No changes to the pile cushion thickness should be permitted near final driving. The required penetration resistance for pile acceptance should only be allowed after the first 100 blows after cushion replacement.

Inspection of splices is important for pile integrity. Poorly made splices are a potential source of problems and possible pile damage during driving. In some cases damage may be detected from the blow count records. Dynamic pile testing can be useful in questionable cases.

Pile driving stresses should be kept within specified limits. If dynamic monitoring equipment was used during test pile driving, the developed driving criteria should keep driving stresses within specified limits. If periodic dynamic tests are made, a check that the driving stresses are within the specified limits can be provided. Adjustments of the ram stroke for all hammer types may be necessary to avoid pile damage. For concrete piles, cushion thicknesses or driving procedures may need adjustment to control tension and compression stresses. If dynamic testing is not used, a wave equation analysis is essential to evaluate the anticipated driving stresses.

Driving of piles at high penetration resistances, above 120 blows per 250 mm (10 blows per inch), should be avoided by matching the driving system with the pile type, length and subsurface conditions. This should have been accomplished in the design phase by performing wave equation analysis. However, conditions can change across the project due to site variability.

All piles should be checked for damage after driving is completed. The driving records for all pile types can be compared with adjacent piles for unusual records or vastly different penetrations. Piles suspected of damage (including timber, H, and solid concrete piles) could be tested to confirm integrity and/or determine extent and location of damage using the pile driving analyzer, or for concrete piles, low strain integrity testing methods. These methods are discussed in Chapter 17. Alternatively, the pile could be replaced or repaired, if possible.

Check for water leakage for closed end pipe piles before placing concrete. The concrete mix should have a high slump and small aggregate. A pipe pile can be easily checked for damage and sweep by lowering a light source inside the pile.

The driving sequence of piles in a pier or bent can be important. The driving sequence can affect the way piles drive as well as the influence the new construction has on adjacent structures. This is especially true for displacement piles. For non-displacement piles the driving sequence is generally not as critical.

The driving sequence of displacement pile groups should be from the center of the group outward or from one side to the other side. The preferred driving sequence of the

displacement pile group shown in Figure 23.16 would be (a) by the pile number shown, (sequence 1), (b) by driving each row starting in the center and working outward (sequence 2), or (c) by driving each row starting on one side of the group and working to the other side (sequence 3).

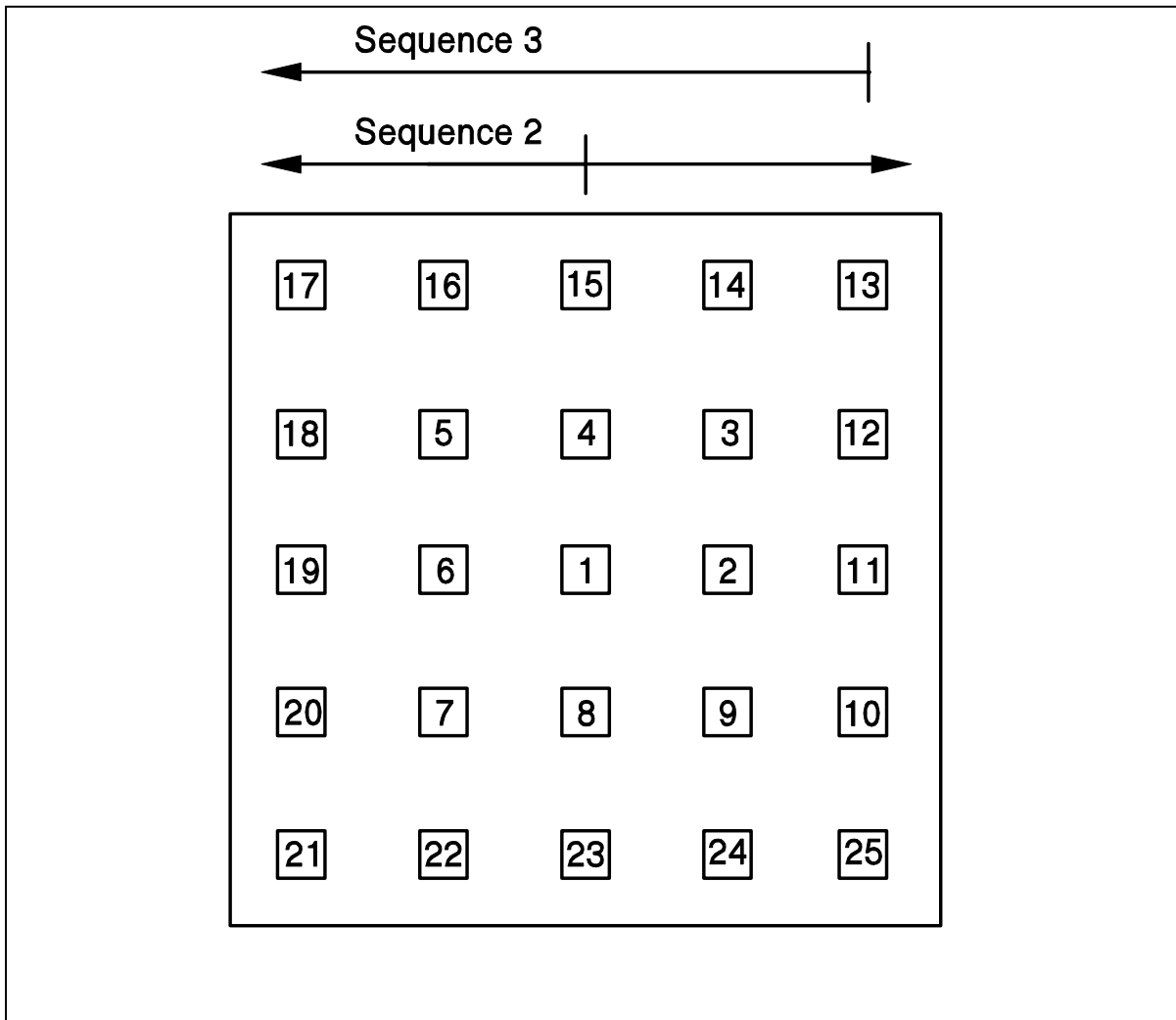


Figure 23.16 Driving Sequence of Displacement Pile Groups (after Passe, 1994)

Pile groups should not be driven from the outside to the center (the reverse of sequences 1 or 2). If groups are driven in that order, displaced soils becomes trapped and compacted in the center of the pile group. This can cause problems with driving the piles in the center of the group.

When driving close to an existing structure, it is generally preferable to drive the piles nearest the existing structure first and work away. For example, if a structure was located on the right side of the pile group shown in Figure 23.16, the piles should be driven by

sequence 3. This reduces the amount of soil displaced toward the existing structure. The displacement of soil toward an existing structure has caused problems before. It can be especially critical next to a bascule bridge where, very small movements can prevent the locking mechanism from locking.

On some projects, vibration measurements may be required to ascertain if pile driving induced vibrations are within acceptable and/or specified maximum levels. Woods (1997) noted that vibration damage is relatively uncommon at a distance of one pile length away from driving. However, damage from vibration induced settlement of loose, clean sands can be a problem up to 400 m (1300 ft) away from driving. To document existing conditions of nearby structures, a preconstruction survey of structures within 120 m (400 ft) of pile driving activities is often performed prior to the start of construction. The preconstruction survey generally consists of photographing or videotaping existing damage, as well as affixing crack gages to existing cracks in some cases. Woods also noted that damage to freshly placed concrete from pile driving vibrations may not be a risk but further research on the setting and curing of concrete may be warranted.

A cold hammer should not be used when restriking piles after a setup period. Twenty hammer blows are usually sufficient to warm up most hammers. Also be sure to record the restrike penetration resistance for each 25 mm (1 inch) during the first 0.25 m (or 1 ft) of restrike.

A summary of common pile installation problems and possible solutions is presented in Table 23-5.

TABLE 23-5 COMMON PILE INSTALLATION PROBLEMS & POSSIBLE SOLUTIONS

Problem	Possible Solutions
<p>Piles encountering refusal penetration resistance (blow count) above minimum pile penetration requirements.</p>	<p>Have wave equation analysis performed and check that pile has sufficient driveability and that the driving system is matched to the pile. If the pile and driving system are suitably matched, check driving system operation for compliance with manufacturer's guidelines. If no obvious problems are found, dynamic measurements should be made to determine if the problem is driving system or soil behavior related. Driving system problems could include preignition, preadmission, low hammer efficiency, or soft cushion. Soil problems could include greater soil strength than anticipated, temporarily increased soil resistance with later relaxation (requires restrike to check), large soil quakes, or high soil damping.</p>
<p>Piles driving significantly deeper than estimated pile penetration depths.</p>	<p>Soil resistance at the time of driving probably is lower than anticipated or driving system performance is better than anticipated. Have wave equation analysis performed to assess ultimate pile capacity based on the blow count at the time of driving. Perform restrike tests after an appropriate waiting period to evaluate soil strength changes with time. If the ultimate capacity based on restrike blow count is still low, check drive system performance and restrike capacity with dynamic measurements. If drive system performance is as assumed and restrike capacity low, the soil conditions are weaker than anticipated. Foundation piles will probably need to be driven deeper than originally estimated or additional piles will be required to support the load. Contact the structural engineer/designer for recommended change.</p>

TABLE 23-5 COMMON PILE INSTALLATION PROBLEMS & POSSIBLE SOLUTIONS (CONTINUED)	
Problem	Possible Solutions
Abrupt change or decrease in penetration resistance (blow count) for bearing piles.	If borings do not indicate weathered profile above bedrock/bearing layer then pile toe damage is likely. Have wave equation analysis performed and evaluate pile toe stress. If calculated toe stress is high and blow counts are low, a reduced hammer energy (stroke) and higher blow count could be used to achieve capacity with a lower toe stress. If calculated toe stress is high at high blow counts, a different hammer or pile section may be required. For piles that allow internal inspection, reflect light to the pile toe and tape the length inside the pile for indications of toe damage. For piles that cannot be internally inspected, dynamic measurements could be made to evaluate problem or pile extraction could be considered for confirmation of a damage problem.
Penetration resistance (blow count) significantly lower than expected during driving.	Review soil borings. If soil borings do not indicate soft layers, pile may be damaged below grade. Have wave equation analysis performed and investigate both tensile stresses along pile and compressive stresses at toe. If calculated stresses are within allowable limits, investigate possibility of obstructions / uneven toe contact on hard layer or other reasons for pile toe damage. If pile was spliced, re-evaluate splice detail and field splicing procedures for possible splice failure.
Vertical (heave) or lateral movement of previously installed piles when driving new piles.	Pile movements likely due to soil displacement from adjacent pile driving. Contact geotechnical engineer for recommended action. Possible solutions include redriving of installed piles, change in sequence of pile installation, or predrilling of pile locations to reduce ground movements. Lateral pile movements could also result from adjacent slope failure in applicable conditions.

TABLE 23-5 COMMON PILE INSTALLATION PROBLEMS & POSSIBLE SOLUTIONS (CONTINUED)	
Problem	Possible Solutions
Piles driving out of alignment tolerance.	Piles may be moving out of alignment tolerance due to hammer-pile alignment control or due to soil conditions. If due to poor hammer-pile alignment control, a pile gate, template or fixed lead system may improve the ability to maintain alignment tolerance. Soil conditions such as near surface obstructions (see subsequent section) or steeply sloping bedrock having minimal overburden material (pile point detail is important) may prevent tolerances from being met even with good alignment control. In these cases, survey the as-built condition and contact the structural engineer for recommended action.
Piles driving out of location tolerance.	Piles may be moving out of location tolerance due to hammer-pile alignment control or due to soil conditions. If due to poor hammer-pile alignment control, a pile gate, template or fixed lead system may improve the ability to maintain location tolerance. Soil conditions such as near surface obstructions (see subsequent section) or steeply sloping bedrock having minimal overburden material (pile point detail is important) may prevent tolerances from being met even with good alignment control. In these cases, survey the as-built condition and contact the structural engineer for recommended action.
Piles encountering shallow obstructions.	If obstructions are within 3 m (10 ft) of working grade, obstruction excavation and removal is probably feasible. If obstructions are at deeper depth, are below the water table, or the soil is contaminated, excavation may not be feasible. Spudding or predrilling of pile locations may provide a solution with method selection based on the type of obstructions and soil conditions.

TABLE 23-5 COMMON PILE INSTALLATION PROBLEMS & POSSIBLE SOLUTIONS (CONTINUED)	
Problem	Possible Solutions
Piles encountering obstructions at depth.	If deep obstructions are encountered that prevent reaching the desired pile penetration depth, contact the structural engineer/designer for remedial design. Ultimate capacity of piles hitting obstructions should be reduced based upon pile damage potential and soil matrix support characteristics. Additional foundation piles may be necessary.
Concrete piles develop complete horizontal cracks in easy driving.	Have wave equation analysis performed and check tension stresses along pile (extrema tables) for the observed blow counts. If the calculated tension stresses are high, add cushioning or reduce stroke. If calculated tension stresses are low, check hammer performance and/or perform dynamic measurements.
Concrete piles develop complete horizontal cracks in hard driving.	Have wave equation analysis performed and check tension stresses along pile (extrema table). If the calculated tension stresses are high, consider a hammer with a heavier ram. If the calculated tension stresses are low, perform dynamic measurements and evaluate soil quakes which are probably higher than anticipated.
Concrete piles develop partial horizontal cracks in easy driving.	Check hammer-pile alignment since bending may be causing the problem. If the alignment appears to be normal, tension and bending combined may be too high. The possible solution is as above with complete cracks.
Concrete pile spalling or slabbing near pile head.	Have wave equation analysis performed. Determine the pile head stress at the observed blow count and compare predicted stress with allowable material stress. If the calculated stress is high, increase the pile cushioning. If the calculated stress is low, investigate pile quality, hammer performance, and hammer-pile alignment.

TABLE 23-5 COMMON PILE INSTALLATION PROBLEMS & POSSIBLE SOLUTIONS (CONTINUED)	
Problem	Possible Solutions
Steel pile head deforms.	Check helmet size/shape, steel yield strength, and evenness of the pile head. If all seem acceptable, have wave equation analysis performed and determine the pile head stress. If the calculated stress is high and blow counts are low, use reduced hammer energy (stroke) and higher blow count to achieve capacity. If the calculated stress is high at high blow counts, a different hammer or pile type may be required. Ultimate capacity determination should not be made using blow counts obtained when driving with a deformed pile head.
Timber pile head mushrooms	Check helmet size/shape, the evenness of the pile head, and banding of the timber pile head. If all seem acceptable, have wave equation analysis performed and determine the pile head stress. If the calculated stress is high and blow counts are low, use reduced hammer energy (stroke) and higher blow count to achieve capacity. Ultimate capacity determination should not be made using blow counts obtained when driving with a mushroomed pile head.

23.9 DRIVING RECORDS AND REPORTS

Pile driving records vary with the organization performing the inspection service. A typical pile driving record in SI or US units is presented in Figure 23.17a and 23.17b, respectively. The following is a list of items that appear on most pile driving records:

1. Project identification number.
2. Project name and location.
3. Structure identification number.

STATE PROJECT NO.: _____ DATE: _____
 JOB LOCATION: _____ BENT / PIER NO.: _____ PILE NO.: _____
 PILE TYPE: _____ LENGTH: _____ COATING.: _____ ULTIMATE CAPACITY.: _____
 HAMMER: _____ RATED ENERGY _____ OPERATING RATE: _____ HELMET WEIGHT: _____
 HAMMER CUSHION TYPE: _____ t = _____ PILE CUSHION TYPE: _____ t = _____
 REF. ELEV.: _____ MIN TOE ELEV.: _____ FINAL TOE ELEV.: _____ PILE CUTOFF ELEV.: _____
 WEATHER: _____ TEMP.: _____ START TIME: _____ STOP TIME: _____

METERS	BLOWS	STROKE / PRESSURE	REMARKS	METERS	BLOWS	STROKE / PRESSURE	REMARKS
0 - 0.25				8.00 - 8.25			
0.25 - 0.50				8.25 - 8.50			
0.50 - 0.75				8.50 - 8.75			
0.75 - 1.00				8.75 - 9.00			
1.00 - 1.25				9.00 - 9.25			
1.25 - 1.50				9.25 - 9.50			
1.50 - 1.75				9.50 - 9.75			
1.75 - 2.00				9.75 - 10.00			
2.00 - 2.25				10.00 - 10.25			
2.25 - 2.50				10.25 - 10.50			
2.50 - 2.75				10.50 - 10.75			
2.75 - 3.00				10.75 - 11.00			
3.00 - 3.25				11.00 - 11.25			
3.25 - 3.50				11.25 - 11.50			
3.50 - 3.75				11.50 - 11.75			
3.75 - 4.00				11.75 - 12.00			
4.00 - 4.25				12.00 - 12.25			
4.25 - 4.50				12.25 - 12.50			
4.50 - 4.75				12.50 - 12.75			
4.75 - 5.00				12.75 - 13.00			
5.00 - 5.25				13.00 - 13.25			
5.25 - 5.50				13.25 - 13.50			
5.50 - 5.75				13.50 - 13.75			
5.75 - 6.00				13.75 - 14.00			
6.00 - 6.25				14.00 - 14.25			
6.25 - 6.50				14.25 - 14.50			
6.50 - 6.75				14.50 - 14.75			
6.75 - 7.00				14.75 - 15.00			
7.00 - 7.25				15.00 - 15.25			
7.25 - 7.50				15.25 - 15.50			
7.50 - 7.75				15.50 - 15.75			
7.75 - 8.00				15.75 - 16.00			

PILE SUPPLIER: _____ PILE CAST OR ROLLING DATE _____
 PILE TOE ATTACHMENTS: _____ FINAL PILE HEAD CONDITION: _____
 FINAL ALIGNMENT: _____ FINAL PLUMBNESS: _____ INTERNAL INSPECTION: _____
 INSPECTORS NAME AND SIGNATURE: _____

Figure 23.17a Pile Driving Log (SI Version)

STATE PROJECT NO.: _____ DATE: _____

JOB LOCATION: _____ BENT / PIER NO.: _____ PILE NO.: _____

PILE TYPE: _____ LENGTH: _____ COATING: _____ ULTIMATE CAPACITY: _____

HAMMER: _____ RATED ENERGY: _____ OPERATING RATE: _____ HELMET WEIGHT: _____

HAMMER CUSHION TYPE: _____ t = _____ PILE CUSHION TYPE: _____ t = _____

REF. ELEV.: _____ MIN TOE ELEV.: _____ FINAL TOE ELEV.: _____ PILE CUTOFF ELEV.: _____

WEATHER: _____ TEMP.: _____ START TIME: _____ STOP TIME: _____

FEET	BLOWS	STROKE / PRESSURE	REMARKS	FEET	BLOWS	STROKE / PRESSURE	REMARKS
0 - 1				35 - 36			
1 - 2				36 - 37			
2 - 3				37 - 38			
3 - 4				38 - 39			
4 - 5				39 - 40			
5 - 6				40 - 41			
6 - 7				41 - 42			
7 - 8				42 - 43			
8 - 9				43 - 44			
9 - 10				44 - 45			
10 - 11				45 - 46			
11 - 12				46 - 47			
12 - 13				47 - 48			
13 - 14				48 - 49			
14 - 15				49 - 50			
15 - 16				50 - 51			
16 - 17				51 - 52			
17 - 18				52 - 53			
18 - 19				53 - 54			
19 - 20				54 - 55			
20 - 21				55 - 56			
21 - 22				56 - 57			
22 - 23				57 - 58			
23 - 24				58 - 59			
24 - 25				59 - 60			
25 - 26				60 - 61			
26 - 27				61 - 62			
27 - 28				62 - 63			
28 - 29				63 - 64			
29 - 30				64 - 65			
30 - 31				65 - 66			
31 - 32				66 - 67			
32 - 33				67 - 68			
33 - 34				68 - 69			
34 - 35				69 - 70			

PILE SUPPLIER: _____ PILE CAST OR ROLLING DATE: _____

PILE TOE ATTACHMENTS: _____ FINAL PILE HEAD CONDITION: _____

FINAL ALIGNMENT: _____ FINAL PLUMBNESS: _____ INTERNAL INSPECTION: _____

INSPECTORS NAME AND SIGNATURE: _____

Figure 23.17b Pile Driving Log (US Version)

4. Date and time of driving (start, stop, and interruptions).
5. Name of the contractor.
6. Hammer make, model, ram weight, energy rating. The actual stroke and operating speed should also be recorded whenever it is changed.
7. Hammer cushion description, size and thickness, and helmet weight.
8. Pile cushion description, size and thickness, depth where changed.
9. Pile location, type, size and length.
10. Pile number or designation matching pile layout plans.
11. Pile ground surface, cut off, and final penetration elevations and embedded length.
12. Penetration resistance data in blows per 0.25 meter (or blows per foot) with the final 0.25 meter (or foot) normally recorded in blows per 25 mm (blows per inch).
13. Graphical presentation of driving data (optional).
14. Cut-off length, length in ground and order length.
15. Comments or unusual observations, including reasons for all interruptions.
16. Signature and title of the inspector.

The importance of maintaining detailed pile driving records can not be overemphasized. The driving records form a basis for payment and for making engineering decisions regarding the adequacy of the foundation to support the design loads. Great importance is given to driving records in litigations involving claims. Sloppy, inaccurate, or incomplete records encourage claims and result in higher cost foundations. The better the pile driving is documented, the lower the cost of the foundation will probably be and the more likely it will be completed on schedule.

In addition to the driving records, the inspector should be required to prepare a daily inspection report. The daily inspection report should include information on equipment working at the site, description of construction work accomplished, and the progress of work. Figure 23.18 shows an example of a daily inspection report.

DAILY INSPECTION REPORT

Project No.: _____

Date: _____

Project: _____

Weather Conditions: _____

Contractor: _____

Contractor's Personnel Present: _____

Equipment Working: _____

Description of Work Accomplished: _____

Special Persons Visiting Job: _____

Test Performed: _____

Special Comments: _____

Figure 23.18 Daily Inspection Report

23.10 SAFETY

Pile driving involves the use of heavy equipment and heavy loads. The pile driving inspector should be cognizant of these activities and position his or herself accordingly. One of the more dangerous operations during pile driving is the lifting of the pile and the positioning of it under the hammer for driving. The inspector should remember that a 30 m (100 ft) pile can fall 30 m (100 ft) from the pile location during positioning. It is better to have a planned escape route prior to pile positioning rather than attempt to quickly determine one should difficulties arise during the pile lifting and positioning process.

The area beneath a suspended load should be avoided. If the hoisting device fails or slips, serious injury could occur. The inspector should also avoid the area behind the crane and be cognizant whenever the crane is moving or swinging.

The inspector should select a position for maintain the pile driving record that is a sufficient distance away from the pile location during driving. The area immediately in front of the pile should be avoided. Heavy pieces sometimes fall from a pile hammer or helmet during operation that could cause serious injury if the inspector were positioned under or near the hammer. All pile types can be also damaged during driving. Concrete and timber piles can break suddenly, and long steel piles can buckle. A sudden pile break or buckling can make the area around the pile location quite dangerous due to the broken or buckled section. A sudden loss of resistance beneath an operating pile hammer can also overload the hammer line causing it to break and the hammer to fall. Damage to the head of a concrete pile during driving can also result in heavy concrete pieces falling due to hammer-pile alignment problems or due to pile cushion deterioration. Standing beneath the hammer and monitoring the final pile penetration resistance by placing marks on the pile every 10 or 20 hammer blows should be avoided for the above reasons. The final penetration resistance can be determined instead by marking the pile prior to driving with 25 mm (1 inch) marks over the anticipated final penetration depth.

Safety devices such as a hard hat, ear protection, steel toed work boots, eye protection, safety vest, fall protection harness, and life jacket should be worn as job conditions dictate. Additional site specific, state, or federal safety rules may also apply and these should be reviewed.

REFERENCES

- Associated Pile and Fitting Corporation. Design and Installation of Driven Pile Foundations.
- Canadian Geotechnical Society (1978). Canadian Foundation Engineering Manual. Part 3, Deep Foundations.
- Deep Foundations Institute (1981). Glossary of Foundation Terms.
- Deep Foundations Institute (1995). A Pile Inspector's Guide to Hammers, Second Edition, Deep Foundations Institute.
- Fuller, F.M. (1983). Engineering of Pile Installations. McGraw-Hill Book Company.
- Passe, Paul D. (1994). Pile Driving Inspector's Manual. State of Florida Department of Transportation.
- Rausche, F., Likins, G.E., Goble, G.G., Hussien, M. (1986). The Performance of Pile Driving Systems; Inspector's Manual.
- Williams Earth Sciences (1995). Inspector's Qualification Program for Pile Driving Inspection Manual. State of Florida Department of Transportation.
- Woods, R.D. (1997). Dynamic Effects of Pile Installations on Adjacent Structures. NCHRP Synthesis 253, National Cooperative Highway Research Program, Transportation Research Board, Washington, D.C.

APPENDIX A

List of FHWA Pile Foundation Design and Construction References

- Briaud, J-L. (1989). The Pressuremeter Test for Highway Applications. Report No. FHWA IP-89-008, U.S. Department of Transportation, Federal Highway Administration, Office of Implementation, McLean, 156.
- Briaud, J-L. and Miran, J. (1991). The Cone Penetrometer Test. Report No. FHWA-SA-91-043, U.S. Department of Transportation, Federal Highway Administration, Office of Technology Applications, Washington, D.C., 161.
- Briaud, J-L. and Miran, J. (1992). The Flat Dilatometer Test. Report No. FHWA-SA-91-44, U.S. Department of Transportation, Federal Highway Administration, Office of Technology Applications, Washington, D.C., 102.
- Briaud, J-L., Tucker, L., Lytton, R.L. and Coyle, H.M. (1985). Behavior of Piles and Pile Groups in Cohesionless Soils. Report No. FHWA/RD-83/038, U.S. Department of Transportation, Federal Highway Administration, Office of Research - Materials Division, Washington, D.C., 233.
- Cheney, R.S. and Chassie, R.G. (2000). Soils and Foundations Workshop Reference Manual. Publication No. FHWA HI-00-045, U.S. Department of Transportation, National Highway Institute, Federal Highway Administration, Office of Engineering, Washington, D.C., 358.
- Goble, G.G., and Rausche, F. (1986). Wave Equation Analysis of Pile Driving - WEAP86 Program. U.S. Department of Transportation, Federal Highway Administration, Implementation Division, McLean, Volumes I-IV.
- Kyfor, Z.G., Schnore, A.S., Carlo, T.A. and Bailey, P.F. (1992). Static Testing of Deep Foundations. Report No. FHWA-SA-91-042, U.S. Department of Transportation, Federal Highway Administration, Office of Technology Applications, Washington, D.C., 174.

- Lam, I.P. and Martin, G.R. (1986). Seismic Design of Highway Bridge Foundations. Volume II - Design Procedures and Guidelines, Report No. FHWA/RD-86/102, U.S. Department of Transportation, Federal Highway Administration, Office of Engineering and Highway Operations, McLean, 181.
- Mathias, D. and Cribbs, M. (1998). DRIVEN 1.0: A Microsoft Windows™ Based Program for Determining Ultimate Vertical Static Pile Capacity. Report No. FHWA-SA-98-074, U.S. Department of Transportation, Federal Highway Administration, Office of Technology Applications, Washington D.C. 112.
- Osterberg, J.O. (1995). The Osterberg Cell for Load Testing Drilled Shafts and Driven Piles. Report No. FHWA-SA-94-035, U.S. Department of Transportation, Federal Highway Administration, Office of Technology Applications, Washington, D.C., 92.
- Rausche, F., Likins, G.E., Goble, G.G. and Miner, R. (1985). The Performance of Pile Driving Systems. Main Report, U.S. Department of Transportation, Federal Highway Administration, Office of Research and Development, Washington, D.C., Volumes I-IV.
- Reese, L.C. (1984). Handbook on Design of Piles and Drilled Shafts Under Lateral Load. Report No. FHWA-IP-84 11, U.S. Department of Transportation, Federal Highway Administration, Office of Implementation, McLean, 386.
- Wang, S-T, and Reese, L.C. (1993). COM624P - Laterally Loaded Pile Analysis Program for the Microcomputer, Version 2.0. Report No. FHWA-SA-91-048, U.S. Department of Transportation, Federal Highway Administration, Office of Technology Applications, Washington, D.C., 504.

APPENDIX B

List of ASTM Pile Design and Testing Specifications

DESIGN

Standard Specification for Welded and Seamless Steel Pipe Piles.
ASTM Designation: A 252

Standard Specification for Round Timber Piles.
ASTM Designation: D 25

Standard Method for Establishing Design Stresses for Round Timber Piles.
ASTM Designation: D 2899

Standard Methods for Establishing Clear Wood Strength Values.
ASTM Designation: D 2555

TESTING

Standard Method for Testing Piles under Axial Compressive Load.
ASTM Designation: D 1143

Standard Method for Testing Individual Piles under Static Axial Tensile Load.
ASTM Designation: D 3689

Standard Method for Testing Piles under Lateral Load.
ASTM Designation: D 3966

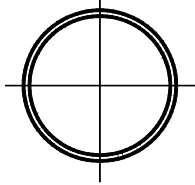
Standard Test Method for High Strain Dynamic Testing of Piles.
ASTM Designation: D 4945

Standard Test Method for Low Strain Dynamic Testing of Piles.
ASTM Designation: D 5882

APPENDIX C-1

Information and Data on Various Pile Types, Metric Units

	Page
Dimensions and Properties of Pipe Piles	C1-3
Data for Steel Monotube Piles.....	C1-17
Typical Prestressed Concrete Pile Sections.....	C1-18
Dimensions and Properties of H-Piles.....	C1-21



PIPE PILES

Approximate Pile Dimensions and Design Properties

Designation and Outside Diameter	Wall Thickness	Area A	Weight per Meter	Section Properties			Area of Exterior Surface	Inside Cross Sectional Area	Inside Volume	External Collapse Index
				I	S	r				
mm	mm	mm ²	N	mm ⁴ x 10 ⁶	mm ³ x 10 ³	mm	m ² /m	mm ²	m ³ /m	*
PP203	3.58	2,245	173	11.197	110.12	70.61	0.64	30,193	0.0301	266
	4.17	2,607	200	12.903	127.00	70.36	0.64	29,806	0.0298	422
	4.37	2,729	210	13.486	132.74	70.36	0.64	29,677	0.0296	487
	4.55	2,839	218	13.985	137.82	70.36	0.64	29,613	0.0296	548
	4.78	2,974	229	14.651	144.21	70.10	0.64	29,484	0.0293	621
	5.56	3,452	266	16.857	165.51	69.85	0.64	28,968	0.0291	874
PP219	2.77	1,884	145	10.989	100.45	76.45	0.69	35,806	0.0359	97
	3.18	2,155	166	12.570	114.55	76.45	0.69	35,548	0.0356	147
	3.58	2,426	187	14.069	128.47	76.20	0.69	35,290	0.0354	212
	3.96	2,678	206	15.484	141.42	75.95	0.69	35,032	0.0351	288
	4.17	2,813	216	16.233	148.30	75.95	0.69	34,903	0.0349	335
	4.37	2,949	227	16.982	155.02	75.95	0.69	34,774	0.0349	388
	4.55	3,065	236	17.648	160.92	75.95	0.69	34,645	0.0346	438
	4.78	3,213	247	18.481	168.79	75.69	0.69	34,452	0.0344	508
	5.16	3,465	266	19.813	180.26	75.69	0.69	34,258	0.0341	623
	5.56	3,729	287	21.269	195.01	75.44	0.69	33,935	0.0339	744
	6.35	4,245	326	24.017	219.59	75.18	0.69	33,419	0.0334	979
	7.04	4,684	360	26.389	240.89	74.93	0.69	33,032	0.0331	1,180
	7.92	5,258	404	29.344	267.11	74.68	0.69	32,452	0.0324	1,500
	8.18	5,420	417	30.177	275.30	74.68	0.69	32,258	0.0324	1,600
	8.74	5,775	444	31.967	291.69	74.42	0.69	31,935	0.0319	1,820
	9.53	6,271	482	34.506	314.63	74.17	0.69	31,419	0.0314	2,120
10.31	6,775	520	36.920	337.57	73.91	0.69	30,903	0.0309	2,420	
11.13	7,291	559	39.417	358.88	73.66	0.69	30,452	0.0304	2,740	
12.70	8,259	633	44.121	401.48	73.15	0.69	29,484	0.0293	3,340	
PP254	2.77	2,187	168	17.232	135.68	88.90	0.80	48,516	0.0484	62
	3.05	2,400	185	18.939	148.96	88.65	0.80	48,258	0.0482	83
	3.40	2,678	206	21.020	165.51	88.65	0.80	48,000	0.0479	116

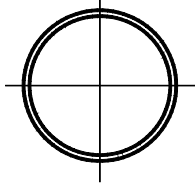
Pile design data converted to SI units from US units published in 1985 version of this manual.

Note: Designer must confirm section properties and local availability of selected pile section.

Material Specifications - ASTM A252

Example of suggested method of designation: PP219 x 2.77

* The External Collapse Index is a non-dimensional function of the diameter to wall thickness ratio and is for general guidance only. The higher the number, the greater is the resistance to collapse.



PIPE PILES

Approximate Pile Dimensions and Design Properties

Designation and Outside Diameter	Wall Thickness	Area A	Weight per Meter	Section Properties			Area of Exterior Surface	Inside Cross Sectional Area	Inside Volume	External Collapse Index
				I	S	r				
mm	mm	mm ²	N	mm ⁴ x 10 ⁶	mm ³ x 10 ³	mm	m ² /m	mm ²	m ³ /m	*
	3.58	2,820	217	22.102	173.70	88.65	0.80	47,871	0.0479	135
	3.81	2,994	230	23.434	185.17	88.39	0.80	47,677	0.0477	163
	4.17	3,271	251	25.515	201.56	88.39	0.80	47,419	0.0474	214
	4.37	3,426	263	26.680	209.75	88.39	0.80	47,226	0.0472	247
	4.55	3,562	274	27.721	217.95	88.14	0.80	47,097	0.0472	279
	4.78	3,742	287	29.053	229.42	88.14	0.80	46,903	0.0469	324
	5.16	4,033	310	31.217	245.81	87.88	0.80	46,645	0.0467	409
	5.56	4,342	334	33.507	263.83	87.88	0.80	46,322	0.0464	515
	5.84	4,555	350	35.088	276.94	87.88	0.80	46,129	0.0462	588
	6.35	4,942	380	37.919	298.24	87.63	0.80	45,742	0.0457	719
PP273	2.77	2,349	181	21.478	157.32	95.50	0.86	56,193	0.0562	50
	3.05	2,587	199	23.559	172.06	95.50	0.86	56,000	0.0559	67
	3.18	2,690	207	24.516	180.26	95.50	0.86	55,871	0.0559	76
	3.40	2,884	222	26.223	191.73	95.25	0.86	55,677	0.0557	93
	3.58	3,032	233	27.513	201.56	95.25	0.86	55,548	0.0554	109
	3.81	3,226	248	29.219	214.67	95.25	0.86	55,355	0.0554	131
	3.96	3,349	258	30.343	222.86	95.25	0.86	55,226	0.0552	148
	4.17	3,516	271	31.800	232.70	95.00	0.86	55,032	0.0549	172
	4.37	3,691	284	33.299	244.17	95.00	0.86	54,839	0.0549	199
	4.55	3,832	295	34.589	254.00	95.00	0.86	54,710	0.0547	224
	4.78	4,026	310	36.212	265.47	94.74	0.86	54,516	0.0544	260
	5.16	4,342	334	38.959	285.13	94.74	0.86	54,193	0.0542	328
	5.56	4,679	359	41.623	306.44	94.49	0.86	53,871	0.0539	414
	5.84	4,904	377	43.704	321.19	94.49	0.86	53,677	0.0537	480
	6.35	5,323	409	47.450	347.41	94.23	0.86	53,226	0.0532	605
	7.09	5,923	455	52.445	383.46	93.98	0.86	52,645	0.0527	781
	7.80	6,517	500	57.024	419.51	93.73	0.86	52,064	0.0522	951
	8.74	7,226	558	63.267	465.39	93.47	0.86	51,290	0.0514	1,180

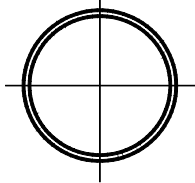
Pile design data converted to SI units from US units published in 1985 version of this manual.

Note: Designer must confirm section properties and local availability of selected pile section.

Material Specifications - ASTM A252

Example of suggested method of designation: PP219 x 2.77

* The External Collapse Index is a non-dimensional function of the diameter to wall thickness ratio and is for general guidance only. The higher the number, the greater is the resistance to collapse.



PIPE PILES

Approximate Pile Dimensions and Design Properties

Designation and Outside Diameter	Wall Thickness	Area A	Weight per Meter	Section Properties			Area of Exterior Surface	Inside Cross Sectional Area	Inside Volume	External Collapse Index
				I	S	r				
mm	mm	mm ²	N	mm ⁴ x 10 ⁶	mm ³ x 10 ³	mm	m ² /m	mm ²	m ³ /m	*
	9.27	7,678	591	67.013	489.97	93.22	0.86	50,903	0.0509	1,320
	11.13	9,162	704	78.668	576.82	92.71	0.86	49,419	0.0494	1,890
	12.70	10,389	799	88.241	645.65	92.20	0.86	48,193	0.0482	2,380
PP305	3.40	3,226	248	36.587	240.89	106.68	0.96	69,677	0.0697	67
	3.58	3,387	261	38.460	252.36	106.43	0.96	69,677	0.0695	78
	3.81	3,600	277	40.791	267.11	106.43	0.96	69,677	0.0695	94
	4.17	3,936	303	44.537	291.69	106.43	0.96	69,032	0.0690	123
	4.37	4,123	317	46.618	304.80	106.17	0.96	69,032	0.0687	142
	4.55	4,291	330	48.283	317.91	106.17	0.96	68,387	0.0687	161
	4.78	4,503	346	50.780	332.66	106.17	0.96	68,387	0.0685	186
	5.16	4,852	373	54.526	357.24	105.92	0.96	68,387	0.0682	235
	5.56	5,233	402	58.689	383.46	105.92	0.96	67,742	0.0677	296
	5.84	5,484	422	61.186	403.12	105.66	0.96	67,742	0.0675	344
	6.35	5,955	458	66.181	435.90	105.66	0.96	67,097	0.0670	443
	7.14	6,646	513	74.089	485.06	105.16	0.96	66,451	0.0662	616
7.92	7,420	568	81.581	534.22	104.90	0.96	65,806	0.0655	784	
PP324	2.77	2,794	215	36.004	222.86	113.54	1.02	79,355	0.0795	30
	3.18	3,200	246	41.124	254.00	113.28	1.02	79,355	0.0793	45
	3.40	3,426	264	44.121	272.03	113.28	1.02	78,710	0.0790	56
	3.58	3,607	277	46.202	285.13	113.28	1.02	78,710	0.0788	65
	3.81	3,832	295	49.115	303.16	113.29	1.02	78,710	0.0785	78
	3.96	3,981	306	50.780	314.63	113.03	1.02	78,710	0.0785	88
	4.17	4,181	322	53.278	329.38	113.03	1.02	78,064	0.0783	103
	4.37	4,387	337	55.775	345.77	113.03	1.02	78,064	0.0780	118
	4.55	4,562	351	58.272	358.88	113.03	1.02	78,064	0.0778	134
	4.78	4,787	368	60.770	376.90	112.78	1.02	77,419	0.0775	155
	5.16	5,162	397	65.765	404.76	112.78	1.02	77,419	0.0773	196
5.56	5,562	428	70.343	435.90	112.52	1.02	76,774	0.0768	246	

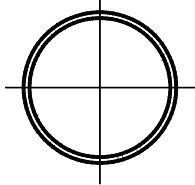
Pile design data converted to SI units from US units published in 1985 version of this manual.

Note: Designer must confirm section properties and local availability of selected pile section.

Material Specifications - ASTM A252

Example of suggested method of designation: PP219 x 2.77

* The External Collapse Index is a non-dimensional function of the diameter to wall thickness ratio and is for general guidance only. The higher the number, the greater is the resistance to collapse.



PIPE PILES

Approximate Pile Dimensions and Design Properties

Designation and Outside Diameter	Wall Thickness	Area A	Weight per Meter	Section Properties			Area of Exterior Surface	Inside Cross Sectional Area	Inside Volume	External Collapse Index
				I	S	r				
mm	mm	mm ²	N	mm ⁴ x 10 ⁶	mm ³ x 10 ³	mm	m ² /m	mm ²	m ³ /m	*
	5.84	5,839	449	73.673	455.56	112.52	1.02	76,774	0.0765	286
	6.35	6,336	487	79.916	493.25	112.27	1.02	76,129	0.0760	368
	7.14	7,097	546	89.074	550.61	112.01	1.02	75,484	0.0753	526
	7.92	7,871	605	98.231	606.32	111.76	1.02	74,193	0.0745	684
	8.38	8,323	639	103.225	639.10	111.51	1.02	74,193	0.0740	776
	8.74	8,646	665	107.388	663.68	111.51	1.02	73,548	0.0737	848
	9.53	9,420	723	116.129	717.75	111.25	1.02	72,903	0.0730	1,010
	10.31	10,131	781	124.869	771.83	111.00	1.02	72,258	0.0722	1,170
	11.13	10,905	840	133.610	825.91	110.74	1.02	71,613	0.0715	1,350
	12.70	12,389	955	150.676	929.15	109.98	1.02	69,677	0.0700	1,760
PP356	3.40	3,768	290	58.272	327.74	124.47	1.12	95,484	0.0956	42
	3.58	3,962	305	61.186	345.77	124.47	1.12	95,484	0.0953	49
	3.81	4,213	324	65.348	367.07	124.46	1.12	94,839	0.0951	59
	3.96	4,374	337	67.846	380.18	124.21	1.12	94,839	0.0948	66
	4.17	4,600	354	71.176	399.84	124.21	1.12	94,839	0.0948	77
	4.37	4,820	371	74.505	417.87	124.21	1.12	94,193	0.0946	89
	4.55	5,013	386	77.419	434.26	124.21	1.12	94,193	0.0943	101
	4.78	5,265	405	81.165	455.56	123.95	1.12	94,193	0.0941	117
	5.16	5,678	436	86.992	489.97	123.95	1.12	93,548	0.0936	147
	5.33	5,871	451	89.906	506.36	123.95	1.12	93,548	0.0936	163
	5.56	6,116	470	93.652	527.66	123.70	1.12	92,903	0.0933	815
	5.84	6,420	494	98.231	552.24	123.70	1.12	92,903	0.0928	215
	6.35	6,968	536	106.139	598.13	123.44	1.12	92,258	0.0923	277
	7.14	7,807	601	118.626	666.95	123.19	1.12	91,613	0.0916	395
	7.92	8,646	666	130.697	735.78	122.94	1.12	90,968	0.0906	542
	8.74	9,549	732	143.184	806.24	122.68	1.12	89,677	0.0898	691
	9.53	10,389	796	155.254	873.43	122.43	1.12	89,032	0.0890	835
	11.13	12,065	926	178.563	1,006.17	121.92	1.12	87,097	0.0873	1,130

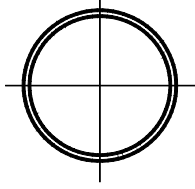
Pile design data converted to SI units from US units published in 1985 version of this manual.

Note: Designer must confirm section properties and local availability of selected pile section.

Material Specifications - ASTM A252

Example of suggested method of designation: PP219 x 2.77

* The External Collapse Index is a non-dimensional function of the diameter to wall thickness ratio and is for general guidance only. The higher the number, the greater is the resistance to collapse.



PIPE PILES

Approximate Pile Dimensions and Design Properties

Designation and Outside Diameter	Wall Thickness	Area A	Weight per Meter	Section Properties			Area of Exterior Surface	Inside Cross Sectional Area	Inside Volume	External Collapse Index
				I	S	r				
mm	mm	mm ²	N	mm ⁴ x 10 ⁶	mm ³ x 10 ³	mm	m ² /m	mm ²	m ³ /m	*
	11.91	12,839	989	190.218	1,070.08	121.67	1.12	86,451	0.0865	1,280
	12.70	13,678	1,052	201.456	1,132.35	121.41	1.12	85,806	0.0855	1,460
PP406	3.40	4,310	331	87.409	430.98	142.49	1.28	125,161	1.2542	28
	3.58	4,529	348	91.987	452.28	142.49	1.28	125,161	0.1252	33
	3.81	4,820	371	97.814	480.14	142.24	1.28	125,161	0.1249	39
	3.96	5,007	385	101.560	499.81	142.24	1.28	124,516	0.1247	44
	4.17	5,265	405	106.555	524.39	142.24	1.28	124,516	0.1244	52
	4.37	5,516	424	111.550	548.97	142.24	1.28	124,516	0.1242	60
	4.55	5,742	441	115.712	570.27	141.99	1.28	123,871	0.1239	67
	4.78	6,026	463	121.540	598.13	141.99	1.28	123,871	0.1237	78
	5.16	6,517	500	130.697	644.01	141.99	1.28	123,226	0.1232	98
	5.56	7,033	539	140.686	693.17	141.73	1.28	122,580	0.1227	124
	5.84	7,355	565	147.346	725.95	141.73	1.28	122,580	0.1224	144
	6.35	8,000	614	159.833	786.58	141.48	1.28	121,935	0.1217	185
	7.14	8,968	688	178.563	878.35	141.22	1.28	120,645	0.1207	264
	7.92	9,936	763	196.877	970.11	140.97	1.28	120,000	0.1199	362
	8.74	10,905	839	216.024	1,061.88	140.72	1.28	118,709	0.1189	487
	9.53	11,873	913	233.922	1,152.01	140.46	1.28	118,064	0.1179	617
	11.13	13,807	1,062	270.134	1,328.99	139.70	1.28	116,129	0.1159	874
	11.91	14,775	1,135	287.616	1,414.20	139.45	1.28	114,838	0.1149	1,000
12.70	15,679	1,208	304.681	1,499.42	139.19	1.28	114,193	0.1141	1,130	
PP457	3.58	5,104	392	131.113	573.55	160.27	1.44	159,355	0.1590	23
	4.37	6,213	478	159.417	696.45	160.02	1.44	158,064	0.1580	42
	4.78	6,775	522	173.569	760.36	160.02	1.44	157,419	0.1573	55
	5.16	7,291	563	186.888	817.71	159.77	1.44	156,774	0.1568	69
	5.56	7,871	607	201.456	879.99	159.77	1.44	156,129	0.1563	87
	5.84	8,259	637	211.029	922.59	159.51	1.44	156,129	0.1558	101
	6.35	8,968	692	228.511	999.61	159.51	1.44	155,484	0.1553	129

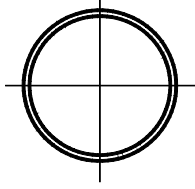
Pile design data converted to SI units from US units published in 1985 version of this manual.

Note: Designer must confirm section properties and local availability of selected pile section.

Material Specifications - ASTM A252

Example of suggested method of designation: PP219 x 2.77

* The External Collapse Index is a non-dimensional function of the diameter to wall thickness ratio and is for general guidance only. The higher the number, the greater is the resistance to collapse.



PIPE PILES

Approximate Pile Dimensions and Design Properties

Designation and Outside Diameter	Wall Thickness	Area A	Weight per Meter	Section Properties			Area of Exterior Surface	Inside Cross Sectional Area	Inside Volume	External Collapse Index
				I	S	r				
mm	mm	mm ²	N	mm ⁴ x 10 ⁶	mm ³ x 10 ³	mm	m ² /m	mm ²	m ³ /m	*
	7.14	10,065	776	255.566	1,117.60	159.26	1.44	154,193	0.1540	184
	7.92	11,163	860	282.205	1,235.58	158.75	1.44	152,903	0.1530	253
	8.74	12,323	947	309.676	1,353.57	158.50	1.44	151,613	0.1518	341
	9.53	13,420	1,030	335.899	1,468.28	158.24	1.44	150,967	0.1508	443
	10.31	14,452	1,113	361.705	1,581.35	157.99	1.44	149,677	0.1498	559
	11.13	15,615	1,199	387.928	1,704.25	157.73	1.44	148,387	0.1485	675
	11.91	16,646	1,281	413.318	1,802.58	157.48	1.44	147,742	0.1475	788
	12.70	17,743	1,364	437.043	1,917.29	157.23	1.44	146,451	0.1465	900
PP508	3.58	5,678	436	180.644	711.20	178.31	1.60	196,774	0.1969	17
	4.37	6,904	531	219.354	863.60	178.05	1.60	195,483	0.1957	30
	4.78	7,549	581	238.917	940.62	177.80	1.60	194,838	0.1952	40
	5.16	8,130	626	257.647	1,014.36	177.80	1.60	194,838	0.1947	50
	5.56	8,775	675	277.210	1,091.38	177.55	1.60	194,193	0.1939	63
	6.35	10,002	769	314.671	1,238.86	177.29	1.60	192,903	0.1926	94
	7.14	11,226	864	352.132	1,386.35	177.04	1.60	191,613	0.1914	134
	7.92	12,452	957	389.176	1,532.19	176.78	1.60	190,322	0.1901	184
	8.74	13,678	1,054	428.718	1,687.87	176.53	1.60	189,032	0.1889	247
	9.53	14,904	1,147	462.017	1,818.96	176.28	1.60	187,742	0.1879	321
	10.31	16,130	1,240	499.478	1,966.45	176.02	1.60	186,451	0.1866	409
	11.13	17,357	1,335	536.939	2,113.93	175.77	1.60	185,161	0.1854	515
	11.91	18,583	1,428	570.237	2,245.03	175.51	1.60	183,871	0.1841	618
12.70	19,743	1,520	607.698	2,392.51	175.26	1.60	183,225	0.1829	719	
PP559	4.37	7,613	585	292.611	1,047.13	196.09	1.76	237,419	0.2375	23
	4.78	8,323	639	318.833	1,142.18	195.83	1.76	236,774	0.2370	30
	5.56	9,678	743	370.030	1,324.07	195.58	1.76	235,483	0.2355	47
	6.35	11,034	847	420.394	1,504.33	195.33	1.76	234,193	0.2343	70
	7.14	12,389	951	470.342	1,687.87	195.07	1.76	232,903	0.2328	100
	7.92	13,744	1,055	520.289	1,868.13	194.82	1.76	231,612	0.2315	138

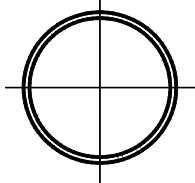
Pile design data converted to SI units from US units published in 1985 version of this manual.

Note: Designer must confirm section properties and local availability of selected pile section.

Material Specifications - ASTM A252

Example of suggested method of designation: PP219 x 2.77

* The External Collapse Index is a non-dimensional function of the diameter to wall thickness ratio and is for general guidance only. The higher the number, the greater is the resistance to collapse.



PIPE PILES

Approximate Pile Dimensions and Design Properties

Designation and Outside Diameter	Wall Thickness	Area A	Weight per Meter	Section Properties			Area of Exterior Surface	Inside Cross Sectional Area	Inside Volume	External Collapse Index
				I	S	r				
mm	mm	mm ²	N	mm ⁴ x 10 ⁶	mm ³ x 10 ³	mm	m ² /m	mm ²	m ³ /m	*
	8.74	15,099	1,161	570.237	2,048.38	194.56	1.76	230,322	0.2303	185
	9.53	16,454	1,264	620.185	2,212.25	194.31	1.76	229,032	0.2288	241
	10.31	17,743	1,366	670.133	2,392.51	194.06	1.76	227,741	0.2275	306
	11.13	19,162	1,472	715.918	2,572.77	193.55	1.76	225,806	0.2260	386
	11.91	20,454	1,574	765.866	2,736.64	193.29	1.76	224,516	0.2248	475
	12.70	21,809	1,675	811.651	2,900.51	193.04	1.76	223,225	0.2235	571
PP610	4.37	8,323	639	380.436	1,248.69	213.87	1.91	283,870	0.2834	18
	4.78	9,097	698	414.983	1,361.77	213.87	1.91	282,580	0.2834	23
	5.56	10,582	812	482.828	1,579.71	213.61	1.91	281,290	0.2809	36
	6.35	12,065	925	549.425	1,802.58	213.36	1.91	279,999	0.2809	54
	7.14	13,486	1,039	611.860	2,015.61	213.11	1.91	278,064	0.2784	77
	7.92	14,970	1,152	678.457	2,228.64	212.85	1.91	276,774	0.2759	106
	8.74	16,517	1,268	745.054	2,441.67	212.34	1.91	275,483	0.2759	142
	9.53	17,937	1,381	807.489	2,654.70	212.09	1.91	274,193	0.2734	185
	10.31	19,421	1,493	869.924	2,867.74	211.84	1.91	272,258	0.2734	235
	11.13	20,904	1,608	936.521	3,080.77	211.58	1.91	270,967	0.2709	296
	11.91	22,388	1,720	998.955	3,277.41	211.33	1.91	269,677	0.2684	364
	12.70	23,809	1,831	1,061.390	3,474.06	211.07	1.91	267,741	0.2684	443
PP660	6.35	13,033	1,003	699.269	2,113.93	231.14	2.08	329,677	0.3286	43
	7.14	14,646	1,126	782.515	2,359.74	230.89	2.08	327,741	0.3286	61
	7.92	16,259	1,249	865.761	2,621.93	230.63	2.08	326,451	0.3261	83
	8.74	17,872	1,376	949.008	2,884.12	230.38	2.08	324,515	0.3236	112
	9.53	19,485	1,498	1,032.254	3,129.93	230.12	2.08	323,225	0.3236	145
	10.31	21,034	1,620	1,111.338	3,375.74	229.87	2.08	321,290	0.3211	184
	11.13	22,711	1,745	1,194.584	3,621.54	229.62	2.08	319,999	0.3211	232
	11.91	24,260	1,866	1,277.830	3,867.35	229.36	2.08	318,064	0.3186	286
	12.70	25,873	1,987	1,356.914	4,113.15	229.11	2.08	316,774	0.3161	347
	14.27	28,969	2,228	1,510.920	4,588.38	228.60	2.08	313,548	0.3135	495

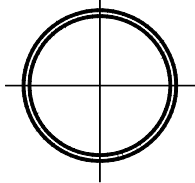
Pile design data converted to SI units from US units published in 1985 version of this manual.

Note: Designer must confirm section properties and local availability of selected pile section.

Material Specifications - ASTM A252

Example of suggested method of designation: PP219 x 2.77

* The External Collapse Index is a non-dimensional function of the diameter to wall thickness ratio and is for general guidance only. The higher the number, the greater is the resistance to collapse.



PIPE PILES

Approximate Pile Dimensions and Design Properties

Designation and Outside Diameter	Wall Thickness	Area A	Weight per Meter	Section Properties			Area of Exterior Surface	Inside Cross Sectional Area	Inside Volume	External Collapse Index
				I	S	r				
mm	mm	mm ²	N	mm ⁴ x 10 ⁶	mm ³ x 10 ³	mm	m ² /m	mm ²	m ³ /m	*
PP711	15.88	32,132	2,472	1,669.088	5,063.60	227.84	2.08	310,322	0.3110	656
	17.48	35,292	2,714	1,823.094	5,522.44	227.33	2.08	307,096	0.3060	814
	19.05	38,389	2,951	1,977.099	5,981.28	226.82	2.08	303,870	0.3035	970
	6.35	14,065	1,081	874.086	2,458.06	249.17	2.23	383,225	0.3838	34
	7.14	15,807	1,214	978.144	2,753.03	248.92	2.23	381,290	0.3813	48
	7.92	17,486	1,346	1,082.202	3,047.99	248.67	2.23	379,999	0.3788	66
	8.74	19,291	1,483	1,190.422	3,342.96	248.41	2.23	378,064	0.3788	89
	9.53	20,969	1,615	1,294.480	3,637.93	248.16	2.23	376,128	0.3763	116
	10.31	22,711	1,746	1,394.375	3,916.51	247.90	2.23	374,838	0.3737	147
	11.13	24,453	1,881	1,498.433	4,211.48	247.65	2.23	372,902	0.3737	185
	11.91	26,195	2,012	1,598.329	4,506.44	247.40	2.23	370,967	0.3712	228
	12.70	27,874	2,143	1,698.224	4,785.02	246.89	2.23	369,677	0.3687	277
	14.27	31,229	2,403	1,898.015	5,342.18	246.38	2.23	365,806	0.3587	395
	15.88	34,713	2,667	2,097.806	5,899.34	245.87	2.23	362,580	0.3612	544
	17.48	38,068	2,929	2,293.435	6,440.12	245.36	2.23	359,354	0.3587	691
	19.05	41,423	3,185	2,480.739	6,980.89	244.86	2.23	356,128	0.3562	835
PP762	6.35	15,099	1,159	1,078.039	2,818.58	266.70	2.39	440,644	0.4415	28
	7.14	16,904	1,302	1,207.071	3,162.70	266.70	2.39	439,354	0.4390	39
	7.92	18,775	1,444	1,336.103	3,506.83	266.70	2.39	437,418	0.4365	54
	8.74	20,646	1,590	1,465.135	3,850.96	266.70	2.39	435,483	0.4365	72
	9.53	22,517	1,731	1,594.166	4,178.70	266.70	2.39	433,548	0.4340	94
	10.31	24,324	1,873	1,719.036	4,522.83	266.70	2.39	431,612	0.4314	120
	11.13	26,261	2,018	1,848.068	4,850.57	266.70	2.39	429,677	0.4289	150
	11.91	28,066	2,159	1,972.937	5,178.31	264.16	2.39	427,741	0.4289	185
	12.70	29,874	2,299	2,097.806	5,506.05	264.16	2.39	426,451	0.4264	225
	14.27	33,550	2,578	2,343.383	6,145.15	264.16	2.39	422,580	0.4214	321
15.88	37,228	2,861	2,588.959	6,800.63	264.16	2.39	418,709	0.4189	443	
17.48	40,907	3,143	2,834.536	7,439.73	264.16	2.39	415,483	0.4164	584	

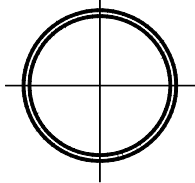
Pile design data converted to SI units from US units published in 1985 version of this manual.

Note: Designer must confirm section properties and local availability of selected pile section.

Material Specifications - ASTM A252

Example of suggested method of designation: PP219 x 2.77

* The External Collapse Index is a non-dimensional function of the diameter to wall thickness ratio and is for general guidance only. The higher the number, the greater is the resistance to collapse.



PIPE PILES

Approximate Pile Dimensions and Design Properties

Designation and Outside Diameter	Wall Thickness	Area A	Weight per Meter	Section Properties			Area of Exterior Surface	Inside Cross Sectional Area	Inside Volume	External Collapse Index
				I	S	r				
mm	mm	mm ²	N	mm ⁴ x 10 ⁶	mm ³ x 10 ³	mm	m ² /m	mm ²	m ³ /m	*
PP813	19.05	44,454	3,419	3,071.788	8,062.44	261.62	2.39	411,612	0.4114	719
	6.35	16,065	1,237	1,306.967	3,211.86	284.48	2.55	502,580	0.5017	23
	7.14	18,067	1,389	1,465.135	3,605.15	284.488	2.55	500,644	0.5017	32
	7.92	20,067	1,541	1,623.303	3,998.44	284.48	2.55	498,709	0.4992	44
	8.74	22,067	1,697	1,785.633	4,391.73	284.48	2.55	496,773	0.4967	60
	9.53	24,067	1,848	1,939.638	4,768.64	284.48	2.55	494,838	0.4942	77
	10.31	26,002	1,999	2,093.644	5,145.54	284.48	2.55	492,902	0.4916	98
	11.13	28,003	2,155	2,251.812	5,538.83	284.48	2.55	490,967	0.4916	124
	11.91	30,003	2,305	2,401.655	5,915.73	281.94	2.55	489,031	0.4891	152
	12.70	31,937	2,455	2,555.661	6,292.63	281.94	2.55	487,096	0.4866	185
	14.27	35,810	2,754	2,855.348	7,030.05	281.94	2.55	483,225	0.4841	264
	15.88	39,744	3,056	3,155.034	7,767.47	281.94	2.55	479,354	0.4791	364
	17.48	43,680	3,358	3,454.721	8,504.89	281.94	2.55	475,483	0.4741	487
19.05	47,488	3,653	3,741.921	9,209.53	281.94	2.55	471,612	0.4716	617	
PP864	6.35	17,099	1,315	1,569.192	3,637.93	302.26	2.71	568,386	0.5694	19
	7.14	19,228	1,477	1,760.659	4,080.38	302.26	2.71	566,450	0.5669	27
	7.92	21,293	1,638	1,947.963	4,522.83	302.26	2.71	564,515	0.5644	37
	8.74	23,485	1,804	2,143.592	4,965.28	302.26	2.71	562,580	0.5619	50
	9.53	25,551	1,965	2,330.896	5,391.34	302.26	2.71	559,999	0.5594	64
	10.31	27,615	2,126	2,518.200	5,833.79	302.26	2.71	558,063	0.5569	82
	11.13	29,808	2,291	2,705.504	6,276.25	302.26	2.71	556,128	0.5569	103
	11.91	31,873	2,451	2,888.646	6,702.31	302.26	2.71	554,192	0.5544	127
	12.70	33,938	2,611	3,071.788	7,111.99	299.72	2.71	551,612	0.5518	154
	14.27	38,068	2,929	3,433.909	7,964.11	299.72	2.71	547,741	0.5468	219
	15.88	42,262	3,251	3,800.193	8,799.85	299.72	2.71	543,225	0.5443	303
	17.48	46,454	3,572	4,158.152	9,635.59	299.72	2.71	539,354	0.5393	405
	19.05	50,519	3,887	4,495.299	10,438.56	299.72	2.71	535,483	0.5343	527
22.23	58,779	4,517	5,202.893	12,044.49	297.18	2.71	527,096	0.5268	767	

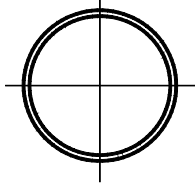
Pile design data converted to SI units from US units published in 1985 version of this manual.

Note: Designer must confirm section properties and local availability of selected pile section.

Material Specifications - ASTM A252

Example of suggested method of designation: PP219 x 2.77

* The External Collapse Index is a non-dimensional function of the diameter to wall thickness ratio and is for general guidance only. The higher the number, the greater is the resistance to collapse.



PIPE PILES

Approximate Pile Dimensions and Design Properties

Designation and Outside Diameter	Wall Thickness	Area A	Weight per Meter	Section Properties			Area of Exterior Surface	Inside Cross Sectional Area	Inside Volume	External Collapse Index
				I	S	r				
mm	mm	mm ²	N	mm ⁴ x 10 ⁶	mm ³ x 10 ³	mm	m ² /m	mm ²	m ³ /m	*
PP914	25.40	67,102	5,143	5,868.863	13,617.65	297.18	2.71	518,709	0.5192	1,010
	6.35	18,130	1,393	1,868.879	4,080.38	320.04	2.87	638,708	0.6396	16
	7.14	20,325	1,564	2,093.644	4,571.99	320.04	2.87	636,128	0.6371	23
	7.92	22,582	1,735	2,318.409	5,063.60	320.04	2.87	634,192	0.6346	31
	8.74	24,840	1,912	2,547.336	5,571.60	320.04	2.87	631,612	0.6321	42
	9.53	27,098	2,082	2,772.101	6,063.21	320.04	2.87	629,676	0.6296	54
	10.31	29,292	2,252	2,992.704	6,538.44	320.04	2.87	627,096	0.6271	69
	11.13	31,550	2,428	3,221.631	7,046.44	320.04	2.87	625,160	0.6246	87
	11.91	33,808	2,597	3,438.072	7,521.66	320.04	2.87	623,225	0.6221	107
	12.70	36,002	2,766	3,658.674	7,996.89	320.04	2.87	620,644	0.6221	129
	14.27	40,390	3,104	4,087.393	8,947.34	317.50	2.87	616,128	0.6171	184
	15.88	44,841	3,446	4,536.923	9,897.79	317.50	2.87	611,612	0.6120	254
	17.48	49,230	3,786	4,953.154	10,831.85	317.50	2.87	607,741	0.6070	341
	19.05	53,616	4,120	5,369.385	11,749.52	317.50	2.87	603,225	0.6020	443
	22.23	62,326	4,790	6,201.848	13,568.49	314.96	2.87	594,192	0.5945	674
	25.40	70,972	5,455	7,034.311	15,338.29	314.96	2.87	585,805	0.5870	900
31.75	87,747	6,770	8,574.367	18,845.12	312.42	2.87	568,386	0.5694	1,380	
PP965	6.35	19,099	1,471	2,197.702	4,555.60	337.82	3.03	709,676	0.7124	14
	7.14	21,485	1,652	2,464.090	5,112.76	337.82	3.03	709,676	0.7099	19
	7.92	23,809	1,833	2,730.478	5,653.54	337.82	3.03	709,676	0.7074	26
	8.74	26,261	2,019	3,001.029	6,227.08	337.82	3.03	703,224	0.7049	35
	9.53	28,582	2,199	3,263.254	6,767.86	337.82	3.03	703,224	0.7023	46
	10.31	30,971	2,379	3,525.480	7,308.63	337.82	3.03	703,224	0.6998	59
	11.13	33,358	2,564	3,796.031	7,865.79	337.82	3.03	696,773	0.6973	74
	11.91	35,680	2,743	4,054.094	8,406.56	337.82	3.03	696,773	0.6973	90
	12.70	38,002	2,922	4,328.807	8,930.95	337.82	3.03	696,773	0.6923	110
	14.27	42,649	3,279	4,828.285	9,996.11	335.28	3.03	690,321	0.6898	156
15.88	47,359	3,641	5,327.762	11,061.27	335.28	3.03	683,870	0.6848	216	

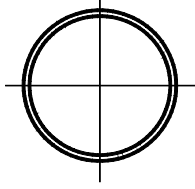
Pile design data converted to SI units from US units published in 1985 version of this manual.

Note: Designer must confirm section properties and local availability of selected pile section.

Material Specifications - ASTM A252

Example of suggested method of designation: PP219 x 2.77

* The External Collapse Index is a non-dimensional function of the diameter to wall thickness ratio and is for general guidance only. The higher the number, the greater is the resistance to collapse.



PIPE PILES

Approximate Pile Dimensions and Design Properties

Designation and Outside Diameter	Wall Thickness	Area A	Weight per Meter	Section Properties			Area of Exterior Surface	Inside Cross Sectional Area	Inside Volume	External Collapse Index
				I	S	r				
mm	mm	mm ²	N	mm ⁴ x 10 ⁶	mm ³ x 10 ³	mm	m ² /m	mm ²	m ³ /m	*
	17.48	52,003	4,001	5,827.240	12,110.04	335.28	3.03	677,418	0.6798	289
	19.05	56,649	4,354	6,326.718	13,142.43	335.28	3.03	677,418	0.6748	376
	22.23	65,810	5,063	7,325.673	15,174.42	332.74	3.03	664,515	0.6647	590
	25.40	74,843	5,767	8,283.005	17,206.42	332.74	3.03	658,063	0.6572	805
	31.75	92,909	7,160	10,156.047	20,975.44	330.20	3.03	638,708	0.6396	1,230
	38.10	110,974	8,533	11,945.842	24,744.47	327.66	3.03	620,644	0.6221	1,780
PP1016	7.92	25,098	1,930	3,188.333	6,276.25	355.60	3.20	787,095	0.7851	23
	8.74	27,679	2,126	3,508.831	6,898.95	355.60	3.20	780,644	0.7826	30
	9.53	30,131	2,316	3,812.680	7,505.28	355.60	3.20	780,644	0.7801	39
	10.31	32,583	2,505	4,120.691	8,111.60	355.60	3.20	780,644	0.7776	50
	11.13	35,099	2,701	4,453.676	8,734.31	355.60	3.20	774,192	0.7751	63
	11.91	37,551	2,890	4,745.038	9,324.24	355.60	3.20	774,192	0.7726	77
	12.70	40,002	3,078	5,036.400	9,914.17	355.60	3.20	767,740	0.7701	94
	14.27	44,906	3,454	5,619.124	11,094.04	353.06	3.20	767,740	0.7651	134
	15.88	49,874	3,836	6,243.471	12,273.91	353.06	3.20	761,289	0.7600	185
	17.48	54,842	4,215	6,826.195	13,453.78	353.06	3.20	754,837	0.7550	247
	19.05	59,681	4,588	7,408.919	14,600.87	353.06	3.20	748,386	0.7500	321
	22.23	69,682	5,336	8,574.367	16,878.68	350.52	3.20	741,934	0.7425	514
	25.40	79,360	6,078	9,698.192	19,172.86	350.52	3.20	729,031	0.7324	719
	31.75	98,070	7,549	11,904.219	23,433.50	347.98	3.20	709,676	0.7124	1,130
38.10	116,781	9,001	14,026.999	27,530.27	345.44	3.20	696,773	0.6923	1,620	
44.45	135,492	10,433	16,024.910	31,627.03	342.90	3.20	677,418	0.6748	2,140	
PP1067	7.92	26,389	2,027	3,696.135	6,931.73	373.38	3.35	864,514	0.8679	20
	8.74	29,034	2,233	4,066.581	7,619.98	373.38	3.35	864,514	0.8654	26
	9.53	31,615	2,433	4,412.053	8,291.85	373.38	3.35	864,514	0.8629	34
	10.31	34,260	2,632	4,786.661	8,947.34	373.38	3.35	864,514	0.8604	43
	11.13	36,905	2,837	5,161.270	9,635.59	373.38	3.35	858,063	0.8579	54
	11.91	39,486	3,036	5,494.255	10,291.08	373.38	3.35	851,611	0.8554	67

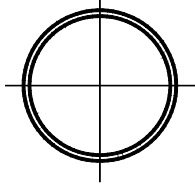
Pile design data converted to SI units from US units published in 1985 version of this manual.

Note: Designer must confirm section properties and local availability of selected pile section.

Material Specifications - ASTM A252

Example of suggested method of designation: PP219 x 2.77

* The External Collapse Index is a non-dimensional function of the diameter to wall thickness ratio and is for general guidance only. The higher the number, the greater is the resistance to collapse.



PIPE PILES

Approximate Pile Dimensions and Design Properties

Designation and Outside Diameter	Wall Thickness	Area A	Weight per Meter	Section Properties			Area of Exterior Surface	Inside Cross Sectional Area	Inside Volume	External Collapse Index
				I	S	r				
mm	mm	mm ²	N	mm ⁴ x 10 ⁶	mm ³ x 10 ³	mm	m ² /m	mm ²	m ³ /m	*
	12.70	42,067	3,234	5,827.240	10,946.56	373.38	3.35	851,611	0.8528	81
	14.27	47,229	3,630	6,534.833	12,257.52	373.38	3.35	845,160	0.8478	116
	15.88	52,390	4,030	7,242.427	13,568.49	370.84	3.35	838,708	0.8403	159
	17.48	57,616	4,430	7,950.020	14,863.07	370.84	3.35	838,708	0.8353	213
	19.05	62,713	4,822	8,615.991	16,141.26	370.84	3.35	832,256	0.8303	277
	22.23	72,908	5,608	9,947.931	18,681.25	368.30	3.35	819,353	0.8202	443
	25.40	83,231	6,390	11,279.872	21,139.31	368.30	3.35	812,902	0.8102	641
	31.75	103,232	7,939	13,818.883	25,891.56	365.76	3.35	793,547	0.7901	1,030
	38.10	123,233	9,468	16,316.272	30,643.81	363.22	3.35	767,740	0.7701	1,460
	44.45	142,589	10,978	18,688.791	35,068.32	360.68	3.35	748,386	0.7500	1,970
	50.80	161,945	12,468	20,978.064	39,328.95	360.68	3.35	729,031	0.7324	2,470
PP1118	8.74	30,453	2,341	4,661.792	8,373.79	391.16	3.51	948,385	0.9507	23
	9.53	33,163	2,550	5,078.023	9,111.21	391.16	3.51	948,385	0.9482	30
	10.31	35,873	2,759	5,494.255	9,832.24	391.16	3.51	941,934	0.9457	38
	11.13	38,647	2,974	5,910.486	10,586.04	391.16	3.51	941,934	0.9432	47
	11.91	41,357	3,182	6,326.718	11,323.46	391.16	3.51	941,934	0.9406	58
	12.70	44,067	3,390	6,742.949	12,044.49	391.16	3.51	935,482	0.9381	70
	15.88	54,971	4,225	8,324.629	14,928.62	388.62	3.51	929,030	0.9256	138
	19.05	65,810	5,056	9,906.308	17,698.03	388.62	3.51	916,127	0.9156	241
	22.23	76,779	5,881	11,487.987	20,483.83	388.62	3.51	903,224	0.9055	384
	25.40	87,102	6,702	12,986.420	23,269.63	386.08	3.51	896,772	0.8930	571
	31.75	108,394	8,328	15,983.287	28,513.49	383.54	3.51	870,966	0.8729	941
PP1219	38.10	129,040	9,936	18,855.284	33,757.35	381.00	3.51	851,611	0.8528	1,300
	44.45	149,686	11,524	21,602.411	38,673.47	381.00	3.51	832,256	0.8303	1,810
	50.80	170,333	13,092	24,266.292	43,425.72	378.46	3.51	812,902	0.8102	2,290
	57.15	190,334	14,641	26,846.927	48,014.10	375.92	3.51	793,547	0.7901	2,770
	8.74	33,228	2,555	6,076.979	9,979.72	426.72	3.84	1,135,482	1.1338	18
	9.53	36,196	2,784	6,618.080	10,864.62	426.72	3.84	1,129,030	1.1313	23

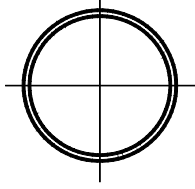
Pile design data converted to SI units from US units published in 1985 version of this manual.

Note: Designer must confirm section properties and local availability of selected pile section.

Material Specifications - ASTM A252

Example of suggested method of designation: PP219 x 2.77

* The External Collapse Index is a non-dimensional function of the diameter to wall thickness ratio and is for general guidance only. The higher the number, the greater is the resistance to collapse.



PIPE PILES

Approximate Pile Dimensions and Design Properties

Designation and Outside Diameter	Wall Thickness	Area A	Weight per Meter	Section Properties			Area of Exterior Surface	Inside Cross Sectional Area	Inside Volume	External Collapse Index
				I	S	r				
mm	mm	mm ²	N	mm ⁴ x 10 ⁶	mm ³ x 10 ³	mm	m ² /m	mm ²	m ³ /m	*
	10.31	39,164	3,012	7,159.181	11,733.14	426.72	3.84	1,129,030	1.1288	29
	11.13	42,196	3,247	7,700.281	12,634.43	426.72	3.84	1,122,578	1.1263	36
	11.91	45,164	3,474	8,241.382	13,502.94	426.72	3.84	1,122,578	1.1212	45
	12.70	48,132	3,702	8,740.860	14,371.46	426.72	3.84	1,116,127	1.1187	54
	15.88	60,004	4,615	10,863.640	17,861.90	426.72	3.84	1,109,675	1.1087	106
	19.05	71,617	5,523	12,944.797	21,139.31	424.18	3.84	1,096,772	1.0962	185
	22.23	83,876	6,427	14,984.331	24,580.60	424.18	3.84	1,083,869	1.0836	295
	25.40	95,490	7,325	16,982.242	27,858.01	421.64	3.84	1,070,966	1.0711	443
	31.75	118,717	9,108	20,894.818	34,248.96	419.10	3.84	1,051,611	1.0485	787
	38.10	141,299	10,871	24,682.524	40,476.05	416.56	3.84	1,025,804	1.0259	1,130
	44.45	163,881	12,614	28,345.360	46,539.26	416.56	3.84	1,006,450	1.0034	1,530
	50.80	186,463	14,339	31,883.327	52,274.73	414.02	3.84	980,643	0.9808	1,970
	57.15	208,400	16,043	35,296.425	57,846.34	411.48	3.84	961,288	0.9582	2,410
	63.50	230,336	17,729	38,626.276	63,254.07	408.94	3.84	935,482	0.9381	2,850

Pile design data converted to SI units from US units published in 1985 version of this manual.

Note: Designer must confirm section properties and local availability of selected pile section.

Material Specifications - ASTM A252

Example of suggested method of designation: PP219 x 2.77

* The External Collapse Index is a non-dimensional function of the diameter to wall thickness ratio and is for general guidance only. The higher the number, the greater is the resistance to collapse.

MONOTUBE PILES

Standard Monotube Weights and Volumes

TYPE	SIZE POINT DIAMETER x BUTT DIAMETER x LENGTH	Weight (N) per m				EST. CONC. VOL. m ³
		9 GA.	7 GA.	5 GA.	3 GA.	
F Taper 3.6 mm per Meter	216 mm x 305 mm x 7.62 m	248	292	350	409	0.329
	203 mm x 305 mm x 9.14 m	233	292	336	394	0.420
	216 mm x 356 mm x 12.19 m	277	321	379	452	0.726
	203 mm x 406 mm x 18.29 m	292	350	409	482	1.284
	203 mm x 457 mm x 22.86 m	-	379	452	511	1.979
J Taper 6.4 mm per Meter	203 mm x 305 mm x 5.18 m	248	292	336	394	0.244
	203 mm x 356 mm x 7.62 m	263	321	379	438	0.443
	203 mm x 406 mm x 10.06 m	292	350	409	467	0.726
	203 mm x 457 mm x 12.19 m	-	379	438	511	1.047
Y Taper 10.2 mm per Meter	203 mm x 305 mm x 3.05 m	248	292	350	409	0.138
	203 mm x 356 mm x 4.57 m	277	321	379	438	0.260
	203 mm x 406 mm x 6.10 m	292	350	409	482	0.428
	203 mm x 457 mm x 7.62 m	-	379	452	511	0.657

Extensions (Overall Length 0.305 m Greater than indicated)

TYPE	DIAMETER + LENGTH	9 GA.	7 GA.	5 GA.	3 GA.	m ³ /m
N 12	305 mm x 305 mm x 6.10 / 12.19 m	292	350	409	482	0.065
N 14	356 mm x 356 mm x 6.10 m / 12.19 m	350	423	496	598	0.088
N 16	406 mm x 406 mm x 6.10 m / 12.19 m	409	482	569	671	0.113
N 18	457 mm x 457 mm x 6.10 m / 12.19 m	-	555	642	759	0.145



Note: Designer must confirm section properties of selected pile section.

Pile design data converted to SI units from US units published in Monotube Pile Corporation Catalog 592.

MONOTUBE PILES

Physical Properties

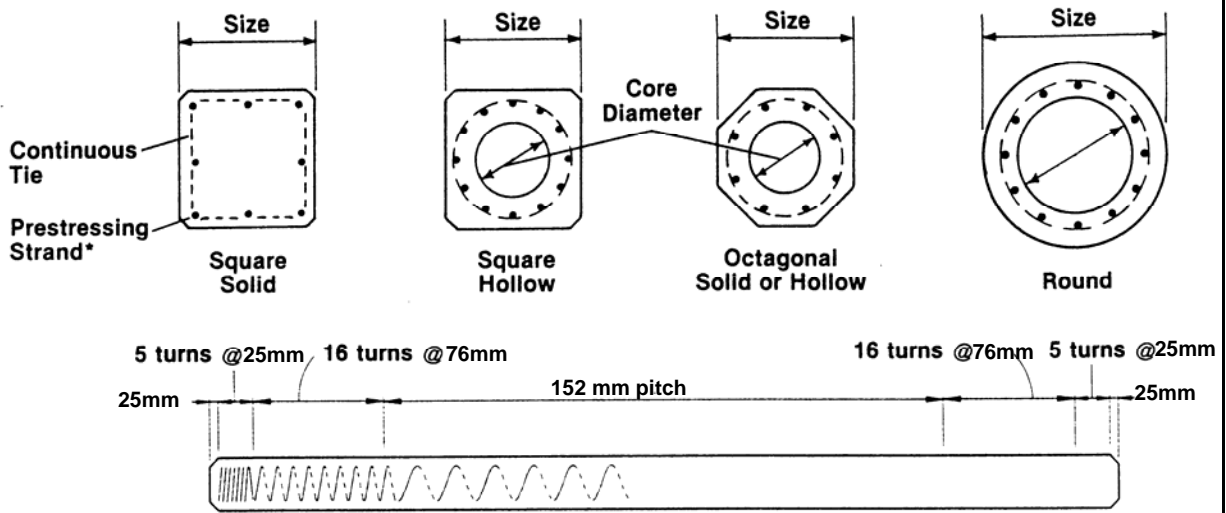
STEEL THICKNESS	POINTS		BUTTS OF PILE SECTIONS							
	203 mm	216 mm	305 mm				356 mm			
	A mm ²	A mm ²	A mm ²	I mm ⁴ x 10 ⁶	S mm ³ x 10 ³	r mm	A mm ²	I mm ⁴ x 10 ⁶	S mm ³ x 10 ³	r mm
9 GAUGE 3.797 mm	2,342	2,535	3,748	42.456	267.109	106	4,355	66.181	360.515	123
7 GAUGE 4.554 mm	2,839	3,077	4,497	50.780	319.548	106	5,252	80.749	437.535	124
5 GAUGE 5.314 mm	3,348	3,619	5,277	60.354	376.902	107	6,129	94.485	507.999	124
3 GAUGE 6.073 mm	3,787	4,245	5,781	61.602	396.567	103	6,839	99.479	550.605	121
CONCRETE AREA mm ²	27,290	30,518	65,161				87,742			

STEEL THICKNESS	POINTS		BUTTS OF PILE SECTIONS							
	203 mm	216 mm	406 mm				457 mm			
	A mm ²	A mm ²	A mm ²	I mm ⁴ x 10 ⁶	S mm ³ x 10 ³	r mm	A mm ²	I mm ⁴ x 10 ⁶	S mm ³ x 10 ³	r mm
9 GAUGE 3.797 mm	2,342	2,535	4,929	96.566	463.754	140	-	-	-	-
7 GAUGE 4.554 mm	2,839	3,077	5,923	115.712	555.521	140	6,710	168.157	712.837	158
5 GAUGE 5.314 mm	3,348	3,619	6,968	136.940	555.521	140	7,871	198.959	839.018	159
3 GAUGE 6.073 mm	3,787	4,245	7,742	144.849	706.282	137	8,774	209.781	907.843	155
CONCRETE AREA mm ²	27,290	30,518	113,548				144,516			

Note: Designer must confirm section properties of selected pile section.

Pile design data converted to SI units from US units published in Monotube Pile Corporation Catalog 592.

PRECAST/PRESTRESSED CONCRETE PILES



* Strand pattern may be circular or square.

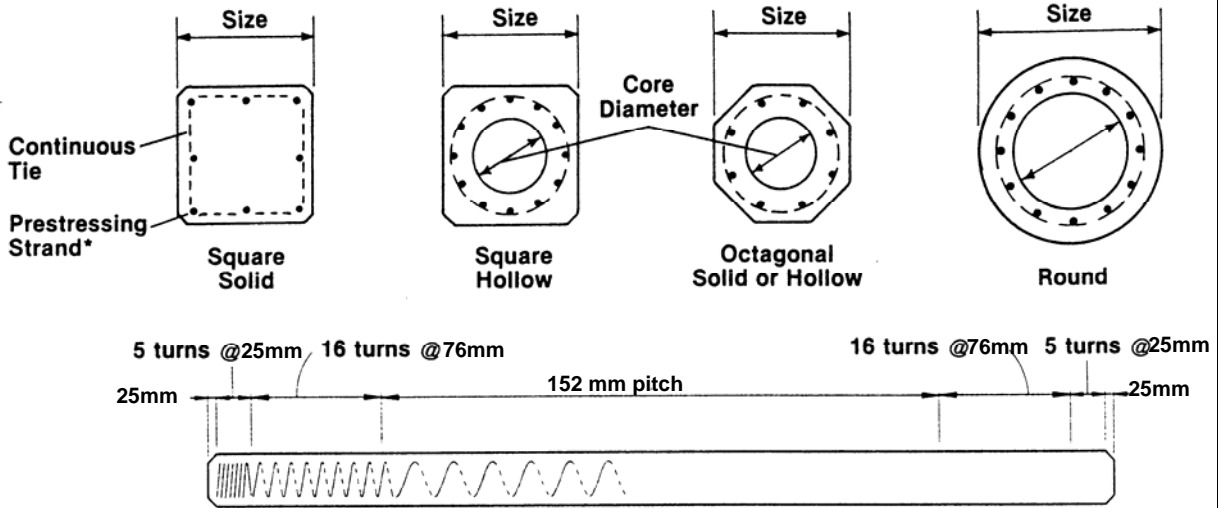
Typical Elevation

Size mm	Core Diameter mm	Section Properties					
		Area mm ²	Weight N/m	Moment of Inertia mm ⁴ x 10 ⁶	Section Modulus mm ³ x 10 ³	Radius of Gyration mm	Perimeter m
Square Piles							
254	Solid	64,516	1,518	346.721	2,736.640	73.4	1.015
305	Solid	92,903	2,189	719.248	4,719.474	87.9	1.219
356	Solid	126,451	2,977	1,332.357	7,488.888	102.6	1.423
406	Solid	165,161	3,896	2,273.040	11,192.365	117.3	1.625
457	Solid	209,032	4,932	3,641.193	15,928.226	132.1	1.829
508	Solid	258,064	6,085	5,549.614	21,843.956	146.6	2.033
508	279 mm	196,774	4,641	5,250.759	20,680.475	163.3	2.033
610	Solid	371,612	8,756	11,507.966	37,755.795	176.0	2.438
610	305 mm	298,709	7,034	11,084.243	36,362.895	192.5	2.438
610	356 mm	272,258	6,406	10,722.954	35,183.026	198.4	2.438
610	381 mm	257,419	6,056	10,473.631	34,363.673	201.7	2.438
762	457 mm	416,773	9,807	25,950.781	68,121.025	249.4	3.048
914	457 mm	672,257	15,834	56,114.240	122,739.109	289.1	3.658

Note: Designer must confirm section properties for a selected pile. Form dimensions may vary with producers, with corresponding variations in section properties.

Data converted to SI units from US unit properties in PCI (1993), Precast/Prestressed Concrete Institute Journal, Volume 38, No. 2, March-April, 1993.

PRECAST/PRESTRESSED CONCRETE PILES



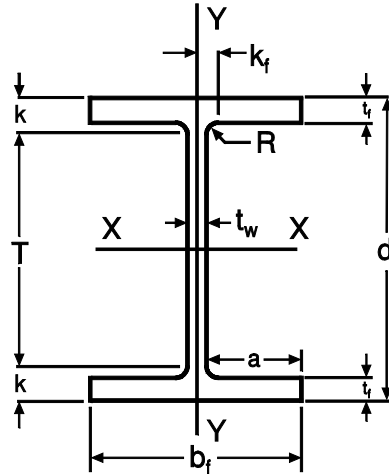
* Strand pattern may be circular or square.

		Section Properties					
Size mm	Core Diameter mm	Area mm ²	Weight N/m	Moment of Inertia mm ⁴ x 10 ⁶	Section Modulus mm ³ x 10 ³	Radius of Gyration mm	Perimeter m
Octagonal Piles							
254	Solid	53,548	1,240	231.008	1,818.964	65.8	0.841
305	Solid	76,774	1,824	472.006	3,097.155	78.5	1.009
356	Solid	104,516	2,466	876.167	4,932.506	91.4	1.180
406	Solid	136,774	3,210	1,495.103	7,357.792	104.6	1.347
457	Solid	172,903	4,086	2,374.600	10,471.334	117.1	1.515
508	Solid	213,548	5,035	3,650.350	14,371.455	130.8	1.682
508	279 mm	152,258	3,575	3,350.663	13,191.587	148.3	1.682
559	Solid	258,709	6,129	5,343.163	19,123.704	143.8	1.853
559	330 mm	172,903	4,086	4,761.688	17,042.547	165.9	1.853
610	Solid	307,741	7,224	7,567.087	24,826.402	156.7	2.021
610	381 mm	193,548	4,597	6,533.168	21,434.280	183.6	2.021
Round Piles							
914	660 mm	314,193	7,399	24,976.799	54,634.471	281.9	2.874
1,067	813 mm	374,838	8,829	42,153.005	79,034.810	335.3	3.353
1,219	965 mm	435,483	10,259	65,856.969	108,023.526	388.9	3.831
1,372	1118 mm	496,773	11,704	97,137.176	141,633.394	442.2	4.310
1,676	1372 mm	729,676	17,191	213,954.191	255,261.296	541.5	5.267

Note: Designer must confirm section properties for a selected pile. Form dimensions may vary with producers, with corresponding variations in section properties.

Data converted to SI units from US unit properties in PCI (1993), Precast/Prestressed Concrete Institute Journal, Volume 38, No. 2, March-April, 1993.

H-PILES



C1-20

Section Designation	Area A	Depth d	Web Thickness t_w	Flange		Distance				Fillet Radius R	Elastic Properties					
				Width b_f	Thickness t_f	T	k	k_f	a		X-X			Y-Y		
											l	S	r	l	S	r
mm x kg/m	mm ²	mm	mm	mm	mm	mm	mm	mm	mm	mm	mm ⁴ x 10 ⁶	mm ³ x 10 ³	mm	mm ⁴ x 10 ⁶	mm ³ x 10 ³	mm
HP360 x 174	22,200	361	20.4	378	20	277	42	30.2	179	20	511	2,830	152	183	968	91
HP360 x 152	19,400	356	17.9	376	18	277	40	29.0	179	20	442	2,480	151	158	840	90
HP360 x 132	16,900	351	15.6	373	16	277	37	27.8	179	20	378	2,150	150	135	724	89
HP360 x 108	13,800	346	12.8	370	13	277	34	26.4	179	20	306	1,770	148	108	584	88
HP310 x 125	15,800	312	17.4	312	17	244	34	23.7	147	15	270	1,730	131	88	565	75
HP310 x 110	14,000	308	15.4	310	15	244	32	22.7	147	15	236	1,530	130	77	497	74
HP310 x 93	11,800	303	13.1	308	13	244	30	21.6	148	15	196	1,290	129	64	414	74
HP310 x 79	9,970	299	11.0	306	11	244	28	20.5	148	15	162	1,080	127	53	343	73
HP250 x 85	10,800	254	14.4	260	14	196	29	20.2	123	13	123	969	107	42	325	63
HP250 x 62	7,980	246	10.5	256	11	96	25	18.3	123	13	88	711	105	30	234	61
HP200 x 53	6,810	204	11.3	207	11	158	23	15.7	98	10	50	487	86	17	161	50

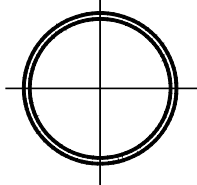
Note: Designer must confirm section properties for a selected pile.

Data obtained from FHWA Geotechnical Metrication Guidelines (1995) FHWA-SA-95-035.

APPENDIX C-2

Information and Data on Various Pile Types, US Units

	Page
Dimensions and Properties of Pipe Piles	C2-3
Data for Steel Monotube Piles.....	C2-17
Typical Prestressed Concrete Pile Sections.....	C2-19
Dimensions and Properties of H-Piles.....	C2-21



PIPE PILES

Approximate Pile Dimensions and Design Properties

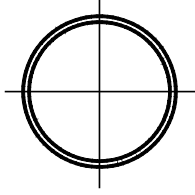
Designation and Outside Diameter	Wall Thickness	Area A	Weight per Foot	Section Properties			Area of Exterior Surface	Inside Cross Sectional Area	Inside Volume	External Collapse Index
				I	S	r				
in	in	in ²	lb	in ⁴	in ³	in	ft ² /ft	in ²	ft ³ /ft	*
PP8	0.141	3.48	11.83	26.9	6.72	2.78	2.09	46.8	0.0120	266
	0.164	4.04	13.72	31.0	7.75	2.77	2.09	46.2	0.0119	422
	0.172	4.23	14.38	32.4	8.10	2.77	2.09	46.0	0.0118	487
	0.179	4.40	14.95	33.6	8.41	2.77	2.09	45.9	0.0118	548
	0.188	4.61	15.69	35.2	8.80	2.76	2.09	45.7	0.0117	621
	0.219	5.35	18.20	40.5	10.1	2.75	2.09	44.9	0.0116	874
PP8-5/8	0.109	2.92	9.91	26.4	6.13	3.01	2.26	55.5	0.0143	97
	0.125	3.34	11.35	30.2	6.99	3.01	2.26	55.1	0.0142	147
	0.141	3.76	12.78	33.8	7.84	3.00	2.26	54.7	0.0141	212
	0.156	4.15	14.11	37.2	8.63	2.99	2.26	54.3	0.0140	288
	0.164	4.36	14.82	39.0	9.05	2.99	2.26	54.1	0.0139	335
	0.172	4.57	15.53	40.8	9.46	2.99	2.26	53.9	0.0139	388
	0.179	4.75	16.15	42.4	9.82	2.99	2.26	53.7	0.0138	438
	0.188	4.98	16.94	44.4	10.3	2.98	2.26	53.4	0.0137	508
	0.203	5.37	18.26	47.6	11.0	2.98	2.26	53.1	0.0136	623
	0.219	5.78	19.66	51.1	11.9	2.97	2.26	52.6	0.0135	744
	0.250	6.58	22.36	57.7	13.4	2.96	2.26	51.8	0.0133	979
	0.277	7.26	24.70	63.4	14.7	2.95	2.26	51.2	0.0132	1180
	0.312	8.15	27.70	70.5	16.3	2.94	2.26	50.3	0.0129	1500
	0.322	8.40	28.55	72.5	16.8	2.94	2.26	50.0	0.0129	1600
	0.344	8.95	30.42	76.8	17.8	2.93	2.26	49.5	0.0127	1820
	0.375	9.72	33.04	82.9	19.2	2.92	2.26	48.7	0.0125	2120
0.406	10.50	35.64	88.7	20.6	2.91	2.26	47.9	0.0123	2420	
0.438	11.3	38.30	94.7	21.9	2.90	2.26	47.2	0.0121	2740	
0.500	12.8	43.39	106.0	24.5	2.88	2.26	45.7	0.0117	3340	

Note: Designer must confirm section properties and local availability of selected pile section.

Material Specifications - ASTM A252

Example of suggested method of designation: PP8 x 0.141

* The External Collapse Index is a non-dimensional function of the diameter to wall thickness ratio and is for general guidance only. The higher the number, the greater is the resistance to collapse.



PIPE PILES

Approximate Pile Dimensions and Design Properties

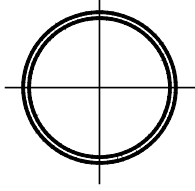
Designation and Outside Diameter	Wall Thickness	Area A	Weight per Foot	Section Properties			Area of Exterior Surface	Inside Cross Sectional Area	Inside Volume	External Collapse Index
				I	S	r				
in	in	in ²	lb	in ⁴	in ³	in	ft ² /ft	in ²	ft ³ /ft	*
PP10	0.109	3.39	11.51	41.4	8.28	3.50	2.62	75.2	0.0193	62
	0.120	3.72	12.66	45.5	9.09	3.49	2.62	74.8	0.0192	83
	0.134	4.15	14.12	50.5	10.10	3.49	2.62	74.4	0.0191	116
	0.141	4.37	14.85	53.1	10.60	3.49	2.62	74.2	0.0191	135
	0.150	4.64	15.78	56.3	11.30	3.48	2.62	73.9	0.0190	163
	0.164	5.07	17.23	61.3	12.30	3.48	2.62	73.5	0.0189	214
	0.172	5.31	18.05	64.1	12.80	3.48	2.62	73.2	0.0188	247
	0.179	5.52	18.78	66.6	13.30	3.47	2.62	73.0	0.0188	279
	0.188	5.80	19.70	69.8	14.00	3.47	2.62	72.7	0.0187	324
	0.203	6.25	21.24	75.0	15.00	3.46	2.62	72.3	0.0186	409
	0.219	6.73	22.88	80.5	16.10	3.46	2.62	71.8	0.0185	515
	0.230	7.06	24.00	84.3	16.90	3.46	2.62	71.5	0.0184	588
	0.250	7.66	26.03	91.1	18.20	3.45	2.62	70.9	0.0182	719
PP10-3/4	0.109	3.64	12.39	51.6	9.60	3.76	2.81	87.1	0.0224	50
	0.120	4.01	13.62	56.6	10.50	3.76	2.81	86.8	0.0223	67
	0.125	4.17	14.18	58.9	11.00	3.76	2.81	86.6	0.0223	76
	0.134	4.47	15.19	63.0	11.70	3.75	2.81	86.3	0.0222	93
	0.141	4.70	15.98	66.1	12.30	3.75	2.81	86.1	0.0221	109
	0.150	5.00	16.98	70.2	13.10	3.75	2.81	85.8	0.0221	131
	0.156	5.19	17.65	72.9	13.60	3.75	2.81	85.6	0.0220	148
	0.164	5.45	18.54	76.4	14.20	3.74	2.81	85.3	0.0219	172
	0.172	5.72	19.43	80.0	14.90	3.74	2.81	85.0	0.0219	199
	0.179	5.94	20.21	83.1	15.50	3.74	2.81	84.8	0.0218	224
	0.188	6.24	21.21	87.0	16.20	3.73	2.81	84.5	0.0217	260
	0.203	6.73	22.87	93.6	17.40	3.73	2.81	84.0	0.0216	328

Note: Designer must confirm section properties and local availability of selected pile section.

Material Specifications - ASTM A252

Example of suggested method of designation: PP8 x 0.141

* The External Collapse Index is a non-dimensional function of the diameter to wall thickness ratio and is for general guidance only. The higher the number, the greater is the resistance to collapse.



PIPE PILES

Approximate Pile Dimensions and Design Properties

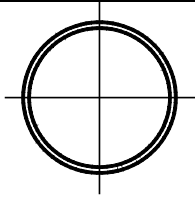
Designation and Outside Diameter	Wall Thickness	Area A	Weight per Foot	Section Properties			Area of Exterior Surface	Inside Cross Sectional Area	Inside Volume	External Collapse Index
				I	S	r				
In	in	in ²	lb	in ⁴	in ³	in	ft ² /ft	in ²	ft ³ /ft	*
PP10-3/4 (cont'd)	0.219	7.25	24.63	100.0	18.7	3.72	2.81	83.5	0.0215	414
	0.230	7.60	25.84	105.0	19.6	3.72	2.81	83.2	0.0214	480
	0.250	8.25	28.04	114.0	21.2	3.71	2.81	82.5	0.0212	605
	0.279	9.18	31.20	126.0	23.4	3.70	2.81	81.6	0.0210	781
	0.307	10.10	34.24	137.0	25.6	3.69	2.81	80.7	0.0208	951
	0.344	11.20	38.23	152.0	28.4	3.68	2.81	79.5	0.0205	1180
	0.365	11.90	40.48	161.0	29.9	3.67	2.81	78.9	0.0230	1320
	0.438	14.20	48.24	189.0	35.2	3.65	2.81	76.6	0.0197	1890
	0.500	16.10	54.74	212.0	39.4	3.63	2.81	74.7	0.0192	2380
PP12	0.134	5.00	16.98	87.9	14.7	4.20	3.14	108.0	0.0278	67
	0.141	5.25	17.86	92.4	15.4	4.19	3.14	108.0	0.0277	78
	0.150	5.58	18.98	98.0	16.3	4.19	3.14	108.0	0.0277	94
	0.164	6.10	20.73	107.0	17.8	4.19	3.14	107.0	0.0275	123
	0.172	6.39	21.73	112.0	18.6	4.18	3.14	107.0	0.0274	142
	0.179	6.65	22.60	116.0	19.4	4.18	3.14	106.0	0.0274	161
	0.188	6.98	23.72	122.0	20.3	4.18	3.14	106.0	0.0273	186
	0.203	7.52	25.58	131.0	21.8	4.17	3.14	106.0	0.0272	235
	0.219	8.11	27.55	141.0	23.4	4.17	3.14	105.0	0.0270	296
	0.230	8.50	28.91	147.0	24.6	4.16	3.14	105.0	0.0269	344
	0.250	9.23	31.37	159.0	26.6	4.16	3.14	104.0	0.0267	443
	0.281	10.30	35.17	178.0	29.6	4.14	3.14	103.0	0.0264	616
	0.312	11.50	38.95	196.0	32.6	4.13	3.14	102.0	0.0261	784
PP12-3/4	0.109	4.33	14.72	86.5	13.6	4.47	3.34	123.0	0.0317	30
	0.125	4.96	16.85	98.8	15.5	4.46	3.34	123.0	0.0316	45
	0.134	5.31	18.06	106.0	16.6	4.46	3.34	122.0	0.0315	56
	0.141	5.59	18.99	111.0	17.4	4.46	3.34	122.0	0.0314	65

Note: Designer must confirm section properties and local availability of selected pile section.

Material Specifications - ASTM A252

Example of suggested method of designation: PP8 x 0.141

* The External Collapse Index is a non-dimensional function of the diameter to wall thickness ratio and is for general guidance only. The higher the number, the greater is the resistance to collapse.



PIPE PILES

Approximate Pile Dimensions and Design Properties

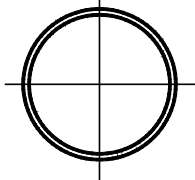
Designation and Outside Diameter	Wall Thickness	Area A	Weight per Foot	Section Properties			Area of Exterior Surface	Inside Cross Sectional Area	Inside Volume	External Collapse Index
				I	S	r				
in	in	in ²	lb	in ⁴	in ³	in	ft ² /ft	in ²	ft ³ /ft	*
PP12-3/4 (cont'd)	0.150	5.94	20.19	118	18.5	4.46	3.34	122	0.0313	78
	0.156	6.17	20.98	122	19.2	4.45	3.34	122	0.0313	88
	0.164	6.48	22.04	128	20.1	4.45	3.34	121	0.0312	103
	0.172	0.68	23.11	134	21.1	4.45	3.34	121	0.0311	118
	0.179	7.07	24.03	140	21.9	4.45	3.34	121	0.0310	134
	0.188	7.42	25.22	146	23.0	4.44	3.34	120	0.0309	155
	0.203	8.00	27.20	158	24.7	4.44	3.34	120	0.0308	196
	0.219	8.62	29.31	169	26.6	4.43	3.34	119	0.0306	246
	0.230	9.05	30.75	177	27.8	4.43	3.34	119	0.0305	286
	0.250	9.82	33.38	192	30.1	4.42	3.34	118	0.0303	368
	0.281	11.00	37.42	214	33.6	4.41	3.34	117	0.0300	526
	0.312	12.20	41.45	236	37.0	4.40	3.34	115	0.0297	684
	0.330	12.90	43.77	248	39.0	4.39	3.34	115	0.0295	776
	0.344	13.40	45.58	258	40.5	4.39	3.34	114	0.0294	848
	0.375	14.60	49.56	279	43.8	4.38	3.34	113	0.0291	1010
	0.406	15.70	53.52	300	47.1	4.37	3.34	112	0.0288	1170
	0.438	16.90	57.59	321	50.4	4.36	3.34	111	0.0285	1350
0.500	19.20	65.42	362	56.7	4.33	3.34	108	0.0279	1760	
PP14	0.134	5.84	19.84	140	20.0	4.90	3.67	148	0.0381	42
	0.141	6.14	20.87	147	21.1	4.90	3.67	148	0.0380	49
	0.150	6.53	22.19	157	22.4	4.90	3.67	147	0.0379	59
	0.156	6.78	23.07	163	23.2	4.89	3.67	147	0.0378	66
	0.164	7.13	24.23	171	24.4	4.89	3.67	147	0.0378	77
	0.172	7.47	25.40	179	25.5	4.89	3.67	146	0.0377	89
	0.179	7.77	26.42	186	26.5	4.89	3.67	146	0.0376	101
	0.188	8.16	27.73	195	27.8	4.88	3.67	146	0.0375	117
	0.203	8.80	29.91	209	29.9	4.88	3.67	145	0.0373	147
	0.210	9.10	30.93	216	30.9	4.88	3.67	145	0.0373	163

Note: Designer must confirm section properties and local availability of selected pile section.

Material Specifications - ASTM A252

Example of suggested method of designation: PP8 x 0.141

* The External Collapse Index is a non-dimensional function of the diameter to wall thickness ratio and is for general guidance only. The higher the number, the greater is the resistance to collapse.



PIPE PILES

Approximate Pile Dimensions and Design Properties

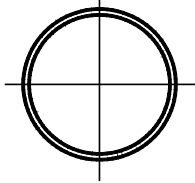
Designation and Outside Diameter	Wall Thickness	Area A	Weight per Foot	Section Properties			Area of Exterior Surface	Inside Cross Sectional Area	Inside Volume	External Collapse Index
				I	S	r				
in	in	in ²	lb	in ⁴	in ³	in	ft ² /ft	in ²	ft ³ /ft	*
PP14 (cont'd)	0.219	9.48	32.23	225	32.2	4.87	3.67	144	0.0372	815
	0.230	9.95	33.82	236	33.7	4.87	3.67	144	0.0370	215
	0.250	10.80	36.71	255	36.5	4.86	3.67	143	0.0368	277
	0.281	12.10	41.17	285	40.7	4.85	3.67	142	0.0365	395
	0.312	13.40	45.61	314	44.9	4.84	3.67	141	0.0361	542
	0.344	14.80	50.17	344	49.2	4.83	3.67	139	0.0358	691
	0.375	16.10	54.57	373	53.3	4.82	3.67	138	0.0355	835
	0.438	18.70	63.44	429	61.4	4.80	3.67	135	0.0348	1130
	0.469	19.90	67.78	457	65.3	4.79	3.67	134	0.0345	1280
	0.500	21.20	72.09	484	69.1	4.78	3.67	133	0.0341	1460
PP16	0.134	6.68	22.71	210	26.3	5.61	4.19	194	0.5000	28
	0.141	7.02	23.88	221	27.6	5.61	4.19	194	0.0499	33
	0.150	7.47	25.39	235	29.3	5.60	4.19	194	0.0498	39
	0.156	7.76	26.40	244	30.5	5.60	4.19	193	0.0497	44
	0.164	8.16	27.74	256	32.0	5.60	4.19	193	0.0496	52
	0.172	8.55	29.08	268	33.5	5.60	4.19	193	0.0495	60
	0.179	8.90	30.25	278	34.8	5.59	4.19	192	0.0494	67
	0.188	9.34	31.75	292	36.5	5.59	4.19	192	0.0493	78
	0.203	10.10	34.25	314	39.3	5.59	4.19	191	0.0491	98
	0.219	10.90	36.91	338	42.3	5.58	4.19	190	0.0489	124
	0.230	11.40	38.74	354	44.3	5.58	4.19	190	0.0488	144
	0.250	12.40	42.05	384	48.0	5.57	4.19	189	0.0485	185
	0.281	13.90	47.17	429	53.6	5.56	4.19	187	0.0481	264
	0.312	15.40	52.27	473	59.2	5.55	4.19	186	0.0478	362
	0.344	16.90	57.52	519	64.8	5.54	4.19	184	0.0474	487
	0.375	18.40	62.58	562	70.3	5.53	4.19	183	0.0470	617
	0.438	21.40	72.80	649	81.1	5.50	4.19	180	0.0462	874
	0.469	22.90	77.79	691	86.3	5.49	4.19	178	0.0458	1000
0.500	24.30	82.77	732	91.5	5.48	4.19	177	0.0455	1130	

Note: Designer must confirm section properties and local availability of selected pile section.

Material Specifications - ASTM A252

Example of suggested method of designation: PP8 x 0.141

* The External Collapse Index is a non-dimensional function of the diameter to wall thickness ratio and is for general guidance only. The higher the number, the greater is the resistance to collapse.



PIPE PILES

Approximate Pile Dimensions and Design Properties

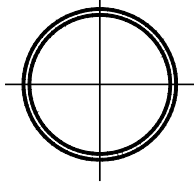
Designation and Outside Diameter	Wall Thickness	Area A	Weight per Foot	Section Properties			Area of Exterior Surface	Inside Cross Sectional Area	Inside Volume	External Collapse Index
				I	S	r				
in	in	in ²	lb	in ⁴	in ³	in	ft ² /ft	in ²	ft ³ /ft	*
PP18	0.141	7.91	26.89	315	35.0	6.31	4.71	247	0.0634	23
	0.172	9.63	32.75	383	42.5	6.30	4.71	245	0.0630	42
	0.188	10.50	35.76	417	46.4	6.30	4.71	244	0.0627	55
	0.203	11.30	38.58	449	49.9	6.29	4.71	243	0.0625	69
	0.219	12.20	41.59	484	53.7	6.29	4.71	242	0.0623	87
	0.230	12.80	43.65	507	56.3	6.28	4.71	242	0.0621	101
	0.250	13.90	47.39	549	61.0	6.28	4.71	241	0.0619	129
	0.281	15.60	53.18	614	68.2	6.27	4.71	239	0.0614	184
	0.312	17.30	58.94	678	75.4	6.25	4.71	237	0.0610	253
	0.344	19.10	64.87	744	82.6	6.24	4.71	235	0.0605	341
	0.375	20.80	70.59	807	89.6	6.23	4.71	234	0.0601	443
	0.406	22.40	76.29	869	96.5	6.22	4.71	232	0.0597	559
	0.438	24.20	82.15	932	104.0	6.21	4.71	230	0.0592	675
	0.469	25.80	87.81	993	110.0	6.20	4.71	229	0.0588	788
	0.500	27.50	93.45	1050	117.0	6.19	4.71	227	0.0584	900
PP20	0.141	8.80	29.91	434	43.4	7.02	5.24	305	0.0785	17
	0.172	10.70	36.42	527	52.7	7.01	5.24	303	0.0780	30
	0.188	11.70	39.78	574	57.4	7.00	5.24	302	0.0778	40
	0.203	12.60	42.92	619	61.9	7.00	5.24	302	0.0776	50
	0.219	13.60	46.27	666	66.6	6.99	5.24	301	0.0773	63
	0.250	15.50	52.73	756	75.6	6.98	5.24	299	0.0768	94
	0.281	17.40	59.18	846	84.6	6.97	5.24	297	0.0763	134
	0.312	19.30	65.60	935	93.5	6.96	5.24	295	0.0758	184
	0.344	21.20	72.21	1030	103.0	6.95	5.24	293	0.0753	247

Note: Designer must confirm section properties and local availability of selected pile section.

Material Specifications - ASTM A252

Example of suggested method of designation: PP8 x 0.141

* The External Collapse Index is a non-dimensional function of the diameter to wall thickness ratio and is for general guidance only. The higher the number, the greater is the resistance to collapse.



PIPE PILES

Approximate Pile Dimensions and Design Properties

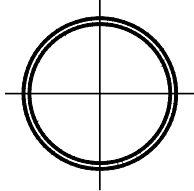
Designation and Outside Diameter	Wall Thickness	Area A	Weight per Foot	Section Properties			Area of Exterior Surface	Inside Cross Sectional Area	Inside Volume	External Collapse Index
				I	S	r				
in	in	in ²	lb	in ⁴	in ³	in	ft ² /ft	in ²	ft ³ /ft	*
PP20 (cont'd)	0.375	23.10	78.60	1110	111.0	6.94	5.24	291	0.0749	321
	0.406	25.00	84.96	1200	120.0	6.93	5.24	289	0.0744	409
	0.438	26.90	91.51	1290	129.0	6.92	5.24	287	0.0739	515
	0.469	28.80	97.83	1370	137.0	6.91	5.24	285	0.0734	618
	0.500	30.60	104.13	1460	146.0	6.90	5.24	284	0.0729	719
PP22	0.172	11.80	40.10	703	63.9	7.72	5.76	368	0.0947	23
	0.188	12.90	43.80	766	69.7	7.71	5.76	367	0.0945	30
	0.219	15.00	50.94	889	80.8	7.70	5.76	365	0.0939	47
	0.250	17.10	58.07	1010	91.8	7.69	5.76	363	0.0934	70
	0.281	19.20	65.18	1130	103.0	7.68	5.76	361	0.0928	100
	0.312	21.30	72.27	1250	114.0	7.67	5.76	359	0.0923	138
	0.344	23.40	79.56	1370	125.0	7.66	5.76	357	0.0918	185
	0.375	25.50	86.61	1490	135.0	7.65	5.76	355	0.0912	241
	0.406	27.50	93.63	1610	146.0	7.64	5.76	353	0.0907	306
	0.438	29.70	100.86	1720	157.0	7.62	5.76	350	0.0901	386
	0.469	31.70	107.85	1840	167.0	7.61	5.76	348	0.0896	475
PP24	0.500	33.80	114.81	1950	177.0	7.60	5.76	346	0.0891	571
	0.172	12.90	43.77	914	76.2	8.42	6.28	440	0.1130	18
	0.188	14.10	47.81	997	83.1	8.42	6.28	438	0.1130	23
	0.219	16.40	55.62	1160	96.4	8.41	6.28	436	0.1120	36
	0.250	18.70	63.41	1320	110.0	8.40	6.28	434	0.1120	54
	0.281	20.90	71.18	1470	123.0	8.39	6.28	431	0.1110	77
	0.312	23.20	78.93	1630	136.0	8.38	6.28	429	0.1100	106
	0.344	25.60	86.91	1790	149.0	8.36	6.28	427	0.1100	142
0.375	27.80	94.62	1940	162.0	8.35	6.28	425	0.1090	185	

Note: Designer must confirm section properties and local availability of selected pile section.

Material Specifications - ASTM A252

Example of suggested method of designation: PP8 x 0.141

* The External Collapse Index is a non-dimensional function of the diameter to wall thickness ratio and is for general guidance only. The higher the number, the greater is the resistance to collapse.



PIPE PILES

Approximate Pile Dimensions and Design Properties

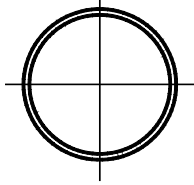
Designation and Outside Diameter	Wall Thickness	Area A	Weight per Foot	Section Properties			Area of Exterior Surface	Inside Cross Sectional Area	Inside Volume	External Collapse Index
				I	S	r				
In	in	in ²	lb	in ⁴	in ³	in	ft ² /ft	in ²	ft ³ /ft	*
PP24 (cont'd)	0.406	30.10	102.31	2090	175	8.34	6.28	422	0.109	235
	0.438	32.40	110.22	2250	188	8.33	6.28	420	0.108	296
	0.469	34.70	117.86	2400	200	8.32	6.28	418	0.107	364
	0.500	36.90	125.49	2550	212	8.31	6.28	415	0.107	443
PP26	0.250	20.20	68.75	1680	129	9.10	6.81	511	0.131	43
	0.281	22.70	77.18	1880	144	9.09	6.81	508	0.131	61
	0.312	25.20	85.60	2080	160	9.08	6.81	506	0.130	83
	0.344	27.70	94.26	2280	176	9.07	6.81	503	0.129	112
	0.375	30.20	102.63	2480	191	9.06	6.81	501	0.129	145
	0.406	32.60	110.98	2670	206	9.05	6.81	498	0.128	184
	0.438	35.20	119.57	2870	221	9.04	6.81	496	0.128	232
	0.469	37.60	127.88	3070	236	9.03	6.81	493	0.127	286
	0.500	40.10	136.17	3260	251	9.02	6.81	491	0.126	347
	0.562	44.90	152.68	3630	280	9.00	6.81	486	0.125	495
	0.625	49.80	169.38	4010	309	8.97	6.81	481	0.124	656
	0.688	54.70	185.99	4380	337	8.95	6.81	476	0.122	814
PP28	0.250	21.80	74.09	2100	150	9.81	7.33	594	0.153	34
	0.281	24.50	83.19	2350	168	9.80	7.33	591	0.152	48
	0.312	27.10	92.26	2600	186	9.79	7.33	589	0.151	66
	0.344	29.90	101.61	2860	204	9.78	7.33	586	0.151	89
	0.375	32.50	110.64	3110	222	9.77	7.33	583	0.150	116
	0.406	35.20	119.65	3350	239	9.76	7.33	581	0.149	147
	0.438	37.90	128.93	3600	257	9.75	7.33	578	0.149	185
	0.469	40.60	137.90	3840	275	9.74	7.33	575	0.148	228

Note: Designer must confirm section properties and local availability of selected pile section.

Material Specifications - ASTM A252

Example of suggested method of designation: PP8 x 0.141

* The External Collapse Index is a non-dimensional function of the diameter to wall thickness ratio and is for general guidance only. The higher the number, the greater is the resistance to collapse.



PIPE PILES

Approximate Pile Dimensions and Design Properties

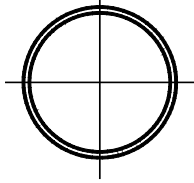
Designation and Outside Diameter	Wall Thickness	Area A	Weight per Meter	Section Properties			Area of Exterior Surface	Inside Cross Sectional Area	Inside Volume	External Collapse Index
				I	S	r				
In	in	in ²	lb	in ⁴	in ³	in	ft ² /ft	in ²	ft ³ /ft	*
PP28 (cont'd)	0.500	43.20	146.85	4080	292	9.72	7.33	573	0.147	277
	0.562	48.40	164.69	4560	326	9.70	7.33	567	0.143	395
	0.625	53.80	182.73	5040	360	9.68	7.33	562	0.144	544
	0.688	59.00	200.68	5510	393	9.66	7.33	557	0.143	691
	0.750	64.20	218.27	5960	426	9.64	7.33	552	0.142	835
PP30	0.250	23.40	79.43	2590	172	10.50	7.85	683	0.176	28
	0.281	26.20	89.19	2900	193	10.50	7.85	681	0.175	39
	0.312	29.10	98.93	3210	214	10.50	7.85	678	0.174	54
	0.344	32.00	108.95	3520	235	10.50	7.85	675	0.174	72
	0.375	34.90	118.65	3830	255	10.50	7.85	672	0.173	94
	0.406	37.70	128.32	4130	276	10.50	7.85	669	0.172	120
	0.438	40.70	138.29	4440	296	10.50	7.85	666	0.171	150
	0.469	43.50	147.92	4740	316	10.40	7.85	663	0.171	185
	0.500	46.30	157.53	5040	336	10.40	7.85	661	0.170	225
	0.562	52.00	176.69	5630	375	10.40	7.85	655	0.168	321
	0.625	57.70	196.08	6220	415	10.40	7.85	649	0.167	443
	0.688	63.40	215.38	6810	454	10.40	7.85	644	0.166	584
	0.750	68.90	234.29	7380	492	10.30	7.85	638	0.164	719
PP32	0.250	24.90	84.77	3140	196	11.20	8.38	779	0.200	23
	0.281	28.00	95.19	3520	220	11.20	8.38	776	0.200	32
	0.312	31.10	105.59	3900	244	11.20	8.38	773	0.199	44
	0.344	34.20	116.30	4290	268	11.20	8.38	770	0.198	60
	0.375	37.30	126.66	4660	291	11.20	8.38	767	0.197	77
	0.406	40.30	136.99	5030	314	11.20	8.38	764	0.196	98
	0.438	43.40	147.64	5410	338	11.20	8.38	761	0.196	124
	0.469	46.50	157.94	5770	361	11.10	8.38	758	0.195	152

Note: Designer must confirm section properties and local availability of selected pile section.

Material Specifications - ASTM A252

Example of suggested method of designation: PP8 x 0.141

* The External Collapse Index is a non-dimensional function of the diameter to wall thickness ratio and is for general guidance only. The higher the number, the greater is the resistance to collapse.



PIPE PILES

Approximate Pile Dimensions and Design Properties

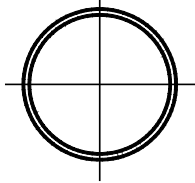
Designation and Outside Diameter	Wall Thickness	Area A	Weight per Foot	Section Properties			Area of Exterior Surface	Inside Cross Sectional Area	Inside Volume	External Collapse Index
				I	S	r				
in	in	in ²	lb	in ⁴	in ³	in	ft ² /ft	in ²	ft ³ /ft	*
PP32 (cont'd)	0.500	49.50	168.21	6140	384	11.10	8.38	755	0.194	185
	0.562	55.50	188.70	6860	429	11.10	8.38	749	0.193	264
	0.625	61.60	209.43	7580	474	11.10	8.38	743	0.191	364
	0.688	67.70	230.08	8300	519	11.10	8.38	737	0.189	487
	0.750	73.60	250.31	8990	562	11.10	8.38	731	0.188	617
PP34	0.250	26.50	90.11	3770	222	11.90	8.90	881	0.227	19
	0.281	29.80	101.19	4230	249	11.90	8.90	878	0.226	27
	0.312	33.00	112.25	4680	276	11.90	8.90	875	0.225	37
	0.344	36.40	123.65	5150	303	11.90	8.90	872	0.224	50
	0.375	39.60	134.67	5600	329	11.90	8.90	868	0.223	64
	0.406	42.80	145.67	6050	356	11.90	8.90	865	0.222	82
	0.438	46.20	157.00	6500	383	11.90	8.90	862	0.222	103
	0.469	49.40	167.95	6940	409	11.90	8.90	859	0.221	127
	0.500	52.60	178.89	7380	434	11.80	8.90	855	0.220	154
	0.562	59.00	200.70	8250	486	11.80	8.90	849	0.218	219
	0.625	65.50	222.78	9130	537	11.80	8.90	842	0.217	303
	0.688	72.00	244.77	9990	588	11.80	8.90	836	0.215	405
	0.750	78.30	266.33	10800	637	11.80	8.90	830	0.213	527
	0.875	91.10	309.55	12500	735	11.70	8.90	817	0.210	767
1.000	104.00	352.44	14100	831	11.70	8.90	804	0.207	1010	
PP36	0.250	28.10	95.45	4490	249	12.60	9.42	990	0.255	16
	0.281	31.50	107.20	5030	279	12.60	9.42	986	0.254	23
	0.312	35.00	118.92	5570	309	12.60	9.42	983	0.253	31
	0.344	38.50	131.00	6120	340	12.60	9.42	979	0.252	42

Note: Designer must confirm section properties and local availability of selected pile section.

Material Specifications - ASTM A252

Example of suggested method of designation: PP8 x 0.141

* The External Collapse Index is a non-dimensional function of the diameter to wall thickness ratio and is for general guidance only. The higher the number, the greater is the resistance to collapse.



PIPE PILES

Approximate Pile Dimensions and Design Properties

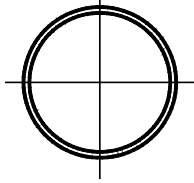
Designation and Outside Diameter	Wall Thickness	Area A	Weight per Foot	Section Properties			Area of Exterior Surface	Inside Cross Sectional Area	Inside Volume	External Collapse Index
				I	S	r				
in	in	in ²	lb	in ⁴	in ³	in	ft ² /ft	in ²	ft ³ /ft	*
PP36 (cont'd)	0.375	42.00	142.68	6660	370	12.60	9.42	976	0.2510	54
	0.406	45.40	154.34	7190	399	12.60	9.42	972	0.2500	69
	0.438	48.90	166.35	7740	430	12.60	9.42	969	0.2490	87
	0.469	52.40	177.97	8260	459	12.60	9.42	966	0.2480	107
	0.500	55.80	189.57	8790	488	12.60	9.42	962	0.2480	129
	0.562	62.60	212.70	9820	546	12.50	9.42	955	0.2460	184
	0.625	69.50	236.13	10900	604	12.50	9.42	948	0.2440	254
	0.688	76.30	259.47	11900	661	12.50	9.42	942	0.2420	341
	0.750	83.10	282.35	12900	717	12.50	9.42	935	0.2400	443
	0.875	96.60	328.24	14900	828	12.40	9.42	921	0.2370	674
	1.000	110.00	373.80	16900	936	12.40	9.42	908	0.2340	900
PP38	1.250	136.00	463.91	20600	1150	12.30	9.42	881	0.2270	1380
	0.250	29.60	100.79	5280	278	13.30	9.95	1100	0.2840	14
	0.281	33.30	113.20	5920	312	13.30	9.95	1100	0.2830	19
	0.312	36.90	125.58	6560	345	13.30	9.95	1100	0.2820	26
	0.344	40.70	138.35	7210	380	13.30	9.95	1090	0.2810	35
	0.375	44.30	150.69	7840	413	13.30	9.95	1090	0.2800	46
	0.406	48.00	163.01	8470	446	13.30	9.95	1090	0.2790	59
	0.438	51.70	175.71	9120	480	13.30	9.95	1080	0.2780	74
	0.469	55.30	187.99	9740	513	13.30	9.95	1080	0.2780	90
	0.500	58.90	200.25	10400	545	13.30	9.95	1080	0.2760	110
	0.562	66.10	224.71	11600	610	13.20	9.95	1070	0.2750	156
	0.625	73.40	249.48	12800	675	13.20	9.95	1060	0.2730	216
0.688	80.60	274.16	14000	739	13.20	9.95	1050	0.2710	289	

Note: Designer must confirm section properties and local availability of selected pile section.

Material Specifications - ASTM A252

Example of suggested method of designation: PP8 x 0.141

* The External Collapse Index is a non-dimensional function of the diameter to wall thickness ratio and is for general guidance only. The higher the number, the greater is the resistance to collapse.



PIPE PILES

Approximate Pile Dimensions and Design Properties

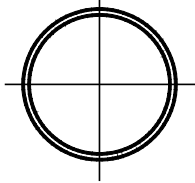
Designation and Outside Diameter	Wall Thickness	Area A	Weight per Foot	Section Properties			Area of Exterior Surface	Inside Cross Sectional Area	Inside Volume	External Collapse Index
				I	S	r				
in	in	in ²	lb	in ⁴	in ³	in	Ft ² /ft	in ²	ft ³ /ft	*
PP38 (cont'd)	0.750	87.8	298.37	15200	802	13.20	9.95	1050	0.269	376
	0.875	102.0	346.93	17600	926	13.10	9.95	1030	0.265	590
	1.000	116.0	395.16	19900	1050	13.10	9.95	1020	0.262	805
	1.250	144.0	490.61	24400	1280	13.00	9.95	990	0.255	1230
	1.500	172.0	584.73	28700	1510	12.90	9.95	962	0.248	1780
PP40	0.312	38.9	132.25	7660	383	14.00	10.50	1220	0.313	23
	0.344	42.9	145.69	8430	421	14.00	10.50	1210	0.312	30
	0.375	46.7	158.70	9160	458	14.00	10.50	1210	0.311	39
	0.406	50.5	171.68	9900	495	14.00	10.50	1210	0.310	50
	0.438	54.4	185.06	10700	533	14.00	10.50	1200	0.309	63
	0.469	58.2	198.01	11400	569	14.00	10.50	1200	0.308	77
	0.500	62.0	210.93	12100	605	14.00	10.50	1190	0.307	94
	0.562	69.6	236.71	13500	677	13.90	10.50	1190	0.305	134
	0.625	77.3	262.83	15000	749	13.90	10.50	1180	0.303	185
	0.688	85.0	288.86	16400	821	13.90	10.50	1170	0.301	247
	0.750	92.5	314.39	17800	891	13.90	10.50	1160	0.299	321
	0.875	108.0	365.62	20600	1030	13.80	10.50	1150	0.296	514
	1.000	123.0	416.52	23300	1170	13.80	10.50	1130	0.292	719
	1.250	152.0	517.31	28600	1430	13.70	10.50	1100	0.284	1130
1.500	181.0	616.77	33700	1680	13.60	10.50	1080	0.276	1620	
1.750	210.0	714.89	38500	1930	13.50	10.50	1050	0.269	2140	
PP42	0.312	40.9	138.91	8880	423	14.70	11.00	1340	0.346	20
	0.344	45.0	153.04	9770	465	14.70	11.00	1340	0.345	26
	0.375	49.0	166.71	10600	506	14.70	11.00	1340	0.344	34
	0.406	53.1	180.35	11500	546	14.70	11.00	1340	0.343	43

Note: Designer must confirm section properties and local availability of selected pile section.

Material Specifications - ASTM A252

Example of suggested method of designation: PP8 x 0.141

* The External Collapse Index is a non-dimensional function of the diameter to wall thickness ratio and is for general guidance only. The higher the number, the greater is the resistance to collapse.



PIPE PILES

Approximate Pile Dimensions and Design Properties

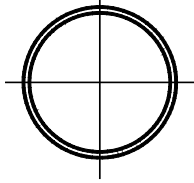
Designation and Outside Diameter	Wall Thickness	Area A	Weight per Foot	Section Properties			Area of Exterior Surface	Inside Cross Sectional Area	Inside Volume	External Collapse Index
				I	S	r				
in	in	in ²	lb	in ⁴	in ³	in	Ft ² /ft	in ²	ft ³ /ft	*
PP42 (cont'd)	0.438	57.2	194.42	12400	588	14.70	11.00	1330	0.342	54
	0.469	61.2	208.03	13200	628	14.70	11.00	1320	0.341	67
	0.500	65.2	221.61	14000	668	14.70	11.00	1320	0.340	81
	0.562	73.2	248.72	15700	748	14.70	11.00	1310	0.338	116
	0.625	81.2	276.18	17400	828	14.60	11.00	1300	0.335	159
	0.688	89.3	303.55	19100	907	14.60	11.00	1300	0.333	213
	0.750	97.2	330.41	20700	985	14.60	11.00	1290	0.331	277
	0.875	113.0	384.31	23900	1140	14.50	11.00	1270	0.327	443
	1.000	129.0	437.88	27100	1290	14.50	11.00	1260	0.323	641
	1.250	160.0	544.01	33200	1580	14.40	11.00	1230	0.315	1030
	1.500	191.0	648.81	39200	1870	14.30	11.00	1190	0.307	1460
PP44	1.750	221.0	752.27	44900	2140	14.20	11.00	1160	0.299	1970
	2.000	251.0	854.40	50400	2400	14.20	11.00	1130	0.292	2470
	0.344	47.2	160.39	11200	511	15.40	11.50	1470	0.379	23
	0.375	51.4	174.72	12200	556	15.40	11.50	1470	0.378	30
	0.406	55.6	189.03	13200	600	15.40	11.50	1460	0.377	38
	0.438	59.9	203.78	14200	646	15.40	11.50	1460	0.376	47
	0.469	64.1	218.04	15200	691	15.40	11.50	1460	0.375	58
	0.500	68.3	232.29	16200	735	15.40	11.50	1450	0.374	70
	0.625	85.2	289.53	20000	911	15.30	11.50	1440	0.369	138
	0.750	102.0	346.43	23800	1080	15.30	11.50	1420	0.365	241
0.875	119.0	403.00	27600	1250	15.30	11.50	1400	0.361	384	
1.000	135.0	459.24	31200	1420	15.20	11.50	1390	0.356	571	

Note: Designer must confirm section properties and local availability of selected pile section.

Material Specifications - ASTM A252

Example of suggested method of designation: PP8 x 0.141

* The External Collapse Index is a non-dimensional function of the diameter to wall thickness ratio and is for general guidance only. The higher the number, the greater is the resistance to collapse.



PIPE PILES

Approximate Pile Dimensions and Design Properties

Designation and Outside Diameter	Wall Thickness	Area A	Weight per Foot	Section Properties			Area of Exterior Surface	Inside Cross Sectional Area	Inside Volume	External Collapse Index
				I	S	r				
in	in	in ²	lb	in ⁴	in ³	in	Ft ² /ft	in ²	ft ³ /ft	*
PP44 (cont'd)	1.250	168.0	570.71	38400	1740	15.10	11.50	1350	0.348	941
	1.500	200.0	680.85	45300	2060	15.00	11.50	1320	0.340	1300
	1.750	232.0	789.65	51900	2360	15.00	11.50	1290	0.331	1810
	2.000	264.0	897.12	58300	2650	14.90	11.50	1260	0.323	2290
	2.250	295.0	1003.25	64500	2930	14.80	11.50	1230	0.315	2770
PP48	0.344	51.5	175.08	14600	609	16.80	12.60	1760	0.452	18
	0.375	56.1	190.74	15900	663	16.80	12.60	1750	0.451	23
	0.406	60.7	206.37	17200	716	16.80	12.60	1750	0.450	29
	0.438	65.4	222.49	18500	771	16.80	12.60	1740	0.449	36
	0.469	70.0	238.08	19800	824	16.80	12.60	1740	0.447	45
	0.500	74.6	253.65	21000	877	16.80	12.60	1730	0.446	54
	0.625	93.0	316.23	26100	1090	16.80	12.60	1720	0.442	106
	0.750	111.0	378.47	31100	1290	16.70	12.60	1700	0.437	185
	0.875	130.0	440.38	36000	1500	16.70	12.60	1680	0.432	295
	1.000	148.0	501.96	40800	1700	16.60	12.60	1660	0.427	443
	1.250	184.0	624.11	50200	2090	16.50	12.60	1630	0.418	787
	1.500	219.0	744.93	59300	2470	16.40	12.60	1590	0.409	1130
	1.750	254.0	864.41	68100	2840	16.40	12.60	1560	0.400	1530
	2.000	289.0	982.56	76600	3190	16.30	12.60	1520	0.391	1970
	2.250	323.0	1099.37	84800	3530	16.20	12.60	1490	0.382	2410
2.500	357.0	1214.85	92800	3860	16.10	12.60	1450	0.374	2850	

Note: Designer must confirm section properties and local availability of selected pile section.

Material Specifications - ASTM A252

Example of suggested method of designation: PP8 x 0.141

* The External Collapse Index is a non-dimensional function of the diameter to wall thickness ratio and is for general guidance only. The higher the number, the greater is the resistance to collapse.

Monotube Piles

Standard Monotube Weights and Volumes

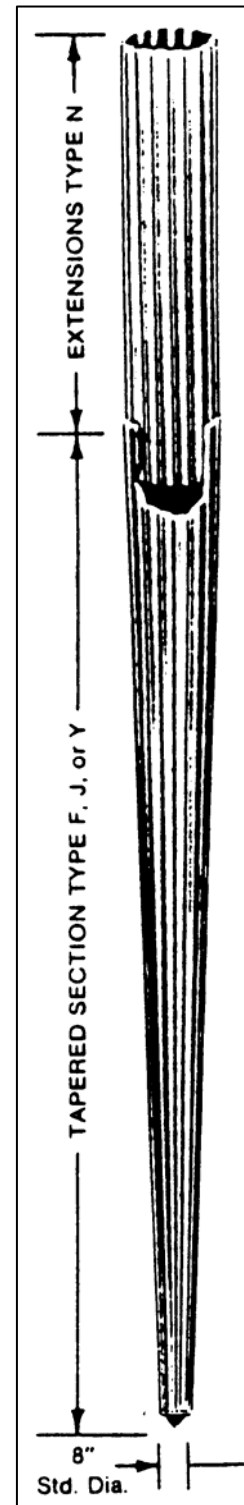
TYPE	SIZE POINT DIAMETER x BUTT DIAMETER x LENGTH	Weight (N) per m				EST. CONC. VOL. yd ³
		9 GA.	7 GA.	5 GA.	3 GA.	
F Taper 0.14 inch per foot	8½" x 12" x 25'	17	20	24	28	0.43
	8" x 12" x 30'	16	20	23	27	0.55
	8½" x 14" x 40'	19	22	26	31	0.95
	8" x 16" x 60'	20	24	28	33	1.68
	8" x 18" x 75'	--	26	31	35	2.59
J Taper 0.25 inch per foot	8" x 12" x 17'	17	20	23	27	0.32
	8" x 14" x 25'	18	22	26	30	0.58
	8" x 16" x 33'	20	24	28	32	0.95
	8" x 18" x 40'	--	26	30	35	1.37
Y Taper 0.40 inch per foot	8" x 12" x 10'	17	20	24	28	0.18
	8" x 14" x 15'	19	22	26	30	0.34
	8" x 16" x 20'	20	24	28	33	0.56
	8" x 18" x 25'	--	26	31	35	0.86

Extensions (Overall Length 1 Foot than indicated)

TYPE	DIAMETER + LENGTH	9 GA.	7 GA.	5 GA.	3 GA.	yd ³ /ft
N 12	12" x 12" x 20' / 40'	20	24	28	33	0.026
N 14	14" x 14" x 20' / 40'	24	29	34	41	0.035
N 16	16" x 16" x 20' / 40'	28	33	39	46	0.045
N 18	18" x 18" x 20' / 40'	--	38	44	52	0.058

Note: Designer must confirm section properties of selected pile section.

Pile design data converted to SI units from US units published in Monotube Pile Corporation Catalog 592.



MONOTUBE PILES

Physical Properties

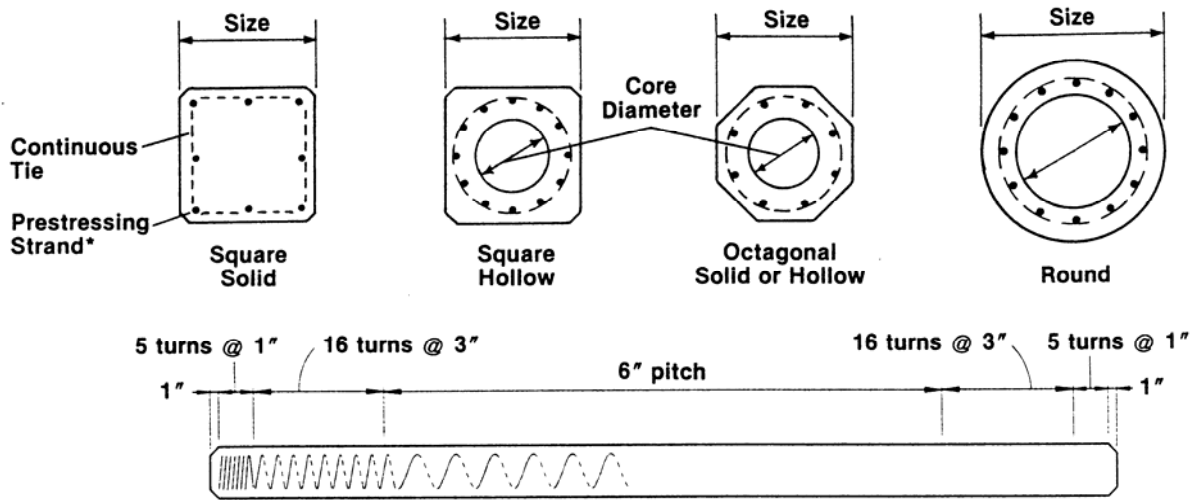
STEEL THICKNESS	POINTS		BUTTS OF PILE SECTIONS							
	8 in	8 ½ in	12 in				14 in			
	A in ²	A in ²	A in ²	I in ⁴	S in ³	r in	A in ²	I in ⁴	S in ³	r in
9 GAUGE (0.1495")	3.63	3.93	5.81	102	16.3	4.18	6.75	159	22.0	4.86
7 GAUGE (0.1793")	4.40	4.77	6.97	122	19.5	4.18	8.14	194	26.7	4.89
5 GAUGE (0.2391")	5.19	5.61	8.18	145	23.0	4.21	9.50	227	31.0	4.88
3 GAUGE (0.2391")	5.87	6.58	8.96	148	24.2	4.07	10.60	239	33.6	4.77
CONCRETE AREA in ²	42.3	47.3	101				136			

STEEL THICKNESS	POINTS		BUTTS OF PILE SECTIONS							
	8 in	8 ½ in	16 in				18 in			
	A in ²	A in ²	A in ²	I in ⁴	S in ³	r in	A in ²	I in ⁴	S in ³	r in
9 GAUGE (0.1495")	3.63	3.93	7.64	232	28.3	5.50	--	--	--	--
7 GAUGE (0.1793")	4.40	4.77	9.18	278	33.9	5.51	10.4	404	43.5	6.23
5 GAUGE (0.2391")	5.19	5.61	10.8	329	33.9	5.53	12.2	478	51.2	6.26
3 GAUGE (0.2391")	5.87	6.58	12.0	348	43.1	5.40	13.6	504	55.4	6.10
CONCRETE AREA in ²	42.3	47.3	176				224			

Note: Designer must confirm section properties of selected pile section.

Pile design data converted to SI units from US units published in Monotube Pile Corporation Catalog 592.

PRECAST/PRESTRESSED CONCRETE PILES



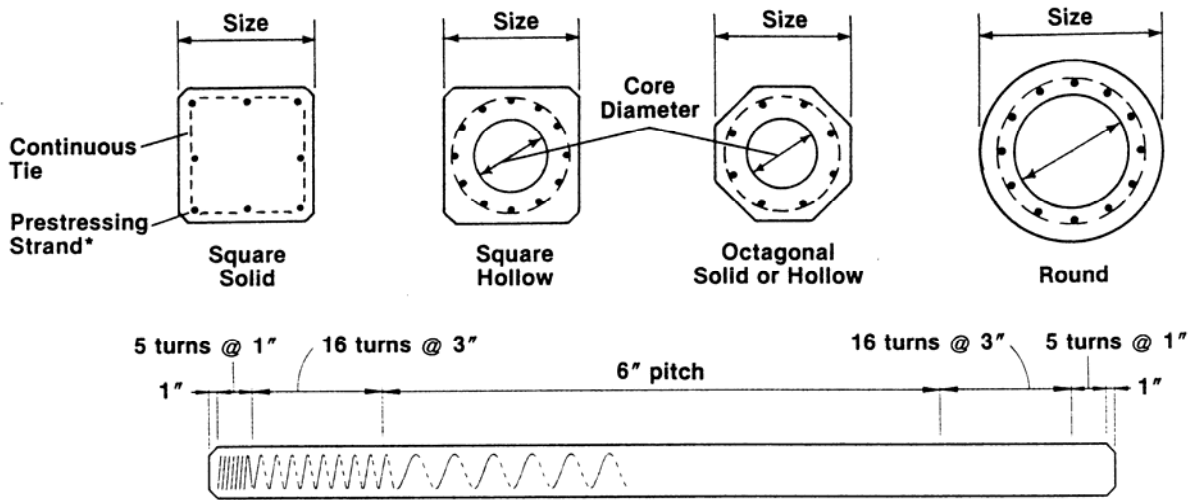
* Strand pattern may be circular or square.

Size in	Core Diameter in	Section Properties					
		Area in ²	Weight lb/ft	Moment of Inertia in ⁴	Section Modulus in ³	Radius of Gyration in	Perimeter ft
Square Piles							
10	Solid	100	104	833	167	2.89	3.33
12	Solid	144	150	1,728	288	3.46	4.00
14	Solid	196	204	3,201	457	4.04	4.67
16	Solid	256	267	5,461	683	4.62	5.33
18	Solid	324	338	8,748	972	5.20	6.00
20	Solid	400	417	13,333	1,333	5.77	6.67
20	11	305	318	12,615	1,262	6.43	6.67
24	Solid	576	600	27,648	2,304	6.93	8.00
24	12	463	482	26,630	2,219	7.58	8.00
24	14	422	439	25,762	2,147	7.81	8.00
24	16	399	415	25,163	2,097	7.94	8.00
30	18	646	672	62,347	4,157	9.82	10.00
36	18	1,042	1085	134,815	7,490	11.38	12.00

Note: Designer must confirm section properties for a selected pile. Form dimensions may vary with producers, with corresponding variations in section properties.

PCI (1993), Precast/Prestressed Concrete Institute Journal, Volume 38, No. 2, March-April, 1993.

PRECAST/PRESTRESSED CONCRETE PILES



* Strand pattern may be circular or square.

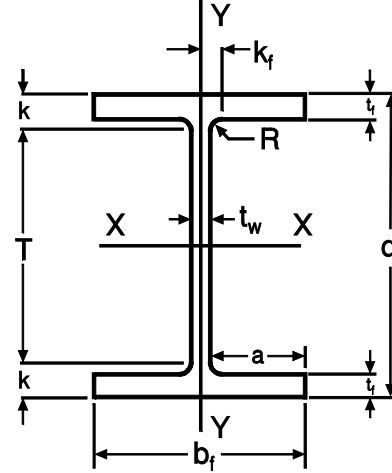
Typical Elevation

Size in	Section Properties						
	Core Diameter in	Area in ²	Weight lb/ft	Moment of Inertia in ⁴	Section Modulus in ³	Radius of Gyration in	Perimeter ft
Octagonal Piles							
10	Solid	83	85	555	111	2.59	2.76
12	Solid	119	125	1,134	189	3.09	3.31
14	Solid	162	169	2,105	301	3.60	3.87
16	Solid	212	220	3,592	449	4.12	4.42
18	Solid	268	280	5,705	639	4.61	4.97
20	Solid	331	345	8,770	877	5.15	5.52
20	11	236	245	8,050	805	5.84	5.52
22	Solid	401	420	12,837	1167	5.66	6.08
22	13	268	280	11,440	1040	6.53	6.08
24	Solid	477	495	18,180	1515	6.17	6.63
24	15	300	315	15,696	1308	7.23	6.63
Round Piles							
36	26	487	507	60,007	3,334	11.10	9.43
42	32	581	605	101,273	4,823	13.20	11.00
48	38	675	703	158,222	6,592	15.31	12.57
54	44	770	802	233,373	8,643	17.41	14.14
66	54	1,131	1,178	514,027	15,577	21.32	17.28

Note: Designer must confirm section properties for a selected pile. Form dimensions may vary with producers, with corresponding variations in section properties.

PCI (1993), Precast/Prestressed Concrete Institute Journal, Volume 38, No. 2, March-April, 1993.

H-PILES



C2-20

Section Designation	Area A	Depth d	Web Thickness t_w	Flange		Distance				Fillet Radius R	Elastic Properties					
				Width b_f	Thickness t_f	T	k	k_f	a		X-X			Y-Y		
											I	S	r	I	S	r
in x lb/ft	in ²	in	in	in	in	in	in	in	in	in	in ⁴	in ³	in	in ⁴	in ³	in
HP14 x 117	34.4	14.21	0.805	14.885	0.805	10.91	1.65	1.19	7.05	0.79	1220	172	5.96	443	59.5	3.59
HP14 x 102	30.0	14.01	0.705	14.785	0.705	10.91	1.57	1.14	7.05	0.79	1050	150	5.92	380	51.4	3.56
HP14 x 89	26.1	13.83	0.615	14.695	0.615	10.91	1.46	1.09	7.05	0.79	904	131	5.88	326	44.3	3.53
HP14 x 73	21.4	13.61	0.505	14.585	0.505	10.91	1.34	1.04	7.05	0.79	729	107	5.84	261	35.8	3.49
HP12 x 84	24.6	12.28	0.685	12.295	0.685	9.61	1.34	0.93	5.79	0.59	650	106	5.14	213	34.6	2.94
HP12 x 73	21.8	12.13	0.605	12.215	0.610	9.61	1.26	0.89	5.79	0.59	569	93	5.11	186	30.4	2.92
HP12 x 63	18.4	11.94	0.515	12.125	0.515	9.61	1.18	0.85	5.83	0.59	472	79	5.06	153	25.3	2.88
HP12 x 53	15.5	11.78	0.435	12.045	0.435	9.61	1.10	0.81	5.83	0.59	393	66	5.03	127	21.1	2.86
HP10 x 57	16.8	9.99	0.565	10.225	0.565	7.72	1.14	0.80	4.84	0.51	294	59	4.18	101	19.7	2.45
HP10 x 42	12.4	9.70	0.415	10.075	0.420	3.78	0.98	0.72	4.84	0.51	210	43	4.13	72	14.2	2.41
HP8 x 36	10.6	8.02	0.445	8.155	0.445	6.22	0.91	0.62	3.86	0.39	119	30	3.36	41	9.88	1.95

Note: Designer must confirm section properties for a selected pile.

AISC (1989), Manual of Steel Construction, Allowable Stress Design. Ninth Edition, American Institute of Steel Construction, Inc. 1989.

APPENDIX D

Pile Hammer Information

Table D-1 DIESEL HAMMER LISTING (sorted by Rated Energy)	D-3
Table D-2 EXTERNAL COMBUSTION HAMMER LISTING (sorted by Rated Energy)	D-11
Table D-3 VIBRATORY HAMMER LISTING (sorted by Power)	D-25
Table D-4 COMPLETE HAMMER LISTING (sorted by GRLWEAP ID Numbers)	D-29

Note: GRLWEAP hammer ID numbers correspond to those contained in Version 2003-1 of the GRLWEAP program.

TABLE D-1: DIESEL HAMMER LISTING (sorted by Rated Energy)									
Hammer Description				SI Units			US Units		
GRLWEAP ID	Hammer Manufacturer	Hammer Name	Hammer Type	Rated Energy kJ	Ram Weight kN	Eq. Rated Stroke m	Rated Energy ft-kips	Ram Weight kips	Eq. Rated Stroke ft
81	LINKBELT	LB 180	CED	10.98	7.70	1.43	8.10	1.73	4.68
120	ICE	180	CED	11.03	7.70	1.43	8.13	1.73	4.70
146	MKT	DE 10	OED	11.93	4.90	3.35	8.80	1.10	11.00
1	DELMAG	D 5	OED	14.24	4.90	2.93	10.51	1.10	9.62
36	DELMAG	D 6-32	OED	18.31	5.87	3.12	13.50	1.32	10.23
82	LINKBELT	LB 312	CED	20.36	17.18	1.19	15.02	3.86	3.89
147	MKT	DE 20	OED	21.70	8.90	2.74	16.00	2.00	9.00
402	BERMINGH	B200	OED	24.41	8.90	2.74	18.00	2.00	9.00
578	APE	D 8-32	OED	24.41	7.83	3.12	18.00	1.76	10.25
83	LINKBELT	LB 440	CED	24.68	17.80	1.39	18.20	4.00	4.55
122	ICE	440	CED	25.17	17.80	1.41	18.56	4.00	4.64
142	MKT 20	DE333020	OED	27.12	8.90	3.51	20.00	2.00	11.50
2	DELMAG	D 8-22	OED	27.25	7.83	3.67	20.10	1.76	12.05
151	MKT	DA 35B	CED	28.48	12.46	2.29	21.00	2.80	7.50
167	MKT	DA 35C	CED	28.48	12.46	2.29	21.00	2.80	7.50
422	BERMINGH	B2005	OED	28.48	8.90	3.20	21.00	2.00	10.50
148	MKT	DE 30	OED	30.37	12.46	3.05	22.40	2.80	10.00
50	FEC	FEC 1200	OED	30.50	12.24	2.49	22.50	2.75	8.18
127	ICE	30-S	OED	30.51	13.35	2.34	22.50	3.00	7.67
3	DELMAG	D 12	OED	30.65	12.24	3.29	22.61	2.75	10.80
401	BERMINGH	B23	CED	31.17	12.46	2.50	22.99	2.80	8.21
414	BERMINGH	B23 5	CED	31.17	12.46	2.50	22.99	2.80	8.21
121	ICE	422	CED	31.35	17.80	1.76	23.12	4.00	5.78

TABLE D-1: DIESEL HAMMER LISTING (sorted by Rated Energy)									
Hammer Description				SI Units			US Units		
GRLWEAP ID	Hammer Manufacturer	Hammer Name	Hammer Type	Rated Energy kJ	Ram Weight kN	Eq. Rated Stroke m	Rated Energy ft-kips	Ram Weight kips	Eq. Rated Stroke ft
149	MKT	DA35B SA	OED	32.27	12.46	3.96	23.80	2.80	13.00
150	MKT	DE 30B	OED	32.27	12.46	3.05	23.80	2.80	10.00
61	MITSUBIS	M 14	OED	34.23	13.22	2.59	25.25	2.97	8.50
350	HERA	1250	OED	34.37	12.50	2.75	25.35	2.81	9.02
101	KOBE	K 13	OED	34.48	12.77	2.70	25.43	2.87	8.86
139	ICE	32-S	OED	35.27	13.35	3.25	26.01	3.00	10.67
415	BERMINGH	B250 5	OED	35.60	11.13	3.20	26.25	2.50	10.50
84	LINKBELT	LB 520	CED	35.68	22.56	1.58	26.31	5.07	5.19
4	DELMAG	D 15	OED	36.74	14.69	3.29	27.09	3.30	10.80
51	FEC	FEC 1500	OED	36.74	14.69	2.50	27.09	3.30	8.21
143	MKT 30	DE333020	OED	37.97	12.46	3.51	28.00	2.80	11.50
62	MITSUBIS	MH 15	OED	38.15	14.73	2.59	28.14	3.31	8.50
403	BERMINGH	B225	OED	39.66	13.35	2.97	29.25	3.00	9.75
360	ICE	I-12	OED	40.95	12.55	3.51	30.20	2.82	11.50
123	ICE	520	CED	41.18	22.56	1.83	30.37	5.07	5.99
351	HERA	1500	OED	41.22	15.00	2.75	30.40	3.37	9.02
152	MKT	DA 45	CED	41.66	17.80	2.34	30.72	4.00	7.68
37	DELMAG	D 12-32	OED	42.48	12.55	3.60	31.33	2.82	11.81
153	MKT	DE 40	OED	43.39	17.80	3.05	32.00	4.00	10.00
144	MKT 33	DE333020	OED	44.75	14.69	3.51	33.00	3.30	11.50
38	DELMAG	D 12-42	OED	45.16	12.55	3.60	33.30	2.82	11.81
39	DELMAG	D 14-42	OED	46.84	13.75	3.60	34.55	3.09	11.81
154	MKT	DE 42/35	OED	47.46	15.58	4.11	35.00	3.50	13.50

TABLE D-1: DIESEL HAMMER LISTING (sorted by Rated Energy)									
Hammer Description				SI Units			US Units		
GRLWEAP ID	Hammer Manufacturer	Hammer Name	Hammer Type	Rated Energy kJ	Ram Weight kN	Eq. Rated Stroke m	Rated Energy ft-kips	Ram Weight kips	Eq. Rated Stroke ft
423	BERMINGH	B2505	OED	48.00	13.35	3.60	35.40	3.00	11.80
161	MKT	DA 55B	CED	51.80	22.25	2.33	38.20	5.00	7.64
168	MKT	DA 55C	CED	51.80	22.25	2.33	38.20	5.00	7.64
579	APE	D 16-32	OED	53.37	15.71	3.43	39.36	3.53	11.25
128	ICE	40-S	OED	54.24	17.80	3.10	40.00	4.00	10.17
145	MKT 40	DE333020	OED	54.24	17.80	3.51	40.00	4.00	11.50
160	MKT	DA55B SA	OED	54.24	22.25	3.66	40.00	5.00	12.00
5	DELMAG	D 16-32	OED	54.51	15.66	3.58	40.20	3.52	11.76
404	BERMINGH	B300	OED	54.66	16.69	3.28	40.31	3.75	10.75
410	BERMINGH	B300 M	OED	54.66	16.69	3.28	40.31	3.75	10.75
6	DELMAG	D 22	OED	55.06	21.85	2.90	40.61	4.91	9.50
124	ICE	640	CED	55.08	26.70	2.06	40.62	6.00	6.77
155	MKT	DE 42/35	OED	56.95	18.69	4.11	42.00	4.20	13.50
129	ICE	42-S	OED	56.96	18.20	3.18	42.00	4.09	10.42
40	DELMAG	D 19-32	OED	57.55	17.80	3.58	42.44	4.00	11.76
159	MKT	DE 50B	OED	57.63	22.25	3.35	42.50	5.00	11.00
571	APE	D 19-32	OED	58.07	18.65	3.12	42.82	4.19	10.25
580	APE	D 19-42	OED	58.07	18.65	3.23	42.82	4.19	10.60
63	MITSUBIS	M 23	OED	58.32	22.52	2.59	43.01	5.06	8.50
361	ICE	I-19	OED	58.56	17.84	3.75	43.19	4.01	12.30
412	BERMINGH	B400 4.8	OED	58.58	21.36	2.74	43.20	4.80	9.00
35	DELMAG	D 19-52	OED	58.63	17.80	3.61	43.24	4.00	11.86
41	DELMAG	D 19-42	OED	58.63	17.80	3.61	43.24	4.00	11.86

TABLE D-1: DIESEL HAMMER LISTING (sorted by Rated Energy)									
Hammer Description				SI Units			US Units		
GRLWEAP ID	Hammer Manufacturer	Hammer Name	Hammer Type	Rated Energy kJ	Ram Weight kN	Eq. Rated Stroke m	Rated Energy ft-kips	Ram Weight kips	Eq. Rated Stroke ft
349	HERA	1900	OED	60.23	18.65	3.23	44.41	4.19	10.60
413	BERMINGH	B400 5.0	OED	61.02	22.25	2.74	45.00	5.00	9.00
103	KOBE	K22-Est	OED	61.49	21.58	2.85	45.35	4.85	9.35
64	MITSUBIS	MH 25	OED	63.51	24.52	2.59	46.84	5.51	8.50
416	BERMINGH	B350 5	OED	64.00	17.80	3.60	47.20	4.00	11.80
7	DELMAG	D 22-02	OED	65.77	21.58	4.10	48.50	4.85	13.44
8	DELMAG	D 22-13	OED	65.77	21.58	4.10	48.50	4.85	13.44
52	FEC	FEC 2500	OED	67.79	24.48	2.77	50.00	5.50	9.09
157	MKT	DE 50C	OED	67.80	22.25	3.96	50.00	5.00	13.00
163	MKT 50	DE70/50B	OED	67.80	22.25	3.66	50.00	5.00	12.00
352	HERA	2500	OED	68.74	25.01	2.75	50.69	5.62	9.02
9	DELMAG	D 22-23	OED	69.45	21.58	4.10	51.22	4.85	13.44
104	KOBE	K 25	OED	69.86	24.52	2.85	51.52	5.51	9.35
85	LINKBELT	LB 660	CED	70.01	33.69	2.08	51.63	7.57	6.82
125	ICE	660	CED	70.01	33.69	2.08	51.63	7.57	6.82
405	BERMINGH	B400	OED	72.89	22.25	3.28	53.75	5.00	10.75
411	BERMINGH	B400 M	OED	72.89	22.25	3.28	53.75	5.00	10.75
46	DELMAG	D 21-42	OED	75.59	20.60	4.27	55.75	4.63	14.00
53	FEC	FEC 2800	OED	75.93	27.41	2.77	55.99	6.16	9.09
353	HERA	2800	OED	76.93	27.99	2.75	56.74	6.29	9.02
581	APE	D 25-32	OED	78.45	24.52	3.20	57.86	5.51	10.50
417	BERMINGH	B400 5	OED	80.00	22.25	3.60	59.00	5.00	11.80
162	MKT	DE 70B	OED	80.68	31.15	3.66	59.50	7.00	12.00

TABLE D-1: DIESEL HAMMER LISTING (sorted by Rated Energy)									
Hammer Description				SI Units			US Units		
GRLWEAP ID	Hammer Manufacturer	Hammer Name	Hammer Type	Rated Energy kJ	Ram Weight kN	Eq. Rated Stroke m	Rated Energy ft-kips	Ram Weight kips	Eq. Rated Stroke ft
11	DELMAG	D 30	OED	80.99	29.37	2.90	59.73	6.60	9.50
130	ICE	60-S	OED	81.35	31.15	3.18	59.99	7.00	10.42
65	MITSUBIS	M 33	OED	83.68	32.31	2.59	61.71	7.26	8.50
54	FEC	FEC 3000	OED	85.47	29.37	2.91	63.03	6.60	9.55
66	MITSUBIS	MH 35	OED	88.98	34.35	2.59	65.62	7.72	8.50
12	DELMAG	D 30-02	OED	89.76	29.37	4.10	66.20	6.60	13.44
13	DELMAG	D 30-13	OED	89.76	29.37	4.10	66.20	6.60	13.44
10	DELMAG	D 25-32	OED	89.96	24.52	4.19	66.34	5.51	13.76
131	ICE	70-S	OED	94.92	31.15	3.10	70.00	7.00	10.17
158	MKT	DE 70C	OED	94.92	31.15	3.96	70.00	7.00	13.00
164	MKT 70	DE70/50B	OED	94.92	31.15	3.66	70.00	7.00	12.00
572	APE	D 30-32	OED	95.01	29.41	3.23	70.07	6.61	10.60
354	HERA	3500	OED	96.26	35.02	2.75	70.99	7.87	9.02
107	KOBE	K 35	OED	97.88	34.35	2.85	72.18	7.72	9.35
126	ICE	1070	CED	98.45	44.50	2.21	72.60	10.00	7.26
55	FEC	FEC 3400	OED	98.99	33.29	2.97	73.00	7.48	9.76
14	DELMAG	D 30-23	OED	100.06	29.37	4.10	73.79	6.60	13.44
362	ICE	I-30	OED	102.27	29.41	3.84	75.42	6.61	12.60
15	DELMAG	D 30-32	OED	102.29	29.37	4.18	75.44	6.60	13.73
418	BERMINGH	B450 5	OED	105.61	29.37	3.60	77.88	6.60	11.80
132	ICE	80-S	OED	108.48	35.60	3.79	80.00	8.00	12.42
67	MITSUBIS	M 43	OED	109.04	42.10	2.59	80.41	9.46	8.50
16	DELMAG	D 36	OED	113.66	35.29	3.22	83.82	7.93	10.57

TABLE D-1: DIESEL HAMMER LISTING (sorted by Rated Energy)									
Hammer Description				SI Units			US Units		
GRLWEAP ID	Hammer Manufacturer	Hammer Name	Hammer Type	Rated Energy kJ	Ram Weight kN	Eq. Rated Stroke m	Rated Energy ft-kips	Ram Weight kips	Eq. Rated Stroke ft
17	DELMAG	D 36-02	OED	113.66	35.29	3.96	83.82	7.93	12.98
18	DELMAG	D 36-13	OED	113.66	35.29	6.09	83.82	7.93	19.98
573	APE	D 36-32	OED	113.98	35.29	3.23	84.06	7.93	10.60
68	MITSUBIS	MH 45	OED	115.84	44.72	2.59	85.43	10.05	8.50
421	BERMINGH	B550 C	OED	119.33	48.95	2.44	88.00	11.00	8.00
19	DELMAG	D 36-23	OED	120.00	35.29	3.96	88.50	7.93	12.98
133	ICE	90-S	OED	122.04	40.05	3.10	90.00	9.00	10.17
21	DELMAG	D 44	OED	122.25	42.28	2.90	90.16	9.50	9.52
20	DELMAG	D 36-32	OED	122.80	35.29	4.01	90.56	7.93	13.14
363	ICE	I-36	OED	122.96	35.33	3.69	90.67	7.94	12.10
419	BERMINGH	B500 5	OED	124.81	34.71	3.60	92.04	7.80	11.80
110	KOBE	K 45	OED	125.77	44.14	2.85	92.75	9.92	9.35
24	DELMAG	D 46-13	OED	130.90	45.12	3.94	96.53	10.14	12.94
134	ICE	100-S	OED	135.60	44.50	3.66	100.00	10.00	12.00
136	ICE	200-S	OED	135.60	89.00	1.83	100.00	20.00	6.00
355	HERA	5000	OED	137.48	50.02	2.75	101.38	11.24	9.02
420	BERMINGH	B550 5	OED	144.01	40.05	3.60	106.20	9.00	11.80
22	DELMAG	D 46	OED	145.20	45.12	3.22	107.08	10.14	10.57
23	DELMAG	D 46-02	OED	145.20	45.12	3.94	107.08	10.14	12.94
25	DELMAG	D 46-23	OED	145.20	45.12	3.94	107.08	10.14	12.94
574	APE	D 46-32	OED	145.75	45.12	3.23	107.48	10.14	10.60
364	ICE	I-46	OED	146.17	45.17	3.69	107.79	10.15	12.12
165	MKT 110	DE110150	OED	149.16	48.95	4.11	110.00	11.00	13.50

TABLE D-1: DIESEL HAMMER LISTING (sorted by Rated Energy)									
Hammer Description				SI Units			US Units		
GRLWEAP ID	Hammer Manufacturer	Hammer Name	Hammer Type	Rated Energy kJ	Ram Weight kN	Eq. Rated Stroke m	Rated Energy ft-kips	Ram Weight kips	Eq. Rated Stroke ft
356	HERA	5700	OED	156.68	57.00	2.75	115.55	12.81	9.02
135	ICE	120-S	OED	162.72	53.40	3.79	120.00	12.00	12.42
26	DELMAG	D 46-32	OED	165.69	45.12	3.99	122.19	10.14	13.10
27	DELMAG	D 55	OED	169.51	52.78	3.40	125.00	11.86	11.15
357	HERA	6200	OED	170.38	61.99	2.75	125.65	13.93	9.02
112	KOBE	KB 60	OED	176.53	58.87	3.00	130.18	13.23	9.84
140	ICE	120S-15	OED	179.60	66.75	3.73	132.45	15.00	12.25
70	MITSUBIS	MH 72B	OED	183.26	70.76	2.59	135.15	15.90	8.50
71	MITSUBIS	MH 80B	OED	202.86	78.32	2.59	149.60	17.60	8.50
166	MKT 150	DE110150	OED	203.40	66.75	4.11	150.00	15.00	13.50
358	HERA	7500	OED	206.09	74.98	2.75	151.99	16.85	9.02
28	DELMAG	D 62-02	OED	206.72	60.79	3.87	152.45	13.66	12.71
29	DELMAG	D 62-12	OED	206.72	60.79	3.87	152.45	13.66	12.71
575	APE	D 62-22	OED	218.94	60.79	3.60	161.46	13.66	11.82
30	DELMAG	D 62-22	OED	223.20	60.79	4.04	164.60	13.66	13.26
365	ICE	I-62	OED	223.71	64.97	4.34	164.98	14.60	14.25
137	ICE	205-S	OED	230.52	89.00	3.20	170.00	20.00	10.50
113	KOBE	KB 80	OED	235.37	78.50	3.00	173.58	17.64	9.84
359	HERA	8800	OED	241.93	88.02	2.75	178.42	19.78	9.02
31	DELMAG	D 80-12	OED	252.55	78.41	3.92	186.24	17.62	12.87
576	APE	D 80-23	OED	267.12	78.41	3.41	196.99	17.62	11.18
366	ICE	I-80	OED	288.01	78.77	4.11	212.40	17.70	13.50
32	DELMAG	D 80-23	OED	288.15	78.41	3.98	212.50	17.62	13.05

TABLE D-1: DIESEL HAMMER LISTING
(sorted by Rated Energy)

Hammer Description				SI Units			US Units		
GRLWEAP ID	Hammer Manufacturer	Hammer Name	Hammer Type	Rated Energy kJ	Ram Weight kN	Eq. Rated Stroke m	Rated Energy ft-kips	Ram Weight kips	Eq. Rated Stroke ft
577	APE	D 100-13	OED	333.98	98.03	3.41	246.30	22.03	11.18
33	DELMAG	D100-13	OED	360.32	98.21	4.11	265.72	22.07	13.50
43	DELMAG	D120-42	OED	409.23	117.70	3.60	301.79	26.45	11.81
582	APE	D 125-32	OED	416.69	122.64	3.40	307.29	27.56	11.15
45	DELMAG	D125-42	OED	425.29	122.64	4.15	313.63	27.56	13.60
44	DELMAG	D150-42	OED	511.66	147.16	3.60	377.33	33.07	11.81
42	DELMAG	D200-42	OED	667.21	196.20	5.13	492.04	44.09	16.83

TABLE D-2: EXTERNAL COMBUSTION HAMMER LISTING (sorted by Rated Energy)									
Hammer Description				SI Units			US Units		
GRLWEAP ID	Hammer Manufacturer	Hammer Name	Hammer Type	Rated Energy kJ	Ram Weight kN	Eq. Rated Stroke m	Rated Energy ft-kips	Ram Weight kips	Eq. Rated Stroke ft
301	MKT	No. 5	ECH	1.36	0.89	1.52	1.00	0.20	5.00
302	MKT	No. 6	ECH	3.39	1.78	1.91	2.50	0.40	6.25
303	MKT	No. 7	ECH	5.63	3.56	1.58	4.15	0.80	5.19
205	VULCAN	VUL 02	ECH	9.84	13.35	0.74	7.26	3.00	2.42
220	VULCAN	VUL 30C	ECH	9.84	13.35	0.74	7.26	3.00	2.42
521	DAWSON	HPH1200	ECH	11.82	10.24	1.16	8.72	2.30	3.79
304	MKT	9B3	ECH	11.87	7.12	1.67	8.75	1.60	5.47
305	MKT	10B3	ECH	17.78	13.35	1.33	13.11	3.00	4.37
522	DAWSON	HPH1800	ECH	18.62	14.69	1.27	13.73	3.30	4.16
567	HMC	19D	ECH	18.98	15.58	1.22	14.00	3.50	4.00
306	MKT	C5-Air	ECH	19.26	22.25	0.87	14.20	5.00	2.84
171	CONMACO	C 50	ECH	20.34	22.25	0.91	15.00	5.00	3.00
204	VULCAN	VUL 01	ECH	20.34	22.25	0.91	15.00	5.00	3.00
251	RAYMOND	R 1	ECH	20.34	22.25	0.91	15.00	5.00	3.00
221	VULCAN	VUL 50C	ECH	20.48	22.25	0.92	15.10	5.00	3.02
307	MKT	C5-Steam	ECH	21.97	22.25	0.99	16.20	5.00	3.24
380	BSP	HH 1.5	ECH	22.02	14.69	1.50	16.24	3.30	4.92
308	MKT	S-5	ECH	22.04	22.25	0.99	16.25	5.00	3.25
514	UDDCOMB	H2H	ECH	22.49	19.58	1.15	16.59	4.40	3.77
523	DAWSON	HPH2400	ECH	23.47	18.65	1.26	17.30	4.19	4.13
541	BANUT	3 Tonnes	ECH	23.48	29.41	0.80	17.32	6.61	2.62
309	MKT	11B3	ECH	25.97	22.25	1.17	19.15	5.00	3.83

TABLE D-2: EXTERNAL COMBUSTION HAMMER LISTING (sorted by Rated Energy)									
Hammer Description				SI Units			US Units		
GRLWEAP ID	Hammer Manufacturer	Hammer Name	Hammer Type	Rated Energy kJ	Ram Weight kN	Eq. Rated Stroke m	Rated Energy ft-kips	Ram Weight kips	Eq. Rated Stroke ft
222	VULCAN	VUL 65C	ECH	26.00	28.93	0.90	19.18	6.50	2.95
172	CONMACO	C 65	ECH	26.44	28.93	0.91	19.50	6.50	3.00
206	VULCAN	VUL 06	ECH	26.44	28.93	0.91	19.50	6.50	3.00
252	RAYMOND	R 1S	ECH	26.44	28.93	0.91	19.50	6.50	3.00
253	RAYMOND	R 65C	ECH	26.44	28.93	0.91	19.50	6.50	3.00
254	RAYMOND	R 65CH	ECH	26.44	28.93	0.91	19.50	6.50	3.00
223	VULCAN	VUL 65CA	ECH	26.53	28.93	0.92	19.57	6.50	3.01
550	ICE	70	ECH	28.48	31.15	0.91	21.00	7.00	3.00
561	HMC	28B	ECH	28.48	31.15	0.91	21.00	7.00	3.00
311	MKT	C826 Air	ECH	28.75	35.60	0.81	21.20	8.00	2.65
335	IHC	SC-30	ECH	29.57	16.73	1.77	21.81	3.76	5.80
542	BANUT	4 Tonnes	ECH	31.33	39.25	0.80	23.11	8.82	2.62
255	RAYMOND	R 0	ECH	33.05	33.38	0.99	24.38	7.50	3.25
310	MKT	C826 Stm	ECH	33.09	35.60	0.93	24.40	8.00	3.05
224	VULCAN	VUL 80C	ECH	33.19	35.60	0.93	24.48	8.00	3.06
256	RAYMOND	R 80C	ECH	33.19	35.60	0.93	24.48	8.00	3.06
257	RAYMOND	R 80CH	ECH	33.19	35.60	0.93	24.48	8.00	3.06
449	MENCK	MHF3-3	ECH	33.55	31.37	1.07	24.75	7.05	3.51
515	UDDCOMB	H3H	ECH	33.74	29.37	1.15	24.88	6.60	3.77
173	CONMACO	C 550	ECH	33.90	22.25	1.52	25.00	5.00	5.00
192	CONMACO	C 50E5	ECH	33.90	22.25	1.52	25.00	5.00	5.00
235	VULCAN	VUL 505	ECH	33.90	22.25	1.52	25.00	5.00	5.00
320	IHC	S-35	ECH	34.61	29.50	1.17	25.53	6.63	3.85

TABLE D-2: EXTERNAL COMBUSTION HAMMER LISTING (sorted by Rated Energy)									
Hammer Description				SI Units			US Units		
GRLWEAP ID	Hammer Manufacturer	Hammer Name	Hammer Type	Rated Energy kJ	Ram Weight kN	Eq. Rated Stroke m	Rated Energy ft-kips	Ram Weight kips	Eq. Rated Stroke ft
225	VULCAN	VUL 85C	ECH	35.24	37.91	0.93	25.99	8.52	3.05
175	CONMACO	C 80	ECH	35.26	35.60	0.99	26.00	8.00	3.25
207	VULCAN	VUL 08	ECH	35.26	35.60	0.99	26.00	8.00	3.25
312	MKT	S-8	ECH	35.26	35.60	0.99	26.00	8.00	3.25
591	APE	5.4mT	ECH	35.31	53.40	0.66	26.04	12.00	2.17
381	BSP	HH 3	ECH	35.31	29.41	1.20	26.04	6.61	3.94
530	Bruce	SGH-0312	ECH	35.31	29.41	1.20	26.04	6.61	3.94
535	BANUT	3000	ECH	35.31	29.41	1.20	26.04	6.61	3.94
481	JUNTTAN	HHK 3	ECH	36.00	29.46	1.22	26.55	6.62	4.01
560	HMC	28A	ECH	37.97	31.15	1.22	28.00	7.00	4.00
568	HMC	38D	ECH	37.97	31.15	1.22	28.00	7.00	4.00
543	BANUT	5 Tonnes	ECH	39.15	49.04	0.80	28.87	11.02	2.62
336	IHC	SC-40	ECH	40.50	24.52	1.65	29.86	5.51	5.42
551	ICE	75	ECH	40.68	33.38	1.22	30.00	7.50	4.00
313	MKT	MS-350	ECH	41.77	34.35	1.22	30.80	7.72	3.99
450	MENCK	MHF3-4	ECH	41.98	39.25	1.07	30.96	8.82	3.51
174	CONMACO	C 565	ECH	44.07	28.93	1.52	32.50	6.50	5.00
176	CONMACO	C 100	ECH	44.07	44.50	0.99	32.50	10.00	3.25
193	CONMACO	C 65E5	ECH	44.07	28.93	1.52	32.50	6.50	5.00
208	VULCAN	VUL 010	ECH	44.07	44.50	0.99	32.50	10.00	3.25
236	VULCAN	VUL 506	ECH	44.07	28.93	1.52	32.50	6.50	5.00
258	RAYMOND	R 2/0	ECH	44.07	44.50	0.99	32.50	10.00	3.25
314	MKT	S 10	ECH	44.07	44.50	0.99	32.50	10.00	3.25

TABLE D-2: EXTERNAL COMBUSTION HAMMER LISTING (sorted by Rated Energy)									
Hammer Description				SI Units			US Units		
GRLWEAP ID	Hammer Manufacturer	Hammer Name	Hammer Type	Rated Energy kJ	Ram Weight kN	Eq. Rated Stroke m	Rated Energy ft-kips	Ram Weight kips	Eq. Rated Stroke ft
506	HPSI	650	ECH	44.07	28.93	1.52	32.50	6.50	5.00
372	FAIRCHLD	F-32	ECH	44.14	48.28	0.91	32.55	10.85	3.00
226	VULCAN	VUL 100C	ECH	44.61	44.50	1.00	32.90	10.00	3.29
516	UDDCOMB	H4H	ECH	44.99	39.16	1.15	33.18	8.80	3.77
544	BANUT	6 Tonnes	ECH	47.00	58.87	0.80	34.66	13.23	2.62
536	BANUT	4000	ECH	47.12	39.25	1.20	34.75	8.82	3.94
482	JUNTTAN	HHK 4	ECH	47.96	39.25	1.22	35.37	8.82	4.01
227	VULCAN	VUL 140C	ECH	48.79	62.30	0.78	35.98	14.00	2.57
337	IHC	SC-50	ECH	49.92	32.44	1.54	36.81	7.29	5.05
177	CONMACO	C 115	ECH	50.68	51.18	0.99	37.38	11.50	3.25
315	MKT	S 14	ECH	50.88	62.30	0.82	37.52	14.00	2.68
552	ICE	110-SH	ECH	51.15	51.18	1.00	37.72	11.50	3.28
553	ICE	115-SH	ECH	51.46	51.18	1.01	37.95	11.50	3.30
441	MENCK	MHF5-5	ECH	52.45	49.04	1.07	38.68	11.02	3.51
451	MENCK	MHF3-5	ECH	52.45	49.04	1.07	38.68	11.02	3.51
209	VULCAN	VUL 012	ECH	52.88	53.40	0.99	39.00	12.00	3.25
178	CONMACO	C 80E5	ECH	54.24	35.60	1.52	40.00	8.00	5.00
237	VULCAN	VUL 508	ECH	54.24	35.60	1.52	40.00	8.00	5.00
545	BANUT	7 Tonnes	ECH	54.82	68.66	0.80	40.43	15.43	2.62
259	RAYMOND	R 3/0	ECH	55.09	55.63	0.99	40.63	12.50	3.25
517	UDDCOMB	H5H	ECH	56.23	48.95	1.15	41.47	11.00	3.77
182	CONMACO	C 140	ECH	56.95	62.30	0.91	42.00	14.00	3.00
210	VULCAN	VUL 014	ECH	56.95	62.30	0.91	42.00	14.00	3.00

TABLE D-2: EXTERNAL COMBUSTION HAMMER LISTING (sorted by Rated Energy)									
Hammer Description				SI Units			US Units		
GRLWEAP ID	Hammer Manufacturer	Hammer Name	Hammer Type	Rated Energy kJ	Ram Weight kN	Eq. Rated Stroke m	Rated Energy ft-kips	Ram Weight kips	Eq. Rated Stroke ft
382	BSP	HH 5	ECH	58.88	49.04	1.20	43.42	11.02	3.94
531	Bruce	SGH-0512	ECH	58.88	49.04	1.20	43.42	11.02	3.94
537	BANUT	5000	ECH	58.88	49.04	1.20	43.42	11.02	3.94
801	DKH	PH-5	ECH	58.88	49.04	1.20	43.42	11.02	3.94
316	MKT	MS 500	ECH	59.66	48.95	1.22	44.00	11.00	4.00
501	HPSI	110	ECH	59.66	48.95	1.22	44.00	11.00	4.00
489	JUNTTAN	HHK 5A	ECH	59.77	49.04	1.22	44.08	11.02	4.00
483	JUNTTAN	HHK 5	ECH	59.98	49.08	1.22	44.23	11.03	4.01
338	IHC	SC-60	ECH	60.96	59.19	1.03	44.95	13.30	3.38
371	FAIRCHLD	F-45	ECH	61.02	66.75	0.91	45.00	15.00	3.00
282	MENCK	MRBS 500	ECH	61.12	49.04	1.25	45.07	11.02	4.09
554	ICE	115	ECH	62.38	51.18	1.22	46.00	11.50	4.00
562	HMC	62	ECH	62.38	51.18	1.22	46.00	11.50	4.00
442	MENCK	MHF5-6	ECH	62.97	58.87	1.07	46.44	13.23	3.51
452	MENCK	MHF3-6	ECH	62.97	58.87	1.07	46.44	13.23	3.51
524	DAWSON	HPH6500	ECH	63.66	45.61	1.40	46.95	10.25	4.58
183	CONMACO	C 160	ECH	66.11	72.31	0.91	48.75	16.25	3.00
211	VULCAN	VUL 016	ECH	66.11	72.31	0.91	48.75	16.25	3.00
260	RAYMOND	R 150C	ECH	66.11	66.75	0.99	48.75	15.00	3.25
261	RAYMOND	R 4/0	ECH	66.11	66.75	0.99	48.75	15.00	3.25
271	MENCK	MH 68	ECH	66.68	34.35	1.94	49.18	7.72	6.37
518	UDDCOMB	H6H	ECH	67.48	58.74	1.15	49.76	13.20	3.77
179	CONMACO	C 100E5	ECH	67.80	44.50	1.52	50.00	10.00	5.00

TABLE D-2: EXTERNAL COMBUSTION HAMMER LISTING (sorted by Rated Energy)									
Hammer Description				SI Units			US Units		
GRLWEAP ID	Hammer Manufacturer	Hammer Name	Hammer Type	Rated Energy kJ	Ram Weight kN	Eq. Rated Stroke m	Rated Energy ft-kips	Ram Weight kips	Eq. Rated Stroke ft
238	VULCAN	VUL 510	ECH	67.80	44.50	1.52	50.00	10.00	5.00
507	HPSI	1000	ECH	67.80	44.50	1.52	50.00	10.00	5.00
228	VULCAN	VUL 200C	ECH	68.07	89.00	0.77	50.20	20.00	2.51
321	IHC	S-70	ECH	69.49	34.40	2.02	51.25	7.73	6.63
592	APE	7.2mT	ECH	69.64	72.09	0.97	51.35	16.20	3.17
191	CONMACO	C 160 **	ECH	70.21	76.81	0.91	51.78	17.26	3.00
538	BANUT	6000	ECH	70.68	58.87	1.20	52.13	13.23	3.94
484	JUNTTAN	HHK 6	ECH	71.94	58.87	1.22	53.05	13.23	4.01
443	MENCK	MHF5-7	ECH	73.44	68.66	1.07	54.16	15.43	3.51
453	MENCK	MHF3-7	ECH	73.44	68.66	1.07	54.16	15.43	3.51
339	IHC	SC-75	ECH	74.30	54.07	1.37	54.80	12.15	4.51
262	RAYMOND	R 5/0	ECH	77.12	77.88	0.99	56.88	17.50	3.25
180	CONMACO	C 115E5	ECH	77.97	51.18	1.52	57.50	11.50	5.00
184	CONMACO	C 200	ECH	81.36	89.00	0.91	60.00	20.00	3.00
212	VULCAN	VUL 020	ECH	81.36	89.00	0.91	60.00	20.00	3.00
231	VULCAN	VUL 320	ECH	81.36	89.00	0.91	60.00	20.00	3.00
239	VULCAN	VUL 512	ECH	81.36	53.40	1.52	60.00	12.00	5.00
317	MKT	S 20	ECH	81.36	89.00	0.91	60.00	20.00	3.00
502	HPSI	150	ECH	81.36	66.75	1.22	60.00	15.00	4.00
383	BSP	HH 7	ECH	82.44	68.66	1.20	60.79	15.43	3.94
532	Bruce	SGH-0712	ECH	82.44	68.66	1.20	60.79	15.43	3.94
802	DKH	PH-7	ECH	82.44	68.66	1.20	60.79	15.43	3.94
803	DKH	PH-7S	ECH	82.44	68.66	1.20	60.79	15.43	3.94

TABLE D-2: EXTERNAL COMBUSTION HAMMER LISTING (sorted by Rated Energy)									
Hammer Description				SI Units			US Units		
GRLWEAP ID	Hammer Manufacturer	Hammer Name	Hammer Type	Rated Energy kJ	Ram Weight kN	Eq. Rated Stroke m	Rated Energy ft-kips	Ram Weight kips	Eq. Rated Stroke ft
503	HPSI	154	ECH	83.53	68.53	1.22	61.60	15.40	4.00
490	JUNTTAN	HHK 7A	ECH	83.69	68.66	1.22	61.72	15.43	4.00
485	JUNTTAN	HHK 7	ECH	83.96	68.71	1.22	61.91	15.44	4.01
444	MENCK	MHF5-8	ECH	83.96	78.50	1.07	61.92	17.64	3.51
181	CONMACO	C 125E5	ECH	84.75	55.63	1.52	62.50	12.50	5.00
555	ICE	160-SH	ECH	86.78	71.20	1.22	64.00	16.00	4.00
556	ICE	160	ECH	86.78	71.20	1.22	64.00	16.00	4.00
563	HMC	86	ECH	86.78	71.20	1.22	64.00	16.00	4.00
322	IHC	S-90	ECH	89.36	44.23	2.02	65.90	9.94	6.63
283	MENCK	MRBS 750	ECH	91.90	73.56	1.25	67.77	16.53	4.10
272	MENCK	MH 96	ECH	94.14	49.04	1.92	69.43	11.02	6.30
384	BSP	HH 8	ECH	94.24	78.50	1.20	69.50	17.64	3.94
539	BANUT	8000	ECH	94.24	78.50	1.20	69.50	17.64	3.94
445	MENCK	MHF5-9	ECH	94.43	88.29	1.07	69.64	19.84	3.51
263	RAYMOND	R 30X	ECH	101.70	133.50	0.76	75.00	30.00	2.50
446	MENCK	MHF5-10	ECH	104.90	98.08	1.07	77.36	22.04	3.51
385	BSP	HH 9	ECH	106.00	88.29	1.20	78.17	19.84	3.94
491	JUNTTAN	HHK 9A	ECH	107.61	88.29	1.22	79.36	19.84	4.00
504	HPSI	200	ECH	108.48	89.00	1.22	80.00	20.00	4.00
512	HPSI	2000	ECH	108.48	89.00	1.22	80.00	20.00	4.00
595	APE	10-60	ECH	108.48	89.00	1.22	80.00	20.00	4.00
264	RAYMOND	R 8/0	ECH	110.18	111.25	0.99	81.25	25.00	3.25
340	IHC	SC-110	ECH	111.04	77.70	1.43	81.89	17.46	4.69

TABLE D-2: EXTERNAL COMBUSTION HAMMER LISTING (sorted by Rated Energy)									
Hammer Description				SI Units			US Units		
GRLWEAP ID	Hammer Manufacturer	Hammer Name	Hammer Type	Rated Energy kJ	Ram Weight kN	Eq. Rated Stroke m	Rated Energy ft-kips	Ram Weight kips	Eq. Rated Stroke ft
519	UDDCOMB	H8H	ECH	111.45	78.32	1.42	82.19	17.60	4.67
508	HPSI	1605	ECH	112.55	73.87	1.52	83.00	16.60	5.00
447	MENCK	MHF5-11	ECH	115.42	107.91	1.07	85.12	24.25	3.51
804	DKH	PH-10	ECH	117.75	98.08	1.20	86.84	22.04	3.94
520	UDDCOMB	H10H	ECH	117.81	98.12	1.20	86.88	22.05	3.94
533	Bruce	SGH-1012	ECH	117.81	98.12	1.20	86.88	22.05	3.94
540	BANUT	10000	ECH	117.81	98.12	1.20	86.88	22.05	3.94
557	ICE	220	ECH	119.33	97.90	1.22	88.00	22.00	4.00
564	HMC	119	ECH	119.33	97.90	1.22	88.00	22.00	4.00
486	JUNTTAN	HHK 10	ECH	119.90	98.12	1.22	88.42	22.05	4.01
323	IHC	S-120	ECH	121.19	59.99	2.02	89.37	13.48	6.63
185	CONMACO	C 300	ECH	122.04	133.50	0.91	90.00	30.00	3.00
213	VULCAN	VUL 030	ECH	122.04	133.50	0.91	90.00	30.00	3.00
232	VULCAN	VUL 330	ECH	122.04	133.50	0.91	90.00	30.00	3.00
505	HPSI	225	ECH	122.04	100.13	1.22	90.00	22.50	4.00
448	MENCK	MHF5-12	ECH	125.89	117.70	1.07	92.84	26.45	3.51
285	MENCK	MRBS 850	ECH	126.49	84.37	1.50	93.28	18.96	4.92
509	HPSI	2005	ECH	128.96	84.64	1.52	95.10	19.02	5.00
386	BSP	HH11-1.2	ECH	129.56	107.91	1.20	95.55	24.25	3.94
186	CONMACO	C 5200	ECH	135.60	89.00	1.52	100.00	20.00	5.00
194	CONMACO	C 200E5	ECH	135.60	89.00	1.52	100.00	20.00	5.00
240	VULCAN	VUL 520	ECH	135.60	89.00	1.52	100.00	20.00	5.00
265	RAYMOND	R 40X	ECH	135.60	178.00	0.76	100.00	40.00	2.50

TABLE D-2: EXTERNAL COMBUSTION HAMMER LISTING (sorted by Rated Energy)									
Hammer Description				SI Units			US Units		
GRLWEAP ID	Hammer Manufacturer	Hammer Name	Hammer Type	Rated Energy kJ	Ram Weight kN	Eq. Rated Stroke m	Rated Energy ft-kips	Ram Weight kips	Eq. Rated Stroke ft
492	JUNTTAN	HHK 12A	ECH	141.31	117.70	1.20	104.21	26.45	3.94
273	MENCK	MH 145	ECH	142.11	73.56	1.93	104.80	16.53	6.34
487	JUNTTAN	HHK 12	ECH	143.88	117.75	1.22	106.10	26.46	4.01
341	IHC	SC-150	ECH	148.28	108.14	1.37	109.35	24.30	4.50
558	ICE	275	ECH	149.16	122.38	1.22	110.00	27.50	4.00
565	HMC	149	ECH	149.16	122.38	1.22	110.00	27.50	4.00
324	IHC	S-150	ECH	149.24	73.87	2.02	110.06	16.60	6.63
805	DKH	PH-13	ECH	153.12	127.54	1.20	112.92	28.66	3.94
229	VULCAN	VUL 400C	ECH	154.04	178.00	0.87	113.60	40.00	2.84
393	BSP	HH11-1.5	ECH	161.78	107.91	1.50	119.31	24.25	4.92
214	VULCAN	VUL 040	ECH	162.72	178.00	0.91	120.00	40.00	3.00
233	VULCAN	VUL 340	ECH	162.72	178.00	0.91	120.00	40.00	3.00
387	BSP	HH14-1.2	ECH	164.87	137.33	1.20	121.59	30.86	3.94
493	JUNTTAN	HHK 14A	ECH	164.87	137.33	1.20	121.59	30.86	3.94
286	MENCK	MRBS1100	ECH	167.37	107.91	1.55	123.43	24.25	5.09
488	JUNTTAN	HHK 14	ECH	167.86	137.37	1.22	123.79	30.87	4.01
454	MENCK	MHF10-15	ECH	169.01	147.12	1.15	124.64	33.06	3.77
287	MENCK	MRBS1502	ECH	183.86	147.16	1.25	135.59	33.07	4.10
566	HMC	187	ECH	187.13	153.53	1.22	138.00	34.50	4.00
388	BSP	HH16-1.2	ECH	188.43	156.95	1.20	138.96	35.27	3.94
494	JUNTTAN	HHK 16A	ECH	188.43	156.95	1.20	138.96	35.27	3.94
274	MENCK	MH 195	ECH	191.36	98.12	1.95	141.12	22.05	6.40
325	IHC	S-200	ECH	197.49	97.90	2.02	145.64	22.00	6.62

TABLE D-2: EXTERNAL COMBUSTION HAMMER LISTING (sorted by Rated Energy)									
Hammer Description				SI Units			US Units		
GRLWEAP ID	Hammer Manufacturer	Hammer Name	Hammer Type	Rated Energy kJ	Ram Weight kN	Eq. Rated Stroke m	Rated Energy ft-kips	Ram Weight kips	Eq. Rated Stroke ft
461	MENCK	MHUT 200	ECH	199.85	117.75	1.70	147.38	26.46	5.57
187	CONMACO	C 5300	ECH	203.40	133.50	1.52	150.00	30.00	5.00
195	CONMACO	C 300E5	ECH	203.40	133.50	1.52	150.00	30.00	5.00
241	VULCAN	VUL 530	ECH	203.40	133.50	1.52	150.00	30.00	5.00
266	RAYMOND	R 60X	ECH	203.40	267.00	0.76	150.00	60.00	2.50
394	BSP	HH14-1.5	ECH	205.88	137.33	1.50	151.83	30.86	4.92
342	IHC	SC-200	ECH	206.80	134.39	1.54	152.51	30.20	5.05
510	HPSI	3005	ECH	209.23	137.33	1.52	154.30	30.86	5.00
495	JUNTTAN	HHK 18A	ECH	212.00	176.58	1.20	156.34	39.68	3.94
275	MENCK	MHU 220	ECH	215.70	111.83	1.93	159.07	25.13	6.33
455	MENCK	MHF10-20	ECH	225.29	196.11	1.15	166.14	44.07	3.77
395	BSP	HH16-1.5	ECH	235.30	156.95	1.50	173.53	35.27	4.92
389	BSP	HH 20	ECH	235.56	196.20	1.20	173.71	44.09	3.94
390	BSP	HH 20S	ECH	235.56	196.20	1.20	173.71	44.09	3.94
511	HPSI	3505	ECH	239.06	156.91	1.52	176.30	35.26	5.00
230	VULCAN	VUL 600C	ECH	243.27	267.00	0.91	179.40	60.00	2.99
215	VULCAN	VUL 060	ECH	244.08	267.00	0.91	180.00	60.00	3.00
234	VULCAN	VUL 360	ECH	244.08	267.00	0.91	180.00	60.00	3.00
288	MENCK	MRBS1800	ECH	257.39	171.68	1.50	189.81	38.58	4.92
242	VULCAN	VUL 540	ECH	271.20	182.01	1.49	200.00	40.90	4.89
326	IHC	S-280	ECH	278.40	133.77	2.08	205.31	30.06	6.83
806	DKH	PH-20	ECH	294.15	196.20	1.50	216.92	44.09	4.92
188	CONMACO	C 5450	ECH	305.10	200.25	1.52	225.00	45.00	5.00

TABLE D-2: EXTERNAL COMBUSTION HAMMER LISTING (sorted by Rated Energy)									
Hammer Description				SI Units			US Units		
GRLWEAP ID	Hammer Manufacturer	Hammer Name	Hammer Type	Rated Energy kJ	Ram Weight kN	Eq. Rated Stroke m	Rated Energy ft-kips	Ram Weight kips	Eq. Rated Stroke ft
290	MENCK	MRBS2502	ECH	306.39	245.24	1.25	225.95	55.11	4.10
291	MENCK	MRBS2504	ECH	306.39	245.24	1.25	225.95	55.11	4.10
391	BSP	HA 30	ECH	353.31	294.28	1.20	260.55	66.13	3.94
289	MENCK	MRBS2500	ECH	355.43	284.49	1.25	262.11	63.93	4.10
276	MENCK	MHU 400	ECH	392.64	225.66	1.74	289.55	50.71	5.71
327	IHC	S-400	ECH	396.77	196.69	2.02	292.60	44.20	6.62
462	MENCK	MHUT 400	ECH	400.18	234.52	1.71	295.12	52.70	5.60
243	VULCAN	VUL 560	ECH	406.80	278.13	1.46	300.00	62.50	4.80
245	VULCAN	VUL 3100	ECH	406.80	445.00	0.91	300.00	100.00	3.00
292	MENCK	MRBS3000	ECH	441.19	294.28	1.50	325.36	66.13	4.92
807	DKH	PH-30	ECH	441.19	294.28	1.50	325.36	66.13	4.92
392	BSP	HA 40	ECH	471.11	392.40	1.20	347.43	88.18	3.94
189	CONMACO	C 5700	ECH	474.60	311.50	1.52	350.00	70.00	5.00
328	IHC	S-500	ECH	496.41	246.09	2.02	366.09	55.30	6.62
596	APE	HI 400U	ECH	542.40	356.00	1.52	400.00	80.00	5.00
463	MENCK	MHUT 500	ECH	550.59	294.28	1.87	406.04	66.13	6.14
277	MENCK	MHU 600	ECH	588.01	343.36	1.71	433.64	77.16	5.62
808	DKH	PH-40	ECH	588.29	392.40	1.50	433.85	88.18	4.92
329	IHC	S-600	ECH	601.44	298.15	2.02	443.54	67.00	6.62
294	MENCK	MRBS4600	ECH	676.56	451.27	1.50	498.94	101.41	4.92
246	VULCAN	VUL 5100	ECH	678.00	445.00	1.52	500.00	100.00	5.00
190	CONMACO	C 6850	ECH	691.56	378.25	1.83	510.00	85.00	6.00
293	MENCK	MRBS3900	ECH	696.09	386.53	1.80	513.34	86.86	5.91

TABLE D-2: EXTERNAL COMBUSTION HAMMER LISTING (sorted by Rated Energy)									
Hammer Description				SI Units			US Units		
GRLWEAP ID	Hammer Manufacturer	Hammer Name	Hammer Type	Rated Energy kJ	Ram Weight kN	Eq. Rated Stroke m	Rated Energy ft-kips	Ram Weight kips	Eq. Rated Stroke ft
464	MENCK	MHUT700U	ECH	699.88	413.09	1.69	516.13	92.83	5.56
295	MENCK	MRBS5000	ECH	735.40	490.52	1.50	542.33	110.23	4.92
468	MENCK	MHU 800S	ECH	799.02	441.44	1.81	589.25	99.20	5.94
465	MENCK	MHUT700A	ECH	839.60	413.09	2.03	619.18	92.83	6.67
297	MENCK	MRBS7000	ECH	856.18	685.30	1.25	631.40	154.00	4.10
330	IHC	S-900	ECH	892.73	442.55	2.02	658.36	99.45	6.62
466	MENCK	MHUT1000	ECH	999.25	588.74	1.70	736.91	132.30	5.57
278	MENCK	MHU 1000	ECH	1000.32	565.02	1.77	737.70	126.97	5.81
247	VULCAN	VUL 5150	ECH	1017.00	667.50	1.52	750.00	150.00	5.00
296	MENCK	MRBS6000	ECH	1029.52	588.60	1.75	759.23	132.27	5.74
298	MENCK	MRBS8000	ECH	1176.66	784.85	1.50	867.74	176.37	4.92
469	MENCK	MHU 1200	ECH	1202.34	657.62	1.83	886.68	147.78	6.00
331	IHC	S-1200	ECH	1208.27	598.97	2.02	891.05	134.60	6.62
299	MENCK	MRBS8800	ECH	1294.34	863.34	1.50	954.53	194.01	4.92
332	IHC	S-1800	ECH	1586.93	738.70	2.15	1170.30	166.00	7.05
279	MENCK	MHU 1700	ECH	1666.35	922.17	1.81	1228.87	207.23	5.93
280	MENCK	MHU 2100	ECH	2098.53	1138.31	1.84	1547.59	255.80	6.05
467	MENCK	MHU2100S	ECH	2100.02	1010.51	2.08	1548.69	227.08	6.82
300	MENCK	MBS12500	ECH	2144.96	1226.33	1.75	1581.83	275.58	5.74
333	IHC	S-2300	ECH	2280.09	1130.30	2.02	1681.48	254.00	6.62
248	VULCAN	VUL 6300	ECH	2440.80	1335.00	1.83	1800.00	300.00	6.00
281	MENCK	MHU 3000	ECH	2944.75	1618.73	1.82	2171.65	363.76	5.97

TABLE D-3: VIBRATORY HAMMER LISTING (sorted by Power)									
Hammer Description				SI Units			US Units		
GRLWEAP ID	Hammer Manufacturer	Hammer Name	Hammer Type	Power kW	Ram Weight kN	Frequency Hz	Power kW	Ram Weight kips	Frequency Hz
770	APE	3	VIB	10.58	0.00	38.30	10.58	0.00	38.30
771	APE	6	VIB	10.58	0.04	38.30	10.58	0.01	38.30
700	ICE	23-28	VIB	21.00	0.45	26.70	21.00	0.10	26.70
720	HMC	3+28	VIB	21.00	0.49	26.80	21.00	0.11	26.80
750	MKT	V-2B	VIB	52.00	0.67	30.00	52.00	0.15	30.00
721	HMC	3+75	VIB	56.00	0.49	36.10	56.00	0.11	36.10
772	APE	15	VIB	59.67	0.49	30.00	59.67	0.11	30.00
773	APE	20	VIB	59.67	0.67	38.30	59.67	0.15	38.30
774	APE	20E	VIB	59.67	0.67	38.30	59.67	0.15	38.30
701	ICE	216	VIB	130.00	2.05	26.70	130.00	0.46	26.70
702	ICE	216E	VIB	130.00	2.05	26.70	130.00	0.46	26.70
751	MKT	V-5C	VIB	138.00	1.91	28.33	138.00	0.43	28.33
722	HMC	13+200	VIB	149.00	1.56	26.70	149.00	0.35	26.70
723	HMC	13S+200	VIB	149.00	1.56	26.70	149.00	0.35	26.70
703	ICE	11-23	VIB	164.00	2.05	31.70	164.00	0.46	31.70
724	HMC	13H+200	VIB	164.00	1.56	29.80	164.00	0.35	29.80
725	HMC	25+220	VIB	164.00	2.71	20.90	164.00	0.61	20.90
775	APE	50	VIB	194.00	1.02	30.00	194.00	0.23	30.00
776	APE	50E	VIB	194.00	1.02	30.00	194.00	0.23	30.00

TABLE D-3: VIBRATORY HAMMER LISTING (sorted by Power)									
Hammer Description				SI Units			US Units		
GRLWEAP ID	Hammer Manufacturer	Hammer Name	Hammer Type	Power kW	Ram Weight kN	Frequency Hz	Power kW	Ram Weight kips	Frequency Hz
777	APE	100	VIB	194.00	1.42	30.00	194.00	0.32	30.00
778	APE	100E	VIB	194.00	0.62	30.00	194.00	0.14	30.00
704	ICE	223	VIB	242.00	2.05	38.30	242.00	0.46	38.30
705	ICE	416L	VIB	242.00	4.09	26.70	242.00	0.92	26.70
708	ICE	44-30	VIB	242.00	5.79	20.00	242.00	1.30	20.00
726	HMC	26+335	VIB	242.00	3.16	25.60	242.00	0.71	25.60
727	HMC	26S+335	VIB	242.00	3.16	25.60	242.00	0.71	25.60
728	HMC	51+335	VIB	242.00	5.38	19.50	242.00	1.21	19.50
752	MKT	V-20B	VIB	242.00	35.60	28.33	242.00	8.00	28.33
779	APE	100HF	VIB	260.00	0.62	43.00	260.00	0.14	43.00
780	APE	150	VIB	260.00	0.62	30.00	260.00	0.14	30.00
781	APE	150T	VIB	260.00	0.76	30.00	260.00	0.17	30.00
706	ICE	812	VIB	375.00	8.10	26.70	375.00	1.82	26.70
707	ICE	815	VIB	375.00	8.19	26.70	375.00	1.84	26.70
709	ICE	44-50	VIB	377.00	5.79	26.70	377.00	1.30	26.70
729	HMC	51+535	VIB	377.00	5.38	26.40	377.00	1.21	26.40
730	HMC	51S+535	VIB	377.00	5.38	26.40	377.00	1.21	26.40
753	MKT	V-30	VIB	448.00	6.54	28.33	448.00	1.47	28.33
782	APE	150HF	VIB	466.00	1.42	43.00	466.00	0.32	43.00
783	APE	200	VIB	466.00	1.29	30.00	466.00	0.29	30.00

TABLE D-3: VIBRATORY HAMMER LISTING (sorted by Power)									
Hammer Description				SI Units			US Units		
GRLWEAP ID	Hammer Manufacturer	Hammer Name	Hammer Type	Power kW	Ram Weight kN	Frequency Hz	Power kW	Ram Weight kips	Frequency Hz
784	APE	200T	VIB	466.00	1.51	30.83	466.00	0.34	30.83
714	ICE	1412C	VIB	470.00	8.99	23.00	470.00	2.02	23.00
710	ICE	44-65	VIB	485.00	5.79	27.50	485.00	1.30	27.50
711	ICE	66-65	VIB	485.00	8.68	21.70	485.00	1.95	21.70
731	HMC	51+740	VIB	485.00	5.38	27.50	485.00	1.21	27.50
732	HMC	76+740	VIB	485.00	8.10	21.70	485.00	1.82	21.70
754	MKT	V-35	VIB	485.00	7.12	28.33	485.00	1.60	28.33
712	ICE	66-80	VIB	597.00	8.68	26.70	597.00	1.95	26.70
713	ICE	1412B	VIB	597.00	9.08	21.00	597.00	2.04	21.00
733	HMC	76+800	VIB	597.00	8.10	26.10	597.00	1.82	26.10
734	HMC	115+800	VIB	597.00	6.01	20.40	597.00	1.35	20.40
785	APE	200T HF	VIB	738.00	1.51	43.00	738.00	0.34	43.00
786	APE	300	VIB	738.00	1.51	25.00	738.00	0.34	25.00
787	APE	400B	VIB	738.00	3.47	23.33	738.00	0.78	23.33
788	APE	600	VIB	800.00	4.67	23.30	800.00	1.05	23.30
810	MGF	RBH 2400	VIB	975.00	23.99	23.50	975.00	5.39	23.50
735	HMC	230+1600	VIB	1193.00	11.97	20.40	1193.00	2.69	20.40
755	MKT	V-140	VIB	1341.00	20.78	23.33	1341.00	4.67	23.33
789	APE	Tan 400	VIB	1476.00	6.10	23.33	1476.00	1.37	23.33
790	APE	Tan 600	VIB	1800.00	9.39	23.30	1800.00	2.11	23.30

TABLE D-4: COMPLETE HAMMER LISTING (sorted by GRLWEAP ID Numbers)									
Hammer Description				SI Units			US Units		
GRLWEAP ID	Hammer Manufacturer	Hammer Name	Hammer Type	Rated Energy kJ	Ram Weight kN	Eq. Rated Stroke m	Rated Energy ft-kips	Ram Weight kips	Eq. Rated Stroke ft
1	DELMAG	D 5	OED	14.24	4.90	2.93	10.51	1.10	9.62
2	DELMAG	D 8-22	OED	27.25	7.83	3.67	20.10	1.76	12.05
3	DELMAG	D 12	OED	30.65	12.24	3.29	22.61	2.75	10.80
4	DELMAG	D 15	OED	36.74	14.69	3.29	27.09	3.30	10.80
5	DELMAG	D 16-32	OED	54.51	15.66	3.58	40.20	3.52	11.76
6	DELMAG	D 22	OED	55.06	21.85	2.90	40.61	4.91	9.50
7	DELMAG	D 22-02	OED	65.77	21.58	4.10	48.50	4.85	13.44
8	DELMAG	D 22-13	OED	65.77	21.58	4.10	48.50	4.85	13.44
9	DELMAG	D 22-23	OED	69.45	21.58	4.10	51.22	4.85	13.44
10	DELMAG	D 25-32	OED	89.96	24.52	4.19	66.34	5.51	13.76
11	DELMAG	D 30	OED	80.99	29.37	2.90	59.73	6.60	9.50
12	DELMAG	D 30-02	OED	89.76	29.37	4.10	66.20	6.60	13.44
13	DELMAG	D 30-13	OED	89.76	29.37	4.10	66.20	6.60	13.44
14	DELMAG	D 30-23	OED	100.06	29.37	4.10	73.79	6.60	13.44
15	DELMAG	D 30-32	OED	102.29	29.37	4.18	75.44	6.60	13.73
16	DELMAG	D 36	OED	113.66	35.29	3.22	83.82	7.93	10.57
17	DELMAG	D 36-02	OED	113.66	35.29	3.96	83.82	7.93	12.98
18	DELMAG	D 36-13	OED	113.66	35.29	6.09	83.82	7.93	19.98
19	DELMAG	D 36-23	OED	120.00	35.29	3.96	88.50	7.93	12.98

TABLE D-4: COMPLETE HAMMER LISTING (sorted by GRLWEAP ID Numbers)									
Hammer Description				SI Units			US Units		
GRLWEAP ID	Hammer Manufacturer	Hammer Name	Hammer Type	Rated Energy kJ	Ram Weight kN	Eq. Rated Stroke m	Rated Energy ft-kips	Ram Weight kips	Eq. Rated Stroke ft
20	DELMAG	D 36-32	OED	122.80	35.29	4.01	90.56	7.93	13.14
21	DELMAG	D 44	OED	122.25	42.28	2.90	90.16	9.50	9.52
22	DELMAG	D 46	OED	145.20	45.12	3.22	107.08	10.14	10.57
23	DELMAG	D 46-02	OED	145.20	45.12	3.94	107.08	10.14	12.94
24	DELMAG	D 46-13	OED	130.90	45.12	3.94	96.53	10.14	12.94
25	DELMAG	D 46-23	OED	145.20	45.12	3.94	107.08	10.14	12.94
26	DELMAG	D 46-32	OED	165.69	45.12	3.99	122.19	10.14	13.10
27	DELMAG	D 55	OED	169.51	52.78	3.40	125.00	11.86	11.15
28	DELMAG	D 62-02	OED	206.72	60.79	3.87	152.45	13.66	12.71
29	DELMAG	D 62-12	OED	206.72	60.79	3.87	152.45	13.66	12.71
30	DELMAG	D 62-22	OED	223.20	60.79	4.04	164.60	13.66	13.26
31	DELMAG	D 80-12	OED	252.55	78.41	3.92	186.24	17.62	12.87
32	DELMAG	D 80-23	OED	288.15	78.41	3.98	212.50	17.62	13.05
33	DELMAG	D100-13	OED	360.32	98.21	4.11	265.72	22.07	13.50
35	DELMAG	D 19-52	OED	58.63	17.80	3.61	43.24	4.00	11.86
36	DELMAG	D 6-32	OED	18.31	5.87	3.12	13.50	1.32	10.23
37	DELMAG	D 12-32	OED	42.48	12.55	3.60	31.33	2.82	11.81
38	DELMAG	D 12-42	OED	45.16	12.55	3.60	33.30	2.82	11.81
39	DELMAG	D 14-42	OED	46.84	13.75	3.60	34.55	3.09	11.81
40	DELMAG	D 19-32	OED	57.55	17.80	3.58	42.44	4.00	11.76
41	DELMAG	D 19-42	OED	58.63	17.80	3.61	43.24	4.00	11.86

TABLE D-4: COMPLETE HAMMER LISTING (sorted by GRLWEAP ID Numbers)									
Hammer Description				SI Units			US Units		
GRLWEAP ID	Hammer Manufacturer	Hammer Name	Hammer Type	Rated Energy kJ	Ram Weight kN	Eq. Rated Stroke m	Rated Energy ft-kips	Ram Weight kips	Eq. Rated Stroke ft
42	DELMAG	D200-42	OED	667.21	196.20	5.13	492.04	44.09	16.83
43	DELMAG	D120-42	OED	409.23	117.70	3.60	301.79	26.45	11.81
44	DELMAG	D150-42	OED	511.66	147.16	3.60	377.33	33.07	11.81
45	DELMAG	D125-42	OED	425.29	122.64	4.15	313.63	27.56	13.60
46	DELMAG	D 21-42	OED	75.59	20.60	4.27	55.75	4.63	14.00
50	FEC	FEC 1200	OED	30.50	12.24	2.49	22.50	2.75	8.18
51	FEC	FEC 1500	OED	36.74	14.69	2.50	27.09	3.30	8.21
52	FEC	FEC 2500	OED	67.79	24.48	2.77	50.00	5.50	9.09
53	FEC	FEC 2800	OED	75.93	27.41	2.77	55.99	6.16	9.09
54	FEC	FEC 3000	OED	85.47	29.37	2.91	63.03	6.60	9.55
55	FEC	FEC 3400	OED	98.99	33.29	2.97	73.00	7.48	9.76
61	MITSUBIS	M 14	OED	34.23	13.22	2.59	25.25	2.97	8.50
62	MITSUBIS	MH 15	OED	38.15	14.73	2.59	28.14	3.31	8.50
63	MITSUBIS	M 23	OED	58.32	22.52	2.59	43.01	5.06	8.50
64	MITSUBIS	MH 25	OED	63.51	24.52	2.59	46.84	5.51	8.50
65	MITSUBIS	M 33	OED	83.68	32.31	2.59	61.71	7.26	8.50
66	MITSUBIS	MH 35	OED	88.98	34.35	2.59	65.62	7.72	8.50
67	MITSUBIS	M 43	OED	109.04	42.10	2.59	80.41	9.46	8.50
68	MITSUBIS	MH 45	OED	115.84	44.72	2.59	85.43	10.05	8.50
70	MITSUBIS	MH 72B	OED	183.26	70.76	2.59	135.15	15.90	8.50
71	MITSUBIS	MH 80B	OED	202.86	78.32	2.59	149.60	17.60	8.50

TABLE D-4: COMPLETE HAMMER LISTING (sorted by GRLWEAP ID Numbers)									
Hammer Description				SI Units			US Units		
GRLWEAP ID	Hammer Manufacturer	Hammer Name	Hammer Type	Rated Energy kJ	Ram Weight kN	Eq. Rated Stroke m	Rated Energy ft-kips	Ram Weight kips	Eq. Rated Stroke ft
81	LINKBELT	LB 180	CED	10.98	7.70	1.43	8.10	1.73	4.68
82	LINKBELT	LB 312	CED	20.36	17.18	1.19	15.02	3.86	3.89
83	LINKBELT	LB 440	CED	24.68	17.80	1.39	18.20	4.00	4.55
84	LINKBELT	LB 520	CED	35.68	22.56	1.58	26.31	5.07	5.19
85	LINKBELT	LB 660	CED	70.01	33.69	2.08	51.63	7.57	6.82
101	KOBE	K 13	OED	34.48	12.77	2.70	25.43	2.87	8.86
103	KOBE	K22-Est	OED	61.49	21.58	2.85	45.35	4.85	9.35
104	KOBE	K 25	OED	69.86	24.52	2.85	51.52	5.51	9.35
107	KOBE	K 35	OED	97.88	34.35	2.85	72.18	7.72	9.35
110	KOBE	K 45	OED	125.77	44.14	2.85	92.75	9.92	9.35
112	KOBE	KB 60	OED	176.53	58.87	3.00	130.18	13.23	9.84
113	KOBE	KB 80	OED	235.37	78.50	3.00	173.58	17.64	9.84
120	ICE	180	CED	11.03	7.70	1.43	8.13	1.73	4.70
121	ICE	422	CED	31.35	17.80	1.76	23.12	4.00	5.78
122	ICE	440	CED	25.17	17.80	1.41	18.56	4.00	4.64
123	ICE	520	CED	41.18	22.56	1.83	30.37	5.07	5.99
124	ICE	640	CED	55.08	26.70	2.06	40.62	6.00	6.77
125	ICE	660	CED	70.01	33.69	2.08	51.63	7.57	6.82
126	ICE	1070	CED	98.45	44.50	2.21	72.60	10.00	7.26
127	ICE	30-S	OED	30.51	13.35	2.34	22.50	3.00	7.67
128	ICE	40-S	OED	54.24	17.80	3.10	40.00	4.00	10.17

TABLE D-4: COMPLETE HAMMER LISTING (sorted by GRLWEAP ID Numbers)									
Hammer Description				SI Units			US Units		
GRLWEAP ID	Hammer Manufacturer	Hammer Name	Hammer Type	Rated Energy kJ	Ram Weight kN	Eq. Rated Stroke m	Rated Energy ft-kips	Ram Weight kips	Eq. Rated Stroke ft
129	ICE	42-S	OED	56.96	18.20	3.18	42.00	4.09	10.42
130	ICE	60-S	OED	81.35	31.15	3.18	59.99	7.00	10.42
131	ICE	70-S	OED	94.92	31.15	3.10	70.00	7.00	10.17
132	ICE	80-S	OED	108.48	35.60	3.79	80.00	8.00	12.42
133	ICE	90-S	OED	122.04	40.05	3.10	90.00	9.00	10.17
134	ICE	100-S	OED	135.60	44.50	3.66	100.00	10.00	12.00
135	ICE	120-S	OED	162.72	53.40	3.79	120.00	12.00	12.42
136	ICE	200-S	OED	135.60	89.00	1.83	100.00	20.00	6.00
137	ICE	205-S	OED	230.52	89.00	3.20	170.00	20.00	10.50
139	ICE	32-S	OED	35.27	13.35	3.25	26.01	3.00	10.67
140	ICE	120S-15	OED	179.60	66.75	3.73	132.45	15.00	12.25
142	MKT 20	DE333020	OED	27.12	8.90	3.51	20.00	2.00	11.50
143	MKT 30	DE333020	OED	37.97	12.46	3.51	28.00	2.80	11.50
144	MKT 33	DE333020	OED	44.75	14.69	3.51	33.00	3.30	11.50
145	MKT 40	DE333020	OED	54.24	17.80	3.51	40.00	4.00	11.50
146	MKT	DE 10	OED	11.93	4.90	3.35	8.80	1.10	11.00
147	MKT	DE 20	OED	21.70	8.90	2.74	16.00	2.00	9.00
148	MKT	DE 30	OED	30.37	12.46	3.05	22.40	2.80	10.00
149	MKT	DA35B SA	OED	32.27	12.46	3.96	23.80	2.80	13.00
150	MKT	DE 30B	OED	32.27	12.46	3.05	23.80	2.80	10.00
151	MKT	DA 35B	CED	28.48	12.46	2.29	21.00	2.80	7.50

TABLE D-4: COMPLETE HAMMER LISTING (sorted by GRLWEAP ID Numbers)									
Hammer Description				SI Units			US Units		
GRLWEAP ID	Hammer Manufacturer	Hammer Name	Hammer Type	Rated Energy kJ	Ram Weight kN	Eq. Rated Stroke m	Rated Energy ft-kips	Ram Weight kips	Eq. Rated Stroke ft
152	MKT	DA 45	CED	41.66	17.80	2.34	30.72	4.00	7.68
153	MKT	DE 40	OED	43.39	17.80	3.05	32.00	4.00	10.00
154	MKT	DE 42/35	OED	47.46	15.58	4.11	35.00	3.50	13.50
155	MKT	DE 42/35	OED	56.95	18.69	4.11	42.00	4.20	13.50
157	MKT	DE 50C	OED	67.80	22.25	3.96	50.00	5.00	13.00
158	MKT	DE 70C	OED	94.92	31.15	3.96	70.00	7.00	13.00
159	MKT	DE 50B	OED	57.63	22.25	3.35	42.50	5.00	11.00
160	MKT	DA55B SA	OED	54.24	22.25	3.66	40.00	5.00	12.00
161	MKT	DA 55B	CED	51.80	22.25	2.33	38.20	5.00	7.64
162	MKT	DE 70B	OED	80.68	31.15	3.66	59.50	7.00	12.00
163	MKT 50	DE70/50B	OED	67.80	22.25	3.66	50.00	5.00	12.00
164	MKT 70	DE70/50B	OED	94.92	31.15	3.66	70.00	7.00	12.00
165	MKT 110	DE110150	OED	149.16	48.95	4.11	110.00	11.00	13.50
166	MKT 150	DE110150	OED	203.40	66.75	4.11	150.00	15.00	13.50
167	MKT	DA 35C	CED	28.48	12.46	2.29	21.00	2.80	7.50
168	MKT	DA 55C	CED	51.80	22.25	2.33	38.20	5.00	7.64
171	CONMACO	C 50	ECH	20.34	22.25	0.91	15.00	5.00	3.00
172	CONMACO	C 65	ECH	26.44	28.93	0.91	19.50	6.50	3.00
173	CONMACO	C 550	ECH	33.90	22.25	1.52	25.00	5.00	5.00
174	CONMACO	C 565	ECH	44.07	28.93	1.52	32.50	6.50	5.00
175	CONMACO	C 80	ECH	35.26	35.60	0.99	26.00	8.00	3.25

TABLE D-4: COMPLETE HAMMER LISTING (sorted by GRLWEAP ID Numbers)									
Hammer Description				SI Units			US Units		
GRLWEAP ID	Hammer Manufacturer	Hammer Name	Hammer Type	Rated Energy kJ	Ram Weight kN	Eq. Rated Stroke m	Rated Energy ft-kips	Ram Weight kips	Eq. Rated Stroke ft
176	CONMACO	C 100	ECH	44.07	44.50	0.99	32.50	10.00	3.25
177	CONMACO	C 115	ECH	50.68	51.18	0.99	37.38	11.50	3.25
178	CONMACO	C 80E5	ECH	54.24	35.60	1.52	40.00	8.00	5.00
179	CONMACO	C 100E5	ECH	67.80	44.50	1.52	50.00	10.00	5.00
180	CONMACO	C 115E5	ECH	77.97	51.18	1.52	57.50	11.50	5.00
181	CONMACO	C 125E5	ECH	84.75	55.63	1.52	62.50	12.50	5.00
182	CONMACO	C 140	ECH	56.95	62.30	0.91	42.00	14.00	3.00
183	CONMACO	C 160	ECH	66.11	72.31	0.91	48.75	16.25	3.00
184	CONMACO	C 200	ECH	81.36	89.00	0.91	60.00	20.00	3.00
185	CONMACO	C 300	ECH	122.04	133.50	0.91	90.00	30.00	3.00
186	CONMACO	C 5200	ECH	135.60	89.00	1.52	100.00	20.00	5.00
187	CONMACO	C 5300	ECH	203.40	133.50	1.52	150.00	30.00	5.00
188	CONMACO	C 5450	ECH	305.10	200.25	1.52	225.00	45.00	5.00
189	CONMACO	C 5700	ECH	474.60	311.50	1.52	350.00	70.00	5.00
190	CONMACO	C 6850	ECH	691.56	378.25	1.83	510.00	85.00	6.00
191	CONMACO	C 160 **	ECH	70.21	76.81	0.91	51.78	17.26	3.00
192	CONMACO	C 50E5	ECH	33.90	22.25	1.52	25.00	5.00	5.00
193	CONMACO	C 65E5	ECH	44.07	28.93	1.52	32.50	6.50	5.00
194	CONMACO	C 200E5	ECH	135.60	89.00	1.52	100.00	20.00	5.00
195	CONMACO	C 300E5	ECH	203.40	133.50	1.52	150.00	30.00	5.00
204	VULCAN	VUL 01	ECH	20.34	22.25	0.91	15.00	5.00	3.00

TABLE D-4: COMPLETE HAMMER LISTING (sorted by GRLWEAP ID Numbers)									
Hammer Description				SI Units			US Units		
GRLWEAP ID	Hammer Manufacturer	Hammer Name	Hammer Type	Rated Energy kJ	Ram Weight kN	Eq. Rated Stroke m	Rated Energy ft-kips	Ram Weight kips	Eq. Rated Stroke ft
205	VULCAN	VUL 02	ECH	9.84	13.35	0.74	7.26	3.00	2.42
206	VULCAN	VUL 06	ECH	26.44	28.93	0.91	19.50	6.50	3.00
207	VULCAN	VUL 08	ECH	35.26	35.60	0.99	26.00	8.00	3.25
208	VULCAN	VUL 010	ECH	44.07	44.50	0.99	32.50	10.00	3.25
209	VULCAN	VUL 012	ECH	52.88	53.40	0.99	39.00	12.00	3.25
210	VULCAN	VUL 014	ECH	56.95	62.30	0.91	42.00	14.00	3.00
211	VULCAN	VUL 016	ECH	66.11	72.31	0.91	48.75	16.25	3.00
212	VULCAN	VUL 020	ECH	81.36	89.00	0.91	60.00	20.00	3.00
213	VULCAN	VUL 030	ECH	122.04	133.50	0.91	90.00	30.00	3.00
214	VULCAN	VUL 040	ECH	162.72	178.00	0.91	120.00	40.00	3.00
215	VULCAN	VUL 060	ECH	244.08	267.00	0.91	180.00	60.00	3.00
220	VULCAN	VUL 30C	ECH	9.84	13.35	0.74	7.26	3.00	2.42
221	VULCAN	VUL 50C	ECH	20.48	22.25	0.92	15.10	5.00	3.02
222	VULCAN	VUL 65C	ECH	26.00	28.93	0.90	19.18	6.50	2.95
223	VULCAN	VUL 65CA	ECH	26.53	28.93	0.92	19.57	6.50	3.01
224	VULCAN	VUL 80C	ECH	33.19	35.60	0.93	24.48	8.00	3.06
225	VULCAN	VUL 85C	ECH	35.24	37.91	0.93	25.99	8.52	3.05
226	VULCAN	VUL 100C	ECH	44.61	44.50	1.00	32.90	10.00	3.29
227	VULCAN	VUL 140C	ECH	48.79	62.30	0.78	35.98	14.00	2.57
228	VULCAN	VUL 200C	ECH	68.07	89.00	0.77	50.20	20.00	2.51
229	VULCAN	VUL 400C	ECH	154.04	178.00	0.87	113.60	40.00	2.84

TABLE D-4: COMPLETE HAMMER LISTING (sorted by GRLWEAP ID Numbers)									
Hammer Description				SI Units			US Units		
GRLWEAP ID	Hammer Manufacturer	Hammer Name	Hammer Type	Rated Energy kJ	Ram Weight kN	Eq. Rated Stroke m	Rated Energy ft-kips	Ram Weight kips	Eq. Rated Stroke ft
230	VULCAN	VUL 600C	ECH	243.27	267.00	0.91	179.40	60.00	2.99
231	VULCAN	VUL 320	ECH	81.36	89.00	0.91	60.00	20.00	3.00
232	VULCAN	VUL 330	ECH	122.04	133.50	0.91	90.00	30.00	3.00
233	VULCAN	VUL 340	ECH	162.72	178.00	0.91	120.00	40.00	3.00
234	VULCAN	VUL 360	ECH	244.08	267.00	0.91	180.00	60.00	3.00
235	VULCAN	VUL 505	ECH	33.90	22.25	1.52	25.00	5.00	5.00
236	VULCAN	VUL 506	ECH	44.07	28.93	1.52	32.50	6.50	5.00
237	VULCAN	VUL 508	ECH	54.24	35.60	1.52	40.00	8.00	5.00
238	VULCAN	VUL 510	ECH	67.80	44.50	1.52	50.00	10.00	5.00
239	VULCAN	VUL 512	ECH	81.36	53.40	1.52	60.00	12.00	5.00
240	VULCAN	VUL 520	ECH	135.60	89.00	1.52	100.00	20.00	5.00
241	VULCAN	VUL 530	ECH	203.40	133.50	1.52	150.00	30.00	5.00
242	VULCAN	VUL 540	ECH	271.20	182.01	1.49	200.00	40.90	4.89
243	VULCAN	VUL 560	ECH	406.80	278.13	1.46	300.00	62.50	4.80
245	VULCAN	VUL 3100	ECH	406.80	445.00	0.91	300.00	100.00	3.00
246	VULCAN	VUL 5100	ECH	678.00	445.00	1.52	500.00	100.00	5.00
247	VULCAN	VUL 5150	ECH	1017.00	667.50	1.52	750.00	150.00	5.00
248	VULCAN	VUL 6300	ECH	2440.80	1335.00	1.83	1800.00	300.00	6.00
251	RAYMOND	R 1	ECH	20.34	22.25	0.91	15.00	5.00	3.00
252	RAYMOND	R 1S	ECH	26.44	28.93	0.91	19.50	6.50	3.00
253	RAYMOND	R 65C	ECH	26.44	28.93	0.91	19.50	6.50	3.00

TABLE D-4: COMPLETE HAMMER LISTING (sorted by GRLWEAP ID Numbers)									
Hammer Description				SI Units			US Units		
GRLWEAP ID	Hammer Manufacturer	Hammer Name	Hammer Type	Rated Energy kJ	Ram Weight kN	Eq. Rated Stroke m	Rated Energy ft-kips	Ram Weight kips	Eq. Rated Stroke ft
254	RAYMOND	R 65CH	ECH	26.44	28.93	0.91	19.50	6.50	3.00
255	RAYMOND	R 0	ECH	33.05	33.38	0.99	24.38	7.50	3.25
256	RAYMOND	R 80C	ECH	33.19	35.60	0.93	24.48	8.00	3.06
257	RAYMOND	R 80CH	ECH	33.19	35.60	0.93	24.48	8.00	3.06
258	RAYMOND	R 2/0	ECH	44.07	44.50	0.99	32.50	10.00	3.25
259	RAYMOND	R 3/0	ECH	55.09	55.63	0.99	40.63	12.50	3.25
260	RAYMOND	R 150C	ECH	66.11	66.75	0.99	48.75	15.00	3.25
261	RAYMOND	R 4/0	ECH	66.11	66.75	0.99	48.75	15.00	3.25
262	RAYMOND	R 5/0	ECH	77.12	77.88	0.99	56.88	17.50	3.25
263	RAYMOND	R 30X	ECH	101.70	133.50	0.76	75.00	30.00	2.50
264	RAYMOND	R 8/0	ECH	110.18	111.25	0.99	81.25	25.00	3.25
265	RAYMOND	R 40X	ECH	135.60	178.00	0.76	100.00	40.00	2.50
266	RAYMOND	R 60X	ECH	203.40	267.00	0.76	150.00	60.00	2.50
271	MENCK	MH 68	ECH	66.68	34.35	1.94	49.18	7.72	6.37
272	MENCK	MH 96	ECH	94.14	49.04	1.92	69.43	11.02	6.30
273	MENCK	MH 145	ECH	142.11	73.56	1.93	104.80	16.53	6.34
274	MENCK	MH 195	ECH	191.36	98.12	1.95	141.12	22.05	6.40
275	MENCK	MHU 220	ECH	215.70	111.83	1.93	159.07	25.13	6.33
276	MENCK	MHU 400	ECH	392.64	225.66	1.74	289.55	50.71	5.71
277	MENCK	MHU 600	ECH	588.01	343.36	1.71	433.64	77.16	5.62
278	MENCK	MHU 1000	ECH	1000.32	565.02	1.77	737.70	126.97	5.81

TABLE D-4: COMPLETE HAMMER LISTING (sorted by GRLWEAP ID Numbers)									
Hammer Description				SI Units			US Units		
GRLWEAP ID	Hammer Manufacturer	Hammer Name	Hammer Type	Rated Energy kJ	Ram Weight kN	Eq. Rated Stroke m	Rated Energy ft-kips	Ram Weight kips	Eq. Rated Stroke ft
279	MENCK	MHU 1700	ECH	1666.35	922.17	1.81	1228.87	207.23	5.93
280	MENCK	MHU 2100	ECH	2098.53	1138.31	1.84	1547.59	255.80	6.05
281	MENCK	MHU 3000	ECH	2944.75	1618.73	1.82	2171.65	363.76	5.97
282	MENCK	MRBS 500	ECH	61.12	49.04	1.25	45.07	11.02	4.09
283	MENCK	MRBS 750	ECH	91.90	73.56	1.25	67.77	16.53	4.10
285	MENCK	MRBS 850	ECH	126.49	84.37	1.50	93.28	18.96	4.92
286	MENCK	MRBS1100	ECH	167.37	107.91	1.55	123.43	24.25	5.09
287	MENCK	MRBS1502	ECH	183.86	147.16	1.25	135.59	33.07	4.10
288	MENCK	MRBS1800	ECH	257.39	171.68	1.50	189.81	38.58	4.92
289	MENCK	MRBS2500	ECH	355.43	284.49	1.25	262.11	63.93	4.10
290	MENCK	MRBS2502	ECH	306.39	245.24	1.25	225.95	55.11	4.10
291	MENCK	MRBS2504	ECH	306.39	245.24	1.25	225.95	55.11	4.10
292	MENCK	MRBS3000	ECH	441.19	294.28	1.50	325.36	66.13	4.92
293	MENCK	MRBS3900	ECH	696.09	386.53	1.80	513.34	86.86	5.91
294	MENCK	MRBS4600	ECH	676.56	451.27	1.50	498.94	101.41	4.92
295	MENCK	MRBS5000	ECH	735.40	490.52	1.50	542.33	110.23	4.92
296	MENCK	MRBS6000	ECH	1029.52	588.60	1.75	759.23	132.27	5.74
297	MENCK	MRBS7000	ECH	856.18	685.30	1.25	631.40	154.00	4.10
298	MENCK	MRBS8000	ECH	1176.66	784.85	1.50	867.74	176.37	4.92
299	MENCK	MRBS8800	ECH	1294.34	863.34	1.50	954.53	194.01	4.92
300	MENCK	MBS12500	ECH	2144.96	1226.33	1.75	1581.83	275.58	5.74

TABLE D-4: COMPLETE HAMMER LISTING (sorted by GRLWEAP ID Numbers)									
Hammer Description				SI Units			US Units		
GRLWEAP ID	Hammer Manufacturer	Hammer Name	Hammer Type	Rated Energy kJ	Ram Weight kN	Eq. Rated Stroke m	Rated Energy ft-kips	Ram Weight kips	Eq. Rated Stroke ft
301	MKT	No. 5	ECH	1.36	0.89	1.52	1.00	0.20	5.00
302	MKT	No. 6	ECH	3.39	1.78	1.91	2.50	0.40	6.25
303	MKT	No. 7	ECH	5.63	3.56	1.58	4.15	0.80	5.19
304	MKT	9B3	ECH	11.87	7.12	1.67	8.75	1.60	5.47
305	MKT	10B3	ECH	17.78	13.35	1.33	13.11	3.00	4.37
306	MKT	C5-Air	ECH	19.26	22.25	0.87	14.20	5.00	2.84
307	MKT	C5-Steam	ECH	21.97	22.25	0.99	16.20	5.00	3.24
308	MKT	S-5	ECH	22.04	22.25	0.99	16.25	5.00	3.25
309	MKT	11B3	ECH	25.97	22.25	1.17	19.15	5.00	3.83
310	MKT	C826 Stm	ECH	33.09	35.60	0.93	24.40	8.00	3.05
311	MKT	C826 Air	ECH	28.75	35.60	0.81	21.20	8.00	2.65
312	MKT	S-8	ECH	35.26	35.60	0.99	26.00	8.00	3.25
313	MKT	MS-350	ECH	41.77	34.35	1.22	30.80	7.72	3.99
314	MKT	S 10	ECH	44.07	44.50	0.99	32.50	10.00	3.25
315	MKT	S 14	ECH	50.88	62.30	0.82	37.52	14.00	2.68
316	MKT	MS 500	ECH	59.66	48.95	1.22	44.00	11.00	4.00
317	MKT	S 20	ECH	81.36	89.00	0.91	60.00	20.00	3.00
320	IHC	S-35	ECH	34.61	29.50	1.17	25.53	6.63	3.85
321	IHC	S-70	ECH	69.49	34.40	2.02	51.25	7.73	6.63
322	IHC	S-90	ECH	89.36	44.23	2.02	65.90	9.94	6.63
323	IHC	S-120	ECH	121.19	59.99	2.02	89.37	13.48	6.63

TABLE D-4: COMPLETE HAMMER LISTING (sorted by GRLWEAP ID Numbers)									
Hammer Description				SI Units			US Units		
GRLWEAP ID	Hammer Manufacturer	Hammer Name	Hammer Type	Rated Energy kJ	Ram Weight kN	Eq. Rated Stroke m	Rated Energy ft-kips	Ram Weight kips	Eq. Rated Stroke ft
324	IHC	S-150	ECH	149.24	73.87	2.02	110.06	16.60	6.63
325	IHC	S-200	ECH	197.49	97.90	2.02	145.64	22.00	6.62
326	IHC	S-280	ECH	278.40	133.77	2.08	205.31	30.06	6.83
327	IHC	S-400	ECH	396.77	196.69	2.02	292.60	44.20	6.62
328	IHC	S-500	ECH	496.41	246.09	2.02	366.09	55.30	6.62
329	IHC	S-600	ECH	601.44	298.15	2.02	443.54	67.00	6.62
330	IHC	S-900	ECH	892.73	442.55	2.02	658.36	99.45	6.62
331	IHC	S-1200	ECH	1208.27	598.97	2.02	891.05	134.60	6.62
332	IHC	S-1800	ECH	1586.93	738.70	2.15	1170.30	166.00	7.05
333	IHC	S-2300	ECH	2280.09	1130.30	2.02	1681.48	254.00	6.62
335	IHC	SC-30	ECH	29.57	16.73	1.77	21.81	3.76	5.80
336	IHC	SC-40	ECH	40.50	24.52	1.65	29.86	5.51	5.42
337	IHC	SC-50	ECH	49.92	32.44	1.54	36.81	7.29	5.05
338	IHC	SC-60	ECH	60.96	59.19	1.03	44.95	13.30	3.38
339	IHC	SC-75	ECH	74.30	54.07	1.37	54.80	12.15	4.51
340	IHC	SC-110	ECH	111.04	77.70	1.43	81.89	17.46	4.69
341	IHC	SC-150	ECH	148.28	108.14	1.37	109.35	24.30	4.50
342	IHC	SC-200	ECH	206.80	134.39	1.54	152.51	30.20	5.05
349	HERA	1900	OED	60.23	18.65	3.23	44.41	4.19	10.60
350	HERA	1250	OED	34.37	12.50	2.75	25.35	2.81	9.02
351	HERA	1500	OED	41.22	15.00	2.75	30.40	3.37	9.02

TABLE D-4: COMPLETE HAMMER LISTING (sorted by GRLWEAP ID Numbers)									
Hammer Description				SI Units			US Units		
GRLWEAP ID	Hammer Manufacturer	Hammer Name	Hammer Type	Rated Energy kJ	Ram Weight kN	Eq. Rated Stroke m	Rated Energy ft-kips	Ram Weight kips	Eq. Rated Stroke ft
352	HERA	2500	OED	68.74	25.01	2.75	50.69	5.62	9.02
353	HERA	2800	OED	76.93	27.99	2.75	56.74	6.29	9.02
354	HERA	3500	OED	96.26	35.02	2.75	70.99	7.87	9.02
355	HERA	5000	OED	137.48	50.02	2.75	101.38	11.24	9.02
356	HERA	5700	OED	156.68	57.00	2.75	115.55	12.81	9.02
357	HERA	6200	OED	170.38	61.99	2.75	125.65	13.93	9.02
358	HERA	7500	OED	206.09	74.98	2.75	151.99	16.85	9.02
359	HERA	8800	OED	241.93	88.02	2.75	178.42	19.78	9.02
360	ICE	I-12	OED	40.95	12.55	3.51	30.20	2.82	11.50
361	ICE	I-19	OED	58.56	17.84	3.75	43.19	4.01	12.30
362	ICE	I-30	OED	102.27	29.41	3.84	75.42	6.61	12.60
363	ICE	I-36	OED	122.96	35.33	3.69	90.67	7.94	12.10
364	ICE	I-46	OED	146.17	45.17	3.69	107.79	10.15	12.12
365	ICE	I-62	OED	223.71	64.97	4.34	164.98	14.60	14.25
366	ICE	I-80	OED	288.01	78.77	4.11	212.40	17.70	13.50
371	FAIRCHLD	F-45	ECH	61.02	66.75	0.91	45.00	15.00	3.00
372	FAIRCHLD	F-32	ECH	44.14	48.28	0.91	32.55	10.85	3.00
380	BSP	HH 1.5	ECH	22.02	14.69	1.50	16.24	3.30	4.92
381	BSP	HH 3	ECH	35.31	29.41	1.20	26.04	6.61	3.94
382	BSP	HH 5	ECH	58.88	49.04	1.20	43.42	11.02	3.94
383	BSP	HH 7	ECH	82.44	68.66	1.20	60.79	15.43	3.94

TABLE D-4: COMPLETE HAMMER LISTING (sorted by GRLWEAP ID Numbers)									
Hammer Description				SI Units			US Units		
GRLWEAP ID	Hammer Manufacturer	Hammer Name	Hammer Type	Rated Energy kJ	Ram Weight kN	Eq. Rated Stroke m	Rated Energy ft-kips	Ram Weight kips	Eq. Rated Stroke ft
384	BSP	HH 8	ECH	94.24	78.50	1.20	69.50	17.64	3.94
385	BSP	HH 9	ECH	106.00	88.29	1.20	78.17	19.84	3.94
386	BSP	HH11-1.2	ECH	129.56	107.91	1.20	95.55	24.25	3.94
387	BSP	HH14-1.2	ECH	164.87	137.33	1.20	121.59	30.86	3.94
388	BSP	HH16-1.2	ECH	188.43	156.95	1.20	138.96	35.27	3.94
389	BSP	HH 20	ECH	235.56	196.20	1.20	173.71	44.09	3.94
390	BSP	HH 20S	ECH	235.56	196.20	1.20	173.71	44.09	3.94
391	BSP	HA 30	ECH	353.31	294.28	1.20	260.55	66.13	3.94
392	BSP	HA 40	ECH	471.11	392.40	1.20	347.43	88.18	3.94
393	BSP	HH11-1.5	ECH	161.78	107.91	1.50	119.31	24.25	4.92
394	BSP	HH14-1.5	ECH	205.88	137.33	1.50	151.83	30.86	4.92
395	BSP	HH16-1.5	ECH	235.30	156.95	1.50	173.53	35.27	4.92
401	BERMINGH	B23	CED	31.17	12.46	2.50	22.99	2.80	8.21
402	BERMINGH	B200	OED	24.41	8.90	2.74	18.00	2.00	9.00
403	BERMINGH	B225	OED	39.66	13.35	2.97	29.25	3.00	9.75
404	BERMINGH	B300	OED	54.66	16.69	3.28	40.31	3.75	10.75
405	BERMINGH	B400	OED	72.89	22.25	3.28	53.75	5.00	10.75
410	BERMINGH	B300 M	OED	54.66	16.69	3.28	40.31	3.75	10.75
411	BERMINGH	B400 M	OED	72.89	22.25	3.28	53.75	5.00	10.75
412	BERMINGH	B400 4.8	OED	58.58	21.36	2.74	43.20	4.80	9.00
413	BERMINGH	B400 5.0	OED	61.02	22.25	2.74	45.00	5.00	9.00

TABLE D-4: COMPLETE HAMMER LISTING (sorted by GRLWEAP ID Numbers)									
Hammer Description				SI Units			US Units		
GRLWEAP ID	Hammer Manufacturer	Hammer Name	Hammer Type	Rated Energy kJ	Ram Weight kN	Eq. Rated Stroke m	Rated Energy ft-kips	Ram Weight kips	Eq. Rated Stroke ft
414	BERMINGH	B23 5	CED	31.17	12.46	2.50	22.99	2.80	8.21
415	BERMINGH	B250 5	OED	35.60	11.13	3.20	26.25	2.50	10.50
416	BERMINGH	B350 5	OED	64.00	17.80	3.60	47.20	4.00	11.80
417	BERMINGH	B400 5	OED	80.00	22.25	3.60	59.00	5.00	11.80
418	BERMINGH	B450 5	OED	105.61	29.37	3.60	77.88	6.60	11.80
419	BERMINGH	B500 5	OED	124.81	34.71	3.60	92.04	7.80	11.80
420	BERMINGH	B550 5	OED	144.01	40.05	3.60	106.20	9.00	11.80
421	BERMINGH	B550 C	OED	119.33	48.95	2.44	88.00	11.00	8.00
422	BERMINGH	B2005	OED	28.48	8.90	3.20	21.00	2.00	10.50
423	BERMINGH	B2505	OED	48.00	13.35	3.60	35.40	3.00	11.80
441	MENCK	MHF5-5	ECH	52.45	49.04	1.07	38.68	11.02	3.51
442	MENCK	MHF5-6	ECH	62.97	58.87	1.07	46.44	13.23	3.51
443	MENCK	MHF5-7	ECH	73.44	68.66	1.07	54.16	15.43	3.51
444	MENCK	MHF5-8	ECH	83.96	78.50	1.07	61.92	17.64	3.51
445	MENCK	MHF5-9	ECH	94.43	88.29	1.07	69.64	19.84	3.51
446	MENCK	MHF5-10	ECH	104.90	98.08	1.07	77.36	22.04	3.51
447	MENCK	MHF5-11	ECH	115.42	107.91	1.07	85.12	24.25	3.51
448	MENCK	MHF5-12	ECH	125.89	117.70	1.07	92.84	26.45	3.51
449	MENCK	MHF3-3	ECH	33.55	31.37	1.07	24.75	7.05	3.51
450	MENCK	MHF3-4	ECH	41.98	39.25	1.07	30.96	8.82	3.51
451	MENCK	MHF3-5	ECH	52.45	49.04	1.07	38.68	11.02	3.51

TABLE D-4: COMPLETE HAMMER LISTING (sorted by GRLWEAP ID Numbers)									
Hammer Description				SI Units			US Units		
GRLWEAP ID	Hammer Manufacturer	Hammer Name	Hammer Type	Rated Energy kJ	Ram Weight kN	Eq. Rated Stroke m	Rated Energy ft-kips	Ram Weight kips	Eq. Rated Stroke ft
452	MENCK	MHF3-6	ECH	62.97	58.87	1.07	46.44	13.23	3.51
453	MENCK	MHF3-7	ECH	73.44	68.66	1.07	54.16	15.43	3.51
454	MENCK	MHF10-15	ECH	169.01	147.12	1.15	124.64	33.06	3.77
455	MENCK	MHF10-20	ECH	225.29	196.11	1.15	166.14	44.07	3.77
461	MENCK	MHUT 200	ECH	199.85	117.75	1.70	147.38	26.46	5.57
462	MENCK	MHUT 400	ECH	400.18	234.52	1.71	295.12	52.70	5.60
463	MENCK	MHUT 500	ECH	550.59	294.28	1.87	406.04	66.13	6.14
464	MENCK	MHUT700U	ECH	699.88	413.09	1.69	516.13	92.83	5.56
465	MENCK	MHUT700A	ECH	839.60	413.09	2.03	619.18	92.83	6.67
466	MENCK	MHUT1000	ECH	999.25	588.74	1.70	736.91	132.30	5.57
467	MENCK	MHU2100S	ECH	2100.02	1010.51	2.08	1548.69	227.08	6.82
468	MENCK	MHU 800S	ECH	799.02	441.44	1.81	589.25	99.20	5.94
469	MENCK	MHU 1200	ECH	1202.34	657.62	1.83	886.68	147.78	6.00
481	JUNTTAN	HHK 3	ECH	36.00	29.46	1.22	26.55	6.62	4.01
482	JUNTTAN	HHK 4	ECH	47.96	39.25	1.22	35.37	8.82	4.01
483	JUNTTAN	HHK 5	ECH	59.98	49.08	1.22	44.23	11.03	4.01
484	JUNTTAN	HHK 6	ECH	71.94	58.87	1.22	53.05	13.23	4.01
485	JUNTTAN	HHK 7	ECH	83.96	68.71	1.22	61.91	15.44	4.01
486	JUNTTAN	HHK 10	ECH	119.90	98.12	1.22	88.42	22.05	4.01
487	JUNTTAN	HHK 12	ECH	143.88	117.75	1.22	106.10	26.46	4.01
488	JUNTTAN	HHK 14	ECH	167.86	137.37	1.22	123.79	30.87	4.01

TABLE D-4: COMPLETE HAMMER LISTING (sorted by GRLWEAP ID Numbers)									
Hammer Description				SI Units			US Units		
GRLWEAP ID	Hammer Manufacturer	Hammer Name	Hammer Type	Rated Energy kJ	Ram Weight kN	Eq. Rated Stroke m	Rated Energy ft-kips	Ram Weight kips	Eq. Rated Stroke ft
489	JUNTTAN	HHK 5A	ECH	59.77	49.04	1.22	44.08	11.02	4.00
490	JUNTTAN	HHK 7A	ECH	83.69	68.66	1.22	61.72	15.43	4.00
491	JUNTTAN	HHK 9A	ECH	107.61	88.29	1.22	79.36	19.84	4.00
492	JUNTTAN	HHK 12A	ECH	141.31	117.70	1.20	104.21	26.45	3.94
493	JUNTTAN	HHK 14A	ECH	164.87	137.33	1.20	121.59	30.86	3.94
494	JUNTTAN	HHK 16A	ECH	188.43	156.95	1.20	138.96	35.27	3.94
495	JUNTTAN	HHK 18A	ECH	212.00	176.58	1.20	156.34	39.68	3.94
501	HPSI	110	ECH	59.66	48.95	1.22	44.00	11.00	4.00
502	HPSI	150	ECH	81.36	66.75	1.22	60.00	15.00	4.00
503	HPSI	154	ECH	83.53	68.53	1.22	61.60	15.40	4.00
504	HPSI	200	ECH	108.48	89.00	1.22	80.00	20.00	4.00
505	HPSI	225	ECH	122.04	100.13	1.22	90.00	22.50	4.00
506	HPSI	650	ECH	44.07	28.93	1.52	32.50	6.50	5.00
507	HPSI	1000	ECH	67.80	44.50	1.52	50.00	10.00	5.00
508	HPSI	1605	ECH	112.55	73.87	1.52	83.00	16.60	5.00
509	HPSI	2005	ECH	128.96	84.64	1.52	95.10	19.02	5.00
510	HPSI	3005	ECH	209.23	137.33	1.52	154.30	30.86	5.00
511	HPSI	3505	ECH	239.06	156.91	1.52	176.30	35.26	5.00
512	HPSI	2000	ECH	108.48	89.00	1.22	80.00	20.00	4.00
514	UDDCOMB	H2H	ECH	22.49	19.58	1.15	16.59	4.40	3.77
515	UDDCOMB	H3H	ECH	33.74	29.37	1.15	24.88	6.60	3.77

TABLE D-4: COMPLETE HAMMER LISTING (sorted by GRLWEAP ID Numbers)									
Hammer Description				SI Units			US Units		
GRLWEAP ID	Hammer Manufacturer	Hammer Name	Hammer Type	Rated Energy kJ	Ram Weight kN	Eq. Rated Stroke m	Rated Energy ft-kips	Ram Weight kips	Eq. Rated Stroke ft
516	UDDCOMB	H4H	ECH	44.99	39.16	1.15	33.18	8.80	3.77
517	UDDCOMB	H5H	ECH	56.23	48.95	1.15	41.47	11.00	3.77
518	UDDCOMB	H6H	ECH	67.48	58.74	1.15	49.76	13.20	3.77
519	UDDCOMB	H8H	ECH	111.45	78.32	1.42	82.19	17.60	4.67
520	UDDCOMB	H10H	ECH	117.81	98.12	1.20	86.88	22.05	3.94
521	DAWSON	HPH1200	ECH	11.82	10.24	1.16	8.72	2.30	3.79
522	DAWSON	HPH1800	ECH	18.62	14.69	1.27	13.73	3.30	4.16
523	DAWSON	HPH2400	ECH	23.47	18.65	1.26	17.30	4.19	4.13
524	DAWSON	HPH6500	ECH	63.66	45.61	1.40	46.95	10.25	4.58
530	Bruce	SGH-0312	ECH	35.31	29.41	1.20	26.04	6.61	3.94
531	Bruce	SGH-0512	ECH	58.88	49.04	1.20	43.42	11.02	3.94
532	Bruce	SGH-0712	ECH	82.44	68.66	1.20	60.79	15.43	3.94
533	Bruce	SGH-1012	ECH	117.81	98.12	1.20	86.88	22.05	3.94
535	BANUT	3000	ECH	35.31	29.41	1.20	26.04	6.61	3.94
536	BANUT	4000	ECH	47.12	39.25	1.20	34.75	8.82	3.94
537	BANUT	5000	ECH	58.88	49.04	1.20	43.42	11.02	3.94
538	BANUT	6000	ECH	70.68	58.87	1.20	52.13	13.23	3.94
539	BANUT	8000	ECH	94.24	78.50	1.20	69.50	17.64	3.94
540	BANUT	10000	ECH	117.81	98.12	1.20	86.88	22.05	3.94
541	BANUT	3 Tonnes	ECH	23.48	29.41	0.80	17.32	6.61	2.62
542	BANUT	4 Tonnes	ECH	31.33	39.25	0.80	23.11	8.82	2.62

TABLE D-4: COMPLETE HAMMER LISTING (sorted by GRLWEAP ID Numbers)									
Hammer Description				SI Units			US Units		
GRLWEAP ID	Hammer Manufacturer	Hammer Name	Hammer Type	Rated Energy kJ	Ram Weight kN	Eq. Rated Stroke m	Rated Energy ft-kips	Ram Weight kips	Eq. Rated Stroke ft
543	BANUT	5 Tonnes	ECH	39.15	49.04	0.80	28.87	11.02	2.62
544	BANUT	6 Tonnes	ECH	47.00	58.87	0.80	34.66	13.23	2.62
545	BANUT	7 Tonnes	ECH	54.82	68.66	0.80	40.43	15.43	2.62
550	ICE	70	ECH	28.48	31.15	0.91	21.00	7.00	3.00
551	ICE	75	ECH	40.68	33.38	1.22	30.00	7.50	4.00
552	ICE	110-SH	ECH	51.15	51.18	1.00	37.72	11.50	3.28
553	ICE	115-SH	ECH	51.46	51.18	1.01	37.95	11.50	3.30
554	ICE	115	ECH	62.38	51.18	1.22	46.00	11.50	4.00
555	ICE	160-SH	ECH	86.78	71.20	1.22	64.00	16.00	4.00
556	ICE	160	ECH	86.78	71.20	1.22	64.00	16.00	4.00
557	ICE	220	ECH	119.33	97.90	1.22	88.00	22.00	4.00
558	ICE	275	ECH	149.16	122.38	1.22	110.00	27.50	4.00
560	HMC	28A	ECH	37.97	31.15	1.22	28.00	7.00	4.00
561	HMC	28B	ECH	28.48	31.15	0.91	21.00	7.00	3.00
562	HMC	62	ECH	62.38	51.18	1.22	46.00	11.50	4.00
563	HMC	86	ECH	86.78	71.20	1.22	64.00	16.00	4.00
564	HMC	119	ECH	119.33	97.90	1.22	88.00	22.00	4.00
565	HMC	149	ECH	149.16	122.38	1.22	110.00	27.50	4.00
566	HMC	187	ECH	187.13	153.53	1.22	138.00	34.50	4.00
567	HMC	19D	ECH	18.98	15.58	1.22	14.00	3.50	4.00
568	HMC	38D	ECH	37.97	31.15	1.22	28.00	7.00	4.00

TABLE D-4: COMPLETE HAMMER LISTING (sorted by GRLWEAP ID Numbers)									
Hammer Description				SI Units			US Units		
GRLWEAP ID	Hammer Manufacturer	Hammer Name	Hammer Type	Rated Energy kJ	Ram Weight kN	Eq. Rated Stroke m	Rated Energy ft-kips	Ram Weight kips	Eq. Rated Stroke ft
571	APE	D 19-32	OED	58.07	18.65	3.12	42.82	4.19	10.25
572	APE	D 30-32	OED	95.01	29.41	3.23	70.07	6.61	10.60
573	APE	D 36-32	OED	113.98	35.29	3.23	84.06	7.93	10.60
574	APE	D 46-32	OED	145.75	45.12	3.23	107.48	10.14	10.60
575	APE	D 62-22	OED	218.94	60.79	3.60	161.46	13.66	11.82
576	APE	D 80-23	OED	267.12	78.41	3.41	196.99	17.62	11.18
577	APE	D 100-13	OED	333.98	98.03	3.41	246.30	22.03	11.18
578	APE	D 8-32	OED	24.41	7.83	3.12	18.00	1.76	10.25
579	APE	D 16-32	OED	53.37	15.71	3.43	39.36	3.53	11.25
580	APE	D 19-42	OED	58.07	18.65	3.23	42.82	4.19	10.60
581	APE	D 25-32	OED	78.45	24.52	3.20	57.86	5.51	10.50
582	APE	D 125-32	OED	416.69	122.64	3.40	307.29	27.56	11.15
591	APE	5.4mT	ECH	35.31	53.40	0.66	26.04	12.00	2.17
592	APE	7.2mT	ECH	69.64	72.09	0.97	51.35	16.20	3.17
595	APE	10-60	ECH	108.48	89.00	1.22	80.00	20.00	4.00
596	APE	HI 400U	ECH	542.40	356.00	1.52	400.00	80.00	5.00
700	ICE	23-28	VIB	21.00	0.45	8.14	21.00	0.10	26.70
701	ICE	216	VIB	130.00	2.05	8.14	130.00	0.46	26.70
702	ICE	216E	VIB	130.00	2.05	8.14	130.00	0.46	26.70
703	ICE	11-23	VIB	164.00	2.05	9.66	164.00	0.46	31.70
704	ICE	223	VIB	242.00	2.05	11.67	242.00	0.46	38.30

TABLE D-4: COMPLETE HAMMER LISTING (sorted by GRLWEAP ID Numbers)									
Hammer Description				SI Units			US Units		
GRLWEAP ID	Hammer Manufacturer	Hammer Name	Hammer Type	Rated Energy kJ	Ram Weight kN	Eq. Rated Stroke m	Rated Energy ft-kips	Ram Weight kips	Eq. Rated Stroke ft
705	ICE	416L	VIB	242.00	4.09	8.14	242.00	0.92	26.70
706	ICE	812	VIB	375.00	8.10	8.14	375.00	1.82	26.70
707	ICE	815	VIB	375.00	8.19	8.14	375.00	1.84	26.70
708	ICE	44-30	VIB	242.00	5.79	6.10	242.00	1.30	20.00
709	ICE	44-50	VIB	377.00	5.79	8.14	377.00	1.30	26.70
710	ICE	44-65	VIB	485.00	5.79	8.38	485.00	1.30	27.50
711	ICE	66-65	VIB	485.00	8.68	6.61	485.00	1.95	21.70
712	ICE	66-80	VIB	597.00	8.68	8.14	597.00	1.95	26.70
713	ICE	1412B	VIB	597.00	9.08	6.40	597.00	2.04	21.00
714	ICE	1412C	VIB	470.00	8.99	7.01	470.00	2.02	23.00
720	HMC	3+28	VIB	21.00	0.49	8.17	21.00	0.11	26.80
721	HMC	3+75	VIB	56.00	0.49	11.00	56.00	0.11	36.10
722	HMC	13+200	VIB	149.00	1.56	8.14	149.00	0.35	26.70
723	HMC	13S+200	VIB	149.00	1.56	8.14	149.00	0.35	26.70
724	HMC	13H+200	VIB	164.00	1.56	9.08	164.00	0.35	29.80
725	HMC	25+220	VIB	164.00	2.71	6.37	164.00	0.61	20.90
726	HMC	26+335	VIB	242.00	3.16	7.80	242.00	0.71	25.60
727	HMC	26S+335	VIB	242.00	3.16	7.80	242.00	0.71	25.60
728	HMC	51+335	VIB	242.00	5.38	5.94	242.00	1.21	19.50
729	HMC	51+535	VIB	377.00	5.38	8.05	377.00	1.21	26.40
730	HMC	51S+535	VIB	377.00	5.38	8.05	377.00	1.21	26.40

TABLE D-4: COMPLETE HAMMER LISTING (sorted by GRLWEAP ID Numbers)									
Hammer Description				SI Units			US Units		
GRLWEAP ID	Hammer Manufacturer	Hammer Name	Hammer Type	Rated Energy kJ	Ram Weight kN	Eq. Rated Stroke m	Rated Energy ft-kips	Ram Weight kips	Eq. Rated Stroke ft
731	HMC	51+740	VIB	485.00	5.38	8.38	485.00	1.21	27.50
732	HMC	76+740	VIB	485.00	8.10	6.61	485.00	1.82	21.70
733	HMC	76+800	VIB	597.00	8.10	7.96	597.00	1.82	26.10
734	HMC	115+800	VIB	597.00	6.01	6.22	597.00	1.35	20.40
735	HMC	230+1600	VIB	0.00	11.97	6.22	0.00	2.69	20.40
750	MKT	V-2B	VIB	52.00	0.67	9.14	52.00	0.15	30.00
751	MKT	V-5C	VIB	138.00	1.91	8.63	138.00	0.43	28.33
752	MKT	V-20B	VIB	242.00	35.60	8.63	242.00	8.00	28.33
753	MKT	V-30	VIB	448.00	6.54	8.63	448.00	1.47	28.33
754	MKT	V-35	VIB	485.00	7.12	8.63	485.00	1.60	28.33
755	MKT	V-140	VIB	0.00	20.78	7.11	0.00	4.67	23.33
770	APE	3	VIB	10.58	0.00	11.67	10.58	0.00	38.30
771	APE	6	VIB	10.58	0.04	11.67	10.58	0.01	38.30
772	APE	15	VIB	59.67	0.49	9.14	59.67	0.11	30.00
773	APE	20	VIB	59.67	0.67	11.67	59.67	0.15	38.30
774	APE	20E	VIB	59.67	0.67	11.67	59.67	0.15	38.30
775	APE	50	VIB	194.00	1.02	9.14	194.00	0.23	30.00
776	APE	50E	VIB	194.00	1.02	9.14	194.00	0.23	30.00
777	APE	100	VIB	194.00	1.42	9.14	194.00	0.32	30.00
778	APE	100E	VIB	194.00	0.62	9.14	194.00	0.14	30.00
779	APE	100HF	VIB	260.00	0.62	13.11	260.00	0.14	43.00

TABLE D-4: COMPLETE HAMMER LISTING (sorted by GRLWEAP ID Numbers)									
Hammer Description				SI Units			US Units		
GRLWEAP ID	Hammer Manufacturer	Hammer Name	Hammer Type	Rated Energy kJ	Ram Weight kN	Eq. Rated Stroke m	Rated Energy ft-kips	Ram Weight kips	Eq. Rated Stroke ft
780	APE	150	VIB	260.00	0.62	9.14	260.00	0.14	30.00
781	APE	150T	VIB	260.00	0.76	9.14	260.00	0.17	30.00
782	APE	150HF	VIB	466.00	1.42	13.11	466.00	0.32	43.00
783	APE	200	VIB	466.00	1.29	9.14	466.00	0.29	30.00
784	APE	200T	VIB	466.00	1.51	9.40	466.00	0.34	30.83
785	APE	200T HF	VIB	738.00	1.51	13.11	738.00	0.34	43.00
786	APE	300	VIB	738.00	1.51	7.62	738.00	0.34	25.00
787	APE	400B	VIB	738.00	3.47	7.11	738.00	0.78	23.33
788	APE	600	VIB	800.00	4.67	7.10	800.00	1.05	23.30
789	APE	Tan 400	VIB	1476.00	6.10	7.11	1476.00	1.37	23.33
790	APE	Tan 600	VIB	1800.00	9.39	7.10	1800.00	2.11	23.30
801	DKH	PH-5	ECH	58.88	49.04	1.20	43.42	11.02	3.94
802	DKH	PH-7	ECH	82.44	68.66	1.20	60.79	15.43	3.94
803	DKH	PH-7S	ECH	82.44	68.66	1.20	60.79	15.43	3.94
804	DKH	PH-10	ECH	117.75	98.08	1.20	86.84	22.04	3.94
805	DKH	PH-13	ECH	153.12	127.54	1.20	112.92	28.66	3.94
806	DKH	PH-20	ECH	294.15	196.20	1.50	216.92	44.09	4.92
807	DKH	PH-30	ECH	441.19	294.28	1.50	325.36	66.13	4.92
808	DKH	PH-40	ECH	588.29	392.40	1.50	433.85	88.18	4.92
810	MGF	RBH 2400	VIB	975.00	23.99	7.16	975.00	5.39	23.50

